

Understanding Quantum Technologies

Fifth edition

Volume 1: physics, computing

2022

Olivier Ezratty



le lab quantique

cover back page

#QEI
the quantum energy initiative

discover the [QEI](#) in page 251

Understanding Quantum Technologies

Fifth edition

Volume 1

2022

Olivier Ezratty

About the author

Olivier Ezratty

consultant and author



[0000-0003-3944-2896](https://orcid.org/0000-0003-3944-2896)

[olivier \(at\) oezratty.net](mailto:olivier(at)oezratty.net), www.oezratty.net, [@olivez](https://twitter.com/olivez)

+33 6 67 37 92 41

Olivier Ezratty advises and trains businesses and public services in the development of their innovation strategies in the quantum technologies realm. He brings them a 360° understanding of these: scientific, technological, marketing as well as the knowledge of the quantum ecosystems.

He has covered many other topics since 2005, with among others digital television, Internet of things and artificial intelligence. As such, he carried out various strategic advisory missions of conferences or training in different verticals and domains such as the **media and telecoms** (Orange, Bouygues Telecom, TDF, Médiamétrie, BVA, Astra), **finance and insurance** (BPCE group, Caisse des Dépôts, Société Générale, Swiss Life, Crédit Agricole, Crédit Mutuel-CIC, Generali, MAIF), **industry and services** (Schneider, Camfil, Vinci, NTN-STR, Econocom, ADP, Air France, Airbus) and the **public sector** (CEA, Météo France, Bpifrance, Business France).

In the quantum realm:

- He is a keynote speaker in a large number of quantum technology events since 2018.
- He published the reference book **Understanding Quantum Technologies** (September 2021 and 2022) following three previous editions in French in 2018, 2019 and 2020. The 2021 and 2022 editions are also available in paperback version on Amazon.
- He runs **two series of podcasts** on quantum technologies with Fanny Bouton (in French): a monthly « Quantum » on tech news (since September 2019) and Decode Quantum, with entrepreneurs and researchers since March 2020, with a total of over 80 episodes.
- He is a trainer on quantum technologies for **Capgemini Institut** and for **CEA INSTN**. In September 2021, he took in charge an elective curriculum on quantum technologies for **EPITA**, an IT engineering school in France.
- He is the cofounder of the **Quantum Energy Initiative** with Alexia Auffèves (CNRS MajuLab Singapore) and Robert Whitney (CNRS LPMMC).
- He is advising **Bpifrance** on quantum projects evaluations, a member of the strategic committee for **France 2030**, the French government innovation strategy plan and also a lecturer at IHEDN.

He also lectures in various universities such as CentraleSupélec, Ecole des Mines de Paris, Télécom Paristech, EPITA, Les Gobelins, HEC, Neoma Rouen and SciencePo, on artificial intelligence, quantum technologies as well as entrepreneurship and product management, in French and English as needed. He is also the author of many open source ebooks in French on entrepreneurship (2006-2019), the CES of Las Vegas yearly report (2006-2020) and on artificial intelligence (2016-2021).

Before all that, Olivier Ezratty started in 1985 at **Sogitec**, a subsidiary of the Dassault group, where he was successively Software Engineer, then Head of the Research Department in the Communication Division. He initialized developments under Windows 1.0 in the field of editorial computing as well as on SGML, the ancestor of HTML and XML. Joining **Microsoft France** in 1990, he gained experience in many areas of the marketing mix: products, channels, markets and communication. He launched the first version of Visual Basic in 1991 and Windows NT in 1993. In 1998, he became Marketing and Communication Director of Microsoft France and in 2001, of the Developer Division, which he created in France to launch the .NET platform and promote it to developers, higher education and research, as well as to startups.

Olivier Ezratty is a software engineer from **Centrale Paris** (1985), which became CentraleSupélec in 2015.

This document is provided to you free of charge and is licensed under a "Creative Commons" license.
in the variant "Attribution-Noncommercial-No Derivative Works 2.0".



see <http://creativecommons.org/licenses/by-nc-nd/2.0/> - web site [ISSN 2680-0527](http://www.issn.org/ISSN_2680-0527)

Credits

Cover illustration: personal creation associating a Bloch sphere describing a qubit and the symbol of peace (my creation, first published in 2018) above a long list of over 400 scientists and entrepreneurs who are mentioned in the ebook.

This document contains over 1600 illustrations. I have managed to give credits to their creators as much as possible. Most sources are credited in footnotes or in the text. Only scientists' portraits are not credited since it's quite hard to track it. I have added my own credit in most of the illustrations I have created. In some cases, I have redrawn some third-party illustrations to create clean vector versions or used existing third-party illustrations and added my own text comments. The originals are still credited in that case.

Table of contents

| | |
|--|------------|
| Volume 1 | i |
| Foreword..... | vii |
| Why | 1 |
| A complex domain in search of pedagogy | 3 |
| A new technology wave | 4 |
| Reading guide | 4 |
| First and second quantum revolutions applications | 6 |
| Why quantum computing? | 8 |
| History and scientists | 18 |
| Precursors..... | 21 |
| Founders..... | 27 |
| Post-war | 46 |
| Quantum technologies physicists..... | 52 |
| Quantum information science and algorithms creators..... | 65 |
| Research for dummies..... | 72 |
| Quantum physics 101..... | 84 |
| Postulates | 86 |
| Quantization..... | 89 |
| Wave-particle duality | 95 |
| Superposition and entanglement | 102 |
| Indetermination | 105 |
| Measurement..... | 105 |
| No-cloning | 107 |
| Tunnel effect | 108 |
| Quantum matter | 109 |
| Extreme quantum..... | 133 |
| Gate-based quantum computing..... | 142 |
| In a nutshell..... | 142 |
| Linear algebra | 144 |
| Qubits..... | 162 |
| Bloch sphere..... | 165 |
| Registers..... | 169 |
| Gates | 171 |
| Inputs and outputs | 181 |
| Qubit lifecycle..... | 183 |
| Measurement..... | 185 |
| Quantum computing engineering..... | 196 |
| Key parameters | 197 |
| Quantum computers segmentation..... | 200 |
| Qubit types | 204 |
| Architecture overview..... | 212 |
| Processor layout | 214 |
| Error correction..... | 216 |
| Quantum memory | 244 |
| Quantum technologies energetics | 249 |

| | |
|--|------------|
| Economics..... | 264 |
| Quantum uncertainty..... | 265 |
| Quantum computing hardware | 273 |
| Quantum annealing | 277 |
| Superconducting qubits..... | 292 |
| Quantum dots spins qubits | 344 |
| NV centers qubits..... | 365 |
| Topological qubits..... | 376 |
| Trapped ions qubits..... | 384 |
| Neutral atoms qubits | 404 |
| NMR qubits..... | 421 |
| Photons qubits..... | 424 |
| Quantum enabling technologies..... | 464 |
| Cryogenics | 464 |
| Qubits control electronics | 485 |
| Thermometers | 522 |
| Vacuum | 522 |
| Lasers | 523 |
| Photonics..... | 529 |
| Fabs and manufacturing tools | 534 |
| Other enabling technologies vendors..... | 551 |
| Raw materials..... | 554 |
| Volume 2 | 571 |
| Content..... | 577 |
| Quantum algorithms..... | 579 |
| Algorithms classes | 583 |
| Basic algorithms toolbox | 589 |
| Higher level algorithms..... | 601 |
| Hybrid algorithms | 624 |
| Quantum inspired algorithms..... | 628 |
| Complexity theories | 629 |
| Quantum speedups | 640 |
| Quantum software development tools..... | 646 |
| Development tool classes..... | 646 |
| Research-originated quantum development tools..... | 659 |
| Quantum vendors development tools..... | 665 |
| Cloud quantum computing..... | 677 |
| Quantum software engineering | 680 |
| Benchmarking | 684 |
| Quantum computing business applications | 701 |
| Market forecasts..... | 701 |
| Healthcare | 707 |
| Energy and chemistry..... | 714 |
| Transportation and logistics | 720 |
| Retail..... | 725 |
| Telecommunications | 725 |
| Finance..... | 726 |
| Insurance | 732 |

| | |
|--|------------|
| Marketing | 733 |
| Content and media | 733 |
| Defense and aerospace | 735 |
| Intelligence services | 737 |
| Industry | 738 |
| Science | 738 |
| Software and tools vendors | 740 |
| Service vendors | 764 |
| Unconventional computing..... | 768 |
| Supercomputing | 769 |
| Digital annealing computing | 775 |
| Reversible and adiabatic calculation..... | 780 |
| Superconducting computing | 784 |
| Probabilistic computing | 790 |
| Optical computing..... | 790 |
| Chemical computing | 796 |
| Quantum telecommunications and cryptography | 798 |
| Public key cryptography | 799 |
| Quantum cryptanalysis threats | 801 |
| Quantum Random Numbers Generators | 810 |
| Quantum Key Distribution..... | 819 |
| Post-quantum cryptography | 837 |
| Quantum homomorphic cryptography | 846 |
| Quantum interconnect..... | 847 |
| Quantum Physical Unclonable Functions | 858 |
| Vendors | 859 |
| Quantum sensing..... | 875 |
| Quantum sensing use-cases and market..... | 875 |
| International System of Measurement | 877 |
| Quantum sensing taxonomy..... | 878 |
| Quantum gravimeters, gyroscopes and accelerometers | 880 |
| Quantum clocks | 886 |
| Quantum magnetometers | 891 |
| Quantum thermometers..... | 895 |
| Quantum frequencies sensing | 896 |
| Quantum imaging..... | 898 |
| Quantum pressure sensors..... | 906 |
| Quantum radars and lidars | 906 |
| Quantum chemical sensors..... | 908 |
| Quantum NEMS and MEMS | 909 |
| Quantum technologies around the world..... | 911 |
| Quantum computing startups and SMEs..... | 912 |
| Global investments..... | 919 |
| North America..... | 924 |
| Europe | 936 |
| Russia..... | 972 |
| Africa, Near and Middle East | 974 |
| Asia-Pacific..... | 977 |
| Corporate adoption..... | 993 |

| | |
|---|-------------|
| Technology screening | 994 |
| Needs analysis..... | 995 |
| Training | 995 |
| Evaluation | 996 |
| Quantum technologies and society | 997 |
| Human ambition..... | 997 |
| Science fiction..... | 998 |
| Quantum foundations..... | 1001 |
| Responsible quantum innovation..... | 1010 |
| Religions and mysticism | 1015 |
| Public education..... | 1016 |
| Professional education | 1017 |
| Jobs impact..... | 1022 |
| Gender balance..... | 1023 |
| Quantum technologies marketing | 1026 |
| Quantum fake sciences | 1029 |
| Quantum biology | 1029 |
| Quantum medicine | 1039 |
| Quantum management | 1047 |
| Other exaggerations | 1050 |
| Conclusion..... | 1056 |
| Bibliography | 1058 |
| Events..... | 1058 |
| Websites and content sources..... | 1061 |
| Podcasts..... | 1062 |
| Books and ebooks | 1062 |
| Comics | 1066 |
| Presentations | 1066 |
| Training..... | 1067 |
| Reports | 1067 |
| Miscellaneous | 1067 |
| Glossary..... | 1068 |
| Index..... | 1091 |
| Table of figures | 1105 |
| Revisions history | 1128 |

Foreword

Quantum technologies hold the promise of major disruptions in computing, communications and sensing. But scientific and technological challenges to their large-scale deployment are still important, and it is quite difficult for public decision makers, users, investors, professionals, and the public at large to anticipate when these will happen. This is of paramount importance for companies to stay competitive, for governments to position their country in this technology race, or for students to make decisions about their career. While some quantum devices are already in use with practical impact, e.g. sophisticated microscopes taking benefit of the exquisite sensitivity of the spin of point defects in diamonds, other technologies will take years if not decades to reach the markets.

But the situation is changing fast. When I co-founded the Quantonation investment fund in 2018, most of the fund's presentation was about the promises of quantum, and about the science. Today, with 21 seed investments made in startups in Europe and North America, the situation has already radically changed since, for the most mature, we are talking about products and customers, and, at least, proofs of concepts. Consulting firms are busy assessing future markets, their size keeps increasing and the horizon is getting closer with significant practical achievements not much further down the road. I'm often asked whether there is not too much "hype" in the field. I don't think so, particularly when I am comparing quantum technologies with other sectors. This is the beginning of market recognition, for a sector which impact is slowly being assessed properly.

But to do that, make proper assessments and keep control of the quantum narrative, we need deep experts who have a proper understanding of all the facets of the technology, from the fundamentals of the science to its applications, including questions about their deployment, their funding, how to teach them, and more. It is necessary to be able to mobilize academic experts to provide an opinion on the science at the base of the innovation, on the ability to make robust products, but we must also be able to imagine their use cases, and scientists alone are not equipped to do so. There is a need for a multidisciplinary collaboration involving scientists, engineers and users capable of taking a forward-looking posture. And here enters my friend Olivier Ezratty, the author of this most wonderful book "Understanding Quantum Technologies", who embodies multidisciplinary. He has the unique ability to listen, question, gather facts, and synthesize his learnings in a book that stands out as unique in the whole world, as far as I know.

I first met Olivier when I started Quantonation back in 2018. From the start I was impressed by his extremely methodic approach that he had applied with success on an earlier publication on artificial intelligence, and his very unique ambition. The book was first published in French, later in English, and it grew with the field he was "decoding" to use the title of Olivier's famous podcast with Fanny Bouton on quantum technologies. The book has gone only better with time, with thorough updates and new chapters about exciting topics e.g. "Quantum Matter" in this new edition. Olivier has also been among the very first supporters of the not-for profit that I co-founded and chaired, Le Lab Quantique. Le Lab Quantique is proud to promote "Understanding Quantum Technologies", an instrument that will benefit its ecosystem building mission.

I am convinced that this book will become a primer for professionals, from scientists to engineers, technicians, investors, and also for teachers, students, and the public at large. We're all extremely lucky to see the second quantum revolution happening before our eyes, science and technology are progressing at an amazing pace and it is essential to invent a new model of knowledge sharing, of collaboration. Olivier Ezratty's book is an indispensable instrument to read this revolution.

Christophe Jurczak, Partner at Quantonation, Paris and co-founder, Le Lab Quantique

Why

This book is the 5th edition of a book originally compiling a series of 18 articles that I published in French between June and September 2018. After two enriched editions in French in 2019 and 2020, I switched to English in the fourth, in September 2021 and here we are with an even larger sequel.

This book is a kaleidoscope for quantum technologies with a 360° perspective encompassing historical, scientific, technological, engineering, entrepreneurial, geopolitical, philosophical, and societal dimensions. It is not a quantum for dummies, babies, or your mother-in-law book. It mainly targets three audiences: information technologies (IT) specialists and engineers who want to understand what quantum physics and technologies are all about and decipher its ambient buzz, all participants to the quantum ecosystem from researchers to industry vendors and policy makers, and at last scientific students who would like to investigate quantum technologies as an exploratory field. For them, this book is also the largest review paper they could imagine with over 3,500 bibliographical references.

“Understanding Quantum Technologies” bears a lot of specificities compared to the existing quantum literature. While being rather technical in many parts, it tries to explain things and translate the complex quantum lingua in other tech’s lingua, particularly for IT and computer science professionals. It looks at the history of science and ideas and pays tribute to key people, from the past and the present. It investigates rarely covered aspects of quantum technologies and quantum engineering like various enabling technologies (cryogenics, cryo-electronics, new materials design, semiconductors, cabling and lasers), their thermodynamic and energetic dimension and what raw materials are used and where they come from. I cover quantum matter and describe how quantum circuits are manufactured. I even explain how research works in general and in the quantum realm and its codes.

It also extensively covers quantum sensing, telecommunications and cryptography. I also crafted a lot of precisely documented custom illustrations. Another differentiation is in the tone, relaxed when possible and calling out the bs and nonsense when necessary. It is abundant, particularly when media, analysts and consultants are fueling the quantum hype. I’m always puzzled by how they sometimes cover vendor news without having a real clue about what they are writing about. It motivated me in the first place back in 2015 to start investigating this field. It is always true as quantum technologies are more commonplace but are still largely misunderstood by general audiences as well as by many IT professionals. One striking example shows up when some folks explain that thanks to quantum cryptography, quantum computers will help make cryptography more secure!

Large vendors and the quantum startups funding craze have elevated quantum technologies to the rank of strategic sectors for developed countries. Most governments have launched their national quantum plans, starting with Singapore, the UK, China, USA, Germany, Japan, Australia, France, Russia, Israel, Taiwan, India and The Netherlands. The worldwide quantum technologies race is on. Countries are embattled to acquire or preserve their technological sovereignty, like if it was the last chance to achieve it, particularly for those countries who felt they lost the digital battle against the USA and Asia (mostly China, South Korea and Taiwan). Also, like many deep techs, quantum technologies are dual-use ones, with both civilian and military use cases, increasing the strategic stakes.

While it has not yet reached the volume and funding of other sectors such as artificial intelligence or the digital cloud, the quantum startups and small business ecosystem continues to expand worldwide. In this book, I mention about 550 such companies in many different categories (hardware, software, telecommunications, cryptography, sensing, enabling technologies, services). In most cases, hardware are in the deep techs realm if not in hard tech territory, with many still at an applied research stage with a rather low technology readiness level. Being still very uncertain, this market remains quite open to opportunities for scientists and creative innovators, while in other markets like with semiconductors and large consumer Internet players, the game looks like it is less open.

Quantum technologies are also surrounded by a fair share of hype. A few scientists, their laboratory's communication department, startups and large vendors frequently exaggerate the impact of their work. Many companies also integrate "quantum" into their positioning if not branding in many fancy ways. Either in a totally artificial way, or based on using technologies from the first quantum revolution.

Transistors, lasers and image sensors are quantum, so most digital technologies can claim to be quantum. As a consequence, we must learn to distinguish the old (first quantum revolution related) from the new (second quantum revolution related). However, even stronger bs shows up elsewhere, with false science-based quantum medicine and other charlatanism. I showcase it in a unique section dedicated to quantum hoaxes and scams, starting page 1029.

This book has another flavor. It is the result of an unprecedented human adventure at the heart of the quantum ecosystem. I started the journey back in 2016. I had then decided to select the theme of quantum computing for my usual techno-screening activities, ranging from preparing conferences and training to writing educational ebooks for professionals. I was joined by my friend **Fanny Bouton** to run a popularization conference on quantum computing in Nantes. She brought and still brings a different perspective, including some science fiction derived inspirations. This led to the conference **Le quantique, c'est fantastique** on June 14th, 2018 ([video](#)) and to numerous subsequent presentations. On top of that, we launched two series of podcasts (in French) covering quantum tech news and with interviews with researchers, entrepreneurs and also users. We also worked on gender balance and contributed as early as possible to this sector feminization and attract new talents¹. Fanny took an interesting turn in 2020, starting to work on **OVHcloud**'s startup program. She plays a key role to embark this European cloud vendor in the quantum adventure and now leads this effort. We both went from a role of observer to a very different one.

In this journey that is still going on, we've had the opportunity to meet with top researchers and entrepreneurs, first in France, and then internationally. It started with **Alain Aspect** (IOGS), **Philippe Grangier** (IOGS), **Daniel Esteve** (CEA), **Patrice Bertet** (CEA), **Maud Vinet** (CEA), **Tristan Meunier** (CNRS Institut Néel), **Eleni Diamanti** (CNRS LIP6), **Iordanis Kerenidis** (CNRS IRIF), **Pascale Senellart** (CNRS & UPS C2N and Quandela), **Elham Kashefi** (CNRS LIP6 and VeriQloud), **Alexia Auffèves** (CNRS Institut Néel in Grenoble and now MajuLab in Singapore), **Philippe Duluc** and **Cyril Allouche** (Atos), **Xavier Waintal** (CEA), **Robert Whitney** (CNRS LPMCM), **Théau Perronnin** (Alice&Bob), **Georges-Olivier Reymond** and **Antoine Browaeys** (Pasqal) and many others afterwards. We also toured almost all quantum **startups** in France. And of course, **Christophe Jurczak** from Quantonation and Le Lab Quantique, who kindly wrote this book foreword.

Our outreach then expanded internationally, particularly in Canada, the USA, the UK, Austria and The Netherlands. I had the opportunity to discuss with **Artur Ekert**, **Peter Knight**, **Tommaso Calarco** and many startup founders, from **PsiQuantum**, **IQM**, **ParityQC**, **ProteinQure**, **Qilimanjaro**, **Qblox**, **Jay Gambetta** from IBM and **Rainer Blatt** from AQT. It is not enough. I want more!

In short, during these years, we have been "embedded" in the scientific and entrepreneurial ecosystem. We also applied one of Heisenberg's principles derivatives, namely that a measurement device may influence the measured quantity. It was and remains a beautiful adventure with real people, passions, convictions, ups and downs, and in the end, a nice result with French and European research and entrepreneurship in quantum technologies that are more dynamic and better positioned than a few years ago. And the adventure is just beginning!

¹ With a one-day training session with Roland Berger and Axelle Lemaire in April 2019, with high school students at Magic Makers in September 2019, with young people and parents at the Startup4Teens event in February 2020, and a debate in early March 2020 with Alexia Auffèves, Elham Kashefi and Pascale Senellart hosted by Fanny Bouton and organized at Talan, another event with a dominant female audience of all ages in the Tech4All event organized by Ecole 42 and Digital Ladies in March 2020, each time in partnership with the association *Quelques Femmes du Numérique ! (Some Digital Women)*.

You may wonder why this book is free and what is its business model. I have published all my books like this since 2006 and fared well so far (on entrepreneurship, artificial intelligence and other technology and science related topics).

I favor distribution breadth over revenue. It makes knowledge easily accessible to broad audiences, particularly with students. Also, being distributed in digital format, books are easy to correct and update. It is quite practical when you mention hundreds of people and organizations, and deal with complicated scientific matters. Afterwards, I sell my time in a rather traditional way with speaking, training and consulting missions. The business model is simple: the (very) long version is free and the (too) short versions are charged. Since the people who don't have time usually have money and the other way around, it works quite well even if it may be counterintuitive in the first place.

A complex domain in search of pedagogy

After having swept through many areas of science and deep techs, I can definitively position quantum physics and quantum computing at the complexity scale apex. Quantum physics is difficult to apprehend since relying on counter-intuitive phenomena like wave-particle duality and entanglement, and on a mathematical formalism that is not obvious to most people, including IT specialists and developers, one of the key audiences for this book. It is still an open challenge to translate this scientific field lingua into natura language for most people, even with a strong engineering background.

There's the rehashed famous quote from **Richard Feynman** who pointed out that when you study quantum physics, if you think you understood everything, you are making a fool of yourself. **Alain Aspect** confirms this, always expressing doubts about his own understanding of the quantum entanglement phenomenon that he experimented with photons in his famous 1982 experiment.

Explaining quantum computing is thus a new and difficult art. When reading quantum physics books, you discover a mathematical formalism and many terms like observables, degeneracy, gentle measurement, Hermitian operators and the likes and wonder how they relate to the physical world. Sometimes, it takes quite a while before being able to make this connection! On the other hand, you hear simplistic descriptions of quantum physics, noticeably on superposition and entanglement, and quantum computing, some coming from quantum computing vendors themselves².

Once you think you understand it after having created a mental view of how it works, your explanations become quickly inaccessible for the profane. How do you avoid this side effect? Probably with finding analogies and use more visual tools to explain things than too much mathematics. I try this in many sections of this book, but, still, mathematics are useful in many parts. Also, to make sure it does not lose its scientific soundness in the process, many parts of this book have been fact-checked and proof-read by quantum scientists. I'd say, not enough. You'll be the judge.

This book frequently responds to questions like what, why, where and how? Particularly with linking theory, maths and the real world. Has Moore's empirical law really stalled? What being "quantum" means for a product or technology? Why are we using this convoluted mathematical formalism? Do we really have objects sitting simultaneously at two different locations? Why parallel opposite vectors in the Bloch sphere are mathematically orthogonal? Why and where density matrices are useful? What are pure and mixed states describing in the physical world? Why superposition and entanglement are the two sides of the same coin? Why do we need to cool many qubit types? How are cryostats working? What is the energy consumption of a quantum computer? How much data sits in quantum registers? How is data loaded in a quantum program? What data is generated by quantum algorithms and how is it decoded? Are quantum computers made for big data applications? How can you compare such and such quantum computer technology? Is Shor algorithm a serious threat for cybersecurity? When will we have a "real" quantum computer? Have we really achieved quantum supremacy?

² See the interesting point in [What Makes Quantum Computing So Hard to Explain?](#) by Scott Aaronson, June 2021.

And on and on... What is the real speedup of quantum algorithms? Are the case studies from D-Wave and the like real production grade applications? Will a quantum Internet replace the existing Internet? Why do many physicists dislike D-Wave and say it is not quantum? Can quantum telecommunications enable either faster than light communications or high-throughput data links? How are classical computing technologies competing with quantum computers? Why are quantum random number generators not that random? Are the Chinese going to kill us (metaphorically) with their (not so) huge R&D investments in quantum technologies? Can Europe take its fair share in this new market? Oh, and if I'm in an organization... what should I do? Am I late in the game by doing nothing?

To properly address this broad laundry list of questions, this book is positioned above the average media coverage of quantum computing, as well as analyst reports, and below classical scientific publications that are generally largely inaccessible to non-specialists, or to specialists from other domains.

A new technology wave

Quantum computing stays on top of the various applications of the second quantum revolution. Quantum sensing is more exotic and fragmented, and quantum telecommunications and cryptography are less fascinating. Why is quantum computing becoming an important topic? Firstly, because large IT companies such as IBM, Google, Intel and Microsoft are making headlines with impressive announcements that we must, however, take with a grain of salt, with a lot of hindsight, and decipher calmly. There's also the obvious impact of Peter Shor's factoring algorithm. It drives fuzzy fears on the future of Internet security and for your own digital privacy.

Above all, it is linked to the broad impact that quantum technologies could have on many scientific fields and digital markets. It may theoretically make it possible to solve problems belonging to classes of complexity that even the largest giant supercomputers will never be able to tackle with. Then, the hype builds exaggerated stories on how quantum computing will for sure fix climate change, predict the weather, cure cancer, and other miracles.

The other reason for this sudden interest is that we are still at the beginning of the story. New leaders will show up. A new ecosystem is being built. This in a field where there are still enormous scientific and technology challenges to overcome. It is a land of opportunities for science, technology and innovation. To resume quantum physics, we are in a highly indeterministic world.

It is quite difficult to evaluate the feasibility of large-scale quantum computing. For most scientists, we are still many decades away from it. Some believe it will never show up. Others are more optimistic. The main enemy is quantum decoherence and qubits errors happening during computing, and which are difficult to avoid and correct. The plan is to fix that with quantum error corrections and logical qubits made of physical qubits. It then becomes, at least, a physical scalability issue with a bunch of complex engineering issues related to cooling, cryo-electronics, cabling, classical computing, miniaturization, as well as fundamental thermodynamic and energetic dimensions.

It is a very interesting living case study of how mankind builds upon scientific progress and addresses the most difficult challenges around. For this respect, it is on par with controlling nuclear fusion.

Reading guide

Here is a tentative to prioritize which parts of this book you could read according to your business and scientific level.

Physicists can find a state-of-the-art tour covering all dimensions of quantum technologies beyond the field they already master.

Computer scientists, engineers and students in various scientific fields are the core target audience for this book, as it presents, popularizes and contextualizes the various scientific, mathematical and engineering concepts used in quantum technologies.

The required mathematical and computer basics level is at the bachelor's degree level for most parts. Afterwards, it can also depend on your age since many of these concepts were not in current programs a couple decades ago unless you were already specialized in quantum physics. Non-technical and decision-makers can still read the sections dealing with usages as well as with how countries are faring and societal issues.

| Book sections | Quantum physicists | Computer scientists and developers | Students in sciences (STEM) | Non technical audiences | Business audiences |
|---|--------------------|------------------------------------|-----------------------------|-------------------------|--------------------|
| Why | | | | | |
| History and scientists | | | | | |
| Quantum Physics 101 | known | optional | | | |
| Gate-based Quantum Computing | | | | | |
| Quantum Computing Engineering | | | | | |
| Quantum Enabling Technologies | | optional | | | |
| Quantum Computing Hardware | | | | | |
| Quantum Algorithms | | | | | |
| Quantum Software Development tools | | | | | |
| Quantum Computing Business applications | | | | | |
| Unconventional computing | | | | | |
| Quantum Telecommunications and Cryptography | | | | | |
| Quantum Sensing | | | | | |
| Quantum Technologies around the world | | | | | |
| Corporate Adoption | | | | | |
| Quantum technologies in society | | | | | |
| Quantum Fake Sciences | | | | | |

Figure 1: Understanding Quantum Technologies parts and audiences relevance. (cc) Olivier Ezratty 2021-2022.

Here's another view of the table of contents showcasing the overall logic between the lower « physics » layers and the upper hardware, software and solutions layers.

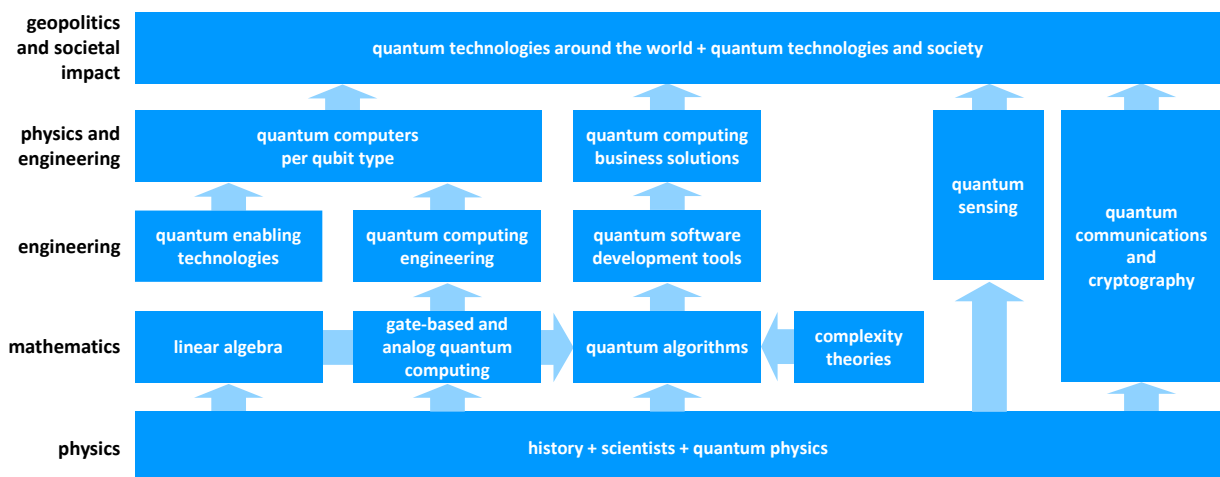


Figure 2: how the topics covered in Understanding Quantum Technologies are related with each other. (cc) Olivier Ezratty.

At last, let's mention one of the reasons why a curious mind may like quantum technologies: they encourage you to explore many scientific disciplines, even human and social sciences, like a scientific Pandora's box.

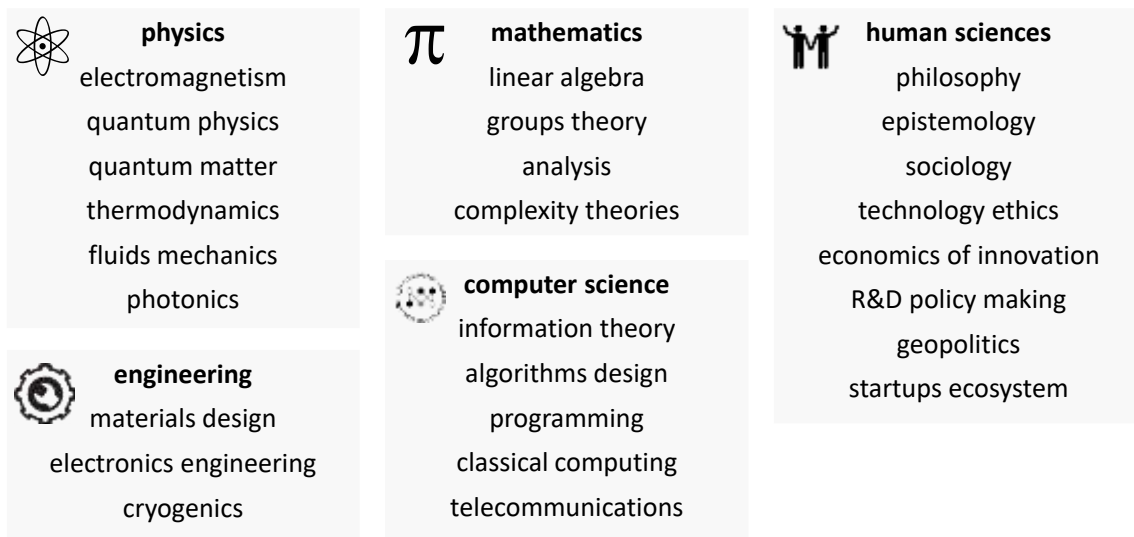


Figure 3: the many scientific domains to explore when being interested in quantum technologies. That's why you'll love this book if you are a curious person. (cc) Olivier Ezratty, 2021-2022.

If you have some scientific background, you'll play in familiar territory but if you've had your degree a couple decades ago, this overview will provide you with some interesting intellectual upgrades. On top of that, learning quantum science is probably more efficient than Sudoku or crosswords to train your brain muscle as it ages!

First and second quantum revolutions applications

Quantum physics has been implemented since the post-war period in almost all products and technologies in electronics, computing and telecommunications.

This corresponds to the **first quantum revolution**. It includes transistors, invented in 1947, which use the field effect and are the basis of all our existing digital world, photovoltaic cells which rely on the pairs of electron holes created by incident photons, and lasers which also exploit the interaction of light and matter and are used in a very large number of applications, particularly in telecommunications and optical storage (CD, DVD and the likes, which are now mostly outdated).

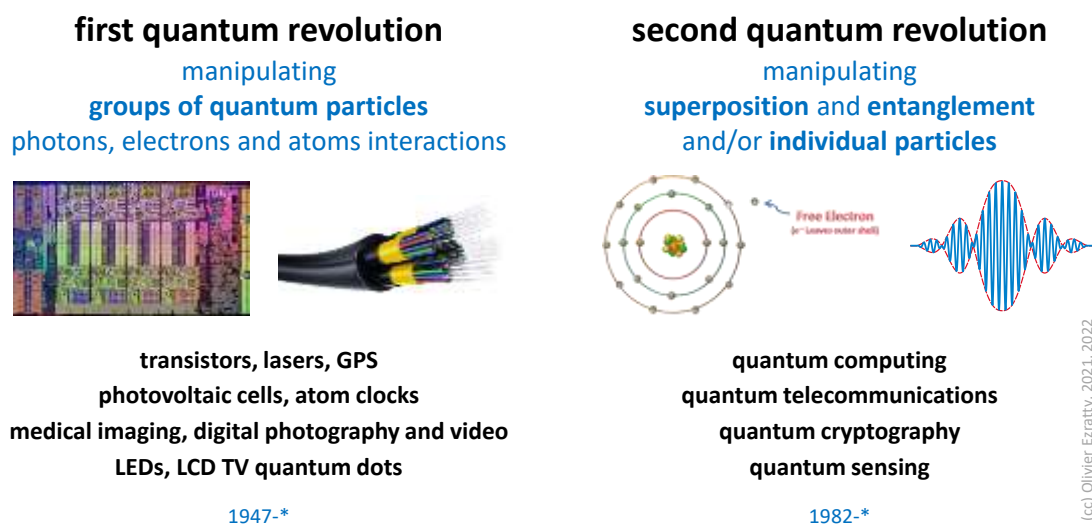


Figure 4: first and second quantum revolution definition and related use cases. (cc) Olivier Ezratty, 2020-2022.

Many medical imaging solutions rely on various quantum effects, including nuclear magnetic resonance imaging (MRI). LEDs are also based on quantum effects. The GPS is relying on atomic clocks synchronization. Quantum dots used in high-end LCD displays and Smart TVs also use variations of the photoelectric effect. The list is long, and we will not detail all these use cases!

The **second quantum revolution** covers the technologies combining all or part of the ability to control individual quantum objects (atoms, electrons, photons), use quantum superposition and/or entanglement. We owe the names of the first and second quantum revolutions to Alain Aspect, Jonathan Dowling and Gerard Milburn in 2003³. The first and the two following ones created it simultaneously and independently. In the United States, the paternity is attributed to the latter, while in France, it is attributed to the former! Who knows why?

The scope of the second quantum revolution covers various recent applications of quantum physics that integrate quantum computing, quantum telecommunications, quantum cryptography and quantum sensing. Said simply, it's about improving our digital world performance and security, and to increase the precision of all sorts of sensors.

- **Quantum computing** is the broad domain of using quantum physics to find solutions to various computing problems. It includes various computing paradigms like gate-based computing, quantum annealing and quantum simulations. Hundred pages are covering this topic in this book.
- **Quantum cryptography** is a mean of communicating inviolable public cryptography keys thanks to quantum physics phenomena and rules, like photon entanglement and the no-cloning theorem. It relies either on fiber optic communications or on space links with satellites as China has tested with its Micius satellite since 2017. **Post-quantum cryptography** is a different field which is intended to replace current classical cryptographic solutions with new solutions that are supposed to be resistant to attacks carried out by future quantum computers. It is not belonging to the second quantum revolution per se but is rather a consequence of it.
- **Quantum telecommunications** enables distributed computing, connecting quantum computers enabling qubit to qubit distant entanglement, and, potentially, quantum sensors, which can be implemented to improve their accuracy. This field still in the making could become the base for a very secure quantum Internet and quantum cloud infrastructures. We cannot exploit it to transmit classic information faster than today⁴. However, it can be used to distribute quantum processing on several quantum processors. It could provide a mean to "scale-out" quantum computers, when it's becoming difficult to "scale-in". This requires a lot of engineering, particularly to convert solid qubits into photon qubits and share entanglement resources.

³ See [Speakable and unspeakable in quantum mechanics](#) by John S. Bell, June 2004 edition (289 pages) which contains a preface by Alain Aspect on the second quantum revolution, dated February 2003, pages 18 to 40. We find the expression in [Quantum technology: the second quantum revolution](#) by Jonathan P. Dowling and Gerard J. Milburn, June 2003 (20 pages) as well as in [Quantum Technology Second Quantum Revolution](#) by Jonathan Dowling, 2011 (60 pages). Dowling's writings make a very large inventory of various quantum technologies embedded in this second quantum revolution. [The Second Quantum Revolution: From Entanglement to Quantum Computing and Other Super-Technologies](#) by Lars Jaeger, 2018 (331 pages) is a broader overview of the different sides of the second quantum revolution.

⁴ But..." *Entangled states cannot be used to communicate from one point to another in space-time faster than light. Indeed, the states of these two particles are only coordinated and do not allow to transmit any information: the result of the measurement relative to the first particle is always random. This is valid in the case of entangled states as well as in the case of non-entangled states. The modification of the state of the other particle, however instantaneous it may be, leads to a result that is just as random. Correlations between the two measurements can only be detected once the results have been compared, which necessarily implies a classical exchange of information, respectful of relativity. Quantum mechanics thus respects the principle of causality*". Source: https://fr.wikipedia.org/wiki/Intrication_quantique.

- **Quantum sensing** makes it possible to measure most physical dimensions with several orders of magnitude better precision than existing classical sensing technologies, even existing atomic clocks. It is a vast scientific field that is the subject of numerous research projects and industrial solutions. It includes ultra-precise atomic clocks⁵, cold atom accelerometers and gyroscopes that use atomic interferometry, SQUIDS (superconducting based) and NV center magnetometers.

Microgravimeters measure gravity with extreme precision, enabling discoveries of underground anomalies like holes, water and various materials. This domain also includes various advanced medical imaging systems with higher precision and non-destructive imaging and measurement tools⁶. A dedicated section of this book is covering quantum sensing, starting page 579. The diversity of quantum sensing solutions or prospect solutions is staggering.

Table 1. Quantum Metrology and Sensing Technologies

| Technology | Technological Readiness ^a | Potential Market |
|--|--------------------------------------|--------------------|
| Measurement | | |
| Atomic clocks | Commercial | \$50-\$500 million |
| Meters for voltage, current, and resistance | Commercial | — |
| Sensors | | |
| Gravimeters and other atomic interferometers | Commercial | < \$50 million |
| Quantum inertial motion units | Medium-term | \$50-\$500 million |
| Atomic magnetometers | Commercial | \$50-\$500 million |
| Magnetoencephalography | Commercial | \$50-\$500 million |
| Quantum electron microscopes | Medium-term | \$50-\$500 million |
| Quantum-assisted nuclear spin imaging | Long-term | < \$50 million |
| Signal measurement | Medium-term | — |

Sources: European Commission (2017) United States Air Force Scientific Advisory Board 2010; interviews.

Figure 5: various quantum sensing use cases. Source: EU and US Air Force, 2015.

Why quantum computing?

The main goal for using quantum computing is to solve complex problems that are and will stay inaccessible to classical computers. This happens when these problems solutions scale exponentially in computing time on classical machines. Problems that scale polynomially on classical hardware are not very interesting for quantum computing. The promise of quantum computing is to address this need. But a big warning and legal disclaimer: it is still a *promise!* We are still far off from delivery.

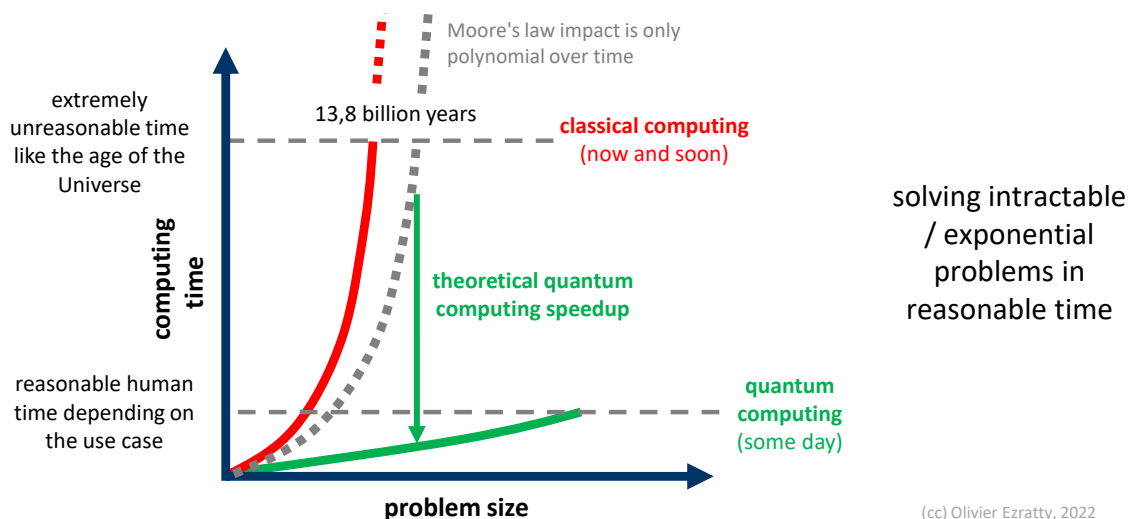


Figure 6: simplified view of the quantum computing theoretical promise. Before delivering this promise, quantum computers may bring other benefits like producing better and more accurate results and/or doing this with a smaller energy footprint. (cc) Olivier Ezratty, 2022.

⁵ See for example this NIST work on an atomic clock based on rubidium, the element most frequently used in atomic clocks. NIST [Team Demonstrates Heart Of Next-Generation Chip-Scale Atomic Clock](#), May 2019.

⁶ See [Quantum camera snaps objects it cannot 'see'](#), by Belle Dume, May 2018. This is a variant of [Diffraction Free Light Source for Ghost Imaging of Objects Viewed Through Obscuring Media](#) by Ronald Meyers, 2010 (22 pages). Yanhua Shih (University of Maryland) US Army Research Laboratory, has been working on the subject since 2005. [Quantum Imaging](#) by Yanhua Shih, 2007 (25 pages). Also, see [Quantum Imaging - UMBC](#) (47 slides).

Quantum computing promise

Typical exponential problems are combinatorial optimization searches and chemical simulations. Their size is usually expressed in a number of items like a number of steps for solving a travelling salesperson problem. Exponential problems are said to be "intractable" because their computation time evolves in crazy proportions with their size.

It starts with various optimization problems such as the above-mentioned traveling salesperson problem, with its contemporary equivalents applied to product delivery or autonomous vehicles routing. Today, you optimize your route with Google Maps or Waze, based on traffic conditions. Traffic conditions are variable and your actual journey time is not always what was planned nor optimal.

With fully autonomous fleets, it may theoretically be possible to optimize the individual path of each and every vehicle based on their departure and destination locations. Conventional algorithms could work with a limited number of vehicles, but beyond a few hundred vehicles and trips, traditional computing capacities would be largely saturated. Quantum computing may then come to the rescue!

Secondly, we have physics and molecular simulations, themselves governed by quantum mechanics equations. It usually boils down to finding the minimum energy configuration of a system, in order to simulate the interaction of atoms in molecules, complex crystal structures or even how magnetism works in various materials. This deals with both classical chemical engineering and biochemistry. Rest assured, this will not go so far as to simulate an entire living being or even a cell. It will already be a fantastic feat when we are able to simulate some simple de-novo protein folding in a better way than what AlphaFold 3 from DeepMind is doing today, the next step being protein interactions simulations⁷.

A third area for quantum computing is the training and inferences of machine learning models and neural networks. It is now within the reach of conventional computers equipped with GPGPUs (general purpose GPUs) such as Nvidia's V100, A100 and H100 and their tensor processing specialized units, optimizing matrices-based operations. Quantum advantage is less obvious in this field, particularly since machine learning must usually be trained with a lot of data. Nowadays, however, using quantum computing for machine learning happens to potentially bring another benefit: creating better solutions instead of creating it faster.



Figure 7: typical quantum computing use cases where a quantum speedup brings clear benefits. These are still "promises" since the capable hardware to implement many of these solutions with a quantum speedup remains to be created and it may take a while up to several decades! (cc) Olivier Ezratty, 2020.

⁷ The competition from classical machine learning is still significant and growing. See [Scientists are using AI to dream up revolutionary new proteins](#) by Ewen Callaway, Nature, September 2022.

Finally, you can't avoid integer factorization, which is of particular interest to the NSA and their peers to break RSA-type public-key encryption security. We'll dig into this in details starting page 801.

Other applications are investigated for different markets such as finance, insurance and even marketing. Many businesses have complex optimization problems to solve. Like with most technology-driven disruptions, businesses will progressively discover quantum computing use case as its market and related skills grow.

“Building a quantum computer is a race between humans and nature, not between countries”

Lu Chaoyang, China
December 2020.

In extreme cases, computing times on conventional computers for exponential problems, even with the most powerful supercomputers of the moment, would exceed the age of the Universe, i.e. 13.85 billion years.

Most of these promises are dependent on the ability to create large scale and fault-tolerant quantum computers, which are years if not decades away. In the interim, we may end-up having quantum systems able to deliver other benefits like producing better and more accurate results and/or doing this with a smaller energy footprint, but not with a real exponential speedup.

Moore's law limitations

Moore's empirical law application, or “More than Moore” as its successor is now labelled, would have a marginal impact, dotted in the graph. First of all, it has been slowing down since 2006, and even if it did not slow down, it would not bring the capacity to solve exponential problems. Computation times for exponential problems would remain exponential despite the supposed doubling of machine power every 18 months to two years. The addition of a single qubit theoretically doubles quantum computers power, both in terms of internal memory space and computing parallelism capacity⁸.

In comparison, quantum computers could theoretically, one of these days, solve these same problems within a reasonable time span on the scale of a human life, in hours, days, weeks or months. Reasonableness obviously depends on the nature of the problem to be solved.

The main benefit of quantum computation is to modify the time scales for solving a problem and turn problems whose classical solution requires some exponential time into quantum solutions requiring at most some polynomial time. It can become useful when the size of the problem is large, sometimes with only about fifty items in a combinatorial optimization search! Quantum computation also makes it possible to gain space, particularly memory, to perform these calculations.

However, the scientific and technological barriers to overcome to make this real are still immense. Some of these use case promises may even be frequently oversold.

Meanwhile, quantum computing is not a “jack of all trades” solution. It is not a replacement tool but more a complement to current High-Performance Computers (HPC). Many, if not most of today's classical computing problems and software are not at all relevant use cases for quantum computing.

From an economy historical perspective, the consequence is that quantum computing won't probably be a Schumpeterian innovation. It will not entirely replace classical legacy technologies. It will complement it. It's an incremental instead of being a replacement technology. You probably won't have a quantum desktop, laptop or smartphone to run your usual digital tasks although quantum technologies can be embedded in these devices like quantum sensors and quantum random number generators.

⁸ One could though argue that adding a single functional qubit to a quantum computer appears to be exponentially difficult with the number of qubits.

Quantum computers will be hidden from users and sit in cloud data centers, like Nvidia GPGPUs racks. This will be even amplified by the progress we can anticipate with wireless telecoms.

When quantum computers will scale after 2030, we'll probably use 6G or 7G networks with even better latency and bandwidth! Of course, it's still hard to anticipate the usages brought by quantum computers when they will scale.

Let's still boil in the fact that, as we'll see later, quantum computers are not excellent to handle big data not for real-time computing. This makes it less relevant to use a local quantum processor, as it makes sense today to have local neural networks capacities to handle your in-camera image recognition processing and voice recognition in smartphones. Less data means more relevance for distant quantum computation done in the cloud.

Classical computing technology developments

How are we currently making progress with conventional computing? We rely on a few known techniques, some of which have not yet been fully explored.

Multi-core architectures enable parallel processing but with limits formalized by **Amdahl's law**, which describes the upper limits of parallel computing systems acceleration.

We have the ongoing sluggish increase of transistors density in processors coupled with so-called **Domain Specific Architectures** using ad-hoc circuits like tensors (matrix multipliers) used to run specialized algorithms like neural networks. One key technology development is to make sure memory is as close as possible to processing units.

Neuromorphic processors mimic biological neurons features with integrated memory and processing using memristors⁹. They can be implemented with spintronics electronics, that imitate how brain cells work with their own memory¹⁰.

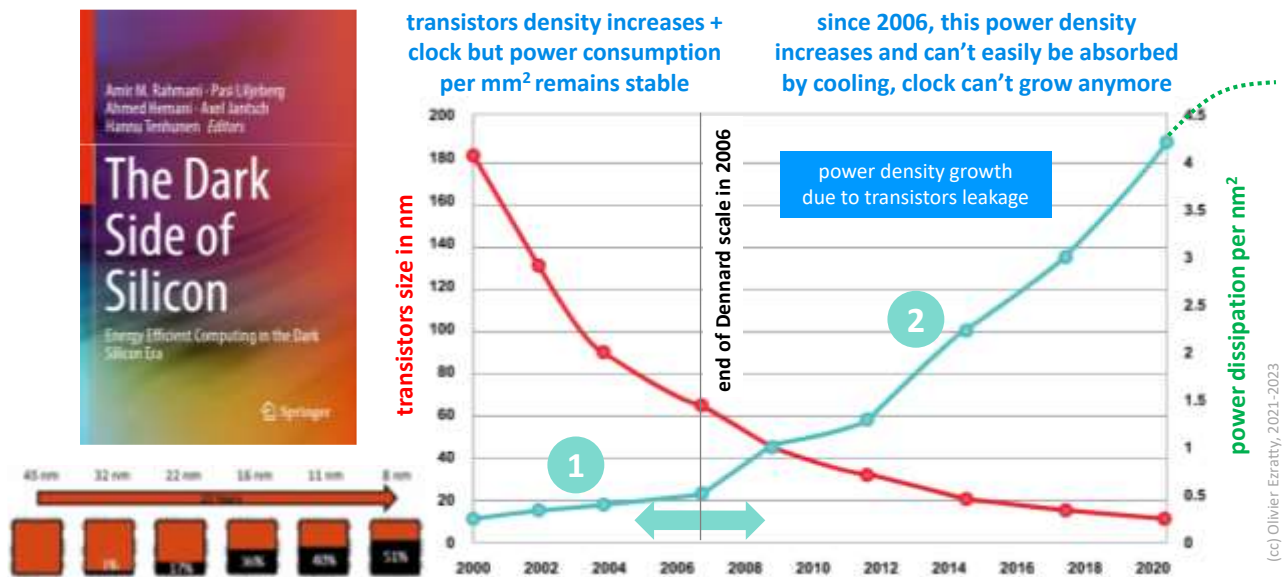


Figure 8: Dennard's scale which explains the dark silicon phenomenon where all CMOS chipsets components cannot be used simultaneously. Compilation (cc) Olivier Ezratty.

⁹ One famous work with neuromorphic processor is the Loihi project from Intel. See [Intel's Neuromorphic Chip Gets A Major Upgrade: Loihi 2 packs 1 million neurons in a chip half the size of its predecessor](#) by Samuel K. Moore, IEEE Spectrum, October 2021.

¹⁰ See the review paper [Quantum materials for energy-efficient neuromorphic computing: Opportunities and challenges](#) by Axel Hoffmann, Julie Grollier et al, April 2022 (24 pages).

The heat barrier limits our capacity to increase processor clock speed beyond 5 GHz. It can reach 6 GHz with liquid cooling¹¹.

This is due to the end, in 2006, of **Robert Dennard's** (1932, American) scale established in 1974. According to this scale or rule, as the transistors density increased, the power consumed per unit area of the chipsets was stable. This happened since the transistors voltage and current could decrease with their density, while increasing the clock frequency. Starting with 65 nm integration, this rule was broken. It comes from an unwanted leakage current between source and drain regions caused by depletion areas interpenetration. That's why, among other phenomena, your laptop computer is also heating your legs when you use it in public transportation or in your coach¹².

The transistors current leaks started to grow and power consumption soared. This is what prevents the growth of processors clock. At the beginning of the 2000s, Intel planned in its roadmaps to raise their CPU clock frequency up to 20 GHz.

Intel then stopped playing this game and instead entered the multicore realm. However, in June 2021, Intel released a new microprocessor for high-end laptops running at a 2.9 GHz base clock but with a 5 GHz turbo mode for a single core, the 4-core i7-1195G7, etched in 10 nm, and with a 28W TDP¹³.

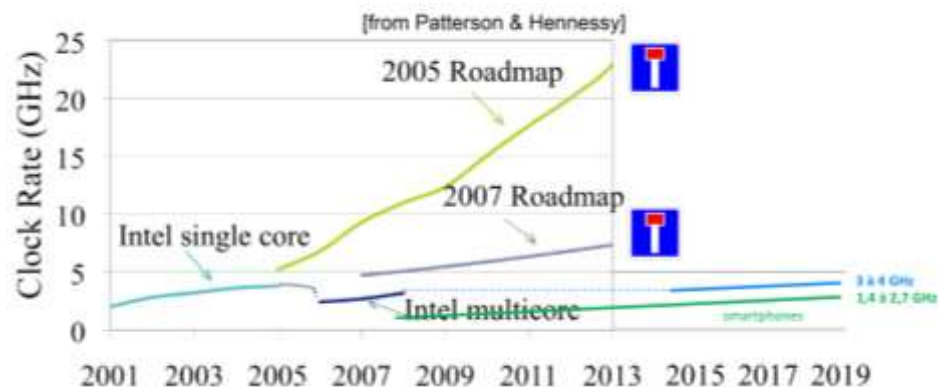


Figure 9: how CMOS chipsets clock was supposed to increase... and didn't. Source: [High Performance Computing - The Multicore Revolution](#) by Andrea Marongiu (41 slides), 2019. Additions: Olivier Ezratty.

The semiconductor demand switched in 2007 towards low-power multi-functions chipsets for smartphones. This opened a boulevard for Arm core-based processors and growth for corporations like **Qualcomm**.

The available computing power per consumed kW increased steadily, doubling every 1.57 years between 1946 and 2009, according to **Jonathan Koomey's** empirical law enacted in 2010. However, this doubling slowed down to 2.6 years after 2000, due to the end of Dennard's scale.

There are many techniques used to optimize classical computing footprint, particularly around memory management, with making sure memory is as close as possible to computing, including in-memory processing¹⁴. After 2006, transistors density still continued to increase.

However, the end of Dennard's scale led to the rarely mentioned **dark silicon** phenomenon. As the chipsets get too hot, it becomes difficult to use it entirely. Various methods are then combined to circumvent this inconvenience: on-demand cores or functions deactivations according to usage needs, a shutdown of certain portions or cores, a voltage drop, or a selective clock frequency adjustment.

¹¹ See on this subject [Minimum Energy of Computing, Fundamental Considerations](#) by Victor Zhirmov, Ralph Cavin and Luca Gamaitoni, 2014 (40 pages) which compares the energy efficiency of living things and electronics.

¹² Another phenomenon is the tunnel effect happening at the thin grid oxide level, that is reduced with using high-dielectric constant oxides ("high k dielectric").

¹³ Thermal dissipation power.

¹⁴ See [Energy Efficient Computing Systems: Architectures, Abstractions and Modeling to Techniques and Standards](#) by Rajeev Muralidhar et al, July 2020 (35 pages) which makes a good inventory of the various ways to save energy with classical computing. And [Processing-in-memory: A workload-driven perspective](#) by S. Ghose et al, IBM Research, 2019 (19 pages).

This is what is used in the Arm core-based processors of smartphone chipsets, whose cores do not use the same clock rates, in the so-called big.LITTLE architectures created in 2011, and replaced with the more flexible DynamIQ architecture in 2017 ¹⁵.

some CMOS density technical challenges

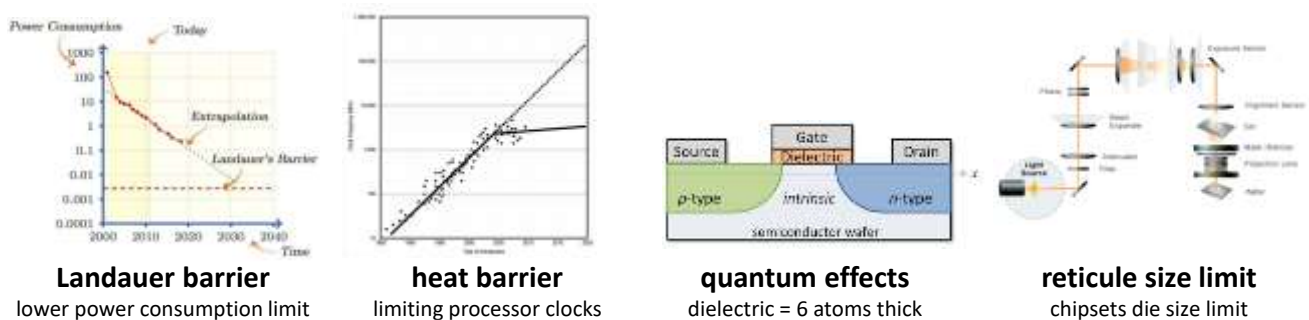


Figure 10: some of the key CMOS density technical challenges to overcome by the semiconductor industry. One source: [Reversible Circuits: Recent Accomplishments and Future Challenges for an Emerging Technology](#) by Rolf Drechsler and Robert Wille, 2012 (8 pages).

To lower transistors density below 10 nm, etching systems using extreme ultraviolet are required, coming from ASML. Etching resolution depends on the wavelength of the light used to project a mask on a photoresist.

current CMOS scaling solutions

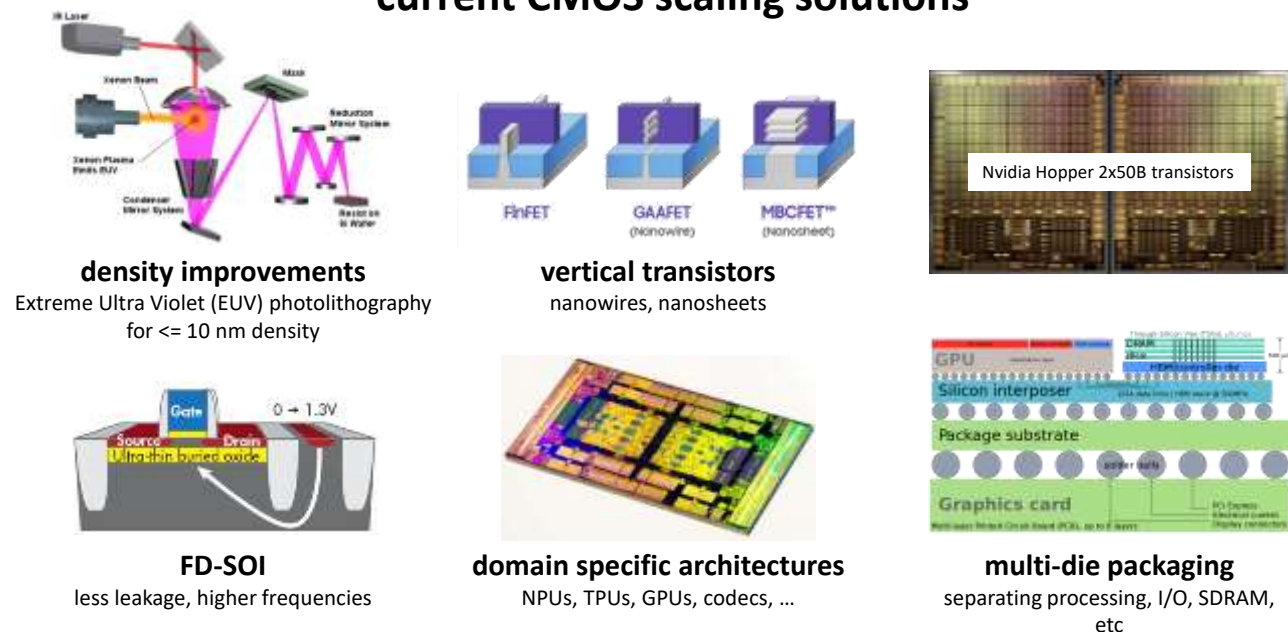


Figure 11: current CMOS scaling solutions adopted by the semiconductor industry. (cc) Olivier Ezratty with uncredited image sources.

Lowering the transistors size requires increasing this frequency to decrease the wavelength, and thus go from the current deep ultra-violet to extreme ultra-violet. It took more than 10 years to develop these EUV lithography systems. It is in production since 2019 in TSMC and Samsung 5 nm nodes fabs. One of key benefits of EUV etching is to reduce the usage of the costly multiple patterning process to improve lithography resolution.

¹⁵ There are many other techniques to improve classical processors energy efficiency. See for example [Energy Efficient Computing Systems: Architectures, Abstractions and Modeling to Techniques and Standards](#) by Rajeev Muralidhar et al, AWS and Melbourne University, July 2020 (35 pages).

ASLM's latest EUV lithography generation is dubbed High-NA (for high numerical aperture). A bit like in photography, High-NA optics will convey more light onto masks and silicon targets and will be required for nodes under 3 nm. It requires both new UV optics but also new light sources. And the EUV machines are much bigger and costly. These machines will be deployed around 2024. The generation after High-NA would be Hyper-NA but even ASML is doubting it will be economically viable¹⁶.

For a while, scientists warned about undesirable quantum effects appearing below 5 nm nodes, with a tunnel effect showing up in the thinner grid oxide. But it didn't prevent going down to 5 nm and then below dimensions. TSMC started producing 2 nm chipsets in 2022, combining EUV etching with the traditional FinFET technology that has been in use for more than 10 years. They are expecting to mass-produce 2 nm chipsets by 2025, thanks to nanowires and nanosheets techniques¹⁷. In July 2021, Intel even announced a new density scale using angstrom sized transistors, with 20Å and 18Å by 2025 (meaning... about 2 nm, given 1 Å = 0,1 nm).

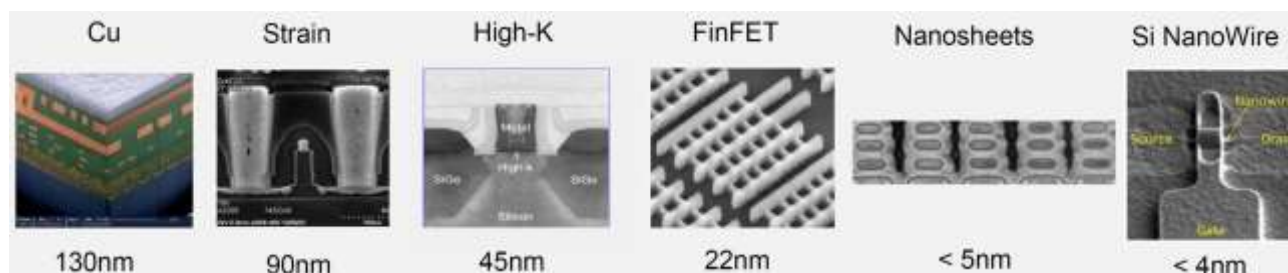


Figure 12: the various CMOS transistor technologies used as density increased.

In May 2021, IBM announced it had prototyped 2 nm nanosheet-based chipsets, manufactured by Samsung, and also using EUV lithography¹⁸.

As far as integration is concerned, two other limits must be taken care of, such as **Rolf Landauer's** (1927-1999, researcher at IBM in 1961) principle which defines the minimum energy required to erase a bit of information. It is a very low theoretical barrier contested by some physicists. And it can be circumvented as we will see with the technique of [adiabatic and reversible computing](#) that is covered page 780. Finally, there is a limit coming from the reticles size, these optical systems used in lithography whose size is physically limited, especially optically. It's explained in below illustration in Figure 13, coming from **ASML**, the world leader in semiconductor lithography. This limit has been reached with the largest recent processors.

The largest single-die processors of 2020 were the **Nvidia** A100 with its 54.4 billion transistors etched in 7 nm, superseded closely in size by the **Graphcore** GC200 with its 59.4 billion transistors and 1,472 cores, launched in July 2020 and the Nvidia H100 launched in 2022 with 80 billion transistors, consolidating two adjacent 4 nm chipsets in a single package.

Cerebras (USA) nevertheless launched in 2019 an amazingly large 21.5 cm x 21.5 cm square processor, fitting in an entire 300 mm wafer, which circumvents the reticle size limit by being etched in several runs, for its 84 main processing units connected by metal layers. The second version of this chipset launched in 2021 contains 2,6 trillion transistors and 40 GB of cache SRAM memory and has a memory bandwidth of 20 PB/s, allowing it to significantly accelerate neural networks training.

¹⁶ See [Hyper-NA after high-NA? ASML CTO Van den Brink isn't convinced](#), Bit Chips, September 2022.

¹⁷ See [Beyond CMOS, Superconductors, Spintronics, and More than Moore Enablers](#) by Jamil Kawa, Synopsys, March 2019 (43 slides), a good presentation describing the various ways to improve the power of components including cold CMOS, semiconductors operating at liquid nitrogen temperature levels (-70°C) and superconducting Josephson effect based transistors.

¹⁸ See [IBM Introduces the World's First 2-nm Node Chip](#) by Dexter Johnson, IEEE Journal, May 2021.



Figure 13: reticle used in photolithography and its related optics, explaining the size limitation of dies in semiconductor manufacturing.

This massive Cerebras chipset, shown in Figure 14, burns about 15 kW/h which are evacuated by a specific water-cooling system. Manufacturing techniques generate defects and more than a couple percent of the 850,000 processing units are defective and are short-circuited during software execution¹⁹. In September 2022, Cerebras announced its own Wafer-Scale Cluster computer using up to 192 15U rack CS-2 systems. It is competing aggressively against Intel/Nvidia and AMD-based supercomputers that are currently dominating the HPC landscape.

Quantum computing may make it possible to overcome the various limitations of current CMOS processors for certain tasks. However, it will not replace them at all for tasks currently performed by today's computers and mobile devices.

The figure shows the Cerebras WSE-2 wafer-scale processor. It is a 21.5 cm square wafer containing 2.6 trillion transistors. The wafer is divided into 84 units, each with 850,000 SLAC cores, 8 ops/clock per core at 1 GHz, and 40 GB SRAM, 15kW TDP*. The wafer is shown next to a 15U rack system (Cerebras CS-2 system rack 15U) and a water movement assembly (top) and air exchanger (bottom). The Cerebras logo and '2016, USA, \$112M' are also present. The first customer / tester is Argonne National Laboratory. A small Nvidia A100 chip is shown for comparison.

WSE-2
2.6 trillion transistors
 84 units on 215x215 mm, 7 nm
 850 000 SLAC cores
 8 ops/clock per core at 1 GHz
 40 GB SRAM, 15kW TDP*

« wafer scale processor »

water movement assembly (top) and air exchanger (bottom)

water movement assembly (top) and air exchanger (bottom)

Cerebras CS-2 system rack 15U

first customer / tester

Argonne NATIONAL LABORATORY

Figure 14: the impressive Cerebras wafer-scale chipset. Source: Cerebras.

¹⁹ With its D1 chipset presented in July 2021, Tesla chose another approach. Engraved in 7 nm, it has a computing capacity of 22.6 TFLOPS FP32, with 50 billion transistors and a 400W TDP. It contains 354 computing units with 1,25 MB SRAM per unit. They assemble these D1 in 25-chipsets tiles, consuming 15 kW, exactly like a Cerebras chipset.

Typically, video and audio compression and decompression are not relevant tasks for quantum computing. They are usually carried out in specialized chipset processing units, known as DSPs (for digital signals processing). Similarly, applications handling very large volumes of data are not suitable for quantum computing for a whole host of reasons that we will study, mainly because data loading speed into qubits is quite low, whatever the qubit type.

As its use cases will be different, it is hard to anticipate the IT landscape that will emerge with powerful quantum computers when they show up. Even with the advent of quantum computers, Ray Kurzweil's singularity predictions, which rely on the ad vitam extension of Moore's empirical law, will need to be adjusted!

Unconventional computing

In a dedicated part starting page 768, we will evaluate some the other avenues considered to overcome the current limitations of classical computing, which may provide some power or efficiency gains positioned between classical and quantum computing. These belong to the broad category of “unconventional computing”.

This includes **superconducting computing** operating at low temperatures (investigated in the USA and Japan), **digital annealing** computing (proposed by **Fujitsu**), **reversible** and/or **adiabatic computing** that could reduce energy consumption and circumvents Dennard’s scale end, **probabilistic computing** as well as different breeds of **optical computing**.

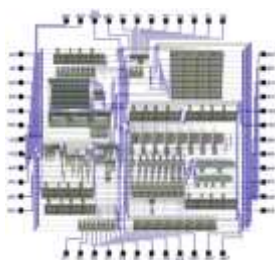
I also delve into some of the inner workings of supercomputers and specialized processors to better understand their strengths and weaknesses. When comparing quantum computers to classical computers, we are better off with knowing both sides of the equation, not just the loud new kid in town!

These are sort of backup solutions, should science fail to create scalable quantum computers. It will also complement quantum computing used in the context of hybrid computing. Interestingly, some unconventional computing avenues, such as superconducting electronics, are potential enabling technologies for scaling certain types of quantum computers.

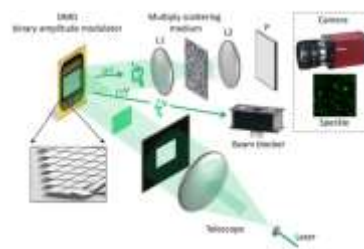
However, at this point, none of these solutions seem positioned to solve intractable problems although some of these are claiming they have this capacity, which is quite hard to fact-check at large scales.



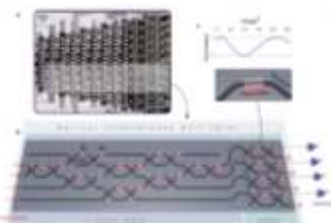
digital annealing



reversible computing



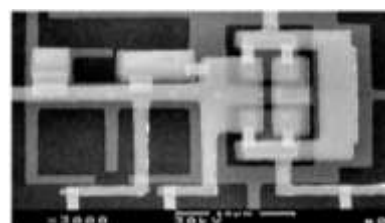
light processors



III/V optonics



probabilistic computing



superconducting logic

Figure 15: various unconventional computing approaches besides quantum computing. (cc) Olivier Ezratty with uncredited images.

The history of technology is about exploring multiple branches. Some do not succeed. Some help each other. Also, some can suddenly wake up after being frozen for decades. The game is open!

Why... key takeaways

- All existing digital technologies are already quantum and belong to the first quantum revolution including transistors, lasers and the likes, leveraging our control of light-matter interactions with large ensembles of quantum objects (electrons, atoms, photons). The second quantum revolution is about using a variable mix of superposition, entanglement and individual quantum objects. It usually contains quantum computing, quantum telecommunications, quantum cryptography and quantum sensing.
- Quantum technologies are at the crossroads of many scientific domains encompassing physics, mathematics, computing, social sciences and the likes. It creates new educational and pedagogy challenges that must be addressed in innovative ways and customized according to various audiences. This book targets broad audiences with some technical background, including computer science engineers.
- Quantum computing promise is to solve so-called intractable problems whose computing complexity grows exponentially with their size. These can't be solved with classical computing, whatever happens with Moore's law. But we're not there yet since there are many challenges to scale quantum computers beyond what can be done today. In the interim, some marginal improvements will come with noisy intermediate scale computers, including better and more precise solutions in various domains.
- Other new technologies may compete with quantum computing, belonging to the broad "unconventional computing" category. Only a very few of these could also bring some exponential computing capacity. Most others bring other benefits compared with classical computing like in the energy consumption domain. Some of these technologies like superconducting electronics and adiabatic/reversible computing could also be helpful as enablers of quantum computing scalability.
- This book is unique in its shape and form. It covers quantum technologies with a 360° approach. It's more scientific than most publications, outside research review papers. It's a good appetizer for those who want to investigate the matter whatever the angle.

History and scientists

After having set the stage, we'll make an history detour to discover the origins of quantum physics. As any scientific and technological endeavor, it's above all a great human story. I pay tribute here to the many scientists who, step by step, made all this possible and are still working on it for those who are still in this world.

Nanoscopic physics. Quantum physics deals with atomic and sub-atomic level particles and with the interactions between electromagnetic waves and matter. It differs from classical Newtonian physics, which predictably governs the dynamics of macrophysical objects, beyond a few microns and up to the size of planets and stars. Classical physics is governed by Newton's laws for matter, by Maxwell's laws for electromagnetic fields and associated forces and by statistical physics which describes continuous media such as gases and fluids and from which the principles of thermodynamics are derived.

When the speed of objects becomes close to the speed of light or when we reach large object's mass, the theory of relativity comes in, explaining the curvature of space-time and modelling the impact of gravity. It helps describing extreme phenomena such as black holes or neutron stars. It allows us to interpret the History of the Universe, but not entirely. But relativistic electrons are also hidden in our body's atoms and in many elements on earth as we'll quickly discover with the weird field of relativistic quantum chemistry.

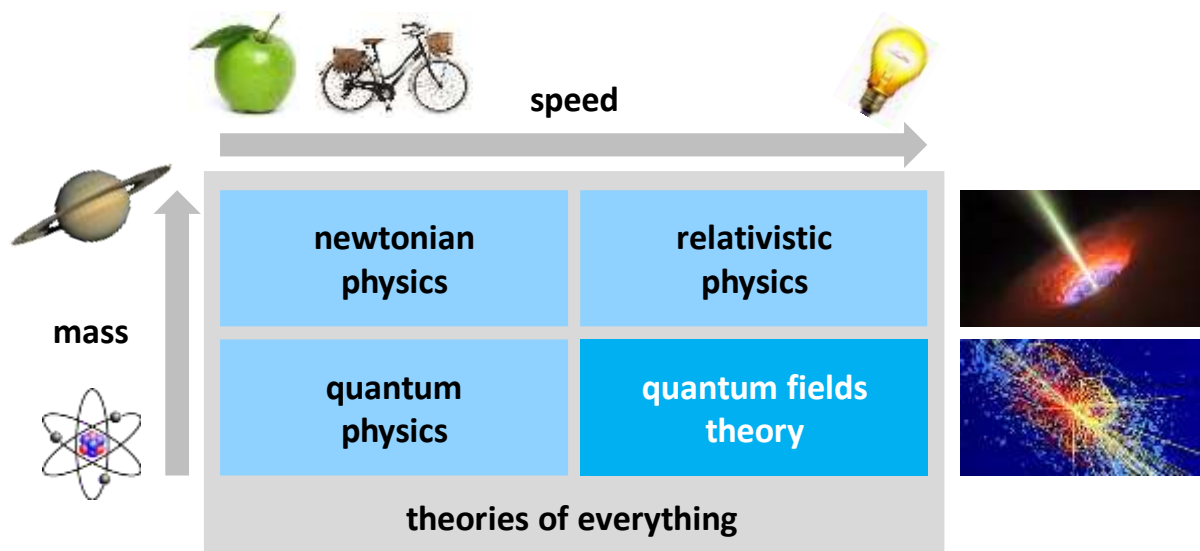


Figure 16: high-level classification of the branches of physics. (cc) Olivier Ezratty, 2020.

The fourth domain of physics in this quadrant is the quantum fields theory. It describes the physics of high-speed elementary particles, such as those observed in particle accelerators like quarks and the famous Higgs boson. Richard Feynman is one of the founders of quantum electrodynamics, a subset of quantum field theory.

In a way, quantum physics was a mean to unify classical matter physics and electromagnetic waves physics. It helps describe how matter was organized at the atomic and electrons levels and how these interacted with quantized electromagnetic waves, aka photons, including visible light.

Unification still in the making. Physics is still not yet complete nor unified. Some observable physical phenomena still resist it. We do not know how to explain the origins of gravitation and we are still looking for the dark matter and energy that would explain the cohesion of galaxies and the Universe current expansion. Scientists would like to explain everything, but some knowledge may never be accessible such as the shape and form of the Universe before the Big Bang.

The so-called theory of everything (ToE) or unification theory sought after by some physicists would be a formalism unifying all the theories of physics and in particular relativity, gravity and quantum physics. This very serious field of physics is still in the making²⁰. Numerous proposals emerge and sorting it out is not easy²¹.

Connecting the dots. This part will help you memorize who's who in the History of quantum physics and quantum computing. It will also cover some important science basics such as the Maxwell and Schrödinger equations that I'll try to explain in layman's terms, at least for readers having basic sciences knowledge. Explaining quantum computing inevitably starts with some quantum physics 101 explanations. Some of its basics, although sometimes quite abstract, must be understood. I still always try to connect the dots between quantum physics and quantum computing from a practical basis. It's a vast puzzle. I'll add its pieces one by one and even though the puzzle may not be fully completed, you'll get a picture enabling you to become fairly well educated on quantum computing.

Experiments and theories. Quantum physics took shape in 1900. Like almost all sciences, it is the result of the incremental work of many scientists with interactions between experimentation, theories and mathematical creativity. Sometimes, quantum physics is better explained with its underlying mathematical models than with incomplete physical interpretations. Representation models such as the broad field of linear algebra plays a key role to describe quantum states and their evolution in space and time. Linear algebra is also an essential tool to understand how quantum computer qubits are manipulated and measured. Even if we can trace the beginning of quantum physics to Max Planck's 1900 quanta discovery, it was based on earlier work from many other scientists who devised about the particle or wave nature of light, on the discovery of electromagnetism and atoms. Quantum physics is a human adventure that brought together immense talents who confronted each other and evolved step by step their understanding of the nanoscopic world. New generations of scientists have always questioned the state of the art built by their predecessors²². Physicists conducted numerous experiments, build theories and then verified it experimentally, sometimes with several decades of latency. They also had to pour philosophy into their work to interpret the deep significance of their discoveries, and quantum physics was not an exception. Despite its constant enrichment, quantum physics has shown an astonishing robustness to stand the test of time and with extreme precision.

Misrepresentations. Many quantum physics scientists are famous even for general audiences, even though their work has been overly simplified. Schrödinger's famous cat and Heisenberg's indeterminacy principle are commonplace... even when their underlying details are quite different from their related clichés. Schrödinger's key work is his non-relativistic particles wave equation, not the 10 lines he wrote in 1935 on his eponymous cat thought experiment that is usually grossly misinterpreted!

²⁰ The American-Japanese physicist Michio Kaku estimates that some theory of everything will be finalized by 2100. See [Michio Kaku thinks we'll prove the theory of everything by 2100](#), April 2019. Michio is at the origin of string theory. He defines very well the connection between the different branches of physics and this theory of everything in [A theory of everything?](#). But for many reasons too long to explain here, he happens to be very optimistic in his prediction!

²¹ This is the case of the Wolfram Physics Project launched in April 2020 by Stephen Wolfram, a prolific Anglo-American physicist, mathematician and computer scientist. Building on his 2002 book "[A new kind of science](#)", the author's idea is to explain everything, the world, physics, the universe, whatever, with cellular automata, graphs and fractals. The world would be discrete on a small scale, including time. His Physics Project focuses on the unification of physics with the same set of tools. See the [hundred pages presentation of the project](#), the [white paper](#) which contains a section on quantum physics. Physicists' views on this theory are more than circumspect. The paper does not develop a theory that would be verifiable with an experimental approach as was the case for quantum physics (superposition, wave function, wave function collapse, atomic transition spectral lines, ...). Wolfram's theory was critically analyzed in 2002 by Scott Aaronson in a 14-page [review](#), particularly about his Bell's inequalities interpretation, and in [A New Kind of Science](#) by Cosma Rohilla Shalizi of Carnegie Mellon University, who does not mince his words. The same "hammer/nail explains everything" approach was created by a team of scientists who describe the Universe physics laws self-learning capabilities with a giant neural network approach, in [The Autodidactic Universe](#) by Stephon Alexander, Jaron Lanier, Lee Smolin et al, 2021 (79 pages).

²² Max Planck's cynically explained in 1950 the evolution of science with the death of old generation of scientists: "*A new scientific truth does not triumph by convincing its opponents and making them see the light, but rather because its opponents eventually die and a new generation grows up that is familiar with it*".

Like life in general, science is a great relay race, with many players. Hundreds of other less-known contributors have also grown the field and must be recognized. Sometimes, genius scientists were so prolific that we forget their contributions. This is the case of John Von Neumann who is better-known for his “Von Neumann model” that is the cornerstone of classical computing and for his contribution to the development of EDVAC in 1949, the first stored program-based computer, rather than for his huge contribution to quantum physics mathematical formalism with density matrices and quantum measurement. It depends on the field you are working in, classical computing or quantum physics.

You won't find here inventors or entrepreneurs *a la* Steve Jobs or Elon Musk, even though the founders of startups like D-Wave, IonQ, Rigetti and PsiQuantum are among the entrepreneurial pioneers of this burgeoning industry, all being high-level scientists with a PhD!

Hall of fame. The History of 20th century quantum physics is embodied in the mythical Fifth **Solvay Conference in 1927**, held at the Institute of Physiology in Brussels. It brought together the greatest mathematicians and physicists of the time including almost all the historical founders of quantum physics with Max Planck, Albert Einstein, Niels Bohr, Louis de Broglie, Erwin Schrödinger, Max Born, Werner Heisenberg and Paul Dirac²³. All this happened as the foundations of 20th quantum physics theories were fairly well laid out. 17 of its 29 participants got a Nobel Prize, 6 of which before the congress (names underlined in green) and the others afterwards (in blue). It was probably one of the largest concentrations and density of scientific brains per square meter in the history of mankind!

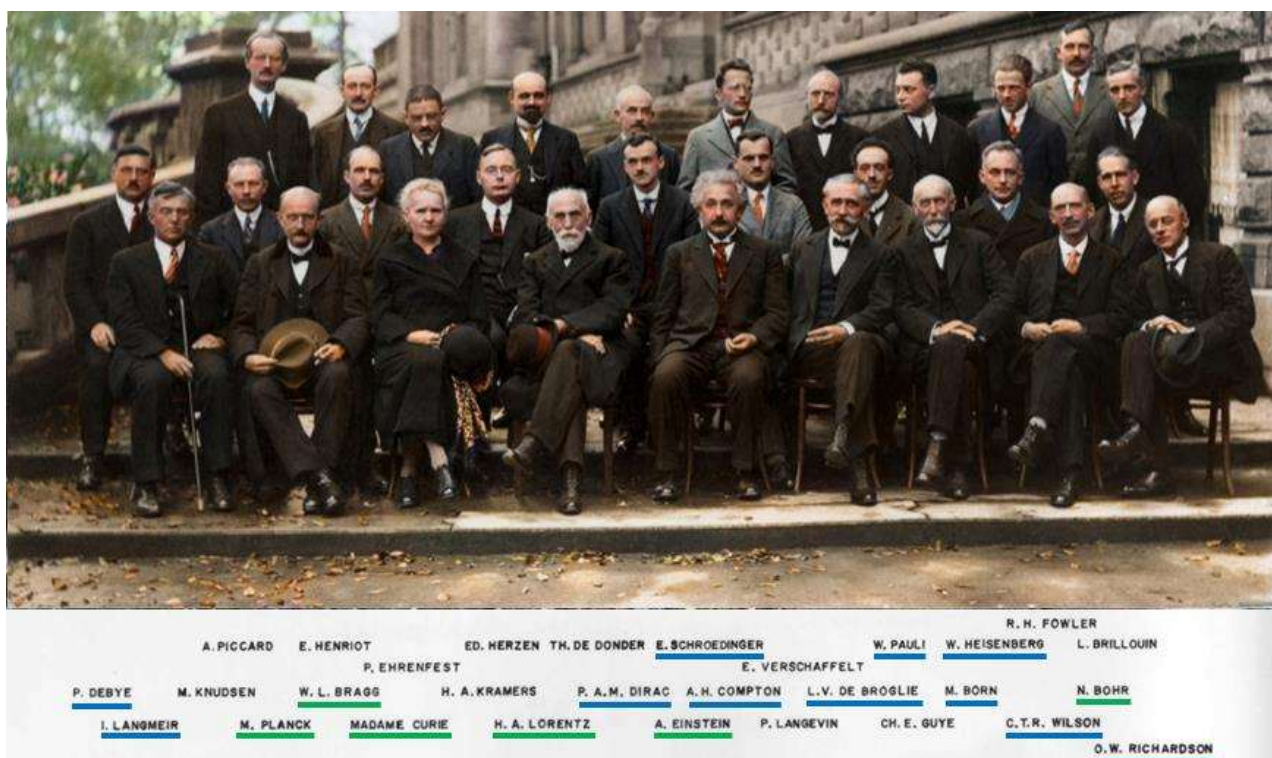


Figure 17: the famous Solvay 1927 conference photo with its 17 Nobel prizes (6 back then, and 11 after the conference). Photo credit: Benjamin Couprie, Institut International de Physique de Solvay.

Solvay conferences on physics are held every 3 to 4 years since their creation in 1911 by the entrepreneur and chemist **Ernest Solvay**. The 1927 congress's topic was electrons and photons, which are at the heart of quantum physics. Half of these conferences are dedicated to quantum physics, the other on different branches of physics. The 28th edition was held in May 2022 and gathered a contemporary hall of fame of quantum scientists from quantum physics to quantum information science.

²³ Only fathers and no mother! Marie Curie was present but was not specialized in quantum physics. She worked on radioactivity.

The major contributions of early scientists in quantum physics are generally arranged in chronological order, with some indication of who influenced whom.

Precursors

We begin with the classical physicists and mathematicians of the 18th and 19th centuries who laid the scientific groundwork that allowed their 20th century successors to formalize the foundations of quantum physics²⁴.



Figure 18: precursor scientists who laid the ground particularly in the electromagnetic fields and mathematics domains.

It's roughly organized in scientific contributions chronological order.



Thomas Young (1773-1829, English) was one of the great sciences and arts polymaths of his time, working in optics, medicine, linguistics, Egyptology and music. He determined that light behaved like a wave, which he proved with the double-slit experiment around 1806, illustrated in Figure 19, that now bears his name. When reducing the size of both slits, it generates interference fringes creating alternating light and dark zones related to the wave nature of light. We had to wait till Albert Einstein's work in 1905 to determine that light was also made of particles.

His experiment used red filtered sunlight going through a first slit. Contemporary experiments use coherent laser light sources. This experiment is one of the cornerstones leading much later to the creation of the electromagnetism theory by James Maxwell.

The slit experiment was implemented with electrons in 1961, with a similar result, illustrating the electron wave-particle duality, devised first by Louis de Broglie in 1924. It was then also done with atoms in 1991 and with various molecules starting in 2002.

Thomas Young also worked on the principles of refraction and human trichromatic vision as well as in fluid mechanics, including on the notion of capillarity and surface tension.

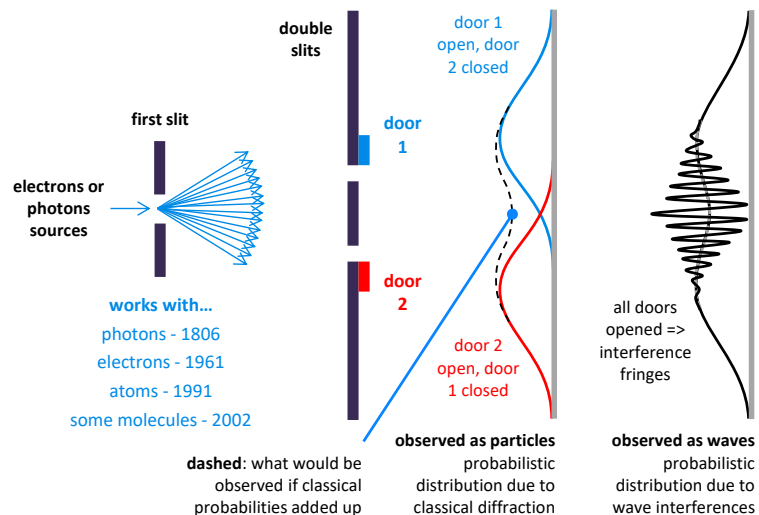


Figure 19: the double-slit experiment principle (cc) Olivier Ezratty, sources compilation.

As an Egyptologist, Thomas Young contributed to the study of the hieroglyphs of the famous Rosetta Stone, which was later used by **Jean-François Champollion** to decipher the whole stone texts. Champollion was then sponsored and helped by a certain **Joseph Fourier**. Yes, the mathematician!

²⁴ I do not always indicate the source of the diagrams used in this text. These are part of common scientific knowledge that are now in the public domain.



William Rowan Hamilton (1805-1865, Irish) was a mathematician and astronomer. He invented around 1827 a set of new mathematical formulations of the laws of physics incorporating electromagnetism. In quantum mechanics, we often speak of Hamiltonians or Hamiltonian functions. These are mathematical operators used to evaluate the total energy of a system of elementary particles including their kinetic and potential energies. This energy is evaluated over time.

Schrödinger's 1926 wave equation describes the evolution of a system's Hamiltonian over time. Among other domains, this concept is used in analog quantum computing with quantum simulators and quantum annealers, like with D-Wave's systems. We'll have the opportunity to cover this in detail in this book, starting page 278.

Hamilton is also behind the creation of quaternions in 1843 which generalize complex numbers, with using i, j and k as imaginary numbers with $i^2 = j^2 = k^2 = ijk = -1$. It can be used to compute three-dimensional rotations and have some applications in quantum computing like for the representation of two-qubit entanglement and of single qubit gates from the Pauli group, in topological quantum computing. This is an exotic domain that we won't cover in this book.



Niels Henrik Abel (1802-1829, Norwegian) is a prolific mathematician at the origin of the so-called Abelian groups. His work focused on the semi-convergence of numerical series, sequences and series of functions, the convergence criteria of generalized integrals, the notion of elliptic functions and integrals (used in cryptography) and the resolution of algebraic equations including his proof of the impossibility of solving general quintic equations.

He died way too early at the age of 26 from tuberculosis while visiting Paris and meeting his fiancée! Along with William Rowan Hamilton, Charles Hermite and Emmy Noether, he is one of the main 'suppliers' of the mathematical foundations used in quantum mechanics.

The adjectives "Abelian" and "non-Abelian" are associated with anyons, the quasiparticles that are the basis of topological quantum computing.

Why do these concepts of quantum mechanics invented long after his death refer to this mathematician? Mainly because the distinction between Abelian and non-Abelian is linked to their commutative mathematical representation. A system with A and B is Abelian when $A*B = B*A$ or non-commutative and non-Abelian when $A*B$ is not equal to $B*A$. The most common non-commutative operations are non-square matrices multiplications. The multiplication of a matrix $(p \times q) * (q \times p)$ will give a matrix $(p \times p)$ whereas in the other direction, $(q \times p) * (p \times q)$ will generate a matrix $(q \times q)$, q and p being here numbers of rows and/or columns.

Non-commutativity is frequently found in quantum physics and particularly with quantum measurement. The order in which quantum objects properties are measured may influence the results because the used measurement operators are non-commutative. In some cases, though, operators are commutative, like with the Measurement-Based Quantum Computing (MBQC) technique that we will have the opportunity to describe later when dealing with photon-based quantum systems.



Charles Hermite (1822-1901, French) was another prolific 19th century mathematician. He worked on numbers theory, quadratic forms, the theory of invariants, orthogonal polynomials, elliptic functions and algebra. His main works were concentrated on the 1848-1860 period. We owe him the notion of Hermitian functions and matrices, which are widely used in quantum physics and quantum computing. A Hermitian matrix is composed of real numbers in the diagonal and can be complex in the rest, and is equal to its transconjugate.

Namely, their transpose matrix whose value of complex numbers has been inverted (i becomes -i and vice-versa).

Quantum measurement operations in quantum physics and computers are defined by Hermitian matrices.

$$A = \begin{bmatrix} 2 & i & -2i \\ -i & 1 & 3 \\ 2i & 3 & -1 \end{bmatrix}^\dagger \quad \bar{A} = \begin{bmatrix} 2 & -i & 2i \\ i & 1 & 3 \\ -2i & 3 & -1 \end{bmatrix} \quad A = \overline{(\bar{A})}^*$$

transposed matrix
Hermitian matrix

matrix equals its transconjugate

Figure 20: how a Hermitian matrix is constructed.

Achille Marie Gaston Floquet (1847-1920, French) was a mathematician who developed mathematical analysis in the theory of differential equations. His name is used in Floquet codes (quantum error correction codes) and we also find him in the physics of quantum matter.



James Clerk Maxwell (1831-1879, Scottish) created in 1865 the theory of electromagnetic fields, combining an electric field and a magnetic field orthogonal to the direction of wave propagation as in the diagram below, and moving at the speed of light. This theory explains light-light interactions such as reflection, diffraction, refraction and interferences. Maxwell's work built on and improved the formalism from Faraday, Gauss, and Ampère.

Maxwell's equations illustrate that when they are constant, electric, and magnetic fields are independent, and in variable regime (with a wavelength λ), it becomes interdependent (\vec{E} and \vec{B}), one generating the other and vice-versa, hence the notion of electromagnetic waves and fields.

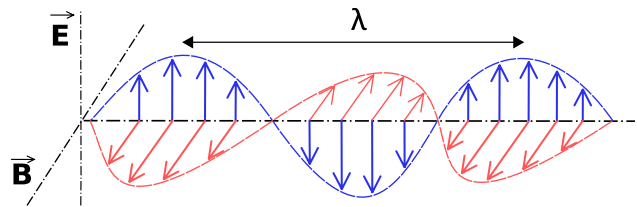


Figure 21: electromagnetic wave electric and magnetic fields components.

In Maxwell's equations, the electromagnetic field is represented by an electromagnetic tensor, a 4x4 matrix whose diagonal is zero and whose half of the components describe the electric field and the other half the magnetic field. These four dimensions correspond to space (3) and time (1).

In fact, there are four main Maxwell equations²⁵:

- The **Maxwell-Gauss** equation describes how an electric field is generated by electric charges. At each point in space, the electric field is directed from positive to negative charges in directions depending on the charges space position.
- The **Maxwell-flux** equation states that a magnetic field is always generated by a dipole with positive and negative charges that are connected and inseparable. Mathematically, this translates into the fact that the divergence of the magnetic field is zero and that there is no magnetic monopole.

$$\text{div}(\vec{E}) = \frac{\rho}{\epsilon_0}$$

electric field
charges distribution
divergent, measures field variation orientation
vacuum dielectric permittivity

Figure 22: Maxwell-Gauss equation describing the electric field created by electric charges.

$$\text{div}(\vec{B}) = 0$$

$$\oiint_{(\Sigma)} \vec{B} \cdot d\vec{S} = 0$$

magnetic field
surface vector Σ derivative
surface integral
closed surface

Figure 23: Maxwell-flux equation.

²⁵ See these well done and visual explanations of Maxwell's equations: [A plain explanation of Maxwell's equations.](#)

Namely, that there is no magnetic field line that escapes to infinity as we have with an electric field.

- The **Maxwell-Faraday** equation describes how the variation of a magnetic field creates an electric field. This is the principle used in electric alternators. The rotational operator using a nabla sign ∇ corresponds to a differential vector operation. It is equal to the first derivative of the magnetic field over time.
- The **Maxwell-Ampere** equation states that magnetic fields are generated by electric currents or by the variation of an electric field. This interdependence between magnetic fields and varying electric fields explains the circulation of self-sustaining electromagnetic waves. On the left of the equation is the rotational magnetic field.

As with Schrödinger's equation, Maxwell's equations have several variations, which may be confusing. Maxwell first published twenty equations with twenty unknown variables in 1865. In 1873, he reduced them to eight equations. In 1884, **Oliver Heaviside** (1850-1925, English) and **Willard Gibbs** (1839-1903, American) downsized the whole stuff to the four partial differential vector equations mentioned above. These four vector equations are reduced to two tensor equations for electromagnetic waves propagated in vacuum.

The non-interaction with other elements explains the independence in this equation between electric and magnetic fields.

Maxwell predicted that electromagnetic waves were travelling at the speed of light.

Electromagnetic waves were only experimentally discovered after Maxwell's death, by **Heinrich Hertz** (1857-1894) between 1886 and 1888. Hertz also discovered the photoelectric effect in 1887. Maxwell's description of electromagnetic waves had a phenomenal impact in electromagnetic telecommunications and optronics. It also served as a foundation for the first quantum physics laws developed by Max Planck in 1900 which led progressively to the quantization of the electromagnetic waves.

Maxwell is also at the origin of the **Maxwell-Boltzmann** statistical law of gas distribution. It models the particle velocity distribution of a perfect gas. It does not take into account the interactions between particles and is not applicable to extreme conditions, such as very low temperatures.

$$\text{rotational} \rightarrow \nabla \times \vec{E} = - \frac{\partial \vec{B}}{\partial t}$$

electric field magnetic field

Figure 24: Maxwell-Faraday equation connecting the magnetic and electric fields.

$$\nabla \times \vec{B} = \mu_0 \vec{j} + \mu_0 \epsilon_0 \frac{\partial \vec{E}}{\partial t}$$

current density vector vacuum magnetic permeability vacuum dielectric permittivity

rotational magnetic field electric field

Figure 25: Maxwell-Ampere equation connecting magnetic field to electric field

$$\frac{1}{c_0^2} \frac{\partial^2 \vec{E}}{\partial t^2} - \nabla^2 \vec{E} = 0$$

second derivative over time of electric field electric field vector second derivative over space of electric field

speed of light

$$\frac{1}{c_0^2} \frac{\partial^2 \vec{B}}{\partial t^2} - \nabla^2 \vec{B} = 0$$

second derivative over time of magnetic field magnetic field pseudo-vector second derivative over space of magnetic field

Figure 26: Maxwell's equations in vacuum.



In particular, it is replaced by the **Bose-Einstein condensate** statistic for bosons (integer spin particles such as helium 4, which can be gathered in the same quantum state and energy level) and by the **Fermi-Dirac** statistic for fermions (particles with half-integer spins such as electrons or helium-3, which cannot cohabit in the same quantum and energy state).

Maxwell is the designer in 1867 of the so-called **Maxwell's demon** thought experiment which would make possible the reversibility of thermodynamic exchange processes and invalidate the second law of thermodynamics.

It rests on two boxes containing two different gases where a gas at two different temperatures is separated by a hole and a closure controlled by a "demon". When the door is opened, the gases mix.

Once mixed (see Figure 27), the demon would control which molecules could go from one box to another, taking advantage of the natural kinetic energy of the gases. This would allow in theory and after a certain time to return to the previous equilibrium in a non-equilibrium situation (on the right in Figure 27).

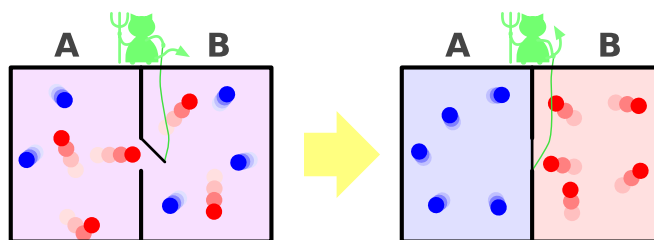


Figure 27: Maxwell's demon principle. Source: Wikipedia.

It took several decades to find the fault, notably via Léo Szilard in 1929 and Léon Brillouin in 1948. Initially, the explanation was that the demon needs to consume some energy to obtain information about the state of the gas molecules to sort them out. Therefore, energy is consumed to modify the stable equilibrium obtained to mix the gases.

The "up to date" explanation is somewhat different. The energy cost comes from resetting the demon's memory, which ultimately consists of a single bit of information²⁶.

All this had repercussions on the notion of the energy value of information and led, much later, to the creation of the field of information thermodynamics, i.e., the study of the energetic and entropic footprints of information, particularly in quantum computing.

This field was then investigated by **Rolf Landauer**, known for his study of irreversible information management circuits heat generation, and by **Charles Bennett** and **Gilles Brassard**, the co-inventors of the QKD based BB84 protocol, which we will discuss later, and then by **Paul Benioff**, who was at the origin of the idea of gate-based quantum computing.

We finally owe Maxwell the creation of color photography in 1855, that was implemented in 1861, based on the three primary colors of human vision.

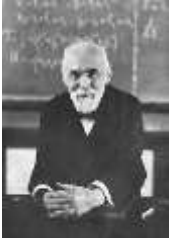
Maxwell's electromagnetic field equations has very well survived the test of time. It's still the basis of classical optics and quantum optics. Even when studying quantized light, researchers and students still rely on Maxwell's equations and their subsequent derivations created since then.

²⁶ Here is the detailed explanation by Alexia Auffèves (CNRS Institut Néel / MajuLab): we can understand the operation of resetting a bit of memory by considering an ultimate Carnot engine, consisting of a single particle that can be located to the left or right of a certain thermostated volume. Left = 0, Right = 1 There are two possible operations. The first one is compression. The particle is initially to the left or to the right of the volume that contains it (we don't know) and we compress the said volume so that at the end it is necessarily on the left. It is an initialization operation where the bit is reset to state 0. As with any compression, you have to pay, here in this ultimate case, the work to be expended is $kT \log 2$. This is Landauer's famous work, which sets an energy bound to all logically irreversible operations. The second operation is relaxation. In the beginning, we know whether the particle is on the left or on the right. We position a wall, a pulley with a mass at the end and let the trigger operate while extracting an elementary work equivalent to $kT \log 2$. This is a Szilard machine. These two manipulations were performed experimentally in 2011 at ENS Lyon. It shows the energy footprint of information and are the ultimate solution to Maxwell's demon paradox. See [Information and thermodynamics: Experimental verification of Landauer's erasure principle](#) by Antoine Bérut, Artyom Petrosyan and Sergio Ciliberto, Université de Lyon and ENS Lyon, 2015 (26 pages).



Ludwig Boltzmann (1844-1906, Austrian) was a physicist, the father of statistical physics, defender of the existence of atoms, facing a strong opposition from scientists until the beginning of the 20th century, and creator of equations describing fluid and gas dynamics in 1872. He is also at the origin of the probabilistic interpretation of the second law of thermodynamics, which establishes the irreversibility of physical phenomena, particularly during thermal exchanges.

Irreversibility is associated with the creation of entropy. Boltzmann tried his hand at philosophy while defending the existence of atoms. Depressed, he died by committing suicide.



Henri Poincaré (1854-1912, French) was a mathematician and physicist, precursor of the theory of relativity and gravitational waves. We owe him a probabilistic function that bears his name, and which is the optical equivalent of the Bloch representation that we will see later, which mathematically describes the state of qubits. He is also the author in 1904 of the mathematical conjecture that bears his name and that was demonstrated in 2003 by the Russian mathematician Grigori Perelman. It is relative to hypersphere bounding the unit ball in a 4-dimensional space.

He was a first cousin of Raymond Poincaré (1860-1934), president of France during the First World War, a lesser-known figure than Georges Clémenceau who was then Prime Minister and drove the war efforts against Germany and with allies from the UK and the USA.



David Hilbert (1862-1943, German) is yet another prolific mathematician who, at the end of the 19th century, was the creator of the mathematical foundations widely used in quantum physics, in particular his so-called Hilbert spaces using vectors to measure lengths, angles and define orthogonality. They are used to represent the state of quantum objects and qubits with vectors and complex numbers with an inner product, distances and an orthonormal basis (see Figure 28). Still, his work had nothing to do with quantum physics, which was not yet formulated at the time.

His work was used by Paul Dirac in 1930 and John Von Neumann in 1932 to lay the groundworks of quantum physics mathematical foundations like the Dirac Bra-Ket notation and the Von Neumann quantum measurement formalism.

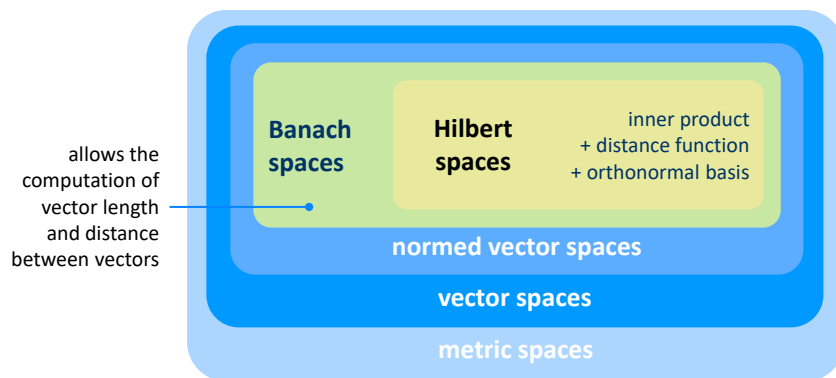


Figure 28: a Hilbert space is a vector space with an inner product. It enables the measurement of vector distances, angles and lengths. Source: compilation Olivier Ezratty, 2022.



Pieter Zeeman (1865-1943, Dutch) was a physicist, Nobel Prize in Physics in 1902 with Hendrik Lorentz, for the discovery of the effect that bears his name between 1896 and 1897. The Zeeman effect occurs when excited atoms are exposed to a magnetic field. This affects their emission or absorption spectrum, that displays many discrete spectral lines. The effect is observed with spectroscopy, which breaks down light rays of different wavelengths with a prism.

In his experiment, spectral lines are broken down into an odd number of lines (normal Zeeman effect, as shown in Figure 29 for cadmium atoms) or an even number of lines (abnormal Zeeman effect). The decomposition depends on the intensity of the magnetic field passing through the analyzed atoms. There is also a nuclear Zeeman effect explained by the spin of atom nucleus.

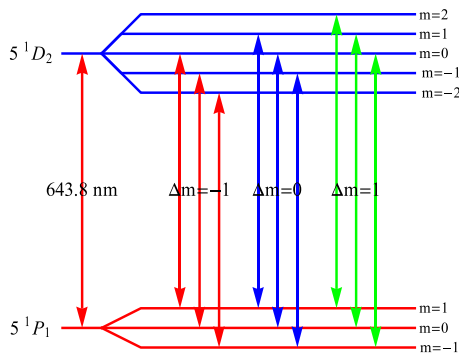


Figure 29: normal Zeeman's effect energy transitions.
Source: [Lecture Note on Zeeman effect in Na, Cd, and Hg](#)
by Masatsugu Sei Suzuki and Itsuko S. Suzuki, 2011.

It is matched by a polarization of the generated light whose nature and intensity depends on the orientation of the magnetic field relative to the light beam as shown here. The Zeeman effect can be explained by Pauli's exclusion principle, elaborated in 1925, and by the transitions in the energy level of the electrons in the same atom layer and having different orbital angular momentum (normal) and spin (abnormal). In astronomy, the Zeeman effect measurement is used to evaluate the intense magnetic fields in stars as well as within the Milky Way. The nuclear Zeeman effect is used in magnetic resonance spectroscopy in MRI scanners.



Hendrik Antoon Lorentz (1853-1928, Dutch) was a physicist who worked on the nature of light and the constitution of matter and made the link between light and Maxwell's electromagnetism equations. We owe him the Lorentz transformations that explain the results of Michelson-Morley's experiments between 1881 and 1887 which showed that the speed of light is stable, whatever the reference frame. With Henri Poincaré and George Francis FitzGerald (1851-1901, Irish), he was a key contributor to the theory of relativity formalized later by Albert Einstein between 1905 and 1915.

Let's also add **Joseph Larmor** (1857-1942, Irish/British) who, among other various contributions, was one of the first to associate electric charges with electron particles in 1894. We also own him the notion of Larmor precession, the rotation of the magnetic moment of an object when it is exposed to an external magnetic field, discovered with protons in 1919 and later extended to electrons.

Founders

The foundations of quantum physics started with Max Planck's black-body explanation with energy quanta and, then took shape over three and a half decades, roughly until 1935. It involved the successive contributions from Einstein, Bohr, De Broglie, Schrödinger, Born, Heisenberg and Dirac to mention only the best-known contributors who were all theoreticians and not experimentalists. In the timeline from Figure 30, the gold coins represent a Nobel prize.

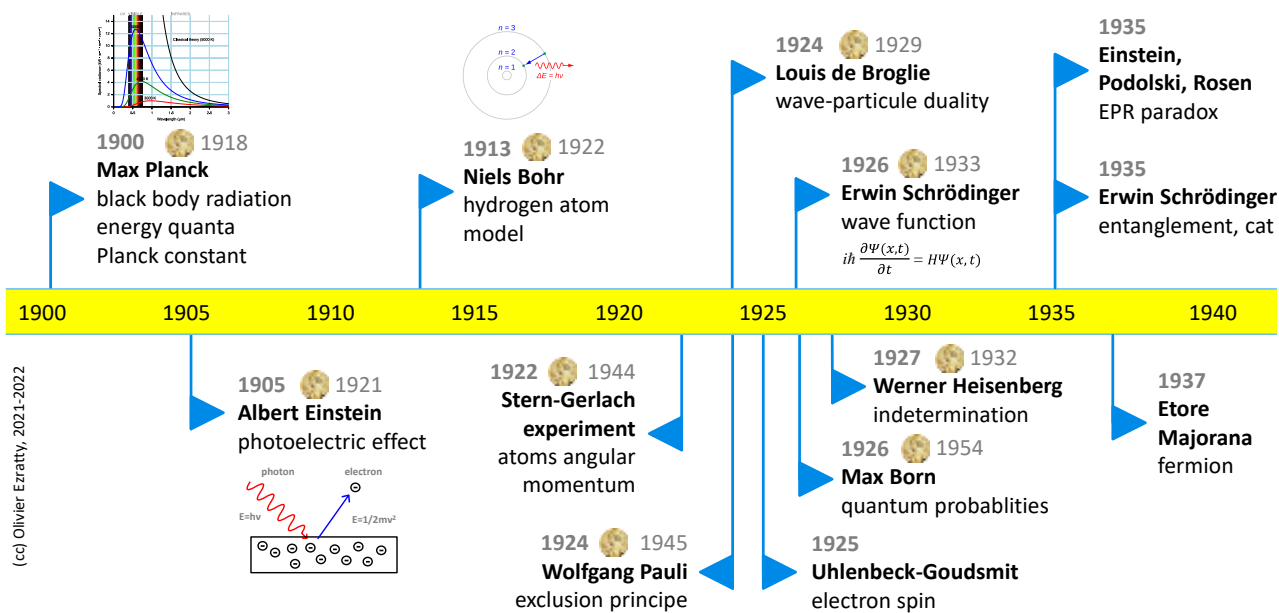


Figure 30: quantum physics foundational years timeline. (cc) Olivier Ezratty, 2021-2022.

Things were relatively quiet during World War II as lots of scientists were focused on creating the atomic bomb in the USA under the umbrella of the then very secret Manhattan project while Europe was not the best place in the world for travel and international scientific collaborations. German scientists who initially led quantum physics became isolated or emigrated to the USA or the UK because they were Jews, like Albert Einstein or Max Born.

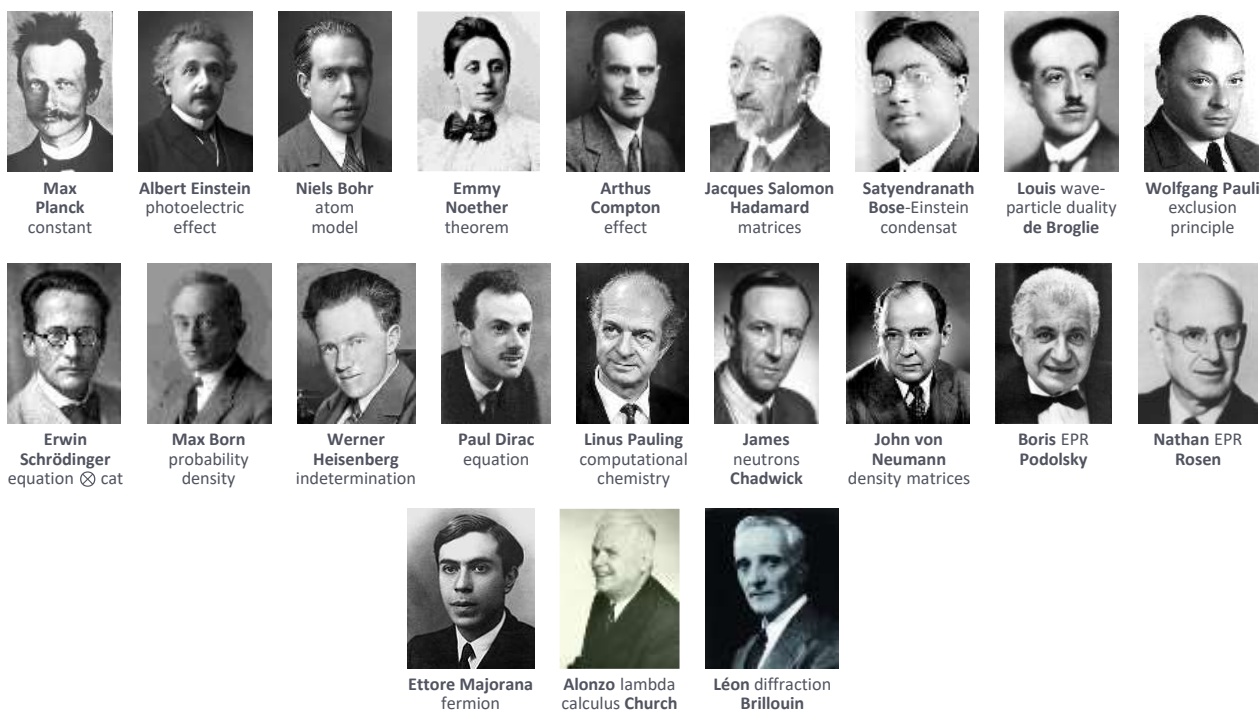


Figure 31: the key founders of quantum physics in the first part of the 20th century. (cc) Olivier Ezratty, 2020.

Here is a broader tour of the great physicists and mathematicians who laid the foundations of quantum physics. They are all Europeans who, some of whom emigrated from Europe to the United States before World War II.



Max Planck (1858-1947, German) was a physicist, initially specialized in thermodynamics. In 1900, he developed the first basis of quantum physics, hypothesizing that energy exchanges between light and matter are made by discrete quanta. This radiation is not continuous but varies by thresholds, in steps of a certain amount of energy, hence the term "quantum" and "quantum physics" or "quantum mechanics". His theory allowed him to roughly explain for the first time the enigmatic radiation of black bodies, that absorbs all incident magnetic radiation.

Examples of black bodies are a closed cavity like an oven, a heated metal that becomes red, orange, then white depending on the temperature, or a star like our own Sun. The spectrum of electromagnetic waves emitted by a black body depends only on its temperature and not at all on its material. The higher the temperature is, the more the electromagnetic spectrum emitted by the black body slides towards higher frequencies on the left, therefore towards purple and ultraviolet. The theory solved the ultraviolet catastrophe.

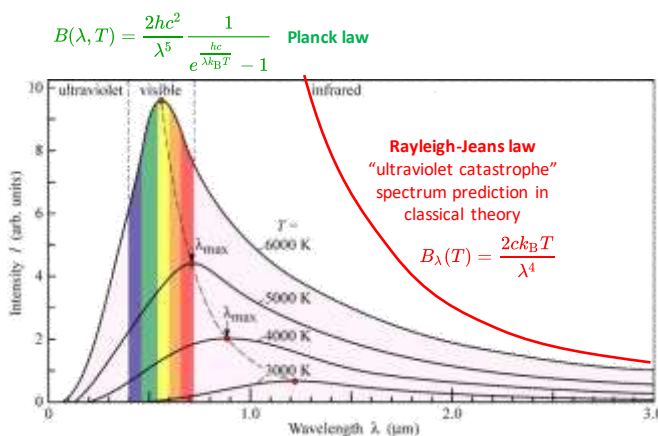


Figure 32: black-body spectrum and the ultra-violet catastrophe.

This so-called ultraviolet catastrophe, an expression **Paul Ehrenfest** (1880-1933, Austrian) created later in 1911, happened with the Rayleigh-Jeans law also proposed in 1900, which was trying to predict the shape of the light spectrum with the black body temperature. It was diverging to infinite values as the temperature was growing. Planck's law solved the problem and avoided the ultraviolet catastrophe. He found his spectrum equation empirically and only then, a related explanation based on harmonic oscillators and energy quanta exchanged between the radiation and the black body "wall". For this work, Max Planck was awarded the Nobel Prize in Physics in 1918.

We also owe him the constant which bears his name (h) and which is used in his blackbody radiation equation. The Planck constant (6.626×10^{-34} Js) was then used in the equation according to which atomic state energy shifts equals to the radiation frequency multiplied by Planck's constant. The constant appears in most quantum physics equations (De Broglie, Schrödinger, Dirac, etc.).

When an electron changes its orbit in a hydrogen atom, it emits or absorbs an electromagnetic wave whose energy is equal to Planck's constant multiplied by the emitted light frequency. More generally, a system can evolve only with multiples of Planck's constant. Despite the numerous experimental validations carried out a few years later, Max Planck expressed until his death a lot of doubts about the very principles of quantum physics!

Planck is also at the origin of several infinitesimal constants as shown in Figure 33: Planck time, which is $t_P = 10^{-44}$ s and Planck distance which is $l_P = 1.616255 \times 10^{-35}$ m. Planck's time is the time it would take for a photon to travel the Planck distance.

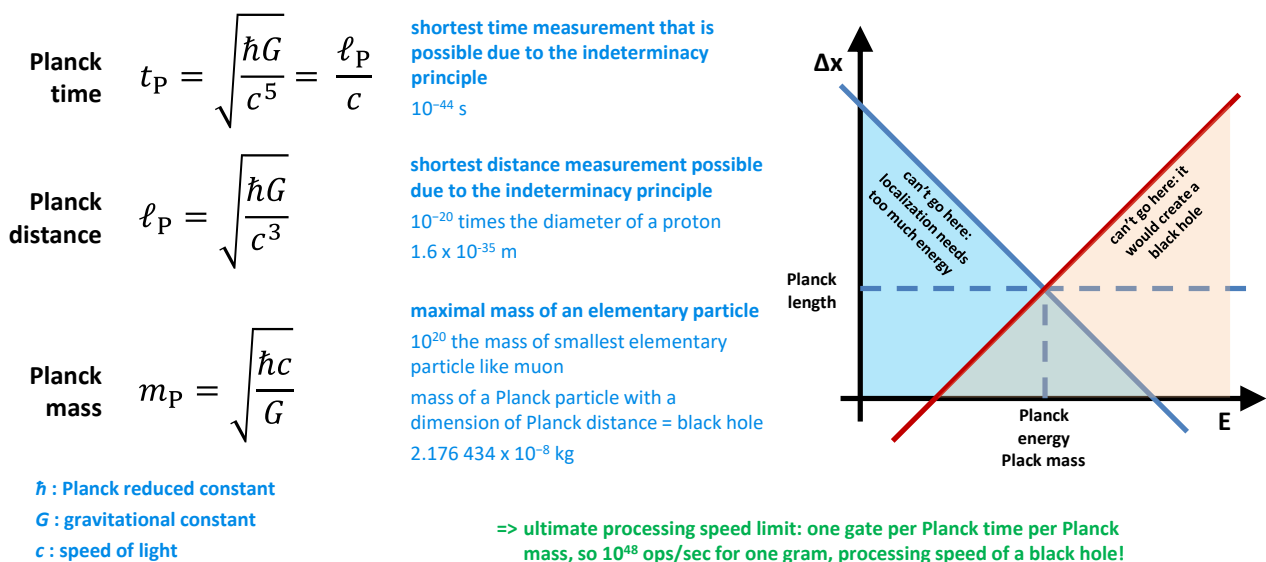


Figure 33: Planck time, distance and mass constants (cc) Olivier Ezratty, 2021.

These are the dimensions of the infinitely small below which any observation would be impossible. The length of Planck l_P is so small that a photon used to observe it would have such a high frequency and energy that it would generate a black hole around it and would therefore become unobservable!

At last, Planck mass is the maximum mass of an elementary particle. A particle with this mass and the size of Planck's distance would be a black hole. These are quite extreme physics. In today's classical cosmology, Planck's wall corresponds in the history of the expansion of the Universe to the moment when 10^{-43} s after the big bang, its size would have been 10^{-35} m, which is respectively the Planck time and Planck distance. Needless to say that the experimental conditions of the big bang are difficult to reproduce. It doesn't prevent some physicists to try to simulate it digitally²⁷.

²⁷ See [A new algorithm that simulates the intergalactic medium of the Universe in seconds is developed](#) by the Instituto de Astrofísica de Canarias, May 2022.



Albert Einstein (1879-1955, German then American) got his Nobel Prize in 1921 for his interpretation of the photoelectric effect in 1905, which became one of the foundations of quantum mechanics after Planck and before De Broglie, Heisenberg and Schrödinger. Einstein determined that Planck's quanta are elementary grains of energy $E = h\nu$ (Planck constant times frequency) with a momentum of $p = h\nu/c$ ²⁸. These were named “photons” in 1926 by **Gilbert Lewis** (1875-1946, American). Symbolically, 1905 is also the year of Jules Verne’s death.

Symmetrically to what Louis De Broglie would later do with electrons, he hypothesized that a photon behaves both as a wave and as a particle.

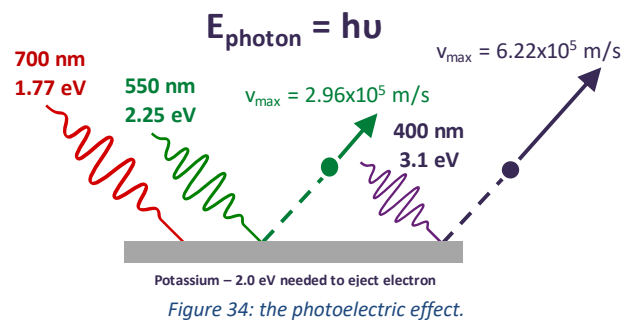
This was coming out of just one out of his four 1905 “annus mirabilis” papers sent between March and June to *Annalen der Physik*, the others being on special relativity, Brownian motion and mass-energy equivalence, published when he was just 26. This was on top of his own 24 pages PhD thesis on a theoretical method to calculate molecular sizes using fluid mechanics and hydrodynamics.

With the photoelectric paper, he reconciled the corpuscular theories of **René Descartes** (1596-1650, French, in 1633) and **Isaac Newton** (1642-1726, English, in 1704) with the wave-based theories of **Christiaan Huygens** (1629-1695, Dutch, in 1678) to describe light.

This was followed by the works from **Augustin-Jean Fresnel** (1788-1827, French), **Léon Foucault** (1819-1868, French, who measured first the speed of light), **Hippolyte Fizeau** (1819-1896, French, who co-discovered the Doppler effect) and of course **James Clerk Maxwell**.

The photoelectric effect corresponds to the capacity of a photon to dislodge an electron from a generally inner orbit of an atom and to create some electric current²⁹.

It is exploited in the cells of silicon-based photovoltaic solar panels. It also explains photosynthesis in plants, which is the metabolic starting point of glucose production.



In addition to Max Planck's work on black body radiation, Einstein's interpretation was based on the earlier work of **Heinrich Hertz** (1857-1894, German) who discovered in 1887 that light can extract an electron out of metal, and **Philipp Lenard** (1862-1947, German) who, in 1902, studied the photoelectric effect and determined that it is only triggered at a certain frequency for the projected light. The latter was awarded the Nobel Prize in Physics in 1905. Becoming a fervent Nazi and opposed to Einstein by scientific rivalry and then by explicit anti-Semitism, he mostly disappeared from quantum physics hall of fame.

Einstein's photoelectric effect equations were then verified by the experiments of **Robert Andrews Millikan** (1868-1953, American) between 1909 and 1914. It enabled him to measure the electric charge of a single electron, which earned him the Nobel Prize in Physics in 1923.

²⁸ In [On a Heuristic Viewpoint Concerning the Production and Transformation of Light](#), 1905.

²⁹ The electron layers of the atoms are numbered from 1 to N, their quantum number. One also starts the numbering by K (first layer close to the nucleus with a maximum of 2 electrons) then L (8 electrons maximum), M (with a maximum of 18 electrons but in practice 8), etc. The photoelectric effect mainly concerns the layers K and L. The ejected electron is then replaced by an electron of external orbit, which generates a new photon, in X-rays or in fluorescence, according to the energy of the incident photon. This then emits an X-ray photon due to the energy differential between electronic layers or an electron called "Auger" from the name of Pierre Auger. This phenomenon was discovered around 1923 by the latter and by Lise Meitner. Another variant of the photoelectric effect is the Compton effect, when the high energy of an incident photon in gamma rays will release an electron from the valence layer and generate another photon. Finally, when the energy of the incident photon is even higher, the interaction takes place at the nucleus of the target atom and generates an electron and a positron.

Of course, Einstein is also at the origin of the special and general theories of relativity. He didn't obtain a Nobel Prize for his work on relativity despite its considerable impact on science.

This is due, among other things, to his theories being based on earlier work from **Hendrick Anton Lorentz** and **Henri Poincaré** as well as the contribution of his former professor **Hermann Minkowski** (1864-1909, German) who created the four-dimensional space-time notion in 1908.

On top of many other contributions in quantum physics, Einstein predicted the photons stimulated emission effect in 1917, that would later lead to the creation of lasers. He also predicted in 1925 a particular behavior of matter, the Bose-Einstein condensate, which occurs when gases are cooled to very low temperatures. Atoms are then in a minimum energy quantum state showing particular physical properties.

This is the case of superfluid helium, discovered in 1938, which is superfluid at very low temperatures, i.e., it can move without dissipating energy. Bose is the name of **Satyendra Nath Bose** (1894-1974, India) with whom Einstein had worked during the 1920s and to whom we owe the "bosons", which verify the characteristics of Bose-Einstein's condensates.

Bosons include elementary particles without mass such as photons and gluons but also certain atoms such as deuterium or Helium 4 as well as certain quasi-particles such as the superconducting electron pairs that are Cooper's pairs. We will see a little later that it is a question of the spin sum of these particles that determines the fact that they are bosons as opposed to fermions.

Albert Einstein also contributed to the philosophical-scientific debates on quantum physics realism, confronting Niels Bohr. He focused on the fact that quantum physics did not seem to completely describe the physical world with its probabilistic bias. Einstein wanted to find a realistic interpretation of quantum physics. He could not be satisfied with a probabilistic description of the state of electrons and other quantum objects. He could not find sufficient the interpretation of quantum physics according to which the observer and the measurement "make" the real world. He thought that the real world exists independently of measurements and observers.

The debate between Albert Einstein and Niels Bohr revolved around various thought experiments on determinism discussed during the 1927 Solvay Congress.

MAY 15, 1935

PHYSICAL REVIEW

VOLUME 47

Can Quantum-Mechanical Description of Physical Reality Be Considered Complete?

A. EINSTEIN, B. PODOLSKY AND N. ROSEN, *Institute for Advanced Study, Princeton, New Jersey*

(Received March 25, 1935)

In a complete theory there is an element corresponding to each element of reality. A sufficient condition for the reality of a physical quantity is the possibility of predicting it with certainty, without disturbing the system. In quantum mechanics in the case of two physical quantities described by non-commuting operators, the knowledge of one precludes the knowledge of the other. Then either (1) the description of reality given by the wave function in

quantum mechanics is not complete or (2) these two quantities cannot have simultaneous reality. Consideration of the problem of making predictions concerning a system on the basis of measurements made on another system that had previously interacted with it leads to the result that if (1) is false then (2) is also false. One is thus led to conclude that the description of reality as given by a wave function is not complete.

Figure 35: the famous EPR paper from Albert Einstein, Boris Podolsky and Nathan Rosen published in 1935.

It culminated later, in 1935, with the famous **EPR paradox** paper, named after its authors Albert Einstein, Boris Podolsky and Nathan Rosen. The paper raised the question of the incompleteness of quantum mechanics at the time³⁰.

³⁰ See [Can Quantum-Mechanical Description of Physical Reality Be Considered Complete?](#), by Albert, Einstein, Boris Podolsky and Nathan Rosen 1935 (4 pages).

It sought to explain the non-locality of the correlated quantum state measurement results of entangled particles which was a consequence of Schrödinger's wave function. It was not yet physically observed as of 1935³¹. For the EPR paper authors, the quantum theory based on Schrödinger's wave function was either incomplete or two quanta could not be instantaneously synchronized at a distance at measurement time. Their measurement outcome being random and correlated, entangled quantum objects had to convey with them a sort of "information switch" indicating where the random measurement should land. A physical theory is complete if each component of reality has a counterpart in the theory that makes it possible to predict its behavior, such as some tuning happening at the source when entangled quanta are created, and transmitted to each one with some hidden variables that would determine the outcome of their measurement. This underlies the notion of determinism, a principle that is absent in Schrödinger's wave function which is entirely probabilistic in nature.

Einstein thought that quantum physics was an incomplete theory that didn't describe reality precisely enough. Einstein was then often credited with the idea that there were hidden variables. It seems, however, that he never mentioned them in his writings despite what John Bell later said. The EPR paper ends with indicating that it should be possible to build a complete theory of quantum mechanics³². Hidden variables are a consequence rather than a hypothesis in the EPR paradox paper.



Figure 36: New York Times coverage of the EPR paper.

The explanation of entanglement by "hidden variables" comes rather from Louis de Broglie with his pilot wave hypothesis elaborated in 1927, an idea later pursued by David Bohm in the 1950s³³. With his "inequalities", John Stewart Bell demonstrated in 1964 that the existence of such hidden local variables was incompatible with the principles of quantum mechanics. Alain Aspect's 1982 experiment on photon entanglement confirmed this hypothesis. In the end, Einstein could not finish his work on his theory of general relativity which was, for him, as incomplete as quantum mechanics. In particular, he wanted to reconcile quantum mechanics and gravity.

Be careful with the simplistic views that Einstein was "against" quantum mechanics, had it all wrong or did not believe in it³⁴. He first questioned the principle of indeterminacy in 1927 and 1930, then estimated that the theory was incomplete to explain entanglement, with the EPR paradox paper published in 1935, and finally, he opposed the lack of realism of quantum theory. This incompleteness is still being discussed more than 80 years later. The origins of entanglement are still not physically explained under certain conditions, particularly with long distance. It is only observed physically and described mathematically³⁵. This remains an open debate as scientists continue to ponder the different possible interpretations of quantum physics. This is part of the field of [quantum foundations and quantum physics philosophy](#) that we cover later in this book, page 1001.

³¹ Einstein's landmark was classical and relativistic physics that acted locally. Gravity is local and is transmitted at the speed of light. All physical theories before quantum physics were local or EPR-local. Remote actions all involve a delay, usually coupled with attenuation with distance as it's the case for gravity.

³² The 1935 New York Times article was published thanks to a "leak" provoked by Boris Podolsky, the youngest of the EPR 3 gang.

³³ See [Albert Einstein, David Bohm and Louis de Broglie on the hidden variables of quantum mechanics](#) by Michel Paty, 2007 (29 pages) which sets the record straight on Albert Einstein's position on the subject of hidden variables. The author, born in 1938, is a physicist and a philosopher of science.

³⁴ This story is well told in [Einstein and the Quantum - The Quest of the Valiant Swabian](#) by A. Douglas Stone, 2013 (349 pages).

³⁵ See the abundant [Einstein Bohr debates](#) and [Interpretations of quantum mechanics](#) pages on Wikipedia, from which the table on the next page is taken.



Niels Bohr (1885-1962, Danish) was a physicist, Nobel Prize in Physics in 1922, who created in 1913, aged 28, a descriptive model of the hydrogen atom with its nucleus made of a proton and an electron rotating around the nucleus on precise orbits corresponding to levels of kinetic energy, multiple of $h/2\pi$, h being Planck's constant and $n = 1, 2, 3$ and so on. This model explained hydrogen spectral lines observed in the experiments of **Johann Balmer** (1825-1898) in 1885, **Theodore Lyman** (1874-1954) in 1906 and **Friedrich Paschen** (1865-1947) in 1908.

It also explained why electrons didn't crash on atom nucleus! Niels Bohr followed the work of **Ernest Rutherford** (1871-1937) who discovered in 1911 the structure of atoms with their positively charged nucleus, thanks to its protons, and their electrons revolving around the nucleus. The latter, with whom Niels Bohr was doing his post-doc in 1911, relied himself on **Hantaro Nagaoka** (1865-1950, Japan) who predicted in 1903 the structure of atoms with a positively charged nucleus and negatively charged electrons revolving around it, called the "Saturnian model".

Electrons had been discovered by **Joseph John Thomson** (1856-1940, English) in 1897 by analyzing the rays emitted by a cathode in a cathode ray tube (CRT), deflected by an electric field as well as by a magnetic field, and detected by a layer of phosphorus. He was awarded the Nobel Prize in Physics in 1906.

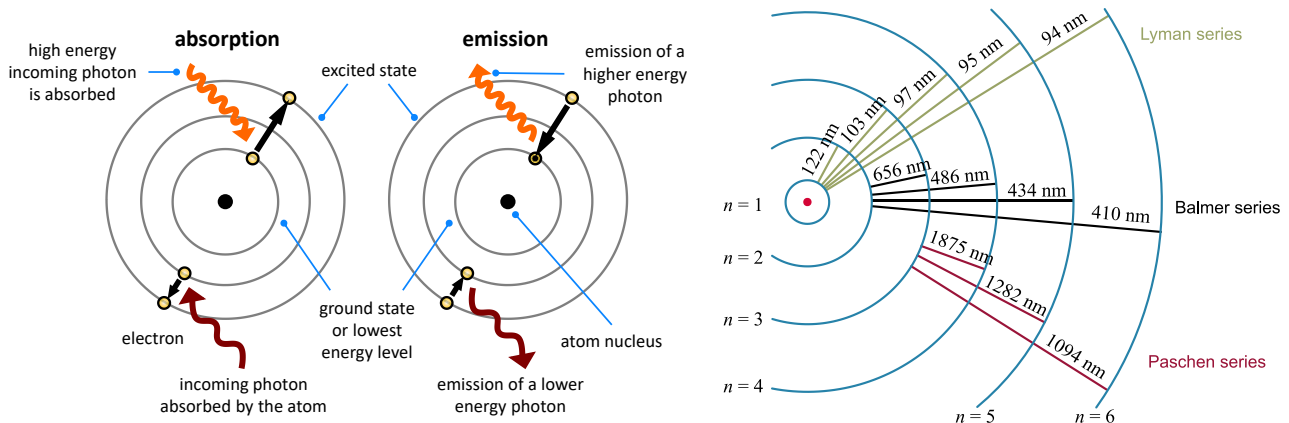


Figure 37: the Bohr atomic model. Source: Wikipedia and other open sources.

Ernest Rutherford had also imagined the existence of neutrons, which was not verified experimentally until 1932 by **James Chadwick** (1891-1974, English). **Marie Curie** (1867-1934, Polish and French) had discovered polonium and radium in 1898 and some effects of radioactivity but not the existence of neutrons.

According to Niels Bohr, electrons emit or absorb a photon when they change orbit. Subsequently, Louis de Broglie's work on wave-particle duality interpreted that the orbits of the electrons were an integer multiple of their associated wavelength.

Together with Werner Heisenberg, Pascual Jordan and Max Born, Niels Bohr is at the origin of the so-called **Copenhagen** interpretation of quantum physics which is based on three key principles³⁶ :

- The description of a wave-particle is realized by its wave function, and no other "hidden" local information or variable can be used to describe its state. We must accept the wave function probabilistic used to describe a quantum state.

³⁶ See also Richard Webb's [Seven ways to skin Schrödinger's cat](#), 2016 which describes the different schools of thought in quantum physics. See also other interpretations of quantum physics in Ethan Siegel's [The Biggest Myth In Quantum Physics Starts With A Bang](#) in Forbes, 2018.

- When a quantum state measurement is performed, its composite wave function of several states is reduced to the wave function of one of the possible states of the quantum with a probability define by Born’s rule (we’ll see that later). This is the collapse of the wave function.
- When two properties are linked by an uncertainty relationship, the two properties cannot be measured with a greater precision than that allowed by the uncertainty relationship (Heisenberg principle of indeterminacy). Moreover, when we measure the position of a particle, we affect its motion, and vice versa. It comes from the bare fact that speed and position do not have any meaning before measurement in quantum physics. Variables linked through an indetermination link are conjugate with regards to actions which can change only by quantum leaps.

This is the main interpretation of quantum mechanics. There are many other interpretations available, listed below in the table from Figure 38. We will have the opportunity to detail the interpretation of Copenhagen towards the end of the book in the part dedicated to the [philosophy of quantum physics](#), page 1001.

| Interpretation | Year published | Author(s) | Deterministic? | Ontologically real wavefunctions? | Unique history? | Hidden variables? | Collapsing wavefunctions? | Observer role? | Local dynamics? | Counterfactually definite? | Existential universal wavefunction? |
|-------------------------------|----------------|---|---------------------|-----------------------------------|------------------------|-------------------|---------------------------|-------------------------------|---------------------|----------------------------|-------------------------------------|
| Ensemble interpretation | 1926 | Max Born | Agnostic | No | Yes | Agnostic | No | No | No | No | No |
| Copenhagen interpretation | 1927 | Niels Bohr, Werner Heisenberg | No | No ¹ | Yes | No | Yes ² | Causal | Yes | No | No |
| de Broglie-Bohm theory | 1927-1952 | Louis de Broglie, David Bohm | Yes | Yes ³ | Yes ⁴ | Yes | Phenomenological | No | No | Yes | Yes |
| Quantum logic | 1936 | Garrett Birkhoff | Agnostic | Agnostic | Yes ⁵ | No | No | Interpretational ⁶ | Agnostic | No | No |
| Time-symmetric theories | 1955 | Saburo Hatanaka | Yes | No | Yes | Yes | No | No | No ⁷⁽¹⁾ | No | Yes |
| Many-worlds interpretation | 1957 | Hugh Everett | Yes | Yes | No | No | No | No | Yes | B-posed | Yes |
| Consistent histories collapse | 1961-1963 | John von Neumann, Eugene Wigner, Henry Stapp | No | Yes | Yes | No | Yes | Causal | No | No | Yes |
| Stochastic interpretation | 1988 | Edward Nelson | No | No | Yes | Yes ⁸ | No | No | No | Yes ⁹⁽¹⁾ | No |
| Many-worlds interpretation | 1987 | H. Dieter Zeh | Yes | Yes | No | No | No | Interpretational ² | Yes | B-posed | Yes |
| Consistent histories | 1984 | Roderik B. Griffiths | No | No | No | No | No | No | Yes | No | Yes |
| Transactional interpretation | 1985 | John G. Cramer | No | Yes | Yes | No | Yes ¹⁰ | No | No ¹¹ | Yes | No |
| Objective collapse theories | 1985-1989 | Graedel–Strohm–Wibaut, Penrose interpretation | No | Yes | Yes | No | Yes | No | No | No | No |
| Relational interpretation | 1994 | Carlo Rovelli | No ¹²⁽¹⁾ | No | Agnostic ¹³ | No | Yes ¹⁴ | Interpretable ¹⁵ | No ¹⁶⁽¹⁾ | No | No |
| QBism | 2011 | Christopher Fuchs, Rüdiger Schack | No | No ¹⁴ | Agnostic ¹⁷ | No | Yes ¹⁸ | Interpretable ¹⁹ | Yes | No | No |

Figure 38: the various interpretation of quantum physics. Source: Wikipedia.

Note that Niels Bohr's son, **Aage Niels Bohr** (1922-2009, Danish), was awarded the Nobel Prize in Physics in 1975 for his work on the structure of atom nucleus³⁷!



Emmy Noether (1882-1935, German) is the creator of the theorem that bears her name in 1915 at the University of Göttingen in Germany and which says that if a system has a continuous symmetry property, then there are corresponding quantities whose values are conserved in time³⁸. At the origin of the field of abstract algebra, it is a foundation to Lagrangian mechanics, precursor of Hamilton's formalism. At that time, she could not teach at the University because this role was forbidden to women. Her theorem was only published in 1918 and she could not officially teach until 1919.

She did not receive a salary from the University until 1923. Her theorem links conservation principles and symmetries. It is one of the foundations of particle physics. Her work helped Albert Einstein to refine the foundations of the theory of general relativity he developed in 1915³⁹. She died relatively young, at 53.

$$\frac{d}{dt} \left(\sum_a \frac{\delta L}{\delta \frac{dq_a}{dt}} \delta q_a \right) = 0$$

Figure 39: Emmy Noether's main equation.

³⁷ See [Quantum Model of the Atom](#) by Helen Klus, 2017.

³⁸ See [In her short life, mathematician Emmy Noether changed the face of physics Noether linked two important concepts in physics: conservation laws and symmetries](#) by Emily Conover, 2018. She created a second important and more general theorem that is the basis of gauge fields theories in quantum fields theory.

³⁹ See [Women in Science: How Emmy Noether rescued relativity](#), by Robert Lea, February 2019.



Arthur Holly Compton (1892-1962, American) was a physicist who got the 1927 Nobel Prize in physics for the discovery in 1922/1923 of the effect which demonstrates that photons can have momentum and behave as particles. His experiment makes a photon interact with a free electron around an atom, validating the photoelectric effect theories of Planck and Einstein. The Compton effect is a variant of this effect, applied to X and gamma rays which are high energy photons.

Compton scattering deals with the reception of an X or gamma photon which has an energy higher than that of the ejected electron. The X ray photon is slowed down and deflected with a lower energy and becomes a scattered photon. This is also called an elastic shock. The effect is used in X-ray radios. X-rays are emitted during electronic transitions between the atomic layers K, L and M (the first around the nucleus of the atom). The emission angles of the ejected electron and the re-emitted photon depend on the energy level of the incident photon.

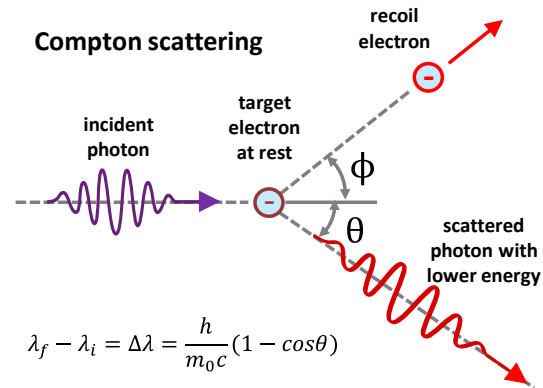


Figure 40: Compton scattering phenomenon.



Otto Stern (1888-1969, German-American) and **Walther Gerlach** (1889-1979, German) respectively conceived in 1921 and together realized in 1922 in Frankfurt the famous Stern-Gerlach experiment which discovered the intrinsic angular momentum quantization in a magnetic field using a beam of electrically neutral silver atoms as shown in Figure 41⁴⁰. In the experiment, this momentum came from the 47th electron spin from heated silver atoms.

It did show that these atoms have a quantized angular dipole that deflects the beam in a given direction upward or downward. It later became known as particle spins. The experiment also did show that spin measurement along a given direction was incompatible with being done in another direction, corresponding to the notion of observables complementarity.

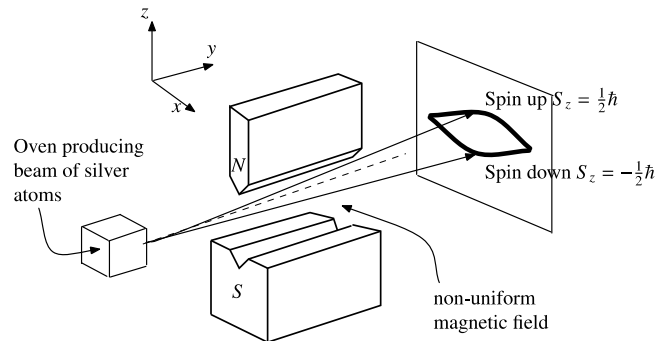


Figure 41: the Stern-Gerlach experiment where an atomic stream of silver is deviated in two discrete directions by a magnetic field.



Jacques Salomon Hadamard (1865-1963, French) was a mathematician who gave his name to the Hadamard gate used in quantum computers and quantum algorithms. He had worked on complex numbers, differential geometry and partial differential equations, particularly during the 1920s. He also became interested in the creative process of mathematicians with studying the creative process of hundreds of colleagues.

⁴⁰ Illustration coming from: [Chapter 6, Particle Spin and the Stern-Gerlach Experiment](#). See [Stern and Gerlach, how a bad cigar helped reorient atomic physics](#) by Bretislav Friedrich and Dudley Herschbach, Physics Today, December 2003 (7 pages). The X, Y and Z components of the electron spin measured in the Stern-Gerlach experiment are complementary variables. Measuring one of the three variables prevents from doing so with the two others.

We owe him in particular the Hadamard transforms, square matrix operations with 2^n complex or integer values on each side. The quantum gate named after Hadamard is used in quantum computation to create a superposition of the states $|0\rangle$ and $|1\rangle$ with a transform of Hadamard of type H1 as described in Figure 42.

This superposition enables computing parallelism in quantum computing, in addition to the principle of entanglement which links the qubits together conditionally and is the real source of quantum exponential acceleration. Superposition is only responsible for a potential polynomial acceleration.

$$\begin{aligned}
 H_0 &= 1 \\
 H_1 &= \frac{1}{\sqrt{2}} \begin{bmatrix} 0 & 1 \\ 1 & 0 \end{bmatrix} \\
 H_2 &= \frac{1}{2} \begin{bmatrix} 1 & 0 & 0 & 0 \\ 0 & 1 & 0 & 0 \\ 0 & 0 & 0 & 1 \\ 0 & 0 & 1 & 0 \end{bmatrix} \\
 H_3 &= \frac{1}{2^{3/2}} \begin{bmatrix} 1 & 0 & 0 & 0 & 0 & 0 & 0 & 0 \\ 0 & 1 & 0 & 0 & 0 & 0 & 0 & 0 \\ 0 & 0 & 1 & 0 & 0 & 0 & 0 & 0 \\ 0 & 0 & 0 & 1 & 0 & 0 & 0 & 0 \\ 0 & 0 & 0 & 0 & 1 & 0 & 0 & 0 \\ 0 & 0 & 0 & 0 & 0 & 1 & 0 & 0 \\ 0 & 0 & 0 & 0 & 0 & 0 & 0 & 1 \\ 0 & 0 & 0 & 0 & 0 & 0 & 0 & 1 \end{bmatrix}
 \end{aligned}$$

Figure 42: Hadamard matrices of various dimensions.



Louis de Broglie (1892-1987, French) was a mathematician and physicist who, in 1923 and 1924, extended the particle-waves duality, then only applied to photons, to massive particles, mainly electrons, and also atoms, protons and neutrons⁴¹. According to this principle, elementary particles behave like particles (with a position, a trajectory and possibly a mass) and like waves (potentially delocalized and scattering in all directions and generating interference) depending on the circumstances.

This is the case of electrons which have a mass and can interfere with each other. Louis de Broglie turned this duality into an equation: $\lambda p = h$, where λ is a wavelength, p is a quantity of motion and h is Planck's constant.

$$\begin{aligned}
 \text{particle energy} & \quad E = h\nu \\
 \text{particle momentum} & \quad p = \frac{h}{\lambda}
 \end{aligned}$$

Figure 43: De Broglie wave-particle equation with electrons.

This earned him the Nobel Prize in Physics in 1929. He is the main French contributor to quantum physics during the inter-war period. The wave-particle duality of electrons was confirmed in 1927.

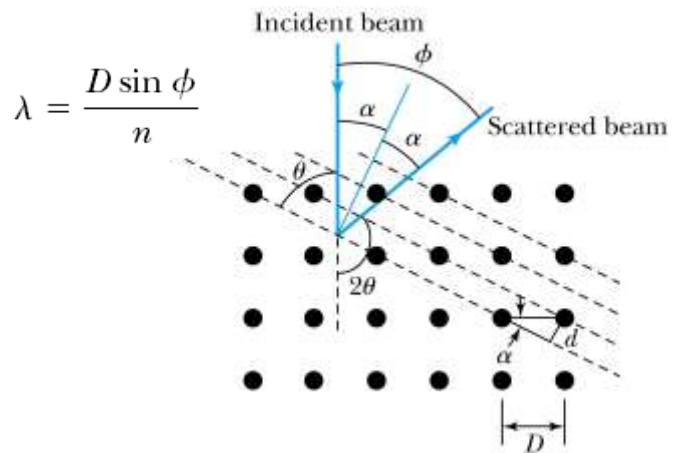
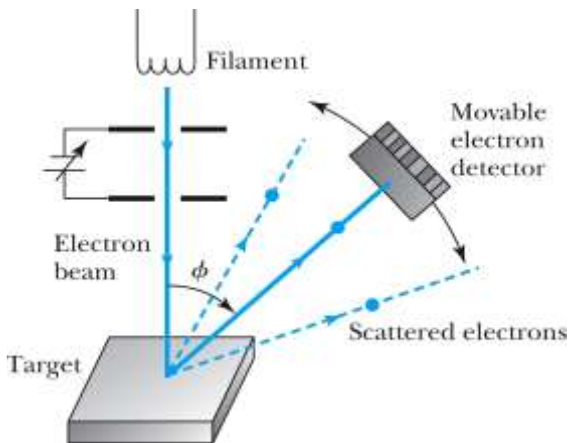


Figure 44: electron wave-particle diffraction experiment. Source: [Wave Properties of Matter and Quantum Mechanics I](#) (48 slides).

It was done as shown above in Figure 44 with a nickel crystal based diffraction experiment by **Clinton Davisson** (1881-1958) and **Lester Germer** (1896-1971) from the Bell Labs in the USA, who shared a Nobel Prize in Physics in 1937.

⁴¹ Louis de Broglie's brother, Maurice de Broglie (1875-1960), was also a physicist. He had studied X-rays and spectrography. Both brothers were members of the Academy of Sciences in France.

George Paget Thomson (1892-1975) from the University of Aberdeen in Scotland did a similar experiment also in 1927. However, the Young double-slit experiment done with electrons was realized much later, in 1961, by **Claus Jönsson** (1939, German).

The confirmation of the wave-particle duality was then verified for neutrons much later in 1988 by **Roland Gähler** and **Anton Zeilinger**⁴² and for atoms in 1991 by **Olivier Carnal** and **Jürgen Mlynek**, using double-slit diffraction and by **Mark Kasevich** and **Steven Chu**, who created the first cold atom interferometer using a light-beam splitter based on Raman transitions. It became the basis of atom interferometry used in quantum absolute gravimeters, using an equivalent of a Mach-Zehnder interferometer replacing light with so-called matter-wave made of atoms⁴³. It is even verifiable with molecules of several atoms.



Wolfgang Pauli (1900-1958, Austrian/American) is at the origin of the principle of exclusion which bears his name elaborated in 1925 and according to which two electrons cannot have the same quantum state in an atom. He had an early role in the discovery of electron spin between 1925 and 1927, as well as the neutrino in 1930, the existence of which was only experimentally proven in 1956, and on works on quantum electrodynamics. He was awarded the Nobel Prize in Physics in 1945. The history of his discoveries is more complex than it seems.

He first discovered in 1924 the atom nucleus spin, used to explain the hyperfine structure of atomic spectra, i.e., the existence of very close spectral lines observed during their excitation. It cannot be explained by the quanta and energy levels of the electron layers in the atoms. He then introduced in 1925 a new degree of freedom for electrons that he did not qualify at first.

It adds to the first three parameters describing the state of an electron in an atom, aka quantum numbers. The first is the energy level of the electron in the atom (the layer where it is located), the second is the azimuthal quantum number (which defines the electron sub-layer) and the third is the magnetic quantum number (which makes it possible to distinguish the orbitals of the electron in the atom)⁴⁴. This fourth degree of freedom was identified by **George Uhlenbeck** (1900-1988, Netherlands/USA) and **Samuel Goudsmit** (1902-1978, Netherlands/USA) as an electron spin⁴⁵.

In 1925, Wolfgang Pauli also formulated the exclusion principle according to which electrons in the same system (an atom) cannot be simultaneously in the same quantum state, a principle that was later extended to all fermions, i.e. half-integer spin particles (electrons have a spin $\frac{1}{2}$ but fermion atoms can have $3/2$, $5/2$, $7/2$ and even $9/2$ spins, like ⁴⁰K).

The quantum state of an electron is defined with the four quantum numbers, or degrees of freedom, that we have just mentioned. An electron spin is described as a direction of magnetic polarization or as an angular rotation of the electron in one direction or the other, but it is only an image and not a physical representation⁴⁶. Electron spins are used in silicon qubits that we cover later, starting page 292.

⁴² See [Single- and double-slit diffraction of neutrons](#) by Anton Zeilinger et al, Review of Modern Physics, 1988 (7 pages).

⁴³ In this setup, the Mach-Zehnder beamsplitter is replaced by a series of three lasers pulses creating a superposition of two atomic energy states driving a diffraction effect, then a mirror effect and at last for a recombination of split wavepackets.

⁴⁴ The second and third electron quantum numbers were introduced by Arnold Sommerfeld (1868-1951, German). Among others, Wolfgang Pauli and Werner Heisenberg were his PhD students. The alpha constant or fine structure constant is also called the Sommerfeld constant per his work from 1916! See [Electron spin and its history](#) by Eugene D. Commins, May 2012 (28 pages).

⁴⁵ Georges Uhlenbeck and Samuel Goudsmit were students of Paul Ehrenfest (1880-1933, Austria/Netherlands). His laboratory had welcomed some illustrious future physicists such as Enrico Fermi, Robert Oppenheimer, Werner Heisenberg and Paul Dirac. Ehrenfest was a specialist in statistical physics. In particular, he contributed to the understanding of phase changes in matter.

⁴⁶ See [How Electrons Spin](#) by Charles T. Sebens, California Institute of Technology, July 2019 (27 pages) which provides a good background on electron spin's physical interpretations, particularly with regards to electron's size. Pauli did demonstrate in 1924 that if the electron spin corresponded to an angular momentum, the electron's rotation would exceed the speed of light.

137 is a number that played a weird role in Pauli's life. It turns out that $1/137$ is a value that roughly corresponds to the fine-structure constant, a ratio that is found in many places in quantum physics and compares data of the same dimension⁴⁷. It is for example the ratio between the velocity of an electron in the lower layer of a hydrogen atom and the speed of light or the probability of emission of the absorption of a photon for an electron ([complete list](#)). "137" is a sort of "42" of quantum physics. Wolfgang Pauli died after some pancreatic cancer surgery, while his hospital room number was 137!



Erwin Schrödinger (1887-1961, Austrian) is a physicist who was awarded the Nobel Prize in 1933 for the creation of his famous wave function in 1926, *aka* Schrödinger equation, which describes the evolution in time and space of the quantum state of a massive quantum particle and the probabilities of finding the quantum at a given place and time. Schrödinger's equation is a variant of the Newtonian mechanics equations that define the total energy of an object as the sum of its kinetic energy and its potential energy. We describe this equation in detail in a dedicated section page 97.

Erwin Schrödinger also created his famous alive and dead cat in a box thought experiment⁴⁸. In the scenario, an opaque box contains a vial of poison, the opening of which is caused by the disintegration of a radioactive radium atom generating alpha particles ("alpha decay"), made of two protons and two neutrons, that are detected by a Geiger counter. Since radium has a 50/50 chance of disintegrating at its mid-life, the cat has a 50/50 chance of being alive and dead, at deadline. When opened, it is either alive or dead. As long as the door is not opened, the cat is said to be superposed in the alive and dead states and entangled with the radium atom state. This story has been repeated ad-nauseam since 1935. But his thought experiment was created to show the absurdity of the measurement postulate, the wave function collapse and Born's rule. Unfortunately, the contrary has been memorized.

The caveat is that a cat can't be superposed in two states because it is a macroscopic object of a size well beyond the quantum/classical limit. It's either alive or dead, never both. These are exclusive states. On top of that, the radium atom disintegration as well as the cat's death are both irreversible processes. They can't be implemented as linear superpositions of waves. When the cat is dead, he's not in a superposition. He's just plain dead.

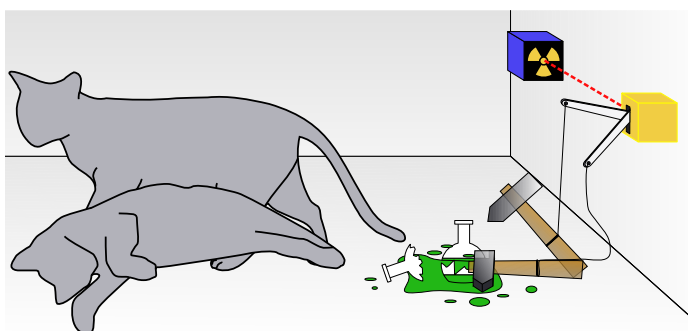


Figure 45: the infamous Schrodinger's cat thought experiment.

We can consider that the cat's death is provoked by a not yet read measurement when the box is closed, corresponding to a non-selective measurement as described page 190. The cat state uncertainty is a classical one, not a quantum one. The cat is in a maximally "mixed state" where the uncertainty of its death is classical, not in a "pure state" where it would be quantum (we define these notions starting page 150). If you used a webcam inside the box and made sure it didn't influence the radium half-life period, you could track the cat state all along, from alive to dead or alive to alive, which are the only two possible paths and observe the absence of superposition.

⁴⁷ The fine-structure constant was measured with a precision of 2.0×10^{-10} in 2020 using cold atoms interferometry. See [Determination of the fine-structure constant with an accuracy of 81 parts per trillion](#) by Léo Morel, 2020 (36 pages).

⁴⁸ The Cat Thought Experiment was published in a series of three papers in 1935, shortly after the publication of the EPR paradox paper by Einstein, Podolsky and Rosen. See [The Present Status of Quantum Mechanics](#) by Erwin Schrödinger, 1935 (26 pages). The history of the cat occupies only nine lines in this long document which deals with superposition, measurement and entanglement. That's even where Schrödinger coined the term entanglement in the first chapter "*The Lifting of Entanglement. The Result Depends on the Will of the Experimenter*". Schrödinger translated himself the German word Verschränkung into entanglement. The cat that appears only three times in all and for all is therefore anecdotal but that is what everyone has remembered. Which is quite normal: the rest is much less easy to apprehend!

This thought experiment was intended to highlight two things. First, that superposition and entanglement only applied to the infinitely small and not to macroscopic objects. History retained the principle of superposition and not this difference between the microscopic and macroscopic worlds. Second, that there was and still is an uncertain limit between the quantum and classical worlds. Schrodinger's thought experiment also dealt with the entanglement between the radium atom and the cat. Could this entanglement work with a macro-object⁴⁹? The paper containing this thought experiment was about entanglement and that was forgotten. Also, this paper's publication was the one generating the publication of the EPR paradox piece by Einstein et al. We should remember that Schrödinger's wave function and the notion of states superposition only make sense at a microscopic scale. Let's leave that poor cat alone in his dreams!



Max Born (1892-1970, German) is a physicist and mathematician who developed the mathematical representation of quantum in a matrix form. We owe him in 1926 the statistical explanation of the probability of finding an electron in a given energy state from its wave function, elaborated by Schrödinger the same year. This principle is applied to qubits, where the sum of the square of the probabilities of the two states of the qubit is equal to 1, given the probabilities are complex numbers.

In 1925, he created the non-commutativity relation of two conjugate quantities, one being the Fourier transform of the other (the commutator $[X,P]=XP-PX=i\hbar I$, where X is a position and P a momentum and I, the identity). It led to the indeterminacy principle creation. He also created the first version of the adiabatic theorem with Vladimir Fock in 1928. He got the Nobel prize in physics in 1954. Fun fact, the British singer Olivia Newton-John is his grand-daughter⁵⁰.



Werner Heisenberg (1901-1976, German) is a physicist, Nobel Prize in Physics in 1932, to whom we owe in 1927 the creation of the famous principle of uncertainty, or rather indeterminacy, according to which one cannot accurately measure both the position and the velocity of an elementary particle, or, more generally, two arbitrary unrelated quantities. He is at the origin, with Max Born and Pascual Jordan in 1925, of the quantum matrix formalism describing physical quantities.

The indeterminacy principle is a consequence of this formalism. It was described mathematically in a simplified manner in 1927 by **Earle Hesse Kennard** (1885-1968, American) in the famous equation in Figure 46, where the product of the standard deviation of position and velocity is greater than half the Dirac (or reduced Planck) constant.

$$\Delta x \Delta p \geq \frac{\hbar}{2}$$

Figure 46: Heisenberg-Kennard inequality, as formulated by Earle Hesse Kennard.

This principle can be used to improve the accuracy of a measurement of any quantity by lowering the accuracy of another quantity characterizing a quantum⁵¹. These quantities can be for example an energy level, a position, a wavelength, or a speed.

One consequence of Heisenberg's principle is that all particles in the Universe are in permanent motion. If they were stable, we would know their position (fixed) and their velocity (zero), violating the indeterminacy principle.

⁴⁹ You can apply this thought experiment to the baking of the half-cooked chocolate. As long as you don't take it out of the oven after the mandatory baking of 9 minutes, but with an oven with an unknown power, you don't know if it is well done or not, and run it through the middle before you take it out. It is in a state of superposition between undercooked, well done and overcooked. On the other hand, if it is overcooked, it will be difficult to go back, like Schrödinger's half-dead cat in case he died. Overcooking as well as the death of the cat are irreversible. It is therefore not a true superposition of quantum states. But here, I have no clue about how the oven and the half-baked chocolate are entangled. It's about statistical physics and thermodynamics, not quantum physics. Even through the oven is a black body! Cheers!

⁵⁰ See [Olivia Newton-John's grandfather Max Born was friend of Albert Einstein](#) by Matthew Alice, 1995.

⁵¹ This measurement technique is used in "quantum squeezing" which is integrated in the latest version of LIGO for the measurement of gravitational waves: [NIST Team Supersizes 'Quantum Squeezing' to Measure Ultra Small Motion](#), 2019.

Another consequence is that a perfect vacuum could not exist because the value and evolution of the magnetic and gravitational fields that pass through it would be stable, violating once again Heisenberg's indeterminacy. This explains the astonishing vacuum quantum fluctuations we discover a [little further](#) starting in page 134. The no-cloning theorem of a qubit state also derives from the principle of indeterminacy.

For some, this indeterminacy principle is a simplified interpretation of the corpuscular nature of matter. It leads to the question of the position and velocity of an electron, when it has no precise position. According to the Copenhagen interpretation of quantum mechanics, we shouldn't try to determine where the electron is located. Try to apply the concepts of classical mechanics to electrons is vain.

In practice, quantum particles are not classical physical particles and therefore their velocity and position cannot be measured. They can only be described by their (Schrödinger) wave function and position probabilities. More generally, in the infinitely small, the measurement device influences the measured quantity. One example illustrates this phenomenon at the macroscopic level: if you illuminate an insect with sunlight and a magnifying glass to better observe it, you may burn it! The same happens with a photon that is used to detect an electron, in the Heisenberg microscope thought experiment, as shown in Figure 47. It will change the speed and position of the electron.

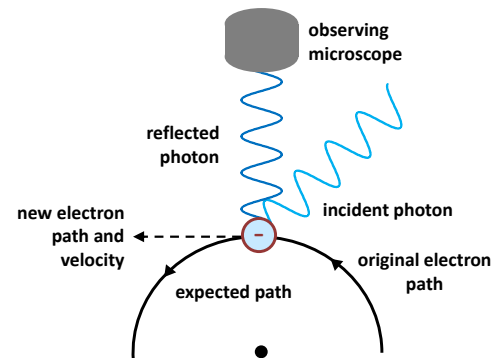


Figure 47: Heisenberg microscope thought experiment. [Source.](#)

Finally, like many of the colleagues of his time, Werner Heisenberg was interested in the links between science, quantum mechanics and philosophy, and as early as 1919. He was assistant to Niels Bohr between 1924 and 1927, before leaving for the University of Leipzig. He also had Max Born as a professor!

During World War II, he was asked with other German scientists to work on the Reich's atomic bomb project. Later revelations did show that he was not very active on this project and did not believe it was an achievable goal.



Paul Dirac (1902-1984, English) is a mathematician and physicist among the founders of 20th century quantum physics. He is credited with the 1928 electron spin equation, which is one of the foundations of relativistic quantum physics (*below*). His equation is a kind of variant of Schrödinger's equation for free relativistic particles, fermions (electrons, protons, neutrons, quarks, neutrinos) which are half-integer spin particles. Relativistic particles are those moving at a speed close to the speed of light, which contains electrons if lower shells of heavy atoms.

In Dirac's equation, the wave function of the electron ψ includes four components of complex numbers that integrate time and space. Dirac's equation enabled him to predict the existence of a particle that was later be called the positron, an opposite of the electron with a positive charge⁵².

$$\left(\beta mc^2 + c \sum_{n=1}^3 \alpha_n p_n \right) \psi(x, t) = i\hbar \frac{\partial \psi(x, t)}{\partial t}$$

Figure 48: Dirac's relativistic wave-function equation.

⁵² Positrons were discovered experimentally by Carl Anderson in 1932. He was awarded the Nobel Prize in Physics in 1936.

Dirac formalized the quantization of the free electromagnetic field in 1927. He also introduced in 1939 the bra-ket notation, known as Dirac's notation, which simplified the notation and manipulation of quantum states and operators in linear algebra (example: $\langle\phi|\psi\rangle$). The Dirac constant also named reduced Planck constant is the Planck constant h divided by 2π , also called "h-bar" for its italicized strikethrough h symbol: \hbar . This Dirac constant is used in the Schrödinger wave function.

Paul Dirac was awarded the Nobel Prize in Physics in 1933, at the age of 31. The Nobel Prizes of the early 20th century were frequently awarded to young scientists, which seems to be out of fashion since then! The youngest Nobel Prize in Physics was awarded to Lawrence Bragg, who won it at the age of 25 in 1915 for his discovery of X-ray refraction at the age of 22⁵³. In which case do we have to deal with relativistic particles, in particular with electrons? It is generally considered that an electron becomes relativistic when the total of its mass and kinetic energy is at least twice the rest mass. This ratio corresponds to the [Lorentz factor](#). It represents a speed of at least 86% of the speed of light. But relativistic phenomena may occur before that speed is reached. In Newtonian equivalent, the speed of an electron around the nucleus of a hydrogen atom is about $c/137$. With electrons from heavy atoms inner shells, this velocity can exceed $c/2$.

This is the case for electrons of the first layer of the gold atom, which move at 85% of the speed of light. This affects the position of relativistic electrons in the low orbits of heavy atoms such as lanthanides, which belong to the rare earths. The Bohr radius that defines the average orbital of an electron decreases inversely proportional to the apparent mass of the electron. Because the electron's apparent mass increases, this Bohr radius is smaller for relativistic electrons. This modifies the structure of the electron orbitals of heavy atoms and the transition energy levels between orbitals that absorb or emit photons.

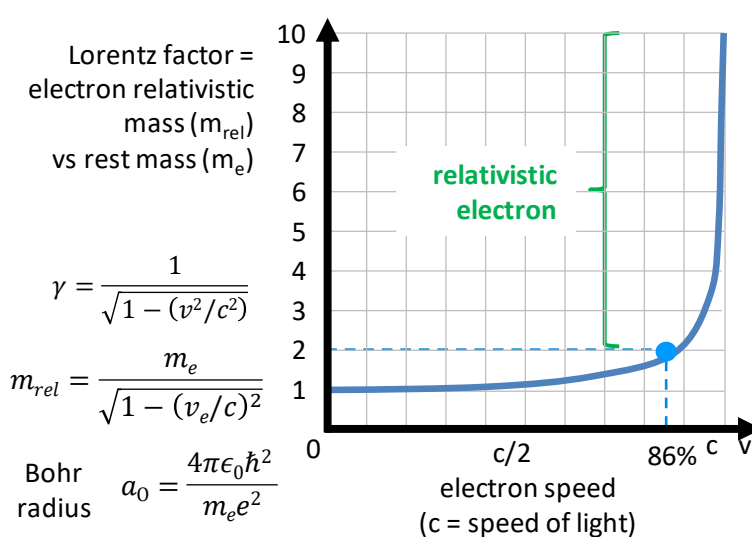


Figure 49: relativistic electrons and Lorentz factor.

This explains the color of gold and silver, due to relativistic modification of orbits of electron layers between which transitions occur due to the absorption of photons. Blue is absorbed in the case of gold, explaining its yellow color. Without the relativistic effect, gold would be white. This has a lot of implications in the chemistry of these materials and with their crystal organization⁵⁴. This quantum relativistic effect also explains why mercury is liquid at room temperature⁵⁵. All this gives rise to a field of chemistry called relativistic quantum chemistry⁵⁶.

⁵³ Paul Dirac was distinguished by his shyness and parsimonious oral expression in meetings or during meals. So much so that his Cambridge colleagues had defined the "dirac" unit as the most concise way to express himself in a meeting, namely, at the rate of a single word per hour. His behavior was equivalent at the Solvay Congresses he attended, notably that of 1927. However, he must have broken a record in his [speech](#) accepting his Nobel Prize at the end of 1933. It is still six pages long! Half, however, of the 12 pages of the speech of Erwin Schrödinger, also winner of the Nobel Prize in Physics that year. Another anecdote: Dirac was married to one of the sisters of Eugene Wigner, Nobel prize in physics in 1963 and famous for his function and also his "friend" paradox.

⁵⁴ See more examples in [Relativistic Effects in Chemistry More Common Than You Thought](#) by Pekka Pyykko, 2012 (24 pages).

⁵⁵ See [Why is mercury liquid? Or, why do relativistic effects not get into chemistry textbooks?](#) by Lars J. Norrby, 2018 (4 pages).

⁵⁶ See [Relativistic quantum chemistry](#) by Trond Saue, 2019 (110 slides) and [An introduction to Relativistic Quantum Chemistry](#) by Lucas Visscher (107 slides). The mathematical formalism of relativistic quantum chemistry is well documented in the voluminous [Introduction to Relativistic Quantum Chemistry](#) by Kenneth Dyall and Knut Faegri, 2007 (545 pages).

It also explains why the size of atoms is not proportional to their number of protons and electrons⁵⁷.

Particles also become relativistic in **particle accelerators** such as the CERN LHC near Geneva (the largest in the world), the ESRF in Grenoble (European Synchrotron Radiation Facility, specialized in the generation of "hard", very high-frequency X-rays) or the SOLEIL light synchrotron located in Saint-Aubin near Saclay just next to the CEA, also in France, or its equivalent from PSI in Switzerland.

The SOLEIL synchrotron uses electrons accelerated to a relativistic speed and inverters that generate beams of light 10,000 times denser than sunlight⁵⁸. Equivalent instruments exist such as the Advanced Photon Source at the Argonne National Laboratory from the US Department of Energy near Chicago.

Free Electron Lasers (FEL) exploit relativistic electron sources. These are lasers generating coherent light (spatially and temporally, the emitted photons have the same frequency, phase and in that case, also polarization) and exploit relativistic electron sources from synchrotrons. The interaction between these electrons and a strong alternating magnetic field makes it possible to generate coherent light in electromagnetic frequency ranges from infrared to X-rays, through visible light and ultraviolet. The FEL are used to explore all sorts of matter, particularly in biomedical research like with X-rays crystallography.

Finally, relativistic particles can be found in **astrophysics** and, for example, in cosmic ray sources as well as in relativistic plasma jets produced at the center of galaxies and quasars⁵⁹.

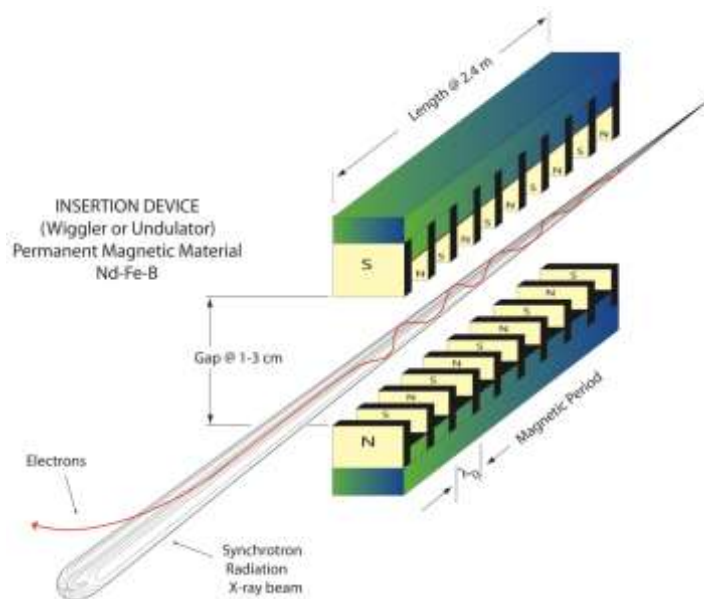


Figure 50: free-electron laser. Source: [X-ray diffraction: the basics](#) by Alan Goldman (31 slides).



Vladimir Fock (1898-1974, Russian) was a theoretician physicist who worked on quantum physics, the theory of gravitation and theoretical optics. We own him the Fock space, representation and state, used in quantum photonics to represent the state of bosons many-body systems having the same quantum state. He co-created the Klein-Gordon equation in 1926, the relativist version of Schrödinger's equation for zero spin massive particles, the adiabatic theorem with Max Born in 1928 and the Hartree–Fock quantum simulation method in 1930. He also worked on quantum electrodynamics and quantum foundations.

⁵⁷ See this [periodic table of elements](#) with an indication of the sizes of the atoms.

⁵⁸ See the conference [Electrons relativists as light sources](#) by Marie-Emmanuelle Couprie, Synchrotron Soleil, 2011 (1h25). Electrons circulate in the synchrotron at a speed close to that of light. SOLEIL powers more than 25 analytical instruments covering the spectrum from infrared to X-rays, with numerous applications in precision microscopy, including a microscopy using very well collimated and polarized white light. These instruments can be used to analyze the three-dimensional structure of organic molecules such as complex proteins, such as the glycoproteins that surround viruses. This even allows one to study how these proteins combine with those of the attacked cells, or ribosomes, which are used to produce the proteins in the cells, are also analyzed.

⁵⁹ Dirac's equation is linked to the **Klein-Gordon equation** (1926) which applies to bosons such as elementary gluon particles and pions, particles having integer or zero spin. Relativistic quantum mechanics is a broad field of physics, used in particular in elementary particles physics. I have not yet found any use cases of this branch of physics in current quantum technologies. See the main foundations of relativistic quantum mechanics in [Relativistic Quantum Mechanics](#) by David J. Miller, University of Glasgow, 2008 (116 slides).



Pascual Jordan (1902-1980, German) was a physicist who collaborated with Max Born and Werner Heisenberg and contributed to laying the mathematical foundations of quantum mechanics, especially in matrix computation. Like Philipp Lenard, he was somewhat forgotten because of his membership in the Nazi Party during the 1930s, although he was rehabilitated after the Second World War thanks to the help of Wolfgang Pauli. He became interested in the philosophical notion of free will.



Linus Pauling (1901-1994, American) was a biochemist known to have co-founded the scientific fields of quantum chemistry and molecular biology. He had the opportunity to meet in Europe the founders of quantum physics like Erwin Schrödinger and Niels Bohr in 1926-1927. He described chemical bonds over a period between 1928 and 1932 and in particular the hybridization of orbitals which explains the geometry of molecules. He published "The Nature of the Chemical Bond" in 1939.

He was awarded the Nobel Prize in Chemistry in 1954 and the Nobel Peace Prize in 1962 for his political activism in favor of nuclear disarmament. He is considered to be at the origin of computational chemistry, which makes it possible to numerically simulate the structure of molecules and which we discuss in the section on quantum applications in health on page 707.



James Chadwick (1891-1974) is an English physicist who was responsible for the discovery of neutrons in 1932, which earned him the Nobel Prize in Physics in 1935. This discovery was late compared to quantum physics and the discovery of electrons. Nuclear physics has indeed progressed in parallel with quantum physics, which was mainly concerned with the interactions between electrons and photons. Before the discovery of neutrons, scientists thought that the nucleus of atoms contained protons and electrons.



John Von Neumann (1903-1957, Hungarian, then American) was a polymath and an extremely prolific mathematician. He participated in the creation of the mathematical foundations of quantum mechanics, notably in the "Mathematical Foundations of Quantum Mechanics" published in 1932. He transposed the main principles of quantum mechanics into models and equations of linear algebra. He devised the key mathematical principles behind quantum measurement models.

This deals, for example, with the representation of quantum states as a position in a Hilbert space, the observables which are projections into Hilbert spaces and the indeterminacy principle which can be explained by the non-commutativity of measurement operators. These principles are also named Birkhoff-von Neumann *quantum logic*, in connection with their seminal paper published in 1936⁶⁰.

Von Neumann also affirmed that the introduction of hidden variables to incorporate determinism was a lost cause because it would contradict other (verified) predictions of quantum physics. Three years before Einstein/Podolsky/Rosen's EPR paper!

We owe him the creation of the notion of entropy (by Von Neumann), in 1932, which is associated with the notions of operators and density matrices that he created in 1927 and which describe the state of a multi-partite quantum system. He participated in the Manhattan Project in the USA.

⁶⁰ See [The Logic of Quantum Mechanics](#) by Garrett Birkhoff and John Von Neumann, 1936 (22 pages).

PRINCETON (VON NEUMAN) ARCHITECTURE

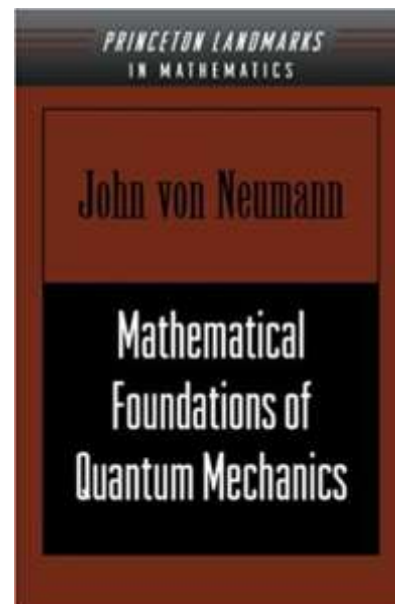
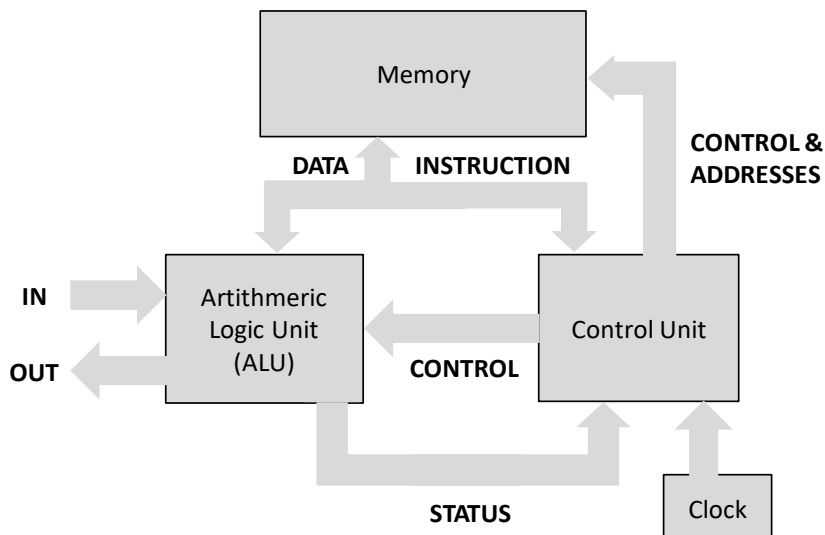


Figure 51: the Von Neuman Princeton architecture which still defines classical computing.

He modelled explosions and lenses for compressing plutonium in A-bombs. He is also responsible for the basic concepts in game theory and classical computers that are still in use. Thus, almost all computers use a Von Neumann architecture with memory, registers, control unit, computing unit, inputs and outputs. What a contribution!



Boris Podolsky (1896-1966, Russian then American) wrote the EPR paradox paper with Albert Einstein and Nathan Rosen in 1935 on quantum entanglement and questions of non-locality of the properties of entangled quanta. He was a specialist in electrodynamics which deals with the analysis of electric and electromagnetic fields. He emigrated to the USA and, according to Russian archives, was a post-war KGB spy and informer of the USSR on the American atomic program between 1942-1943. His code name was... "Quantum".



Nathan Rosen (1909-1995, American then Israeli) is the third EPR paradox author when working as an assistant to Albert Einstein in Princeton. After moving to Israel in 1953, he created the Institute of Physics at Technion University in Haifa. He was mainly working on astrophysics and relativity theory. He devised the concept of wormholes, a theoretical link between different points in space and time. He also thought neutrons were built out of a proton coupled to an electron.



Ettore Majorana (1906-circa 1938, Italian) imagined the existence of a fermion in 1937 based on Dirac's equations, an elementary particle that would be its own anti-particle. The Majorana fermion naming is also abusively applied in condensed matter physics to quasi-particles having similar properties. Their existence was discovered in 2012 and verified in 2016 and then in 2018, even if it is still disputed by many physicists and two related 2018 papers had to be retracted in 2021.

These Majorana quasi-particles (or "Majorana Zero Modes") could make it possible to design universal quantum computers called topological computers that can handle very efficient error correction codes requiring a small number of physical qubits. This is the exploration path chosen by Microsoft after the work of Michael Freedman and Alexei Kitaev in the late 1990s. Ettore Majorana is said to have committed suicide after a depression, because he could hardly stand the pressure of his genius! But his disappearance remains enigmatic because his body has never been found!



Alonzo Church (1903-1995, American) was a mathematician who was a key contributor to the foundations of theoretical computer science and on the notion of computability. Among other things, he created the lambda calculus in 1936, a universal abstract programming language which inspired the creation of LISP. He also created the so-called Church-Turing thesis. For this last one, any automatic calculation can be carried out with a Turing machine. Church and Turing also proved an equivalence between being λ -computable and Turing computable.

Many variations of the Church-Turing thesis were elaborated after them to extend the broad field of complexity theories. For example, the extended Church-Turing thesis states that the computation time of a problem is equivalent at worst to a polynomial depending on the size of the problem. It is not demonstrable.

What about the others, known, unknown or less famous from the 1927 Solvay Congress? Two participants deserve to be mentioned who had some connections with quantum physics.



Léon Brillouin (1889-1969, Franco-American) who is less known in France because of his expatriation to the USA during World War II contributed to advances in quantum physics between the two World Wars. In particular, he brought quantum mechanics closer to crystallography. He especially discovered the phenomena of diffraction of waves traversing crystals, called Brillouin scattering.

And then, finally, **Hendrik Anthony Kramers** (1894-1952, Dutch) who assisted Niels Bohr in the creation of quantum theory. Many of the participants were not quantum physics scientists. They were invited because the Belgium organizers tried to have a stable proportion of Belgians, French, Germans and English participants. Were there, for example, **Émile Henriot** and **Marie Curie** who were focused on radioactivity, **Paul Langevin** (with whom Marie Curie had had an affair in 1910, after the accidental death of her husband Pierre Curie in 1906), as well as a good number of chemists.

What was striking during this prolific period were the way the social network of physicists worked, without smartphones and the Internet. They had many encounters, cross-University tenures, meetings, letter exchanges and conferences. It was slow according to today's references, but the results were still astounding.

At last, here's a simple chart reminding us how young the founders of quantum physics were when they published their seminal work in the key years from 1900 to 1935. Back then, scientific research didn't work the same way. They also were frequently awarded Nobel prizes at less than 40! Nowadays, most of the times, you have to wait until you are at least 50 if not 70.

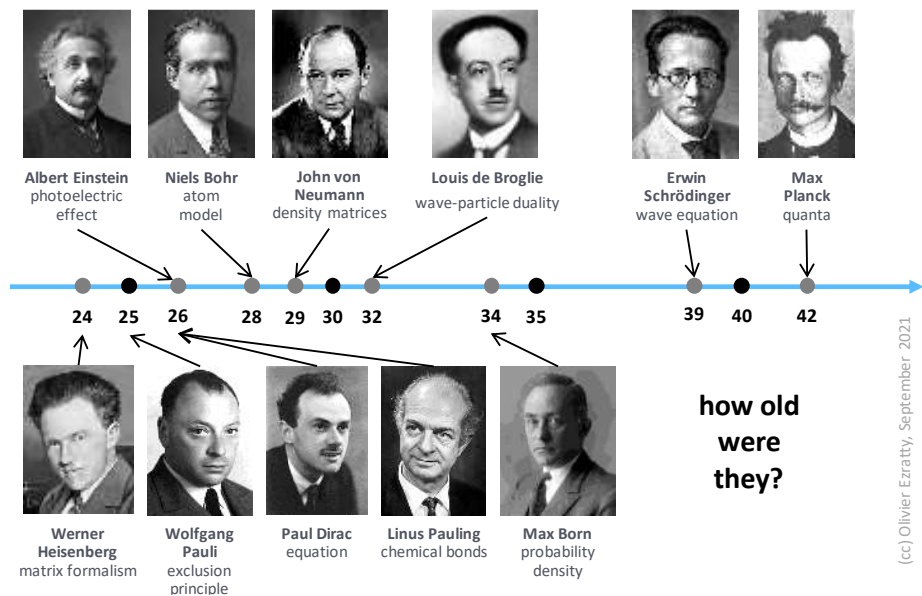


Figure 52: how old were quantum scientists when they were awarded the Nobel prize in physics? (cc) Olivier Ezratty, 2021.

Post-war

As mentioned before, quantum physics developments seemed to slow down between 1935 and 1960. Physicists were then busy with nuclear physics. The Manhattan project mobilized an amazingly large number of physicists like John Von Neumann and **Enrico Fermi** (1901-1954, Italian American, Nobel prize in physics in 1938) whose contributions were centered in nuclear physics and statistical physics, leading to the Fermi-Dirac ideal gas statistics.

Quantum physics still led, after World War II, to an incredible wealth of technologies that revolutionized the world. We can mention three important branches resulting from the applications of the first quantum revolution: **transistors**, invented in 1947 by William Shockley, John Bardeen and Walter Brattain from the Bell Labs⁶¹, **masers** and **lasers** invented between 1953 and 1960 by Gordon Gould, Theodore Maiman, Nikolay Basov, Alexander Prokhorov, Charles Hard Townes and Arthur Leonard Schawlow, only a few of whom received the Nobel Prize associated with these discoveries, **photo-voltaic cells** that convert light into electricity, and the **GPS**. Transistors and lasers are the basis of much of today's digital technology. All our digital devices are already quantum! The field of quantum optics started in the early 1960s with the laser invention and Roy J. Glauber's work, with his seminal work in 1963 on light classification where he formalized the coherent states generated by lasers, *aka* Glauber states.

The post-war period was also dominated in quantum physics by advances made on superconductivity with the BCS theory in 1957 and the Josephson junction in 1962, and by the theoretical work of John Stewart Bell in 1964.

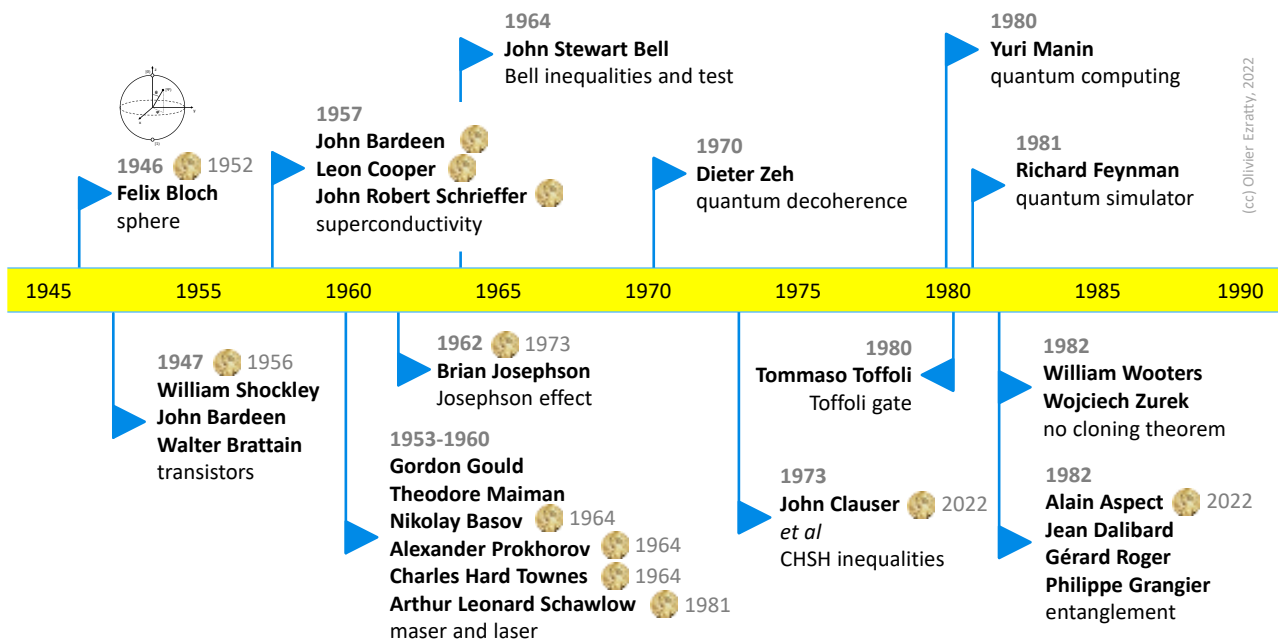


Figure 53: timeline of key events in quantum physics after World-War II. (cc) Olivier Ezratty, 2022.

⁶¹ Transistors are based on many quantum phenomena, particularly the electronic structure of atoms in semiconductor crystals that was discovered during the 1930s and creates forbidden energy levels named band gaps (found by Sir Alan Herries Wilson, UK, in 1931), the impact of defects in crystals leading to doping and the tunneling effect due to the wave-particle duality of electrons. It also uses the field effect, which modulates the electrical conductivity of a material by the application of an external electric field. It was invented by Julius Edgar Lilienfeld (1882-1963, Austro-Hungarian and American) who got a related patent granted in 1926 using copper-sulfide semiconductor materials. It corresponds to what we today call a "Field Effect Transistor" (FET). The first transistor invented in 1947 was made of germanium, not silicon. See [The Transistor, an Emerging Invention: Bell Labs as a Systems Integrator Rather Than a 'House of Magic'](#) by Florian Metzler, October 2020 (57 pages) which shows the flow of discoveries that led to the creation of the first transistor by the Bell labs in 1947. This first computers using transistors was the TRADIC Phase One computer that was built in 1954.

We then have the verification of entanglement by Alain Aspect's experiment in 1982. 1980 and 1981 are other key dates which mark the symbolic beginnings of quantum computing, imagined by Yuri Manin (gate-based quantum computing) and Richard Feynman (quantum simulation).

The term **second quantum revolution** covers advances from the 1990s and later, when the quantum properties of individual particles could be controlled at the level of photons (polarization, ...), electrons (spin) and atoms or ions, as well as superposition and entanglement. This led to the emergence of quantum cryptography and quantum telecommunications, in addition to the premises of quantum computing. The original definition of this second quantum revolution is however not as precise as that ⁶².



Felix Bloch (1905-1983, Swiss then American) is a physicist who created the geometrical representation of a qubit state in a sphere, Bloch's sphere was elaborated in 1946 in a paper on nuclear magnetism, his main specialty. Like other physicists of his time, he contributed to the Manhattan Project, although quite shortly. He was awarded the Nobel Prize in Physics in 1952 for his work on nuclear magnetic resonance and magnons conceptualization. He was also the first director of the international particle physics laboratory CERN in 1954.

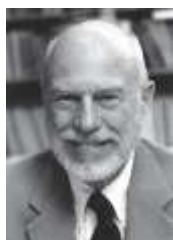


Chien-Shiung Wu (1912-1997, Chinese then American) was a scientist who contributed to the development of nuclear physics and to the Manhattan Project, with her gaseous diffusion process used for separating uranium 238 from uranium 235. She also contributed to the development of quantum physics by conducting the first experiment related to the synchronization of photon pairs and entanglement in 1949, before Alain Aspect's experiment in 1982⁶³.

This experiment was different and was based on the measurement of the angular correlation of gamma ray photons (with very high-frequency and high-energy) generated by the encounter of electrons and positrons.



Hugh Everett (1930-1982, American) is a physicist who created the formulation of relative states and a global wave function of the Universe integrating observations, observers and tools for observing quantum phenomena. He met Niels Bohr with other physicists in Copenhagen in 1959 to present his theory. He was politely listened to, but his interlocutors said that he understood nothing about quantum physics.



Everett was also a contributor to the connections between the theory of relativity and quantum physics, especially around quantum gravitation. He is credited with the hypothesis of multiple or multiverse worlds, or many-worlds interpretation, explaining quantum entanglement and non-locality. It is in fact coming from **Bryce DeWitt** (1922-2004, American) who interpreted his work in 1970. DeWitt also worked on the formulation of quantum gravity theories.

⁶² The second quantum revolution expression was created simultaneously and independently in 2003 by Alain Aspect and by Jonathan Dowling and Gerard Milburn. The latter is also known to be one of the three protagonists of the KLM model of photon-based quantum computing, created in 2001 jointly with Emanuel Knill and Raymond Laflamme.

⁶³ See [The Angular Correlation of Scattered Annihilation Radiation](#), Wu and Shaknov, 1949.



John Wheeler (1911-2008, American) supervised Hugh Everett's thesis. He was a specialist in quantum gravitation. He worked in the field of nuclear physics, notably in the Manhattan project, on the first American H-bombs and on very high-density nuclear matter found in neutron stars. He popularized the term black hole in 1967. He imagined a delayed-choice experiment to decide when a quantum object decides to travel as a wave or as a particle.

He collaborated with Niels Bohr and among his PhD students were Richard Feynman and Wojciech Zurek!



Roy J. Glauber (1925-2018, USA) was a theoretical physicist, teaching at Harvard and at the University of Arizona. He got the Nobel Prize in Physics in 2005 for his foundational work on the quantum theory of optical coherence. He is considered to a father of non-classical light description and of the quantum optics field, with his work in 1963, describing the various types of light (coherent, not coherent, ...). He also worked in the field of high-energy particle physics, which we don't cover in this book since out of scope of the "second quantum revolution".



Philip W. Anderson (1923-2020, USA) was a theoretical physicist who contributed to the theories of localization (*aka* "Anderson localization" according to which extended states can be localized by the presence of disorder in a system), antiferromagnetism and quantum spin liquid, symmetry breaking leading to the creation of the Standard Model, superconductivity (at high-temperature, pseudospin approach to the BCS theory, Anderson's theorem on impurity scattering in superconductors).

He created the "condensed matter physics" naming. He got the Nobel prize in physics in 1977 for his work on the electronic structure of magnetic and disordered systems. He worked at the Bell Labs and was also a teacher at Cambridge University, UK.



John Stewart Bell (1928-1990, Irish) relaunched research in quantum mechanics in the 1960s on the notion of entanglement. We owe him the [Bell inequalities](#) that highlight the paradoxes raised by quantum entanglement. Bell's 1964 theorem indicates that no theory of local hidden variables - imagined by Einstein in 1935 - can reproduce the phenomena of quantum mechanics⁶⁴. He was rather pro-Einsteinian in his approach and favorable to a realistic interpretation of quantum physics⁶⁵.

His Bell inequalities define the means to verify or invalidate the hypothesis of the existence of hidden variables explaining quantum entanglement. Bell's inequalities were violated by the experiments of **Alain Aspect** in 1982, demonstrating the inexistence of these local hidden variables.

Prior to this experiment, Bell's inequalities had been formulated for pairs of entangled photons by **John Clauser** (1942, American, 2022 Nobel prize in physics), **Michael Horne** (1943-2019, American), **Abner Shimony** (1928-2015, American) and **Richard Holt** in 1969 with their so-called CHSH inequalities with some experimental settings proposals⁶⁶.

⁶⁴ See this explanation of Bell's theorem in a paper by Tim Maudlin on the occasion of the 50th anniversary of the theorem: [What Bell Did](#), 2014 (28 pages). And Bell's original document: [On the Einstein-Podolsky-Rosen paradox](#), John S. Bell, 1964 (6 pages). In 1964, Bell worked at the University of Wisconsin.

⁶⁵ See [What Bell Did](#) by Tim Maudlin, 2014 (28 pages) which describes the EPR paradox and Bell's contribution.

⁶⁶ See [Proposed experiment to test local hidden-variable theories](#), 1969 (5 pages).

John Bell's work was completed in 2003 by **Anthony Leggett** (1938, Anglo-American, Nobel Prize in Physics in 2003 for his work on superfluid helium) with his inequalities applicable to hypothetical non-local hidden variables⁶⁷. Anthony Leggett was also an initial key contributor to what led to the creation of superconducting qubits.

Anton Zeilinger (1945, Austrian) managed to experimentally violate these inequalities in 2007. According to Alain Aspect, however, this did not call into question the non-local hidden variable model proposed by David Bohm.



Claude Cohen-Tannoudji (1933, French) is a former student of Ecole Normale Supérieure (ENS Paris) where he followed the teachings of mathematicians Henri Cartan and Laurent Schwartz and physicist Alfred Kastler. He was awarded the Nobel Prize in Physics in 1997 at the same time as Steven Chu, who was later Secretary of Energy during Barack Obama's first term. This Department (DoE, Department of Energy) is one of the federal agencies most invested in quantum technologies, notably because they operate the largest supercomputers in the country.

Claude Cohen-Tannoudji owes his Nobel Prize to his work on atoms laser cooling which made it possible to reach extremely low temperatures, below the milli-Kelvin⁶⁸. Alain Aspect once worked in his team. Alain Aspect says that he discovered quantum physics with reading the reference book on quantum physics by Claude Cohen-Tannoudji, Bernard Diu and Franck Lalœ published in 1973⁶⁹. It totals over 2300 pages. So, this book is quite small in comparison. And also, more accessible!



Serge Haroche (1944, French), Nobel Prize in Physics in 2012, is a founder of Cavity Electrodynamics (CQED) which describes the interaction between photons and atoms in cavities. He used it to create cold atom based qubits. **Jean-Michel Raimond**⁷⁰ and **Michel Brune** were among his key collaborators. Serge Haroche was the first to measure the phenomenon of quantum decoherence (loss of superposition) in an experiment in 1996. This experiment was conducted at the ENS with rubidium atoms. Serge Haroche is also a member of Atos Scientific Council.

CQED was later applied in the field of superconducting qubits with Circuit Electrodynamics (cQED), where atoms are replaced by an artificial atom made with a Josephson junction and the cavity by a planar microwave resonator. Serge Haroche is one of the most circumspect scientists on the future of quantum computing, at least for universal gate computing. He believes more in the advent of quantum simulation⁷¹.

Other scientists brought key contributions in atoms science. **Daniel Kleppner** (1932, American) was the first to create a Bose-Einstein condensate with Rubidium atoms in 1995, and then in 1998 with hydrogen. **Herbert Walther** (1935-2006, German) did pioneering work in cavity quantum electrodynamics and also with trapped ions. He created the Max Planck Institute of Quantum Optics in 1981. **Gerhard Rempe** (1956, German) developed cavity quantum electrodynamics with the control of neutral atoms using microwaves, in connection with **Jeff Kimble** (1949, American, Caltech).

⁶⁷ See [Nonlocal Hidden-Variable Theories and Quantum Mechanics: An Incompatibility Theorem](#) by Anthony Leggett, 2003 (25 pages).

⁶⁸ See his [Nobel lecture](#).

⁶⁹ This book is published in three tomes that were last revised in 2019. The first one is [Quantum Mechanics, Volume 1: Basic Concepts, Tools, and Applications](#). The second deals with [Angular Momentum, Spin, and Approximation Methods](#) and the third one with [Fermions, Bosons, Photons, Correlations, and Entanglement](#). These are classical quantum physics student textbooks.

⁷⁰ See his interesting conference [Quantum Computing or how to use the strangeness of the microscopic world](#), Jean-Michel Raimond, 2015 (1h36mn). See also his [presentation material](#) (56 slides).

⁷¹ See [Quantum Computing: Dream or Nightmare?](#) by Serge Haroche and Jean-Michel Raimond, Physics Today, 1996 (2 pages) who expressed their skepticism about quantum computing. Serge Haroche continues to convey this skepticism.



Alain Aspect (1947, French, 2022 Nobel prize in physics) observed violations of Bell's inequalities with a series of experiments conducted between 1980 and 1982 at the Institut d'Optique (Orsay University in the southern suburb of Paris with Jean Dalibard, Philippe Grangier and Gérard Roger. Taking the principles of quantum physics for granted, it validated the non-locality of quantum properties and “spooky action at a distance”⁷². One other option is you need to reject these principles and use a local variable model to explain the phenomenon. But it is not the only one⁷³.

The experiment avoided any potential synchronization between the polarizers, using a 50 MHz random optical switch on both sides, feeding two orthogonal polarizers and photon detectors. From 1988 to 2015, other experiments were conducted elsewhere and implemented loophole-free Bell tests, first closing individual loopholes and then, in 2015, closing them altogether. It confirmed then that there were no local variables explaining entanglement and validated the non-locality condition: long distance between analyzers to avoid any interactions made possible by special relativity.

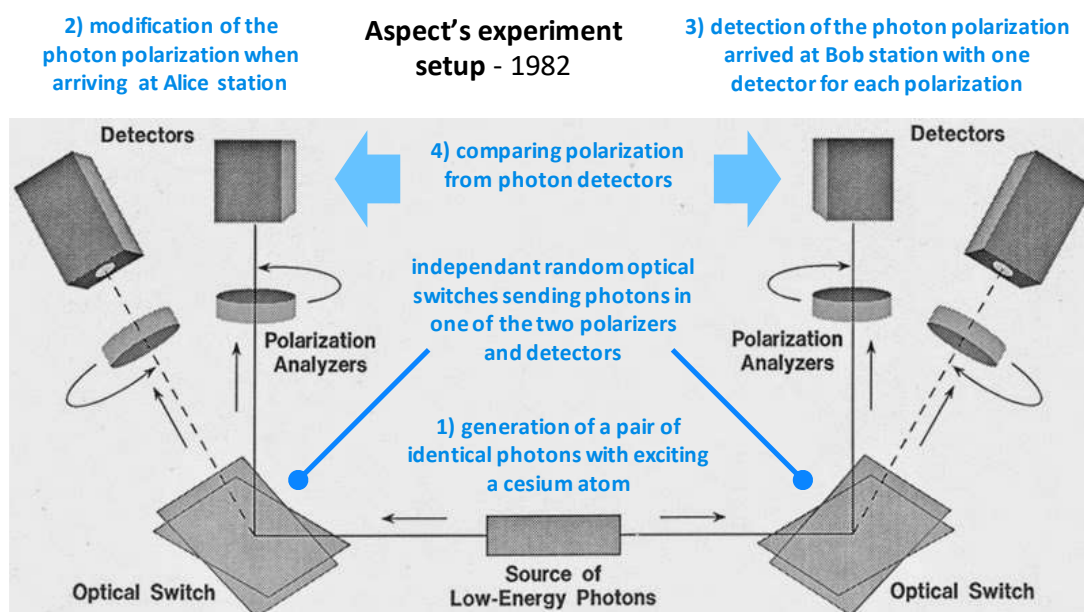


Figure 54: Alain Aspect et al 1982 Bell inequality test experiment setup.

It avoided detection loopholes with high-efficiency photon detectors on top of escaping ‘memory loopholes’, which was already obtained by Alain Aspect et al in their seminal 1982 experiment⁷⁴. After his work on photon entanglement, Alain Aspect shifted gear on cold atoms control with lasers, starting with helium.

⁷² Alain Aspect’s experiments were using calcium atoms as source of photons, using some laser excitement and an atomic cascade generating pairs of entangled photons in the visible spectrum at 551 nm and 423 nm. There were actually several experiments: in 1981 with Philippe Grangier and Gérard Roger with one way polarizers, 1982 also with Grangier and Roger with two-channels polarizers and also 1982, with Jean Dalibard and Gérard Roger, using variable polarizers based on acousto-optical 10 ns switches. These could act faster than light propagation between the polarizers (40 ns) and even than the photons time of flight between the source and each switch (20 ns). See [Experimental Test of Bell's Inequalities Using Time-Varying Analyzers](#) by Alain Aspect, Gérard Roger and Jean Dalibard, PRL, December 1982 (4 pages).

⁷³ You have superdeterminism-based theories promoted by Carl H. Brans, Sabine Hossenfelder and Tim Palmer that are based on the hypothesis of superdeterministic hidden variables theory and could still violate Bell’s inequalities, but also the CSM ontology which pertains that the Psi function is lacking information on the measurement context, like described in [Why \$\psi\$ is incomplete indeed: a simple illustration](#) by Philippe Grangier, October 2022 (2 pages).

⁷⁴ See [Experimental loophole-free violation of a Bell inequality using entangled electron spins separated by 1.3 km](#) by B. Hensen et al, ICFO and ICREA in Spain and Oxford, UK, August 2015 (8 pages) and also [A strong loophole-free test of local realism](#) by Lynden K. Shalm et al, September 2016 (9 pages).

This led to the creation of a promising field of quantum computing in France, using cold atoms, embodied by the startup **Pasqal**, whose scientific director is Antoine Browaeys, a former PhD student of Alain Aspect who also worked with Philippe Grangier.

Along with other scientists, Alain Aspect is also a member of Atos Scientific Council and in the scientific board of **Quandela**. He teaches quantum physics, notably in MOOCs created for Ecole Polytechnique and distributed by Coursera.



Philippe Grangier (1957, French) was a PhD student of Alain Aspect with whom he worked on the 1982 experiment with Gérard Roger and Jean Dalibard. He is one of the world's leading specialists in quantum cryptography, especially on CV-QKD. He was involved in the creation of the associated startup, Sequrnet, in 2008 and closed in 2017, probably created a little too early in relation to the needs of the market. He is also invested in cold atoms control with lasers at IOGS (Institut d'Optique).

At last, he cocreated the CSM ontology of quantum foundations with Alexia Auffèves and Nayla Farouki, starting in 2013 and with a series of 7 foundational papers published between 2015 and 2019. CSM ontology is quickly covered in the [Quantum Foundations section](#).



Jean Dalibard (1958, French) is a research physicist at the ENS and teacher at the Polytechnique and the Collège de France. He is a specialist in quantum optics and interactions between photons and matter⁷⁵. He participated with Philippe Grangier in the set-up of Alain Aspect's experiment in 1982 when he was a contingent scientist at the Institut d'Optique. He created the magneto-optical trap (MOT) system in 1987 that is used to cool neutral atoms using a mix of variable magnetic fields and lasers.



Dieter Zeh (1932-2018, German) is the discoverer of the quantum decoherence phenomenon in 1970. It marks the progressive end of the phenomenon of superposition of quantum states, when particles are disturbed by their environment and their amplitude and phase is modified. The notion of decoherence is key in the design of quantum computers. The objective is to delay it as much as possible resulting from the interaction between quanta and their environment⁷⁶.



Wojciech Zurek (1951, Polish) is a quantum decoherence physicist who contributed to the foundations of quantum physics applied to quantum computers. We owe him the no-cloning theorem, which states that it is impossible to clone a qubit identically without the resulting qubits then being entangled. He is also at the origin of the concept of quantum Darwinism which would explain the link between the quantum world and the macrophysical world.



Maciej Lewenstein (1955, Polish) is a theoretical physicist, specialized in quantum optics of dielectric media and cavity quantum electrodynamics, teaching at ICFO in Spain. He worked with many leading worldwide scientists including Roy J. Glauber (Nobel in Physics in 2005) at Harvard, Thomas W. Mossberg, Andrzej Nowak, Bibb Latané, Anne L'Huillier (CEA, France), Peter Zoller and Eric Allin Cornell (Nobel in Physics in 2001 for his work on Bose-Einstein condensates in 1995), in the USA, France, Spain, Poland and Germany.

⁷⁵ See in particular his lesson on [cold atoms at the Collège de France](#) which describes well how atoms are cooled at very low temperatures with lasers.

⁷⁶ Dieter Zeh is notably the author of [On the Interpretation of Measurement in Quantum Theory](#) in 1970 (8 pages).

His contributions span an incredible number of fields like the physics of ultra-cold gases, quantum information, quantum optical systems, quantum communications, quantum cryptography, quantum computers, mathematical foundations of quantum physics, tensor networks and entanglement theory, laser-matter interactions atto-second physics, quantum optics (cQED), atoms cooling and trapping, non-classical states of light and matter and quantum physics foundations.



Anton Zeilinger (1945, Austrian, 2022 Nobel prize in physics) is a physicist who advanced the field of quantum teleportation in the 2000s. He also proved in 1991 the wave-particle duality of neutrons. He was also the first to experiment a qubit teleportation in 2009. He is a specialist in quantum entanglement, having proved that it is possible to entangle more than two quantum objects or qubits. He created theoretical and experimental foundations for quantum cryptography.

With two colleagues, he also developed the GHZ (Greenberger-Horne-Zeilinger) entangled state, which enables yet another demonstration of the inexistence of hidden variables which would explain quantum entanglement of at least three particles and with a finite number of measurements. The concept was created in 1989 and was validated experimentally in 1999. Anton Zeilinger also supervised the thesis of **Jian-Wei Pan**, who became later the quantum research czar in China with the development of many advances, particularly in quantum communications and photonics.



Frank Wilczek (1951, American) is a professor of physics at MIT and the chief scientist at the Wilczek Quantum Center in Shanghai. He was awarded in 2004 the Nobel Prize for Physics shared with David Gross and H. David Politzer, for his work on the theory of strong interaction and quantum chromodynamics. He is known for his work on quasi-particles and anyons in 1982 and he also predicted the existence of time crystals in 2012.

Quantum technologies physicists

This story now provides an overview of key contributors to the physics of quantum computing. They are often specialized in condensed matter, such as for superconducting qubits, and in photonics.

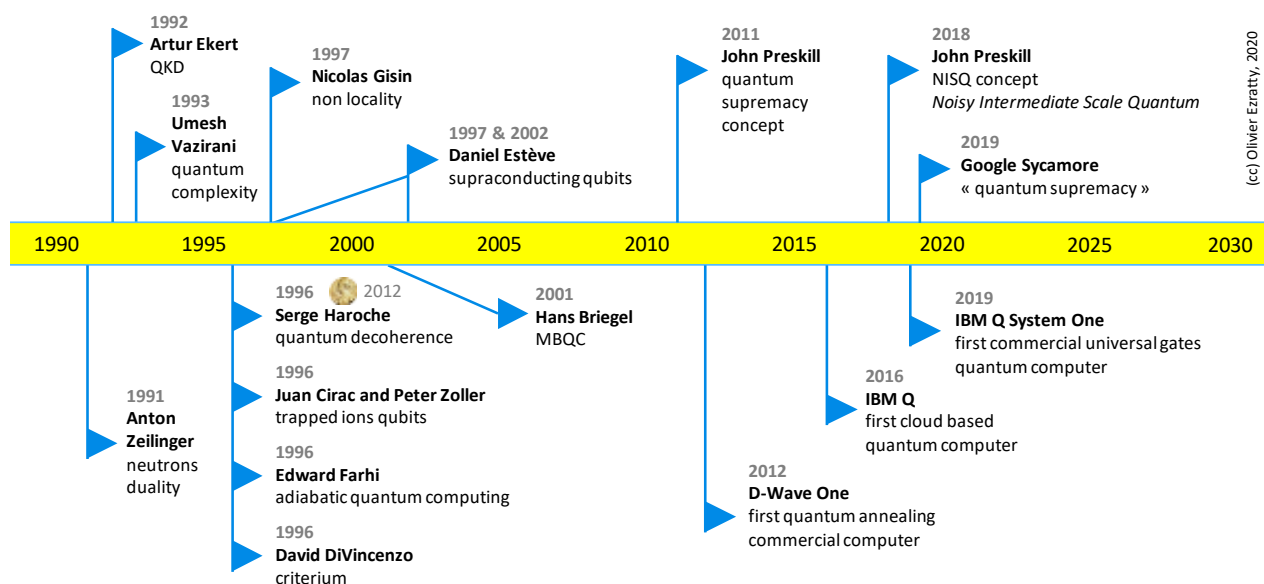


Figure 55: quantum computing key events timeline from 1990 to 2020. (cc) Olivier Ezratty, 2020.

I highlight many European and French physicists, particularly those I have had the opportunity to meet for the last three years in my journey in the quantum ecosystem. This inventory is both objective and subjective.

Objective because it includes a broad and worldwide hall of fame in the field. Subjective because I have added a good dose of physicists I know. It creates a measurement bias which is easy to understand in social science as well as in quantum physics.



Richard Feynman (1918-1988, American) is one of the fathers of quantum electrodynamics, which earned him the Nobel Prize in Physics in 1965. He is at the origin of the quantum explanation of helium superfluidity at very low temperature in a series of papers published between 1953 and 1958. He theorized in 1981 the possibility of creating quantum simulators, capable of simulating quantum phenomena, which would be useful to design new materials and molecules in various fields like chemistry and biotech⁷⁷. He was also known for his great presentation skills.



Wolfgang Paul (1913-1993, Germany), not to be confused with Wolfgang Pauli, is a physicist who conceptualized trapped ions in the 1950s. He got the Nobel Prize in Physics in 1989. We owe him the traps that bear his name and are used to control trapped ions. He shared his Nobel prize with **Hans Georg Dehmelt** (1922-2017, Germany) who codeveloped these traps with him. The physicists **Juan Ignacio Cirac** (1965, Spanish) and **Peter Zoller** (1952, Austria) theorized, designed and tested the first trapped ion qubits in 1996, based on the work of Wolfgang Paul.



Brian Josephson (1940, English) is a physicist from the University of Cambridge. He was awarded the Nobel Prize in Physics in 1973 at the age of 33⁷⁸, for his prediction in 1962 of the effect that bears his name when he was only 22 years old and a PhD student at the University of Cambridge. The Josephson effect describes the passage of current in a superconducting circuit through a thin insulating barrier a few nanometers thick, using tunneling effect, and the associated threshold effects.

Below a certain voltage, the current starts to oscillate. It is generated by electrons with opposite spins organized in Cooper pairs named after Leon Cooper who discovered it in 1952. These pairs behave as bosons.

These electrons pairs have opposite spins (magnetic polarity). The system behaves as a resistance associated with a loop inductance, the oscillation being controllable by a magnetic field and having two distinct energy states. Superconductivity was discovered in 1911 by **Heike Kamerlingh Onnes** (1853-1926, Netherlands). This is the basis of superconducting qubits and their quantum gates!

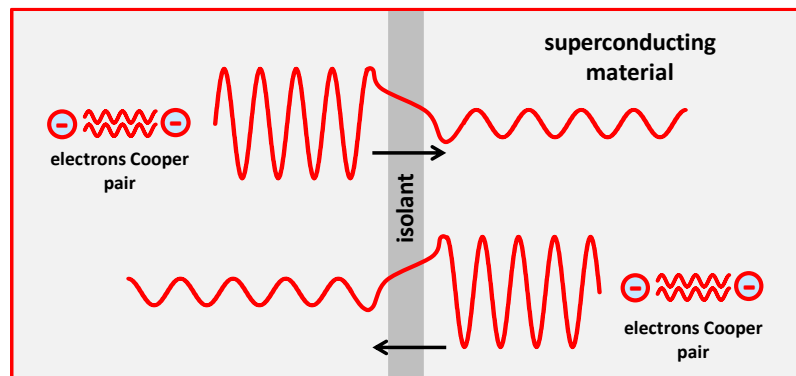


Figure 56: Josephson effect and Cooper pairs of opposite spin electrons.

⁷⁷ See [Simulating Physics with Computers](#) submitted in May 1981 to the International Journal of Theoretical Physics and published in June 1982 and [Quantum Mechanical Computers](#) also by Richard Feynman, published in 1985 (10 pages). He describes how a quantum computer could perform mathematical operations similar to those of traditional computers. He concludes by saying that it should be possible to create computers where a bit would fit into a single atom!

⁷⁸ Brian Josephson shared the 1973 Nobel Prize in Physics with two scientists who had worked before him in the same field: Leo Esaki (1925, Japan, still alive in early 2020) for his discovery of the tunnel effect in semiconductors in 1958 and Ivar Giaever (1929, Norway, also still alive) who found that this effect could occur in superconducting materials in 1960.



Paul Benioff (1930-2022, American) proposed in 1979/1980 the concept of a reversible and non-dissipative quantum Turing machine using 2D lattices of spins $\frac{1}{2}$, based on earlier work from Rolf Landauer on the thermodynamics of computing and Charles Bennett on reversible computing⁷⁹. It was a semi-classical machine concept that didn't yet exploit entanglement and interferences. His work was extended by the "universal quantum computer" concept from David Deutsch in 1985.



Yuri Manin (1937-2023, Russian and German) is a mathematician who proposed the idea of creating gate-based quantum computers, in his 1980 book "Computable and Uncomputable", then in the USSR.

Then, **Richard Feynman** devised in 1981 the idea of a quantum simulator. Feynman and Benioff were participants of the famous "Physics & Computation" conference in 1981 that was co-organized by IBM and the MIT at the MIT Endicott House⁸⁰.

It brought together a number of well-known scientists in quantum information technology such as Tommaso Toffoli and Edward Fredkin.

Rolf Landauer was also among them. It was for this conference that Richard Feynman published his famous paper "Simulating Physics with Computers" which created the concept of quantum simulation⁸¹.



Figure 57: participants of the first quantum computing conference in 1981. Source: [Simulating Physics with Computers](#) by Pinchas Birnbaum and Eran Tromer (28 slides).



Tommaso Toffoli (1943, Italian then American) is an engineer known for the creation, at the beginning of the 1980s, of the quantum gate bearing his name, a conditional gate with three inputs that is widely used in quantum programming. After working at MIT, he became a Boston University professor, where he has served since 1995. Like Stephen Wolfram, his interests include cellular automata and artificial life.



Edward Fredkin (1934, American) is a professor at Carnegie Mellon University. He is the author of the two-way conditional swap quantum gate (SWAP). He is also the designer of the concept of reversible classical computer with Tommaso Toffoli at MIT. He is also a prolific inventor far beyond quantum computing and is the originator of vehicle identification transponders and automotive geonavigation.

⁷⁹ See [The computer as a physical system: A microscopic quantum mechanical Hamiltonian model of computers as represented by Turing machines](#) by Paul Benioff, Journal of Statistical Physics, June 1979, published in May 1980 (30 pages). Paul Benioff was then in a visiting stay at the Centre de Recherche Théorique from CNRS in Marseille, France while being affiliated with the DoE Argonne National Laboratory in the USA. The paper was followed by [Quantum Mechanical Hamiltonian Models of Turing Machines](#) by Paul Benioff, October 1981 and June 1982, also in the Journal of Statistical Physics (32 pages). This theoretical system was based on using a two-dimensional lattice of spin $\frac{1}{2}$ systems (today, it would be electron spins based qubits). Back in the 1980s, the very notion of qubits was not yet in the radar. It appeared much later, in 1995. In Benioff's model, a quantum gate was a Hamiltonian transformation of individual spins that was driven by the Turing quantum machine.

⁸⁰ See [How a 1981 conference kickstarted today's quantum computing era](#) by Harry McCracken, FastCompany, May 2021.

⁸¹ See [Simulating Physics with Computers](#) by Richard Feynman, 1981 (103 pages).

He is also a promoter of the notion of "digital philosophy" which reduces the world and its functioning to a giant quantum program, a theory he shares with Seth Lloyd, an idea that has been revived by Elon Musk who believes that the Universe is a gigantic program and that we live in a simulation. Is the "automatic" respect of elementary physical laws a "program"? A thorny philosophical and semantic question!



Rainer Blatt (1952, Austrian and German) from the University of Innsbruck is an experimental physicist specialized, among other things, in trapped ions qubits. He was the first to entangle the quantum states of two trapped ions in 2004 and then with eight ions in 2006. He co-founded Alpine Quantum Technologies (AQT), whose ambition is to create and commercialize a trapped ions based quantum computer. He also works at TUM in Munich, Germany and is the coordinator of the Munich Quantum Valley since 2021.



David Wineland (1944, American) is a Boulder-based NIST physicist known for his advances in trapped ions and their laser-based cooling in 1978. He also created in 1995 the first single quantum gate operating on a single atom. He was awarded the Nobel Prize in Physics in 2012 jointly with Serge Haroche for his advances in atoms and ions laser cooling, a technique he first experimented in 1978, followed by the first quantum gate applied to a trapped ion in 1995 and the entanglement between four trapped ions in 2000.



Christopher Monroe (1965, American) is an American physicist known for his work on trapped ions and for co-founding IonQ in 2015, one of the two best funded quantum startups worldwide with PsiQuantum. He worked on trapped ions with David Wineland at the NIST Maryland laboratory. He demonstrated the ability to entrap ions, create ions-based quantum memory and create analog quantum simulators. He also ran a laboratory at the University of Michigan in the early 2000s.



Edward Farhi (1952, American) is a theoretical physicist who has worked in many fields, including high-energy particle physics, particularly at the CERN LHC in Geneva and then at MIT. He worked with Leonard Susskind on unified theories with electro-weak dynamical symmetry breaking. He and Larry Abbott proposed a model in which quarks, leptons, and massive gauge bosons are composite. He is the creator of adiabatic quantum algorithms and quantum walks. He also introduced with Peter Shor the concept of quantum money in 2010.



John Preskill (1953, American) is a professor at Caltech. Among many other contributions, he is the creator of quantum supremacy notion in 2011 and of NISQ in 2018, the Noisy Intermediate-Scale Quantum, qualifying current and future noisy quantum computers. He is a regular speaker at conferences where he reviews the state of the art of quantum computing⁸². He's now involved with Amazon and their cat-qubits superconducting project revealed in December 2020.



Daniel Esteve (1954, French) is a physicist in charge of the CEA's Quantronics laboratory in Saclay, France, launched in 1984 with Michel Devoret and Cristian Urbina, and part of the IRAMIS laboratory. He contributed to the development of transmon superconducting qubits. He created a first operational qubit in 1997, the quantonium, followed by another controllable prototype in 2002, with Vincent Bouchiat. He continues to work on improving the quality of superconducting qubits.

⁸² See his presentation that provides an overview of the state of the art of quantum computing [Quantum Computing for Business](#), John Preskill, December 2017 (41 slides).



Michel Devoret (1953, French) is a telecom engineer turned physicist, co-founder of the Quantronics laboratory with Daniel Esteve at the CEA in Saclay between 1985 and 1995, which is one of the world pioneers of superconducting qubits. He is a professor at Yale University since 2002. He was a co-founder of the American startup QCI with his Yale colleague Rob Schoelkopf (1964, USA), which he left in 2019/2020. He preferred to be entirely dedicated to research.

He worked several times with John Martinis, when John was a PhD student in UCSB, then when he was a post-doc at CEA in Saclay in the early 2000s, and at last at the University of Santa Barbara (UCSB), where they wrote together a review paper in 2004 on superconducting qubits⁸³.



Steven Girvin (1950, USA) is a professor of physics at Yale University, specialized in condensed matter physics, and Director of the Co-design center for Quantum Advantage, at Brookhaven University since 2020. He is a key contributor to works on circuit quantum electrodynamics (cQED) and superconducting qubits. At Yale, he works with Robert Schoelkopf and Michel Devoret on the various engineering problems associated with superconducting qubits.



Rob Schoelkopf (1964, USA) a physicist and director of the Yale Quantum Institute. Along with Steve Girvin and Michel Devoret, he made key advances in superconducting qubits. He particularly worked on single-electron devices, being the inventor of the Radio-Frequency Single-Electron Transistor. He also created the field of circuit quantum electrodynamics (cQED) with Andreas Wallraff and Alexandre Blais who were respectively Yale post-doc and PhD student around 2002-2004.

In 2007, with Steven Girvin, he engineered a superconducting communication bus to store and transfer information between distant qubits on a chip. In 2009, their team, also including Alexandre Blais and Jay Gambetta, demonstrated the quantum processor running some quantum computation, with two qubits⁸⁴.



Jay Gambetta (1979, USA) is the scientist leading as a VP since 2019 IBM's research team working on superconducting qubits quantum computers after running the IBM team that created and launched IBM Quantum Experience, Qiskit and the IBM Quantum System One in 2019. He joined IBM in 2011. After a thesis in quantum foundations and non-Markovian open quantum systems done in Australia in 2004, he focused on developing superconducting qubits, first in a post-doc tenure at Yale University and then at the Institute for Quantum Computing in Waterloo. He also worked on quantum validation techniques, quantum codes and applications.



Alexandre Blais (Canada) is a Professor in the Department of Physics and Director of the Université de Sherbrooke's Institut Quantique. He is one of the key contributors to the development of circuit quantum electrodynamics (cQED) that enable the creation of superconducting qubits. He is also a cofounder of Nord Quantique, a Quebec startup developing bosonic code qubits. Like Jay Gambetta, he did a post-doc at Yale, the US epicenter of the early developments of superconducting qubits.

⁸³ In [Implementing Qubits with Superconducting Integrated Circuits](#) by Michel Devoret and John Martinis, 2004 (41 pages).

⁸⁴ See [Demonstration of Two-Qubit Algorithms with a Superconducting Quantum Processor](#) by L. DiCarlo, Rob Schoelkopf et al, 2009 (9 pages).



Irfan Siddiqi (1976, American-Pakistani) is one key contributor to advancements in superconducting qubits. He did his PhD and post-doc at Yale, working initially in aluminum hot-electron bolometers for microwave astronomy and then, high frequency measurement techniques for superconducting qubits. He developed the Josephson Bifurcation Amplifier that uses the non-dissipative and nonlinear nature of the Josephson junction to create high gain and minimal back action readout of qubits.

This led to the creation of superconducting parametric amplifiers and Josephson traveling wave parametric amplifiers. He then moved at Berkeley University and the DoE Lawrence Berkeley National Laboratory. He works on quantum electrodynamics, quantum error correction, multi-partite entanglement generation and single photon detection. He runs there the Advanced Quantum Testbed, an integrated research platform on superconducting qubits and enabling technologies.



Artur Ekert (1961, Polish and English) is a quantum physicist known to be one of the founders of quantum cryptography. He had met Alain Aspect in 1992 to talk to him about this inspiration after discovering the latter's experiments. This is a fine example of step-by-step inventions, one researcher inspiring another! He was the director of the Singapore Center for Quantum Technology from 2007 to 2020. He is also a teacher at Oxford University and a member of Atos's Scientific Council.



Nicolas Gisin (1952, Switzerland) is a physicist specialized in quantum communication. He demonstrated quantum non-locality with an experiment in 1997 over a 10 km distance, extending the performance achieved in the laboratory by Alain Aspect in 1982. He co-founded IDQ in 2001, a Swiss startup initially specialized in quantum random number generators using photons passing through a dichroic mirror. It was acquired by SK Telecom in 2018.



David DiVincenzo (1959, American) was a researcher at IBM and the creator of the criteria that define the minimum requirements for a quantum computer with universal gates. He is now a researcher and professor at the University of Aachen in Germany. He is a member of the Atos Scientific Council, along with Alain Aspect, Serge Haroche, Artur Ekert and Daniel Esteve, among others.



Daniel Loss (1958, Swiss) proposed in 1998 with David DiVincenzo to use electron spins in quantum dots to create a quantum computer. He currently is the Co-Director and founding member of National Center on Spin Qubits (NCCR SPIN) that gathers the University of Basel, EPFL and IBM Zurich, an initiative from the Swiss Nanoscale Center SNI. He is the Director of the Center for Quantum Computing at the University of Basel. After a PhD in theoretical physics at the University of Zurich in 1985 he was a post-doc in the group of Anthony J. Leggett in the USA and at IBM Research. After a stint in Vancouver, he went back to Switzerland.

He works on condensed matter physics and spin-dependent and phase-coherent phenomena in semi-conducting nanostructures and molecular magnets with applications in quantum computing.



Bruce Kane (c. 1958, American) is a researcher at the Joint Quantum Institute from the University of Maryland (a JV with NIST). While he was doing research at UNSW, he presented in 1998 the “donors spin” model, a spin-based qubit concept based on using individual phosphorous atoms in pure silicon lattice structures. This is the principle on which Michelle Simmons works at both UNSW and her startup SQC.

The jury's still out to demonstrate that this technology can scale among the various spin qubits proposals.



Menno Veldhorst (1984, Dutch) is a group leader at QuTech. He got his PhD in 2012 on superconducting and topological hybrids at the University of Twente. He then worked on silicon quantum dots at UNSW where he demonstrated in 2015 the first two qubit operations in silicon. At QuTech, he works on silicon and silicon/germanium (SiGe) qubits to build scalable quantum computers. His team is currently pioneering work on SiGe/Ge qubits with qubits manipulation in arrays up to 16 quantum dots. He proposed a crossbar array architecture to create logical qubits.



Lieven Vandersypen (1972, Belgian) started as a mechanical engineer and a PhD at Stanford, then went to IBM in Almaden, California, where he became interested in MEMS. He demonstrated the use of Shor's algorithm for factoring the number 15 with NMR qubits, and then became a researcher at TU Delft University in the Netherlands and in its QuTech spin-off, which he currently runs. He is a pioneer of electron spin qubits. In this capacity, he works notably with Intel, and is testing their FinFET-based qubit chipsets at QuTech with Intel, which invested \$50M in QuTech in 2015.



Leo Kouwenhoven (1963, Dutch) is a quantum physicist who got his PhD at TU Delft in 1992 and became a professor there in 1999. He led experimental results on the potential "signatures" of Majorana fermion quasiparticles in 2012 and later on their "definitive" existence in 2018. The related Nature paper had to be retracted in 2021 due to experimental data mismanagement and reporting. From 2016 till 2022, he was a researcher at Microsoft Research. He left Microsoft in 2022 and has returned to his home based at QuTech and the Kavli Institute of Nanoscience from TU Delft.



Christophe Salomon (1953, French) is a physicist specialized in photonics and cold atoms, research director at the LKB (Normale Sup in Paris). He is particularly interested in quantum gases superfluidity (Bose-Einstein condensates) and in time measurement with cesium atomic clocks. He did a thesis in laser spectroscopy and then did a post-doc at the joint JILA laboratory between NIST and the University of Colorado. He is also a member of the Academy of Sciences since 2017.



John Martinis (1958, American), is a physicist from UCSB who famously worked at Google between 2014 and 2020 where he led the hardware team in charge of superconducting qubits up to creating the Sycamore processor and its related "quantum supremacy experiment", published in Nature in October 2019. After his thesis at Berkeley on superconducting qubits, he did a post-doc in Daniel Esteve's Quantronics laboratory at the CEA in Saclay.

In September 2020, he started to work with Michelle Simmons at SQC in Australia. He also created Quantala in 2020, a quantum computing company selling IP and protecting his own patents.



Mikhail Lukin (USA) is a Russian born quantum physics professor at Harvard. He's a prolific scientist with a skyrocketing h-index of 163, working on quantum optics, quantum control of atomic and nanoscale solid-state systems, quantum sensing, nanophotonics and quantum information science. He's behind many feats in cold atoms physics as well as in the NV centers field, being the inventor of NV centers based magnetometry.

He cofounded QuEra (USA) that develops a cold atoms gate-based quantum computer, reaching 256 qubits as of 2021. He is also a cofounder and scientific advisor of QDTI (USA).



Andreas Wallraff (German) is a Professor for Solid State Physics at ETH Zurich after having obtained degrees in physics from the London Imperial College and RWTH Aachen in Germany and worked at the Jülich Research Center also in Germany, Yale University in the USA and the LKB in France. He is specialized in the coherent interaction of single photons with quantum electronic circuits and quantum effects as well as on hybrid quantum systems combining microwave control, superconducting circuits and semiconductor quantum dots.



Jürgen Mlynek (1951, German) is a physicist specialized in optonics and interferometry. He was the coordinator of the strategic advisory board behind the launch of the European Flagship project on quantum in 2018. We owe him, as mentioned in connection with Louis De Broglie, the experiment validating the wave-particle duality of atoms carried out using helium in 1990 with Olivier Carnal at the University of Konstanz.



Jian-Wei Pan (1970, China) is the leading quantum physics scientist in China. He is a professor and Executive VP at USTC (University of Science and Technology of China) and a member of CAS (China Academy of Science). He did his PhD in Vienna under the supervision of Anton Zeilinger. He and his team are famous for premiere experiments on photons quantum entanglement in 2004, quantum key distribution over a satellite (2017), with boson sampling (2019) and superconducting qubits (2021).



Marie-Anne Bouchiat (1934, French) is a specialist in rubidium atoms physics and their control by optical pumping. This is the basis for the creation of quantum computers based on cold atoms. Her daughter **Hélène Bouchiat** (1958, French) is also a physicist, specialized in condensed matter at the LPS laboratory of the University Paris-Saclay and member of the Académie des Sciences since 2010, like her mother who has been there since 1988.



Elisabeth Giacobino (1946, French) is a specialist in laser physics, nonlinear optics, quantum optics and superfluidity, particularly in relation to the control of cold atoms. She worked at the CNRS in the ENS LKB (Laboratoire Kastler-Brossel). She is a member of the scientific selection committee of the European Quantum Flagship and also for the ANR (Agence Nationale de la Recherche).



Jacqueline Bloch (1967, French) is a research director at CNRS (PI) in the Centre de Nanosciences et de Nanotechnologies (C2N) lab from CNRS and Université Paris-Saclay, working on polaritons, quasi-particles coupling light and semiconductor matter, mainly built in gallium arsenide (GaAs). These have potential applications in the creation of quantum simulators based on polariton arrays as well as for quantum metrology.



Jean-Michel Gérard (1962, French) is a physicist from the CEA IRIG laboratory in Grenoble and director of the joint PHELIQS laboratory (PHotonics, ELectronics and Quantum Engineering) from UGA (University of Grenoble) and CEA. He works in particular on the creation of single photon sources based on quantum dots as well as single photon detectors based on superconducting nanowires and OPO laser diodes.



Pascale Senellart (1972, French) is a physicist, CNRS research director at the C2N laboratory. She designed and invented a process for manufacturing sources of unique and indistinguishable photons used in quantum telecommunications and computing. These are GaAsAl semiconductor quantum dot trapped in a multi-layered 3D structure, powered by a laser and directly feeding an optical fiber. She co-founded the startup Quandela in 2017 with **Valérien Giesz** (CEO) and **Niccolo Somaschi** (CTO and Chairman) who were a PhD student and a post-doc in her team.

Quandela is selling these photon sources and is creating photon qubit-based quantum computers. She is their scientific advisor. Pascale Senellart also launched the Quantum hub of the University Paris-Saclay in November 2019, which brings together public and private research laboratories as well as higher education institutions. She was awarded the CNRS Silver Medal in 2014.



Maud Vinet (1975, French) started as physics engineer and was granted a PhD in physics from Grenoble University. She then spent 20 years working in silicon technologies development and transfer for the semiconducting industry. She led the silicon qubit project at CEA-Leti in Grenoble. Since 2016, CEA-Leti was focused on silicon spin qubits leveraging the strong relationships between fundamental science and technology in Grenoble ecosystem. In November 2022, Maud Vinet launched **Siquance** along with Tristan Meunier (CNRS) and François Perruchot (CEA-Leti).

The silicon qubit ecosystem in Grenoble involves several laboratories in addition to CEA-Leti: IRIG (also from CEA), CNRS's Institut Néel, LPMMC, and various entities of UGA (Université Grenoble Alpes). Maud is also driving QLSI, the European Quantum Flagship research project on silicon spins qubits, awarded in March 2020, after obtaining with **Tristan Meunier** (1977, French, at CNRS Institut Néel) and **Silvano de Franceschi** (1970, Italian, at CEA IRIG) an ERC funding of €14M in 2018 for the QuCube silicon qubit project. Before her journey in quantum computing, she had previously contributed to the industrialization of the FD-SOI technology with CEA and STMicroelectronics⁸⁵, Globalfoundries and IBM.



Alexia Auffèves (1976, French) is a CNRS research director and the director of Singapore's CNRS MajuLab international laboratory since January 2022 after having conducted her research for over 15 years in Grenoble at CNRS Institut Néel. She is specialized in quantum thermodynamics and collaborates with various teams in France (C2N, ENS Lyon) and around the world (Center for Quantum Technologies in Singapore, Chapman University and Saint-Louis University in the USA, Oxford and Exeter Universities in the UK, Madrid University in Spain, etc.).

Alexia Auffèves started as an experimentalist, doing her PhD thesis at the ENS LKB in Paris, with Serge Haroche. She then became a theoretician although with quite abroad perspective. She developed the CSM ontology of quantum mechanics (Contexts, Systems and Modalities) with Philippe Grangier and the philosopher Nayla Farouki that we cover later in this book, when discussing quantum foundations, page 1001⁸⁶. She launched and coordinated QuEnG (Quantum Engineering Grenoble), the Grenoble quantum ecosystem, which became the QuantAlps federation in January 2022. Her recent work focuses on the energetic aspects of quantum technologies, both from fundamental and full-stack perspectives, which explains why she cofounded the [Quantum Energy Initiative](#) in August 2022 with **Robert Whitney** (a physicist from CNRS LPMMC in Grenoble), **Janine Spettstoesser** (Chalmers University, Sweden) and Olivier Ezratty. Yes, that's me, the writer of this book.

⁸⁵ FD-SOI = Fully-Depleted Silicon on Insulator. The technology uses on the one hand a layer of silicon oxide insulator and on the other hand, channels of undoped silicon between the drain and the source, limiting leakage between the latter two.

⁸⁶ See [Contexts, Systems and Modalities: a new ontology for quantum mechanics](#) by Alexia Auffèves and Philippe Grangier, 2015 (9 pages). See also the [associated Wikipedia](#) page. This work has been articulated on a total of seven papers released between 2015 and 2019.



Antoine Browaeys (c. 1970, French) is a CNRS research director leading the quantum optics-atom team in the Charles Fabry Laboratory at Institut d'Optique specialized in the control of cold atoms. He is also a cofounder and the scientific director of Pasqal, a startup designing a cold atoms computer that will be first used as a quantum simulator, and then, as a universal gates quantum computer. He was awarded the CNRS silver medal in 2021.



Hélène Perrin (c. 1975, French) is CNRS research director working at the Laboratoire de Physique des Lasers (LPL) from Université Sorbonne Paris Nord, working on Bose-Einstein condensates and cold atoms control. Together with Pascal Simon, she drives the Quantum Simulation SIM project, a cold atom-based quantum simulator. She also gives lessons on quantum computing. She did her PhD thesis with Christophe Salomon at the ENS LKB in Claude Cohen-Tannoudji's group. At CEA-Saclay, she also worked on fractional quantum Hall effect. Since 2022, she is the director of QuanTIP, the Paris region quantum ecosystem network.



Eleni Diamanti (1977, Franco-Greek) is a leading specialist and experimenter in the development of photonic resources for quantum cryptography, also working on quantum communication complexity. She's a CNRS research Director and faculty at LIP6 laboratory from Paris-Sorbonne University. She is the vice-director of the Paris Centre for Quantum Computing since April 2020. She is also involved in many European projects around quantum key distribution, like the Quantum Internet Alliance and OpenQKD. She is a recipient of a European Research Council Starting Grant.

At last, she's a cofounder and a scientific advisor with Julien Laurat for the startup WeLinQ, created in 2022 with Tom Darras as CEO, which creates cold atom based quantum memories for quantum computer interconnects and quantum repeaters.



Jason Alicea (American) is a Professor of Theoretical Physics at Caltech University's IQIM (Institute for Quantum Information and Matter). He is specialized in condensed matter physics and topological phase of matter which could lead on creating non-Abelian anyons and Majorana fermions, a qubit type mainly explored by Microsoft.



Michelle Simmons (1967, British-Australian) is a physicist from the University of New Wales in Australia (UNSW), working on silicon spin qubits. She is the director of CQC2T (Centre of Excellence for Quantum Computation and Communication Technology) from UNSW. She is also the co-founder of SQC (Silicon Quantum Computing), the leading quantum computing Australian startup (\$66M), a spin-off from her university and from QQC2T.

In 2019, her team built the first two-qubit gate between phosphorous atom qubits in silicon, operating in only 0.8 ns. It became a full-fledged 10 qubit processor in 2022. She is using STM (scanning tunneling microscopes) to position phosphorus dopants in the silicon substrate.



Andrew S. Dzurak (Australian) is the Director of the Nanotechnology Fabrication Unit at UNSW's Australian National Fabrication Facility from the CQC2T research center. This facility's white room is used to manufacture silicon qubits chipsets. Andrew Dzurak is a pioneer of silicon qubits since 1998. He is leading research at CQC2T on silicon qubit control and reading. He created the first phosphorus-based silicon double qubits in 2015. He was a lead scientist for SQC, founded by Michelle Simmons, but seemingly left the company in 2021.

He created Diraq in 2022, a startup dedicated to the creation of scalable quantum computers using quantum dot silicon spin qubits.



Andrea Morello (1972, Italian) is one of the star researchers at UNSW in Australia. He is Program Manager of the ARC Centre of Excellence at CQC2T and leads the Fundamental Quantum Technologies Laboratory at UNSW. During his studies, he attended the Laboratoire National des Champs Magnétiques Intenses of the CNRS in Grenoble. Today he is one of the specialists in silicon-based qubits. He is also a quantum engineering teacher at UNSW.

His team was the first to demonstrate coherent control and readout of an individual phosphorus atom electron and nuclear spin in silicon and held for many years the record for the longest quantum memory time of 35.6 s in a single solid-state qubit.



Andrew G. White (c. 1970, Australian) is a leading Australian quantum scientist who is the Director of the University of Queensland Quantum Technology Laboratory. He is most known for his work in quantum photonics, including a first demonstration of an optical CNOT entangling gate realized in 2004 and based on the Knill, Laflamme and Milburn (KLM) protocol and linear optics. He is also very eclectic, having also worked on nuclear physics and marine biology. He's a scientific advisor for Quandela.



James Clarke (c. 1971, American) launched Intel's quantum computing research efforts and the Director of Quantum Hardware at Intel since 2015. He's also behind Intel's partnership with QuTech in The Netherlands. He is currently focused with his team of about 100 researchers and engineer on creating scalable quantum computers with silicon and SiGe qubits. He started working at Intel as a process engineer in 2001 after having studied and worked on organic chemistry (PhD in Harvard and post-doc at ETH Zurich).



Christine Silberhorn (1974, German) is a researcher and professor working on photon-based quantum computing at the University of Paderborn located between Dortmund and Hanover. She leads there the Integrated Quantum Optics group. Her laboratory designs and manufactures integrated optoelectronics components, entangled photon sources and quantum array systems. Her team designed a system to convert photon qubits between infrared and visible wavelengths. She also works on optical quantum memories. She was awarded the Leibnitz prize in 2011.

She cofounded It'sQ in 2022, a quantum photonic computing startup and is one of the very few lead researchers in Germany who created a quantum computing hardware company.



Stephanie Wehner (1977, German) is a physicist working on quantum communication protocols, based at the University of Delft in the Netherlands. She coordinates the "Quantum Internet Alliance", one of the projects of the European Quantum Flagship, which plans to deploy a quantum key distribution (QKD) Internet network running in mesh mode. She started her professional life in cybersecurity, detecting system flaws. She is also producing many quantum tech MOOCs.



Perola Milman (c. 1975, French) is a specialist in the theory of quantum computing and in particular with trapped photons and ions. In particular, she has demonstrated the entanglement capacity of molecules. She is a lecturer-researcher at the Laboratory of Quantum Materials and Phenomena of the University Paris Diderot. She is a professor of quantum theory of light and on quantum entanglement.



Sara Ducci (1971, French) is another teacher-researcher at the same Laboratoire Matériaux et Phénomènes Quantiques (MPQ) where she co-founded in 2002 a team in charge of nonlinear optical devices. She is working on producing pairs of entangled photons sources based on III-V semiconductors. She is also interested in the characterization (state measurement...) and manipulation of photons. At last, she teaches quantum physics at Ecole Polytechnique.



Jacqueline Romero (c. 1985, Philippines) is a quantum optics physicist doing research in Australia at the University of Queensland, after completing her PhD in Glasgow, UK. She is working on optical neuromorphic architectures and on dense encoding of information in photons using several of their characteristics in addition to the usual polarization.



Fabio Sciarrino (1978, French Italian) is the director of the Quantum Information Lab at the Sapienza University of Rome and specialized in photonics. His team is at the origin of many advances in the field, notably in boson sampling, a key experiment in the path of photon-based quantum computers. He collaborates with Quandela's team and the C2N of Palaiseau (Pascale Senellart).



Patrice Bertet (c. 1976, France) is part of Daniel Esteve's team at CEA-SPEC. He did his thesis at Serge Haroche on Rydberg atoms and then went to Delft University. He participated in the early days of superconducting qubits (quantronium at CEA and TU Delft). He then worked on QED (quantum electrodynamics) circuits based on cavities and then on transmon qubits. He is working on the association of superconducting qubits and the measurement of their state with electron spins, notably based on NV centers, which can also be used for quantum memories.



Audrey Bienfait (c. 1990, France) is a former PhD student of Patrice Bertet at CEA-SPEC who is now doing her research at ENS Lyon in the team of **Benjamin Huard** (1979, French). She was awarded the Bruker Prize 2018 for her thesis on electron paramagnetic resonance or "ESR - Electron Spin Resonance" in quantum regime and the Michelson Postdoctoral Prize 2019 in March 2020 for her work on the entanglement of superconducting qubits via phonons.



Sébastien Tanzilli (France) is the director of the InPhyNi physics laboratory in Nice and also the CNRS national quantum program director. He works on quantum cryptography with continuous or discrete keys (CV-QKD and DV-QKD), in fundamental quantum optics as well as in hybrid quantum systems for the study and realization of quantum communication networks. He was also the president of the GDR-IQFA, a community of quantum physics researchers in France (IQFA = Information Quantique, Fondements & Applications) from its creation in 2011 until 2021.



Virginia D'Auria (Italy) is a researcher working on quantum optics transmission systems using continuous and discrete variables and DV/QV hybridization. Having worked at the ENS LKB in Paris, she also worked on photon detectors. Since 2010, she is part of the photonics group of InPhyNi and works on discrete and continuous variable quantum communications compatible with optical fibers of telecom operators.



Jelena Vucokic (c. 1975, Serbian) is a research professor at Stanford, working in quantum photonics. She directs the Nanoscale and Quantum Photonics Lab and the Q-FARM (Quantum Fundamentals, ARchitecture and Machines initiative), an interdisciplinary quantum laboratory. She contributes to developments in photonics for the development of optical quantum computers. She did her PhD at Caltech in 2002.



Francesca Ferlino (1977, Italian) is a typically European researcher, having worked in many laboratories from different countries. She is research director at the IQOQI in Innsbruck, Austria, where she leads the Dipolar Quantum Gases laboratory. She is a specialist in cold atoms and erbium-based Bose-Einstein condensates.



Marcus Huber (Austria) is a research group leader at the IQOQI in Vienna, working on quantum entanglement, qubit state measurement and quantum thermodynamics in general. In addition to the IQOQI, he has also worked at the Universities of Bristol, Geneva and Barcelona. He is a great advocate of the open publication of research work, being at the origin of the Quantum-Journal.org website, a kind of arXiv for quantum science.



Tracy Northup (c. 1975, Austria) is a researcher working on trapped ions and optical cavities, one of the major branches of quantum computing. She leads the Quantum Interfaces Group laboratory at the University of Innsbruck, which is one of the most active in the field of trapped ions, a major Austrian specialty.



Anne Matsuura (c. 1970, Japanese-American) is a physicist who is leading the Quantum & Molecular Technologies team from the Intel Quantum Research Laboratory since 2014. She leads the American's efforts in the creation of superconducting and silicon qubits quantum computers, with an overall vision of the hardware architecture. Her impressive career starts with a thesis at Stanford in synchrotrons, then in US Air Force labs and In-Q-Tel (the CIA investment fund). She also directed the European Theoretical Spectroscopy Facility in Belgium.



Sarah Sheldon (c. 1986, American) has been a member of IBM's quantum computing teams based at the Thomas J. Watson Research Center in Yorktown, New York, since 2013. She is particularly active in improving the quality of superconducting qubits, their quantum gates and error correction codes. She obtained her PhD at MIT in 2013 before doing a post-doc with IBM.



Stefanie Barz (c. 1980, German) is a quantum optics professor and researcher at the University of Stuttgart. Her interests include quantum cryptography and quantum telecommunications. She worked in particular on blind computing with Elham Kashefi and Anne Broadbent. She leads the SiSiQ project funded by the German Ministry of Research with €3.6M of European funding, which aims to create quantum communication infrastructure with silicon photonics.



Alexei Grinbaum (1978, Franco-Russian) is a researcher at CEA-Saclay in Etienne Klein's LARSIM laboratory. He works on the quantum foundations and quantum physics philosophy⁸⁷. He is notably the author of the book "Les robots et le mal" (Robots and evil) published in 2018. He is particularly interested in the ethics of science, its acceptance by society and responsible innovation.



Frédéric Grosshans (1976, French) is a CNRS researcher at LIP6 from Université Paris-Sorbonne, specialized in QKD, repeaters and quantum networks. He was the creator with Philippe Grangier of the continuous variable QKD. He is also the co-director with Nicolas Treps (from LKB) of the Quantum Information Center Sorbonne of the Alliance Paris-Sorbonne launched in September 2020, which federates quantum research and training of several Parisian quantum groups.



Jean-François Roch (1964, French) is a quantum physics professor at ENS Paris Saclay. He is a pioneer of the usage of NV centers in many applications, particularly in quantum sensing, including for studying matter and magnetism at very high-pressure, which could be helpful for the discovery of high-temperature superconducting materials. He conducts these researches in partnership with Thales and with the CEA. He also led the founding Wheeler delayed choice experiment in 2006.



Ronald Walsworth (c. 1972, American) is a pioneer in the usage of NV centers for quantum sensing in various fields, from life science to physics and astrophysics like for the detection of dark matter. He leads the Walsworth group at the University of Maryland and is the founding director of the UMD Quantum Technology Center. Several startups emerged from his lab like qdm.io, Hyperfine.io (MRI) and QDTI (which he both cofounded).

He also launched the Quantum Catalyzer quantum startups accelerator (Q-CAT) that creates quantum startups from scratch. He got a PhD in physics from Harvard in 1991.

Quantum information science and algorithms creators

Let's end this long "hall of fame" with some of the main contributors to the creation of quantum information science and algorithms. It is a relatively new discipline that emerged in the early 1990s.



Alexander Holevo (1943, Russian) is a mathematician working in quantum information science and who devised the 1973 Holevo theorem according to which we cannot retrieve more than N bits of useful information from a register of N qubits⁸⁸. This is the consequence of the wave packet reduction that reduces the qubit state to its basis states $|0\rangle$ and $|1\rangle$ after measurement. He also developed the mathematical basis of quantum communications.

⁸⁷ See [Narratives of Quantum Theory in the Age of Quantum Technologies](#) by Alexei Grinbaum, 2019 (20 pages).

⁸⁸ This theorem indirectly validates the fact that it is difficult to do "big data" with a quantum computer in the sense of storing and analyzing large volumes of information. On the other hand, Grover's algorithm makes it possible to quickly find a needle in a haystack, as we will see later.



David Deutsch (1953, Israeli and English) is a physicist from the Quantum Computing Laboratory at Oxford University in the UK. He devised in 1985 the idea of creating a universal quantum computer using a quantum Turing machine which led him to create in 1989 the gate-based circuits programming model, completing Yuri Manin's and Paul Benioff's 1980 ideas⁸⁹. He is also the author of a search algorithm, with two variants, a first one from 1985 and a second one in 1992 that he co-created with Richard Jozsa.



Umesh Vazirani (1945, Indian-American) is a professor at the University of Berkeley. He is one of the founders of quantum computing, with his paper co-authored in 1993 with his student Ethan Bernstein, [Quantum Complexity Theory](#). He is also the creator of the Quantum Fourier Transform (QFT) algorithm, which was used less than a year later by Peter Shor to create his famous integer factoring algorithm that served as a spur to funding research in quantum computing in the USA. The QFT is a founding algorithm used in many other quantum algorithms.



Peter Shor (1959, American) is a mathematician who became the father of the algorithm of the same name in 1994 which allows the factorization of integers into prime numbers, based on quantum Fourier transforms (QFT). Before that, he created the first quantum discrete-log algorithm (dlog) and, later, the famous nine-qubit flip error and phase error correction algorithm for quantum computers called the "Shor code"⁹⁰. We indirectly owe to him the whole movement of post-quantum cryptography (PQC).

PQC is about creating cryptography codes resisting to public keys breaking using the Shor algorithm and other quantum algorithms... with quantum computers that do not yet exist. Peter Shor created his famous factorization algorithm while working at Bell Labs. He has been teaching applied mathematics at MIT since 2003.

Daniel R. Simon (American) is the creator of another search algorithm in 1994, bearing his name. Precisely, his quantum algorithm solves the hidden subgroup problem (HSP) using an oracle based model, providing an exponential acceleration compared to classical computing⁹¹. Daniel Simon worked at Microsoft Research when he created his famous algorithm. He later worked on cybersecurity research until his retirement, always with Microsoft Research.



Lov Grover (1961, Indian-American) is a computer scientist who created the seminal quantum algorithm in 1996 that is said to be a search algorithm in a database but has many more use cases as we'll see in the quantum algorithms part of this book (page 591). He currently works in the Department of Mathematics of the Guru Nanak Dev University, in Punjab, India. His full name is Lovleen Kumar Grover.

⁸⁹ See [Quantum theory, the Church-Turing principle and the universal quantum computer](#) by David Deutsch, 1985 (21 pages). This is a foundational paper describing a lot of concepts, including the unitaries used in single qubit gates, the notion of quantum computing complexity, etc. It was also followed by [Quantum computational networks](#) by David Deutsch, September 1989 where networks correspond to series of gate operations. Back then, the very name of qubit didn't exist yet, and was created only in 1995.

⁹⁰ See the excellent [The Early Days of Quantum Computation](#) by Peter Shor, August 2022 (10 pages) where Peter Shor recount the history of the early years of quantum computing and how he discovered his various algorithms with try and error.

⁹¹ See [On the power of quantum computation](#) by Daniel Simon, 1994 (11 pages) also updated in 1997.



Michael Freedman (1951, American) is a mathematician who founded and runs the Microsoft Station Q laboratory in Santa Barbara, California. He is one of the fathers of topological quantum computing along with Alexei Kitaev. He was also awarded the Fields Medal in 1986 for his work on the Poincaré conjecture, later demonstrated in 2006 by Grigori Perelman.



Alexei Kitaev (1963, Russian and American) is with Michael Freedman one of the fathers of the topological quantum computer concept in 1997, investigated by Microsoft. He was a researcher at Microsoft Research in the early 2000s and is now working at Caltech University and with Google. He has also done a lot of work on error correction codes, including the creation of toric codes, surface codes and magic states distillation (with **Sergey Bravyi**) and the Quantum Phase Estimate algorithm, used in Shor's integer factorization algorithm.



Aram Harrow (American) is a prolific specialist in quantum algorithms. He teaches both quantum physics and quantum computing at MIT. At MIT, he is surrounded by Peter Shor and Charles Bennett. He is the co-author of the HHL quantum algorithm used to solve linear equations which he created jointly with Avinatan Hasidim and Seth Lloyd⁹². He is also interested in the creation of hybrid classical/quantum algorithms.



Daniel Gottesman (1970, American) is a physicist from the Perimeter Institute in Waterloo, Canada. He did his PhD thesis at Caltech under the supervision of John Preskill. He is known for his work on quantum error correction codes (QEC) and is co-author of the famous Gottesman-Knill's theorem according to which a quantum algorithm using only Clifford gates can be efficiently simulated (meaning, polynomially) on a classical computer.

Clifford group quantum gates are based on half and quarter-turn rotations (of the qubit in the Bloch sphere), Hadamard gate and the C-NOT conditional gate. This theorem thus indirectly proves that a basic gate set is insufficient to generate an exponential quantum advantage. We need to add a T gate to make it possible to approximate any arbitrary unitary transformation, meaning, any move within the Bloch sphere for single qubit operations. This is particularly important for the Shor algorithm.



Gil Kalai (1955, Israeli) is a professor of mathematics at the Hebrew University of Jerusalem and at Yale University. His main ambition is to demonstrate mathematically that it will be impossible to create real universal quantum computers, due to their error rate, even with error correction codes and the notion of logical qubits that assemble physical qubits. He also questioned the reality of the October 2019 Google supremacy performance in several of his writings and conference talks.



Andrew Steane (1965, English) is a Professor of Physics at Oxford University. He created the so-called Steane quantum error correction code in 1996. This code corrects flip and phase errors on a single qubit. Looking at how it works provides good insights on the inner workings of quantum error correction codes, although this particular code will probably not be used when we'll have scalable quantum computers. Other more sophisticated QEC codes are investigated like color codes, surface codes and Floquet codes.

⁹² See [Quantum algorithm for linear systems of equations](#), 2009 (24 pages).



Scott Aaronson (1981, American) teaches information science at the University of Austin in Texas. He is a leading expert in quantum algorithms and complexity theories. He is notably at the origin of a quantum algorithm used for boson sampling, a way to demonstrate some quantum advantage for photonic based experiments. Bosons are integer spin particles such as photons, while particles such as electrons, neutrons and protons are fermions, with a spin $1/2$.



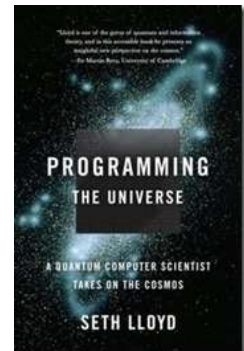
Dorit Aharonov (1970, Israeli) is a quantum algorithms researcher. She received her PhD in Computer Science in 1999 at the Hebrew University of Jerusalem on "Noisy Quantum Computation" and then did a post-doc at Princeton and Berkeley. She is credited with the "quantum threshold theorem" co-demonstrated with Michael Ben-Or which states that below a certain error rate threshold, error correction codes can be recursively applied to obtain an arbitrarily low error rate of logical qubits.

This is a very theoretical mathematical approach that doesn't take into account the way noise is also scaling as we increase the number of qubits. Dorit Aharonov's uncle is **Yakir Aharonov** (1932, Israeli), a physicist who had worked with David Bohm, among others.



Seth Lloyd (1960, American) is a professor at MIT who is a prolific contributor to quantum information and quantum algorithms. He is the initiator of Quantum Machine Learning, of the concept of qRAM (quantum random access memory), of continuous variables gates-based quantum computing (1999), of quantum radars (2008). He's also the L in the famous HHL quantum linear equation solving algorithm and worked on quantum error correction codes and quantum biology.

In his 2006 book, *Programming the Universe*, Lloyd contends that the universe itself is one big quantum computer producing what we see around us, and ourselves, as it runs a cosmic program. According to Lloyd, once we understand the laws of physics completely, we will be able to use small-scale quantum computing to understand the universe completely as well. In about 600 years.



Seth Lloyd was laid off from MIT in 2019 then put on leave, then on disciplinary actions for a period of five years starting in 2020 because he had not informed his management of some Jeffrey Epstein originated funding.

In 2016, he created Turing (2016, USA) with Michele Reilly, a software company working on hybrid classical-NISQ software solutions using AI and quantum machine learning techniques.



Alán Aspuru-Guzik (circa-1978, American) is a research director at the University of Toronto, formerly at Harvard, who, among other things, created various quantum chemistry algorithms, a topic we will cover in the section dedicated on quantum algorithms. He is also the co-founder of the Zapata Computing, a startup developing quantum computing software frameworks, particularly in chemical simulation.



Robert Raussendorf (c. 1975, German) is well known for having invented one-way quantum computing and measurement-based quantum computing (MBQC) along with **Hans Briegel** (1962, German) in the early 2000's. He is an Associate Professor at the Department of Physics and Astronomy of the University of British Columbia. He did his thesis at the Ludwig Maximilians University in Munich, Germany in 2003 on MBQC.



Elham Kashefi (1973, British Iranian) is a research director at CNRS in France, in the LIP6 laboratory from Sorbonne University. She is also the co-founder with Marc Kaplan of VeriQloud, a secure quantum telecommunications startup, and teaching quantum information science at the University of Edinburgh. Originally a mathematician and computer scientist, she became a specialist in quantum communication protocols and quantum algorithms, around topics like code verification and blind quantum computing.

She did her PhD thesis “Complexity Analysis and Semantics for Quantum Computation” at the Imperial College of London in 2003 under the co-supervision of Peter Knight. She created the BFK blind computing protocol in 2009 with Anne Broadbent and Joe Fitzsimons (who created Horizon Quantum Computing in Singapore). With her team at LIP6, she is at the origin of the creation of a site on the zoo of quantum communication protocols⁹³. And as this was not enough, she is also versed in Quantum Physical Unclonable Functions (QPUF), physical identifiers of quantum and tiltable objects, a topic we briefly cover in this book in page 858.

In November 2022, Elham Kashefi was appointed as Chief Scientist for NQCC, the UK National Quantum Computing Center, and will chair its Technical Advisory Group.



Anne Broadbent (Canadian) is a mathematician from the University of Ottawa specialized in quantum computing, quantum cryptography and quantum information. She was a student of Alain Tapp and Gilles Brassard at the Université de Montréal. She created the BFK blind computing protocol in 2009 along with Elham Kashefi and Joe Fitzsimons.



Maria Schuld (c. 1989, German) is a senior researcher and software developer at Xanadu since 2017, based in South Africa at the University of KwaZulu-Natal in Durban where she got her PhD in quantum machine learning and was then a post-doc after a short internship at Microsoft Research in the USA. She is a key contributor to the development of quantum machine learning algorithms, particularly in the field of pattern recognition.



Mazyar Mirrahimi (circa 1980, Iranian) is a mathematician who moved to quantum physics. He is currently the director of Inria's Quantic laboratory, which specializes in error correction codes and quantum algorithms, among other topics. He did his post-doc with Michel Devoret at Yale University. Back in 2013, he published a seminal paper on cat-qubits.

These are physical qubits using a cavity and a superconducting qubit that self-corrects some errors, starting with flip errors. These cat-qubits are used by the startup Alice&Bob as well as by Amazon, as announced in December 2020.



Zaki Leghtas (Morocco/France) is a researcher based in France in Mazyar Mirrahimi's team and is also specialized in error correction codes and systems. He is notably one of the creators of cat-qubits mentioned above. These are supposed to enable the creation of logical qubits with fewer than 100 physical qubits. He worked in Michel Devoret's laboratory at Yale University before joining Inria's Quantic team in 2015. He is also affiliated with ENS and Mines ParisTech.

⁹³ See the [Protocol Library wiki](#).



Shi Yaoyun (1976, Chinese) is a professor at the University of Michigan and also leading the Alibaba Quantum Laboratory which develops fluxionium superconducting qubit computers. He created various records of quantum simulation on server clusters that we will describe in this book. He earned a computer science PhD from Stanford. He also worked on quantum cryptography and certifiable randomness.



Kristel Michielsen (circa-1969, Belgian) is a physicist working at the University of Aachen in Germany and at the Jülich Supercomputing Centre (JSC) where she leads the Quantum Information Processing (QIP) research group. She has contributed to numerous works in quantum computing both in physics and algorithms. She created the [QTRL scale](#), for Quantum Technology Readiness Level, that is used to evaluate the level of maturity of quantum technologies and which we will discuss in the section dedicated to [practices in research](#).



John Watrous (Canadian) is a researcher working at the University of Waterloo, Canada, specialized in quantum algorithms and complexity theory. He demonstrated some complexity classes equivalencies like QIP is in EXP and QIP=PSPACE . He also worked on cellular automata. He had previously collaborated with Scott Aaronson. He is the author of the voluminous [The Theory of Quantum Information](#), 2018 (598 pages).



Ryan Babbush (circa-1989, American) is a Google researcher working on quantum simulation algorithms. His goal is to create commercial quantum chemistry solutions. In a February 2020 [presentation](#), he did show that chemical simulation with Google's Sycamore 53 qubits processor could not use more than 12 qubits because of its high error rate.



Matthias Troyer (1968, Austrian) is Professor of Computational Physics at ETH Zurich. He joined Microsoft Research in Redmond at the beginning of 2017. He is one of the creators of the Q# language for quantum programming and of the open source framework ProjectQ launched in 2016 by ETH Zurich. He is particularly interested in chemical simulation with quantum computers. He received his PhD from ETH Zurich in 1994.



Krysta Svore (c.1978, American) is currently the general manager of quantum software at Microsoft. She has a Ph.D. in Computer Science from Columbia University. Her contribution in quantum information science covers a broad range of topics: MBQC, quantum machine learning, contributing to the creation of the $|\text{LIQ}^i\rangle$ quantum programming language, surface codes, fault-tolerance quantum computing.



Jordanis Kerenidis (c. 1980, Greek) is a director of research from CNRS at IRIF (Institut de Recherche en Informatique Fondamentale), working on cryptography, quantum communication, quantum complexity theories and quantum machine learning, his latest specialty. He did his thesis at MIT under the supervision of Peter Shor and worked in the same office as Scott Aaronson and also worked at Berkeley with Umesh Vazirani. He is part of the founding team of QC Ware.

There he leads the R&D in quantum algorithms. He also co-leads the Paris Quantum Ecosystem (PCQC) with Eleni Diamanti. He was one of the members of the parliamentary mission on quantum technologies led by MP Paula Forteza between April 2019 and January 2020.



Frédéric Magniez (French) is the Director of the CNRS IRIF laboratory mentioned above. He also did run a Chair at Collège de France in Spring 2021. His research focuses on the design and analysis of randomized algorithms for processing large datasets, as well as the development of quantum computing, particularly algorithms, cryptography and its interactions with physics. In 2006, he founded and led the national working group for quantum computing, bringing together 20 research groups.



Benoît Valiron (1980, France) is a researcher at the CNRS LIR laboratory from Université Paris-Saclay and teaching quantum programming and algorithms, including at CentraleSupélec. This quantum programming specialist is the co-author of the open source quantum programming language Quipper, which he contributed to create while being at the University of Pennsylvania.



Bettina Heim (c. 1980) is a Microsoft developer specializing in quantum software. She is responsible for the development of the quantum programming language Q# compiler, promoted by Microsoft since 2017 and which is part of their Quantum Development Kit, currently running on quantum emulators on traditional processors and now supported on third party hardware proposed on the cloud, including IonQ and Honeywell trapped ion based quantum processors.



Cristian Calude (1952, Romanian/New Zealander) and **Elena Calude** (Romanian/New Zealander) are researchers from the Institute of Information Sciences, University of Albany in Auckland, New Zealand. They work on quantum algorithms, hybrid quantum algorithms and complexity theories.



Sophia Economou (c. 1980, Greek-American) is an Associate Professor in the Department of Physics at Virginia Tech College of Science. She previously worked at the US Naval Research Laboratory. She is a physicist specialized in the control of quantum dot semiconductor spins and their spin-photon interfaces. She is also a creator of advanced molecular simulation algorithms on quantum computers.



Ewin Tang (2000, American) published in July 2018 a paper demonstrating a classical recommendation algorithm as efficient as an algorithm designed for D-Wave quantum computers by Iordanis Kerenidis and Anupam Prakash in 2016⁹⁴. They responded by finding a flaw in the reasoning. On close inspection, the quantum algorithm would scale better in some extreme conditions. She was 18 years old at the time. Ewin Tang is now a computer scientist at the University of Washington.



Cyril Allouche (French) has been leading Atos R&D efforts in Quantum Computing since its beginning in 2015. Cyril Allouche are the "implementers" of the quantum vision of Thierry Breton, CEO of Atos until 2019. His work encompasses developing the aQASM (Atos Quantum Assembly Language) quantum programming language and the myQLM quantum programming emulator running on regular personal computers and servers.

⁹⁴ See [A quantum-inspired classical algorithm for recommendation systems](#), Ewin Tang, July 2018 (32 pages) and [Major Quantum Computing Advance Made Obsolete by Teenager](#) by Kevin Harnett, July 2018.

Here we are. We've covered a whole lot of people and probably missed many who should be in this hall of fame list! I'll update it whenever required. We will encounter many of these scientists in this book.

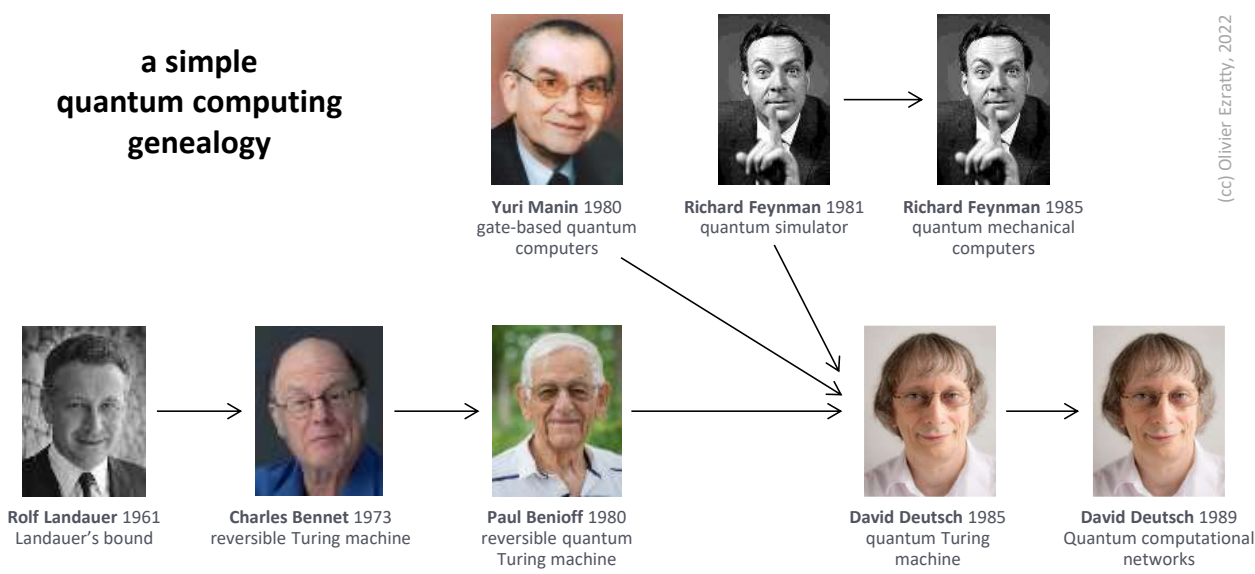


Figure 58: quantum computing genealogy to remind us that other scientists than Richard Feynman have to be remembered for their contribution. (cc) compilation Olivier Ezratty, 2022.

Research for dummies

As I investigated the broad quantum science and technology landscape, I learned more on how fundamental and applied research was operating.

I did not know much about it before this adventure. Working in the 'digital world', as a developer, marketer and in the entrepreneurial ecosystem doesn't necessarily make you look deeply into the inner workings of research. I discovered many aspects that I am detailing here, particularly with regards to practices, lingua-franca, careers and evaluations.

If you're a researcher, this is very basic stuff that you already know fairly well. For others, it will clarify some of vague understanding you might have on how research works.

Long-term

The first key point is the long-term approach in quantum technologies. It can also be found in other branches of physics and so-called deep-tech related sciences. Time scales are measured in decades. It starts with intuitions, creativity, passion, rigor and hard work. These ideas are not always broadly adopted right away. There's always some resistance with the current scientific establishment.

This long-term history can be observed in condensed matter physics. Brian Josephson devised the Josephson junction in 1962. IBM tried to use it unsuccessfully to build superconducting computers. Anthony Leggett made significant discoveries in the early 1980s which led to the creation of the first superconducting qubits in the early 2000s and to Google and IBM's superconducting machines between 2016 and 2020. And we're not done there since this technology's scalability has not yet been proven.

Alain Aspect's work, which started in the late 1970s and culminated with his 1982 experiment had no immediate industrial application. Fortunately, he was well supported by many laboratories, particularly to build the necessary instrumentation. His work led to the creation of many of the branches of quantum technology. For example, Artur Ekert was inspired by Alain Aspect's work to advance the field of quantum cryptography in the early 1990s.

All of this cannot be meticulously planned in advance. Research serendipity must prevail. Commercialization comes later, through meetings between specialists from different and complementary disciplines. Innovators are either the researchers themselves, or more generally others, engineers and entrepreneurs, who know how to detect research work having some business potential. Hence the importance of bringing them together in innovation ecosystems. However, in its current shape, the quantum startup ecosystem is mostly made of researchers turned into entrepreneurs.

This generates its share of misunderstandings with public authorities. They are tempted to over-evaluate and measure the performance of basic research, if not to fund it, using only criteria from the business world. On the other hand, and this is particularly true for quantum technologies, research work requires peer reviews. This may give the impression that researchers are both judge and jury. To prevent this from driving decision-makers and people suspicious, research work must honestly be translated in layman's terms. This should encourage researchers to communicate with broader audiences than their peers. It requires leadership. Scientists must be more involved there, particularly in those times where people are more and more skeptic on science and innovation.

Publications

This book contains many references to scientific publications. I do this almost systematically and always look for the original scientific publication whatever the news.

Research is now frequently published first in open access in the famous **arXiv** site managed by Cornell University. These are articles pre-prints that have not yet gone through peer reviewing and be published in peer-reviewed journals. These articles must sometimes be taken with a grain of salt. However, they allow authors to collect comments from informed readers. Their quantity and quality depend on the author's fame, the topic and the number of researchers who master it⁹⁵.

Between 9 and 18 months later, a paper publication in a peer-reviewed journal may follow. If the delay is too short, it may mean the journal is a predatory one. It is usually published mostly as is, includes some revisions suggested by the "referees" of the review committees, or even with a change of title. In these cases, the version published on arXiv is not necessarily the most recent. It is sometimes updated. The benefits are openness and free access.

As a general rule, when I discover the existence of an article, I search for it on Google Search with the name followed by "filetype:PDF" and I find it free of charge in more than 90% of the cases on arXiv or on the ResearchGate site, the researchers' reference social network.

Quantum technologies peer-reviewed⁹⁶ journals include **Nature** and its various thematic variations like **Nature Communications**, **Science**, **Physical Review X**, **Physical Review Research**, **Physical Review Letters**, **Quantum Science and Technology**, **Journal of Applied & Computational Mathematics**, **International Journal of Quantum Information**, **Quantum Engineering**, **Advanced Quantum Technologies**, **Quantum Journal**, **Quantum Information Processing**, **IEEE Journal of Quantum Electronics**, and **IEEE Transactions on Quantum Engineering**. Fortunately, in this field, there are only a few predatory journals that do not have peer-review process and charge researchers for their work publication.

⁹⁵ See [Comment bien lire et comprendre une étude scientifique](#) par Gary Dagorn, Mathilde Damgé et Bessma Sikouk, May 2021. It provides a lot of insights on how to read a scientific paper. You can translate this article in French in your browser. Also look at [Ten simple rules for reading a scientific paper](#) by Maureen A. Carey, Kevin L. Steiner and William A. Petri Jr, July 2020.

⁹⁶ In peer-reviews journals, the reviewers are unknown to the paper authors. They provide some feedback on the paper and expect a paper update. The authors provide an updated version and comments that are either accepted or rejected by the reviewer. It can lead authors to modify their claims and even their paper title. When everything's finalized, the paper can be published. Nowadays, the initial paper published on arXiv is also updated to reflect these changes. There is also a special double-blind review process where the authors are unknown from the reviewers to avoid any reviewer bias. I have bumped only once on such a case in quantum technologies, on a QML algorithm: [On the universal approximability and complexity bounds of deep learning in hybrid quantum-classical computing](#), 2021 (15 pages).



Figure 59: some key quantum physics peer-review publications.

In most scientific fields, including quantum science, there are many publications but not enough skilled reviewers. This job is sometimes done by PhD students. Sometimes, innovative papers are locked by reviewers, particularly when they are cross-discipline, which is frequently the case with quantum science and is a problem when publications are over-segmented.

arXiv is unlocking this situation and is now common practice. It enables fast turnaround for debates between scientists⁹⁷. It also makes it easier for students and others to create their bibliography and review papers. It however doesn't seem that quantum research is prone to significant paper-milling or even to papers being retracted⁹⁸. On the **RetractionWatch** [database](#), you can find only a few retracted papers in quantum physics, mostly coming from China and India (102 items with “quantum” in the title). It includes the famous retracted papers from The Netherlands and Denmark on Majorana fermions.

There are other sites for pre-prints like arXiv, with for example **engrXiv** on engineering (with some papers related to quantum technologies). And **viXra** is an arXiv for the preprints that will never be published in peer-reviews publication and are too fringe to be accepted on arXiv (vixra.org/quant).

PhD theses are easier to retrieve and are generally published freely. These are usually good sources of bibliographical information. Beyond the main thesis goal that is to advance science in a usually narrow domain, it generally starts with making an inventory of the state of the art, like in review papers. Review papers present a state of the art of a field. Their bibliography is generally impressive, sometimes as long as the paper itself. They are a good starting point to study a subject, especially if the paper is not too old. I provide links to many such review papers, particularly on specific qubit types. If the author's pedagogy is good, it can be very useful for learning on your own. A bibliography generally allows you to go deeper into the subject by discovering the need-to-know fundamental texts.

Several authors are usually mentioned in scientific papers, up to a very large number. In general, beyond three authors, the first is the one who was the owner and done the bulk of the work. It's usually a PhD student or a post-doc. He/she has processed the experience and written a large part of the document, but this may depend on countries, laboratories and thesis supervisors. The last one is the thesis or research laboratory supervisor⁹⁹. In the latter case, the penultimate author is the thesis director who supervised the work. In between are the other contributors, experimenters or simple reviewers.

⁹⁷ Like with [Reply to arXiv:2203.14555](#) by Margaret Hawton, May 2022 (1 page) that is a reply to [A Comment on the "Photon position operator with commuting components"](#) by Margaret Hawton and A. Jadczyk, March 2022 (4 pages). See also [Is the Moon there if nobody looks: A reply to Gill and Lambare](#) by Marian Kupczynski, September 2022 (8 pages) which is typical of the debates going on with quantum foundation topics and on the nature of reality.

⁹⁸ See [The fight against fake-paper factories that churn out sham science](#), Nature, March 2021.

⁹⁹ This is the case of these hundreds of publications with the famous Didier Raoult who is cited as the last contributor, as laboratory director but not necessarily thesis director.

Some papers have a very large number of authors. It is typical from the papers published by Google AI which can have upwards of 80 coauthors, which means about half of their whole team. They probably all contributed to the published work but certainly not equally¹⁰⁰.

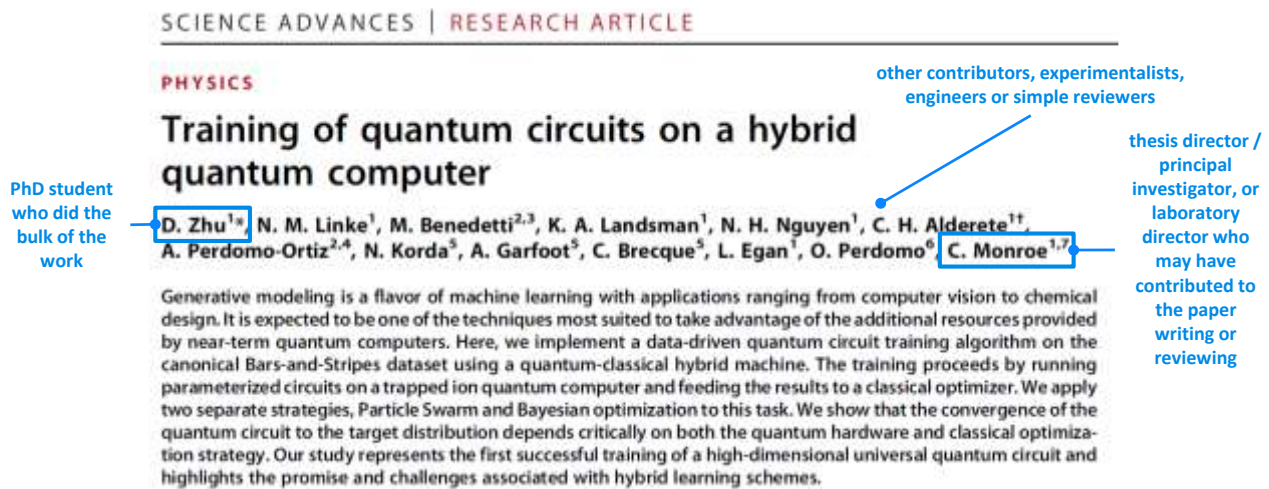


Figure 60: typical presentation of scientific paper's co-authorship. Source: [Training of quantum circuits on a hybrid quantum computer](#) by D. Zhu, Christopher Monroe et al, 2019 (7 pages).

Well crafter papers don't forget to mention the respective contribution of all the authors, like in the example below. It also mentions reviewers (not those from a peer-review publication), research funding source, any potential competing interest, how the research data can be accessed and the availability of any supplemental material, that is now usually placed at the end of papers in their pre-print format. These supplemental materials can contain technical details and can be very interesting, like for example, to describe the experimental setup and its hardware and/or software engineering.

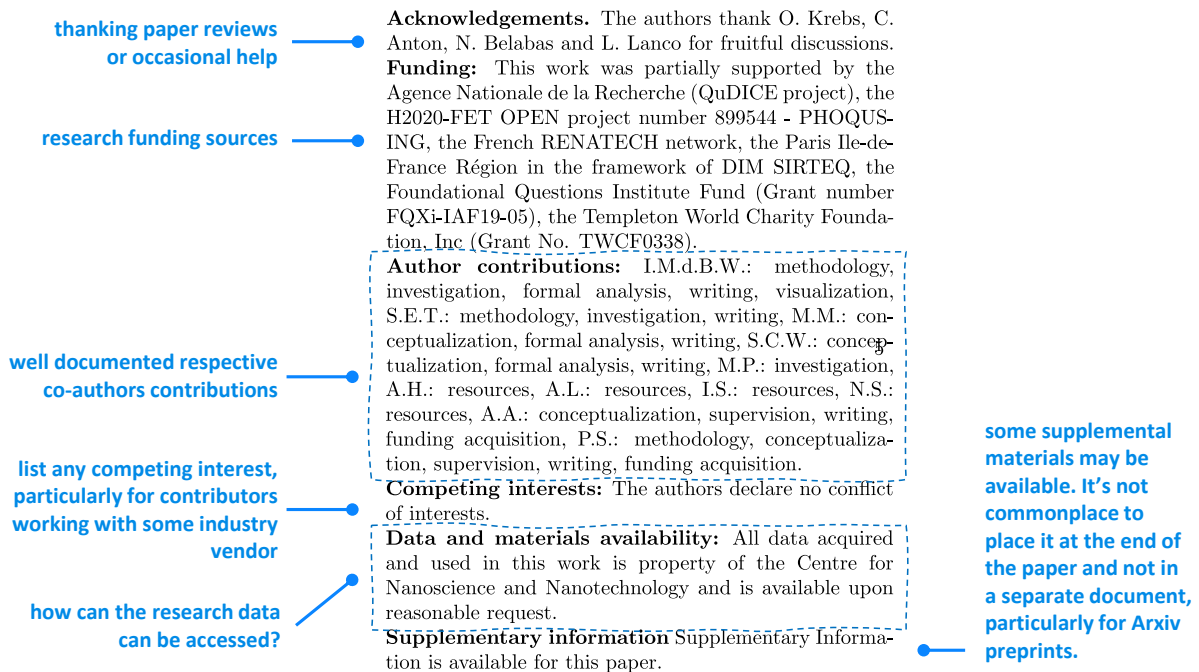


Figure 61: typical credits at the end of a scientific paper. Source: [Coherence-powered work exchanges between a solid-state qubit and light fields](#) by Ilse Maillette De Buy Wenniger, Maria Maffei, Niccolo Somaschi, Alexia Auffèves, Pascale Senellart et al, April 2022 (17 pages). This is the typical requirement for some peer-reviewed publications like Nature.

¹⁰⁰ I found out this extreme case in [Search for a massless dark photon in \$\Lambda_c^+ \rightarrow \text{py}'\$ decay](#) by BESIII Collaboration, August 2022 (8 pages) with 573 authors from 75 research organizations, in China. For just 8 pages!

The other extreme case is a paper having only a single author. It means first that it is probably not a PhD student, otherwise his PhD supervisor would be a coauthor, or the author is a PhD but he lost the support of his/her supervisor for whatever reason, which is bad omen and very rare. Second, you can look at whether he/she works in a research institution and his CV. At last, you can assess the author's network if he/she mentions and thanks reviewers or contributors. The author may be already famous like say a John Preskill, Peter Shor, Seth Lloyd or Scott Aaronson, so no problem. Other cases with no attached institution, record or network may mean that the author may be working on some fringe theories in a very isolated fashion, particularly if there's no mention of any help or thanks to anybody for the research.

In many countries, such as the USA, it is common practice to mention authors with the initials of their first and middle names initials. It does not make it easy to search them online, especially for Chinese authors. This is particularly the case when there are many contributors. I try to quote authors with their first name when they are easy to be found.

In the thousand footnotes in this book, I otherwise take the liberty of not using the cryptic description convention that is used in the abundant bibliographies of scientific publications, sometimes using authors, publication references but not the paper title!

¹⁷K. O'Brien, C. Macklin, I. Siddiqi, and X. Zhang, *Phys. Rev. Lett.* **113**, 157001 (2014).

¹⁸T. C. White, J. Y. Mutus, I.-C. Hoi, R. Barends, B. Campbell, Y. Chen, Z. Chen, B. Chiaro, A. Dunsworth, E. Jeffrey *et al.*, *Appl. Phys. Lett.* **106**, 242601 (2015).

¹⁹C. Macklin, K. O'Brien, D. Hover, M. E. Schwartz, V. Bolkhovskiy, X. Zhang, W. D. Oliver, and I. Siddiqi, *Science* **350**, 307 (2015).

Figure 62 : why (t.h.) these long bibliographies do not contain any title?

I use a clear title convention followed by first author/authors, sometimes their research laboratories or companies, publication date and then number of pages or slides, which helps you identify at a glance the volume and depth of the referenced documents. And footnotes may be cumbersome, but they prevent you from looking at bibliographical references at the end of the document, which is never very practical whether you read a paperback or electronic version of the document. When I don't mention all a paper's contributors, I use the expression "*et al*" which is an abbreviation of the Latin "*et alia*", meaning "*and the others*". I'm usually selecting the first and last authors, then in the middle those I happen to know some way or the other, as described in Figure 63.

³⁸⁶ See [Correlated charge noise and relaxation errors in superconducting qubits](#) by C.D. Wilne, Roger McDermott et al, Nature, December 2020 on Arxiv and June 2021 in Nature (19 pages) which describes the correlated errors appearing in superconducting qubits and how it could impact the architecture of quantum error correction codes and [A potential hangup for quantum computing: Cosmic rays - For quantum chips, the problems they cause are too big for error correction](#) by John Timmer, ArsTechnica, December 2021, referring to [Resolving catastrophic error bursts from cosmic rays in large arrays of superconducting qubits](#) by Matt McEwen, Rami Barends et al, Google AI, Nature Physics, December 2021 (13 pages) who developed a test protocol to assess the impact of radiations on 26 qubits in its Sycamore processor.

³⁸⁷ See [Impact of ionizing radiation on superconducting qubit coherence](#) by Antti P. Vepsäläinen, William D Oliver et al, August 2020 (24 pages), the source of the illustration.

Figure 63: bibliographical references as presented in this book. I find it more practical although it doesn't seem to be orthodoxal.

Paper communication

These scientific publications can be discovered by following the RSS feeds of arXiv, reference specialized papers, in addition, from scientific news feeds of online media or popular scientific press. I also discover new interesting papers with scanning scientific conferences presentations¹⁰¹.

In the case of quantum technologies, the "tech" media often broadcasts scientific news dressed-up with sensationalism and exaggerations. This often stems from the propensity of laboratory communicators or sometimes researchers themselves to make shortcuts between their work and its potential

¹⁰¹ Here is an example with a list of many IEEE [superconducting technologies presentations](#).

usage that may be very long-term¹⁰². It is even stronger when the communication comes from a large company such as Google or when the article was written by the laboratory's communication branch.

The job of the technology screener consists in sorting this out. When your local non-English speaking media broadcasts such information, it is often necessary to start by identifying the original paper which is possibly quoted at the end of the article. Sometimes, you discover blatant translation error that entirely twists the scope of the covered scientific advance.



this would mean they are building some sort of quantum computer...

... but it's just about a new sensor measuring the quality of superconducting qubits using some new materials

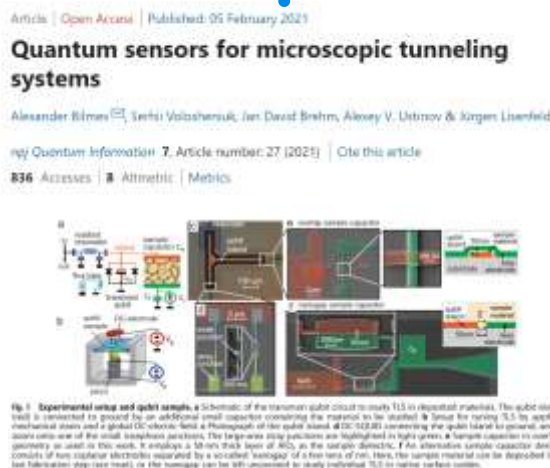


Figure 64: example of a scientific paper presented with outrageous claims by its lab communication department. Sources: [Scientists Take Step Towards Quantum Supremacy](#), MISIS, March 2021 and [Quantum sensors for microscopic tunneling systems](#) by Alexander Bilmes et al, February 2021 (6 pages).

Analysis and classification

Next, one must find the original scientific article with the methods described above. Once all this has been done, the bulk of the work consists in classifying the information: what is it about and how does it fit into the web of quantum technologies? As far as I know, no artificial intelligence can automatize this process¹⁰³. This classification task is a tedious one and you can be easily misled with reading a paper title or press release too quickly. Here is one interesting example with a post from James Dargan in The Quantum Insider which wrongly described the European LSQuanT project as an initiative to provide quantum computing solutions to the transportation industry¹⁰⁴. Wrong! It is a project related to fundamental quantum physics and digital simulation of quantum transport, a condensed matter phenomenon!

What is the actual progress made with regards to the state of the art? You can rely on classical recommendations: read the introduction and not just the abstract, identify the problem that the writers are trying to solve and how they are advancing the state of the art, look at the data and identify any missing data, and read the conclusion. If you can't decipher the paper content, make a search of other more generalists web sites mentioning it.

¹⁰² The example below comes from [Scientists take step towards quantum supremacy](#) by National University of Science and Technology MISIS, March 2021. The supremacy from the article title is very far away considering the paper is about some sensing technology to measure the efficiency of some superconducting qubit.

¹⁰³ Various tools attempt to automate this sorting work, such as [In Layman's Terms: Semi-Open Relation Extraction from Scientific Texts](#) by Ruben Kruiper et al, May 2020 (13 pages). It is currently applied to the field of biology.

¹⁰⁴ See [LSQuant: Novel Initiative Created To Improve Quantum Transport Methodologies](#), May 2021.

In general, a paper presenting a breakthrough that will allow the quantum computer to be realized at room temperature or ahead of all others becomes a simple very one-time breakthrough in the development of a particular type of qubit. It looks like your tiny hairy dog after the shower! In many cases, quantum science-related papers are inaccessible, requiring solid mathematical and/or physics background. Even quantum science specialists have a hard time interpreting many papers.

You frequently come across a set of Russian dolls concepts with unknown concepts referring to other unknown concepts, and so on. This is some sort of involuntary humor of scientific complexity¹⁰⁵. However, hopefully, some papers do not use too much jargon and manage to deal with a big fundamental question by making it understandable to many specialists in their discipline and well beyond. This is often the case with publications in Nature.

How can I check the whole thing, particularly given the specialists in my own network have not yet had the time to do so? You either need to be patient, do it on your own, or look for someone who has done the job. For big news related to quantum computing, one can wait for the next post from Scott Aaronson or a laconic tweet from John Preskill.

Finally, I use arXiv as soon as I come across a startup that defines in too broad terms what it does without any technology specifics. It's so commonplace now! A search starts with finding the startup scientific founder, then with identifying their research work that they are probably willing to package in their freshly created startup. In their bibliography building work, researchers also look at **Google Scholar** and also on **SciRate**, where discussions take place around pre-print papers published on arXiv.

We must recognize our limits and understand that we're not protected from believing scientific hoaxes like the famous one created by **Alan D. Sokal** in 1996. It merged social sciences and quantum gravity and was published in a social science publication, not a quantum physics one¹⁰⁶.

Hopefully, quantum scientific publications are way more serious than most of the quantum hype that is conveyed by general news with their amazing amplification capabilities. You'll read time and again that quantum computing will drive autonomous cars, create quantum intelligent robots, reduce CO₂ emissions, cure cancers, help Tesla (but not others) build top-notch batteries or that quantum communications will teleport your data faster than light around the Earth. Most of these assertions will flourish when the IBMs and Googles of this world make fancy announcement or after your government launches its own "billion dollars" national quantum plan. But they are at least unproven if not entirely false. Who's going to reveal it to you?

Roles

In most countries and in all disciplines, several roles can be distinguished in research organizations.

Doctoral students are students who are undertaking a doctoral thesis (PhD, for Philosophy Doctorate, for any science). It lasts from three to five years depending on the country. This thesis completes a higher education program in the University.

¹⁰⁵ Here are a couple interesting examples of papers whose title refers to mostly unknown concepts: [The Franke-Gorini-Kossakowski-Lindblad-Sudarshan \(FGKLS\) Equation for Two-Dimensional Systems](#) by Alexander A. Andrianov et al, April 2022 (27 pages), [Floquet integrability and long-range entanglement generation in the one-dimensional quantum Potts model](#) by A.I. Lotkov et al, October 2021-April 2022 (24 pages), [Probing Lorentz-Invariance-Violation Induced Nonthermal Unruh Effect in Quasi-Two-Dimensional Dipolar Condensates](#) by Zehua Tian et al, May 2022 (12 pages), [Emergent quantum mechanics of the event-universe, quantization of events via Denrographic Hologram Theory](#) by Oded Shor et al, August 2022 (12 pages) and [Emergent Sasaki-Einstein geometry and AdS/CFT](#) by Robert J. Berman et al, Nature Communications, January 2022 (8 pages) which I found has some connections with [Exploring uberholography](#) by Dmitry S. Ageev, August-September 2022 (14 pages) which deals with some quantum error correction code. To some extent, this complexity can be fun. See also [Variational quantum algorithm for measurement extraction from the Navier-Stokes, Einstein, Maxwell, Boussinesq-type, Lin-Tsien, Camassa-Holm, Drinfeld-Sokolov-Wilson, and Hunter-Saxton equations](#) by Pete Rigas, September 2022 (144 pages) which requires a significant mathematical background.

¹⁰⁶ See [Transgressing the Boundaries: Towards a Transformative Hermeneutics of Quantum Gravity](#) by Alan D. Sokal, 1996 (39 pages).

Post-docs or post-doctoral researchers are researchers who, after having obtained their PhD, conduct research in a laboratory under a fixed-term contract. They sometimes do several post-docs in different locations, frequently out of their originating country. It is the anteroom of a full-time research position.

Researchers have a full-time tenure in a research organization whether in the industry or with government funded research organizations. In many countries, they are also civil servant researchers recruited through some open competitions process .

Habilitation to Direct Research (HDR in France) allows a tenured researcher to direct the thesis of one or more doctoral students as a thesis director and to obtain a university professorship. The rules vary from country to country, such as having completed two doctoral theses and having published internationally recognized work in one's field¹⁰⁷.

Research Directors are researchers with the possibility to autonomously determine the field of their research work. They supervise several doctoral students and post-docs when they are successful with finding the related public and/or private funding. They are also selected by competition in research institutions. Depending on the country and research organization, there are several grades in the function, linked to advancement over time and merit.

Principal Investigators are lead researchers who are in charge of the preparation, conduct, resources allocation and administration of a research grant for which they are the project lead researcher and main holder. Sometimes, a PI is synonym of laboratory director or research group leader.

In addition to these roles, let's not forget the **laboratory technicians** who set up the experiments and about whom less is said and the **engineers** who can play a role in the creation of many scientific instruments.

h-index

The h-index, named after its creator Jorge Hirsch in 2005, is an index that quantifies a researcher's productivity and scientific impact. It is based on the level of citations of his scientific publications in peer-reviewed journals. It is a bit like a PageRank for a website, but a simpler one. It is an integer corresponding to the number of papers h that have each obtained more h citations in other papers.

The level of h-index can be used as a quantitative data for obtaining a position as a resident researcher (10-12), professor (>18) or member of an academy of science (>45). As with any composite index¹⁰⁸, it generates side effects: a race to “publish or perish” papers of little incremental value, cross-referencing between researchers, self-citation, an abundance of co-authors¹⁰⁹, etc.

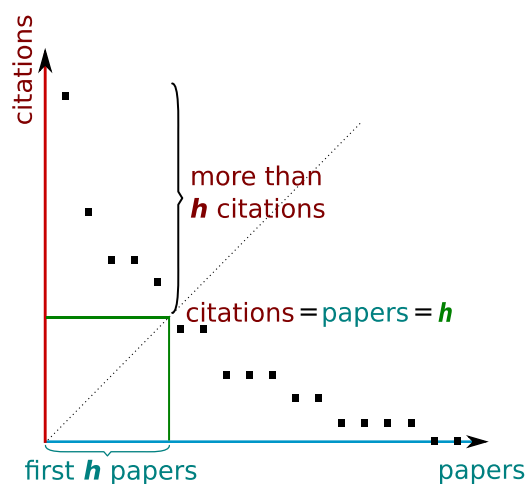


Figure 65: h-index explained graphically.

The discrepancy of h-index is quite high with researchers with a Nobel prize in physics with low index like with John Clauser (29, Nobel in 2022) and Brian Josephson (22, Nobel in 1973) and very high index like Anton Zeilinger (139, Nobel in 2022) or David Wineland (122, Nobel in 2012).

¹⁰⁷ This habilitation replaced the Doctorat d'Etat in 1984 in France. The HDR is considered to be a diploma. It is awarded on free application by the research commission of the Universities which deliberates in the form of a jury.

¹⁰⁸ The Shanghai ranking list of universities comes to mind.

¹⁰⁹ In this paper from Google, we have no less than 85 co-authors: [Implementing a quantum approximate optimization algorithm on a 53-qubit NISQ device](#) by Bob Yirka, February 2021 (19 pages). It's a bit too much and we can wonder about their all contributions!

Some alternatives indexes have been proposed like the recent h-frac, but not yet adopted¹¹⁰. It remains, however, an interesting indicator of the influence of researchers and their production volume.

On average, the h-index of a researcher in physics is close to the length of his career since his PhD. It obviously evolves over time. It is full of flaws like all quantitative indicators. For example, the basic h-index does not distinguish between main author and co-author. Hence the abundance of authors cited in many papers, some of them having made only marginal contributions.

The index is usually calculated from **Google Scholar** data, but it is sometimes found calculated only on the SemanticScholar website. The most serious index is provided by the Website of **Science** because its database is the cleanest.

Open research

On top of being published in open source as pre-prints, research results and datasets can be published in various platforms like **Zenodo**, which was developed under the European OpenAIRE program and is operated by CERN. The deposits can contain research papers, the experiments data sets, research software, detailed reports and any other digital artefacts. Using this sort of service is becoming common practice, to make sure experiments are reproducible. Other services like **OSF** (Open Science Framework) also promote open research practices.

Fake news

Science is not exempt of fake news. In all scientific fields, some researchers may publish questionable results for their experiments, aggregate and compile tinkered data, or simply avoid taking into account embarrassing data, generating a survivor bias. This can happen in quantum technologies, particularly when evaluating the quality of experimental qubits or, for instance, finding Majorana zero modes, *aka* fermions. In general, you need to be an expert in the field to identify this kind of abuse. They however seem rare in quantum technologies.

With a generalist technological knowledge in the domain, one can start to detect tricks of the trade or exaggerations. This is easier to do with commercial vendors like with IBM and their quantum volume, Honeywell and their "*most powerful quantum computer in the world*" or with the Google and Chinese quantum supremacy experiments.

Poster sessions

In a scientific conference, a "poster session" is usually a part of the conference dedicated to the presentation of researchers' projects during a break, in a dedicated area.

Researchers display a poster describing their research work and talk with conference participants as they stroll through the conference exhibition area during dedicated breaks. It is an exercise in humility reminding what Jehovah's witnesses are doing in the streets.

Figures of merit

This common expression broadly describes a set of specifications and the success metrics to be achieved to bring a given technology to fruition. DiVincenzo's qubit technology criteria can be considered a figure of merit for success for quantum computing. It usually provides a roadmap and set of goals for researchers and technology vendors.

¹¹⁰ See [The h-index is no longer an effective correlate of scientific reputation](#) by Vladlen Koltun and, David Hafner, Intel Labs, February 2021 (26 pages). Among other things, the authors found out that the correlation between h-index and scientific awards in physics is declining. They propose an alternative index named [h-frac](#), for h-fractional, that improves the correlation between the index and other scientometric measures like scientific awards. It allocates citations fractionally and evenly among all coauthors of scanned papers to avoid the phenomenon of low-contribution hyperauthors.

International

Nowadays, all modern countries have crafted their “quantum national plan” with a certain willingness to better control their sovereignty. It’s like being the first with the atomic bomb during World War II.

But let’s remember that international collaboration between researchers is intense. Most of those I met in French laboratories collaborate with colleagues either in Europe within the framework of Europe 2020 projects, the European Flagship or for some ERCs.

They also collaborate with researchers outside the European Union, particularly in Asia (Japan, Singapore), as well as in the USA, UK, Switzerland and Australia¹¹¹.

Quantum science knowledge is quite open and is rather well shared on a global scale. This is encouraged by many international scientific conferences where knowledge is being built, researchers get to know each other, and joint projects are being launched. This is one of the reasons why I don't believe in the existence of a supposed quantum computer whose capabilities would defy understanding and which would be hidden in the basement of a secret NSA datacenter to break all the RSA keys of the Internet.

Scientific nationalism in quantum technologies finally comes into play further downstream of research, when it comes to transforming it into industrial advantage. Technologies often have their "magic sauce", as in semiconductor manufacturing processes. This has always been the case in digital technologies.

Technology Readiness Level

This technology readiness level notion is commonly used in deep techs. It describes the level of maturity of a technology with a scale from 1 to 9. It follows a relatively standardized classification initially created by NASA in 1975¹¹², then used by the European Union and various other organizations. It was initially mainly used in the aerospace, defense and energy industries.

This scale can have several use cases. It is used to assess the level of risk and maturity for an investor in a startup. Very advanced deep techs are also the playground of TRL and quantum technologies are no exception.

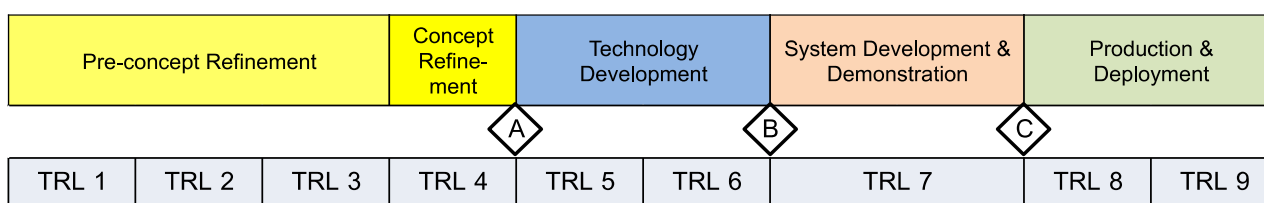


Figure 66: the scale of technology readiness level. Source: [Some explanations on the TRL \(Technology readiness level\) scale](#), DGA, 2009 (15 pages).

The TRL scale has 9 levels¹¹³:

- **TRL 1:** basic principles are described or observed, at the theoretical or experimental stage.
- **TRL 2:** technological concepts are formulated and not yet necessarily tested.
- **TRL 3:** proof of concept is carried out in a laboratory, at the level of the technical process.
- **TRL 4:** the technology is validated in the laboratory as a whole.

¹¹¹ This can also take the form of CNRS International Mixed Units such as those established in Japan and Singapore.

¹¹² See [Technology Readiness Levels at 40: A Study of State-of-the-Art Use, Challenges, and Opportunities](#) by Alison Olechowski et al, 2015 (11 pages) which is the source of the diagram.

¹¹³ See [Technology Development Stages and Market Readiness](#) by Surya Raghu, June 2017 (35 slides).

- **TRL 5:** a technology model in a production grade environment is created.
- **TRL 6:** a technology prototype is demonstrated in an environment representative of the intended use case.
- **TRL 7:** a prototype is evaluated in an operational environment.
- **TRL 8:** a complete system has been evaluated and qualified.
- **TRL 9:** a complete system is operational and qualified in production.

The relevance of the solution to market needs is missing at this scale, but it is a marketing rather than a technical consideration¹¹⁴. Most of the time, it more or less coincides with TRL levels 7 to 9 since reaching this scale requires funding and finding customers willing to test the solution.

Kristel Michielsen has proposed a scale suitable for quantum computing, the **QTRL**, for the Quantum Technology Readiness Level in Figure 67. Her assessment of some technologies can be argued. For example, she positions D-Wave's quantum-annealed computers in TRL 8 and 9. This is commercially correct since these computers are well marketed. This being said, if they are well available physically, it is not proven that they are of much use at the moment.

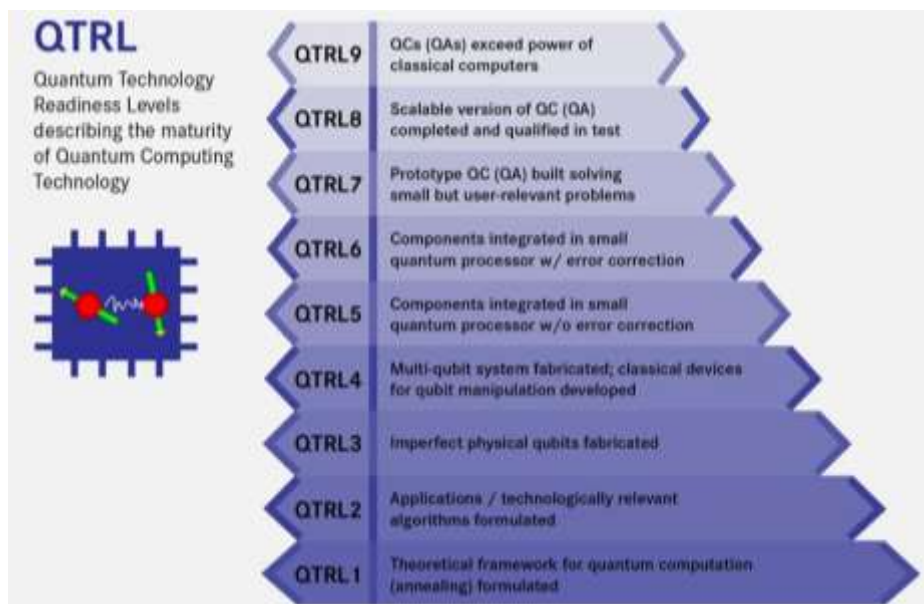


Figure 67: the quantum TRL scale, created by Kristel Michielsen. Source: [Simulation on/of various types of quantum computers](#) by Kristel Michielsen, March 2018 (40 slides).

The specificity of quantum technologies is that many hardware startups are created with very low TRLs. This is particularly true for those who are starting to design qubits using technologies that have not yet been proven, even in the labs. In quantum technologies, the notions of "MVP" (minimum viable product) are very different from the classical digital world. It's based on scientific rather than functional metrics. We have many such startups around in quantum technologies because of the famous FOMO (fear of missing out) syndrome with investors.

This shows up with investors who fear of missing the future golden goose or unicorn. They are ready to overinvest in companies they perceived will be the future market champion. This explains for example the level of funding for startups like **Rigetti** and **PsiQuantum** or the new SPAC funding mechanism (special purpose acquisition company) implemented by **IonQ**, **Rigetti** and **D-Wave** and the recent quantum business spin-off from **Honeywell** and its merger with **CQC** (becoming **Quantinuum** in December 2021).

¹¹⁴ See [TRL, MRL, POC, WTF?](#) by Massis Sirapian of the Defense Innovation Agency, April 2019.

Quantum physics history and scientists key takeaways

- A first wave of 19th century scientists laid the groundwork that helped create quantum physics afterwards (Young, Maxwell, Boltzmann, mathematicians). The photoelectric effect, black body spectrum and atoms emission or absorption spectrum were not explained with the current theoretical frameworks.
- Starting with Max Planck, a second wave of scientists (Einstein, De Broglie, Schrodinger, Heisenberg, Dirac, Born, Von Neumann) created quantum physics to describe light/matter interactions, energy quantification and wave-particle duality. It solved most of the 19th century unexplained physics experiments.
- These scientists were theoreticians while many lesser-known researchers were experimentalists with landmark discoveries (superconductivity, electron interferences, Stern-Gerlach experiment, ...).
- After World War II all digital technologies (transistors, lasers, telecommunications) were based and are still based on quantum physics, as part of what is now called the first quantum revolution.
- Since the 1980s and thanks to advances in individual quantum objects control and the usage of quantum superposition and entanglement, new breeds of technologies were created, most of them belonging to the “quantum information science” field and being part of the second quantum revolution.
- Many of these research programs were funded by governments after Peter Shor’s integer factoring algorithm was created.
- While the first quantum revolution was driven by research coming mostly out of Europe, the last wave comes out of all developed countries across several continents (North America, Europe, Asia/Pacific).

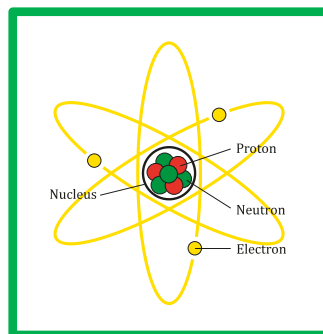
Quantum physics 101

After a historical review of quantum physics and computing with its most important contributors, let's look at the fundamentals of quantum physics in a more structured way. Whatever the ups and downs, this field has gone through the test of time for nearly a whole century. Thousands of experiments have validated the theory and mathematical formalism behind it even though we still can't explain what's happening at a physical level, particularly with quantum entanglement or, even, with the wave-particle duality phenomenon with electrons and photons.

Several years of undergraduate and graduate studies are usually necessary to master quantum physics notwithstanding its rich mathematical foundations. This part will save you some of this time and provide some scientific background knowledge that will help you better understand the various quantum information systems exposed in the remainder of this book.

As seen before, quantum physics appeared at the beginning of the 20th century to explain the dynamics of elementary particles, particularly to study how **photons**, **electrons** and **atoms** behave and interact¹¹⁵. Quantum physics also deals with elementary particles from the standard model like quarks and neutrinos, but it's out of scope in the second quantum revolution and quantum information science¹¹⁶. In some cases, we still care about atom nucleus spins, which relate to proton spins, itself linked to its quark constituents. Nucleus spin plays a role in NV centers-based technologies. We also care about it with electron spin-based qubits since nucleus spin can have a detrimental impact on electron spins handling qubits information. It relates to the kinds of isotopes of carbon and silicon that are used in carbon nanotubes and silicon wafers used to create electron spin qubits.

quantum physics deals with atomic and sub-atomic particles, and photons at this scale, matter behaves differently than macro objects in classical physics



atoms and electrons

elementary particles standard model

| | three generations of matter (fermions) | | | interactions / force carriers (bosons) | |
|--------|---|---------------------------------------|--------------------------------------|--|----------------------------|
| | I | II | III | | |
| mass | ≈2.2 MeV/c ² | ≈1.28 GeV/c ² | ≈173.1 GeV/c ² | 0 | ≈124.97 GeV/c ² |
| charge | 2/3 | 2/3 | 2/3 | 0 | 0 |
| spin | 1/2 | 1/2 | 1/2 | 0 | 0 |
| | u up | c charm | t top | g gluon | H higgs |
| | d down | s strange | b bottom | γ photon | |
| | e electron | μ muon | τ tau | Z Z boson | |
| | ν_e electron neutrino | ν_μ muon neutrino | ν_τ tau neutrino | W W boson | |

Labels on the right side of the table: GAUGE BOSONS (VECTOR BOSONS), SCALAR BOSONS.

Figure 68: what particles are we dealing with quantum physics? All of them, but in the second quantum revolution, we mainly use electrons, photons and atoms. Source: Wikipedia.

Quantum physics first helped explain various observations such as the **black-body radiation** (solved by Max Planck in 1900), the **photoelectric effect** (solved by Albert Einstein in 1905) and the **sharp spectral lines** observed with excited atoms like hydrogen (solved by Niels Bohr and its atom model in 1913).

¹¹⁵ As a reminder, here are the dimensions of elementary particles: 10⁻¹⁰m for an atom, 10⁻¹⁵m for the diameter of a hydrogen atom nucleus, thus of a single proton, and 10⁻¹⁸m for that of an electron.

¹¹⁶ See [Neutrinos as Qubits and Qutrits](#) by Abhishek Kumar Jha et al, March 2022 (30 pages) which makes a proposal to use neutrinos for quantum computing, without taking care of the related engineering problems. It's very hard to contain and control neutrinos!

Later on, in the mid 1920's, quantum physics was built upon a **mathematical formalism** using multi-dimensional Hilbert spaces and vectors. It centered around the **Schrödinger wave equation** which describes how a massive particle like the electron behaves over space and time, using complex number probability amplitudes and differential equations over time and space.

These provide a probabilistic insight on the outcome of the measurement of a particle's energy, momentum, and many other physical properties.

Quantum mechanics differs from classical physics with demonstrating how and why particles energy, momentum, angular momentum and other metrics are restricted to discrete values (**quantization**), objects can behave as particles or waves depending on the context (**wave-particle duality**), and there are limits to how accurately the value of a physical quantity can be predicted prior to its measurement, given a complete set of initial conditions (**indeterminacy principle**).

It also refers to **state superposition** which is at the basis of qubit operations and one of the sources of the quantum computers processing parallelism, **entanglement** which is a direct consequence of superposition applied to several quantum objects and is used with multi-qubits quantum gates and is also related to quantum communications and cryptography. Quantum objects **no-cloning** is a particular aspect of quantum physics that limits what we can do with qubits and how memory is managed. At last, **quantum tunnelling effect** has some impact in quantum technologies, like with the Josephson junctions used in superconducting qubits and with D-Wave quantum annealers.

Quantum physics explains other physical phenomena belonging to the broad **quantum matter** category, like **superconductivity** which plays a key role in superconducting qubits, **superfluidity**, used with liquid helium in dilution refrigerators and **quantum vacuum fluctuation** and its role in quantum decoherence. It also enabled the creation of **lasers**, used in many places like for controlling cold atom and trapped ion qubits and for all photonic based quantum computing and telecommunications. At last, **polaritons** are sets of interactions between light and semiconductors which could become useful in quantum sensing and quantum simulation. The quantum objects bestiary also includes **skyrmions** and **magnons**!

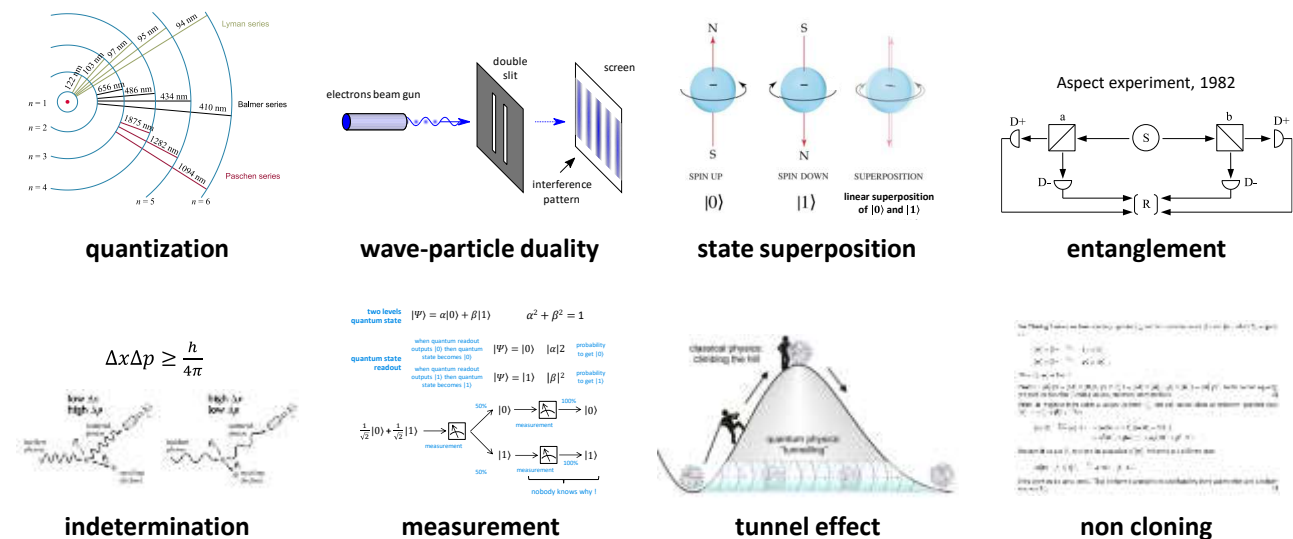


Figure 69: eight key dimensions of quantum physics that we are dealing with. (cc) compilation Olivier Ezratty, 2021.

Postulates

Quantum physics formalism is based on a set of postulates that follows¹¹⁷. Why are these postulates and not laws? Mainly because they describe a mathematical formalism that cannot be proved per se.

One of the other reasons is that quantum physics does not rely on an ontology describing the physical objects it's based upon. I'll try whenever possible to connect these postulates with some physical meaning. If all of this seems gibberish for you, skip it!

Postulate I - Quantum state: the state of an isolated physical system is represented, at a given time t , by a state vector $|\psi\rangle$ (psi) belonging to a Hilbert space H called the state space with vectors of length 1, using complex numbers. This is the canonical definition of a quantum state. The $|\psi\rangle$ vector contains the knowledge we can have of a quantum system, represented by the values taken by its measurable and compatible properties. A broader definition of a quantum state is the ensemble of values taken by compatible physical properties of a system made of one or several quantum objects. These compatible properties must be measurable simultaneously or in any order. The $|\psi\rangle$ vector is a mathematical object that helps determine and predict over time the probabilistic distribution of the various values of the quantum object compatible properties. The immediate consequence of this first postulate is the notion of superposition where a linear combination of several $|\psi\rangle$ vectors can form another valid quantum state. For a generic qubit, its quantum state defines its amplitude and phase as we'll see later in the Bloch sphere description. $|\psi\rangle$ is then a vector in a two-dimensional Hilbert vector space combining the $|0\rangle$ and $|1\rangle$ basis states with their related complex amplitudes.

Postulate II - Physical quantities: are related in quantum physics with observables that are mathematical operators \hat{A} acting on the $|\psi\rangle$ vector as $\hat{A}|\psi\rangle$. With the quantum matrix formalism, \hat{A} is a Hermitian (linear) matrix operator acting on the state vector $|\psi\rangle$ to evaluate quantized or continuous physical properties of quantum objects. This operator is a self-adjoint matrix, with the implication that several consecutive measurements generate the same (vector) result. A projector operator like a Pauli matrix σ_x , σ_y or σ_z used to measure a qubit state is a specific case of an observable operator.

By the way, let's clearly define properties and their variations:

Properties correspond to a quantum system's various observables. For a photon, it can be, for example its phase, polarization, and wavelength. In quantum physics, it is not possible to evaluate the values of all properties of quantum systems to describe it, due to Bohr's complementarity principle. Properties can also be continuous like a quantum object momentum or position.

Exclusive property values are the possible results of a quantum measurement of a quantized property. The classical examples are vertical and horizontal polarization for a photon or spin up or down for an electron spin along a projection axis. These are mutually exclusive since it corresponds to two results of a physical measurement. Mathematically speaking, two properties are exclusive if their projector operators (*aka* observables...) are orthogonal. Otherwise, these are non-exclusive properties.

Compatible properties of a quantum system can be measured in any order or simultaneously¹¹⁸. In that case, their observable operators A and B commute ($AB=BA$), or their commutator is equal to zero ($[A,B]=AB-BA=0$)¹¹⁹.

¹¹⁷ Source: [Wikipedia](#).

¹¹⁸ The notion of properties compatibility must not be confused with complementarity. There is complementarity between incompatible properties, like position and momentum! Incompatible observables are related to conjugate variables, defined by one being a Fourier transform of the other and Heisenberg's indeterminacy principle being consequently applied to both these variables measurement. See [Bohr's Complementarity and Kant's Epistemology](#) by Michel Bitbol and Stefano Osnaghi, 2013 (22 pages) which lay out well these different concepts.

¹¹⁹ Compatible properties are well explained in [Mathematical Foundations of Quantum Mechanics: An Advanced Short Course](#) by Valter Moretti, 2016 (103 pages).

Compatible properties have commuting observables. Measuring a complete set of commuting observables (CSCO) constitutes the most complete measurement of a quantum system.

Incompatible properties aka conjugate variables cannot be measured simultaneously and their observable operators A and B do not commute ($AB \neq BA$ or $[A,B] \neq 0$). This is a particularity of quantum mechanics.

However, revealing one property value with a measurement doesn't exclude revealing another property afterwards. But it is not possible to obtain exact knowledge of both properties at the same time (in the probabilistic sense and following Born's rule). At least one will be totally probabilistic. For a single particle, one example of incompatible properties or observables are two different spin components (X and Y or X and Z). After measuring the X spin component, a Z measurement will yield a random result. Also, the energy and position of an electron are incompatible properties.

Postulate III - Measurement: is the result of a physical quantity measurement with an observable operator A. The measurement result is one of the observable operator eigenvalues. We define eigenvalues [later](#) starting page 146 and cover the related mathematical formalism in the [measurement section](#) of this book starting page 184. This postulate is sometimes embedded or associated with the previous one. The observable operator doesn't generate a measurement result per se. It helps create a probabilistic distribution of the possible measurement outcomes of a property given what is mathematically known of the quantum object state vector. When applied to a quantum object vector, it creates another state vector along the eigenvectors of the observable operator. It can then serve to create a series of real numbers describing the probabilities of the various exclusive values a given property can take. The **expectation value**, or **predicted mean value**, is the average value of repeated measurements that would be obtained with the physical implementation of the observable. We'll come back to this [later](#) starting page 152. The measurement postulate is also named the Von Neumann measurement postulate.

Postulate IV - Born rule: when the physical quantity A is measured on a system in a normalized state $|\psi\rangle$, the probability of obtaining an eigenvalue α_n for discrete values or α for continuous values of the corresponding observable A is given by its squared amplitude of the related wave function. It is a projection on the corresponding eigenvector. This is related to Max Born's probability rule. A quantum state can be generally represented by a density operator, which is a square matrix, nonnegative self-adjoint operator ρ normalized to be of trace 1. The average expected value of A in the state ρ is $tr(A\rho)$, the trace (sum of diagonal matrix values) of the observable operator applied to the density matrix¹²⁰. This postulate is sometimes merged with the measurement postulate. This postulate is associated with the principle of spectral decomposition. For a single qubit, the Born rule is simple to describe with α^2 being the probability of getting a $|0\rangle$ and β^2 of getting a $|1\rangle$ when the qubit state is described as $|\psi\rangle = \alpha|0\rangle + \beta|1\rangle$ with α and β being complex numbers. And due to probabilities normalization, $\alpha^2 + \beta^2 = 1$.

Postulate V - State collapse: only one result is obtained after a quantum measurement. Two sequential measurements based on the same observable operator will always output the same value. For a qubit, after we measure its state, whatever it is, we get a $|0\rangle$ or a $|1\rangle$ and this becomes the new qubit state after measurement.

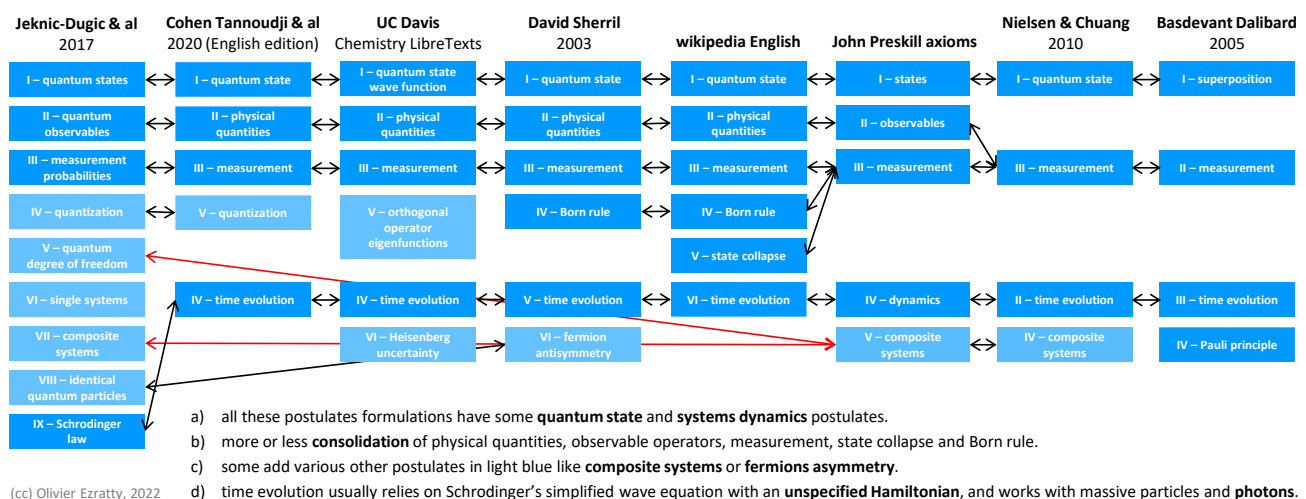
¹²⁰ There are variations of this postulate for various quantum spectrum (discrete and nondegenerate, discrete and degenerate, continuous and non-degenerate). Degenerate spectrum is defined in the glossary.

Postulate VI - Time evolution: the time evolution of the state vector $|\psi(t)\rangle$ is governed by the Schrödinger wave equation¹²¹. We don't directly deal much with time evolutions to understand quantum computing with qubits and gates, but it still plays a key role in quantum annealing and quantum simulation and, behind the scenes, in gate-based computing, with qubits decoherence, quantum noise, quantum error corrections mechanisms and measurement.

There is also a **Composition** postulate, which defines the notion of tensor product applied to separable composite quantum systems. *Aka* "Composite Systems" with John Preskill's axioms. We'll talk about it abundantly when covering [linear algebra](#) starting page 144 and [qubit registers](#) starting page 169.

There are indeed many variations of these postulates in shape, form, name and number, which ranges from 4 to 9 depending on the source¹²². Quantum State can become State Space and Physical Quantities become Unitary Dynamics¹²³. John Preskill lists five 'axioms', considering that postulates are axioms since they are not contradicted experimentally¹²⁴. There is not really a single "bible" of quantum postulates even when reading quantum physics founders writings (Bohr, Heisenberg and others) who didn't agree on all of it. I have consolidated below a table with some of these variations of postulates. Imagine if there were various versions of the Bible with 5, 7, 9, 10 and 12 commandments!

quantum physics postulates variations



(cc) Olivier Ezratty, 2022

Figure 70: a compilation of various inconsistent lists of quantum postulates and axioms. (cc) Olivier Ezratty, 2022.

Mostly covered in [linear algebra](#) section starting page 144, the main related quantum physics mathematical tools are:

- **Linear algebra:** complex numbers, eigenvectors, eigenvalues and eigenstates.
- **Functional analysis:** Hilbert spaces, Hermitian matrices, linear operators, spectral theory.
- **Differential equations:** partial differential equations, separation of variables, ordinary differential equations, Sturm–Liouville problems, eigenfunctions.
- **Harmonic analysis:** Fourier transforms and series.

¹²¹ As a result, the postulates are applicable for massive non-relativistic particles. Relativistic massive particles time evolution is described by the Dirac and Klein-Gordon equations while photons are covered by Maxwell's equations and their various derivations.

¹²² 9 postulates are listed in [Axiomatic quantum mechanics: Necessity and benefits for the physics studies](#) by J. Jeknic-Dugic et al, 2017 (23 pages).

¹²³ In [Quantum mechanics distilled](#) by Andy Matuschak and Michael Nielsen on the [Quantum Country](#) site.

¹²⁴ See [Lecture Notes for Ph219/CS219: Quantum Information Chapter 2](#) by John Preskill, California Institute of Technology, July 2015 (53 pages).

Quantization

In quantum physics, material or immaterial quantum objects have some physical properties that are discontinuous and not continuous like distances in classical physics. This frequently corresponds to the orbits of electrons around atomic nuclei which are defined in a discrete way, to atom energy levels, but also deals with photons various properties, electrons and atom nucleons and nucleus spins, and other properties of matter and waves as well as other particles from the standard model (quarks, gluons, neutrinos, ...) that are studies in the physics of high energy particles (HEP).

Principle

There is a correspondence between the discontinuous energetic transitions of electrons in orbit around atoms and the related absorbed or emitted photons. Quantization shows up in other various places like in crystals. Atoms also form harmonic oscillators and vibrate at quantified amplitudes in crystal-line structures, according to a model Einstein developed in 1907.

You'll actually find many quantum oscillators all over the place, like with superconducting qubits.

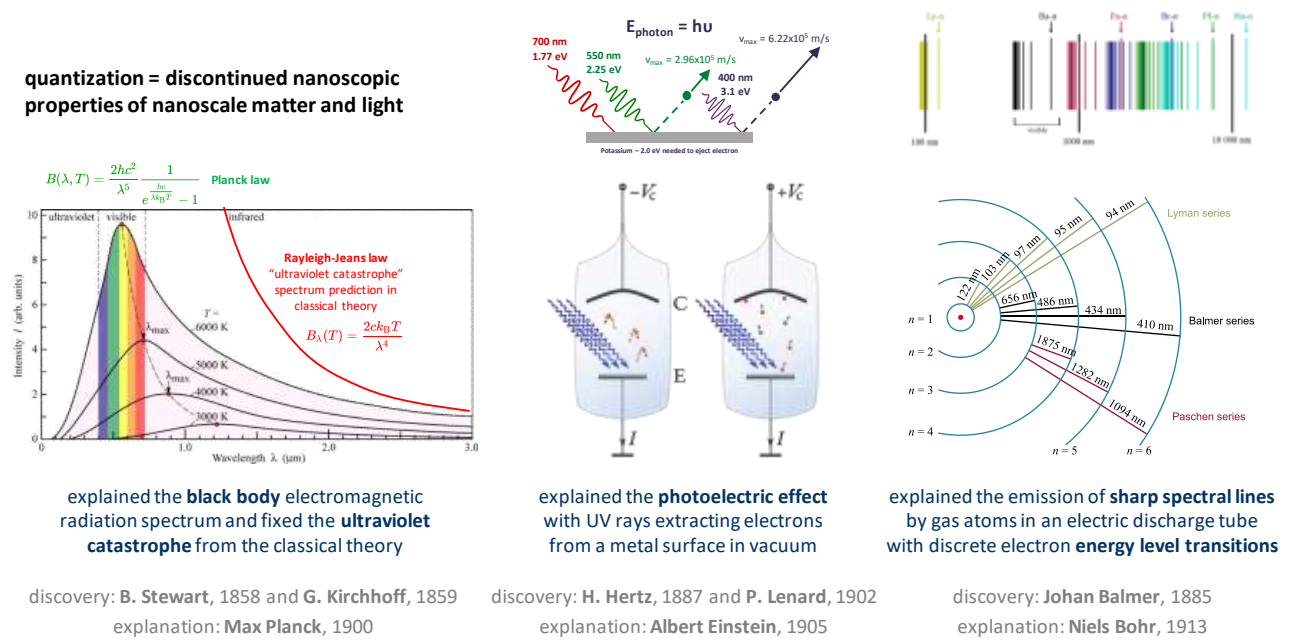


Figure 71: the three fundamental 19th century electro-magnetic waves experimental results which were later explained by quantum physics, all explained by quantization of the electro-magnetic wave field. (cc) Olivier Ezratty compilation. Various schema sources.

Quantization was a way to progressively explain experiments done beforehand, the first being the blackbody radiation spectrum. This one marked the beginnings of quantum physics.

Before explaining black body spectrum, let's recall the three kinds of spectrum that can be usually found experimentally and are pictures in Figure 72.

- A **continuous spectrum** comes from a hot and dense body like the sun, a heated solid or a perfect such body *aka* black body. It contains light in all visible frequencies that come from the random excitement of atoms in the examined body.
- An **absorption spectrum** is usually made of a continuous source of light traversing an absorbing medium like a cold gas. The resulting spectrum will be a continuous one with black lines corresponding to the frequencies absorbed by the medium.
- An **emission spectrum** is created by some rarified hot gas. It shows discrete spectrum lines corresponding to photons emitted by the excited gas atoms at specific frequencies.

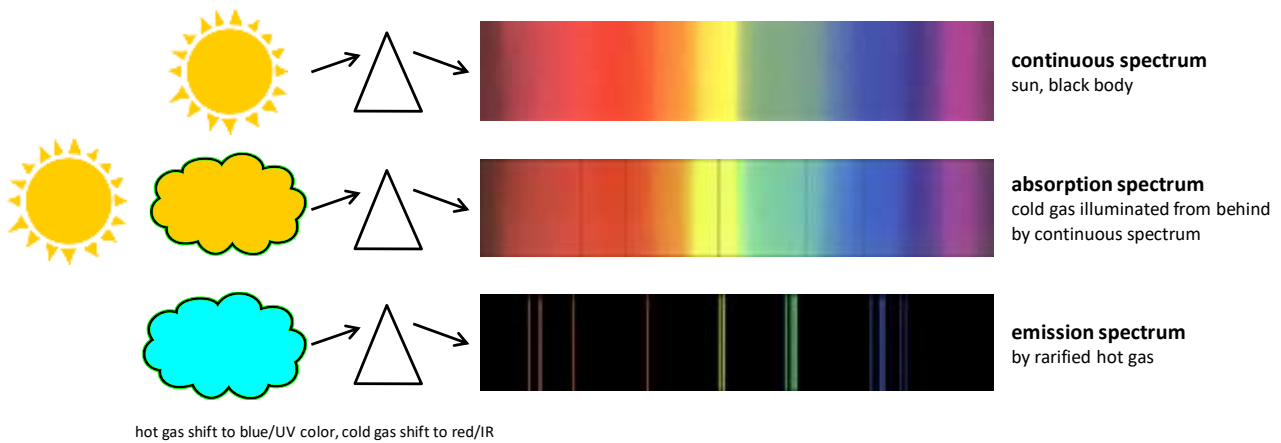


Figure 72: differences between continuous spectrum, absorption spectrum and emission spectrum.

Black bodies were theorized by **Gustav Kirchhoff** in 1859. These are ideal physical bodies in thermal equilibrium that absorb all incident electromagnetic waves radiations and reflects or transmits none. Since it absorbs all wavelengths, it's supposed to be black, although stars like the Sun are good approximations of black bodies and are not black at all. In usual experiments, a black body has a little hole that emits radiations which are analyzed by a spectrograph. The challenge which took four decades to be resolved was to evaluate the spectrum of the cavity radiation.

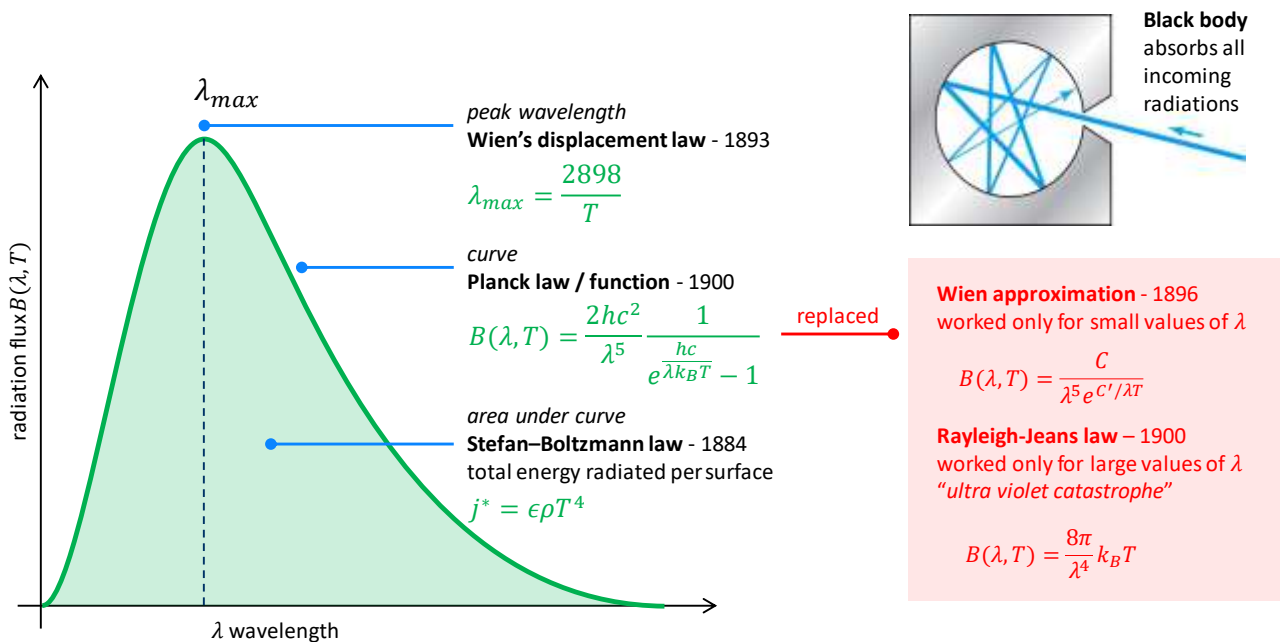


Figure 73: blackbody spectrum explanations over time. Compilation (cc) Olivier Ezratty, 2021.

It was first discovered that the spectrum didn't depend on the body radiation and only on its temperature T and wavelength λ (lambda). It also proved that thermal radiation was an electromagnetic one. Hot objects like lightbulbs and heated metals are close to black bodies.

As the temperature increases, the black body color, corresponding to the spectrum peak shown in Figure 73, shifts from red to blue. There were various attempts to explain the blackbody radiation with thermodynamics and oscillators and to predict the spectrum curve.

Before Planck's work, Stefan-Boltzmann's law (1884) described the relation between temperature and total energy radiated per surface area ($\epsilon \rho T^4$) and Wien's displacement law (1893) described the relationship between peak wavelength and temperature. These two laws worked well. **Wilhelm Wien** (1864-1926, Germany) even won the 1911 Nobel Prize in physics for this discovery.

Predicting the spectrum curve didn't work so well. First, Wien devised another law in 1896, Wien's approximation or radiation law that didn't work well with large wavelengths. The Rayleigh-Jeans formula created in 1900 didn't work for small wavelengths, leading to the so-called ultra-violet catastrophe. It was based on Boltzmann's statistical methods.

To make a better curve prediction, Max Planck guessed that the energy of the oscillators in the cavity was quantized and was a multiple of some quantity with the formula $E = nh\nu$, n being an integer, h being Planck's constant and ν the wave frequency. With this discretization, oscillators couldn't afford having many energy quanta for high energy levels. Thus, their number decreased as the frequency increased instead of growing exponentially as in Rayleigh-Jeans law. See the details in Figure 73.

But, at this point in time, there was no clear explanation on the origin of these quanta. The second step was Albert Einstein's work on the photoelectric effect in 1905, explaining how light and electrons interacted in quantized form. He guessed that the energy from an electromagnetic field is not spread over a spherical wavefront but is localized in individual directional quanta, which were later described as wave packets with a speed (of light) and length. But light quantization can show up in many other photon's characteristics: their polarization, their frequency, their phase and other various characteristics.

Electrons quantum numbers

At last, the Niels Bohr's atomic model in 1913 helped describe the electron energy transitions within atoms that explained the various hydrogen emission spectrums discovered by **Johan Balmer** in 1885, **Theodore Lyman** in 1906 and **Friedrich Paschen** in 1908, corresponding to transitions starting from the second, first and third atom electron layers. These are known as Balmer series, Lyman series and Paschen series. But other energy transitions like those from the **Zeeman** effect could only be explained by the existence of other quantum numbers.

During the 1920s, a better understanding of the quantum nature of electrons was achieved. It was progressively discovered that electrons had actually four quantum numbers:

- $n =$ **principal quantum number** corresponding to their energy level or electron shell in the atom electron shells, numbered from 1=K, 2=L, 3=M to n , n being very high for so-called Rydberg (high-energy) states close to atom ionization¹²⁵. This number may correspond to some energy levels used in cold atoms and trapped ions qubits. It corresponds to the rows shown in Figure 74.
- $\ell =$ **orbital angular momentum** numbered from 0 to $n-1$ or letters (s, p, d, f, g, h, i, etc.) also named azimuthal or orbital quantum number, describes the electron subshell. It corresponds to different types of elliptic orbitals around the atom and to the columns shown in Figure 74.
- $m_\ell =$ **magnetic quantum number** describing the electron energy level within its subshell. Its value is an integer between $-\ell$ and ℓ which describes the number of different orbitals in the subshell and their orientation.
- $m_s =$ **spin projection quantum number** being either $+1/2$ or $-1/2$, in a given spatial direction (usually x, y or z in an orthonormal basis), called spin component, also named intrinsic angular momentum. This is the property used in so-called electron spin or silicon qubits. But... what is the unit of the spin? It is rarely mentioned but the spin unit is the Dirac constant \hbar , which equals the Planck constant h divided by 2π . What physical property is it describing? Nobody really knows. It's an intrinsic property which doesn't depend on the situation like temperature. It doesn't describe a rotation of the electron around an axis. Spin is the only quantum number that has no physical meaning equivalent in the macroscopic world.

¹²⁵ The principal quantum number is limited to 7 for non-excited atoms and is theoretically illimited with excited atoms. A record of $n=766$ was observed with hydrogen atoms in interstellar medium.

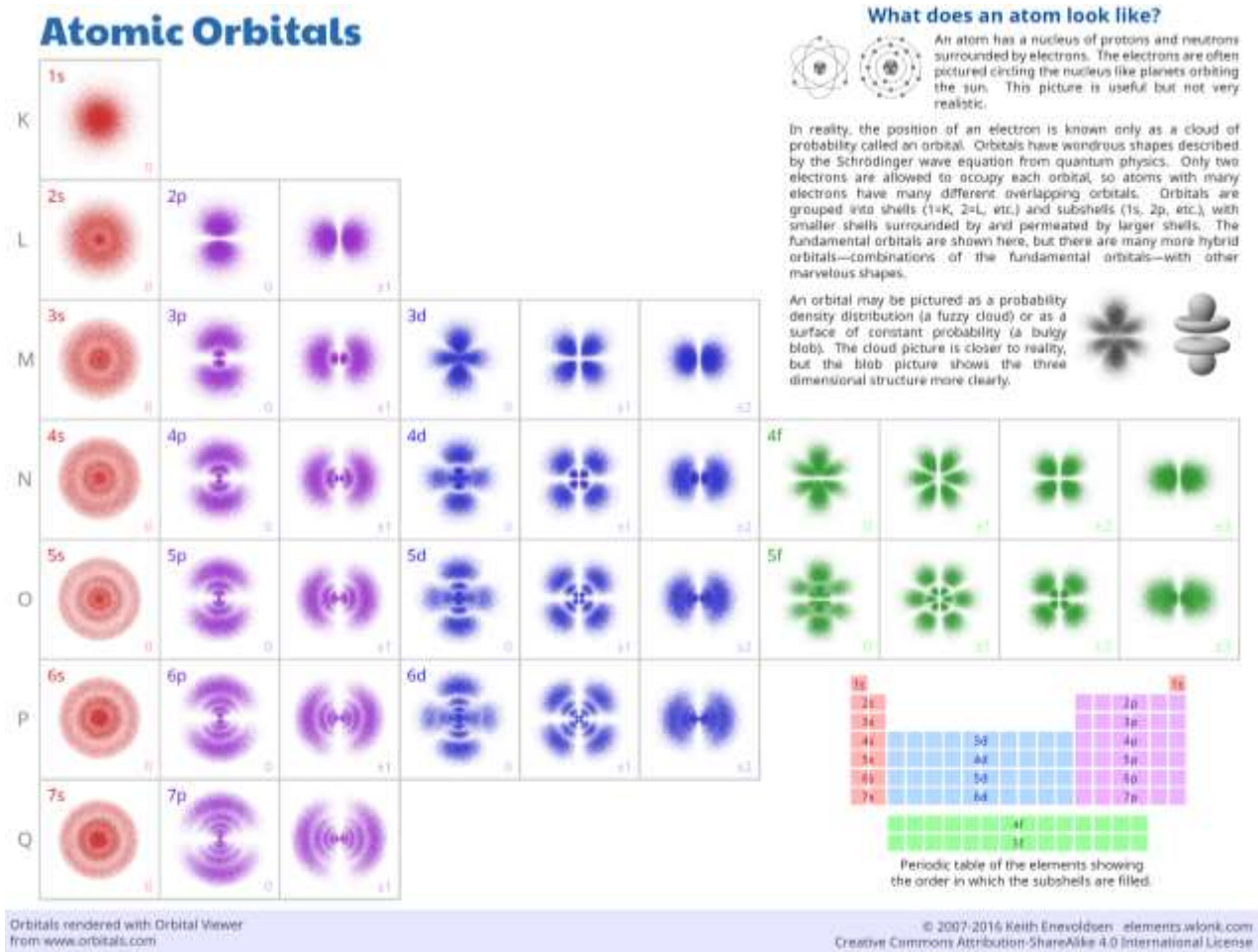


Figure 74: electron atomic orbitals corresponding to their angular momentum quantum number. Source: [Keith Enevoldsen](#).

It's key to understand the effect of these various electron quantum numbers in many fields like with NV centers and silicon spin qubits, quantum dot photon sources and many others.

Nucleons and nucleus quantum numbers

Not only electrons have a spin but also atom nucleus and their nucleons constituents that are neutrons and protons. An atom nucleus has Z protons corresponding to the element atomic number and N neutrons which add up to a total of $A=Z+N$ nucleons. Protons and neutron have a spin of $1/2$. The nucleus has a half-integer spin ($1/2, 3/2, 5/2, \dots$) when the number of neutrons plus the number of protons is odd, an integer spin ($1, 2, 3, \dots$) when the number of neutrons and protons are both odd and no spin at all when its number of neutrons and protons are both even.

Nucleus spins are either something we need to avoid like in silicon qubits produced with ^{28}Si , the silicon isotope with a null spin, or that we use to store qubit information like in NV centers and SiC cavities and also electron donor qubits based on atoms like phosphorus where there is a coupling between some atom nucleus spins and some free electrons.

But how is it possible to have a zero spin when you add-up the spins of protons and neutrons which are positive? Let's take a pause and provide some answer. This is due to way a nuclear spin is calculated.

Nucleons have quantum numbers that are similar to electrons quantum numbers, but with different possible values bounds and meanings:

- $n =$ **nucleon shell number** or layer with integer values ranging from 0 to 6. It is bounded and there is no equivalent of Rydberg states in nucleus with large principal quantum number. The nuclear shell model is the equivalent of the atomic Bohr model related to electron shells.
- $\ell =$ **orbital angular momentum** quantum number which is also quantized with an integer value starting at 0, the angular momentum itself being $L^* = \hbar\sqrt{\ell(\ell + 1)}$.
- $m_\ell =$ **magnetic quantum number** with integer values ranging from $-\ell$ to ℓ . In each nucleon shell, nucleons of the same type have a tendency to regroup by pairs with opposite magnetic quantum number.
- $m_s =$ **spin quantum number**, being either $+1/2$ or $-1/2$, in each spatial direction, also named intrinsic angular momentum. A nucleon spin s equal to $1/2$ is the size of the vector \vec{s} . The spin angular momentum is $S^* = \hbar\sqrt{s(s + 1)}$ with $s=1/2$.

A nucleon total angular momentum is a vector $\vec{j} = \vec{\ell} + \vec{s}$ and $j = \ell + s$ in scalar representation with ℓ being the nucleon orbital angular momentum and $s = 1/2$ its intrinsic angular momentum or spin. The scalar representation is a good approximation of the vector representation since nucleons move in an average magnetic field orienting them in a similar direction. In the end, the atom's **nuclear spin** is the sum of its nucleon's total angular momentum j .

As atom nucleus size grows, nucleus shells are filled progressively. Filled layers have a number of neutrons or protons called “magic numbers” (2, 8, 20, 28, 50, 82, 126) as shown below in Figure 75. Atoms with entirely filled layers of either neutrons or protons are more stable. Nucleons pair in orbits with projections $\pm m_\ell$ such that their momenta cancel. The notion of layer magic number applies separately for protons and for neutrons. For example, ^{116}Sn (selenium) has a magic number of 50 protons and ^{54}Fe (iron) has a magic number of 28 neutrons. Filled shells have a total angular momentum of zero since made of pairs of neutrons or protons with opposite projections of total angular momentum. That's why an even number of protons and neutrons lead us to have a zero nuclear spin. And when you have both a magic number of neutrons and protons, your nucleus is doubly magic like with ^{40}Ca and ^{208}Pb , and has an exceptional stability. All this refers to atoms and nucleus in their ground state.

On top of these numbers, nucleus have a parity that is $\lambda = (-1)^\ell$ where ℓ is the total orbital angular momentum of the nucleus. Its value corresponds to the symmetrical or asymmetrical structure of the nucleus.

Analyzing some material nuclear spin is the basis of **NMR spectroscopy**. It exposes it to a strong homogeneous magnetic field, usually generated with cooled superconducting magnets which create it thanks to their support of large electric currents with no resistance. A sample is then irradiated by a radiofrequency (RF) field around the Larmor precession frequency of the searched elements, in the hundred MHz range. This is the frequency of the nucleus spin vector rotation in a cone around the axis of the ambient magnetic field. A receiver captures the transmitted RF signal, amplifies it and pass it through a quadrature demixer fed by a reference frequency tone. It down converts the signal to a lower frequency and decomposes it into its in-phase and quadrature which is then converted into digital format through with ADCs (analog-to-digital converters) before being analyzed digitally.

Two other notions are related to atom's nucleus and are frequently mentioned elsewhere in this book:

Spin-orbit coupling or spin-orbit interaction is a relativistic interaction of a particle's spin with its motion inside a potential. One example if the shifts in an electron's energy levels that due to electro-magnetic interaction between the electron's magnetic dipole, its orbital motion and the electrostatic field of the atom nucleus.

Hyperfine structure are small differences in otherwise degenerate (equivalent, equal) energy levels in atoms, molecules and ions that are explained by the electromagnetic multipole interaction between the nucleus and electron clouds. In atoms, hyperfine structure come from the energy of the nuclear magnetic dipole moment interacting with the magnetic field generated by the atom electrons and the energy of the nuclear electric quadrupole moment in the electric field gradient due to the distribution of charge within the atom.

nucleus shell and magic numbers

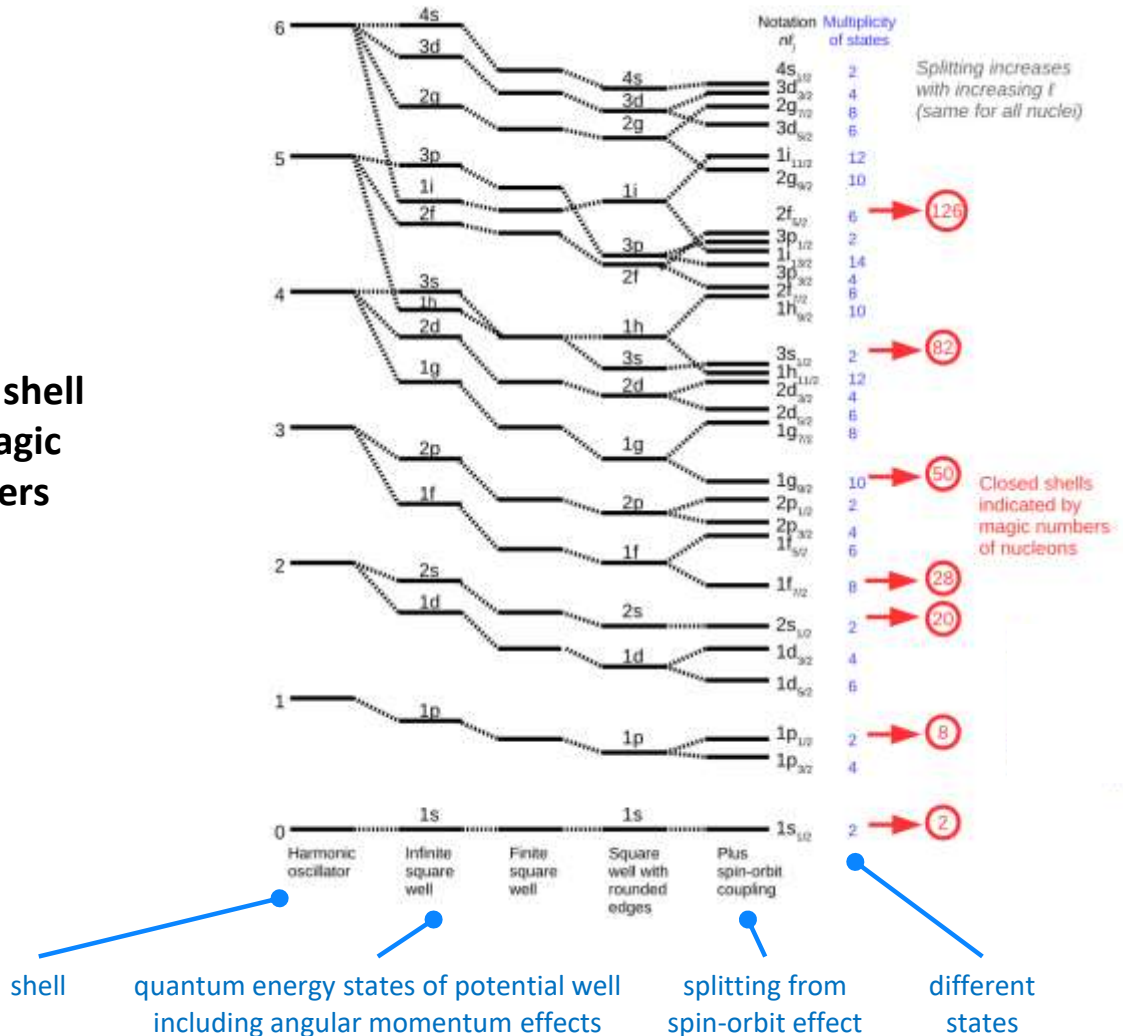


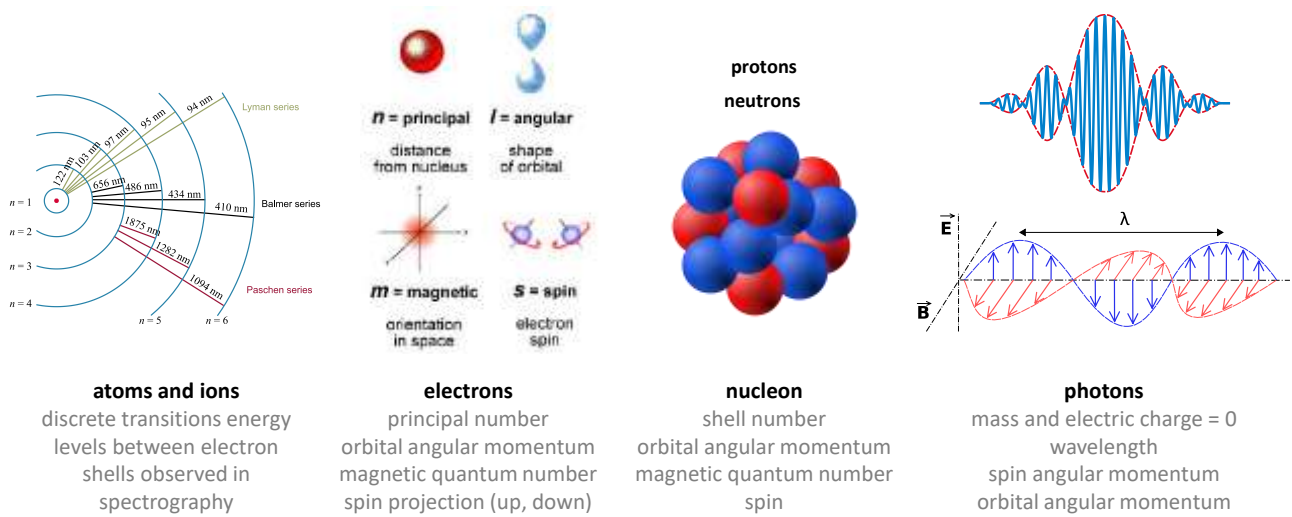
Figure 75 : nucleus shells and magic numbers. Source: [Particle and Nuclear Physics Handout #3 by Tina Potter](#), 2022 (124 slides).

The cohesion of atom's nucleus comes from the strength of the nuclear force that binds nucleons together. It is countered by Coulomb's force that creates a repulsion between same charge particles like protons. The relative value of the nuclear force and the Coulomb repulsion force explain nuclear fusion for small atoms and fission for large atoms, iron being in the neutral zone in the elements table.

Photon quantum numbers

Photons also have their quantum numbers but they are different than with electrons and nucleons. We describe it in the section dedicated to [photon qubits](#), starting page 427.

In quantum information systems, we use quantum objects which can usually have two different separable states that can be initialized, modified and measured. Even superconducting loops in superconducting qubits rely on two systems levels clearly distinct for the oscillating current flowing through their Josephson effect insulator.



=> used to created qubits with distinct states and at the particle scale (atoms, electrons, photons).

Figure 76: quantization applied to atoms, ions, electrons and photons. (cc) Olivier Ezratty, 2022, with Wikipedia images source.

Wave-particle duality

We often read and hear that quantum objects like photons and electrons are both waves and particles. The right manner to describe this would be to say that they behave differently depending on the way they are observed. In some experiments, these quantum objects behave like classical waves, are not localized in space and generate interferences when added together, a bit like colors can mix (photons) and sounds can mix (acoustic waves). In other experiments, they behave as classical particles and can be localized in space and have a kinetic momentum and mass¹²⁶. One simpler way to interpret things is to say that quantum objects act as a particle when observed and as waves when not observed.

Various experiments such as Young's double-slit experiment show that both photons and electrons behave both as particles and as waves depending on the context and measurement system, generating interference fringes when observed as waves. You can observe the path of a quantum object or the interferences it creates, but not both simultaneously.

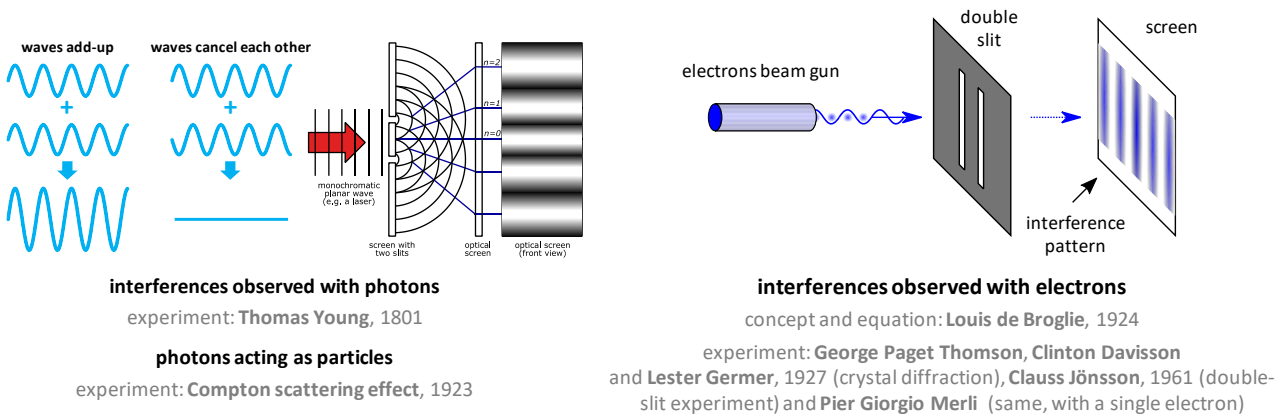


Figure 77: experiments showing wave-particle duality with photons and electrons.

This is the Bohr's principle of complementarity according to which it is not possible to apply observables simultaneously in terms of particles and waves. It shows up in the Young experiment: if we let the quantum object traverse both slits, it behaves like a wave and creates interferences.

¹²⁶ Usually, it is impossible to observe these two behaviors simultaneously although there are some exceptions.

If we detect the quantum object in each of the slits, practically done with closing one of the slits, it creates a measurement-based decoherence and the quantum object behaves and is observed as a particle. And the classical probabilities of particle observation don't add up to make for the interferences observed with the wave observation. This wave-particle duality is linked to the quantum physics mathematical formalism that relies on vectors that can add up linearly like waves.

It led to a still unsolved mystery, the “which-way” question. When interference fringes appear on the screen, by superposition of paths coming from the two slits, which path did the single photon or electron take?

The wave-particle duality is used in many quantum computers to make physical qubits such as trapped ions interact with energy in the form of photons emitted by lasers. Qubits can also interfere with each other thanks to interferences.

Delayed choice experiment

John Wheeler proposed various thought experiments between 1978 and 1984 to determine if light chooses its path with sensing the experimental devices. The Wheeler's delayed-choice or which-way experiment asked the question: when does a quantum object decide to travel as a wave or as a particle?

It led to various experiments like the 1999 quantum eraser but the most decisive experiment was conducted by a team of French researchers in 2006 as shown in Figure 78¹²⁷.

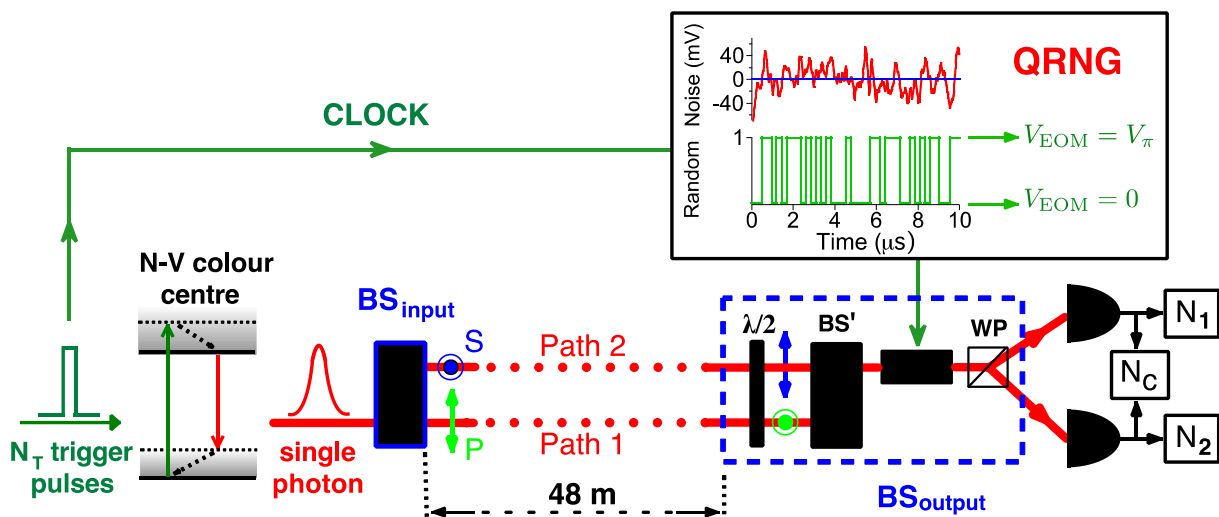


Figure 78: delayed choice experiment and its quantum eraser. Source: [Experimental realization of Wheeler's delayed-choice GedankenExperiment](#) by Vincent Jacques, Frédéric Grosshans, Philippe Grangier, Alain Aspect, Jean-François Roch et al, 2006 (9 pages).

They generated pulses of single photons with an NV centers source created by Jean-François Roch, a pioneer in this domain, that were sent through a first beam splitter (BS_{input}) and a delay line of 48 meters. Then, the two beams traversed a dynamic-controlled beam-splitter by electro-optical modulator driven (BS_{output}) by a quantum random number generator (QRNG).

At last, two photon detectors (N_1 and N_2) could determine if the photon behaved as a particle (no interference due to the inactive beamsplitter) or as a wave (with interferences due to the activated beamsplitter).

¹²⁷ See [Experimental realization of Wheeler's delayed-choice GedankenExperiment](#) by Vincent Jacques, Frédéric Grosshans, Philippe Grangier, Alain Aspect, Jean-François Roch et al, 2006 (9 pages). The experiment used a single photon source using NV centers. The experiment has been reproduced many times since then with many variations. See for example [A generalized multipath delayed-choice experiment on a large-scale quantum nanophotonic chip](#) by Xiaojiong Chen et al, 2021 (10 pages) which is based on a nanophotonic component.

The QRNG clock was near the photon source, but the QRNG was positioned close to the dynamic beamsplitter. The experiment determined that the wave/particle behavior of the photons in the interferometer was dependent on the choice of the measured observable at the end of the photon journey, not the beginning.

And even when that choice was made at a position and a time sufficiently separated from the entrance of the photons in the interferometer. Although it's still debated, it does not require a backward in time effect explanation.

Other more delayed-choice sophisticated experiments are regularly done. A Chinese team demonstrated a generalized multipath wave-particle duality implemented by a large-scale silicon-integrated multipath interferometers¹²⁸.

Schrödinger's wave equation

The wave-particle duality led Schrödinger to create his famous wave equation which describes a massive non-relativistic quantum object with a wave function with the probabilities of finding the particle at a particular position in space at a given time. Ladies and gentlemen, here is this wave equation and its constituents, unleashed below in Figure 79.

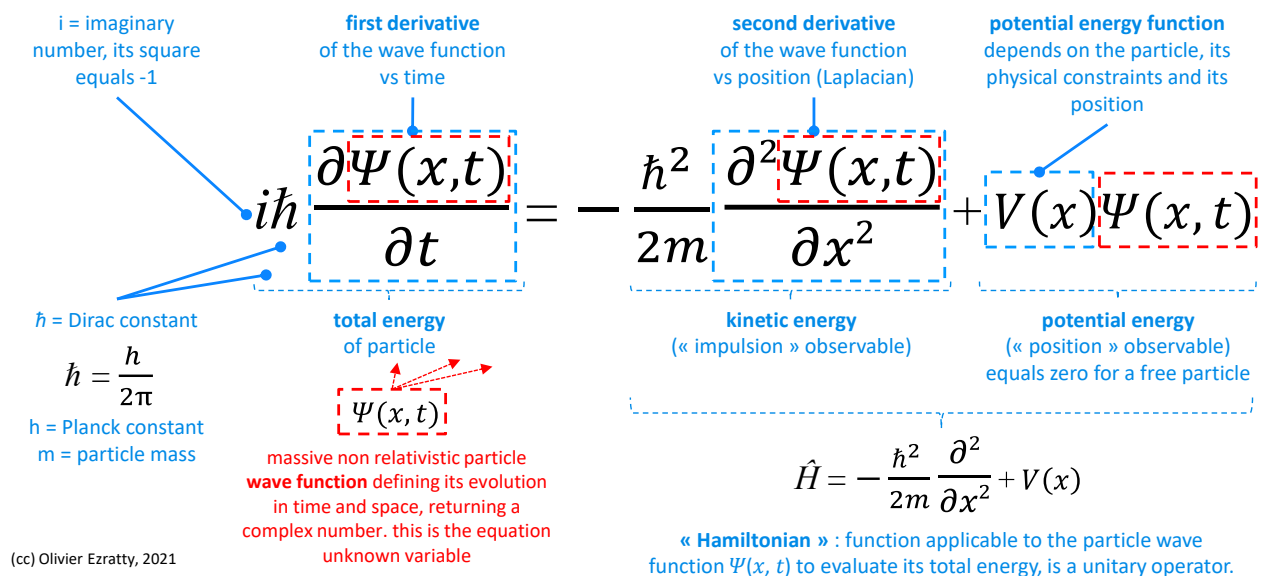


Figure 79: the famous Schrodinger's wave equation explained in detail (cc) Olivier Ezratty, 2021.

Here's how to understand the components of this equation and their implications:

- Its **unknown** is the wave function of the particle $\psi(x, t)$ that describes its probabilistic behavior in space and time. x indicates the position of the particle in space, with one, two or three dimensions depending on its constraints, and t is the time. This function returns a complex number that encodes the wave amplitude and phase.
- The full Schrodinger wave equation illustrates the principle of **energy conservation**. The item to the left of the equation describes the total energy of the particle at a given time and place. The element on the right includes the kinetic energy of the particle and its potential energy. Like said about the quantum physics [postulates](#), starting page 86, the Schrodinger's Hamiltonian, which is a time-dependent unitary matrix operator, is expressed differently with photons and with relativistic massive particles.

¹²⁸ See [A generalized multipath delayed-choice experiment on a large-scale quantum nanophotonic chip](#) by Xiaojiong Chen et al, 2021 (10 pages).

- The **wave function square** is equal to the probability of finding the particle at location x at time t . For an electron, which is the most commonly analyzed particle with this equation, it is an indication of the probability of finding it at a given distance from the nucleus of the atom around which it orbits. Logically, as a result, the sum of the probabilities of finding the particle somewhere is equal to 1.

This is called a normalization constraint. One of its derivatives is the Max Born function that we will see later. The modulus of a complex number is the size of its vector. If $z = a + ib$, the modulus $|z|$ of z is thus the square root of the sum of the squares of a and b , see *below*.

- It is a **partial differential** equation, i.e. it connects its components via derivative functions, in this case of first degree (a slope on a curve) and second degree (an acceleration). The particle wave function appears three times in the equation: to the left of the equation with a first derivative on the time of the wave function, to the right with a second derivative on its position and with a simple multiplication with the function $V(x)$.

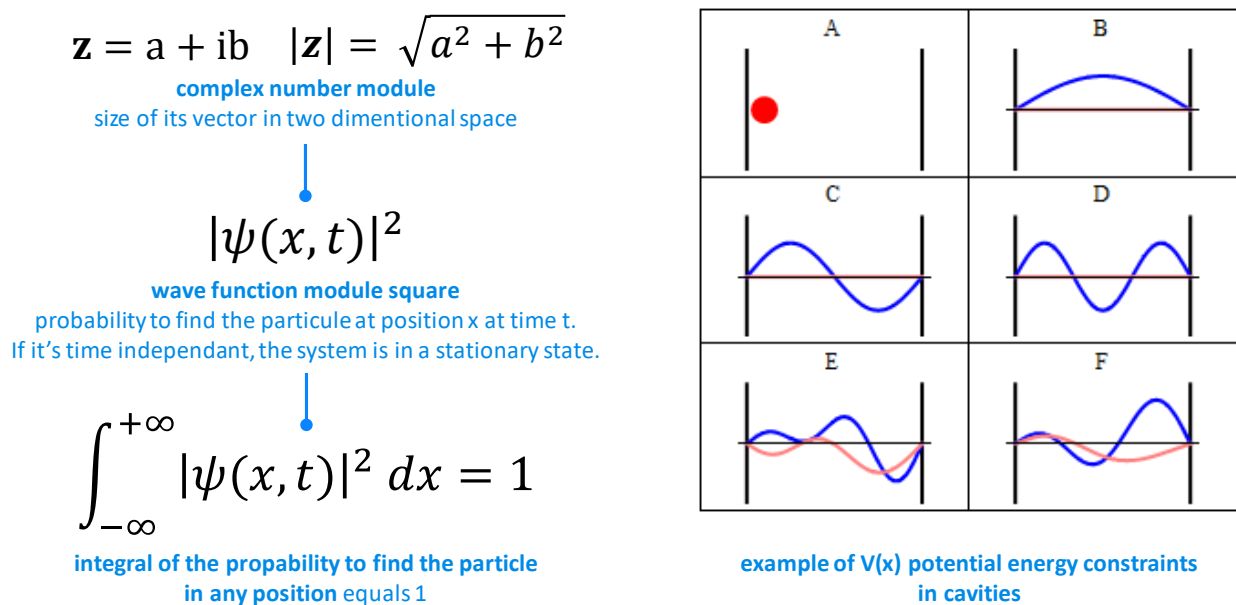


Figure 80: constraints of the Schrodinger's equation (cc) Olivier Ezratty, 2021.

- The **potential energy of the particle** is defined by the function $V(x)$ which depends only on the particle position in space and its physical constraints, in particular electromagnetic ones. When a particle is free and moves without constraints, this function returns zero. This function $V(x)$ is the main variable of Schrödinger's equation.
- Schrödinger's equation is **analytically solved** in a limited number of cases such as for the electron of a hydrogen atom, a free particle, a particle in a potential well or box or a quantum harmonic oscillator. In the most complex cases, the resolution of the equation requires non-analytical methods, raw calculation and simulation. It is one of the fields of application of quantum simulators to solve the Schrödinger equation in cases where analytical methods are not available. Any micro or macro-object has a Schrödinger wave function, all the way to the entire Universe. But the equation only makes practical sense for nanoscopic objects.
- The equation is **linear** over time. This means, among other things, that any combination of solutions of the equation becomes a new solution of the equation. This makes it possible to decompose a wave function into several elementary wave functions that are called the "eigenstates" of the quantum object. They correspond to the different energy levels of the particle that are discrete when the particle is constrained in space, like the electrons in an atom.

One can indeed in this case derive the notion of quantification of the particle states from the Schrödinger equation ([demonstration](#)). The linearity of this equation has a lot of consequences like superpositions, entanglement as well as the no-cloning theorem.

- The operator who acts on the right side and accumulates the second derivative and the potential energy function is called a **Hamiltonian**, which describes the total energy of the system. We find this expression in the quantum annealing calculation with D-Wave and with quantum simulators.
- This equation is a **general postulate** that has been experimentally validated in a large number of cases. Its interpretation has given rise to much debate, namely, is it a simple probabilistic model or does it describe reality? We deal with this in the chapter on the [philosophy of quantum physics](#).
- The generic Schrödinger equation presented so far is said to be **time dependent**. This equation is presented in various ways depending on the needs and annotations. The second derivative of the wave function on the position of the particle is sometimes presented with the nabla sign squared (∇^2).

A nabla operates a derivative on a scalar or vector function. The ∇^2 operates a second derivative, also called Laplacian. The most concise form of Schrödinger's equation is on the bottom right, with a Hamiltonian operator on the left (\hat{H}) and the energy operator on the right (\hat{E}), both of which apply to the particle wave function.

$$\left[-\frac{\hbar^2}{2m} \nabla^2 + V \right] \Psi = i\hbar \frac{\partial}{\partial t} \Psi$$

$$\hat{H}\psi(x, t) = \hat{E}\psi(x, t)$$

Figure 81: concise versions of Schrodinger's wave equation.

- There is a **time-independent** form of Schrödinger's equation that applies to particles in a stationary state¹²⁹. In this version of Schrödinger's equation, the energy operator E is a simple constant, a real number.

$$\left[-\frac{\hbar^2}{2m} \nabla^2 + V(r) \right] \Psi(r) = \hat{E}\Psi(r)$$

Figure 82: time-dependent version of the Schrodinger's equation.

- The Schrödinger equation is **symmetric** or **antisymmetric** depending on the particle type. When applied to two quantum objects r_1 and r_2 , $\psi(r_1, r_2) = \psi(r_2, r_1)$ when the equation is symmetric (meaning, the wave equation is not differentiated by the given particles order) and $\psi(r_1, r_2) = -\psi(r_2, r_1)$ when it's antisymmetric. The first case corresponds to bosons which can be indistinguishable and "live" together and have a zero or integer spin and the second, to fermions, which can't cohabit with the same quantum state at the same location and have half-integer spins. All this is a consequence of Pauli's exclusion principle.
- The $\psi(x, t)$ function must be a **continuous function** and "filled" everywhere in space. Its value is bounded by 0 and 1, with no infinite value anywhere. It also has a single value, even in the case of superposition. In that case, the $\psi(x, t)$ is a linear superposition of two Psi functions and is itself a psi function. A quantum superposition is just another wave function.

For a system with several quantum objects, the wave function describes the quantum system state, or quantum state. According to the Copenhagen interpretation of quantum physics, the wave function from the Schrödinger equation contains the best description possible of a quantum system.

¹²⁹ According to Wikipedia: "A standing wave is the phenomenon resulting from the simultaneous propagation in opposite directions of several waves of the same frequency and amplitude, in the same physical medium, which forms a figure, some elements of which are fixed in time. Instead of seeing a wave propagating, we see a standing vibration but of different intensity at each observed point. The characteristic fixed points are called pressure nodes. ».

If electrons and photons both can behave as waves, they have not the same wavelengths. Indeed, a photon with an energy of 1 eV (electron-volt) has a wavelength λ of 1240 nm (in the infrared spectrum) while an electron with the same energy has a much shorter wavelength of 1.23 nm (in the X-ray spectrum). This short wavelength explains why we use electron microscopes to probe matter with a much better resolution than light-based microscopes.

Relativistic particles obey to Dirac and Klein-Gordon wave equations while photons are described with Maxwell's equations combined with a formalism coming from the so-called second quantization which regroups superposed photons, use photon numbers, and creation/annihilation operators.

Large objects wave behavior

The wave-particle duality was verified with atoms in 1991 in interferometry experiments involving lasers and classical optics. A Young double-slit experiment was also carried out in Austria in 2002 with fullerene molecules (C_{60} , formed of 60 carbon atoms as in Figure 83¹³⁰, but also with a 70 atoms variant) and in 2012 with molecules containing 58 and 114 atoms, the latter named $F_{24}PcH_2$ being made of fluorine, carbon, oxygen, hydrogen and nitrogen¹³¹. Figure 84 shows the shape of the molecule. In 2019, the same kind of experiment was done with a slightly more complex molecule, a polypeptide of 15 amino acids which serves as an antibiotic, gramicidin A1¹³².



Figure 83: C_{60} fullerene molecule.

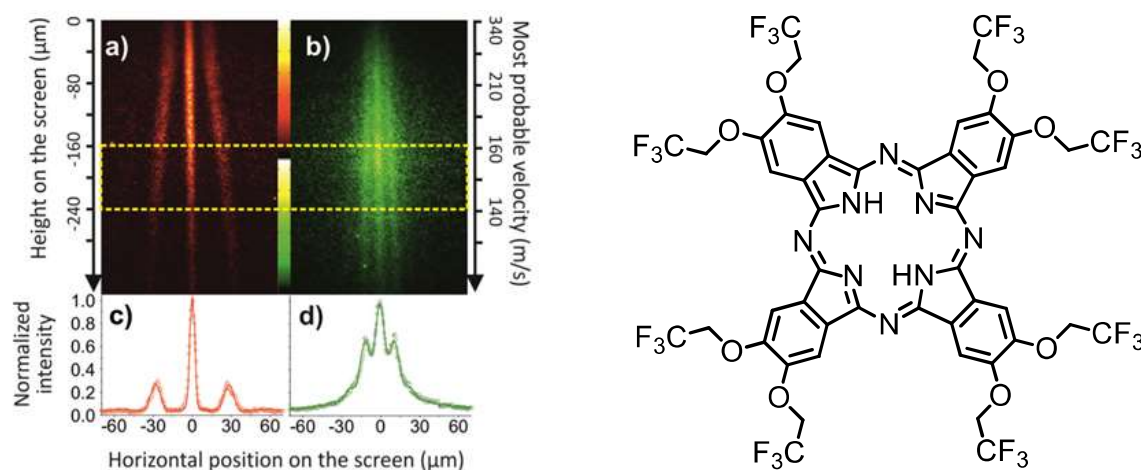


Figure 84: $F_{24}PcH_2$ made of fluorine, carbon, oxygen, hydrogen and nitrogen. Sources: [Real-time single-molecule imaging of quantum interference](#) by Thomas Juffmann et al, 2012 (16 pages) and [Highly Fluorinated Model Compounds for Matter-Wave Interferometry](#) by Jens Tüxen, 2012 (242 pages).

In 2021, other experiment led to the creation of larger quantum objects, sized 100 and 140 nm, and cooled at ultra-low temperatures¹³³.

¹³⁰ See [Quantum interference experiments with large molecules](#) by Olaf Nairz, Markus Arndt and Anton Zeilinger, 2002 (8 pages).

¹³¹ See [Real-time single-molecule imaging of quantum interference](#) by Thomas Juffmann et al, 2012 (16 pages). See also the [video of the experiment](#). [Highly Fluorinated Model Compounds for Matter-Wave Interferometry](#) by Jens Tüxen, 2012 (242 pages) describes the experimental device for the verification of the wave-matter duality of large molecules.

¹³² See [A natural biomolecule has been measured acting like a quantum wave for the first time](#), November 2019, which refers to [Matter-wave interference of a native polypeptide](#) by Armin Shayeghi et al, October 2019 (10 pages).

¹³³ See [How Big Can the Quantum World Be? Physicists Probe the Limits](#) by Philip Ball, Quanta Magazine, July 2021, Real-time optimal quantum control of mechanical motion at room temperature by Lorenzo Magrini et al, July 2021 (36 pages) and [Quantum control of a nanoparticle optically levitated in cryogenic free space](#) by Felix Tebbenjohanns et al, Nature, July 2021 (26 pages).

Photon's wave-particle duality

On the other hand, photons can behave under certain conditions like particles. When they reach an atom, they can transmit it some kinetic motion. This is what makes it possible to generate the somewhat counter-intuitive physical phenomenon of atoms laser cooling using lasers and a Doppler effect. Temperature is related to the movement of atoms in their gaseous, liquid or solid medium. Lowering the temperature means slowing down the movement of atoms. A Doppler effect is used to do this. The moving atoms are illuminated with a laser whose frequency is tuned just below the energy absorption level of the atoms.

The atoms moving towards the light will absorb the photons because these have an apparent frequency that is higher than the absorption level. This reduces the kinetic energy of the atoms receiving the photon.

The photons moving in the other direction will not absorb them because the apparent frequency of the incident photon is below the absorption level, so it's unable to change the energy state of the atoms.

Thanks to the random movement of the atoms in all directions, after a certain time, the overall temperature drops. This phenomenon slows down once the velocity of the atoms falls below a certain threshold, which explains the Doppler effect attenuation ("Doppler shift").

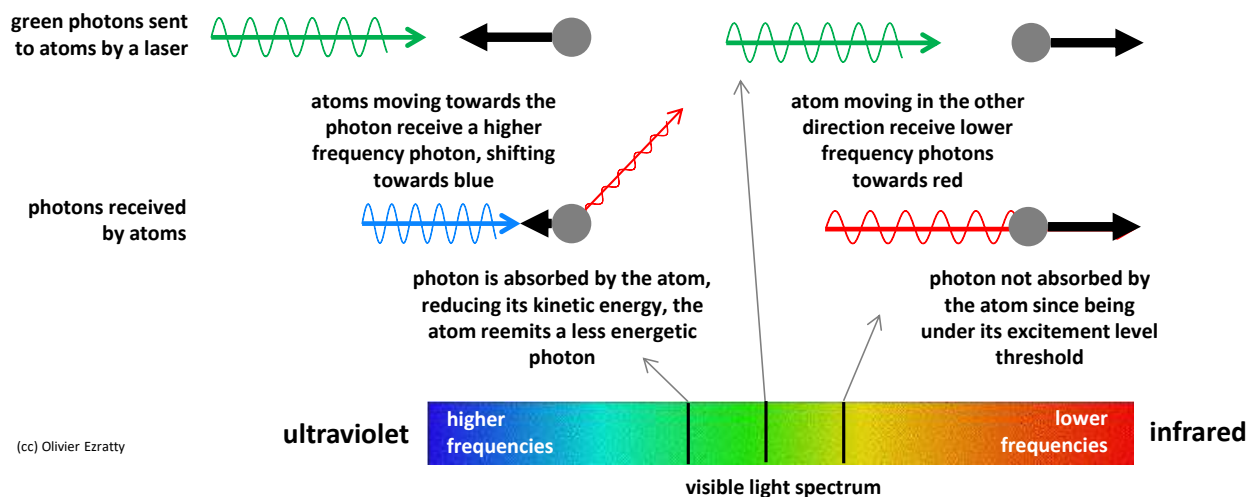


Figure 85: explanation of Doppler effect with photons, (cc) Olivier Ezratty, 2021.

These techniques are used to cool atoms to temperatures close to absolute zero. It is used to prepare cold atoms and trapped ions used in certain types of quantum computers, often in combination with magnetic and/or electronic traps to control the atoms position¹³⁴.

The record low temperature was reached in 2019 with 50 nK, achieved by researchers from JILA, the joint laboratory of NIST and the University of Colorado¹³⁵.

¹³⁴ Doppler measurement is also used to evaluate the speed at which stars and galaxies move away from each other and to evaluate the rate of expansion of the Universe. Other atoms laser-based cooling methods crafted to reach lower temperatures include Sisyphus cooling first proposed by Claude Cohen-Tannoudji in 1989 and using two counter-propagating lasers using orthogonal polarization, evaporative cooling using magneto-optical traps (MOT) and optical molasses with 3D Doppler effect.

¹³⁵ See [JILA Researchers Make Coldest Quantum Gas of Molecules](#), February 2019. The 50 nK record was obtained with laser cooling of a gas containing 25,000 potassium-rubidium molecules.

Superposition and entanglement

Superposition and entanglement are directly related to the wave nature of quantum objects and to the linearity of the underlying mathematical models expressed in quantum physics postulates.

Superposition

The strawman's version of superposition is that quantum objects can be simultaneously in several states or locations, such as the direction of electron spin, upward or downward, the linear polarization of photons, horizontal or vertical, or the frequency, phase or energy of an oscillating current in a superconducting loop crossing the barrier of a Josephson junction. It is not correct according to canonical interpretations of quantum mechanics. It is more related to quantum objects behaving as waves when not being measured. Superposition is also a mathematical consequence of quantum postulates and wave-particle duality. It results from the fact that a linear combination of solutions to the Schrödinger equation is also a solution to this equation.

A quantum states of a given quantum object can be added together or superposed. Superposition explains the interferences obtained with electrons in the 1961 double-slit experiment.

A quantum object is not per se in a superposition of various states. It has a single and predictable quantum state described by a probability distribution of given observables. Measuring this property can provide different values according to the probability distribution. That's all.

According to the Copenhagen interpretation of quantum physics, one shouldn't try to give a physical meaning to superposition before any measurement. In a classical physics interpretation, superposition could be explained by a very high frequency of quantum state changes. It is considered to be totally inaccurate for specialists, but it is still an intuitive way to figure out how superposition looks like in the physical world.

quantum objects can be in superposed states

it is a consequence of wave-particle duality.

since the Schrödinger wave equation is linear, any linear combination of solutions is also a solution.

qubit example: $|\Psi\rangle = \alpha|0\rangle + \beta|1\rangle$

corresponds to a linear superposition of $|0\rangle$ and $|1\rangle$ with complex amplitudes α and β containing information on their phase difference.

=> handles information in qubits and qubits registers.

=> enables parallelism on registers superposed states.

concept: Paul Dirac, 1930

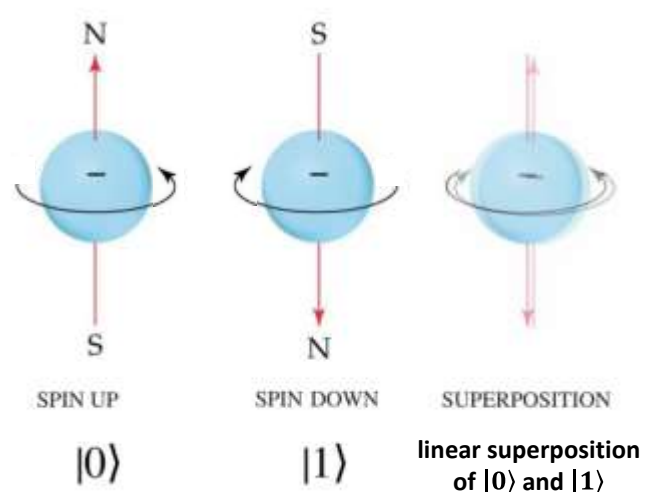


Figure 86: electron spin superposition. (cc) Compilation Olivier Ezratty, 2021.

Superposition can happen with various weird situations, as we'll later see. For example, you can create superposition between several photon Fock-states, meaning, superposing 0 photon, 1 photon and 2 photons, or even photon frequencies. You can even superpose temperatures¹³⁶ and thermodynamic evolutions with opposite time arrows¹³⁷ which can challenge your willingness to visualize what's it all about!

¹³⁶ See [Quantum Superposition of Two Temperatures](#) by Arun Kumar Pati and Avijit Misra, December 2021 (7 pages).

¹³⁷ See [Quantum superposition of thermodynamic evolutions with opposing time's arrows](#) by Giulia Rubino, Gonzalo Manzano and Časlav Brukner, November 2021 (10 pages).

In quantum computing, superposition shows up with qubits, allowing which have an internal “value” linearly combining their basis states $|0\rangle$ and $|1\rangle$ with complex amplitudes instead of having one of the two values as with classical bits. This mathematical view is expanded to N qubits whose internal state is characterized by 2^N complex amplitude values. This contributes to the massive parallelism enabled by quantum computers. It looks like it should enable some exponential computing capacity but it’s not the case. As we’ll investigate later in this book, superposition alone is not sufficient. We also need entanglement and some specific quantum gates to really bring some exponential acceleration.

In the case of a single quantum object, superposition is a combination of states corresponding to several exclusive states of an observable. Coherence is another name describing a superposition. And decoherence is a phenomenon that destroys superposition, particularly with quantum measurement.

Entanglement

The simplest way to describe an entangled state of two quantum object is to say these have a correlated state, whatever the distance between them. They form sort of a single object. You touch one, it will affect the other. You measure one object, then the other, and the related results will be correlated. This can be checked with repeated tests on a system repeatedly prepared in a similar way, using a so-called Bell test.

Entanglement can also be described with a mathematical viewpoint based on superposition. The mathematical representation of a quantum system AB made of two subsystems A and B is the tensor product of the two subsystems, meaning, a large vector or matrix: $H_{AB} = H_A \otimes H_B$. We’ll described the form of the matrices representing quantum systems a little later. In that case, the system AB can be described by or decomposed with its individual parts A and B . There are however situations where you can linearly combine several of these composite quantum states, which becomes a new quantum state. In many cases, such a composite state can’t anymore be decomposed as the tensor product of two states. The composite quantum state becomes inseparable. That’s where entanglement shows up! Entanglement is a direct consequence of superposition applied to multi-object systems.

Entangled quantum objects cannot be considered as separated objects. With a pair of entangled quantum objects, a measurement made on one quantum will instantly have an effect on the other quantum, without waiting for a delay in the transmission of information at the speed of light between the two quanta. This is the principle of the "non-locality" of quantum properties that disturbed Einstein in 1935 and spurred his famous EPR paper with Rosen and Podolsky.

Using qubit’s representation that we’ll describe later, classical entangled two-qubit states are Bell pairs, like $\frac{|00\rangle+|11\rangle}{\sqrt{2}}$ or $\frac{|01\rangle+|10\rangle}{\sqrt{2}}$. You see that they are a simple linear combination of separable states ($|00\rangle$ and $|11\rangle$ or $|01\rangle$ and $|10\rangle$). If you measure the first qubit in both cases, you have an even 50%/50% chance to get a $|0\rangle$ or a $|1\rangle$. When you measure the second qubit, you then have a 100% chance to get respectively the same value of the opposite values $|1\rangle$ or $|0\rangle$. But you can’t decide in advance what is the first measurement outcome (on Alice’s side). So, you observe some synchronicity between two measurements but no determinism on the first readout value. It’s all about having two simultaneous synchronized random values. It is described as the “no-signaling principle”: there is no statistical difference between a “first” or “second” measurement of entangled pairs, meaning Bob doing the measurement before or after Alice and Alice didn’t send any actual pre-determined information to Bob when doing the measurement on her side.

But that is a mathematical representation of entanglement. You can wonder how these composite objects are created in the real world. Of course, some physical interaction must be created to entangle electrons, atoms and/or photons. Photons can be prepared to be entangled with being generated by some excitement of atoms like cesium which generates photon couples of different wavelengths but with some correlated properties like their polarization. Neutral atoms can be entangled with exciting them with lasers, raising their energy levels to a so-called Rydberg state. Electron spins are entangled with lowering a potential energy barrier between them. Quantum objects of different types can also be entangled, like photons with atoms or electrons with photons¹³⁸.

These entangled particles are not linked by chance. They usually had a common past or some past interactions. For example, two entangled photons can be produced with a birefringent mirror and separated by dichroic mirrors, creating two photons of orthogonal polarizations. The action on one of the two photons has an impact on the other photon as demonstrated by Alain Aspect in his famous 1982 experiment. But the values that are generated are completely random!

It is not defined at one end and transmitted to the other end. It is a random value that can be uncovered at two different places with some quantum measurement.

A 2019 experiment conducted at the University of Glasgow has even allowed to photograph a representation of the state of entangled photons¹³⁹. Nevertheless, we are still able to entangle particles that do not necessarily have a common past¹⁴⁰. Bell's inequalities were first validated with photons in the visible spectrum. It's been extended to other parts of the spectrum, of course in the infrared bands that are used in fiber optics and free space quantum communications and even in the X-ray band¹⁴¹. It has also been done with all sorts of qubits (superconducting, silicon spin, trapped ions, neutral atoms).

Despite its randomness, entanglement is a very powerful resource. It helps generate random secret keys for two parties with the QKD (quantum key distribution) protocols. It powers quantum computing with creating interdependencies between qubits. Multi-qubits quantum gates conditionally link them together. Once entangled, qubits have inseparable quantum states. Without it, no useful quantum algorithm could work. But quantum entanglement does not mean we can transmit some useful information faster than light since the entangled objects properties are random.

How are we checking that a quantum system is entangled? This is done with correlation statistic tests. With two quantum objects, it's a **Bell inequality test** or Bell experiment (see [glossary](#), page 1068) that looks at the statistical correlation between the states of two quantum objects, with an experiment done a large number of times with the same settings. This test was extended with the **Mermin inequalities test** created by David Mermin in 1990 to extend Bell's inequalities test to the entanglement of a higher number of quantum object like a GHZ state with three or more qubits¹⁴². These tests are very costly as you increase the number of correlated quantum objects. Another variation is to conduct a state tomography for a set of qubits as described page 188. Again, its cost grows exponentially with the number of qubits, which explains why most qubit tomographies are not done beyond 6 qubits.

¹³⁸ In 2017, researchers in Warsaw were able to entangle a photon with billions of rubidium atoms. See [Quantum entanglement between a single photon and a trillion of atoms](#), 2017.

¹³⁹ See [Scientists unveil the first-ever image of quantum entanglement](#) by Paul-Antoine Moreau, July 2019.

¹⁴⁰ See [Qubits that never interact could exhibit past-future entanglement](#) by Lisa Zyga, July 2012.

¹⁴¹ See [Entangled X-ray Photon Pair Generation by Free Electron Lasers](#) by Linfeng Zhang et al, August 2022 (13 pages).

¹⁴² See [Extreme quantum entanglement in a superposition of macroscopically distinct states](#) by David Mermin. PRL, 1990 (no free access).

In science at the frontier of science fiction, some imagine exploiting quantum entanglement to analyze a quantum state inside a black hole¹⁴³! This is beyond the scope of this book¹⁴⁴!

Indetermination

Heisenberg's principle of indeterminacy or indetermination states that one cannot accurately measure both the position and velocity of a particle or two complementary quantities describing a quantum object state. It is mathematically described as an inequality showing that the multiplication of both precisions can't be lower than the Planck constant divided by 4π . Surprisingly, this inequality was not created by Werner Heisenberg but devised and demonstrated by **Earle Hesse Kennard** in 1927 as he was doing a sabbatical at the University of Göttingen. It is even named the Kennard inequality or Heisenberg-Kennard inequality¹⁴⁵.

The indeterminacy principle has another consequence: one cannot observe at the same time a quantum object in its particle state and in its wave state, per the principle of complementarity enacted by Niels Bohr around 1928, that we already mentioned in the wave-particle duality section. It also explains vacuum quantum fluctuations that we cover later in page 134.

For purists, the notions of particle speed and position are even meaningless for electrons. Its characterization is based on its wave nature and its probabilistic description via Schrödinger's wave function. Don't even try to understand where it is at a given place and time.

When it deals with velocity and position or waves, Heisenberg's indeterminacy principle is closely related to a characteristic of Fourier transforms: a nonzero function and its Fourier transform cannot both be sharply concentrated, so, precisely measurable. The more concentrated a signal is in the time domain, the more spread out it is in the frequency domain and vice-versa. We have here a mathematical balance between a pulse length precision and its spectral analysis precision.

Since complementary (or incompatible) properties can't both be measured with an arbitrary precision, we can improve one property measurement precision with decreasing the measurement precision of the complementary property. It's being implemented with the so-called photons squeezing technique. This technique is implemented in the latest LIGO (USA) and VIRGO (Italy) huge interferometers that are used to measure gravitational waves generated by huge astrophysical phenomena like dual black hole collapses. These instruments increase the precision of photons time arrival in the interferometer at the price of a greater imprecision in the number of photons¹⁴⁶.

Measurement

Measuring quantum object properties follows a very different path than with classical physics due to the back action induced by quantum measurement on the measured system and to its probabilistic dimension.

With classical mechanics, you can usually predict over time the results of the measurement of macro-objects properties (dimension, speed, position) based on their dynamics. In quantum mechanics, given the knowledge of the position of the measured object, one cannot measure precisely its momentum.

¹⁴³ See [Can entangled qubits be used to probe black holes?](#) by Robert Sanders, 2019.

¹⁴⁴ Superposition also happens within benzene C_6H_6 with two carbon-carbon links with their neighbors, using one or two electrons.

¹⁴⁵ See [The Uncertainty Principle, Stanford Encyclopedia of Philosophy](#), 2001 (14 pages).

¹⁴⁶ See [Squeezing More from Gravitational-Wave Detectors](#), December 2019. Kip Thorne (1940, USA), Rainer Weiss and Barry C. Barish got the Nobel Prize in Physics in 2017 for their contributions to the creation of the LIGO detector and the observation of gravitational waves.

More generally, the knowledge we have about two non-commuting observables is bounded such that we can never assign them a well define value simultaneously, due to the Heisenberg uncertainty principle.

Moreover, a quantum measurement readout requires some interaction with a macroscopic object that selects automatically one specific outcome. In strawman language, quantum measurement is in the eye of the beholder! Measuring the same initial state several times can lead to different outcomes. However, even if each measurement yields a probabilistic result, when repeated several times, their statistical distribution is not probabilistic. It corresponds to the knowledge that can be obtained from the evaluated quantum state created experimentally in a similar way several times.

Before measurement, a single isolated quantum object is said to be in a pure state, represented by a vector in a Hilbert space, or its “Psi” (ψ) vector. It is a superposition, or linear combination of basis states or one of the object basis state, like “ground state” or “excited”. When a quantum object is measured against one observable, the state of the quantum object become one of the observable basis states, like a spin direction up or down or a discrete energy level. The quantum object collapses in a probabilistic way into one of the available basis states. If we conduct another measurement, we’ll always get the same result being the basis state that was obtained beforehand in the first measurement. This is also called "*Schrödinger wave function collapse*" or "*wave packet collapse*" which however works only with so-called projective measurement, as defined by John Von Neumann.

With a photon of intermediate polarization between horizontal or vertical linear polarization, it will become a horizontally or vertically polarized photon after its polarization measurement.

In quantum computing, this principle of reduction is implemented when measuring the state of a qubit. It modifies its value by collapsing it to the basis states $|0\rangle$ or $|1\rangle$.

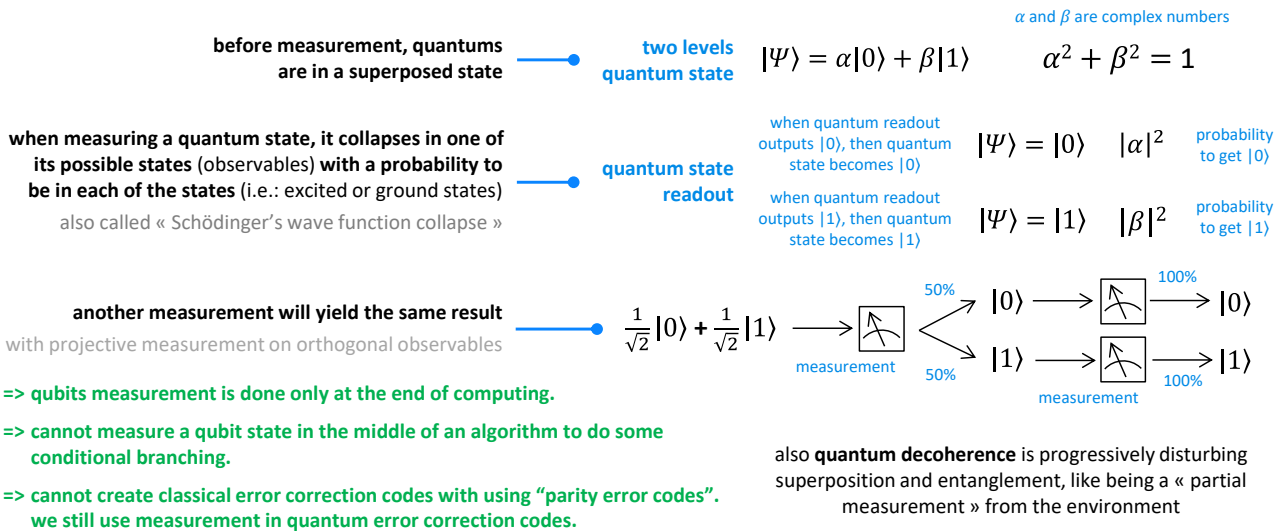
The outcome is probabilistic with a chance of retrieving a $|0\rangle$ or a $|1\rangle$ depending on the qubit state. However, when the quantum state is a basis state, say $|0\rangle$ or $|1\rangle$ for a qubit, its measurement should return this basis state in 100% of the cases and is therefore not probabilistic but deterministic. This works however only in a perfect world without any quantum noise. Even when a qubit is in a basis state, its measurement doesn’t return a perfect basis state 100% all the time. You get a % that is inferior to 100% and corresponds to the readout qubit fidelity. It turns a basis state measurement into a probabilistic one.

The subtle information contained in a qubit that is represented by a complex number or a two-dimensional vector is reduced to $|0\rangle$ or $|1\rangle$ at the time of its measurement. It becomes a classical bit. A single measurement is then making us lose all the wealth of information contained in the qubit. We turn the equivalent of two floating point numbers to a single bit! However, this measurement is supposed to happen only at the end of quantum algorithms. During computing, the whole wealth of qubit internal information is leveraged, particularly with the creation of interferences between qubits.

All this is illustrated in the diagram below in Figure 87. We will come back to the meaning of α and β complex numbers in the next section on qubits.

This reduction should occur theoretically only at the end of computing. During computing, qubits are modified by quantum gates preserving the richness of their information, the combinatorial nature of their values based on superposition and entanglement. However, quantum measurement is to be implemented during computing with systems implementing quantum error corrections.

The subject of quantum measurement is quite broad. In a [forthcoming more detailed section](#) page 184, we will cover several additional concepts such as projective (Von Neumann) measurement, non-selective measurement, weak measurement, gentle measurement and non-destructive measurement.



formalism: Erwin Schrödinger, 1926

Figure 87: quantum measurement explained with qubits, (cc) Olivier Ezratty, 2021.

No-cloning

The no-cloning theorem prohibits the identical copy of the state of a quantum object onto another quantum object. The theorem is mathematically demonstrated in [six lines](#) in Figure 88. It is also described page 148.

The theorem was demonstrated in 1982 by William Wootters, Wojciech Zurek and Dennis Dieks¹⁴⁷. The article is still not available in open source on a site such as arXiv, self-applying the no-cloning principle¹⁴⁸!

a quantum's state can't be replicated independently onto another quantum

only possible copy is through entangled states creation
easy to demonstrate mathematically ————

- => qubit teleportation.**
- => secures telecommunications with quantum key distribution.**
- => creates significant constraints in quantum computing (memory, cache, error correction, ...).**

discovery : James Park in 1970
then William Wootters and Wojciech Zurek in 1982

No Cloning Assume we have a unitary operator U_{cl} and two quantum states $|\phi\rangle$ and $|\psi\rangle$ which U_{cl} copies, i.e.,

$$\begin{aligned} |\phi\rangle \otimes |0\rangle &\xrightarrow{U_{cl}} |\phi\rangle \otimes |\phi\rangle \\ |\psi\rangle \otimes |0\rangle &\xrightarrow{U_{cl}} |\psi\rangle \otimes |\psi\rangle \end{aligned}$$

Then $\langle\phi|\psi\rangle$ is 0 or 1.

Proof 1: $\langle\phi|\psi\rangle = (\langle\phi| \otimes \langle 0|)(|\psi\rangle \otimes |0\rangle) = (\langle\phi| \otimes \langle\phi|)(|\psi\rangle \otimes |\psi\rangle) = \langle\phi|\psi\rangle^2$. In the second equality we used the fact that U_{cl} , being unitary, preserves inner products. \square

Proof 2: Suppose there exists a unitary operator U_{cl} that can indeed clone an unknown quantum state $|\phi\rangle = \alpha|0\rangle + \beta|1\rangle$. Then

$$\begin{aligned} |\phi\rangle|0\rangle &\xrightarrow{U_{cl}} |\phi\rangle|\phi\rangle = (\alpha|0\rangle + \beta|1\rangle)(\alpha|0\rangle + \beta|1\rangle) \\ &= \alpha^2|00\rangle + \beta\alpha|10\rangle + \alpha\beta|01\rangle + \beta^2|11\rangle \end{aligned}$$

But now if we use U_{cl} to clone the expansion of $|\phi\rangle$, we arrive at a different state:

$$(\alpha|0\rangle + \beta|1\rangle)|0\rangle \xrightarrow{U_{cl}} \alpha|00\rangle + \beta|11\rangle$$

Here there are no cross terms. Thus we have a contradiction and therefore there cannot exist such a unitary operator U_{cl} . \square

Figure 88: no-cloning theorem demonstration, source: Wikipedia.

As a consequence, it is impossible to copy the state of a qubit to exploit it independently of its original, contrarily to a classical bit that can be copied from/to memory and from/to storage. It also prevents quantum computers to implement the Von Neumann computing model with separate processing and memory.

¹⁴⁷ See [A single quantum cannot be cloned](#) by William Wootters and Wojciech Zurek, Nature, 1982.

¹⁴⁸ A summarized version if available in [The no-cloning theorem](#) by William K. Wootters and Wojciech H. Zurek, Physics Today 2009 (2 pages).

In quantum computers, qubits can be duplicated via quantum gates and entanglement, but the resulting qubits are entangled and therefore somehow synchronized, inseparable and... random. Reading the copy destroys the original by projecting the state of the two qubits to the 0 or 1 closest to their initial state and in a probabilistic way.

This has a direct impact on the design of quantum algorithms and in particular on the error correction codes of quantum computers. These error-correction codes use the trick of projective measurement on a different computational basis as we'll see later.

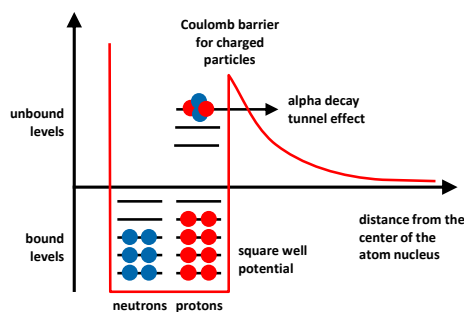
A derivative of no-cloning is non-deleting. In the case of a qubit, it means it's impossible to reset a qubit from an entangled set of two qubits $|\psi\rangle$, meaning to transform $|\psi\rangle|\psi\rangle$ into $|\psi\rangle|0\rangle$.

Tunnel effect

The wave-particle nature of matter allows it to cross physical barriers also known as energy walls in some circumstances, depending on the wall thickness and quantum object wavelength. The transmitted wave is usually attenuated after crossing the barrier and its strength depends on the wavelength with regards to the barrier length and composition.

This phenomenon was first accidentally unveiled by **Henri Becquerel** in 1896 when he discovered radioactivity. It did show up with uranium salts decaying, producing alpha rays comprised of two neutrons and two protons. This phenomenon was explained later thanks to quantum physics and wave-particle duality by **George Gamow** (1904-1968, Ukrainian-Russian-American) in 1928. Just before in 1927, the German physicist **Friedrich Hund** (1896-1997, German) created the formalism explaining electron based tunneling effect.

The tunnel effect is used in superconducting Josephson junctions and exploited in D-Wave quantum annealers where it is used to converge a system of spin qubits ("Hamiltonian", with a given total energy level) towards an energy minimum corresponding to the resolution of a complex combinatorial problem or a search for energy minimum as in chemistry or molecular biology.



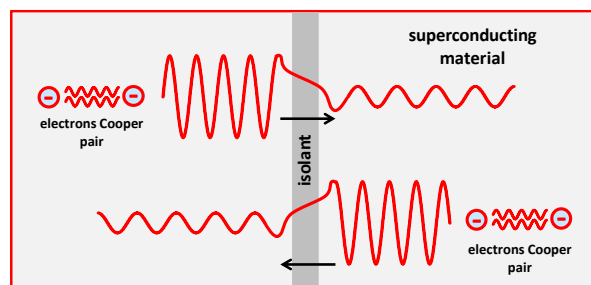
radioactive alpha decay across the Coulomb barrier

=> tunnel effect microscopes.

=> Josephson junctions and superconducting qubits.

=> used in quantum annealing computers (D-Wave).

=> tunnel effect is avoided in most transistor types.



Josephson junction

wave-particle duality enables particles to cross physical barriers

these are energy walls.

wave is usually attenuated after crossing the barrier.

depends on the wave length with regards to the barrier length and composition.

discovery: **Henri Becquerel** with uranium salts, 1896.

explanation: **George Gamow**, 1928.

electron tunneling formalism: **Friedrich Hund**, 1927.

Figure 89: overview of the tunnel effect and its use cases, (cc) Olivier Ezratty, 2021.

But contrarily to what I wrote in the previous editions of this book, the tunnel effect is not exploited in transistors. Most transistors make use of the field effect which was patented by Julius Edgar Lilienfeld in 1926. It is implemented in MOSFETs (metal-oxide-semiconductor field effect transistor) and in CMOS (complementary-metal-oxide-semiconductor, that use variants of MOSFETs). These transistors use a metal gate deposited on a silicon-dioxide (SiO_2) and now a “high-K dielectric” as the gate dimension is decreasing with higher densities, to reduce the tunnel effect. The gate voltage determines the transistor conductivity.

Quantum matter

Quantum matter refers to materials or assemblies of few atoms which, for specific conditions, physical observables such as magnetism, electronic state or optical properties are only described by advanced quantum physics. They are at the crossroads of statistical physics. Iconic quantum materials are superconducting materials in which, below a certain temperature, electrons behave collectively as a sort of fluid dubbed “quantum fluid”. Other known quantum fluids in physics are superfluid helium, Bose-Einstein condensates, polariton condensates and ultra-cold neutral atoms. They all exhibit quantum mechanical effects at a macroscopic collective level. These phenomena are usually reported at very low temperatures, close to -273°C , and sometimes high-pressures but some of them start to emerge in less drastic conditions.

Definitions

Given all standard matter such as metal, semiconductor or insulator rely on quantum description, starting with electrons quantum numbers and the atomic structure, how are quantum materials and quantum matter being accurately defined? Where is the frontier? Well, there’s no real consensus on this, a bit like how postulates are formalized in quantum physics.

One of the reasons is that quantum materials range from yet untested theoretical concepts, to lab-based experiments, up to industry applications like with graphene. It’s an entire new research field that is still in the making with a lot of fundamental research.

It is also a field that is really hard to dig into, even more than many other fields that are covered in that book, like quantum error correction. So, forgive some of the vagueness of this part. I have not really understood *all* the sentences I wrote here!

The simplest definition I found is “*materials where electrons do interesting things*”. Then, I opened quantum matter’s Pandora’s box and found many other definitions.

The US Department of Energy created its own definition in 2016 with “*solids with exotic physical properties that arise from the interactions of their electrons, beginning at atomic and subatomic scales where the extraordinary effects of quantum mechanics cause unique and unexpected behaviors*”¹⁴⁹.

A more precise definition was proposed by Philip Ball in 2017 which is based on materials where electrons are operating collectively as quasi-particles and are frequently confined in some 2D geometries like graphene sheets, with derivatives in 3D assemblies of graphene sheets with small angle rotations called **magic angle**, creating the new field of **twistronics**¹⁵⁰.

¹⁴⁹ Seen in [Basic Research Needs for Quantum Materials](#), DoE, 2016 (4 pages), with a slightly simpler one “*solids with exotic physical properties, arising from the quantum mechanical properties of their constituent electrons; such materials have great scientific and/or technological potential*” seen in [Quantum Materials for Energy Relevant Technology](#) by the DoE Office of Science, 2016 (170 pages).

¹⁵⁰ In [Quantum materials: Where many paths meet](#) by Philip Ball, MRS Bulletin, 2017 (8 pages), [Magic angle, a new twist on](#) by Pablo Jarillo-Herrero and Senthil Todadri, MIT, January 2021 (12 pages) and [Magic-Angle Multilayer Graphene: A Robust Family of Moiré Superconductors](#) by Jeong Min Park, Pablo Jarillo-Herrero, December 2021 (15 pages). This could lead to interesting superconducting effects.

Quantum materials are also grouped as **strongly correlated materials** where magnetism is important and their behavior is “*dictated by quantum mechanical correlations between electrons*”, and **topological materials** where some symmetry of the material lattice provides protected electronic states on the surface or in the bulk of the crystal.

And I didn't try to find any semantic nuance between quantum matter and quantum materials!

In another source¹⁵¹, quantum matter deals with “*novel phases of matter at zero temperature with exotic properties*”. It adds:

“The main ways of characterizing and manipulating quantum matter are with entanglement, symmetry, and topology:

***Entanglement** is the quantum property of correlated physical attributes among particles (position, momentum, spin, polarization).*

***Symmetry** refers to features of particles and spacetime that are unchanged under some transformation, seen as the property of a system looking the same from different points of view (a face, a cube, or the laws of physics) and its partner, symmetry breaking (in phase transitions)¹⁵².*

***Topology** is the property of geometric form being preserved under deformation (bending, stretching, twisting, and crumpling, but not cutting or gluing). Physical systems may have global symmetric and topological properties that remain invariant across system scales”.* Usually, obtaining some topological order requires cooling at very low temperatures like with superconducting materials.

As stated before, quantum matter is characterized with being based on collective excitations. These excitations are composite entities that are analogous in their behavior to a single particle¹⁵³ named quasiparticles

It can be quasiparticles that are assemblies of several fermions, mostly electrons and holes, like two electrons in Cooper pairs explaining superconductivity, polaritons, excitons and vortex magnetic phenomena like skyrmions, etc... It can also be collective excitations of bosons like phonons in crystal lattices. There are over 30 identified quasiparticles classes including some that are very exotic and less talked about like the Bogoliubon (a quasiparticle found in superconductors) and the wrinklön¹⁵⁴.

Philip Ball proposes a classification of these quasiparticles in seven categories¹⁵⁵:

- **Cooper pairs** of electrons in classical superconductivity (high-temperature superconductivity with cuprates requires a more complicated explanation). We cover their various use cases with superconducting qubits and sensors.

¹⁵¹ See [Quantum Matter Overview](#) by Melanie Swan, Renato P. dos Santos and Frank Witte, April 2022 (23 pages). See also [The 2021 Quantum Materials Roadmap](#) by Feliciano Giustino et al, February 2021 (93 pages) and [Introduction to Quantum Materials](#) by Leon Balents, KITP, 2018 (51 slides).

¹⁵² Classical matter phases transitions are traditionally described with Lev Landau's symmetry breaking model elaborated in 1937. It describes in a simplified way what happens at phase transitions (like gas↔liquid and liquid↔solid) with the evolution of a symmetry-breaking order parameter (OP) named η (eta). It also describes various types of ordering phenomena like ferromagnetic, ferroelectric, ferroelastic or other types of electronic orders like Mott or insulator-metal transitions systems. In most cases, quantum matter is described by a “topological order” that can't be explained by Landau's model. Some examples include topological insulators, topological semimetals, fractional quantum Hall states, quantum spin liquids and Fermi liquids. A Mott transition is a particular type of topological phase transition. Mott insulators are materials that are expected to conduct electricity but are insulators, particularly at low temperatures, and under certain conditions which can be controlled, leading to so-called Mott transitions.

¹⁵³ Source: [Webster](#). Quasiparticle were first defined by Lev Landau in the 1930s.

¹⁵⁴ Source : https://en.wikipedia.org/wiki/List_of_quasiparticles.

¹⁵⁵ See Quantum materials: Where many paths meet by Philip Ball, 2017 (8 pages)

- **Relativistic Dirac fermions** such as many-electron excitations in Dirac semimetals and in graphene¹⁵⁶. Graphene has many applications in sensing and electronics. There was even a European Union Graphene Flagship program launched in 2013 with 1B€.
- **Weyl fermions** are massless fermions related to Dirac fermions whose existence was predicted by Herman Weyl in 1929 and discovered in 2015 at Princeton¹⁵⁷. These fermions are massless, have a high degree of mobility and are quasiparticle excitations in Weyl semimetals. Topological semimetals could be used in low-consumption spintronic and magnetic memory devices and ultrafast photodetectors¹⁵⁸.
- **Laughlin quasiparticles** proposed by Robert Laughlin in 1983 and who received the Nobel in Physics in 1998 for his theoretical explanation of the fractional quantum Hall effect, together with Horst Störmer and Daniel Tsui, who discovered the effect experimentally. They relate to the “fractional quantum Hall effect” (FQHE, discovered in 1982) in a 2D “electron gas” placed in a magnetic field. It involves electron quasiparticles behaving like if they had a fractional charge, such as $1/3$, $2/5$ or $3/7$, 1 being the charge of a single electron. One use case is to create an electron interferometer¹⁵⁹.
- **Majorana fermions** are hypothetical particles proposed in 1937 by Ettore Majorana, which are their own antiparticles. Their existence is still questioned. They could lead to creating topological qubits quantum computers with a better resistance to quantum noise and errors.
- **Anyons** are hypothetical particles proposed by Frank Wilczek in 1982. Anyons have quantum statistics positioned in a continuum between fermions ($1/2$ spin) and bosons (integer spin). They could show up in quantum spin liquids¹⁶⁰. These quantum spin liquids which can show up in magnetic materials where electron spins are not orderly aligned but are entangled. The first spin liquids were experimentally detected in 2020¹⁶¹. It could help to create innovative electronic memories. This state of matter was envisioned in 1973 by Philip W. Anderson¹⁶².
- **Skyrmions** take the form of vortex-like topological quasiparticle excitations of spins in some magnetic materials. They were envisioned in 1962.

We could still add here various classes and subclasses of quantum materials:

- **Spin glasses** where electron spins freeze in a disordered fashion at some non-zero temperature. It leads to the notion of **quantum glasses**¹⁶³.
- **Plasmons** which are collective oscillations of electrons on the surface of a conductor that can interact with photons. It could also help creating energy savings and faster data storage solutions.
- **Topological insulators** are materials whose bulk part is insulating and whose surface (2D or 3D) presents counterpropagating spin channels with no charge current. It could help create a new breed of energy-saving and fast-switching transistors.

¹⁵⁶ See the thesis [Relativistic Phases in Condensed Matter](#) by Thibaud Louvet, 2018 (165 pages).

¹⁵⁷ See [After 85-year search, massless particle with promise for next-generation electronics discovered](#) by Morgan Kelly, 2015.

¹⁵⁸ See [Topological Semimetals](#) by Andreas P. Schnyder, 2020 (32 pages).

¹⁵⁹ See [Realization of a Laughlin quasiparticle interferometer: Observation of fractional statistics](#) by F. E. Camino, Wei Zhou and V. J. Goldman, 2005 (25 pages).

¹⁶⁰ See [A Field Guide to Spin Liquids](#) by Johannes Knolle and Roderich Moessner, 2018 (17 pages).

¹⁶¹ See [Scale-invariant magnetic anisotropy in RuCl₃ at high magnetic fields](#) by K. A. Modic et al, October 2020 (32 pages).

¹⁶² See [Quantum Spin Liquids](#) by C. Broholm et al, May 2019 (21 pages).

¹⁶³ See the review paper [Quantum Glasses](#) by Leticia F. Cugliandolo and Markus Müller, Sorbonne Université CNRS LPTHE and Paul Scherrer Institute, August-September 2022 (23 pages).

- **Quantum wires** are conducting wires with quantum confinement effects modifying the transport properties, mostly when the wires have a diameter of a few nanometers, even down to a single atom¹⁶⁴. They are usually called nanowires. Carbon nanotubes are a class of quantum wires.

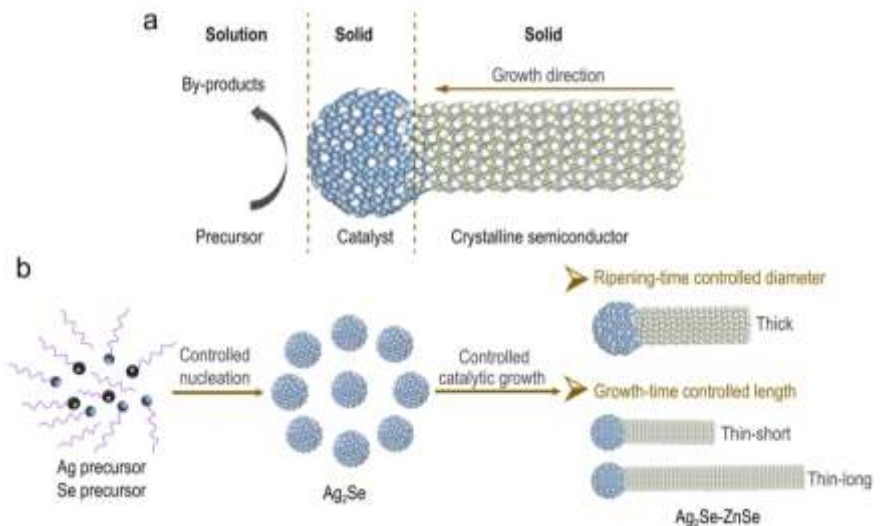


Figure 90: quantum wires. Source: [On demand defining high-quality, blue-light-active ZnSe colloidal quantum wires](#) from Yi Li et al, National Review Science, April 2022 (29 pages).

- **Spin-torque materials** that are already used in some low-power non-volatile magnetic memories (STT-RAM or STT-MRAM).
- **Time crystals** which we'll cover later, and it is the source of a lot of headaches.
- **Wigner crystals** are another very weird phenomenon. Predicted by Eugene Wigner in 1934 (the same Wigner of the Wigner function used in quantum photonics), it consists in crystals made of electrons, of course also at very low temperatures

They were experimentally observed in 2018 by an Israeli-US-Hungarian team in one dimension at 10 mK using carbon nanotubes for their measurement¹⁶⁵ and 2020 in 2D at 80 mK by a team from ETH Zurich (as shown here on the right in Figure 91)¹⁶⁶.

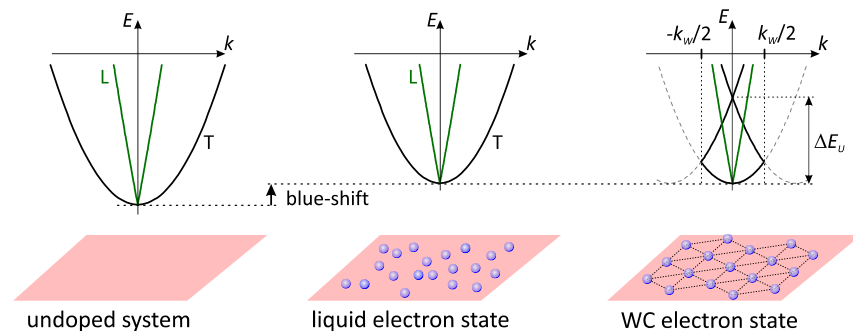


Figure 91: Wigner crystals. Source: [Observation of Wigner crystal of electrons in a monolayer semiconductor](#) by Tomasz Smoleński et al, 2020 (26 pages).

- **Quantum batteries** are still theoretical devices that would be more efficient than traditional batteries with a shorter recharging cycle.

¹⁶⁴ See one recent example of quantum nanowire in [On demand defining high-quality, blue-light-active ZnSe colloidal quantum wires](#) from Yi Li et al, National Review Science, April 2022 (29 pages).

¹⁶⁵ See [Imaging the electronic Wigner crystal in one dimension](#) by I. Shapir et al, Science, 2019 (38 pages).

¹⁶⁶ See [Observation of Wigner crystal of electrons in a monolayer semiconductor](#) by Tomasz Smoleński et al, 2020 (26 pages).

- Quantum dots** that are used in LCD screens and are not considered as being quantum materials since their behavior is explained by single electrons and classical quantum light/matter exchanges. They are made of powder with tiny compound grains of different sizes between 2 and 6 nm which are used to down-convert the blue light coming from LEDs into red and green light, creating a better balanced coverage of primary colors, as shown in Figure 92¹⁶⁷. The main problem is to replace cadmium that is a pollutant. These LCD screens quantum dots must not be confused with the quantum dots used in silicon qubits to trap single electrons and control their spin as well as the quantum dots used in unique photon sources like the ones from Quandela.

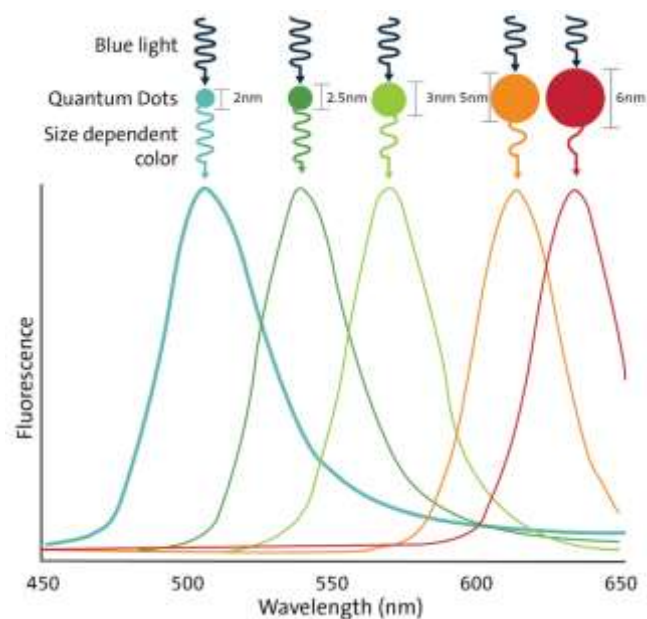


Figure 92: quantum dots used in LCD screen and lighting. Source: [Nanomatériaux et nanotechnologies : quel nanomonde pour le futur?](#) by Pierre Rabu, 2018.

Some other concepts related to quantum matter mandate some explanations:

Many of the quantum matter species happen in crystals. And there are a lot of types of crystals classified by their crystallographic order! There are 230 crystallographic space groups organized in 7 crystal systems named triclinic, monoclinic, orthorhombic, tetragonal, trigonal, hexagonal and cubic and subclasses with primitive centering, centered on a single face, body centered and face centered¹⁶⁸.

Bravais lattices

7 groups and 14 subgroups

P: Primitive centering
 C: Centered on a single face
 I: Body centered
 F: Face centered

1. Cubic P
2. Cubic I
3. Cubic F
4. Tetragonal P
5. Tetragonal I
6. Orthorhombic P
7. Orthorhombic C
8. Orthorhombic I
9. Orthorhombic F
10. Monoclinic P
11. Monoclinic C
12. Triclinic
13. Rhomboedral
14. Hexagonal

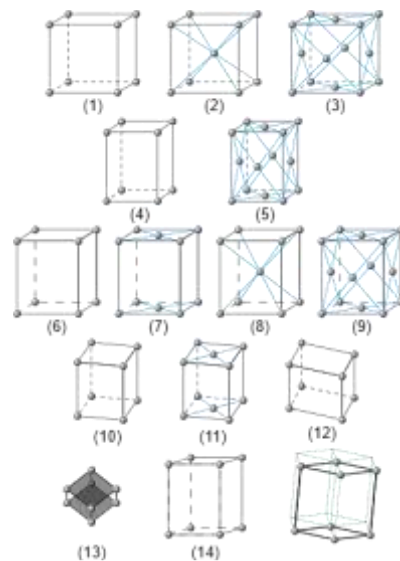


Figure 93: Bravais lattices and crystal structure classification. Source: Wikipedia.

¹⁶⁷ It was first discovered at the end of the 1970s by Alexei Ekimov in Russia and explained in 1982 by Alexander Efros, also from Russia. From [The Quantum Dots Discovery](#). See [Advances in Quantum-Dot-Based Displays](#) by Yu-Ming Huang et al, 2020 (29 pages), schema from [Quantum dots and their potential impact on lighting and display applications](#) by Paul W. Brazis, 2019 (18 pages).

¹⁶⁸ See [Crystal Systems and Space Groups](#) by Paul D. Boyle, University of Western Ontario (44 slides) and [Cristallographie et techniques expérimentales associées](#) (in English) by Béatrice Grenier, 2014 (67 slides).

One key notion in crystallography is chirality which describes how crystal structures break spatial symmetry and are not identical to their mirrored structure¹⁶⁹. There are also 1651 magnetic space groups which describe magnetism configurations at the atom level in crystal lattices¹⁷⁰.

Another key notion in quantum matter is time reversal symmetry. A time reversal symmetry means that the material looks the same when looking at a time scale backwards and forward.

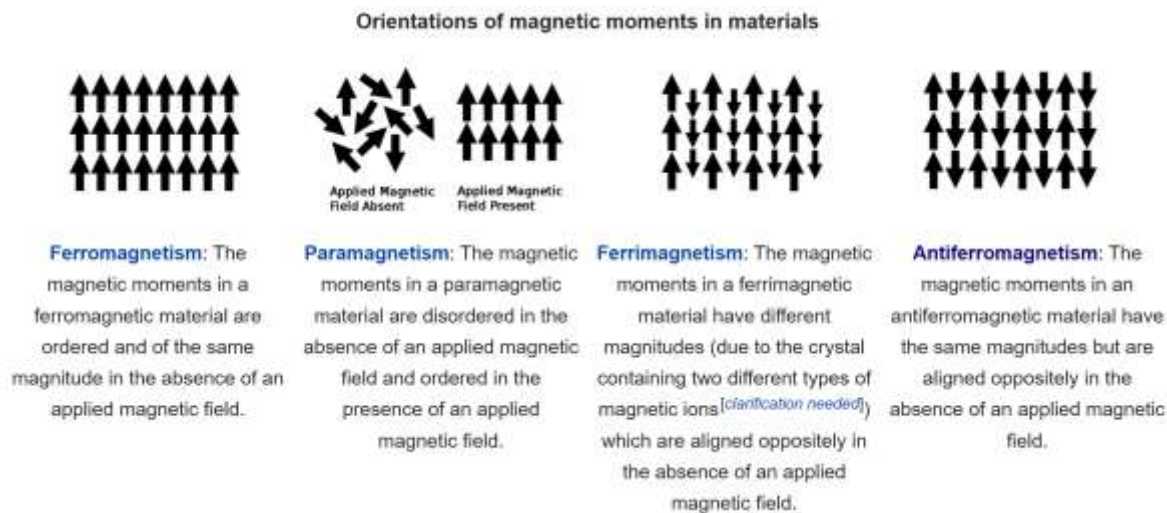


Figure 94: ferromagnetism, paramagnetism, ferrimagnetism and antiferromagnetism explained. Source: Wikipedia.

Reversing time means looking backwards in time only from a mathematical standpoint, not physically reversing time. There's no way you can change the arrow of time backwards. Time reversal is not a time machine!

Figure 95 presents an inventory of some physical properties that change or do not change with time reversal.

time reversal symmetry

| do not change with time reversal | changes with time reversal |
|---|-----------------------------------|
| position of particle in space | time of events |
| particle acceleration in space | particle velocity |
| force on the particle | particle linear momentum |
| particle energy | electric vector potential |
| electric potential and field | magnetic field |
| density of electric charge | electric current density |
| energy density of the EM field | power / rate of work done |

Figure 95: time reversal symmetry explained.

Superconductivity

Superconductivity occurs when under a low-level temperature, some conducting materials no longer oppose resistance to electric current. With usual electric current, electrons move from atom to atom and transform part of their kinetic energy into heat related to the movement of the atoms hit by electrons, also known as the Joule effect.

With superconductivity, electrons arrange themselves in pairs, called Cooper's pairs, circulating between atoms without friction. The structure of the atoms of the conductive metal is also modified. Waves of atoms occur that follow and accompany the movement of Cooper's pairs. These are specific breeds of phonons.

¹⁶⁹ See [A Chirality-Based Quantum Leap](#) by Clarice D. Aiello and many al, November 2021 (93 pages) described in [Chirality and the next revolution in quantum devices](#) by César Tomé López, Mapping Ignorance, May 2022. See also [Topology and Chirality](#) by Claudia Felser and Johannes Gooth, May 2022 (27 pages) which makes a good classification including chiral and topological matter.

¹⁷⁰ See [Magnetic Group Table, Part 2 Tables of Magnetic Groups](#), by Daniel B. Livin, 2014 (11976 pages). I hope the author found some way to automatize the production of all these pages! See also [Exhaustive constructions of effective models in 1651 magnetic space groups](#) by Feng Tang et al, March 2021 (25 pages) and [Structure and Topology of Band Structures in the 1651 Magnetic Space Groups](#) by Haruki Watanabe et al, August 2018 (43 pages).

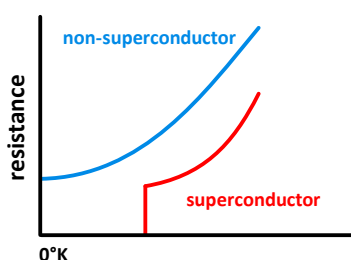
Cooper's pairs are electrons of opposite spins forming composite bosons (ensemble with zero spin), allowing them to have the same quantum state¹⁷¹.

Superconductivity was discovered experimentally in 1911 by **Heike Kamerlingh Onnes** (1853-1926), Cornelis Dorsman, Gerrit Jan Flim and Gilles Holst at the University of Leiden in the Netherlands, with solid mercury at 4.2K. Kamerlingh Onnes also discovered that a magnetic field whose intensity depends on temperature could make the superconducting effect disappear¹⁷². Its interpretation was formulated much later, in 1957.

superconducting elements

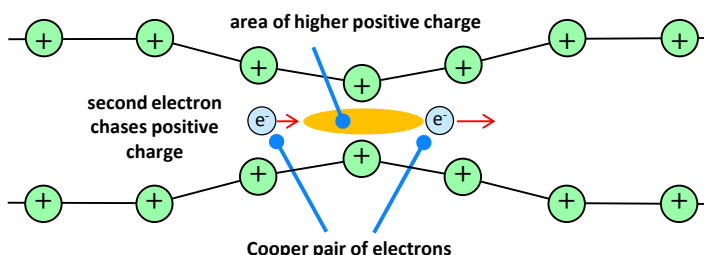
Figure 96: table of chemical elements with those which are superconducting. Source: Wikipedia and various other sources.

It was achieved by **John Bardeen**¹⁷³, **Leon Neil Cooper** and **John Robert Schrieffer** of the University of Illinois. They built the so-called **BCS theory**¹⁷⁴. Later experiments and extrapolations on the persistence of circulating currents injected into macroscopic superconducting rings found that the lower bound of these permanent currents was around 10^5 years.



some materials have zero resistivity below a threshold temperature (T_c)

discovery: **H. Kamerlingh Onnes** et al, 1911



explained by Cooper pairs of electrons with opposed spins flowing in crystal lattice, creating bosons

theory: **Bardeen, Cooper, Schrieffer** (BCS) theory, 1957

Figure 97: superconductivity explained.

¹⁷¹ Cooper's pairs can also be formed with atoms as with helium 3, a fermion, in its superfluid state named a fermionic condensate.

¹⁷² See this detailed presentation: [Superconductivity and Electronic Structure](#) by Alexander Kordyuk, 2018 (145 slides).

¹⁷³ John Bardeen holds two Nobel prizes in physics, one in 1956 for the invention of the transistor with William Shockley and Walter Brattain and the other for the interpretation of superconductivity in 1972 with Leon Neil Cooper and John Robert Schrieffer. Cooper co-created the BCS theory at the age of 27 and won the corresponding Nobel Prize at the age of 42. Born in 1930, he is still with us today.

¹⁷⁴ An accurate timeline of the discovery of the principle of superconductivity is provided in the presentation [50 Years of BCS Theory "A Family Tree" Ancestors BCS Descendants](#), by Douglas James Scalapino, John Rowell and Gordon Baym, 2007 (52 slides). See also the excellent book [The rise of superconductors](#) by P.J. Ford and G.A. Saunders 2005 (224 pages) which tells the story of the discovery and then interpretation of superconductivity. Before the BCS theory, many physicists had broken their teeth on the explanation of superconductivity: Albert Einstein, Niels Bohr, Lev Landau, Max Born, Felix Bloch, Léon Brillouin, John Bardeen (co-inventor of the transistor), Werner Heisenberg and Richard Feynman.

About 50 chemical elements are superconducting at low temperature but the superconductivity temperature and pressure thresholds are very variable. In general, metals that are superconductors are poor conductors in their normal state and most good conductors like copper, gold and silver are not superconductors.

Superconductivity is possible with composite alloys such as germanium, titanium and niobium alloys or copper-based materials (as cuprates). This is particularly the case with aluminum and mercury. The most common superconducting materials are aluminum and a niobium and titanium alloy, used in superconducting wires in MRI imaging systems and superconducting qubit cryostats¹⁷⁵.

The superconducting effect is maximum for atoms that have a large number of valence electrons, i.e., in the last orbital layer, with the highest quantum number. Superconductivity explains unexpected phenomena such as the levitation of magnets above superconductors immersed in liquid nitrogen. Superconducting ceramics, discovered since 1986, can be used in this striking experiment.

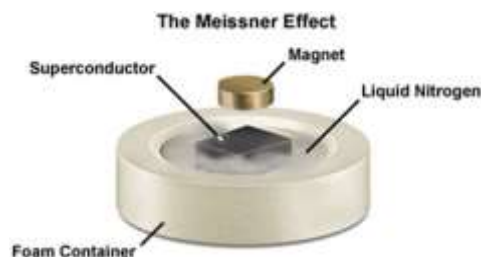


Figure 98: the Meissner effect.

The magnetic field is then expelled from inside the superconducting material. This is the Meissner effect, discovered in 1933 by **Walther Meissner** (1882-1974, German), which only applies to certain so-called type I superconductors. It explains the repulsion demonstrated in numerous experiments. Type II which does not generate this phenomenon includes niobium titanium alloys which are frequently used with a 1:1 ratio of each in the alloy.

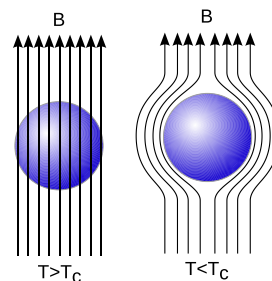


Figure 99: Meissner effect explanation.

In type II superconductors, an intermediate phase between the classical metallic phase and the superconducting phase allows the magnetic field to pass partially. The Holy Grail of superconductivity would be to obtain it at room temperature, allowing, for example, to reduce transmission losses in grid electric power lines¹⁷⁶. Out of the various metals used in quantum technologies, titanium becomes superconducting at 390 mK, aluminum at 1.2K, indium at 3.4K and niobium at 9.26K.

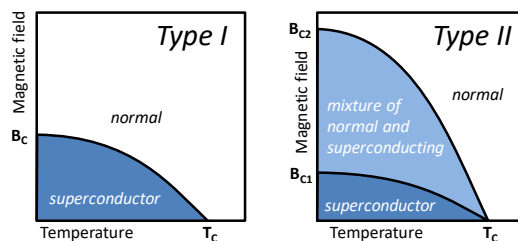


Figure 100: type I and II superconductors characteristics. Source: [Critical Magnetic Field](#), undated.

Scientists from IBM began discovering superconducting metal alloys above 77K (-196°C) in the late 1980s, the temperature of liquid nitrogen.

¹⁷⁵ See [Superconductivity 101](#). The superconducting properties of the niobium-titanium alloy were discovered in 1962. It is widely used in the cooling of MRI scanners but also in many scientific instruments, notably in the ITER experimental nuclear fusion reactor at Caradache. The Periodic Table of Elements comes from Wikipedia.

¹⁷⁶ Type I and II superconductors are mathematically and quantumly explained by the **Ginzburg–Landau** theory created in 1950. See [Theory of Superconductivity](#) by Carsten Timm, TU Dresden, February 2022 (150 pages).

Most of them are cuprates alloys (copper-based). A record was achieved in 2019 with a molecule combining lanthanum and hydrogen (LaH₁₀, illustrated in Figure 101) and at -23°C, thus a near-ambient temperature. In the latter case, however, it works at a huge pressure of 218 GPa, representing more than 2 million times the atmospheric pressure, which is 101,325 Pa¹⁷⁷. Other records were broken with metallic hydrogen in 2020 by CEA, operating at 17°C and at an even greater pressure of 400 GPa¹⁷⁸. Another record of 15°C with 270 GPa was achieved in the USA also in 2020, using a carbonaceous sulfur hydride¹⁷⁹. A less impressive 2022 record was created in China with clathrate calcium hydride (CaH₆) being superconducting at 215K and 172 GPa¹⁸⁰.

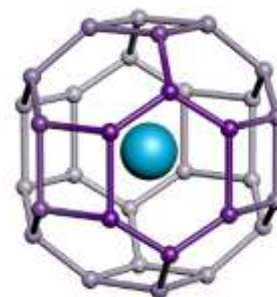


Figure 101: LaH₁₀ high superconducting temperature molecule.

You always see this trade-off between superconducting temperature and pressure. At this very high pressure, practical use cases are not easy to implement! But at lower temperatures, interesting use cases arise like with single photons detectors¹⁸¹.

Hence the willingness to use quantum simulators or computers to run superconductivity quantum equations and identify materials that would be superconducting at room or near-room temperature¹⁸².

By the way, we may wonder why scientists are not using high-temperature superconducting materials to build superconducting qubits? The main reason is that their low temperature of about 15 mK is related to the controlled noise environment linked to using driving micro-waves in the 5-10 GHz range (~0.040 meV). These microwaves have the benefit of being photons adapted to the anharmonic excitement levels of Josephson gates and to be transportable on coaxial cables which are themselves made of superconducting materials like niobium-titanium. The superconducting qubits cooling temperature of 15 mK creates an ambient thermal noise that is one order of magnitude lower than the temperature corresponding to these controlling microwaves (a few kT, with k=Boltzmann constant and T being the temperature = ~0.004 meV).

Superconductivity is commonly used in **MRI scanners**¹⁸³, using large superconducting magnets that are cooled with liquid helium. Scanners are encased in a protective coating to constrain the magnetic field inside the scanner. The niobium-titanium coil wiring is enveloped in a copper matrix.

This combination is also used in large physics instruments like the **CERN LHC** in Geneva with 1200 tons of cables including 470 tons of NbTi (niobium-titanium), the rest being copper, in cables totaling 21 km. Superconductivity creates a current of 11,850 A generating a powerful magnetic field of 8.33 tesla creating a centripetal force holding the accelerated particles. These magnets are cooled by 10,000 tons of superfluid helium-4 at 1.9K. Their cables are made of niobium-titanium filaments surrounded by copper. The whole unit power is 40MW with an electricity consumption estimated at 750 GWh per year according to CERN. It is the largest and most powerful refrigerator in the world!

¹⁷⁷ See [Quantum Crystal Structure in the 250K Superconducting Lanthanum Hydride](#) by Ion Errea, July 2019 (20 pages).

¹⁷⁸ See [Here comes metallic hydrogen - at last!](#) by Jean-Baptiste Veyrieras, May 2020. Another record was broken in 2019 with YH₆ (yttrium hybrid) at a pressure of 110 GPa. See [Anomalous High-Temperature Superconductivity in YH₆](#) by Ivan A. Troyan et al, 2019 (36 pages).

¹⁷⁹ See [Room-temperature superconductivity in a carbonaceous sulfur hydride](#) by Elliot Snider et al, Nature, October 2020 (14 pages).

¹⁸⁰ See [High-Temperature Superconducting Phase in Clathrate Calcium Hydride CaH₆ up to 215 K at a Pressure of 172 GPa](#) by Liang Ma et al, PRL, April 2022 (not open access).

¹⁸¹ See [Single-photon detection using high-temperature superconductors](#) by I. Charaev et al, August 2022 (8 pages).

¹⁸² Another fancy solution consists in lowering the room temperature as described in [Novel approach to Room Temperature Superconductivity problem](#) by Ivan Timokhin and Artem Mishchenko, April 1st, 2020 (4 pages).

¹⁸³ Nuclear magnetic resonance imaging.



Figure 102: MRI principle. Source of illustration on the right: [Helium Reclaiming Magnetic Resonance Imagers](#) by Dan Hazen, MKS Instruments (5 pages).

Superconductivity is operated in the **Chuo Shinkansen** Maglev high-speed train in Japan, which has been undergoing trials since 2013 and is expected to reach a commercial speed of 505 km/hr. It uses a superconductive based magnetic suspension with a rather expensive infrastructure. Power consumption per passenger/kilometer is three times that of traditional Shinkansen, but it is still competitive with airplanes. A 286 km Tokyo-Nagoya line is planned for commercial service in 2027.

Superconductivity has also been studied to improve the efficiency of electric motors and generators with HTS Synchronous Motors (High-Temperature Superconducting). It allows a reduction of motors size and efficiency improvements. It is based on superconducting materials that only require liquid nitrogen cooling, but some systems still use helium-based cooling.

Studies began in the 1980s and these engines and generators are beginning to be deployed in the military navy and in wind power generation, notably at **ASMC**, **Sumitomo Electric**¹⁸⁴ and with the European **EcoSwing** project, which involves Sumitomo's cryostat division.

Superconducting cables have also been introduced to transmit electricity without power loss and greater capacity to meet the ever-increasing demand. They are offered by the French cable manufacturer **Nexans**, which installed one in Long Island. Their 600 m underground cable has been in operation since 2008. It can supply electricity to 300,000 homes¹⁸⁵. But it is rather complex to implement and was not seemingly replicated in many places. The project cost was \$46.9M.



Figure 103: Nexans superconducting cable.

As far as quantum computers are concerned, superconductivity is used in particular in superconducting qubits that exploits the Josephson effect that we have already described in another section. This technology is also used in variations of SQUIDS (superconducting quantum interference device) in quantum sensing. Josephson junctions have a relationship between voltage and frequency which enables the creation of various sensors. It can convert a voltage to frequency as well as a frequency to voltage (with the inverse AC Josephson effect using a microwave impulse). We also find it in the type II niobium-titanium based superconducting cables used for reading the state of superconducting and electron spin qubits.

¹⁸⁴ See [Design of MW-Class Ship Propulsion Motors for US Navy by AMSC](#) by Swarn S. Kalsi, 2019 (50 slides).

¹⁸⁵ Information Source: [Long Island HTS Power Cable](#), Department of Energy, 2008 (2 pages). In addition to Nexans, the cryogenic system was supplied by Air Liquide.

Superconductivity could also be used to create processors operating at low temperatures and capable of operating up to 700 GHz, much faster than current server processors running at a peak 4 to 5 GHz¹⁸⁶. An MIT team announced in July 2019 a proposal for a technique to create spiking neurons with superconducting Josephson effect circuits using nanowires¹⁸⁷.

This is still a research field with very few industry applications at this point. We'll investigate this field in a specific section on unconventional computing. Superconducting electronics could be very useful to create and analyze the microwaves used in superconducting and electron spin qubits.

Superfluidity

Superfluidity is yet another quantum physics phenomenon to cover here. It occurs only with superfluid helium which, at ambient pressure, never freezes, no matter how low the temperature can be.

Superfluid liquid has zero viscosity and flows without any loss of kinetic energy. When poured into a recipient, it tends to rise up by capillary action on its rim and flow out of it. It can even pass through very fine capillaries.

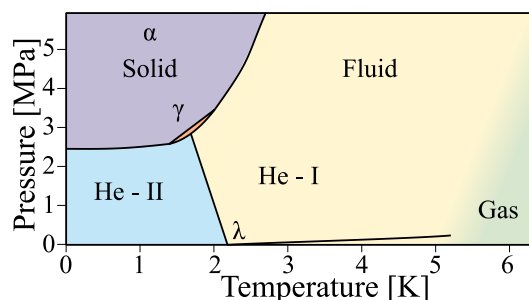


Figure 104: superfluidity. Source: [Wikipedia](#).

Helium was first liquefied in 1908 at 4.2K by Heike Kamerlingh Onnes, the discoverer of superconductivity in 1911. Its superfluidity was highlighted independently in 1938 by **Pyotr Kapitsa** (1894-1984, USSR), **John Frank Allen** (1908-2001, USA) and **Don Misener** (1911-1996, USA)¹⁸⁸.

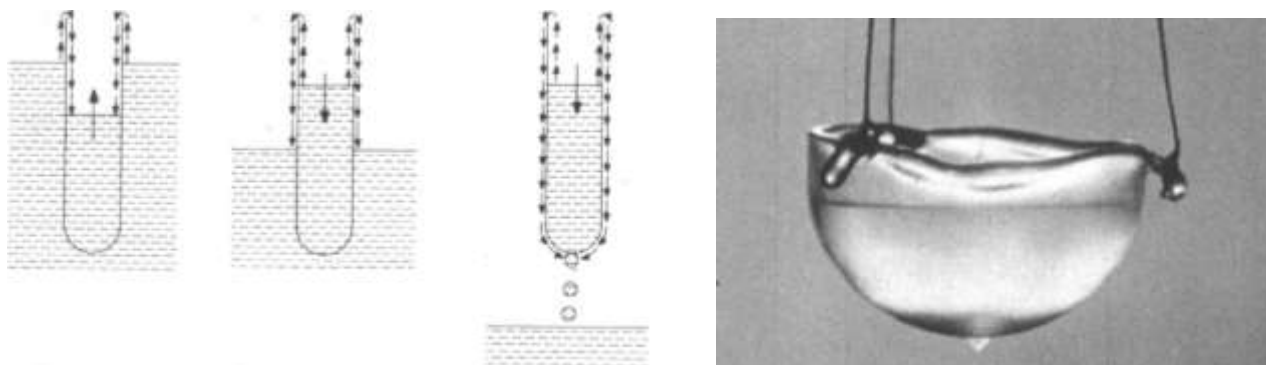


Figure 105: visualization of the superfluidity phenomenon. Source: [Helium 4](#) (14 slides).

There are two isotopes of helium: ^3He with a single neutron, which is the least abundant in nature, and ^4He , with two neutrons, the most common. The latter is a boson, with an integer spin, giving it different properties from helium 3, which is a fermion with a half-integer spin. At low temperature, ^4He behaves like Bose-Einstein condensates since being bosons. ^3He behaves differently, being fermions, and assemble in pairs similar to electron Cooper pairs. It becomes superfluid at lower temperatures than ^4He , at around 1 mK in the absence of a magnetic field (see the phase diagram in Figure 104), vs. 2.17K for ^4He .

¹⁸⁶ See [Superconductor ICs: the 100-GHz second generation](#) by Darren Brock, Elie Track and John Rowell of Hypres, 2000 (7 pages).

¹⁸⁷ See [A Power Efficient Artificial Neuron Using Superconducting Nanowires](#) by Emily Toomey, Ken Segall et Karl Berggren, 2019 (17 pages).

¹⁸⁸ See [Viscosity of Liquid Helium below the \$\lambda\$ -Point](#), Pyotr Kapitsa, Nature (1938) and Flow of liquid helium II, Joan F. Allen, Don Misener, 1938 (1 page). Pyotr Kapitsa was awarded the Nobel Prize in 1978 for his work in the field of low temperatures.

Its superfluidity was only discovered in 1973¹⁸⁹. The different properties of ³He and ⁴He are used to operate the dilution cryogenics systems that equip many quantum computers whose operating temperature is between 10mK and 1K. We will study this in detail in this book, starting page 465.

Industrial demand for helium is spread across many industries: medical imaging for MRI systems magnets cooling, then microelectronics industries.

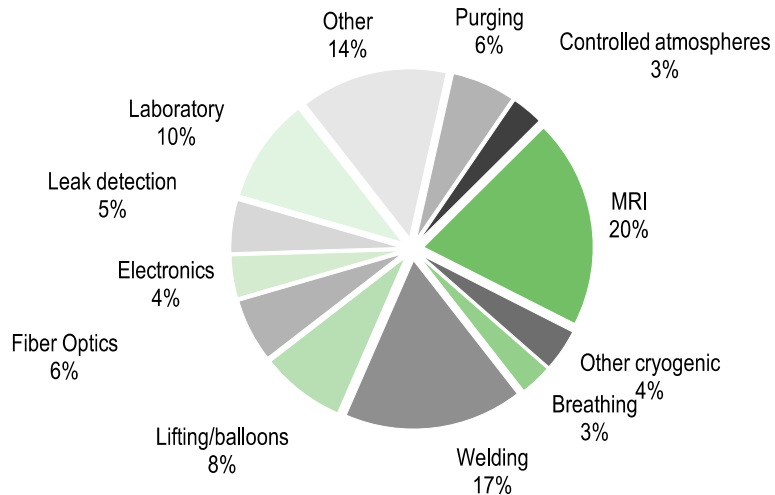
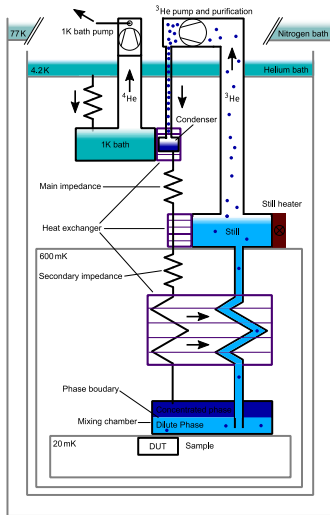
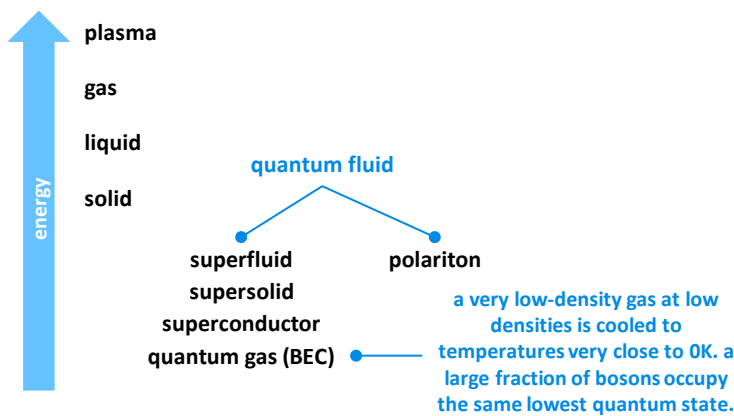


Figure 106: Sources: left diagram: [Wikimedia](#), right diagram: [Edison Investment Research](#), February 2019, referring to [Kornbluth Helium Consulting](#).

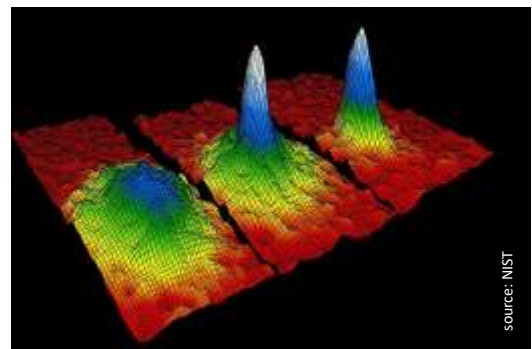
Bose-Einstein Condensates

Bose-Einstein condensates are extremely low-density gases of bosons cooled down to very low temperatures, at the lowest energy level we can set matter in, below solid state. ⁴He is the most famous element that was experimented in this matter state.



=> superconductivity, ferromagnetism, antiferromagnetism and BECs are parts of the condensed matter physics field.

=> BECs laid the groundwork for cold atoms research, quantum sensing and quantum computing using it.



Bose-Einstein condensation at 400, 200 and 50 nK
 prediction: Satyendra Bose and Albert Einstein, 1924
 discovery: Karl Weiman, Wolfgang Ketterle and Eric Cornell, 1995

Figure 107: Bose-Einstein condensates positioned within the various states of matter.

It took a while between the work of Bose and Einstein in 1924 and the experimental discovery of BECs in 1995 by **Carl Wieman**, **Wolfgang Ketterle** and **Eric Cornell** with rubidium 87 at 170 nK. It was cooled with laser-based Doppler effect and magnetic evaporating technique.

¹⁸⁹ David Morris Lee (1931), Douglas Dean Osheroff (1945) and Robert Coleman Richardson (1937-2013) were awarded the Nobel Prize in Physics in 1996 for their discovery of helium-3 superfluidity.

BECs play an important role in quantum technologies. They led to the control of individual atoms that are used in quantum simulators and in quantum gravimeters. Together with superfluids and supersolids, BECs belong to the field of quantum hydrodynamics.

Supersolids

Supersolidity is another weird quantum state of matter showing up at ultracold temperatures, when atoms behave as a crystal and as a superfluid at the same time. This is made possible with crystal lattice with holes (like in an NV center).

The vacancies behave quantumly as bosons and can switch position in a quantum manner like a Bose Einstein Condensate. It's a vacancies quantum tunnelling phenomenon.

This state of matter was predicted in 1969¹⁹⁰ and it was first demonstrated, although debated for a long time, in 2004 with ⁴He at a pressure of about 60 bar and below 170 mK¹⁹¹. The related fundamental research is going on in various places in the world like in the USA, Innsbruck¹⁹², Pisa¹⁹³, Stuttgart, Warsaw, Geneva, and Paris. It is now possible to create supersolids with ultracold dipolar quantum gases of highly magnetic lanthanide atoms like erbium and dysprosium. The supersolidity effect can be controlled by a magnetic field.

There are no known practical applications of this phenomenon to date although it could lead to new forms of quantum simulation systems like the ones using cold atoms.

Polaritons

Polaritons is a field of quantum physics that is rarely mentioned in the context of quantum technologies. It mostly belongs to fundamental research but could be of interest in various fields such as quantum computing and quantum sensing.

Polaritons are quantum quasi-particles in the domain of strong coupling between light and matter. They result from the coupling between photons and an electrical polarization wave.

These waves occur in particular in plasmons (oscillations of free electrons in metals), phonons (oscillations of atoms, especially in crystal structures) and excitons (pairs of electron holes generated by photons in semiconductors¹⁹⁴). The materials can be atoms gas, massive classical semiconductors, thin films inserted in optical cavities or superconducting Josephson junctions.

Excitation photons have a wavelength corresponding to the resonance frequency of the associated medium, often in the visible light or infrared ranges. Polaritons have mixed properties of photons dressed by electronic excitations.

They behave like bosons (having an integer spin) that can occupy the same quantum state and operate in groups, such as superconducting currents forms with paired electrons named Cooper pairs or Bose-Einstein condensates (BEC).

¹⁹⁰ By David J. Thouless (1934-2019, British, 2016 Nobel prize in physics) and, independently, by Alexander Andreev (1939, Russian) and Ilya Mikhailovich Lifshitz (1917-1982, Russian). See [The flow of a dense superfluid](#) by David J. Thouless, 1969 (25 pages) and [Quantum theory of defects in crystals](#) by Alexander Andreev and Ilya Mikhailovich Lifshitz, 1969 (7 pages).

¹⁹¹ See [Probable observation of a supersolid helium phase](#) by E Kim and M H W Chan, 2004, [The enigma of supersolidity](#) by Sébastien Balibar, Nature, 2010 (7 pages) and the review paper [Saga of Superfluid Solids](#) by Vyacheslav I. Yukalov, 2020 (26 pages).

¹⁹² Research in Austria is led by Francesca Ferlaino from the University of Innsbruck, IQOQI.

¹⁹³ See [The supersolid phase of matter](#) by Giovanni Modugno, 2020 (37 slides).

¹⁹⁴ The name of polariton was created by Joseph John Hopfield (1933, American) in 1958 and at that time concerned polariton excitons. See [Theory of the Contribution of Excitons to the Complex Dielectric Constant of Crystals](#) by Joseph John Hopfield, 1958 (14 pages). Hopfield is also known in the field of neural networks in AI with his "Hopfield networks".

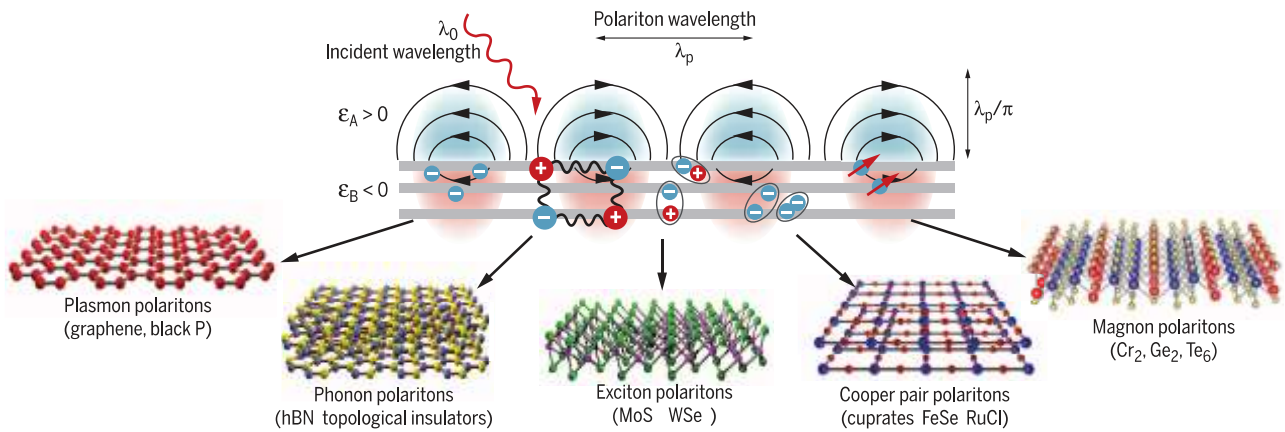


Figure 108: various forms of polaritons. Source: [Polaritons in van der Waals materials](#) by D. N. Basov et al, 2016 (9 pages) which makes a good inventory of different types of polaritons and their fields of application.

Depending on the interaction scale, polaritons operate in a semiclassical or quantum regime. In the first case, the electromagnetic field interacts with a macroscopic polarization field. The polariton field then has the properties of a classical field but its elementary quantum is the result of a dipole-photon "wrapping" that can only be described by quantum mechanics. In the second case, the electromagnetic field interacts with a single polarization field quantum that has been isolated in one way or another, such as a superconducting qubit or an exciton in a quantum box. We are then in the quantum regime of strong coupling, known as the "Jaynes-Cummings Hamiltonian", where the energy levels are discrete and each level correlate to a given number of excitation quanta in the system. Cavity-excited polaritons are generally in the first regime.

In polaritons, semiconductor matter receives photons that excite it. It then emits photons to get out of its excited state, all of this in a very fast iterative cycle, the photons circulating in a closed circuit in the cavity. In practice, electromagnetic and polarization fields co-propagate in the medium in an identical way, notably in polarization and frequency, and with a fixed phase relation (without phase shift or with a 180° phase shift, i.e., π). Polaritons are particularly interesting for generating strong nonlinearities which are searched in photonics¹⁹⁵.

Thanks to the degenerate states in which polaritons can be prepared and to the fact that they interact with each other, polaritons constitute an out-of-equilibrium quantum fluid called "light quantum fluid", often abusively referred to as "liquid light". Polaritons can thus generate surface waves and propagation phenomena typical of quantum fluids such as superfluids. Polaritons also interact with each other, which is not the case for photons in vacuum¹⁹⁶. We can experimentally control the spatial distribution of the density, phase and velocity of these fluids of light¹⁹⁷.

¹⁹⁵ See also this very dense review paper [Quantum Fluids of Light](#) by Iacopo Carusotto and Cristiano Ciuti, 2013 (68 pages).

¹⁹⁶ See the pedagogical presentation [Swimming in a sea of light: the adventure of photon hydrodynamics](#) by Iacopo Carusotto, 2010 (28 slides). Presentation realized with the help of, among others, Elisabeth Giacobino and Alberto Bramati from CNRS. See also the very well-illustrated presentation [Quantum fluids of light](#) by Jacqueline Bloch, February 2020 (58 slides).

¹⁹⁷ Source: description of the ANR project: [Quantum Light Fluids - QFL](#) launched in 2016.

There are many variants of polaritons which depend on the nature of the electronic excitation of the matter:

- **Phonon-polaritons** resulting from the coupling between an infrared photon and an optical phonon caused by the mechanical oscillation of two adjacent ions of opposite charge in a crystalline structure. This oscillation produces an oscillating electric dipole moment. This phenomenon was discovered by **Kirill Tolpygo** (1916-1994, Russian) in 1950 and, independently, by **Kun Huang** (1919-2005, Chinese) in 1951. One application of phonon polaritons are thermal emitted and imagers¹⁹⁸.
- **Exciton-polaritons** result from the coupling of a photon with an exciton in a semiconductor cavity. An exciton is a quasi-particle consisting of an electron-hole pair connected by Coulomb forces, generated by excitation photons. The notion of exciton was created by **Yakov Frenkel** (1894-1952, Russian) in 1931. Like all types of polaritons, these have two energy bands: the high and low polariton. It is a general property of the strong coupling regime between electric dipole and electromagnetic field. Here, the level is high when the photon and the semiconductor are excited and in phase, and low when they are in opposite phase¹⁹⁹.

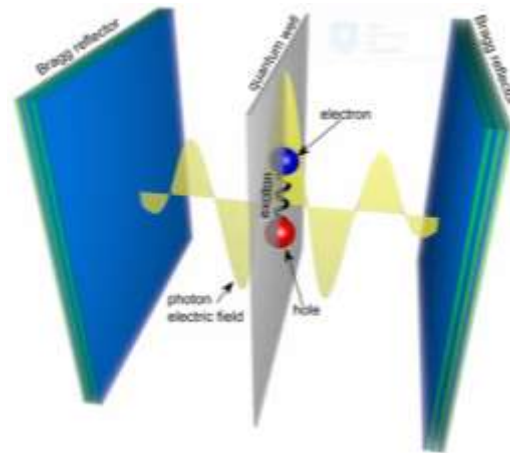


Figure 109: exciton-polariton. Source: [Polariton: The Krizhanovskii Group](#), University of Sheffield.

Researchers are trying to create transistors using polariton-exciton as well as on single quantum control²⁰⁰.

- **Surface plasmon polaritons (SPP)** result from coupling surface plasmons and photons. A plasmon is a quantized oscillation of high-density electron gases. A surface plasmon is a coherent electron oscillation occurring at the interface between two different materials, often a metal and a dielectric or between metal and air. A surface plasmon polariton is an oscillation caused by an incident photon.

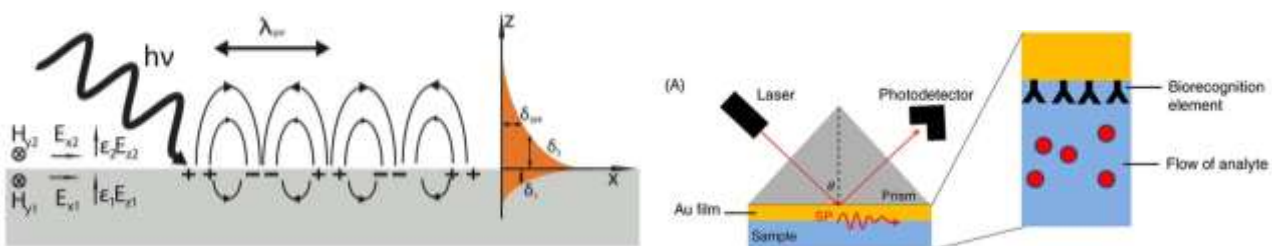


Figure 110: surface-plasmon polariton phenomenon. Source: [Wikipedia](#).

¹⁹⁸ See [Surface phonon polaritons for infrared optoelectronics](#) by Christopher R. Gubbin et al, January 2022 (23 pages).

¹⁹⁹ Source of illustration: Low Dimensional Structures & Devices Group. University of Sheffield, mentioned [here](#).

²⁰⁰ The "polariton blockade" mechanism allows in principle to manipulate excitonic cavity polaritons at the single quantum scale. See [Towards polariton blockade of confined exciton-polaritons](#) by Aymeric Delteil, 2019 (4 pages).

SPPs are used in optical quantum sensors for temperature and for the detection of the concentration of different components by refractivity and then spectroscopy, especially in medtechs (detection of various organic molecules and of interactions between proteins), biological analyses (toxins, drugs, additives) or for the detection of gases²⁰¹.

SPRs (Surface Plasmon Resonance Plasma) can be much more powerful than near-infrared spectroscopy sensors such as those from Scio²⁰². They measure the polarized light reflected from a laser diode in terms of intensity, angle, wavelength, phase and polarization.

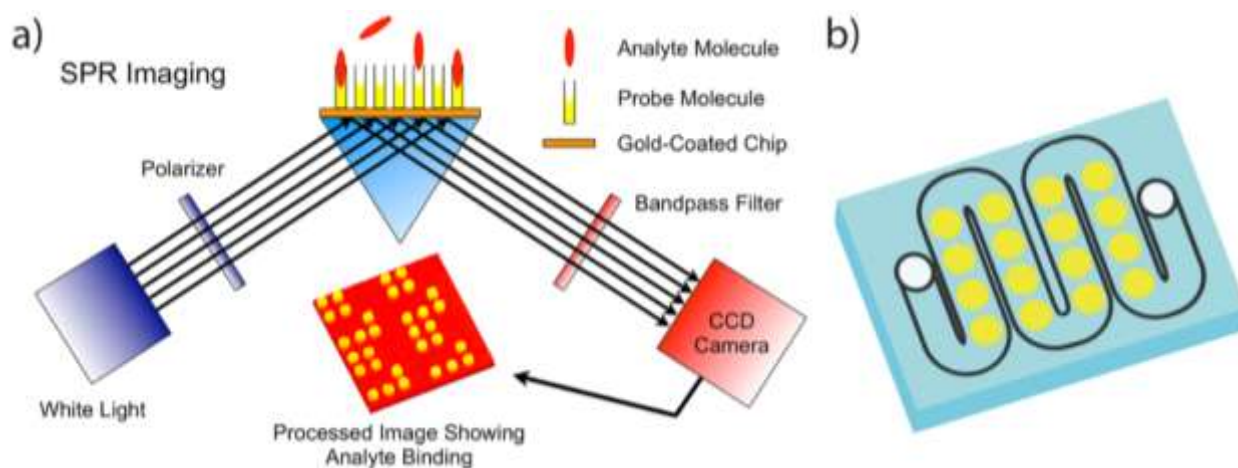


Figure 111: surface plasmon resonance plasma. Source: [Surface Plasmon Resonance \(SPR\)](#) by Lifeasible.

As in many biological analysis systems, it is possible to create 2D matrices (microarrays) integrating many detection molecules and to detect a lot of components in the sample to be analyzed²⁰³.

SPRs are commonly marketed by companies such as **Cytiva** (USA), **Carterra** (USA), **Horiba** (Japan)²⁰⁴, **IBIS Technologies** (Netherlands), **Lifeasible** (USA), **Polaritons Technologies** (Switzerland) and **XanTec** (Germany).

- **Cavity polaritons** are a variant of the polariton excitons where the photon is trapped in a microcavity, and the exciton is confined in a quantum well. They are made of III-V semiconductors like indium, arsenic and gallium.

Photons trapping is often performed using two Bragg mirrors facing each other to create an optical cavity using layers of dielectrics to reflect light very efficiently and of all wavelengths. These mirrors are fabricated from molecular beam epitaxy allowing coherent crystal growth on a gallium arsenide (GaAs) crystal substrate. The result is monocrystalline and can contain more than a hundred layers of different alloys, with thicknesses ranging from 5 nm to 50 nm, controlled to the

²⁰¹ The general principle of this instrument is to use a laser diode to illuminate a gold surface at an angle (via a mechanically controllable angle) and to capture the reflected beam with a detector. The gold surface is coated with a specific molecule ("biorecognition element" in the diagram) that tends to associate itself with a molecule that we want to detect (in the liquid phase "flow of analyte"). The molecules detected can be peptides, polypeptides, proteins, enzymes, vitamins, DNA or RNA sequences, or antibodies (in particular for cancers diagnosis). The association modifies the reflectivity of gold and allows the detection of the target molecule.

²⁰² See [Recent advances in Surface Plasmon Resonance for bio sensing applications and future prospects](#) by Biplob Mondal and Shuwen Zeng, August 2020 (31 pages). The second author is from the Limoges XLIM laboratory in France.

²⁰³ See [Surface Enzyme Chemistries for Ultra sensitive Microarray Biosensing with SPR Imaging](#) by Jennifer B. Fasoli et al, 2015 (10 pages) where the associated illustration comes from.

²⁰⁴ Horiba's European research center is located in Palaiseau next to the C2N of the CNRS, Télécom Paris, Thales and the Institut d'Optique. Horiba is specialized in spectrometers and various other optical instruments like [near-IR photoluminescence](#) characterization of InGaAs/GaAs quantum dots. They acquired Yvon Jobin, a French optical instruments manufacturer in 1997.

nearest atomic monolayer²⁰⁵. These microcavity polaritons were discovered in 1992 by Claude Weisbuch (France)²⁰⁶.

- **Intersubband-polaritons** result from the coupling of an infrared or terahertz photon with an intersubband excitation. They can be used to create infrared detectors.
- And then **Bragg-polaritons** (Braggortons), **plexcitons** (plasmons + excitons), **magnon polaritons** (magnon, spin waves in ferromagnetic materials + photons) and **similaritons** (amplified photons in optical fibers).

In short, all these "*-ons" are the result of the interaction between photons and different forms of matter, noticeably electrons. What does this have to do with quantum computing? Polaritons are used in various optical devices related to photon qubits, including photon transport and single photon detectors.

They could eventually allow the creation of photon qubits that can interact with each other. This is what emerged from an MIT and Harvard publication by Vladan Vuletić and Mikhail Lukin in 2018 which demonstrated the interaction of three photons in an atom placed in a Rydberg state, constituting a "Rydberg polariton"²⁰⁷. Another research project in Singapore uses polariton excitons to create photon qubits with the particularity of being able to operate at room temperature, using single-qubit gates and $\sqrt{\text{SWAP}}$ two-qubits gates²⁰⁸.

Microcavities polaritons can be used to create quantum simulators²⁰⁹. They are implanted in III-V semiconductor structures as 2D arrays. One field of application is the simulation of gravitational structures such as a Hawking radiation on the horizon of a black hole. And why not, to simulate the operation of a dilution refrigerator associating helium 3 and 4 at very low temperature.

Polaritons are also the field of topological behaviors of matter and are perhaps an alternative way to the Majorana fermions to create error corrected qubits. These are longer term pathways than the qubit technologies studied in this book, but worthy of interest.

Other applications, already mentioned, target the very diverse field of quantum sensing, including optomechanical systems²¹⁰.

In France, polaritons are the specialty of Cristiano Ciuti (UPC MPQ), **Elisabeth Giacobino** (CNRS LKB), **Jacqueline Bloch** (CNRS C2N²¹¹), **Alberto Bramati** (ENS LKB), **Alberto Amo** (PhLAM CNRS Lille), **Le Si Dang** and **Maxime Richard** (CNRS Institut Néel Grenoble).

²⁰⁵ See [Cavity polaritons for new photonic devices](#) by Esther Wertz, Jacqueline Bloch, Pascale Senellart et al, 2010 (12 pages).

²⁰⁶ See [Observation of the coupled exciton-photon mode splitting in a semiconductor quantum microcavity](#) by Claude Weisbuch et al, 1992 (4 pages).

²⁰⁷ See [Physicists create new form of light](#) by Jennifer Chu, 2018 referencing [Observation of three-photon bound states in a quantum non linear medium](#) by Qi-Yu Liang et al, 2018 (5 pages).

²⁰⁸ We will define this type of quantum gate in a [dedicated section](#) of this book. See [Quantum computing with exciton- polariton condensates](#) by Sanjib Ghosh and Timothy C. H. Liew, October 2019 (6 pages). Tim Liew is a researcher at the joint MajuLab laboratory between CNRS and the National University of Singapore.

²⁰⁹ See [Microcavity Polaritons for Quantum simulation](#) by Thomas Boulier, Alberto Bramati, Elisabeth Giacobino, Jacqueline Bloch et al, May 2020 (21 pages) as well as [Polaritonic XY-Ising machine](#) by Kirill P. Kalinin, Alberto Amo, Jacqueline Bloch and Natalia G. Berloff, 2020 (12 pages).

²¹⁰ See [Enhanced Cavity Optomechanics with Quantum-well Exciton Polaritons](#) by Nicola Carlon Zambon, Zakari Denis, Romain De Oliveira, Sylvain Ravets, Cristiano Ciuti, Ivan Favero and Jacqueline Bloch, February-September 2022 (22 pages).

²¹¹ The clean room of the C2N in Palaiseau, France, allows the prototyping of a whole bunch of nanostructures. The semiconductors used to manage polaritons are moreover manufactured with techniques similar to the single photon sources of Pascale Senellart's team, also from the C2N, and the associated startup, Qandela.

Magnons

Quantum matter also includes **magnons**, a category of quasi-particles that take the form of quantized spin waves in magnetic materials, usually crystalline lattices. Magnons were conceptualized by **Felix Bloch** in 1930 and experimentally detected in 1957 by **Bertram Brockhouse** (1918-2003, Canadian). These objects which behave as bosons could be used in quantum information systems.

Current physics experiments are done at the control low-level like with controlling these magnons with microwaves²¹² or measured with superconducting qubits²¹³. Magnons can also be used at low temperature to create some topological materials²¹⁴ and even for some species of SiC-based spin qubit control²¹⁵.

Skyrmions

Order is not restricted to the periodic atomic array of a crystal and can also be associated with magnetic order in a solid where spins align parallel to each other in ferromagnets and antiparallel in anti-ferromagnets. More complex magnetic nanostructures are skyrmions that form mesoscopic magnetic vortex with particle-like properties²¹⁶.

Then, how do you distinguish between magnons and skyrmions which are both magnetic quasiparticles? Magnons are quantized dynamic magnetic excitations that travel through magnetic materials while skyrmions are static.

The skyrmion naming comes from **Tony Hilton Royle Skyrme** (1922-1987) who in 1961 formulated a nonlinear field theory of massless pions in which particles can be represented by topological solitons. Skyrmions existence in magnetic materials was predicted in 1989 by Bogdanov et al²¹⁷. In 2008, **Sebastian Mühlbauer** discovered skyrmions in MnSi crystals at the Munich reactor using neutrons²¹⁸.

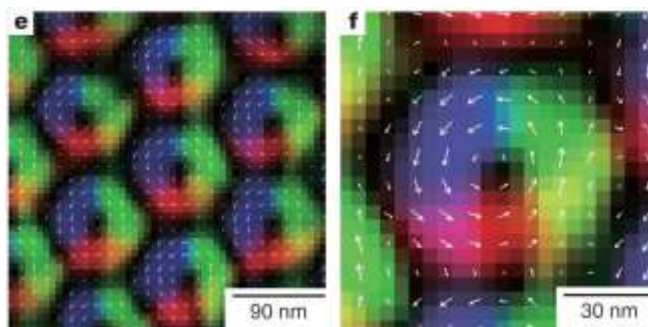


Figure 112: visualizing a skyrmion. Source: [Real-space observation of a two-dimensional skyrmion crystal](#) by X. Z. Yu et al, 2010, *Nature* (5 pages).

Then, Japanese and Korean researchers implement real-space imaging of a two-dimensional hexagonally arranged skyrmion lattices spaced by 90 nm in a thin film of $\text{Fe}_{0.5}\text{Co}_{0.5}\text{Si}$ and exposed to a magnetic field of 50–70mT, using Lorentz transmission electron microscopy²¹⁹. This helicoidal structure can also be 3D and create superposition of various magnetic skyrmion states.

²¹² See [Floquet Cavity Electromagnonics](#) by Jing Xu et al, Argonne Lab and University of Chicago, October 2020 (9 pages).

²¹³ See [Dissipation-Based Quantum Sensing of Magnons with a Superconducting Qubit](#) by S. P. Wolsk et al, University of Tokyo, September 2020 (6 pages).

²¹⁴ See [Topological Magnons: A Review](#) by Paul McClarty, 2021 (21 pages).

²¹⁵ See [Nonlinear magnon control of atomic spin defects in scalable quantum devices](#) by Mauricio Bejarano et al, August 2022 (17 pages).

²¹⁶ I found these insights on skyrmions in the presentation [Introduction to Contemporary Quantum Matter Physics Lecture 11: Skyrmions I](#) by Marc Janoschek and Johan Chang, 2021 (26 slides) and [Part II](#) (24 slides). See also the review paper [The 2020 skyrmionics roadmap](#) by C Back et al, 2020 (38 pages).

²¹⁷ See [Thermodynamically stable "vortices" in magnetically ordered crystals. The mixed state of magnets](#) by A. N. Bogdanov and D. A. Yablonskii, 1989 (3 pages).

²¹⁸ See [Skyrmion Lattice in a Chiral Magnet](#) by S. Mühlbauer et al, *Science*, 2009 (44 pages) which also mentions hedgehogs or instantons, composed of two merons. An endless story. These skyrmions are observed at a critical temperature of 29.5K. And [Instantons: thick-wall approximation](#) by V. F. Mukhanov and A.S. Sorin, June 2022 (12 pages).

²¹⁹ See [Real-space observation of a two-dimensional skyrmion crystal](#) by X. Z. Yu et al, 2010, *Nature* (5 pages).

This could lead to the creation of new ultra-high-density memories²²⁰ particularly with the room-temperature Néel skyrmions that can be made with thin-film systems²²¹, to in-memory processing architectures²²², to create QRNGs²²³, in low-power spintronic applications²²⁴ and in a new breed of qubits with skyrmions in magnetic nano disks bounded by electrical contacts, where static electric and magnetic fields control the skyrmions quantized energy levels corresponding to their helicity. You may probably then need to find a way to entangle them²²⁵!

Topological matter

The very concept of topological quantum states leading to topological matter was discovered with a specific insulating phenomenon that can be explained by the **quantum Hall effect**, with electrons moving through a strong magnetic field and accumulating in some parts of the material depending on its shape. This electron conductivity is quantized, as discovered in 1980 by **Klaus von Klitzing** (Germany) who was awarded the Nobel Prize in Physics in 1985. This “integer” quantum Hall effect was later completed by the discovery of the fractional quantum Hall effect by Tsui et al. in 1982 in two-dimensional electron systems in semiconductor devices, followed by the theoretical discovery of the entangled gapped quantum spin-liquid state of integer-spin “quantum spin chains” by **Frederick Duncan** and **Michael Haldane** in 1981, who was awarded the Nobel prize in physics in 2016 along with **David J. Thouless** and **J. Michael Kosterlitz**²²⁶.

In 2005, **Eugene Mele** and **Charles Kane** predicted that topological insulation could happen in graphene sheet submitted to strong spin-orbit coupling creating the quantum Hall effect without any applied magnetic field²²⁷. This phenomenon is named the “quantum spin Hall effect” and relates to the Kane-Mele invariant²²⁸. It was demonstrated to occur in wafers of mercury telluride. It was experimented by **Shou-Cheng Zhang** et al from Stanford University in 2007²²⁹. The same year, the first 3D topological insulator was discovered by **Zahid Hasan** from Princeton²³⁰.

²²⁰ See for example [Skyrmion-Electronics: Writing, Deleting, Reading and Processing Magnetic Skyrmions Toward Spintronic Applications](#) by Xichao Zhang et al, 2019 (80 pages).

²²¹ See [Mobile Néel skyrmions at room temperature: status and future](#) by Wanjun Jiang et al, 2016 (15 pages) and [Observation of Robust Néel Skyrmions in Metallic PtMnGa](#) by Abhay K. Srivastava et al, Advanced Materials, December 2019 (5 pages).

²²² See [Skyrmion Logic-In-Memory Architecture for Maximum/Minimum Search](#) by Luca Gnoli et al, January 2021 (15 pages) and [Robust and programmable logic-in-memory devices exploiting skyrmion confinement and channeling using local energy barriers](#) by Naveen Sisodia et al, May 2022, UGA, CNRS and CEA (11 pages).

²²³ See [Single skyrmion true random number generator using local dynamics and interaction between skyrmions](#) by Kang Wang et al, Nature Communications, 2022 (8 pages).

²²⁴ See [The skyrmion switch: turning magnetic skyrmion bubbles on and off with an electric field](#) by Marine Schott et al, CNRS Institut Néel, UGA and CEA IRIG, 2016 (31 pages).

²²⁵ See [Skyrmion qubits: A new class of quantum logic elements based on nanoscale magnetization](#) by Christina Psaroudaki and Christos Panagopoulos, Caltech and NTU Singapore, PRL, August 2021 (11 pages) and also [Universal quantum computation based on nanoscale skyrmion helicity qubits in frustrated magnets](#) by Jing Xia et al, April 2022 (7 pages).

²²⁶ See [Topological Quantum Matter](#) by F. Duncan M. Haldane, Nobel Lecture, December 2016 (23 pages).

²²⁷ See [Quantum spin Hall effect in graphene](#) by Charles Kane and Eugene Mele, University of Pennsylvania, 2005 (4 pages).

²²⁸ See [Topological Insulators and the Kane-Mele Invariant: Obstruction and Localisation Theory](#) by Severin Bunk and Richard J. Szabo, 2019 (81 pages) and [Quantum spin Hall effect: a brief introduction](#) (34 slides).

²²⁹ See [Quantum Spin Hall Insulator State in HgTe Quantum Wells](#) by Markus Koenig, Shou-Cheng Zhang et al, October 2007 (16 pages).

²³⁰ See [A topological Dirac insulator in a quantum spin Hall phase \(experimental realization of a 3D Topological Insulator\)](#) by D. Hsieh, Zahid Hasan et al, Princeton University, 2009 (12 pages).

Since then, over 20 topological insulators materials were discovered and there are probably hundreds of them²³¹. A French American research team devised in 2020 a machine learning model to detect such topological insulators out of an initial database of 4009 candidates²³². Again, spintronics are a potential use case of topological insulators to create power-saving electronics where the on/off of a bit would be an electron spin instead of the on/off path of an electron stream.

In topology, an invariant can be described by a single winding number which describes the type of structure with its domain walls, vortices and vector order. It related to the **Chern number**. This number changes over quantum phase transitions. These are other various physics concepts to consider, way beyond what I can do at this point in my quantum journey²³³.

It is interesting to note that some materials can showcase 3D topological behavior at ambient temperature, like bismuth-selenide (Bi_2Se_3). It is a semiconductor and a thermoelectric material that has a topological insulator ground-state. It could be used in targeted cancer treatments and X-ray to mammography²³⁴. You can also potentially build **magnetic monopoles** quasiparticles, breaking the convention that magnetism always shows up with dipoles²³⁵.

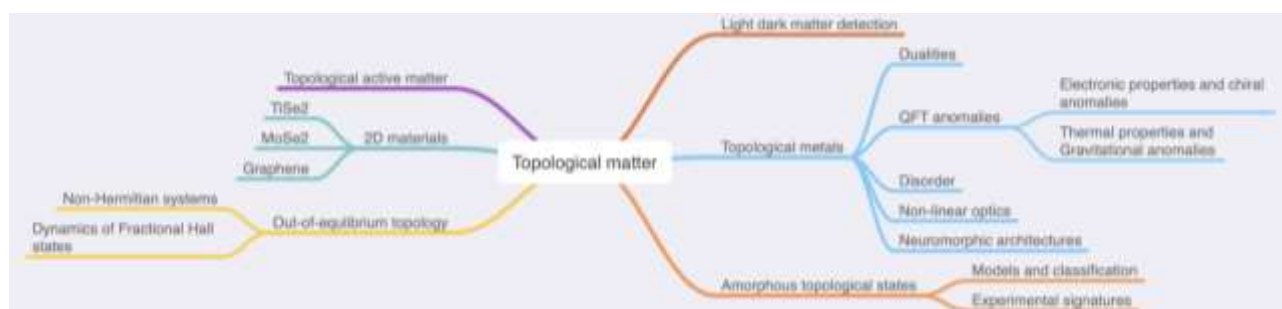


Figure 113: a classification of topological matter. Source: [Research Lines - Theory of Topological Matter](#) by Adolfo Grushin, CNRS.

Like me, you're certainly willing to "visualize" the different types of topological materials identified. I found this nice and highly detailed table showing their great diversity in a review paper, below in Figure 114.

Topological matter can have several applications related to light-matter interactions in the Terahertz regime. It can help create waveguides, optical isolators and diodes who are more resistant to their environment perturbations in the recent field of **topological photonics** which is related to polaritons²³⁶.

²³¹ See [Topological phases of amorphous matter](#) by Adolfo G. Grushin, January 2021 (45 pages) which describes the physics of topological phases and [Introduction to topological Phases in Condensed Matter](#) by Adolfo G. Grushin (28 pages) which provides some background information on the way to classify topological matter.

²³² See [Detection of Topological Materials with Machine Learning](#) by Nikolas Claussen et al, ENS Paris, Princeton, June 2020 (15 pages).

²³³ See [Topological Materials : Some Basic Concepts](#) by Ion Garate, 2016 (35 slides), [Core Concept: Topological insulators promise computing advances, insights into matter itself](#) by Stephen Ornes, 2016 and [Topological phases](#) by Nicholas Read, Physics Today, 2012 (6 pages).

²³⁴ See [Topological insulator bismuth selenide as a theranostic platform for simultaneous cancer imaging and therapy](#) by Juan Li and al, 2013 (7 pages).

²³⁵ See [Emergent magnetic monopoles isolated using quantum-annealing computer](#) by Los Alamos National Laboratory, Physorg, July 2021, which refers to [Qubit spin ice](#) by Andrew D. King, Science, July 2021 (18 pages) which simulates a new topological material with a D-Wave quantum annealer.

²³⁶ See [Roadmap on Topological Photonics](#) by Hannah Price et al, Journal of Physics, 2022 (63 pages), the well illustrated presentation [Introduction to Topological Photonics](#) by Mikael C. Rechtsman, Penn State, AMOLF Nanophotonics Summer School, June 2019 (42 slides), [Topological photonic crystals: a review](#) by Hongfei Wang et al, 2020 (23 pages) and [Topological photonic crystals: physics, designs and applications](#) by Guo-Jing Tang et al, January 2022 (60 pages).

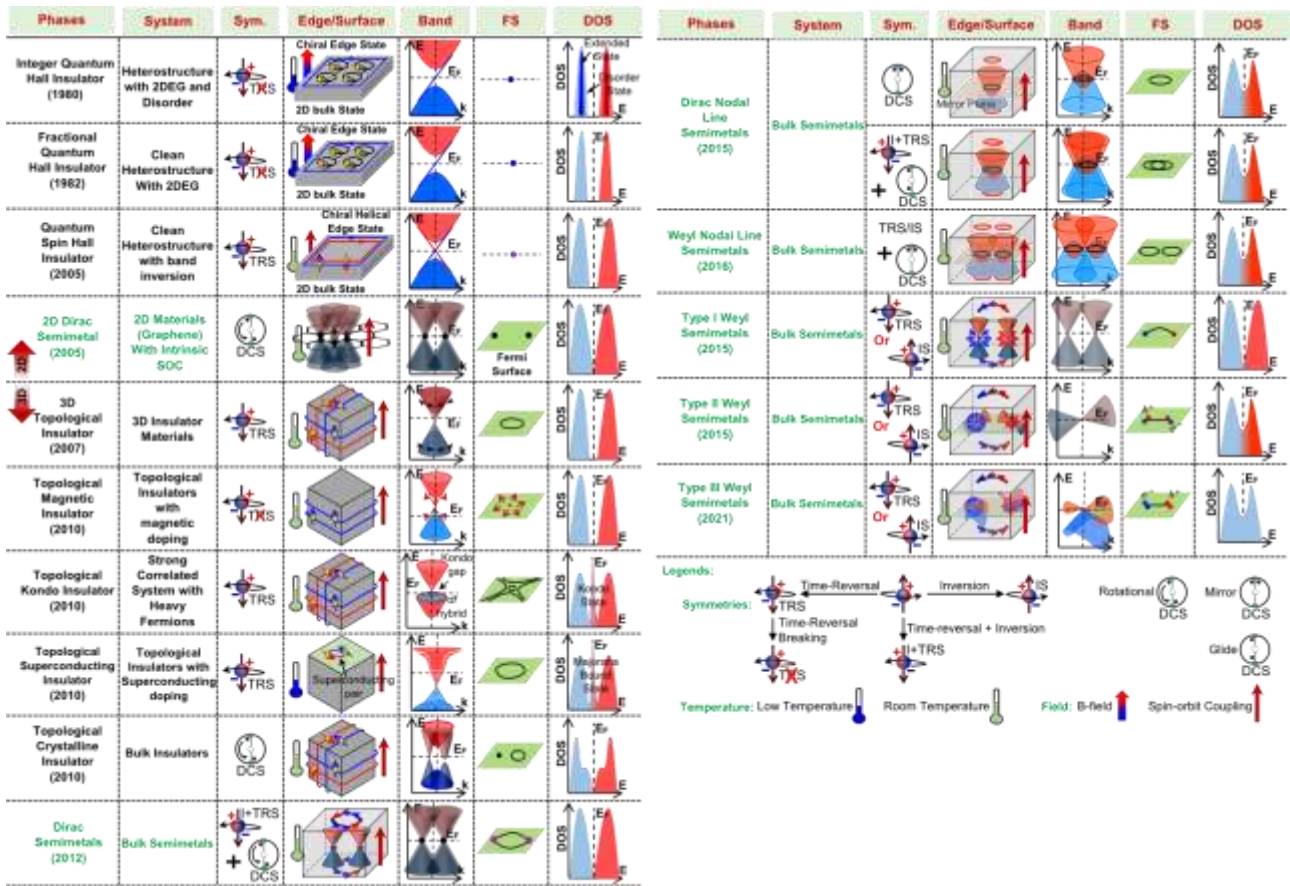


Figure 114: a table with a classification of various topological materials in 2D and 3D, and indicating time reversal and operating temperature. Source: [Topological Quantum Matter to Topological Phase Conversion: Fundamentals, Materials, Physical Systems for Phase Conversions, and Device Applications](#) by Md Mobarak Hossain Polash et al, February 2021 (83 pages).

We even have **topological lasers**²³⁷, which can for example consolidate multiple sources in a coherent way, leading to even more powerful lasers, using a topological insulator vertical-cavity surface-emitting array (VCSEL)²³⁸.

Then of course, one key application of topological matter is topological qubits, often associated with Majorana fermions sought after by Microsoft. But topological qubits are way more diverse with many competing definitions and architectures. For example, you also can count with Fibonacci anyons²³⁹.

Time crystals

Time crystals is a beast we hear a lot about since mid-2021, when Google announced it had created such thing in its Sycamore processor²⁴⁰. It shed some light on this weird phenomenon that was devised in a 2012 paper by Frank Wilczek from the MIT (and 2004 Nobel prize in physics) and by another paper by him and Alfred Shapere from the University of Kentucky²⁴¹.

²³⁷ See [Topological lasing](#), PhLAM Laboratory, Lille France.

²³⁸ See [Topological-cavity surface-emitting laser](#) by Lechen Yang et al, Nature Photonics, 2021 (6 pages) and [Topological insulator vertical-cavity laser array](#) by Alex Dikopoltsev et al, Science, 2021 (5 pages).

²³⁹ See [Fibonacci Anyons Versus Majorana Fermions: A Monte Carlo Approach to the Compilation of Braid Circuits in SU\(2\)_k Anyon Models](#) by Emil G eneta Johansen and Tapio Simula, 2021 (23 pages).

²⁴⁰ See [Eternal Change for No Energy: A Time Crystal Finally Made Real](#) by Natalie Wolchover, July 2021 referring to [Observation of Time-Crystalline Eigenstate Order on a Quantum Processor](#) by Xiao Mi et al, Google, July 2021 (24 pages) and [Realizing topologically ordered states on a quantum processor](#) by K. J. Satzinger et al, Google AI, April 2021 (6 pages).

²⁴¹ See [Quantum Time Crystals](#) by Frank Wilczek, MIT, 2012 (6 pages) and [Classical Time Crystals](#) by Alfred Shapere and Frank Wilczek, PRL, 2012 (5 pages).

This thing is somewhat linked to the history of the search for a perpetuum mobility, an isolated object supposed to keep in motion indefinitely. It was dismissed by the French Academy of Science in 1775 due to the limits of friction and, later, to the second law of thermodynamics²⁴².

In classical crystals, the atoms are periodically arranged in space structured according to one of the 230 structures already described. In time crystals, these atoms are periodically arranged in both space and time. It simply means that their structure is in a permanent oscillating mode with a given period, for so-called discrete time crystals²⁴³.

But the scientific description of the phenomenon is the less explicit “spontaneous time symmetry breaking”. Then, you quickly lose ground with common wisdom²⁴⁴.

Time crystals do not lose energy to the environment. They are the stage of motion without energy. It is a type or phase of non-equilibrium matter. But they are still initially driven, sometimes even out of their equilibrium level. Some real time crystals were first observed in lab experiments, starting in 2017 with some constantly rotating ring of charged ions spin (which by the way, shows some signal damping, in Figure 115)²⁴⁵. It can also happen with some continuous change of spin for some particles, when the change periods is up to 100 times longer than the system drive period. It was tested in 2021 by a QuTech team in The Netherlands using controllable ¹³C nuclear spins in diamond structures²⁴⁶.

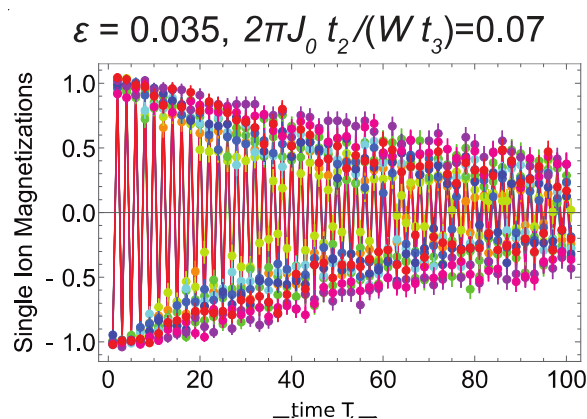


Figure 115: time crystal oscillations over time. Source: [Observation of a Discrete Time Crystal](#) by J. Zhang, Christopher Monroe et al, September 2016 (9 pages).

So why all this fuss around time crystals and how could they become useful? Some think they may be useful to create some form of quantum memory.

Things get complicated when you learn that time crystals have also been experimented with superconducting qubits like with the Google 2021 experiments and other subsequent ones with a continuous line of 57 qubits in a 65 qubits IBM QPU²⁴⁷. How could a series of connected superconducting qubits become a “crystal” per se?

They may behave as a continuously oscillating system but are not a single crystal since they are a complex assembly of Josephson junctions, capacitances, resonators and microwave drives mixing various elements (aluminum, aluminum-oxide, niobium, titanium...).

Quantum batteries

Quantum matter research is leading some labs to investigate the possibility of creating innovative batteries for energy storage relying on some quantum phenomenon including entanglement.

²⁴² See [A Decade of Time Crystals: Quo Vadis?](#) by Peter Hannaford and Krzysztof Sacha, April 2022 (8 pages) and [A Brief History of Time Crystals](#) by Vedika Khemani et al, Harvard, October 2019 (79 pages).

²⁴³ There are also continuous time crystals that were observed first in 2022 in Germany. See [Observation of a continuous time crystal](#) by Phatthamon Kongkhambut et al, February-August 2022 (13 pages).

²⁴⁴ There’s even an acronym for this, TTSB which means time translation symmetry breaking.

²⁴⁵ See [Observation of a Discrete Time Crystal](#) by J. Zhang, Christopher Monroe et al, September 2016 (9 pages).

²⁴⁶ See [Many-body-localized discrete time crystal with a programmable spin-based quantum simulator](#) by J. Randall et al, QuTech, Science, November 2021 (7 pages).

²⁴⁷ See [Realization of a discrete time crystal on 57 qubits of a quantum computer](#) by Philipp Frey and Stephan Rachel, January 2022 (12 pages).

Work in this field started around 2012 with some fundamental research by Robert Alicki and Mark Fannes from Poland and Belgium on how much work could be stored and extracted from quantum batteries²⁴⁸. Quantum batteries could store energy in high energy states of quantum objects and extracted efficiently. Some of these batteries rely on various quantum principles, some of them being not far from classical quantum photonics. This is a different field than classical batteries whose design could be improved with using quantum computers, as covered page 717 in this book.

All the papers I've found in that field are very theoretical and quite far from practical batteries. The main benefit of these quantum batteries seems to be fast charging, with the caveat of fast discharging, which is quite inconvenient²⁴⁹. I have not found yet any quantum battery that would improve energy density in a real documented manner with a full-stack product packaging, one of the main showstoppers for various use cases like for long distance electric vehicles or aerial vehicles. So, you're far from buying your next Tesla equipped with a 1000-mile range quantum battery²⁵⁰.

So, what do we have in-store here? Mainly scientific work with very low TRLs.

Scientists from Australia and Italy are working on an **organic battery** with fast charging using a process called superextensive scaling of absorption, meaning that the larger the system is, the faster it absorbs energy²⁵¹. It's based on of a thin active layer of a low-mass molecular semiconductor named LFO (Lumogen F-orange) that is dispersed into a polymer matrix that is sandwiched between two dielectrics made of 8 and 10 pairs of Bragg mirrors, creating a microcavity. The battery cell is then controlled by a laser in the 500 nm red-light range, a noncollinear optical parametric amplifier, beam splitters and delay lines and a detector. In a word, we could say it's a "light" battery, absorbing energy as light, and rendering it as light, in a different wavelength. Like in many other papers of this kind, it's quite difficult to infer the practicality of these quantum batteries.

If researchers are not overselling it, the news media are doing it, touting "*batteries with one million miles autonomy*"²⁵².

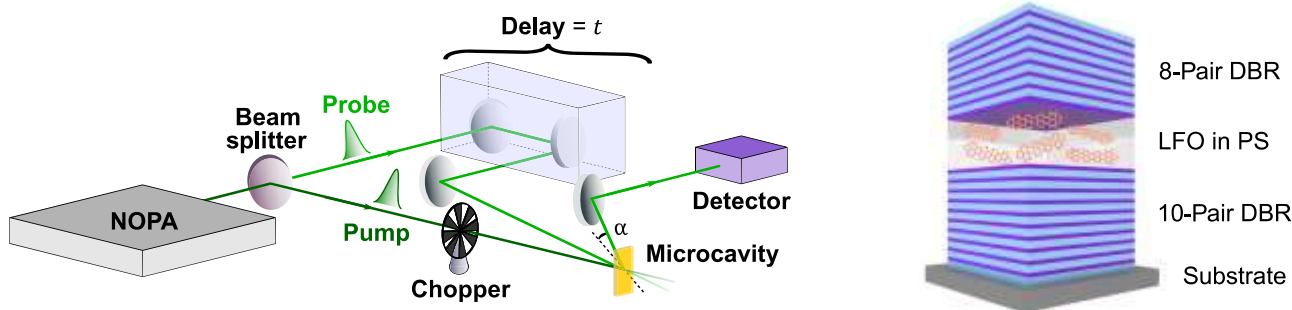


Figure 116: source: [Superabsorption in an organic microcavity: Toward a quantum battery](#) by James Q. Quach et al, Heriot-Watt University, 2022 (9 pages).

²⁴⁸ See [Extractable work from ensembles of quantum batteries. Entanglement helps](#) by Robert Alicki and Mark Fannes, Physical Review E, November 2012 (4 pages).

²⁴⁹ See [Sizing Up the Potential of Quantum Batteries](#) by Sourav Bhattacharjee, Indian Institute of Technology, April 2022.

²⁵⁰ Despite what you can read in [Quantum technology could make charging electric cars as fast as pumping gas](#) by Institute for Basic Science, March 2022 that is linked to [Quantum charging advantage cannot be extensive without global operations](#) by J.-Y. Gyhm et al, PRL, April 2022 (13 pages).

²⁵¹ See [Superabsorption in an organic microcavity: Toward a quantum battery](#) by James Q. Quach et al, Heriot-Watt University, 2022 (9 pages).

²⁵² See [How quantum batteries could lead to EVs that go a million miles between charges](#), The Next Web, June 2022.

This comes from another paper, authored by Canadian scientists and an engineer from Tesla which proposes an improved Li-Ion battery that could last 1.5 million miles over its lifespan but, of course, not with a single recharge²⁵³. And it's even not a quantum battery.

In another approach, other scientists from Australia are looking at ways to store energy in light-induced spin state trapping in spin crossover materials²⁵⁴. And a team from Italy and Korea wants to use micromasers to store energy²⁵⁵.

Another paper from a Korean American German Singaporean team describes quantum batteries as isolated quantum systems undergoing unitary charging protocols (unitary in the mathematical sense)²⁵⁶. With ensembles of such batteries, some collective effects enhance work extraction or boost the charging power thanks to entanglement between the component quantum batteries. The described system is based on an Otto engine which can serve as an engine and as a refrigerator.

In another work from US and Japanese researchers, we are closer to classical battery designs. It's about using lithium-doped samarium nickelate, a quantum crystalline material with strongly correlated electron systems²⁵⁷.

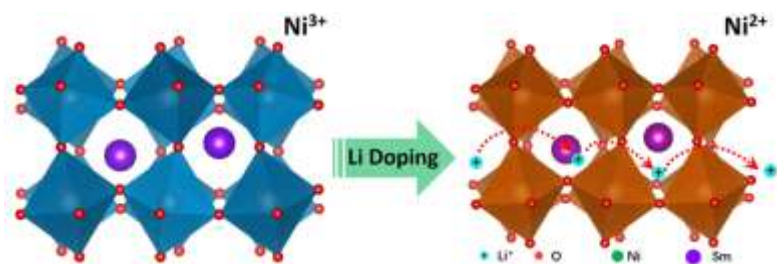


Figure 117: lithium-doped samarium nickelate quantum battery. Source: [Strongly correlated perovskite lithium ion shuttles](#) by Yifei Sun et al, 2018 (6 pages).

Lithium ions are usually the main compound of batteries electrolytes.

The quantum crystal structure improves the conduction of these ions that could also be sodium ions. It could enable better electrolytes but another effect of the structure where additional electron modifies the material conductivity could be used in neuromorphic synapses for storing neural networks connections weights.

Other research work deal with microscopic batteries which don't seem to be useful for energy storage²⁵⁸. They can help better understand the thermodynamics of qubits manipulation and provide innovative insights on how to fight decoherence and noise²⁵⁹.

Higher TRLs can be found with rather classical batteries that would use topological semi-metallic porous carbon materials as potential more efficient anodes for Li-Ion, sodium-ion and potassium-ion batteries. Other topological materials could be useful for supercapacitors.

²⁵³ See [A Wide Range of Testing Results on an Excellent Lithium-Ion Cell Chemistry to be used as Benchmarks for New Battery Technologies](#) by Jessie E. Harlow, J.R. Dahn et al, 2019 (15 pages).

²⁵⁴ See [UQ discovery paves the way for faster computers, longer-lasting batteries](#), June 2022 referring to [Toward High-Temperature Light-Induced Spin-State Trapping in Spin-Crossover Materials: The Interplay of Collective and Molecular Effects](#) by M. Nadeem, Jace Cruddas, Gian Ruzzi and Benjamin J. Powell, May 2022 (55 pages). A similar spin-based approach is described in [Quantum advantage in charging cavity and spin batteries by repeated interactions](#) by Raffaele Salvia et al, April 2022 (14 pages).

²⁵⁵ See [Micromasers as Quantum Batteries](#) by Vahid Shaghghi et al, April 2022 (6 pages).

²⁵⁶ See [Charging Quantum Batteries via Otto machines: The influence of monitoring](#) by Jeongrak Son et al, May 2022 (16 pages). Hard to understand what are the characteristics of this kind of battery and how it performs compared to classical Li-ion batteries!

²⁵⁷ See [Quantum material is promising 'ion conductor' for research, new technologies](#) by Emil Venere, Physorg, 2018. Pointing to [Strongly correlated perovskite lithium ion shuttles](#) by Yifei Sun et al, 2018 (6 pages).

²⁵⁸ Like with [IBM Quantum Platforms: A Quantum Battery Perspective](#) by Giulia Gemme et al, April 2022 (13 pages) which is using an IBM superconducting processor to store energy in qubits. It's actually using the Armonk processor which has exactly one qubit. A similar experiment done in China is described in [Optimal charging of a superconducting quantum battery](#) by Chang-Kang Hu et al, August 2021 (4 pages).

²⁵⁹ Like with [Coherence-powered work exchanges between a solid-state qubit and light fields](#) by Ilse Maillette De Buy Wenniger, Maria Maffei, Niccolo Somaschi, Alexia Auffèves, Pascale Senellart et al, April 2022 (17 pages).

Topological materials could also be useful to create more efficient catalyzers for water electrolysis, with the production of hydrogen in sight coming from renewable originated electricity²⁶⁰.

Extreme quantum

Beyond the basics of quantum physics, many other branches of quantum physics deserve to be examined in this book. They can have various impacts on quantum technologies, noticeably on quantum sensing. They are also used in cosmology. Finally, they are unfortunately used by many false sciences and scams that we will discuss in the section dedicated to [quantum hoaxes](#), starting page 1029.

Quantum field theory

Quantum Field Theory (QFT²⁶¹) is a branch of quantum physics that deals with the physics of elementary particles in the relativistic realm, including their creation or disappearance during various interactions, such as electron and positron pairs. These phenomena are generally reproduced in particle accelerators²⁶².

QFT also covers the mechanisms of condensed matter such as Bose-Einstein condensates or superfluid helium and more generally, the behavior of quasiparticles, complex collective behaviors such as Cooper's (electron) pairs in superconducting materials.

QFT combines elements of quantum mechanics, special relativity, and classical notions of electromagnetic fields. It is based on a mathematical formalism that is even more difficult to assimilate than the one of non-relativistic quantum physics.

It exploits the notion of Lagrangian and Lagrangian integrals over time describing the evolution of fields and the interactions between the fields of several particles.

QFT is used to explain or modelize the fine structure of the hydrogen atom (corresponding to close spectral lines not explainable by classical quantum energy jumps), the existence of particle spin (which explains these spectral lines), the spontaneous emission of photons by atoms during their return to their fundamental state and the mechanisms of radioactivity.

The foundations of QFT were created by many scientists starting in 1928: **Paul Dirac**, **Wolfgang Pauli**, **Vladimir Fock** (1898-1974, Russian), **Shin'ichirō Tomonaga** (1906-1979, Japanese), **Julian Schwinger** (1918-1994, American), **Richard Feynman** and **Freeman John Dyson** (1923-2020, American²⁶³). Shin'ichirō Tomonaga, Julian Schwinger and Richard Feynman received the 1965 Nobel Prize in Physics for their work on quantum electrodynamics which is part of QFT.

In the early 1950s, they solved the problem of infinite energy values generated by the initial QFT models by using an adjustment technique called **renormalization**.

Physicists are still struggling to integrate the theory of general relativity into the QFT, preventing it from becoming a "theory of the whole" or unified theory explaining all known physical phenomena in the Universe.

QFT operates in three main areas:

- In the physics of **high-energy particles** explored in particle accelerators such as the CERN LHC. It has been supplemented on this point by the standard model that we will see below.

²⁶⁰ See [Topological quantum materials for energy conversion and storage](#) by Huixia Luo, Peifeng Yu, Guowei Li and Kai Yan, Nature Review Physics, July 2022 (14 pages).

²⁶¹ Later on, we'll use the QFT acronym with another meaning, Quantum Fourier Transform!

²⁶² See [The History of QFT](#), a Stanford site, which summarizes the history of QFT.

²⁶³ It also gave rise to the notion of the Dyson sphere, which dimensions the level of technological control of energy sources by extra-terrestrial civilizations, with a sphere capturing the totality of a star's energy.

- In the **physics of condensed matter** with superconductivity, superfluidity and the quantum Hall effect. This is the framework of **QED** (quantum electrodynamics), launched by Paul Dirac in 1928, which studies in particular the production of positrons and positron/electron interactions (attraction, annihilation, pair creation, Compton effect). The **CQED** (cavity QED) sub-branch studies the relations between matter and photons in optical cavities. It is used by condensed matter physicists working on superconducting qubits.
- In **cosmology** to contribute to modeling the origin and evolution of the Universe as well as certain mechanisms of interaction between black holes and quantum fields.

Quantum vacuum fluctuation

One of the consequences of QFT is the notion of quantum vacuum fluctuation, also called vacuum energy. Based on Heisenberg's principle of indeterminacy that quantum fields are in perpetual fluctuation, QFT models zero-point fluctuations or vacuum energy, which is the minimum energy level of quantum systems.

In this framework, Heisenberg's principle can be considered as a generalized predicate. According to these models, total vacuum cannot exist. Elementary fluctuations lead to spontaneous electromagnetic waves creation, given all fields are fluctuating.

One scenario devised by Paul Dirac is the creation of pairs of virtual electron and positron particles, which rapidly annihilate each other, generating photons in the process. But this is not the only solution to his equations. It can come from electromagnetic fields moving at the speed of light.

Under the influence of a surrounding electromagnetic field, this leads to a polarization of the vacuum. The latter even leads to make the vacuum birefringent, its refractive index depending on the polarization of the light that gets through it. The phenomenon is however potentially observable only with some very intense electromagnetic field.

Theoretical models initially indicated that this vacuum energy would be infinite on the scale of the Universe. They were then corrected using the renormalization method, already mentioned above. These elementary vacuum fluctuations would explain the spontaneous emission of radiation by the electrons in the atoms as well as the spontaneous radioactivity²⁶⁴.

The concept of vacuum energy originated with **Max Planck** in 1911 when he published an article containing an energy equation for a medium containing a fixed constant, a kind of energy floor for this medium, without being able to interpret it. It was not until 1916 that the chemist **Walther Nernst** (1864-1941, German²⁶⁵) interpreted this constant as the energy level of the vacuum in the absence of any radiation. It happens when you cool down a black body to a very low temperature, below a couple millikelvins (mK).

According to the QFT, the Universe is a vast soup containing constantly fluctuating fields, both fermions (leptons and quarks) and bosons (force fields like gluons mediate the strong force that stick together the quarks that are the elementary constituents of protons and neutrons, and photons, and the cohesion between nucleons is coming from a residual force from strong interactions). This notion of minimum energy level is a modern version of the notion of ether - a not completely empty void - which dominated 19th century physics, notably for James Clerk Maxwell. The electromagnetic bath in which the vacuum is immersed, supplemented by the energy of the vacuum, would give vacuum some viscosity properties.

²⁶⁴ In addition to these elementary fluctuations, vacuum is constantly traversed, even in the remotest regions of space, by electromagnetic waves, not to mention the effects of gravitation. The Universe is thus filled with radiations including the cosmological background noise which is a remnant of the big bang, having a temperature of 2.7K. It is the same in a vacuum-packed box because all matter emits radiation.

²⁶⁵ Walther Nernst played a key role in launching the Solvay Congresses from 1911 onwards.

Still, these theories are less complete than classical quantum mechanics. One of the solutions is to assume that fermions have a negative vacuum energy and bosons have a positive vacuum energy, both balancing each other. But this has not been demonstrated experimentally, particularly with non-relativistic energy particles.

Some link could be found between vacuum energy and the dark energy of the Universe as well as gravity²⁶⁶. This is very speculative. It could help explain the 73% of the energy contained in the Universe, sometimes called dark energy. Its density is very low, at 10^{-13} Joules/cm².

There are different ways to verify the existence of quantum vacuum fluctuations. The best-known is related to the Casimir effect that we will study in the next part. Recently, French and German scientists have also managed to interact with this quantum vacuum fluctuation in a semiconductor²⁶⁷.

Casimir effect

The physicist **Hendrik Casimir** (1909-2000, Dutch) predicted in 1948 the existence of an attractive force between two parallel electrically conductive and uncharged plates²⁶⁸. He obtained his PhD in 1931 at the University of Leiden in the Netherlands. He also visited Niels Bohr in Copenhagen and was a research assistant to Wolfgang Pauli in 1938. The Casimir effect is interpreted as being related to the existence of quantum vacuum energy. The experiment imagined by Casimir uses parallel mirrored metal surfaces that are as perfectly flat as possible. They create a Fabry-Perot cavity similar to the one that used in lasers.

The Casimir effect is commonly attributed to quantum fluctuations in vacuum. Temporary changes in the energy level at points in the space between the two mirrors would spontaneously generate pairs of very short-lived particles and antiparticles and photons associated with their annihilation. These vacuum fluctuations take place in and out of the volume of the cavity.

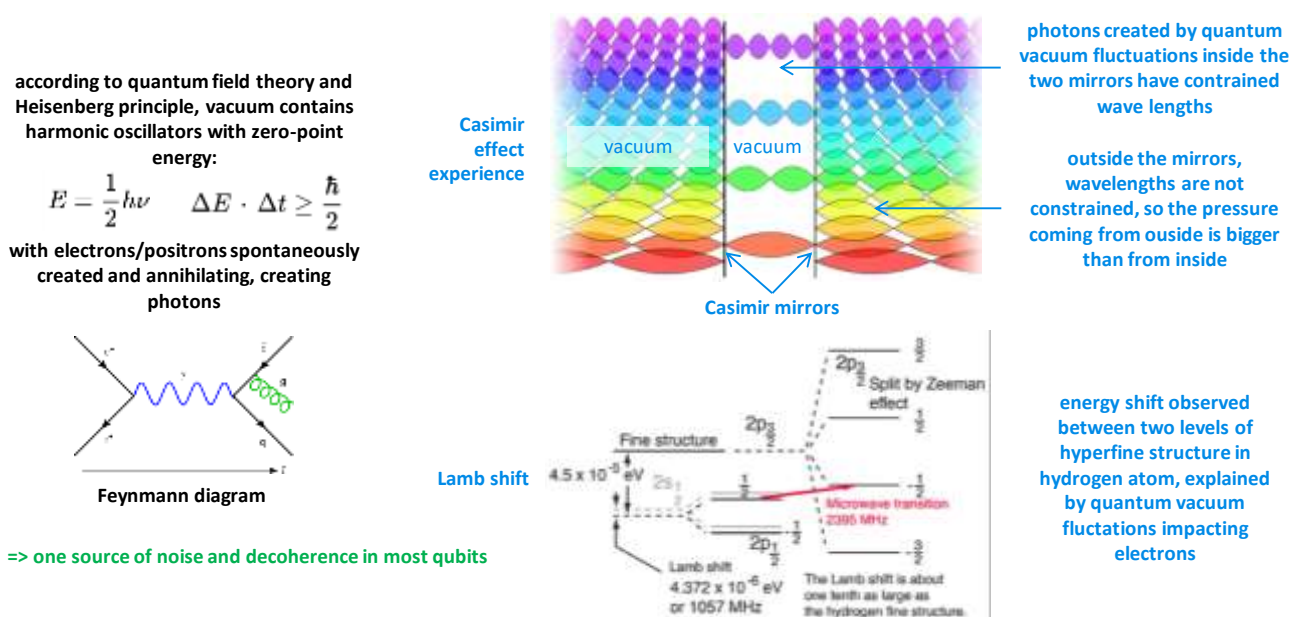


Figure 118: vacuum fluctuations measurement. Sources: [The Lamb Shift](#) and [The Casimir Effect](#) by Kyle Kingsbury, 2014 (82 slides).

²⁶⁶ See [Casimir cosmology](#) by Ulf Leonhardt, February 2022 (41 pages).

²⁶⁷ See [Understanding vacuum fluctuations in space](#), August 2020 and [Electric field correlation measurements on the electromagnetic vacuum state](#) by Ileana-Cristina Benea-Chelmus, Jérôme Faist et al, 2018/2020.

²⁶⁸ See [On the attraction between two perfectly conducting plates](#) by Hendrik Casimir, 1948 (3 pages) and [Electromagnetic vacuum fluctuations, Casimir and Van der Waals forces](#) by Cyriaque Genet, Astrid Lambrecht et al, 2004 (18 pages).

Because of the interference effect induced by the cavity, fluctuations at certain frequencies are reduced. The density of electromagnetic energy in the cavity is thus lower than the density of energy outside the cavity as shown above in Figure 118²⁶⁹. These are spontaneous quantum fluctuations.

The effect cannot be explained by the simple pressure that is higher on the outside than the pressure between the two plates. In detail, the wavelengths of the photons generated by the vacuum outside the plates can be of any size and especially long while inside the plates, these wavelengths are constrained by the distance between the plates and can only be 1/n of this distance.

The spontaneous electromagnetic spectrum of the vacuum is therefore wider outside the plates than inside, creating a stronger pressure inside than outside, which therefore tends to make the plates move closer together, but very slightly.

For two parallel mirrors of surface A and a distance L between the two mirrors, the force of attraction between the two mirrors follows the formula on the right. In practice, L is between 0.2 μm and 5 μm and is usually 1 μm. This is a "macroscopic" scale.

$$F_{Cas} = \frac{\hbar c \pi^2 A}{240 L^4}$$

According to Heisenberg's principle, which is used to explain the effect, energy and time can be linked by the formula on the right. It shows indirectly that during a very short time, a small amount of energy can be created.

$$\Delta E \cdot \Delta t \geq \frac{\hbar}{2}$$

The macroscopic accumulation of these operations is annihilated, making it possible to avoid a violation of the energy conservation principle. So, be uber-skeptic when hearing anyone claiming they can harvest energy from vacuum to produce free electricity.

The experiments are not necessarily 100% conclusive and the data generated do not fit perfectly with the models unlike many classical quantum mechanics experiments. The reason for this is that it is difficult to obtain perfect surfaces.

The first experiments validating the Casimir effect were carried out almost 50 years after the definition of this effect²⁷⁰. The first one is that of **Steve Lamoreaux** (American) in 1996, using parallel plates.

His measurement gave a result that was 5% off the predictions. The precision instruments used then detected a force of one billionth of a Newton. The model was improved in other experiments carried out in 1998 and again in 2012 using an electrode geometry combining a plane and a polystyrene sphere with a diameter of 200 μm and covered with gold (diagrams *below*)²⁷¹. The differences between the models and the measurements decreased to 1%, which remains significant in physics.

The Casimir effect could explain several other commonly observed physical phenomena such as the electron's abnormal magnetic moment and the Lamb shift. The first phenomenon describes a drift of this magnetic moment with respect to Dirac's equations.

The second comes from **Willis Eugene Lamb** (1913-2008, American), Nobel Prize in Physics in 1955, who had done his thesis under the supervision of Robert Oppenheimer. Lamb shift is an energy gap observed between two levels of fine structure of the hydrogen atom, two very close energy levels.

²⁶⁹ See a good panorama of the Casimir effect with [The Casimir effect and the physical vacuum](#) by G. Takács, 2014 (111 slides). See also [The Casimir Effect](#) by Kyle Kingsbury, 2014 (82 slides) which describes well the experimental devices for the evaluation of the Casimir effect and evokes some cases of use in MEMS. And then [Zero-Point Energy and Casimir Effect](#) by Gerold Gründler, 2013 (47 pages), which casts the history of the Casimir effect, going back to Planck's work in 1911.

²⁷⁰ The experimental difficulty consists in cancelling out all the other forces between the two plates and they are all much larger than the Casimir effect, particularly electrostatic and van der Waals forces.

²⁷¹ See [Physicists solve Casimir conundrum](#) by Hamish Johnston, 2012 which refers to [Casimir Force and In Situ Surface Potential Measurements on Nanomembranes](#) by Steve Lamoreaux et al, 2012 (6 pages).

The effect is explained with the perturbations coming from vacuum fluctuations and affecting the electron in these two neighboring energy levels, creating the spontaneous generation of photons that are rapidly absorbed by the electron.

The effect was discovered in 1947 by Willis Eugene Lamb and interpreted the same year by **Hans Bethe** (1906-2005, German) for the hydrogen spectrum using the idea of mass renormalization. It was used in the development of post-war quantum electrodynamics.

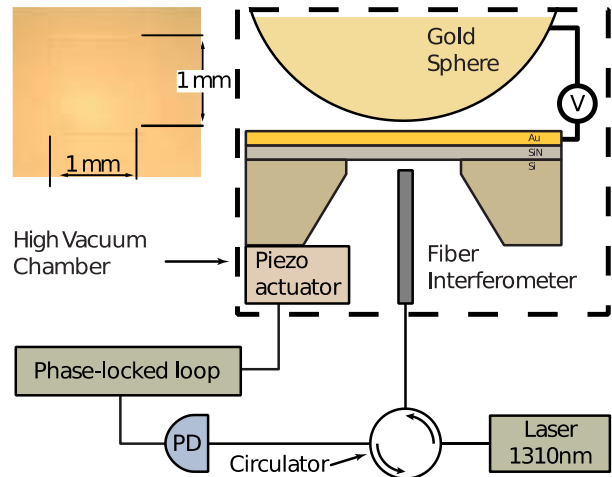
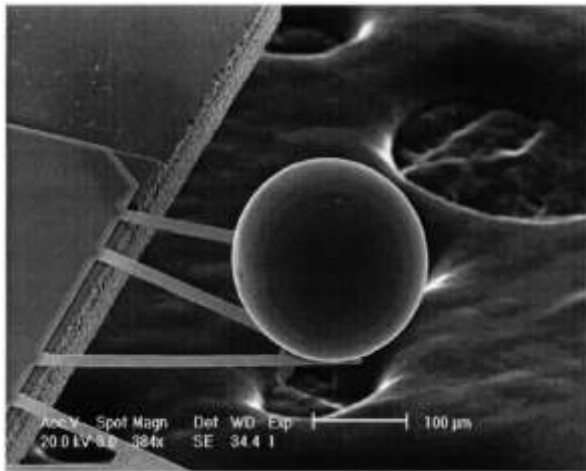


Figure 119: vacuum source measurement with a dynamic Casimir effect. Sources: [The Casimir Effect](#) by Kyle Kingsbury, 2014 (82 slides) and [Casimir Force and In Situ Surface Potential Measurements on Nanomembranes](#) by Steve Lamoreaux et al, 2012 (6 pages).

The polarization of vacuum explains part of this shift at 27 MHz for a total of 1057 MHz²⁷². The calculation uses the fine-structure constant α (about 1/137) which describes the contribution of vacuum energy to the electron's anomalous magnetic moment. The α constant is also used to quantify the strength of the electromagnetic interaction between elementary charged particles.

There is also a **Dynamic Casimir Effect** (DCE), discovered by **Gerald Moore** in 1969. It generates pairs of particles by the movement of the mirrors used in the Casimir experiment²⁷³.

As with the Casimir Effect, the energy observed is infinitesimal. For the energy to be significant, the mirrors would have to move at relativistic velocities, which is not very practical. And there is no problem with energy conservation, the necessary energy being provided by the mirror movement. The vacuum simply serves as a nonlinear medium!

The interpretation of the Casimir effect is still debated. Some physicists explain it by other mechanisms than vacuum energy.

They rely on the **van der Waals** (1837-1923, another Dutch) forces, where atoms attract or repel each other depending on their distances²⁷⁴. However, this infinitesimal force works at a microscopic scale, where the Casimir effect operates at a macroscopic scale.

²⁷² This phenomenon of vacuum polarization in the Lamb effect is described in [The Vacuum Polarisation Contribution to the Lamb Shift Using Non-Relativistic Quantum Electrodynamics](#) by Jonas Frafjord, 2016 (61 pages).

²⁷³ See [Electro-mechanical Casimir effect](#) by Mikel Sanz, Enrique Solano et al, 2018 (10 pages).

²⁷⁴ See [The origin of Casimir effect: Vacuum energy or van der Waals force?](#) by Hrvoje Nikolic, 2018 (41 slides) and the even more skeptic [The Casimir-Effect: No Manifestation of Zero-Point Energy](#) by Gerold Gründler, 2013 (15 pages) and [All wrong with the Casimir effect](#) by Astrid Karnassnigg, 2014 (3 pages). Then, [The Casimir effect: a force from nothing](#) by Astrid Lambrecht, 2007 (5 pages).

French physicists are quite active in the field, and, in particular **Astrid Lambrecht**, formerly director of the INP of the CNRS, the Institute of Physics which oversees the physics laboratories of the CNRS²⁷⁵.

The Casimir effect could be of interest in quantum metrology to create sensors and in particular NEMS/MEMS.

These theories on quantum vacuum fluctuation and the Casimir effect are also fraudulently exploited by the creators of so-called machines capable of capturing vacuum energy, which collect nothing at all in practice. The fluctuation-dissipation theorem ensures that quantum vacuum fluctuations does not violate the second principle of thermodynamics. No energy can be recovered thanks to these fluctuations! Forget it.

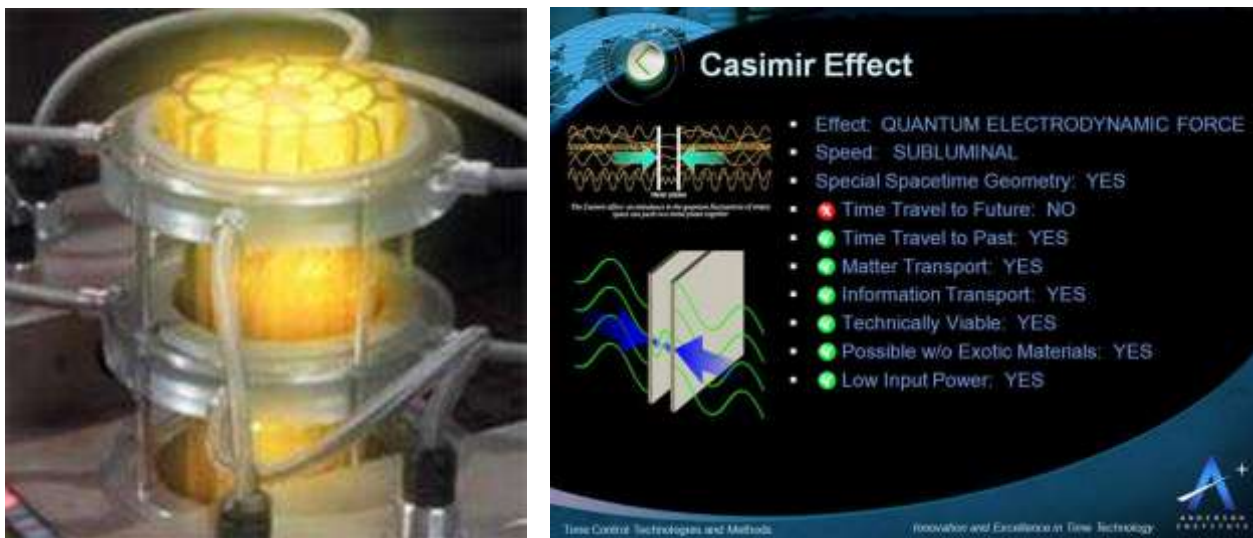


Figure 120: Anderson Institute claims about using the Casimir effect.

For example, you have a certain **David Lewis Anderson**, who started the **Anderson Institute** in 1990, who claims to be able to use the Casimir effect to travel back in time and create a "free" electricity generator²⁷⁶.

In other cases, the Casimir effect is exploited in a scientific but borderline way to imagine science fiction scenarios like ways to cross wormholes²⁷⁷.

The **NASA** even explored the idea to use sails and vacuum fluctuation to propel a space vessel between 1996 and 2002, to no avail. It was one of the ideas explored as part of the fancy Breakthrough Propulsion Physics Program, which was awarded a tiny budget of \$1.2M and later cancelled.

²⁷⁵ See [The Casimir effect theories and experiments](#) by Romain Gu erout, Astrid Lambrecht and Serge Reynaud, LKB, 2010 (28 slides) and [Casimir effect and short-range gravity tests](#), LKB, 2013 (15 slides). Astrid Lambrecht chaired the [Casimir RNP](#) group, which brought together researchers from around the world working on the Casimir effect. The group was active between 2009 and 2014.

²⁷⁶ Its website seems to be inactive since 2012. See this radio interview from 2019 with the guy who defies the laws of bullshit in his talk. It shows how an interviewer lacking some scientific background can be fooled by a good talker. In [See Is Time Travel Real?](#) 2019 and the [Anderson Institute](#) website.

²⁷⁷ See [One Theory Beyond the Standard Model Could Allow Wormholes that You Could Actually Fly Through - Universe Today](#) by Matt Williams, August 2020, mentioning [Humanly traversable wormholes](#) by Juan Maldacena and Alexey Milekhin, August 2020.

Unifying theories

The quest of a **unified theory** has occupied many physicists for nearly a century. Its goal would be to consolidate all the physics theories and in particular, quantum physics, relativity and gravity into a single formalism. In addition to the QFT, a very large number of explanatory and unifying theories of physics have been developed.

No such theory is considered today as being complete. Here's a rough map showing how these different theories are related.

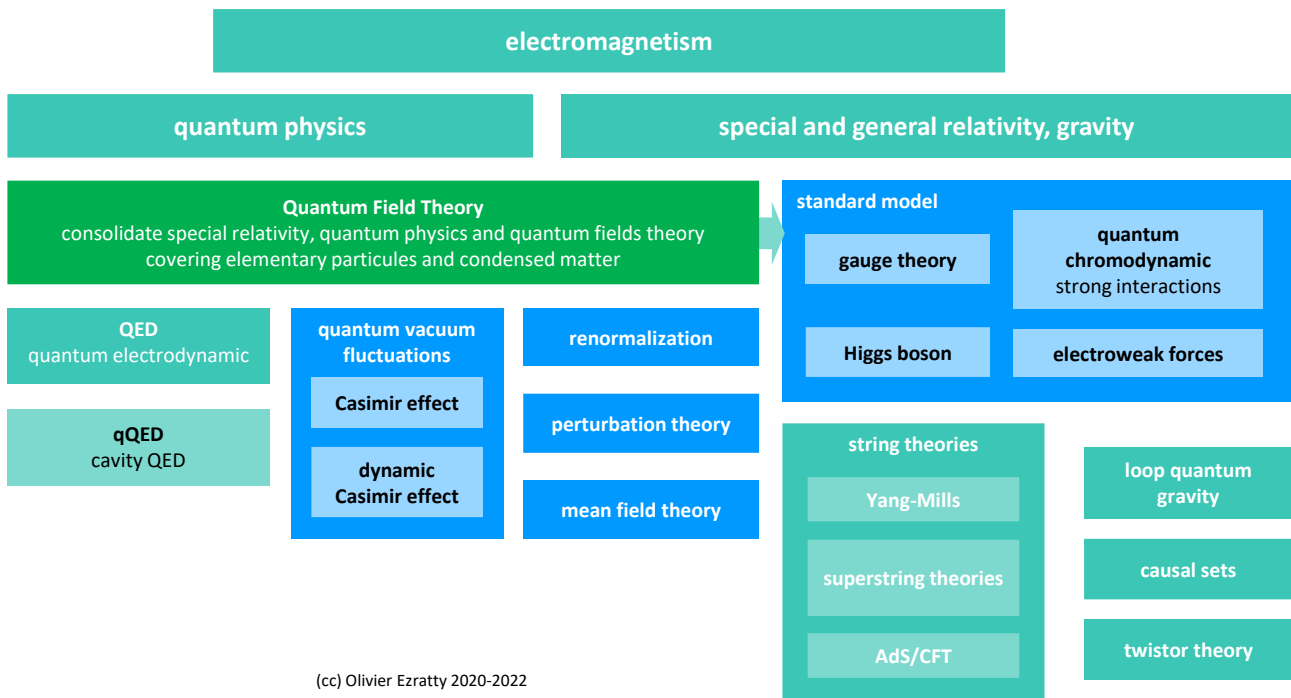


Figure 121: vague classification of quantum physics theories and unification theories. (cc) Olivier Ezratty, 2020.

Quantum chromodynamics provides a description of the strong interactions binding quarks together via gluons to form particles called hadrons, namely, protons and neutrons. Murray Gell-Mann (1929-2019, American, Nobel Prize in Physics in 1969) and Georges Zweig (1935, Russian then American, former PhD student of Richard Feynman) each proposed the existence of quarks in 1963. Quantum chromodynamics is an extension of the quantum field theory developed in 1972 by Murray Gell-Mann and Harald Fritzsch.

Standard model describes the architecture of known elementary particles and their interactions. It models the fundamental weak and strong electromagnetic forces. It only lacks gravity to be complete. This model predicted the existence of quarks, these massive particles forming neutrons and protons, in addition to other elementary particles such as the famous Higgs boson whose existence was proven at CERN's LHC in 2012. The expression “standard model” was created in 1975. It relies on a gauge theory because of its mathematical symmetries.

It is not the first of its kind because Maxwell's electromagnetism is also a gauge theory, between magnetic and electric fields. The standard model particles do not cover the famous dark matter whose nature is not yet known.

String theory combines general relativity and quantum physics to propose a quantum explanation of gravity, using a new massless particle, the graviton. According to this theory, elementary particles are tiny strings, open or closed, with vibration types defining the nature of the particle. Their size is of the order of magnitude of 10^{-35} m, the Planck length. According to this theory, the Universe would be a set of vibrating strings.

The graviton would join the three other forces of nature intermediated by particles without mass: electromagnetic waves mediated by photons, strong interactions mediated by gluons that link quarks together in protons and neutrons and weak interactions mediated by W and Z bosons that govern atomic nuclei and in particular radioactivity²⁷⁸. String theory essentially covers bosons of all kinds.

Superstring theory is an extension of the string theory that adds fermions to the code theory model that focused on bosons. It tries to consolidate the description of all forces in a single unified theory. It quantifies gravity and ties it to other forces. It is based on the notion of supersymmetry which extends the standard model by making each type of boson correspond to a type of fermion. The theory took shape in 1943 with Werner Heisenberg in the form of the S-matrix theory, and then was reborn in 1984. It uses 10 dimensions to describe physics, far beyond the four classical dimensions (three for position and one for time). It also uses the notion of "branes" which describes point particles in these multidimensional spaces. However, this theory is not unique since there are five variants, which some people try to unify in the **M-theory**, which is based on 11 dimensions. A never-ending story!

Loop quantum gravity theory is another tentative to explain gravity with a quantum model. It discretizes the effects of gravity by presenting space as a meshed structure with quantized areas and volumes of space, and gravitational field quanta connected to each other by links characterized by a spin (that has nothing to do with usual particles spin)²⁷⁹. For this theory created in the 1980s, the Universe would be a gigantic spin foam. Its main promoters are **Carlo Rovelli** (Center for Theoretical Physics in Marseille) and **Lee Smolin** (Perimeter Institute for Theoretical Physics in Waterloo²⁸⁰). The seeds of the theory date back to 1952, with many intermediate stages as described in Figure 122. It is, above all, a mathematical and topological model. It does not seem to formulate an experimental validation method even though it is used to model that the big bang was coming after a big bounce in a cyclical phenomenon with contractions and expansions. It may be possible to detect some fossil signature of these phenomenon.

A brief history of quantum gravity:

- 1952 Flat space quantization (Rosenfeld, Pauli, Fierz, Gupta,...)
- 1959 Canonical structure of general relativity (Dirac, Bergmann, Arnowit, Deser, Misner)
- 1964 Penrose introduces the idea of spin networks
- 1967 Wheeler-DeWitt equation
- 1974 Hawking radiation and black hole entropy
- 1984 String theory
- 1986 New variables for general relativity (Ashtekar, Sen)
- 1988 Loop representation and solutions to the Wheeler-DeWitt equation (Jacobson, Smolin)
- 1989 Extra dimensions from string theory
- 1995 Hilbert space of loop quantum gravity, geometric operators
- 2000' Spin foam models, group field theory, loop quantum cosmology,...

Figure 122: history of quantum gravity. Source: [The philosophy behind loop quantum gravity](#) by Marc Geiller, 2001 (65 slides).

²⁷⁸ A proton has two up quarks and one down quark. A neutron has two down quarks and one up quark. An up quark can desintegrate in a down quark, a positron and a neutrino via a W boson and a down quark can disintegrate in an up quark, one electron, one antineutrino and a W boson. A quark has a size close to that of an electron, about 10^{-16} cm. Radioactivity emits alpha rays via strong forces, particles comprising two protons and two neutrons (helium 4 atom without electron), beta rays generated by weak forces which are electrons or positrons and finally gamma rays which are photons of very high energy level.

²⁷⁹ It is reminiscent of the recent theory of the whole built by Stephen Wolfram and published in 2020.

²⁸⁰ See [Lee Smolin Public Lecture Special: Einstein's Unfinished Revolution](#), 2019 (1h13mn) where he describes the shortcomings of quantum mechanics.

These are only a few of the many theories being devised. Some amateurs also try to create their own theory of the whole, without usually obtaining any feedback from the scientific community²⁸¹.

Quantum physics 101 key takeaways

- Quantum physics is based on a set of postulates and a strong linear algebra mathematical formalism. Surprisingly, there are many variations of these postulates. There is not a single bible or reference for these, illustrating the diversity of pedagogies and opinions in quantum physics. But although deemed incomplete, the theory has been validated by an incredible number of experiments.
- Quantum physics describe the behavior of matter and light at nanoscopic levels. It deals not only with atoms, electrons and photons which are used in quantum information technologies but also with all elementary particles from the standard model (quarks, ...).
- Quantumness comes from the quantification of many properties of light and matter that can take only discrete values, from the wave-particle duality of massive (atoms, electrons) and non-massive (photons) particles, and from wave-particle duality and its consequences like superposition and entanglement. By the way, a cat can't be both alive and dead since it's not a nanoscopic quantum object. Forget the cat and instead, learn Schrodinger's equation!
- Indetermination principle states it's impossible to measure with an infinite precision quantum objects properties that are complementary like speed and position. You can use this principle to improve measurement precision in one dimension at the expense of the other. It is used in photons squeezing, itself applied in the LIGO giant gravitational waves interferometer.
- Quantum matter and fluids are showing up with composite elements associating light and matter, or with superfluidity and superconductivity where boson quantum objects can behave like a single quantum object. You find there a wealth of strange phenomenon such as skyrmions, magnons, topological insulators and quantum batteries. They could lead to a new chapter in the second quantum revolution.
- Quantum physics also explains weird effects like vacuum quantum fluctuation, although it doesn't violate the second principle of thermodynamics, nor can it lead to the creation of some free energy sources.
- Most of quantum physics phenomena as described in this section have or will have some use cases in quantum information science and technologies.

²⁸¹ See, for example, the [Unified Theory Research Team](#) website, which announced the publication in September 2020 of a theory model of the whole called MME for Model of Material and Energy. The site claims that its model, which is presented as an algorithmic approach, can explain everything, from the functioning of all particles to the bricks of life. The team behind this project includes two Pierre and Frédéric Lepeltier from France. The first has been the CEO of the Unified Theory Research Team for 32 years.

Gate-based quantum computing

As a computer scientist, you may have skipped all the previous parts to get here right away. One can indeed understand how quantum computers operate without delving too deeply into quantum physics beyond grasping its basic mechanisms. Some mathematical knowledge is however required on trigonometry and linear algebra, including vectors, matrices and complex numbers²⁸².

The first basic element of a quantum computer is its inevitable qubit. You've probably already heard about this mysterious object having “simultaneously” the values 0 and 1. As a result, you’ve been told that a set of N qubits create an exponential 2^N superposed state that explains the power of quantum computing. Unfortunately, most explanations usually stop there and you then end up wondering how it actually works to make some calculation. What comes in and out of a quantum computer? How is it programmed? How do you feed it with data and code? Where is it useful? This book is there to provide you with some educated answers to all these critical questions.

We will cover here the logical and mathematical aspects of qubits, qubit registers, quantum gates and measurement²⁸³. Each and every time, when possible, we’ll draw parallels with traditional computing. In the following part, we’ll look at quantum computer engineering and hardware and even describe the complete architecture of a superconducting qubits quantum computer.

In a nutshell

Before digging into qubits, qubit registers and the likes, here’s a tentative to summarize the key elements of gate-based quantum computing that we’ll cover in detail afterwards. It shows how physics and mathematics are intertwined.

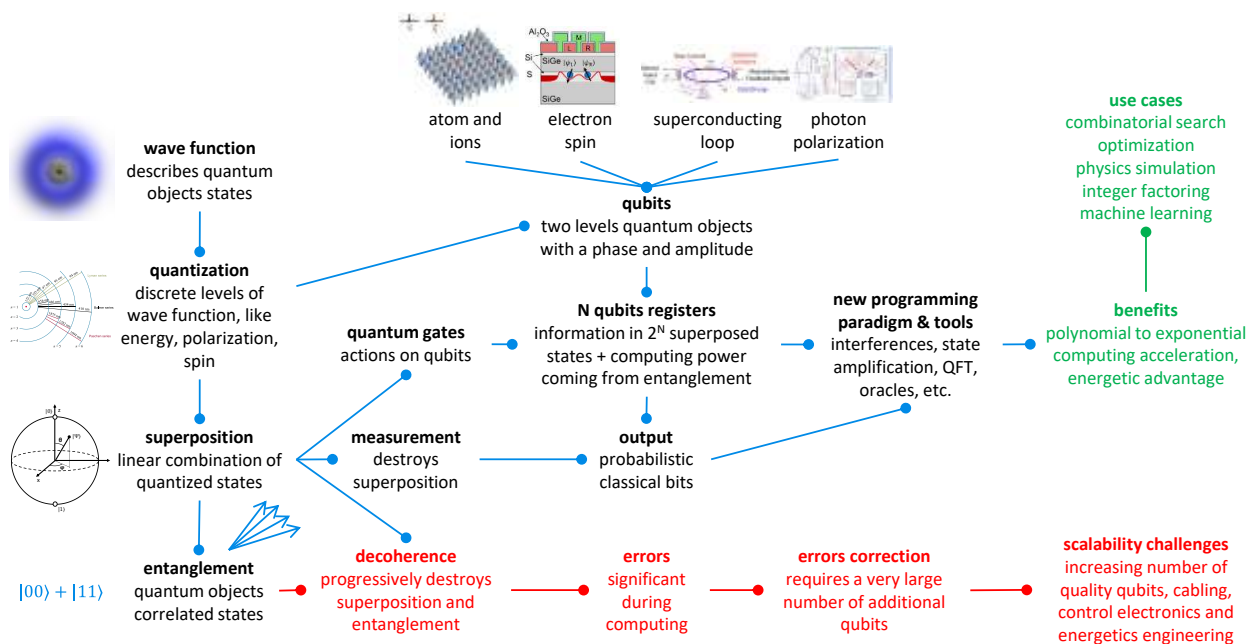


Figure 123: a single schematic to describe quantum physics and quantum computing. (cc) Olivier Ezratty, 2021.

²⁸² Complex numbers were created by the polymath Girolamo Cardano (1501-1576, Italian) and the Algerian mathematician Raffaele Bombelli (1526-1572, Italian) between 1545 and 1569. They were used to solve polynomial equations associating cubes and squares that kept Italian mathematicians busy since the end of the fifteenth century. See [A Short History of Complex Numbers](#) by Orlando Merino, 2006 (5 pages).

²⁸³ The name qubit, for ‘quantum’ and ‘bit’, appeared in 1995 in [Quantum coding](#) by Benjamin Schumacher, April 1995 (34 pages).

Wave function

mother equation of quantum physics, created by Erwin Schrödinger. It describes particles properties probabilities in space and time with a complex number. This equation is specific to non-relativistic massive particles like electrons. We also use photons in quantum computing, whose properties are defined by Maxwell's electromagnetic equations and the second quantization equations (Glauber states, Wigner function, Fock states, etc.).

Quantization

properties of quantum objects, having discrete, not continuous and exclusive values. It enables the creation of qubit physical and logical objects having two levels.

Superposition

qubits are quantized quantum objects having two basis computational states $|0\rangle$ and $|1\rangle$. These can be combined linearly, thanks to the linearity over space of Schrödinger's wave equation. Solutions of this equation can be linearly combined with complex numbers. Thus, a wave adding two solution waves is still a solution. This doesn't mean the qubit is really simultaneously in two states.

Entanglement

often presented as a situation where several quantum objects have properties that are correlated. Actually, entanglement is the consequence of superposition of multiple qubit states. This is the phenomenon that provides both a real theoretical exponential acceleration to quantum computing but also enables conditional relations between qubits. Without it, qubits would be independent and no useful computing could be done.

Qubits

mathematical objects with two levels 0 and 1. It's described by two complex number amplitudes. But due to normalization and getting rid of their global phase (we'll explain all of that), they are described by two real numbers for their amplitude and phase. Physical qubits are based on massive (electron, controlled atoms, superconducting currents) or non massive quantum objects (photons) and one of their quantum properties or observables (spin, energy level, current direction of phase, polarity).

Registers

physical and logical assemblies of several qubits. With N qubits, they can handle computing on a space 2^N computational basis states together represented by complex number amplitudes. Each basis state is one of the possible combinations of N 0s and 1s. Computing power comes from entanglement.

Quantum gates

logical operations exerted on qubits. We have single qubit gates which are changing single qubit states and several qubit gates conditionally changing one or two qubits based on the state of a control qubit, and leveraging entanglement. Gates are the only mechanism used to feed a quantum register with data and instructions. These are not separated as in classical computing based on a Von Neumann / Turing machine model.

Programming paradigms

quantum programming is based on very different paradigms than classical programming. In a nutshell, it's analog-based. We play with interferences, states amplification, quantum Fourier transforms and the concept of oracles.

Measurement

the way to extract information from qubits. Unfortunately, you can't read the two real numbers describing the qubit state nor the combination of qubit registers computational basis states. You get just classical 0s and 1s for each qubit. Quantum algorithms toy with the wealth of superposition and entanglement during computing to recover a simple result at the end. Measurement is also used during quantum error corrections. Since qubit measurement output is probabilistic, you generate a deterministic output with running your algorithm several times (up to several thousand times) and computing an average of the obtained results.

Output

for a register of N qubits, you get N 0s and 1s. But these are probabilistic results. You usually need to run your algorithm several times and compute an average of the results to get a deterministic result. Noise and decoherence are additional reasons why you need to do this several times.

Benefit

an acceleration of computing time compared to the best classical computers. Accelerations can be from polynomial to exponential. The benefit can also be economic like with the energetic cost of quantum computing that many expect to be fairly low compared to classical computing.

Use cases

quantum computing will not replace most use cases of classical computing. It brings value for complex combinatorial problems, optimization problems, quantum physics simulation, some machine learning problems and at last, fast integer factoring.

Decoherence

the enemy with quantum computing. This is when qubit states is degraded, both for superposition and entanglement. It results from the interactions between the qubits and their environment despite of all the care implemented to isolate it.

Errors

result of decoherence and other perturbations affecting the qubits. Other sources of errors are the imprecision of the control electronics driving qubit gates. Qubit phase and amplitude is degraded over time. Existing error rates are many order of magnitude higher than with classical computing. These are the reasons why we don't have yet quantum computers with a very high number of functional qubits.

Error corrections

set of techniques used to correct these errors. It requires assembling so-called logical qubits made of a great number of physical qubits. The needed ratio at this point is ranging from 30 to 10,000 physical qubits to create a logical qubit. The ratio depends on the qubit quality and technology but also on the target logical qubit fidelity (from 10^{-8} to 10^{-15} error rates).

Scalability challenges

assembling these huge logical qubit is the mother of all the challenges with quantum computing. It's not easy to assemble that many qubits and keeping them stable, limit their decoherence and the likes. On top of that, assembling a great number of qubits creates huge engineering challenges with cryogenics cooling power, thermal dissipation, cabling and control electronics. These are the reason why quantum computers don't scale yet to bring their expected benefits.

(cc) Olivier Ezratty, 2021-2022

Figure 124: the key concepts behind gate-based quantum computing in one page. (cc) Olivier Ezratty, 2021-2022.

Linear algebra

Quantum physics and computing require some understanding of a whole bunch of concepts of linear algebra that we will quickly scan here. They are associated with a mathematical formalism describing quantum phenomena. This mathematical formalism is also the cornerstone of quantum physics postulates, already covered in an earlier section, page 86. It is also essential to create quantum algorithms.

I will try to explain some of these concepts and mathematical conventions that are used with quantum computing. This will mainly allow you to find your way through some of the scientific publications I mention in this book.

Linearity

Linear algebra is the branch of mathematics using vector spaces, matrices and linear transformations. In the case of quantum physics and computing, it also deals with complex numbers.

A phenomenon is linear if its effects are proportional to its causes. This translates into the verification of two simple equations pertaining to homogeneity and additivity as shown in Figure 125.

homogeneity $f(\lambda x) = \lambda f(x)$ for all $x \in \mathbb{R}$
additivity $f(x + y) = f(x) + f(y)$ for all $x, y \in \mathbb{R}$

Figure 125: homogeneity and additivity in linear algebra.

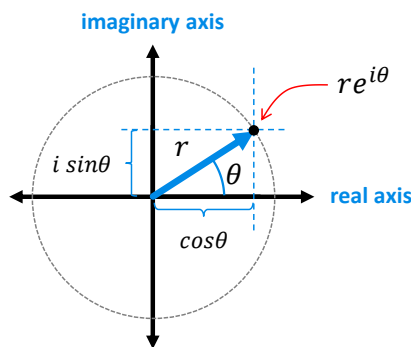
\mathbb{R} being a vector space, λ a real number, x being a vector of the vector space \mathbb{R} and $f(x)$ a function applying to this vector. In a one-dimensional space, a classic example of a linear function is $f(x) = ax$. A polynomial function of the type $f(x) = ax^2 + b$ is obviously not linear because it evolves non-proportionally to x . Even $f(x) = ax + b$ is not linear, and for the same reason.

As already defined, an observable is a mathematical operator, a Hermitian matrix, used to measure (mathematically) a property of a physical system. It's frequently assimilated to the measured property. For a qubit, it corresponds to some measurable value by a sensor on a quantum object outputting a classical 0 or 1. The measurement causes the qubit quantum object wave function to collapse on one of the basis states. If the state of a quantum or qubit is measured twice, the measurement will yield the same result. With qubits, observables are usually based on projections on a two-level properties system, mathematically materialized by a $|0\rangle$ or $|1\rangle$, aka qubit computational basis states. But, if the physics permits it, other computational basis can be used. It's the case with photons and polarization measurement where their angle can be easily made different in different parts of an experiment.

Hilbert spaces and orthonormal basis

A quantum state of a single or several quantum objects can be described by a vector in a Hilbert space. A qubit state is represented in a two-dimensional orthonormal space formed with the basis states vectors $|0\rangle$ and $|1\rangle$. It is a vector of complex numbers in a two-dimensional Hilbert space allowing lengths and angles measurements. A complex number is defined as $a+ib$ where a and b are real and $i^2=-1$.

Complex numbers are very useful in quantum physics. It relates to the wave-particle duality of all quantum objects and to the need to handle their amplitude (complex number norm, vector length or modulus) and phase (the complex number angle when using polar coordinates).



r = amplitude, modulus, norm

θ = phase angle

Euler formula

$$e^{i\theta} = \cos\theta + i \sin\theta$$

phase angles add up

$$e^{i\theta_1} e^{i\theta_2} = e^{i(\theta_1+\theta_2)}$$

Figure 126: complex number explained by geometry and trigonometry.

With qubits, it is represented with the complex numbers α and β associated with the states $|0\rangle$ and $|1\rangle$ and whose sum of squares makes 1. This linear combination of the states $|0\rangle$ and $|1\rangle$ describes the phenomenon of superposition within a qubit.

This two-dimensional space replaces the infinite-dimensional space that characterizes a Schrödinger wave function $f(x)$, where x can take any value in space. It is thus a simplified representation of the quantum state of a qubit. By manipulating these symbols, the vectors and matrices, we forget a little the wave-like nature of the manipulated quanta, even though it is still present in the phase information embedded in the imaginary part of α and β for one qubit. It also can deal with photons which do not obey to Schrödinger's equation but to Maxwell's electromagnetic equations.

An orthonormal basis of a vector space consists of base vectors which are all mathematically orthogonal with each other and whose length is 1. In the representation of a qubit state, the most common orthonormal basis is made of the states $|0\rangle$ and $|1\rangle$.

Other orthonormal reference basis can be used for measurement, particularly with photons, and polarization references different from the starting reference ($0^\circ/90^\circ$ then $45^\circ/135^\circ$, obtained with rotating a simple polarizer).

Another example of an orthonormal basis is the states located on the Bloch sphere on the x-axis and represented with $|+\rangle$ and $|-\rangle$. These are often called Schrodinger cats.

$$|+\rangle = \frac{|0\rangle + |1\rangle}{\sqrt{2}} \quad |-\rangle = \frac{|0\rangle - |1\rangle}{\sqrt{2}}$$

Figure 127: another orthonormal basis.

Dirac Notation

In Dirac notation, a quantum object state is represented by $|\Psi\rangle$, the **ket** of quantum state Ψ . The **bra** of the same state vector, represented by $\langle\Psi|$ is the conjugate (or transconjugate, or adjoint) transpose of the "ket". It is the "horizontal" vector $[\bar{\alpha}, \bar{\beta}]$ where $\bar{\alpha}$ and $\bar{\beta}$ are the conjugates of α and β , inverting the sign of the imaginary part of the number (-i instead of +i, or the opposite).

The **scalar product** of two qubits $\langle\Psi_1|\Psi_2\rangle$ is the mathematical projection of the state vector Ψ_2 onto the vector Ψ_1 . This yields a complex number. When the vectors are orthogonal, the scalar product is equal to 0. When the two vectors are identical, $\langle\Psi|\Psi\rangle$ is Ψ 's norm and is always equal to 1. A scalar product is also named an inner product.

An **inner product** is a generalization of a dot vector product applied to complex number vectors, according to the sigma in Figure 130.

The **outer product** of two vectors representing a qubit, one in bra and the other in ket, gives an operator or density matrix which is a 2x2 matrix.

When the bra corresponds to the transconjugate of the ket, it is a density operator of a pure state. This notion of density operator will then be extended to a combination of qubits.

$$\begin{array}{l} \text{vectors} \\ \text{Dirac} \\ \text{notation} \end{array} \quad |\Psi\rangle = \begin{bmatrix} \alpha \\ \beta \end{bmatrix} \quad \begin{array}{l} \bar{\alpha} = \alpha^* \\ \langle\Psi| = [\bar{\alpha}, \bar{\beta}] \\ \Psi \text{ bra} \end{array}$$

$$(1 + i)^* = 1 - i$$

complex number conjugate

Figure 128: introduction to Dirac vector notation.

$$\langle\Psi_1|\Psi_2\rangle = [\bar{\alpha}_1, \bar{\beta}_1] \times \begin{bmatrix} \alpha_2 \\ \beta_2 \end{bmatrix} = \bar{\alpha}_1\alpha_2 + \bar{\beta}_1\beta_2$$

inner scalar product: vector similarity

$$\langle\Psi|\Psi\rangle = [\bar{\alpha}, \bar{\beta}] \times \begin{bmatrix} \alpha \\ \beta \end{bmatrix} = \alpha^2 + \beta^2 = 1$$

Figure 129: inner scalar product.

$$\begin{array}{l} \text{complex vectors} \\ \text{dot product} \end{array} \quad A \cdot B = \sum_i a_i \bar{b}_i$$

Figure 130: dot product.

$$|\Psi\rangle\langle\Psi| = \begin{bmatrix} \alpha \\ \beta \end{bmatrix} \times [\bar{\alpha}, \bar{\beta}] = \begin{bmatrix} \alpha\bar{\alpha} & \alpha\bar{\beta} \\ \beta\bar{\alpha} & \beta\bar{\beta} \end{bmatrix}$$

Figure 131: outer product.

What are the use cases of this Dirac notation? It is particularly helpful for [manipulating quantum states](#), to simplify tensor products representations and with measurement, which we'll cover [later](#) starting page 184.

Eigenstuff

We also need to define the notions of **eigenvector**, **eigenvalue**, **eigenstate** and **eigenspace** which are often used in quantum mechanics and quantum computing as well as in machine learning, particularly in dimension reduction algorithms such as PCA (Principal Components Analysis). These notions allow to define the structure of certain square matrices²⁸⁴.

For a square matrix A , an eigenvector x or eigenvector of A is a vector that verifies the equation $Ax = \lambda x$, λ being a complex number called eigenvalue.

These eigenvectors have the particularity of not changing direction once multiplied by the matrix A . For an eigenvalue λ , the associated eigenspace, or eigenspace, is the set of vectors x that satisfy $Ax = \lambda x$. These eigenvalues are evaluated by calculating the determinant of the matrix $A - \lambda I$, where I is the identity matrix (1 in the diagonal boxes and 0 elsewhere). We then find the values of which solves $0 = A - \lambda I$. It is a polynomial equation having a degree less than or equal to the size of the square matrix²⁸⁵.

The reference eigenvectors of a matrix A allow to reconstitute an orthonormal space linked to the matrix. For example, a projection matrix in a 3D plane will have as main eigenvectors two orthogonal vectors located in the plane and one vector orthogonal to the plane. This multiplication gives λx with λ being non-zero if the eigenvector is in the plane in question and 0 if the vector is orthogonal to the plane²⁸⁶. A matrix A can be that of a quantum gate. An eigenvector of a quantum gate is therefore a ket whose value is not modified by the quantum gate.

This is easy to imagine for the S gate, phase change, which we will see later. The $|0\rangle$ and $|1\rangle$ kets being in the rotation axis, they are not modified by it.

They are thus eigenvectors of the S gate and the corresponding eigenvalues are 1 and -1. This is always the case for quantum gate matrices since the vectors representing the quantum states, the kets, always have a length of 1. These eigenvalues are the only ones enabling this!

The search for the eigenvectors and eigenvalues of a matrix A is like diagonalizing it. For this it must be diagonalizable ("non-defective"). Hermitian and unitary matrices commonly used in quantum physics are all non-defective and diagonalizable. The diagonalization of a square matrix consists in finding the matrix which will multiply it to transform it into a matrix filled only in its diagonal. A matrix A is diagonalizable if we can find a matrix P and a diagonal matrix D such that $P^{-1}AP = D$ (P^{-1} being the inverse matrix of P , such that $P^{-1}P = PP^{-1} = I$, I being the matrix identity with 1's in the diagonal and 0's elsewhere). A square matrix of dimension n is diagonalizable if it has n mutually independent eigenvectors. The diagonalized matrix diagonal contains the eigenvalues λ_i of the origin matrix, with $i=1$ to N being the size of the matrix.

A diagonalized quantum state of a quantum object can look like $A = \sum_i \lambda_i |i\rangle\langle i|$. This decomposition of a pure state vector in a Hilbert space in eigenstates $|i\rangle$ and eigenvalues λ_i is also named a **spectral decomposition**. It's linked to the wave-duality aspect of all quantum objects.

²⁸⁴ See a good quick review of linear algebra in [Linear Algebra Review and Reference](#) by Zico Kolter and Chuong Don 2015 (26 pages).

²⁸⁵ See this nice visual explanation of eigenvectors and eigenvalues: [Eigenvectors and eigenvalues | Chapter 14, Essence of linear algebra](#), 2016 (17 minutes).

²⁸⁶ This is well explained in [Gilbert Strang's](#) lecture at MIT, 2011 (51 minutes).

A quantum object is indeed decomposed into a coherent superposition of elementary waves. In the case of photons, it's easy to grasp with several photons of different frequencies being superposed and forming a gaussian wave packet. It constitutes a coherent superposition of the electromagnetic field. These wave packets are commonly generated by femtosecond pulse lasers²⁸⁷.

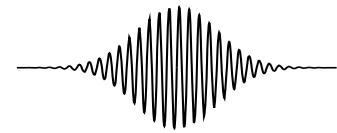


Figure 132: a photon gaussian wave packet.

And the eigenstates? This is another name given to eigenvectors, but by physicists!

Tensor products

The tensor product of two vectors of dimension m and n gives a vector of dimension m*n while the tensor product of a matrix of dimension m*n by a matrix of dimension k*l will give a matrix of dimension mk*nl. Tensor products use the sign \otimes .

$$\begin{bmatrix} v_1 \\ v_2 \\ \vdots \\ v_n \end{bmatrix} \otimes \begin{bmatrix} w_1 \\ w_2 \\ \vdots \\ w_m \end{bmatrix} = \begin{bmatrix} v_1 w_1 & \cdots & v_1 w_m \\ \vdots & \ddots & \vdots \\ v_n w_1 & \cdots & v_n w_m \end{bmatrix}$$

tensor product of two vectors

$$|i\rangle = \alpha_i|0\rangle + \beta_i|1\rangle = \begin{bmatrix} \alpha_i \\ \beta_i \end{bmatrix}$$

$$|\Psi\rangle = \bigotimes_{n=1}^N |i\rangle$$

qubits register state before any entanglement is a tensor product of each qubit 2 dimension vector
dimensionality of 2^N real numbers (N qubits $\times 2$)

these states can be linearly combined

$$|\Psi_1\rangle = \{000 \dots 000\}$$

$$|\Psi_{2^N}\rangle = \{111 \dots 111\}$$

$$\sum_{i=1,2^N} \lambda_i |\Psi_i\rangle$$

$$\begin{bmatrix} \lambda_1 \\ \lambda_2 \\ \vdots \\ \lambda_{2^N} \end{bmatrix}$$

n qubits register pure state $|\Psi\rangle$ of N qubits $|i\rangle$ is a point in a Hilbert space with a basis of 2^N orthogonal vectors $|\Psi_i\rangle$, these being combinations of N $|0\rangle$ and $|1\rangle$, dimensionality of $2^{N+1} - 1$ real numbers

a qubit register pure state $|\Psi\rangle$ representation with its computational basis state vectors amplitudes

Figure 133: tensor products construction. (cc) Olivier Ezratty, 2020.

Tensor products are used to compute “manually” the state of quantum registers containing several unentangled qubits. The state of a register of N non-entangled qubits is the tensor product of these N qubits represented by their vertical ket vector.

This gives a ket, a vertical vector that has 2^N different values, each representing the complex number weight of different combinations of 0s and 1s. A quantum register is a superposition of these 2^N different states complex amplitudes. The sum of these squared amplitudes gives 1 per the Born rule. By the way, the tensor product of qubits is represented by a vector, after vectorization of the tensor product matrix of 2^N dimensions.

Entanglement

Quantum states are separable when they are mathematically the result of the tensor product of each of the pure states that compose it. But these values can be assembled linearly to create another quantum state, modulo a normalization rule. This combines several vectors resulting from tensor products. These combinations can become inseparable.

²⁸⁷ And when the carrier frequency is growing or decreasing through the pulse, it's named a chirp pulse.

That's when entanglement comes into play. An entangled state of two or more qubits occurs when it cannot be factorized as the tensor product of two pure states. In other words, it cannot be the combination of independent qubits. The qubits become dependent.

This is demonstrated mathematically for the states $|00\rangle$ and $|11\rangle$ of a register of two qubits. In these pairs, the measurement of the value of one of the qubits determines that of the other, here identical. The creation of such entangled pairs of qubits requires preparation operations like using a combination of Hadamard and CNOT gates.

Two qubits placed side by side are not magically entangled! The pair used in the example can be generated by two quantum gates, an H gate (Hadamard) and a CNOT gate, as shown just below.

an entangled EPR pair can't be a tensor product of two qubits $|\Psi_1\rangle$ and $|\Psi_2\rangle$

$$|\Psi_1\rangle = \alpha_1|0\rangle + \beta_1|1\rangle \quad |\Psi_2\rangle = \alpha_2|0\rangle + \beta_2|1\rangle$$

$$|\Psi_1\rangle \otimes |\Psi_2\rangle = (\alpha_1|0\rangle + \beta_1|1\rangle)(\alpha_2|0\rangle + \beta_2|1\rangle)$$

$$\frac{1}{\sqrt{2}}(|00\rangle + |11\rangle) = \alpha_1\alpha_2|00\rangle + \alpha_1\beta_2|01\rangle + \beta_1\alpha_2|10\rangle + \beta_1\beta_2|11\rangle$$

$$\alpha_1\beta_2 = 0 \text{ and } \beta_1\alpha_2 = 0$$

$$\text{are incompatible with } \alpha_1\alpha_2 = \frac{1}{\sqrt{2}} \text{ and } \beta_1\beta_2 = \frac{1}{\sqrt{2}}$$

$$\text{if } \alpha_1 = 0 \text{ then } \alpha_1\alpha_2 = 0$$

$$\text{if } \beta_2 = 0 \text{ then } \beta_1\beta_2 = 0$$

implications: the density matrix mathematical representation of qubits registers

Figure 134: non separability of two entangled qubits.

We will define this CNOT gate [later on](#), after page 171. This is described as both qubits having correlated values. But these values are... random since being a perfect superposition of 0 and 1!

Only multi-qubit quantum gates generate entangled qubits in a qubit register, besides the SWAP gate which doesn't. Here with an example of creating a Bell pair associating the states $|00\rangle$ and $|11\rangle$ with a mix of Hadamard and CNOT gates.

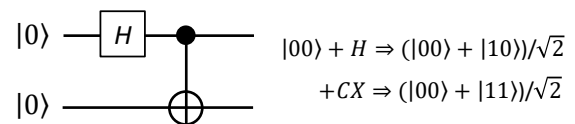


Figure 135: a Bell pair.

A so-called **GHZ** state (for Greenberger-Horne-Zeilinger, distinguishable from GHZ frequencies with a capital Z) with three entangled qubits is superposing the states $|000\rangle$ and $|111\rangle$. It is a generalization of the 2-qubit Bell state $(|00\rangle + |11\rangle)/\sqrt{2}$. A GHZ is usually prepared with a Hadamard gate and two consecutive CNOTs.

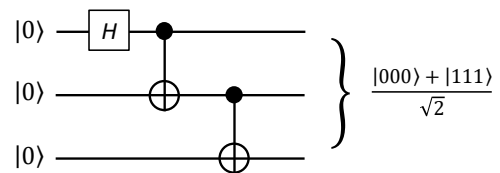


Figure 136: a GHZ state.

These pairs of Bell and GHZ states are used in error correction codes as well as in telecommunications, among other things.

Another typical entangled state is the **W state**, created in 2000, that has the property of being maximally entangled and robust against particle loss. It is a generalized version of another of the four possible Bell states, $(|01\rangle + |10\rangle)/\sqrt{2}$ ²⁸⁸:

$$|W\rangle = \frac{1}{\sqrt{3}}(|001\rangle + |010\rangle + |100\rangle)$$

Figure 137: a W state.

At last, the level of entanglement of a qubit register depends on the Hamming distance between the basis states involved in the linear superposition of basis states. The far apart they are, with the greater number of non-identical 0s and 1s, the greatest the entanglement is.

²⁸⁸ See [Three qubits can be entangled in two inequivalent ways](#) by Wolfgang Dür (which explains the W in W states), G. Vidal, and J. Ignacio Cirac, 2000 (12 pages) and the thesis [Symmetry and Classification of Multipartite Entangled States](#) by Adam Burchardt, September 2021 (126 pages).

Matrices

Various matrix transformations must be understood here:

- **Matrix conjugate** when all complex number see their complex part negated, or $a_{ij} = a_{ij}^*$.
- **Matrix transpose** when all matrix a_{ij} values are transformed into a_{ji} value, with i =line and j =column indices of matrix “cells”.
- **Matrix transconjugate** which is a conjugate of the transpose or vice-versa, also named adjoint. It's notated as A^\dagger , for A « dagger ».
- **Matrix traces** are the sum of their diagonal values, usually normalized to 1, like with density matrices. It is also the sum of their eigenvalues.

We also have three important classes of matrices:

- **Hermitian matrices** are equal to their transconjugate, meaning that $a_{ij} = a_{ji}^*$.

- **Projectors** are matrix operators using a Hermitian matrix that is equal to its square. A diagonalized projector contains only zeros and a single 1. A projector is a non-unitary operation. It relates with the irreversibility of quantum measurement.

If $|\psi\rangle$ is a unit vector, the outer product $|\psi\rangle\langle\psi|$ is a projector that can project any vector $|\phi\rangle$ on $|\psi\rangle$.

| Notation | Description |
|--|--|
| z^* | Complex conjugate of the complex number z . $(1+i)^* = 1-i$ |
| $ \psi\rangle$ | Vector. Also known as a <i>ket</i> . |
| $\langle\psi $ | Vector dual to $ \psi\rangle$. Also known as a <i>bra</i> . |
| $\langle\varphi \psi\rangle$ | Inner product between the vectors $ \varphi\rangle$ and $ \psi\rangle$. |
| $ \varphi\rangle \otimes \psi\rangle$ | Tensor product of $ \varphi\rangle$ and $ \psi\rangle$. |
| $ \varphi\rangle \psi\rangle$ | Abbreviated notation for tensor product of $ \varphi\rangle$ and $ \psi\rangle$. |
| A^* | Complex conjugate of the A matrix. |
| A^T | Transpose of the A matrix. |
| A^\dagger | Hermitian conjugate or adjoint of the A matrix, $A^\dagger = (A^T)^*$. $\begin{bmatrix} a & b \\ c & d \end{bmatrix}^\dagger = \begin{bmatrix} a^* & c^* \\ b^* & d^* \end{bmatrix}$. |
| $\langle\varphi A \psi\rangle$ | Inner product between $ \varphi\rangle$ and $A \psi\rangle$. Equivalently, inner product between $A^\dagger \varphi\rangle$ and $ \psi\rangle$. |

Figure 138: linear algebra key rules. Source: [Quantum Computation and Quantum Information](#) by Nielsen and Chuang, 2010 (10th edition, 704 pages).

Indeed, $(|\psi\rangle\langle\psi|)|\phi\rangle = |\psi\rangle(\langle\psi||\phi\rangle) = (\langle\psi|\phi\rangle)|\psi\rangle$, given $\langle\psi|\phi\rangle$ is a real number being the inner product of both vectors. Some of these elements are summarized in Figure 138.

- **Unitary matrices** are square matrices whose inverse equals their transconjugate ($A^\dagger = A$). A unitary matrix has several properties, one of which is to have orthogonal eigenvectors and to be diagonalizable. Unitary matrices define the reversible gates applied to qubits or sets of qubits.

$$A = \begin{bmatrix} 2 & i & -2i \\ -i & 1 & 3 \\ 2i & 3 & -1 \end{bmatrix}^\dagger \quad \bar{A} = \begin{bmatrix} 2 & -i & 2i \\ i & 1 & 3 \\ -2i & 3 & -1 \end{bmatrix} \quad A^\dagger = \overline{(A)}^* = \begin{bmatrix} 2 & i & -2i \\ -i & 1 & 3 \\ 2i & 3 & -1 \end{bmatrix} \quad \begin{array}{l} U|x\rangle = |y\rangle \\ |x\rangle = U^\dagger|y\rangle \end{array}$$

transposed matrix
hermitian matrix
transconjugate = identity
unitary reversibility

Figure 139: unitary matrices. (cc) Olivier Ezratty, 2021.

A unitary operation is the application of a unitary matrix to a computational state vector that we'll later see. Quantum computing reversibility comes from this unitary property. A unitary matrix U can also be expressed as $U = e^{iH}$, with H being a Hermitian matrix, but finding H given U is a complicated calculation problem.

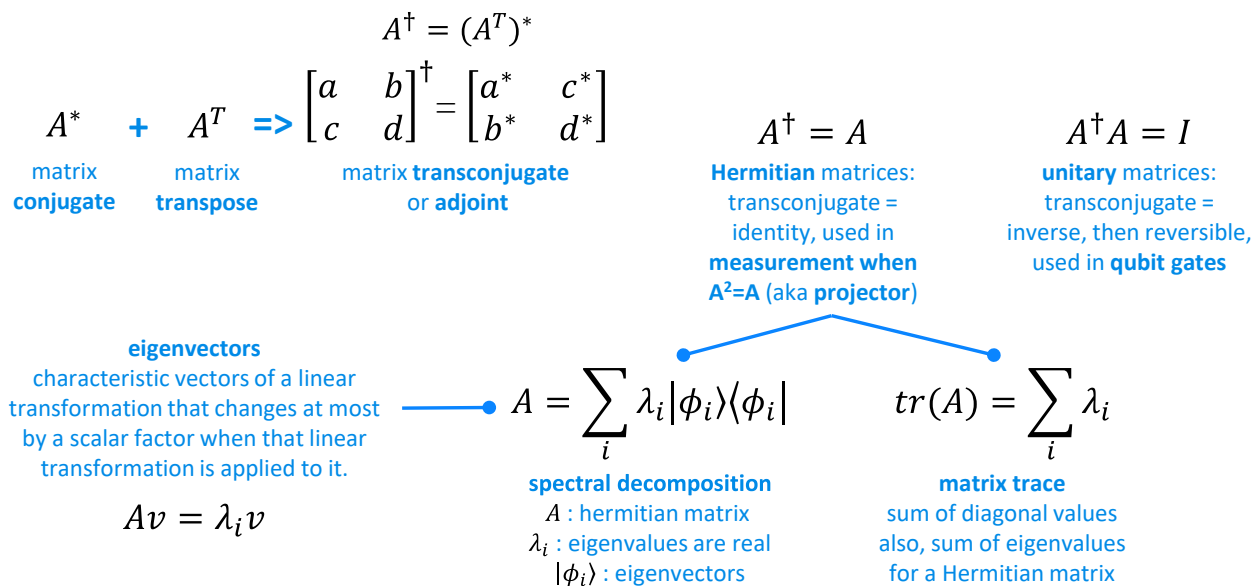


Figure 140: difference between unitary matrices and Hermitian matrices. (cc) Olivier Ezratty, 2021.

Pure and mixed states

Let's now explain what the three main states of quantum objects are, basis, pure and mixed. We'll apply it to the case of qubits, given these notions are valid with any quantum system. We are dealing with mathematical models that describe quantum objects states²⁸⁹.

| | basis states | pure states | mixed states |
|---|---|---|--|
| definitions | aka computational basis states, are N dimensions vectors combining 0s and 1s, with 2^N different such vectors for a N qubits register. | vectors in a Hilbert space of norm 1, specified by a single ket describing coherent superpositions of basis states with complex numbers. | or statistical mixture of pure states, are classical statistical ensemble of combination p_i of pure states Ψ_i . Ψ_i can be any combination of pure states but is usually a set of computational basis states. |
| randomness origin | no randomness with perfect qubits | quantum | quantum and classical |
| with a single qubit | $ 0\rangle$ and $ 1\rangle$ | $ \Psi\rangle = \alpha 0\rangle + \beta 1\rangle$ $ \alpha ^2 + \beta ^2 = 1$ | $p_1 \psi_1\rangle, p_2 \psi_2\rangle$ we don't add them, it's just a statistical ensemble, statistical mixture or convex sum of several systems. |
| with a N qubits register $i = 1$ to 2^N | $ i\rangle$ 01101011> for N=8 all $ i\rangle$ form the computational basis states of the N qubits register, contains N combinations of 0 and 1, all basis states are mathematically orthogonal. | $ \Psi\rangle = \sum_i \alpha_i i\rangle$ $\sum_i \alpha_i^2 = 1$ $\alpha_i = \text{complex number}$ a pure state is a linear superposition of computational basis states. | $\{(p_i \Psi_i\rangle)\}$ <small>ensemble notation</small> $\sum_i p_i = 1$ $p_i = \text{positive real number probability to find } \Psi_i \text{ in the mixed state given all } p_i \text{ are } 0 \text{ or } 1 \text{ in a pure state.}$ |

Figure 141: differences between basis states, pure states and mixed states. (cc) Olivier Ezratty, 2021.

Basis states correspond to given combinations of 0 and 1 values in a qubit register. For a single qubit, these are the states $|0\rangle$ and $|1\rangle$. For a register of N qubits, it is one of the 2^N different basis states combinations of 0s and 1s, or a tensor product of N single qubit basis states. It constitutes the computational basis in a complex numbers Hilbert space of dimension 2^N .

²⁸⁹ See [The Many Inconsistencies of the Purity-Mixture Distinction in Standard Quantum Mechanics](#) by Christian de Ronde and César Massri, August 2022 (19 pages) that provides an interesting historical perspective on the pure and mixed states nuances and shortcomings.

The vectors of this basis are all mathematically orthogonal. A basis state is also named a computational basis state. When measuring individual qubits in these states, you get a deterministic result, at least with theoretically perfect qubits.

Pure states describe the state of an isolated quantum system of one or several objects as a linear superposition of the states from its computational basis. It's a vector in a Hilbert space. That's when superposition and entanglement come in. With massive particles, basis and pure states are solutions to Schrödinger's equation. It's applicable to one or several quantum objects or qubits. During computation, a qubit register is theoretically in a pure state, but quantum decoherence will gradually turn it into a mixed state. A pure state is also presented as a quantum state where we have exact information about the quantum system. This information corresponds to the famous ψ vector in the Hilbert space. When preparing a quantum state, we indeed know the parameters of the vector ψ even though actual property measurements will generate random results if the quantum state is not measured along with one of its eigenstates. The information we have about measurement potential results is their probabilistic distribution.

Mixed states are weird beasts. Literally, these are “*statistical ensembles of classical probabilistic combinations of pure states*”, these being usually computational basis states, but they can also be expressed as real number linear combinations of any pure states. Basis states and pure states describe the information available for a single quantum object or qubit, or a group of such objects. A mixed state describes a large number of such systems, prepared in a similar manner, and the states they could be in when repeating an experiment followed by some measurement.

However, a pure state measurement generating random results most of the time, we still also experimentally prepare and measure it on a repeated basis to have an idea of its state probability distribution. In the end, both pure states and mixed states describe the information we can extract from a system after doing repeated experiments and measurements. Their difference lies with the origin of measurement randomness. Its origin is entirely quantum for pure states and both quantum and classical (or “non-quantum”) for mixed states. Got it? If not, we have a couple practical examples below to figure out what it looks like in the real world!

Typically, mixed states provide the available information describing two sorts of systems:

Random quantum objects like photons coming from an unpolarized photons source, or, when photons with different polarities are merged like in the below illustration on the right. The photon polarization at this point is a statistical mixture of horizontal and vertical polarization photons. Let's say this is the case where quantum objects that are prepared differently and are then mixed together. The two sources are not “coherently” prepared. In the example in the left, a 45° polarizing beam splitter applied to horizontalized prepared photons produces superposed H and V photons in a pure state. On the right, the polarizing beam splitter creates 50% vertically and 50% horizontally polarized photons that can be merged by a 45° non-polarizing beam splitter. They are statistically merged, but not superposed, thus creating a mixed state.

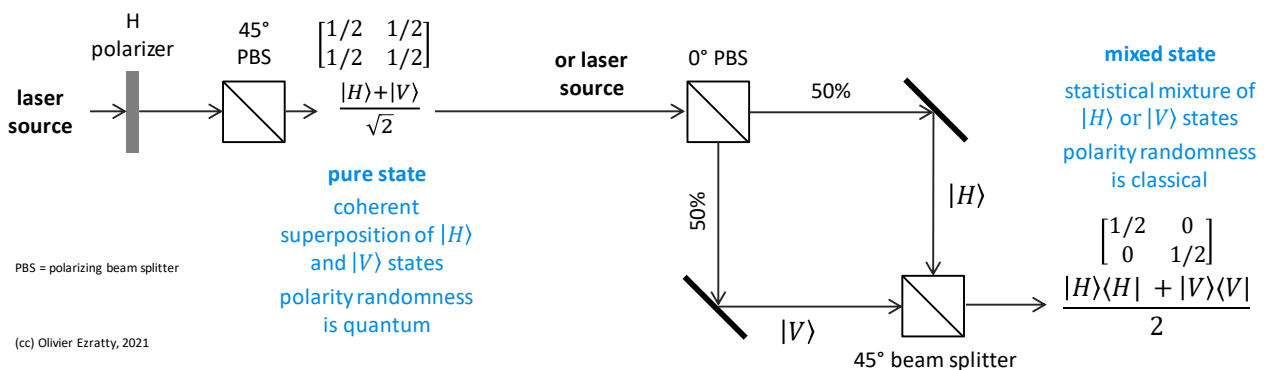


Figure 142: how to generate mixed states with photons. (cc) Olivier Ezratty, 2021.

In this other example, two lasers are preparing coherent light that is polarized respectively horizontally and vertically and then merged by a beam combiner. The resulting photons represent a totally mixed state with uncorrelated and incoherent photons. Their statistical distribution is entirely classical with a density matrix void of any off-diagonal values.

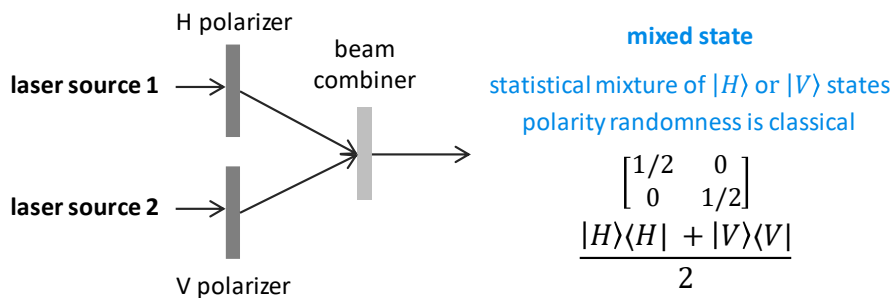


Figure 143: another method to generate a mixed state with photons. (cc) Olivier Ezratty, 2021.

Subsystems of an inseparable entangled system of several quantum objects. It helps understand what we are measuring at the end of computing when the resulting qubits are still entangled. One particular case is a set of qubits affected by decoherence coming from interactions with the environment. It helps understand the effect of decoherence on the state of a qubits register during computing and how error correction codes are mitigating it. Decoherence comes from the entanglement between a system and its environment, thus, the observed system is not yet isolated and becomes a subsystem of a larger entangled system. Thus, it becomes a mixed state. Want to grasp it clearly? You need to toy with density matrices representations of these pure and mixed states.

Note that these concepts are applicable to both a single qubit and a register of N qubits.

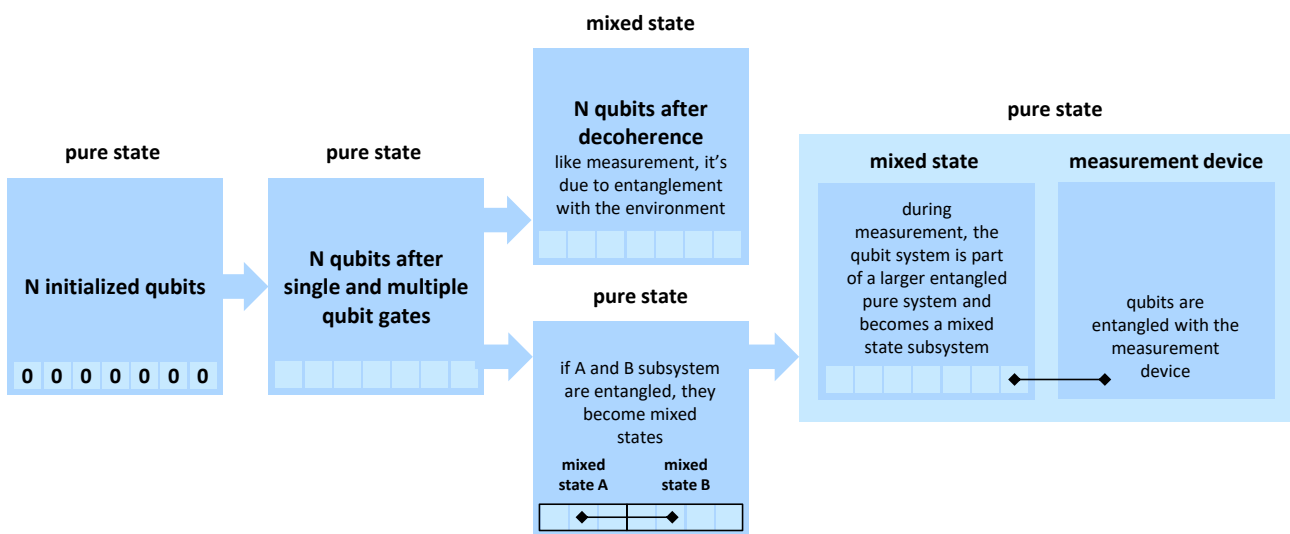


Figure 144: mixed states and pure states when using qubits. (cc) Olivier Ezratty, 2021.

Density matrices

Density matrices, also named density operators, were introduced in 1927 by **John von Neumann** and **Lev Landau** and later expanded by **Felix Bloch**. Von Neumann created this formalism to develop his theory of quantum measurements.

A density matrix is a mathematical tool used to describe quantum systems in pure or mixed states. Compared to the state vector that we saw earlier, a density matrix is the only way to mathematically describe a mixed state. It consolidates all the physically significant information that could be retrieved from a set of quantum objects given what we know about them. Quantum and classical probabilities are boiled in the density matrix.

Usually represented by the sign ρ (rho), a density matrix is a square matrix of complex numbers used to describe a quantum system, like a register of several qubits. Its size is $2^N \times 2^N$ where N is the number of qubits in the register.

The density matrix of a quantum register in **pure state** is the outer product of its computational basis state vector $|\Psi\rangle\langle\Psi|$ as described below, with an example using a Bell pair of two qubits. There is no more information in the density matrix than in the basis state vector at this stage.

A density matrix for a **mixed state** adds several pure states matrices with real probability coefficients p_i . The $|\Psi_i\rangle$ pure states that are combined to form a mixed state can be themselves states from the computational basis (combination of 0s and 1s) but not necessarily. They can be any vector in the 2^N Hilbert space and made of (normalized) linear superpositions of these basis states. Mathematically speaking, a pure state density matrix is a special case of mixed state density matrix where only one p_i is not zero.

We'll repeat here what was said with pure and mixed states: a mixed state density matrix consolidates both **quantum uncertainties** (that persists even when the system state is well known) and **classical uncertainties** (due to a lack of knowledge of individual quantum sources and preparation conditions) when a pure state density matrix contains only information pertaining to **quantum uncertainties**.

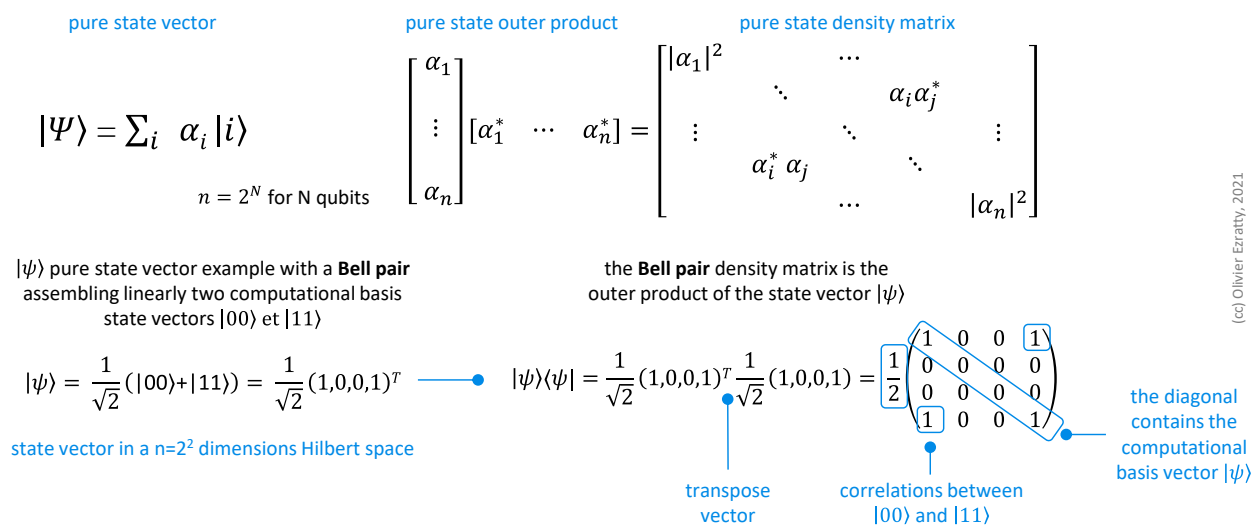


Figure 145: how a pure state matrix is constructed. (c) Olivier Ezratty, 2021.

A density matrix has several mathematical properties as described *below* and detailed afterwards with some differences between pure and mixed states density matrices.

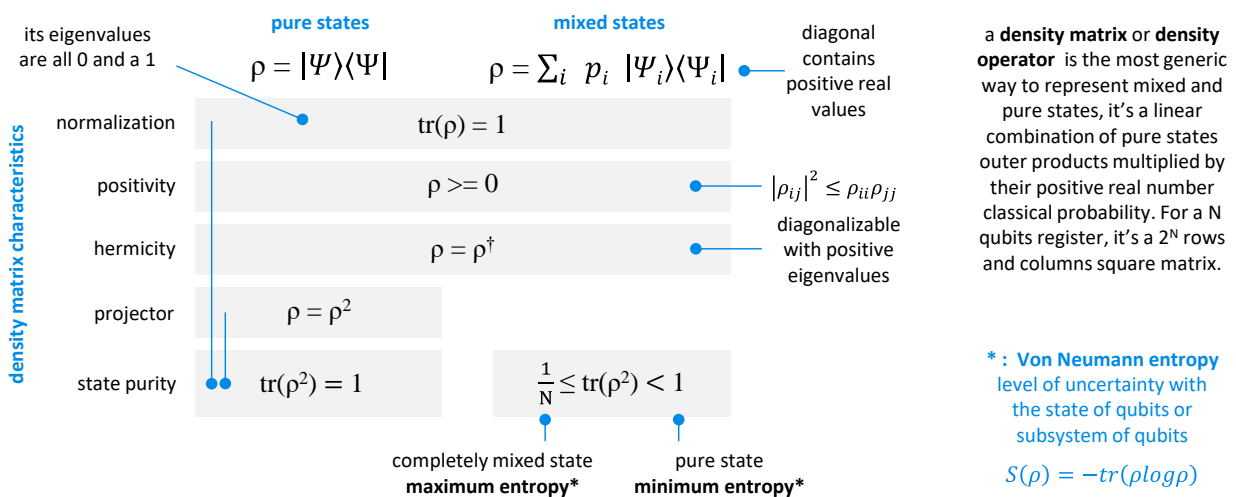


Figure 146: the various mathematical properties of pure and mixed states density matrices.

Hermicity. A density matrix is Hermitian, meaning that it's equal to its transconjugate matrix. As a consequence, the density matrix can be diagonalized in a different basis, with positive real number eigenvalues. Hermicity comes from the density matrix construction: it's real number linear sum of Hermitian matrices resulting from the Hermitian inner product of pure states vectors. One consequence is that it removes any global phase from the quantum system it describes. You can easily understand it by evaluating on your own a density matrix of a given qubit and its global phase.

Positivity. A density matrix M is positive semi-definite, meaning that $\langle x|M|x\rangle \geq 0$ for all x vectors. It's also defined as a symmetric matrix with non-negative eigenvalues (meaning... positive or zero). These eigenvalues being the values in the diagonal after matrix diagonalization. But even before diagonalization, all density matrices diagonal values are positive due to hermicity and the way they are constructed as positive probabilities combinations of outer products of pure states whose diagonal are always containing positive values.

Normalization. A density matrix trace equals 1 for both pure and mixed states. A density operator is said to be “normalized to unit trace”. That's the sum of its diagonal values which are all positive real numbers. It comes from two rules: Born's rule applied to a pure state ($\sum_i \alpha_i^2 = 1$) and classical probabilities rules applied to the mixed state ($\sum_i p_i = 1$). As a result, a density matrix diagonal value at position $j = \sum_i p_i \alpha_{ij}^2$, α_{ij} being the weight α_j from the pure state i composing the mixed state. The diagonal is also referred to as a statistical mixture or as a population.

There are some differences between pure and mixed states density matrices.

Projector. A pure state density matrix is a projector, i.e. equal to its square and the trace of its square density matrix ρ^2 is equal to 1. Being a projector means that its eigenvalues are all zeros except a single one that is 1. The eigenvector associated with the eigenvalue one is the state vector of the system. Being a projector means the density matrix can be used as the way to measure a quantum state using this vector as a basis reference. In a single qubit system and the Bloch sphere, it would be any vector in the sphere and the related measurement observable, a geometrical projection of the evaluated qubit on this vector. In the case of a mixed state, the density matrix trace is inferior to 1 and its minimum is $1/N$, when the state is maximally mixed with equal probabilities for all basis values. The average value obtained with applying an observable A to a pure state quantum system state vector ψ is evaluated with the formula $\langle \psi|A|\psi\rangle$, also named an expectation value. In other words, it's the dot vector product of ψ and the vector obtained by applying matrix A to vector ψ . The expectation value of a mixed state represented by a density matrix ρ is $tr(\rho A)$, a trace of the density matrix multiplied by the observable A matrix.

Off-diagonal elements can have a time-dependent phase that will describe the evolution of coherent superpositions. These elements are also named “coherences”. As decoherence starts due to interactions with the environment, any pure state will progressively turn into a mixed state and the off-diagonal values will be affected. This evolution follows the Liouville–von Neumann equation.

$$\frac{|0\rangle\langle 0| + |1\rangle\langle 1|}{2} = \frac{|+\rangle\langle +| + |-\rangle\langle -|}{2} = \begin{bmatrix} 1/2 & 0 \\ 0 & 1/2 \end{bmatrix} = \frac{1}{2}\mathbb{I}$$

Mixedness defines how much “mixed” is a quantum state defined by its density matrix. It's computed with $tr(\rho^2)$ and is equal to 1 for a pure state and $1/N$ for a mixed state with N quantum objects. As a result, any time-dependent unitary transformation U applied to this quantum state won't affect the mixedness. Indeed, the density matrix over time is $\rho(t) = U(t, t_0)\rho(t_0)U^\dagger(t, t_0)$. Its mixeness is $tr(\rho^2(t)) = tr(U(t, t_0)\rho(t_0)U^\dagger(t, t_0)U(t, t_0)\rho(t_0)U^\dagger(t, t_0))$ which equals $tr(\rho^2(t_0))$.

Combinations. A mixed state can be the result of an infinite number of combinations of pure states, the most common example being, for two qubits, the half-identity mixed state being an equally mixed state of both $|0\rangle$ and $|1\rangle$ or $|+\rangle$ and $|-\rangle$. Given a density matrix, you can't compute the pure states that were combined to create it. Said otherwise, quantum states with the same density matrix can't be distinguished operationally (i.e. by a set of measurements). Also, when a unitary operation U (defined later, sorry) is applied to a mixed state defined by its density matrix ρ , the resulting state density matrix is $U\rho U^\dagger$.

For the fun of a better understanding, I've added below in Figure 147 a graphical segmentation of all the various matrix types we've been mentioning in the previous pages and how they are related with each other.

We forgot to define a **non-defective matrix**, which is a diagonalizable matrix. And a normal matrix A verifies $AA^\dagger = A^\dagger A$. A **trivial** matrix is both Hermitian and unitary and have orthonormal eigenvectors with eigenvalues being +1 or -1.

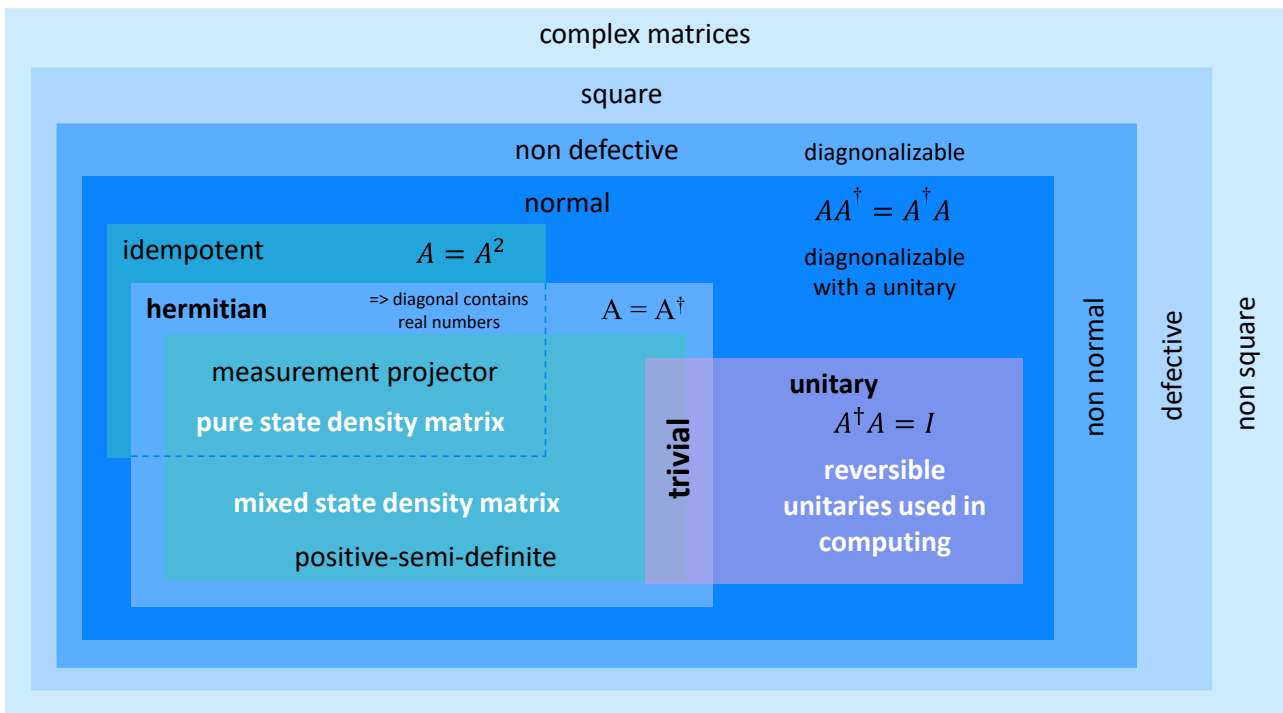


Figure 147: a Russian dolls map of matrices. (cc) Olivier Ezratty, 2021.

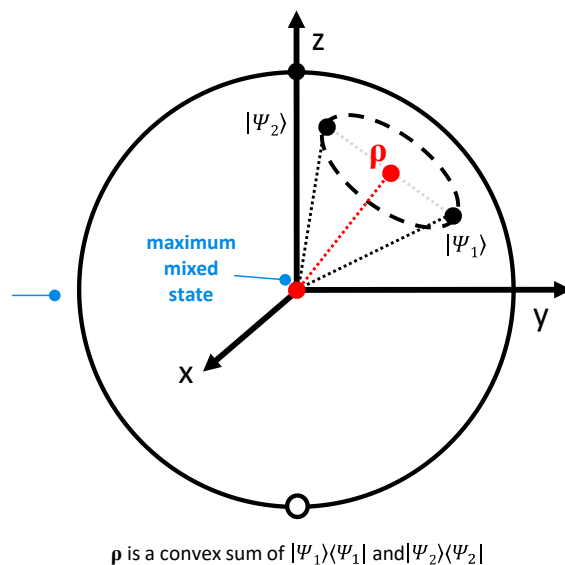
Single qubit mixed states can be represented by a point inside the Bloch sphere as shown below in a “Death Star” representation, with a statistical mixture of two pure qubit states. The mixed state is a convex sum of pure states inner products, ‘convex’ meaning it’s a sum using positive real coefficients that sum up to 1. The geometric representation is a good way to figure out why a given mixed state can result from an infinite number of combinations of two pure states. We can combine more than two pure states to create a mixed state. By the way, the Bloch sphere becomes a Bloch ball.

Density matrix dimensionality. Although it contains 2^{2N} complex values, due to normalization, the dimensionality of a density matrix is $2^{2N}-1$ real numbers. The explanation is reconstructed below. For a starter, we have 2^{2N} complex values which is the square or 2^N , the number of lines and columns in the density matrix. We separate the matrix diagonal from the off-diagonal values. The diagonal values are real numbers because they are the positive probability sums of the diagonal values of pure states density matrices, themselves being positive as $|\alpha_i|^2$.

a single qubit mixed state can be **represented** by points inside the Bloch sphere with 3 degrees of freedom: its two usual angles and the vector length.

a **maximum mixed state** is at the center of the Bloch sphere with equiprobability of $|0\rangle$ and $|1\rangle$.

a mixed state can result from an infinite number of **combinations** of various pure states as shown in the sphere. the **state purity** is measured by its proximity to the Bloch sphere surface.



ρ is a convex sum of $|\psi_1\rangle\langle\psi_1|$ and $|\psi_2\rangle\langle\psi_2|$

ket

$$\frac{|0\rangle+|1\rangle}{\sqrt{2}} \Rightarrow \begin{bmatrix} 1/2 & 1/2 \\ 1/2 & 1/2 \end{bmatrix}$$

pure state superposition of $|0\rangle$ and $|1\rangle$
pure state superposition of $|0\rangle$ and $|1\rangle$

$$\frac{|0\rangle\langle 0| + |1\rangle\langle 1|}{2} = \begin{bmatrix} 1/2 & 0 \\ 0 & 1/2 \end{bmatrix}$$

(maximum) mixed state of $|0\rangle$ and $|1\rangle$



Figure 148: representation of a single qubit mixed state in the Bloch sphere. (cc) Olivier Ezratty, 2021.

The matrix trace equals 1, removing another useful dimension. The off-diagonal values are redundant since the matrix is equal to its transadjoint. So, we divide by two their dimensionality. Since these are complex numbers, we multiply it by two to get a number of real numbers. When summing this up, we find $2^{2N} - 1$ different real numbers. This dimensionality is usually presented as 2^{2N-1} complex numbers or 2^{2N} real numbers, avoiding the minus 1 which is quickly negligible as N grows.

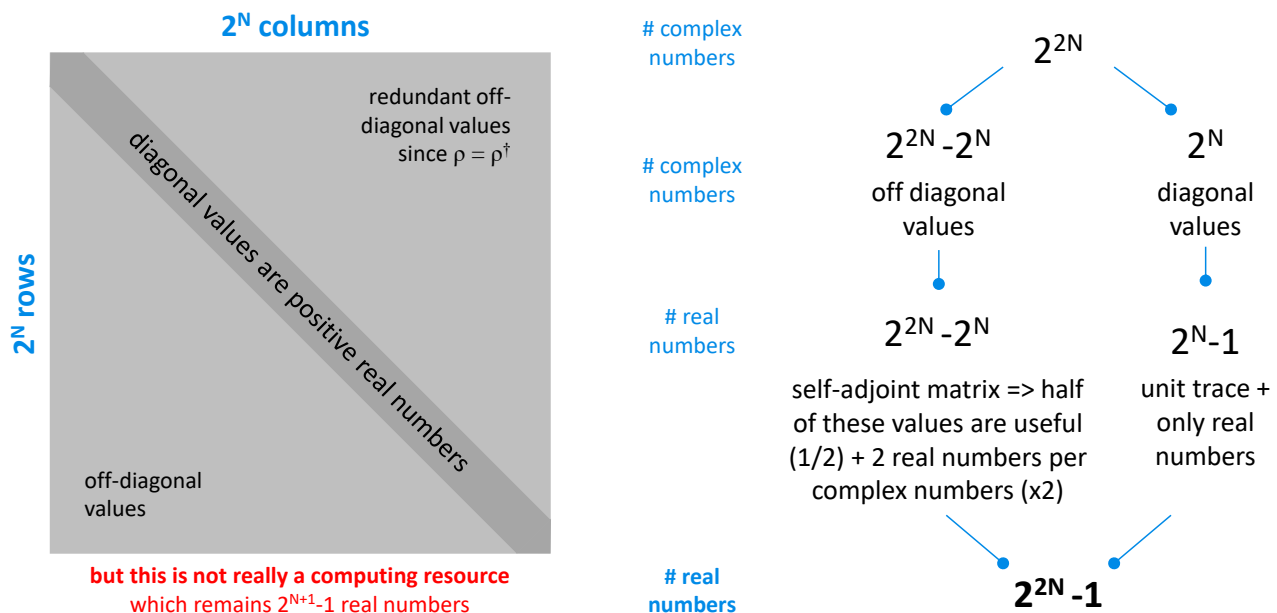


Figure 149: computing the dimensionality of a density matrix. (cc) Olivier Ezratty, 2021.

However, this dimensionality does not correspond to some useful computing resource in standard gate-based programming models although some work has been done to exploit it, but with no additional computing acceleration²⁹⁰.

²⁹⁰ See [Quantum Circuits with Mixed States](#) by Dorit Aharonov, Alexis Kitaev and Noam Nissam, 1998 (20 pages). It describes a model using not only unitary matrix operator-based quantum gates. It enables the usage of subroutines in programming. But this programming model doesn't seem adopted so far except for quantum error correction codes which implement measurement during computing. Mixed states based programming is implemented in the qGCL extension of the language pGCL as described in [Quantum programming with mixed states](#) by Paolo Zuliani, 2005 (14 pages).

A theoretical perfect gate-based quantum computer is using qubits registers that are in a pure state until measurement, representing thus a dimensionality of $2^{N+1}-1$ real numbers, the -1 standing for the normalization constraint of the computational basis vector²⁹¹. So why do we care about these density matrices for mixed states? These are mostly used to understand the effects of decoherence and measurement and with qubits registers tomography which helps determine their fidelities.

The sequence of quantum gates in a quantum circuit can also be represented by a large unitary matrix of dimension $2^N * 2^N = 2^{2N}$ complex numbers. So, with a dimensionality close to a density matrix. But this is not an actual computing resource. It deals more with the extensive computing resources required to emulate in-memory an entire unitary algorithm in a classical computer instead of just executing gates one by one on the computational state vector.

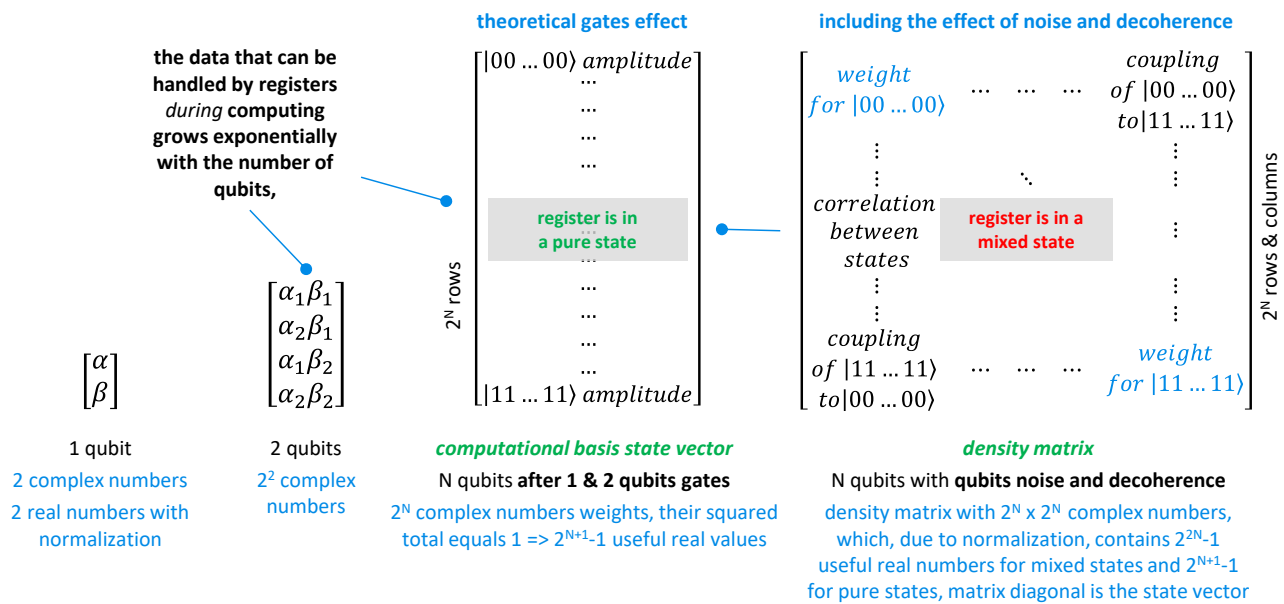


Figure 150: dimensionality of a qubit register. (cc) Olivier Ezratty, 2022.

There are many other subtleties with density matrices that we can't detail in the book. For example:

Diagonalization is possible for any mixed state density matrix. It will decompose the state into classical probabilistic combination of pure states eigenvectors forming an orthonormal basis.

Reduced density matrices are the density matrices of subsystems of composite systems. The reduced density matrix for an entangled pure state is a mixed state or mixed ensemble.

Mixed state purification consists, inversely, in integrating a mixed state in a larger system to create or reconstruct a pure state. It is used in some error-correcting codes.

Bipartite pure states are tensor products of two systems that are not entangled. A pure state system is entangled if and only if some of its reduced states are mixed rather than pure. If all were pure, it would mean that the pure state density matrix ρ would be separable into several pure states, one for each qubit in the case of a qubits register.

Schmidt decompositions are used to decompose bipartite systems and evaluate their level of entanglement. This level of entanglement can be determined with the Schmidt coefficients coming from the Schmidt decomposition.

²⁹¹ Thus, wrong is the statement that "A calculation using n number of qubits on a quantum computer would need 2ⁿ classical bits on a standard computer" as seen in [Simulating subatomic physics on a quantum computer](#) by Sarah Charley, October 2020. Why? Because one of the 2^N quantum amplitudes in a N qubit register cannot be stored or emulated on a single bit!

Matrix rank. A matrix rank is the number of non-zero values in its diagonalized version. The rank of a density matrix gives an indication of the purity of the state it represents. A pure state density matrix has a rank 1, since it can be diagonalized into a matrix where only one value in the diagonal is non-zero. A maximally mixed state has a rank of 2^N , i.e. the number of lines and columns in the density matrix representing N qubits.

Schmidt rank is an indication of the level of entanglement in a density matrix. Not to be confused with the matrix rank which deals with its purity level.

Quantum Channels are transformations of a quantum state resulting from any kind of interaction with a quantum environment. They are modeled with an operator, called a superoperator, transforming a density matrix into another density matrix. Technically speaking, a superoperator is a completely positive (we've defined that already) and trace-preserving operator (self-explainable), or CPTP. Its form is a linear map from one Hilbert space to another Hilbert space. Its dimension is a square matrix with 2^{2N} columns and as many rows, so with 2^{4N} (or 16^N) complex numbers, before normalization, N being the number of qubits. It is useful to modelize quantum subsystems (which are in mixed state), decoherence, quantum error correction and qubits noise²⁹². It is even possible to build a tomography with a superoperator, aka a quantum process tomography (QPT). One for example can build a QPT of a quantum gate to detect its imperfections. A QPT can also be done for a more complex operation, or unitary applied to a set of qubits, like a Quantum Fourier Transform²⁹³.

Grad, curls and divs

In the equations of Maxwell, Schrödinger, Dirac and others that we have seen are used notations good to remember here around the symbol nabla: ∇ , sometimes used with an arrow $\vec{\nabla}$.

Nabla generally designates the gradient of a scalar or vector function, i.e. its first derivative. A scalar function applies to a vector, often of three dimensions x, y and z of a Euclidean space. It returns a number. A vector function returns a vector! This leads to the notions of **gradient** and **Laplacian** which apply to a scalar function and correspond to first and second derivatives in space, and to divergence and rotational (or curl) which apply to a vector function. A Laplacian can also be applied to a vector function. We won't go far in this book with respect to these functions.

| | | | |
|---|---|---|--|
| $\nabla = \left(\frac{\partial}{\partial x}, \frac{\partial}{\partial y}, \frac{\partial}{\partial z} \right)$ | $\nabla f = \left(\frac{\partial f}{\partial x}, \frac{\partial f}{\partial y}, \frac{\partial f}{\partial z} \right)$ | $\nabla \cdot \vec{G} = \left(\frac{\partial G_x}{\partial x}, \frac{\partial G_y}{\partial y}, \frac{\partial G_z}{\partial z} \right)$ | $\nabla \times \vec{G} = \left(\frac{\partial G_z}{\partial y} - \frac{\partial G_y}{\partial z}, \frac{\partial G_x}{\partial z} - \frac{\partial G_z}{\partial x}, \frac{\partial G_y}{\partial x} - \frac{\partial G_x}{\partial y} \right)$ |
| <p>del or nabla operator, first space derivative of a vector</p> | <p>scalar function gradient, scalar field vector of space variations</p> | <p>vector function divergence, showing its local evolution</p> | <p>rotational or curl of a vector function G transforming a vector field in a vector field describing the field variation in space</p> |
| $\nabla^2 f = \nabla \cdot \nabla f = \left(\frac{\partial^2 f}{\partial x^2}, \frac{\partial^2 f}{\partial y^2}, \frac{\partial^2 f}{\partial z^2} \right)$ | | $\nabla^2 \vec{G} = \left(\frac{\partial^2 G_x}{\partial x^2} + \frac{\partial^2 G_x}{\partial y^2} + \frac{\partial^2 G_x}{\partial z^2}, \frac{\partial^2 G_y}{\partial x^2} + \frac{\partial^2 G_y}{\partial y^2} + \frac{\partial^2 G_y}{\partial z^2}, \frac{\partial^2 G_z}{\partial x^2} + \frac{\partial^2 G_z}{\partial y^2} + \frac{\partial^2 G_z}{\partial z^2} \right)$ | |
| <p>scalar function Laplacian</p> | | <p>vector function Laplacian</p> | |

Figure 151: del, nabla, gradient, divergence, rotational, curl, Laplacian. You won't need them in the rest of this book, sort of. This is just informative.

²⁹² See [Quantum Channels](#) by Stéphane Attal (65 pages).

²⁹³ See [Quantum Process Tomography of the Quantum Fourier Transform](#) by Yaakov S. Weinstein, Seth Lloyd et al, 2004 (45 pages).

Permanent and determinant

This inventory would not be complete without describing an even stranger mathematical object: the **permanent** of a square **matrix** $n \times n$, invented by Louis Cauchy in 1812. The formula in Figure 152 describes its content.

$$\text{per}(A) = \sum_{\sigma \in \mathfrak{S}_n} \prod_{i=1}^n a_{i,\sigma(i)}$$

Figure 152: a permanent.

The \prod denotes a multiplication of values from the index matrix i and $\sigma(i)$. σ is a permutation function of integers between 1 and n , the dimension of the matrix (number of columns and rows). The sigma relates to the set of σ functions of the permutation group \mathfrak{S}_n (also called symmetrical group) which has a size of $n!$ (factorial of n). The values $a_{i,\sigma(i)}$ are the cells of the coordinate matrix i and $\sigma(i)$.

Here is what it gives with $n=2$ and $n=3$ knowing that beyond that, it becomes less readable:

$$\text{perm} \begin{pmatrix} a & b \\ c & d \end{pmatrix} = ad + bc \quad \text{perm} \begin{pmatrix} a & b & c \\ d & e & f \\ g & h & i \end{pmatrix} = aei + bfg + cdh + ceg + bdi + afh$$

Figure 153: computing the permanent of 2x2 and 3x3 matrices.

The permanent is therefore a real number resulting from $n!$ (factorial of n) additions of multiplications of n values of the matrix. The permanents are notably used to evaluate matrices that represent graphs.

They are also used in the classical numerical simulation of boson sampling that we will describe in the section dedicated to [photon qubits](#), page 445²⁹⁴. Contrary to the calculation of the determinant, in Figure 154, which can be simplified, that of the permanent remains a classical intractable problem.

The **determinant of a matrix** is a variant of its permanent. $\text{sgn}(\sigma)$ is the sign of permutations, which is +1 if the number of permutations needed to create the permutation is even and -1 if it is odd. Olé!

$$\det(A) = \sum_{\sigma \in \mathfrak{S}_n} \left(\text{sgn}(\sigma) \prod_{i=1}^n a_{i,\sigma(i)} \right)$$

Figure 154: a determinant.

And this is what it gives for $n=3$. Note that the group of permutations includes the permutation that does not change the order of the elements.

$$\det \begin{pmatrix} a & b & c \\ d & e & f \\ g & h & i \end{pmatrix} = aei + bfg + cdh - ceg - bdi - afh$$

Figure 155: computing the determinant of a 3x3 matrix.

Determinants have particular properties such as $\det(AB)=\det(A).\det(B)=\det(B).\det(A)=\det(BA)$ which can facilitate the calculation of the determinant of a matrix if it can be factorized into several matrices. Also, the determinant of a matrix is the product of its eigenvalues.

So much for the definition of the basics of the linear algebra of quantum computing. I've skipped a lot of other definitions and rules of computation. It was a question of clarifying certain notions that are frequently used in the scientific literature on quantum computing and in many of the reference works cited in this book. What we have just seen may be useful for you to compare some of the scientific literature on quantum computing.

If you like maths, linear algebra and complexity, you can have some fun exploring type III factors algebra that describes the observables in relativistic quantum fields theory²⁹⁵! Classical quantum physics and computing is based on a simplistic type I factors algebra. Simpler, but still complicated.

²⁹⁴ The calculation time of a permanent increases faster than an exponential of a fixed value (Mn) as soon as n becomes very large compared to M . So, for example, with $M=2$, $2n$ is much smaller than $n!$ as soon as n is greater than 4. As the numerical simulation of the boson requires a determinant that depends on the size of the simulation, it is even more cumbersome to compute than an exponential problem.

²⁹⁵ See [The Role of Type III Factors in Quantum Field Theory](#) by Jakob Yngvason, 2004 (15 pages).

Fourier transforms

Since quantum physics deals a lot with wave-particle duality and particularly with waves, waves signals decomposition is a key mathematical tool. That's the role of a Fourier transform that we mentioned already when dealing with Heisenberg's indeterminacy principle. It's about maths but not linear algebra.

The Fourier Transform implements a mathematical decomposition of a function $f(x)$ into a function $\hat{f}(\xi)$ returning a complex number containing an amplitude and phase for single frequencies ξ . It's a more generic version of Fourier series which work with periodic signals. Fourier transform are Fourier series where the signal period can approach infinite.

It can be used for example to decompose a wave packet pulse signal that is concentrated in time. A Fourier transform usually operates in the time domain with x being a time in second and ξ a frequency in Hertz.

$$\hat{f}(\xi) = \int_{-\infty}^{\infty} f(x)e^{-2\pi i x \xi} dx$$

Figure 156: a Fourier transform in the time domain.

It can be decomposed using Euler's formula in its real and complex parts separating the amplitude and phase of the Fourier transformed signal:

$$\hat{f}(\xi) = \int_{-\infty}^{\infty} f(x) \cos(2\pi i x \xi) dx - i \int_{-\infty}^{\infty} f(x) \sin(2\pi i x \xi) dx$$

Figure 157: Fourier transform decomposed in real and complex part.

The inverse Fourier transforms that frequency decomposition function $\hat{f}(\xi)$ back into its original compound time domain signal $f(x)$.

$$f(x) = \int_{-\infty}^{\infty} \hat{f}(\xi)e^{2\pi i x \xi} d\xi$$

Figure 158: inverse Fourier transform.

All of this is easier to understand with examples like in the schema below decomposing a time domain signal into five frequencies constituents with their respective magnitude and (equal) phases.

Computing Fourier series and transforms is done in many ways:

Discrete-time Fourier Transform (DTFT) is a form of Fourier analysis that is applicable to a sequence of values. It is often used to analyze samples of a continuous function. The term discrete-time refers to the fact that the transform operates on discrete data, often samples whose interval has some units of time.

Discrete Fourier Transform (DFT) converts a finite sequence of equally-spaced samples of the function into a same-length sequence of equally-spaced samples of the Discrete-Time Fourier transform (DTFT). The samples are complex numbers coming from a DTFT.

Fast Fourier Transform (FFT) computes the discrete Fourier transform (DFT) of a sequence, or its inverse (IDFT). It's an efficient variation of the DFT.

Quantum Fourier Transform (QFT) is a linear transformation applied on qubits. It is the quantum analogue of the DFT and reverse DFT. A QFT is a Discrete Fourier Transform applied to the data stored in the 2^n computational basis states of a n qubits register. The Quantum Fourier Transform, implements a DFT on the complex amplitudes of a quantum state. We cover it [later](#) page 595.

Fourier series were created by **Joseph Fourier** (1768-1830, French) as part of his work in the book "The Analytical Theory of Heat" published in 1822. Beforehand, he accompanied Napoleon Bonaparte in his 1798-1801 Egyptian expedition as a scientific advisor. He then became a Prefect for the Isère department, based in Grenoble. Afterwards, he also drove the young Jean-François Champollion to get interested in deciphering the Rosetta Stone.

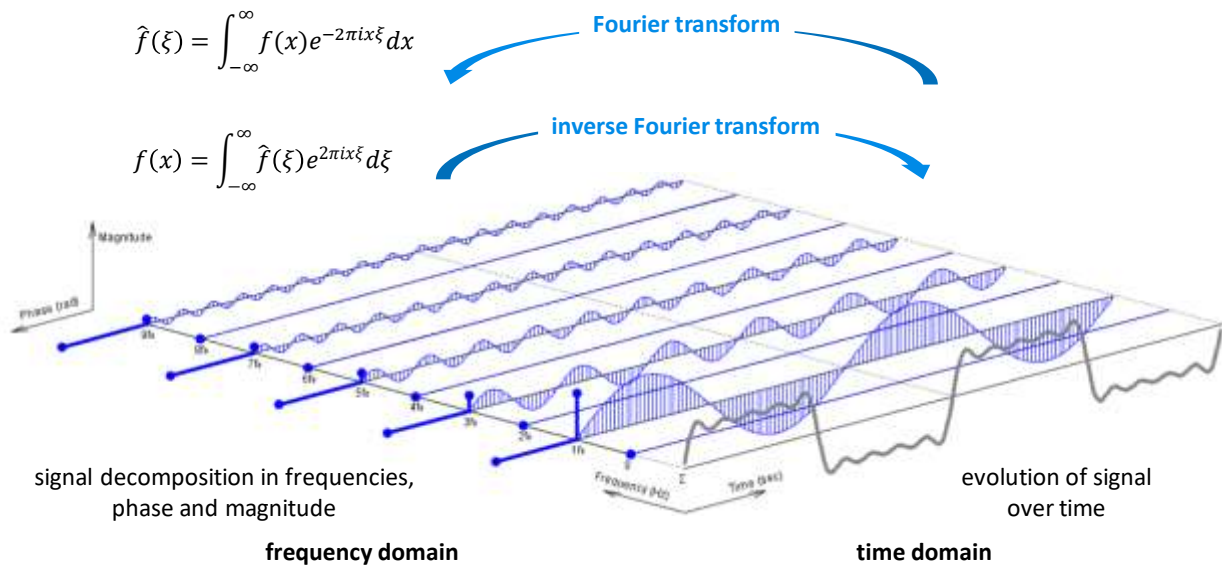


Figure 159: Fourier transform and inverse Fourier transform and signal decomposition. Source: <https://www.tomasboril.cz/files/myprograms/screenshots/fourierseries3d.png>, comments (cc) by Olivier Ezratty, 2021.

Nonlinearities

We often hear about nonlinearities with quantum physics, particularly with the difficulty to implement it with qubits. It's also used in neural networks activation functions in classical computing. But their meaning is not the same in these different scenarios.

Superconducting qubits exploit the Josephson effect and an anharmonic oscillator to prevent the energy states of the superconducting loop oscillating current from being separated by the same energy level. This is a nonlinear effect linked to the way harmonic oscillators work when dampened in a certain way. It enables microwaves controls for changing qubits state between $|0\rangle$ and $|1\rangle$ with a larger frequency than the one that would allow a switch from the $|1\rangle$ state to the $|2\rangle$ state, which is what we are trying to avoid.

Nonlinearities are also sought after in photonics, especially to create quality two-photon quantum gates. Nonlinearities occur when solid media modify the characteristics of photons such as their polarization P and in a nonlinear way with respect to the electric field applied to the solid. The dominant $\chi^{(i)}$ of a nonlinear medium defines its order. A $\chi^{(3)}$ is a third order nonlinear medium.

$$P = \epsilon_0(\chi^{(1)}E + \chi^{(2)}E^2 + \chi^{(3)}E^3 + \dots)$$

with ϵ_0 being the vacuum permittivity.

This phenomenon happens in the Kerr effect which sees some materials refractive index changing in a nonlinear (quadratic, second order $\chi^{(2)}$ medium) manner as a function of the electric field applied to them. Conversely, the Pockels effect used in optical modulators sees the refraction changed in a linear manner as a function of the electric field applied. This nonlinearity in optics also occurs in many devices such as power lasers.

Finally, nonlinearities are classically used in neural networks activation functions. These are, for example, sigmoid based on exponential fractions.

So how can such activation functions be performed in quantum computation that relies only on linear algebra? One of the first imagined solutions consists in using a nonlinear, non-reversible and dissipative quantum gate called D ²⁹⁶. Others consists in handling the nonlinearity part of algorithms in their classical parts before feeding a quantum algorithm. That's what can be done in algorithms solving Navier-Stokes fluid mechanics equations.

²⁹⁶ Method proposed by Sanjay Gupta in [Quantum Neural Networks](#), 2001 (30 pages) and [Quantum Algorithms for Deep Convolutional Neural Network](#), by Iordanis Kerenidis et al, 2020 (36 pages).

Qubits

Qubits are the basic elements of data manipulation in quantum computers. They are the quantum equivalents of classical computing bits. With them, we move from a deterministic to a probabilistic world but with the capability to handle more information during computing.

In conventional computing, bits used in processing units like microprocessors correspond to circulating electrical charges that reflect the passage or absence of an electrical current. A classical bit has a value of 1 if the current is flowing or 0 if the current is not flowing. The logic is transistors based. A bit readout gives 1 or 0 and deterministically, i.e. if the read operation is repeated several times, or the read operation is repeated after a re-edition of the calculation, it will yield the same result. This is true for data storage of information, for its transport and processing. This is valid modulo the errors that can occur during this journey. These most often occur in storage and memory and are corrected via error correction systems using some data redundancy, usually with some parity bits for each stored byte, so with a rather low data overhead. In data storage, complicated redundancy systems are used like RAID disks organization mixing and matching several disks and parity error codes to consider the physical errors coming from storage.

In a qubit, everything is different! While qubits are usually initialized at $|0\rangle$, operations on them called quantum gates create a mathematical linear superposition between states $|0\rangle$ and $|1\rangle$. These two states correspond to two different discrete possible values of a physical property of a quantum object like an electron spin (up or down in a given direction), a photon polarization or an atom energy level. Qubits are represented mathematically by a vector in a two-dimension Hilbert space which describes its amplitude and phase, reminding us of the “wave” nature of quantum objects.

We’ll see later how we use the Bloch sphere geometrical representation to understand how amplitude and phase are visualized. And it gets more complicated when we conditionally connect qubits together using multi-qubits quantum gates implementing quantum entanglement.

At the end of computing, we read the value of a qubit. Like all quantum object measurement, it results in a wave packet collapse onto one of the two qubit basis states. So, we get a $|0\rangle$ or a $|1\rangle$ and the result is probabilistic, not deterministic. The wealth of information handled by a qubit during computing is lost at the end of calculation.

| | | bits: 0 or 1 | | qubits: 0 and 1 |
|------------------------------|------------------|---|--------------------|---|
| states | mathematical bit | 2 possible exclusive states, 0 or 1 | mathematical qubit | linear combination of $ 0\rangle$ and $ 1\rangle$ |
| initialization | | 0 or 1 | | $ 0\rangle$ basis state |
| dimensionality | | 1 binary digit => two possible values | | 2 real numbers => one point on Bloch sphere |
| modifications | | logic decision tables, irreversible | | reversible unitary transformations |
| readout | | 0 or 1, deterministic | | 0 or 1, probabilistic |
| errors | | no error, perfect mathematical object | | no error, perfect mathematical object |
| physical implementation | physical bit | current/no current in a logic electronic circuit and two states memory device bit | physical qubit | quantum object with two exclusive states for one property |
| computing vs memory | | separate devices and parts of processors | | all done in qubits and with quantum gates |
| computing operations | | transistors based logic | | amplitude and phase change + entanglement |
| errors sources | | cosmic rays, transistors leakage | | decoherence, thermal, electromagnetic, radioactivity... |
| error levels | | 2.5×10^{-11} bit per hour error rate | | usually $\gg 0,1\%$ with qubit gates and readout |
| information redundancy | logical bit | parity bits | logical qubit | large number of physical per logical qubits, 10^2 to 10^6 |
| error correction | | ECC (memory), MCA (CPU), RAID (storage) | | quantum error correction codes |
| error level after correction | | negligible | | under an acceptable threshold for fault tolerance |

(cc) Olivier Ezratty, September 2021

Figure 160: detailed comparison between classical bits and qubits with separating the mathematical logic, the physical implementation and error correction techniques. (cc) Olivier Ezratty, 2021.

The role of a quantum algorithm is to leverage this wealth of information during computing so that a simple result is generated at the end. We turn this probabilistic outcome in a deterministic one with executing the algorithm a great number of times, up to thousand times, and averaging the obtained results. It's also dependent on the structure of quantum algorithms which are designed to generate a result with qubits being as close as possible to their so-called "computational basis states", namely, $|0\rangle$ and $|1\rangle$.

To sort things out, it's still useful to differentiate three levels of 'qubit objects' used in computing as described in Figure 160:

Mathematically. Bits and qubits are idealized mathematical objects that implement a pure mathematical formalism with no errors. What is named a "qubit" is above all a mathematical object. Its dimensionality is different than with a bit. It's represented by two complex numbers, the amplitudes α and β from the qubit quantum state description $\alpha|0\rangle + \beta|1\rangle$. Due to normalization ($\alpha^2 + \beta^2 = 1$) and getting rid of the qubit global phase, its dimensionality becomes two real numbers, usually represented by two angles in the Bloch sphere. Bits and qubit measurement are both mathematical and physical operations. With qubits, it's mathematically based on a projective measurement on the computational basis comprised of $|0\rangle$ and $|1\rangle$, using a Hermitian matrix. Physically, it's using a measurement apparatus operating on the qubit quantum object.

Physically. Bits and qubits are implemented with different sorts of physical devices. With bits, we use to say they correspond to currents circulating or not circulating in transistor-based devices. While this is true with processing, this is different with memory and storage²⁹⁷. Qubits are implemented with quantum systems comprised of a single quantum object (atom, electron, photon) or several quantum objects (particularly with superconducting qubits and topological matter qubits like Majorana fermions). The $|0\rangle$ or a $|1\rangle$ states correspond to two exclusive states for one given property of a quantum object or system, that is clearly separable at measurement, like a photon polarization that is detected with a polarizer and a photon detector or an electron spin that can be detected with some magnetic sensor and a technique called electron spin resonance (ESR). These are also called two-level systems (TLS).

Physical qubits processing is using physical operations: **amplitude and phase changes** implemented by single-qubit gates and provoking **superposition** and **entanglement** which conditionally connects qubits together with two or more qubits gates, **interferences** resulting from the previous operations and are at the core of most quantum algorithms, and **quantum measurement** yielding $|0\rangle$ or $|1\rangle$ for each qubit when computing has ended or when executing quantum error correction codes. Both bits and qubit physical objects are prone to physical errors. While error rates are very small with classical bits, it's currently quite high with qubits. One simple operation like a two qubits quantum gate can generate over 0,4% error rates, which is unacceptable for most algorithms.

Qubits errors, namely decoherence, come from the various interactions between the qubit quantum objects and their environment like thermal noise, electro-magnetic noise, cosmic rays and gravity²⁹⁸. These errors require quantum error correction codes, which, as we'll later see, require a significant overhead of physical qubits.

²⁹⁷ These rely on electronic systems storing information like some magnetic encoding in hard disks drives or with two states transistor-based objects in SRAM (used in processors), DRAM (used around processors) or Flash memory (used in SSD and your usual USB memory key).

²⁹⁸ It explains why many qubit types requires some sort of isolation: vacuum and low temperature to avoid thermal and electro-magnetic noise and multi-layered shielding to avoid other sources of electromagnetic noise. But we'll see later that for superconducting and electron spin qubits, the required low temperature is also linked to the microwaves used to control qubits.

Logically. Error correction is thus required to create usable computing devices. In classical computing and telecommunications, “bits” are corrected with different techniques including using parity bits²⁹⁹. Bits are processed, stored and transmitted with a very low-level of errors.

Qubits must be assembled in groups called logical qubits, which are physical assemblies of a much great number of physical qubits, up to 10 000’s³⁰⁰. Redundancy overhead becomes much bigger than with parity bits used in classical computing. In logical qubits, physical qubits are processed with quantum error correcting codes. The number of physical qubits assembled into logical qubits depends on their physical error rate and on the logical qubit error rate that is expected to enable practical quantum computing. For example, the famous integer factoring Shor algorithm is very demanding since using very precise small angles phase rotation gates.

While qubits are everywhere in quantum computing, these are not the only quantum objects available to manage quantum information.

Quantum computers can also theoretically be built with **qutrits** (with three possible quantum states), **ququarts** (with four possible states) and more generically, with **qudits** (d being the number of possible quantum states of the qubit underlying quantum system)³⁰¹.

It can deliver some computing power with a smaller number of quantum objects than with qubits. These are still mostly research labs tools. For example, researchers at Berkeley are investigating superconducting qudits with more than two levels³⁰².

The most common qudits are implemented with photons by managing several of their properties.

Using qudits would have an impact on quantum algorithms design and programming. Most of quantum algorithms are designed for quantum computers using qubit-based gates. However, compilers could probably automatically transform classical quantum gates into qudits-based gates.

The record so far is about creating quvigints, qudits with 20 different exclusive values for photons, that are efficiently measured with state tomography³⁰³.

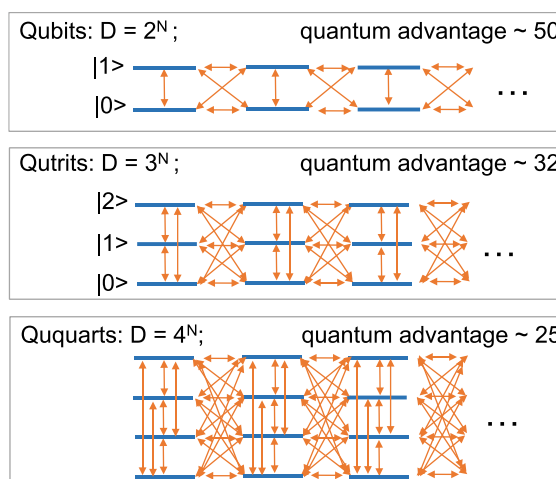


Figure 161: qubits, qutrits and ququarts. Source: [Quantum Simulations with Superconducting Qubits](#) by Irfan Siddiqi, 2019 (66 slides).

²⁹⁹ ECC (error correcting codes) are used in memories. Some systems are used in processors like the Intel MCA (Machine Check Architecture) which detects and reports errors in microprocessor. Other systems correct errors in storage like RAID redundancy for hard-disk drives and SSDs. We also have error correction codes used in classical telecoms.

³⁰⁰ As of 2021, there are no commercial computers using real logical qubits. The reason is simple: the number of available physical qubits in gate-based processing units, topping at 127 with IBM’s last generation of superconducting qubits, is still *under* the number of physical qubits required to build just one logical qubit!

³⁰¹ See for example [Ultracold polar molecules as qudits](#) by JM Hutson et al, 2020 which deals with qudits using fluorine-calcium and rubidium-cesium diatomic molecules allowing four quantum levels per molecule. This reduces the number of necessary qubits of $\log_2(d)$, d being the number of state levels of the qubits.

³⁰² See [Quantum Simulations with Superconducting Qubits](#) by Irfan Siddiqi, 2019 (66 slides).

³⁰³ See [Finding quvigints in a quantum treasure map](#) by University of Queensland, March 2021 and [Robust and Efficient High-Dimensional Quantum State Tomography](#) by Markus Rambach et al, March 2021 (6 pages).

Bloch sphere

Let's first dig into the mathematical models of qubit representation. These models do not depend on the qubits underlying quantum object types. Physical qubit types have an impact on their error level and types as well as on the low-level quantum gates operations available to control qubits.

In a classical probabilistic model, a probabilistic pbit would have a probability p of having the value 0 and $1-p$ of having the value 1³⁰⁴. It would be a linear probabilistic model. We cover the niche market of probabilistic computers in a [dedicated section](#), page 790.

Well, with qubits, these probabilistic laws are quite different!

A qubit vector state is defined by two complex numbers α and β according to the formula describing the qubit quantum object state $|\Psi\rangle$ as $\alpha|0\rangle + \beta|1\rangle$. Quantumly speaking, $|\Psi\rangle$ is a linear superposition of basis states $|0\rangle$ and $|1\rangle$ with coefficients α and β , aka amplitudes. α is a complex number whose square describes the probability of having the state $|0\rangle$ and β is a complex number whose square describes the probability of having the state $|1\rangle$.

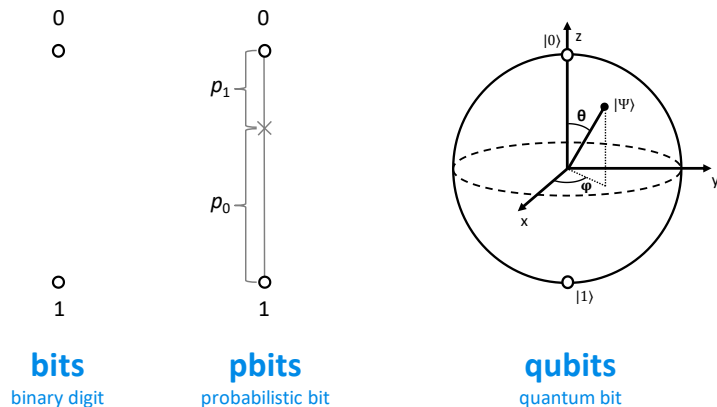


Figure 162: bits, probabilistic bits and qubits.

The sum of the probabilities of the two basis states must give 1. It is indeed not $\alpha + \beta$ but $\alpha^2 + \beta^2$ that give 1. It comes from the generic probabilistic model developed by **Max Born** in 1926 and from one of the postulates of quantum physics. It gives to the square of the modulus of the wave function of a quantum the meaning of a probability density of the presence of an elementary particle in space (mostly, for electrons).

The mathematical representation model of the state of a qubit is based on complex numbers and on the geometrical metaphor of the famous **Bloch sphere**. This model is linked to the representation of the state of a qubit or any two-state quantum by a two-dimensional vector whose length, called "norm", is always 1.

Angles. The qubit state $|0\rangle$ is a length 1 vector going from the center of the sphere to the North pole of the sphere and the state $|1\rangle$ is a vector going from the center of the sphere to its South pole. An arbitrary qubit state $|\Psi\rangle$ is represented by a vector with an angle θ (0 to π , latitude) with respect to the vertical z-axis and an angle ϕ (0 to 2π , longitude) with respect to the x-axis located from the center of the sphere to its equator and around the z-axis. θ corresponds to the qubit amplitude and ϕ to its phase.

Orthogonality. The basis states $|0\rangle$ and $|1\rangle$ are opposite in the Bloch sphere and are mathematically orthogonal. This is highly counter-intuitive and linked to the angle θ that is divided by two in the formulae. When θ equals π , corresponding to a half turn in the sphere, moving from $|0\rangle$ to $|1\rangle$, $\cos(\theta/2) = \cos(90^\circ) = 0$ illustrating the fact that $|0\rangle$ and $|1\rangle$ are indeed mathematically orthogonal states. This is true for any opposing states within the sphere as with the $|\Psi\rangle$ and $|\Psi'\rangle$ examples below in Figure 163.

³⁰⁴ Linear probabilistic models are used in the probabilistic processors discussed in a small [dedicated chapter of this book](#).

These opposite states are antiparallel or antipodal, meaning parallel but in opposite directions. It explains why angle θ is halved in the equations describing a quantum state in Bloch sphere in the sine and cosine calculations of the formulas giving α and β ³⁰⁵!

So, we divide θ by 2 to link the geometric representation in the sphere with the mathematical representation of the qubit state, and to allow a spreading of all the states of a qubit over the whole sphere. The whole sphere occupation of qubits representations makes it easier to describe how single qubit gates work as we'll show later in a graphical way.

By the way, $\sin(\theta)$ is a marker of the qubit coherence or level of superposition. It's easy to grasp since the sinus will be equal to zero when the qubit is in the $|0\rangle$ and $|1\rangle$ states. It will be maximal, at 1, when the qubit vector will sit on the equator in the Bloch sphere with an even superposition of $|0\rangle$ and $|1\rangle$.

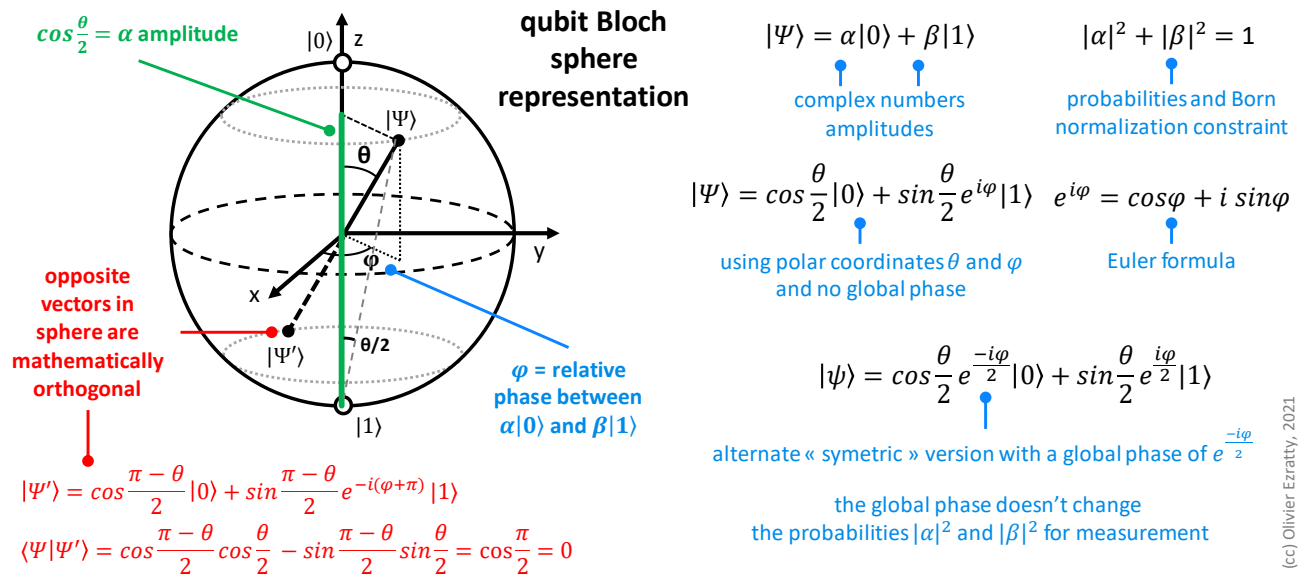


Figure 163: a thorough explanation of the Bloch sphere representation of qubits. (cc) Olivier Ezratty, 2021.

Global phase. A qubit representation is usually independent of its global phase. It can be removed from the equation to turn α into a real number. Still, a qubit is sometimes represented with a global phase of $\frac{-i\varphi}{2}$ as shown in Figure 163. When removing the global phase from α , the complex part of β integrates the phase difference between the amplitudes α and β . In that case, β is a complex number when the qubit is not in the plane crossing the x-axis ($\theta = 0$) and the z-axis ($\varphi = 0$) of the Bloch sphere, meaning it has a non-zero phase. This complex number associates a real part for the direction z and a complex part for the dimensions x and y which are orthogonal to z. Applying a rotation around the z-axis will generally reintroduce a complex number in the α of the transformed qubit, which we do not necessarily factorize to remove the global phase of the qubit when doing hand calculations.

Information. The paradox to be understood is the following: since there is an infinite number of positions in Bloch's sphere, a single qubit could theoretically store a large amount of information, at least much more than a bit. Let's say it could be two floating point numbers, like the two angles θ and φ in the Bloch sphere.

³⁰⁵ This is deciphered in [Ian Glendinning's The Bloch Sphere](#), 2005 (33 slides) which explains this by the mathematical orthogonality of the two states $|0\rangle$ and $|1\rangle$ which are nevertheless opposed in the Bloch sphere. It is even better explained in [Why is theta/2 used for a Bloch sphere instead of theta?](#) which definitely clears up this mystery.

Unfortunately, we can only obtain a classical 0 or 1 after measurement because of that damn Holevo theorem³⁰⁶! We could theoretically retrieve some floating-point number with averaging the results of a large number of runs of the algorithm. Their precision will depend on several factors: the number of runs or “shots”, the qubit error rates and the efficiency of quantum error correction codes. Given the overhead of all of this, forget about using qubits as a high-precision floating-point number storage device!

When the state vector of the qubit is horizontal in the Bloch sphere, i.e. it sits in its equator, and we have an even superposition of $|0\rangle$ and $|1\rangle$, but with a variable relative phase between the $|0\rangle$ and $|1\rangle$ amplitudes which is related to the horizontal angle of the vector φ with respect to the z axis as in the diagram on the right. Two usually superposed states are $|+\rangle$ and $|-\rangle$.

These are orthogonal states. These equatorial states share the same α component of $1/\sqrt{2}$ but opposite β values. This qubit-rich information is then modified by phase rotation quantum gates. If all qubits in the equator share the same 50%/50% amplitude probabilities, they have a different phase.

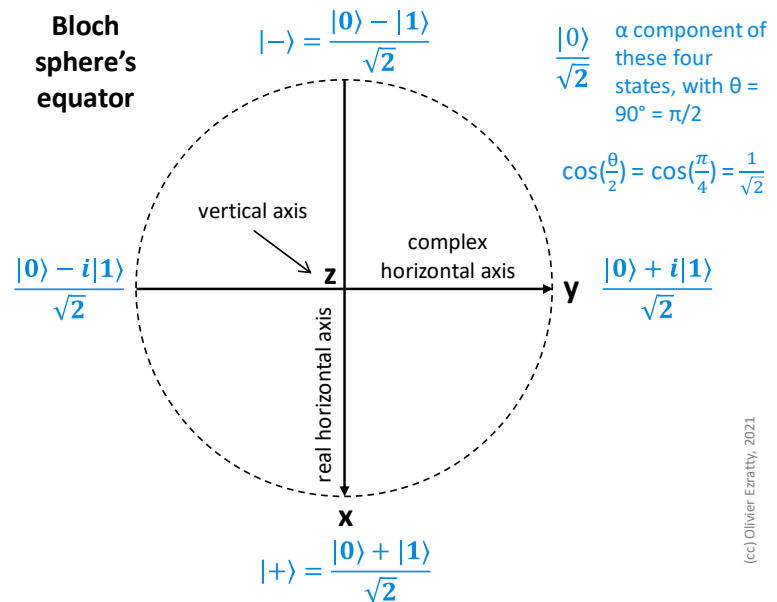


Figure 164: Bloch sphere equator and superposed states (cc) Olivier Ezratty, 2021.

A significant part of the quantum computing power comes with playing with the qubit phase that generates interferences between qubits. We’ll see that later with algorithms such as phase amplitude and phase kickback.

As a general rule, most quantum gates do not generate all vector positions in the Bloch sphere. They are often half or quarter turns. The points of the sphere most often used are the cardinal points: the $|0\rangle$, $|1\rangle$, then the four points corresponding to the superposition of $|0\rangle$ and $|1\rangle$ on the equator.

To obtain all the quantum computing power, we need to make smaller turns than quarter turns, with the variable-phase R gates, usually composed with T gates, which we will see later and is outside the so-called Clifford gates group. Only these gates are supposed to enable some exponential speedup with gate-based quantum computing. Another way to look at this is that quantum advantage comes from using the full power of “analog” qubits.

Origins. We owe this Bloch sphere to three scientists: **Erwin Schrödinger** for his wave function of 1926, **Max Born** for his associated probabilistic model, created the same year, and to **Felix Bloch** (1903-1983, Switzerland) who represented the state of a two-level quantum on the sphere in 1946.

³⁰⁶ To learn more and with a better scientific accuracy, you can consult the Wikipedia sheet of the [wave function](#) and [amplitude probability](#). Other explanations can be found in the example of the electron orbit levels in the hydrogen atom in [Quantum Mechanics and the hydrogen atom](#) (19 slides). The physical interpretation of Max Born's statistical rule remains in any case open, as explained in Arkady Bolotin's June 2018 paper, [Quantum probabilities and the Born rule in the intuitionistic interpretation of quantum mechanics](#) (14 pages).

Bloch's sphere is frequently assimilated to **Poincaré's sphere**, named after **Henri Poincaré** (1854-1912, France) and created in 1892³⁰⁷. It is used to describe the polarization of light. The sphere polar coordinates represent the various types of light polarization: linear polarization (on the sphere equator), left elliptical polarization (upper hemisphere), right elliptical polarization (lower hemisphere) then left and right circular polarization (North and South poles).

The vertical axis (circular polarization) and one of the horizontal axis (linear polarization) represent two observables for a photon. All other states can be described as linear superpositions of these couples of basis states. And contrarily to massive particle-based quantum objects whose quantum probabilities are described by Schrödinger's equation, light equations used here are just Maxwell's electromagnetic waves equations.

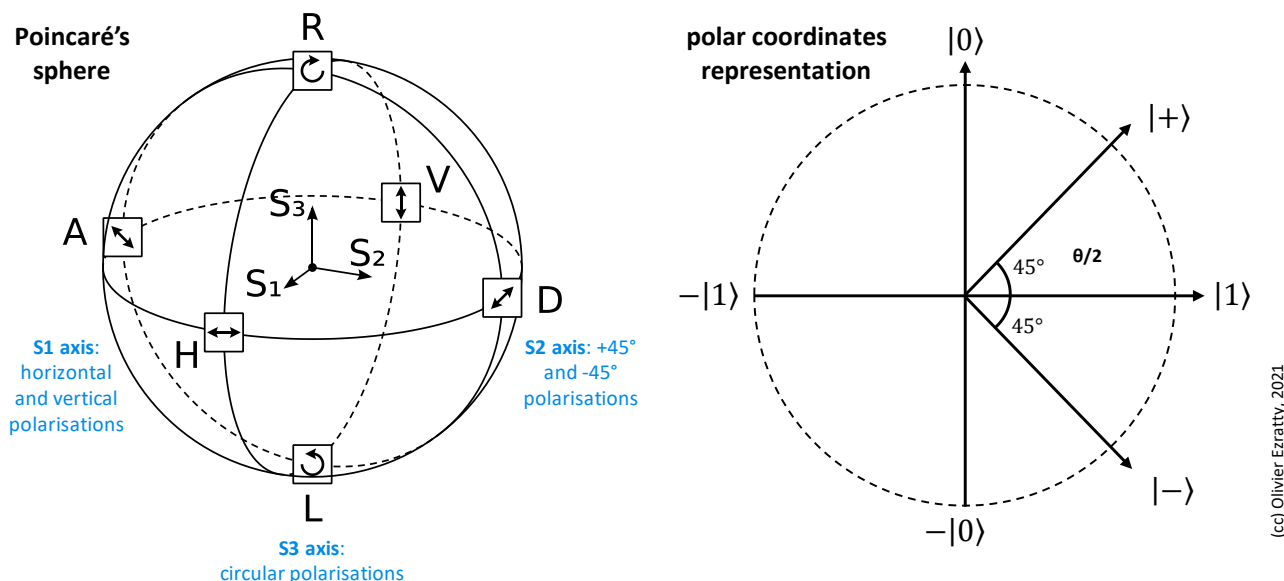


Figure 165: the Poincaré photon sphere which inspired the Bloch sphere creation and another, Euclidian, representation of a qubit.

The Bloch sphere representation is also used for representing an electron spin measured along three orthogonal axis (X, Y, Z), showing how superposition works with spins.

Sometimes, a system of polar coordinates is used on one circle, positioning the computational basis states of $|0\rangle$ and $|1\rangle$ as geometrically orthogonal vectors. It somewhat duplicates values since of $-|0\rangle$ and $-|1\rangle$ are similar to $|0\rangle$ and $|1\rangle$, with just a different global phase. Only the right half of the circle is useful.

Many other fancy qubits representations have been created with projection of the Bloch sphere onto a plane, representations of several qubit states with many Bloch spheres, even some representation of quantum entanglement with three Bloch spheres for two qubits³⁰⁸ or with tetrahedrons³⁰⁹. None of these have been standardized and have a practical value for most quantum developers.

³⁰⁷ Here are some sources of information associated with this section: [Lectures on Quantum Computing](#) by Dan C. Marinescu and Gabriela M. Marinescu, 2003 (274 pages), [The Bloch Sphere](#) by Ian Glendinning, 2005 (33 slides), [The statistical interpretation of quantum mechanics](#), Max Born's 1954 Nobel Prize acceptance speech in physics (12 pages) and the excellent book [The mathematics of quantum mechanics](#) by Martin Laforest, 2015 (111 pages), which describes the mathematical basics of quantum computing with complex numbers, vectors, matrices and everything.

³⁰⁸ See [Two-Qubit Bloch Sphere](#) by Chu-Ryang Wie, 2020 (14 pages).

³⁰⁹ See [Geometry of Qubits - A picture book](#) by Yosi Avron and Oded Kenneth, 2018 (20 slides).

Registers

In a quantum computer, qubits are organized in registers: a bit like the 32- or 64-bit registers of today's classical processors. One key difference is for now, a quantum computer has only one register and not many as with current classical microprocessors.

The main difference between an n-qubit register and a traditional n-bit register is the amount of information that can be manipulated simultaneously. In conventional computers, 32- or 64-bit registers store integers or floating-point numbers on which elementary mathematical operations are performed.

A register of n qubits is a vector in a 2^n dimensional space of complex numbers. Its dimensionality is exponentially larger than a n-bits register. Let's take for instance a register of 3 bits and 3 qubits. The first one will store one value at a time as 101 (5 in base 2) while the register of three qubits will contain complex numbers attached to each of the possible values of this register, 2 to the power of 3, i.e. 8, aka computational state basis. These complex numbers are the amplitude of each computational state. The total of their squares equals 1 since these are probabilities.

| | n bits register | n=3 example | n qubits register | |
|-----|--|--------------------|---|-----|
| 101 | 2^n possible states once at a time | | 2^n possible states linearly superposed | 000 |
| | evaluable | | partially evaluable | 001 |
| | independent copies | | no copy | 010 |
| | individually erasable | | non individually erasable | 011 |
| | non destructive readout | | value changed after readout | 100 |
| | deterministic | | probabilistic | 101 |
| | | | | 110 |
| | | | | 111 |

aka register pure states

Figure 166: key differences between a classical bit register and a qubit register. (cc) Olivier Ezratty, 2021.

However, these 2^n states amplitudes do not really constitute some information storage capacity. Quantum algorithm's main goal is to amplify the computational basis state amplitude that is the sought result, while reducing all the other amplitudes to near zero. Logically, it is like testing many hypotheses in parallel to bring out the best one.

The output information is a set of n classical bits. The 2^n amplitudes handled during computation are not some useful information that we exploit outside the register. We'll always end with one computational state and its related classical bits. So, in the end, you don't really process "big data" with quantum computing or at least, you don't output any big data. You may still use some sort of big data to prepare the state of the register before or during calculation³¹⁰.

But it's not to the advantage of quantum computing since feeding a quantum register with classical data is quite slow³¹¹.

³¹⁰ However, exceptions are beginning to appear with hybrid methods for accelerating database access combining traditional computer-based and quantum algorithms. See [Quantum computers tackle big data with machine learning](#) by Sarah Olson, Purdue University, October 2018.

³¹¹ It's well explained in the excellent overview [Quantum Computing: Progress and Prospects](#) from the US Academy of Sciences, 2019 (272 pages) : "Large data inputs cannot be loaded into a QC efficiently. While a quantum computer can use a small number of qubits to represent an exponentially larger amount of data, there is not currently a method to rapidly convert a large amount of classical data to a quantum state (this does not apply if the data can be generated algorithmically). For problems that require large inputs, the amount of time needed to create the input quantum state would typically dominate the computation time, and greatly reduce the quantum advantage."

The graphic representation below in Figure 167 was built using the Quirk open source simulator. It is a sample of a quantum Fourier transform algorithm run on 4 qubits. The column numbers vector is showing the computational base probabilities. In the beginning we have a 100% $|0000\rangle$.

After applying an X gate on the first qubit, we get a 100% amplitude for a $|1000\rangle$. After applying Hadamard gates to all qubits, we get even amplitudes of 6,3% for all computational basis states. Then the QFT finds out the result, $|1001\rangle$ which shows up on the last column³¹².

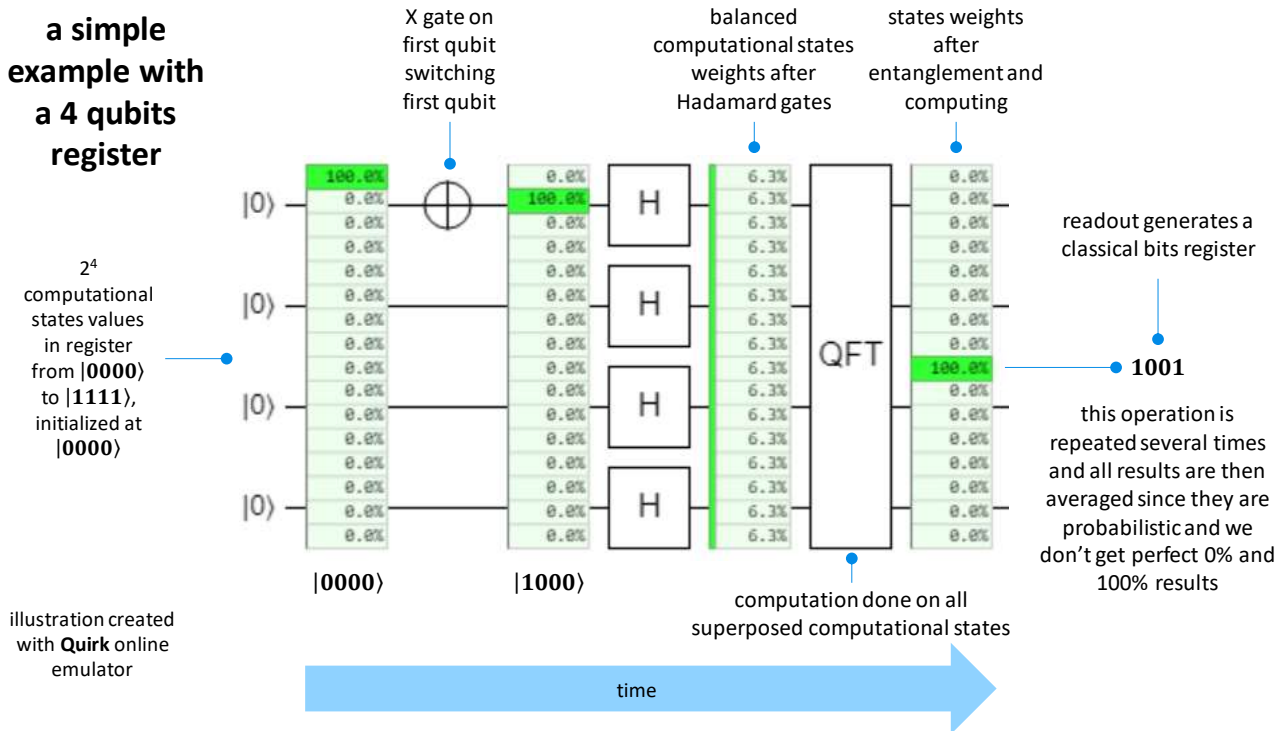


Figure 167: manipulating a 4-qubit register vector state with Quirk. (cc) Olivier Ezratty, 2021.

Another way of presenting things is a little simpler and more graphical: all the register states are on the left, the calculation generates interference between these states to make one of the states on the right come out which is the answer to the problem posed³¹³. The example is based on the use of only two qubits that give four different "binary" states of the qubits.

So, we do not recover 2^n values in practice, but n bits. The operation can be repeated several times to obtain an average in the form of floating numbers. But it depends on the algorithms. For the majority of them, a binary output is sufficient, as for Peter Shor's integer factorization algorithm.

We are anyway constrained by **Holevo's theorem** of 1973 which proves that with n qubits, we cannot recover more than n bits of information after a quantum calculation!

At the current stage of qubit development, one and two-qubit gates error rate is between 0,1% and 0.5% and ideally it should be less than 0.0001%. This error rate can be evaluated for each isolated qubit.

³¹² In [A quantum computer only needs one universe](#) by Andrew Steane, 2003 (10 pages), the latter insists on the key role of entanglement. He considers that entanglement does not so much explain the gain in quantum computing power.

³¹³ See [Introduction to Quantum Computing](#) by William Oliver from MIT, December 2019 (21 slides).

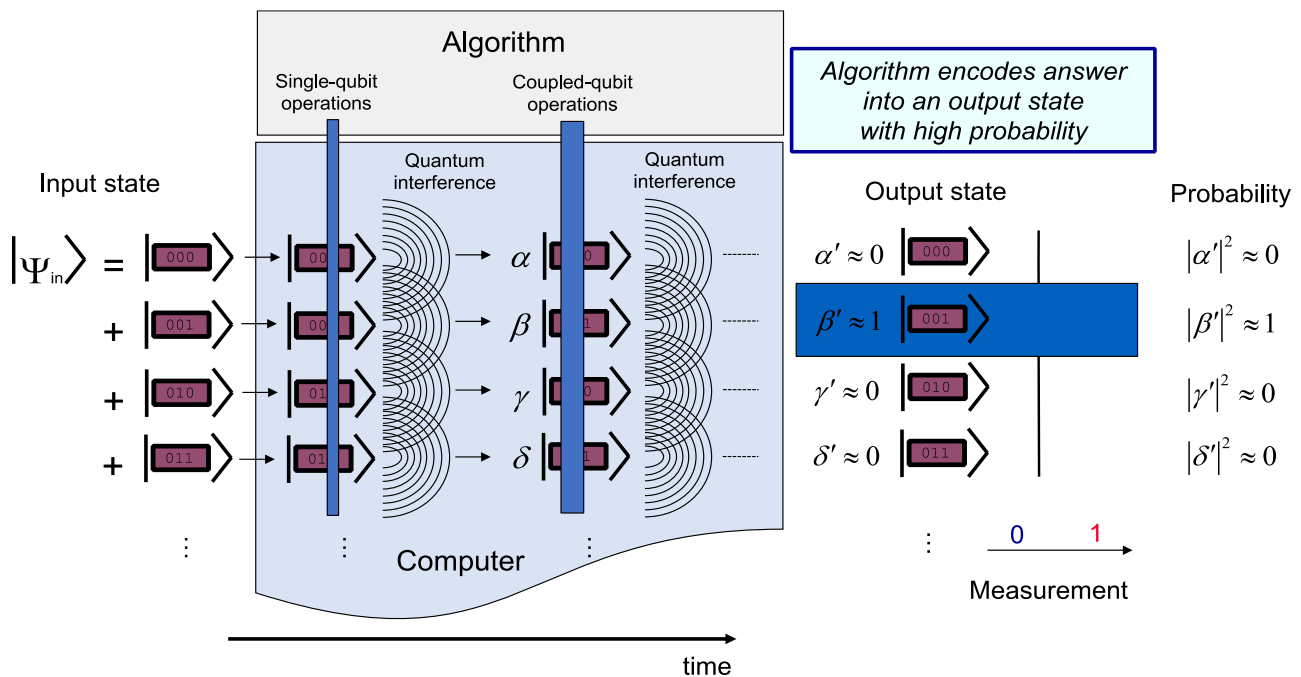


Figure 168: representing qubits manipulations with interferences. Source: [Introduction to Quantum Computing](#) by William Oliver from MIT, December 2019 (21 slides).

By the way, don't believe the nonsense that is the comparison of the exponential size of the qubit registers computational basis state with the number of particles in the Universe. These are not equivalent dimensions. A number of objects combination is not homothetic with a number of objects! With a given number of objects, combinations of these objects will always represent a number that is much higher than the number of objects taken as a reference. And... exponentially!

On the other hand, besides this exponential combination sizing, qubits have a lot of drawbacks in total opposition with classical bits. One can neither copy classically nor erase the value of qubits individually. Their measurement modifies their values. These are probabilistic objects that are difficult to manipulate.

Ancilla qubits. Universal gate quantum computing uses ancilla qubits or control qubits that can be combined with the computing qubits. The value of these qubits is not read at the end of the processing. It is a kind of trash can of qubits used during computations. They are used in various algorithms as well as to implement the error correction codes (QEC) explained later. We still always use a single qubit register. It can be just logically partitioned between computation qubits and ancilla qubits, these last playing more or less the role of classical registers in a microprocessor. Their content may be scrapped at the end of some parts of computing. It's sometimes done using the "uncompute trick" which reverses part of the processing affecting these ancilla without erasing the other qubits containing the intermediate computing result.

Gates

In classical computing, logic gates execute Boolean algebra using bit-dependent decision tables as an input. Several types of logic gates with one and two inputs are used, including the NAND gate which is interesting because it is universal and uses only two transistors. The other one- and two-bit Boolean gates can theoretically be created with NAND gates. In general, however, logic gates are mixed in the circuits.

An Intel Core i5/7 processor with over 10 billion transistors contains several billion logic gates. A processor is obviously very complex, with gates managing access to a cache memory and registers, and instruction pipeline executing the code defining the gates to be used in calculations. These operations are generated at the processor's clock frequency, most often expressed in GHz.

The classic two-bit logic gates (NAND, NOR, XOR, AND, OR) are irreversible because they destroy information during their execution.

Qubits undergo operations via quantum gates that can be applied to one or more qubits.

Single-qubit gates apply a 2×2 unitary matrices of complex numbers to the qubit state vector containing the famous α and β complex amplitudes. These always generate some rotation of the qubit vector in the Bloch sphere. The norm of the vector remains stable at 1 at least, before any decoherence happens. And quantum gates modify qubits information without reading it. A single qubit gate on a register of N qubits is a unitary operator, a large square matrix of 2^N lines and columns which results from the tensor product of the gate matrix applied to a qubit and the identity operator acting on all the other qubits, in the qubits order.

Two qubit gates apply 4×4 unitary matrices to the computational basis state vector containing 4 entries (2^2).

Three qubit gates apply a 8×8 matrix to a state vector containing $8=2^3$ entries.

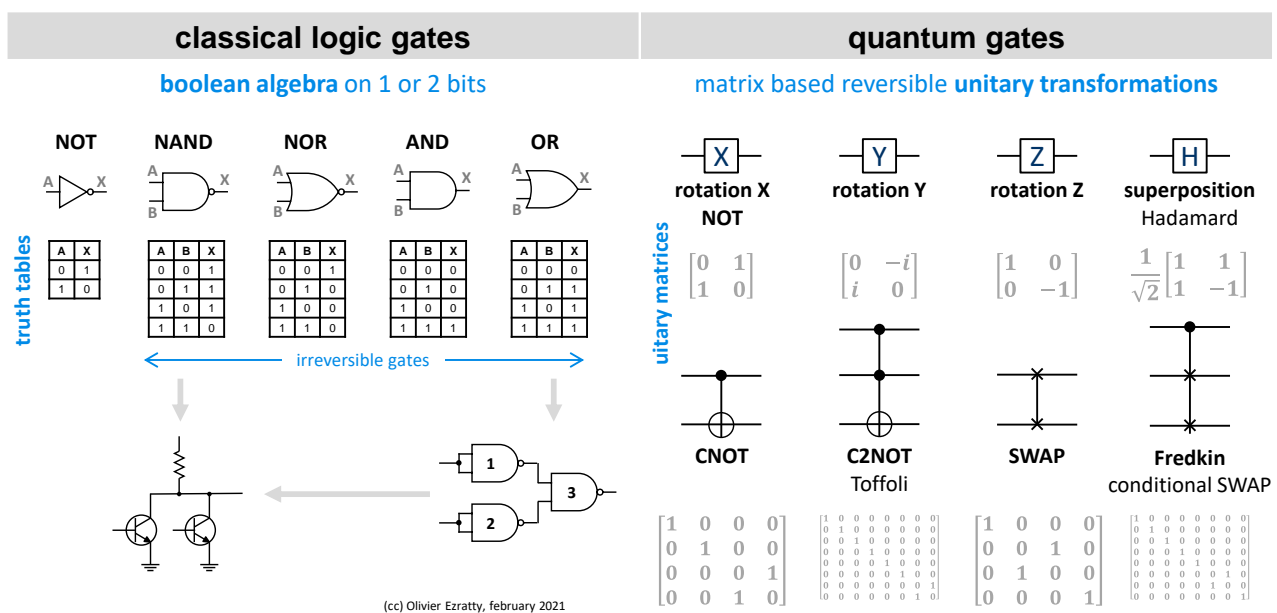


Figure 169: comparison between classical logic gates and qubit gates. (cc) Olivier Ezratty, 2021.

We'll now look at the various quantum gates made available to quantum developers³¹⁴. The variations come from the rotation axis in the Bloch sphere (usually, X, Y or Z) and the angle of the rotation ($1/2$ turn, $1/4$ turn, $1/8$ turn or arbitrary rotation angle)³¹⁵.

- **X gate (or NOT)** performs an inversion or bit flip. A $|0\rangle$ becomes $|1\rangle$ and vice-versa. Mathematically, it inverts the α and the β of the two-component vector that represents qubit state. It generates a 180° rotation in the Bloch sphere around the X axis.

This gate is often used to initialize to $|1\rangle$ the state of a qubit at the beginning of a process which is by default initialized at $|0\rangle$.

$$X = \begin{bmatrix} 0 & 1 \\ 1 & 0 \end{bmatrix}$$

- **Y gate** performs a 180° rotation around the Y-axis in the Bloch sphere. It also turns a $|0\rangle$ into $|1\rangle$.

$$Y = \begin{bmatrix} 0 & -i \\ i & 0 \end{bmatrix}$$

³¹⁴ Single qubit gates can be classified in XY and Z gates. XY gates are rotations around an axis in Bloch's sphere equator and can be viewed as amplitude change gates while Z gates are rotations around the Z axis and can be described as phase change gates.

³¹⁵ The formalism and classification of quantum gates is more sophisticated, as very well explained in the excellent lecture notes [Gates, States, and Circuits - Notes on the circuit model of quantum computation](#) by Gavin E. Crooks, January 2022 (79 pages).

- **Z** gate applies a sign change to the β component of the qubit vector (phase flip), i.e. a phase inversion and a 180° rotation with respect to the Z axis. The X, Y and Z gates complemented by the identity I are the **Pauli gates**.

$$Z = \begin{bmatrix} 1 & 0 \\ 0 & -1 \end{bmatrix}$$

They have several characteristics like $ZX=iY$ and $X^2=Y^2=Z^2=I$. Their unitary matrices are noted σ_x , σ_y and σ_z . Any single qubit unitary transformation can be written as a linear combination of Pauli gates with real number coefficients, plus the identity I.

- **S** gate generates a phase change, or a quarter turn rotation around the Z-axis (vertical). This is the equivalent of a half Z-gate. It is also called a "phase gate".
- **T** gate equivalent to a half S, which generates a phase change of one eighth of a turn. With two of these gates, an S gate is generated. This gate that is not part of Clifford's group (defined ... later) has the particularity of allowing by approximation the creation of any rotation in Bloch's sphere.

$$S = \begin{bmatrix} 1 & 0 \\ 0 & i \end{bmatrix}$$

$$T = \begin{bmatrix} 1 & 0 \\ 0 & e^{\frac{i\pi}{4}} \end{bmatrix}$$

It's the key to universal gate-based quantum computing. It is indispensable to run a quantum Fourier transform and all derived algorithms like Shor integer factoring, HHL (linear algebra) and most quantum machine learning algorithms.

- **R** phase shift gates are variations of Pauli gates, with an arbitrary rotation angle in the Bloch sphere. The R_z gate rotates around the z axis, R_x around the x axis and R_y around the y axis³¹⁶. A $R_z(\text{angle})$ gate is also called a P_{angle} gate (P for phase).

$$R_m = \begin{bmatrix} 1 & 0 \\ 0 & e^{\frac{2i\pi}{2^m}} \end{bmatrix}$$

When the x, y and z axes are not specified, it is z, the vertical axis of the Bloch sphere, as in the matrix above. When x, y and z are specified without an angle or m, it is 90° or $\pi/2$. The rotation is carried out on a complete round divided by m. The R_z gates modify the phase of a qubit and not its amplitude. Thus, the measurement of its state $|0\rangle$ or $|1\rangle$ is not affected by this gate. It will return both $|0\rangle$ or $|1\rangle$ with the same proportions, before and after the use of an R_z gate. Only two points of a sphere do not move during a rotation around an axis connecting them.

- **H** gate aka Hadamard-Walsh: puts a qubit at $|0\rangle$ or $|1\rangle$ in a superposed state " $|0\rangle$ and $|1\rangle$ ". It is fundamental to generate this superposition in the registers.

$$H = \frac{1}{\sqrt{2}} \begin{bmatrix} 1 & 1 \\ 1 & -1 \end{bmatrix}$$

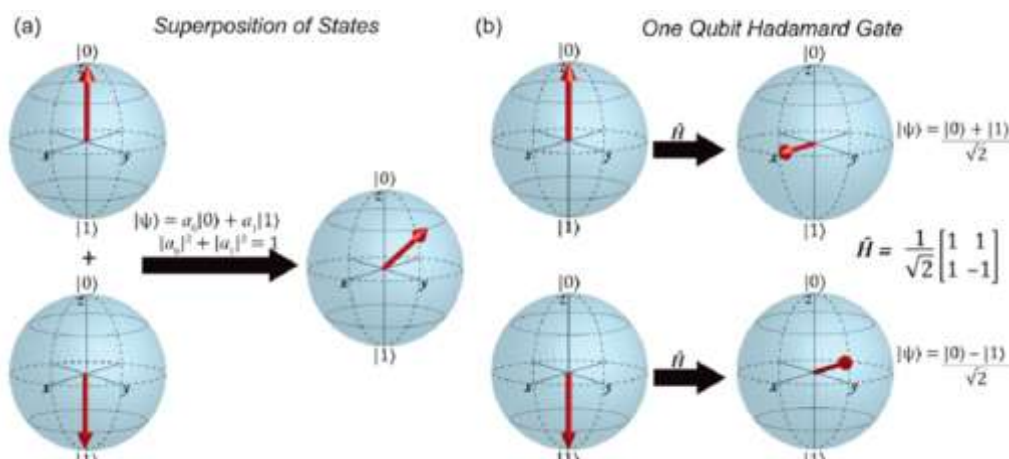


Figure 170: example of application of an Hadamard gate on $|0\rangle$ or $|1\rangle$ qubits. Source: [Molecular spin qubits for quantum algorithms](#) by Eufemio Moreno-Pineda, Clément Godfrin, Franck Balestro, Wolfgang Wernsdorfer and Mario Ruben, 2017 (13 pages).

³¹⁶ This is well explained in [The Prelude](#), Microsoft, 2017.

It is often used to initialize a quantum register before executing an oracle-based algorithm like Grover or Simon algorithms. Here is a representation of the effect of this gate on a qubit initialized at $|0\rangle$ or $|1\rangle$. If we apply two Hadamard gates to a qubit, we return to the starting point. In other words: $HH = I$ ($I =$ identity operator)³¹⁷.

- **I** gate is the identity gate. It may be used as a pause. In the real physical world, a real I gate is not an exact identity due to decoherence! If you “run” 20 identity gates on a $|1\rangle$ qubit, you’ll end up having some amplitude flipping error transforming progressively the qubit into a $|0\rangle$.
- **|0** reset gate is sometimes indicated at the beginning of an algorithm to indicate that we start with initialized qubits. It is obviously irreversible.

$$I = \begin{bmatrix} 1 & 0 \\ 0 & 1 \end{bmatrix}$$

$$|0\rangle = \begin{bmatrix} 1 & 0 \\ 0 & 0 \end{bmatrix}$$

The mathematical formalism applied to a single qubit simply illustrates this. But this works only in theory, only if the gate error rate is zero. Since it is not zero, you don’t ever a perfect $|0\rangle$ or $|1\rangle$.

A qubit reset operation may also be used to clean up ancilla qubits after their usage, when we are not using the uncompute trick, which is a way to cleanly reset ancilla qubits and remove potential entanglements with other qubits.

Below are representations of the effect of these single qubit gates, also labelled unary gates, on qubits initialized in $|0\rangle$ for the gates H, X, Y, R_x and R_y and with $|+\rangle$ for the phase change gates S, T, Z and R_z . Indeed, phase shift gates have no effect on $|0\rangle$ as well as on $|1\rangle$. For $|1\rangle$, it may just change the qubit global phase, and not its relative phase between the qubit amplitudes α and β , with no material impact on most algorithms. In the examples, the R gates use an angle of 90° or $\pi/2$.

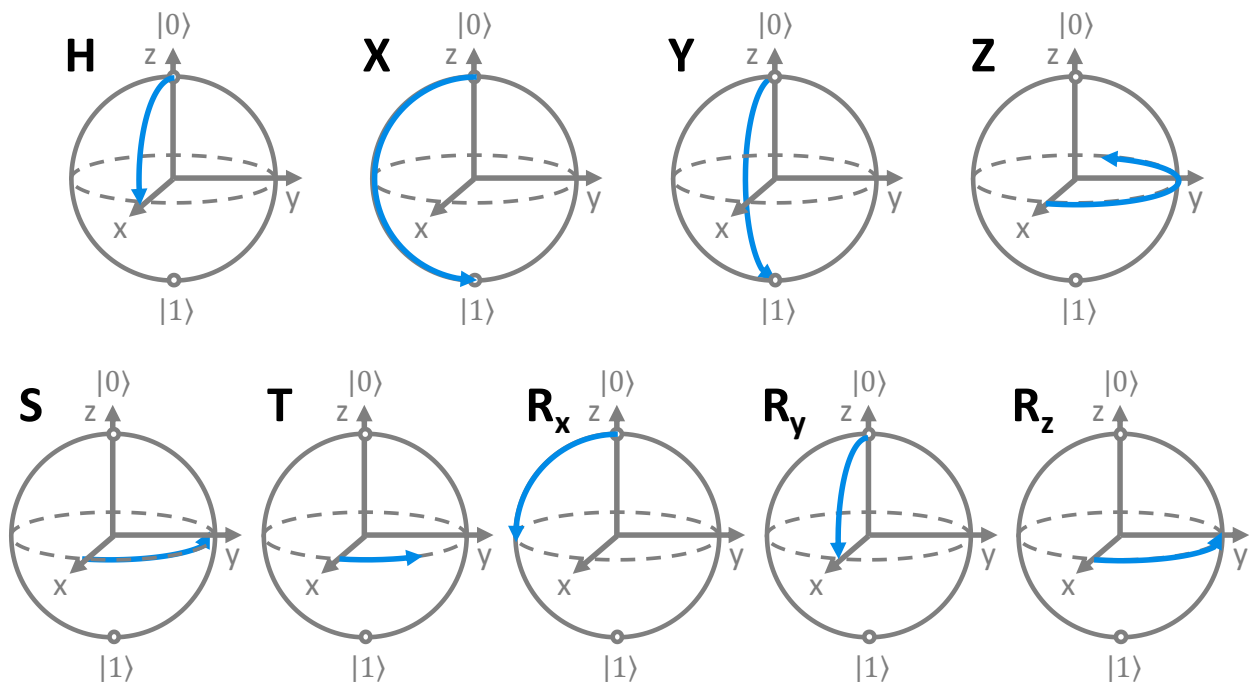


Figure 171: Bloch sphere representation of various single-qubit gates. (cc) Olivier Ezratty, 2021.

³¹⁷ This is also valid with X, Y and Z gates. In the usual notation, an H gate applied to $|0\rangle$ gives a state $|+\rangle$ and an H gate applied to $|1\rangle$ gives a state $|-\rangle$.

We now cover two and three qubit gates. Apart from the SWAP gate, all of these gates are conditional gates that apply a transformation of the state of one or two target qubits according to the state of one control qubit. These conditional gates create entanglement between the qubits that are in play. The entanglement between the involved qubits is persistent after executing these gates.

- **CNOT gate** is an inversion of the value of a qubit conditioned by the $|1\rangle$ value of another qubit. It is a quantum equivalent of the XOR gate in classical computing. Formerly called Feynman gate (C).
- **C2NOT** or **Toffoli gate** is an inversion of the value of a qubit conditioned by the $|1\rangle$ value of two other qubits.
- **CZ gate**, or Control-Z, is a conditional phase change Z gate.
- **CS gate**, or Control-S, allows a phase change of a qubit controlled by the state of a qubit.
- **SWAP gate** inverts the quantum values of two qubits. It can be generated from the chaining of three consecutive CNOT gates. The SWAP gate is the only two-qubit gate that is not creating a new entanglement between the two qubits. If they were separable before the gate, they will still be separable afterwards.

$$\text{SWAP} = \begin{bmatrix} 1 & 0 & 0 & 0 \\ 0 & 0 & 1 & 0 \\ 0 & 1 & 0 & 0 \\ 0 & 0 & 0 & 1 \end{bmatrix}$$

Figure 172: the two-qubit SWAP gate unitary matrix.

The key role of SWAP gates is to connect qubits that are physically distant in the register physical layout. A SWAP gate may also displace some entanglement. For example, if qubits A and B are entangled, but C is not entangled with A and B, a SWAP between B and C will displace entanglement to A and C and leave B unentangled with A and C. SWAP is usually a costly gate. It is not used a lot when the qubit topology enables all to all qubits direct connections like with some trapped ions qubits. As a consequence, most SWAP gates are created by compilers.

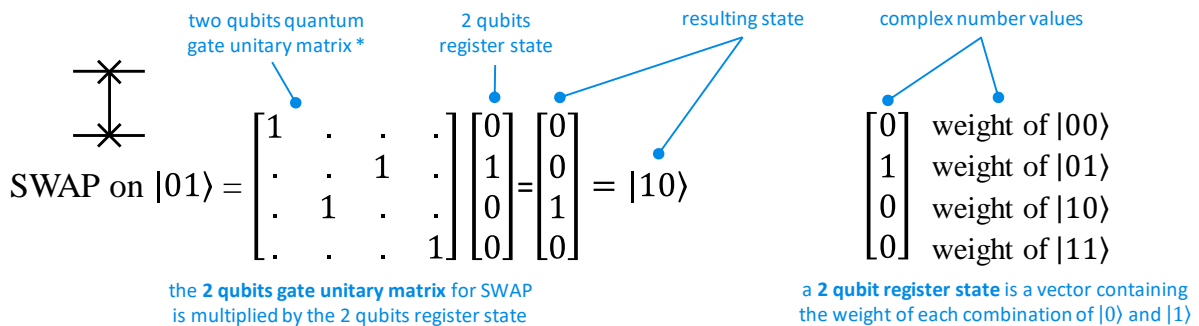


Figure 173: example of SWAP gate operation. (cc) Olivier Ezratty, 2021.

- **Fredkin gate** is a SWAP gate between two qubits that is conditioned by the state of a third qubit. So it has three inputs.
- **Generic Control-U gate** is a two qubits gate applying a generic one qubit unitary to a qubit based on the state of a control qubit.

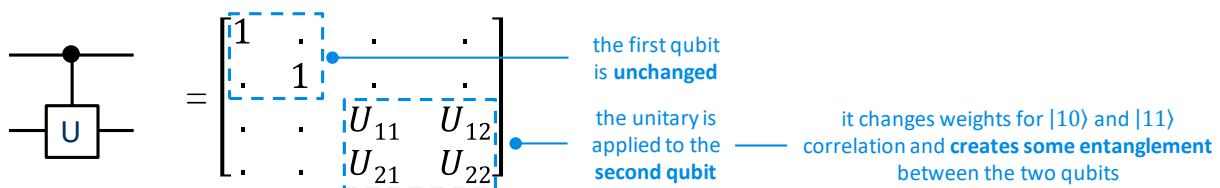


Figure 174: control-U two-qubit gate unitary matrix. (cc) Olivier Ezratty, 2021.

- **Phase-controlled R gates** are the equivalent of single-qubit phase-change R gates, conditioned by the state of a control qubit. If the algorithm, like a quantum Fourier transform, requires m to be large, it is not easy to ensure the reliability of the gate because the required precision becomes very large compared to the phase errors generated by the quantum system. However, phase errors are difficult to correct!

A precision record of such a gate seems to have been reached by Honeywell with its ion trapped qubits presented in 2020 which have a rotation precision of 1/500 turn. This reminds us that during operations, quantum computing is analog. It is digital only at the level of commands and measured results, which become classical bits again³¹⁸.

There are some reasons to get confused with S, T and R phase gates angles. For example, a S gate is sometimes branded as a $\pi/2$ and sometimes as a $\pi/4$. The same is applied to a T gate that is sometimes a $\pi/4$ and sometimes a $\pi/8$. The explanation is in the chart below and is related to the way a global phase is applied to the gate unitary operator. We can split hairs with using a “rotation” for the large one and a “round” for the small one.

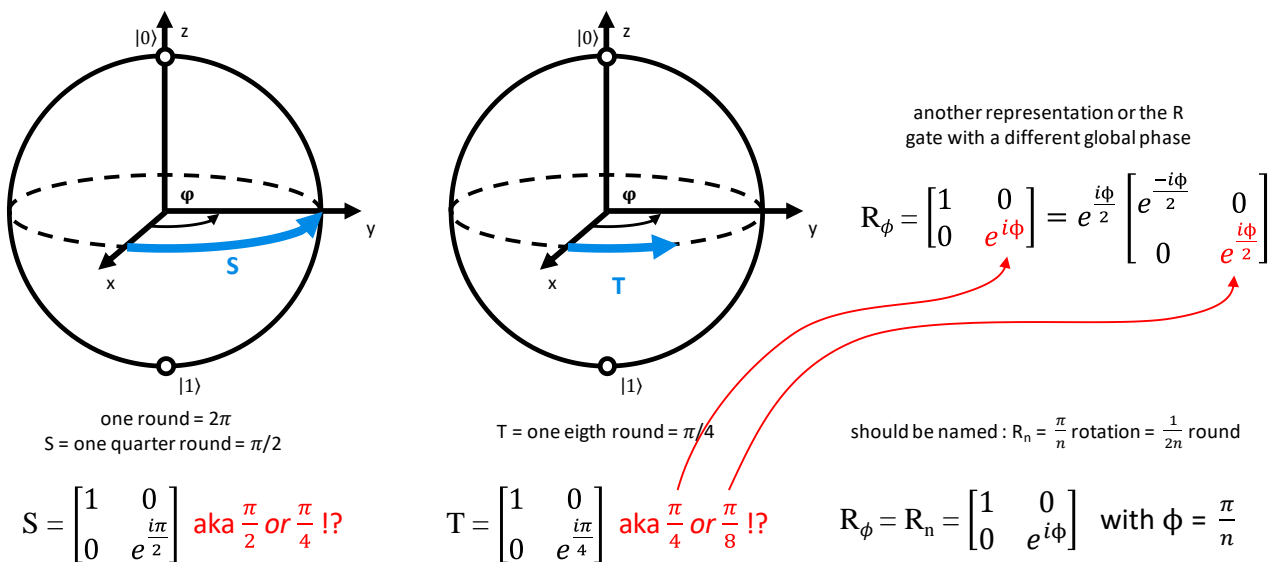


Figure 175: solving the ambiguity of phase gates labelling. (cc) Olivier Ezratty, 2021.

The effect of two-qubit gates is mostly always presented with using $|0\rangle$ s and $|1\rangle$ s as starting points in the control qubit, like with “a CNOT inverts the state of a target qubit when the control qubit is $|1\rangle$ ». But the CNOT will always have an effect on the target qubit when the control qubit is not exactly in the $|0\rangle$ state.

You just need to have a non-null β complex amplitude component in the first qubit. So, the only case a CNOT will do nothing on the target qubit is when the control qubit is exactly a $|0\rangle$.

To fully understand the effect of these gates on any qubit state and computational basis vectors for several qubits, you have to look at the unitary matrices implementing these gates and their linear effects on the qubits and/or register computational basis vectors.

³¹⁸ Here are a few sources of information on the subject of quantum gates: [Gates, States, and Circuits](#) by Gavin E. Crooks, July 2021 (82 pages), [Universality of Quantum Gates](#) by Markus Schmassmann, 2007 (22 slides), [An introduction to Quantum Algorithms](#) by Emma Strubell, 2011 (35 pages), [Equivalent Quantum Circuits](#) by Juan Carlos Garcia-Escartin and Pedro Chamorro-Posada, 2011 (12 pages), [The Future of Computing Depends on Making It Reversible](#) by Michael P. Frank, 2017.

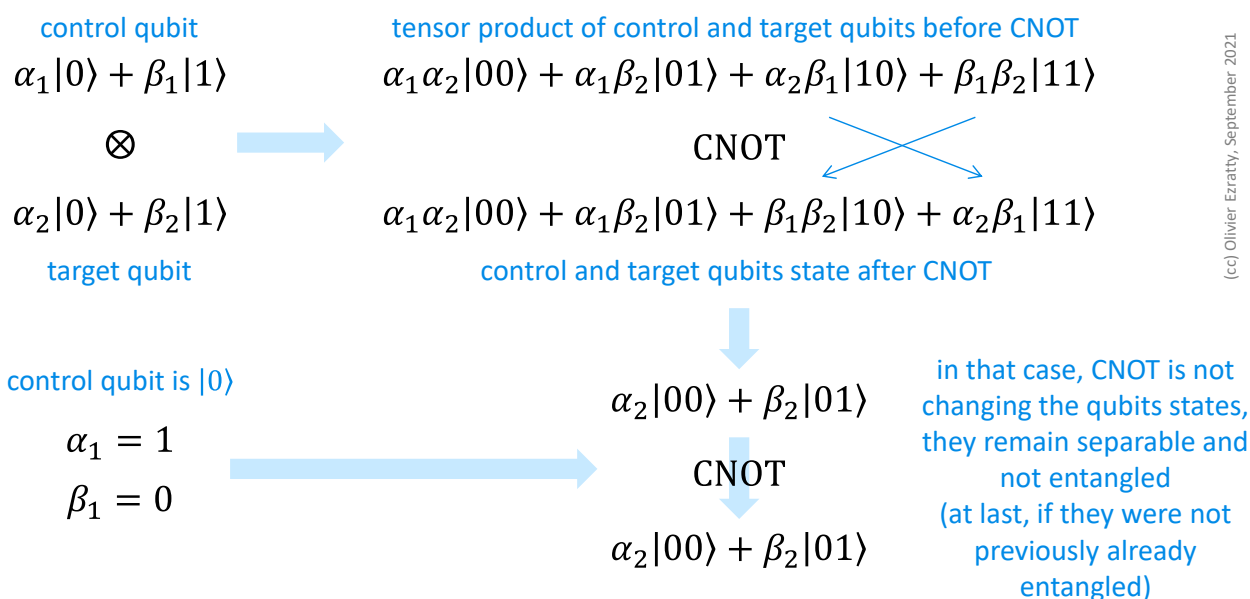


Figure 176: visualization of a CNOT two-qubit gate effect, generically and with a control qubit at $|0\rangle$, the only case when it won't generate any qubit entanglement. (cc) Olivier Ezratty, 2021.

In other words, and as demonstrated in Figure 176, unless the control qubit is $|0\rangle$, a CNOT gate will create some new entanglement between the control and target qubit. But one could argue two things: first, after a couple of operations, we never have a perfect $|0\rangle$ and are rapidly off-bounds, creating tiny entanglements with CNOT gates in that case, and second, most CNOT gates are run after a Hadamard gate was applied on the control qubit, getting off the $|0\rangle$ state!

Let's add a number of two-qubit gates which play a particular role. These are physical gates implemented at the lowest control level depending on the qubit type. They are not necessarily directly useful for developers but are the basis of some specific universal gates sets with some qubit types.

- **$\sqrt{\text{SWAP}}$ gate**, or square root SWAP, stops halfway through a SWAP. It is a physical level gate used to entangle electron spin qubits.
- **iSWAP gate** is a two-qubit gate that is implemented in superconducting qubits like those from IBM.
- **XY gate** is a generic two-qubits gate implementing a rotation by some angles β and θ between the states $|01\rangle$ and $|10\rangle$ and $\text{iSWAP} = \text{XY}(0, \pi)$. It's a physical gate proposed by Rigetti that can be implemented on superconducting qubits to reduce the number of two-qubits gates required to run many algorithms³¹⁹.
- **ZZ gate** that is implement with qubits coupling is a technique that can be used with qubit couplers to connect two superconducting qubits and implement as a CZ gate³²⁰.

$$\sqrt{\text{SWAP}} = \begin{bmatrix} 1 & 0 & 0 & 0 \\ 0 & \frac{1}{2}(1+i) & \frac{1}{2}(1-i) & 0 \\ 0 & \frac{1}{2}(1-i) & \frac{1}{2}(1+i) & 0 \\ 0 & 0 & 0 & 1 \end{bmatrix}$$

Figure 177: a $\sqrt{\text{SWAP}}$ unitary matrix.

$$\text{XY}(\beta, \theta) = \begin{bmatrix} 1 & 0 & 0 & 0 \\ 0 & \cos(\frac{\theta}{2}) & i \sin(\frac{\theta}{2})e^{i\beta} & 0 \\ 0 & i \sin(\frac{\theta}{2})e^{-i\beta} & \cos(\frac{\theta}{2}) & 0 \\ 0 & 0 & 0 & 1 \end{bmatrix}$$

Figure 178: an $\text{XY}(\theta, \pi)$ two-qubit gate unitary matrix.

³¹⁹ See [Implementation of the XY interaction family with calibration of a single pulse](#) by Deanna M. Abrams et al, 2019 (13 pages).

³²⁰ See [Implementation of Conditional Phase Gates Based on Tunable ZZ Interactions](#) by Michele C. Collodo, Andreas Wallraff et al, PRL, May 2020 (10 pages).

- R_{xx} , R_{yy} and R_{zz} are two-qubit gates that are implemented natively in some trapped ion quantum computers as a Mølmer-Sørensen gate. They are called Ising coupling gates. The gate R_{xx} is implemented natively in IonQ systems. These gates were also created for the first NMR quantum computing systems.
- **Mølmer-Sørensen gate**, **Cirac-Zoller gate (C-NOT)**, **AC Stark shift gate** and **Bermudez gate** are various two-qubit gates implemented at the physical level with trapped ions qubits. The Mølmer-Sørensen gate is a “mixed-species” entangling gate that can couple different breeds of ions. It is also less sensitive to motion temperature. It’s the main entangling gate for IonQ trapped ion computers.

| | atoms | | electrons & spins | | | | photons |
|--------------------|-----------------------|---------------------------------|---|----------------------|------------|-------------------|------------------------------------|
| qubit type | trapped ions | cold atoms | super-conducting | silicium | NV centers | Majorana fermions | photons |
| single qubit gates | rotations | $U_{xyz}(\theta, \psi, \mu)$ | $R_x(\pm\pi/2), R_z(\lambda)$ (IBM, Rigetti) | R_x, R_y | R_x, R_y | T, H | X, Z, H X, Z, R, CZ (Xanadu) |
| two qubit gates | XX Mølmer-Sorensen | C-Z $C-U_{xy}(\theta, \psi)$ | CNOT, iSWAP (IBM) C-Z (Rigetti) | $\sqrt{\text{SWAP}}$ | CNOT | CNOT | CNOT |

(cc) Olivier May, July 2021

Figure 179: examples of physical qubit gates implement by specific qubit types. Consolidation (cc) Olivier Ezratty, 2021.

Logical reversibility. Quantum gates have the particularity of being logically reversible. It can easily be visualized for a single qubit gate, which is a simple rotation in the Bloch’s sphere and therefore, reversible with the inverse rotation. A multi-qubit gate is a rotation in a wider dimensional space, with 2^N dimensions, N being the number of qubits. Likewise, it’s logically reversible with an inverse rotation, but harder to visualize.

We can rewind some parts of algorithms by applying in reverse order the quantum gates that have just been applied to a set of qubits³²¹. One benefit of this process is the so-called uncompute trick used in some oracle-based algorithms. It enables resetting the ancilla qubits used in computation without doing any reading. It avoids damaging the useful qubits that we need to use for the rest of the algorithm.

That being said, qubits can undergo other operations. They could be stored, meaning transferred, in or from quantum memory. They can also be used to encode two bits instead of one, in what is called "superdense coding", which is mainly used in quantum telecommunications³²².

Gates classes. The science of quantum gates has led to the creation of many concepts, theorems about groups of quantum gates. They are associated with the notion of **universal gate sets**, capable of generating all other quantum gates.

Figure 180 contains a custom diagram summarizing these classes of quantum gates. In short, $SU(2^n)$ is the space of unitary transformations applicable on n qubits. It covers all the quantum computations that can be performed on n qubits. $SU(2)$ includes all the unitary transformations that can be performed on one qubit (with $n=1!$). Clifford’s group includes gates with one and discrete qubits quarter-turn rotation plus conditional gates. T (eighth turn) and R as Control-R gates with different angles from π and $\pi/2$ are not in Clifford’s group. They are needed to cover $SU(2)$ and $SU(2^n)$ well. In practice, the addition of the T gate is enough to create a universal gate set with using approximations.

³²¹ See [Synthesis and Optimization of Reversible Circuits - A Survey](#) by Mehdi Saeedi and Igor Markov, 2011 (34 pages), which reviews the algorithmic impact of reversibility in both classical and quantum computing.

³²² See [From Classical to Quantum Shannon Theory](#), 2019 (774 pages) which describes the application of Shannon’s information theory to quantum computing. As well as [On superdense coding](#), August 2018, by Fred Bellaïche, an Econocom engineer who publishes very interesting and popularized scientific articles on quantum.

The classification of the gates begins with the **Pauli gates** that apply half-turn rotations around the X, Y and Z axes of the Bloch sphere of representation of the qubits.

Pauli group includes the gates resulting from the combination of these three Pauli gates and the sign inversion operations on the α or the β of the qubits (± 1 and $\pm i$). On one qubit, the Pauli group includes the gates $\pm I$, $\pm iI$, $\pm X$, $\pm iX$, $\pm Y$, $\pm iY$, $\pm Z$, and $\pm iZ$ (where I is the identity).

Clifford group includes single and multiple qubit gates that standardize the Pauli group applicable to n qubits, i.e., the U gates of this group combined with the Pauli group gates σ with $U\sigma U^*$ generate Pauli group gates. A Clifford gate is a quantum gate that can be decomposed into Clifford group gates. These include Pauli gates (X, Y, Z) and H, S (90° rotation) and CNOT (also called CX for *control-X*) gates. The Clifford group is very large as soon as $n > 1$. Its size is respectively 24, 11,520 and 92,897.280 elements for $n=1, 2$ and 3 ³²³. It is usually said that Clifford group gates are digital quantum gates while non-Clifford gates are analog.

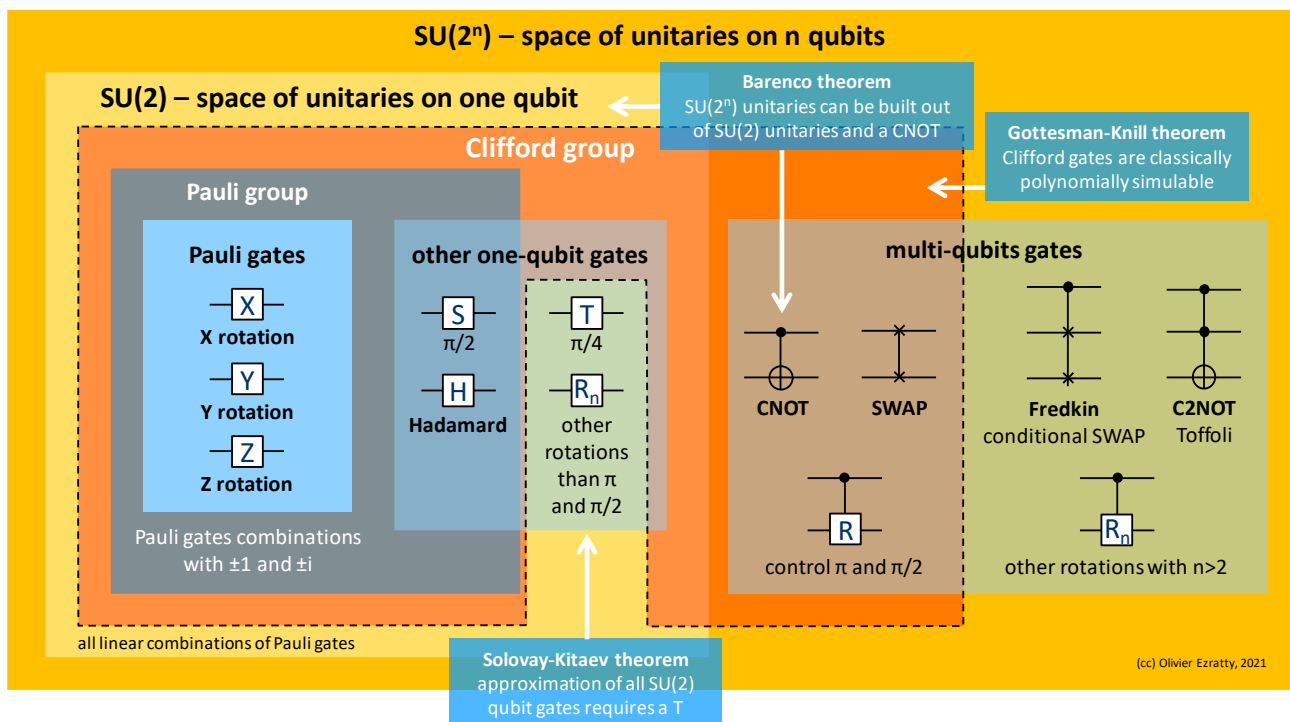


Figure 180: a visual taxonomy of qubit gates explaining the Pauli gates, the Pauli group, the Clifford group and the role of T and R gates to create a universal gate set. (cc) Olivier Ezratty, 2021.

Gottesman-Knill's theorem demonstrates that algorithms using gates in the Clifford group can be simulated in polynomial time on classical computers. It means that they are insufficient to provide an exponential speedup compared to classical computing³²⁴. Another variant of this theorem from Leslie G. Valiant defines conditions for a quantum algorithm to be classically simulable in polynomial time on a classical computer³²⁵.

³²³ See [Clifford group](#) by Maris Ozols, 2008 (4 pages). Clifford is the name of an English mathematician, William Kingdon Clifford (1845-1879) who is not related to the group that bears his name.

³²⁴ See [Positive Wigner Functions Render Classical Simulation of Quantum Computation Efficient](#) by A. Mari and J. Eisert, December 2021 (7 pages) that generalizes the Gottesman-Knill theorem to quantum systems that preserve the positivity of the Wigner function (aka, do not use non-Gaussian photon states). It creates additional constraints on how to obtain exponential speedups with photon based quantum computers. It is also discussed in [Quantum computational advantage implies contextuality](#) by Farid Shahandeh, December 2021 (6 pages).

³²⁵ See [Quantum Computers that can be Simulated Classically in Polynomial Time](#) by Leslie G. Valiant, 2002 (10 pages).

So, how can we obtain an exponential acceleration? It is necessary to use gates with more than two qubits implementing entanglement to obtain this acceleration like the Toffoli gate³²⁶. This can also be achieved with using phase-controlled R gates that are not part of Clifford's group, which can be approximated with adding a T gate. These non-Clifford gates have a particularity: they are difficult to correct with quantum error correction codes and to be implemented in a fault-tolerant manner. We'll see that [later](#) in page 235. On top of that, a maximally entangled state is required among the used qubits which makes sense since separable subsets of the qubit register wouldn't provide a large Hilbert space for computation. To create a universal gate set, you need to use two gates that don't commute or anticommute. T and H gates don't commute whereas all Pauli gates anticommute ($XY=-YX$, $ZX=-XZ$, $YZ=-ZY$). Geometrically, commuting and anticommute happens when the related gates rotation axis are respectively parallel (like S and T) and orthogonal in the Bloch sphere (X and Y, or X and Z). With T and H, they are neither parallel or orthogonal but separated by a 45° turn³²⁷.

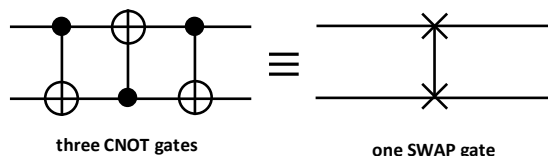
Continuous gates make it possible to generate rotations of any angle in the Bloch sphere. The latter allow to generate all the phase-controlled R gates we have just seen and which are indispensable for QFT (Quantum Fourier Transform) based algorithms. Only a few qubits technologies can generate these gates at the hardware level, and usually with a poor precision.

Discrete gates are sets of (Hadamard, Z, S, CNOT) that make at best only half and quarter turns in the Bloch sphere.

Universal gate set is a group of gates that has the property of allowing the creation of all unitary operations on a set of qubits. From a practical point of view, also it allows to create all known quantum gates for one, two and three qubits. Such a gate-set must be able to create superpositions, entanglement and it must have at least one gate with no-real parameters (i.e. complex numbers instead of real numbers).

Here are some known sets of universal gates:

- CNOT + all single qubit unitaries can enable the creation of any unitary transformation on any number of qubits. This is demonstrated in the **Barenco theorem** according to which $SU(2^n)$ unitaries can be built out of $SU(2)$ unitaries and a CNOT two qubit gate³²⁸. It also demonstrates that any unitary transformation $SU(2^n)$ on n qubits can be built with a maximum of 4^n elementary quantum gates.
- CNOT + T (eighth of turn) + Hadamard, using approximations, linked to the **Solovay-Kitaev's theorem**. It proves that a dense and finite set of quantum gates in $SU(2)$ space allows can be used to reconstruct any gate in this space with a maximum error rate ϵ .



a set of universal gates can be combined to create all sorts of quantum gates. it requires at least one two-qubit gates like a CNOT.

Figure 181: how to create a SWAP gate with three CNOT gates.

The number of gates to be chained is a polynomial order of magnitude of $\log(1/\epsilon)$. The $SU(2)$ space is the Special Unitary group of dimension two.

It includes unit matrices (from determinant 1) with complex coefficients and dimension 2.

$$SU(2) = \left\{ \begin{pmatrix} \alpha & -\bar{\beta} \\ \beta & \bar{\alpha} \end{pmatrix} : \alpha, \beta \in \mathbb{C}, |\alpha|^2 + |\beta|^2 = 1 \right\}$$

³²⁶ See [On the role of entanglement in quantum computational speed-up](#) by Richard Jozsa et Noah Linden, 2002 (22 pages).

³²⁷ See [Quantum computing 40 years later](#) by John Preskill, June 2021 (49 pages).

³²⁸ See [Elementary gates for quantum computation](#) by Adriano Barenco, Charles Bennett, David DiVincenzo, Peter Shor and al, 1995 (31 pages).

This search for a set of discrete quantum gates allowing by approximation to generate a set of continuous gates of arbitrary rotations is important for some algorithms that we will see later, notably the discrete Fourier transform that is exploited in Shor's algorithm. You can see below in Figure 182 the effect of the sequence of T and H gates which, according to the combinations, allow to cover the different positions of Bloch's sphere, validating **Solovay-Kitaev's theorem**³²⁹. Transpilers are the parts of quantum code compilers that convert any quantum gate in the underlying universal gate set implemented by the quantum processor and handle related optimizations.



Figure 182: a visual description of Solovay-Kitaev's theorem. Source: TBD.

Inputs and outputs

Traditional microprocessors are composed of fixed logic gates, etched into the silicon, and 'moving' bits, which are electrical pulses that propagate through the circuit through the various gates. All this at a certain frequency, often in GHz, set by a quartz clock.

In a quantum computer, the first stage of processing consists of resetting the quantum register into an initial state. This is called "preparing the system". The various registers are first physically configured in the $|0\rangle$ state. The following initialization consists in using different operators such as the Hadamard transformation to create $|0\rangle+|1\rangle$ superposition or the X gate to change this value $|0\rangle$ to $|1\rangle$. Sometimes, more preparation is required to prepare a denser register state, like with quantum machine learning algorithms. Once this initialization is done, computing gates operations are sequentially applied to the qubits according to the algorithm to be executed.

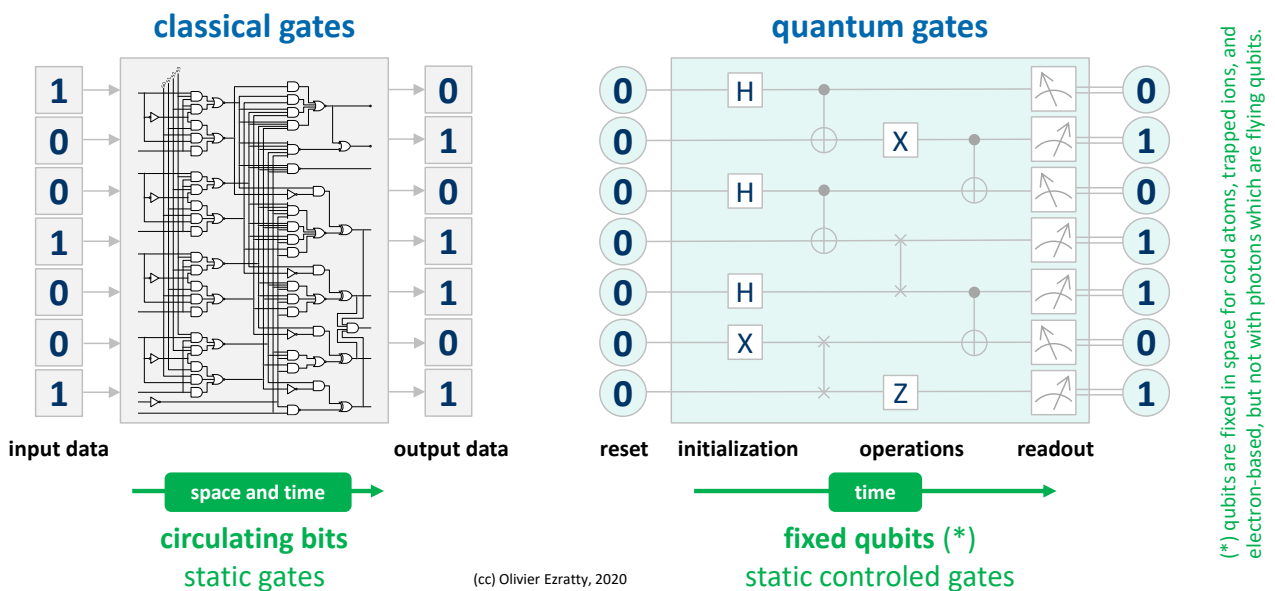


Figure 183: time and space differences with classical logic and quantum gates. (cc) Olivier Ezratty, 2021.

³²⁹ See [Shorter quantum circuits](#) by Vadym Kliuchnikov et al, Microsoft, Facebook and the Universities of Birmingham, Oxford, Bristol and Brussels, March 2022 (83 pages) which proposes an efficient method to generate any unitary with fewer gates, and [T-count and T-depth of any multi-qubit unitary](#) by Vlad Gheorghiu, Michele Mosca, Priyanka Mukhopadhyay, October 2021-October 2022 (28 pages) which defines lower bounds for these T gate usage.

They always include some multi-qubits gates implementing entanglement between qubits. Finally, qubits are measured at the end of the processing, which has the effect of modifying their quantum state.

Quantum algorithms diagrams for universal gates computers (*below right*) are most often time diagrams, whereas for classical logic gates it is also a physical diagram. In the right part describing a quantum algorithm, there are no physical wires connecting the qubits between an input and an output, the gates being in their path. It is a time-based schema!

A quantum algorithm is the description of a quantum circuit made of a series of sequenced timely quantum gates operating on 1, 2 and sometimes 3 qubits. It's the way to create a large unitary transformation on the initialized qubits.

Now, let's toy a little bit with qubits and gates with Quirk, particularly to identify pure and mixed states with single or two qubits. It also shows the role of off-diagonal values in density matrices.

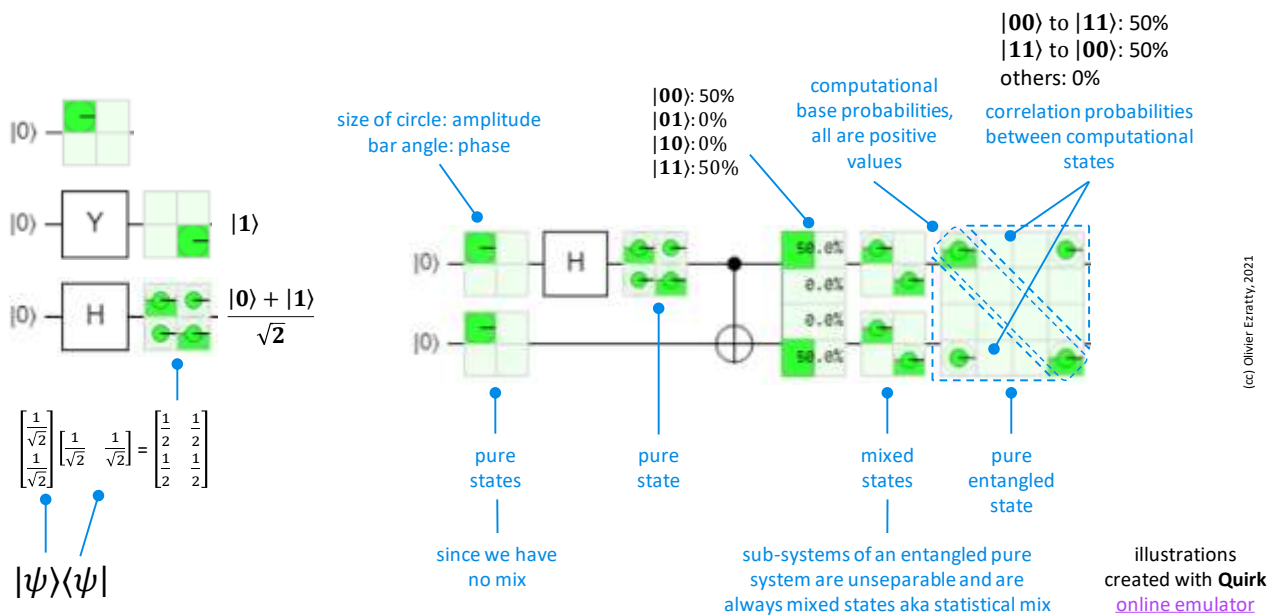


Figure 184: on examples of toying with Quirk to see how pure and mixed states look with two qubits. (cc) Olivier Ezratty, 2021.

Here, we describe a mixed state generated on two qubits after one of them is entangled with a third qubit.

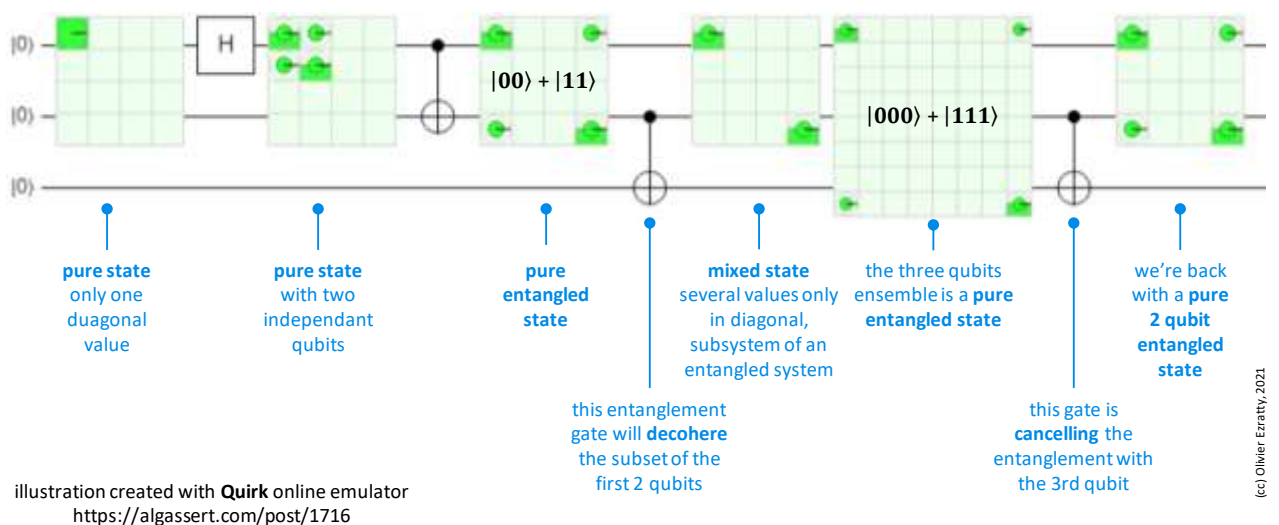


Figure 185: three examples of toying with Quirk to see how pure and mixed states look with three qubits. (cc) Olivier Ezratty, 2021.

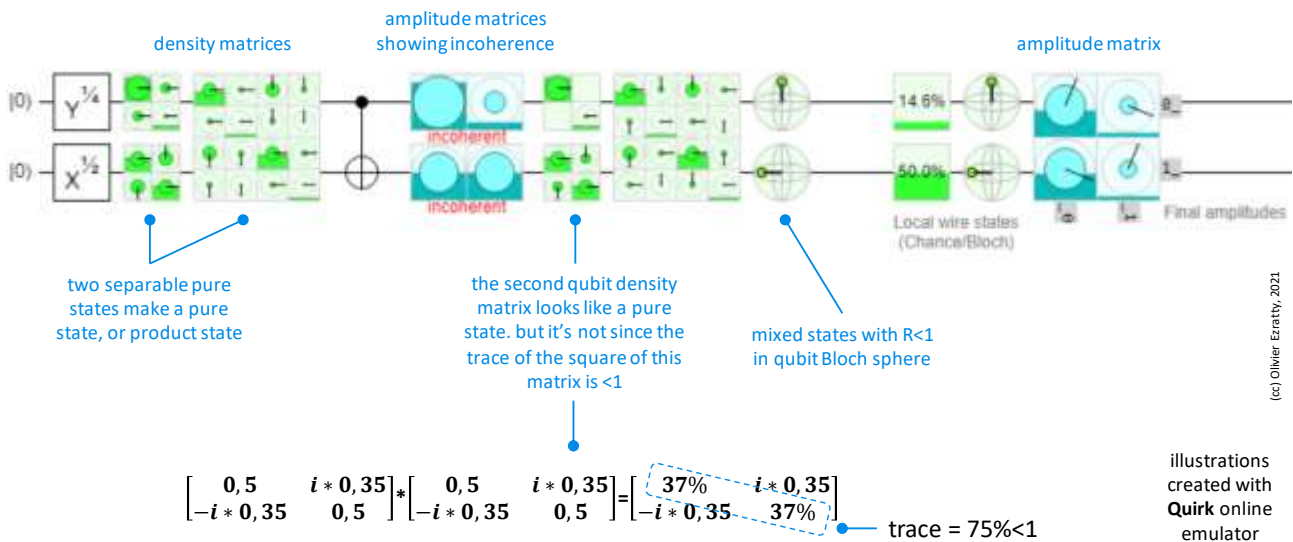


Figure 186: three examples of toying with Quirk to see how pure and mixed states look with two qubits. (cc) Olivier Ezratty, 2021.

Qubit lifecycle

One way to understand how a universal gates quantum computer works is to track the life of a qubit during processing:

Initialization. A qubit is always initialized at $|0\rangle$, corresponding to the base state, usually at rest, of the qubit. This initialization consumes some energy with all known types of qubits.

Preparation. It is then programmatically prepared with quantum gates to adjust its values that are vectors in the Bloch sphere. The Hadamard gate is one of the most common one and creates a superposed state of $|0\rangle$ and $|1\rangle$. Single qubit gates apply a rotation of the qubit vector in the Bloch sphere. These rotations are based on unitaries, 2×2 complex number matrix operations applied to the qubit vector $[\alpha, \beta]$. These unitaries have a trace of 1, maintaining the vector length of 1. For most quantum algorithms, qubit preparation is usually simple with a set of X gates to set them and H gates to create superposed states. In some cases, like with quantum machine learning, qubit states preparation can be more complex, requiring a lot of gates.

Multiple-qubit gates then conditionally link qubits together. Without these quantum gates, little could be done with qubits.

Data manipulation. The qubits information that is manipulated during computing is "rich" with a dimension of two real numbers, the angles θ and ϕ , or the vector $[\alpha, \beta]$ for each qubit. But a set of N qubits holds 2^N complex number values, representing the proportion of each of the computational basis states made of the various combinations of N 0s and 1s. It creates a dimensionality of $2^{N+1} - 1$ real numbers, to take into account the normalization constraint for the computational basis states amplitudes. As these gates are operated on the qubits, quantum computing works in an analog way³³⁰.

Measurement. When we measure the value of a qubit, we obtain a classical binary 0 or 1 with a probabilistic return depending on the qubit state. So, for each qubit, we have a 0 as input, a 0 or a 1 as output, and an infinite number of states in between during calculations.

³³⁰ This is the position stated in [Harnessing the Power of the Second Quantum Revolution](#) by Ivan H. Deutsch, November 2020 (13 pages). Or more precisely, the author states that gate-based quantum computers are both digital and analog.

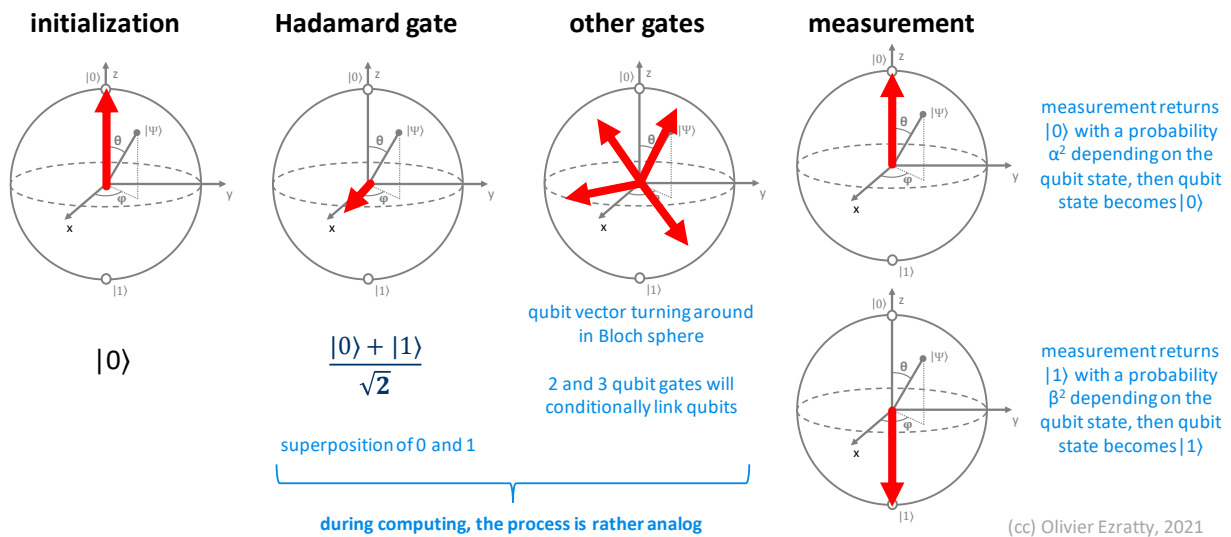


Figure 187: the effect of measurement on a single qubit. (cc) Olivier Ezratty, 2021.

All this to say that the mathematical richness of qubit-based quantum computing happens only during processing. This is the life cycle of the qubit illustrated in the above diagram in Figure 187.

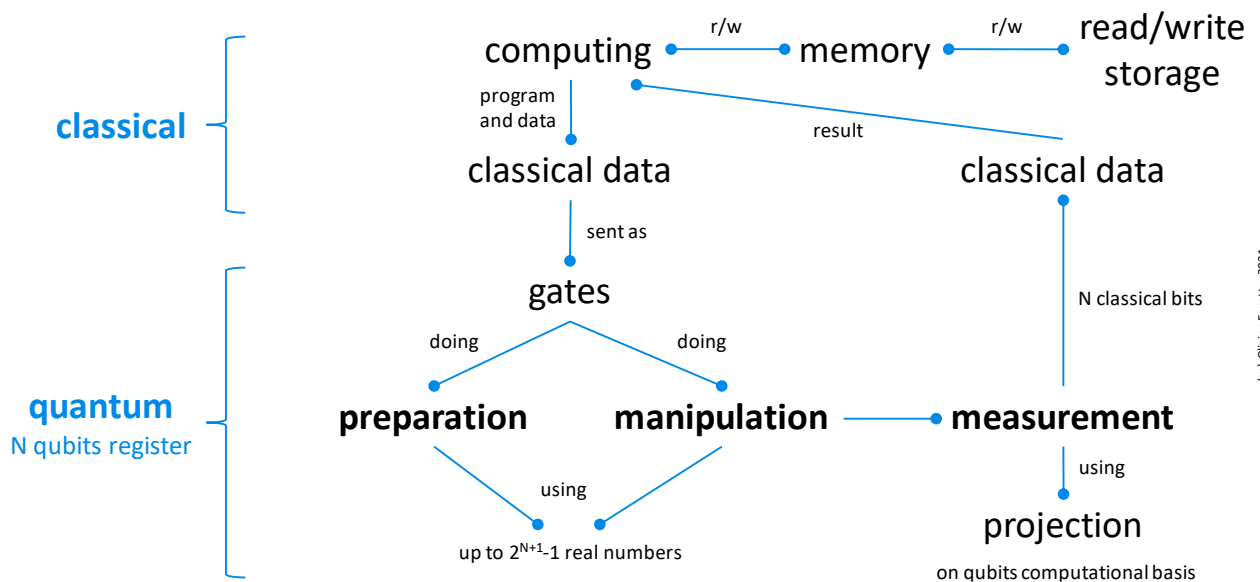


Figure 188: classical and quantum data flow in gate-based quantum computing. (cc) Olivier Ezratty, 2021.

Another schematic view of how classical and quantum computing are intertwined and the format of data that is handled is provided in Figure 188. What is specific to quantum computing is that the same instructions handle data and computing, i.e. quantum gates. The wealth of data in registers exists only during computing but not at the end, after measurement, where it is back in classical mode, turning the computational basis state vector of dimension $2^{N+1}-1$ real numbers to a meager N classical bits.

Quantum switch is a curious artefact worth mentioning here. It consists in creating a series of qubit transformations that can be implemented simultaneously in different orders. Like say, A then B and B then A, on a given register state. It defies logic and understanding of time flow, creating an indefinite causal order³³¹.

³³¹ See [Comparing the quantum switch and its simulations with energetically-constrained operations](#) by Marco Fellous-Asiani, Raphaël Mothe, Léa Bresque, Hippolyte Dourdent, Patrice A. Camati, Alastair Abbott, Alexia Auffèves and Cyril Branciard, August 2022 (20 pages).

It can even be a useful resource for improving reliability of quantum communications³³².

Measurement

We'll now look into quantum measurement, a much broader topic than you may think. We have already explained that quantum measurement is assimilated to a wave function collapse onto basis states, in the case of qubits, $|0\rangle$ or $|1\rangle$. We've also seen that quantum computing is highly probabilistic, requiring executing several times your calculation and making an average of the obtained results.

But quantum measurement is way more subtle than that. We'll see here what can be measured in qubits and when, what is a projective measurement, what is a POVM, a CPTP map, what are gentle and weak measurements, non-selective and selective measurement, state tomography and the likes. Some of these techniques are related to quantum computing, including error corrections and some hardware benchmarking tasks and others with quantum telecommunications.

Projective measurement

A projective measurement is the most generic form of measurement used in quantum computing. We'll first describe it geometrically and then with some mathematical formalism. Projective measurement is also named a von Neumann measurement since **John Von Neumann** elaborated its formalism in 1932.

It's easy to intuitively understand what it looks like with using the Bloch sphere for a qubit. A projective measurement consists in doing a geometrical vector projection of your qubit pure state on any axis in the Bloch sphere.

The simplest case of all is a projection on the z axis containing the $|0\rangle$ and $|1\rangle$ orthogonal vectors. It's about doing a measurement in the qubit computational basis. It could also be, theoretically, a projection on any other axis, like the $|+\rangle$ and $|-\rangle$ states that sit on the Bloch sphere equator along the x axis. We'll see later how to achieve this feat.

While quantum gates are reversible operations based on unitary operators, reading the state of the qubits is an irreversible operation. It is not a rotation in Bloch's sphere but a projection on an axis, which will yield a binary result with a probability depending on the qubit state. The projection is using a self-adjoint matrix operator, meaning that if executed several times, you'll always get the same result. Of course, the measurement of the qubit modifies its state unless it's already a perfect $|0\rangle$ or $|1\rangle$.

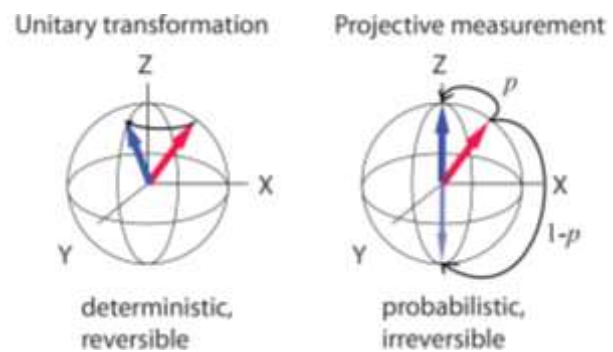


Figure 189: visual difference between a unitary transformation (gate) and a projective measurement. Source: [A computationally universal phase of quantum matter](#) by Robert Raussendorf (41 slides).

After a projective measurement on the Z axis, the qubit will irreversibly collapse in the states $|0\rangle$ or $|1\rangle$. Qubits measurement is reversible only in the case when they are already perfectly in the computational basis states $|0\rangle$ or $|1\rangle$. In that case, the measurement along the Z axis is not changing the qubit value and is therefore reversible since it's an identity operation.

Mathematically, a projective measurement is using Projection-Valued Measures (PVMs) on a closed system. On a given qubit, it uses two orthogonal measurement operators, in the form of 2x2 self-adjointed (Hermitian) matrices.

³³² See [Improvement in quantum communication using quantum switch](#) by Arindam Mitra, Himanshu Badhani and Sibasish Ghosh, September 2022 (14 pages).

When measuring a qubit along the Z axis, also named the observable Z with eigenvalues +1 and -1 and eigenvectors $|0\rangle$ and $|1\rangle$ (the observable Z is the matrix representation of a Z single qubit quantum gate!), these PVMs operators are respectively:

$$M_0 = |0\rangle\langle 0| = \begin{bmatrix} 1 & \\ & 0 \end{bmatrix} \begin{bmatrix} 1 & 0 \\ & 0 \end{bmatrix} = \begin{bmatrix} 1 & 0 \\ 0 & 0 \end{bmatrix} \quad \text{and} \quad M_1 = |1\rangle\langle 1| = \begin{bmatrix} 0 & \\ & 1 \end{bmatrix} \begin{bmatrix} 0 & 1 \\ & 0 \end{bmatrix} = \begin{bmatrix} 0 & 0 \\ 0 & 1 \end{bmatrix}$$

Given the Z observable operator is $Z=M_0 - M_1$, which returns +1 for $|0\rangle$ and -1 for $|1\rangle$.

On a general basis, with a quantum object with several distinct states, a measurement operator is a matrix M_m and the probability to get the outcome m (with $m=0$ and 1 in the case of a qubit, or $m=0$ to $N-1$ in the case of a N states quantum object) is $p(m) = \langle \psi | M_m^\dagger M_m | \psi \rangle$ with the completeness constraint $\sum_m M_m^\dagger M_m = I$ (I being the identity matrix).

For $m=0$, it reads as $p(0) = [\alpha \ \beta] \begin{bmatrix} 1 & 0 \\ 0 & 0 \end{bmatrix} \begin{bmatrix} 1 & 0 \\ 0 & 0 \end{bmatrix} \begin{bmatrix} \alpha \\ \beta \end{bmatrix} = [\alpha \ \beta] \begin{bmatrix} \alpha \\ 0 \end{bmatrix} = \alpha^2$! Since $\beta^2 = 1 - \alpha^2$ due to the Born normalization rule, only one measurement is required to get both α^2 and β^2 , these being not individual measurement results but their respective probabilities.

Any global phase added to $|\psi\rangle$ will disappear during measurement. If we define $|\psi'\rangle = e^{i\theta} |\psi\rangle$ and apply a measurement operator M_m on $|\psi'\rangle$:

$$p'(m) = \langle \psi' | M_m^\dagger M_m | \psi' \rangle = \langle \psi' | e^{-i\theta} M_m^\dagger M_m e^{i\theta} | \psi' \rangle = \langle \psi' | M_m^\dagger M_m | \psi' \rangle = p(m)$$

After the measurement with the operator M_m , the system state $|\psi\rangle$ becomes the projection of $|\psi\rangle$ on M_m divided by the probability of getting state m:

$$\frac{M_m |\psi\rangle}{\sqrt{\langle \psi | M_m^\dagger M_m | \psi \rangle}} \quad \text{also often written} \quad \frac{M_m |\psi\rangle}{\sqrt{\langle \psi | M_m | \psi \rangle}}$$

since $M_m^\dagger = M_m$ (self-adjoint matrix) and $M_m M_m = M_m$ (projector matrix)

All these measurement equations are part of the measurement postulate (usually the third) from quantum mechanics postulates.

In Figure 190, let's make a pause to understand the $\langle A|B|C \rangle$ Dirac notation. You usually read it from the right. The ket on the right is a vertical vector that is multiplied by the middle object that is a square matrix. It creates a similar vertical vector. Then, you multiply it with the bra on the left which is a horizontal vector. It is a dot product of an inner scalar product. The result is a complex number and it is a real number when $\Psi = \phi$.

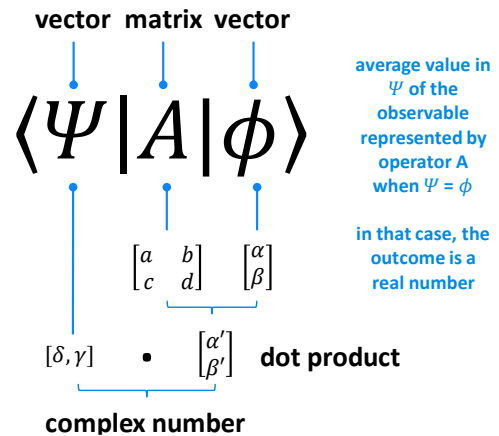


Figure 190: understanding the $\langle A|B|C \rangle$ Dirac notation.

Now, let's be a bit practical.

How can we change the measurement basis with qubits, for implementing a measurement along another axis than Z? At least two options are available:

- It may be possible to *physically* implement a measurement on a different basis than the computational basis. This is, for example, the case with polarization-based photon qubits where the polarizer angle can be dynamically and programmatically modified with some electrically controlled optical settings. It looks more difficult to implement for other types of qubits.

- When the *only* supported measurement is a projective measurement in the computational basis $|0\rangle$ and $|1\rangle$, any another projective measurement can be implemented with first applying a unitary transformation to the qubit that creates a rotation in the Bloch sphere equivalent to moving the measurement axis to the Z axis ($|0\rangle$ and $|1\rangle$). When we say we do an “X” or “Y measurement”, it means that we first apply a H or HS^\dagger single gate rotation (H = Hadamard gate and S = half a Z gate or quarter phase turn) to handle this axis rotation and then, apply a (computational basis) Z-axis measurement. This is what is regularly done with quantum error correction codes as well as with MBQC (measurement-based quantum computing).

With QECs (quantum error correction codes), this sort of projective measurement is applied to ancilla qubits, these additional qubits that detect errors in entangled computing qubits. So, when physicists say they are doing a measurement on a basis of two orthogonal vectors, they mean they are applying first a unitary transformation and then a measurement on the computational basis.

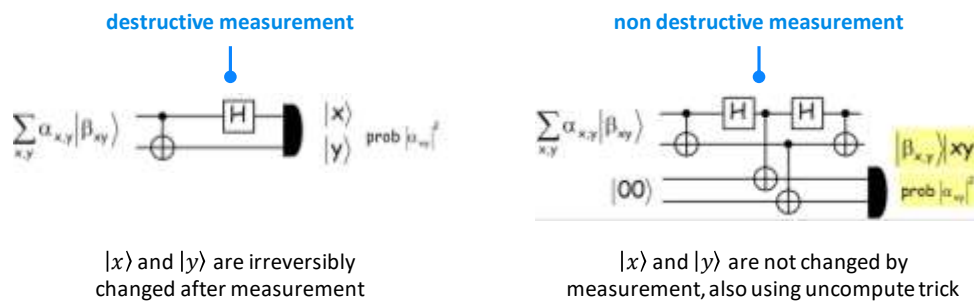


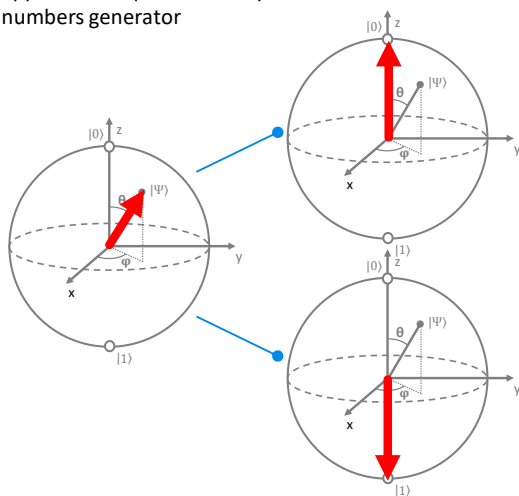
Figure 191: how a projective measurement in a different basis can implement non-destructive measurement. Which is actually different from the notion of QND (quantum-non-destructive measurement) that we'll define later.

Qubits register measurement

So far, we've just elaborated on measurement mathematical underlying tools and dealt with only one qubit. How about measuring a whole qubit register?

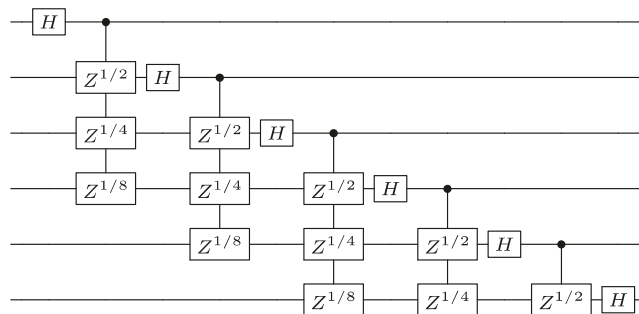
A N qubit register has 2^N possible computational basis states, from $|00\dots00\rangle$ to $|11\dots11\rangle$. When measuring once a qubit register, you get one of these states, being a combination of N 0s and 1s.

a single qubit measurement is probabilistic
 i.e.: a qubit register after a Hadamard gate applied to all qubits is a simple random numbers generator



on a practical basis:

- the algorithm is executed many times, up to 8000 for IBM Q Experience
- an average of qubits results is computed, producing a real number
- the averaged result is theoretically deterministic
- modulo the error generated by noise and decoherence



x1000 to x8000 shots required in NISC computers

Figure 192: a qubit probabilistic measurement and the notion of computing shots. (cc) Olivier Ezratty, 2021.

You could stop there and think, that's my result, fine, I'm done! Well, no! Since the measurement outcome is probabilistic and prone with errors, you need to run your algorithm a certain number of times and count the number of times you'll get each computational basis state. If doing so a great number of times, you'll end up recovering a probability distribution for each computational basis state and reconstruct a full state vector. But to do that, you'll need to execute your algorithm an exponential number of times with regards to the number of qubits, losing any gain coming from quantum computing.

The process you'll implement will depend on what data you want to extract from your prepared qubits register and the run algorithm. Usually, a quantum algorithm is supposed to generate a simple computational basis state (one given combination of 0s and 1s) and not a combination of several states and their respective probabilities.

measurement is using a collection $\{M_m\}$ of operators acting on the measured system state space $|\psi\rangle$, with probability of m being: $p(m) = \langle\psi|M_m^\dagger M_m|\psi\rangle$

system state after measurement becomes:

$$\frac{M_m|\psi\rangle}{\sqrt{\langle\psi|M_m^\dagger M_m|\psi\rangle}} \quad \text{with:} \quad \sum_m M_m^\dagger M_m = I$$

a measurement is **projective** if all measurement operators or projectors M_m are satisfying $M_m^2 = M_m$, aka « idempotency »

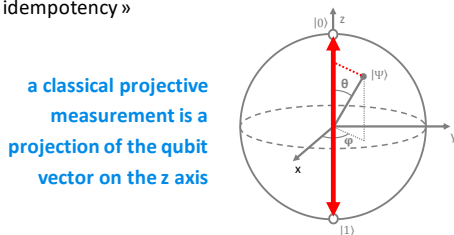


Figure 193: another explanation of projective measurement on a different basis and its usage in non-destructive measurement techniques like with error correction codes. (cc) Olivier Ezratty, 2021.

You can then run several times your algorithm and compute the average values of each qubit, giving a % of 0/1 for each then round up to the nearest 0 and 1. And there you are. What is "several"? It depends. IBM proposes to run your algorithm a couple thousand times on its cloud Q Experience platform with 5 to 65 qubits and states that this number will grow with the number of qubits, we hope linearly. I have not yet found the rule of thumbs used to define the number of runs, or "shots".

All in all, you must remember that one run of an algorithm is **probabilistic** and with many runs, you'll converge progressively to a **deterministic** solution being the average of all runs results.

From computational vector state to full state tomography

What are we measuring? A single computational state, a statistical weight of 0 and 1 or a full vector state? It depends on the algorithm and also on the actual technical need of the undertaken measurement. For most algorithms, a series of runs and qubit measurement and their average will output after roundup the found computational basis state.

For algorithms debugging with a reasonable number of qubits and for characterizing the quality of a small group of qubits, it may be useful to compute either a histogram of the whole computational state vector or even, a so-called quantum state tomography which will reconstitute the density matrix of the quantum register.

the z basis is qubit's **computational basis**:

$$M_{0=} |0\rangle\langle 0| = \begin{bmatrix} 1 & \\ & 0 \end{bmatrix} \quad [1 \quad 0] = \begin{bmatrix} 1 & 0 \\ 0 & 0 \end{bmatrix} \quad M_{1=} |1\rangle\langle 1| = \begin{bmatrix} 0 & \\ & 1 \end{bmatrix}$$

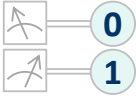
probabilities $p(0) = |\alpha|^2$ $p(1) = |\beta|^2$ removed global phase

state after measurement $\frac{\alpha}{|\alpha|}|0\rangle = e^{i\phi}|0\rangle$ $\frac{\beta}{|\beta|}|1\rangle = e^{i\phi}|1\rangle$

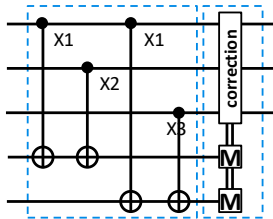
when **another basis projection** is required like x or y axis or any axis in the Bloch sphere, gates are applied to the qubit that change the qubit basis. we then measure qubits using the $|0\rangle$ and $|1\rangle$ basis.

for example, if we want to make a qubit measurement on the $|+\rangle$ and $|-\rangle$ basis, we first apply a X rotation on the qubit and then do a measurement in the $|0\rangle$ and $|1\rangle$ basis.

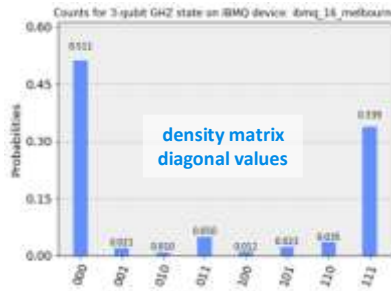
it enables **non destructive measurement** for the initial qubit and is used in most error correction codes that we'll see later.



qubits are measured at the end of computation on each qubit computational basis, several times and averaged: in the general case when the algorithm must generate a pure state.



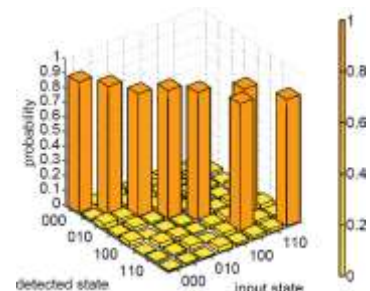
projective measurement on another basis (after X, Y, Z, R_x, R_y or R_z gates): such as with error correcting codes



an histogram with a 2^N probability split of qubits registers computational basis => useful when the algorithm result combines several states, mostly in the middle of an algorithm for debugging purpose.

at the end of computing, we are supposed to have only one bar with a value close to 1, which is easier the measure with a simple measurement method.

this histogram is possible to compute only for a **reasonable number of qubits** because of its exponential quantum computing cost.



fredkin gate tomography example

a quantum state tomography is a richer visualization with the full system density matrix => used to assess the quality of qubit gates, entanglement and measurement. more complicated to generate (more repeat projections/measurement). tomography is usually possible for a number of qubits ≤ 6.

Figure 194: from a vector state to a full density matrix, the various ways to measure the state of a qubit register. Compilation (cc) Olivier Ezratty, 2021.

The computational state vector is assembled with a lot of repeat runs and measurements with a number growing exponentially with the number of qubits. It will eventually provide the statistical distribution of each and every computational basis states. Since the number of runs grows exponentially, you understand quickly why it won't make sense to use this technique when we'll exploit a large number of qubits.

Development tools like IBM Quantum Experience dumps the vector state of your qubits only for helping you learn about how their system work and also understand the impact of noise and decoherence.

| | | | | | | |
|---|--|---|---|---|---|---|
| <p>computational basis states</p> <ul style="list-style-type: none"> 0000> 0001> 0010> 0011> 0100> 0101> 0110> 0111> 1000> 1001> 1010> 1011> 1100> 1101> 1110> 1111> <p>4 qubits example</p> | <p>computational state</p> <ul style="list-style-type: none"> α₁ α₂ α₃ α₄ α₅ α₆ α₇ α₈ α₉ α₁₀ α₁₁ α₁₂ α₁₃ α₁₄ α₁₅ α₁₆ <p>α_i : complex numbers</p> | <p>if we measure one qubit at position j, the returned value will be 0 with the probability:</p> $\sum_{i \in I_{q_j=0}} \alpha_i ^2$ <p>I_{q₁=0} contains the computational base states where the first qubit is 0</p> <p>probability to get a 1</p> $\sum_{i \in I_{q_j=1}} \alpha_i ^2$ <p>in this example, when all measurements returned 0, we got a 0000>. with repeating the operation several times, we get different computational basis states. after thousands runs, we obtain a rough distribution of α_i ² probabilities for all i. the intermediate Σ's and a lot of computing and matrix inversion may enable us to reconstruct a density matrix.</p> | <p>j=1</p> <ul style="list-style-type: none"> 0000> 0001> 0010> 0011> 0100> 0101> 0110> 0111> <p>when measuring the next qubit, we'll get a subset of probabilities for computational states where i ∈ I_{q₁=0}</p> | <p>j=2</p> <ul style="list-style-type: none"> 0000> 0001> 0010> 0011> 0100> 0101> 0110> 0111> 1000> 1001> 1010> 1011> 1100> 1101> 1110> 1111> <p>returned value for 2nd qubit</p> | <p>j=3</p> <ul style="list-style-type: none"> 0000> 0001> 0010> 0011> 0100> 0101> 0110> 0111> 1000> 1001> 1010> 1011> 1100> 1101> 1110> 1111> <p>returned value for 3th qubit</p> | <p>j=4</p> <ul style="list-style-type: none"> 0000> 0001> 0010> 0011> 0100> 0101> 0110> 0111> 1000> 1001> 1010> 1011> 1100> 1101> 1110> 1111> <p>returned value for 4th qubit</p> |
|---|--|---|---|---|---|---|

Figure 195: what happens to your qubits when you progressively measure them. (cc) Olivier Ezratty, 2021.

Reconstituting the whole system density matrix is a more tedious process. In the most basic technique used, we are keeping track of all intermediate measurements leading to getting the computational state vector and some matrix inversion is required to create it in the end. The process requires even more quantum and classical computation than for reconstituting the computational state vector. And it scales with 2^{3N}, N being the number of qubits!

This is usually applied with up to 6 qubits, and particularly with 2 qubits to characterize the quality of two qubit gates. A record state tomography of 8 qubits was achieved in 2005 with trapped ions by Rainer Blatt's group in Innsbruck³³³.

The graphical representation of these density matrices is often used to evaluate the fidelity of 2 or 3-qubit gates in research publications. The example in Figure 196 illustrates this with comparing the theoretical state of a density matrix for 2 and 4 qubits and measurement results. It also helps qualify the quality of qubits entanglement. Various techniques are proposed to speed-up quantum state tomographies and achieve it with a better precision.

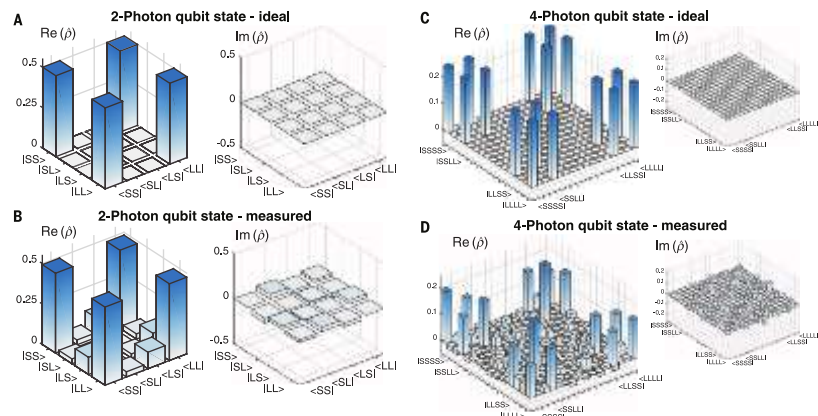
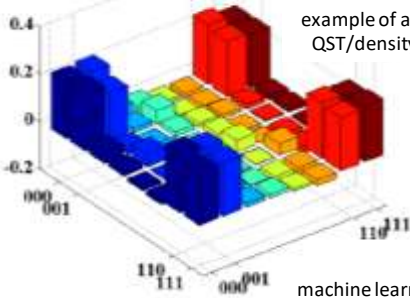


Figure 196: the difference between an ideal 2 and 4-photon density matrices and as measured in experiments. Source: [Generation of multiphoton entangled quantum states by means of integrated frequency combs](#) by Christian Reimer et al, Science, 2016 (7 pages).

However, this is a tool for researchers and hardware designers, not for quantum software developers³³⁴. The next step is a Quantum Process Tomography which qualifies the quantum channel of a given process, like a series of gates, one gate, or quantum noise and decoherence. It creates an even richer matrix with 2^{2N} columns and rows, representing a linear operator on the system density matrix, aka a superoperator.

reconstruction of a quantum system density matrix
via repeated measurements and statistical analysis of a large number of copies, or done with digital simulation. is using POVM measurement technique and matrix inversion. This is also done at the gate level (GST).

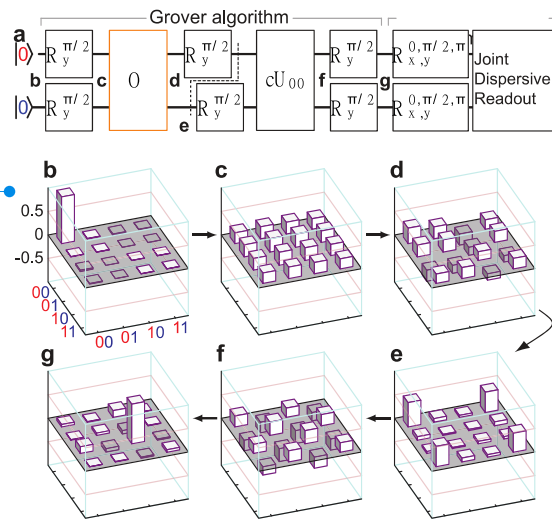
used to evaluate the functionality of qubits, quantum operations and entanglement quality



example of a 3-qubits QST/density matrix

machine learning and SVM may be used to determine the state

Figure 197: how do you reconstruct a quantum system density matrix.



source: Demonstration of Two-Qubit Algorithms with a Superconducting Quantum Processor by L.DiCarlo et al, 2009

Non-selective and selective measurements

A non-selective measurement is a measurement that is physically done but not yet read. For any reason, its outcome is not available either because it wasn't yet used or because it's really inaccessible when measurement is done by the environment. How is it different from a real measurement? It deals

³³³ See [Scalable multi-particle entanglement of trapped ions](#) by H. Haffner, Rainer Blatt et al, 2006 (17 pages).

³³⁴ See for example [Quantum process tomography via completely positive and trace-preserving projection](#) by George C. Knee et al, UK, 2020 (13 pages). But it requires some background knowledge!

with the information available about the quantum states we are evaluating. This is explained in the example below using photons polarization and relates with pure states and mixed states.

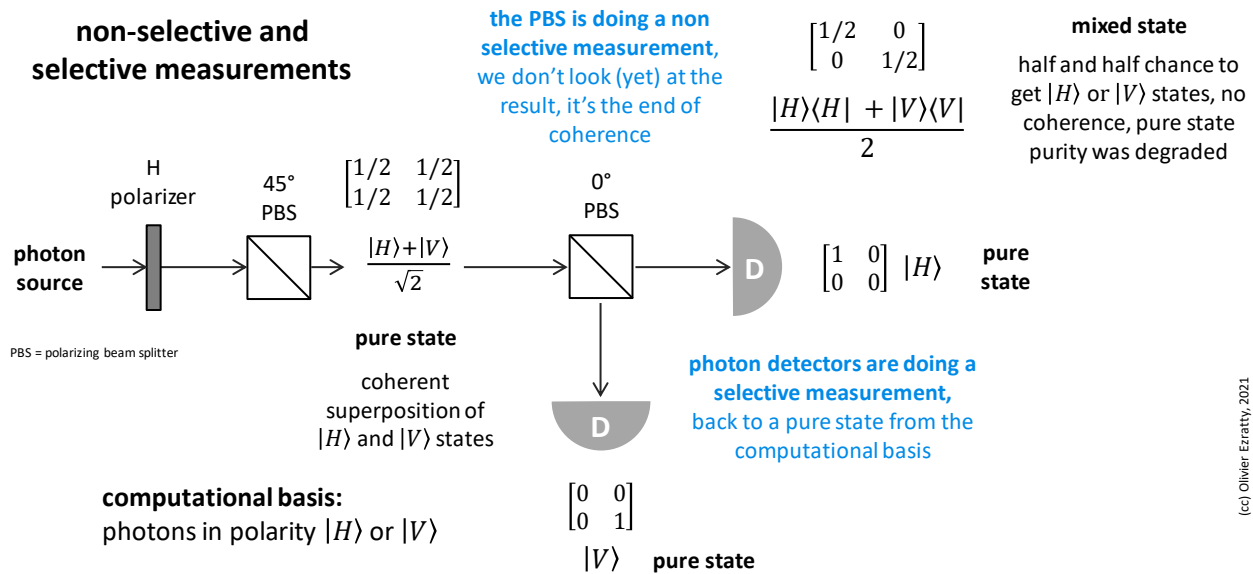


Figure 198: non-selective and selective measurements. (cc) Olivier Ezratty, 2021.

A single photons source generates photons that traverse first a horizontal polarizing filter and then a 45° polarizing beam splitter (PBS). The PBS create a pure state coherent superposition of $|H\rangle$ and $|V\rangle$ states (horizontally and vertically polarized photons). Then, this coherent superposition traverses a 0° PBS. The outcome can be measured in the two PBS exits with single photon detectors. Before being measured, this output is a mixed state of $|H\rangle$ and $|V\rangle$.

There is no more coherent superposition (exit the pure state) and we don't know yet what both detectors will read. But we know that there's a 50% chance that the detector on the PBS horizontally polarized exit will detect a photon and 50% for the other detector. After detection, we'll end up with finding a single photon on one of the detectors, giving a related pure state. And nothing for the other.

This means that after measurement of a qubit in a given basis, the coherences in its density matrix in the measurement basis are erased. There's no more any coherence and superposition. This happens before looking at any measurement outcomes. In other words, a non-selective measurement of a pure state degrades its purity by turning it into a totally mixed state.

This could be used in a new updated Schrodinger' cat thought experiment, replacing the disintegrating radium atom by a simple qubit in a superposed state (after a H gate). A measurement at time T would trigger the poison release if the result is $|1\rangle$. All this in a closed box. Keeping the box closed at time T+whatever would be an equivalent of a non-selective measurement, then opening the box at time T+after whatever, would become a classical measurement of an already totally mixed state.

Positive Operator-Valued Measurement (POVM)

A Positive Operator-Valued Measure (POVM) is a quantum measure generalizing Projection-Valued Measures (PVMs) which is useful when the measurement basis is not made of orthogonal states in their Hilbert space. It is of particularly interest when measuring a photon qubit in a telecommunication link with two non-orthogonal polarization basis (0° and 45° like in the BB84 protocol). Like in PVMs, the measurement operators of a POVM add up to identity matrix. POVMs are also interesting when measuring a subsystem of an open system.

POVMs that are not PVMs are called non-projective measurements. They have many use cases like enhancing quantum states tomography, help detect entanglement and allow unambiguous state discrimination of non-orthogonal states, with applications in quantum cryptography and randomness generation³³⁵.

Other measurements concepts

I'll cover here other measurement-related tools and concepts I have encountered in various courses and scientific papers. You probably don't need to understand this if you are just a quantum software developer. It may be interesting, however, if you are involved in designing quantum systems, error correction systems, measurement systems, quantum firmware and the likes.

Gentle or Weak Measurement. It is one type of quantum measurement that retrieves little information of the measured system in average with the benefit of only slightly disturbing it. In a weak measurement, the correlations in the off-diagonal values of the system density matrix are only slightly altered. The system purity and entanglement remain mostly unaltered.

Postselected Measurement. It is a measurement where the result is chosen by the user, usually after a weak measurement. Surprising! As all measurements, it also turns a pure state into a mixed state. It refers to the process of conditioning on the outcome of a measurement on some other qubit values. The process consists in throwing away any outcome which does not allow you to do what you want to do. If the outcome you are trying to select has probability $0 < p < 1$, you will have to try an expected number $1/p$ times before you manage to obtain the outcome you are trying to select. If $p = 1/2^n$ for some large integer n , you may be waiting a very long time.

This weird technique is noticeably used to better understand quantum physics and phenomenon like measurement non-commutativity³³⁶.

CPTP map. A Completely Positive and Trace Preserving map also referenced as a quantum channel is used to describe non-selective measurements, conditional expectations and quantum filters, as well as feedback networks in quantum control theory. It corresponds to the most generic operation that can be applied to a quantum system. The state of the target system is associated to a trace-one, positive semidefinite density operator and, under the assumption that no initial correlations are present with the environment, its evolution over some specified time interval is described by a completely positive, trace-preserving (CPTP) linear map.

For open quantum systems, however, the interaction between the system and environment leads to non-unitary evolution of the system (e.g., dissipation), which requires CPTP maps for full characterization³³⁷.

In other words, a CPTP map is the mathematical operation that transforms the density matrix ρ of a quantum system during a measurement on the basis $\langle m_k |$ into the density matrix ρ' as described in Figure 199. A CPTP map is a superoperator of dimension 2^{4N} complex numbers.

$$\rho' = \sum_k M_k \rho M_k^\dagger = \sum_k p_k |m_k\rangle\langle m_k|$$

with $p_k = \langle m_k | \rho | m_k \rangle$

Figure 199: defining a CPTP map.

³³⁵ See [Understanding the basics of measurements in Quantum Computation](#) by Nimish Mishra, 2019. But what is $\delta_{mm'}$ in these formulas? It is the Kronecker Delta function which is equal to 0 when $m \neq m'$ and equal to 1 when $m = m'$. Meaning that inner product of all measurement operators is equal to 0 when they are different. This is the definition of orthonormality between a set of operators.

³³⁶ See for example [Quantum advantage in postselected metrology](#) by David R. M. Arvidsson-Shukur, Seth Lloyd et al, Nature Communications, 2020 (9 pages).

³³⁷ Source: [Quantum and classical resources for unitary design of open-system evolutions](#) by Francesco Ticozzi and Lorenza Viola, 2017 (27 pages).

Quantum Non-Demolition measurement. It is a type of measurement in which the uncertainty of the measured observable does not increase from its measured value during the subsequent normal evolution of the system. For a qubit measurement, it means that after its measurement, its value won't change anymore in subsequent measurements. QND measurements are the least disturbing type of measurement in quantum mechanics. QND measurements are extremely difficult to implement. Note that the term "non-demolition" does not imply that the wave function fails to collapse³³⁸. It can be implemented with photons, particularly to measure a photon number (number of photons in a superposed states of similar photon, or a single-mode Fock state), using a secondary probe field interfering with the signal field³³⁹. It has also been experimented to measure an electron spin with an additional ancilla quantum dot next to an operational quantum dot³⁴⁰. It also currently works well with superconducting qubits. What would be a "demolition measurement"? It would be one that, after retrieving the result, would create so significant a back-action on the measured quantum that it would either destroy it (like a classical photon counting device that absorbs the counted photons) or turn it into a state outside the computational basis (such as a different energy level than ground/excited levels for a qubit).

Quantum Steering is a quantum measurement phenomenon when one subsystem can influence the wave function of another subsystem by performing specific measurements. It is a variation of non-local correlations intermediate between Bell nonlocality and quantum entanglement³⁴¹.

Quantum Measurement Thermodynamics. We have already mentioned the theoretical reversible aspect of gates-based quantum computing which relates to the unitary transformations applied with quantum gates. But most of the time, particularly with solid qubits, there is always some energy exchanges between qubits and their control as well as measurement devices. Fundamental research is undertaken to better understand the evolution of the thermodynamic equilibrium of qubit operations particularly during entanglement and also, measurement and error correction. Since measurement is done on a repeated basis due to the implementation of quantum error correction codes, it makes sense to wonder whether this could be optimized. Depending on the qubit state (ground level or excited level, and also in intermediate states), measurement can absorb or release some energy that is quantum and microscopic in nature and it's also powered by entanglement³⁴².

³³⁸ QND was initially introduced in 1975 by VB Braginsky and YI Vorontsov in USSR. Source: [Quantum Nondemolition Measurement](#), Wikipedia. See also [Quantum Non-Demolition Measurement of Photons](#) by Keyu Xia, March 2018. It was demonstrated with the detection of a single photon as described in [Seeing a single photon without destroying it](#) by G. Nogues et al, 1999 (4 pages).

³³⁹ See [Detecting an Itinerant Optical Photon Twice without Destroying It](#) by Emanuele Distanto et al, Max Planck Institute, June 2021 (6 pages) which deals with detecting twice a photon with some non demolition quantum measurement. The detectors use a single atom coupled to an optical cavity. Other methods consist in using the cross-Kerr effect where a measured photon traverses an optical medium and changes its refraction index. It provokes a phase shift for a probe photon traversing the same media, its phase being measured with a Mach-Zehnder interferometer. See a description of this old technique in [Quantum non-demolition measurements in optics](#) by Philippe Grangier, Juan Ariel Levenson and Jean-Philippe Poizat, 1998 (7 pages).

³⁴⁰ See [Quantum non-demolition readout of an electron spin in silicon](#) by J. Yoneda et al, Nature, 2020 (7 pages).

³⁴¹ See [Quantum Steering](#) by Roope Uola et al, 2020 (43 pages) and [Quantum steering on IBM quantum processors](#) by Lennart Maximilian Seifert et al, PRA, April 2022 (11 pages) which shows poor entanglement with 15 qubits.

³⁴² See also [Probing nonclassical light fields with energetic witnesses in waveguide quantum electrodynamics](#) by Maria Maffei, Patrice Camati and Alexia Auffèves, September 2021 (6 pages) which studies the thermodynamics of a qubit coupled to a waveguide, which relates well to superconducting qubit gates and readout operations but also other qubit operations (photons, cold atoms). They demonstrate that the work performed by a coherent pulse on the qubit is always larger than the work that can later be extracted from the qubit, aka its ergotropy. But this classical ergotropy bound is violated if the input field is a resonant single-photon pulse. This opens the door to some energy recovery at the end of computing.

This research field could lead to a better understanding of the whereabouts of the energetic footprints of quantum measurement and entanglement and how it can impact the energy cost of quantum computing, particularly as it scales up³⁴³.

Quantum Reservoir Engineering is a set of qubits management techniques using a quantum bath in order to reduce its energetic footprint, its measurement readout times and enable quantum non-demolition measurement³⁴⁴. It's about tightly controlling the qubit coupling with its environment. It is connected to quantum error correction techniques. The approach was initially imagined for NMR qubits, leveraging the Nuclear Overhauser effect. Then it was tested with trapped ions, using some coupling between the qubit harmonic oscillator and a reservoir of oscillator with laser radiations³⁴⁵. The technique is also branded “quantum bath”, “engineered dissipation”, “autonomous feedback” and “coherent feedback”. It has since been tested with superconducting qubits and is the basis of the cat-qubits from Inria, Alice&Bob and Amazon³⁴⁶.

Algorithmic Cooling is a related technique also named heat-bath algorithmic cooling, which consists in balancing the entropy transfers between qubits and with ancilla qubits as part of error correction codes³⁴⁷. It is used to improve the purity of a target subset of qubits quantum states in a qubit register.

³⁴³ The thermodynamics of quantum measurement is involving a few groups worldwide including the team of Alexia Auffèves from Institut Néel in Grenoble, France, IQOQI and the University of Innsbruck in Austria and Andrew Jordan's team at the University of Rochester, USA. See [A two-qubit engine powered by entanglement and local measurements](#) by Ingrid Fadelli, April 2021 which refers to [Two-Qubit Engine Fueled by Entanglement and Local Measurements](#) by Léa Bresque, Andrew Jordan, Alexia Auffèves et al, March 2021, PRL (5 pages), [Alternative experimental ways to access entropy production](#) by Zheng Tan, Alexia Auffèves, Igor Dotsenko et al, May 2021 (15 pages) and the colloquium [A short story of quantum and information thermodynamics](#) by Alexia Auffèves, March 2021 (14 pages). See also [Stochastic Thermodynamic Cycles of a Mesoscopic Thermoelectric Engine](#) by R David Mayrhofer, Cyril Elouard, Janine Splettstoesser and Andrew Jordan, October 2020 (18 pages) and [Thermodynamics of quantum measurements](#) by Noam Erez, 2018 (3 pages).

³⁴⁴ Quantum Reservoir Engineering must not be confused with Quantum Reservoir Computing which is an entirely different beast. Introduced by Keisuke Fujii and Kohei Nakajima in 2017, it is the quantum equivalent of a similar technique used in classical deep learning where a low-dimensional data input is projected onto a higher-dimensional dynamical system, the reservoir, generating transient dynamics that facilitates the separation of input states. It is particularly useful to analyze time series of complex data structures. See [Quantum reservoir computing: a reservoir approach toward quantum machine learning on near-term quantum devices](#) by Keisuke Fujii and Kohei Nakajima, November 2020 (13 pages).

³⁴⁵ See [Quantum Reservoir Engineering](#) by J.F. Poyatos, J.I. Cirac and Peter Zoller, 1996 (14 pages) and the associated presentation [Quantum Reservoir Engineering](#) by Peter Zoller, 2013 (86 slides).

³⁴⁶ See [Measurement, Dissipation, and Quantum Control with Superconducting Circuits](#) by Patrick Michael Harrington, 2020 (154 pages), [Reservoir engineering using quantum optimal control for qubit reset](#) by Daniel Basilewitsch et al, 2019 (13 pages), [Reservoir \(dissipation\) engineering and autonomous stabilization of quantum systems](#), Quantic team, Inria, 2018 and [Quantum reservoir engineering and single qubit cooling](#) by Mazyar Mirrahimi, Zaki Leghtas and Uri Vool, 2013 (6 pages).

³⁴⁷ See [Novel Technique for Robust Optimal Algorithmic Cooling](#) by Sadegh Raeisi, Mária Kieferová and Michele Mosca, June 2019 (10 pages).

Gate-based quantum computing key takeaways

- Gate-based quantum computing is the main quantum computing paradigm. It relies on qubits and finite series of quantum gates acting on individual qubits or two and three qubits. The main other paradigms belong to analog quantum computing and include quantum simulators and quantum annealers.
- To understand the effect of qubits and quantum gates, you need to learn a bit of linear algebra. It deals with Hilbert vector spaces made of vectors in highly multidimensional spaces, matrices and complex numbers. The Dirac Bra-Ket notation helps manipulate vectors and matrices in that formalism.
- A qubit is usually represented in a Bloch sphere, reminding us of the wave nature of quantum objects during computation. This wave nature is exploited with qubits phase control and entanglement which provokes interferences between qubits. Qubits entanglement is created by conditional multi-qubit gates like the CNOT.
- A qubit register of N qubits can store a linear superposition of 2^N basis states corresponding to the qubit computational basis, each associated with a complex number. But surprisingly, this exponential growth in size is not enough to create an exponential speedup for quantum computing.
- While the computational space grows exponentially with the number of qubits, a qubit register measurement at the end of quantum algorithms yields only N classical bits. You have to deal with it when designing quantum algorithms.
- Computation must usually be done a great number of times and its results averaged due to the probabilistic nature of qubits measurement.
- Qubits measurement can be done in various ways, the main one being a classical projective measurement, if possible a non-demolition one (QND) that will maintain the qubit in its collapsed state after measurement. Other techniques are used that are useful for qubits quality characterization and for quantum error corrections.

Quantum computing engineering

After reviewing the basic principles of quantum physics and the logical dimension of gate-based quantum computing, let's look at the operational and physical operations of a quantum computer³⁴⁸.

Quantum computer architectures depend closely on the characteristics of their qubits. In this section, we will rely on the most common universal quantum gate computer architecture, that of superconducting qubits based on the Josephson effect. It is notably used by IBM, Google, Intel, Rigetti and IQM. However, many of the architectural principles mentioned here are applicable to quantum computers using other types of qubits.

First and as a reminder, here are the main components of a classical computer that you also find in various shapes and forms in smartphones, tablets, personal computers, game consoles and servers. Its key component is its microprocessor. It retrieves data and programs from a storage system and copies them to memory (RAM) entirely or on the fly as needed. The microprocessor then reads the program's instructions from memory in its cache to execute it one after the other and use conditional branching.

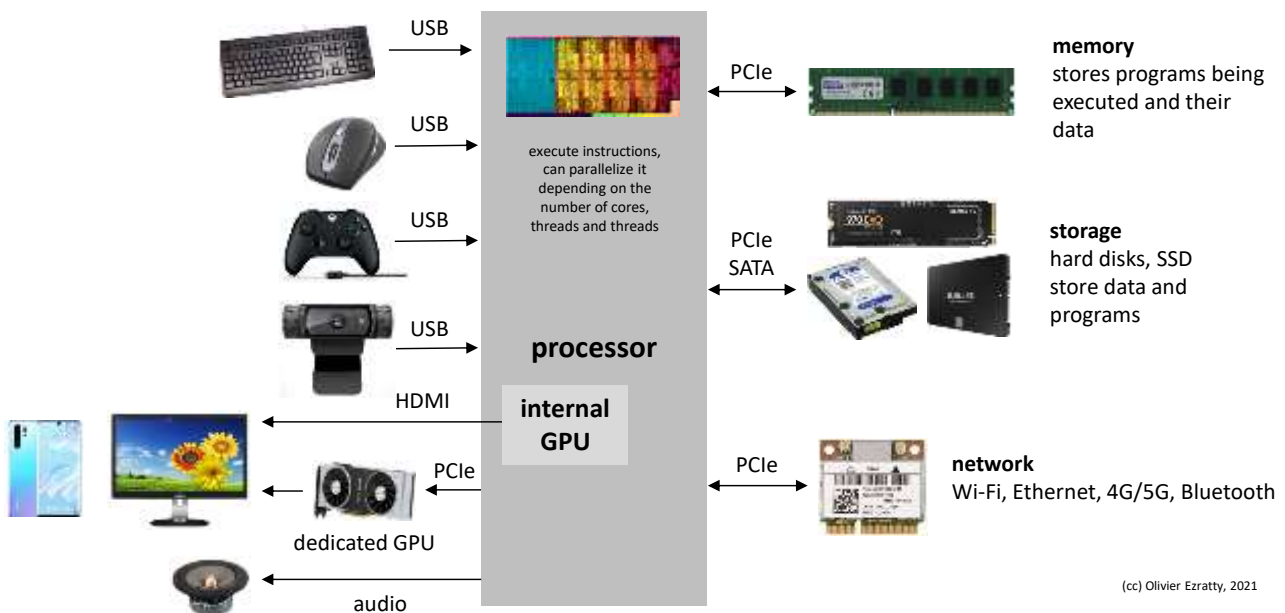


Figure 200: a classical personal computer hardware architecture. (cc) Olivier Ezratty, 2021.

Data and programs can be retrieved remotely over a network and from remote servers on the Internet. The whole system is controlled by physical interfaces at input (keyboard, mouse, touchpad, joystick, webcam, microphones, scanners) and generates output (displays, audio, printers, other peripherals). The processor can be complemented by a graphics processor (GPU). It is either external to the microprocessor, for demanding requirements such as in CAD and video games or integrated into the microprocessor as is the case for all most laptops and most desktops processors.

Depending on the configuration, the processor is surrounded by a variable number of external components that are soldered in the motherboard.

³⁴⁸ I consulted a very large number of information sources to carry out this part, both on the research side and on the supplier side, such as IBM or D-Wave. Note [Quantum Computing Gentle Introduction](#) from MIT, published in 2011 (386 pages) which describes precisely some mechanisms of quantum computers such as qubit state reading methods. It also describes quite well the mathematical foundations used in quantum computers. You can also enjoy an [8-minute video](#) from Dominic Walliman, who explains the basics of the quantum computer!

This is the case of the Intel chipsets like the Z390, which complements the core processors and manages a large part of the computer's inputs/outputs. Wi-Fi and cellular modems are associated with antennas. Of course, an internal and external power supply and a battery for mobile devices must be added.

On the energy side, it is the processor and GPU that heat up the most and require passive or active cooling depending on their power drain. In embedded systems such as smartphones, this is done with heat conducts and air. In PCs, it is supplemented by one or more fans. In the most extreme cases, liquid cooling uses a water circuit to improve heat dissipation. One of the reasons why heat is generated by classical processing is the non-reversibility of classical computing.

Key parameters

Let's look at the definition of the key performance indicators of gate-based quantum computers. The best-known set of indicators was created by **David DiVincenzo** in 2000 when he was an IBM researcher. He is now a research professor at the University of Aachen in Germany³⁴⁹.

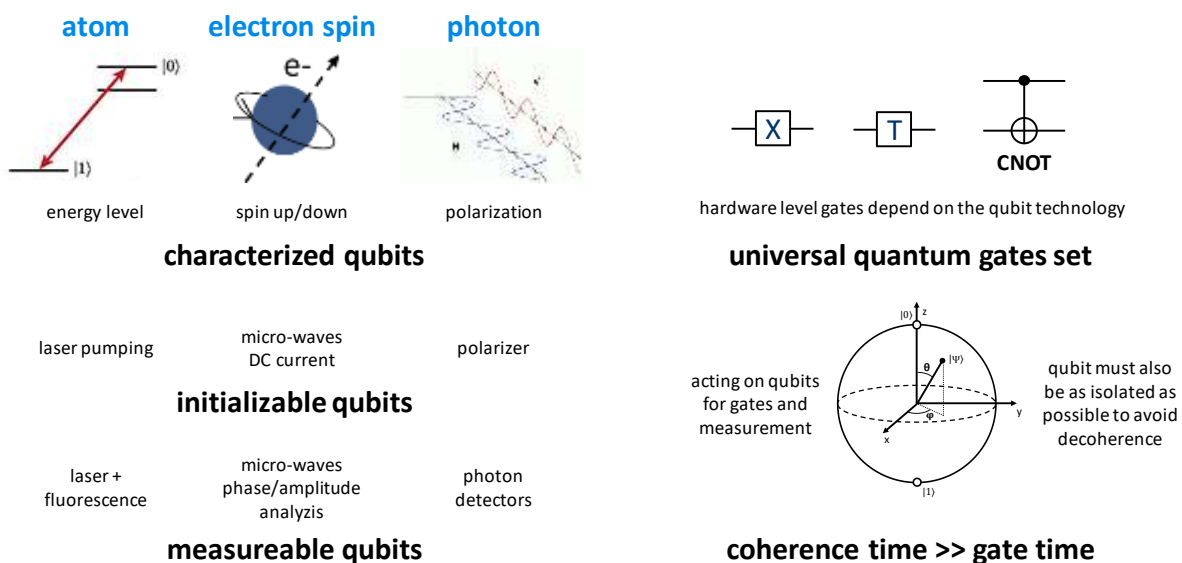


Figure 201: DiVincenzo gate-based quantum computing criteria. (cc) Olivier Ezratty, 2021, inspired by Pascale Senellart.

While individual qubits barely existed, he defined the basic technical characteristics of a universal gate-based quantum computer as follows:

Well-characterized qubits. Quantum computers use qubits that exploit quantum objects that can have two distinct and measurable states. Their physical characteristics are well known. The architecture is scalable in the sense that it can exploit many physical qubits and then, logical qubits relying on these physical qubits and quantum error correction codes.

Initializable qubits. In general, to the value $|0\rangle$ often called "ground state" for the associated quantum objects, corresponding, for example, to the lowest energy level of an elementary particle or an artificial atom as for superconducting qubits.

Coherence times. It must be greater than quantum gates activation times. The time during which the qubits are in a coherent state must be greater than the quantum gates activation time in order to be able to execute an algorithm containing a sufficiently long sequence of quantum gates. Error correction codes using a large number of physical qubits have the benefit of extending this usable computing time.

³⁴⁹ See [The Physical Implementation of Quantum Computation](#) by David DiVincenzo, 2000 (9 pages).

Universal quantum gates set. The quantum hardware must allow the creation of a universal gate set. It depends on the qubit technology. It requires a minimum set of single-qubit gates allowing the creation of any rotation in the Bloch sphere, completed by a CNOT two-qubits gate.

Measurement. With the ability to measure qubits state at the end of computing, which seems obvious. This measurement should not influence the state of other qubits in the system. Ideally, the measurement error rate should be well below 0.1%.

David DiVincenzo added two other optional criteria that are used instead for quantum communications:

Flying qubits conversion. The ability to convert static qubits into flying qubits, who are usually photons, and sometimes electrons.

Transport these moving qubits. from one point to another reliably and remotely. This will allow to manage quantum telecommunications, distributed architectures of quantum computers and to set up *blind computing* architectures allowing to distribute treatments while protecting their confidentiality. The technology will quickly become essential to enable the distribution of quantum computations over several quantum processors, a bit like we do with multi-core chipsets or with processing distribution architectures over several CPUs and several servers. Some vendors like IonQ have announced that they will rely on this architecture. This will be useful for qubit architectures that will be limited in the number of qubits, which may only be able to consolidate a few hundred at most. It will thus be necessary to be able to link remote processor qubits and keep them entangled. Different quantum interconnection techniques are possible. The most generic is optical and is not much constrained by distance. At rather short distances, microwave links are possible, particularly to couple superconducting qubits, as well as shuttling electrons³⁵⁰.

DiVincenzo's criteria are quite basic. From a practical and operational point of view, quantum computers can also be characterized by another set of parameters as follows:

Number of qubits. It will condition the available computing power. As this power theoretically increases exponentially with the number of qubits, it is a key parameter. As of late 2021, the commercial record was 127 qubits with the largest IBM Quantum System available in the cloud. The number of qubits should be evaluated in its capacity to scale. Some technologies are easier to miniaturize and scale than others. It is necessary to integrate in this miniaturization both the quantum qubit chipsets and the elements that control them. On top of that, we must ensure that decoherence and noise does not increase as the number of qubits is growing. Today, trapped ions qubits have an excellent fidelity but don't scale well. Superconducting qubits seem to scale-up better but their fidelity is not stable as the number of qubits grows with existing industry vendors hardware although it could change in the future. Cold atom qubits scale a little better but with some practical limits in the number of controllable atoms. Electron spins qubits could scale best in theory.

Qubits connectivity. It will condition the quantum algorithms execution speed. The greater this physical connectivity, the faster the code execution will be. With a low connectivity, the compiler of the quantum code will have to add a lot more operations to link the qubits together, particularly relying on SWAP gates. This connectivity varies greatly from one technology to another. In 2D technologies, as with superconducting and silicon qubits, it is limited to neighboring qubits. It seems better with some types of trapped ion qubits.

Qubit parallel operation. How qubit gates can be parallelized over different qubit zones without disruption will also condition the speed of execution of quantum algorithms.

³⁵⁰ Princeton University and Konstanz University in Germany are working on optical interconnection between CMOS quantum processors. This is documented in [Quantum Computing Advances With Demo of Spin-Photon Interface in Silicon](#), 2018. The magic consists in transferring the quantum state of an electron spin to a photon at its phase level.

Qubits fidelities. When executing quantum gates and reading their state, qubit fidelity conditions the ability to execute long algorithms. It has a direct impact on the supported algorithm depth. It also impacts the capacity to run quantum error correction codes and create logical qubits with an arbitrary fidelity level.

Execution time. For both quantum gates and qubit state measurement. The first is obviously important to make the algorithms run as fast as possible. But the second is equally important because it is involved in error correction codes and therefore conditions the execution time of all algorithms.

Operating temperature. For the processor and their equipment which is very dependent on the type of qubits. The Holy Grail is of course to operate at room temperature. The currently operational quantum computers based on superconductors operate at a very low temperature of 15 mK (1 mK = 1 milli-kelvin, 0 kelvin = -273.15°C), but some types of qubits still in the research stage are supposed to operate at room temperature, such as those based on photons and NV centers (cavities in nitrogen-doped diamond structures like with Quantum Brilliance). However, this is not necessarily the case for associated equipment such as photon generators and detectors for photon qubits. Operating at very low temperature is a way to preserve the coherence of the qubits. But the lower the temperature, the smaller the energy that can be radiated by the qubits and their control electronics. Operating qubits at 100 mK or 1K, like with electron spin qubits, creates a much larger available cooling budget to control the qubits than operation at 15 mK.

Total energy consumption. We will investigate this and study it in a global manner with incorporating all quantum computer components: the processor itself, all its control electronics as well as the involved cryogenic systems, starting page 259. As of 2022, quantum computers had a power drain sitting between 2 kW and 35 kW depending on the qubit type and number of qubits.



Figure 202: datacenters integration topics quantum for quantum computers. (cc) Olivier Ezratty, 2021.

System rackability. How will quantum computers be deployed in data centers? Does it fit in standard rack systems? It is notably planned by the startup Pasqal, as well as for Quandela's photon generators and LightOn's optical processors, as well as micro-wave external electronics from companies like Zurich Instruments and Qblox. Alpine Quantum Technologies from Austria also announced in 2021 it would fit its trapped ion computing in two standard 19-inch racks. It is associated with issues of weight, space, cooling and power supply. What kind of fluids must be used for cooling, usually cold water, connected to the first stage compressor of cryostats, whatever their size? Quantum computers must also withstand the usual data centers conditions like vibrations, dust and electromagnetic environment, or be separated in special isolated facilities. They could site in the modular building blocks used in the most recent data centers.

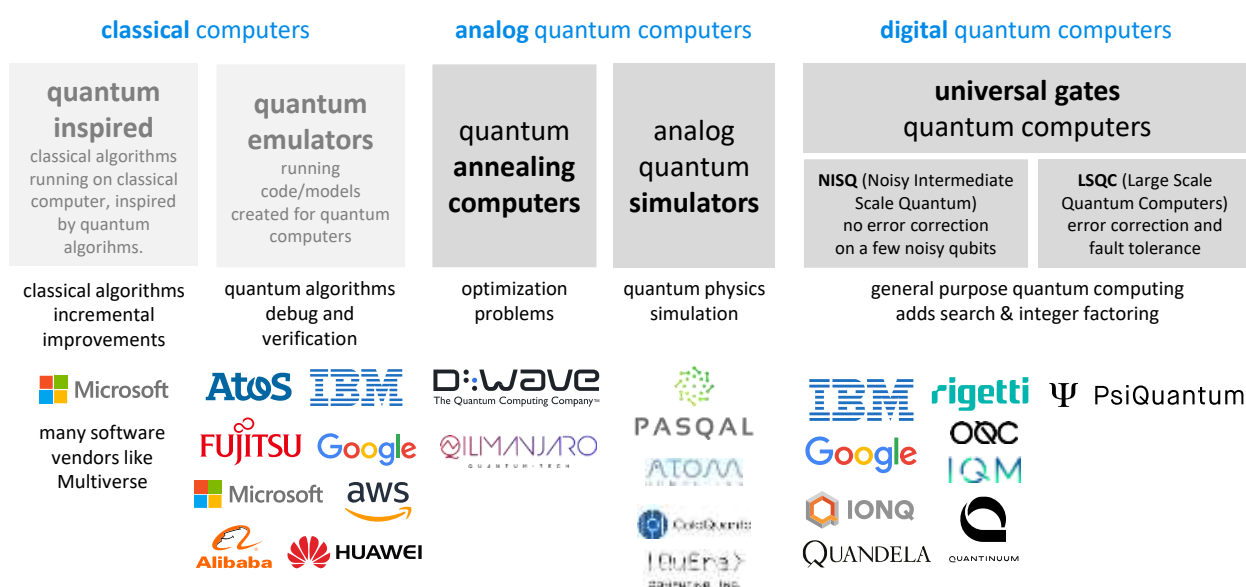
These last three operational parameters play a role when deploying computers or quantum accelerator in data centers. It plays a critical role since, for most applications, quantum computers will be offered through cloud services.

All these considerations to gauge the capabilities of a quantum computer involve the discipline of quantum computers benchmarking! As Kristel Michielsen points out, benchmarks can be used when the number of qubits is below 50 when comparing the rendering of algorithms between quantum computers and their emulation on supercomputers³⁵¹. Beyond that, it will be more difficult.

Benchmarked quantum computers will generally have dissimilar characteristics: different universal quantum gates requiring compilers to assemble different quantum gates to execute the same algorithm, and different error correction codes, adapted to the error rate of the qubits and quantum gates of the compared computers. The dissimilarities will be much greater than between two Intel and AMD processors or two smartphone chipsets!

Quantum computers segmentation

There is not just one category of quantum computers, but many. We must at least distinguish gate-based quantum computers and analog computers, including quantum annealing computers such as the ones from D-Wave.



© Olivier Ezratty, 2022

Figure 203: the different computing paradigms with quantum systems, hybrid systems and classical systems. (cc) Olivier Ezratty, 2022.

But there are at least six categories of quantum computers:

Quantum emulators. These are used to execute quantum algorithms on traditional computers ranging from simple laptops to supercomputers, depending on the number of qubits to be emulated. They execute these algorithms, quantum gates and qubits with the processing capabilities of traditional computers, using large vectors and matrices. It is used to test quantum algorithms without quantum computers. Quantum emulators are sometimes called quantum simulators, but this name should be avoided to prevent the confusion with... quantum simulators. These are analog quantum computers simulating quantum physics phenomena, for example magnetism or the tridimensional structure of molecules. Quantum emulators may however also simulate qubit noise model like Atos QLM emulator³⁵². They can also reproduce the (quantum) physical characteristics of various qubits and in that case, they also implement some form of digital quantum simulation. To date, supercomputers can fully emulate up to the equivalent of 40 to 50 qubits. We detail this starting page 652.

³⁵¹ In [Benchmarking gate-based quantum computers](#), 2017 (33 pages).

³⁵² We can make a distinction between an exact digital simulation and approximate digital simulation, emulating a digital error rate that is equal or below NISQ hardware. This can help simulate a greater number of qubits.

Records have however been broken with more than 100 qubits, with a low number of quantum gates and using various techniques like tensor compression. Emulating quantum computers requires a lot of power both on the memory side, to store 2^N quantum register states for N qubits, if not the full 2^{2N} real numbers of the density matrix, and for the associated processing that relies on floating-point matrix multiplications. Still, records in this field are regularly broken.

Quantum inspired computing is about using classical algorithms running on classical hardware that are inspired by quantum algorithms and bring some new efficiencies. They are not about emulating quantum code on a classical computer. Typical quantum inspired algorithms use tensor network libraries.

Quantum annealing computers use the adiabatic theorem which consists in using a slow and controlled evolution of a set of qubits linked together according to a particular topology ("Chimera", "Pegasus" or for the new generation "Zephyr" in the case of D-Wave). The process is first initialized in the ground state of the Hamiltonian and the adiabatic theorem guarantees the convergence of the system towards a low energy state, ideally the ground state. This technique is used to search for an energy minimum in a complex problem, such as the simulation of atomic interactions in molecules or the optimization of the duration of a path. The coefficients of the Hamiltonian are the couplings (weights of the interactions between qubits) and the self-couplings (weights of the qubits) and the variables of an instance are the spins of each qubit. Many optimization and quantum simulation algorithms can be translated into quantum annealing algorithms. Until now, D-Wave seems to bring interesting gains in computation time but this is strongly disputed by some specialists.

Quantum simulators serve as simulators of quantum phenomena without using gates-based qubit systems. They work in an analog and not digital way, i.e., the parameters linking the qubits together are continuous. For the moment, they are mainly laboratory tools. The most commonly used technique are neutral atoms cooled and controlled by lasers, like the ones from Pasqal, ColdQuanta and Atom Computing. Trapped ions, superconducting qubits, spin qubits³⁵³ and other qubit types can also be used in simulators but no commercial vendor is promoting it when they can also implement gate-based quantum computing which is supposed to be more generic³⁵⁴.

Universal quantum computers use qubits with quantum gates capable of executing all quantum algorithms. At a later time, it will provide a speedup compared to the best classical algorithms running on supercomputers as well as vs quantum annealers. They are currently limited to 127 qubits. The quantum noise levels of qubits is detrimental to computing and requires the usage of logical qubits made of many physical qubits and quantum error correction codes (QEC). While waiting for these fault-tolerant quantum computers to ramp up with logical qubits, we are using non corrected qubits in the so-called NISQ for "Noisy Intermediate-Scale Quantum", an expression from John Preskill³⁵⁵. It describes existing and future general-purpose quantum computers supporting 50 to a few hundred physical qubits. These can run algorithms with a limited circuit depth due to the qubit error rates like variational quantum circuits and quantum machine learning algorithms driven by classical algorithms in so-called hybrid algorithms. They are supposed at some point to exceed supercomputers computing capacities for specific algorithms. Then, much later, we'll have fault tolerant (FTQC) and large scale quantum computers (LSQC), with a very large number of physical qubits and over 100 logical qubits compatible with quantum software requirements.

There are now several other variations of universal quantum computers that deserve some description:

³⁵³ See [Analog Quantum Simulation of the Dynamics of Open Quantum Systems with Quantum Dots and Microelectronic Circuits](#) by Chang Woo Kim, John M. Nichol, Andrew N. Jordan and Ignacio Franco, March-October 2022 (20 pages).

³⁵⁴ Amazon is investigating it, in [A scalable superconducting quantum simulator with long-range connectivity based on a photonic bandgap metamaterial](#) by Xueyue Zhang, Oskar Painter et al, August 2022 (34 pages).

³⁵⁵ In [Quantum Computing in the NISQ era and beyond](#) in 2018.

Continuous variables quantum computers, or analog quantum computers with universal gates. They use qubits that store variable quantities between 0 and 1 and can be manipulated with quantum gates, also named ‘qunats’³⁵⁶.

Direct Variable vs Continuous Variable encoding of quantum information

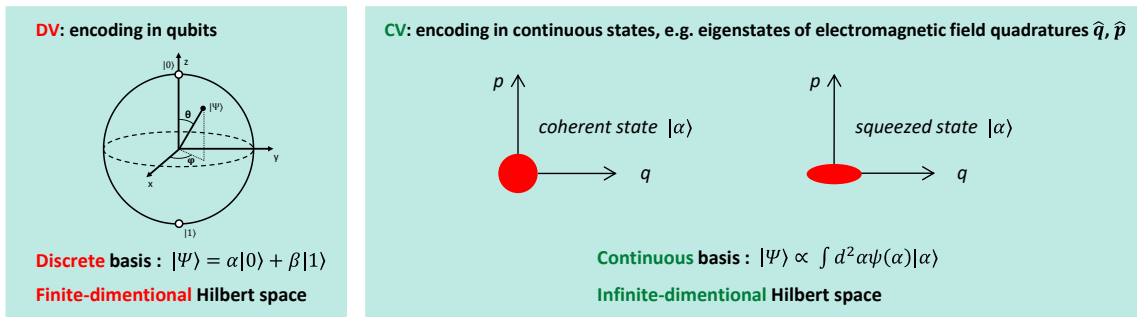


Figure 204: direct variable and continuous variable encoding of quantum information. inspired from [Sub-Universal Models of Quantum Computation in Continuous Variables](#) by Giulia Ferrini, Chalmers University of Technology, Genova, June 2018. (35 slides).

This category of quantum computing was proposed in 1999 by Seth Lloyd and Samuel L. Braunstein³⁵⁷. They are usually based on continuous variable photons but other qubit types like trapped are used.

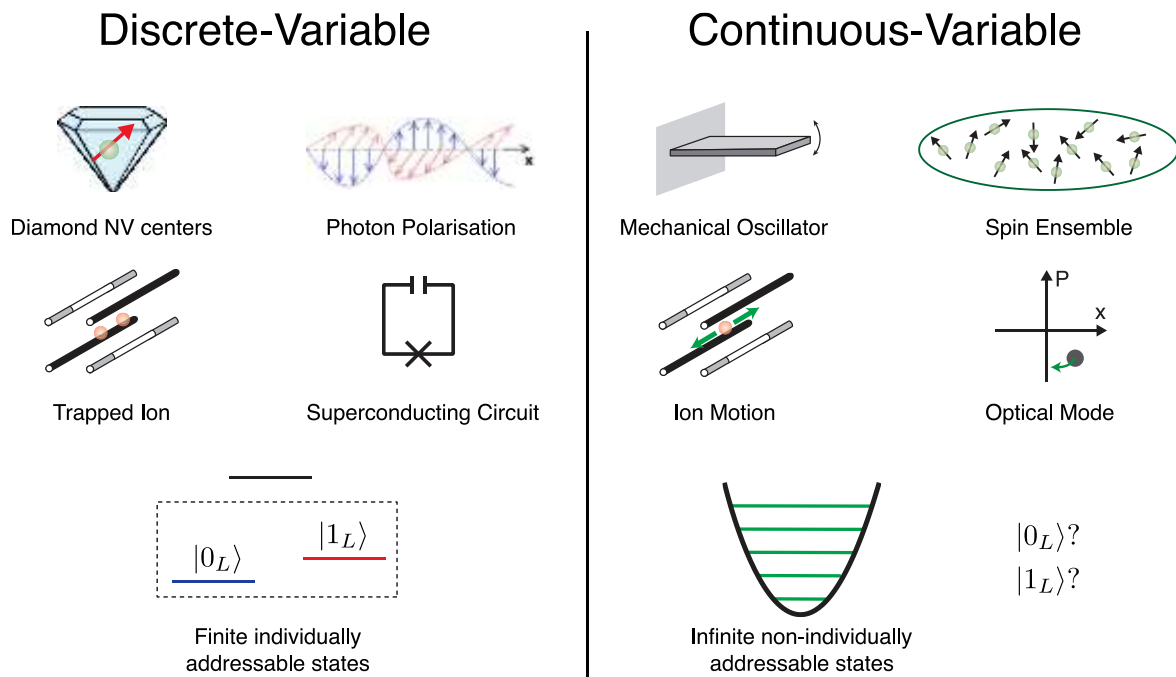


Figure 205: various implementations of discrete-variable and continuous-variable quantum computing. Source: TBD.

MBQCs, or Measurement Based Quantum Computers, is an architecture variant of NISQ/LSQ adapted to flying qubits and particularly to photon qubits which can't easily be entangled with two qubits gates. The process consists in entangling all qubits at the beginning of computing. It's followed by qubits readouts in an ordered way, enabling the implementation of traditional gates. MBQC also implements some massive parallelism, adapted to the limited and finite processing depth of flying qubits. The startup PsiQuantum plans to use a variant of this technique named FBQC.

³⁵⁶ See [Universal Quantum Computing with Arbitrary Continuous-Variable Encoding](#) by Hoi-Kwan Lau and Martin B. Plenio, 2016 (5 pages) as well as [Continuous-variable quantum computing in the quantum optical frequency comb](#) by Olivier Pfister, 2019 (16 pages).

³⁵⁷ See [Quantum Computation over Continuous Variables](#) by Seth Lloyd and Samuel L. Braunstein, February 1999 (9 pages).

Topological quantum computing is based on specific anyon qubits that are self-corrected. The low-level programming model of these qubits is much different from universal quantum computers. This is the path chosen by Microsoft, together with QuTech. Its development seems to be quite sluggish.

Here's another segmentation of these models with two dimensions: discrete or continuous data encoding and discrete or continuous variables computing given the vendor position is rough, some being positioned in various slots (Pasqal also wants to do gate-based computing)³⁵⁸:

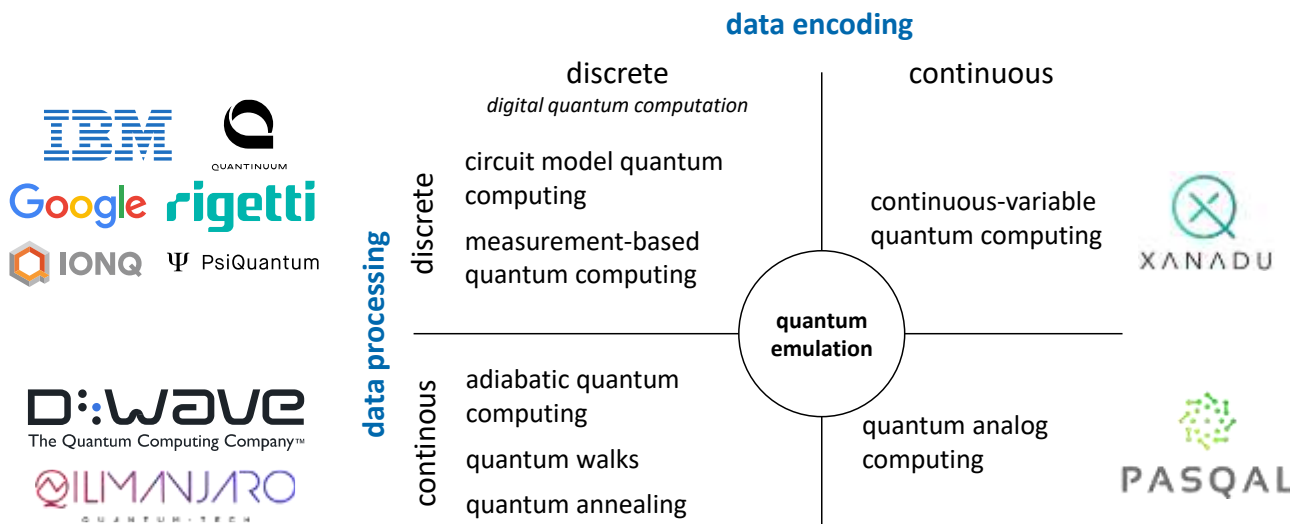


Figure 206: discrete vs continuous data encoding vs data processing. Source: [Quantum computing using continuous-time evolution](#) by Viv Kendon, 2020 (19 pages).

Quantum Accelerator. It is a quantum computer used as a complement to a supercomputer or HPC, usually to run hybrid algorithms like VQE (Variational Quantum Eigensolvers) combining a classical part that prepares the data structure that feeds a quantum accelerator³⁵⁹. The QPU serve as an accelerator for the HPC which can be a node or the whole HPC, using CPU and/or GPUs/TPUs. GPUs/TPUs are themselves also accelerators for the CPUs. There are some design issues requiring tight integration between the HPC and the QPU, particularly with regards to batch loading and to the way the quantum algorithm is executed multiple times. A QPU contains itself a classical computer. It converts digital signals (gates) into analog signals (the micro-waves or lasers controlling the qubits and handling their readout). This QPU computer will need to be as close as possible to the HPC computing capacities to improve the turnaround. It may lead to create custom designs integrating an HPC and one or several quantum accelerators³⁶⁰.

Other quantum accelerator designs contain more or less generic upper software layers with connectors driving various quantum and classical architectures (annealers, gate-based, emulators)³⁶¹.

This inventory is only an appetizer. We will have the opportunity to detail these architectures.

And we are always in for many surprise and new programming paradigms that nearly nobody in the ecosystem is evaluating like the “dark path holonomic qudit computation” coming from Sweden³⁶².

³⁵⁸ See [Quantum computing using continuous-time evolution](#) by Viv Kendon, 2020 (19 pages).

³⁵⁹ See [Quantum Accelerators for High-performance Computing Systems](#) by Keith A. Britt et al, 2017 (7 pages).

³⁶⁰ See [Quantum Accelerator Stack: A Research Roadmap](#) by K. Bertels et al, 2021 (39 pages) which proposes a detailed architecture for a quantum accelerator and See [QPU-System Co-Design for Quantum HPC Accelerators](#) by Karen Wintersperger, Hila Safi and Wolfgang Maurer, Siemens AG and Technical University of Applied Sciences Regensburg, September 2022 (15 pages).

³⁶¹ See for example the proposals in [Quantum Computer Architecture: Towards Full-Stack Quantum Accelerators](#) by Koen Bertels et al, 2019 (20 pages).

³⁶² See [Dark path holonomic qudit computation](#) by Tomas André and Erik Sjoqvist, August 2022 (6 pages).

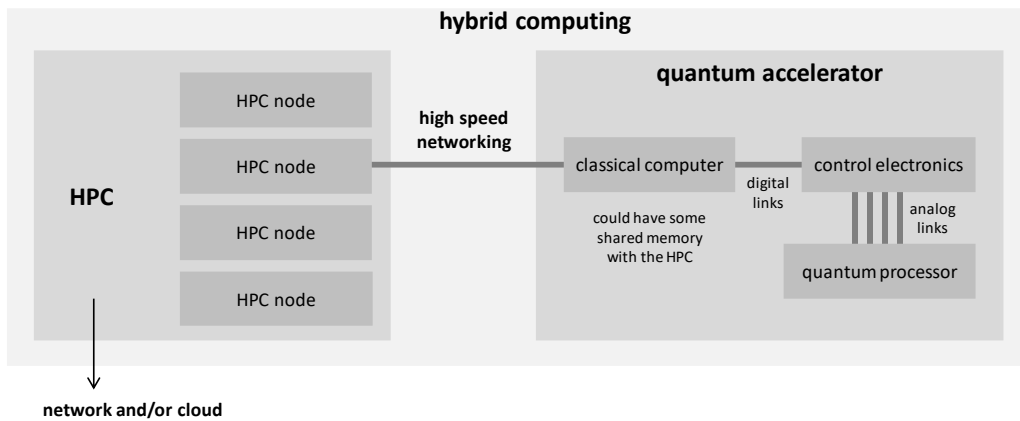


Figure 207: basics of a hybrid classical/quantum computing hardware architecture. (cc) Olivier Ezratty, 2021.

Qubit types

Quantum computers physical qubits are devices that handle particles or quasiparticles with one physical property or observable that can have two possible mutually exclusive states, that can be initialized, modified with quantum gates and then measured.

They are sometimes individual quantum objects, as with atoms (trapped ions and cold atoms), electrons (quantum dots silicon qubits) or photons! And only one at a time! In the case of superconducting qubits or Majorana fermions, the quantum state is based on a large number of electrons arranged in Cooper pairs that share the same quantum state, the pairs of electrons that are created at superconducting temperature. With NV centers and some exotic qubits, qubits are constructed with ensembles of quantum objects or with heterogeneous quantum objects like mixing electron spins and atom nuclear spins.

Qubits can also be classified in two meta-breeds: stationary or moving (flying). Those based on trapped ions, cold atoms, electrons spin, NV centers and superconducting loops are stationary. Flying qubits are based on photons that physically circulate from quantum gate to quantum gate as well as on flying electrons. They move around from a source, through physical devices implementing quantum gates and land on detectors. In all cases, the quantum gates are dynamically activated by electronic circuits or lasers and operate on the qubits where they are (stationary qubits) or in the path of their transit (flying qubits).

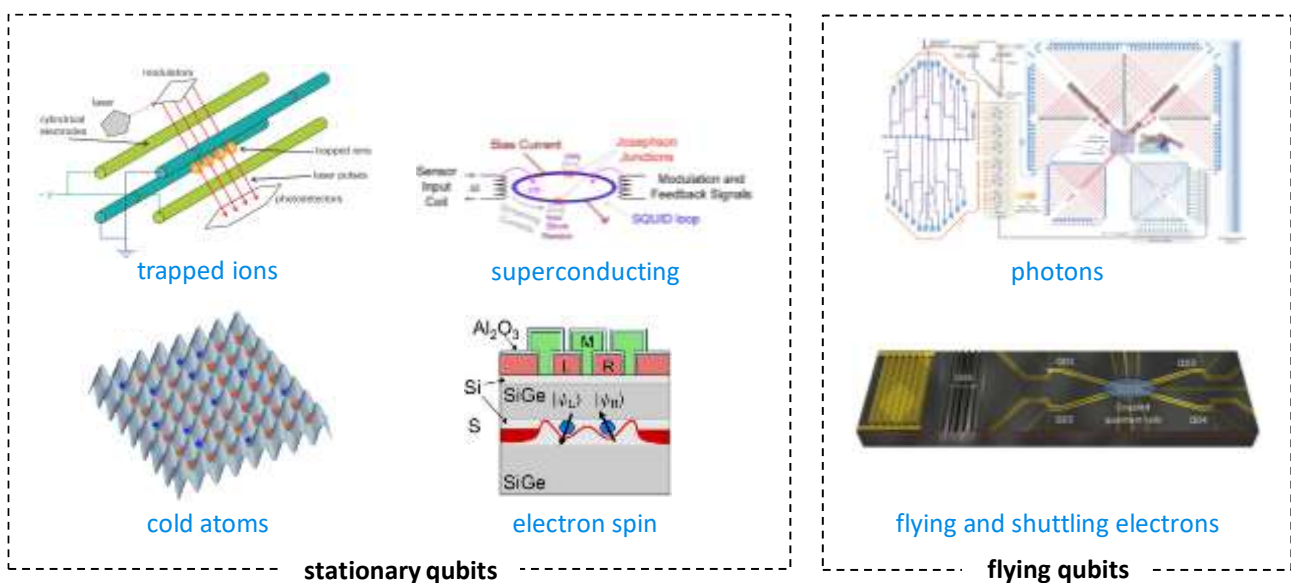


Figure 208: separating stationary and flying qubits. (cc) Olivier Ezratty, 2021.

Here are the main types of qubits that are currently being studied, tested and sometimes commercialized³⁶³. We'll detail [later](#) starting in page 273 and with much details all these different options. Looking at these technologies reminds me of the Wacky Races movie and cartoons vehicles as well as the Tatooine podracers in Star Wars I, with an amazing technology diversity and true believers in their fate. The only difference is we may end up with no single winner but several winners if not some forms of technology hybridization. Can we compare it to the Manhattan project from 1940-1945? It had only two main uranium and plutonium combustible options and some variations with the explosives. Here, with quantum computing, the world is looking at many more options.

Controlled atoms

This is one of the oldest types of qubits. It consists in controlling atoms in vacuum with lasers, one qubit per atom. Cold atoms are neutral while trapped ions are ionized atoms. One key difference is how these atoms are controlled in space. Ions can be positioned with electrodes and magnetic fields while non-ionized atoms are only controlled by lasers. They both share a similar measurement technique using laser excitation, fluorescence and visual readout with some CCD or CMOS imaging sensor.

Trapped ions are atom ions that are kept in a vacuum and suspended by electrostatic suspension. Their initialization is done with laser optical pumping.

Lasers are used to cool and stabilize the ions, exploiting the Doppler effect, with different energy transitions than those used to modify the state of the qubits. The most frequently used ions are calcium and strontium. Single-qubit quantum gates are activated by microwaves, lasers or magnetic dipoles. Lasers or electrodes are used for two-qubit quantum gates. While trapped ions are best-in-class for qubits fidelity and connectivity, it seems currently difficult to scale it beyond a hundred ions. And it's very slow.

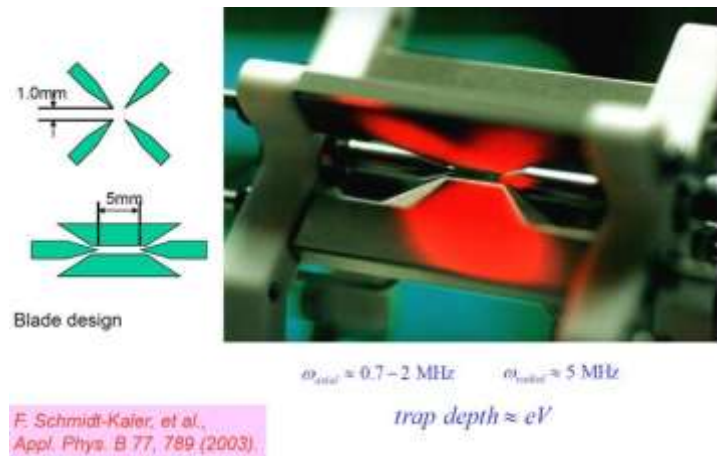


Figure 209: a typical Paul trap for trapped ions, created in 2003.

Cold atoms are cooled at very low temperatures, also using the Doppler effect and other laser-based techniques. The used atoms are neutral atoms and quite often rubidium, an alkaline metal. The quantum state of these cold atoms is their energy level, which can use their Rydberg high-excitation states on some occasions. Cold atoms are used to create both gate-based quantum computer and analog quantum simulators.

Nuclear magnetic resonance (NMR) qubits were tested over 20 years ago and are nearly completely abandoned. Most of the time, they are based on using ensemble of atoms or molecules. They do not scale at all. It is a good demonstration that qubits research must remain open and cannot be settled too early around one or two technologies. Even now, it's too early to tell which qubit type will really scale to create useful quantum computers.

Controlled electrons

This other category of qubits is about electrons that are controlled most of the time in solid-state circuits instead of vacuum like with cold atoms and trapped ions.

³⁶³ See [Roadmap on quantum nanotechnologies](#) by Arne Laucht et al, 2021 (49 pages) which reviews some of these qubit types.

Superconducting qubits are based on the state of a superconducting current that crosses a very thin barrier in a loop, usually a metal oxide such as aluminum, using the Josephson effect³⁶⁴. There are several types of superconducting qubits: flux, phase and charge.

The most common one is the transmon, a variation of charge superconducting qubits. In all cases, qubit observables are two very distinct states of a high-frequency oscillating current flowing through the Josephson junction.

The oscillation is made possible by the fact that the loop integrates the equivalent of an inductance and a capacitance. The current oscillation is activated by microwave pulses using frequencies between 4 and 8 GHz and transmitted by coaxial wires. In transmon qubits, the qubit observable is measured with a resonator integrated in the circuit which receives a microwave and sends it back. The readout electronic system splits out the amplitude and phase of the readout microwave to detect the qubit value. On the right is a schematic of two superconducting Google Sycamore qubits, themselves connected by a third qubit - in green - which acts as a dynamic coupler between two qubits, to create controlled entanglement.

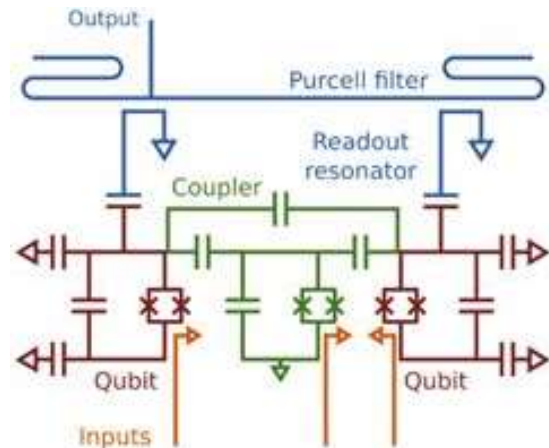


Figure 210: Google Sycamore superconducting electronic architecture. Source: Google.

In some transmons, individual qubits activation frequency is tuned by a direct current flux bias line.

Superconducting qubits are relatively easy to manufacture because they are based on semiconductor circuit creation techniques even if some of the materials are different, such as niobium and aluminum³⁶⁵. They are built on a dielectric substrate, usually with silicon or sapphire. These qubits are operating at 15 mK, requiring a dilution refrigerator. This temperature is required for a chain of reasons: qubits are driven by microwaves in the 4-8 GHz range and the current thermal noise is constrained by order of magnitude below the temperature corresponding to these microwaves' energy. The 4-8GHz corresponds to off-the-shelf microwave generation equipment and to the size of the capacitor and resonator used in the vicinity of the qubit Josephson junctions.

Superconducting qubits have many challenges dealing with scalability. The microwave RF generators are usually located outside the cryogenic enclosure of the quantum processor, which create a lot of wiring with about 3 to 4 cables per qubit. Qubits control frequencies must be different and tuned for adjacent qubits. Their fidelity is not best-in-class and seems to decrease as we grow the number of qubits.

Quantum dots electron spin qubits are developed with scalability in sight. Most of them use two electrons trapped in a quantum well, one containing the qubit and the other one used to measure it. These qubits are usually manufactured using silicon-based CMOS circuits. Silicon is often supplemented with various dopants. They benefit from the reuse of CMOS manufacturing processes that are already well mastered. These qubits are easy to miniaturize down to below 100 nm. They work at temperatures between 100 mK and 1K, higher than superconducting qubits, allowing the use of more electronics around the chipset, to generate the microwaves and other electric signals required to create qubit gates and handle qubit readout. This promising technology is however less mature than superconducting qubits. No lab or company has really exceeded 15 functional qubits as of 2022.

³⁶⁴ See [Digital readout and control of a superconducting qubit](#) by Caleb Jordan Howington, 2019 (127 pages).

³⁶⁵ See [Practical realization of Quantum Computation Superconducting Qubits](#) (36 slides).

NV centers (Nitrogen Vacancy) are artificial diamond structures in which a carbon atom has been replaced by a nitrogen atom near a carbon atom gap. Qubit states and control rely on a combination of electron, nitrogen and carbon ^{13}C nucleus spins. Qubit gates are implemented with microwaves, a magnetic field and an electric field. Entanglement is handled with photons, magnetic coupling or with controlling the core spin of neighboring ^{13}C carbon atoms via the use of microwaves to create a CNOT gate. Qubit readout is using a laser and fluorescence detection.

Majorana fermions are anyons or quasi-particles which are particular states of Cooper's pairs in condensed matter at very low temperature.

These qubits use braiding, a special topology that makes it possible to implement error correction at the qubit level. The promise is to enable the creation of scalable fault-tolerant quantum computers. These must also be cooled to a temperature close to absolute zero, around 10mK. This is the path chosen by Microsoft. The existence of the fermions of Majorana is not yet proven. It is one of the most hazardous paths to quantum computing. Majorana fermions are often discussed but they belong to a broader category named "topological matter" and "many-body systems".

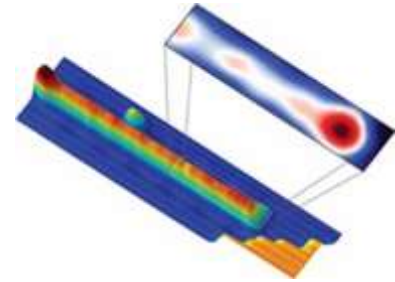


Figure 211: researchers may have seen Majorana fermions, but that's not really sure.

The main problem is... we are not sure these anyons and Majorana fermions really exist. It's still work in progress with ups and downs.

Flying qubits

Flying qubits are special because they travel from the place where they originated, traverse physical devices acting on them and terminate their journey on a sensor measuring one observable. They have a limited time available to run any computing, including a finite and small number of quantum gates.

Photons are the most common flying qubit and there are many varieties of implementations. One type is based on a horizontal/vertical polarization observable. Others use continuous variables qubits. Boson sampling systems use multi-modes photons. It is quite difficult to implement two qubit gates with these photon qubits, thus the alternative of the MBQC architecture that is an interesting work-around. Also, photon generation follows a probabilistic pattern which makes things complicated when the number of qubits grows. Most of these qubits operate at room temperature, but the photon sources and their detectors must however usually be cooled to temperatures between 4K and 10K, which is much less demanding than the 15 mK of superconducting qubits or the 1K of silicon qubits.

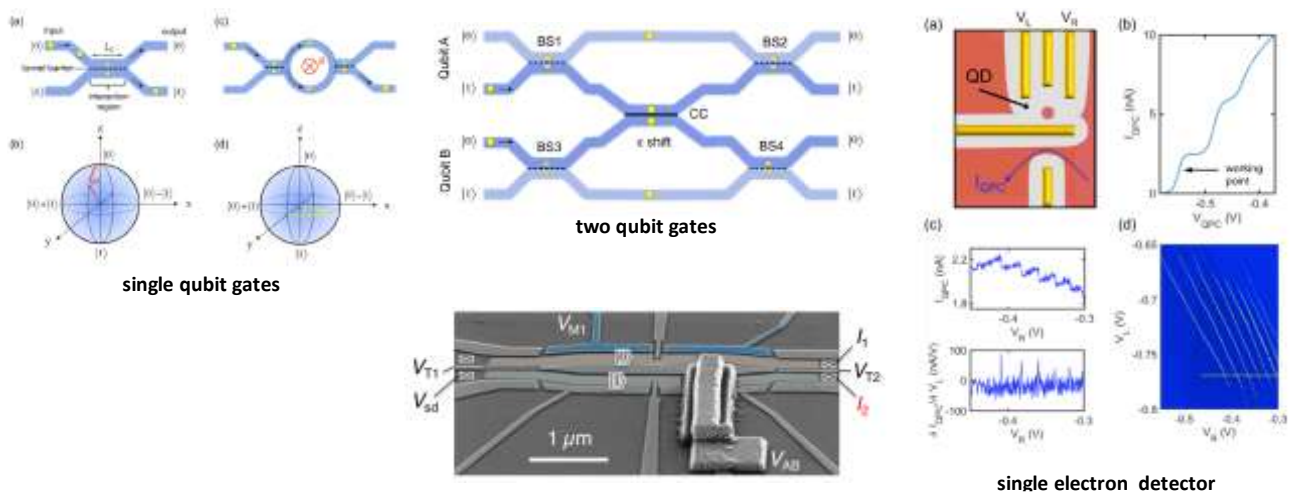


Figure 212: flying electrons in their waveguides. Their circuit architecture has some commonalities with photon circuits. Source: [Coherent control of single electrons: a review of current progress](#) by Christopher Bäuerle, Xavier Waintal et al, 2018 (35 pages).

Flying electrons are at a pure research stage qubit technology using traveling electrons³⁶⁶. It is based on using single-electron transport circulating on wave guide nanostructures build on semiconductors circuits, mostly GaAs, leveraging Coulomb coupling, quantum charge Hall effect and surface acoustic waves. Single- and two-qubit quantum gates can be realized on such circuits. Electrons can fly on distance of 6 to 250 microns. Electrons are created with producing THz photons which are converted into electrons. One qubit uses two-electron paths for states $|0\rangle$ or $|1\rangle$ ³⁶⁷. At the end of processing, these flying electrons are detected by a quantum dot.

This technique could also be used to create shuttling electrons qubits connecting static quantum dots-based qubits together. A few labs in the world are working on this including NPL in the UK, Ruhr-Universität Bochum, ERATO-JST and AIST in Japan, CEA-Leti and Institut Néel in Grenoble, France.

Exotic qubits

Many research labs are working on using exotic qubits of various kinds. Most of the time, these qubits are at the fundamental research stage and far away from industrialization or even, sometimes, are now yet materialized with a real single functional qubit.

In the **atom realm**, we can count with rare-earth ions in an insulating solid-state matrix³⁶⁸, molecular ions³⁶⁹, cold atom ensembles³⁷⁰, 2D organic molecule networks³⁷¹, LCD base nematic qubits³⁷² and chemical compounds that have photon-controlled state transitions³⁷³.

Molecular magnets are being explored, one variant being made with terbium and with four possible spin related quantum levels, creating qudits, with $d=4$. The small name of these magnets is SMM for Single-Molecule Magnets. The molecule used is TbPc2 also called bis (phthalocyaninato) terbium(III). Their state is measured with a phase-measuring interferometer. Their advantage is their stability. But they are relatively difficult to control³⁷⁴.

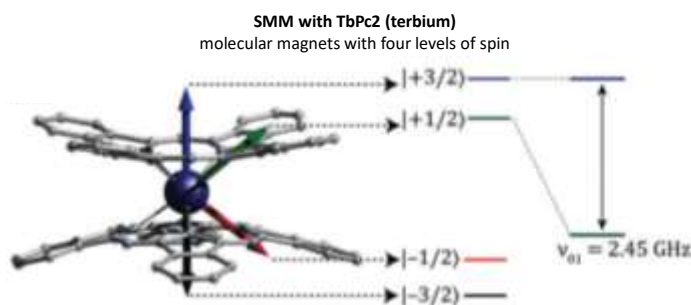


Figure 213: TbPc2 is a molecular magnet molecule used in prototype quantum processors. Source: [Molecular spin qudits for quantum algorithms](#) by Eufemio Moreno-Pineda, Clément Godfrin, Franck Balestro, Wolfgang Wernsdorfer and Mario Ruben, 2017 (13 pages).

³⁶⁶ See the review paper [Semiconductor-based electron flying qubits: Review on recent progress accelerated by numerical modelling](#) by Hermann Edlbauer, Xavier Waintal, et al, July 2022 (44 pages).

³⁶⁷ See [Electrical control of a solid-state flying qubit](#) by Michihisa Yamamoto, Christopher Bäuerle et al, 2017 (17 pages), [Coherent control of single electrons: a review of current progress](#) by Christopher Bäuerle, Xavier Waintal et al, 2018 (35 pages) and [Macroscopic Electron Quantum Coherence in a Solid-State Circuit](#) by H. Duprez et al, 2019 (10 pages).

³⁶⁸ See [Universal Quantum Computing Using Electronuclear Wavefunctions of Rare-Earth Ions](#) by Manuel Grimm et al, 2021 (19 pages).

³⁶⁹ See the review paper [Molecular-ion quantum technologies](#) by Mudit Sinhal and Stefan Willitsch, University of Basel, April 2022 (15 pages). Difficult to cool molecules with lasers. Destructive measurement.

³⁷⁰ See [Quantum supremacy with spin squeezed atomic ensembles](#) by Yueheng Shi et al, April 2022 (12 pages)

³⁷¹ See [Blueprint of optically addressable molecular network for quantum circuit architecture](#) by Jiawei Chang et al, September 2022 (11 pages).

³⁷² See [Nematic bits and universal logic gates](#) by Ziga Kos and Jörn Dunkel, August 2022 (10 pages).

³⁷³ See [Functionalizing aromatic compounds with optical cycling centres](#) by Guo-Zhu Zhu et al, UCLA, Nature Chemistry, July 2022 (6 pages).

³⁷⁴ See [Molecular spin qudits for quantum algorithms](#) by Eufemio Moreno-Pineda, Clément Godfrin, Franck Balestro, Wolfgang Wernsdorfer and Mario Ruben, 2017 (13 pages). This work was carried out in partnership with the Karlsruhe Institute of Technology in Germany. And also the thesis [Quantum information processing using a molecular magnet single nuclear spin qudit](#) by Clement Godfrin, 2017 (191 pages).

In the **electrons realm**, various topological materials³⁷⁵, various forms of graphene based qubits³⁷⁶, carbon nanotubes-based mechanical oscillators³⁷⁷, electron spin in magnetic materials in Van der Waals crystals made of chromium³⁷⁸, electrons on solid neon³⁷⁹, quantum neural networks using variations of superconducting qubits³⁸⁰, quantum memristors³⁸¹, toponomic quantum computing which is a variant of topological computing³⁸² and various qubit hybridization techniques to couple fast operating qubits and long coherence time qubits for implementing some sort of quantum memories, like with associating superconducting qubits with NV centers, or superconducting qubits with yttrium iron garnet magnons³⁸³.

Figuring out the TRL of these proposals is usually easy: it is very low! Particularly when you don't have any published one and two qubit fidelities data.

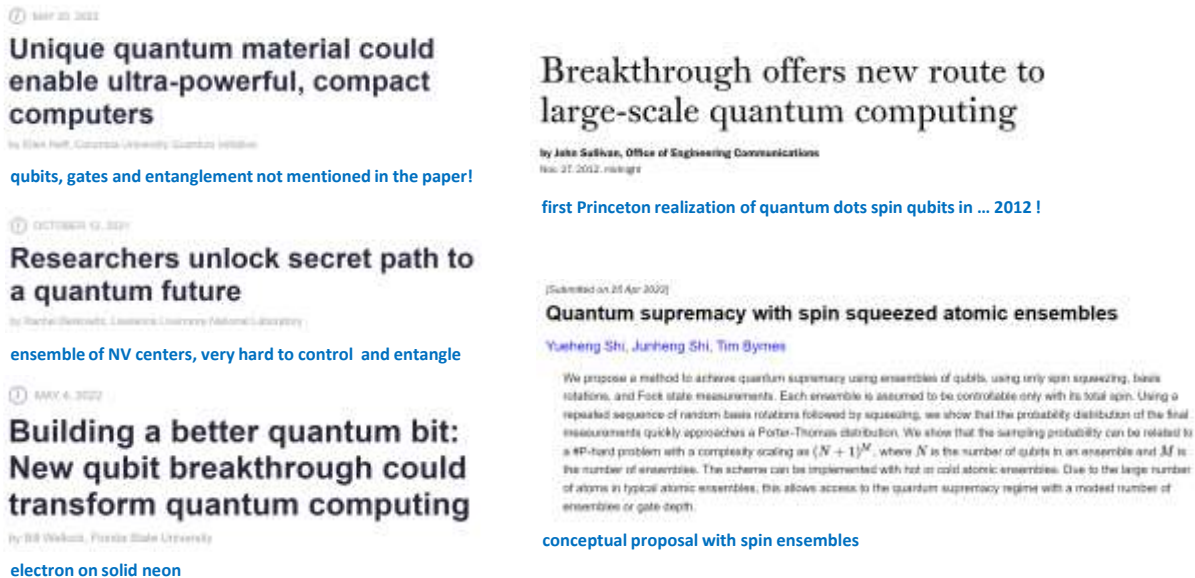


Figure 214: examples of research laboratories communication on new exotic qubits with very low TRL!

³⁷⁵ See [Anomalous normal fluid response in a chiral superconductor UTe₂](#) by Seokjin Bae et al, July 2021 (5 pages) and [Multicomponent superconducting order parameter in UTe₂](#) by I. M. Hayes, July 2021.

³⁷⁶ See [Visualization and Manipulation of Bilayer Graphene Quantum Dots with Broken Rotational Symmetry and Non trivial Topology](#) by Zhehao Ge et al, 2021 (19 pages).

³⁷⁷ See [Proposal for a nanomechanical qubit](#) by F. Pistolesi, Andrew Cleland, A. Bachtold, August 2021 (19 pages).

³⁷⁸ See [Unique quantum material could enable ultra-powerful, compact computers](#) by Ellen Neff, Columbia University Quantum Initiative, May 2022, referring to [Coupling between magnetic order and charge transport in a two-dimensional magnetic semiconductor](#) by Evan J. Telford et al, Nature Materials, May 2022 (15 pages). The initial title is of course quite overselling. One simple indication in the scientific paper: the words qubits, gates and entanglement are not even mentioned. So, a powerful quantum computer is very far in this roadmap even though it could operate at 132 K which is considered to be “hot” in quantum computing (ambient temperature is 300K)!

³⁷⁹ See [Building a better quantum bit: New qubit breakthrough could transform quantum computing](#) by Bill Wellock, Florida State University, May 2022, referring to [Single electrons on solid neon as a solid-state qubit platform](#) by Xianjing Zhou, David I. Schuster et al, Nature, May 2022 (16 pages). The team created its qubit by freezing neon gas into a solid at very low temperatures, spraying electrons from a light bulb onto the solid and trapping a single electron there.

³⁸⁰ See [Coherently coupled quantum oscillators for quantum reservoir computing](#) by Julien Dudas, Julie Grollier and Danijela Marković, April 2022 (4 pages), a quantum reservoir neural network implementation on a Josephson parametric converter.

³⁸¹ See [Quantum Memristors with Quantum Computers](#) by Y.-M. Guo, F. Albarrán-Arriagada, H. Alaeian, E. Solano, G. Alvarado Barrios, PRA, December 2021 -August 2022(7 pages) and [Entangled quantum memristors](#) by Shubham Kumar, Enrique Solano et al, arXiv and PRA, July & December 2021 (9 pages).

³⁸² See [Toponomic Quantum Computation](#) by C. Chryssomalakos et al, February 2022 (5 pages).

³⁸³ See [Analog quantum control of magnonic cat states on-a-chip by a superconducting qubit](#) by Marios Kounalakis et al, PRL, TU Delft, Tohoku University and CAS in China, July 2022 (14 pages).

These are most of the time interesting physics experiments but no functional qubit, a fortiori, entangled qubits and related fidelities. Sometimes, there are real use cases but not in quantum computing and more in quantum sensing. It won't of course present research laboratories communications departments to fuel the hype with their stack of overpromises.

Figures of merits

Let's now inventory the various figures of merit of these qubit architectures:

Qubits stability which is evaluated with their coherence time (the T_1 we'll describe later when discussing error correction page 216). Associated with quantum gate times and error rate, it conditions the number of quantum gates that can be chained in an algorithm. The most stable qubits so far are trapped ions based but as far as you don't have too many of them.

Qubits fidelity is related to the errors level that is evaluated with single and double gates as well as with measurement. Again, the best-in-class are trapped ions. We cover that starting 220.

Qubits connectivity is the way they are linked together, which will condition many parameters such as the execution speed and the depth of the algorithms that can be exploited. Best-in-class qubits for this respect are again trapped ions in 1D structures, although it does not scale well.

Large scale entanglement if possible, without being limited to the immediately neighboring qubits. So far, nobody does it really well.

Operating temperature and for the accompanying electronics. The best are NV centers which are supposed to work at ambient temperature, and the worst are superconducting qubits, requiring 15 mK.

Qubits density and their control electronics which impacts scalability. This rather favors quantum dots electron spin qubits.

Manufacturing process which depends on many parameters. In the case of cold atoms, for example, it is not necessary to create specialized circuits, whereas it is necessary for all other technologies.

Scalability potential which depends on many systems parameters, both at the fundamental level with the qubit stability and fidelities at large scale but also with the various enabling technologies. Unfortunately for your forecasting, scalability potentials do not align with qubits technologies present maturities!

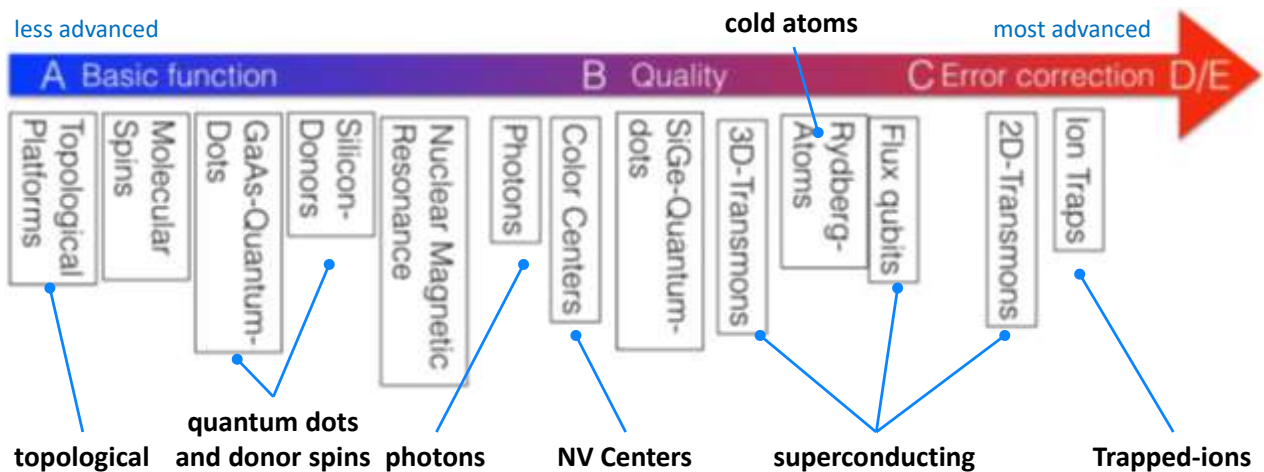


Figure 215: degree of maturity of various qubit technologies. *Entwicklungsstand* Quantencomputer (State of the art of quantum computing, in English, June 2020 (266 pages).

The level of qubits is evolving rapidly. It is described in this excellent document from the German cybersecurity agency³⁸⁴. It mentions other technologies not listed in this inventory.

Here's another way to put it³⁸⁵. It segments the types of qubits according to three dimensions: the clock frequency of the quantum gates (roughly, the gates number that can be executed per second), the number of operations before errors occur, and the quantum gates fidelity (separating the one- and two-qubit gates). These last two axis are roughly homothetic because the number of operations before errors are generated depends on the error rate.

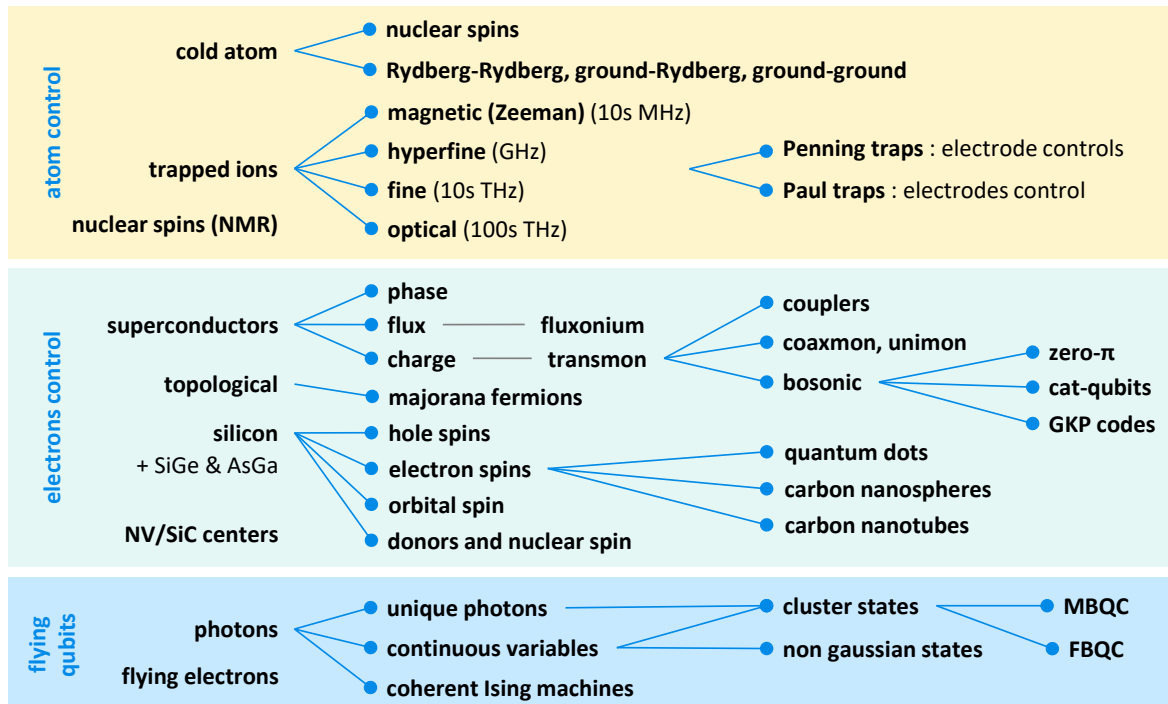


Figure 216: rough zoology of qubits classes and sub-classes. (cc) Olivier Ezratty, 2022.

Trapped ions have better gates than superconducting qubits but are quite slow. Silicon qubits are for the moment quite fast (at least, as fast as superconducting qubits). Cold atoms are slower. A last axis is missing: the number of qubits as of today and technology scalability. The chart was made in 2019 and may be outdated for some qubit types. In the section devoted to quantum computing commercial vendors, we cover with more detail the science and technology behind each of these types of qubits, starting page 292.

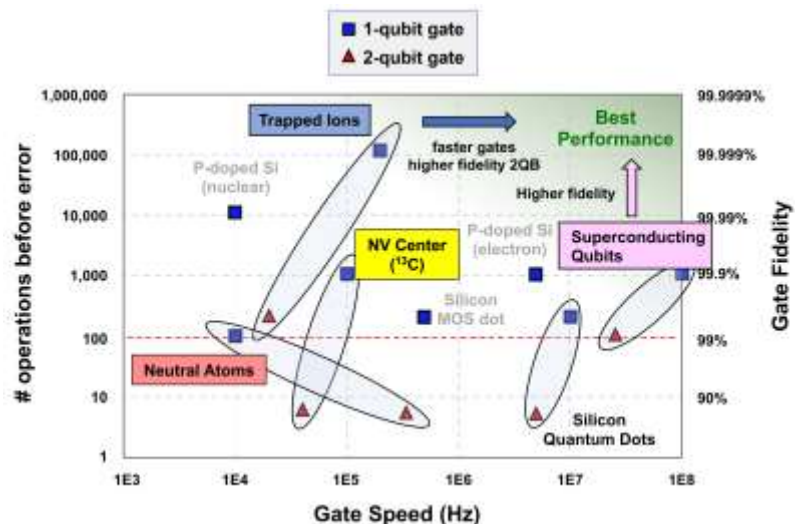


Figure 217: comparison of qubit computing depth and gate speed. Source: [Engineering Quantum Computers](#) by William D. Oliver, December 2018 (15 slides).

³⁸⁴ See [Entwicklungsstand Quantencomputer](#) (State of the art of quantum computing, in English, June 2020 (266 pages).

³⁸⁵ See [Introduction to Quantum Computing](#) by William Oliver from MIT, December 2019 (21 slides) and [Engineering Quantum Computers](#) by William D. Oliver, December 2018 (15 slides).

Architecture overview

We will provide here an overview of the general architecture of a quantum computer, using the example of a superconducting qubit accelerator.

First of all, a bit like some external GPUs, quantum computers are implemented as co-processors or accelerators of classical computers that power and control them. A quantum computer is always driven by a classical computer, as can be a GPU for video games or for training neural networks in deep learning. These conventional computers are used to run the programs that are driving the quantum processor with physical operations to be performed on the qubits and are interpreting qubits readout results.

The classical computer closely controls the operation of the quantum computer by triggering at a precise rate the operations on the qubits that are performed by various electronic devices creating various electronics and photonic signals controlling quantum gates and quantum readout. It takes into account quantum gates execution time and the known qubits coherence time, i.e., the time during which the qubits remain in a state of superposition and entanglement. You will always need a classical computer to drive all of these tasks, unless you are Donald Trump, who can certainly do this with his thoughts.

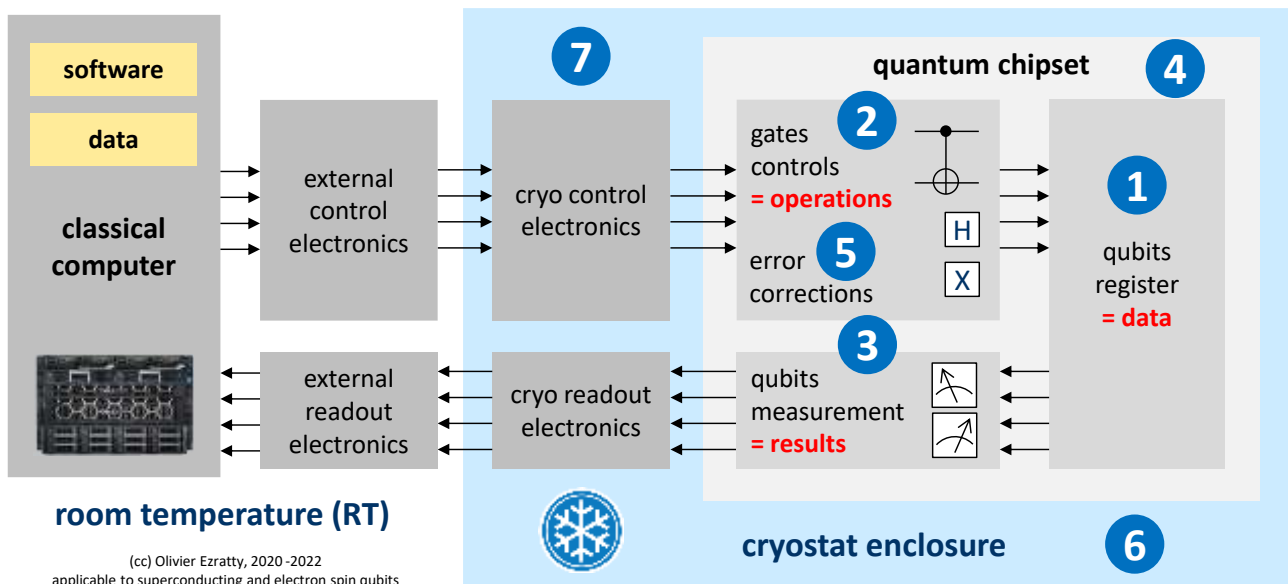


Figure 218: typical high-level architecture of a gate-based quantum computer. (cc) Olivier Ezratty, 2020.

In addition to its classical control computer, our quantum computer includes at least the components labeled from 1 to 7 that we will describe one by one, first with an overview below, then later, with a more detailed view. The other types of quantum computers have similarities and differences that we will mention whenever relevant.

1 Quantum registers are collections of qubits. In 2021, the benchmarked record was 65 superconducting qubits with IBM. Quantum registers store the information manipulated in the computer and exploit the principle of superposition and entanglement allowing simultaneous operations on a large number of register values. To make a parallel with classical computing, this is memory. But processing is done directly in memory.

2 Quantum gate controllers are physical devices that act on the quantum register qubits, both to initialize them and to perform quantum gates on them. These gates are applied iteratively, according to the algorithms to be executed. They can also be used to manage error correction codes. Quantum gates feed registers with both data and instruction. These are not separated operations like with classical microprocessors.

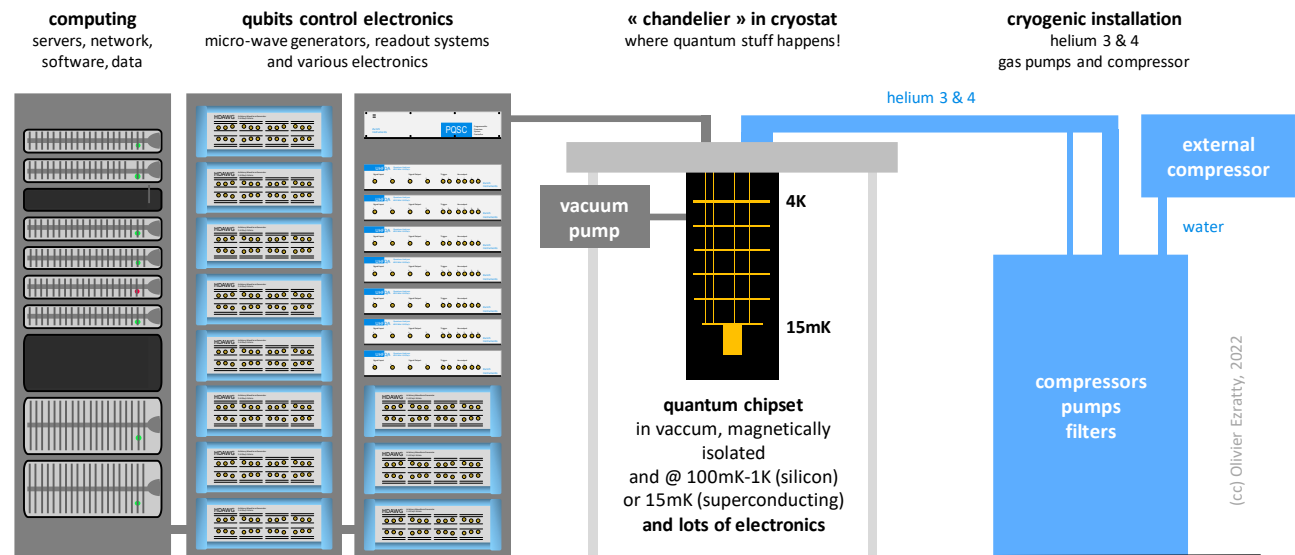
③ **Measurement** qubit states is used to obtain the result at the end of the sequential execution of an algorithm's quantum gates and to evaluate error syndromes during quantum error correction. This cycle of initialization, calculation and measurement is usually applied several times to evaluate an algorithm result. The result is then averaged to a value between 0 and 1 for each qubit in the quantum computer's registers. The signals coming from qubit readout are then converted into digital values and transmitted to the conventional computer which controls the whole and implements results interpretation. In common cases, such as with D-Wave and IBM, computing is repeated at least a couple thousand times. The reading devices are connected to their control electronics via superconducting wires in the case of superconducting computer qubits.

④ **Quantum chipset** usually includes quantum registers, quantum gates controls and measuring devices when it comes to superconducting or electron spin qubits. These are fed by microwaves coming from outside the chipset. Devices are more heterogeneous for other types of qubits, such as those that use lasers for initialization, quantum gates and qubit measurement like with trapped ions and cold atoms. Current chipsets are not very large. They have the size of a full-frame or dual-format photo sensor for the largest of them. Each qubit is relatively large, their size being measured in microns for superconducting qubits or down to 100 nm for electron spin qubits whereas modern CMOS processor transistors now have transistor sizes around 5 nanometers. The chipset for superconducting and electron spin qubits is a chip of a few square centimeters. It is usually integrated in an OFHC (Oxygen-Free High thermal Conductivity) copper packaging which is purified and freed from oxygen, limiting thermal conductivity. This package is fitted with coaxial connectors so that it can be fed by the microwaves controlling qubit gates. In the latest superconducting processors from IBM and Google with 53 qubits, more than 160 of these connectors are required. The chipset package is integrated in two small concentric aluminum and Cryoperm (from **MuShield**) magnetically insulated enclosures.

⑤ **Error correction** is implemented with special code operating on a large number of consolidated qubits named logical qubits. They can be physically organized to optimize error correction, such as with surface codes and color codes. It's one of the biggest challenges ahead for creating scalable quantum computers. As of 2021, no quantum computer is large enough to accommodate logical qubits, given the number of physical per logical qubits exceeds the maximum number of qubits currently available.

⑥ **Cryogeny** usually keeps the qubit chipset and its surrounding control electronics at a temperature close to absolute zero. It contains part of the control electronics and the quantum chip(s) to avoid generating disturbances that prevent the qubits from working. The Holy Grail would be to operate qubits at room temperature but the corresponding architectures such as in NV centers are not yet operational and there are still practical performance reasons to operate it at low-temperatures. The cryostat uses a mix of helium 3 and 4 to cool the components inside the chandelier while its compressor is itself cooled with cold water coming from another compressor, similar to the compressors used in classical air conditioning. Other types of qubits use cryostats in different places: with cooling photon sources or detectors in photon qubits systems, or for cooling ultra-vacuum pumps with cold atoms.

⑦ **Control electronics** in the cryostat enclosure. The qubit control electronics drive the physical devices used to initialize, modify, and read the qubit status. In superconducting qubits, quantum gates are activated with microwave generators of frequencies between 4 and 8 GHz generally located outside the cryostat. These microwaves are transmitted on coaxial electrical wires between their source and the quantum processor, with superconducting cables below 4K. Their generators still take up a lot of space. They are not very miniaturized at this stage. Interesting work aims at integrating these microwave generators and readers inside the cryostat enclosure, if only to limit the wiring. These are frequently based on cryo-CMOS technology, CMOS components that are tailored to work at low temperature, 4K for many and as low as 20 mK for some. Figure 219 provides a rough representation of an entire superconducting qubits based quantum computer. The blue equipment corresponds to the microwave generators and analyzers from Zurich Instruments.



for superconducting or electron spin qubits

Figure 219: typical physical components of a superconducting qubit quantum computer. It contains a classical computer that drives the whole system. (cc) Olivier Ezratty, 2020-2022.

Processor layout

To better understand the previous explanation, here is a chipset layout with 8 superconducting qubits, from ETH Zurich. Although it's already a few years old, the underlying concepts are generic.

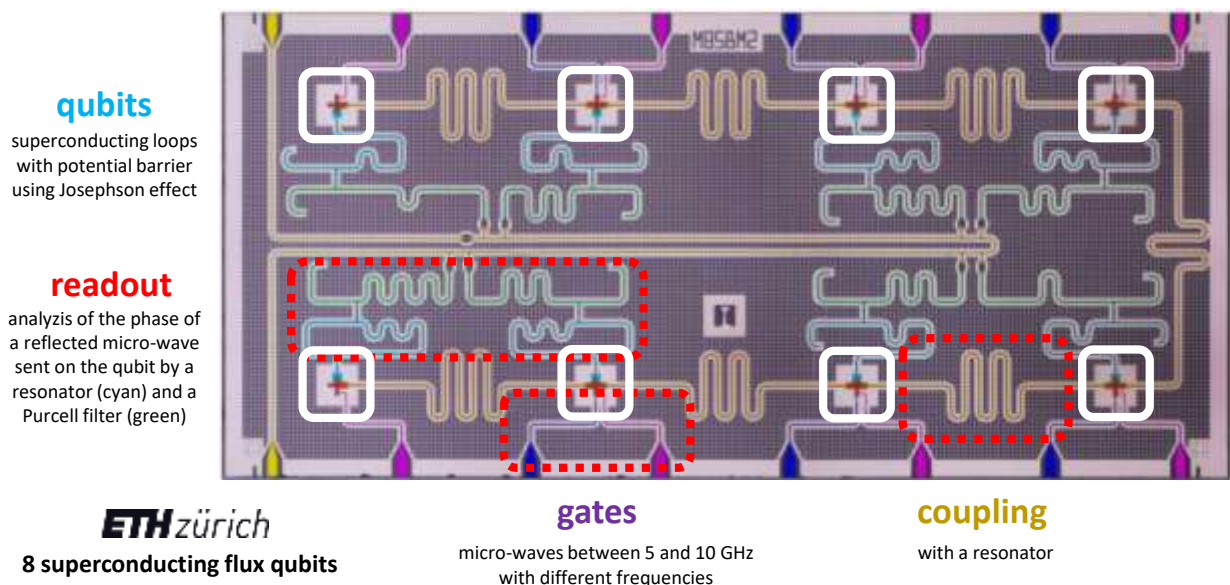


Figure 220: a small 8-qubit superconducting processor from ETH Zurich showing its various components controlling the qubits. source: [The European Quantum Technologies Roadmap](#), 2017 (30 pages) and the thesis [Digital quantum computation with superconducting qubits](#) by Johannes Heinsoo, ETH Zurich, 2019 (271 pages).

- **Qubits** are located in the white rectangles. These are tiny Josephson effect superconducting circuit loop.
- **Coupling circuits** link them together. It's used to control entanglement between pairs of qubits.
- **Single-qubit gates** use the blue and purple contacts. It sends microwaves to the qubits. These pins are powered via cables by very high frequency current sources, sending microwaves photons, between 4 and 8 GHz. These frequencies must be different between adjacent qubits of the same circuit to avoid crosstalk. It is the combination of these frequencies that will trigger different types of quantum gates and entanglements between adjacent qubits.

- **Measurement** takes place with other circuits, also fixed in the component. In superconducting qubits, these are magnetometers which are then connected to the outside of the vacuum chamber and cooled by superconducting cables. These are driven by microwaves.

Qubits must interact with each other but as little as possible with their environment until measurement. This is one of the reasons why they are usually cooled to a temperature close to absolute zero and magnetically isolated from the outside. The choice of materials for the chipsets also plays a role in minimizing the noise that could affect the qubits and bring them out of their coherent state.

In the diagram below is the how and why of the relationship between qubit gates time and coherence time during which the qubits remain stable. The orders of magnitude of these times for a typical quantum computer, particularly with superconducting qubits, give at best a ratio of 1 to 500 between gate times and coherence time. This means that the number of quantum gates that can be used in an algorithm is limited on NISQ systems. In the first generations of IBM quantum computers, the X, Hadamard and CNOT gates lasted 130 ns, 130 ns and 650 ns respectively.

These indications provide an upper limit on the number of gates that can be chained in a quantum algorithm. Note that these times are longer for quantum computers with ion traps, but the gate times are also longer. In CMOS qubits, coherence times are longer and gate times are low.

However, the available computing time is more limited by the quantum gates error rate. It constrains what is called the computation depth, i.e. the number of quantum gates that can be chained together without the error rate of the gates mitigating the results. Algorithms must therefore optimize the number of gate cycles to be executed, which is furthermore constrained by the physical connectivity between qubits.

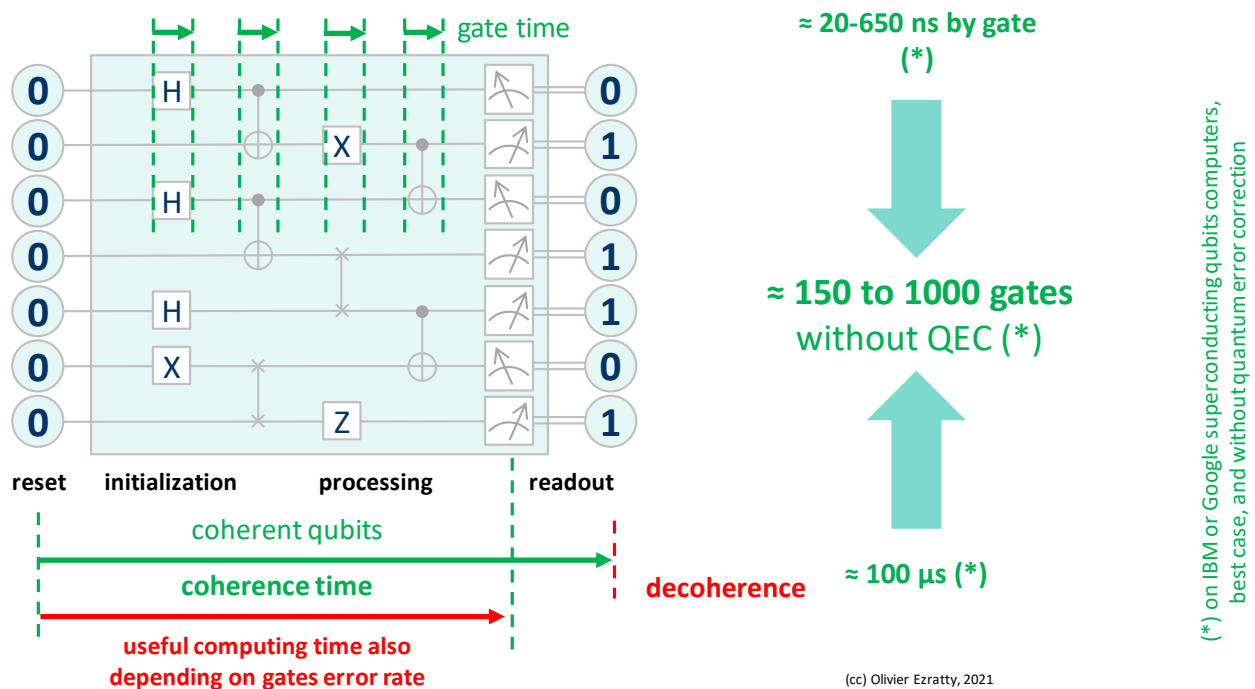


Figure 221: a timeline showing the relation between useful computing time and gate coherence time and fidelities. (cc) Olivier Ezratty, 2021.

In diagrams describing quantum algorithms, such as the one in Figure 221, the double bar after measuring the state of a qubit conventionally indicates that a normal bit has been recovered, at 0 or 1. By the way, all this reminds us that there are as many output qubits as input qubits in a quantum computation since they are physically the same!

Error correction

One of the pitfalls of existing qubits is their significant error rates generated with quantum gates and measurement and coming mostly from the fateful quantum decoherence.

Decoherence is mostly generated by the interactions between the qubits and their environment. It progressively destroys the quantum information sitting in the qubits, and particularly the entanglement between these. It leads to an inevitable failure in computation after a short time. Error rates for each operation and readouts are commonly between 0.1% and several %, depending on the qubit type and quality. But even 0.1% is an intolerable level for most calculations.

In conventional computing, errors are way less frequent but must still be corrected. While some errors may be detected and fixed during computing in microprocessors, most errors are happening in memory, storage and telecommunications. These errors are discrete, corresponding to some unwanted bit flip. In quantum technologies, errors happen first and foremost in computing and within qubits and they are continuous and analog by nature.

So, we correct them with various techniques that we'll cover here, without necessary going into their details. This field is quite broad and very technical. We'll describe the various Quantum Error Correction (QEC) techniques that will be related to Fault-Tolerant Quantum Computing and Quantum Error Mitigation techniques that will be applicable in the near-term NISQ generation of quantum computers.

Errors sources and typologies

A qubit register is coherent when its qubits superposition and entanglement is preserved over some period of time. At the individual qubit level, qubit stability is measured against its amplitude and phase stability, related to flip and phase error rates. Qubits coherence time is an indication of how long register qubits remain coherent, with stable superposition. Qubits amplitude stability is evaluated with a T_1 time while phase stability is measured with a T_2 and a T_2^* , these being sometimes confused with each other in the literature³⁸⁶.

Real single qubit errors can be decomposed as linear combinations of these flip and phase errors³⁸⁷. Quantum error corrections codes are designed to separately correct flip and phase errors, the integration of which corrects any linear combination of both error types.

- **Flip errors** as shown in the Bloch sphere in Figure 222, are amplitude errors that tend to push the amplitude back to $|0\rangle$. These errors correspond mathematically to a decay of the diagonal part of the qubit density matrix in its eigenstate basis. It is related to the T_1 , which is linked to a loss of amplitude ("energy relaxation"). It is also called "longitudinal coherence time", "spontaneous emission time", "population lifetime" or "amplitude damping" and corresponds to a loss of energy in qubits. It is a dissipative process that releases some energy³⁸⁸.

³⁸⁶ I found a good explanations in [Dancing with qubits](#) by Robert Sutor, pages 415 to 421, 2019 (516 pages).

³⁸⁷ More precisely, single qubits errors can be decomposed in quantum channels: depolarizing channel (with a bit flip error, a phase flip error or a combination of both, in which case, the qubit remains in a pure state, and the qubit moves with some rotation in the Bloch sphere), a dephasing or phase damping channel (vanishing off-diagonal values in the qubit density matrix, in which case the qubit moves in a mixed state and inside the Bloch sphere) and an amplitude-damping channel. Source: [Lecture Notes for Ph219/CS219: Quantum Information Chapter 3](#) by John Preskill, Caltech, October 2018 (65 pages).

³⁸⁸ In superconducting qubit circuits, T_1 is proportional to the circuit quality factor $Q = \omega_q T_1$, which itself is proportional to the ratio between the energy stored in the qubit resonator and its rate of energy loss. T_1 comes from different phenomena: spontaneous emission, quasiparticle tunneling, flux coupling and dielectric losses in the Josephson junction. The Purcell effect is a spontaneous emission through the readout cavity. The Purcell decay rate is related to the speed of this phenomenon. It is reduced with using a Purcell filter which suppresses signal propagation at the qubit transition frequency. The filter is a pass-through with the readout cavity frequency that protects the qubit from decoherence channels while enabling its readout

The flip error is measured with a simple experiment with using an X gate and measuring the result n times at different t times. T_1 corresponds to the time when the probability of obtaining a $|1\rangle$ reaches $1/e$. Such an error can damage the entanglement of the qubits related to the one affected by this error.

T_1 : flip error (relaxation, dampening)

- qubit energy loss the the environment.
- spontaneous emission, quasiparticle tunneling, flux coupling, dielectric losses and control electronics imprecision.
- more important at qubit readout.
- time to decay from $|1\rangle$ to $|0\rangle$.
- decay of qubit density matrix diagonal.

$T_2 - T_2^*$: phase error (dephasing, decoherence time)

- environment creates loss of phase memory.
- control electronics imprecision.
- important during computation.
- tied to number of consecutive gates.
- decay of qubit density matrix off-diagonal values.

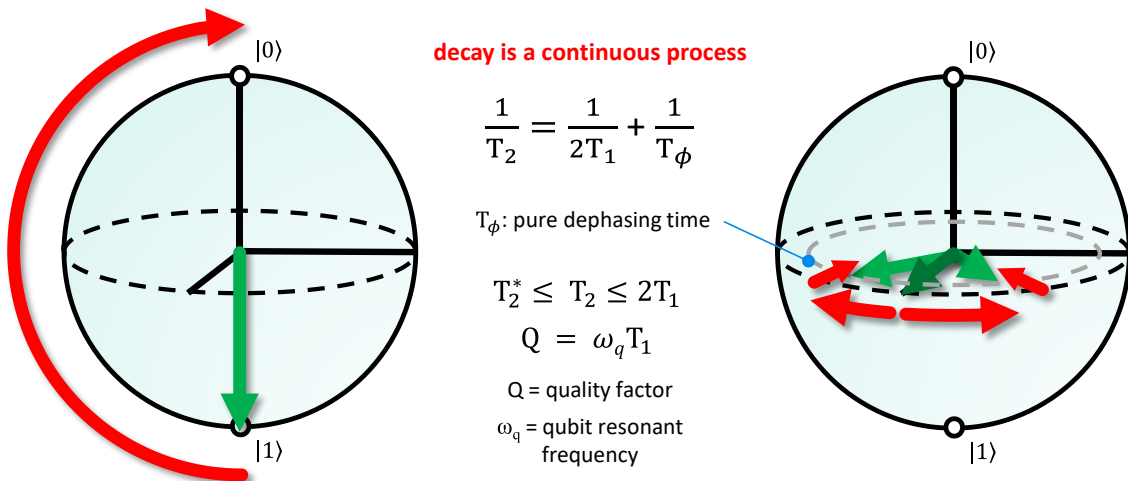


Figure 222: flip error and phase errors and their effect in the qubit Bloch sphere. (cc) Olivier Ezratty, 2022.

- **Phase errors** are rotations around the z-axis in the Bloch sphere (coherent noise, mostly due to control electronics imprecision) coupled with a move of the qubit vector within the sphere (decoherence noise, pure dephasing). These errors are not dissipative, meaning, they are thermodynamically neutral. Pure dephasing is related to the decay of the non-diagonal part of the qubit density matrix, creating a mixed state explaining why the qubit state moves inside the Bloch sphere. Coherent phase errors are measured in two manners, with T_2^* and T_2 and are also called the “transverse coherence time”, “transverse relaxation”, “phase coherence time” or “phase damping”. T_2^* is evaluated with a Ramsey experiment, applying one Hadamard gate, wait time t , then apply another Hadamard gate, and measure the output. Without phase errors, the probability should look like a sinusoidal curve. With it, the curve slowly converges around a probability 0.5. T_2^* is obtained when the probability reaches $1/e$. On the other hand, T_2 is obtained with a Hahn echo experiment where an X gate is added at $t/2$, which removes some error sources not pertaining to qubit defects.
- **Leakage errors** is a third error type that sees a qubit drifting and stabilizing in another energy state than the basic $|0\rangle$ or $|1\rangle$. This can occur in the $|2\rangle$ level of a superconducting qubit, which we are trying to avoid, or with variations in the hyperfine energy levels of trapped ion qubits. This type of error can be corrected with specific reset protocols³⁸⁹. You don’t observe such leakage errors with photon qubits using polarization as information encoding.

³⁸⁹ See an example in [Removing leakage-induced correlated errors in superconducting quantum error correction](#) by M. McEwen et al, Google AI, February 2021 (12 pages).

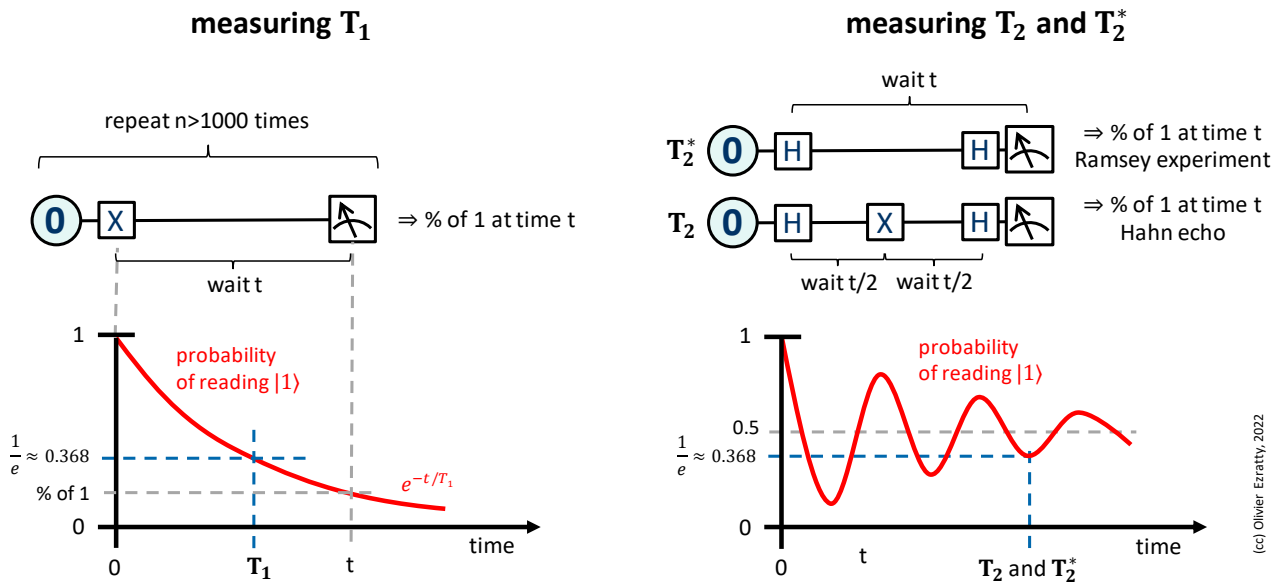


Figure 223: how are measured T_1 , T_2 and T_2^* . (cc) Olivier Ezratty, 2022.

The goal of having long qubit energy relaxation times is in competition with that of achieving high-fidelity qubit control and measurement. One key concern is to be able to apply error corrections as fast as possible after they are detected and before qubits decoherence takes effect or gets amplified. This is the reason why readout gates and phase detection electronics (for superconducting/quantum dots spin qubits) must be as fast as possible. But fast gates and readouts can drive leakage errors! They also require high-bandwidth microwave pulses, which reduce the capacity to frequency multiplex it in readout microwave circuits.

Error sources are multiple³⁹⁰, leading notably to the progressive decoherence of qubits which affects qubits superposition and entanglement. They are linked to the various interactions between qubits and their immediate environment³⁹¹. These include:

- **Control electronics** imperfections like clock, phase and amplitude jitter. It can be triggered by calibration errors of quantum gates that occur in particular in the calibration of superconducting qubits. They can notably trigger leakage errors. These small errors can create imprecisions with qubit operations. They are mitigated with improving the precision of control electronics. With superconducting and quantum dots spin qubits, it's mainly located at the local oscillators, mixers, AWG (arbitrary wave generation) and DAC levels (digital to analog conversion). These are coherent errors while other errors drive qubits decoherence.
- **Thermal noise** from components around the qubits. This is the reason for the existence of attenuators around superconducting qubits. It comes among other things from shocks between atoms.
- **Electrical and magnetic noise** which can have many origins depending on the qubits. It explains why D-Wave isolates its quantum computer with 16 metal layers to limit the impact of terrestrial magnetism on its qubits. Most solid state quantum processors are packaged in tight metal shielding.
- **Material defects** which are commonplace with solid state qubits (superconducting, quantum dots spins, NV centers). One common defect comes from dielectric losses in the Josephson junction of superconducting qubits.

³⁹⁰ Here is a small inventory of noise sources for superconducting qubits: [Sources of decoherence](#), ETH Zurich, 2005 (23 slides).

³⁹¹ Any operation will generate an error. An error can be generated at the time of correction, at the time of detection or at the time of application of a gate. Doing nothing on a qubit can also generate errors because of its finite coherence time.

- **Vacuum quantum fluctuations** originating errors which we studied quickly in a previous section, page 134³⁹². It's an endogamous source of errors within qubits while all others are exogamous.
- **Radioactivity**, particularly coming from cosmic rays. Radiations can be X-rays, gamma rays (whose electromagnetic nature was discovered in 1914), beta particles and their ionizing effects. The phenomenon is now well characterized. It creates phonons quasi-particles in the chipset substrate that can propagate to many surrounding qubits, endangering the efficiency of quantum error correction codes³⁹³. Radioactivity is one of the many sources of long range correlated noise. Envisioned solutions are to shield the qubit processing unit with lead³⁹⁴ or copper backside metallization³⁹⁵, to trap phonons using high impedance resonators made of granular aluminum³⁹⁶ and to implement distributed error corrections schemes³⁹⁷.

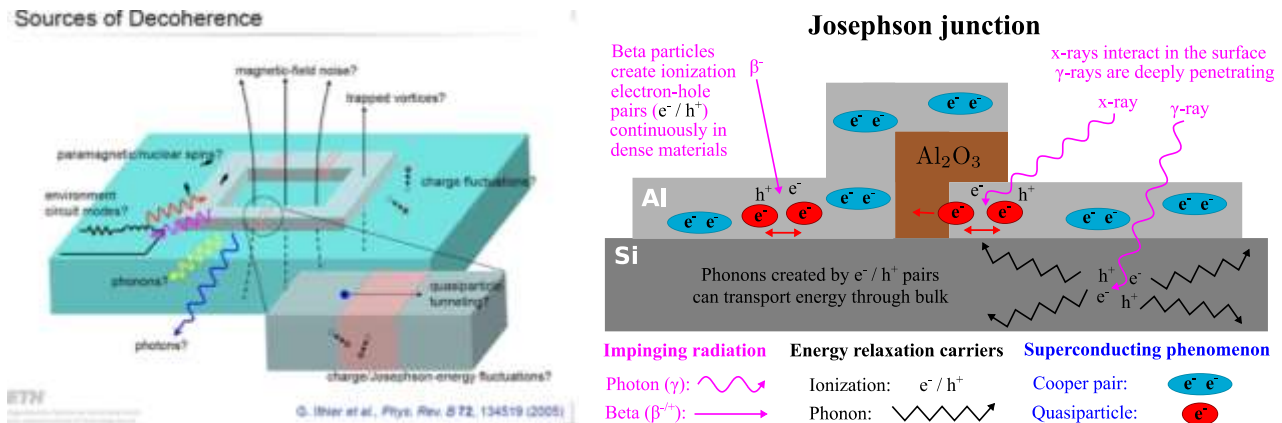


Figure 224: sources of decoherence and cosmic radiations affecting superconducting qubits. Sources: [Sources of decoherence](#), ETH Zurich, 2005 (23 slides) and [Impact of ionizing radiation on superconducting qubit coherence](#) by Antti P. Vepsäläinen, William D Oliver et al, August 2020 (24 pages).

- **Gravity**, given this type of error and vacuum fluctuation ones appear to be minor compared to the previous ones³⁹⁸.

Generally speaking, errors are generated by various interactions, electromagnetic or mechanical, between qubits and their immediate environment and are associated with the phenomenon of quantum decoherence. The first objective of physicists is obviously to reduce these physical sources of error. They are progressing steadily but are barely managing to gain one or two orders of magnitude in error rates, whereas in an ideal world, we would need ten orders of magnitude improvements.

³⁹² See [Observation of quantum many-body effects due to zero point fluctuations in superconducting circuits](#) by Sébastien Léger, Nicolas Roch et al, Institut Néel, 2019 (8 pages) which describes the phenomenon on superconducting qubits.

³⁹³ See [Correlated charge noise and relaxation errors in superconducting qubits](#) by C.D. Wilne, Roger McDermott et al, Nature, December 2020-June 2021 (19 pages) which describes the correlated errors appearing in superconducting qubits and how it could impact the architecture of quantum error correction codes, [Resolving catastrophic error bursts from cosmic rays in large arrays of superconducting qubits](#) by Matt McEwen, Rami Barends et al, Google AI, Nature Physics, December 2021 (13 pages) who developed a test protocol to assess the impact of radiations on 26 qubits in its Sycamore processor and [TLS Dynamics in a Superconducting Qubit Due to Background Ionizing Radiation](#) by Ted Thorbeck et al, IBM, October 2022 (14 pages) which identifies the impact of ionizing radiations on qubit lifetimes.

³⁹⁴ See [Impact of ionizing radiation on superconducting qubit coherence](#) by Antti P. Vepsäläinen, William D Oliver et al, August 2020 (24 pages).

³⁹⁵ See [Phonon downconversion to suppress correlated errors in superconducting qubits](#) by V. Iaia, Robert McDermott et al, Wisconsin and Syracuse Universities, March 2022 (21 pages).

³⁹⁶ See [Phonon traps reduce the quasiparticle density in superconducting circuits](#) by Fabio Henriques et al, Applied Physics Letters, 2019 (14 pages).

³⁹⁷ See [Distributed quantum error correction for chip-level catastrophic errors](#) by Qian Xu, Lian Jiang et al, March 2022 (11 pages).

³⁹⁸ See about gravity: [A model of quantum collapse induced by gravity](#) by Franck Laloë, 2020 (14 pages) and [Gravitational Decoherence](#), 2017 (78 pages).

Some of these effects are avoided by cooling the qubits to a temperature close to absolute zero, but this is not enough. Researchers are therefore working hard to ensure that the noise affecting the qubits is as low as possible so that qubits coherence time can be as long as possible.

We have to manage this contradiction: qubits remain coherent, in a state of superposition and entanglement, if we do not disturb them, but we spend our time disturbing them with quantum gates operations! There are three ways to address these issues: improving gates fidelity, implementing quantum error correction codes and at last, reduce the number of gates needed to run algorithms.

Qubits fidelities

In a gate-based quantum computer, three types of errors (or related fidelities) are usually evaluated: errors in single-qubit quantum gates, errors in two-qubit gates, and errors with qubits readout. These error rates are currently sitting between 0.1% and several 1%, which is much higher than the current error rates of traditional computing, which are negligible³⁹⁹. Qubits "fidelity" for any of these three dimensions is 100% minus the related error rate. In typical quantum parlance, when a "three-nines" 2 qubit-fidelity is mentioned, it means that it is better than 99,9%.

The chart below in Figure 225 consolidates a comparison of some fidelity levels of superconducting, trapped ion and cold atom quantum computer qubits, this information being provided by their vendors⁴⁰⁰. Qubit fidelities encompasses these three fidelities/errors dimensions (1Q, 2Q, readout).

Two-qubit gates and readout error rates are generally higher than one-qubit gates error rates⁴⁰¹. We must therefore always pay attention to two-qubit gates, particularly given these gates are the source of much of the quantum computing power.

But these fidelities are not always measured in the same conditions. Some are measured with only a couple interacting qubits while others are done with all the register's qubits being active. It can create significant differences favoring the first kind of measurements, particularly due to the significant crosstalk between qubits.

The best fidelity achieved as of 2022 was 99.989% for Honeywell's 4 ion trapped single-qubit gate and 99.91% for IBM's Falcon R10 (27 qubit) dual-qubit gates⁴⁰². Google's Sycamore single qubit gates fidelity is 99.84% with 53 qubits. The two-qubit CZ gates fidelity of China's Zuchongzhi 2.1 66 qubits superconducting processor is 99.4%⁴⁰³.

Another observation relates to IBM's most recent fidelities with their best-in-class 27, 65 and 127 qubit systems as of November 2021. It did show 2-gates and readout fidelities that are lower as the number of qubits grows. Still, for a given a qubits number, IBM improves its processor fidelities over time.

³⁹⁹ In classical calculation, errors are very rare. We talk about single particle perturbations (PPI) and single event upset (SEU) which trigger "soft errors" or logical errors. The SER (Soft Error Rate) combines the SDC (Silent Data Corruption, not detected) and the DUE (Detected and Unrecoverable Error, detected but not correctable). The unit of error measurement is the FIT (Failure in Time), which corresponds to one error per billion hours of use. The MTBF of electronic equipment (Mean Time Between Failure) is generally measured in years or decades. Errors are generally caused by isolated particles (ions, electrons, photons), particularly from cosmic rays like high-energy gamma rays. This affects in particular the electronics used in aerospace, which must be hardened to withstand them, as well as those used on Earth but at altitude. Memory is often more affected than processors. Hence error correction systems that use for example a parity bit and cyclic redundancy check used in telecommunications.

⁴⁰⁰ Source for qubit reliability data mainly comes from [Qubit Quality on Quantum Computing Report](#) website, 2020. Plus some additional data coming from vendor sites.

⁴⁰¹ See [An introduction to quantum error correction](#) by Mazyar Mirrahimi, 2018 (31 slides) as well as [Introduction to quantum computing](#) by Anthony Leverrier and Mazyar Mirrahimi, March 2020 (69 slides) which completes it well.

⁴⁰² See the NASA and Google paper describing Google's performance: [Quantum Supremacy Using a Programmable Superconducting Processor](#) by Eleanor G. Rieffel et al, August 2019 (12 pages).

⁴⁰³ Data source: [Superconducting Quantum Computing](#) by Xiaobo Zhu, June 2019 (53 slides).

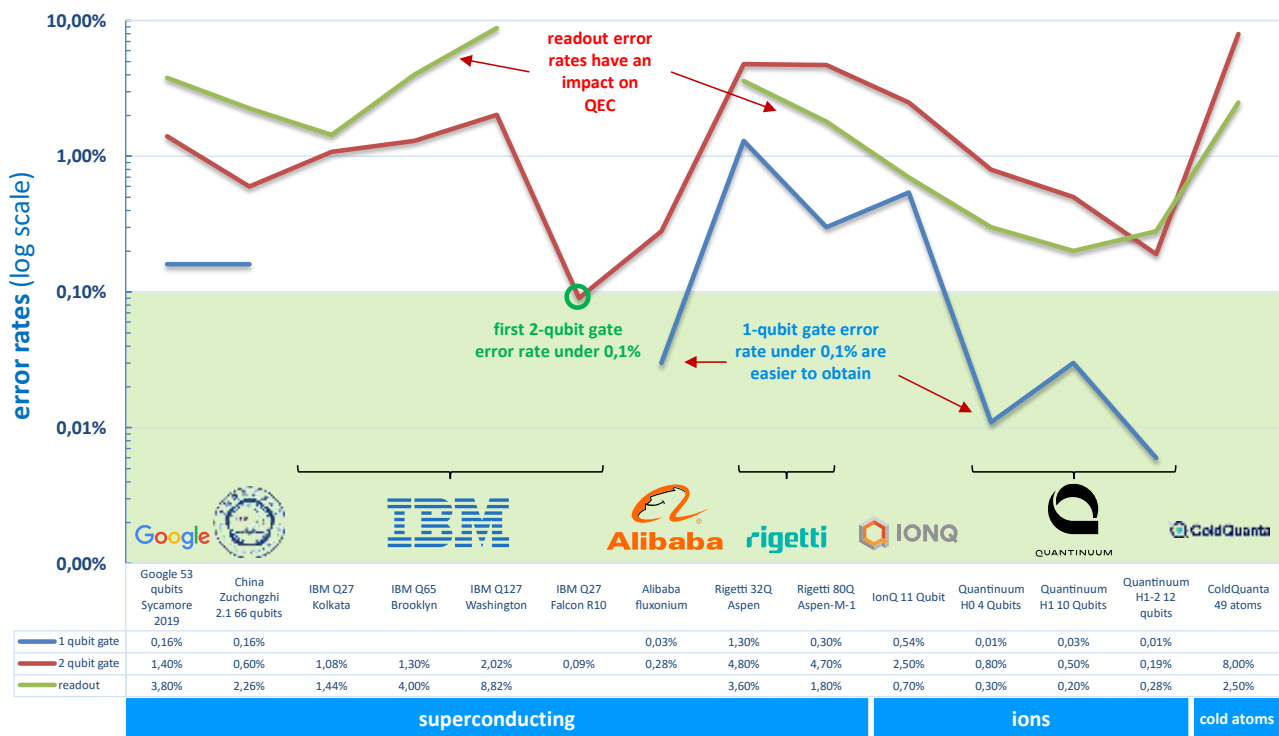


Figure 225: comparison of some qubit error rates with recent quantum processors. The most important rate is the two-qubit error rate. At this point, only IBM has a 2QB error rate below 0,1% with an experimental Falcon R10 27-qubit QPU. Compilation (cc) Olivier Ezratty, 2022.

These error rates are currently prohibitive when executing many quantum gates in a row. With each operation, error rates add up and the reliability rate decreases. Imagine chaining a few dozen two-qubit gates! At this rate, the error rate can very fast exceed 50% at the end of a rather simple algorithm and, generally, well before the fateful qubit coherence time limit.

Hence the fact that the power of a quantum computer is always evaluated not simply by the number of available qubits but by the number of operations that can be done with a reasonable error rate at the end of the calculation. To avoid this quantitative constraint, we should have qubits with quantum gate error rates of 10^{-10} or even 10^{-15} .

Figure 226 illustrates this discrepancy between today's physical qubits and the need to perform reliable calculations (without error correction).

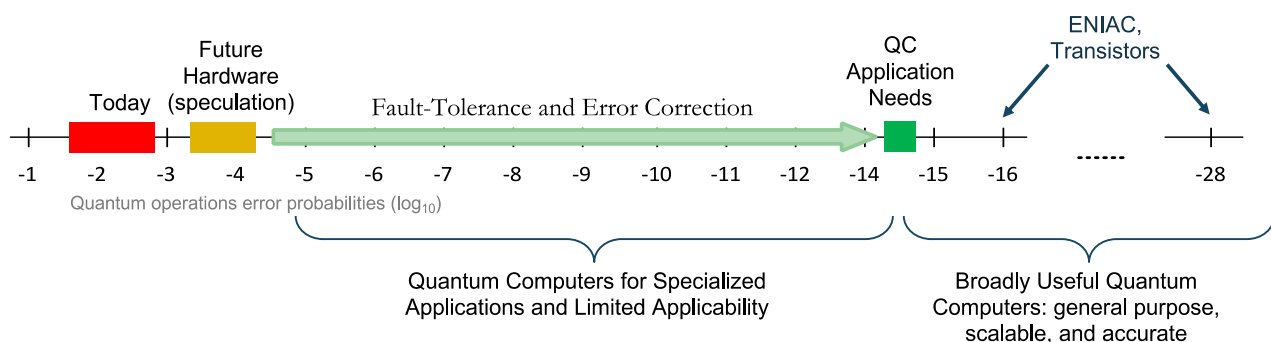


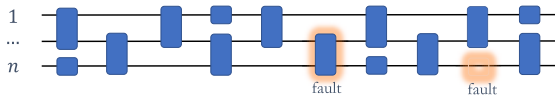
Figure 226: comparison of error levels between existing quantum hardware and what is required, with error correction codes. Source: [How about quantum computing?](#) by Bert de Jong, DoE Berkeley Labs, June 2019 (47 slides).

A formula is used to evaluate the dependency between quantum gates error rates (ϵ), the number of qubits (n) and the number of usable gates (d), called "circuit depth": $nd < 1/\epsilon$. As the error rate decreases, the usable circuit depth increases, and the range of usable algorithms expands.

Circuit depth in the Noisy Intermediate-Scale Quantum Technology Era

Noise sets a limit on the maximum size of a computation without error correction.

Rough estimate: $nd \ll 1/\epsilon$
 n = number of qubits (width)
 d = circuit depth
 ϵ = error rate



Deep circuits → few qubits → efficient classical simulation.

Shallow circuits → many qubits → potential for a quantum advantage.

Shallow circuits and their potential

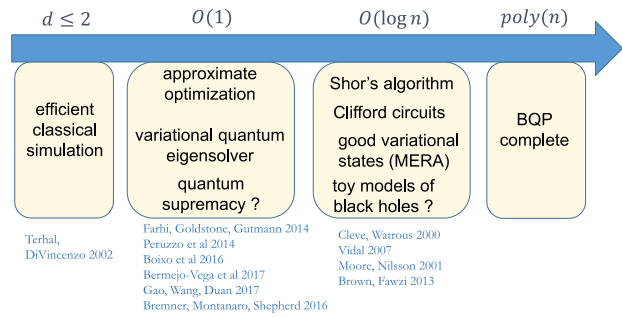


Figure 227: relationship between circuit depth and their use case. Source: [Quantum advantage with shallow circuits](#) by Robert König, 2018 (97 slides).

It is presented in another way in this **Quantum Benchmark** diagram, with the number of qubits on the abscissa and the depth of the circuits on the ordinate (number of gates that can be linked in a quantum calculation), conditioned by the skewed dotted lines that correspond to the error rates of the quantum gates.

The white zone is the *quantum supremacy* zone, also known as the *quantum discovery regime*⁴⁰⁴.

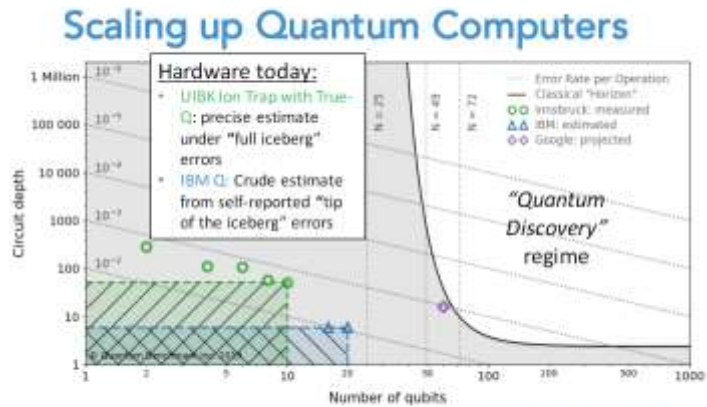


Figure 228: circuit depth vs number of qubits. Source: Joseph Emerson, *Quantum Benchmark*. 2019.

For a quantum computer to be useful and scalable, you need a lot of qubits, a low error rate for quantum gates and qubits readout, and a long qubit coherence time to be able to execute algorithms without much time constraints although quantum error correction codes are indispensable workarounds for this last constraint.

How are quantum gates and measurement error rates evaluated? We've seen previously how individual qubits flip and phase error rates are usually measured. Other methods are required to have an idea of the fidelities of registers with entangled qubits.

One method is the **Randomized Benchmarking (RBM)** process which consists in chaining a random sequence of quantum gates whose result is known in advance and with comparing the results obtained with the right responses. Usually, a random sequence of Clifford gates is launched and then executed backwards. The error rate increases with the number of chained quantum gates and depends on their type. We can evaluate the error rate of a given gate with the **Interleaved RBM** which injects the gate periodically into the random gate set used. We then measure the difference in error rate between the sequence with and without these added quantum gates⁴⁰⁵.

⁴⁰⁴ Slides presented by Joseph Emerson of Quantum Benchmark at the Quantum Computing Business conference organized in Paris on June 20, 2019 by Bpifrance. They position Google very close to the area of interest with their 72 qubits, but public benchmarks of these qubits have not yet been published after their announcement in March 2018. The 53 qubits of the Sycamore generation announced in October 2019 are however at about the same place (purple diamond).

⁴⁰⁵ See [Efficient measurement of quantum gate error by interleaved randomized benchmarking](#) by Easwar Magesan, Jay Gambetta et al, March 2012 (5 pages). And [Quantum Computing: Progress and Prospects](#), 2018 (206 pages), page 2-20. The process of benchmarking quantum gates is detailed in [Randomized benchmarking for individual quantum gates](#) by Emilio Onorati et al, 2018 (16 pages). The origin of the method is [Scalable noise estimation with random unitary operators](#) by Joseph Emerson et al, 2005 (8 pages).

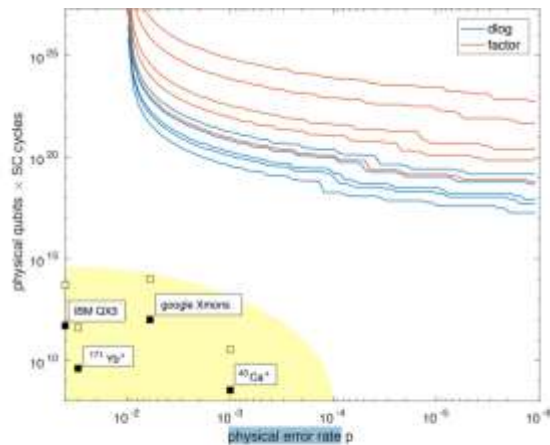


Figure 24: Comparison of algorithmic demands with currently achieved hardware performance. The plot shows required resources as number of qubits times rounds of error correction in the surface code for diag (blue) and factoring (orange) for common key sizes as a function of the physical error rate p . The squares show current realizations assuming one day run time (solid) or 100-days (empty), the yellow area shows expected near-term progress. Both scales are logarithmic.

Strategies for Characterizing Noise

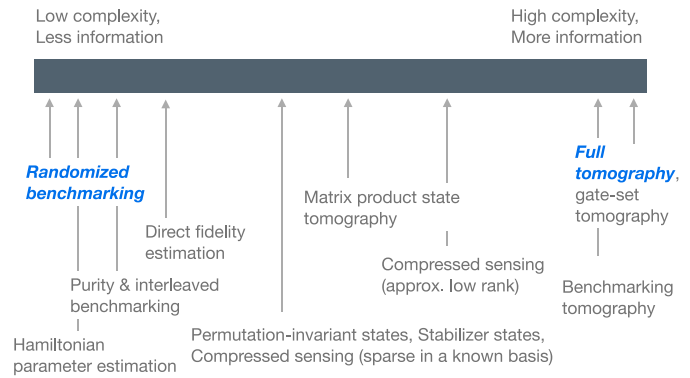


Figure 229: source: [Entwicklungsstand Quantencomputer](#), 2018.

Figure 230: comparing the various strategies to characterize qubit noise.

Source: [Characterization of quantum devices](#) by Steve Flammia, University of Sydney, 2017 (118 slides).

You'll have to look elsewhere to find out more data⁴⁰⁶. The RBM method has some drawbacks for clean noise quantification. It is apparently not suitable for the detection of any noise patterns⁴⁰⁷.

Several other methods exist, such as **quantum state tomography** (QST) that we already covered in the [section](#) dedicated to measurement, page 184, which is based on a repeated measurement of qubit states that allows the reconstruction of a mean density matrix and the associated errors, for one or two qubits after a calculation.

Another method is used to assess the reset/gate/readout cycle, **SPAM** (state preparation and measurement). SPAM measures the cumulative fidelities of a single qubit state preparation and readout. It's used and advertised by Quantinuum. It however doesn't provide any indication on multiple qubit gates and qubits entanglement quality and scaling⁴⁰⁸.

Yet another method exists that is based on some mathematical tools identifying a match between the noise rate of one and two-qubit gates of an algorithm and the total noise rate of the complete algorithm. In short, it links macro noise (algorithm) to micro noise (quantum gates).

Error correction codes zoo

Quantum error correction can't work the same as classical error correction. Qubits cannot be independently replicated with some measurement that would be performed on one replicated qubit. On top of that, we are correcting analog errors in multiple dimensions, not just a 0/1 error flip that could be labelled as a simple "digital error"⁴⁰⁹.

⁴⁰⁶ As in the aforementioned German report [Entwicklungsstand Quantencomputer](#) (*State of the art of quantum computing*), which dates from 2018 and highlights the huge gap between the performance of qubits, particularly at IBM and Google, and the need for integer factorization to break common RSA keys. See also [Efficient learning of quantum noise](#) by Robin Harper et al, Nature Communications, 2019 (15 pages) and [Characterization, certification and validation of quantum systems](#) by Martin Kliesch, April 2020 (87 pages).

⁴⁰⁷ See [Characterization of quantum devices](#) by Steve Flammia, University of Sydney, 2017 (118 slides) which provides an excellent overview of the various qubits benchmarking techniques.

⁴⁰⁸ See [99.9904% SPAM Fidelity with barium-137 sets the standard and creates a further step towards solving some of the world's most intractable problems](#) by Kortny Rolston-Duce, Quantinuum, March 2022.

⁴⁰⁹ The stakes of QEC are very well explained in [Approaches to Quantum Error Correction](#) by Julia Kempe, 2005 (29 pages). See also the review paper [Quantum Error Correction for Quantum Memories](#) by Barbara M. Terhal, April 2015 (47 pages) and the excellent [Introduction to Quantum Error Correction and Fault Tolerance](#) by Steven M. Girvin, August 2022 (99 pages) which is a transcript from a lecture at Les Houches Summer School in 2019 and (brilliantly) covers both classical and quantum error correction techniques.

The techniques explored for more than two decades consists in implementing quantum error correction codes called **QEC** for Quantum Error Correction or rather **QECC** for QEC Codes ⁴¹⁰. Most of these QEC schemes correct errors that are small and independent, meaning, not correlated between several close and distant qubits.

Error correction codes apply to both universal gate quantum computing and quantum telecommunications. In the first case, they are integrated into the concept of fault-tolerance quantum computing (**FTQC**). Error correction is a mean to slow down qubits decoherence and extend the available computation time.

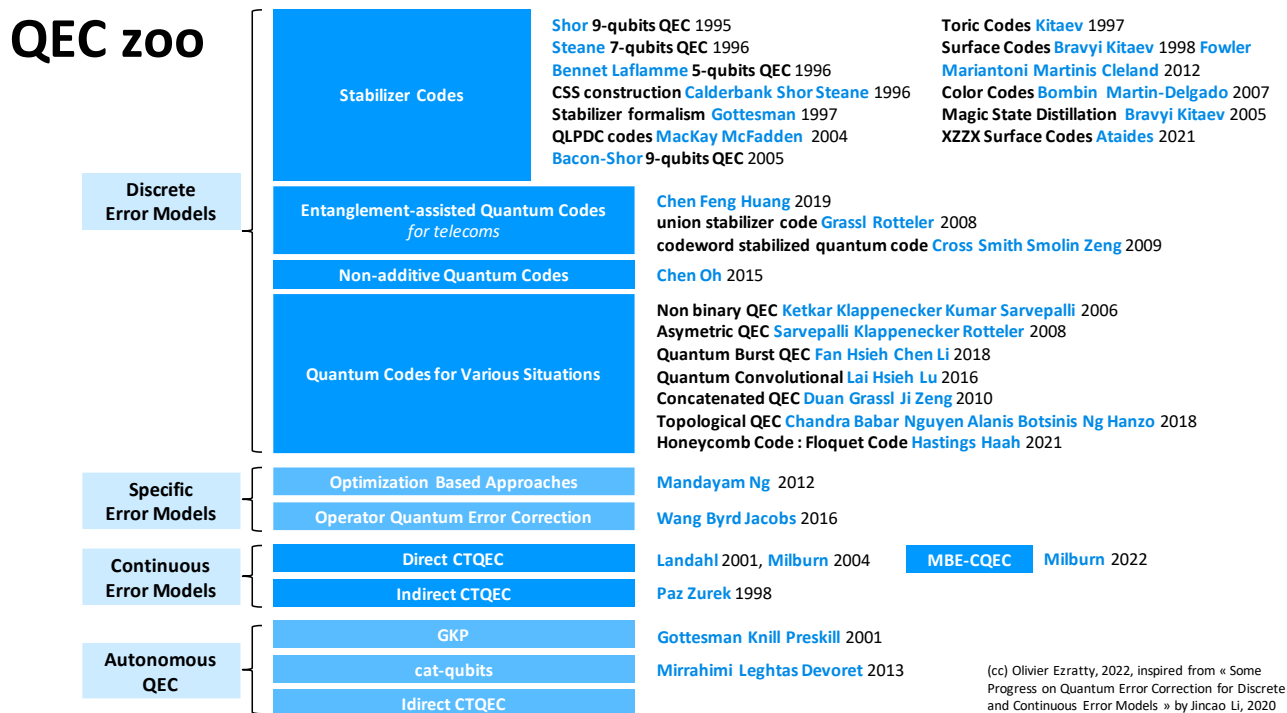


Figure 231: inventory of key quantum error correction codes. (cc) Olivier Ezratty, 2022, inspired from [Some Progress on Quantum Error Correction for Discrete and Continuous Error Models](#) by Jincao Li, 2020 (16 pages).

The chart in Figure 231 makes an inventory of the main quantum error correction codes with their origin and date of creation⁴¹¹. This error correction zoo is very dense⁴¹².

It is a very rich scientific field of quantum technologies and has been growing regularly since 1995. It includes several families of error correction codes.

The most important QEC codes family are the **stabilizer codes**. The first ones correct flip and/or phase errors with three, five (Laflamme), seven (Steane) or nine qubits (Shor). These codes replicate qubits several times with entanglement. They follow the same processing in parallel. Then, the code compares the results at the output of algorithms to keep the statistically dominant results. All this is done without reading the value of the qubits which would make the whole system collapse. This is implemented with ancilla qubits that are used to detect error syndromes without affecting the qubits used in calculation.

⁴¹⁰ This theme has, like many quantum specialties, its own conference. See [International Conference on Quantum Error Correction](#) and the [videos](#) with all the presentations of the 2019 edition.

⁴¹¹ Illustration inspired by a scheme discovered in [Some Progress on Quantum Error Correction for Discrete and Continuous Error Models](#) by Jincao Li, 2020 (15 pages).

⁴¹² See the Error Correction zoo and its [section](#) on quantum error correction codes. And [Quantum Error Correction for Beginners](#) by Simon J. Devitt, William J. Munro, and Kae Nemoto, 2013 (41 pages).

The trick consists in duplicating the information on several qubits and do qubits rotations in the Bloch sphere then some projective measurement. This will not deteriorate the information contained in the qubits. This measurement enables the detection of error syndromes. We then use single-qubit gates to correct the qubits for which an error was detected. It goes through some classical processing that must be as fast as possible.

Stabilizers codes have many variants including:

Topological codes including **surface codes** and **color codes**⁴¹³ themselves derived from **toric codes**⁴¹⁴, and many other specimens such as the **DFS** (Decoherence Free Subspaces) protocol encode quantum information in a subspace that is unaffected by physical errors or so-called holographic codes⁴¹⁵ and also **Fractal Surface Codes**⁴¹⁶. Color codes have much less overhead than surface codes and render possible the implementation of FTQC (Fault-Tolerant Quantum Computing). It is due to one key feature of these correction codes: they can be implemented with the transversal gates described in the section on FTQC. It could be used with superconducting and quantum dots spin qubits. However, what is “colored” in these colored codes and how does it work? I have no clear idea⁴¹⁷.

Magic state distillation. A Shor and Steane code can correct any Pauli error, including Y gate, which is equal to iZX . It can correct any linear combination of I, X, Y and Z gates with complex numbers. This comes from the fact that any unit operation on a qubit can be expressed as a combination of IXYZ with complex factors: $U = aI + bX + cY + dZ$. This means, indirectly, that these QECs should be able to correct analog and continuous errors such as slight variations in amplitude or phase, i.e. rotations of a few degrees in the Bloch sphere. To correct these errors corresponding to gates outside the Clifford group such as a T gate (eighth of rotation in the Bloch sphere, these gates that provide an exponential speedup for gate-based computing), however, magic states are also used which feed circuits made with gates from the Clifford group. These states are prepared by a process called magic state distillation⁴¹⁸. It has an enormous overhead with the number of required physical qubits to create a single logical qubit, of about two orders of magnitude (x100). Magic state distillation is implemented in surface codes. This overhead could be avoided or reduced with using 3D correction codes, which are difficult to implement with actual qubits at this time.

ZXXZ surface code that would reduce the number of required physical qubits to create a logical qubit thanks to a lower error threshold. In April 2021, University of Sydney science undergraduate Pablo Bonilla Ataides ZXXZ paper published in Nature Communications brought the attention of Amazon researchers⁴¹⁹.

⁴¹³ This is however not the only solution to the magic state distillation physical qubits cost. See [Fault-tolerant magic state preparation with flag qubits](#) by Christopher Chamberland and Andrew Cross, IBM, May 2019 (26 pages) which describes an alternative using more ancilla qubits (“flag qubits”).

⁴¹⁴ See [Fault-tolerant quantum computation by anyons](#) by Alexei Kitaev, 1997 and 2008 (27 pages).

⁴¹⁵ Color codes are variations of stabilizing codes. See some explanations in [The Steep Road Towards Robust and Universal Quantum Computation](#) by Earl T. Campbell, Barbara M. Terhal and Christophe Vuillot, 2016 (10 pages).

⁴¹⁶ See [Topological Order, Quantum Codes, and Quantum Computation on Fractal Geometries](#) by Guanyu Zhu, Tomas Jochym-O’Connor, and Arpit Dua, IBM, PRX, Quantum, September 2022 (55 pages).

⁴¹⁷ See for example [The ABCs of the color code](#) by Aleksander Marek Kubica, 2018 (205 pages), a rich thesis done under the supervision of John Preskill at Caltech with the help from Jason Alicea, Fernando Brandão and Alexei Kitaev. And [The cost of universality: A comparative study of the overhead of state distillation and code switching with color codes](#), by Michael E. Beverland, Aleksander Kubica and Krysta M. Svore, 2021 (69 pages).

⁴¹⁸ See [Universal quantum computation with ideal Clifford gates and noisy ancillas](#) by Sergey Bravyi and Alexei Kitaev, 2004 (15 pages). There are other solutions such as [A fault-tolerant non-Clifford gate for the surface code in two dimensions](#) by Benjamin J. Brown, May 2020, which applies to surface codes.

⁴¹⁹ See [Student’s physics homework picked up by Amazon quantum researchers](#) by Marcus Strom, University of Sydney, April 2021, [Sydney student helps solve quantum computing problem with simple modification](#) by James Carmody April 2021 and [The XZZX surface code](#) by J. Pablo Bonilla Ataides et al, April 2021, Nature Communications (12 pages).

This surface code could be used by Amazon who made a choice to use a relatively low number of photons per cat qubit (8 to 10, compared to about 30 for Alice&Bob), still requiring some first level bit-flip error correction on top of phase-flip correction. That's where a ZXXZ surface code QEC could come into play. ZXXZ QEC codes are indeed mentioned as an option QEC technique in Amazon's technical paper from December 2020. A team from Amazon, Caltech and the University of Chicago improved these codes in 2022 to work with biased noise (which has more phase than flip noise)⁴²⁰.

Planar Honeycomb Code, aka Floquet Code, was created by Matthew B. Hastings and Jeongwan Haah from Microsoft in 2021 to simplify toric codes with fewer qubits and stabilizers⁴²¹. It is adapted to qubits architectures implementing pair-wise qubit measurements (XX, YY, ZZ) like with Majorana fermions. The technique was improved by Google researchers⁴²², by Christophe Vuillot from Inria Nancy⁴²³ and with the XYZ² variant in 2022⁴²⁴.

Quantum LDPC codes that are inspired by classical LDPC (low-density parity check) codes used in telecommunications (Wi-Fi, 5G, DVB) and seem to scale better than surface codes⁴²⁵. They are also adapted to Majorana fermions but for a longer term. But they require an increased connectivity between qubits that is not possible on a 2D layout and which will require 3D circuitry to create distance connections between qubits.

Autonomous QEC. Here, we must distinguish "logical error correction codes" and "physical codes" that are directly managed at the qubit hardware level. Also branded "autonomous QEC", these contain **bosonic codes**, including GKP error codes⁴²⁶, binomial codes, 0- π and cat-codes⁴²⁷. The latter implementation in a cavity a "Schrödinger cat" that allows to manage a projection space used for error correction, as in the error correction algorithms based on stabilizing codes that we will see later. It usually corrects flip errors autonomously, but new variations are able to correct both flip and phase errors⁴²⁸.

Continuous error correction. In opposition to discrete quantum error correction codes (DQEC) that we've covered, there are alternative QEC using continuous measurement and correction. Juan Pablo Paz and Wojciech Zurek proposed in 1998 a continuously operating error correction code, the CTQEC, for "continuous-time QEC", or CQEC, based on differential equations and acting at reduced time intervals.

⁴²⁰ See [Tailored XZZX codes for biased noise](#) by Qian Xu, Lian Jiang et al, March 2022 (16 pages). Biased noises is well explained in the thesis [Quantum Error Correction with Biased Noise](#) by Peter Brooks, Caltech, 2013 (198 pages).

⁴²¹ See [Dynamically Generated Logical Qubits](#) by Matthew B. Hastings and Jeongwan Haah, Microsoft, October 2021 (18 pages).

⁴²² See [Benchmarking the Planar Honeycomb Code](#) by Craig Gidney and Michael Newman, Google, February-September 2022 (16 pages).

⁴²³ See [Planar Floquet Codes](#) by Christophe Vuillot, Inria, December 2021 (16 pages) and [A Pair Measurement Surface Code on Pentagons](#) by Craig Gidney, June 2022 (16 pages).

⁴²⁴ See The [XYZ² hexagonal stabilizer code](#) by Basudha Srivastava et al, Chalmers, April 2022 (15 pages).

⁴²⁵ See [Quantum Low-Density Parity-Check Codes](#) by Nikolas P. Breuckmann and Jens Niklas Eberhardt, October 2021 (17 pages), [Qubits Can Be as Safe as Bits, Researchers Show](#) by Mordechai Rorvig, January 2022 referring to See [Asymptotically Good Quantum and Locally Testable Classical LDPC Codes](#) by Pavel Panteleev and Gleb Kalachev, 2022 (51 pages).

⁴²⁶ See [Encoding a qubit in an oscillator](#) by Daniel Gottesman, Alexei Kitaev and John Preskill, PRA, 2001 (22 pages) and the perspective [Quantum error correction with the Gottesman-Kitaev-Preskill code](#) by Arne Grimsmo and Shruti Puri, PRX Quantum, June 2021 (20 pages).

⁴²⁷ Cat-codes are used by the startup Alice&Bob. Knowing that their creation goes back to the work of Mazyar Mirrahimi and Zaki Leghtas in 2013, with whom the founders of Alice&Bob worked. Error correction codes are constantly being updated. Thus, a proposal recently emerged from QEC that goes further than cat-code and does not depend on hardware architecture. See [Novel error-correction scheme developed for quantum computers](#), March 2020 which refers to [Quantum computing with rotation-symmetric bosonic codes](#) by Arne L. Grimsmo, Joshua Combes and Ben Q. Baragiola, September 2019.

⁴²⁸ See [Quantum error correction using squeezed Schrödinger cat states](#) by David S. Schlegel et al, January 2022 (20 pages) which provides protection for both flip and phase errors.

There are two methods for acting directly on the information (direct CTQEC) or via auxiliary qubits (indirect CTQEC). CQEC avoids using ancilla qubits to measure the stabilizer operators by weakly measuring the physical qubits. It also enables faster measurements and error detection, reducing undetected errors.

These methods were later improved by various contributors including Andrew J. Landahl and Gerard J. Milburn⁴²⁹. The later recently proposed to use some real-time measurement-based estimator (MBE) of the real logical qubit to be protected to accurately track the actual errors occurring within the real qubits in real-time. This leads to the **MBE-CQEC** scheme that protects the logical qubit to a high degree and allows the error correction to be applied either immediately or at a later time.

Quantum Error Mitigation. At last, one other solution being considered deals with using NISQ, for Noisy Intermediate Scale Quantum computers, those current quantum computers that use noisy and uncorrected qubits. This is done with algorithms, often hybrid classical/quantum algorithms, which are supposed to be errors resilient and with using some Quantum Error Mitigation techniques (QEM). We detail it later in this section.

Error correction principles

The general principle of a classical quantum error correction code is illustrated in the diagram in Figure 232 with a six-step correction⁴³⁰:

1. **Encoding:** the qubit to be corrected will first be replicated a certain number of times via CNOT gates on several auxiliary qubits (here 2). The resulting qubits are entangled. In the example, we get the state $\alpha|000\rangle + \beta|111\rangle$ for an input state $|\psi\rangle = \alpha|0\rangle + \beta|1\rangle$.
2. **Processing:** it will potentially generate an error coming from various sources of noise. This can be a calculation as well as some telecom transmission of a qubit.
3. **Detection:** one or more error syndromes are detected via quantum gates that associate qubits with other ancilla qubits. In the example below, it detects pure flip errors.
4. **Measurement:** the state of these ancilla qubits is measured to become classical bits in the syndrome extraction process. It helps create the index of the qubit to be corrected in the replicated entangled qubits. This is some non-destructive measurement for the corrected entangled qubits since it's done in a different basis. These measurements are labelled "mid-circuit measurements" since they occur before the end of your circuit execution, only on a subset of the register qubits and without changing the quantum state of other qubits in the register.
5. **Correction:** the address obtained with syndrome measurement is used to correct the faulty qubits with an X gate (for a phase error, we'd use a Z gate). There are alternative forms of QEC that do not involve the measurement of the syndrome by qubit reading but by its direct use with quantum gates that correct the defective qubit without going through conventional bits.
6. **Consolidation:** finally, the corrected qubits are disentangled to recreate an isolated corrected qubit $|\psi\rangle$. This consolidation seems to be used with error correction for quantum telecommunications. When applied to quantum computing, the corrected entangled qubits can be kept to move on to the next step, i.e. another computing operation to be corrected.

"Whatever comes out of these gates, we have a better chance to survive if we work together. You understand?"

"We stay together, we survive."
General Maximus Decimus Meridius
(Russell Crowe) in *Gladiator*, 2000.

⁴²⁹ See [Continuous quantum error correction via quantum feedback control](#) by Charlene Ahn, Andrew C. Doherty and Andrew J. Landahl, PRA, March 2002 (12 pages), [Practical scheme for error control using feedback](#) by Mohan Sarovar, Charlene Ahn, Kurt Jacobs and Gerard Milburn, PRA, May 2004 (12 pages) and [Measurement based estimator scheme for continuous quantum error correction](#) by Sangkha Borah, Gerard Milburn et al, March 2022 (9 pages).

⁴³⁰ Based on [A Tutorial on Quantum Error Correction](#) by Andrew M. Steane, 2006 (24 pages). See also [An introduction to quantum error correction](#) by Mazyar Mirrahimi, 2018 (31 slides).

7. **Reuse:** the correct qubit or qubits can now be used for subsequent operations that will also be corrected with the same process.

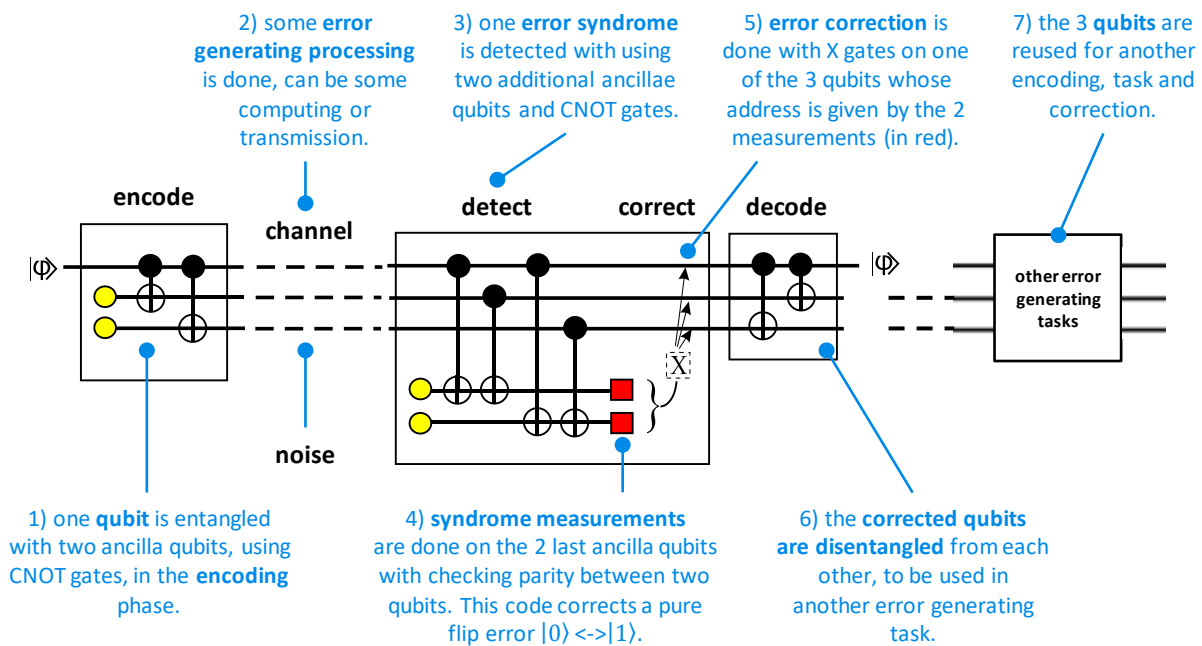


Figure 232: a simple error correction code, adapted from [A Tutorial on Quantum Error Correction](#) by Andrew M. Steane, 2006 (24 pages).

adapted from « A Tutorial on Quantum Error Correction » by Andrew M. Steane, 2006

Error correction codes charts such as Shor's on [Wikipedia](#) are usually not complete. They usually lack the measure/correction steps. They can also rely on direct error correction⁴³¹.

They also do not specify where to place the error correction codes in a quantum algorithm. It seems that this is required at each stage of some quantum computation. Error correction codes will be repeated several times that is roughly proportional to the computational depth of the quantum algorithm. It will be the role of the compilers to position QEC in the code executed on the quantum processor. It may depend on their knowledge of the fidelity rates of the quantum gates used in the hardware. In the end, the QEC will increase computation time by one to several orders of magnitude depending on the ratio of physical qubits per logical qubits and the qubit life-extension obtained with the code. It has to be taken into account when evaluating the time-based quantum computing advantage brought by a given algorithm.

Looking at the genealogy of these error correction codes, we must start with the simplest ones that correct qubit sign errors with three qubits like the example in Figure 232 from Andrew Steane. A similar QEC corrects qubit phase errors by exploiting Hadamard gates.

The 1995 **Shor's 9-qubit error correction code** consolidates these two methods, with the corrected qubit being replicated 8 times. This code corrects both flip and phase errors⁴³². It uses a total of 15 qubits. What such a complete code looks like is shown in Figure 233. In the first phase the corrected qubit is replicated two times and each resulting qubit is again replicated two times with CNOT gates. The first three blocks of 3 qubits implement a flip error correction. It outputs 3 qubits which then implement a phase error correction.

⁴³¹ See [Quantum Error Correction An Introductory Guide](#) by Joschka Roffe, 2019 (29 pages) which explains the generic operation of error correction codes and [Quantum Error Correction for Beginners](#) by Simon Devitt, William Munro and Kae Nemoto, 2013 (41 pages). These are the two main sources of information that allowed me to write these pages on QEC. See also a description of various error correction codes in [Software for Quantum Computation](#), a thesis by Daniel Matthias Herr from ETH Zurich, 2019 (164 pages).

⁴³² The details of the process are well documented in the [Wikipedia sheet of quantum error correction](#).

full Shor 9 error correction code

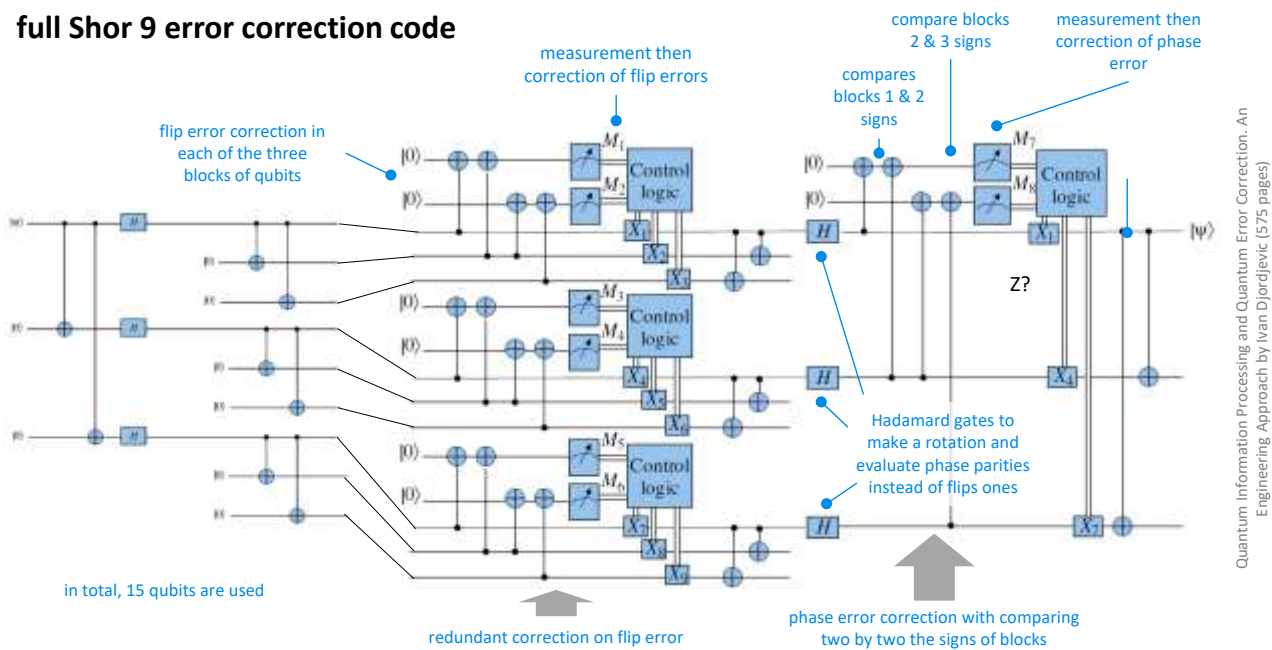


Figure 233: a full Shor 9 error correction code correcting both flip and phase errors. Source: [Quantum Information Processing and Quantum Error Correction. An Engineering Approach](#) by Ivan Djordjevic (575 pages).

Raymond Laflamme (1960, Canada) demonstrated in 1996 that at least five physical qubits are needed to create a "logical qubit" integrating flip and phase error correction. With **Emanuel Knill**, he also demonstrated that any single qubit error was a linear combination of flip and phase errors, leading to factoring error correction to flip and phase errors corrections⁴³³.

In practice, the 7-qubit **Steane** code is the most referenced because it is not redundant like the Shor code. These 3-, 5-, 7- and 9-qubit codes are part of a generic group called **stabilizer codes** formalized by **Daniel Gottesman** in 1997. We are now going to dig a little deeper into how they operate.

We will better understand how an error correction works without reading the state of the qubit to be corrected. Let's take the case of a simple flip error correction code with three qubits.

These three entangled qubits can have an error X_1 , X_2 or X_3 or no error (I =identity). X is an amplitude inversion Pauli gate. It creates an amplitude inversion of the corresponding entangled qubit as shown in the equations in Figure 234. These new states correspond to three errors and the absence of errors.

$$\begin{aligned}
 |\psi_L\rangle &= \alpha|000\rangle + \beta|111\rangle \xrightarrow{I} \alpha|000\rangle + \beta|111\rangle, \\
 |\psi_L\rangle &= \alpha|000\rangle + \beta|111\rangle \xrightarrow{X_1} \alpha|100\rangle + \beta|011\rangle, \\
 |\psi_L\rangle &= \alpha|000\rangle + \beta|111\rangle \xrightarrow{X_2} \alpha|010\rangle + \beta|101\rangle, \\
 |\psi_L\rangle &= \alpha|000\rangle + \beta|111\rangle \xrightarrow{X_3} \alpha|001\rangle + \beta|110\rangle.
 \end{aligned}$$

Figure 234: amplitude inversions.

These four states have the interest of being mathematically orthogonal for all the values of the α and β defining the state of the qubit to be corrected. The trick is to perform a measurement of these values in the vector space corresponding to these four values and not in the original qubit computational base. This will not deteriorate the superposition of the original qubit. The syndrome extraction is called a "Stabilizer code" or "stabilization code", which will feed the ancilla qubits. The process is the same to evaluate and correct a phase error but with Z gates instead of X gates.

⁴³³ This is demonstrated in [A Theory of Quantum Error-Correcting Codes](#) by Emanuel Knill and Raymond Laflamme, 1996 (34 pages). But also independently in [Mixed State Entanglement and Quantum Error Correction](#) by Charles Bennett, David DiVincenzo, John A. Smolin and William K. Wootters, 1996 (82 pages). See also [Magic States](#) by Nathan Babcock (28 slides).

3 qubits flip error correction code

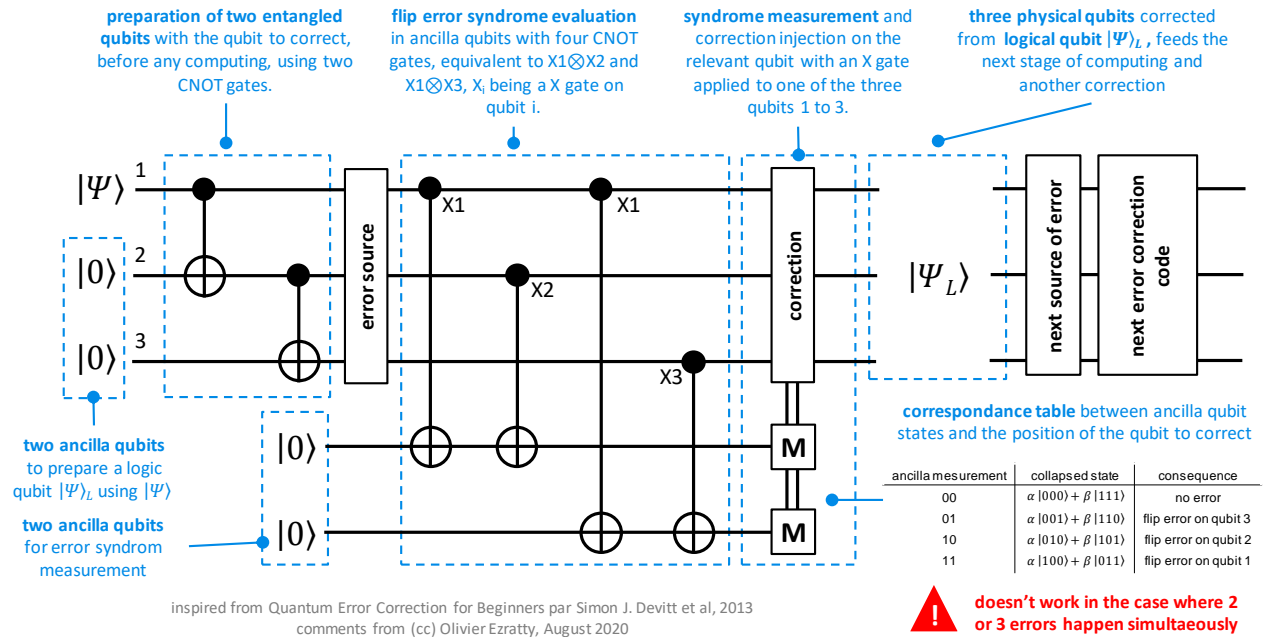


Figure 235: 3 qubits flip error correction code explained. (cc) Olivier Ezratty, 2021.

The disadvantage of the solution is that it cannot detect errors that would occur at the same time on two or three of the entangled qubits. No error-correcting code can correct all errors!

The stabilizer codes formalism generically describes the error correction codes we have just studied with three parameters: $[[n, k, d]]$ with:

- **k** = number of logical qubits, usually 1 which is the qubit that needs to be corrected.
- **n** = number of physical qubits used in the code, with $n > k$. The $n-k$ qubits store the redundant information thanks to entanglement.
- **d** = smallest number of simultaneous qubit errors that can transform one valid codeword into another, *aka* the **code distance**. The complete definition is actually more complicated.

More precisely, an error correction code with a code distance d can correct errors for up to $(d - 1)/2$ (replicated) qubits, or say differently $d \geq 2m+1$, m being the number of redundant qubits that can be corrected. You need d to be at least 3 to correct both flip and phase errors.

In this notation, Shor's 9 qubit code is a $[[9, 1, 3]]$, Steane's is a $[[7, 1, 3]]$ and Laflamme's is a $[[5, 1, 3]]$. They all have a code distance of 3. A simple 3-qubit flip or phase correction code is a $[[3, 1, 1]]$ stabilizer code with a code distance of 1. There are larger cases like with the $[[512, 174, 8]]$ CSS code⁴³⁴.

The stabilizer codes use a syndrome table that provides a match between the errors on each qubit and the detected syndrome. The number of ancilla qubits used to create this table must therefore be sufficient to identify the qubits to be corrected in the logical qubit. In the example in Figure 236 with a logical qubit with 7 physical qubits, the 3 ancilla qubits allow the identification of eight scenarios, sufficient to determine which of the 7 physical qubits must be corrected. The 8th scenario is the absence of error, therefore needing no correction.

⁴³⁴ See [Classical product code constructions for quantum Calderbank-Shor-Steane codes](#) by Dimiter Ostrev et al, 2022 (19 pages).

7 qubits error correction code named $[[7,1,3]]$ in the stabilizers formalism

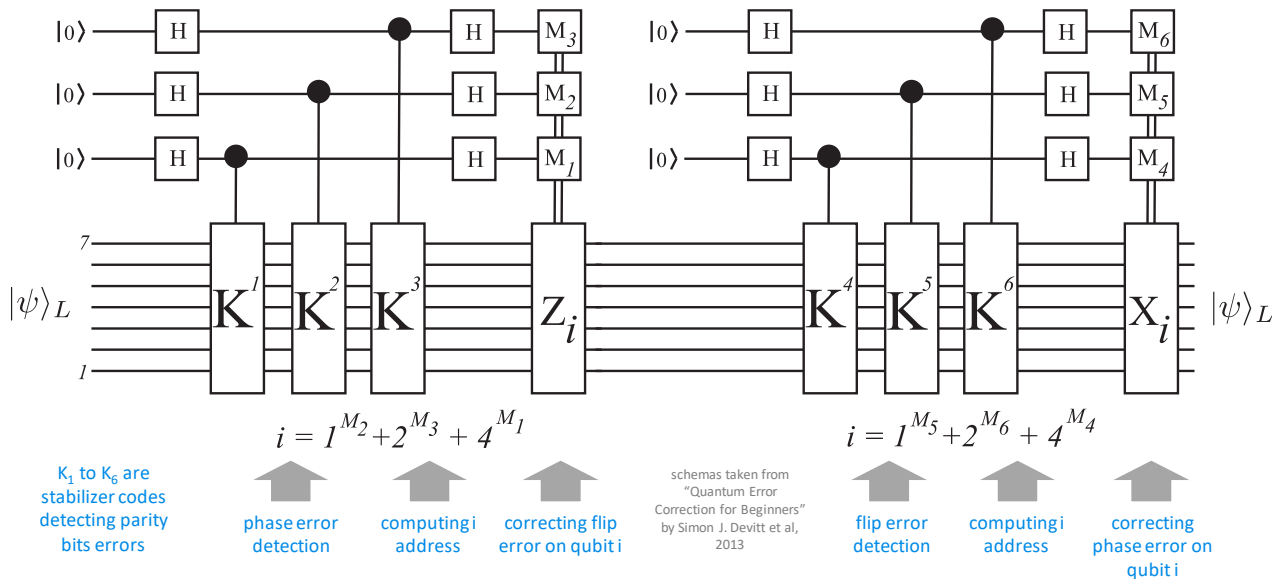


Figure 236: 7 qubits correction code with a code distance 3. Source: [Quantum error corrections for beginners](#) by Simon J. Devitt et al, 2013.

It seems that the qubits correction can be applied in two manners: the one presented so far with a measurement of ancilla parity qubits generating classical bits allowing to determine on which qubits to apply a quantum error correction gate, and other methods allowing this without the measurement and to apply the correction directly with quantum gates⁴³⁵. The first solution seems to be more commonly used. So why is the second solution less used or even recommended?

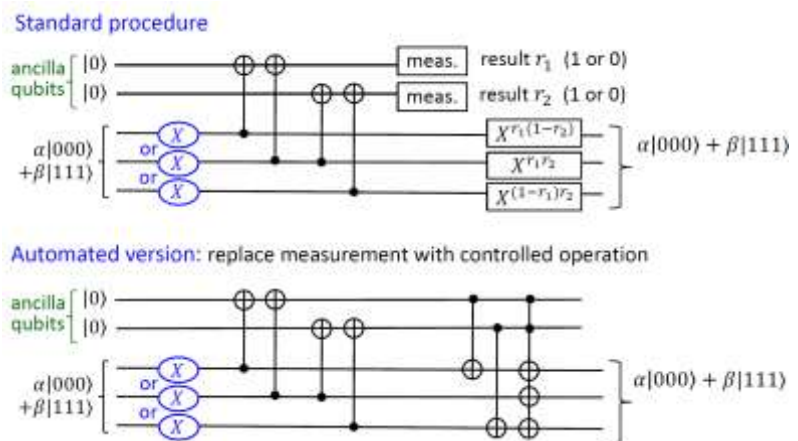


Figure 237: error correction replacing measurement with a controlled operation. Source: [Quantum error correction \(QEC\)](#) by Alexander Korotkov, 2017 (39 slides).

The autonomous method also branded **aQEC** (autonomous quantum error correction) would be more energy and time saving (comparison in Figure 237⁴³⁶). It is also a way to possibly run the error correction autonomously within a quantum processor, without going through the classical part, should qubits control be performed very close to the qubits. But in that case, the ancillas can't be reused. Some energy dissipation must be handled, using a technology called reservoir engineering, which is actually implemented in cat-qubits⁴³⁷. Otherwise, whatever, the ancilla qubits used in QEC must be reset to $|0\rangle$ and this reset is a dissipative process. The thermal bath is just elsewhere!

⁴³⁵ Like the "No ancilla error detection" code (NAED), an error detection scheme that does not employ ancilla qubits or mid-circuit measurements and encodes qubits in pairs of qubits with $|0\rangle_L = |01\rangle$ and $|1\rangle_L = |10\rangle$. See [Quantum Error Detection Without Using Ancilla Qubits](#) by Nicolas J. Guerrero and David E. Weeks, US Air Force Institute of Technology, April 2022 (8 pages).

⁴³⁶ Seen in [Quantum error correction \(QEC\)](#) by Alexander Korotkov, 2017 (39 slides). [List of all courses](#) on quantum computing.

⁴³⁷ See [Protecting a Bosonic Qubit with Autonomous Quantum Error Correction](#) by Jeffrey M. Gertler et al, University of Massachusetts-Amherst and Northwestern University, October 2020 (23 pages). This study investigates autonomous QEC on bosonic codes qubits using reservoir engineering. See also [Autonomous quantum error correction and quantum computation](#) by Jose Lebreuilly et al, Yale University, Amazon and University of Chicago, March 2021 (18 pages) and [Autonomous quantum error correction with superconducting qubits](#) by Joachim Cohen, ENS Paris, 2017 (164 pages).

Logical Qubits

With quantum computers available online such as those from IBM having up to a few dozen qubits, it is the role of software to implement dynamic error correction codes and more precisely, compilers that will transform the developer's code into executable machine code at the physical level of the qubits and integrating QEC code. Given that we have at this point just enough qubits to test small QEC like Steane's 7-qubits codes or small sized surface codes.

Conceptually, a logical qubit sits between a physical qubit (with a small lifetime and prone to significant error rates) and a mathematically perfect qubit (with infinite computing time and zero error). It lasts longer than a physical qubit and should have an error rate in the range 10^{-8} to 10^{-15} that is compatible with the constraints of your algorithm. This error rate is more or less the inverse of the number of quantum gates in your circuit.

At one point in time, logical qubits will maybe be implemented entirely in the hardware architecture, exposing logical qubits to the classical computer driving the quantum accelerator. This will simplify the connection between the classical control computer and the quantum processor.

A QEC (Quantum Error Correction) could be performed at the hardware level by creating qubit assemblies that generate ready-to-use physical logical qubits. Here is an old example with seven superconducting physical qubits to create one simple logical qubit.

The number of physical qubits to be assembled to create a logical qubit depends on the error rate of the qubits.

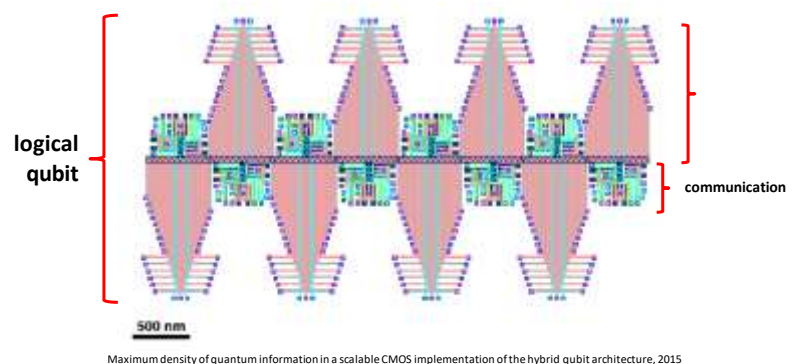


Figure 238: a concept of logical qubit implemented at the physical level. Source: [Maximum density of quantum information in a scalable CMOS implementation of the hybrid qubit architecture, 2015 \(17 pages\)](#).

The higher the qubit error rate, the more qubits must be assembled. This number can reach several thousand qubit physical qubits⁴³⁸. But QEC seems to be bound to be implemented mainly with software and on generic QPU architectures. The number of physical qubits in a logical qubit depend on many factors such as the quantum error correction code used, the underlying physical qubits fidelities, their connectivity and their target error rate.

We're still a long way from that! Current estimates are around 1,000 physical qubits to create a logical qubit. This corresponds to the plans published by **IBM**, **Google** and **PsiQuantum** with 100 logical qubits created out of one million physical qubits. On the physical architecture side, **topological qubits** are an analog version of surface codes that should allow to reduce this ratio of logical/physical qubits, just like cat-qubits, which are forecasted to require fewer than 100 physical qubits to create one logical qubit.

Trapped ions can use **lattice surgery** to connect and entangle these topologically corrected physical qubits⁴³⁹.

⁴³⁸ See [What determines the ultimate precision of a quantum computer?](#) by Xavier Waintal, 2019 (6 pages) which describes the limits of error correction codes. Other useful contents on error correction include: [Error mitigation in quantum simulation](#), Xiao Yuan, IBM Research, 2017 (42 minutes), [Code Used To Reduce Quantum Error In Logic Gates For First Time](#), 2019, [Scientists find a way to enhance the performance of quantum computers](#) by the University of Southern California, 2018 and [Cramming More Power Into a Quantum Device](#) by Jay Gambetta and Sarah Sheldon, March 2019 about the error level of the IBM Q System One announced in January 2019.

⁴³⁹ See [Error protected quantum bits entangled](#), University of Innsbruck, January 2021 referring to [Entangling logical qubits with lattice surgery](#) by Alexander Erhard et al, Nature, 2020 (15 pages).

IonQ is planning to create logical qubits corrected with a Bacon-Shor QEC (a variation of Shor's code with 13 qubits⁴⁴⁰) thanks to their much better fidelities⁴⁴¹.

For qubits that can be physically well connected with their immediate neighbors, the most often considered error correction is the **surface code**, created between 1998 and 2001.

As shown in the diagram in Figure 241, it uses matrices of processing qubits (in white) connected to measuring qubits (in black) via **Pauli X** (amplitude flip) and **Pauli Z** (phase flip) gates operating on these data qubits as shown in yellow and green. This gives two ancilla qubits for two physical qubits organized to detect and correct flip and phase errors over 4 replicated qubits. This constitutes a stabilizer code of type $[[5, 1, 2]]$ using four blocks with four cycles.

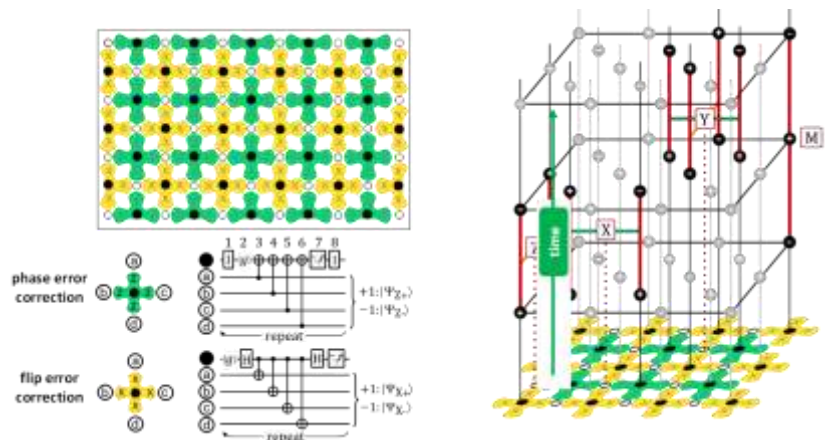


Figure 239: surface code physical layout and process. Source: [Surface codes: Towards practical large-scale quantum computation](#) by Austin G. Fowler, Matteo Marianton, John M. Martinis and Andrew Cleland, 2012 (54 pages).

A surface code with distance d requires d^2 replicated qubits and $d^2 - 1$ measurement qubits, so a total of $2d^2 - 1$ physical qubits to correct a single qubit. d being usual odd, you then have an even number of measurement qubits divided in two equal parts with flip (Z) measurement) and phase (X) measurement qubits as shown below with two example of distance 3 and 5 surface codes. A surface code logical qubit error rate is $P_L \approx 0.03(p/p_{th})^{d_e}$ with p being the physical qubit error rate, p_{th} being the threshold physical error rate below which logical errors falls with d , and d_e being linked to the surface code distance d with $d_e = d/2$ when d is even, and $= (d + 1)/2$ when d is odd. Evaluating how many physical qubits are required to create a logical qubit of a given fidelity is quite complicated with many logarithms using qubit fidelities ratios with fidelities threshold and surface code distance. How are logical qubits delimited and logical gates implemented is another (complicated) story.

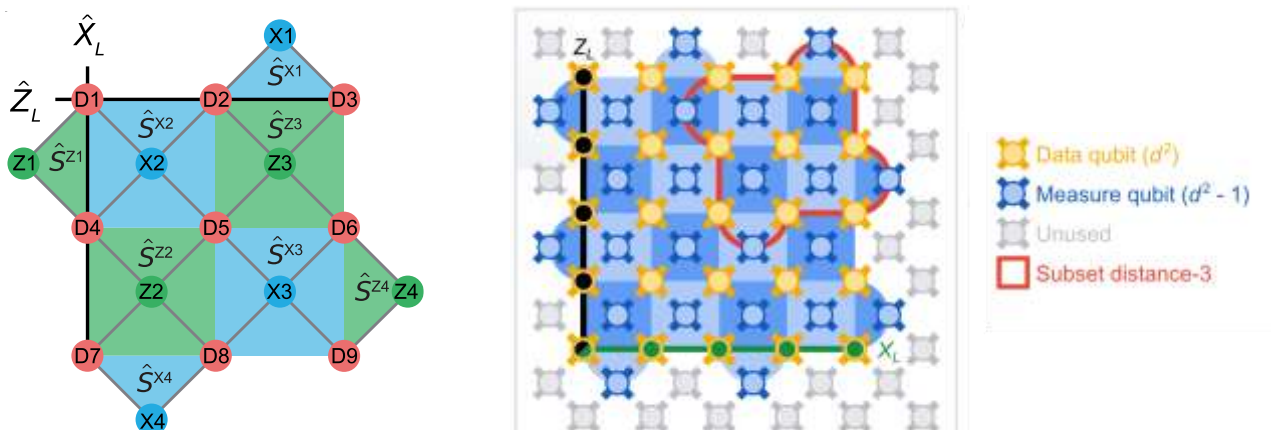


Figure 240: two examples of surface codes, with a distance 3 using 17 qubits (left) and 5 using 49 qubits (right). On the left, the replicated qubits are in red and the measurement qubits are in green (Z, for flip error correction) and blue (X, for phase error correction). Sources: [Realizing Repeated Quantum Error Correction in a Distance-Three Surface Code](#) by Sebastian Krinner, Alexandre Blais, Andreas Wallraff et al, December 2021 (28 pages) and [Suppressing quantum errors by scaling a surface code logical qubit](#) by Rajeev Acharya et al, Google AI, July 2022 (44 pages).

⁴⁴⁰ Bacon-Shor code is documented in [Operator Quantum Error Correcting Subsystems for Self-Correcting Quantum Memories](#) by Dave Bacon, 2006 (17 pages).

⁴⁴¹ And [Fault-Tolerant Operation of a Quantum Error-Correction Code](#) by Laird Egan, Christopher Monroe et al, 2020 (23 pages).

A quantum error correcting code has a certain **threshold** level that defines the higher bound of physical qubit error rates when a logical qubit will have an error rate inferior to that of the physical qubits. It depends on the code itself and on the qubit type.

Surface codes have a higher threshold in the 1% range and are thus tolerant to higher qubit error rates. But they require a larger number of physical qubits per logical qubits. Also, physical qubits must be connected to their immediate neighbors in a 2D structure or with honeycomb variations⁴⁴².

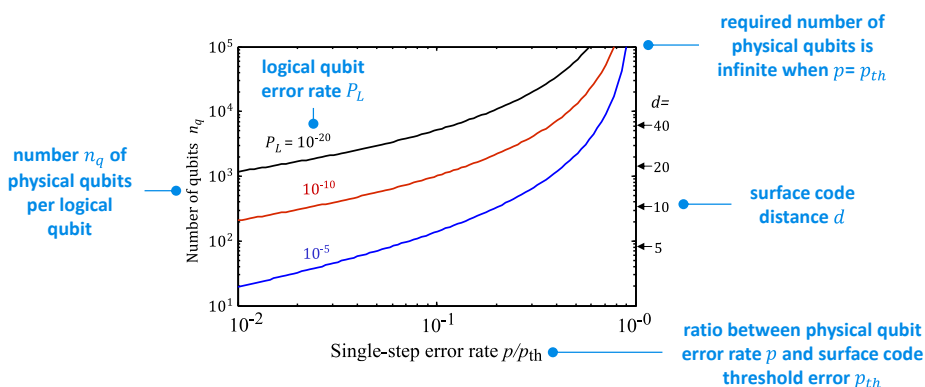


Figure 241: relationship between physical and logical qubit error rate with the number of physical qubits in a logical qubit and the surface code distance. Source: the excellent review paper [An introduction to the surface code](#) by Andrew Cleland, University of Chicago, 2022 (68 pages).

How about real implementations of logical qubits? They are now plentiful but are not yet creating logical qubits with higher fidelities than their underlying physical qubits.

- A team from **Maryland** led by Christopher Monroe implemented in January 2021 a logical qubit using a Bacon-Shor 13 code with a chain of 15 trapped ytterbium ions that was correcting single qubit errors⁴⁴³. They then used two such logical qubits in a configuration of 32 qubits to implement fault-tolerant 2-qubit gates.
- **Google** announced in July 2021 the creation of their first logical qubits with 5 and 21 physical qubits, showing a x100 improvement in the error rate between the 5 and 21 version⁴⁴⁴.
- **Quantinuum** created a single Steane color-code also using 10 trapped ion qubits. They defined the pseudothreshold as a crossover point where the logical qubit error rates is below the physical level error rates. They created a logical qubit with better fidelities than their underlying physical qubits in August 2022⁴⁴⁵.
- A **China** research team implemented a distance 3 surface code using 17 physical qubits ($=3^2+(3^2-1)$) on the 66 qubits Zuchongzhi 2.1 superconducting qubits QPU. It implements repeated error corrections and post-processing error corrections⁴⁴⁶.

⁴⁴² Surface codes are well documented in [Surface codes: Towards practical large-scale quantum computation](#), by Austin G. Fowler, Matteo Mariantoni, John M. Martinis and Andrew Cleland, 2012 (54 pages) but their source of inspiration is older and comes from [Quantum codes on a lattice with boundary](#) by Sergey Bravyi and Alexei Kitaev, 1998 (6 pages). In practice, the structure of surface codes is quite complex and involves activated and deactivated substructures in the qubit matrix.

⁴⁴³ See [Fault-tolerant control of an error-corrected qubit](#) by Laird Egan, Christopher Monroe et al, January 2021 (9 pages). The 15 used qubits contain the 9 for the Bacon-Shor correction code, 4 for the stabilizers ancilla and two unused ions at the edges of the 1D set of ions.

⁴⁴⁴ For Google's logical qubit, see [Exponential suppression of bit or phase errors with cyclic error correction](#) by Zijun Chen et al, February 2021 in arXiv and in Nature in July 2021 (6 pages) and [supplemental materials](#) (30 pages).

⁴⁴⁵ See [Realization of Real-Time Fault-Tolerant Quantum Error Correction](#) by C. Ryan-Anderson et al, PRX, December 2021 (29 pages), a follow-up from the previous paper. It uses a 10 qubit trapped ion quantum computer to encode a single logical qubit using the Steane $[[7, 1, 3]]$ color code. They later implemented a $[[7, 1, 3]]$ color code with 20 qubits with a transversal CNOT gate on two logical qubits in [Implementing Fault-tolerant Entangling Gates on the Five-qubit Code and the Color Code](#) by C. Ryan-Anderson et al, August 2022 (17 pages) and could obtain a logical qubit with 99.94% fidelity, compared to 99.68% for the underlying physical qubits.

⁴⁴⁶ See [Realization of an Error-Correcting Surface Code with Superconducting Qubits](#) by Youwei Zhao et al, PRL, December 2021 (10 pages). "Future work will concentrate on realizing larger-scale surface codes, to achieve the important goal of suppressing the logical error rate as the code distance increases. This necessitates further improvements to the quantum computing system's performance, such as the number and quality of qubits, the fidelity of quantum gate operations, and rapid feedback of digital electronics".

- A team led by **Andreas Wallraff** from ETH Zurich did a similar experiment a little later⁴⁴⁷.
- Another team in **Austria** and **Germany** developed a proof of concept of two logical qubits made with trapped ions and using a T gate and magic state distillation⁴⁴⁸.
- A joint **QuTech-Fujitsu-Element Six** team demonstrated in 2022 a fault-tolerant operation of a NV centers based QPU with logical qubits made of 5 physical spin qubits and two additional measurement qubits in a 29-qubit QPU running at 10K⁴⁴⁹.
- In 2022, **Google AI** created a distance 5 surface code logical qubit with 49 qubits ($=5^2+(5^2-1)$) that improves logical qubit error rates as physical qubits per logical qubits grows. But they have not yet reached the QEC efficiency threshold where logical qubit errors would be lower than physical qubit errors⁴⁵⁰. Google researchers indicate that their logical qubits would be better than their underlying physical qubit starting with a distance 7 surface code, requiring about 100 physical qubits, which they are not far from obtaining.

What are the figures of merit of a quantum error correction code and a logical qubit architecture? A key one is the logical qubit fidelities. You can't claim the creation of a logical qubit without adding its target fidelity. The end goal is to reach between 10^{-9} and 10^{-15} error rates. These rates differ according to the target algorithms. 10^{-9} may be enough for condensed matter and Hubbard models simulations, 10^{-15} is required for Shor's integer factoring for 2048-bit RSA keys while even better error rates are required for complex chemical simulations. The inverse of these error rates corresponds approximatively to the number of T gates to execute in these algorithms, which are the costlier to correct in surface codes. Then comes the overhead with the number of physical qubits per logical qubit but also code time cost, meaning, how will it slow down quantum computing. A logical qubit must also be able to implement non-Clifford quantum gates in a fault-tolerant manner, an aspect we'll describe in the next part.

Fault-tolerant quantum computing

FTQC (fault-tolerance quantum computing) was defined by Peter Shor in 1997⁴⁵¹ and is based on a few general principles related to implementing a practically useful QEC scheme with logical qubits: error-tolerant state preparation, error-tolerant quantum gates, error-tolerant measurement and error-tolerant error correction. Error correction codes can themselves introduce errors since they use quantum gates and state measurements which themselves generate errors. Moreover, error correction codes do not correct all possible errors. They just increase the apparent fidelity rate of the corrected qubits.

Also, QEC codes used repeatedly during long calculations must not introduce more errors than are corrected and should not spread errors in an uncontrollable way to various qubits in the computing register. As Peter Shor recounts: *"To be able to build a quantum computer, it's not enough to be able to correct errors with noiseless gates; you need to be able to correct errors using noisy gates. This means you have to correct the errors faster than you introduce new ones"*⁴⁵². This is where you understand why qubit gates, qubit readout time and the classical processing of readout data have all to be as fast as possible.

⁴⁴⁷ See [Realizing Repeated Quantum Error Correction in a Distance-Three Surface Code](#) by Sebastian Krinner, Alexandre Blais, Andreas Wallraff et al, Nature, December 2021-May 2022 (28 pages).

⁴⁴⁸ See [Demonstration of fault-tolerant universal quantum gate operations](#) by Lukas Postler, Rainer Blatt et al, Nature, December 2021 (14 pages).

⁴⁴⁹ See [QuTech and Fujitsu realise the fault-tolerant operation of a qubit](#) by Qutech, May 2022.

⁴⁵⁰ See [Suppressing quantum errors by scaling a surface code logical qubit](#) by Rajeev Acharya et al, Google AI, July 2022 (44 pages).

⁴⁵¹ See [Fault-tolerant quantum computation](#) by Peter Shor, March 1997 (11 pages).

⁴⁵² In [The Early Days of Quantum Computation](#) by Peter Shor, August 2022 (10 pages).

FTQC theoretically allows the execution of algorithms of arbitrary length, whereas without it, we are limited to a few series of gates. The challenge is to ensure that the calculation and QEC prevents errors from cascading. We must avoid linking one qubit with too many qubits with multi qubit gates in QECs. For this respect, a 7-qubits Steane code is appropriate.

And let's not forget that a CNOT gate propagates flip errors from the control qubit to the target qubit and phase errors from the target to the control. From an operational standpoint, FTQCs creation involves minimizing the number of ancilla qubits and optimizing the choice of QECs according to the type of errors generated by each type of qubit and quantum gates⁴⁵³.

Transversal gates are implemented with FTQC to avoid propagating errors beyond the corrected qubits. It is an arrangement of links between logical qubits linked together by two-qubit gates.

The diagram on the right illustrates these links between two logic qubits using a 7 qubit Steane code via CNOT gates. Each of the physical qubits of the logical qubits is connected one by one between the two logical qubits. This is still very theoretical, besides trapped ions, no qubit topology enables this kind of connectivity.

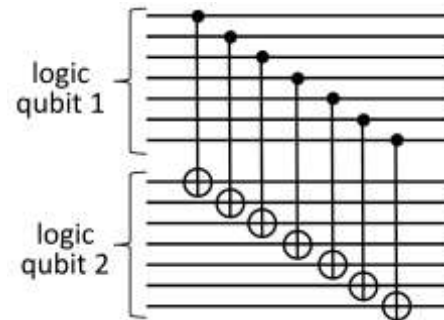


Figure 242: how transversality connects two logical qubits.

However, transversal gates can only be implemented within the Clifford group. According to the **Eastin-Knill** no-go theorem, no QEC code can transversally implement a universal gate set. That's why we usually need a costly QEC named **magic state distillation** to implement FTQC with T and Toffoli gates which lie outside the Clifford group. It has a huge cost of two orders of magnitude for physical per logical gates, explaining why it's often estimated said that logical qubits require over 10K physical qubits (on top of the effect of code concatenations or surface code)⁴⁵⁴.

One of the problems is that error correction generates an overhead that grows faster than the exponential gain of the quantum computer (2^{4n} vs 2^n according to Quantum Benchmark).

We can get some comfort from the **threshold theorem** demonstrated by Dorit Aharonov and Michael Ben-Or in 1999 according to which it is possible to perform error correction up to an arbitrary desired apparent error rate if the error rate of the single-qubit gates is below a given threshold which is dependent on the error correction code used and the characteristics of the qubits⁴⁵⁵.

Concatenation of codes C_1 (size n_1) and C_2 (size n_2)

We construct a code of size $n_1 n_2$, where each qubit of C_2 is replaced by a block of n_1 qubits encoded in C_1 .

Higher order QEC by concatenation

| Level of concatenation | Error probability |
|-------------------------------|---|
| Physical qubits | $q_0 = p$ |
| 1 st encoded level | $q_1 = cp^2 = c^{-1}(cp)^2$ (*) |
| 2 nd encoded level | $q_2 = c(cp^2)^2 = c^{-1}(cp)^{2^2}$ |
| ⋮ | ⋮ |
| r th encoded level | $q_r = c(q_{r-1})^2 = c^{-1}(cp)^{2^r}$ |

(*) For the Steane code $c \in 10^4$

Figure 243: how concatenated codes are reducing the error rate. Source: [Introduction to quantum computing](#) by Anthony Leverrier and Mazyar Mirrahimi, March 2020 (69 slides).

⁴⁵³ See [A Comparative Code Study for Quantum Fault Tolerance](#) by David DiVincenzo, Barbara Terhal and Andrew Cross, 2009 (34 pages).

⁴⁵⁴ See [Roads towards fault-tolerant universal quantum computation](#) by Earl T. Campbell et al, 2018 (9 pages).

⁴⁵⁵ See [Fault-Tolerant Quantum Computation With Constant Error Rate](#) by Dorit Aharonov and Michael Ben-Or, 1999 (63 pages).

This rate would be between 0.1% and 1% but is subject to change. The consequence of this theorem is to allow the application of error correction codes recursively until reaching the desirable error rate to execute a given algorithm. This is however based on the assumption that qubit fidelities are stable as their number is growing, a feat that is not yet achievable!

It also doesn't take into account various sources of errors like isotropic errors affecting simultaneously several qubits⁴⁵⁶. On the other hand, a variation of the threshold theorem was recently demonstrated that takes into account a stable percentage of defects in planar arrays of qubits and includes a QEC protocol for large arrays of defective qubits⁴⁵⁷.

The standard specification in vendor roadmaps for FTQC QPUs is one million physical qubits with 99.9% two-qubit gate fidelity running a surface code QEC. It might enable 100 to 1000 logical qubits, taking into account the significant overhead of T-gates or Toffoli gates synthesis and correction.

How about the number of logical qubits of a FTQC QPU? It should provide a space-related quantum advantage vs classical computing so we need at least 50 to 55 data qubits. Most algorithms requiring an equivalent of about 50 additional qubits (ancilla, transit, ...), we end up with needing about 100 logical qubits and a number of physical qubits that depends on the architecture, ranging from 30 to 10.000 physical qubits per logical qubits. The sheer number of qubits required to build a FTQC awarded it another nickname: Fairy-Tale Quantum Computing!

QEC concatenation is exploiting this recursivity of error correction codes. A QEC generates logical qubits which can then be used as virtual physical qubits for a new QEC, and so on. With each recursion, the apparent error rate decreases. We stop concatenating QEC codes when we reach an error rate compatible with the expected usage of the qubits. Concatenation can be optimized by using different types of QEC at each level of recursivity⁴⁵⁸. This theorem was demonstrated only for a 7-qubit Steane error correction code and for error rates that are not growing with the number of physical qubits. This is unfortunately not what is currently observed with the majority of qubit types! Surface codes and their various derivatives are not concatenated but rather expanded in 2D with a growing number of qubits. But their relative noise and number of qubit scaling are different.

With concatenated codes, the noise is reduced by the exponential law ϵ^{2^k} with a number of qubits in X^k , ϵ being the error rate, k the number of concatenations and X the number of qubits within a single concatenation, which can reach about 91 depending on the implementation and on the way ancilla qubits are managed and recycled, using Steane's method (not to be confused with Steane's code)⁴⁵⁹. But concatenated codes threshold is quite low, in the range of 10^{-6} , which is currently inaccessible for all breeds of qubits.

⁴⁵⁶ See [Quantum codes do not increase fidelity against isotropic errors](#) by J. Lacalle et al, January 2022 (18 pages).

⁴⁵⁷ See [Quantum computing is scalable on a planar array of qubits with fabrication defects](#) by Armands Strikis, Simon C. Benjamin and Benjamin J. Brown, November 2021 (16 pages).

⁴⁵⁸ See [Dynamic Concatenation of Quantum Error Correction in Integrated Quantum Computing Architecture](#) by Ilkwon Sohn et al, 2019 (7 pages).

⁴⁵⁹ 91 is based on using a Steane 7-qubit $[[7; 1; 3]]$ code, including the ancilla factory and $4 \times 7 = 28$ qubits ancilla factory times 3 because the preparation, verification and measurement of ancillas is three times longer than the data qubit operations (9 versus 3 time-steps). Hence, while ancillas are in used for a given gate, ancillas must be being prepared for the next two gates. Thus each level of error correction replaces one qubit by 91 qubits (7 data qubits and 3×28 ancilla qubits). Source: [Optimizing resource efficiencies for scalable full-stack quantum computers](#) by Marco Fellous-Asiani, Jing Hao Chai, Yvain Thonnart, Hui Khoon Ng, Robert S. Whitney and Alexia Auffèves, arXiv, September 2022 (39 pages). Flag qubits could reduce this significant overhead and reduce X . But this doesn't take into account T gates magic state distillation that adds a minimum of 15 qubits! See [Fault-tolerant quantum error correction on near-term quantum processors using flag and bridge qubits](#) by Lao Lingling et al, 2020 (12 pages) and [Fault-tolerant quantum error correction for Steane's seven-qubit color code with few or no extra qubits](#) by Ben W. Reichardt, April 2018 (11 pages). See [Overhead analysis of universal concatenated quantum codes](#) by Christopher Chamberland, Raymond Laflamme et al, 2017 (25 pages) which describes a fault-tolerant QEC of 105 qubits.

With surface codes, the noise is reduced according to $\frac{d}{\epsilon^2}$ and the number of required physical qubits grows by d^2 , d being the distance of the surface code, more or less corresponding to the edge of the surface code squares as shown in Figure 240 for distances 3 and 5.

All in all, concatenated error correction codes have a better impact on noise, but at the expense of a large number of physical qubits while surface codes scale slower in error reduction and physical qubits requirements. It seems that surface codes are more appropriate for more noisy physical qubits while concatenated codes will be better, for less noisy qubits.

Qubits lifetime extension. A nagging question may arise: if we need to accumulate error correction codes, don't we risk running into the wall of qubit decoherence, particularly with superconducting qubits? Well, no. As said before, error correction codes have the direct effect of artificially extending the coherence time of the qubit registers by several orders of magnitude⁴⁶⁰. Each correction is equivalent to a reset of the qubits decoherence times T_1 (flip) and T_2 (phase). This explains how Google could publish an optimized version of the Shor integer factoring algorithm with 20 million qubits and requiring 8 hours of run-time, which is many orders of magnitude longer than their qubits coherence time that sits way under a tiny 100 μ s.

Instruction bandwidth bottleneck is yet another engineering challenge for FTQC and error correction. Thousands of physical qubits must be driven by software-based quantum error correction. It creates a digital workload from the classical control computer down to the physical qubits and their many ancilla qubits, in a range exceeding several tens of TB/s just for factoring a 1024 bits integer with Shor's algorithm! Specific architectures can be designed to handle QEC as close as possible to the physical qubits, ideally in cryo-electronics components and with some microcode sitting at the lowest possible stage in the cryostat (for solid-state qubits), starting at 4K⁴⁶¹.

Approximate QEC

One QEC group named Approximate QEC or Quasi-Exact fault-tolerant Quantum (QEQ) computation sits in-between NISQ and FTQC⁴⁶². It is an intermediate solution implementing some error correction, but not to a point of creating perfect logical qubits. It still uses some variations of stabilizers and surface codes. One of these methods named NISQ+ combines aQEC and SFQ driving circuits⁴⁶³. It can help boost the "simple" quantum volume of NISQ QPUs. The simple quantum volume is computed with multiplying the number of useful qubits and a number of doable quantum gates under a certain error threshold.

The related paper raises an interesting point: slow QEC decoders make applications take exponential time to complete, which is kind of problematic! It's explained by the ratio between QEC data generation and QEC data processing is around 2 for syndrome data processing ratio using classical controls. With superconducting SFQ circuits, the ratio is of 0.125 thanks to a very low latency. The proposed SFQ circuit uses a circuit map similar to the qubit circuits topology. It implements an "Approximate SFQ decoder" stabilizer-based algorithm using a union-find algorithm, resets (stopping signal propagation once pairs are found), boundaries (match signals to boundaries) and tie-breaking (chooses single paths among an equal set).

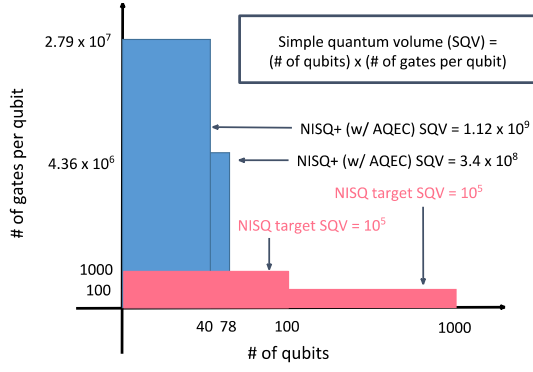
⁴⁶⁰ See [Extending the lifetime of a quantum bit with error correction in superconducting circuits](#) by Nissim Ofek, Zaki Leghtas, Mazhar Mirrahimi, Michel Devoret et al, 2016 (5 pages) which shows that thanks to a cat-code-based QEC, the lifetime of superconducting qubits can be extended by a factor of 20!

⁴⁶¹ See the QuEST architecture proposal in [Taming the Instruction Bandwidth of Quantum Computers via Hardware Managed Error Correction](#) by Swamit Tannu et al, GeorgiaTech, Stanford and Microsoft, 2017 (13 pages slides).

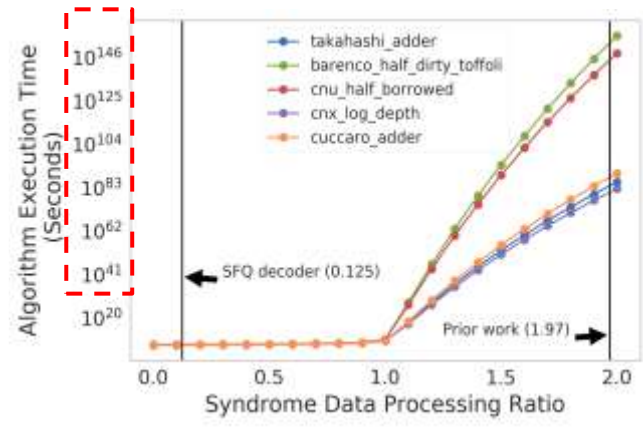
⁴⁶² See [Theory of quasi-exact fault-tolerant quantum computing and valence-bond-solid codes](#) by Dong-Sheng Wang, Raymond Laflamme et al, May 2021 (22 pages).

⁴⁶³ See [NISQ+: Boosting quantum computing power by approximating quantum error correction](#) by Adam Holmes et al, Intel, University of Chicago and USC, April 2020 (13 pages) and explained in this [video](#) (21 mn).

NISQ+ could enable a 78 logical qubits with a computing depth of 4.36×10^6 gates, using 1000 physical qubits



prohibitive exponential times with classical QEC



NISQ+/SFQ advantage threshold

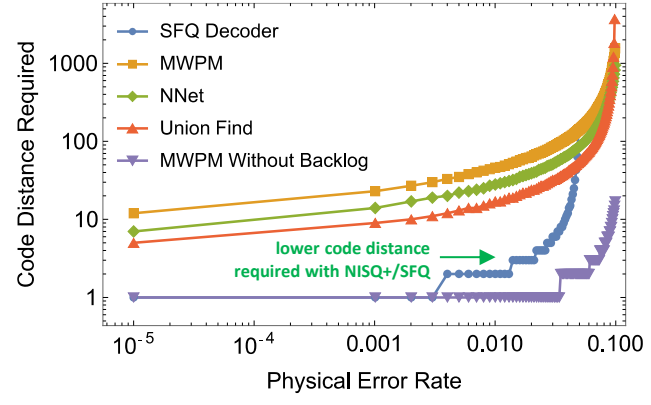
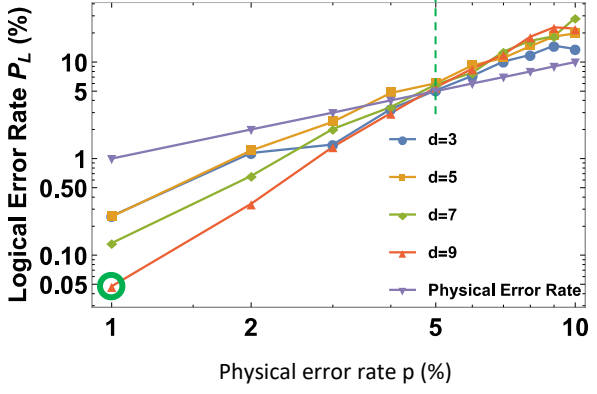


Figure 244: the NISQ+ architecture and benefits. Source: [NISQ+: Boosting quantum computing power by approximating quantum error correction](#) by Adam Holmes et al, Intel, University of Chicago and USC, April 2020 (13 pages).

The accuracy threshold of this SFQ circuit is at 5% of physical error rate and significantly interesting at 1%, yielding then a logical qubit error rate of 0,05% with a code distance of $d=9$. It is a much lower required code distance compared to other correction techniques like those using neural networks.

The SFQ circuit power consumption is $13 \mu\text{W}$ for a full circuit with a logical depth of 6, has a real-estate of 1.3 mm^2 and a latency of 20 ns for QEC. It seems made to run at 4K. It could enable the creation of a 78 logical qubits system using 1000 physical qubits and a computing depth of $4,36 \times 10^6$ gates.

In another work, a team led by Microsoft created a concept architecture to implement a FTQC with a scalable decoder running the QEC, but without details on the required hardware (room temperature or cryoelectronics, CMOS or SFQ)⁴⁶⁴.

Quantum error mitigation

Quantum error mitigation (QEM) is about reducing quantum algorithms errors with combining classical post-processing techniques with some potential circuits modifications on top of running the algorithm several times and averaging its results (*aka* the “*expectation values of an observable*”, i.e., the combination of 0s and 1s). QEM has a much lower overhead in qubits and running time vs QEC but its scalability is still questioned. It is a NISQ-era solution aiming at creating a quantum computing advantage before FTQC shows up in the longer term. QEM reduces the influence of quantum errors using multiple runs and subsequent measurements coupled to some classical processing as opposed to QEC-based active qubits measurement and fast feedback-based corrections impacting the results of individual runs.

⁴⁶⁴ See [A Scalable Decoder Micro-architecture for Fault-Tolerant Quantum Computing](#) by Poulami Das, Krysta Svore, Nicolas Delfosse et al, Microsoft, GeorgiaTech and Caltech, January 2020 (19 pages).

QEM proposals started to pop-up around 2016⁴⁶⁵. Most of them consist in learning the effects of noise on qubit evolutions and create predictive (if not linear) noise models that can be applied to tune the results of quantum computations. It is adapted to rather shallow circuits⁴⁶⁶ and we're not really sure yet it brings a quantum advantage on useful problems. Most QEM methods do not increase the required qubits count for a given algorithm. You'll notice that many contributions in the QEM space come from IBM Research.

Here are some identified QEM techniques:

Zero noise extrapolation (ZNE) builds error models based on solving linear equations. It supposes the noise is stable. It cancels noise perturbations by an application of Richardson's deferred approach to the limit and works on short-depth (or shallow) circuits⁴⁶⁷. A similar protocol was designed for (hybrid) variational quantum simulators used to simulate the dynamics of quantum systems⁴⁶⁸.

Probabilistic error cancellation is about detecting circuit bias with finding noise quantum channels, represented as density matrices for quantum gates, using quasi-probability decomposition. There's a sampling overhead in the process. It then inverts a well-characterized noise channel to produce noise-free estimates of the algorithm observables (the 0s and 1s they're supposed to generate)⁴⁶⁹. It's also called Bayesian error mitigation and Bayesian read-out error mitigation (BREM).

Learning Based Methods QEM are based on machine learning techniques using training data to learn the effect of quantum noise in various situations. It's proposed by companies like QuantroOx (UK), by the University of Erlangen in Germany⁴⁷⁰ and by Quantum Machines (Israel). One of these is Clifford circuit learning or Clifford Data Regression is a variation of the previous technique that learns the effect of noise from Clifford gates using data comparing quantum emulation on classical hardware and runs on quantum processors. It then uses rather simple linear regression techniques to correct errors in post-processing⁴⁷¹. It can also be applicable to fault-tolerant T gates⁴⁷². You have also QuantumNAS, a noise adaptative search method⁴⁷³ as well as some specific deep reinforcement learning techniques to improve qubit control precision⁴⁷⁴.

⁴⁶⁵ See the review papers [Hybrid Quantum-Classical Algorithms and Quantum Error Mitigation](#) by Suguru Endo, Zhenyu Cai, Simon C. Benjamin and Xiao Yuan, 2020 (39 pages), [Quantum Error Mitigation](#) by Zhenyu Cai, Ryan Babbush, Simon C. Benjamin et al, October 2022 (40 pages) and [Testing platform-independent quantum error mitigation on noisy quantum computers](#) by Vincent Russo, Andrea Mari, Nathan Shammah, Ryan LaRose and William J. Zeng, October 2022 (17 pages).

⁴⁶⁶ See [Fundamental limits of quantum error mitigation](#) by Ryuji Takagi et al, npj, September 2022 (11 pages).

⁴⁶⁷ See the beginning of [Error mitigation for short-depth quantum circuits](#) by Kristan Temme, Sergey Bravyi and Jay M. Gambetta, 2016 (15 pages) and [Scalable error mitigation for noisy quantum circuits produces competitive expectation values](#) by Youngseok Kim, Jay M. Gambetta, Kristan Temme et al, August 2021 (7 pages).

⁴⁶⁸ See [Efficient Variational Quantum Simulator Incorporating Active Error Minimization](#) by Ying Li and Simon C. Benjamin, PRX, 2017 (14 pages).

⁴⁶⁹ See the second part of [Error mitigation for short-depth quantum circuits](#) by Kristan Temme, Sergey Bravyi and Jay M. Gambetta, 2016 (15 pages), [Probabilistic error cancellation with sparse Pauli-Lindblad models on noisy quantum processors](#) by Ewout van den Berg, Zlatko K. Mineev, Abhinav Kandala and Kristan Temme, January 2022 (30 pages), [Probabilistic error cancellation with sparse Pauli-Lindblad models on noisy quantum processors](#) by Ewout van den Berg et al, IBM, January 2022 (30 pages) and [Unfolding Quantum Computer Readout Noise](#) by Benjamin Nachman et al, October 2019-May 2020 (13 pages).

⁴⁷⁰ See [Neural networks enable learning of error correction strategies for quantum computers](#), October 2018 and [Reinforcement Learning with Neural Networks for Quantum Feedback](#), Thomas Fösel et al, 2018 (7 pages).

⁴⁷¹ See [Error mitigation with Clifford quantum-circuit data](#) by Piotr Czarnik et al, May 2020 (16 pages) and [Improving the efficiency of learning-based error mitigation](#) by Piotr Czarnik, Michael McKerns, Andrew T. Sornborger and Lukasz Cincio, April 2022 (13 pages).

⁴⁷² See [Error mitigation for universal gates on encoded qubits](#) by Christophe Piveteau, David Sutter, Sergey Bravyi, Jay M. Gambetta and Kristan Temme, IBM Research, March 2021 (11 pages).

⁴⁷³ See [QuantumNAS: Noise-Adaptive Search for Robust Quantum Circuits](#) by Hanrui Wang et al, January 2022 (19 pages).

⁴⁷⁴ See [Deep Reinforcement Learning for Quantum State Preparation with Weak Nonlinear Measurements](#) by Riccardo Porotti, Antoine Essig, Benjamin Huard and Florian Marquardt, June 2021 (15 pages).

Error suppression by derangement (ESD) which provides an exponential error suppression with increasing the qubit count by $n \geq 2$ but is still adapted to NISQ architecture and shallow circuits⁴⁷⁵.

Dynamic Decoupling involves decoupling idle qubits from other qubits under certain conditions. The technique is proposed by IBM⁴⁷⁶. It seems that under certain circumstances, it can generate a good quantum speedup for oracle-based algorithms⁴⁷⁷.

Other methods include symmetry constraints verification, distillation using randomized benchmarking⁴⁷⁸, randomized compiling⁴⁷⁹, applying gates simulating the reverse effect of errors⁴⁸⁰, depolarizing noise⁴⁸¹, quantum verification and post-selection⁴⁸², virtual distillation with derangement operators⁴⁸³, using matrix product operators⁴⁸⁴, read-out noise mitigation and also mixing various QEM and QEC techniques⁴⁸⁵. Detailing and comparing these various methods is way above my quantum computing pay grade!

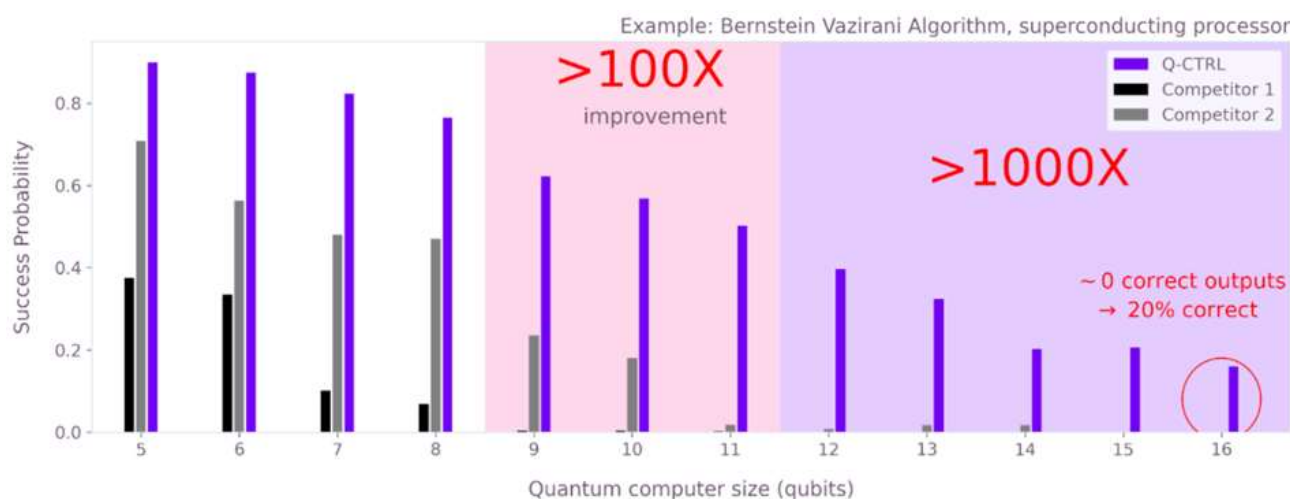


Figure 245: charting the Q-CTRL improvements. [Firing up quantum algorithms - boosting performance up to 9,000x with autonomous error suppression](#) by Michael J. Biercuk, March 2022 and [Experimental benchmarking of an automated deterministic error suppression workflow for quantum algorithms](#) by Pranav S. Mundada, Michael J. Biercuk, Yuval Baum et al, September 2022 (16 pages).

⁴⁷⁵ See [Exponential error suppression for near-term quantum devices](#) by Balint Koczor, PRX, 2021 (34 pages).

⁴⁷⁶ See [Pulse-level Noise Mitigation on Quantum Applications](#) by Siyuan Niu and Aida Todri-Sainal, LIRMM Montpellier France, April 2022 (11 pages) and [Analyzing Strategies for Dynamical Decoupling Insertion on IBM Quantum Computer](#) by Siyuan Niu and Aida Todri-Sainal, LIRMM France, April 2022 (11 pages).

⁴⁷⁷ See [Demonstration of algorithmic quantum speedup](#) by Bibek Pokharel and Daniel A. Lidar, July 2022 (12 pages).

⁴⁷⁸ See [Shadow Distillation: Quantum Error Mitigation with Classical Shadows for Near-Term Quantum Processors](#) by Alireza Seif, Liang Jiang, March 2022 (16 pages) and [Virtual Distillation for Quantum Error Mitigation](#) by William J. Huggins et al, Google AI, PRX, 2021 (25 pages).

⁴⁷⁹ See [Crucial leap in error mitigation for quantum computers](#) by Monica Hernandez and William Schulz, Lawrence Berkeley National Laboratory, December 2021, referring to [Randomized Compiling for Scalable Quantum Computing on a Noisy Superconducting Quantum Processor](#) by Akel Hashim, Irfan Siddiqi et al, 2021 (12 pages).

⁴⁸⁰ See [Quantum Error Mitigation via Quantum-Noise-Effect Circuit Groups](#) by Yusuke Hama et al, May 2022 (22 pages).

⁴⁸¹ See [Mitigating Depolarizing Noise on Quantum Computers with Noise-Estimation Circuits](#) by Miroslav Urbanek, Benjamin Nachman, Vincent R. Pascuzzi, Andre He, Christian W. Bauer, and Wibe A. de Jong, PRA, December 2021 (7 pages).

⁴⁸² See [Mitigating errors by quantum verification and post-selection](#) by Rawad Mezher, James Mills and Elham Kashefi, September 2021 and May 2022 (15 pages).

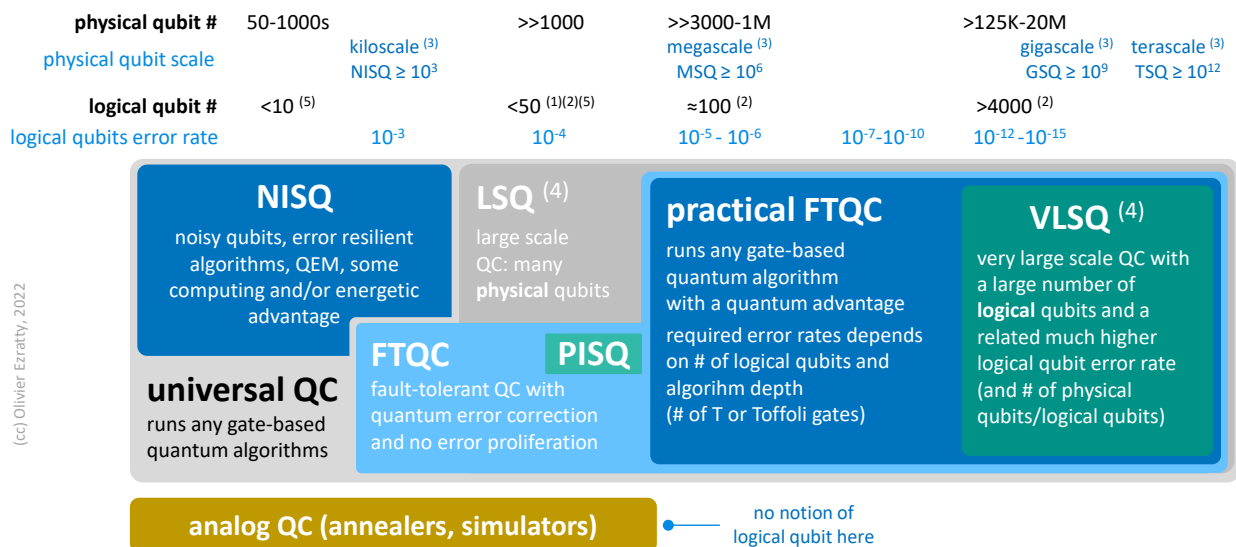
⁴⁸³ See [Virtual Distillation for Quantum Error Mitigation](#) by William J. Huggins, Ryan Babbush et al, August 2021 (26 pages).

⁴⁸⁴ See [Quantum error mitigation via matrix product operators](#) by Yuchen Guo et al, January-October 2022 (13 pages) which accounts for correlated errors between different gates.

⁴⁸⁵ Like in [Quantum error mitigation as a universal error-minimization technique: applications from NISQ to FTQC eras](#) by Yasunari Suzuki, October 2021 (33 pages).

In the commercial world, QEM can lead some vendors to display some outlandish claims like when Q-CTRL announces that its error correction scheme boosts algorithms performance by up to 9000x thanks to some autonomous error correction⁴⁸⁶. Why not, but 9000x of what? Looking at the details, this is achieved with back-end and front-end optimization compilation and some error mitigation techniques. When you read their chart, shown in Figure 245, you find that the x9000 ratio pertains to the success rate of running a Bernstein-Vazirani algorithm on a superconducting qubits processor, in the case of 16 qubits. But the related success factor is below 20% and is an extreme case.

You must remind yourself that 16 qubits can be easily emulated on your own laptop and is way below any quantum computing advantage. If you were to extend their chart beyond 30 qubits, you'd be hundreds of thousands better than their competitors but with a very small success probability.



(cc) Olivier Ezratty, 2022

(1) 100 logical qubits # is based on a mathematical advantage starting with about 55 qubits and for a similar number of ancilla qubits for most algorithms (QFT, HHL, QML).
 (2) the # of logical qubits depends on autonomous error correction and the number of physical qubits required per logical qubits, the best case being with cat-qubits.
 (3) this scale was presented in March 2022 by Dave Bacon from Google. It positions NISQ above the 1000 physical qubits threshold.
 (4) VLSQ is an equivalent to VLSI in classical semiconductors computing.
 (5) a few <50 logical qubits are not sufficient to run a quantum gate-based algorithm with some quantum computing advantage. Thus, the practical FTQC threshold at 100 logical qubits.

Figure 246: positioning all the concepts: NISQ, PISQ, LSQ, FTQC, Universal quantum computing and the related error correction codes. (cc) Olivier Ezratty, 2022.

I summarized these various gate-based computing classes in the above schema in Figure 246.

It requires a lot of comments and annotations and is still work in progress:

- **Universal quantum computing** is the quantum computing paradigm in which all quantum algorithms can be implemented from a mathematical standpoint. It must support non-Clifford quantum gates. This feature is implemented at a narrow and noisy scale with NISQ systems and with FTQC.
- **NISQ** definition is not really agreed upon. Is it starting today, or will we need more physical qubits and generate some proven generic quantum computing advantage? I added in blue a scale proposal presented by Dave Bacon at Google in March 2022⁴⁸⁷, which deals with a simple scale of number of physical qubits with NISQ being in the thousand, MSQ in the million, GSQ in the billion and TSQ in the tera number of qubits. NISQ is powered by quantum error mitigation in the near term and with approximated QEC in the mid-term. It will extend the usability of quantum computers with a larger number of qubits and circuit depth.

⁴⁸⁶ See [Firing up quantum algorithms - boosting performance up to 9,000x with autonomous error suppression](#) by Michael J. Biercuk, March 2022.

⁴⁸⁷ See [QIP 2022 | Software of QIP, by QIP, and for QIP](#) by Dave Bacon from Google, March 2022 (1 hour).

- **LSQ** stands for large scale quantum computer and is about having a QPU with a large number of qubits. But are these physical or logical qubits and how does it relate to FTQC? The dust has not yet settled for its definition. What we know is a large scale quantum system without error correction would not be very usable. On average, the depth of gate-based computing is limited by qubit error rates and many quantum algorithms have a breadth (number of qubits) that is in line with their depth (number of gate cycles). So, we have a sort of gap between the upper stages of NISQ and early stages of practical FTQC with logical qubits.
- **FTQC** can start with a few logical qubits of average error correction with target error rates of about 10^{-3} to 10^{-4} . We'll maybe have a continuum in the FTQC progress with error rates growing progressively until it reaches 10^{-15} in the long term as the number of logical qubits will grow. These error rates will have to shrink at a faster rate than the increase of logical qubit numbers.
- **Practical FTQC** is about FTQC providing a generic quantum advantage. It would require at least 100 logical qubits given half of them are used for data with a space exceeding the memory capabilities of equivalent classical systems, and the other half providing the ancilla qubits required for many algorithms like the QFT and its derivatives. The number of physical qubits corresponding to the logical qubit thresholds depend on autonomous error correction and the number of physical qubits required per logical qubits, the best case being with cat-qubits⁴⁸⁸. The target error rate of 10^{-5} to 10^{-6} is a rough estimate, below the inverse square of the number of logical qubits.
- **PISQ** for Perfect Intermediate Scale Quantum is a proposal from Qutech scientists that corresponds to the arrival of 50+ FTQC “perfect” qubits QPUs. They advocate to get ready for it in parallel with all the efforts related to NISQ systems⁴⁸⁹.
- **VLSQ**: this is large scale FTQC with several orders of magnitude larger number of logical qubits used to run chemical simulations, Shor integer factoring and large scale optimization and industry scale algorithms. So, in the above chart in Figure 246, I position these various definitions for universal quantum computing, FTQC, LSQ and VLSQ, with one scale for physical qubits and one for logical qubits as well as with logical qubit error rates.
- **FTDQC** is a new term, meaning « fault tolerant distributed quantum computation », which could potentially be implement with long distance quantum communication, even with satellites⁴⁹⁰.

QEC impact on computing time

There are only a few studies and research done to evaluate how long it would take to execute specific quantum algorithms in an “end-to-end” fashion. We know that, theoretically, with a FTQC of 20 million qubits, we could factorize an RSA 2048 bits key in 8 hours with superconducting qubits. Gate time is quite variable from 12 ns for superconducting qubits to 100 μ s for trapped ions qubits.

You can get an idea of the timing overhead coming from three mechanisms:

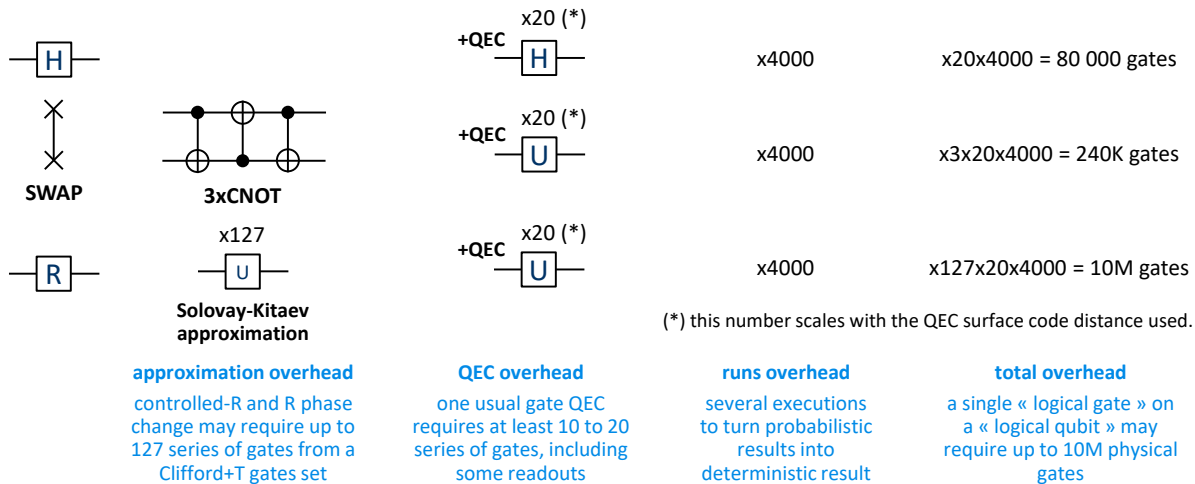
- **Non-Clifford gates** creation overhead like R/Control-R gates with arbitrary phases, based on the Solovay-Kitaev theorem. It creates a x127 to x235 gates overhead!
- **Quantum error correction (QEC)** overhead in the case of FTQC. It creates a x10 to x20 gates overhead, minimum! It may be much bigger for large surface codes and concatenated codes. With surface code QEC, this runtime overhead scales with the code distance.

⁴⁸⁸ I saved you the EFTQC variation, for early FTQC that is used in [On proving the robustness of algorithms for early fault-tolerant quantum computers](#) by Rutuja Kshirsagar et al, September 2022 (27 pages) which deals with an interesting question: what is the error rate of logical qubits in the FTQC realm that would be required for some key algorithms?

⁴⁸⁹ See [Quantum Computing -- from NISQ to PISQ](#) by Koen Bertels et al, April 2022 (11 pages).

⁴⁹⁰ See [Upper Bounds for the Clock Speeds of Fault-Tolerant Distributed Quantum Computation using Satellites to Supply Entangled Photon Pairs](#) by Hudson Leone et al, University of Technology Sidney, August 2022 (9 pages).

- **Number of runs** or shots required to average probabilistic results. IBM advises using 4000 runs but this number may grow with the number of used qubits. So, a x4000 overhead! We can anticipate that this number will remain high with logical (error corrected) qubits given quantum computing will always have a probabilistic dimension, even with error correction.



one performance indicator of quantum computing is the quantum gates speed (CLOPS for IBM).

it depends on the qubit types and implementation: 12 ns to 300 ns for superconducting qubits, 1 μs for cold atoms, 10 ns to 5 μs for electron spins, 100 μs for trapped ions and 1 ms for photon qubits (which may rely on an MBQC technique, making these numbers irrelevant).

Figure 247: assessing the overhead of quantum error correction on a practical basis. (cc) Olivier Ezratty, 2021.

I tentatively added these three mechanisms for three scenarios: an H gate, a SWAP gate assembled with three CNOT gates and an arbitrary R gate created with a Clifford gate set plus a T gate using the Solovay-Kitaev approximation theorem. Adding all these timing overheads, you obtain between 80K and 10M gates to run to execute a single physical gate. That's quite significant!

Interestingly, the longer the gates, like with trapped ions qubits, the better fidelity they have, creating a balancing effect between the QEC overhead and the gates times. All this should be taken into account when dealing with so-called quantum algorithms speedups, particularly with non-exponential speedups.

But these estimates are very raw and deserve scrutiny. It depends on the QEC technique that is being used, on the qubit type, on their fidelities, and so on.

Quantum memory

We would guess that quantum memory is some memory capable of storing the quantum state of qubits and then using them to feed quantum computer registers⁴⁹¹. It should be able to store superposed and entangled qubits and deliver it to whatever computing is needed. But it is part of a broader category defined as “quantum RAM” or qRAM, which is able to store either classical or quantum data, the data being queried with superposed quantum addresses.

Quantum memory is also required in quantum key distribution repeaters⁴⁹² and can be useful in various situations like with quantum sensing and for creating deterministic sources of photons⁴⁹³.

⁴⁹¹ See [Architectures for a quantum random access memory](#), by the Italians Vittorio Giovannetti and Lorenzo Maccone and the American Seth Lloyd, 2008 (12 pages).

⁴⁹² Here's one example with [One-hour coherent optical storage in an atomic frequency comb memory](#) by Yu Ma et al, April 2021 (6 pages) and another one with [Space-borne quantum memories for global quantum communication](#) by Mustafa Gündoğan et al, 2020 (11 pages).

⁴⁹³ See [Quantum memories - A review based on the European integrated project “Qubit Applications \(QAP\)”](#) by C. Simon et al, 2010 (22 pages).

However, we focus here on the first category of quantum memory, aimed at quantum computing. It is a very diverse one with different logical and physical architectures. We'll look at quantum memories for repeaters in the section dedicated to quantum telecommunications hardware.

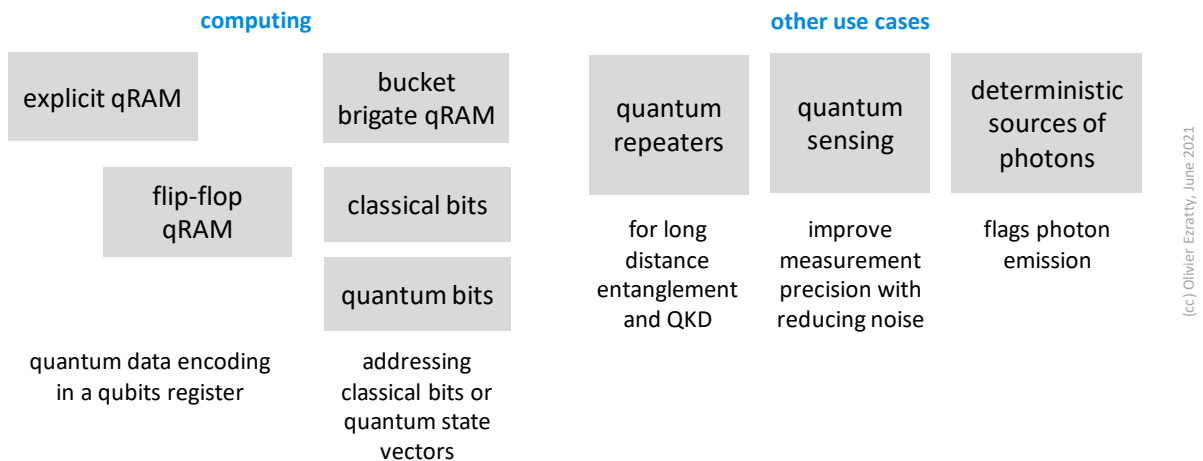


Figure 248: various classes of quantum memories and use cases. (cc) Olivier Ezratty, 2021.

Quantum algorithms requirements

One anticipated usage of quantum memory is to temporarily store the state of a qubit register during a data preparation process, a usual lengthy process, before transferring it to a faster quantum processing unit. With N qubits, this memory would be able to store in theory 2^N different computational vector states amplitude values.

According to the no-cloning theorem, the content of this memory cannot be the copy of the state of other quantum registers. In computing, quantum memory is used to store data into some quantum memory to be later used in quantum processing. Data preparation and encoding depends on the algorithm. It is necessary for certain types of quantum algorithms such as Grover's search and quantum machine learning algorithms that we will describe later on⁴⁹⁴.

The most demanding encoding is when you encode a vector of 2^N values (well, minus 1 for normalization constraints) in the whole computational state vector⁴⁹⁵. This creates a superposition with all or some of the basis states from the computational basis. Namely, we encode a vector \mathbf{x} containing 2^N real (or even complex) number values from \mathbf{x}_0 to \mathbf{x}_{2^N-1} with the normalization constraint that the square of these values is equal to 1. It ends up creating the state vector on the right with 2^N amplitudes x_i associated with the vectors $|i\rangle$ from the computational basis. This is called amplitude encoding.

$$\sum_{i=1, 2^N} x_i^2 = 1$$

normalization constraint

$$\sum_{i=1, 2^N} x_i |i\rangle = \begin{bmatrix} x_0 \\ x_1 \\ \vdots \\ x_{2^N-1} \end{bmatrix}$$

encoded state vector

Since this data encoding grows exponentially with the number of qubits, it may erase any computing speedup we would gain later. So, this is efficient only if we find a way to make this fast. One solution is to encode sparse vectors where only a few values are nonzero.

⁴⁹⁴ See [Quantum Machine Learning and qRAM](#) by Behnam Kia, 2018 (59 slides) as well as [Quantum Algorithms for Linear Algebra and Machine Learning](#) by Anupam Prakash, 2014 (91 pages).

⁴⁹⁵ See [Quantum 101: Do I need a quantum RAM?](#) by Olivia Di Matteo, May 2020 (58 slides).

Quantum memory types

There are several types of qRAM and other quantum memory types:

- **Explicit qRAM** encodes data in physical qubits and then, use quantum circuits to extract the encoded data⁴⁹⁶. There is no specific addressing system to selectively access parts of this memory. This is the scenario depicted above. Also named QAQM for Quantum Access Quantum Memory and Quantum Access Memory⁴⁹⁷.
- **Flip-flop qRAM** is a variant of explicit qRAM based on qubits circuit algorithms used to efficiently load classical data in a qubit register⁴⁹⁸.
- **Implicit qRAM** was proposed by Seth Lloyd et al in 2008 with the **bucket brigade** addressing system, based on a qutrits tree (three states quantum objects) containing wait/left/right flags⁴⁹⁹, sort of decision trees to reach the right memory cell. Also named QACM for Quantum Access Classical Memory.

This quantum addressing system can be used for accessing both *classical* bits and *coherent states* in qubits. The first case may be useful when building some oracles for algorithms like a Grover search. In the full quantum case, the coherent superposition of these addresses enables a readout of a superposition of many state amplitudes in the computational basis. Namely, we can query a given amplitude α_i of the computational basis vector at the i address, encoded in binary with N classical bits or several of these, encoded in superposition⁵⁰⁰.

$$\sum_j \alpha_j |j\rangle |0\rangle$$

α_j weighted superposition of addresses corresponding to computational basis states $|j\rangle$

$$\sum_j \alpha_j |j\rangle |b_j\rangle$$

result of query, weights are applied to $|b_j\rangle$ j -th memory location

In classical RAM, the memory array of N bits (2^N) is usually organized in a 2-dimensional lattice which requires $O(\sqrt{N})$ switches, precisely, usually a fixed number of address data to address lines and columns in memory chipsets.

In bucket brigade qRAM, this can decrease to $O(\log N)$ to address a particular computational basis vector amplitude. But this has to take into account the burden of any quantum error correction⁵⁰¹.

⁴⁹⁶ See [Optimal QRAM and improved unitary synthesis by quantum circuits with any number of ancillary qubits](#) by Pei Yuan and Shengyu Zhang, Tencent Quantum Laboratory, February 2022 (19 pages) proposes an optimized method for feeding QRAM with amplitude QSP (quantum state preparation).

⁴⁹⁷ See [Quantum Associative Memory](#) by Dan Ventura and Tony Martinez, 1998 (31 pages) and this implementation proposal that sees quite optimistic despite the support of prestigious folks like John Preskill, in [Quantum Data Center: Theories and Applications](#) by Junyu Liu et al, University of Chicago, Caltech and AWS, July 2022 (24 pages).

⁴⁹⁸ See [Circuit-based quantum random access memory for classical data with continuous amplitudes](#) by Tiago M. L. de Veras et al, 2020 (11 pages) referring to [Circuit-based quantum random access memory for classical data with continuous amplitudes](#) by Daniel K. Park et al, 2019 (9 pages).

⁴⁹⁹ See [Quantum random access memory](#) by Vittorio Giovannetti, Seth Lloyd et al, 2008 (4 pages) and [Architectures for a quantum random access memory](#) by Vittorio Giovannetti, Seth Lloyd and Lorenzo Maccone, 2008 (12 pages).

⁵⁰⁰ See [Circuit-Based Quantum Random Access Memory for Classical Data](#) by Daniel K. Park et al, Nature, 2019 (8 pages) which proposes an optimized implementation.

⁵⁰¹ The QEC burden may be significant. also [On the Robustness of Bucket Brigade Quantum RAM](#) by Srinivasan Arunachalam et al, 2015 (19 pages) which shows that the timing advantage of qRAM bucket brigade addressing may be quickly lost due to QEC overhead. See also [Quantum Random Access Memory](#) by Aaron Green and Emily Kaplitz, 2019 (12 pages) and [Methods for parallel quantum circuit synthesis, fault-tolerant quantum RAM, and quantum state tomography](#) by Olivia Di Matteo, 2019 (111 pages) and [Fault tolerant resource estimation of quantum random-access memories](#) by Olivia Di Matteo et al, 2020 (14 pages).

Various implementations of the bucket brigade solution have been proposed so far, including one using quantum walks, with the benefit of being more robust to decoherence and easier to parallelize⁵⁰².

Before any qRAM data transfer to computation qubits can be done, an uncompute processing must be implemented that remove the selected computational basis vectors addresses from the related data.

- There are also proposals for creating **Quantum Read Only Memories (QROM)** which allows only retrieval of stored quantum information; the stored information cannot be updated⁵⁰³.
- **Probabilistic Quantum Memory (PQM)** stores and simultaneously analyzes r patterns while using only n qubits. A quantum computer therefore would need $O(n)$ qubits as opposed to $O(rn)$ bits of associative memory on a classical computer⁵⁰⁴.

In the end, when quantum data is transferred from quantum memory to computing qubits, it is achieved with teleporting the memory qubits to the computing one by one, usually with using entangled photons and, in many cases, some conversion from solid qubits to photon qubits (spin or charge to photons and the other way around). This teleportation is supposed to preserve the superposition and entanglement between the memory qubits during this transfer. Given there must be some errors generated during the transfer, which will require their own error correction codes.

Quantum memory physical implementations

None of the different quantum memory architectures studied over the last two decades is working yet. However, research is making progress, with targeted use cases that are more related to secure telecommunications and for quantum optical repeaters. At this stage, the advent of qRAM for quantum computing is more difficult to predict than scalable quantum computing!

The most promising quantum memory technologies are coupling cold atoms and photon polarization⁵⁰⁵:

- **Cold atoms and light polarization.** Chinese scientists used in 2019 the storage of the circular polarization state of a single photon trapped in a laser-cooled rubidium structure in a magneto-optical trap and thus made transparent⁵⁰⁶.

Rubidium atoms are cooled with lasers to 200 μK . The same year, another team in China created a 105 qubits memory using 210 memory cells and dual-rail representation of a photon-based qubits with fidelities of 90% but these qubits seem not entangled and thus, not able to store a full state vector with 2^N values, but only a N or $2N$ values using basis encoding in each individual qubit⁵⁰⁷. Other techniques are based on cesium with fidelities reaching 99%⁵⁰⁸.

⁵⁰² See [Quantum random access memory via quantum walk](#) by Ryo Asaka et al, 2021 (13 pages).

⁵⁰³ See [Optimization of Quantum Read-Only Memory Circuits](#) by Koustubh Phalak et al, PennState and IBM, April 2022 (6 pages). It uses amplitude encoding with qubits for address and qubits for memory.

⁵⁰⁴ See [Probabilistic Quantum Memories](#) by Carlo A. Trugenberger, PRL, 2000 (4 pages) and a recent implementation improvement proposal in [EP-PQM: Efficient Parametric Probabilistic Quantum Memory with Fewer Qubits and Gates](#) by Mushahid Khan et al, University of Toronto, January 2022 (27 pages).

⁵⁰⁵ As in [Highly-efficient quantum memory for polarization qubits in a spatially-multiplexed cold atomic ensemble](#), 2017 (13 pages), a paper to which Julien Laurat from CNRS contributed.

⁵⁰⁶ As reported in [HKUST Physicist Contributes To New Record Of Quantum Memory Efficiency](#), 2019, which refers to [Efficient quantum memory for single-photon polarization qubits](#) by Yunfei Wang et al, 2019 (8 pages).

⁵⁰⁷ See [Experimental realization of 105-qubit random access quantum memory](#) by N. Jiang et al, 2019 (6 pages).

⁵⁰⁸ See [Highly-efficient quantum memory for polarization qubits in a spatially-multiplexed cold atomic ensemble](#) by Pierre Vernaz-Gris, Julien Laurat et al, Nature Communications, January 2018 (6 pages) and [Efficient reversible entanglement transfer between light and quantum memories](#) by M. Cao, Julien Laurat et al, LKB France, April 2021 (6 pages).

This is also the technique developed by Julien Laurat at ENS LKB in Paris and implemented by WeLinQ.

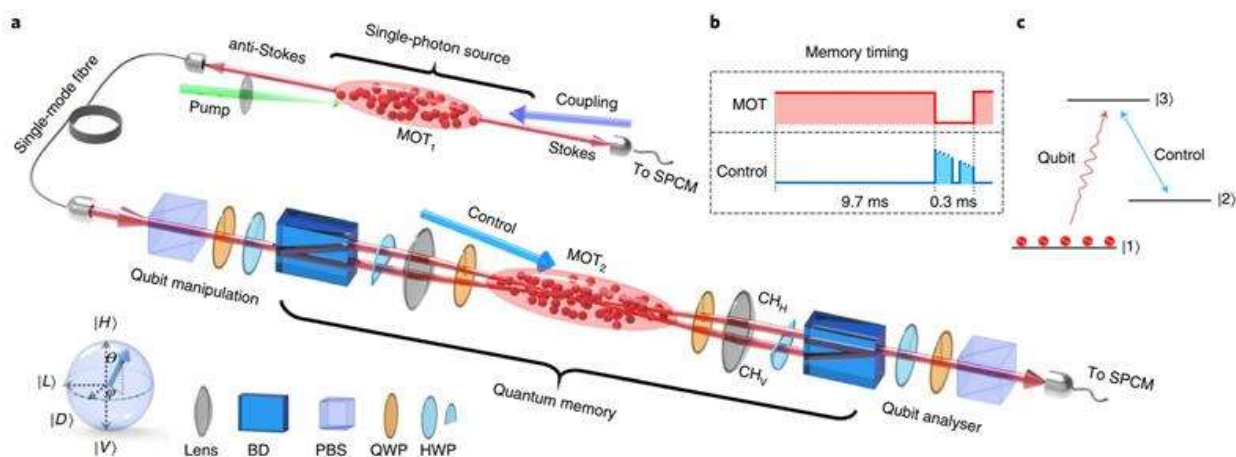


Fig. 1 | Experimental set-up and energy level scheme of the single-photon quantum memory. **a**, Schematic of the experimental optical set-up. The cold atoms in the first magneto-optical trap (MOT₁) serve as a nonlinear optical medium for producing time-frequency entangled photon pairs, while the cold atoms in the second magneto-optical trap (MOT₂) are the medium for the quantum memory. The anti-Stokes photon is coded with an arbitrary polarization state through the QMU consisting of a QWP and HWP. After the QMU, the two orthogonal linear polarizations are separated into two beams by a polarization beam displacer (BD) that are coupled into the two balanced spatial channels CH_H and CH_V of the quantum memory. The memory read-outs are recombined at the second BD and the polarization state is measured by the qubit analyser. **b**, The memory operation timing shows the MOT sequence and the optimized control laser intensity time-varying profile in each experimental cycle. **c**, The atomic energy level scheme of the quantum memory based on EIT.

Figure 249: a cold atom base single qubit memory. Source: [Efficient quantum memory for single-photon polarization qubits](#) by Yunfei Wang et al, 2019 (8 pages).

- A related work in **Canada** is dynamically controlling rubidium's transparency to trap single photons⁵⁰⁹. In practice, photons are stored for a thousandth of a second, but this would be sufficient for optical telecommunication repeaters. Another work in France from the Pasqal team used cold atoms to store quantum information⁵¹⁰.
- **Optical memories** are also tested with ytterbium⁵¹¹, a rare earth that can be controlled at high frequency. The process is similar to the previous one and consists in preserving the polarization of a single photon in a magnetic trap, rather for optical repeater applications in long-distance secure communication lines⁵¹².
- The storage of quantum states is also possible in **electron spins**⁵¹³ and **donors spins**⁵¹⁴.

⁵⁰⁹ See [Physicists create new, simpler-than-ever quantum 'hard drive for light'](#), by Kate Willis, University of Alberta, 2018, which refers to [Coherent storage and manipulation of broadband photons via dynamically controlled Autler-Townes splitting](#), October 2017 (17 pages).

⁵¹⁰ See [Storage and Release of Subradiant Excitations in a Dense Atomic Cloud](#) by Giovanni Ferioli, Antoine Glicenstein, Loic Henriot, Igor Ferrier-Barbut and Antoine Browaeys, PRX, May 2021 (12 pages).

⁵¹¹ See [Nuclear spin-wave quantum register for a solid-state qubit](#) by Andrei Ruskuc et al, Caltech, Nature, February 2022 (32 pages). It uses ytterbium nuclear spin in yttrium orthovanadate crystal (YVO₄, V for vanadium) arranged in nanophotonic cavity. It stores polarization information in spin ensembles. Bell states are created with ytterbium and vanadium. Control is made with 675 and 991 MHz microwaves and optical readout at 984 nm. It operated at 460 mK.

⁵¹² See [Simultaneous coherence enhancement of optical and microwave transitions in solid-state electronic spins](#), December 2017 (10 pages). This is a joint work between the University of Geneva, notably Nicolas Gisin, and the CNRS in France.

⁵¹³ See [Researchers achieve on-demand storage in integrated solid-state quantum memory](#) by Liu Jia, Chinese Academy of Sciences, January 2021.

⁵¹⁴ See [Random-access quantum memory using chirped pulse phase encoding](#) by James O'Sullivan, March 2021-June 2022 (27 pages) which deals with using ensembles of bismuth donors spin in natural silicon, coupled to a planar superconducting niobium resonator, all operating at 100 mK with a resonant frequency of 7.093 GHz. Pulses are made of 1,200 photons. It seems to be used with individual qubits memory, not entangled qubits and amplitude encoding.

- **NV centers**⁵¹⁵ and other crystal defects are also tested, storing qubits in **nuclear spins**⁵¹⁶.
- Passively **corrected quantum memory** can be implemented with cat-qubits⁵¹⁷.
- **Photons** trapped in cavities⁵¹⁸.
- **Trapped ions** as experimented in 2022 in China with 218 ions in a 1D trap with over 300 ms stability⁵¹⁹.
- Memory with **error correction** using the honeycomb technique or Floquet codes⁵²⁰.

Many new quantum memory proposals pop up from time to time. An interesting one from the University of Cambridge stores some quantum bit information in an electron spin hidden in haystack of 100,000 atom nuclei. The electron spin and the whole haystack are controlled by a laser. But the nuclei surrounding the electron make it difficult to entangle several qubits. End of story⁵²¹!

Quantum technologies energetics

The main motivation for creating quantum computers is their computing capacity, which theoretically increases exponentially with their number of high fidelity qubits. This should make it possible to perform calculations that will someday be inaccessible to conventional supercomputers. In some other cases, like with some NISQ architecture using quantum error mitigation, it will only be “just” faster or sometimes, provide better results, like in quantum machine learning or quantum physics simulations.

How does this computing capacity translate in terms of energy consumption is a key question. At first glance, it looked like the energetic cost of quantum computing was several orders of magnitude lower than classical computers. That was a naïve interpretation of Google Sycamore's 2019 quantum supremacy demonstration which did show a ratio of about one to one million in energy consumption compared to the IBM Summit supercomputer that was used as a comparison, and even when using the optimized algorithm and configuration proposed afterwards by IBM.

But the benchmark was comparing apples and oranges with a randomized benchmark with no input data nor any useful output data. It was later shown by Waintal et al that, with accounting for its high error rate and noise and using tensor networks, Sycamore's performance could be emulated on a rather simpler classical server cluster⁵²².

⁵¹⁵ See [Storing quantum information in spins and high-sensitivity ESR](#), by two researchers including Patrice Bertet of the Quantronics group at CEA/CNRS, September 2017 (13 pages). See also [A Ten-Qubit Solid-State Spin Register with Quantum Memory up to One Minute](#) by C. E. Bradley et al, QuTech and TU Delft, 2019 (12 pages) and [Multiplexed control of spin quantum memories in a photonic circuit](#) by D. Andrew Golter et al, MITRE Corporation, Sandia Labs, University of Arizona, September 2022 (18 pages).

⁵¹⁶ See [Nuclear Spin Quantum Memory in Silicon Carbide](#) by Benedikt Tissot et al, April-August 2022 (12 pages). It uses an all-optical O-band (in the 1260 nm-1360 nm range, adapted to long distance communication) to control vanadium defect spins in SiC

⁵¹⁷ See [Candidate for a self-correcting quantum memory in two dimensions](#) by Simon Lieu et al, May 2022 (11 pages).

⁵¹⁸ See [Toward a Quantum Memory in a Fiber Cavity Controlled by Intracavity Frequency Translation](#) by Philip J. Bustard et al, March 2022 (7 pages). Here, the memory traps photons in a low-loss cavity.

⁵¹⁹ See [Experimental realization of a 218-ion multi-qubit quantum memory](#) by R. Yao et al, September 2022 (6 pages).

⁵²⁰ See [A Fault-Tolerant Honeycomb Memory](#) by Craig Gidney et al, August 2021 (17 pages).

⁵²¹ See [Light used to detect quantum information stored in 100,000 nuclear quantum bits](#) by University of Cambridge, February 2021 and [A different type of cloud computing: Quantum breakthrough uses lasers to find data in a giant cloud of atomic nuclei](#) by Daphne Leprieux-Ringuet, February 2021. And [Quantum sensing of a coherent single spin excitation in a nuclear ensemble](#) by D. M. Jackson et al, Nature Physics, 2021 (21 pages).

⁵²² See [What limits the simulation of quantum computers?](#) by Yiqing Zhou, Edwin Miles Stoudenmire and Xavier Waintal, PRX, November 2020 (14 pages) and [A density-matrix renormalization group algorithm for simulating quantum circuits with a finite fidelity](#) by Thomas Aryal, Thibaud Louvet, Yiqing Zhou, Cyprien Lambert, E. Miles Stoudenmire and Xavier Waintal, August 2022 (25 pages).

On the other hand, another commonplace view is that the sheer power of about 15kW that is required for cooling superconducting qubits processors is a showstopper. It gives the impression that quantum computers will be high-power consuming devices. This may not be true and forgets that a rack of Nvidia GPGPUs used for machine learning tasks has a power consumption above 30kW.

Real comparisons should be made in the future, with large-scale quantum computers that will bring a quantum computing advantage to classical supercomputers. These will require a large number of physical qubits to implement error correction. Controlling these qubits uses energy-consuming conventional electronics. The question remains open: will quantum computers provide some energy advantage on top of a computing advantage, or do they risk to turn into energy hogs⁵²³?

The same questions should be asked for other quantum technologies that could potentially be deployed at a large scale like quantum telecommunications and cryptography as well as quantum sensors.

Digital energy footprint

Quantum computers are usually compared in performance and energy footprint with supercomputers. So, what are we dealing with? The world's largest supercomputers consume several MW (megawatts) like the recent Frontier from the DoE Oak Ridge Laboratory in Tennessee and its 21 MW for 1.1 exaflops and 700 petabytes of storage, 9,400 AMD CPUs and 37,000 AMD GPUs.

It followed the IBM Summit in 2019 and its 13 MW of peak power for 200 petaflops, including 3.9 MW just for cooling. These MW came from the thousands of Power9s CPU chipsets and general purpose Nvidia GPUs requiring a complex water-cooling system that uses two tons of water per minute. IBM Summit occupies 500 m² and weighs 349 tons, compared to about 2 tons for a superconducting quantum computer that fits into a room of about 20 m², the device being a square cube of about 2.75m, which also gives a "mass advantage" and a "surface advantage" in its current state, provided we also obtain a computing advantage, which has yet to be proven.

New supercomputers are launched each and every year, but their scale doesn't change fast. These supercomputers won't be replaced by quantum computers. Many of the scientific applications they are used for are not suitable for quantum computing, like any digital simulation requiring large sets of data such as in weather forecasts or using the finite elements method and other methods to solve differential equations. We will always need them. On the other hand, when quantum computers scale up, they will be able to perform computations inaccessible to conventional supercomputers, like molecular simulations and, probably with a smaller energy footprint.

The energy efficiency of classical systems is the ratio of their performance to their energy consumption. A classical server efficiency can be expressed in FLOPS/W, where FLOPS is the number of floating-point operations per second. Since the birth of computing, this efficiency has doubled about every 18 months.

This is Koomey's law, with a current record for supercomputers of 52 GFLOPS/W for the DoE's full size Frontier HPC launched in 2022⁵²⁴.

However, this sort of amazing progress has not prevented an explosion in global energy consumption to power digital technologies. Digital technologies now consume 11% of the world's electricity, with computer datacenters accounting for a quarter of this energy footprint⁵²⁵.

⁵²³ Like in this evaluation of Shor's energetic cost seen in [Energy Cost of Quantum Circuit Optimisation: Predicting That Optimising Shor's Algorithm Circuit Uses 1 GWh](#) by Alexandru Paler et al, ACM Transactions on Quantum Computing, March 2022.

⁵²⁴ See <https://www.top500.org/> and the June 2022 Top 500 charts. See also [Compute and energy consumption trends in deep learning inference](#) by R. Desislavov, F. Martinez-Plumed, and J. Hernandez-Orallo, 2021 (26 pages).

⁵²⁵ See [Spintronic devices for energy-efficient data storage and energy harvesting](#) by Jorge Puebla et al, Communication Materials, 2020 (9 pages).

It is increasing as usage grows. These phenomena are simply a new manifestation of the rebound effect, formalized by William Stanley Jevons in 1865.

Efficiency gains automatically lead to a decrease in the cost of resources. Without regulation of markets and uses, they lead to an increase in global consumption (see Figure 250). However, this does not mean that improving the energy efficiency of computers is inherently wrong. On the contrary, it is the only solution to maintain performance with limited energy and material resources.

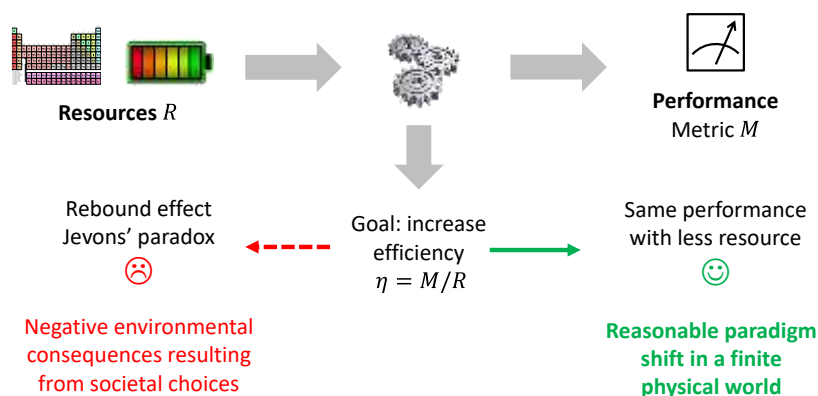


Figure 250 Energy efficiency and the rebound effect. A machine consumes material and energy resources to perform a task with a performance M . Its efficiency is defined by the ratio $\eta = M/R$. Source: Alexia Auffèves, France Quantum June 2022 [presentation](#).

The debate is also raging about the potentially large energetic footprint of cryptocurrencies, with various more or less questionable comparison methodologies⁵²⁶. And let's forget about the metaverse which may itself be yet another digital energetic hog.

Quantum Energy Initiative

Scaling quantum computing is one of the most challenging scientific and technology endeavors ever launched by mankind on top of space exploration, nuclear fusion and DNA sequencing and genome based therapies creations.

It should be undertaken with behaving responsibly as early as possible. One way is to embed in research and systems design an approach integrating the environmental footprint of quantum technologies. This footprint is of course energetic but also encompasses raw materials, manufacturing processes and product lifecycle handling. Addressing these questions are both scientific, technology and societal challenges.

We can learn a couple lessons from what happened with artificial intelligence and deep learning. It became trendy starting in 2012 with a peak around 2020 when deep learning use cases became mainstream and embedded from smartphones to cloud datacenters. Suddenly, it was discovered that AI had a significant energetic cost, both for training large deep learning models and to run them whether on end-user devices or on servers⁵²⁷. The “frugal AI” topic then emerged. Solutions were proposed to reduce the energetic footprint on AI mainly with less data-hungry machine learning models⁵²⁸, so-called data “quantization” (using 8-bit and even 1-bit numbers instead of 16-32-64 floating-point numbers) and also with optimizing the power consumption of dedicated hardware like GPGPUs and embedded systems chipsets (in smartphones, connected objects and also cars). What if the environmental footprint of AI had been taken care of earlier?

⁵²⁶ On [Bitcoin's Energy consumption: a quantitative approach on a subjective question](#) by Rachek Rybarczyk, Galaxy Digital Mining, May 2021 (13 pages) and [Fact sheet: Climate and Energy Implications of Crypto-Assets in the United States](#), White House, September 2022. In the Blockchain realm, Ethereum switched in September 2022 from proof-of-work to proof-of-stake for mining, with a significant energy saving of several orders of magnitude. See [Ethereum energy consumption](#), Ethereum, September 2022 which provides a lot of energy consumption related data for various Internet services.

⁵²⁷ See [Compute and Energy Consumption Trends in Deep Learning Inference](#) by Radosvet Desislavov, 2021 (26 pages) which describes how GLOPS/W have recently evolved depending on the type of AI problem (CNN for convolutional networks, NLP for natural language processing).

⁵²⁸ See [Frugal Machine Learning](#) by Mikhail Evchenko, Joaquin Vanschoren, Holger H. Hoos, Marc Schoenauer and Michèle Sebag, November 2021 (31 pages).

The same question deserves to be asked for quantum technologies. Why not take care right now of their environmental footprint? One could argue that the first challenge is scientific before being environmental. Some are advocating to first obtain high-fidelity qubits and useful fault-tolerant quantum computers and later address the environmental problem. Looking at how research labs and industry vendors were working until now on addressing the scalability challenges of quantum computers demonstrate that despite its relative technology immaturity and high scientific uncertainty, it is time to take environmental concerns into account right now. In a world of doubts on the role of science and technology, it's also a way to demonstrate that in emerging technologies, it's possible to implement responsible innovation practices from the start and not as afterthoughts and under pressure.



All of this is the reasoning behind the creation of the **Quantum Energy Initiative (QEI)** in 2022⁵²⁹. The idea came out from a research team in France led by Alexia Auffèves (MajuLab in Singapore) with Robert Whitney (CNRS LPMCM in Grenoble) and Olivier Ezratty (myself).

It quickly got the support of researchers (in quantum computing and also quantum telecommunications) and industry vendors (in quantum computing and enabling technologies) throughout the world. It's about bringing a scientific and technology community together to address these issues in a concerted way and foster a cross-disciplinary research-industry collaboration.

The QEI is first about answering several key questions related to quantum computing:

- Is there a **quantum energy advantage** as the processors scale up and how different is it from the quantum computational advantage?
- What is the fundamental **minimal energetic cost** of quantum computing?
- How to **avoid energetic dead-ends** on the road to large scale quantum computing? Can we create optimization tools and models for qubit technology, enabling technologies and software engineering?

The seed of Quantum Energy Initiative is described in a thorough perspective paper from Alexia Auffèves published in PRX Quantum in June 2022⁵³⁰. It lays the ground for a transversal initiative, connecting quantum thermodynamics, quantum information science, quantum physics and engineering. It makes the connection between classical and quantum thermodynamics, qubit architectures, qubit noise models, room temperature control electronics and cryo-electronics, quantum error correction codes, algorithms and compiler designs. It proposes a methodology to assess the energetic performance of quantum technologies, dubbed MNR⁵³¹.



Figure 251: the QEI position paper. [Quantum technologies need a Quantum Energy Initiative](#) by Alexia Auffèves, PRX Quantum, June 2022 (11 pages).

⁵²⁹ See the QEI website: <https://quantum-energy-initiative.org/>. It contains a poll (“Join us”) to build the QEI community and a Manifesto that quantum professionals can sign to support the initiative. As of the publishing of this book late September 2022, about 200 signatures had been collected coming from 32 countries.

⁵³⁰ See [Quantum technologies need a Quantum Energy Initiative](#) by Alexia Auffèves, PRX Quantum, June 2022 (11 pages).

⁵³¹ See also the thesis [The resource cost of large scale quantum computing](#) by Marco Fellous-Asiani, November 2021 (215 pages).

After having first modeled the energy consumption of a scalable fault-tolerant superconducting qubits quantum computer and learned some lessons on the conditions of a related energetic advantage, the QEI aims to apply this methodology to all types of qubits developed by research laboratories and companies around the world. This includes silicon spin qubits, trapped ion qubits, neutral atom qubits and photon qubits. The three main paradigms of quantum computing will also need to be evaluated, namely programmable quantum gate computing, quantum annealing and quantum simulation. This will allow the energy dimension to be exploited for comparison and scaling. These efforts also involve the entire quantum computing software chain, in particular error correction codes, algorithms and compilers.

This work could lead to the implementation of a "Q-Green 500" type benchmarking system to compare the best quantum computers in terms of their energy efficiency. They will also provide a basis for the creation of tools and models to dimension quantum computer architectures from an energy point of view by integrating all their hardware components - quantum and classical - and software. They will provide roadmap elements and specifications for companies in the enabling technology sector, such as benchmarks for the energy consumption of control electronics systems.

The QEI self-mandate is not limited to quantum computing. It goes beyond and is intended to expand to all quantum technologies, namely quantum telecommunications⁵³² and quantum sensing.

Modeling a quantum computing energetic advantage

Thanks to quantum coherence, superposition and entanglement, quantum computers could showcase an exponential computing speedup compared to their classical counterparts, depending on the size and nature of the problems to be solved and on the used quantum algorithm. This computational advantage is usually predicted for ideal, error-free processors. In reality, quantum processors are noisy, with error rates currently exceeding 0.1% per operation, a prohibitive level for most algorithms and many quantum error correction codes.

In the short term, algorithms are created that can run on such noisy processors in the quantum computing paradigm called NISQ (Noisy Intermediate Scale Quantum) and with using quantum error mitigation techniques.

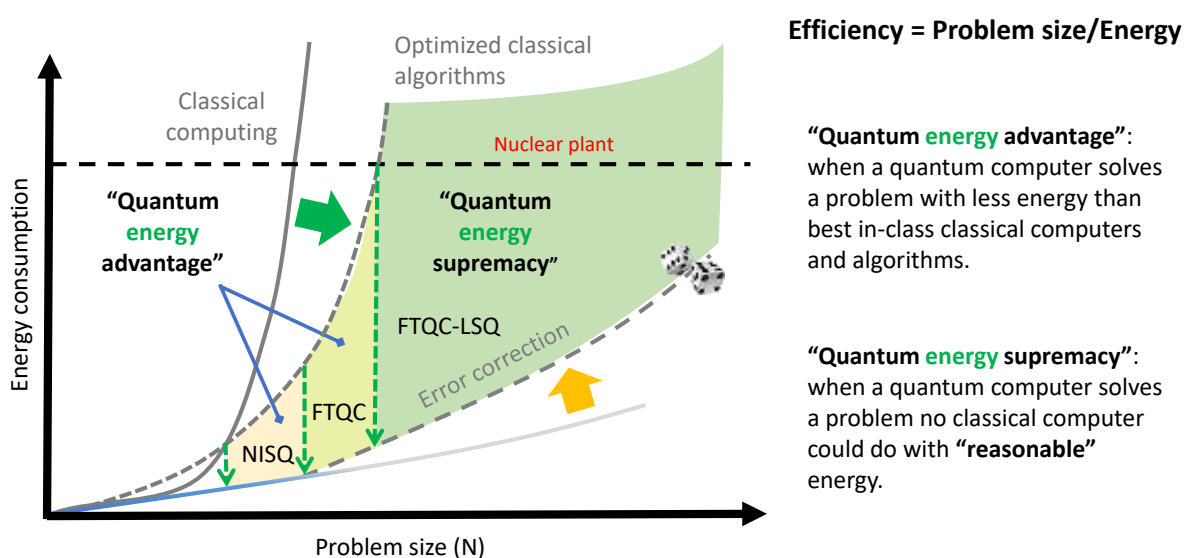


Figure 252 Different regimes of quantum energy advantage. Source: Alexia Auffèves and Olivier Ezratty, 2022.

(cc) Alexia Auffèves & Olivier Ezratty, 2022.

⁵³² Work has already started there. See for example [Reducing energy consumption of fiber networks via quantum communication technology](#) by Janis Notzel and Matteo Rosati, February 2022 (25 pages). With some proposal of a quantum receiver that would reduce the power consumption of classical fiber optic lines amplifiers.

In the longer term, we'll rely on quantum error correction using a large number of so-called physical qubits assembled as logical qubits, that will enable longer calculations and at an acceptable error rate. This number varies from 30 to 10,000 depending on the qubit technology. The associated error correction mechanisms also considerably increase the number of calculation steps.

In both cases, demonstrating a computational advantage for real quantum processors is an open question. In some cases, quantum computers could be less energy-intensive than conventional computers to solve the same problem as illustrated in Figure 252.

With larger scale FTQC could emerge a sort of quantum energy supremacy when a quantum computer solves a problem that no classical computer could process with a reasonable energy footprint like what comes out of a nuclear plant reactor (1 GW)⁵³³.

Modeling and optimizing the energetic efficiency of quantum computers must take into account the resources used for control and error correction. As a ratio of a performance to a resource, this energy efficiency is a hybrid quantity:

- Computational performance emerges at the fundamental quantum level, and results from the ability to control the noisy quantum processor to perform an algorithm with a certain accuracy. Understanding and optimizing these mechanisms is a matter of quantum control, quantum thermodynamics, quantum error correction, algorithms and compilers.
- Establishing satisfactory control at the quantum level requires the provision of resources at the macroscopic level, which determines the energy consumption necessary to carry out the calculation. This is the domain of enabling technologies including cryogenics, control electronics, cabling, lasers, amplifiers, detectors, whose mix depends on the qubit type.

It is essential to set up a full-stack quantum computer model coupling these different levels, as well as common language and concepts⁵³⁴. On this basis, the methodology proposed in the QEI is simple.

It sets a target performance at the microscopic level defining an implicit relationship between the different parameters of the model and a macroscopic energy consumption that is then minimized under this constraint. It was applied on a superconducting qubits model and considered typical algorithms used for optimization, physical simulations, quantum machine learning, and cryptanalysis for integer factorization.

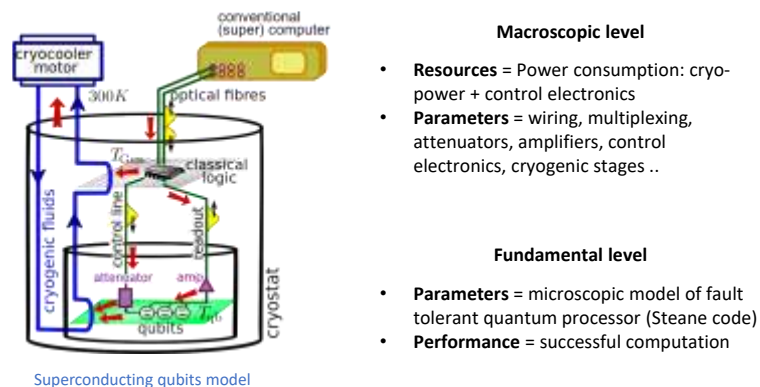


Figure 253 Full-stack model of a superconducting quantum computer coupling a quantum level and a macroscopic level of description. Source: Alexia Auffèves and Robert Whitney.

(cc) Alexia Auffèves & Robert Whitney, 2022

⁵³³ Interestingly, one paper shows how Shor algorithm is reaching this exact threshold, in [Energy Cost of Quantum Circuit Optimisation: Predicting That Optimising Shor's Algorithm Circuit Uses 1 GWh](#) by Alexandru Paler and Robert Basmadjian, ACM Transactions on Quantum Computing, March 2022 (no free access).

⁵³⁴ See [Energy use in quantum data centers: Scaling the impact of computer architecture, qubit performance, size, and thermal parameters](#) by Michael James Martin et al, NREL, 2021 (18 pages) that proposes a modelling of quantum processors energy consumption but not in a full-stack manner. It doesn't take into account the characteristics of the algorithm and is very generic with regards to all enabling technologies where many technology choices can impact the total system power consumption.

A full-stack modeling integrates the sources of quantum noise affecting qubits, the conventional qubit control resources such as electronics that generate microwave pulses and voltages, filters and attenuators, cryogenics, cables and amplifiers used for reading the state of the qubits, then the sources of heat dissipation involved in the whole material chain and in particular in the cryostat (see Figure 253). At last, it takes into account the size of the error correction code, initially a concatenated Steane code and then a surface code.

The model establishes a relationship between microscopic processor parameters such as qubit fidelity, with macroscopic qubit control parameters. It allows to minimize the energy consumption of the whole computer, under the constraint of reaching a targeted computational performance⁵³⁵.

Naturally, the results depend strongly on the qubits fidelity. A gain of a factor of 10 could lead to an energy gain of a factor of 100. The model can help find out the optimal temperature for control electronics. For CMOS type technologies and even with a highly optimistic assumed power consumption of 2mW per qubit⁵³⁶, room temperature is preferable to run the electronics. It would be similar with higher power drains electronics. The technological constraint then lies in the wiring, which must be simplified, essentially by using advanced (and future) multiplexing techniques. Another option is to use superconducting electronics running at the processor level or at the 4K stage.

With this model, the possibility of an energy-based quantum advantage was investigated. It computes the minimum energy consumption of a fault-tolerant quantum computer to factor an N-bit integer and compare it to the classical record⁵³⁷.

A classical record was obtained in 2021 by an Inria team on a Germany-based supercomputer, for factoring a 829-bit key⁵³⁸ with a consumption of 965 GJ, or 1.3MW of power over 8.6 days.

The models show that a quantum computer operating with qubits 2000 times more faithful than Google Sycamore, combined with Steane's code would require $2.7\text{GJ} = 2.9\text{MW}$ for 16 minutes, which is the amount of energy contained in about 75 liters of fuel oil. That would be 350 times less energy than used on the supercomputer. Breaking a 2048-bit RSA key is beyond the reach of a conventional supercomputer. On a quantum computer of the same type as above, the energy consumption would be $38\text{GJ} = 7\text{MW}$ for 1.5 hours. Using surface codes error correction would lighten the constraint of qubit fidelities.

Estimations were made for different key sizes in the classical and quantum cases (see Figure 254), giving access to an energy efficiency in each case. An energetic quantum advantage is clear with $N=848$.

⁵³⁵ All of this modeling comes out of [Optimizing resource efficiencies for scalable full-stack quantum computers](#) by Marco Fellous-Asiani, Jing Hao Chai, Yvain Thonnart, Hui Khoon Ng, Robert S. Whitney and Alexia Auffèves, arXiv, September 2022 (39 pages). See also the thesis [The resource cost of large scale quantum computing](#) by Marco Fellous-Asiani, November 2021 (215 pages).

⁵³⁶ A [Scalable Cryo-CMOS 2-to-20GHz Digitally Intensive Controller for 4x32 Frequency Multiplexed Spin Qubits/Transmons in 22nm FinFET Technology for Quantum Computers](#) by Bishnu Patra et al, 2020 (4 pages). This consumption model should still be full stack, up to analyzing readout microwaves after traversing parametric amplifiers, HEMTs and ADCs. It is not sure 2 mW are enough to do all of this. One key question to ask is what is the theoretical lower bound of microwave packets generation energetic costs?

⁵³⁷ The method is different from the one proposed in [Is quantum computing green? An estimate for an energy-efficiency quantum advantage](#) by Daniel Jaschke and Simone Montangero, November 2022 (13 pages) which compares NISQ systems and their classical emulation equivalent, but not best in-class classical algorithms equivalents. This makes the energetic reasoning incomplete. They also remind us that a quantum advantage comes from maximally entangled states, the overarching question of quantum computing scalability.

⁵³⁸ See [The State of the Art in Integer Factoring and Breaking Public-Key Cryptography](#) by Fabrice Boudot, Pierrick Gaudry, Aurore Guillevic, Nadia Heninger, Emmanuel Thomé and Paul Zimmermann, June 2022 (9 pages).

This energy advantage is different in nature from the computational advantage, which considers only the computation time⁵³⁹.

Both advantages are thus achieved for different key sizes. Let us recall that the proposed corrector code is resource-intensive and that the result would be much lower with, for example, a surface code.

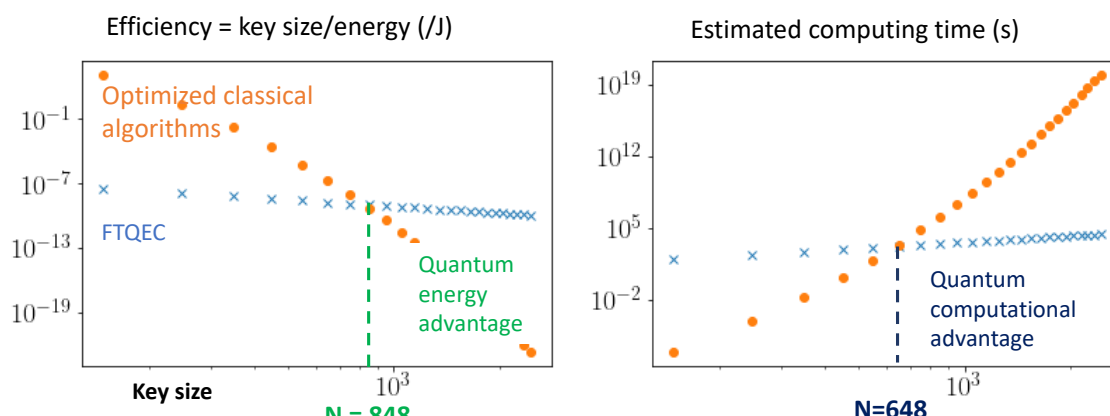


Figure 254 First results for estimating the quantum energy advantage. Source: Marco Fellous-Asiani, Alexia Auffèves, Robert Whitney.

This is a theoretical model with many optimistic technology assumptions and complex interdependencies that have to be discussed with many stakeholders, particularly in the enabling technologies vendor space. The beauty of the model is to highlight these interdependencies, which can help make sound choices in quantum computer design.

Microscopic energetics of quantum technologies

The fundamental quantum level mentioned before is already a rich field of research⁵⁴⁰. The energy and entropy at stake when dealing with quantum systems are the kingdom of quantum thermodynamicians⁵⁴¹. Some of them even investigate the interconnection and optimization of qubit technologies and the energetic cost of quantum computing and other quantum technologies like quantum communications.

As Kater Murch & al write in a review paper⁵⁴² “*Quantum information processing relies on precise control of non-classical states in the presence of many uncontrolled environmental degrees of freedom—requiring careful orchestration of how the relevant degrees of freedom interact with that environment. These interactions are often viewed as detrimental, as they dissipate energy and decohere quantum states. Nonetheless, when controlled, dissipation is an essential tool for manipulating quantum information: Dissipation engineering enables quantum measurement, quantum state preparation, and quantum state stabilization*”.

⁵³⁹ This is the topic of [The impact of hardware specifications on reaching quantum advantage in the fault tolerant regime](#) by Mark Webber et al, September 2021 (16 pages) which shows that the number of qubits to achieve a given task that is inaccessible to a classical computer depends on the target precision and computing time. 13 to 317 million qubits would be necessary to break Bitcoin signatures (which has no real use case...) and about the same order of magnitude to simulate FeMoCo (with potential use cases in reducing the energetic footprint of fertilizers production). See also [Nitrogen, Bitcoin, and Qubits The Shape of Transmons to Come](#) by The Observer, September 2021, and [From FeMoco to Bitcoin: Universal Quantum answers two major quantum advantage questions](#) by Universal Quantum, January 2022, which advertises the benefits of trapped ions qubits, and points to [Blueprint for a microwave trapped ion quantum computer](#) by Bjoern Lekitsch et al, 2017 (12 pages).

⁵⁴⁰ See the colloquium [A short story of quantum and information thermodynamics](#) by Alexia Auffèves, March 2021 (14 pages).

⁵⁴¹ See for example [Third law of thermodynamics and the scaling of quantum computers](#) by Lorenzo Buffoni et al, March-October 2022 (9 pages) which looks a fundamental issue related to the limits of the preparation of a qubit ground state.

⁵⁴² See the review papers [Engineered Dissipation for Quantum Information Science](#) by Patrick M. Harrington, Erich Mueller and Kater Murch, February 2022 (28 pages) and [Energy dynamics, heat production and heat-work conversion with qubits: towards the development of quantum machines](#) by Liliana Arrachea, May 2022 (63 pages).

There are many quantum thermodynamics concepts in play in qubits inner working and with other quantum technologies. Each qubit technology comes with its own assets and challenges with regard to their energy consumption.

Superconducting qubits are a well investigated area where qubits microwaves spontaneous emission is a dissipative process engendering errors and decoherence, with energy exchanges between the qubit and its controlling microwave during a qubit gate operation⁵⁴³, error mitigation which can make use (among various other techniques) engineering dissipation with energy baths whether it is handled with bosonic qubits like cat-qubits or with programmed error correction, engineering dissipation which can also help efficiently prepare (entangled) Bell states with two qubits, the Zeno effect with measurement backactions, how to optimize the measurement operation with various types of microwave light (single photon, coherent light, thermal light)⁵⁴⁴, the connection between quantum measurement and error correction⁵⁴⁵ and ways to purify the state of a single qubit with a quantum thermodynamic method⁵⁴⁶. There are also specific cooling mechanisms for superconducting qubits and even some connections between qubit thermodynamics and the way to optimize computing at the compiler level. At last, in the internal debates between the types of superconducting qubits, let's note that fluxonium qubits have a lower energy consumption since being driven by lower frequency microwaves and need less cooling, but at the price of various constraints.

Silicon spin energetics are also studied. Their operating parameter and controls are a bit different than with superconducting qubits, with a richer mix of microwave pulses and direct current and operations at a potentially higher temperature. Some quantum energetic advantage can even be found at the scale of one-qubit full added implemented with a three quantum dots silicon spin qubits with a three orders of magnitude gain⁵⁴⁷ and with entanglement generation between electron spin and photons in devices mixing static and flying qubits like quantum memories, repeaters and interconnections between quantum computing units⁵⁴⁸.

Trapped-ions qubits operations can also be optimized with regards to the energetics of their gates⁵⁴⁹.

Photon qubits are different beasts with regards to the thermodynamics of the whole food chain between single photon generations, entanglement preparation, computing (usually, using MBQC) and photon readout. A first seed of optical computing energetics was launched in Pascale Senellart's C2N team⁵⁵⁰. Also, the H2020 OPTologic project aims to create light-induced and controlled topology for energy-efficient logic operations in quantum photonic computing systems.

⁵⁴³ See [Energetics of a Single Qubit Gate](#) by J. Stevens, Andrew Jordan, Audrey Bienfait, Alexia Auffèves, Benjamin Huard et al, PRL, September 2021-September 2022 (19 pages).

⁵⁴⁴ See [Energetic cost of measurements using quantum, coherent, and thermal light](#) by Xiayu Linpeng, Léa Bresque, Maria Maffei, Andrew N. Jordan, Alexia Auffèves and Kater W. Murch, PRL, June 2022 (13 pages).

⁵⁴⁵ There are also debates about what are heat and work in quantum thermodynamics and qubits.

⁵⁴⁶ See [Quantum thermodynamic method to purify a qubit on a quantum processing unit](#) by Andrea Solfanelli, Alessandro Santini and Michele Campisi, March 2022 (5 pages).

⁵⁴⁷ See [Quantum dynamics for energetic advantage in a charge-based classical full-adder](#) by João P. Moutinho, Silvano De Franceschi et al, July 2022 (18 pages).

⁵⁴⁸ See [Energy-efficient entanglement generation and readout in a spin-photon interface](#) by Maria Maffei, Andrew Jordan, Alexia Auffèves et al, May 2022 (6 pages).

⁵⁴⁹ See [Classical Half-Adder using Trapped-ion Quantum Bits: Towards Energy-efficient Computation](#) by Sagar Silva Pratapsi et al, October 2022 (7 pages).

⁵⁵⁰ See [Coherence-Powered Charge and Discharge of a Quantum Battery](#) by Ilse Maillette de Buy Wenniger, M. Maffei, N. Somaschi, A. Auffèves, P. Senellart et al, February 2022 (19 pages).

And in general, there is a direct link between quantum thermodynamics and physics with the speed of the quantum gates a quantum computer could execute, with fundamental Quantum Speed Limits (QSL)⁵⁵¹.

Quantum sensing is also an interesting field of research with regards to quantum thermodynamics and energetics, particularly to find theoretical lower bounds of energy consumption in quantum sensors⁵⁵². Quantum thermodynamics can also help optimize quantum sensors precision.

About the reversibility of classical and quantum calculations

Here we study the impact of theoretical reversibility of gate-based quantum computing on its energetic cost. We first need to define the notion of logical reversibility of computation and its thermodynamic impact.

Logical reversibility of a calculation is linked to the ability to reverse it after one or more operations and recover input data from output data. This can be done at the scale of a classical logic gate or an elementary quantum gate and then up to a complete calculation. If logical reversibility is possible at the level of any gate used, then it becomes ipso-facto doable for a complete calculation⁵⁵³. Today's classical computers are logically irreversible. They rely on two-bit logic gates that destroy information since they generate one bit with two bits and we don't keep the information from the two initial qubits. One bit is thrown away every time. You can't reverse a simple NAND, OR or AND logic operation. We could use reversible logic gates that do not destroy information and generate as many output bits as input bits. This would lead to a logically reversible calculation. All of this was theorized by Charles Bennett in 1973 and Tommaso Toffoli in 1980. Classical computing is a big energy spender because logic gates are not logically reversible. The lower bound of energy consumption of current classical computing comes from Landauer's famous limit of $kT \ln(2)$ energy dissipated per irreversible bit operation, which can be the erasure of a bit or the merging of two computation paths. Even though we are far off this limit with current classical computing technologies, this lower bound could be avoided with logical reversible computing.

The implementation of this logical reversibility by rewinding calculations would reduce the energetic cost of classical computing, the energy spent in the forward calculation being potentially recovered in the reverse calculation. It was not a chosen path for various reasons. First was the steadiness of Moore's empirical law for many decades. Second is reversible classical architecture have significant overhead in the number of transistors used.

Thermodynamic reversibility is another matter and can be obtained when the system is continuously balanced with its thermal bath. It requires handling operations in a quasi-static way, namely, slowly and with logical gates requiring a minimum energy spending. This is the field of adiabatic computing.

Gate-based quantum computing is logically reversible because it uses unitary operations which are all mathematically reversible. Qubits readout is the only logically irreversible operation when it collapses qubit states to a basis state⁵⁵⁴.

⁵⁵¹ See [From quantum speed limits to energy-efficient quantum gates](#) by Maxwell Aifer and Sebastian Deffner, February 2022 (19 pages). It mentions that Amazon Web Services (AWS) classical computing is charged with about 4×10^{-13} cents per classical floating point operation when a single quantum circuit evaluation currently costs 1 cent on an AWS-owned Rigetti QPU ([pricing source](#)).

⁵⁵² See [Thermodynamic principle for quantum metrology](#) by Yaoming Chu and Jianming Cai, Huazhong University of Science and Technology, March 2022 (19 pages) and [Notes on Thermodynamic Principle for Quantum Metrology](#) by Yaoming Chu and Jianming Cai, Huazhong University of Science and Technology, August 2022 (6 pages).

⁵⁵³ See these detailed explanations on the reversibility of classical calculus: [Synthesis of Reversible Logic Circuits](#) by Vivek Shende et al, 2002 (30 pages).

⁵⁵⁴ Measurement Based Quantum Computing, which relies mainly on measurement during the entire calculation, is irreversible by construction. This is why it is also called 1WQC for one way quantum computing.

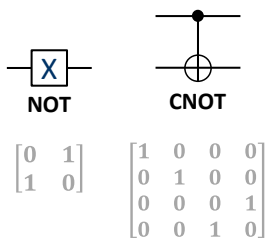
Qubits readout is reversible only when the qubit states are perfectly aligned with the basis qubit states $|0\rangle$ and $|1\rangle$, i.e., when the readout doesn't change the qubit quantum state.

However, quantum computing is not really thermodynamically reversible. It would be reversible in the absence of noise and if measurements were not changing qubit's internal states. Achieving physical irreversibility would also mandate that all non-quantum qubit control electronics rely on physically and thermodynamically reversible processes or at least be energy-saving operations.

One way to achieve this would be to use adiabatic and reversible electronic components working from within the cryostat, but it's not really possible, particularly at the DAC/ADC levels, given these analog/digital pulse signals conversions are not reversible processes.

Another explored avenue is ABQC for **Asynchronous Ballistic Quantum Computing**, promoted by Michael P. Frank's team at the DoE Sandia Labs in the USA. They plan to implement it with Josephson junction circuits⁵⁵⁵.

all quantum gates are mathematically reversible, this is a property of the matrix linear transformations



we could theoretically run an algorithm and rewind it entirely to return to the initial state, which could help recover part of the energy spent in the system

can be useful for some sub-parts of algorithms run before the end of computing and measurement, used in the "uncompute trick" at the end of some algorithms like for solving linear equations with HHL. it keeps the result x with resetting all other qubits without any measurement.

on a practical basis:

- the gates are not physically and thermodynamically reversible due to some irreversible processes like microwave generations and DACs (digital analog converters) and because gates are analog and noisy.
- part of the digital processes taking place before microwaves generation and after their readout conversion back to digital could be implemented in classical adiabatic / thermodynamically reversible fashion.
- being investigated at Sandia Labs, Wisconsin University and with SeeQC, with their RSFQ superconducting based logic, microwaves DACs and ADCs.

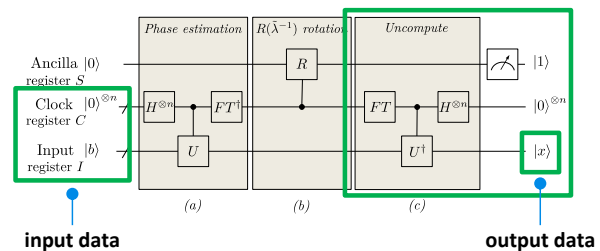


Figure 255:reversibility in quantum computing. Source: Olivier Ezratty, 2021.

Quantum reversible computing can also be used in quantum memory and with the uncompute trick of results that are no longer necessary, such as those sitting in ancilla qubits⁵⁵⁶. However, quantum reversibility is not the key to reducing the energy consumption of quantum computing.

Macroscopic energetics of quantum computing

We'll look here into more details about the "classical" and "macroscopic" power consumption of a quantum computer, taking first the example of a superconducting qubits QPU.

To date, the energy consumption of a quantum computer is relatively reasonable. A current quantum computer with superconducting qubits consumes about 25 kW, of which 16 kW comes from cryogenics. Cold atoms or photons quantum computers consume even less energy, in particular because they do not require cryogenic cooling to 15 mK.

⁵⁵⁵ See [Pathfinding Thermodynamically Reversible Quantum Computation](#) by Karpur Shukla and Michael P. Frank, January 2020 (28 slides) and [Asynchronous Ballistic Reversible Computing using Superconducting Elements](#) by Michael P. Frank et al, April 2020 (27 slides).

⁵⁵⁶ See [Putting Qubits to Work - Quantum Memory Management](#) by Yongshan Ding and Fred Chong, July 2020.

Photon qubits only require photon sources and detectors cooled at between 3K and 10K which is less energy hungry in face-value provided it scales well with the number of used qubits.

When thousands of qubits will fit in these machines, their power consumption will increase due to the energetic cost of qubit control for initialization, quantum gates, error correction and qubit readout⁵⁵⁷. Most of qubits energetic costs come from the signals used for gate activations and readout. These signals are microwaves pulses, direct current pulses and laser beams. The related spent power seems to increase linearly with the number of qubits. But error correction requires a large number of physical qubits per logical qubits, adding another power consumption multiplying factor. It will depend on the fidelity of the physical qubits and the ratio of physical qubits per logical qubits. The higher the fidelity, the lower this ratio will be. On top of that, the cryogenic cost of the qubits grows very fast as the temperature is lower in proportion of the mass to cool.

Let's breakdown the power consumption of a typical quantum computer:

Control electronics power consumption varies greatly from one technology to another and depends on the number of physical qubits managed, which will be counted in millions with large scale quantum computers (LSQC). It is currently high for the control of superconducting qubits based on microwaves produced outside the cryostat with electronics coming from Zurich Instruments, Qblox, Quantum Machines and the likes. Microwave readouts is costly in bandwidth, requiring Gbits/s of data streams per qubit. Microwave production with cryo-CMOS components sitting in the cryostat looks promising and is studied at Google, Intel, Microsoft, CEA-LIST and elsewhere. It can significantly reduce microwave generation related power consumption and may make sense for silicon spin qubits who run at higher temperatures than superconducting qubits and have a higher cooling budget of 500 to 1500 μ W at 100 mK. Trapped ion-based qubits control is performed with lasers and conventionally generated microwave pulses. With cold atoms, qubits control exploits a couple lasers and an SLM matrix that potentially supports a thousand qubits with modest power consumption. With photon qubits, the power drain seems more important for photon detection (about 7.5W per qubit) than for photon generation (about 1mW per qubit, source: Quandela). Superconducting based photon detectors are more demanding with cooling.

Cryogenics consumes up to 16 kW⁵⁵⁸ for superconducting and silicon qubits and a little less for other types of qubits due to higher temperatures, such as the 3K to 10K of photon generators and detectors used with photon qubits. Cryogenics will be required for cold atoms at the ultra-vacuum pump level, but will not significantly scale with the number of injected atoms. These are cooled with laser beams and tweezers and under ultra-high vacuum.

The cryogenics consumption is usually continuous, without variations between thermalization and production. Thermalization lasts about 24 hours for dilution refrigerator systems used with superconducting and electron spins qubits.

Vacuum is generated with superconducting and silicon spin qubits while cold atoms and trapped ions qubits use ultra-high vacuum. Photons do not need it. With superconducting and silicon qubits, vacuum comes from pumps and dilution refrigeration cooling. Cold atoms require only 100W for the ultra-vacuum pump plus about 300W for its cooling at 4K. Trapped ions systems use heating strips covering the vacuum chamber with a process that can take weeks. This is a fixed cost because when vacuum is in place, heating is stopped, and vacuum remains stable during computations.

⁵⁵⁷ This is the thesis of Joni Ikonen, Juha Salmilehto and Mikko Mottonen in [Energy-Efficient Quantum Computing](#) 2016 (12 pages).

⁵⁵⁸ This cooling power usually doesn't take into account the cost of cooling the water circulating in the cryostat compressor.

Computer control is used with all types of qubits. They all require one to three control servers that drive the qubit gates and readout devices by exploiting compiled quantum software, that transforms qubit gates into low-level instructions for qubits initialization, control and readout. These servers are networked, either on premise or in the cloud and via conventional network switches. They represent a limited fixed cost with an estimated consumption of between 300W and 1 kW. Part of the control computing could be moved into the cryostat for superconducting and electron spin qubits, in order to implement autonomous error correction codes. The control computer would then only drive logical qubits and not the physical qubits of the configuration.

Error correction is an important parameter that will condition the power consumption of a quantum computer. The key parameter is the ratio between the number of physical qubits and logical qubits, which depends on physical qubit fidelities. The higher this one is, the lower the ratio of physical/logical qubits. It also depends on the algorithm size and its target performance. To perform LSQC (large scale quantum computing), the number of qubits to control will be multiplied and generate high energy consumption. However, error correction codes may run up against another wall: the scale dependence of qubit noise. Namely, qubit gates and readout fidelities usually decrease with the number of qubits.

This may have the consequence of reversing the effect of increasing the number of qubits used in error correction. The error rate of logical qubits gates then increases, instead of decreasing⁵⁵⁹. The same problem arises with surface codes although their overhead seems lower than with concatenated codes. For error correction codes to be effective, the error rate of qubits should be at least ten times lower than their current level. In addition, we must also consider the fact that quantum algorithms are executed thousands of times and their result are then averaged. This increases the power drain of a quantum computation because it extends its duration by three orders of magnitude, at least, for the time being. In their work modelling a full-stack energetic cost of a superconducting qubits computer, Fellous-Asiani, Whitney, Auffèves et al found out that, from the energetic footprint standpoint, it is way more efficient to use room temperature electronics than cryo-CMOS due to the overhead cost of their cooling. This result moves the scalability burden cost on the wiring and its multiplexing. On top of that, control electronics have an energetic bill that is much bigger than the cryogeny used for the electronic components sitting in the cryostat (cables, filters, attenuators, qubit chipsets, circulators, amplifiers).

Many of these quantum computer components have a variable energy cost depending on the number of qubits, including the cryogenic side. Indeed, the electronics embedded in cryostats release heat in approximate proportion to the number of physical qubits used. This heat must be evacuated within the cryostat. The consumption of the control electronics also generally depends on the number of qubits. It seems that, up to a thousand qubits, this control electronics is a fixed cost for cold atoms. Only vacuum creation and the control computer seem to be fixed costs.

In the entrepreneurial scene, it's interesting to observe that the total power consumption of a quantum computer recently starting to become a selling point, although not yet being perceived as being an important one. For example, AQT (trapped ions) explain that their 20-qubit system can be attached to a regular 220V/110W plug with their <2kW power drain, similar to a kitchen oven. Pasqal is using a similar selling point for its Fresnel quantum simulator.

Creating a scalable quantum computer is clearly an optimization problem taking into account many energetic constraints. Qubits systems that operate at cryogenic temperature are constrained by the cryostat cooling power and by the heat released within the cryostat.

⁵⁵⁹ This is what comes out of [Limitations in quantum computing from resource constraints](#) by Marco Fellous-Asiani, Jing Hao Chai, Robert S. Whitney, Alexia Auffèves and Hui Khoon Ng, PRX Quantum, November 2021 (8 pages).

Superconducting and silicon spins qubits are the most challenging for that respect. Heat is generated by the inbound cable microwave attenuation filters and in the qubit readout related microwave amplifiers. In addition, the part of microwave generation and readout systems that is integrated in the cryostat have their own thermal footprint. All this must fit into the current thermal budget of the cryostats that is currently limited to 1W at the 4K stage and to about 25 μ W at the lower 15 mK stage. We will probably be able to create even more powerful cryostats with more pulse heads and as dilutions with a gain of an order of magnitude for the available cooling power. Other optimizations can be implemented to increase the available cooling power at very low temperature with getting closer to the theoretical Carnot efficiency. which seems possible with large cryostats. These are still constraints for the scalability in number of qubits, particularly for LSQC (large scale quantum computers) which will require millions of physical qubits!

Several options are investigated to reduce the power consumption of the qubits-related classical electronics. An interesting one is superconducting components such as those from SeeQC. D-Wave has integrated its own superconducting controls in its own quantum processor. With cryo-CMOS control electronics, the heat dissipation is greater.

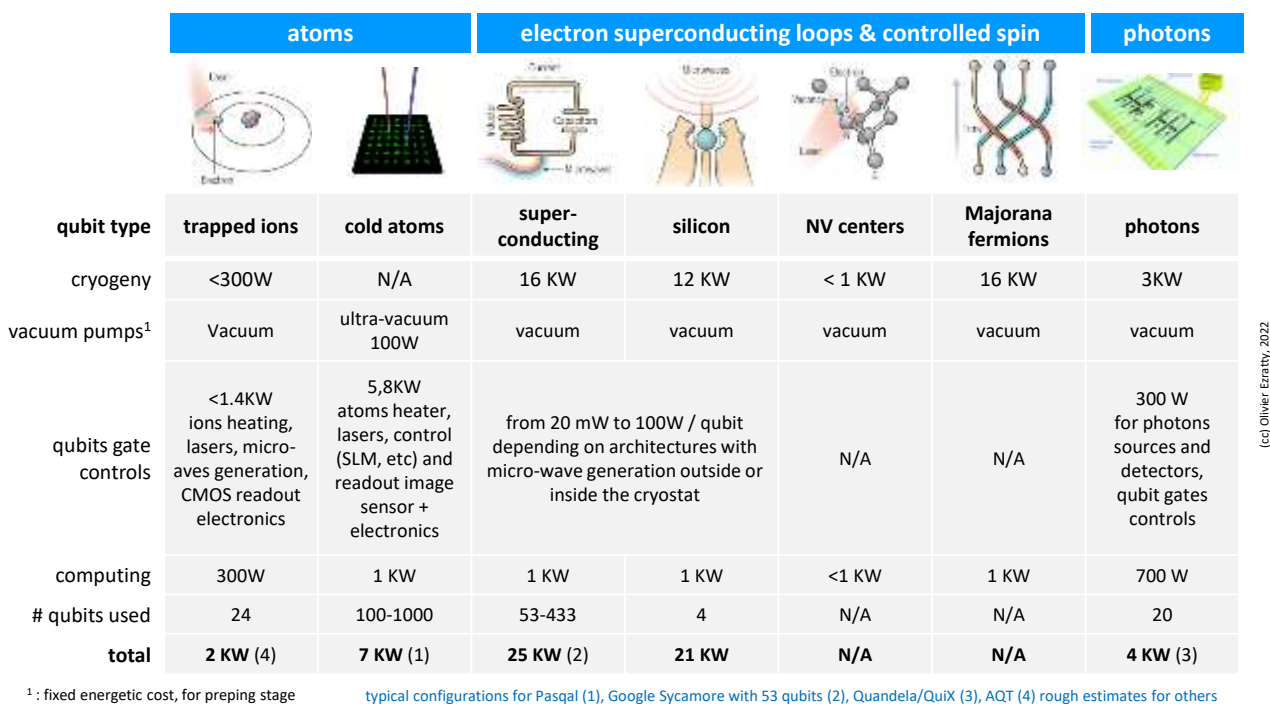


Figure 256: current quantum computers total power and decomposition. (cc) Olivier Ezratty, 2022.

The other way to be less constrained is to run the qubits at higher temperatures. This is what is possible with silicon spin qubits, which only require a temperature between 100mK and 1K instead of 15 mK for superconductors. This increases the thermal budget for the control electronics at the qubit stage.

Some significant engineering is required to optimize a multi-parameter system, at least with superconducting and silicon spin qubits:

1. Physical scalability requires putting as much as possible **qubits control electronics inside the cryostat**... but it is not efficiency energy wise unless control electronics are of the superconducting breed (SFQ).
2. These electronics thermal dissipation is **constrained** by the available cryostat cooling power.
3. Two paths must be investigated simultaneously: increase the available **cryostat cooling power** and reduce these **electronics thermal footprint** as low as possible.

4. Find an efficient way to **handle digital communication** between the inside and outside of the cryostat. Fiber optics, wireless, multiplexing, up/down signal conversions, whatever!
5. Look at various ways to **reduce qubits power drain**, with optimizing their own quantum thermodynamics, particularly when implementing error correction codes. It can also come from algorithm and compiler designs. Reducing the number of physical qubits per logical qubits is an option pursued for example with bosonic codes and cat-qubits who are self-correcting flip errors.
6. With **scale-out solutions** involving connecting several quantum computing processing units with some microwaves and photonic links, look at the energetic footprint of this connectivity, on top of its probable impact on qubit links fidelity.

Energetic cost of distributed architectures

The temptation is great to create ever larger quantum computers, with giant cryostats in the case of superconducting qubits, like we'll see with IBM and Google's roadmaps. Another approach would be to create distributed architectures of quantum computers linked together by quantum connection based on entangled photons, a choice made by IonQ with their trapped ions qubits, noticeably because it is difficult to scale these qubits beyond a couple dozens.

In theory, this would make it possible to create computing clusters that, seen from the outside, would create a single computer, a bit like a large classical server cluster.

This will be conditioned by the capability of converting qubits states to photons qubits states and by the resulting qubit connectivity between the various quantum processors units of this quantum cluster. But this is not just about "connecting" qubits. Interconnect architectures are about creating fragile entangled states between qubits using the intermediary of photons. These may create some statistical overhead on their own, which has to be boiled in for both assessing the real obtained quantum computing scalability and the related energetic footprint.

Use cases energetic assessment

Another longer-term question deserves to be asked: does the potential energetic advantage of quantum computing depend on algorithms and applications? What will happen if and when quantum computing becomes widespread? Are we finally going to create a new source of energy consumption that will be added to existing sources, which are already growing fast in the digital world? What will be its impact? How can it be limited?

At this stage, it is too early to have a clear idea. Answers will largely come from the emergence or not of quantum solutions for volume applications, such as autonomous vehicle routing or personalized health solutions.

Without volume-oriented applications, quantum computers will be dedicated to niche applications equivalent to those of current supercomputers, which are mainly used in fundamental and applied research or for public services like weather forecasts.

On their end, volume applications will only be achievable once the quantum computing scalability will work and millions of low-noise qubits can be operated. This scalability will probably come from fixing some of energetic consumption issues of quantum computing. And we'll close the loop!

Then, we'll have to look at the externalities of these applications and potential Jevon's effects. Namely, some new solutions will have a given quantum computing energetic cost but may help reduce the environmental footprint in other domains like in transportation. If it's well balanced, that's fine. If, on the other hand, the externalities are not positive, like, say in finance portfolio optimization tasks, you will have to think about it.

Economics

Given we are at the very early stage of the quantum computing era, it's still difficult to assess the economics of this industry. It's too small to generate economies of scale giving some indications on the cost and price of a regular quantum computer. Still, we can make some projections based on a couple assumptions.

The only "priced" quantum computers on the market today are coming from D-Wave. Their units are priced at about \$14M. They have sold only a few of these. Most D-Wave customers are using D-Wave computers sitting on the cloud either with D-Wave itself or with Amazon. Some customers pay in excess of \$200K per year to benefit from a premium access to these machines. As far as we know, the other "volume" manufacturer of quantum computers is IBM, but they haven't sold any unit so far, at least publicly. They installed a couple ones in Germany, South Korea, Japan and Canada in their own facilities, to serve these markets through various local research, university and industry partners. The rest is provided through their own cloud services.

One can economically make a distinction between **cost** (of R&D, goods and manufacturing), **price** (how much is it sold or rented) and **value** (what value is it bringing to customers, particularly, compared with existing classical computing solutions). Right now, the equation is simple: costs are high, prices are high as well when computers are sold (particularly superconducting qubits ones) and value is low at this point, and is positioned in the educational and proof-of-concept realms.

A quantum computer cost and price depend on several parameters including its underlying R&D, bill of materials of off-the-shelf and custom-designed components, manufacturing and integration costs, economies of scale, marketing and sales costs, the cost of maintenance and consumables if any, and finally, the manufacturer's profit. The higher the sales volume, the greater the economies of scale. Volumes are currently very low given most quantum computers are just prototypes that are not yet useful for production-grade applications.

At some point, when and if we reach some quantum advantage threshold, useful applications will emerge. It will first target niche b2b and government markets⁵⁶⁰. Then, when applications and innovation ramp-up, we may have a larger number of corporate users. It will justify scaling manufacturing capacities. R&D fixed costs will then be easier to amortize with volume. Cost of goods may also decrease, particularly if technology progress can help get rid of the complicated wirings and electronics that we have today in some of these devices.

Let's look one by one at the major hardware components of a quantum computer looking at how it will benefit from economies of scale:

- **Control computer(s)**: these are standard rack-mounted servers as well as the associated networking connection. These are the most generic parts of a quantum computer.
- **Chipset**: quantum registers chipsets are the cornerstone of electron-based quantum computers, such as with superconducting and electron spin qubits. Even if they are manufactured in CMOS or similar technologies, their manufacturing volume is very low. Economies of scale are therefore almost non-existent. You don't need such components with cold atoms and trapped ions qubits. It is replaced by specialized optical components to direct the laser beams controlling the qubit atoms. With NV centers, chipsets can be cheap to manufacture if done in volume.

⁵⁶⁰ Some economists think that quantum computers may offer an economic advantage compared to classical computing even without reaching a computing advantage, thanks to asymmetries in cost structures. This still is conjecture based since these economists didn't really analyze the real possibility of pre-quantum-advantage NISQ computers to bring any usefulness. The proposed model is only based on economies of scale and the effects of competition. See [Quantum Economic Advantage](#) by Francesco Bova, Avi Goldfarb and Roger G. Melko, National Bureau of Economic Research, February 2022 (28 pages).

- **Electronic components:** these are used to create, process, transmit and send the quantum gate signals to the qubits. Their technology depends on the type of qubit. These signals are microwaves for superconducting and electron spins qubits, laser-based photons for cold atoms and trapped ions, and some other varieties of electro-magnetic signals otherwise. Standard and expensive laboratory equipment are used for microwave generations such as those from Rohde&Schwarz. More integrated equipment is sold by companies like Zurich Instruments, Qblox, Quantum Machines and Keysight. It's using customized FPGA and rather standard electronic components. When these tools are miniaturized as ASICs running at room temperature or cryo-CMOS running at temperatures below 4K, their small economies of scale make it rather expensive.
- **Cabling:** niobium-titanium superconducting cabling used to feed superconducting and electron spin qubits with microwaves are very expensive, costing about \$3K each. And we need about three such cables for each and every qubit. This drives high-costs for manufacturing superconducting and electron-spin based qubits systems. The main companies providing these cables are Coax&Co and Delft Circuits.
- **Cryogenics:** these are standard systems but marketed in low volumes. They can cost up to \$1M for superconducting and silicon qubits. Their cost is one to two orders of magnitude lower for the cryogenics of components such as photon qubits. Large cryostats use an enclosed cooled system with many cylindrical layers of protection, a GHS (gas handling system), a compressor (such as those coming from CryoMech and Sumitomo) and another compressor used to cool the water feeding the primary compressor.
- **Consumables:** in quantum computers operating at very low temperatures, there is at least some liquid nitrogen and gaseous helium 3 and 4. The latter two are not consumables and operate in a closed circuit in dry dilution systems. It's still expensive.
- **Casing:** this is about steel, glass and design with some specifics linked to vibrations isolation.

As quantum technologies mature, some cost structures will increase and others will decrease. Economies of scale will do the rest. We can therefore forecast that the \$15M D-Wave computer price tag will remain for some time in the top range of quantum computers prices, at least at superconducting qubits. Some computers will be less expensive than \$1M. In practice, many quantum computers will be usable as resources in the cloud and at a more moderate cost. This is what IBM, Rigetti, D-Wave, Microsoft and Amazon (with third-party machines for the latter two) are already offering. Microsoft and Amazon quantum cloud pricing is already quite high. Then, one can wonder about its added value.

Quantum uncertainty

Estimating if and when scalable and useful quantum computers will be available is a difficult art and science. The opinion spread between optimists and pessimists is quite large. Some entrepreneurs expect to achieve miracles in less than one decade while some scientists, on the other hand, think that this will never happen. In between, other scientists are moderately optimists and expect the wait to last at least a couple decades. Let's look at these various opinions.

Optimism

Google said it achieved quantum supremacy in October 2019. It was not a true supremacy since their Sycamore setting was doing no programmable computing solving a specific problem. It was found later that, due to the qubit noise in their system, it was relatively easy to emulate it on a classical server cluster, and discussed [here](#) in this book, starting page 694. So much for any quantum supremacy or advantage! It was the same with the so-called boson sampling experiments quantum advantages coming from China in 2019 and 2020. These were unprogrammable random photon mixers. Later boson sampling experiments in 2021 and 2022, like withy Xanadu, were programmable, but did not show a practical computing advantage.

As published in their 2020 roadmaps, Google, IBM and Amazon expect to achieve true quantum supremacy relatively quickly and create a quantum computer with 100 logical qubits in less than a decade.

Kenneth Regan thought in 2017 that an industry vendor - probably Google - would claim to have reached quantum supremacy in 2018 and that it would quickly be contradicted by the scientific community⁵⁶¹. This happened in 2019 and the contradictions came fast. That was quite a good prediction! For the specialists who can dissect their scientific publications, the view is obviously more nuanced, especially concerning the reliability of the qubits they generate. They communicate a lot about their efforts to reduce the noise of qubits to make them more reliable⁵⁶².

Alain Aspect does not see any strong scientific obstacle preventing the creation of reliable quantum computers. He believes that the uncertainty is mostly a technological and engineering one, but that it will take a few decades to create one reliable advantage-grade quantum computer. However, there is nothing to prevent this process from being accelerated, if it is fueled by good talent and public/private investments. **John Preskill** has the same opinion: it will work, but it will take several decades. **Nicolas Gisin** estimates that the pace to quantum usability is accelerating⁵⁶³. **Jian-Wei Pan** is even more optimistic, forecasting some regular quantum advantage before 2027⁵⁶⁴.

Optimists also include the many hardware quantum computing startups, all with solutions that are expected to work on a large scale within the next five years. They are found in all types of qubits: superconductors (IQM, QCI), electron spins (Quantum Motion, SQC), cold atoms (Pasqal, Atom Computing, ColdQuanta, QuEra), trapped ions (IonQ, Quantinuum, Universal Quantum) and photons (PsiQuantum which predicts one million qubits in less than five to ten years, Orca Computing, Qandela, Xanadu).

At last, you have ultra-optimists like **Michio Kaku**, a Japanese physicist turned into a futurist and best-selling author and who cocreated the string field theory seems affected by a variant of the Nobel disease. His upcoming book “Quantum Supremacy”, to be published in 2023, predicts that quantum computing will soon “*solve some of humanity's biggest problems, like global warming, world hunger, and incurable disease*”. That’s a little overpromising!

Pessimism

Pessimism comes from a few researchers, who are not necessarily specialized in the field in which they express themselves. Above all, they are pessimistic about the ability to fix the noise that affects qubits, whatever their type⁵⁶⁵.

The first and best-known of these pessimists is the Israeli researcher **Gil Kalai** who believes that we will never be able to create quantum computers with a low error rate⁵⁶⁶. According to him, we cannot create stable quantum computers because of the noise that affects the qubits. This is illustrated in the scale below in Figure 257, which sets the lowest reasonably achievable noise level well above the level required to create a scalable quantum computer.

⁵⁶¹ In [Predictions we didn't make](#), January 2018.

⁵⁶² See [The Era of quantum computing is here.Outlook: cloudy](#) by Philipp Ball, in Science, April 2018.

⁵⁶³ See [Quantum computing at the quantum advantage threshold: a down-to-business review](#) by A.K. Fedorov, Nicolas Gisin, Sergei Belousov et al, March 2022 (55 pages).

⁵⁶⁴ See [Jian-Wei Pan Sees Routine Quantum Advantage Within Five Years](#) by Matt Swayne, The Quantum Insider, February 2022.

⁵⁶⁵ See [The different forms of quantum computing skepticism](#) by Boaz Barak, 2017.

⁵⁶⁶ See [Why Quantum Computers Cannot Work](#), 2013 (60 slides) illustrating [How Quantum Computers Fail: Quantum Codes, Correlations in Physical Systems, and Noise Accumulation](#), 2011 (16 pages) and [The Argument Against Quantum Computers](#) by Katia Moskwitch, February 2017. Gil Kalai declares: "My expectation is that the ultimate triumph of quantum information theory will be in explaining why quantum computers cannot be built".

He is working on the creation of some mathematical model that would prove the impossibility of overriding these errors, even with quantum error correction codes. In 2022, he published another paper to prove his point, with a philosophical approach related to the notion of free will⁵⁶⁷.

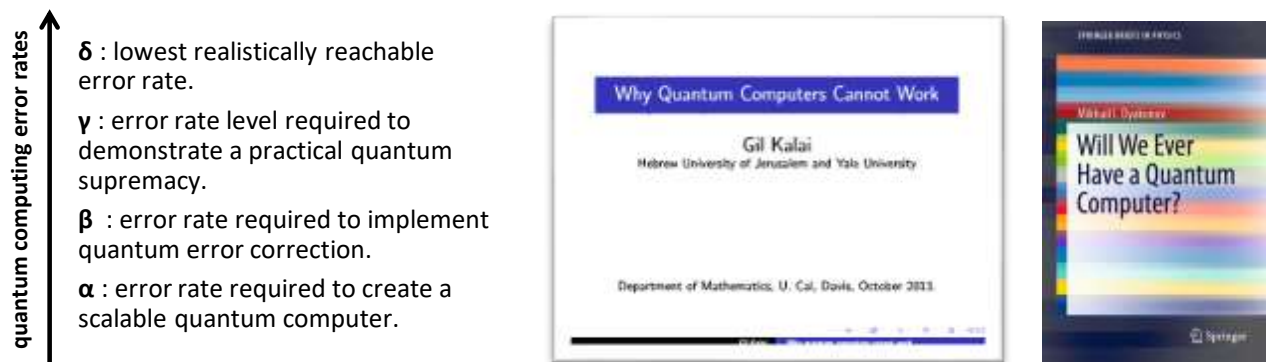


Figure 257: Gil Kalai's quantum computing errors complexity scale.

Another skeptic of quantum computing is the **Mikhail Dyakonov** (born in 1940 in the USSR) who works in the Charles Coulomb Laboratory (L2C) of the CNRS and the University of Montpellier in France. He detailed his views in an article at the end of 2018, which he later turned into a book⁵⁶⁸. His argument is more intuitive but less documented than the work of Gil Kalai⁵⁶⁹.

We also have **Serge Haroche** for whom universal quantum computing is an unreachable dream, also because of that damned noise. On the other hand, he thinks that the path of quantum simulation, especially based on cold atoms, is reasonable and realistic.

Xavier Waintal (CEA-IRIG in Grenoble, France) also has serious reservations about the possibility of creating large-scale quantum computers. Here again, the culprit is noise. His reasoning is based on physical explanations different from those of Gil Kalai. Qubit operations are relying on very complex n-body quantum problems and error correction codes generally deal with only two types of errors (flip, phase) but not with all sources of error. He recommends exploiting the mean-fields theory which allows to model the complex interactions between qubits and their environment⁵⁷⁰. These are very fundamental questions to address. I'd say his arguments are both the most documented I've seen but which, well used, may fuel interesting research to find solutions.

Cristian Calude and **Alastair Abbott** point out that the advantage of the main quantum algorithms usable in practice would generate a modest quadratic acceleration (square root of classical computing time) that could be achieved on classical computers with heuristic approaches⁵⁷¹.

Quantum skepticism is also evident in **Ed Sperling's** November 2017 review of the field, which included a reminder of all the obstacles to be overcome⁵⁷².

⁵⁶⁷ See [Quantum Computers, Predictability, and Free Will](#) by Gil Kalai, April 2022 (33 pages).

⁵⁶⁸ See [The Case Against Quantum Computing](#), 2018. He even made a short book about it, [Will We Ever Have a Quantum Computer?](#), 2020 (54 pages, free download). As well as a debate on the subject launched by Scott Aaronson in [Happy New Year! My response to M. I. Dyakonov](#). See also [Skepticism of Computing](#) by Scott Aaronson who dissects 11 objections on quantum computing capabilities. See also [Noise stability, noise sensitivity and the quantum computer puzzle](#) by Gil Kalai, 2018 (1h04mn).

⁵⁶⁹ See a response to this argument in [The Case Against 'The Case Against Quantum Computing'](#) by Ben Crige, January 2019 and a highly documented response from Scott Aaronson in [Happy New Year! My response to M. I. Dyakonov](#), 2013.

⁵⁷⁰ See [What determines the ultimate precision of a quantum computer?](#) by Xavier Waintal, 2017 (6 pages) that we have already mentioned. Xavier Waintal has notably developed classical algorithms for the simulation of N-body problems. They are used by various teams of researchers in condensed matter physics, notably those working on topological matter and Majorana fermions. They run on laptops and supercomputers.

⁵⁷¹ In [The development of a scientific field](#) by Alastair Abbott and Cristian Calude, June 2016.

⁵⁷² In [Quantum Madness](#) by Ed Sterling, November 2017.

Leonid Levin (a Russian scientist who defined the NP complete complexity class in 1973) and **Oded Goldreich** (an Israeli professor in computer science from the Weizmann Institute) are other quantum computing skeptics mentioned by Scott Aaronson in [Lecture 14: Skepticism of Quantum Computing](#).

Another argument against scalable quantum computing deals with the computational state vector amplitudes values becoming tiny as the number of qubits grows. After just applying a set of H gates on N qubits, this amplitude becomes $1/2^N$ for each computational basis state in the qubits register. It becomes quite small as N grows beyond 50. Are these values corresponding to some physical observable that would have a value way below the physical error rate in the system? Or even below some physical Planck constant? Well, this is good food for thought. At least, the computational state vector always has a norm of 1. And the physical observables in the system remain based on the individual qubits basis states $|0\rangle$ and $|1\rangle$.

“For me, the most important application of a quantum computer is disproving the people who said it’s impossible. The rest is just icing on the cake.”
 Scott Aaronson
 2019.

Managing uncertainty

One key challenge is to make a distinction between scientific unfeasibility, scientific uncertainty and technological uncertainty. This set of uncertainties raises existential questions about how to manage such a long innovation cycle. When should we invest? When are market positions being settled? Is fundamental research decoupled from industrialization? Is quantum computing a simple engineering matter? Or, on the other hand, will it be impossible to control very large swaths of maximally entangled physical qubits?

Note that the pessimists quoted above are not Americans and most of the optimists are. Is there a cultural bias here? These variations in innovation and economic cultures have an impact on industry approaches. Major IT companies such as IBM, Google, Intel, Amazon and Microsoft can fund quantum computing R&D investments with a very long-term vision. They have the profitability, the cash and the ability to attract skills to do so. You may still note that, at this point in time, these large IT vendors have not yet engaged in a startup acquisition spree like they did in the fields of artificial intelligence and other emerging technologies.

Rose law (2003)
“quantum Moore’s law”

not yet applicable to qubits numbers
 not follow-up since 2016

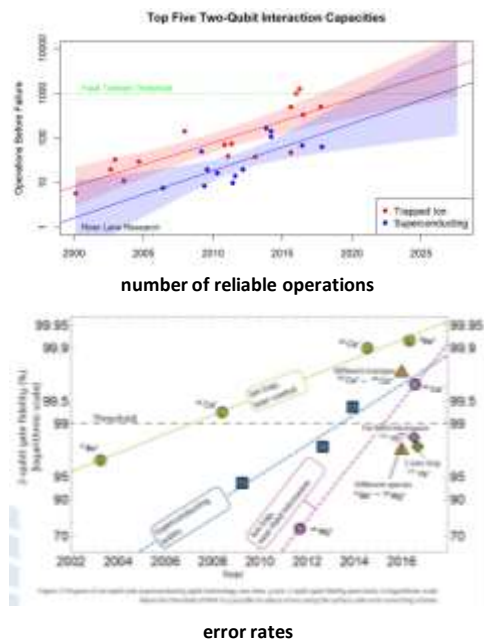
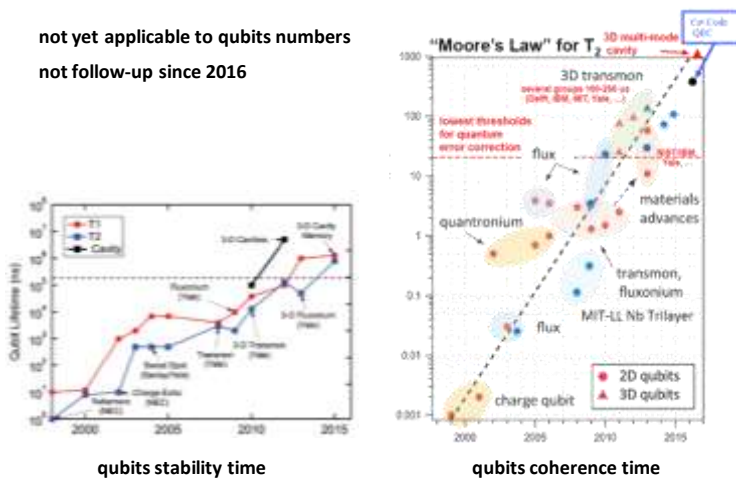


Figure 258: a compilation of the putative equivalents of Moore’s law in quantum computing. They all need updates! Otherwise, you can’t prove there’s a real ongoing acceleration of progress in quantum computing science and technology.

Well-funded startups such as D-Wave, Rigetti, IonQ, PsiQuantum, OQC and IQM can also adopt a fairly long-term view, even if it still depends on their ability to commercialize quantum computer prototypes and to attract long-term oriented investors. The corresponding amounts are not necessarily crazy.

The engineering problems to be solved deal with qubits materials and manufacturing techniques, quantum error correction, control electronics, large-scale cryogenics and of course algorithmic and software advances. The required approach is multidisciplinary with mathematics, fundamental quantum physics, thermodynamics and chemistry, and finally, code, including machine learning which is notably used for qubits calibration.

We can try to extrapolate the evolutions of the last ten years in quantum computing. When he was the co-founder of D-Wave, Geordie Rose enacted in 2003 his own equivalent of Moore's empirical law, [Rose's Law](#), predicting a doubling every year of the number of qubits in a quantum computer, as show in Figure 258. Since 2007, D-Wave delivered well on this promise but the progress has been sluggish for gate-based quantum computers.

Most of these charts have not been updated and some even include numbers corresponding to nonoperational systems like Google's 2018 72-qubit Bristlecone or IonQ's 129 qubits which never saw the day of light. You then understand why you must be cautious when interpreting these "exponential charts" with looking at a similar chart created in 2015 that positioned NMR qubits as best-in-class for their scalability potential⁵⁷³. In reality, NMR qubits didn't really scale well.

Some exponential law can however be observed in the evolution of other operating parameters of quantum computers such as the stability time of qubits, their error rate and the number of consecutive operations performed reliably⁵⁷⁴. Recently, **Rob Schoelkopf** from Yale University created his own law showcasing the progress with superconducting qubits coherence times and gates fidelities and times.

I tried to understand why the predictions of creating viable quantum computers were always quite long-term, between 5 and 50 years. One of the answers comes from the length of cycles in the associated research and manufacturing processes.

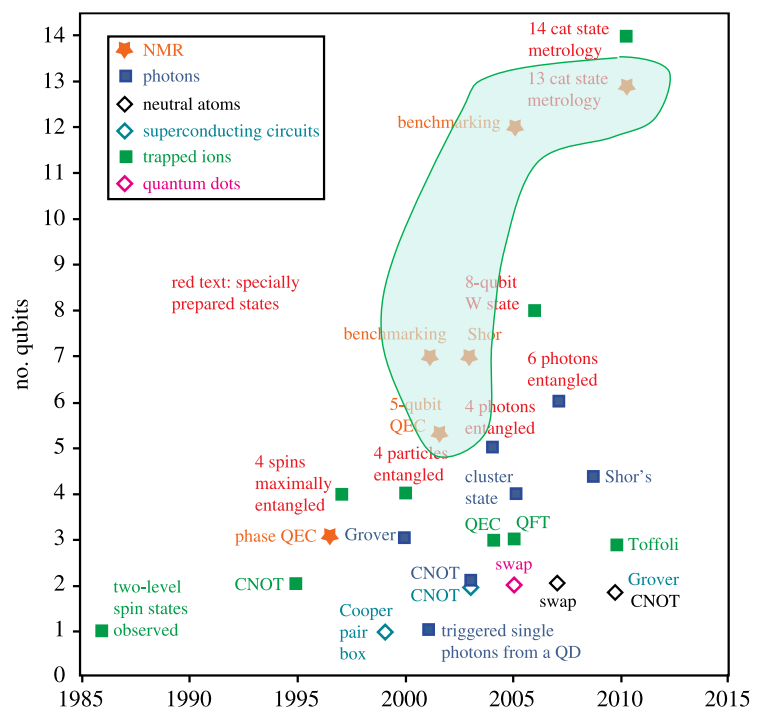


Figure 259: a chart with number of qubits per technology and year, as of 2015. It gave the impression, back then, that NMR qubits were the most scalable. They are not! Source: [Recent advances in nuclear magnetic resonance quantum information processing](#) by Ben Criger, Gina Passante, Daniel Park and Raymond Laflamme, The Royal Society Publishing, 2015 (16 pages).

⁵⁷³ See [Recent advances in nuclear magnetic resonance quantum information processing](#) by Ben Criger, Gina Passante, Daniel Park and Raymond Laflamme, The Royal Society Publishing, 2015 (16 pages).

⁵⁷⁴ Some of the diagrams below come from the [Technical Roadmap for Fault-Tolerant Quantum Computing](#), a UK report published in October 2016 and from [this other source](#).

For example, creating a prototype silicon-based qubit chipset takes up to nine months of manufacturing with up to 160 manufacturing steps. After this manufacturing process, component characterization and packaging stage add more time.

Components characterization qualitatively tests and selects the manufactured components. This can last up to a month and in the best case down to a week. Then, to carry out the tests, the thermalization of the computer takes about 24 hours and the change of the chipset to be tested takes at least 3 to 7 hours as we'll discovered in the section on cryogenics, page 473.

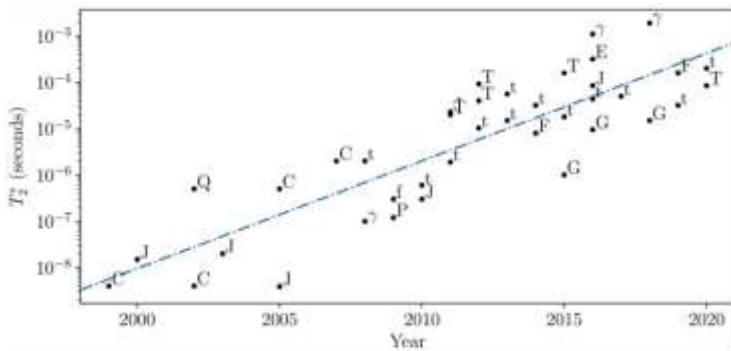


Figure 6.9 Qubit coherence times T_2 (or T_2 measured after spin echo) across the years. Letters signify: charge qubit (C), flux qubit (J), fluxonium (f for 2D, F for 3D), phase qubit (P), transmon (t for 2D, T for 3D), photon encoded qubit (γ), error corrected bosonic qubit (E), gatemon (G).

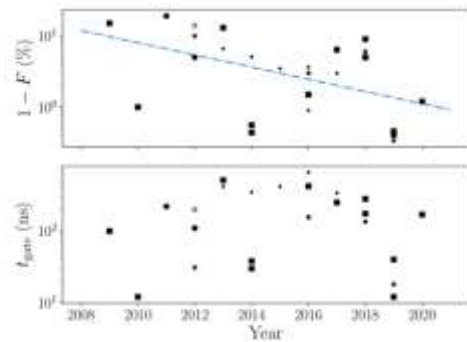


Figure 8.5 (a) Two-qubit gate fidelities and (b) two-qubit gate speeds, for transmon qubits. The type of marker denotes the type of gate: CZ (square), CNOT (circle), cross-resonance (dot), ISWAP (star).

Figure 260: Rob Schoelkopf charts on progress with superconducting qubits coherence times and gates fidelities and times, [Twitter source](#) (didn't find a better one), August 2020.

The design to manufacturing whole cycle lasts about 2,5 years. Finally, the *test & learn* cycles are often very long, much longer than with software! This long cycle may be shorter with other solid-state qubits like superconducting qubits, and also with photon qubits for which semiconducting photonic circuits are also required.

Challenges ahead

Whether you are an optimist or a pessimist with regards to the advent of scalable quantum computers, you need to adopt an educated view of the challenges ahead. Over time, as my understanding of these challenges was growing, I tended to shift from “optimism” to “neutralism” or, at least, to being a “documented optimist”. Some of the challenges ahead are indeed enormous.

Xavier Waintal uses the scale shown in Figure 261, with 5 difficulty levels, to build a quantum computing machine. It positions where we are right now and the challenges ahead. It goes beyond large scale computing given some quantum memory would be mandatory for some key algorithms like QML and HHL.

| difficulty scale | technology | use cases | examples |
|------------------|--|--|---------------------------|
| 1 | quantum simulator (analog-no gates) | quantum simulations | D-Wave, Pasqal |
| 2 | gates-based analog systems, low fidelity | system validation NISQ algorithms | Google, IBM, Rigetti, ... |
| 3 | gates-based analog systems, low fidelity | variational calculations in quantum chemistry | Possibly PsiQuantum |
| 4 | ideal quasi-deterministic gates-based systems (FTQC/LSQ) | factoring large numbers, exact quantum chemistry | TBD |
| 5 | 4 + quantum memory | quantum machine learning, linear algebra (HHL) | TBD |

Figure 261: Source: Xavier Waintal.

My chart in Figure 262 goes into some details with laying out some of these challenges, most of which being covered extensively in various parts of this document.

Two things come to mind: one is that quantum computers scalability is the most challenging issue to tackle with. If quantum computing capacity is known to theoretically scale exponentially with the number of qubits, you may wonder whether the scale challenge itself is also an exponential one.

One way to grasp it is to look at IBM and Google's progress with their superconducting qubits. It's been sluggish since 2019 with 72/127 qubits, given that most benchmarks show that only fewer than 20 qubits are practically usable⁵⁷⁵. There's still some hope with bosonic codes and cat-qubits which could limit the logical/physical scaling overhead. Also, scale-out options with qubits interconnect options using microwaves or photons are interesting but have their own scalability challenges. Other qubit types like electron spins and photons also look promising.

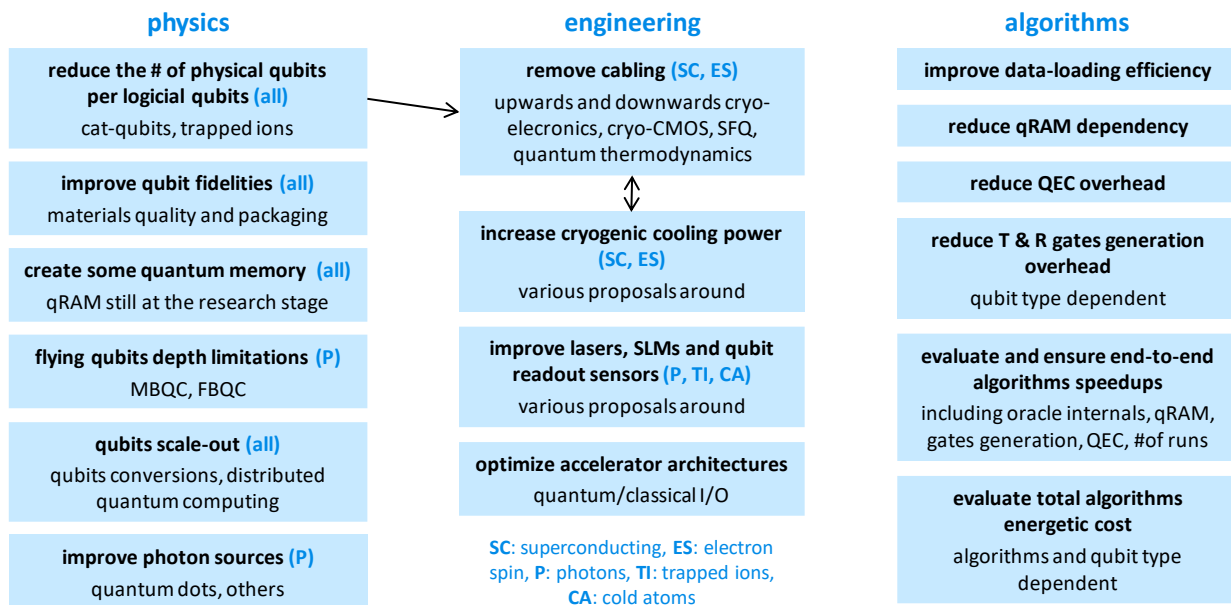


Figure 262: a map of the various challenges to make quantum computing a practical reality. (cc) Olivier Ezratty, 2021.

The second challenge deals with real algorithms speedups. Not all algorithms showcase an exponential theoretical speedup. Grover's algorithm speedup is only polynomial. All non-exponential speedups may end-up being useless due to their implementation cost. The trick of the trade is that all speedups are theoretical but not yet practical. Another way to look at this is to envision, even with moderate algorithms speedups, an energetic advantage for quantum computing, as discussed in the related part that we just saw, starting on page 249.

These speedups are never documented with taking into account all the quantum computing food chain: data preparation, oracle operations, quantum memory access when it is required, quantum error correction, non-Clifford group quantum gates generation (particularly for all algorithms using a quantum Fourier transform, and there are many) and the number of shots/runs required (with or without quantum error corrections).

I wish somebody did produce such evaluations with actual and projected data on these different aspects of gate-based quantum computing, even if it brings bad news! When bad news travel fast, fixes arrive faster, if there are any! And this is valid for the dominant wave of NISQ hybrid algorithms.

One broader challenge for the industry is to spur developer creativity for the design of even more algorithms and ways to assemble many quantum algorithms to create innovative solutions.

In the end, it looks like quantum simulators may be one very viable short-term option but we also still lack data to prove it. Some algorithms are being evaluated to run on these quantum simulators, like the ones from Pasqal and ColdQuanta but they have only been tested so far on classical computers emulators. The quantum software ecosystem will have to look at this!

⁵⁷⁵ See one example here from Google with experiments on Sycamore stopping at 20 qubits: [Efficient and Noise Resilient Measurements for Quantum Chemistry on Near-Term Quantum Computers](#) by William J. Huggins et al, Google AI, June 2020 (17 pages).

Quantum annealing and photonic coherent Ising machines could also bring their share of hope. The debate is still out to assess what is the quantum advantage of D-Wave with its latest annealer generation, relying on their 5000 qubits Pegasus chipset.

I still count on two things to reach quantum computing scalability and practicality. One is the great diversity of paths chosen by scientists and entrepreneurs. I have never seen so many variations in hardware technologies than in the quantum space. This creates a sort of fault-tolerance for innovation. The second, more generally, is I still believe and bet on scientists and engineers' creativity to solve these highly complicated problems. It is still a very generic commonplace reasoning that has not much value per se.

Quantum computing engineering key takeaways

- A quantum computer is based on physical qubits of different nature, the main ones being superconducting qubits, electron spin qubits, NV centers, cold atoms, trapped ions and photons. They all have pros and cons and no one is perfect at this stage. Future systems may combine several of these technologies.
- Many key parameters are required to create a functional quantum computer. It must rely on two-states quantum objects (qubits). These must be initializable and manipulable with a set of universal gates enabling the implementation of any linear transformation of qubit states. Qubits must be measurable at the end of algorithms. Their coherence time must allow the execution of a sufficient number of quantum gates. Decoherence and errors must be as low as possible.
- Most quantum computers are composed of several parts: the qubit circuit (for solid-state qubits), vacuum enclosures (particularly with cold atoms and trapped ions) or waveguides (photons), usually housed in a cryogenic vacuum chamber (with the exceptions of photons and NV centers), some electronics sending laser rays or coaxial cables guided microwaves or direct currents onto qubits and a classical computer driving these electronic components.
- Since qubits are noisy, scientists have devised quantum error correcting schemes. These rely on creating logical "corrected" qubits composed of a lot of physical qubits, up to 10,000. This creates huge scalability challenges, many of them with classical enabling technologies like cabling, electronics and cryogeny. The science of quantum error correction, quantum error mitigation (a new section in this edition) and fault-tolerant quantum computing is a realm in itself.
- Many quantum algorithms also require some form of quantum memory, either for data preparation and loading (such as with quantum machine learning) or to access efficiently classical data (such as with oracle based algorithms like a Grover search). These quantum memories don't exist yet.
- The energetic cost of quantum computing is both a potential benefit but also an immense challenge, particularly when a large number of physical qubits are required to create large scale fault-tolerant computers. All components must be carefully designed to take into account the cryogenic cooling power as well as the available space to house cabling and cryo-electronics. This explains the creation of the Quantum Energy Initiative by Alexia Auffèves, Olivier Ezratty and Robert Whitney, which creates a community of researchers and industry vendors and organizations working collectively on this topic.
- The economics of quantum computers are still uncertain due to their immaturity and the current low manufacturing volume. Uncertainty is also strong with regards to the feasibility of scalable quantum computers. The scalability challenges ahead are enormous. One of them is to benefit from actual algorithm speedups when including all end-to-end computing operations.

Quantum computing hardware

In a bottom-up approach, we've covered successively the basics of quantum physics, the mathematical aspects of gate-based quantum computing, then quantum computing engineering and enabling technologies. Let's now move to the last stack, quantum computers, with focusing on their specifics depending on the types of physical qubits they are using. We are dealing here with all sorts of players: public research laboratories, large established companies as well as startups.

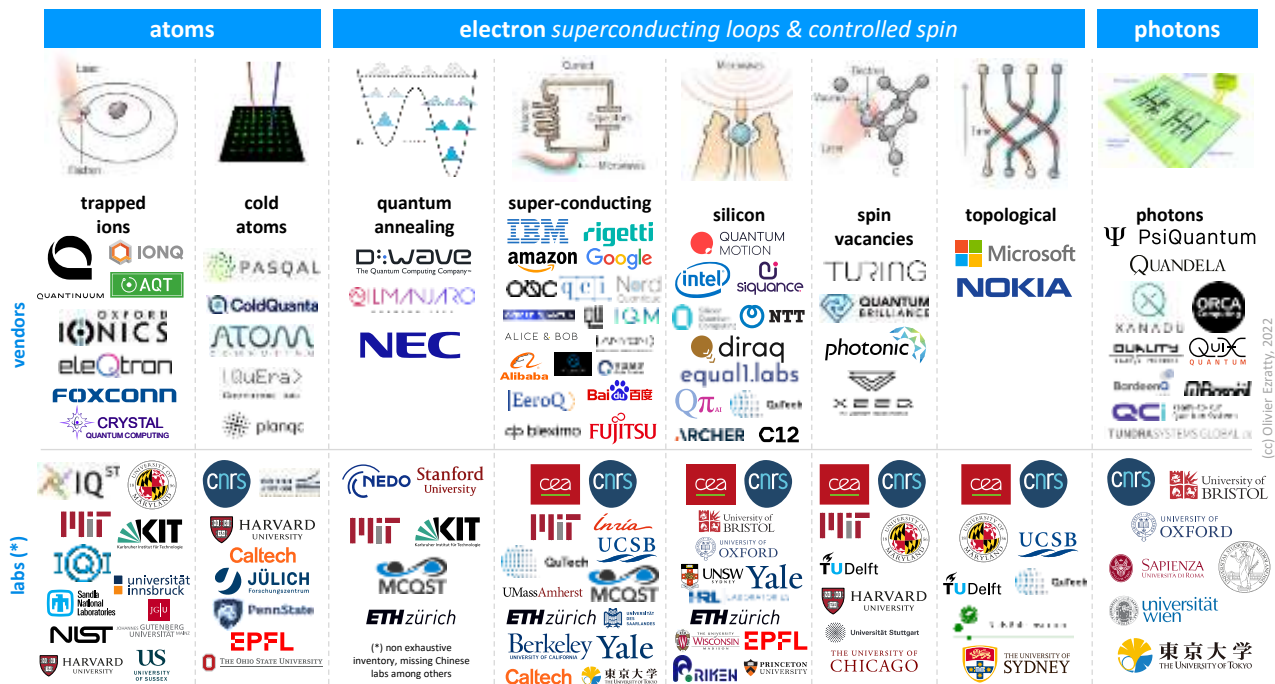


Figure 263: a map of key research lab and industry vendors in quantum computing hardware per qubit type. (cc) Olivier Ezratty, 2022. Qubits drawing source: [Scientists are close to building a quantum computer that can beat a conventional one](#) by Gabriel Popkin in Science Mag, December 2016. I consolidated the logos lists since 2018. It's incomplete for the research labs at the bottom but rather exhaustive for the vendors at the top.

There number startups in this inventory keeps growing, in Figure 263. They do not shy away from Google and IBM. There are not many Chinese startups yet. For the moment, the country's investments in quantum computing are concentrated in well-funded public research like with Jian Wei-Pan's giant lab in Hefei and with large cloud companies like Baidu, Alibaba and Alibaba. Notice that Chinese labs are missing in the chart. There are eight main categories of quantum computers grouped into three categories:

Atoms:

- **Trapped ions** found in particular at IonQ, a spin-off from the University of Maryland, as well as at Honeywell and the Austrian startup Alpine Quantum Technologies.
- **Cold atoms** like rubidium, cesium and strontium are used by Pasqal, QuEra, ColdQuanta and Atom Computing to create both analog quantum computers and gate-based quantum computers.
- **Nuclear Magnetic Resonance**, which is nearly abandoned as a path for quantum computing, NISQ or beyond despite one China company selling a desktop version for educational use cases.

Electrons:

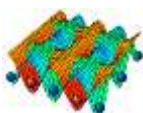


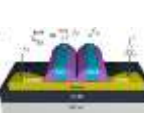
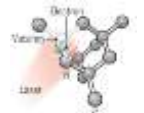

- **NV centers** with only a few industrial players like Quantum Brilliance. Most NV centers applications are in quantum sensing.

- **Superconducting** effect qubits are used in IBM's, Google, Rigetti, OQC and IQM quantum computers as well as in D-Wave quantum annealers. This is a broad category with Josephson qubits (transmon, fluxonium, coaxmon, unimon, ...) and photon cavities-based qubits using superconducting control qubits (cat-qubits, GKP) with Alice&Bob, Amazon, Nord Quantique and QCI.
- **Quantum dots spins qubits** pushed notably by Intel, Quantum Motion, SQC, C12, Archer and the consortium between CEA-Leti CNRS Institut Néel and CEA-IRIG in France. There are many variations there as well.
- **Topological qubits** with the hypothetical Majorana fermions from Microsoft whose existence is yet to be proven. Other topological qubits avenues are investigated in research laboratories at the fundamental research level.

Flying qubits:

- **Photon qubits**, with a lot of variations like with the use of [MBQC](#) architectures to circumvents the difficulty to handle two-qubit gates and the limited computing depth of flying qubits, boson sampling and coherent Ising machines. The current main photon qubit vendors are PsiQuantum, Xanadu, Orca Computing and Quandela.
- **Flying electrons**, a separate track of qubits, with no commercial vendor yet involved in it. It's a fundamental research field.

Solid-states qubits usually refer to the electron qubits category with superconducting and electron spin qubits. However, trapped ions and photon qubit also rely on semiconductor circuits for their operations. But the “ions” are flying above their control circuits and the photons are circulating in nanophotonic circuits.

| | atoms | | electrons superconducting & spins | | | photons |
|----------------------------------|---|---|---|--|---|---|
| |  |  |  |  |  |  |
| | cold atoms | trapped ions | superconducting | silicon | NV centers | photons |
| qubit size | about 1 μm space between atoms | about 1 μm space between atoms | (100μ) ² | (100nm) ² | <(100nm) ² | nanophotonics waveguides lengths, MZI, PBS, etc |
| best two qubits gates fidelities | 99.4% | 99.9% | 99.97% (IBM Falcon R10) | >99% (SiGe) | 99.2% | 98% |
| best readout fidelity | 99.1% | 99.9% | 99.4% | 99% (SiGe) | 98% | 50% |
| best gate time | 1 ns | 100 μs | 20 ns - 300 ns | ≈5 μs | 10-700 ns | <1 ns |
| best T ₁ | > 1 s | 0,2s-10mn | 100-400μs | 20-120μs | 2.4 ms | ∞ & time of flight |
| qubits temperature | < 1mK 4K for vacuum pump | <1mK 4K cryostat | 15mK dilution cryostat | 100mK-1K dilution cryostat | 4K to RT | RT 4K-10K cryostats for photons gen. & det. |
| operational qubits | 324 (Pasqal) | 32 (IonQ) 20 (AQT) | 127 (IBM) 56-66 (China) | 15 (Delft) in SiGe | 5 (Quantum Brilliance)-10 | 216 modes GBS (Xanadu) |
| scalability | up to 10,000 | <50 | 1000s | millions | 100s | 100s-1M |

(cc) Olivier Ezratty, 2022. RT = room temperature.

Figure 264: figures of merit per qubit type. Best gate time covers only the electronics drive part but not the whole classical drive computing time. Best T₁ is the best qubit relaxation time. (cc) Olivier Ezratty, 2022. Data sources: cold atoms (ColdQuanta summer 2022, [In situ equalization of single-atom loading in large-scale optical tweezer arrays](#) by Kai-Niklas Schymik, Florence Nogrette, Antoine Browaeys, Thierry Lahaye et al, PRA, August 2022 and [Ultrafast energy exchange between two single Rydberg atoms on a nanosecond timescale](#) by Y. Chew et al, Nature Photonics, 2022 (7 pages)), trapped ions ([Trapped Ion Quantum Computing: Progress and Challenges](#), 2019, [Materials Challenges for Trapped Ion Quantum Computers](#), 2020, [Infineon, IonQ and Quantinuum](#)), silicon ([Roadmap on quantum nanotechnologies](#), 2020), superconducting (IBM papers), NV centers ([Quantum computer based on color centers in diamond](#), 2021). I list only the most demanding two qubit gates and readouts fidelities. Cold atoms systems are usually simulators, but data pertains to gate-based implementations.

Many of the commercial companies in this panorama are associated with American or European research laboratories. Google collaborates with the University of Santa Barbara in California, IBM and Microsoft with the University of Delft in the Netherlands, and IBM with the University of Zurich, among other publicly funded research organizations.

These categories of technologies have different levels of maturity. Superconducting qubits are the most proven to date. Trapped ions are best-in-class with regards to fidelity and connectivity but do not scale well. Neutral atoms are starting to scale better. Linear optics and NV centers have also some difficulties to scale. Electron spin-based systems could scale but are less mature. Finally, Majorana fermions are still in limbo. But other qubit types are looming around and may become promising (other topological materials, Silicon Carbide, etc.). Creating assessment on the maturity of these technology pertains more to weather forecast than climate change predictions. Meaning, while you can forge some ideas on the relative maturity of these technologies with a short term view, it's much harder to make sound predictions in the longer term. For example, scaling these various technologies face very different challenges. As such, the table in Figure 264 is a sketchy and probably highly questionable comparison between these different qubits, particularly with cold atoms which are so far, used in quantum simulation mode and not gate-based architectures.

Another way of comparing qubit classes is to look at where the industry bucks are going. I created the chart below in Figure 265 with doing some guesswork on how much was invested by the large IT companies (IBM, Google, Microsoft, Amazon, Intel). But again, investors are not necessary in position to guess which technology will really scale.

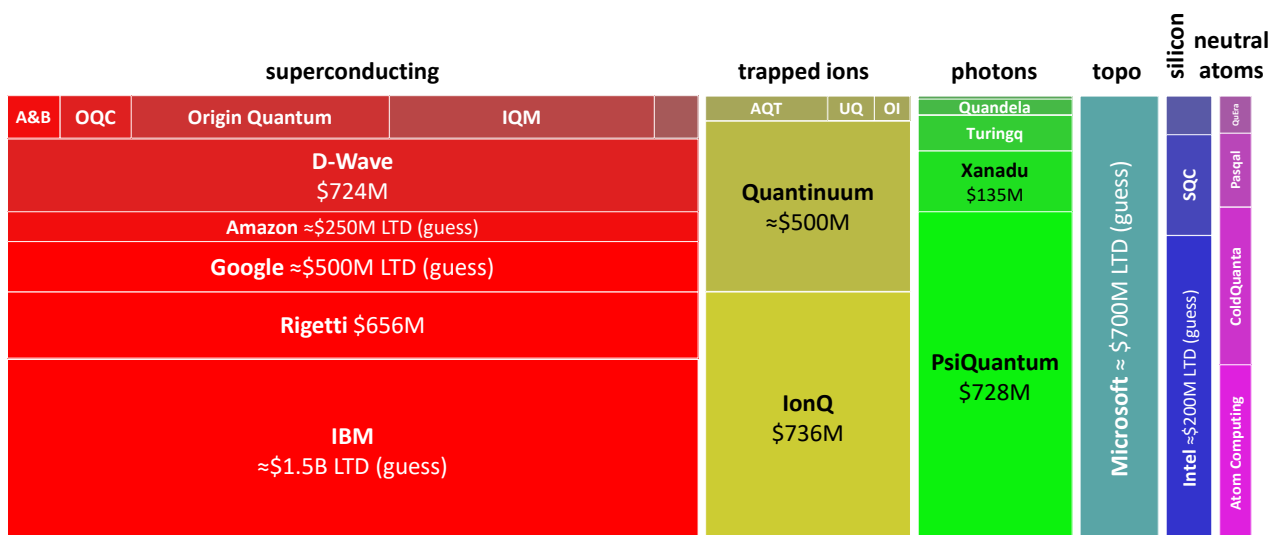


Figure 265: fuzzy logic assessment of industry investments per qubit type mixing capital investment for startups and internal investments for legacy companies. LTD=life to date. UQ = Universal Quantum. OI = Oxford Ionics. cc Olivier Ezratty, 2022.

These numbers are approximate and if you have some information to correct or update it, I'll take it! For startups, it's easier and consolidate the amount publicly raised either in venture capital or through a SPAC (for D-Wave, IonQ and Rigetti). What do you learn from this chart? That superconducting qubits are kings, followed by trapped ions and photon qubits. Therefore, silicon and cold atoms qubits seem under invested. Both because it seems Intel has not yet invested much in silicon qubits that have a rather low TRL and since not large company invested in cold atoms. I would seriously advise not to determine future winners based on these amounts.

There is so much scientific and technology uncertainty! Some solutions even not in this chart could show up in the future, either in the topological qubits space, beyond Microsoft's sole endeavor, or with SiC and other variations of spin cavities (beyond NV centers which don't show up in the chart due to the very small amount raised by the couple startups from this field).

Another summary view, below, shows how various qubit types have use cases beyond quantum computing and even, within the three paradigm of quantum computing with all qubit types being usable for quantum simulations although it seems it is only available with neutral atom qubits with commercial vendors. Photons, cavity spins and cold atoms have the broadest use cases given they have many applications in quantum sensing. Silicon qubits seem to have a narrower usage scope but don't discount them too soon. They may showcase one of the best scalability potential for quantum computing.





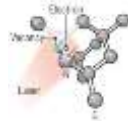

| | atoms | | superconducting & controlled spin | | | photons |
|------------------------|---|---|---|--|---|---|
| |  |  |  |  |  |  |
| quantum objects | trapped ions | cold atoms | superconducting | quantum dots spins | cavity spins (NV, SiC) | photons |
| gate-based computing | Green | Orange | Green | Green | Orange | Green |
| quantum simulation | Green | Green | Green | Green | Green | Green |
| quantum annealing | | | Green | | | |
| quantum memory | Orange | Green | | | in repeaters | with cold atoms |
| quantum telecoms & QKD | | | | | in repeaters | Green |
| quantum sensing | | Green | SQUIDs | | | Green |

Figure 266: qubit types and their use cases in all quantum computing paradigms and on telecommunications and sensing. Orange means: less commonplace and/or harder to implement. (cc) Olivier Ezratty, 2022.

At last, here is a summary of the scalability challenges faced by the main qubit types around (I left aside topological and NV centers qubits). All these topics are detailed in this part⁵⁷⁶.

| | superconducting | neutral atoms | trapped ions | silicon spins | photons |
|-------------------|---|---|---|---|---|
| challenges | <ul style="list-style-type: none"> noise and crosstalk \nearrow with # of qubits. electronics energetic cost. cabling. scaling cryostats. | <ul style="list-style-type: none"> atom controls beyond 10,000 qubits. harder to implement gate-based QC. SLM resolution. | <ul style="list-style-type: none"> entanglement beyond 30 qubits. overall scaling beyond 40 qubits. | <ul style="list-style-type: none"> controlled electrostatic potential. error correction. qubits entanglement. | <ul style="list-style-type: none"> photon sources power. photon statistics. creating large cluster states of entangled photons. |
| solutions | <ul style="list-style-type: none"> materials improvement. 3D chipset stacking. cryo-CMOS or SFQ. microwave signals multiplexing. scale-out with photons. more powerful cryostats. | <ul style="list-style-type: none"> scale-out with atoms/photon conversion. higher resolutions SLMs. various atoms controls (microwaves, lasers). | <ul style="list-style-type: none"> ions shuttling. switched to baryum (IonQ). Rydberg states ions (Crystal Quantum Computing). QPU photonic interconnect. | <ul style="list-style-type: none"> material and interfaces improvement. integrated cryoelectronics. more powerful cryostats. | <ul style="list-style-type: none"> MBQC. bright and deterministic photon sources (Quandela). deterministic sources of cluster states. integrated nanophotonics. |
| caveats | <ul style="list-style-type: none"> photonic interconnect overhead and statistics. energetic cost of microwave multiplexing. | <ul style="list-style-type: none"> precision of gate control. potential applicability limited to mid-scale simulations. | <ul style="list-style-type: none"> photonic interconnect viability. photonic interconnect statistics and impact on speedups. | <ul style="list-style-type: none"> long learning & chipset prod. cycles. scalability potential is capital intensive. fidelities still improving. | <ul style="list-style-type: none"> photon statistics. small cluster states so far. |

Figure 267: the various pathways to scalability in quantum computing per qubit type. (cc) Olivier Ezratty, 2022.

⁵⁷⁶ See [2022 Roadmap for Materials for Quantum Technologies](#) by Christoph Becher et al, February 2022 (38 pages) which provides an overview of many qubit types and their various challenges.

Quantum annealing

Quantum annealing is a particular quantum computing paradigm and technology that is also based on quantum physics and qubits but works entirely differently compared to gate-based quantum computing as we'll detail here. It has characteristics and performance levels that are intermediate between traditional supercomputers and general-purpose (fault-tolerant) gate-based quantum computers. D-Wave is the main commercial player in this category. Some research laboratories are also involved in quantum annealing but not as many as those involved in the different types of gate-based quantum computers.

In the 2000s, the interest in Shor's factoring algorithm created more traction for gates-based quantum computing, at the expense of quantum annealing. Ironically, the largest integer factoring (of 6 digits: 376,289) by a quantum processor was achieved in 2018 on a D-Wave quantum annealer and not with Shor's algorithm on a gate-based system and it is still the record to date⁵⁷⁷.

History

The quantum annealing paradigm (QA) is an optimization process for finding the global minimum of a given objective function by a process using quantum fluctuations and the tunnel effect⁵⁷⁸. It is mostly used for solving problems like combinatorial optimization problems where the search space is discrete, with many local minima. It is still usable for chemical simulations and non-discrete problems.

The idea to implement quantum annealing using quantum tunnelling effect came first in 1988 and 1989 in Italy and Germany⁵⁷⁹. It was then perfected in Japan by **Tadashi Kadowaki** and **Hidetoshi Nishimori** in 1998 with the *“introduction of quantum fluctuations into the simulated annealing process of optimization problems, aiming at faster convergence to the optimal state. Quantum fluctuations cause transitions between states and thus play the same role as thermal fluctuations in the conventional approach. The idea is tested by the transverse Ising model, in which the transverse field is a function of time similar to the temperature in the conventional method. The goal is to find the ground state of the diagonal part of the Hamiltonian with high accuracy as quickly as possible”*⁵⁸⁰.

As described in Wikipedia: *“Quantum annealing starts from a quantum-mechanical superposition of all possible states (candidate states) with equal weights. Then, the system evolves following the time-dependent Schrödinger equation [...]. The amplitudes of all candidate states keep changing, realizing a quantum parallelism, according to the time-dependent strength of the transverse field, which causes quantum tunneling between states. If the rate of change of the transverse field is slow enough, the system stays close to the ground state of the instantaneous Hamiltonian. The transverse field is finally switched off, and the system is expected to have reached the ground state of the classical Ising model that corresponds to the solution to the original optimization problem”*. In here, what is a “transverse field”? It is a transverse magnetic field that is applied in an homogenous way on qubits and then slowly decreased to control the evolution of the Ising model⁵⁸¹.

A year after Tadashi Kadowaki and Hidetoshi Nishimori's paper, **D-Wave** was created in Canada and it produced its first commercial annealer 13 years later, in 2012. But Japan did not surrender to the idea to create annealing industry solutions.

⁵⁷⁷ See [Quantum Annealing for Prime Factorization](#) by Shuxian Jiang et al, 2018 (9 pages).

⁵⁷⁸ Source: https://en.wikipedia.org/wiki/Quantum_annealing

⁵⁷⁹ See [A numerical implementation of quantum annealing](#) by S. Albeverio et al, University of Milan, July 1988 (10 pages) which refers to [Quantum stochastic optimization](#) by Bruno Apolloni et al, 1989 (12 pages).

⁵⁸⁰ See [Quantum annealing in the transverse Ising model](#) by Tadashi Kadowaki and Hidetoshi Nishimori, 1998 (9 pages).

⁵⁸¹ An Ising model is a statistical physics model created to solve problems of simulation of ferromagnetic and para-magnetic materials associating particles having two state levels (a magnetic moment +1 or -1) which are linked together.

It took the form of a digital annealer created by **Fujitsu** and plans by **NEC** to create a quantum annealer. Also, many Japanese software startups are dedicated to quantum annealing.

At some point, John Martinis was working on creating a quantum annealer at **UCSB** but the idea was abandoned in favor of gate-based superconducting qubits when he started working at Google in 2004⁵⁸². In Europe, **Qilimanjaro** (Spain) is in the process of creating a quantum annealer that would have greater capacities than the ones from D-Wave.

In 2000, **Edward Farhi** et al from the MIT created an algorithm to solve a SAT problem using adiabatic evolution which is considered an algorithmic cornerstone of quantum annealing⁵⁸³.

In 2013, Google and NASA set-up a joint quantum computing lab, QUAIL, and toyed with D-Wave systems. It drove some awareness on the first supposed and oversold “quantum advantage” in 2015. Quantum annealing and D-Wave drove relatively bad press in the quantum community. They oversold their capacity and didn’t explain well how it worked. Things fared better starting in 2017 and 2020 with their latest 2000 and 5000 qubit releases.

Science

We must start here with explaining the following schema which connects the (quantum) adiabatic theorem and the various forms of digital simulated and quantum annealing:

- The **adiabatic theorem** states if you are in the ground state of a slowly varying quantum system, you stay in the ground state. It was created by Max Born and Vladimir Fock in 1928.
- The **diabatic theorem** is related to quick Hamiltonian evolutions and can be implemented in gate-based quantum computing although a recent proposal emerged to implement it with a quantum annealer using a locally managed transverse field⁵⁸⁴.
- It can be implemented to solve various optimization and simulation problems in three manners:
 - Classically digitally with a **simulated annealer** (including Fujitsu’s digital annealers),
 - With a **quantum annealer** (D-Wave).
 - With a **gate-based quantum computer**, using a time discretization of the system Hamiltonian evolution.

Quantum annealing is faster than digital annealing as found in a 2022 benchmark⁵⁸⁵. It was also found that digitized simulated annealing can be used for more efficient integer factoring on NISQ QPUs than with Shor’s algorithm⁵⁸⁶.

- **Quantum annealing** is implemented with converting an optimization problem into a generic **QUBO** optimization problem (Quadratic unconstrained binary optimization) which itself can be turned into solving an **Ising model** on a quantum annealer.
- **Reverse annealing** uses classical methods such as simulated annealing to find a trivial solution and find better solutions using quantum annealing. This has been recently implemented with D-Wave annealers and is more efficient than classical quantum annealing.

⁵⁸² See the thesis [Superconducting flux qubits for high-connectivity quantum annealing without lossy dielectrics](#) by Christopher M. Quintana, 2017 (413 pages), directed by John Martinis who was then at Google.

⁵⁸³ See [Quantum Computation by Adiabatic Evolution](#) by Edward Farhi, Jeffrey Goldstone, Sam Gutmann and Michael Sipser, MIT and Northwestern University, 2000 (24 pages).

⁵⁸⁴ See [Locally Suppressed Transverse-Field Protocol for Diabatic Quantum Annealing](#) by Louis Fry-Bouriaux et al, UCL October 2021 (18 pages).

⁵⁸⁵ See [Benchmarking Quantum\(-inspired\) Annealing Hardware on Practical Use Cases](#) by Tian Huang et al, March 2022 (35 pages).

⁵⁸⁶ See [Digitized Adiabatic Quantum Factorization](#) by Narendra N. Hegade, Enrique Solano et al, November 2021 (10 pages).

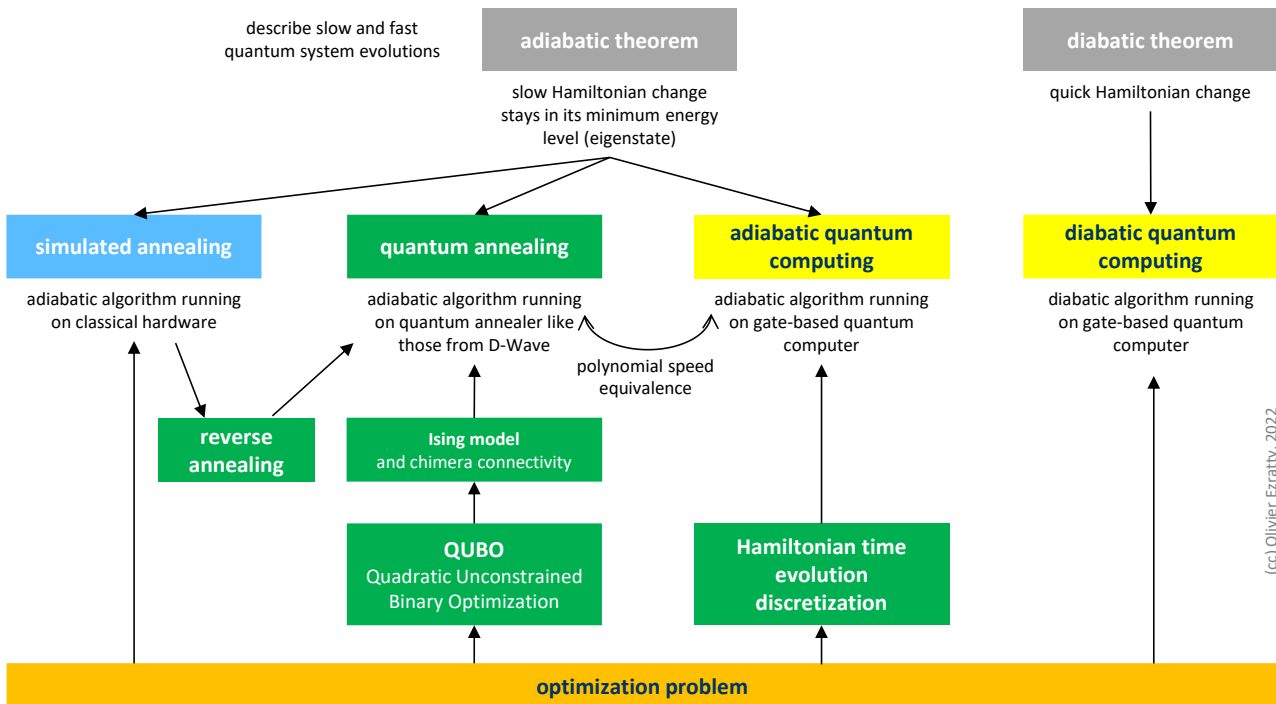


Figure 268: from the adiabatic theorem to quantum annealing. (cc) Olivier Ezratty, 2022. And some references found in [Adiabatic quantum computation](#) by Tameem Albash and Daniel A. Lidar, 2018 (71 pages).

Quantum annealing starts with preparing a system of interconnected qubits with establishing links between them using weights that are defined by couplers, a bit like in neural networks used in artificial intelligence. It sets the relative qubits connections energy in the longitudinal field (z) and the absolute qubits energy as a linear coefficient or bias on each qubit. These values h_i and J_{ij} are discretized depending on the capabilities of the DACs integrated in the chipset. It was using a 4 bit encoding in the first commercial D-Wave systems with values ranging from -1 to +1 by steps of 1/8. The precision of these DACs has since then improved with each new generation of D-Wave annealer.

2-local Ising Hamiltonian initialization
defines h_i and J_{ij} and set all σ_i^z at +1

net qubits energy
longitudinal interactions

$$\mathcal{H}_p = \sum_{i=0}^N h_i \sigma_i^z$$

qubits connections energy
longitudinal field

$$+ \sum_{i<j}^N J_{ij} \sigma_i^z \sigma_j^z$$

problem variables

- h_i linear coefficient (bias) on qubit usually discretized
- J_{ij} coupling between vertices V_i and V_j discretized and implemented with couplers non zero values limited by coupling topology

problem unknowns

- σ_i^z qubits values : +1 or -1 (« spin orientation »)
- σ_i^z and σ_i^x are Pauli operators

quantum annealing process
increases $B(s)$ and decreases $A(s)$ gradually

Ising model Hamiltonian → \mathcal{H}_p

unknown effect of noise → $\mathcal{H}_n(t)$

effect from the variation of a transverse field → $A(s)$

trivial initial state all qubits at +1 in x direction → $\sum_{i=0}^N \sigma_i^x$

$$\mathcal{H}_s(t) = \underbrace{\mathcal{H}_p \frac{B(s)}{2}}_{\text{final Hamiltonian}} + \underbrace{\mathcal{H}_n(t) - \frac{A(s)}{2} \sum_{i=0}^N \sigma_i^x}_{\text{initial Hamiltonian}}$$

annealing time operators

- t time
- t_f total annealing time, about 5 μ s
- s fraction of annealing time= t/t_f
- $A(s)$ tunneling energy at anneal fraction s reduced over time as a $\Gamma(t)$ transverse magnetic field applied to all qubits is reduced
- $B(s)$ problem Hamiltonian energy at anneal fraction s increases over time during annealing

qubits connectivity
coefficients and couplings

qubits topology

- V_i vertices containing qubit i
- E_{ij} edge connecting qubits i and j

system energy

- \mathcal{H}_p initial system Hamiltonian
- $\mathcal{H}_n(t)$ system noise Hamiltonian
- $\mathcal{H}_s(t)$ total Hamiltonian

Figure 269: uncovering a quantum annealing Hamiltonian. (cc) Olivier Ezratty, 2022.

The system is then initialized with setting the qubits at $|+\rangle$, a perfect superposition between $|0\rangle$ and $|1\rangle$, corresponding to the lowest-energy state of the system, also called the tunneling Hamiltonian.

The annealing process then takes place with progressively reducing this magnetic transverse field down to zero, which, thanks to the quantum tunnel effect, will drive the system to an equilibrium state that corresponds to a minimum energy level. In the equations in Figure 269, it means reducing the value of scalar $A(s)$ and increasing the value of $B(s)$ accordingly, usually not linearly. This leads to automatically modifying the values of the qubits (spin up or down in the z direction) towards a result that corresponds to the solution of the submitted problem. This annealing process is a magnetic equivalent of a classical thermal annealing.

From the mathematical standpoint, the system Hamiltonians \mathcal{H}_p , \mathcal{H}_S and \mathcal{H}_n described in Figure 269 are square matrix operators of dimension 2^N , N being the number of used qubits. The σ_j^z notation in the Ising and annealing Hamiltonian are somewhat confusing. It is actually the tensor product of the identity operator for all qubits non equal to j and the Pauli z operator for the given qubit j , as follows. A Pauli operator is a 2×2 matrix equivalent to the X, Y and Z single-qubit gates from gate-based quantum computing. Thus, σ_j^z is a simplified notation of the whole tensor product of dimension 2^N , the full version being the following, I_k being identity matrices of dimension 2×2 for all k between 1 and N at the exception of j :

$$\sigma_j^z = I_1 \otimes \dots \otimes I_{j-1} \otimes \sigma_j^z \otimes I_{j+1} \otimes \dots \otimes I_N$$

The same can be said of the product $\sigma_i^z \sigma_j^z$ which is also a tensor product of dimension 2^N using the following equation with I_k for all k between 1 and N at the exception of i and j :

$$\sigma_i^z \sigma_j^z = I_1 \otimes \dots \otimes I_{i-1} \otimes \sigma_i^z \otimes I_{i+1} \otimes \dots \otimes I_{j-1} \otimes \sigma_j^z \otimes I_{j+1} \otimes \dots \otimes I_N$$

System Hamiltonian matrix eigenvalues are the possible energy levels of the system. The annealing process has the effect of maintaining the system in its minimum energy level. It doesn't compute these eigenvalues but finds the qubit spin values (σ_i^z) that are minimizing the Hamiltonian. Another notation of the effect of quantum annealing is to find the combination of N spins noted $\hat{\sigma}$ that minimizes the Hamiltonian. The searched space is Ω_N that contains all N combinations of -1 and $+1$: $\{-1, +1\}^N$.

$$\hat{\sigma} = \arg \min_{\sigma \in \Omega_N} \left(\sum_{i=0}^N h_i \sigma_i^z + \sum_{i < j}^N J_{ij} \sigma_i^z \sigma_j^z \right)$$

At the end of the annealing, the qubits state is read and generates a $+1$ or a -1 for each of them depending on the direction of the magnetic flux of the superconducting loop (and, by the way, we don't care about it being a QND – aka non demolition - measurement). As a result, the solved problem search space is discrete and finite. The process is however iterative with several annealing passes and results being averaged. Like with gate-based quantum computing, the process is also probabilistic, and not just because noise gets involved with an unknown time-evolving Hamiltonian $\mathcal{H}_n(t)$.

quantum annealers

- mature **development tools** offering.
- large number of **software startups**, particularly in Japan and Canada.
- quantum annealers are available in the **cloud** by D-Wave and Amazon Web Services.
- the greatest number of well documented **case studies** in many industries although still at the proof of concept stage.
- most universal qubits gates algorithms can be have an equivalent on quantum annealing.

- only **one operational commercial vendor**, D-Wave.
- computing **high error rate**.
- **no operational proof** of quantum advantage.
- **most commercial applications** are still at the pilot stage and not production-scale grade but this is also the case for all gate-based quantum computers.
- **all algorithms are hybrid**, requiring some preparation on classical computers.

Figure 270: quantum annealers pros and cons. (cc) Olivier Ezratty, 2022.

There are variations in this model's implementation with regards to the qubits coupling mechanism. It can be made on one degree (z for D-Wave) or two and three degrees of freedom (x, y and z, in a so-called Heisenberg model) like what **Qilimanjaro** (Spain) is planning to implement.

Qubit operations

Using a quantum annealer works as described in Figure 271. Algorithms are prepared classically with converting the given problem into a QUBO problem that is then translated in an Ising model with setting up the links between qubits in the initialization process and the qubits "weights".

The annealing process then takes place with controlled evolutions of A(s) and B(s) as described in the previous chart, with tuning the magnetic transverse field affecting the qubits chipset. When s=1, the system proceeds with reading the qubits values +1 or -1.

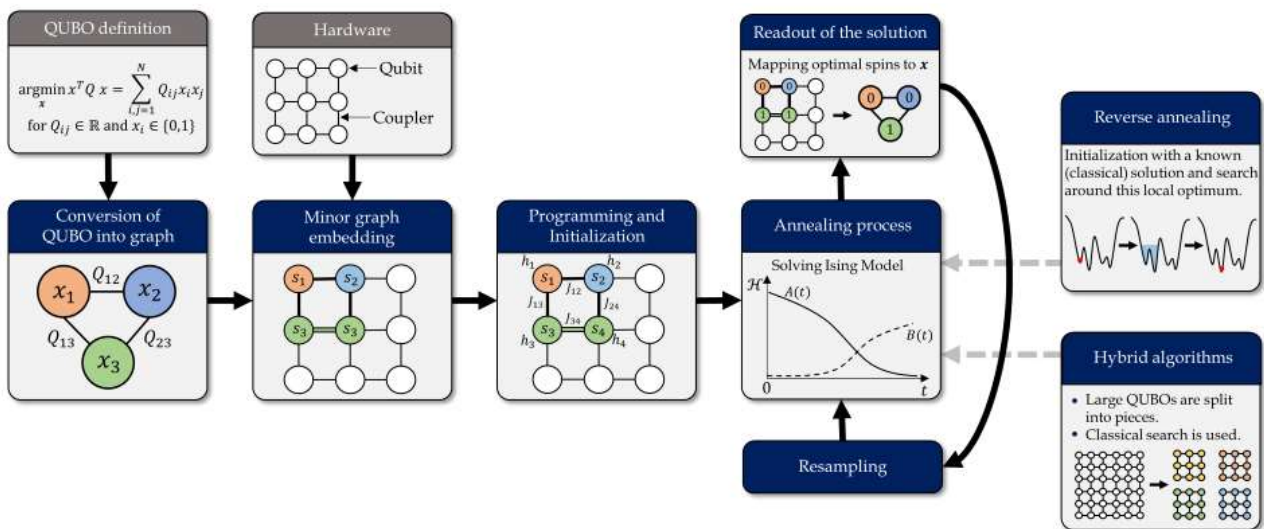


Figure 271: a quantum annealing computing process. Source: [Quantum Annealing for Industry Applications: Introduction and Review](#) by Sheir Yarkoni et al, Leiden University and Honda Research, December 2021 (43 pages).

D-Wave qubits are niobium-based rf-SQUID exploiting superconducting current loops interrupted by two Josephson effect barriers that are controlled by variable magnetic fluxes.

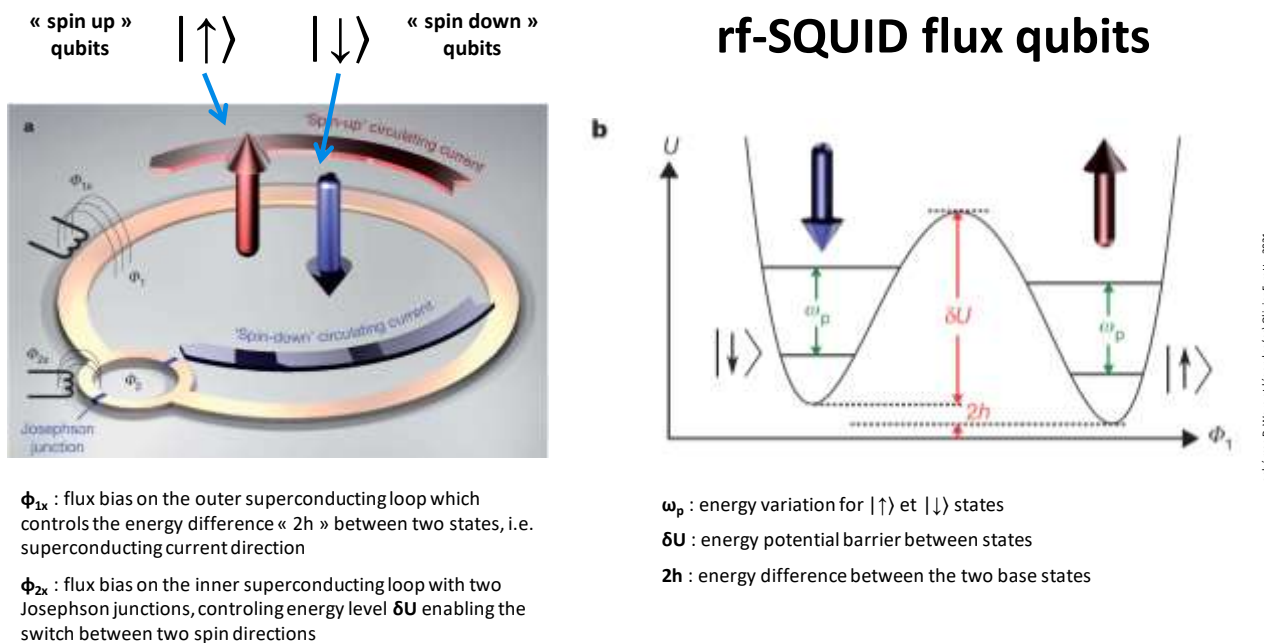


Figure 272: rf-SQUIDs used in a D-Wave quantum annealer. Source: D-Wave.

Taking always the example of D-Wave annealers, we can dig into how the qubits are controlled to prepare and handle an annealing process⁵⁸⁷. The process needs to control several parameters:

- J_{ij} the coupling between vertices V_i and V_j is controlled by DACs (digital to analog converters). These couplers are set with a static DC flux current applied to their compound-junction.
- h_i the energy between two states of qubits i is also controlled via a DAC. But other DACs are there to correct the drift created by the annealing process.
- $A(s)$ is a transverse magnetic field applied to all qubits and controlled in the chipset by analog lines via the CCJJ DACs.
- $B(s)$ increases over time during annealing, also controlled by CCJJ analog lines in the chipset.

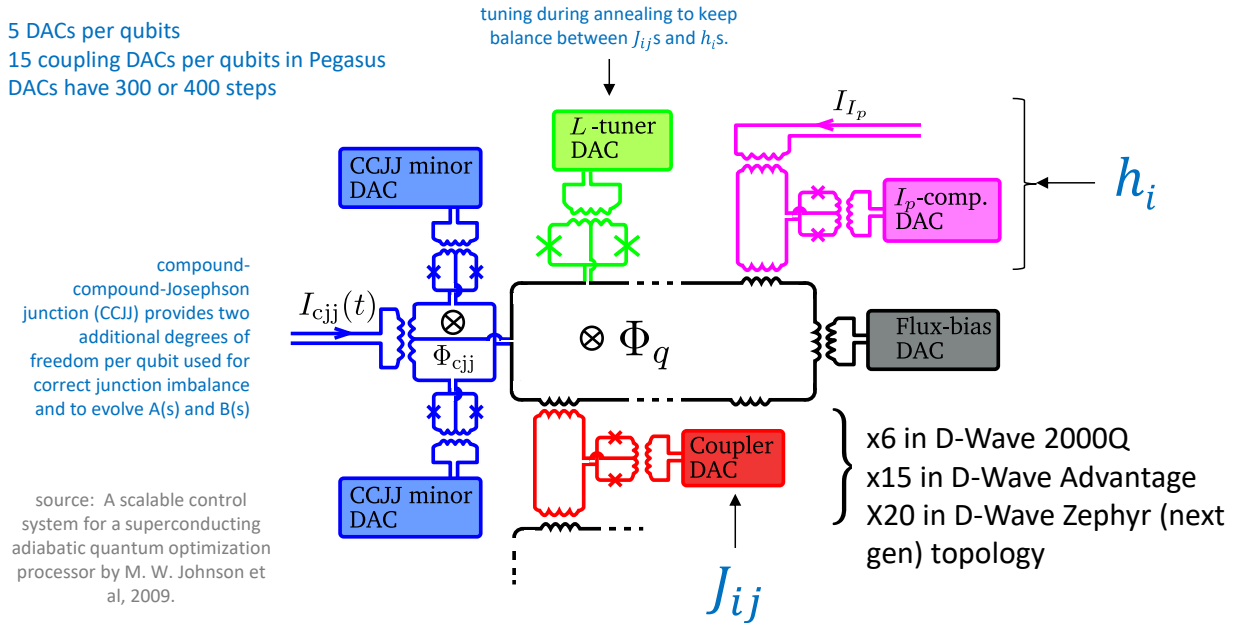


Figure 273: source: how D-Wave qubits are controlled at the physical level. Source: [A scalable control system for a superconducting adiabatic quantum optimization processor](#) by M. W. Johnson et al, 2009.

These are optimization problems where the variables J_{ij} can only take two values (-1 or +1 for solving an Ising model or 0 and 1 for solving a QUBO problem) and where they are linked together by different fixed parameters which are defined as floating numbers (FP32) with the boundary constraints $-1 \leq J_{ij} \leq 1$ and $-2 \leq h_i \leq 2$. However, the related DACs introduce significant sampling noise due to their sampling rate with a couple hundred different steps. In the end, the precision of the data of the problem to be solved is much lower, probably below one single byte. We're far from high-precision floating point scientific computation. It should be mentioned that D-Wave systems require frequent recalibration.

The initialization of a D-Wave 2000Q takes 25 ms, the annealing itself usually lasts 20 μ s but can be extended to 2 ms, and readout time is 260 μ s. If we repeat the annealing process a thousand times, we end-up running the whole thing in less than a second. Between each run, some time was required to enable heat dissipation, with the chipset temperature rising to 500 mK with early generations of D-Wave annealers.

⁵⁸⁷ The electronics architecture of superconducting qubits control is described in [A scalable control system for a superconducting adiabatic quantum optimization processor](#) by M. W. Johnson et al, 2009 (14 pages) and [Architectural considerations in the design of a superconducting quantum annealing processor](#) by P. I. Bunyk et al, 2014 (9 pages).

The initialization signals of the Hamiltonian are multiplexed and sent in digital format from the outside to the chip. A chipset requires an order of magnitude of $O(\sqrt[3]{N})$ external control lines for N qubits, using signals multiplexing.

This greatly simplifies the cabling of the cryogenic enclosure of the computer compared to the superconducting IBM and Google computers, as shown in the *adjacent* illustration of a 2000Q. Most of what can be seen in the intermediate stages in the cryostat corresponds to the dilution cryogenics system.



Figure 274: Inside a D-Wave system, with the cryostat open. Source: D-Wave.

Annealers don't need to send microwave pulses to qubits and thus, avoid the related coaxial cables used in gate-based superconducting qubits. Some of the magic comes from the integrated DC ramp pulses generation circuits that are sitting in the quantum chip. These circuits use SFQ components implementing DACs, basically superconducting transistors using Josephson junctions close to those of the qubits. Still, these components are noisy and may contribute to the noise affecting the qubits in this architecture⁵⁸⁸.

Research

Let's mention some research work beyond what D-Wave is doing.

Quantum annealing was explored in 2016 by the IARPA agency in its **Quantum-Enhanced Optimization** (QEO) project, which aimed to create an adiabatic computer void of some of the limitations from D-Wave, particularly in terms of connectivity and quality of qubits. Appropriately, in view of IARPA's mission, the goal was to accelerate the production of quantum computers capable of executing Shor's integer factoring algorithm to break the public keys coming from intercepted communications. This project was folded into DARPA's **QAFS** project (Quantum Annealing Feasibility Study) in February 2020 which produced a 25 coherent annealer system.

Stanford University is also working on quantum annealing. In 2016, they created a prototype photonic based annealer with 100 qubits having an all-to-all connectivity (so... 10,000 connections)⁵⁸⁹. This connectivity is what makes such a system "coherent". This research was still going on in 2021 and involves **NTT** in Japan.

At last, the H2020 European project **AVaQus** (Annealing-based VARIational QUantum processorS) launched in October 2020 brings together five research laboratories (Institut de Física d'Altes Energies of Barcelona, Karlsruhe Institut für Technologie (KIT) of Karlsruhe, CNRS Institut Néel in France, the University of Glasgow and the Consejo Superior de Investigaciones Científicas in Madrid), associated with three startups **Delft Circuits** (Netherlands), **Qilimanjaro** (Spain) and **HQS** (Germany). The project is scheduled to end in 2023 and got a funding of €3M, independently of the Quantum Flagship program.

⁵⁸⁸ See [Analog errors in quantum annealing: doom and hope](#) by Adam Pearson, 2019 (9 pages).

⁵⁸⁹ See [A fully-programmable 100-spin coherent Ising machine with all-to-all connections](#) by Peter L. McMahon, Yoshihisa Yamamoto et al, 2016 (9 pages).

Vendors

We'll of course start with D-Wave and will follow-on with Qilimanjaro and NEC.



Located in Vancouver, **D-Wave** (1999, Canada, \$724M + SPAC) was for a very long time the only supplier of commercial quantum processors.

D-Wave was created by Geordie Rose (their first CTO and for some time also their CEO⁵⁹⁰), Haig Farris, Bob Wiens and Alexandre Zagoskin, formerly in charge of research. Geordie Rose received his PhD in Materials Physics in the mid-1990s from the University of British Columbia. The creation of D-Wave is a direct result of this work. He met Haig Farris during his studies while the latter was teaching economics.

It took D-Wave eight years to prototype its first chip containing four qubits and a total of 13 years to sell their first quantum computer, the D-Wave One. During these years, they raised \$31M, then \$1.2M in 2012 from InQTel, the CIA's investment fund. In 2011, D-Wave signed a partnership with Lockheed Martin, which does some work for the NSA. All in all, the startup went through 13 rounds of funding, ending with a SPAC finalized in 2022!

In February 2022, D-Wave announced its own SPACification via the dedicated investment fund **DPCM Capital** created by Eric Schmidt (former Google, now SandboxAQ chairman), Peter Diamandis (Singularity University), Shervin Pishenar (Hyperloop One founder)⁵⁹¹. They were to raise \$340M, including \$40M coming from a Canadian pension fund, PSP Investments. Were also involved Goldman Sachs and NEC Corporation. This valued the company at \$1.6B which was IPOed in August 2022. They have another funding source with \$150M coming from Lincoln Park Capital. Public financial information uncovered that in 2021, D-Wave revenue was \$11M with losses of \$59M. The company expects a fast growth starting in 2025, generating a \$551M turnover in 2026. As of early 2022, they had a staff of 180 including 36 PhDs and a 200 patents portfolio.

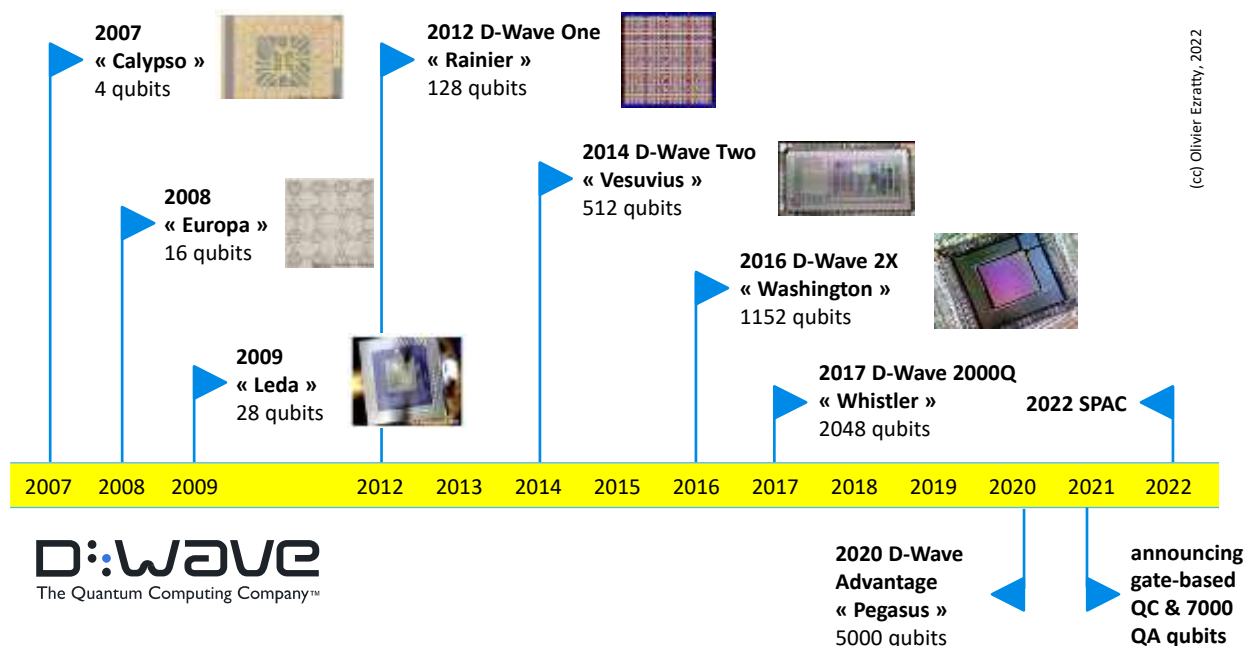


Figure 275: timeline of D-Wave's history. (cc) Olivier Ezratty, 2022.

⁵⁹⁰ Co-founder Geordie Rose then created **Kindred.ai**, a startup that aims to integrate General Intelligence (GIA) into robots. He left Kindred.ai in 2018 to create **Sanctuary**, a spin-off of Kindred, dedicated to AGI, the quest for the Holy Grail of general artificial intelligence.

⁵⁹¹ See their [February 2022 investor presentation](#) (25 slides).

D-Wave's 2021 management team is quite different. Only one of the co-founders is still part of it, Eric Ladizinsky, who is their Chief Scientist. The CEO from 2009 to 2020 was Vern Brownell. Their CTO Alan Baratz joined the company in 2017 and became CEO in 2020.

Although quantum annealing accelerators have technical limitations compared to general-purpose quantum computers, they have the advantage of being available and are surrounded by a strong software ecosystem. However, most of the 250+ case studies solutions published by D-Wave and their customers and partners seem to be proofs of concept. Few seem to have been deployed, be production-grade, or at least provide a proven quantum advantage over classical computing. D-Wave has developed its end-to-end quantum annealing computer solution. It is the first full-featured quantum computer in history with a design that allows it to be easily integrated into a clean room.

Their roadmap has progressed steadily with the first three generations of prototypes created between 2007 and 2009 and then, starting from 2012, five generations of commercial computers, starting with the D-Wave One in 2012 with 128 qubits, the D-Wave 2000Q in 2017 with 2048 qubits and 128,000 Josephson junctions on a $(5.5 \text{ mm})^2$ chipset and a list price of \$15M, up to the D-Wave Advantage with the Pegasus chipset launched in September 2020 with 5,640 qubits and one million Josephson junctions⁵⁹², each qubit being coupled to 15 other qubits compared to 6 in the 2000Q⁵⁹³. It allows more complex problems to be solved with an equivalent number of qubits. It is a performance given gate-based superconducting qubits have a 1 to 3 (IBM) to 1 to 4 (Google) connectivity at best. The Pegasus chipset is larger, being a square of 8,5 mm. It is manufactured in the USA in Skywater's cleanrooms (formerly a Cypress Semiconductor fab) located in Bloomington, Minnesota. The embedding graph or qubits connectivity is branded a chimera their D-Wave 2000Q annealers and a Pegasus graph for their D-Wave Advantage annealers⁵⁹⁴.

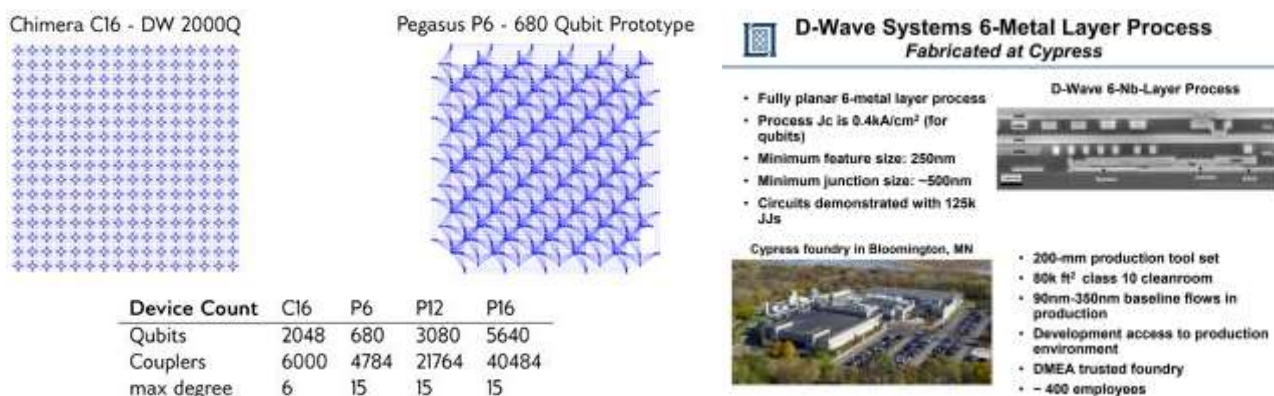


Figure 276: evolution of D-Wave's qubit connectivity. And their chipset manufacturing process. Source: D-wave.

⁵⁹² See [Quantum annealing with manufactured spins](#) by Mark Johnson et al, 2011 (6 pages) which outlines the D-Wave process. As well as [Technical Description of the D-Wave Quantum Processing Unit](#) by D-Wave, 2020 (56 pages) and related [supplemental information](#) (19 pages). The Pegasus architecture from the D-Wave advantage is described in [Next Generation Quantum Annealing System](#) by Mark Johnson, March 2019 (27 slides) and in [Next-Generation Topology of D-Wave Quantum Processors](#) by Kelly Boothby et al, 2019 (24 pages). See [D-Wave Announces General Availability of First Quantum Computer Built for Business](#) by D-Wave, September 2020.

⁵⁹³ The chimera uses cells with 8 qubits with internal and external couplings. It has 4 internal couplings within cells and 2 external couplings in pre-Pegasus chipsets and 12 internal and 3 external couplings in Pegasus chipsets.

⁵⁹⁴ D-Wave's chimera matrix requires a conversion process of its qubit mesh problem. This process is so far mostly exploited for problems that fit well with this qubit organization. For an arbitrary optimization problem, the conversion gives a result that is not convincing in terms of efficiency and acceleration. This is what emerges from the work of Daniel Vert, then PhD student at CEA LIST, in [On the limitations of the chimera graph topology in using analog quantum computers](#) by Daniel Vert, Renaud Sidney and Stéphane Louise, CEA LIST, 2019 (5 pages) and in [Revisiting old combinatorial beasts in the quantum age: quantum annealing versus maximal matching](#) by the same authors, October 2019 (36 pages). D-Wave's chimera structure limits the way a QUBO or other optimization problem can be converted into an Ising problem solvable with D-Wave's chimera structure.

In October 2021, D-Wave made significant announcements as part of their Clarity roadmap with an upcoming Advantage 2 generation codename Zephyr with 7000 qubits to be released by 2024 (with a first 500-qubit prototype which was delivered in June 2022), a 20-way qubits connectivity in a new graph architecture⁵⁹⁵. They announced also the future release of a gate-based QPU that will be implemented in a separate (flux-based) multi-layer superconducting processor architecture, starting with 60 and then 1000 qubits to implement error correction. They plan to use surface code QECs and to use some combination of RSFQ and other cryo-electronics to control these qubits. They could be highly differentiated for that respect and only challenged by other superconducting qubit vendors partnering with SeeQC.

How about error rates? They are not computed the same way as gate-based single and two qubit gate fidelities. The error rate is measured as a precision with the Ising model parameters, which is about 2% given the DACs precision⁵⁹⁶. The high-error rate of D-Wave annealing systems can be mitigated with some quantum error correction technique, created in 2019⁵⁹⁷ and more recently in 2022 for post-processing error correction⁵⁹⁸ and machine learning aided error correction⁵⁹⁹.

Other researchers found that the thermal noise involved in the annealing process could be used as a resource to enable faster and more reliable computations, involving the curious process or reverse annealing⁶⁰⁰. It could help finding a better solution than an existing solution already computed with a regular annealing process.

The qubits operate at 10 to 15 mK like all gate-based superconducting qubits. The cryostat is thus the same, using a dry dilution system. Cryogeny consumes about 16kW out of a total of 25kW. The remaining 9kW is related to traditional computer control systems that are outside the cryostat. The cryogenic part includes an enclosure with five layers of magnetic isolation.

So, what is quantum in D-Wave? Beyond the many Josephson junctions used in their chipset, it comes from the tunnelling effect that allows the system to quickly search for a global energy minimum of an N-body system⁶⁰¹. It is coupled with superposition of the qubit states. According to D-Wave, the system also uses entanglement, which is poor and probably circumvented to nearest neighbor qubits. This has been questioned by some scientists⁶⁰².

Algorithms designed for classical gate-based quantum computers can theoretically be converted into algorithms executable on D-Wave and vice versa at a maximum polynomial time overhead cost, which can be substantial⁶⁰³. However, a similar problem will require many more qubits with D-Wave than with a universal quantum computer.

⁵⁹⁵ See [Zephyr Topology of D-Wave Quantum Processors](#) by Kelly Boothby, Andrew D. King and Jack Raymond, D-Wave, September 2021 (18 pages).

⁵⁹⁶ The question remains open as to whether this architecture is scalable and provides a real quantum advantage. This is questioned in [Fundamental Limitations to the Scalability of Quantum Annealing Optimizers](#) by Tameen Albash et al, 2019. The reasons: issues of noise and thermodynamics.

⁵⁹⁷ See [Analog errors in quantum annealing: doom and hope](#) by Adam Pearson et al, 2019 (16 pages).

⁵⁹⁸ See [Post-Error Correction for Quantum Annealing Processor using Reinforcement Learning](#) by Tomasz Śmierzchalski et al, March 2022 (14 pages).

⁵⁹⁹ See [Boosting the Performance of Quantum Annealers using Machine Learning](#) by Jure Brencic et al, March 2022 (14 pages).

⁶⁰⁰ See [Thermodynamic study of D-Wave processor could lead to better quantum calculations](#) by Hamish Johnston, June 2020.

⁶⁰¹ See the review paper [Quantum Annealing: An Overview](#) by Atanu Rajak et al, India, July 2022 (36 pages).

⁶⁰² Jonathan Dowling thought in the previous reference that the only quantum effects of D-Waves were tunneling and superposition, but without quantum entanglement.

⁶⁰³ This is documented in [Adiabatic quantum computation is equivalent to standard quantum computation](#), 2005 (30 pages) and in [How Powerful is Adiabatic Computation?](#) by Wim van Dam, Michele Mosca and Umesh Vazirani, 2001 (12 pages).

On a D-Wave, the number of qubits would need to be up to 32 times the number of quantum gates of the classical quantum algorithm but it depends on the problem⁶⁰⁴.

According to D-Wave, their annealers can solve NP-complete problems, a category of combinatorial problems theoretically solved in polynomial time on D-Wave but which are solved in exponential time on a classical computer⁶⁰⁵, like routing problems, the traveling salesperson (TSP) problem and the likes. D-Wave annealers can also be used to solve statistical problems⁶⁰⁶.

In 2017, **John Preskill** estimated that there is no convincing theoretical basis for the advantage of quantum annealing, which is one form of adiabatic quantum computing⁶⁰⁷. He thinks this architecture is not theoretically as scalable as general-purpose quantum computers. The arguments about D-Wave's annealers quantumness revolve around the low-scale coherence between qubits which may prevent an efficient implementation of quantum annealing⁶⁰⁸. It is also related to the limited connectivity between qubits⁶⁰⁹. Others think that D-Wave systems can generate at best some quadratic acceleration and not an exponential one, compared to traditional computing⁶¹⁰. **Daniel Lidar** from the University of Southern California is investigating variations of quantum annealing algorithms that could solve intractable problems on classical computers⁶¹¹.

D-Wave's software development environment is Ocean, a suite of open source Python tools and libraries accessible via the Ocean SDK on both the D-Wave GitHub repository and in their Leap quantum cloud service (that is also accessible on Amazon Braket).

It contains a large set of libraries to solve various optimization and constraint satisfaction problems as described on the right. We cover it with more details later in this book in the section dedicated to hardware vendor software development tools.

In October 2021, D-Wave released its **Constrained Quadratic Model** solver (CQM), working with both discrete and continuous variables. It expanded the optimization problems D-Wave's annealers can solve, with up to 100.000 variable constraints⁶¹² on top of the binary quadratic model (BQM) solver problems defined with binary values (0,1) and the discrete quadratic model (DQM) solver for problems on nonbinary (multiple choices) values.

One of the oldest and famous D-Wave publicized case study came from Google and NASA using a 2012 D-Wave annealer to solve an optimization and combinatorial problem in a graph whose algorithm was designed in 1994.

⁶⁰⁴ From "Automatically Translating Quantum Programs from a Subset of Common Gates to an Adiabatic Representation" by Malcolm Regan et al, seen in [Reversible Computation](#), conference proceedings, 11th International Conference, RC 2019, Lausanne, Switzerland, June 2019 (246 pages).

⁶⁰⁵ See [Practical Annealing-Based Quantum Computing](#) by Catherine McGeoch et al of D-Wave, June 2019 (16 pages) which makes an inventory of the benefits of quantum annealing computing, especially in terms of the size of the problems to be solved, which should be neither too small because they are trivial, nor too large because they must then be broken down into sub-problems that are manageable with the capacity of current D-Wave processors. It seems that the problems to be solved must have global minimums and local minimums, the first being difficult to find with classical methods.

⁶⁰⁶ See [Applications of Quantum Annealing in Statistics](#) by Robert C. Foster, 2019 (30 pages).

⁶⁰⁷ In [Quantum Computing for Business](#), 2017 (41 slides).

⁶⁰⁸ See [How "Quantum" is the D-Wave Machine?](#) by Seung Woo Shin, Umesh Vazirani et al, 2014 (8 pages).

⁶⁰⁹ See the example of [Phase-coded radar waveform AI-based augmented engineering and optimal design by Quantum Annealing](#) by Timothé Presles et al, Thales, August 2021 (9 pages). In this use case, no quantum advantage can be seen with D-Wave due to limited qubits connectivity.

⁶¹⁰ This was the opinion of Jonathan P. Dowling in [Schrödinger's Killer App - Race to Build the World's First Quantum Computer](#) by Jonathan P. Dowling, 2013 (445 pages), pages 208 to 216.

⁶¹¹ See his [Adiabatic quantum computing](#) page on USC Quantum Computation and Open Quantum Systems web site.

⁶¹² See [Hybrid Solver for Constrained Quadratic Models](#), 2021 (8 pages).

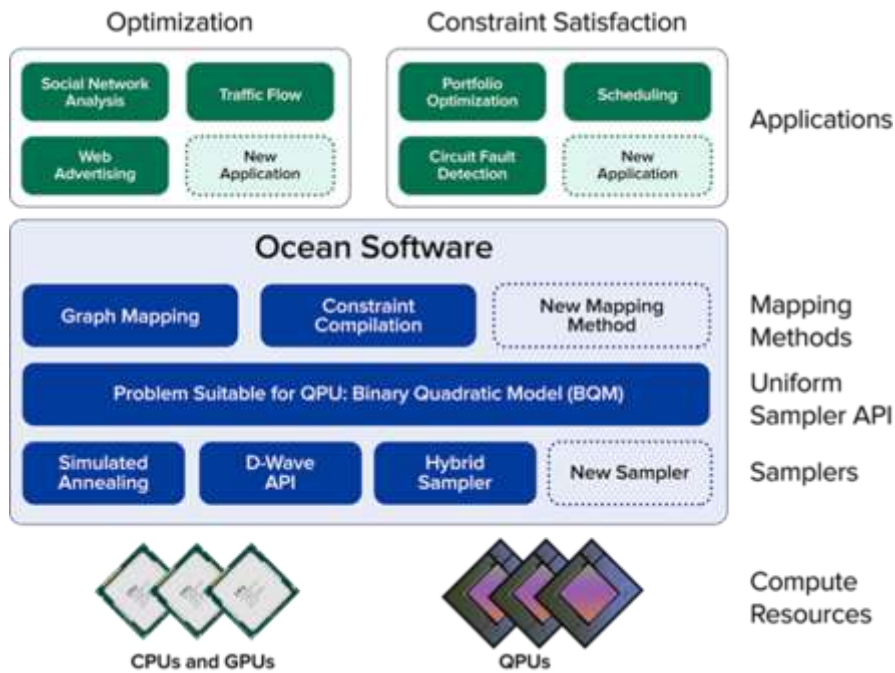


Figure 277: D-Wave Ocean software platform. Source: D-Wave.

Google announced in 2015 that it had achieved a performance 100 million times better than that of traditional computers, a single core of an Intel Xeon server processors⁶¹³. Like many such claims, they were questionable since based on a single optimized algorithm, here, a Quantum Monte Carlo simulating quantum tunneling on a classical computer. Critics abounded about this performance⁶¹⁴. It was a first “hype” moment of quantum computing.

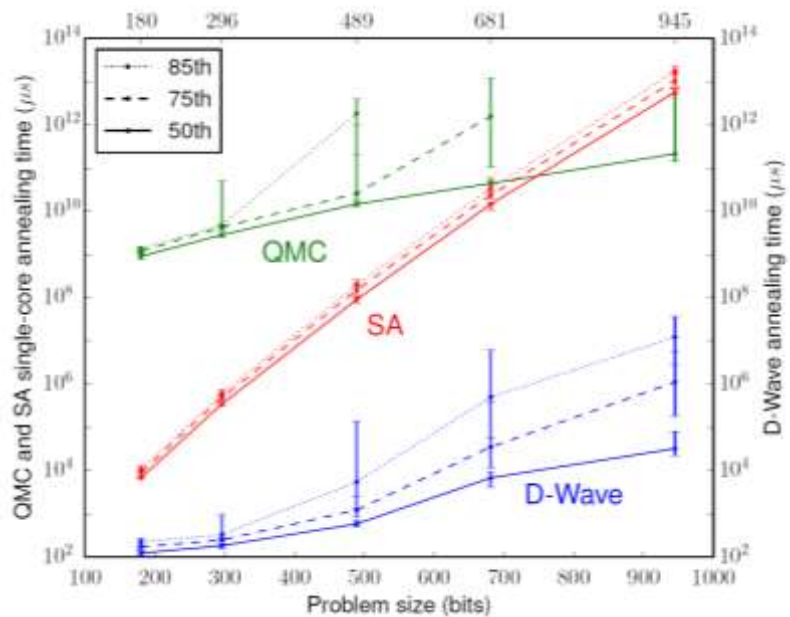


Figure 278: how Google and NASA communicated in 2015 about the performance of a D-Wave annealer. Source: [What is the Computational Value of Finite Range Tunneling](#) by Vasil S. Denchev, John Martinis, Hartmut Neven et al, January 2016 (17 pages).

⁶¹³ In [Google's D-Wave 2X Quantum Computer 100 Million Times Faster Than Regular Computer Chip](#) by Alyssa Navarro in Tech Times, November 2015 and documented in [What is the Computational Value of Finite Range Tunneling](#) by Vasil S. Denchev, Sergio Boixo, Sergei V. Isakov, Nan Ding, Ryan Babbush, Vadim Smelyanskiy, John Martinis and Hartmut Neven, January 2016 (17 pages).

⁶¹⁴ Including [Temperature scaling law for quantum annealing optimizers](#), 2017 (13 pages), which points out the limitations of quantum annealing.

D-Wave communicates on many other of its pilot references⁶¹⁵. Its web site references over 250 case studies, the largest number of any quantum computing vendor⁶¹⁶. Here are a couple ones:

- **Denso**, a Japanese car equipment manufacturer presented at CES 2017 in Las Vegas a system for optimizing a fleet of Toyota delivery vehicles.
- **Biogen**, **1Qbit** and **Accenture** did prototype in 2012 a screening solution to identify molecules for drug retargeting, with a problem of map staining⁶¹⁷. It is difficult to say what this has generated in practice. Their partner **Menten AI** performs protein analysis.
- **Lockheed-Martin** produced in 2014 some validation procedures for its embedded software in 6 weeks instead of 8 months with a D-Wave and its QVTRace tool⁶¹⁸.
- **Volkswagen** simulated the operations of a cab fleet in Beijing, and also a solution to develop new batteries⁶¹⁹. The solution was used in November 2019 to optimize the shuttle route at Lisbon's WebSummit, in partnership with Here and Volkswagen's Data:Lab in Munich.
- **NASA** experimented D-Wave annealers in its joint QUAIL lab with Google in various fields, including the detection of exoplanets by analysis of telescopic observations using the transit method, as well as for various optimization and planning problems⁶²⁰.
- **GE Research** experimented some hybrid maintenance resource allocation optimization application.
- **Ocado**, a British retailer, prototyped some optimization solution for its robots-based warehouse operations.
- **Los Alamos National Laboratory** with **Stanford University** prototyped the detection of the formation of terrorist networks in Syria with analyzing imbalances in social networks⁶²¹.
- **Volkswagen** experimented quantum annealing to optimize car paint-shop processing in order to minimize color switching, but with no clear quantum advantage⁶²².
- **KAIST** and **LG U+** in Korea used D-Wave annealers to optimize data-transfer routing using a fleet of low-earth orbit telecommunications satellites and a QUBO algorithm, with the help of **Qunova Computing**, a Korean quantum software startup⁶²³.
- Researchers in Poland, Hungary, Brazil and the USA found a way to use D-Wave annealers to **optimize trains dispatching** on single-railways lines⁶²⁴.

⁶¹⁵ I found this inventory in [Quantum Applications](#) by D-Wave, May 2019 (96 slides).

⁶¹⁶ See [Quantum Annealing for Industry Applications: Introduction and Review](#) by Sheir Yarkoni et al, Leiden University and Honda Research, December 2021 (43 pages) which provides an overview of how D-Wave annealers are “programmed” and what kinds of problems it can solve.

⁶¹⁷ Described in [Programming with D-Wave Map Coloring Problem](#), 2013 (12 pages).

⁶¹⁸ See [Quantum Computing Approach to V&V of Complex Systems Overview](#), 2014 (31 slides) and [Experimental Evaluation of an Adiabatic Quantum System for Combinatorial Optimization](#), 2013 (11 pages).

⁶¹⁹ See [Forget quantum supremacy: This quantum-computing milestone could be just as important](#) by Steve Ranger, December 2019.

⁶²⁰ See [Quantum Computing at NASA: Current Status](#) by Rupak Biswas, 2017 (21 slides) as well as [Adiabatic Quantum Computers: Testing and Selecting Applications](#) by Mark A. Novotny, 2016 (48 slides).

⁶²¹ See [Using the D-Wave 2X Quantum Computer to Explore the Formation of Global Terrorist Networks](#) by John Ambrosiano et al, 2017 (14 pages).

⁶²² See [Multi-car paint shop optimization with quantum annealing](#) by Sheir Yarkoni et al, September 2021 (7 pages).

⁶²³ See [KAIST & LG U+ Team Up for Quantum Computing Solution for Ultra-Space 6G Satellite Networking](#), KAIST press office, June 2022.

⁶²⁴ See [Quantum annealing in the NISQ era: railway conflict management](#) by Krzysztof Domino et al, December 2021 (23 pages).

- In April 2020, D-Wave opened free access to its cloud computers to researchers looking for **solutions** to the **covid pandemic**⁶²⁵. The solutions developed included solving optimization problems such as optimizing patient routing to hospitals in Japan, modeling the spread of the virus, managing nurses' schedules in hospitals, assessing the rate of virus mutation and screening molecules. It remains to be proven that D-Wave provides a real quantum advantage in solving these different problems.
- In February 2021, D-Wave and Google published a study showcasing a computational advantage of annealing with the **D-Wave Advantage** for simulating some condensed matter physics, 3 million times faster than with classical methods. It didn't exactly describe the classical hardware that is being used as a reference, but it looked like a traditional Intel-based server⁶²⁶. These comparisons with a single narrow algorithm are insufficient to draw any conclusions. Another similar work was published in 2022 with using 2000 qubits for accurate simulations of coherent quantum dynamics at large scales⁶²⁷. This paper did show that there was indeed large scale coherence happening in D-Wave annealers, a key support to solve complex problems.

We can also mention some recent quantum annealing algorithms:

- **Sorting lists** and building search trees or heaps, which can be modeled as QUBO problems⁶²⁸.
- **Neural network training** with using binary encoding the neural network free parameters, polynomial approximation of the activation function and reduction of binary higher-order polynomials into quadratic ones⁶²⁹.
- **Parallelizing annealing** on several quantum annealings with decomposing a problem graph into several graphs with the DBK algorithm, used for the Maximum Clique problem with 120 nodes and 6395 edges⁶³⁰. These smaller disjointed graphs are executed in a D-Wave Advantage.
- **Physical simulations** of topological matter and phase change⁶³¹.

As of 2022, D-Wave had installed fewer than 10 quantum annealers at customer sites⁶³² and operates more than 30 of them in its own facilities, with more than half of them dedicated to their cloud access offering, some of them being available through the Amazon Braket cloud offering.

One D-Wave Advantage was ordered by the DoE Los Alamos National Laboratory in September 2019 and deployed since then⁶³³. In January 2022, a first D-Wave (Advantage) system was deployed in Europe, at the Forschungszentrum Jülich Supercomputing Center. It was also the first D-Wave coupled with a supercomputer as part of the Jülich UNified Infrastructure for Quantum computing (JUNIQ).

⁶²⁵ See [Can Quantum Computers Help Us Respond to the Coronavirus?](#) by Mark Anderson, April 2020.

⁶²⁶ See [Scaling advantage over path-integral Monte Carlo in quantum simulation of geometrically frustrated magnets](#), February 2021 (6 pages).

⁶²⁷ See [Coherent quantum annealing in a programmable 2000-qubit Ising chain](#) by Andrew D. King et al, Nature, February-September 2022 (24 pages).

⁶²⁸ See [QUBOs for Sorting Lists and Building Trees](#) by Christian Bauckhage et al, March 2022 (6 pages).

⁶²⁹ See [Completely Quantum Neural Networks](#) by Steve Abel et al, February 2022 (12 pages).

⁶³⁰ See [Solving Larger Optimization Problems Using Parallel Quantum Annealing](#) by Elijah Pelofske et al, May 2022 (16 pages). See also [Parallel Quantum Annealing](#) by Elijah Pelofske et al, November 2021 (12 pages).

⁶³¹ See [Observation of topological phenomena in a programmable lattice of 1,800 qubits](#), August 2018 (37 slides).

⁶³² Identified customers are the joint Google/NASA Quail research center, USRA (Universities Space Research Association), Lockheed Martin and the University of Southern California sharing one system, and Jülich Supercomputing Centre in Germany (since 2021). Other customers like in pharmaceutical companies are using D-Wave annealers through their Leap cloud offering.

⁶³³ See [Nuclear weapons lab buys D-Wave's next-gen quantum computer](#) by Stephen Shankland, September 2019 and [On the Emerging Potential of Quantum Annealing Hardware for Combinatorial Optimization](#) by Byron Tassef et al, October 2022 (25 pages).

The Julich team has published several benchmarks of various algorithms since then⁶³⁴.

In summary, quantum annealing may be a technique contested by many specialists, but it has the merit of existing and being testable in many use cases⁶³⁵. It will probably make some progress with newly published cases running on its Advantage generation. And we are looking forward at their capabilities to implement gate-based superconducting qubits computing.



Qilimanjaro (2019, Spain) is a startup based in Barcelona created by three physicists coming from different Spanish institutions (Barcelona Supercomputing Center, IFAE, University of Barcelona) and with a strong international experience and two experienced business managers!

The founding team assembles Jose Ignacio Latorre (Chief Science Officer, also now the Director of CQT in Singapore and Chief Research of CRO Quantum at TII in Abu Dhabi, went through MIT, CERN and Niels Bohr Institute), Pol Forn-Díaz (Chief Hardware Architect, TU Delft, MIT, Caltech and IQC Waterloo), Artur Garcia Sáez (Chief Software Architect, ICFO, Stony Brook), plus Víctor Canivell (Chief Business Officer) and Jordi Blasco (Chief Financial & Legal Officer).

They develop their own quantum annealer based on coherent flux qubits. Their differentiation lies with a better qubit coherence, qubits coupling designs and qubits connectivity.

These qubits will be first controlled by classical electronics working at room temperature. In a later stage, they plan to create cryogenic controls on a separate chipset. They rely on two fabs for their qubits designs, the one from IFAE and the one from the Institute of Microelectronics of Barcelona (IMB-CNM, which has similarities with the C2N in Palaiseau, France).

In a full-stack approach, they are also developing **QIBO**, a quantum software platform in the cloud. It is the cloud operating service to run software batches on the future Qilimanjaro quantum annealer, classical quantum emulators and gate-based quantum computers with a design pattern to create classical/quantum hybrid algorithms. But they also plan to sell their hardware to customers willing to use it on-premises.

They initially wanted to launch an ICO (initial coin offering) to fund the company when it was trendy but abandoned it. On top of benefiting from public grants, the company started to work for an unnamed French international company involved in logistics to develop quantum inspired optimization algorithms. They then established a partnership with Abu-Dhabi to help the Emirate create its Quantum Research Centre at the Technology Innovation Institute (QRC-TII). They provide Abu Dhabi with their know-how to build the QCR research lab and team, provide access to their technology with the goal to sell them a multi-qubit quantum processor before 2023, and let them then become self-sufficient. Jose-Ignacio Latorre became their TII's Chief Scientist after the deal was made. In 2020, he also became the director of CQT in Singapore after having been a visiting professor since 2013. CQT may play a role first in Qilimanjaro's software development efforts.

Qilimanjaro also benefits from European funding through the project **AVAQUS** already mentioned. This project coordinator is Pol Forn-Díaz, head of the IFAE Quantum Computing Technologies group on top of his role in Qilimanjaro. It involves the superconducting team from Nicolas Roch at Institut Néel in Grenoble who designs the microwave amplifiers used in flux qubits readouts.

⁶³⁴ Like [Improved variational quantum eigensolver via quasi-dynamical evolution](#) by Manpreet Singh Jattana, Kristel Michielsen et al, February 2022 (19 pages) and [Quantum annealing for hard 2-SAT problems : Distribution and scaling of minimum energy gap and success probability](#) by Vrinda Mehta, Fengping Jin, Hans De Raedt and Kristel Michielsen, February 2022 (17 pages).

⁶³⁵ To learn more about D-Wave, here are their [explanations about the structure of their hardware](#), a [video](#) explaining the structure of D-Wave chipsets, a [video from Linus](#), a blogger who gets into the bowels of a D-Wave 2000Q in quite a detailed way, the [video of Colin Williams's](#) presentation at USI in June 2018 in Paris (33 minutes) as well as [Near-Term Applications of Quantum Annealing](#), 2016, an interesting Lockheed Martin presentation on the uses of a D-Wave computer (34 slides). And testimonials from their customers in [Qubits 2017](#). See also [Brief description on the state of the art of some local optimization methods: Quantum annealing](#) by Alfonso de la Fuente Ruiz, 2014 (21 pages).



At last, let's mention that NEC (Japan) is also developing coherent quantum annealers using parametric oscillators and qubits as couplers.

Their ambition to have an available system by 2023 with an “all-to-all” qubits connectivity (which is actually a nearest-neighbor one)⁶³⁶. They seem to reuse some research work done on superconducting qubits initially aimed at gate-based quantum computing. Meanwhile, they also work on some simulated annealing software running on their classical supercomputer, the SX-Aurora Tsubasa.

Superconducting qubits

After describing superconducting-based quantum annealing, let's move on to gate-based superconducting qubits quantum computers. From a physical point of view, D-Wave's accelerators and superconducting qubits ones have in common to be based on Josephson junctions but their qubit physics, overall architectures, control signals and programming models are way different.

superconducting qubits

- **key technology** in public research and with commercial vendors (IBM, Google, Rigetti, Intel, Amazon, OQC, IQM, etc).
- **record of 127 programmable qubits** with IBM.
- constant progress in **noise reduction**, particularly with the cat-qubits variation which could enable a record low ratio of physical/logical qubits.
- many existing **enabling technologies**: cryostats, cabling, amplifiers, logic, sensors.
- **potentially scalable technology** and deployable in 2D geometries.

- **qubit coherence time usually < 300 μs**.
- **high qubits noise levels** with most vendors.
- **cryogeny constrained** technology at <15 mK.
- **heterogeneous qubits** requiring calibration and complex micro-wave frequency maps.
- **cabling complexity** and many passive and active electronic components to control qubits with micro-waves.
- **qubit coupling limited** to neighbor qubits in 2D structures (as compared with trapped ions).
- **qubits size** and uneasy miniaturization.

Figure 279: superconducting qubits pros and cons. (cc) Olivier Ezratty, 2022.

Superconducting qubits seem to be the kings in quantum computing town, being exploited or chosen by IBM, Google, Rigetti, Amazon, Alibaba, as well as many startups such as IQM (Finland) and OQC (UK). It is the currently best scalable architecture in the gate-based model, even if the results are still modest with a record of 127 operational qubits for with IBM and 66 in China as of mid-2022⁶³⁷.

Like all existing gate-based quantum systems, superconducting qubits computers are in the pre-NISQ or NISQ realm, *aka* noisy intermediate-scale computers, with such a low qubit gates and readout fidelity that they are impractical for most industry use cases.

It is observable with the discrepancy between the number of available physical qubits (72, 80 and 127 with Google, Rigetti and IBM) and the number of qubits that are actually exploited with useful algorithms, that doesn't exceed 20 at this point in time (besides a correction error code using 49 qubits on a 72 qubit chipset by Google in July 2022). IBM's quantum volume is currently capped at 9 useful qubits with their best 27 qubits system using their Falcon R10 chipset.

The short term workaround of low fidelity are quantum error mitigation techniques and adapted quantum algorithms.

⁶³⁶ See [Quantum Computing Initiatives](#), NEC.

⁶³⁷ See a general point on the issue in [Superconducting Qubits: Current State of Play](#) by Morten Kjaergaard et al, MIT & Chalmers, 2020 (30 pages).

Longer term workarounds are quantum error correction and qubits number scalability. It creates problems that are not yet solved with regards to fidelity stabilization with a growing number of qubits, solving the qubits cabling maze with cryogenic electronics or signals multiplexing and scaling cryostats cooling power.

Google and IBM's current approaches to scale their systems are way too optimistic as we'll see later but you can still bet on them solving both fundamental and engineering problems⁶³⁸.

The Josephson effect is used in these qubits to control the flow of a circulating current through a thin nanometric insulating barrier between two superconducting metals, creating a tunnel junction. It creates a nonlinear and nondissipative physical system with a single degree of freedom, the number of Cooper pairs (electron pairs) traversing the tunnel junction conjugated to the superconducting phase difference across it. Superconducting qubits have the particularity of being the only mainstream ones that are macroscopic, in the sense that they are not linked to the control of a single particle as an atom, electron or photon, as in most other qubit technologies.

At superconducting temperature, the superconducting electrons in a Josephson loop look like a single particle, with billions of electron Cooper pairs behaving as bosons which can be condensed into the same quantum state. They form an artificial atom with precisely controllable energy levels according to their parameters comprising a Josephson barrier, some capacitances and inductances connected in series and/or in parallel and some non-destructive readout circuits using a nearby resonator⁶³⁹. One qubit is using about 10^{11} electrons (100 billion).

Superconducting qubits use non dissipative elements: capacitors, inductors and the Josephson junction which act as a nonlinear non-dissipative inductor. Capacitors store energy in the electric field while inductors store energy in the magnetic field. But at any non-zero frequency, superconductors still dissipate some power, through two channels: the transport by the Cooper pairs and by normal charge carriers (quasi-particles), that is proportional to the quasi-particle density, which diminishes exponentially at low temperatures.

History

The history of superconducting qubits started in the mid-1980s but you need to fly back to 1957 with the creation of the **BCS theory** that explained (partially) how pairs of opposite spin electrons - *aka* Cooper pairs - behave at low temperatures, generating the superconducting effect. Then, 1962 marks the Josephson effect discovery by **Brian Josephson**, completed by its experimental proof in 1963 by **Philip Anderson** and **John Rowell**. In 1980, **Antony Leggett** modeled the collective degrees of freedom of superconducting circuits. A bit like a Bose-Einstein condensate of cold atoms, Cooper-pairs of electrons in a superconducting material behave like a single quantum object with its own quantum wave⁶⁴⁰.

In 1985, **John Clarke**, **Michel Devoret** (his post-doc) and **John Martinis** (his PhD), all at Berkeley, implemented the first spectroscopy of such artificial atom, using microwave radiations to excite it, creating the first phase qubit⁶⁴¹. Back then, the JJ (the little nickname for Josephson junctions) was implemented with Nb-NbO_x-PbIn (niobium, lead, indium) and cooled with a He₄-based cryostat.

⁶³⁸ See for example the review paper [A practical guide for building superconducting quantum devices](#) by Yvonne Y. Gao et al, September 2021 (49 pages).

⁶³⁹ This artificial atom property was demonstrated in 1985. See [Energy-Level Quantization in the Zero-Voltage State of a Current-Biased Josephson Junction](#) by John Martinis, Michel Devoret and John Clarke, 1985 (2 pages).

⁶⁴⁰ See [A Brief History of Superconducting Quantum Computing](#) by Steven Girvin, August 2021 (39 mn).

⁶⁴¹ See [Energy-Level Quantization in the Zero-Voltage State of a Current-Biased Josephson Junction](#) by John M. Martinis, Michel H. Devoret and John Clarke, PRL, 1985 (4 pages).

In 1998, **Vincent Bouchiat**, then a PhD in **Michel Devoret**, **Daniel Esteve** and **Cristian Urbina**'s Quantronics group at CEA-Saclay in France, implemented the first Cooper Pairs Box (CPB) in a loop and characterized its ground state.

The first demonstration of quantum coherent superposition with the first excited state was achieved in 1999 by **Yasunobu Nakamura** with **Yuri Pashkin** and **Jaw-Shen Tsai** at NEC Labs in Tsukuba, Japan⁶⁴². It was the first “charge qubit” per se, with a tiny coherence time of 2 ns. They extended it in 2001, implementing the first measurement of Rabi oscillations associated with the transition between two Josephson levels in the Cooper pair box, using the configuration developed by Vincent Bouchiat and Michel Devoret in 1998. A first functional qubit version of the Cooper pair box, the quantronium, was demonstrated by the CEA-Saclay Quantronics team in 2002⁶⁴³.



Figure 280: Daniel Esteve (CEA Quantronics) showing to the author the first operational two-transmon processor in his laboratory, June 2018.

The modern version of the CPB circuit, the transmon, was developed at Yale University in 2006. The Yale University research teams led by **Rob Schoelkopf**, **Michel Devoret** and **Steve Girvin** welcomed many talented theoreticians and experimentalists who were key contributors to the progress of transmon qubits. **Alexandre Blais** and **Andreas Wallraff** developed around 2003-2004 the key principles of circuit QED (cQED)⁶⁴⁴. It allowed quantum non-demolition readout of qubit state in the dispersive regime. A QND readout happens after measurement collapses the wave function onto $|0\rangle$ or $|1\rangle$ and a subsequent readout will yield the same $|0\rangle$ or $|1\rangle$ ⁶⁴⁵. Then, **David Schuster** and **Jay Gambetta** created between 2007 and 2011 2D and 3D cavity resonators designs⁶⁴⁶. **Jens Koch** created Cooper

⁶⁴² See [Coherent control of macroscopic quantum states in a single-Cooper-pair box](#) by Yasunobu Nakamura, Yuri Pashkin and Jaw-Shen Tsai, Nature, 1999 (4 pages).

⁶⁴³ See [Superconducting quantum bits](#) by Hans Mooij, Physics World, December 2004 that provides more technical insights of what was achieved in Japan and France between 1999 and 2022. It took about 12 years to CEA's team to reach 4 qubits as described in the interesting thesis [Design, fabrication and test of a four superconducting quantum-bit processor](#) by Vivien Schmidt, 2015 (191 pages). Back then, IBM and Google teams were also at a similar stage.

⁶⁴⁴ cQED was defined in [Cavity quantum electrodynamics for superconducting electrical circuits: An architecture for quantum computation](#) by Alexandre Blais, Ren-Shou Huang, Andreas Wallraff, Steve Girvin and Rob. Schoelkopf, PRA, 2004 (14 pages) and [Strong coupling of a single photon to a superconducting qubit using circuit quantum electrodynamics](#) by Andreas Wallraff, David Schuster, Alexandre Blais, Steve Girvin, Rob Schoelkopf et al, Nature, 2004 (7 pages). See also [Superconducting Qubits: A Short Review](#) by Michel H. Devoret, Andreas Wallraff and John M. Martinis, 2004 (41 pages) and [Circuit QED and engineering charge based superconducting qubits](#) by Steve Girvin, Michel Devoret and Rob Schoelkopf, 2009 (27 pages).

⁶⁴⁵ QND was created by Vladimir Braginsky (1931-2016) in Russia in the early 1980s.

⁶⁴⁶ See [Circuit Quantum Electrodynamics](#) by David Schuster, 2007 (255 pages), [3D microwave cavity with magnetic flux control and enhanced quality factor](#) by Yarema Reshitnyk et al, 2016 (6 pages) and the foundational paper [Observation of high coherence in Josephson junction qubits measured in a three-dimensional circuit QED architecture](#) by Hanhee Paik, Michel Devoret et al, 2011 (5 pages).

pair boxes with a large shunting capacitance which created a modest reduction in anharmonicity and enabled strong coupling with microwave photons⁶⁴⁷.

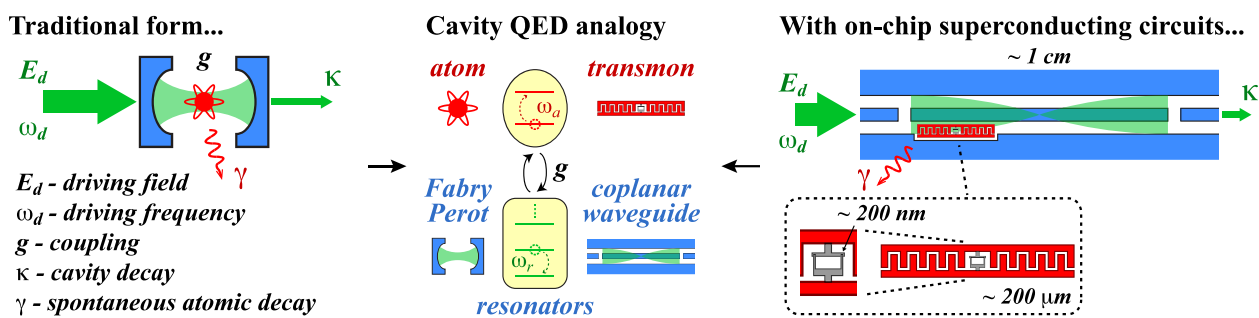


Figure 281: principles of circuit QED. Source: [Circuit QED - Lecture Notes](#) by Nathan K. Langford, 2013 (79 pages).

Jerry Chow was also a key contributor between 2005 and 2010 and has since then been at IBM, now leading their quantum hardware system developments in Jay Gambetta's team. In 2009, Devoret, Schoelkopf, **Leonardo Di Carlo** (now at TU Delft), **Jerry Chow** et al created the first programmable two-qubit processor and implemented a small Grover search on it. **Blake Robert Johnson** proposed in 2011 to use a Purcell filter to protect a qubit from spontaneous emission coming from the Purcell effect that is a relaxation through the readout resonator. It's a mix of low-pass and high-pass microwave filter⁶⁴⁸. **Matt Reagor** and **Hanhee Paik** improved in 2013 the stability of microwaves in 3D resonators used in superconducting qubits⁶⁴⁹. Hanhee Paik has been working as a researcher at IBM since 2014 after a two-year stint at Raytheon BBN. Nowadays, the Yale University team are working on variations of cat-qubits.

Other contributions worth mentioning are **Hans Mooij** (TU Delft) who created a flux-qubit with three Josephson junctions in 1999 with experiments done in 2000. **Andrew Houck** (Princeton) contributed to the development of the transmon qubit. In 2010, **Andrew Cleland**, **John Martinis** and their PhD **Arron O'Connell** were able to entangle three flux superconducting qubits and to control it with a mechanical resonator⁶⁵⁰. It led to the creation of the Xmon tunable qubit in 2013⁶⁵¹, which was later used by Martinis at Google after 2014. **Andrew Cleland** now runs his own lab at the University of Chicago. In 2017, **Peter Leek** then at Oxford created the coaxmon superconducting qubit, where the qubit and resonator are on opposing sides of a single chip, with control and readout wiring being provided by coaxial wiring running perpendicular to the chip plane⁶⁵².

It led the same year to the creation of OQC. At last, in 2022, **Mikko Möttönen** from IQM created the Unimon superconducting qubit with a simpler setting, better nonlinearity and fidelities⁶⁵³.

⁶⁴⁷ See [Charge insensitive qubit design derived from the Cooper pair box](#) by Jens Koch, Terri M. Yu, Jay Gambetta, Andrew. Houck, David Schuster, J. Majer, Alexandre Blais, Michel Devoret, Steve Girvin and Rob Schoelkopf, 2007 (21 pages). That's quite a hall of fame for a paper!

⁶⁴⁸ See [Controlling Photons in Superconducting Electrical Circuits](#) by Blake Robert Johnson, a thesis under the direction of Rob Schoelkopf, 2011 (190 pages) which proposed the Purcell filter. See also [Controlling the Spontaneous Emission of a Superconducting Transmon Qubit](#) by Andrew Houck, Jay Gambetta, Michel Devoret, Rob Schoelkopf et al, 2008 (4 pages) and [Quantum theory of a bandpass Purcell filter for qubit readout](#) by Eyob A. Sete et al, 2015 (15 pages). The spontaneous emission rate (SER) is one key contributor that affects a superconducting qubit coherence time T_1 .

⁶⁴⁹ See [Reaching 10 ms single photon lifetimes for superconducting aluminum cavities](#) by Matt Reagor, Hanhee Paik et al, 2013 (4 pages).

⁶⁵⁰ See [Quantum ground state and single-phonon control of a mechanical resonator](#) by Aaron O'Connell, John Martinis, Andrew Cleland et al, Nature, 2010 (7 pages).

⁶⁵¹ See [Coherent Josephson qubit suitable for scalable quantum integrated circuits](#) by R. Barends, John Martinis and Andrew Cleland, April 2013 (10 pages).

⁶⁵² See [Double-sided coaxial circuit QED with out-of-plane wiring](#) by J. Rahamim, Peter Leek et al, 2017 (4 pages).

⁶⁵³ See [Unimon qubit](#) by Eric Hyppä, Mikko Möttönen et al, March 2022 (37 pages).

superconducting qubits timeline

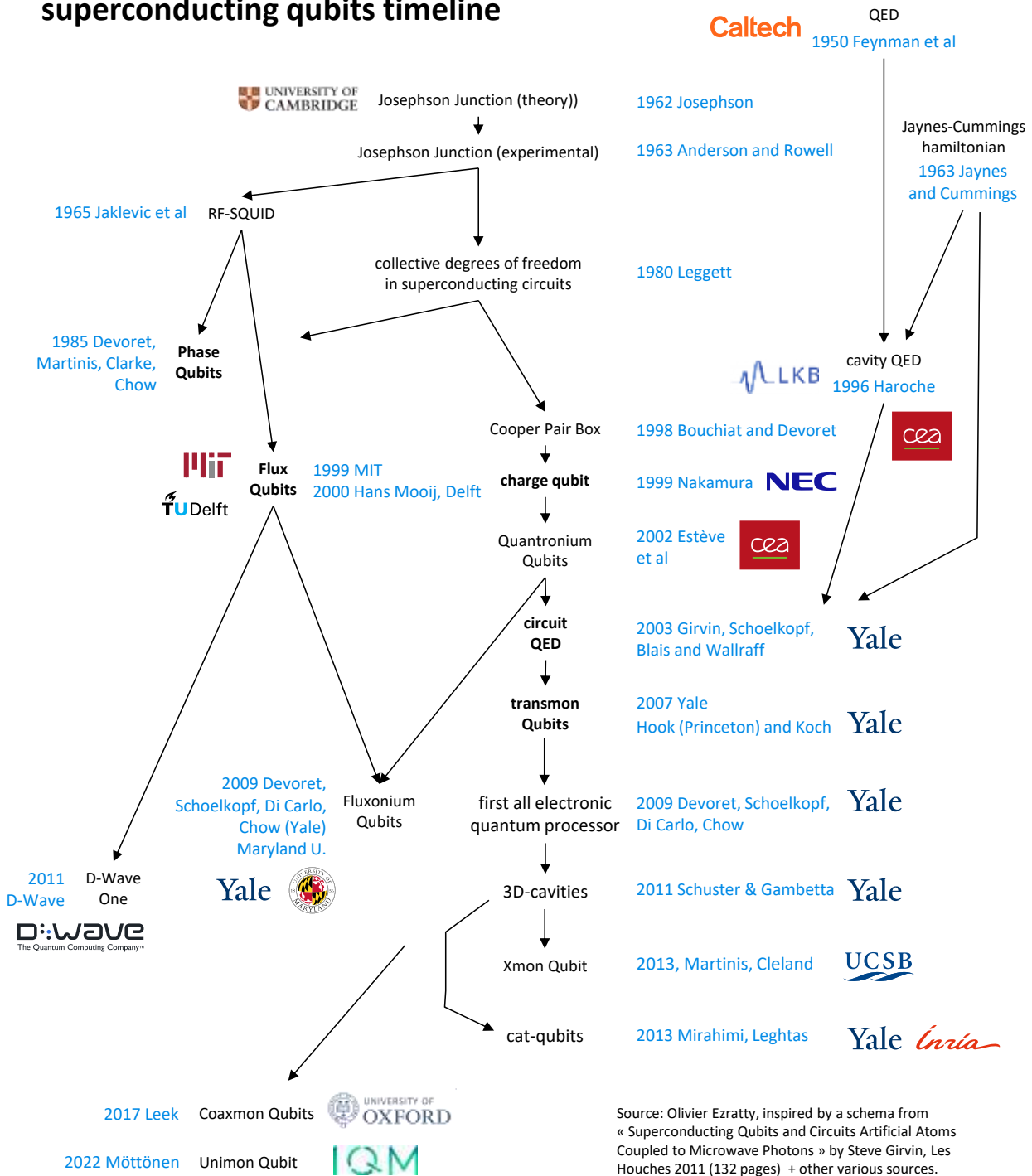


Figure 282: a historical timeline of superconducting qubits. The contribution of scientists at Yale University seems dominant here, thus the nickname of the “Yale gang”. (cc) Olivier Ezratty, 2022.

We’ll also talk later about the cat-qubits, created in 2013 by **Maryar Mirrahimi** and **Zaki Leghtas**.

Let’s now circle back to the different types of superconducting qubits that differ in the way they encode quantum information in two distinct states⁶⁵⁴:

Phase Qubits use larger Josephson junctions than in charge qubits. Their state corresponds to two levels of current energy in a Josephson junction. This approach was tested by NIST in the USA among other places but no commercial vendor seems to use this type of superconducting qubit. John Martinis

⁶⁵⁴ This is well explained in [Practical realization of Quantum Computation](#), (36 slides).

tested such qubits back in 2012 at UCSB in a 5-qubit system used to factorize the number 15⁶⁵⁵. A German (Jülich, University of Munster) and Russian (Kotelnikov Institute) team proposed in early 2020 to use YBa₂Cu₃O_{7-x} nanotubes (also called YBCO, for yttrium, barium, copper and oxide, which is superconducting at 92K) to create phase qubits controllable by a single microwave photon⁶⁵⁶.

Flux Qubits: their states correspond to the direction of flow of the superconducting current in its loop. It couples a capacitor, from one to three Josephson junctions and a superinductor and has high coherence and large anharmonicity which also enable the handling of qutrits instead of qubits like what Rigetti is experimenting. Measuring the state of such a qubit uses a SQUID (superconducting quantum interference device) with two Josephson junctions connected in parallel, a magnetometer that measures the current direction in the qubit, thus its basis state 0 or 1. This type of superconducting qubit is adopted by D-Wave (in annealing mode and soon, gate-based mode) and Qilimanjaro (in annealing mode), Rigetti, Alibaba⁶⁵⁷, Bleximo and Atlantic Quantum in the vendors space. It is studied in research labs at the MIT, TU-Delft (until 2010), the Lawrence Berkeley National Laboratory (Irfan Siddiqi⁶⁵⁸), the University of Berkeley and Yale University (Shruti Puri), the University of Maryland (Vladimir Manucharyan⁶⁵⁹), in Russia⁶⁶⁰.

In recent works, fluxonium qubits generated the best T_1/T_2 with T_1 exceeding 1 ms. They use control frequencies below 1 GHz which lowers down dielectric loss effects and leads to long relaxation time T_1 . Single-qubit gates can have good speed in the range of 10 ns and errors levels around 10^{-4} . In this architecture, both readout and control crosstalk are expected to be small⁶⁶¹. Their main shortcomings are their lower control frequencies and bad protection from both relaxation (T_1) and dephasing (T_2).

Charge Qubits: their states correspond to current flow thresholds in the Josephson junction of the superconducting loop. Small Josephson junctions delimit a superconducting island with a well-defined electrical charge. The basis states of such charge qubits are the states of charge of the island in Cooper pairs. The most common variant is the **transmon**, for “transmission line shunted plasma oscillation qubit”, which reduces the effect of charge noise but with a weaker anharmonicity⁶⁶². With transmons, the Cooper pairs box is operated in the phase regime.

The nonlinear Josephson junction inductance makes the LC resonator slightly anharmonic, and its two lowest energy levels are the basis states of the qubit. Transmons are used by IBM, Google, IQM and others. To date, these are the qubits generating the lowest error rate in superconducting qubits but their low anharmonicity creates a toll on gate and readout speeds.

⁶⁵⁵ See [Computing prime factors with a Josephson phase qubit quantum processor](#) by Erik Lucero, John Martinis et al, 2012 (5 pages).

⁶⁵⁶ See [Energy quantization in superconducting nanowires](#), February 2020, referring to [Energy-level quantization and single-photon control of phase slips in YBa₂Cu₃O_{7-x} nanowires](#) by M. Lyatti, February 2020.

⁶⁵⁷ See [Fluxonium qubits for ultra-high-fidelity and scalable quantum processors](#) by Chunqing Deng, (49 minutes) and [Fluxonium: An Alternative Qubit Platform for High-Fidelity Operations](#) by Feng Bao et al, 2022 (19 pages).

⁶⁵⁸ See [Scalable High-Performance Fluxonium Quantum Processor](#) by Long B. Nguyen, Irfan Siddiqi Singh et al, January 2022 (29 pages).

⁶⁵⁹ See [Millisecond coherence in a superconducting qubit](#) by Aaron Somoroff, Vladimir Manucharyan et al, University of Maryland, March 2021 (14 pages). Not only do they have a T_2 exceeding 1.35 ms but their single-qubit gate fidelity also exceeds 0.9999. See also [The high-coherence fluxonium qubit](#) by Long B. Nguyen, Vladimir E. Manucharyan et al, October 2018 (12 pages).

⁶⁶⁰ See [High fidelity two-qubit gates on fluxoniums using a tunable coupler](#) by Ilya N. Moskalenko, Russia, March 2022 (18 pages) which proposes a fluxonium architecture with two qubits CZ gates fidelities of 99,23%.

⁶⁶¹ See [Transmon and Fluxonium Qubits](#) by Emanuel Hubenschmid, June 2020 (106 slides).

⁶⁶² See [Charge insensitive qubit design derived from the Cooper pair box](#) by Jens Koch, Jay Gambetta, Alexandre Blais, Michel Devoret, Rob Schoelkopf et al, 2007 (21 pages).

They are divided into at least two categories: qubits with a single Josephson junction (single junction transmon, used by IBM) or with two Josephson junctions connected in parallel (spit transmon, used by Google)⁶⁶³.

Then, you have many variations with the **coaxmon** (OQC) and **unimon** (IQM) and the **mergemon** or merged element transmon where the Josephson junction is engineered to act as its own parallel shunt capacitor, reducing the size of the qubit⁶⁶⁴.

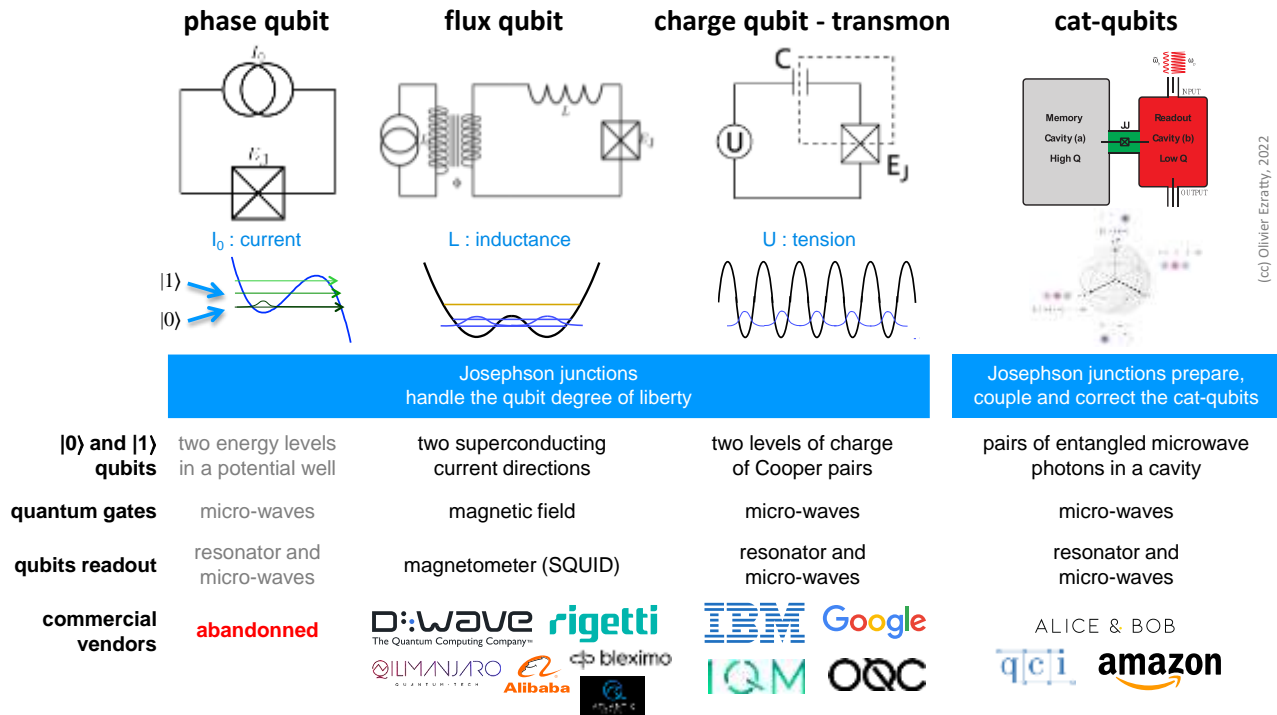


Figure 283: the different types of superconducting qubits and the related industry vendors. inspired from [Implementing Qubits with Superconducting Integrated Circuits](#) by Michel Devoret, 2004 (41 pages) and [Flux Noise in Superconducting Qubits](#), 2015 (44 slides).

Andreev Spin Qubits (ASQ) is a research-level qubit that relies on a localized microscopic excitation of the BCS condensate that natively has only two levels and is based on a nanowire. It is not a collective excitation of the superconducting loop circuit. This qubit type was proposed at and is studied at Chalmers in Sweden⁶⁶⁵ (funded as a H2020 program from 2019 to 2023⁶⁶⁶), at CEA Saclay in France⁶⁶⁷, NBI in Denmark and also QuTech in The Netherlands, among other places.

Since it manipulates electron spins in relation to a superconducting resonator and makes use of circuit electrodynamics (cQED), it sits in between the categories of superconducting and silicon spin qubits.

⁶⁶³ Transmon is a diminutive of "Transmission line shunted plasmon oscillation circuit" created by Rob Schoelkopf, in other words, an oscillator circuit based on shunted Josephson junction. The shunt has become a capacitance that filters low frequencies. A plasmon is the collective behavior of free electrons of metals, here in the form of superconducting Cooper pairs.

⁶⁶⁴ See [Merged-element transmon](#) by R. Zhao et al, December 2020 (8 pages) and [Merged-Element Transmons: Design and Qubit Performance](#) by H. J. Mamin et al, IBM Research, August 2021 (8 pages).

⁶⁶⁵ See the initial proposal in [Andreev Level Qubit](#) by A. Zazunov et al, PRL, 2003 (4 pages), [Dynamics and phonon-induced decoherence of Andreev level qubit](#) by A. Zazunov et al, PRB, 2005 (22 pages) and the thesis [Coherent manipulation of Andreev Bound States in an atomic contact](#) by Camille Janvier, CEA Qnantronic, 2016 (268 pages). And recent research in [Coherent manipulation of an Andreev spin qubit](#) by M. Hays, Michel Devoret et al, Science, 2021 (17 pages) and [Direct manipulation of a superconducting spin qubit strongly coupled to a transmon qubit](#) by Marta Pita-Vidal et al, August 2022 (24 pages).

⁶⁶⁶ See [Andreev qubits for scalable quantum computation](#) with an EU contribution of 3.5M€.

⁶⁶⁷ See [Circuit-QED with phase-biased Josephson weak links](#) by C. Metzger, Christian Urbina, Hugues Pothier et al, January 2021 (22 pages).

cat-qubits are cavity-based qubits connected to a transmon qubit used only for their preparation, readout and/or correction depending on the implementation. The cat-qubit technique was devised by Mazyar Mirrahimi and Zaki Leghtas around 2013, particularly during their work at Yale University with Michel Devoret. It was then adopted by Rob Schoelkopf's team at Yale.

bosonic qubits is a broad category of qubits that are resilient to noise or generating less noise and make it possible to assemble logical qubits with much fewer physical qubits, in the 10-100 range instead of 1,000-10,000 range⁶⁶⁸. It contains cat-qubits and **GKP codes**⁶⁶⁹. Other protected qubits include the **zero- π qubits** of Peter Brooks, Alexei Kitaev and John Preskill which use two Josephson junctions, the **bifluxon**⁶⁷⁰ and other variants⁶⁷¹.

The cat-qubits approach is chosen by **Alice&Bob** (France), **Amazon** (USA) and **QCI** (USA) while **Nord Quantique** (Canada) seems to use another breed of bosonic code. Cat-qubits are also investigated in many other research labs like **RIKEN** in Japan⁶⁷². The **QuCoS** QuantERA collaborative three-year European project is focused on demonstrating the scalability of cat-qubits. It combines the University of Innsbruck (Gerhard Kirchmair), ENS Lyon (Benjamin Huard), Mines ParisTech and ENS Paris (Zaki Leghtas), KIT (Ioan Pop), Inria (Mazyar Mirrahimi), the Romanian National Institute for Research and Development of Isotopic and Molecular Technologies (Luiza Buimaga-Iarinca) and Quantum Machines (Israel).

How about using superconducting qubits for implementing quantum simulations? It is not a common practice. One of the reasons is the lack of generic long-range connectivity that could enable some direct entanglement between all qubits. It would require a different physical arrangement of the qubits and to create specific long-range connections between the qubits. This is possible with using cross-resonance gates that create interactions between qubits with their respective resonance frequencies.

Science

For what follows, we will focus on those transmon qubits that are the most common and exploited by IBM, Google and IQM. They are anharmonic and therefore nonlinear oscillators. Their nonlinearity comes from the Josephson junction which allows to better separate two energy states of the superconducting loop (*on the right in Figure 284*) than with a simple linear resonator coupling a capacitor and an inductor (*on the left in Figure 284*). In a harmonic oscillator, the energy levels are spaced equally and are multiples of the first energy level ($\hbar\omega_r$ in the diagram).

The capacitance has an electrical energy (kinetic) and the inductance has a magnetic energy (potential). With the transmon qubit, the Josephson tunnel junction has a nonlinear inductance which creates its anharmonicity. In both cases, the flowing current is quantized with discrete energy levels corresponding to the horizontal bars in the graph in Figure 284, with corresponding different current phases corresponding to the intersection between these bars and the parabolic (CPB) and cosinusoidal (JJ) curves.

⁶⁶⁸ See [Quantum information processing with bosonic qubits in circuit QED](#) by Atharv Joshi et al, 2021 (24 pages).

⁶⁶⁹ See [Quantum Error Correction with the GKP Code and Concatenation with Stabilizer Codes](#) by Yang Wang, July 2019 (59 pages).

⁶⁷⁰ See [Moving beyond the transmon: Noise-protected superconducting quantum circuits](#) by András Gyenis, Alexandre Blais, Andrew A. Hook, David I. Schuster et al, June 2021 (14 pages).

⁶⁷¹ Like [Superconducting circuit protected by two-Cooper-pair tunneling](#) by W. C. Smith, A. Kou, X. Xiao, U. Vool and M. H. Devoret, 2020 (9 pages) which uses pairs of Cooper pairs to create a qubit that is insensitive to multiple relaxation and dephasing mechanisms. And also [Encoding qubits in multimode grid states](#) by Baptiste Royer, Shraddha Sing and Steven M. Girvin, January 2022 (38 pages) and [Coherent control of a multi-qubit dark state in waveguide quantum electrodynamics](#) by Maximilian Zanner et al, Nature Physics, March 2022 (8 pages).

⁶⁷² See [Fault-Tolerant Multi-Qubit Geometric Entangling Gates Using Photonic Cat Qubits](#) by Ye-Hong Chen et al, RIKEN, 2021 (12 pages). About a realization of Mølmer-Sørensen multi-qubit cat-qubits gates.

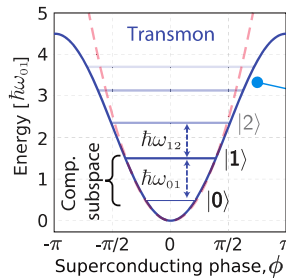
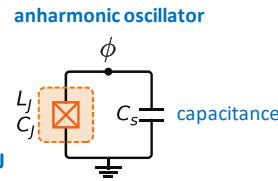
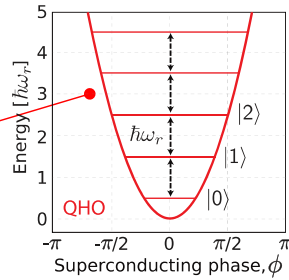
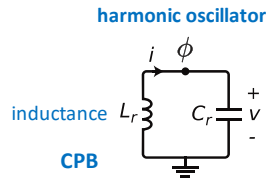
These energy states are usually controlled by microwaves pulses. These interactions between superconducting qubits and microwave photons are part of a branch of quantum physics called **circuit quantum electrodynamics**, or cQED⁶⁷³.

ϕ : oscillator phase
 L_r : linear inductance
 C_r : capacity
 \hbar : Dirac constant
 ω_r : pulse (2π *frequency)
 H : oscillator Hamiltonian

Cooper Pairs Box (CPB)
 inductance+capacitance
 energy parabolic curve =>
 equally spaced energy levels.

$$H = 4E_C n^2 + \frac{1}{2} E_L \phi^2$$

$\hbar\omega_r$: constant energy
 required to switch levels
 => hard to control
 qubits states $|0\rangle$ and $|1\rangle$,
 since a microwave pulse with energy $\hbar\omega_r$
 could switch qubit from state $|1\rangle$ to $|2\rangle$.



Josephson junction with:
 L_J : non linear inductance
 C_J : inductance capacity
 E_C : Coulomb charge energy.
 E_J : Josephson coupling energy.
 E_L : inductance energy.

Josephson Junction (JJ)
 energy cosinusoidal curve =>
 unequally spaced energy levels.

$$H = 4E_C n^2 + E_L \cos(\phi)$$

thanks to the loop non-linearity, energy transitions $\hbar\omega_{nm}$ between adjacent levels are different and are decreasing, so a microwave pulses used to switch from $|0\rangle$ to $|1\rangle$ won't push $|1\rangle$ state to $|2\rangle$ and beyond.

- these oscillators have evenly or unevenly quantized energy levels $|i\rangle$.
- $|0\rangle$ and $|1\rangle$ qubits states are evaluated with the phase of the oscillator.
- the oscillator phase has nothing to do with the qubit relative phase represented in its Bloch sphere representation.

Figure 284: why superconducting qubits use an anharmonic oscillator. (cc) Olivier Ezratty, 2022, with schema from "A Quantum Engineer's Guide to Superconducting Qubits" by Philip Krantz et al, 2019.

Qubits use a linear superposition of the first two energy levels which have a different wave function relating the phase and current probabilities across the Josephson junction. The superposed states in the Bloch sphere equator like $(|0\rangle + |1\rangle)/\sqrt{2}$ and $(|0\rangle - |1\rangle)/\sqrt{2}$ correspond to an oscillating current that is dampened over time, as Rabi oscillations, in the 10 MHz range, shown in Figure 285. The $\hbar\omega_{01}$ energy level between the basis states $|0\rangle$ and $|1\rangle$ correspond to microwave frequencies in the 4 to 8 GHz band.

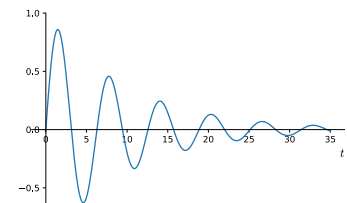


Figure 285: a Rabi oscillation for superposed qubit states, at a frequency in the 10 MHz range.

These frequencies must be well separable from the following ones. This separation is made possible because the (microwave photon) energy sent to move from one level to the other is different from one of these levels to other higher levels. Since the upper levels are less spaced, their related transition energy is lower. As the qubits are activated by microwaves, they are no longer likely to switch to a higher energy level. The anharmonic oscillator in the Josephson loop is provided by a nonlinear inductance L_J . The energy level between $|0\rangle$ and $|1\rangle$ of $\hbar\omega_{01}$ is higher than the energy levels needed to go to the upper levels $\hbar\omega_{12}$ and $\hbar\omega_{23}$. It is also compatible with the cooling temperature of the processor and the ambient noise.

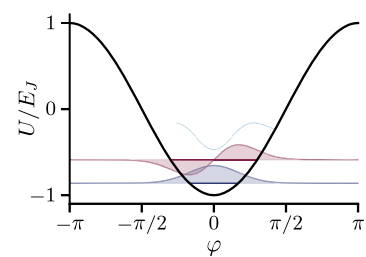


Figure 286: $|0\rangle$ and $|1\rangle$ wave function giving the probability of phase ϕ in blue and green. Source: [Superconducting circuit protected by two-Cooper-pair tunneling](#) by W. C. Smith et al, 2020 (9 pages).

⁶⁷³ See [Circuit-QED with phase-biased Josephson weak links](#) by C. Metzger, Christian Urbina, Hugues Pothier et al, January 2021 (22 pages). Serge Haroche was awarded the Nobel Prize in Physics in 2012 for his work on the interaction between cold atoms and superconducting cavities. See on this subject the excellent [Circuit Quantum Electrodynamics](#) by Alexandre Blais, Andreas Wallraff et al, May 2020 (82 pages).

Those of the superconducting qubits control around 5 GHz have an energy level equivalent to a temperature of about 250 mK, much higher than the 15 mK temperature commonly used⁶⁷⁴. The micro-waves for silicon qubit control are located between 8 and 26 GHz and enable qubit temperatures of 100 mK while some can even reach 1,5K.

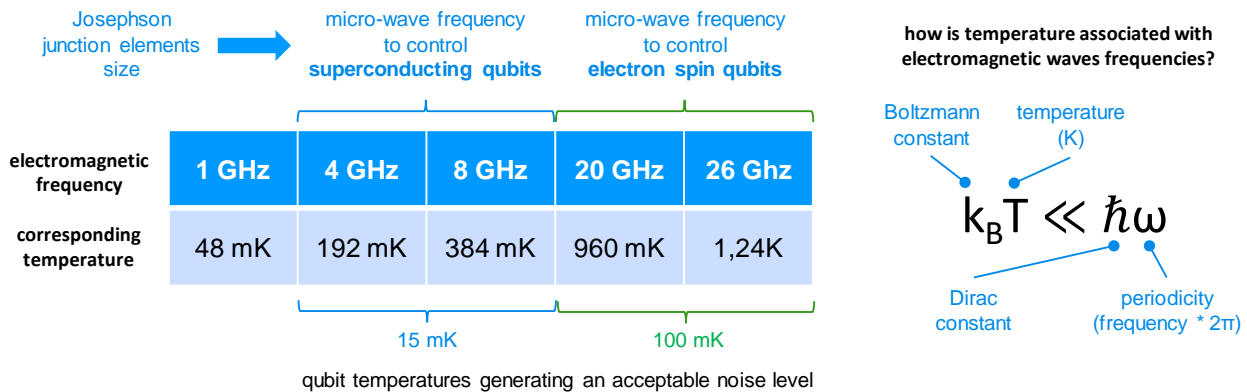


Figure 287: the rationale behind the 15 mK operating temperature of superconducting qubits. (cc) Olivier Ezratty, 2021.

There is another reason for running the qubit at around 15 mK. It takes a certain amount of energy, known as the energy gap, to break up the Cooper pairs running in a superconducting qubit. In aluminum that is the typical material used to create the Josephson junction and its surroundings, the energy gap corresponds to 90 GHz at 20 mK. It is an order of magnitude greater than the energy difference between the two levels in a qubit. It means that the qubit can be driven with lower energies (in the 4-8 GHz range) without breaking up the superconducting current Cooper pairs and altering the quantum coherence of the qubit⁶⁷⁵.

What differentiates phase, charge (transmon) and flux qubits are the relative values of the charge energy (E_C , aka Coulomb charge energy), the Josephson coupling energy (E_J) and the qubit inductance energy (E_L)⁶⁷⁶.

| E_J/E_C | $E_L/(E_J - E_C)$ | | | |
|-------------|-------------------|-----------|-------------|------------|
| | 0 | $\ll 1$ | ~ 1 | $\gg 1$ |
| $\ll 1$ | cooper-pair box | | | |
| ~ 1 | quantronium | fluxonium | | |
| $\gg 1$ | transmon | | | flux qubit |
| $\gg \gg 1$ | | | phase qubit | |

Table 1: “periodic table” of superconducting quantum circuits

Figure 288: periodic table of superconducting circuits. Source: [Introduction to Quantum Electromagnetic Circuits](#) by Uri Vool and Michel Devoret, 2017 (56 pages).

Then, just with transmon qubits, you find other variations with:

- Fixed (IBM, MIT⁶⁷⁷) or tunable (Google) qubit frequencies.
- Tunable couplers (Google).
- Architectures mixing digital and analog superconducting computing⁶⁷⁸.

⁶⁷⁴ See [Why 4-8 GHz? The rationale behind common qubit frequencies](#), The Observer, January 2022, explains the rationale for the microwaves frequencies being used with superconducting qubits. Above 8 GHz, electronics are too expensive and below 4 GHz, the ambient thermal noise is too important.

⁶⁷⁵ Source: [Superconducting quantum bits](#) by Hans Mooij, Physics World, December 2004.

⁶⁷⁶ This is well explained in [Experiments on superconducting qubits coupled to resonators](#) by Marcus Jerger aus Bühl, 2013 (140 pages).

⁶⁷⁷ See [Cancelling microwave crosstalk with fixed-frequency qubits](#) by Wuerkaixi Nuerbolati et al, April 2022 (5 pages).

⁶⁷⁸ See [Superconducting Circuit Architecture for Digital-Analog Quantum Computing](#) by J. Yu, Enrique Solano et al, March 2021 / May 2022 (23 pages).

- Controlled-phase gates with variable amplitude and frequency which could significantly reduce the depth of quantum circuits particularly for implementing a quantum Fourier transform required in many algorithms like Shor, HHL and QML (C-R_θ)⁶⁷⁹.
- New techniques to implement faster qubit readout⁶⁸⁰.
- And techniques using qutrits instead of qubits (with Rigetti).

Of course, many researchers are looking for ways to improve qubits fidelities with better materials and designs⁶⁸¹.

In some cases, researchers invent useless things like with trying to entangle superconducting qubits with tardigrades⁶⁸².

But the physics of a superconducting qubit is much more complicated than that for the neophyte. The qubit itself is coupled to a cavity containing a resonator usually implemented as a **coplanar waveguide** (CPW) resonator on a superconducting circuit. Its length usually corresponds to a quarter-wavelength or the resonator drive frequency. With a 6 GHz drive frequency, it turns into a 1.25 cm resonator that is usually squeezed in a serpentine layout.

$$H = \hbar\omega_r \left(a^\dagger a + \frac{1}{2} \right) + \frac{\hbar\omega_q}{2} \sigma^z + \hbar g (a^\dagger \sigma^- + \sigma^+ a) + \hat{H}_\kappa + \hat{H}_\gamma$$

angular oscillation frequency of the relevant cavity mode
 energy difference of the two qubit levels
 strength of interaction between cavity and qubit
 mediate relaxation and dephasing through coupling to an external bath
 cavity qubit
 total energy of qubit + cavity
 cavity harmonic oscillator energy
 qubit energy
 coherent exchange of excitations between the qubit and cavity
 coupling between cavity and qubit
 coupling to environment
 resonator photons
 a : annihilation operator
 a^\dagger : creation operator
 σ^z : qubit amplitude
 $\sigma^- = \frac{1}{2}(\sigma^x - \sigma^y) = |-\rangle$ superposed state
 $\sigma^+ = \frac{1}{2}(\sigma^x + \sigma^y) = |+\rangle$ superposed state
 $\omega_{rq} = \omega_q - \omega_r$: detuning of qubit from the cavity

Figure 289: Jaynes-Cumming cQED Hamiltonian, (cc) Olivier Ezratty, 2022.

The energy of the ensemble is modeled by a **Jaynes-Cummings Hamiltonian** as shown in Figure 289⁶⁸³.

⁶⁷⁹ See [Extensible circuit-QED architecture via amplitude- and frequency-variable microwaves](#) by Agustin Di Paolo, Alexandre Blais, William D. Oliver et al, MIT, April 2022 (29 pages).

⁶⁸⁰ See [Fast readout and reset of a superconducting qubit coupled to a resonator with an intrinsic Purcell filter](#) by Yoshiki Sunada, Yasunobu Nakamura et al, February 2022 (12 pages) and [Realization of fast all-microwave CZ gates with a tunable coupler](#) by Shaowei Li, Jian-Wei Pan et al, February 2022 (12 pages).

⁶⁸¹ Like with [Engineering superconducting qubits to reduce quasiparticles and charge noise](#) by Xianchuang Pan et al, February 2022 (23 pages) which reduces quasiparticles generation coming from broken Cooper pairs.

⁶⁸² See [Entanglement between superconducting qubits and a tardigrade](#) by K. S. Lee et al, December (19 pages) and the pushback it generated in [Peers dispute claim that tardigrades were entangled with qubits](#) by Bob Yirka, Phys.org, December 2021, [Schrodinger's Tardigrade Claim Incites Pushback At issue: Quantum-entangled water bears?!](#) by Philippe Ross, IEEE Journal, December 2021 and [Frequency Shifts Do Not Imply Quantum Entanglement](#) by Ben Brubaker, January 2022. The arXiv paper was later published in the [New Journal of Physics](#) from IOP Science.

⁶⁸³ See [The Jaynes-Cummings model and its descendants](#) by Jonas Larson and Th. K. Mavrogordatos, February 2022 (237 pages).

This involves many notions like a Jaynes-Cummings spectrum, a resonant regime (the cavity-qubit are interoperating oscillators), dressed states (the different energy levels of the qubits) and a dispersive regime (enabling qubits readout with the resonator)⁶⁸⁴.

Many parameters define a superconducting qubit's characteristics, like its **Q factor**, the ratio between the energy stored in an oscillator and the energy dissipated per oscillation cycle times 2π . It characterizes the stability of a superconducting qubit and determines its T_1 or relaxation time. The greater the Q factor is, the longer T_1 will be⁶⁸⁵ but it can be detrimental to noise sensitivity.

Qubit operations

The general principle of superconducting qubits operations is as follows:

- **Qubit quantum state** in the generic case of a transmon is a two-level charge of Cooper pairs that correspond to a nonlinear oscillator containing at least a Josephson junction and a capacitance laid out in a current loop. A flux bias (direct current pulse) can be used to individually control each qubit resonant frequency if it is frequency tunable. It can help reduce control frequency crosstalk between qubits but at the cost of a lower lifetime (T_1). It is better to have fixed and different qubit frequencies.

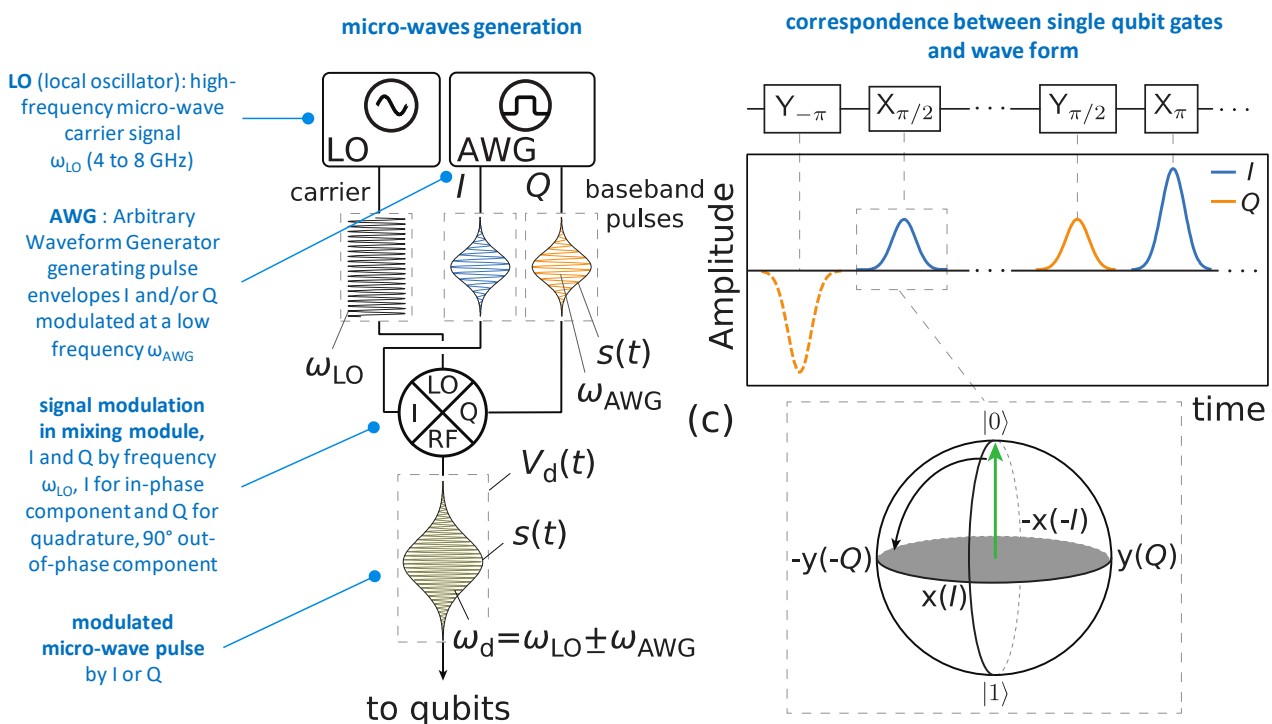


Figure 290: qubit drive microwaves generation. Source: [A Quantum Engineer's Guide to Superconducting Qubits](#), by Philip Krantz et al, 2019 (67 pages).

⁶⁸⁴ Some sources to learn cQED: the review paper [Microwave photonics with superconducting quantum circuits](#) by Xiu Gu et al, 2017 (170 pages) that describes well how superconducting qubits interact with microwaves. [Superconducting Qubits and Circuits Artificial Atoms Coupled to Microwave Photons](#) by Steve Girvin, Les Houches 2011 (132 pages), the review [Practical Guide for Building Superconducting Quantum Devices](#) by Yvonne Y. Gao, Adriaan Rol, Steven Touzard and Chen Wang, November 2021 (48 pages) and [Superconducting qubit in a resonator test of the Leggett-Garg inequality and single-shot readout](#) by Agustin Palacios-Laloy, 2010 (253 pages).

⁶⁸⁵ See [Decoherence benchmarking of superconducting qubits](#) by Jonathan J. Burnett et al, Nature, 2019 (8 pages) and [Extending Coherence in Superconducting Qubits: from microseconds to milliseconds](#) by Adam Patrick Sears, a thesis under the supervision of Rob Schoelkopf, 2013 (178 pages).

- **Single-qubit quantum gates** are generated by microwave pulses sent via coaxial cables on the qubits. Their frequency is adjusted to the energy level $\hbar\omega_{01}$ mentioned above. This frequency is calibrated to be different on adjacent qubits to avoid crosstalk effects⁶⁸⁶. The microwave pulse amplitude controls the rotation angle and its phase adjusts the axis of the gate rotation operation.

This makes it possible to create T, S and R gates with a phase other than a quarter or half turn in the Bloch sphere⁶⁸⁷. In practice, two arbitrary waveform generators create a wave form for “in-phase” and “quadrature” (I and Q) signals which are two microwave pulses that have the same (local-oscillator originated) frequency and are 90° out of phase, as shown in Figure 290.

The I signal is a cosine waveform and the Q signal is a sine waveform. They add-up in the mixer to create a pulse signal with an arbitrary phase depending on the relative amplitudes of the I and Q waveform signals⁶⁸⁸. The mixer then adds the local oscillator signal to the resulting signal⁶⁸⁹. At 5 GHz, an LO pulse lasts 0,2 ns. Most single qubit gate last at least 10 to 20 ns. It means in that case that a generated microwave packet contains about 50 to a hundred 5 GHz pulses shaped by its wave form. Microwave pulses generated at ambient temperature are progressively attenuated and filtered at every stage of the cryostat so that only a couple hundred microwave photons reach the qubit. The attenuators eliminate photons proportionally to the cooling budget available at each cold plate stage.

- **Two-qubit quantum gates** are realized with a coupling circuit positioned between the two qubits, which can be a simple capacitor or a dynamically controllable system. As we will see later, this coupling is managed with an intermediate qubit in Google's Sycamore processor and their Chinese equivalents. IBM is not using couplers but instead cross-resonance gates.
- **Qubits readout** depends on its type. With transmon qubits, a resonator is coupled to the qubit. It transmits a microwave pulse in a resonator that is coupled with the qubit using microwave reflectometry. The qubit state slightly affects the resonator frequency and phase. These readout microwaves are usually amplified in several stages. The method is called “dispersive readout” where for a fixed microwave drive frequency, the resonance frequency of the waveguide resonator shifts depending on the qubit measured state⁶⁹⁰. This measurement technique protects the qubit from all radiations except the readout microwave pulse at ω_r , it amplifies the outgoing signal with the lowest added noise (near the quantum limit). The readout also creates a differentiated phase in the reflected microwave that is analyzed after demixing which generates the in-phase and quadrature signals (I/Q). Measuring the phase of the reflected microwave determines the state of the qubit after measurement without destroying it. It’s a QND readout as already explained.

⁶⁸⁶ A precise calibration of these frequencies is also necessary because of the variability of the behavior of Josephson loops, which are different from one another due to imprecise manufacturing techniques. This variability does not exist for qubits based on single particles such as trapped ions or cold atoms. See [Control and mitigation of microwave crosstalk with frequency-tunable qubits](#) by Ruixia Wang et al, Beijing Academy of Quantum Information Sciences, July 2022 (5 pages) which proposes a quantum error mitigation technique limiting the impact of crosstalk. Static ZZ crosstalk is the one many researchers are working to suppress like in [Frequency adjustable Resonator as a Tunable Coupler for Xmon Qubits](#) by Hui Wang et al, China, August 2022 (12 pages). ZZ crosstalk errors can be described as the amplitude of one qubit influencing the amplitude of other qubits. ZX or ZY errors are linked to the amplitude of a qubit influencing the phase of other qubits.

⁶⁸⁷ These gates can be optimized by modulating the pulsation in an optimal way. See [Implementing optimal control pulse shaping for improved single-qubit gates](#) by J. M. Chow et al., May 2020 (4 pages) which anticipates the capacity to generate single-qubit gates in 1 ns, against a current minimum of around 20 ns.

⁶⁸⁸ See [Radio frequency mixing modules for superconducting qubit room temperature control systems](#) by Yilun Xu, Irfan Siddiqi et al, Lawrence Berkeley National Laboratory, July 2021 (7 pages) that describes the role of a signal mixer.

⁶⁸⁹ Another option consists in mixing the LO signal separately with the I and Q signals and then merge the resulting signal, removing unwanted spurious frequency components. See [Frequency Up-Conversion Schemes for Controlling Superconducting Qubits](#) by Johannes Herrmann, Andreas Wallraff et al, October 2022 (9 pages).

⁶⁹⁰ See [Dispersive Readout, Rabi- and Ramsey-Measurements for Superconducting Qubits](#) by Can Knaut, 2018 (25 slides).

One first stage can use a low-noise superconducting Josephson Parametric Amplifier (JPA) or Traveling Wave Parametric Amplifier (TWPA) operating at the quantum limit, then with a high electron mobility transistor (HEMT) amplifier running at the 4K stage and, at last, with a Low Noise Amplifier (LNA) running at room temperature.

At last, the amplified microwave is converted in digital format with an ADC (analog to digital converter) and analyzed by a FPGA circuit to identify the qubit basis states $|0\rangle$ or $|1\rangle$ with a microwave phase analysis.

Frequency-based multiplexed readout can also be achieved to simplify the wiring exiting the qubit chipset. The readout microwave is modulated with a higher frequency than the quantum gates frequency, above 6 GHz⁶⁹¹.

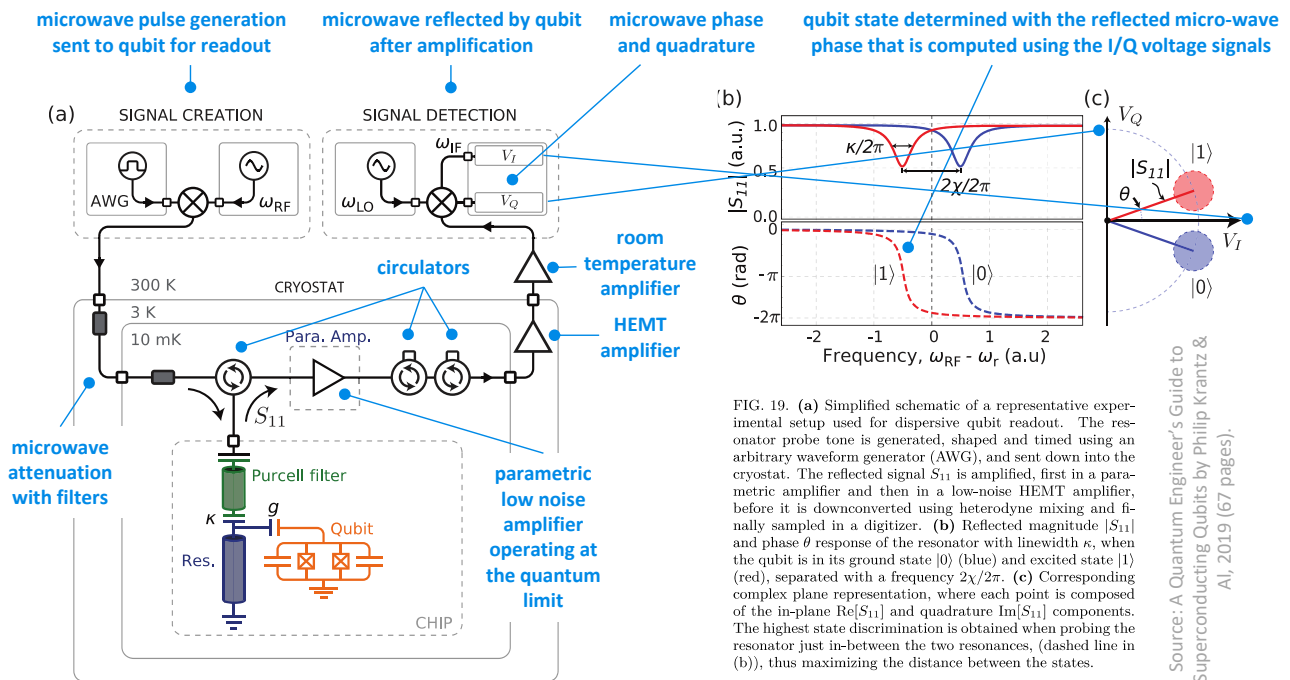


Figure 291: superconducting qubit readout process. Source: [A Quantum Engineer's Guide to Superconducting Qubits](#), by Philip Krantz et al, 2019 (67 pages).

Source: A Quantum Engineer's Guide to Superconducting Qubits by Philip Krantz & AI, 2019 (67 pages).

I have always wondered why measuring a simple phase of a microwave signal was so complicated. This is the most complex part of superconducting qubits engineering. Could it be possible to measure a reflected microwave pulse phase with a simpler analog setting running at the qubit temperature and then transmit a simple 0 or 1? Seemingly not.

- **Connectivity** is an important feature of a quantum processor. The more qubits are connected with each other, the fewer SWAP gates must be run to logically entangle them. With 2D structures, one of the problems to be solved lies in the internal connections in the chipset.

⁶⁹¹ Other techniques for measuring the state of superconducting qubits are being considered, such as the activation of qubit fluorescence. It is done by jumping from the $|0\rangle$ to $|2\rangle$ state of the qubit, the transition to the $|1\rangle$ state not being possible with the fluorescence excitation photon. See the thesis [Energy and Information in Fluorescence with Superconducting Circuits](#) by Nathanaël Cottet, 2018 (227 pages).

3D architectures are used with one layer for qubit readout and another for qubit operations but the qubits topology connectivity is at best with 4 nearest neighbors like with Google's Sycamore. As shown in Figure 292, a Japanese team proposed in 2020 an original solution consisting in flattening the matrix and making it possible to connect the control elements in 2D. But at the price of overlapping part of the links between qubits⁶⁹².

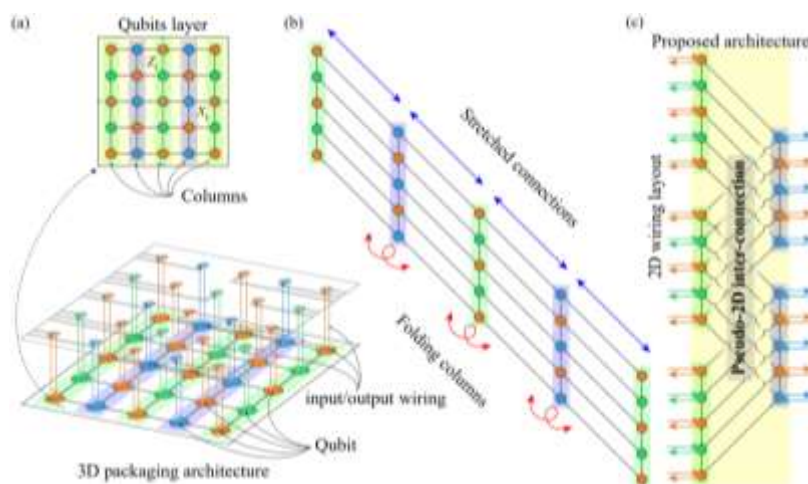


Figure 292: a proposal to improve superconducting qubits connectivity. Source: [Pseudo-2D superconducting quantum computing circuit for the surface code](#) by H. Mukai, February 2019 (8 pages).

- **Digital simulations.** Some software solutions are available to simulate the physical behavior of superconducting qubits at a low level. Among these, **CircuiQ** is a proposal from the MIT, ParityQC and the University of Innsbruck with the participation of Benoît Vermersch (LPMCM, Grenoble)⁶⁹³. It's a Python open source toolbox that can be used for analyzing superconducting circuits at the physical level, using their Hamiltonian. It can help estimate the qubits T_1 under various noise mechanisms.

There are other similar software packages like **scqubits**, developed by researchers from Northwestern University and **SQcircuit** from Stanford⁶⁹⁴.

Setups

In the current state of the art, the cryostats housing these qubits are filled with many cables and microwave attenuators driving the qubits and with first stages amplifiers used in the qubits state readout⁶⁹⁵. Implementing quantum error correction will require 1,000 or 10,000 physical qubits per logical qubit⁶⁹⁶. It will create significant challenges for scaling up the architecture at least, with the existing cabling and external microwave generation and readout systems. Thus, the need for cryogenic electronics and miniaturized microwaves coaxial cabling that we will soon [investigate](#), starting in page 485.

⁶⁹² See [Wiring the quantum computer of the future: A novel simple build with existing technology](#) by Jaw-Shen Tsai (Japan), April 2020 which points to [Pseudo-2D superconducting quantum computing circuit for the surface code](#) by H. Mukai, February 2019 (8 pages).

⁶⁹³ See [CircuiQ: An open source toolbox for superconducting circuits](#) by Philipp Aumann, William D. Olivier et al, March 2022 (14 pages).

⁶⁹⁴ See [Computer-aided quantization and numerical analysis of superconducting circuits](#) by Sai Pavan Chitta, Jen Koch et al, Northwestern University, June 2022 (12 pages) and [Analysis of arbitrary superconducting quantum circuits accompanied by a Python package: SQcircuit](#) by Taha Rajabzadeh1, Zhaoyou Wang, Nathan Lee, Takuma Makihara, Yudan Guo, and Amir H. Safavi-Naeini, June 2022 (23 pages).

⁶⁹⁵ This is well explained in [Superconducting Circuits Balancing Art and Architecture](#) by Irfan Siddiqi of Berkeley Lab, 2019 (34 slides).

⁶⁹⁶ Source: [Surface codes: Towards practical large-scale quantum computation](#) by Austin G. Fowler et al, 2012 (54 pages).

Digital-to-analog converters, aka DACs and Analog-to-Digital converters convert microwaves at room temperature and handle a very large volume of outbound or inbound data of 8 to 14 Gbits/s as shown in the diagram in Figure 293 corresponding to Google's Sycamore.

This data is managed in real time. It does not however seem necessary to store them. It is not a big-data system!

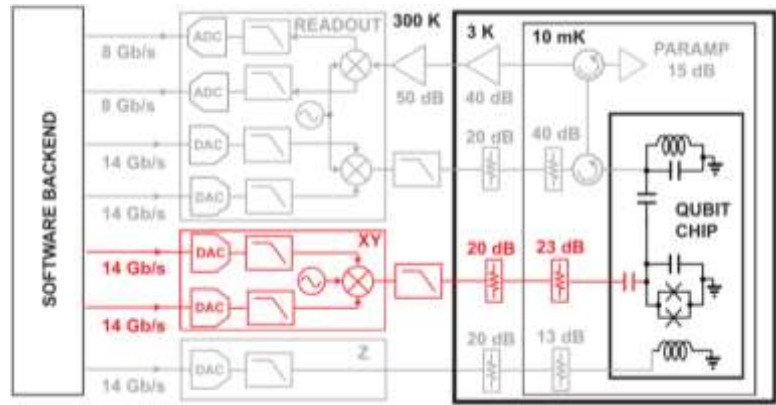


Figure 293: Sycamore's qubit control and readout architecture. Source: Google.

The electronics used in research laboratory equipment is illustrated with the example in Figure 294 of a configuration used to test a 5-qubit superconducting chipset in 2015.

Its uses classical off-the-shelf equipment from **Rohde & Schwarz** or **Tektronix**.

These external generators are appreciated for the quality of the microwave pulses they produce. For a larger number of qubits, multiple microwave generators are used from vendors like **Zurich Instruments**, **Qblox** and **Quantum Motion** that we cover in a [dedicated section](#), page 485. Others, like **SeeQC**, are attempting to miniaturize all or part of these components with superconducting electronics.

5 superconducting qubits lab configuration

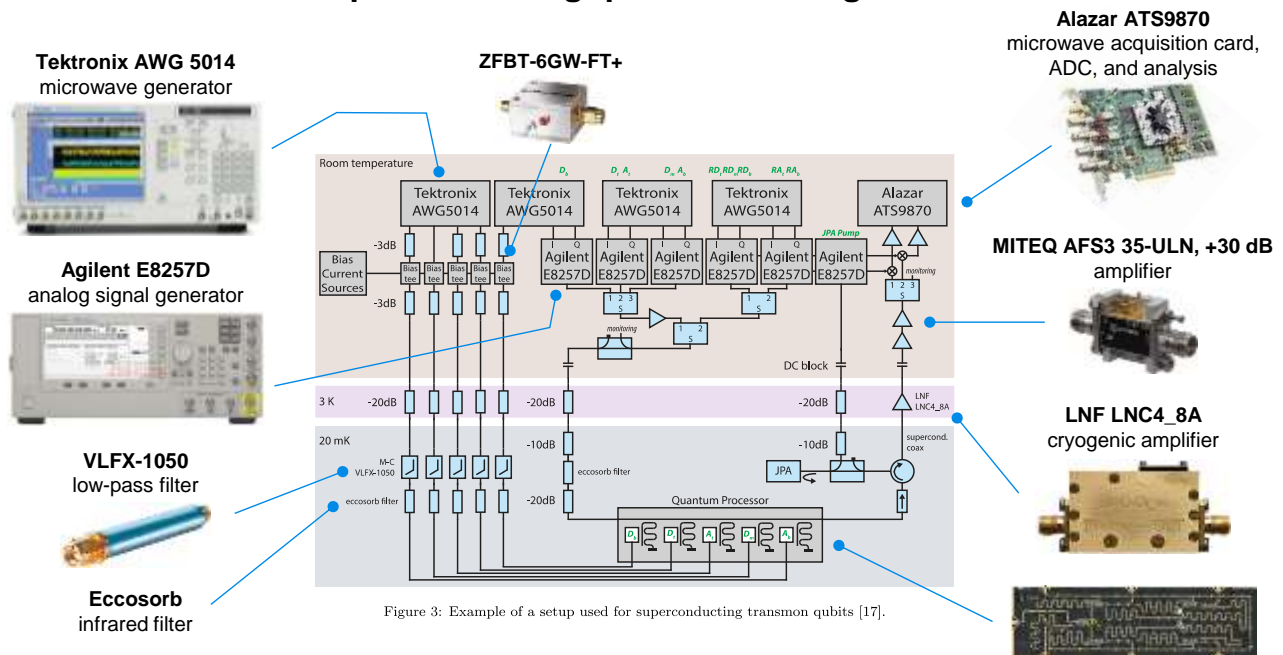


Figure 3: Example of a setup used for superconducting transmon qubits [17].

Figure 294: a superconducting qubits lab configuration. Source: [The electronic interface for quantum processors](#) by J.P.G. van Dijk et al, March 2019 (15 pages). I have added visuals of the electronic components used in the configuration.

Superconducting qubits fidelities are not best-in-class compared to trapped ions. It also decreases with the number of qubits. There is some progress being made to reduce qubit noise. It has several origins such as charge fluctuations, random electrons and materials impurities. Fidelity is currently not high enough to implement error correction codes. Some methods are proposed to improve readout fidelity.

THE TYRANNY OF WIRES

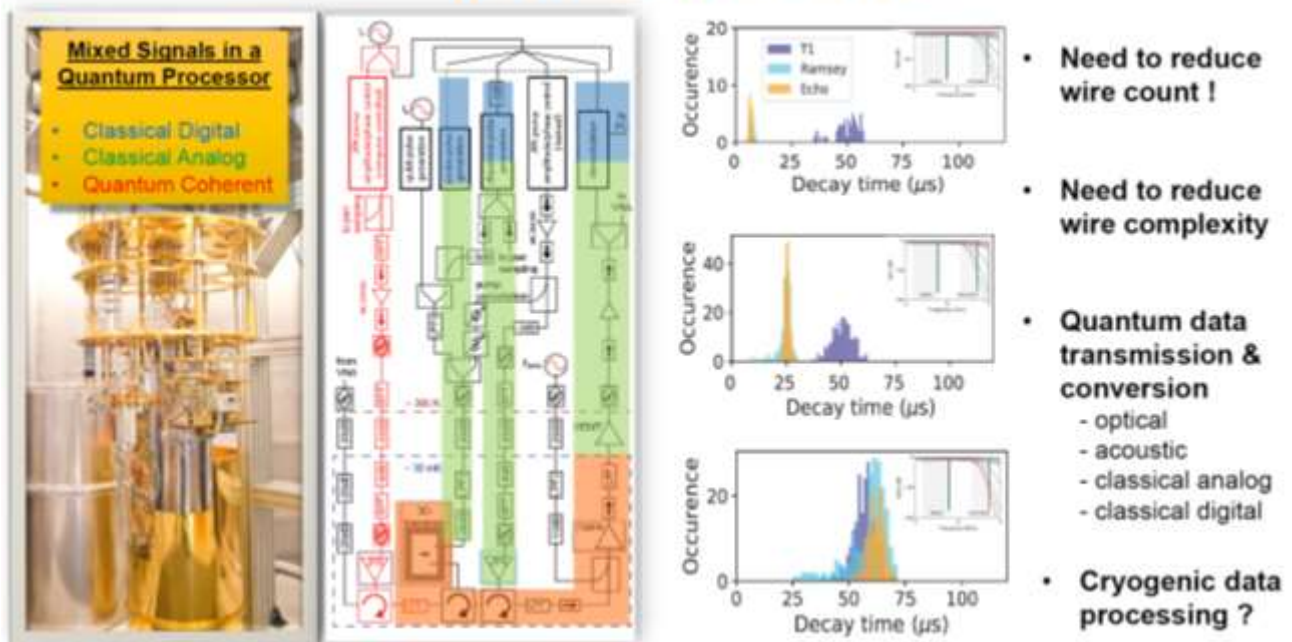


Figure 295: the tyranny of wires in superconducting qubits. Source: [Superconducting Circuits Balancing Art and Architecture](#) by Ifsan Siddiqi of Berkeley Lab, 2019 (34 slides).

A team of Canadian and American researchers is proposing a miniaturizable optical measurement⁶⁹⁷. A variant was proposed in 2018 by Robert McDermott of the University of Wisconsin-Madison, with the objective of improving measurement fidelity to 99%⁶⁹⁸.

The size of superconducting qubits is in the micron range, making it difficult to create large chips with millions of qubits. Miniaturization always seems possible but it is difficult to manage because the quality of the superconducting qubits seems to decrease with their size⁶⁹⁹.

Manufacturing

Superconducting qubits are electronic circuits built with techniques that are not that far from how classical analog circuits are being produced like in the radar and electronics markets, with some similarities with digital electronics, *aka* CMOS chipsets.

We'll describe later the specifics of the manufacturing of superconducting qubits. Most thesis coming out of superconducting labs contain a description of the manufacturing techniques being used although it changes over time⁷⁰⁰.

⁶⁹⁷ See [Heisenberg-limited qubit readout with two-mode squeezed light](#), 2015 (12 pages).

⁶⁹⁸ In [Measurement of a Superconducting Qubit with a Microwave Photon Counter](#), March 2018 (11 pages).

⁶⁹⁹ See [Investigating surface loss effects in superconducting transmon qubits](#) by Jay Gambetta et al, 2016 (5 pages) and [On-chip integrable planar NbN nano SQUID with broad temperature and magnetic-field operation range](#) by Itamar Holzman and Yachin Ivry, Technion, April 2019 (7 pages) who prototyped miniaturized 45 nm x 165 nm SQUIDs.

⁷⁰⁰ See for example [Design, fabrication and test of a four superconducting quantum-bit processor](#) by Vivien Schmitt, 2015 (192 pages).

Materials used for manufacturing superconducting qubits include generally aluminum (for the Josephson junction, at least for the dielectric), niobium (for capacitors and resonators and sometimes the Josephson junction) and indium (for the chipset connectors), bore (in boron-nitride in Josephson junction dielectric⁷⁰¹), titanium nitride (for capacitors, with a better quality factor) and occasionally selenium (associated with niobium and bore in capacitors), silicon or sapphire (for the wafer substrate) and tantalum⁷⁰². While most deposition techniques generate polycrystalline structures⁷⁰³, some are starting to investigate epitaxial deposition to create monocrystalline structures.

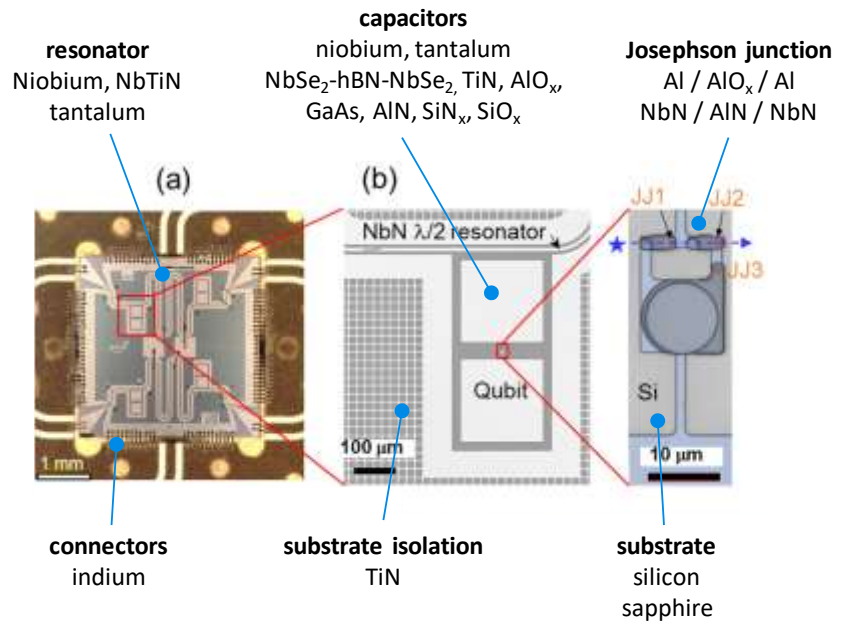


Figure 296: the various components and materials used in a superconducting qubit. Source: [Enhanced coherence of all-nitride superconducting qubits epitaxially grown on silicon substrate](#) by Sunmi Kim et al, September 2021.

IMEC already tests such processes avoiding lift-off and angled evaporation, all done with photolithography. They are part of the related EU project **Matqu** with CEA-Leti and others to build superconducting qubits on 300 mm wafers using existing CMOS fabs.

Superconducting qubits miniaturization is an interesting area of research given they are currently quite large, mainly due to the size of their resonators with a length of $\lambda/4$, λ corresponding to their control wavelength. It can exceed a size of 1 mm^2 . Resonators could be as small as 0.04 mm^2 using special fabrication techniques⁷⁰⁴. Similar efforts are undertaken to miniaturize capacitors with van der Waals materials ($\text{NbSe}_2\text{-hBN-NbSe}_2$)⁷⁰⁵.

⁷⁰¹ See [Hexagonal boron nitride as a low-loss dielectric for superconducting quantum circuits and qubits](#) by Joel I-J. Wang, William D. Oliver et al, MIT, Nature Materials, January 2022 (30 pages) and [Enhanced coherence of all-nitride superconducting qubits epitaxially grown on silicon substrate](#) by Sunmi Kim et al, September 2021 (7 pages).

⁷⁰² See [Towards practical quantum computers: transmon qubit with a lifetime approaching 0.5 milliseconds](#) by Chenlu Wang et al, NPJ, January 2022 (6 pages).

⁷⁰³ See [Microscopic relaxation channels in materials for superconducting qubits](#) by Anjali Premkumar, Andrew A. Houck et al, Nature Communications, July 2021 (9 pages).

⁷⁰⁴ See [Compact superconducting microwave resonators based on Al-AlOx-Al capacitor](#) by Julia Zotova et al, March 2022 (10 pages) and See [Tiny materials lead to a big advance in quantum computing](#) by Adam Zewe, MIT News Office, January 2022. For a 5 GHz pulse, the wavelength is about 6 cm. A quarter wavelength is then 1.5 cm.

⁷⁰⁵ See [Miniaturizing transmon qubits using van der Waals materials](#) by Abhinandan Antony et al, Columbia University and Raytheon BBN. September 2021 (6 pages).

Research

A significant number of research laboratories are working on superconducting qubits all over the world. In the USA, at **Yale University** and **MIT**⁷⁰⁶, in Europe and in Germany, in Sweden at the **WACQT** of Chalmers University, in France at the **CEA**, in Switzerland at **ETH Zurich**⁷⁰⁷, in Finland⁷⁰⁸ and in **Japan**.

Other works aim at lengthening the coherence time of superconducting qubits, notably at Princeton in Andrew A. Houck's team⁷⁰⁹. Indeed, this coherence time of the order of one hundred micro-seconds (μs) is still quite limiting. It generates a constraint on the number of quantum gates that can be executed in a quantum software, even if the accumulated errors become prohibitive before this limit threshold. New records were broken in 2021 with 1.6 ms T_1 at Princeton and Sherbrooke with a $0-\pi$ circuit (but with a 25 μs dephasing time, aka T_2) and 210 μs with transmon qubits at Yale⁷¹⁰. In May 2021, a China team obtained a 300 μs T_1 with a transmon qubit⁷¹¹. IBM reached the 1 ms T_1 barrier with one experimental planar transmon qubit in May 2021 as well (but the related paper is still pending). The best lab-level record was with a 1.48 ms T_2 coherence time on flux qubits at the University of Maryland in Vladimir Manucharyan's team⁷¹². These records are however not necessarily obtained with a great number of functional qubits... when more than 2 are used!

Superconducting qubits lifetime record is still way above this, with 3D SRF cavities (for superconducting radio frequency cavities). These are developed by the DoE Fermilab and have a very high Q-factor.

In 2020, they reached qubit lifetimes of about 2s with special materials design reducing the 2-level system losses. Fermilab researchers plan to implement qubits with these SRFs, packing between 63 and 128 effective qubits into 9 SRF cavities hosting qubits. These cavities are bulky, the size of the device being about one meter long in Figure 297⁷¹³.



Figure 297: the huge SRF superconducting qubits from the DoE Fermilab. Source: [Superconducting Quantum Materials and Systems Center](#) by Anna Grassellino, SQMS Center Director, Fermilab, June 2021 (40 slides),

⁷⁰⁶ See [Quantum Computing @ MIT: The Past, Present, and Future of the Second Revolution in Computing](#) by Francisca Vasconcelos, MIT, February 2020 (19 pages). They have developed a 16-qubit superconducting chipset, manufactured by Lincoln Labs at MIT.

⁷⁰⁷ With Andreas Wallraff's QuSurf team working on superconducting qubits and their error correction codes. This project is funded by the American IARPA agency. In 2019, they were at 7 experimental qubits. It is also supported by the ScaleQIT project (Scalable Superconducting Processors for Entangled Quantum Information Technology) funded by the European Union and by the OpenSuperQ project of the European flagship.

⁷⁰⁸ VTT's goal is to manage 50 to 100 superconducting qubits. VTT has its own circuit manufacturing unit with a 2600 m² clean room of a similar size to CNRS C2V clean room in Palaiseau, France. See [Engineering cryogenic setups for 100-qubit scale superconducting circuit systems](#) by S. Krinner et al, 2019 (29 pages).

⁷⁰⁹ See [New material platform for superconducting transmon qubits with coherence times exceeding 0.3 milliseconds](#) by Alex P. M. Place, Andrew A. Houck et al, February 2020 (37 pages). Qubits are using tantalum instead of niobium and on a sapphire substrate. The paper describes starting page 8 the manufacturing process of these qubits.

⁷¹⁰ See [Experimental Realization of a Protected Superconducting Circuit Derived from the \$0-\pi\$ Qubit](#) by András Gyenis, Alexandre Blais et al, Sherbrooke, Princeton, U. Chicago and Northwestern University, March 2021 (31 pages) and [Direct Dispersive Monitoring of Charge Parity in Offset-Charge-Sensitive Transmons](#) by K Serniak, R Schoelkopf, Michel Devoret et al, Yale University, March 2019 (11 pages) with transmons at a T_1 of 210 μs .

⁷¹¹ See [Transmon qubit with relaxation time exceeding 0.5 milliseconds](#) by Chenlu Wang et al, May 2021 (15 pages).

⁷¹² See [Millisecond coherence in a superconducting qubit](#) by Aaron Somoroff, Vladimir E. Manucharyan et al, University of Maryland, 2021 (14 pages),

⁷¹³ See [Superconducting Quantum Materials and Systems Center](#) by Anna Grassellino, SQMS Center Director, Fermilab, June 2021 (40 slides), [Materials and devices for fundamental quantum science and quantum technologies](#) by Marco Polini et al, January 2022 (19 pages) and [Three-Dimensional Superconducting Resonators at \$T < 20\$ mK with Photon Lifetimes up to \$\tau = 2\$ s](#) by A. Romanenko, R. Pilipenko, S. Zorzetti, D. Frolov, M. Awida, S. Belomestnykh, S. Posen, and A. Grassellino, March 2020 (5 pages).

Other researchers work on using various qubits materials like titanium nitride and tantalum on sapphire substrates, at Princeton, ENS Lyon and Alice&Bob among other locations. These are used in complement to the Al/AIO/Al Josephson junctions, for various other parts of the qubit circuits (isolators, capacitances, resonators).

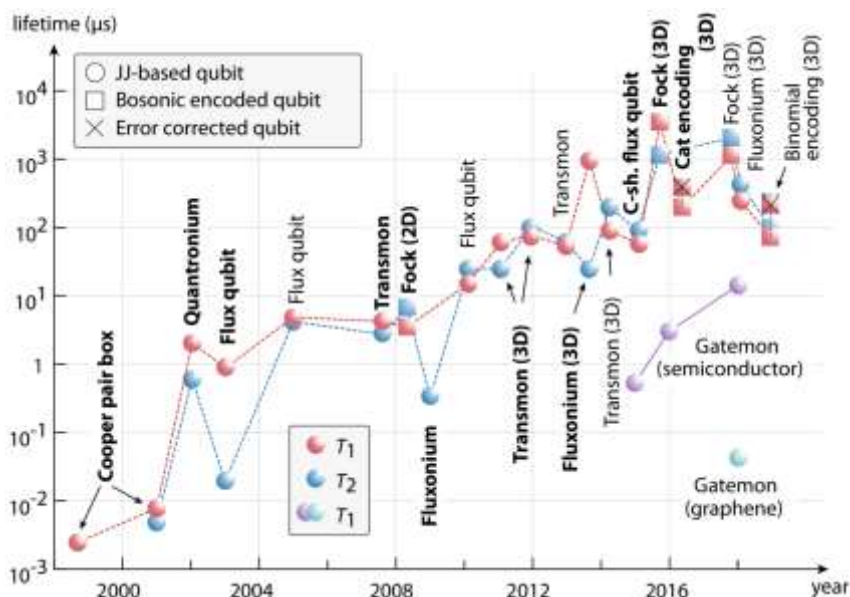


Figure 298: logarithmic evolution of superconducting lifetime over time. Source: [Superconducting Qubits Current State of Play](#) by Morten Kjaergaard et al, 2020 (30 pages).

The Quantronics team at CEA-Saclay uses transmons for its quantum circuits, but now explores another route based on high coherence impurity spins in insulators for making qubits, with superconducting quantum circuits for controlling them. The rationale is that the electro-nuclear spin levels of such systems may indeed provide more robust qubits for which quantum error correction could be more easily manageable than for transmon qubits.

Other research conducted at the CEA consists in associating superconducting qubits with NV centers, linked by microwaves, to be used as quantum memory as well as a means of more precise readout of superconducting qubits. NV centers spins can serve as quantum memory thanks to a spin coherence time that is 1000 times longer than that of superconducting qubits (100 milliseconds vs. 100 microseconds). Another field of research is the coupling of superconducting qubits with nuclear spins (instead of electron spins, on phosphorus or bismuth nuclei) via electron spins.

As with many solid-state qubits, one of the key research goals is to transform these microwave photons into photons in the visible/infrared band to allow their long-distance transport, in particular via fiber optic-based telecommunication, which would become the basis of distributed quantum computing⁷¹⁴.

There is another interesting field of research aimed at simplifying qubit readout that may avoid the burden of parametric microwave amplification and circulators at the 15 mK stage. One of these consists in using microwave photons counting and Josephson photomultipliers (JPM) that are embedded directly in the qubit chipset⁷¹⁵. It has however some shortcomings to overcome like crosstalk and loss of qubit fidelity over time.

⁷¹⁴ See for example [Microwave-to-optical conversion via four-wave mixing in a cold ytterbium together](#) by Jacob P. Covey et al, July 2019 which discusses this conversion.

⁷¹⁵ See [High-Fidelity Measurement of a Superconducting Qubit Using an On-Chip Microwave Photon Counter](#) by A. Opremcak, Roger McDermott et al, PRX, February 2021 (15 pages) and the associated thesis [Qubit State Measurement Using a Microwave Photon Counter](#) by Alexander M. Opremcak, 2020 (159 pages).

In 2021, a **China** research team led by Jian-Wei Pan created a 66 superconducting qubits system and claimed having reached another quantum advantage. In this **Zuchongzhi 2.1** system, they reproduced the Google supremacy experiment with a 2D array of qubits with 13 additional qubits, using the same coupling technology, with 110 couplers⁷¹⁶. Their fidelities were not best-in-class with 99,86% for single qubit gates, 99,24% for two-qubit gates and 95,23% for qubits readout, on top of a rather low T_1 of 30.6 μ s. In their experiment, though, they did use only 56 of their 66 qubits, showing that qubits fidelities are probably not that good when all qubits are activated. In September 2021, they used 60 qubits on 24 cycles with an improved readout fidelity of 97.74%⁷¹⁷. China researchers implemented some quantum neuronal sensing application of quantum many-body states⁷¹⁸.

Vendors



IBM is one of the few major players in the IT world that has been investing in fundamental research for a very long time in quantum computing⁷¹⁹. It is one of the most advanced in universal quantum computing research, having focused on superconducting qubits for a while.

IBM's quantum activity is driven by Jay Gambetta with researchers in their Yorktown, Poughkeepsie, San Jose and Zurich labs, partnering with various American and other countries universities including ETH Zurich and EPFL in Switzerland. IBM has both the most significant full-stack physics, hardware, software tools and cloud R&D investment and strong market presence. Their in-house manufacturing capacity enable them to prototype and produce most of the components needed to build their machines, particularly for their qubit chipsets and control electronics. Their most visible outside vendor is Bluefors although they are also developing an in-house giant “super-fridge” cryostat codenamed Goldeneye. The most recent 2022 update added a scale-out strategy with their QPUs on top of their scale-in roadmap announced in 2020⁷²⁰.

They are also very open and reliable, publishing roadmaps and roadmap updates, respecting their planned milestones and with a steady stream of open research publications showcasing their contribution to the complicated quantum computing field even though it sometimes looks like a puzzle that may be hard to reassemble.

IBM's choice technology is the fixed frequencies transmon superconducting qubits. It is using cross-resonance two-qubit gates which consists in applying a microwave drive to one qubit (the control) at the frequency of another qubit (the target), generating a ZX interaction that is mediated by a bus⁷²¹.

⁷¹⁶ See [Strong quantum computational advantage using a superconducting quantum processor](#) by Yulin Wu, Jian-Wei Pan et al, June 2021 (22 pages).

⁷¹⁷ See [Quantum Computational Advantage via 60-Qubit 24-Cycle Random Circuit Sampling](#) by Qingling Zhu, Jian-Wei Pan et al, September 2021 (15 pages).

⁷¹⁸ See [Quantum Neuronal Sensing of Quantum Many-Body States on a 61-Qubit Programmable Superconducting Processor](#) by Ming Gong et al, January 2022 (14 pages).

⁷¹⁹ Who does fundamental research? Mainly IBM, Microsoft, Google and large telecom companies. The Bell Labs coming from the dismantling of AT&T in 1982 are now part of Nokia after gone through Lucent and Alcatel-Lucent.

⁷²⁰ See [The Future of Quantum Computing with Superconducting Qubits](#) by Sergey Bravyi, Oliver Dial, Jay M. Gambetta, Dario Gil and Zaira Nazario, IBM Quantum, September 2022 (20 pages), a well-crafted paper detailing their scientific roadmap including quantum error correction trade-off choices, chipset manufacturing and scale-in/scale-out architecture.

⁷²¹ See [First-principles analysis of cross-resonance gate operation](#) by Moein Malekakhlagh et al, IBM Research, May 2020 (30 pages) and [Mitigating off-resonant error in the cross-resonance gate](#) by Moein Malekakhlagh et al, August 2021 (20 pages).

Its number of qubits increased steadily from 5 in 2016 to 127 in November 2021. IBM's quantum systems have been running in the cloud since 2016. These are already used by thousands of researchers, students, startups and corporations around the world. After creating laboratory computers, IBM ventured into creating packaged ones when announcing the Q System One in January 2019 at the Las Vegas CES, initially a 20-qubit system⁷²².

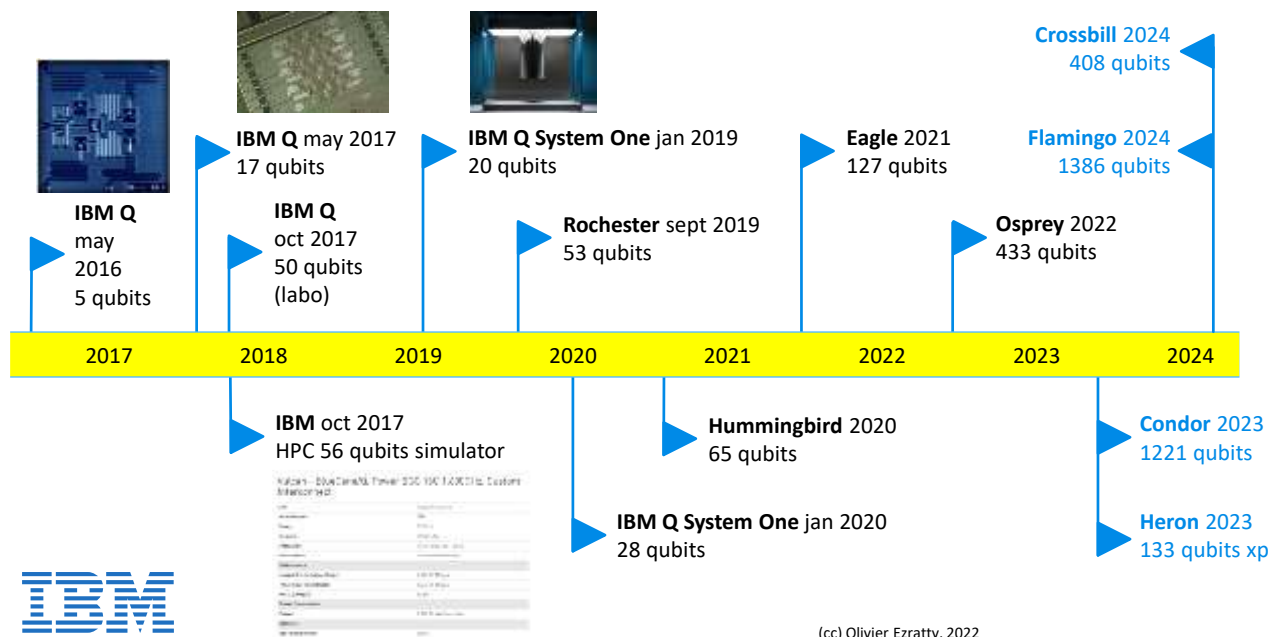


Figure 299: IBM quantum computing timeline. (cc) Olivier Ezratty, 2022.

The Quantum System One is 2.75 m wide, about the size of a D-Wave quantum annealer. In Figure 300, ci-dessous on the right, you can see the Quantum System assembly workshop. IBM is implementing a pre-industrial approach to the production of its quantum computers, despite their very limited capacities and low volume economics. The casing front contains the suspended cryostat while the back contains all the computing, electronics and cryostat compressor and pumps. The Quantum Systems are also self-calibrating. IBM is continuously improving these systems and updating the related qubits lifetime and gates fidelities data on their Quantum Experience web site.

Most of these units are sitting in IBM's own data center in Poughkeepsie, with some extra systems sitting in IBM sites in Germany (operated with the Fraunhofer Institute), Tokyo in Japan, in Korea at Yonsei University, in Canada near Sherbrooke Institut Quantique⁷²³ and supposedly at Cleveland Clinic in the USA. In October 2022, Joe Biden visited the Poughkeepsie facility⁷²⁴ and was presented the Osprey 433 qubit processor that unveiled later in November 2022⁷²⁵. As of October 2022, IBM had already retired 26 quantum computers with 1, 5, 7, 15, 20, 27, 28, 53 and 65 qubits⁷²⁶.

⁷²² Its design was created with the design studios Map Project Office and **Universal Design Studio** (UK) and **Goppion** (Italy), a manufacturer of high-end exhibition devices for museums, which notably designed the protective device for the Mona Lisa in the Louvre Museum and the Queen's jewels in the Tower of London.

⁷²³ See [IBM Research launches the first Discovery Accelerator in Canada](#), IBM, February 2022. This deployment represents in investment of CAN \$65M by IBM matched by the Government of Québec. IBM will team up there with Alexandre Blais' team at Institut Quantique in Sherbrooke.

⁷²⁴ See [U.S. President Biden visits IBM's quantum data center — home of the world's largest fleet of quantum computers](#), IBM, October 2022.

⁷²⁵ See the details of Osprey's November 2022 announcement in [Assessing IBM Osprey 433-qubit quantum computer](#), Olivier Ezratty, November 2022.

⁷²⁶ See [Retired systems](#), IBM. Extracted on October 24th, 2022.



Figure 300: IBM System Q packaging (left) and without packaging (right). Source: IBM.

In September 2020, IBM announced their plan to “scale-in” the number of qubits of their quantum computers⁷²⁷ with a 127 qubits version ("Eagle") introduced in November 2021⁷²⁸, 433 qubits announced in November 2022 and to be put online in 2023 ("Osprey") and 1221 qubits in 2023 ("Condor").

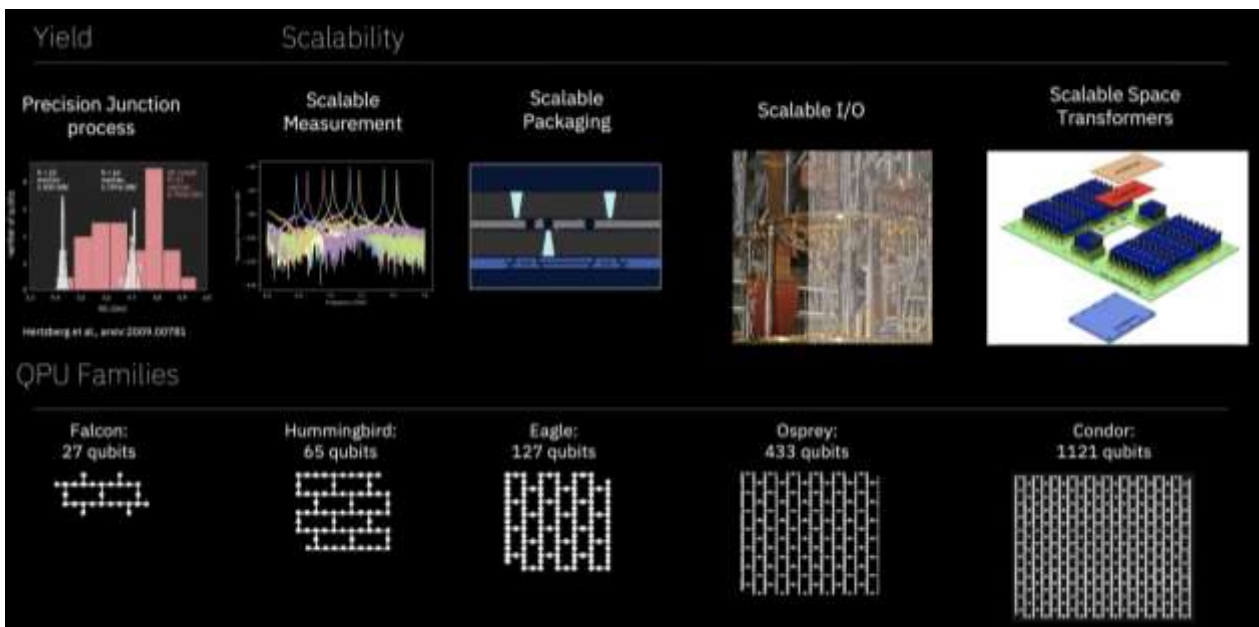


Figure 301: IBM's superconducting roadmap from 2020 to 2023. Source: IBM.

This roadmap was updated in May 2022 with the addition of new processors⁷²⁹.

This was a « scale-out » complementary approach, about how to assemble several quantum chipsets with three-steps: first, Heron (133 qubits, 2023) will be assembled in QPU with many units running the same algorithm in parallel, accelerating the thousands of runs that are necessary with NISQ systems algorithms.

⁷²⁷ See [IBM's Roadmap For Scaling Quantum Technology](#) by Jay Gambetta, September 2020, completed by [IBM publishes its quantum roadmap, says it will have a 1,000-qubit machine in 2023](#) by Frederic Lardinois in TechCrunch. See also [IBM Envisions the Road to Quantum Computing Like an Apollo Mission](#) by Dexter Johnson, September 2020.

⁷²⁸ See [Eagle's quantum performance progress](#) by Oliver Dial, IBM, March 2022.

⁷²⁹ See [Expanding the IBM Quantum roadmap to anticipate the future of quantum-centric supercomputing](#) by Jay Gambetta, May 2022.

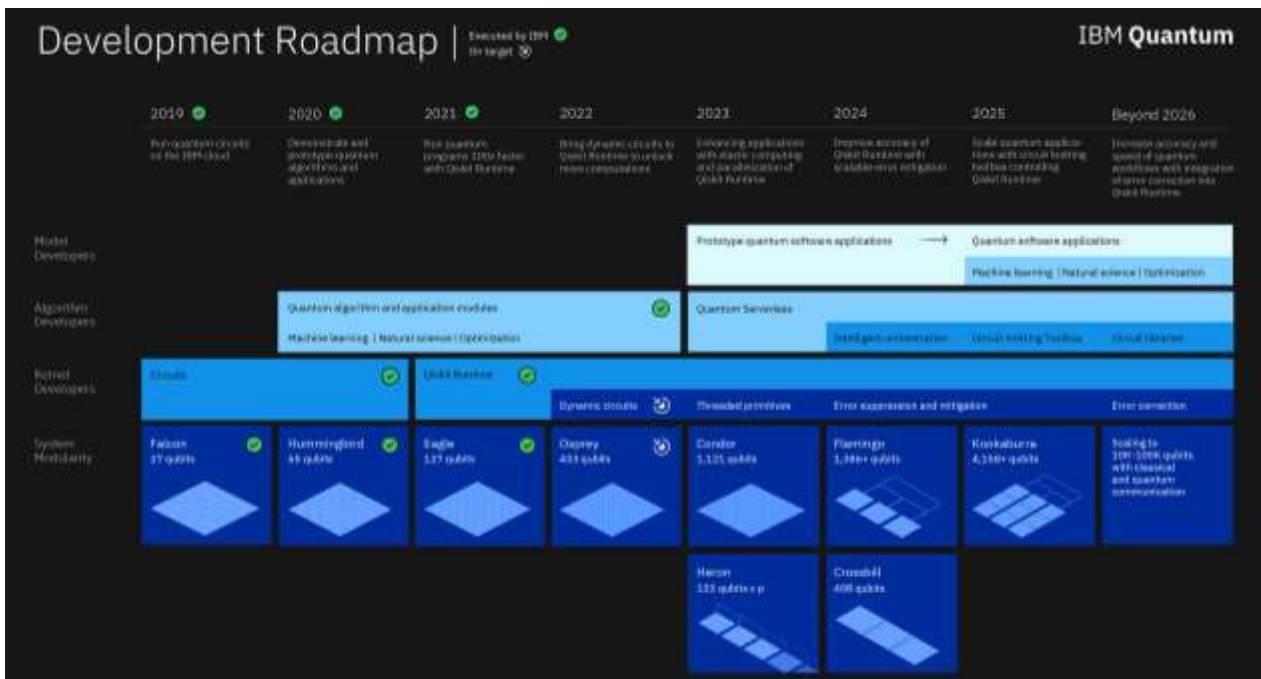


Figure 302: IBM's scale-in and scale-out roadmap. Source: IBM.

Second, Crossbill will assemble three chipsets similar to Heron and total 408 qubits in 2024 ($3 \times 133 = 399$, we can presume that the remaining 9 qubits are explained by some connectivity constraints). These chipsets will be tightly connected with chip-to-chip coupler qubit gates. Then, Flamingo will follow in 2024 with 1386 qubits (3×462) with three chipsets blocks interconnected through some short-range microwave-photonic link (less than one meter). Then, Kookaburra will reach 4158 qubits assembling three blocks of three chipsets associating chip-to-chip micro-wave coupler gates and longer range photonic-based interconnectivity.

We'll now look at the various technology improvements IBM is implementing or planning to implement in its various superconducting qubits systems. IBM is probably the most open industry vendor with regards to its scientific openness. Among others, their presentations at the Chicago APS March Meeting in 2022 was enlightening, particularly with the Industry Session talk from Hanhee Paik and another from Oliver Dial⁷³⁰.

Heavy-Hexagon layout. In July 2021, IBM announced a generalization of their hexagon qubits topology. This heavy-hex lattice is the 4th version of IBM Quantum systems qubits topology and has been used upwards of its Falcon processor (27 qubits) as shown in the schema, where useful computing qubits are in yellow, black qubits in the red zones, the phase (Z) errors correction qubits and the white qubits in blue zones, the flip (X) errors corrections qubits⁷³¹. It uses a hexagonal arrangement with an intermediate qubit on each side of hexagons. The topology is optimized for quantum errors correction, using custom hybrid surface and Bacon-Shor subsystem codes.

The IBM processors qubit numbers can be explained by this architecture and the lattice code distance for error correction (Falcon 27 qubits with a distance 3 code, Hummingbird 65 qubits and a distance 5 code and Eagle with 127 qubits and a distance 7 code). This topology is different from the square lattice chosen by Google in its Sycamore processors, which, however, uses coupling qubits, a solution that IBM was not relying on until it was announced in May 2022 that they would later implement it.

⁷³⁰ See also this [impressive list](#) of over 800 papers from IBM research and its research partners published on arXiv (as of August 2022).

⁷³¹ See [The IBM Quantum heavy hex lattice](#) by Paul Nation et al, IBM Research, July 2021 and [Topological and subsystem codes on low-degree graphs with flag qubits](#) by Christopher Chamberland et al, IBM Research, December 2019 (20 pages). Heavy hex requires some tuning with algorithms like QAOA. See [Scaling of the quantum approximate optimization algorithm on superconducting qubit based hardware](#) by Johannes Weidenfeller et al, IBM, February 2022 (20 pages).

IBM was using fixed frequency qubits when Google uses tunable frequency ones. The hex lattice reduces the effect of frequency collision between qubits.

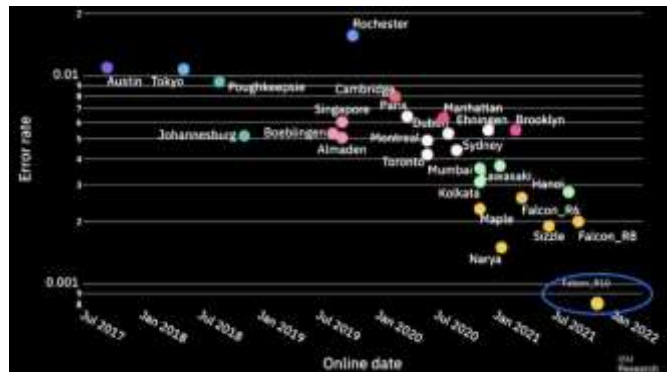
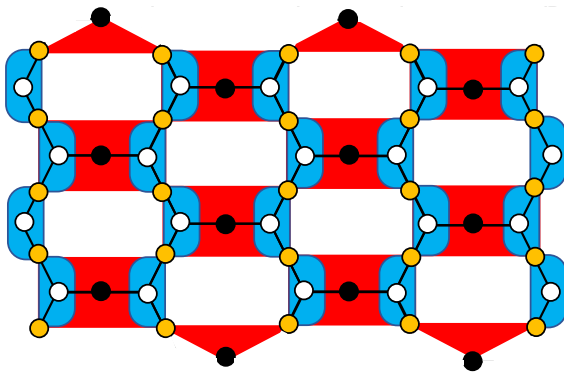


Figure 303: Heavy-Hexagon layout (left) and evolution of IBM's superconducting qubits fidelities over time (right).

Qubit quality. With improving qubit readouts fidelity using low noise amplifiers (QLA for quantum-limited amplifiers)⁷³². They reached fidelities records in November 2021 with Falcon R10 (27 qubits) with less than 0.001 errors (*aka* a “three nines”, meaning 99,9% fidelities for two-qubit gates), but with no scientific paper describing Falcon R10 so far. It enabled them to obtain a quantum volume of 512 in May 2022 with this chipset (meaning: 9 operational qubits).

They also improve coherence times on a regular basis within a class of systems processors (like Falcon for 27 qubits)⁷³³. Their record is a T_1 of 300 μ s with their Falcon R8 processor and 1 ms in research ([source](#)). They also continuously improve qubit physical properties⁷³⁴. Like with using laser annealing in their production⁷³⁵, with new materials design improving their purity and avoiding contaminations and computer aided design⁷³⁶, and with improving chipset vacuum isolation during its assembly⁷³⁷. Metallic superconducting nanowires could also be controlled with applying a moderate voltage to a nearby gate electrode. Switches using this effect would require very little power and could mitigate the well-known negative impact of phonons on the coherence of superconducting qubits⁷³⁸.

IBM researchers are also quite prolific in finding ways to improve gates fidelities. Like with enabling efficient SWAP gates implementation with low crosstalk, using dispersively coupled fixed-frequency transmon qubits and simultaneous driving of the coupled qubits at the frequency of another qubit, with a fast two-qubit interaction equivalent to $ZX + XZ$ entangling gates, implemented without strongly driving the qubits⁷³⁹.

⁷³² See [Rising above the noise: quantum-limited amplifiers empower the readout of IBM Quantum systems](#) by Baleegh Abdo, January 2020.

⁷³³ T_1 and T_2 reached about 260 μ s in September 2021 with their [Peekskill](#) 27 qubit system. It was a 3-times improvement vs previous systems.

⁷³⁴ See [Materials challenges and opportunities for quantum computing hardware](#) by Nathalie P. de Leon et al, Science, April 2021 (x pages).

⁷³⁵ See [High-fidelity superconducting quantum processors via laser-annealing of transmon qubits](#) by Eric J. Zhang et al, December 2020 (9 pages) and [Laser-annealing Josephson junctions for yielding scaled-up superconducting quantum processors](#) by Jared B. Hertzberg et al, August 2021 (8 pages).

⁷³⁶ See [What if We Had a Computer-Aided Design Program for Quantum Computers?](#), IBM, October 2020 and [Qiskit Metal: IBM Community Building a Computer-Aided Program for Quantum Device Design](#) by Matt Swayne, October 2020.

⁷³⁷ See [Ultrahigh Vacuum Packaging and Surface Cleaning for Quantum Devices](#) by M. Mergenthaler et al, 2020 (6 pages).

⁷³⁸ See [Vibrations could flip the switch on future superconducting devices](#) by Markus F. Ritter, Andreas Fuhrer and Fabrizio Nichele, March 2022, pointing to [Out-of-equilibrium phonons in gated superconducting switches](#) by Markus F. Ritter et al, Nature Electronics, March 2022 (7 pages).

⁷³⁹ See [Cross-Cross Resonance Gate](#) by Kentaro Heya and Naoki Kanazawa, IBM Research Japan, PRX, November 2021 (15 pages).

3D circuits. It started with stacked pairs of chipsets separating qubits from microwave controls, using TSV (through-silicon vias) with their 127 qubit systems in 2021⁷⁴⁰.

This 3D chipset layout introduced with Eagle (127 qubits) adds multi-level wiring (MLW) on the backside of the interposer. Control and readout signals are routed as strip lines in the MLW and are well isolated from the interposer and qubit metal levels. Connections between the qubits and this MLW is done via superconducting TSVs (through-silicon vias). It reduces crosstalk when pairing qubits. They also improved readout multiplexing with using 9 lines instead of 5 in Eagle. However, this degrades their CNOT gates fidelity due to collisions between qubit readout frequencies.

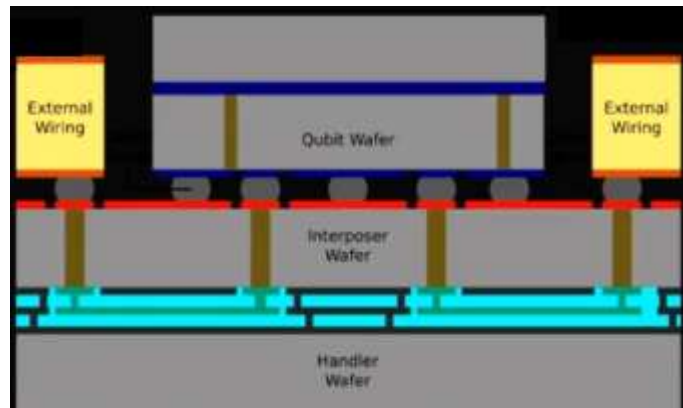


Figure 304: the three stacked die chipset architecture used in Eagle's 127 qubit processor. Source: IBM.

Scalability. With microwaves signals multiplexing and intelligent filtering for qubit states readouts, starting with Hummingbird 65 qubits system in 2020. They are also using microwave flexible cables to reduce the space used by microwave cabling in cryostats. They are also implementing tunable couplers to control qubits entanglement⁷⁴¹.

With Osprey (433 qubits), wires density improved using flexible cables and with control electronics of “generation 3”, using custom-made FPGAs.



Figure 305: IBM's quantum data center in Poughkeepsie, New York State. Source: IBM.

Scalability will also come from qubits miniaturization coming from various paths like a simplification of the readout electronics replacing the usual circulator with a “microwave-controlled qubit readout multichip module” (QRMCM)⁷⁴².

Error Mitigation. They are optimizing their quantum error correction architecture⁷⁴³, particularly to correct T gates errors while using classical QEC for Clifford gates as part of “Quantum readout-error mitigation” (QREM).

⁷⁴⁰ See [Merged-Element Transmons: Design and Qubit Performance](#) by H. J. Mamin et al, March 2021 (7 pages).

⁷⁴¹ See [Tunable Coupling Architecture for Fixed-frequency Transmons](#) by J. Stehlik et al, IBM Research, February 2021 (7 pages) and [With fault tolerance the ultimate goal, error mitigation is the path that gets quantum computing to usefulness](#) by Kristan Temme, Ewout van den Berg, Abhinav Kandala and Jay Gambetta, July 2022.

⁷⁴² See [High-Fidelity Qubit Readout Using Interferometric Directional Josephson Devices](#) by Baleegh Abdo et al, December 2021 (34 pages). Avoiding the magnet-based based circulator for qubit readout using a microwave-controlled qubit readout multichip module (QRMCM) that “integrates interferometric directional Josephson devices consisting of an isolator and a reconfigurable isolator or amplifier device, and an off-chip low-pass filter”. Also, see [Merged-Element Transmons: Design and Qubit Performance](#) by H.J. Mamin et al, PRA, August 2021 (7 pages).

⁷⁴³ Their views on QEC: [Hardware-aware approach for fault-tolerant quantum computation](#) by Guanyu Zhu, 2020.

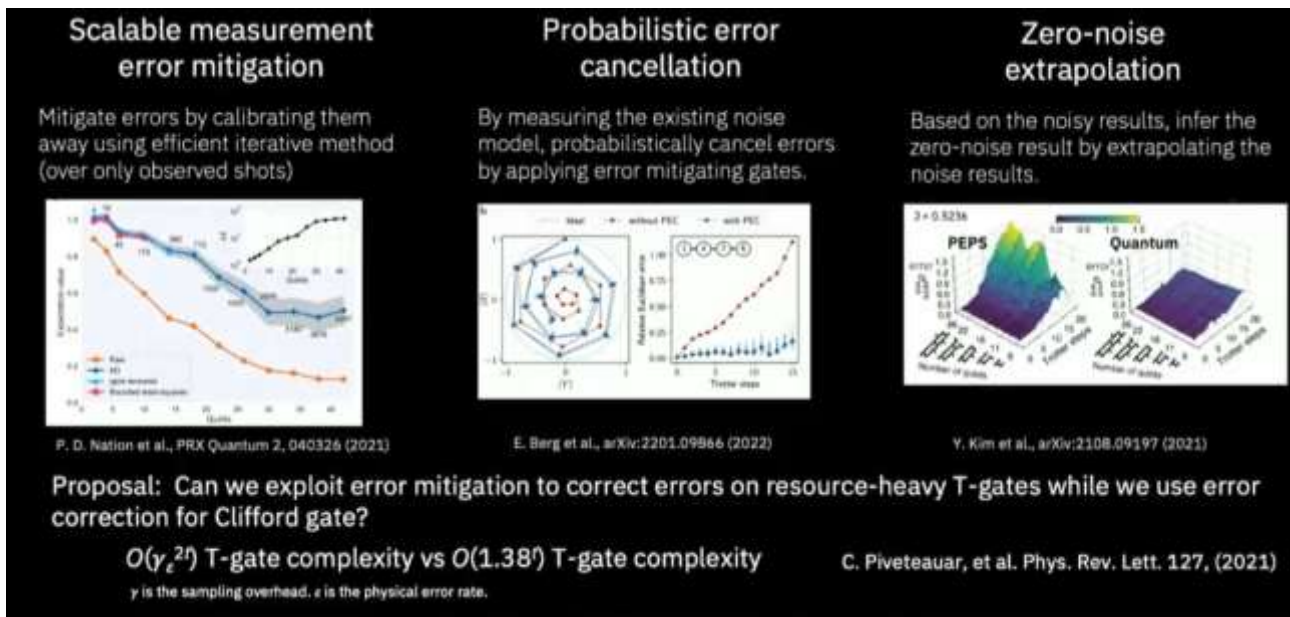


Figure 306: the various quantum error mitigation techniques IBM is working on. Source: IBM.

Various algorithms optimizations. IBM research teams are finding many ways, more or less efficient, to optimize algorithms run-time.

For example, they are allowing more computations with the Bernstein-Vazirani algorithm run on 12 qubits, where SWAP gates are replaced with resets, improving fidelity from 0.0007 to 0.80.

They also propose to use “circuit knitting”, i.e., combining smaller circuits to simulate larger problems using entanglement forging⁷⁴⁴. However, this technique has a strong tendency to strongly attenuate algorithms quantum advantage and parallelism.

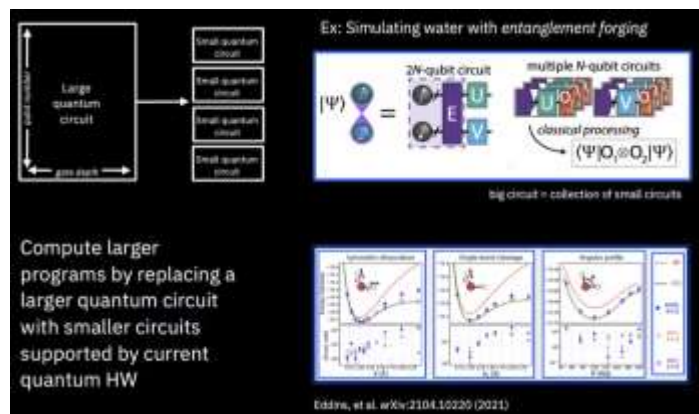


Figure 307: entanglement forging technique. Source : IBM.

Cryogeny. IBM announced in 2020 that it was working on a giant home-made cryostat called "Goldeneye" exceeding current market capacity, to host from a thousand to a million physical qubits⁷⁴⁵, shown in Figure 308. It is due for 2023 and has already been tested as of May 2022 at 25 mK. It has about 12 pulse tubes and 6 dry dilutions with half of the dilution being inverted at the bottom.

⁷⁴⁴ See [Doubling the size of quantum simulators by entanglement forging](#) by Andrew Eddins, Sergey Bravy, Sarah Sheldon et al, April 2021 (17 pages), [Entanglement forging The 2x Gambit: IBM Tech Doubles Qubit Effectiveness](#) by Charles Q. Cho, February 2022, [Simulating Large Quantum Circuits on a Small Quantum Computer](#) by Tianyi Peng, Aram Harrow et al, October 2020, PRL (20 pages), [Quantum Divide and Compute: Exploring The Effect of Different Noise Sources](#) by Thomas Ayril and F.M Le Régent (Atos) with Zain Saleem, Yuri Alexeev, Martin Suchara (DoE Argonne National Laboratory, February 2021 (21 pages) and [Constructing a virtual two-qubit gate by sampling single-qubit operations](#) by Kosuke Mitarai and Keisuke Fujii, Osaka University, JST PRESTO and RIKEN, January 2021 (13 pages).

⁷⁴⁵ See [IBM scientists cool down world’s largest quantum-ready cryogenic concept system](#) by Pat Gumann and Jerry Chow, September 2022. The device is 3m high and 2m wide with 1.7 m³ of experimental volume and 10 internal plates. Its cooling power is of 10 mW at 100 mK and 24W at 4K.

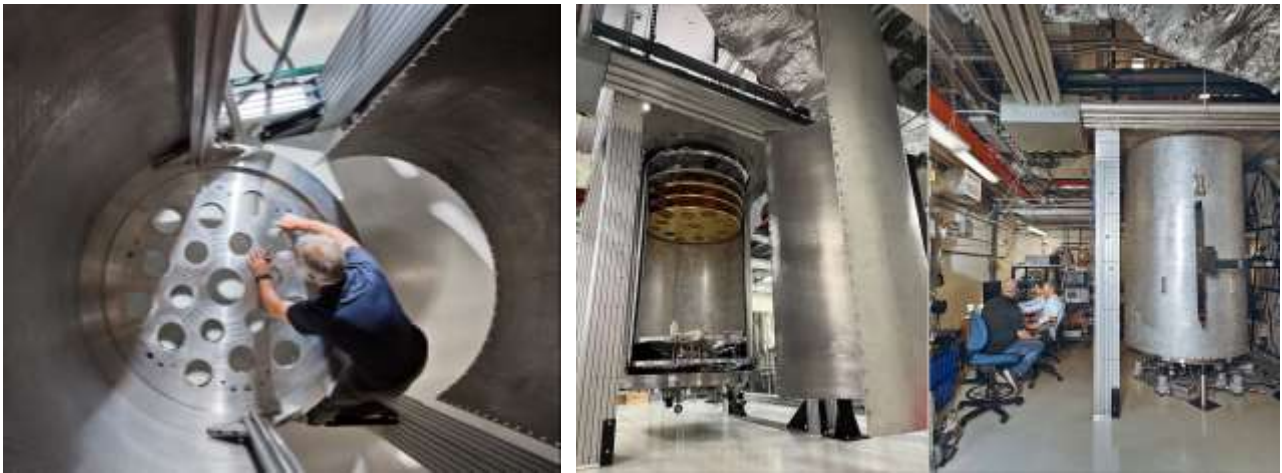


Figure 308: IBM's giant Goldeneye dilution refrigerator. Source: IBM.

QPU interconnect. Beyond 2023 and Condor, scale-out will involve interconnecting quantum processing unit microwave-optical transduction and optical fiber to connect QPUs, with optomechanical coupling or electro-optic coupling. One option is to use optical channels with SiGe/Si optical resonators⁷⁴⁶. These quantum units will be cooled with a new generation of cryostats, designed by Bluefors as part of their KIDE range using a hexagonal form factor, announced in November 2021. It will precede Goldeneye in their roadmap. IBM will start to implement this System Two modular architecture with their 1121 qubits systems in 2023.

MBQC option. Other longer-term plans consist in using constant depth circuits using entanglement and measurements ala “one way quantum computing” and MBQC that is also to be used with flying qubits like photons.

Benchmarking. IBM now uses three key metrics to benchmark its quantum systems. The first one is simply their number of qubits which define the **scale** of their system. The second is the quantum volume that was introduced in 2019 and described in details page 686. It defines their computing **quality**. IBM announced it would double every year.

In April 2022, they obtained a record quantum volume of 256, meaning 8 operational qubits and 8 depths of computing, which increased to 512 in May 2022⁷⁴⁷. There is some inconsistency with IBM's roadmap. They expect to more than double the number of qubits in their system while doubling the available quantum volume every year. This means adding one operational qubit per year! At last, in November 2021, IBM introduced CLOPS (circuit layers operations per seconds) which defines the speed of their processor.



Figure 309: IBM's quantum volume evolution over time. Source: IBM.

⁷⁴⁶ See [Engineering electro-optics in SiGe/Si waveguides for quantum transduction](#) by Jason Orcutt et al, Quantum Science Technology, 2020 and [Ultrahigh-Q on-chip silicon-germanium microresonators](#) by Ryan Schilling, Hanhee Paik et al, Optica, 2022 (4 pages).

⁷⁴⁷ See [Pushing quantum performance forward with our highest Quantum Volume yet](#) by Petar Jurcevic et al, IBM, April 2022.

It currently sits between 800 and 2500 CLOPS⁷⁴⁸.

It is also key to care about the level of large entanglements in these systems, *aka* genuine multipartite entanglement (GME). It was done in 2021 by a team of Australian researchers with fidelities of 54% for 27 qubits with using some quantum readout-error mitigation (QREM)⁷⁴⁹. It was also implemented by IBM Research with a 65-qubit QPU⁷⁵⁰. The schema in Figure 310 shows the history of experimentally prepared quantum states exhibiting N-qubit GME, where $N \geq 3$, with at least 95% confidence in gate-based quantum systems. It illustrates the challenges to create large high-fidelity entangled states.

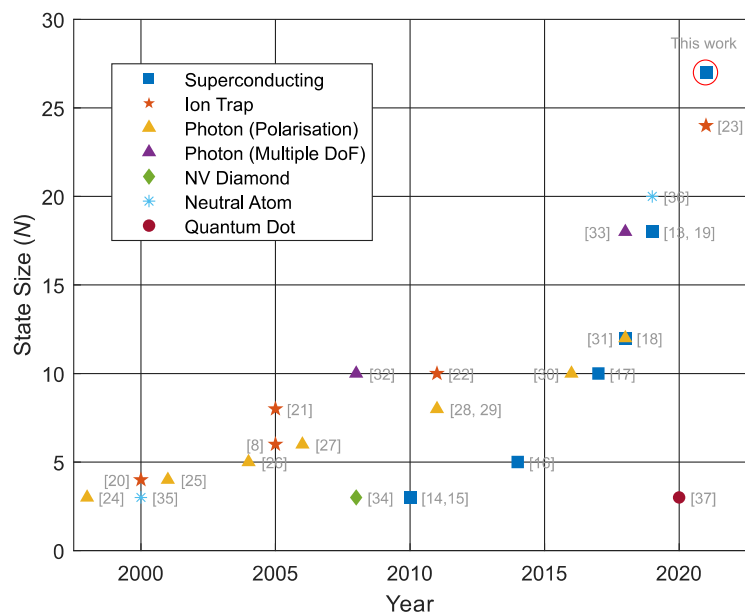


Figure 310: largest multipartite entangled state over time. Source: [Generation and verification of 27-qubit Greenberger-Horne-Zeilinger states in a superconducting quantum computer](#) by Gary J. Mooney et al, August 2021 (16 pages).

Serverless. As part of their May 2022 announcements, IBM explained it is adopted a “serverless” architecture, another name for a cloud service driving both classical and quantum computers with a pay-as-you-go pricing⁷⁵¹. It involves three techniques: circuit knitting that leverages classical resources cut a quantum problem in smaller problems and circuits to run on NISQ QPUs and also use classical processing. This is interesting but reduces the quantum acceleration generated by the QPUs who will run quantum algorithms of smaller Hilbert space. Then, entanglement forging is a way to simplify knitting specific to solving chemistry problems. They then use “quantum embedding” to re-frame a problem and split it between pieces running classically and others quantumly “*for only the classically difficult parts of the problem*”. At last, error mitigation is based on classical post-processing to reduce the impact of some classes of quantum errors.

Deployments and customer evangelism. IBM has been investing a lot since 2016 to build a community of developers and users worldwide. They launched the IBM Quantum network in 2017. It brings together major Fortune 500 companies, research laboratories and startups interested in developing quantum solutions. This network offers access free access to quantum systems with one (crowded) 15 bits system, 8 5-bit systems and a 1-bit small-use system. Commercial systems have respectively 5, 27, 28, 53, 65 and 127 qubits. At last, a quantum emulator (branded a simulator) supports 32 qubits. As of August 2022, they had 27 quantum systems online.

IBM also launched a customer Quantum Computation Center in Poughkeepsie, New York, a quantum center in Montpellier, France, in 2018, and then a partnership in Germany with a Fraunhofer Institute in 2019 plus other quantum centers in Japan and Quebec, Canada.

⁷⁴⁸ See [Quality, Speed, and Scale: three key attributes to measure the performance of near-term quantum computers](#) by Andrew Wack, Hanhee Paik, Jay Gambetta et al, 2021 (8 pages).

⁷⁴⁹ See [Generation and verification of 27-qubit Greenberger-Horne-Zeilinger states in a superconducting quantum computer](#) by Gary J. Mooney et al, August 2021 (16 pages).

⁷⁵⁰ See [Whole-device entanglement in a 65-qubit superconducting quantum computer](#) by Gary J. Mooney et al, October 2021 (15 pages).

⁷⁵¹ See [Introducing Quantum Serverless, a new programming model for leveraging quantum and classical resources](#) by Blake Johnson, Ismael Faro, Michael Behrendt and Jay Gambetta, May 2022

Their task is to evangelize developers and researchers to encourage them to develop software on their Qiskit platform and their quantum systems sitting in the cloud.

IBM publishes amazing data on their developer community activity with over 410,000 developers with a run-rate of 3.5 billion quantum circuits executed each and every day as of April 2022 which doesn't really mean anything.

At last, we should mention the quantum volume benchmark created by IBM in 2017 and updated in 2019. We cover it in detail in the [section dedicated to benchmarks](#), page 684.

In April 2021, IBM finalized the deployment of a 28-qubit Quantum System in its own site near Stuttgart, Germany, in relationship with Fraunhofer as an intermediate to reach out the developer community⁷⁵². It was even inaugurated remotely by Chancellor Angela Merkel on June 15th, 2021.

IBM also announced a partnership of 10 years with Cleveland Clinic in the USA, including the delivery of their 1,121 qubits system around 2024. Meanwhile, the customer will rely on the existing cloud-based Quantum Experience systems⁷⁵³. Then, in June 2021, IBM announced a five year \$300M artificial intelligence and quantum computing research partnership with the UK. They plan to hire 60 scientists as part of the new Hartree National Centre for Digital Innovation (HNCDI)⁷⁵⁴. IBM has however not put all its eggs in the superconducting qubits basket. Their Zurich research center is also investigating electron spins and Majorana fermions qubits at a fundamental research level, working on this with ETH Zurich and EPFL. Also, in February 2022, IBM invested \$25M in Quantinuum⁷⁵⁵.



Google started to invest in quantum computing in the mid-2010s. In 2014/2015, it tested some algorithms on a **D-Wave** quantum annealing system installed in the joint QUAIL laboratory established with NASA and located at the Ames Research Center in Mountain View.

Google initially wanted to create its own quantum annealer *ala* D-Wave but quickly switched gears towards gate-based superconducting qubits quantum computing, under the direction of **Hartmut Neven** since 2006, who manages quantum hardware and software. In 2019, he put forward an empirical law called Dowling-Neven according to which the power of computers doubles exponentially. This was exaggerated when you look at their evaluation method⁷⁵⁶!

Hardware was developed by **John Martinis** et al between 2014 and 2020⁷⁵⁷. All this was done in connection with the University of Santa Barbara in California (UCSB), where he came from with part of his team.

⁷⁵² See [Fraunhofer launches quantum computing research platform in Germany](#), April 2021.

⁷⁵³ See [Cleveland Clinic, IBM launch 10-year quantum computing partnership](#) by Mike Miliard, March 2021.

⁷⁵⁴ See [UK STFC Hartree Centre and IBM Begin Five-Year, £210 Million Partnership to Accelerate Discovery and Innovation with AI and Quantum Computing](#), June 2021.

⁷⁵⁵ See [IBM invests in Quantinuum, and other quantum news updates](#) by Dan O'Shea, Fierce Electronics, February 2022.

⁷⁵⁶ The reasoning is as follows: the number of qubits would so far increase exponentially, and the power doubles with each addition of a single qubit. All this, every six months. Unfortunately, the available data on the actual power of today's quantum computers does not comply with this law. There is no doubling of the number of operational qubits every six months! There is even regression! Google announced 72 qubits in March 2018 and then 53 qubits in October 2019. At IBM, we are in the total confusion between the Q System One which went from 20 to 28 qubits between January 2019 and January 2020, which does not look like a doubling every six months. On the other hand, this doubling could eventually be achieved with other technologies such as Honeywell's trapped ions or Pasqal's cold atoms. In his presentation at Q2B in December 2019, John Preskill highlighted another exponential doubling: gate fidelity rates are steadily improving, which would increase quantum volume exponentially. At the same time, the cost of emulating quantum computing on conventional computers increases exponentially with quantum volume. Hence a doubly exponential evolution of computing power. The bug? Nothing says that the fidelity of quantum gates will continue to improve steadily. See [A New Law to Describe Quantum Computing's Rise?](#), June 2019.

⁷⁵⁷ John Martinis resigned from Google in April 2020 after being demoted to a scientific advisory role mid-2019. He explained this in an exit interview for Forbes: [Google's Top Quantum Scientist Explains In Detail Why He Resigned](#) by Paul Smith-Goodson, 2020. See also [Google's Head of Quantum Computing Hardware Resigns](#) by Tom Simonite, April 2020.

In 2017, Google stated its ambition to obtain some quantum supremacy as defined by John Preskill in 2011⁷⁵⁸. In April 2017 came a first 9 qubits chipset. In 2018, their Foxtail 22 qubits chipset was tested, but in quiet way. Then came in March 2018 the announcement of a record 72 qubits with their Bristlecone generation, promising a two-qubits gates fidelity of 99,56%. It seemed however a dead-end and was abandoned. Then came the famous October 2019 so-called quantum supremacy with their Sycamore processor using 53 qubits and a random algorithm similar to the boson sampling algorithm imagined by Scott Aaronson in 2012⁷⁵⁹.

NASA and Google science papers were mistakenly posted on the Internet in September 2019 and then officially published in the journal Nature in October 2019⁷⁶⁰, filing 70 pages with a level of detail never seen before⁷⁶¹. Google compared their qubits with the most powerful supercomputer of the time, the IBM Summit installed at the Department of Energy's Oak Ridge National Laboratory in Tennessee⁷⁶². Computing for 200 seconds on Sycamore would take 10,000 years once emulated on the IBM Summit. This comparison didn't make much sense as we discuss quantum supremacy and advantages in [another part](#) of this book, page 694.

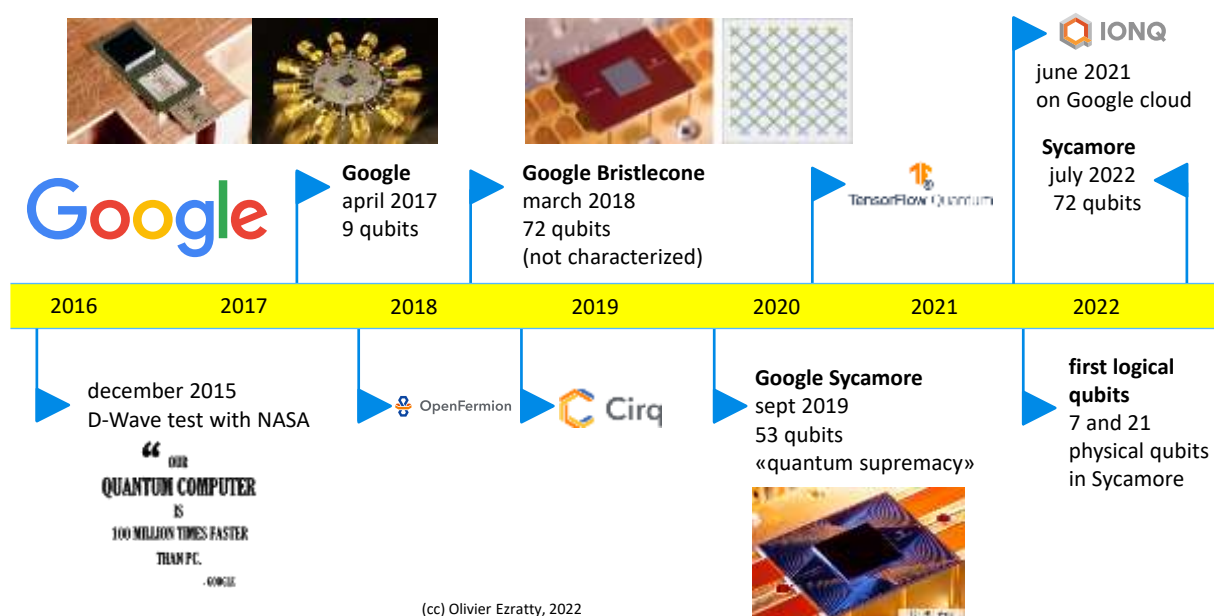


Figure 311: Google's quantum computing timeline. (cc) Olivier Ezratty, 2022.

⁷⁵⁸ See [Google says it is on track to definitively prove it has a quantum computer in a few months' time](#) by Tom Simonite, April 2017. See also [The Question of Quantum Supremacy](#), May 2018 which references two related papers : [Characterizing Quantum Supremacy in Near-Term Devices](#), 2016 (23 pages) and [A blueprint for demonstrating quantum supremacy with superconducting qubits](#), 2017 (22 pages).

⁷⁵⁹ See [Quantum Supremacy Using a Programmable Superconducting Processor](#) by John Martinis, October 2019. The most detailed presentation on Google's hardware engineering with Sycamore is available on [Google's quantum computer and pursuit of quantum supremacy](#) by Ping Yeh, September 2019 (63 slides). See also [Quantum Computer Datasheet](#), Google AI, May 2021 (6 pages) which provides detailed indications of Sycamore's qubit fidelities with the Weber version of the processor.

⁷⁶⁰ See [Hello quantum world! Google publishes landmark quantum supremacy claim](#) by Elizabeth Gibney, October 2019.

⁷⁶¹ See [Quantum supremacy using a programmable superconducting processor](#) by Frank Arute, John Martinis et al, October 2019 (12 pages) and [Supplementary information for "Quantum supremacy using a programmable superconducting processor"](#) by Frank Arute, John Martinis et al, October 2019 (58 pages). See also [Quantum supremacy using a programmable superconducting processor](#), a lecture by John Martinis at Caltech, November 2019 (one hour). And [another version](#), played at QC Ware's Q2B conference in December 2019 (19 slides and 32-minute [video](#)). At last, here is this video promoting Google's supremacy: [Demonstrating Quantum Supremacy](#), October 2019 (4'42").

⁷⁶² See [Google researchers have reportedly achieved "quantum supremacy"](#) by Martin Giles, in the MIT Technology Review, September 2019 and the [source](#) of the paper on the Internet, with illustrations. They use a type of algorithm that is of little use, but which clearly favors quantum computing and requires a limited number of quantum gates, which is good for noise-generating quantum processors. See also [Why I Coined the Term 'Quantum Supremacy'](#) by John Preskill, October 2019.

Let's have a look at Sycamore's engineering and its related supremacy benchmark:

Cross-Entropy Benchmarking (XEB). The benchmark algorithm combined a set of random quantum gates with a homogeneous distribution. This last part scans all the possible values (2^{53}) of qubits superpositions⁷⁶³. In the supremacy regime, the so-called computation has a 0,2% chance to produce the right results. It is executed 3 million times to generate an average measurement mitigating this low fidelity⁷⁶⁴!

It uses superposition on all the qubits (53), allowing maximum performance. Usually, ancilla qubits are necessary to make some calculation. Ancilla qubits are used as buffer values. As a result, the exponential advantage decreases accordingly. Typical algorithms don't benefit from the superposition of 2^{53} states but, for example, a lesser 2^{30} or 2^{40} states. Any quantum advantage would then vanish. This explains why in most vendors roadmap, the end-goal is to create systems with 100 logical qubits and not just between 50 and 55 qubits. The benchmarks use a small 20 quantum gates computing depth. Namely, the algorithm tested at full load only chains 20 sequences of quantum gates executed simultaneously. This is related to the noise generated in the qubits which limits this depth. Many algorithms require a larger number of quantum gates, such as Shor's integer factorization.

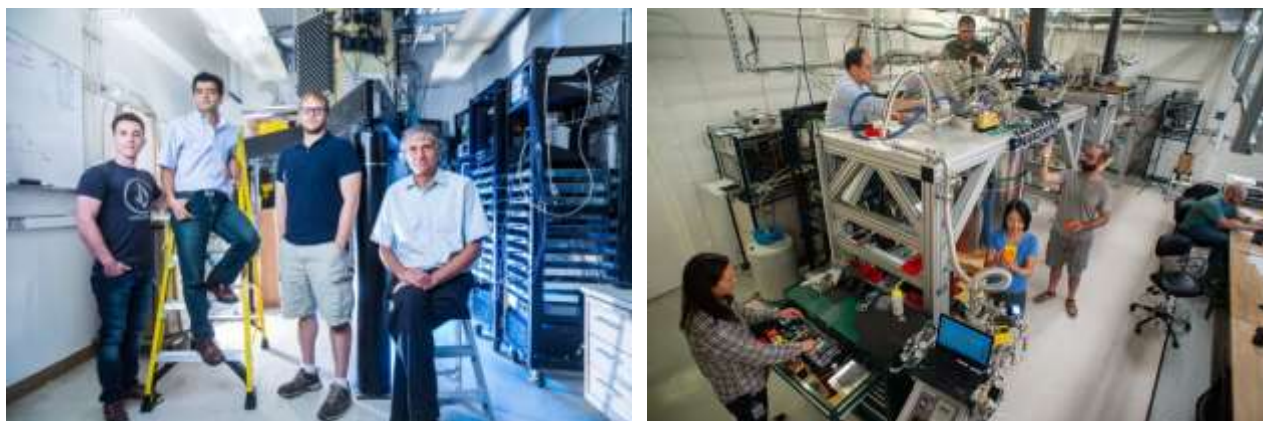


Figure 312: John Martinis and his team when he was at Google and Google's Sycamore's assembly in their lab. Sources: Google.

On October 21, 2019, IBM researchers published an article in which they questioned Google's performance, stating that they could run their algorithm in 2.5 days instead of 10,000 years on the IBM Summit supercomputer⁷⁶⁵. This would require adding 64 PB of SSD to the supercomputer, which they had not tested. That's about 7 racks full of SSDs at 2019 capacity. IBM wanted to contradict Google's claim of quantum supremacy, which they turned into some sort of quantum advantage⁷⁶⁶.

⁷⁶³ The following explanation can be found in Kevin Harnett's [Quantum Supremacy Is Coming: Here's What You Should Know](#) in Quanta Magazine, July 2019.

⁷⁶⁴ See [The Google Quantum Supremacy Demo and the Jerusalem HQCA debate](#) by Gil Kalai, December 2019, where he questions the results of Google's quantum supremacy, particularly its evaluation of qubit noise at large scale.

⁷⁶⁵ See [On "Quantum Supremacy" | IBM Research Blog](#) by Edwin Pednault, October 2019 and [Leveraging Secondary Storage to Simulate Deep 54-qubit Sycamore Circuits](#) by Edwin Pednault et al, October 2019 (30 pages).

⁷⁶⁶ Google's quantum supremacy quibbles have gone a long way, including IBM's response. And then [Has Google Finally Achieved Quantum Supremacy?](#), October 2019, which is quite well documented. Then [Quantum supremacy: the gloves are off](#) by Scott Aaronson, October 2019 where he discusses the fact that this case is the equivalent of Kasparov vs. Deep Blue, with IBM playing the role of Kasparov. Not to mention the debate on supremacy terminology that has once again generated a lot of fuss, as reported in [Academics derided for claiming 'quantum supremacy' is a racist and colonialist term](#) by Sarah Knapton, December 2019.

On top of that, randomized benchmarking used in Google’s experiment is an approach that is not unanimously accepted to establish the superiority of quantum computing over classical computing⁷⁶⁷.

| Metric | Value | Unit | Comments |
|--------------------------------------|-----------|--------------|--|
| Number of qubits | 53 | qubits | Computing qubits |
| Couplers | 86 | couplers | Qubits used for coupling computing qubits |
| Single qubits gates | 1,113 | gates | Number of single qubit gates executed in benchmark |
| Single qubits gates duration | 25 | nano-seconds | Duration of a single qubit gate |
| Single qubit error | 0,16% | percent | |
| Two qubits gates | 430 | gates | Number of two qubits gates executed in benchmark |
| Two qubits gates duration | 12 | nano-seconds | Duration of a two qubit gate |
| Two qubits gates error | 0,93% | percent | |
| Readout error | 3,80% | percent | |
| Gates depth | 20 | cycles | Number of series of quantum gates executed. |
| Gates per cycle | 55,65 | gates/cycle | Number of quantum gates executed per cycle |
| Measured fidelity | 0,20% | percent | Total fidelity of system in supremacy regime |
| Number of iterations | 3,000,000 | iterations | Number of full algorithm executions |
| Computing time | 6,000 | seconds | Total computing time |
| Quantum computing time | 30 | seconds | Total quantum computing time |
| Readout analog to digital convertors | 277 | number | Generating 8 bits at 1 GB/s |

Figure 313: all the figures of merit of Sycamore processor in 2019. Sources: [Quantum supremacy using a programmable superconducting processor](#) by Frank Arute, John Martinis et al, October 2019 (12 pages) and [Supplementary information for "Quantum supremacy using a programmable superconducting processor"](#) by Frank Arute, John Martinis et al, October 2019 (58 pages).

Qubits couplers. Sycamore uses controllable qubit couplers, a technique pioneered by William D. Oliver’s research team at the MIT Lincoln Labs⁷⁶⁸. There are 86 of them in all, connecting the 53 qubits of the chipset. This makes a total of 139 qubits. These couplers are in fact qubits whose frequency is controlled by a direct current line (DC). It allows the implementation of fast two qubits quantum gates, acting in an average 12 ns. They implement CZ and CPHASE two-qubit gates. Sycamore’s processor has qubit readout error ranging from 3% to 7% and two-qubit gates have an error rate ranging from 0.5% to 1.5% while single-qubit gates have error between 0.05% and 0.5%.

Machine Learning based calibration. These qubits and couplers are controlled with microwaves carried by coaxial cables, at frequencies between 5 and 7 GHz, adjusted by a DC flux line. Google developed a deep learning-based qubit calibration code, which has made it possible to refine the qubit microwaves activation frequencies to avoid crosstalk between neighboring qubits.

Isolation: the qubit chipset is protected by some Mu-metal shielding, another one in aluminum and a black coating to absorb infrared photons. The processor is made of aluminum and indium on silicon and includes two dies stacked on top of each other or next to the other.

⁷⁶⁷ See [Lecture 3: Boson sampling](#) by Fabio Sciarrino (63 slides) and [An introduction to boson-sampling](#) by Bryan Gard, Jonathan P. Dowling et al, 2014 (13 pages). See the review [Quantum computers: amazing progress \(Google & IBM\), and extraordinary but probably false supremacy claims \(Google\)](#) by Gil Kalai, September 2019 as well as [The Quest for Quantum Computational Supremacy](#) by Scott Aaronson, September 2019, which was published three weeks before Google’s announcement but was still valid (16 pages).

⁷⁶⁸ See [Tunable Coupling Scheme for Implementing High-Fidelity Two-Qubit Gates](#) by Fei Yan, William D. Oliver et al, MIT Lincoln Labs, PRX, 2018 (10 pages).

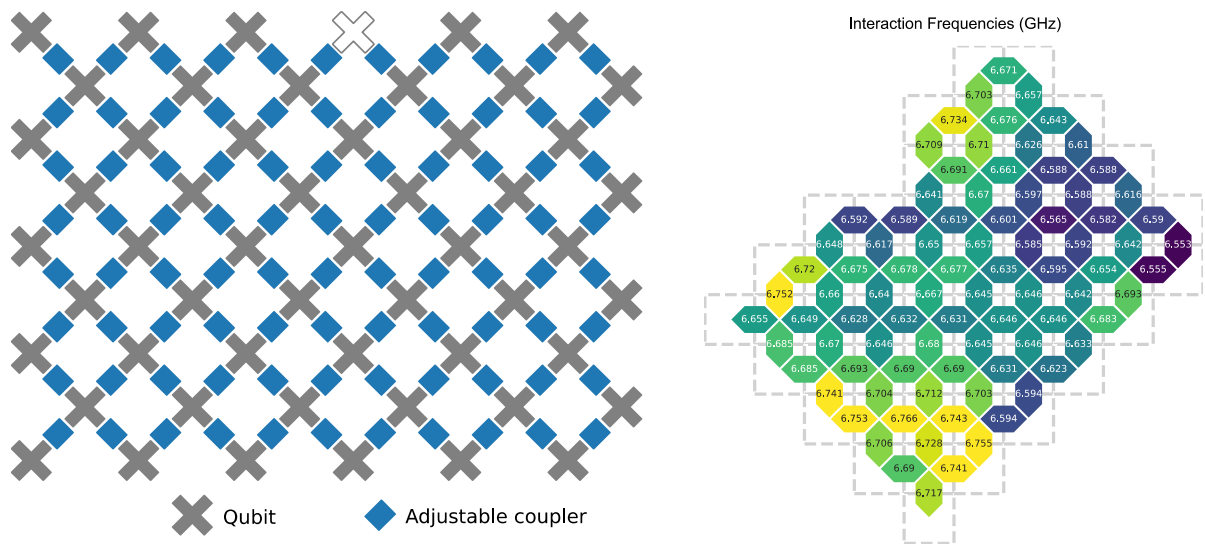


Figure 314: Google's Sycamore qubits layout, with their data qubits and coupler qubits (in blue). On the right, the interaction frequencies with each qubit which were calibrated and optimized using a machine learning solution. Source: Sycamore's papers.

Microwave generation. Below is a set of schematics of the control electronics inside and outside the cryostat. The system uses 54 external microwave signal generators for the single-qubit gates (X and Y), 54 for qubit frequency control and 86 for qubit control. This is completed by 9 readout microwave control signals, meaning they are frequency domain multiplexing readout by chunks of 6 qubits thanks to their use of a wideband parametric amplifier at the 15 mK stage, what they call an IMPA. The control electronics package includes 277 digital-to-analog converters that occupy 14 6U rack-mount cases. There is a similar number of coaxial cables ending in the cryostat.

Z gates: DC flux lines are also used to create Z gates, or phase gates. They are controlled with microwaves in IBM's superconducting qubits. Using DC flux lines is reducing the phase error observed with these gates.

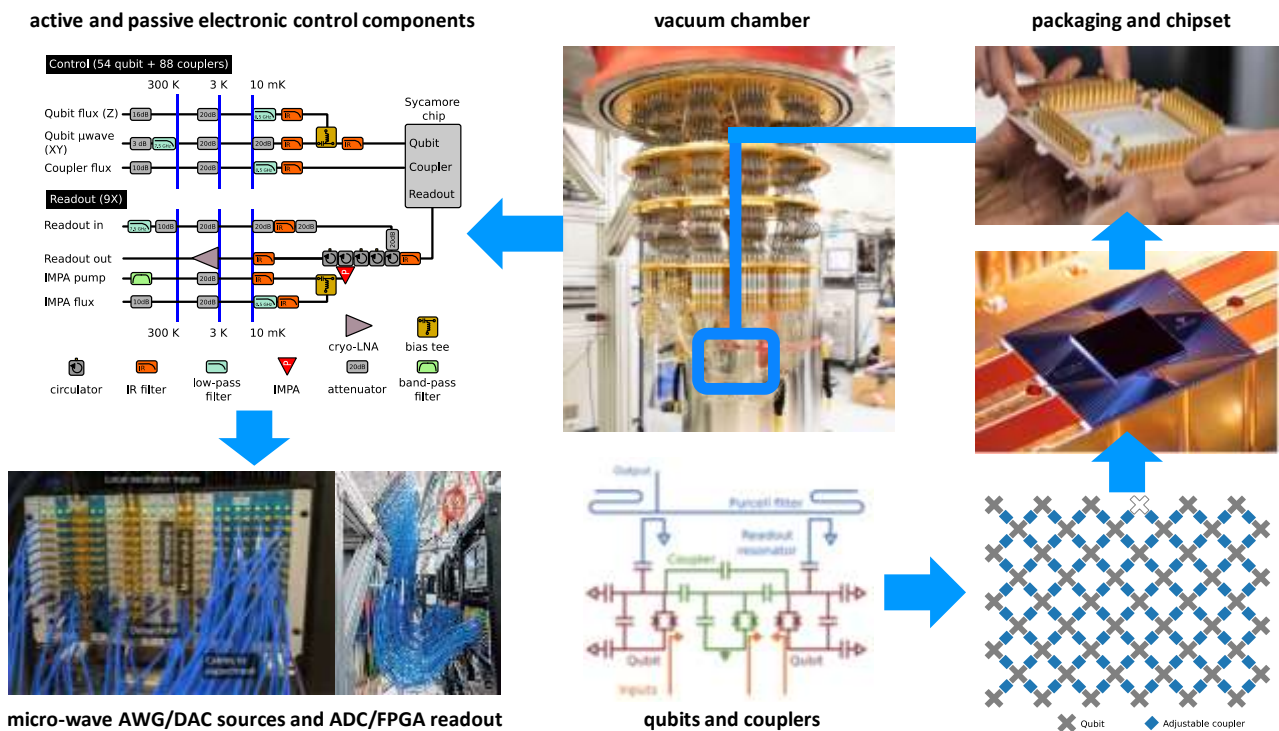


Figure 315: a Russian doll description of Sycamore starting with the qubits and coupler, then with the chipset layout, its size, its packaging and connectors, where it is placed in the cryostat and the surrounding control electronics. Source: Google. Compilation (cc) Olivier Ezratty, 2020-2022 with sources from Google.

Qubit readouts is done with only a few microwave photons sent to the qubits. The result is amplified by 100 dB in several steps, one at the 15 mK processor stage and another at the 3K stage. The resulting amplified microwaves are converted digitally by an ADC (analog-to-digital converter) and analyzed by a FPGA to detect their phase. The system multiplexes in the frequency domain the readout microwaves of 6 qubits groups conveyed by a single cable, between 5 and 7 GHz.

Energetic advantage: Sycamore showcases some energy consumption advantage, with a ratio of about one to a million. Its power consumption is about 25 kW and the ORNL IBM Summit is at 12 MW at full charge, and the computing time ratio is 2.5 minutes vs. 2.5 days (1/1440) in the most favorable IBM Summit case. But we are probably comparing apples and oranges given the supremacy doesn't relate to solving some useful problem with input data and parameters.

Between 2019 and mid-2022, Google had not yet released a new generation processor. Finally, they quietly disclosed that they had created a 72-qubit version of Sycamore in a paper related to surface codes, published in July 2022, as shown in Figure 316. The next step will be a 100+ qubits QPU to implement a distance-7 surface code logical qubit.

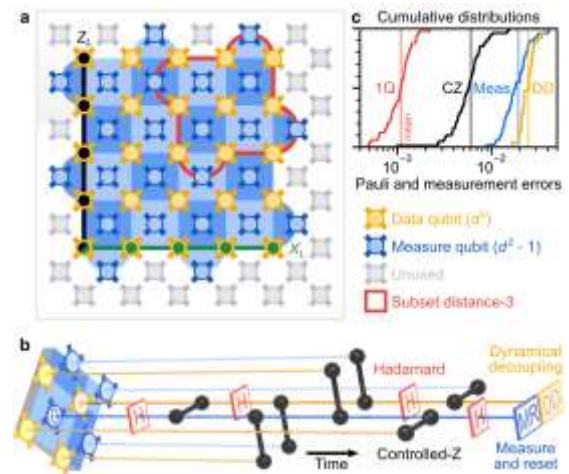


Figure 316: Sycamore's 72 qubit version that implements a distance-5 surface code error correction for a single logical qubit, that is still insufficient to improve qubit fidelities. Source: [Suppressing quantum errors by scaling a surface code logical qubit](#) by Rajeev Acharya et al, Google AI, July 2022 (44 pages).

It wants to reduce qubits error rates and scale up to a hundred logical qubits⁷⁶⁹. In a July 2020 conference, Hartmut Neven announced his 10-year plan to achieve this result, showing impressive mockups of a giant quantum computer containing 100 modules with 10 000 physical qubits each. It would be a giant installation, as shown on the impressive artist's rendering in Figure 317.

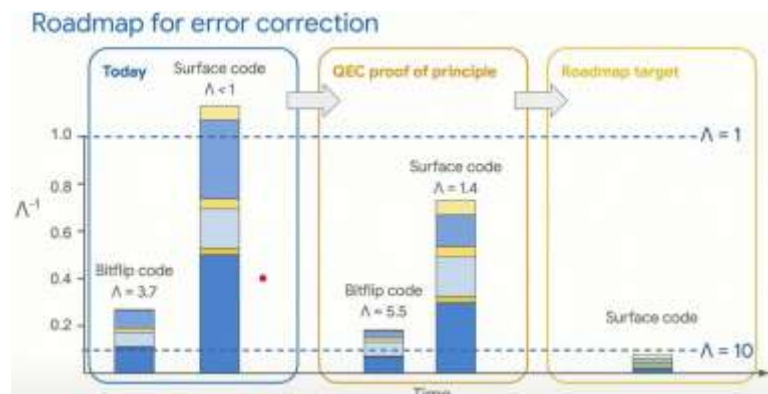


Figure 317: Google's roadmap for error corrections. Source: Hartmut Neven, July 2020.

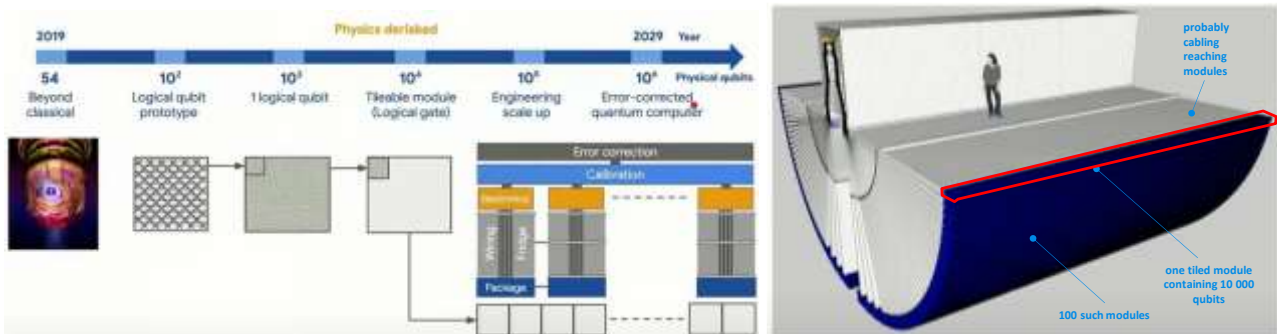
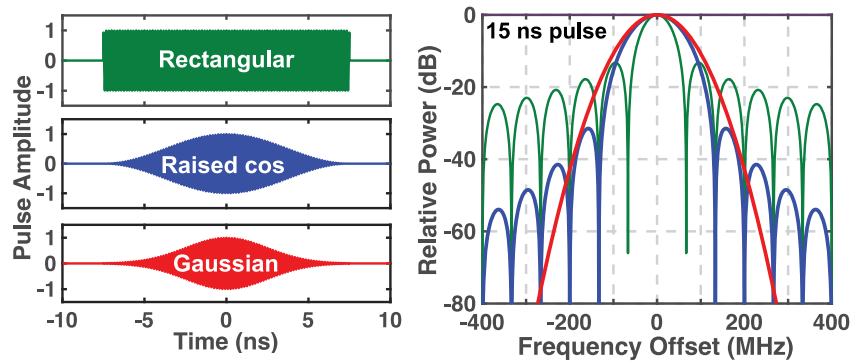


Figure 318: Google's scalability roadmap with logical qubits made of 1000 physical qubits. And a giant system, as envisioned in 2020. Things may have changed since then. Source: Hartmut Neven, July 2020.

⁷⁶⁹ Source of the illustrations shown in Figure 317 and Figure 318: [Day 1 opening keynote by Hartmut Neven \(Quantum Summer Symposium 2020\)](#), July 2020 (30 mn) and the [whole symposium](#).

Cryo-CMOS. To scale up micro-waves generation and put it inside the cryostat, Google published some work on a cryo-CMOS chipset operating at 3K, using simple waveform generators consuming a minimum of energy to create only single qubit gates⁷⁷⁰.

It has however not yet been deployed. It relies on cosinusoidal shape microwaves with the interest of creating spectral "holes" corresponding to the qubits frequencies harmonics of the state $|1\rangle$ to the state $|2\rangle$ transition, that must be avoided. It corresponds to the wavelength known as ω_{12} as seen in the illustration from page 299.



Raised cosine: good compromise between sidelobes and pulse duration

Figure 319: qubit control signals optimization with spectral holes matching qubit frequencies harmonics. Source: [XY Controls of Transmon Qubits](#) by Joseph Bardin, June 2019 (36 slides).

Qubits improvements. Several physical improvements are tested with their qubits. They reset qubits with high fidelity, allowing us to reuse qubits in quantum computations. They also test mid-circuit measurement that makes it possible to keep track of computation within quantum circuits. They also work on addressing cosmic radiation originated noise in circuits⁷⁷¹.

Error correction codes. At the APS March Meeting 2022 in Chicago, Kevin Satzinger provided an update on Google’s ploy with quantum error correction using surface codes. Their mid-term goal is to create a “logical qubit” prototype with 100 physical qubits, then extend it to 1000 physical qubits⁷⁷². The end goal is to build logical qubits with error rates around 10^{-12} , a level that is required to execute many useful gate-based algorithms. With surface codes, these logical qubits are organized in squared arrays of about d^2 physical qubits (in blue, green ones are the qubit couplers) where d is the so-called code distance (5 in the example below).

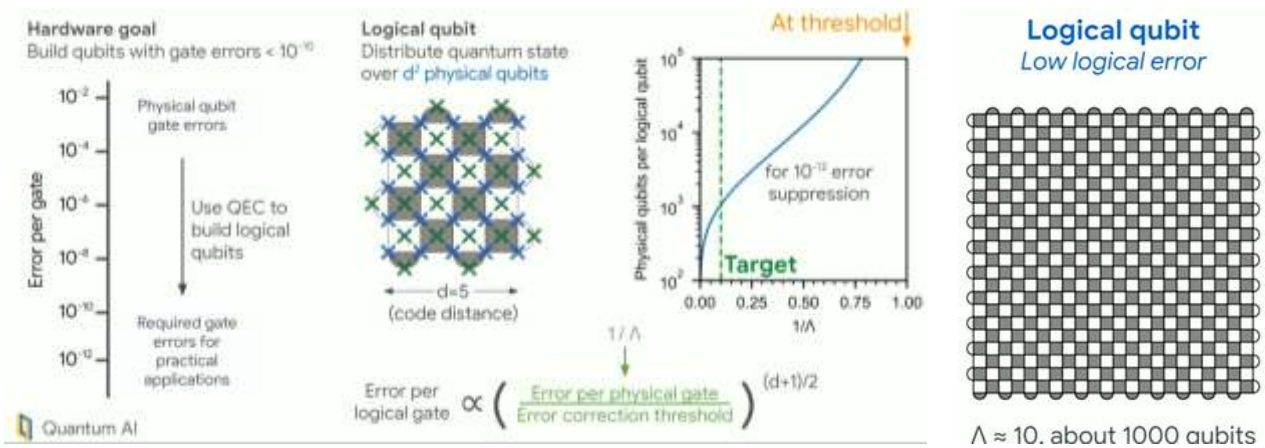


Figure 320: how Google plans to reach an error rate of 10^{-12} with its logical qubits. Source: [APS March Meeting: Google, Intel and Others Highlight Quantum Progress Points](#) by John Russell, HPCwire, March 2022.

⁷⁷⁰ See [Control of transmon qubits using a cryogenic CMOS integrated circuit](#) by Joseph Bardin, March 2020 (35 minutes) and [A 28nm Bulk-CMOS 4-to-8GHz <2mW Cryogenic Pulse Modulator for Scalable Quantum Computing](#) by Joseph Bardin, Craig Gidney, Charles Neil, Hartmut Neven, John Martinis et al, February 2019 (13 pages).

⁷⁷¹ See [Resolving catastrophic error bursts from cosmic rays in large arrays of superconducting qubits](#) by Matt McEwen et al, April 2021 (13 pages).

⁷⁷² See [APS March Meeting: Google, Intel and Others Highlight Quantum Progress Points](#) by John Russell, HPCwire, March 2022.

Kevin Satzinger explained how Google came out with the 1000 physical qubit per logical qubit number. It comes from the way logical gates error are evaluated, per the formula $1/\Lambda$, Λ being the ratio between the threshold (theorem) error level and the physical gate error level. Λ must be at 10 to reach a 10^{-12} error rate with 1000 physical qubits per logical qubits (above, right). They first plan to implement $d=3$ and then $d=5$ surface codes and make sure the latter is better than the former with regards to logical gate errors⁷⁷³.

In 2021, Google experimented two repetition code layouts on Sycamore with 21 qubits in a 1D chain correcting flip or phase errors and a distance-2 surface code of 7 qubits correcting both flip and phase errors. It did show that flip and phase errors could be exponentially suppressed with adding more physical qubits⁷⁷⁴. They did show a 100-factor improvement in error suppression as the size of their logical qubits was growing from 5 to 21 physical qubits. They could assess the impact of a good Λ value.

The next step being to expand these tests on a yet-to-deliver successor of Sycamore and a larger number of qubits and the capacity to implement larger surface codes with $d \geq 3$. They also propose to use “pulse sequence” to correct unwanted crosstalk and dephasing that are disturbing surface codes⁷⁷⁵.

They still have a huge challenge, like with IBM, to grow the number of physical qubits without degrading their fidelities.

Sycamore at work. Since 2020, Google tried to make some good use of Sycamore to test various algorithms. They “*simulated simple models of chemical bonding, high-temperature superconductivity, nanowires, and even exotic phases of matter such as time crystals*”. They also solved some small combinatorial problems and managed a chemical simulation of a molecule of four atoms. In most cases, there was no more touted supremacy. This time, without mentioning the notion of supremacy⁷⁷⁶! Which makes sense given they didn’t use more than 15 qubits to solve these small-scale problems. Other same scale algorithms were published in 2020⁷⁷⁷. Like with IBM’s QPUs, the larger the number of qubits that are used in algorithms, the worse it is with their noise and computing depth. They end-up with using around 15 to 20 qubits for useful purposes. Of course, with that number of qubits, we’re very far from any quantum advantage or supremacy.

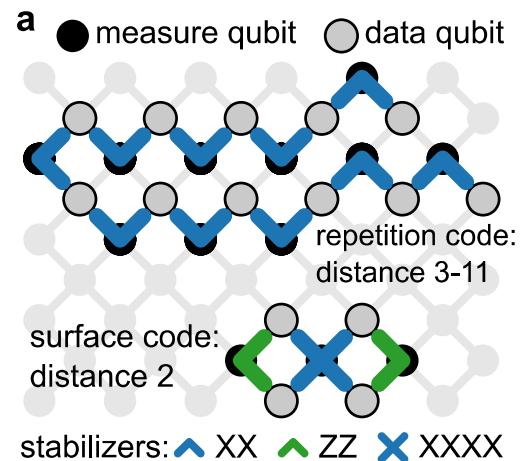


Figure 321: the first logical qubits created on Sycamore in 2021. Source: [Exponential suppression of bit or phase flip errors with repetitive error correction](#) by Zijun Chen et al, Nature, Google AI, July 2021 (32 pages).

⁷⁷³ See also [Progressing superconducting quantum computing at Google](#) by Kevin Satzinger, April 2022 (47 mn).

⁷⁷⁴ See [Demonstrating the Fundamentals of Quantum Error Correction](#) by Jimmy Chen et al, August 2021 and [Exponential suppression of bit or phase flip errors with repetitive error correction](#) by Zijun Chen et al, Nature, July 2021 (32 pages). [Removing leakage-induced correlated errors in superconducting quantum error correction](#) by M. McEwen et al, March 2021, Nature Communications (12 pages) deals with another error reduction technique named “multi-level reset” that consists in “pumping” the excess energy from superconducting qubits that leak to their higher energy levels $|2\rangle$ or $|3\rangle$.

⁷⁷⁵ See [Pulse sequence design for crosstalk mitigation](#) by Murphy Yuezhen Niu.

⁷⁷⁶ See [Quantum Approximate Optimization of Non-Planar Graph Problems on a Planar Superconducting Processor](#) by Google AI Quantum and Collaborators, April 2020 (17 pages) which deals with three families of combinatorial problems with the QAOA algorithm and [Hartree-Fock on a superconducting qubit quantum computer](#) by Google AI Quantum and Collaborators, April 2020 (27 pages) with a diimide ((NH)² molecular simulation algorithm.

⁷⁷⁷ See this theoretical paper on the use of quantum computing, not necessarily with Google qubits, to study black holes. See [Google Scientists Are Using Computers to Study Wormholes](#) by Ryan F. Mandelbaum, November 2019 which refers to [Quantum Gravity in the Lab: Teleportation by Size and Traversable Wormholes](#) by Adam R. Brown et al, November 2019 (20 pages).

In 2021⁷⁷⁸, together with researchers from Columbia University, Google's teams created a chemical simulation classical/quantum hybrid algorithm using a Monte Carlo method⁷⁷⁹. It was used to compute the ground state of two carbon atoms in a diamond crystal, using 16 qubits. The method was however not more efficient than a full classical algorithm.

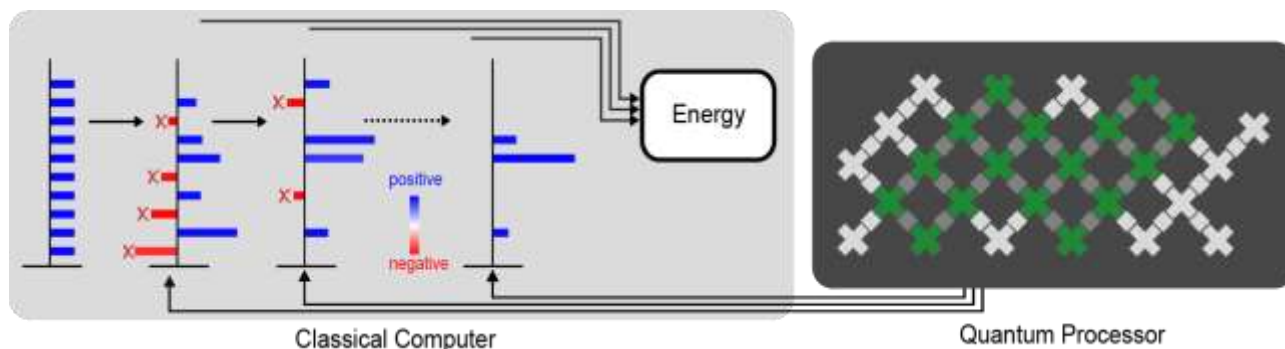


Figure 322: simple schematic of a chemical simulation classical/quantum hybrid algorithm using a Monte Carlo method. Source: [Hybrid Quantum Algorithms for Quantum Monte Carlo](#) by William J. Huggins, March 2022.

In 2022, another simulation of some molecules and materials as published, first with the iron-sulfur clusters of nitrogenase, including the FeMo-cofactor (aka FeMoCo), a component of the natural nitrogen cycle and second with the electronic structure of α -RuCl₃, a candidate material for realizing spin liquid physics⁷⁸⁰. The experiments were using 5 to 11 qubits, far from any quantum advantage territory. All of this was running on Google's 53-qubit Weber processor, the second generation of Sycamore chipsets with slight performance improvements.

In 2021, Google also teamed up with **Caltech** to show some quantum superiority when quantum computers directly exploit quantum data coming from quantum sensors. Fewer experiments are required than if the communication between sensors and the quantum processor was classical. The experiment was done with 40 qubits and 1300 quantum operations⁷⁸¹.

Google software tools. Several Google teams are working on quantum software, including those working on Cirq, on TensorFlow Quantum and another Google X team working on applications, under the leadership of Jack Hidary⁷⁸². They also released a **Fermionic Quantum Simulator** for quantum chemistry applications in collaboration with **QSimulate** (2018, USA) aka qsim. It can simulate noisy quantum circuits with Nvidia GPUs on Google Cloud. Google also published stim, an open source tool providing a 10000x speedup when simulating error correction circuits.

Quantum cloud. At last, it has a quantum cloud offering for quantum algorithm simulation and hosts an IonQ trapped ion system and, surprisingly, none of its Sycamore systems which are only accessible to a handful of academic partners, an outreach strategy that is very different from the broadscale one IBM adopted.



Rigetti (2013, USA, \$656M) is another commercial superconductor vendor. With D-Wave, IonQ and PsiQuantum, it is the fourth best funded startup in the industry.

⁷⁷⁸ See [2021 Year in Review: Google Quantum AI](#) by Emily Mount, December 2021.

⁷⁷⁹ See [Hybrid Quantum Algorithms for Quantum Monte Carlo](#) by William J. Huggins, March 2022 and [Unbiasing Fermionic Quantum Monte Carlo with a Quantum Computer](#) by William J. Huggins, Ryan Babbush, Joonho Lee et al, Nature, July 2021 (28 pages).

⁷⁸⁰ See [Simulating challenging correlated molecules and materials on the Sycamore quantum processor](#) by Ruslan N. Tazhigulov et al, March 2022 (22 pages).

⁷⁸¹ See [Quantum advantage in learning from experiments](#) by Hsin-Yuan Huang et al, December 2021 (52 pages).

⁷⁸² See [Alphabet Has a Second, Secretive Quantum Computing Team](#) by Tom Simonite, January 2020. No secret anymore buddy!

It was launched by Chad Rigetti, who got a PhD and did a post-doc at Yale University on microwave driven two-superconducting qubit gates in 2009⁷⁸³, and then worked as a researcher at IBM between 2010 and 2013.

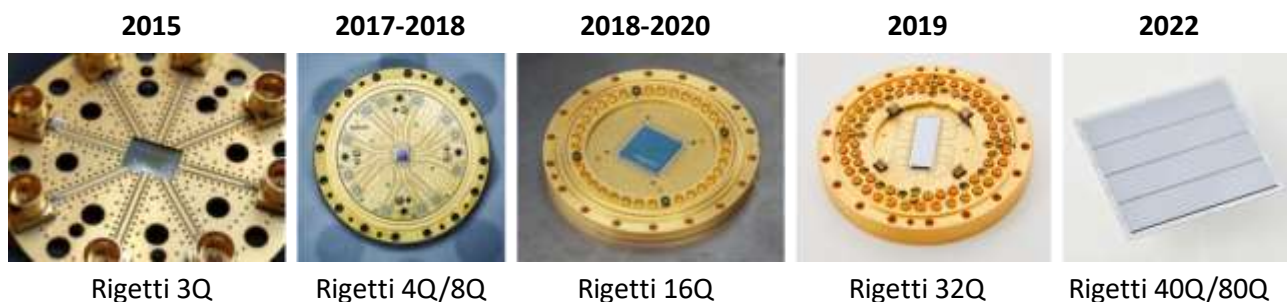


Figure 323: evolution of Rigetti actual chipsets over time. Source: Rigetti investor presentation.

Over about 8 years, their QPUs went from 3 to 80 qubits. They had a tendency to oversell their roadmap, having announced prematurely a 128 qubits test version in August 2018 that was never benchmarked or deployed. They started to deploy their system on Amazon Braket with its Aspen-9 processor of 31 qubits in 2020.

Their Aspen-M 80 qubits chipset was announced in December 2021 and commercially available in February 2022 on Rigetti Quantum Cloud Services and Amazon Braket, and subsequently on Azure Quantum, Strangeworks QC and Zapata Computing's Orquestra platform⁷⁸⁴. Their fidelities are not as good as with IBM and Google but it is continuously improving, even as they increase the number of qubits.

| metric | Aspen-9 | Aspen-11 | Aspen-M-1 |
|---------------------------------|------------|--------------|--------------|
| number of physical qubits | 31 | 40 | 80 |
| median T_1 | 27 μ s | 25.7 μ s | 30.7 μ s |
| median T_2 | 19 μ s | 14.9 μ s | 23.0 μ s |
| median simultaneous 1Q fidelity | 99,80% | 99.50% | 99.70% |
| median 2Q XY fidelity | 95,40 % | 93.70% | 95.30% |
| median 2Q CZ fidelity | 95,80 % | 90.20% | 93.10% |
| median RO fidelity | | 97.10% | 98.20% |
| median active reset fidelity | | 99.20% | 99.80% |

Figure 324: Rigetti qubits figures of merit for their last generation chipset. These number are now fairly well detailed, but they show that it doesn't compete well with IBM at least on two qubit gates. Data source: Rigetti.

In 2022, they demonstrated improved two-qubit gates fidelities of 99,5% but with a 9 qubits prototype⁷⁸⁵. Sideways, they are also experimenting the usage of qutrits with three level anharmonic oscillators in their superconducting loops. It was tested on a 5-transmon chipset with two qutrits entanglement⁷⁸⁶.

So, what is special with Rigetti? Let's look at a couple aspects of their qubits and systems engineering.

Coupling qubits. Their flux qubits are entangled by dynamically configurable couplers, which reminds us of Google Sycamore. It brings more flexibility for managing two qubit gates⁷⁸⁷. These are adjustable transmon qubits using asymmetric SQUIDs (magnetometers).

⁷⁸³ See [Quantum Gates for Superconducting Qubits](#), 2009 (248 pages).

⁷⁸⁴ See [Rigetti Announces Commercial Availability of their 80 Qubit Aspen-M and a Teaming with NASDAQ to Explore Financial Applications of QC](#), February 2022.

⁷⁸⁵ See [Rigetti Computing Reports Fidelities as High as 99.5% on Next-Generation Chip Architecture](#), February 2022.

⁷⁸⁶ See [Beyond Qubits: Unlocking the Third State in Quantum Processors](#) by Alex Hill, Rigetti, December 2021 and [Quantum Information Scrambling on a Superconducting Qutrit Processor](#) by M. S. Blok et al, April 2021 (21 pages).

⁷⁸⁷ This is explained in [Demonstration of Universal Parametric Entangling Gates on a Multi-Qubit Lattice](#) by M. Reagor et al, 2018 (17 pages).

Electronics optimization. Rigetti made efforts to optimize the physical and electrical components of its accelerators. First, by integrating the control and measurement wiring of the qubits in compact sheets that they patented⁷⁸⁸. They developed their own microwave generation electronics. They also found a way to limit crosstalk between qubits⁷⁸⁹. They also work on merging microwave and DC flux lines into the same wires used for respectively XY and Z single qubit gates, between the 10 mK cold plate and the qubit chipset⁷⁹⁰. As a result, they tout performance improvements expressed in CLOPS (circuit layer operations per seconds) for their 40-qubit Aspen-11 and 80-qubit Aspen-M systems. The first had 844 CLOPS while the second reached 892. It can be compared to IBM's 1500 CLOPS on their 65 qubits system and 850 with 127 qubits (as of April 2022)⁷⁹¹.

Modular chipsets. Rigetti is now splitting qubits in multiple semiconductors dies connected with each other with indium-based flip-chip bonded on a single larger carrier die. This reduces qubits crosstalk between modules, at the expense of a smaller fidelity. They first tried this with 4 chips containing each 4 aluminum and niobium-based SQUIDS qubits and 4 tunable couplers, their fidelities are $99.1 \pm 0.5\%$ and $98.3 \pm 0.3\%$ for iSWAP and CZ gates⁷⁹². They then expanded this to two 40 qubits dies in their Aspen M1 chipset released in December 2021.

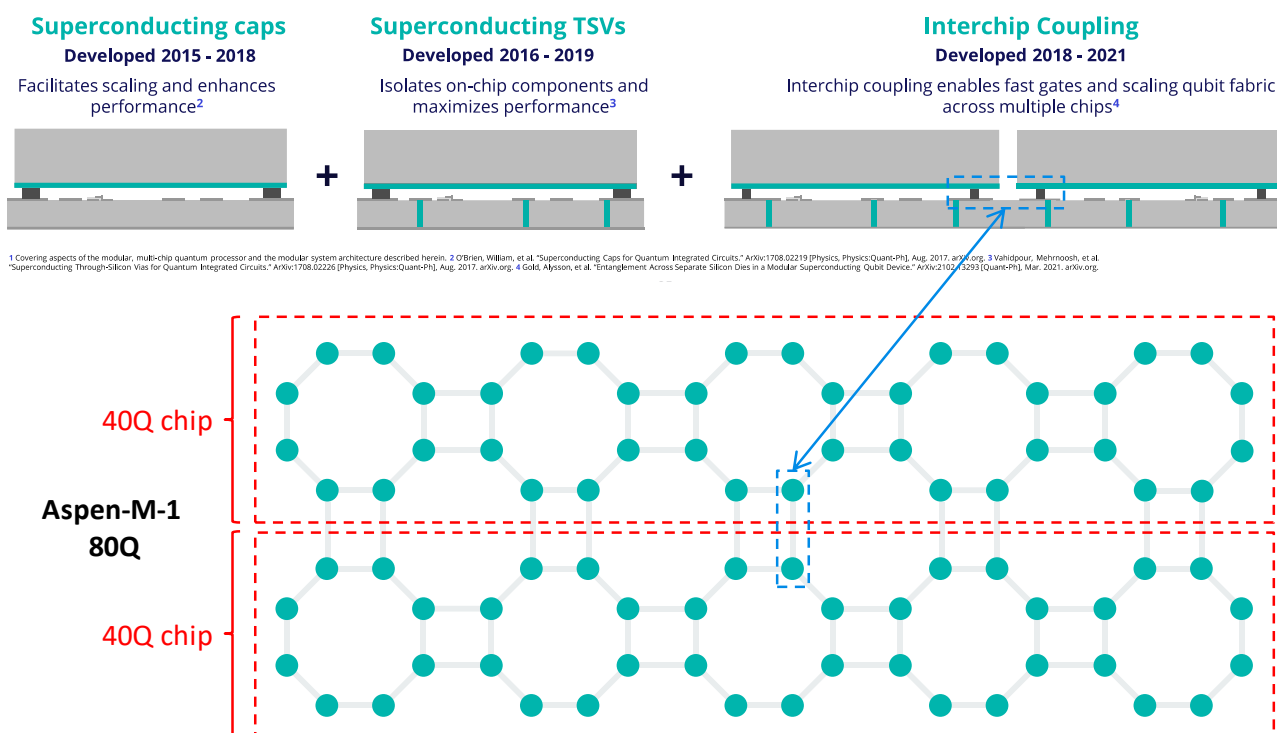


Figure 325: interchip coupling implemented with their Aspen-M-1 80-qubit processor, assembling two dies of 40 qubits.
Source: Rigetti.

Cleanroom. Rigetti have their own small manufacturing unit producing their semiconducting chipsets, named Fab-1. This enables them to create new chipsets with a 5-15 month cycle. The required and initial investment of about \$10M, which is reasonable even for a startup. The creation of superconducting qubit circuits is done with a very low-level of integration.

⁷⁸⁸ See Connecting Electrical Circuitry in a Quantum Computing System, [USPTO 20190027800](#).

⁷⁸⁹ See [Methods for Measuring Magnetic Flux Crosstalk Between Tunable Transmons](#) by Deanna M. Abrams et al, August 2019 (12 pages).

⁷⁹⁰ See [Full control of superconducting qubits with combined on-chip microwave and flux lines](#) by Riccardo Manenti et al, July 2021 (8 pages).

⁷⁹¹ See [Optimizing full-stack throughput and fidelity with Rigetti's Aspen-M generation of quantum processors](#), Rigetti, February 2022.

⁷⁹² See [Entanglement Across Separate Silicon Dies in a Modular Superconducting Qubit Device](#) by Alysson Gold, 2021 (9 pages).

We are far from the \$20B 5 nm fabs from TSMC. In the case of silicon qubits, on the other hand, it is necessary to have an equipment of about \$1B⁷⁹³!



Figure 326: Rigetti's superconducting cleanroom fab line in Fremont, California. Source: Rigetti.

This multi-dies QPU approach is the main driving technology for them to scale their QPUs. The short term roadmap contains the 84-qubit Ankaa for 2023 and the 336-qubit Lyra for late 2023. Then, they plan to create 500 qubits chipsets by 2025 and assemble them in 1000, 4000 and larger QPUs. They have however not yet explained how they will interconnect these multi-dies chipsets⁷⁹⁴.

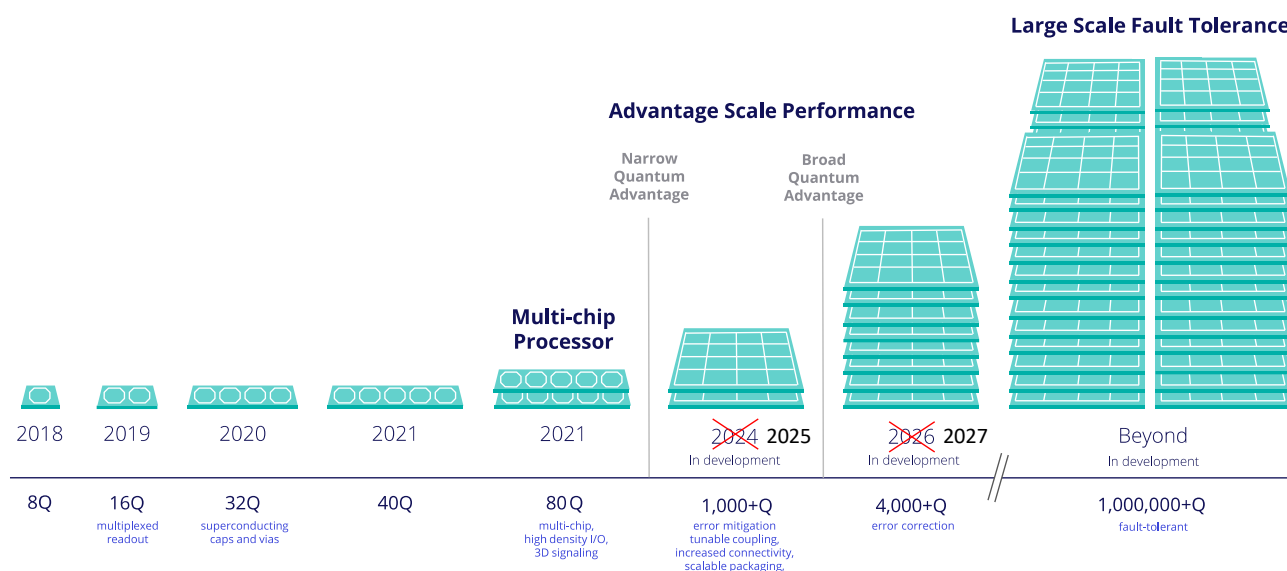


Figure 327: Rigetti's scalability roadmap announced in October 2021. In May 2022, the company announced an additional one-year delay for their 1000 and 4000 qubits QPUs. They also expect to release 84 and 336 qubit chipsets in 2023. Source: Rigetti investor presentation, October 2021 and [Rigetti Computing Reports First Quarter 2022 Financial Results and Provides Business Update](#), May 2022.

Full-stack software development. It includes pyQuil for scripting and Quil for quantum gate management. These are both open source and published on Github. Quil allows to synchronize tasks between quantum and classical computing⁷⁹⁵. In 2018, they demonstrated the use of their quantum computer for a machine learning algorithm that does not require a hybrid algorithm⁷⁹⁶.

⁷⁹³ See [Quantum Cloud Computing Rigetti](#) by Johannes Otterbach, 2018 (105 slides) and the [corresponding video](#), and [Manufacturing low dissipation superconducting quantum processors](#) by Ani Nersisyan et al, Rigetti, 2019 (9 pages).

⁷⁹⁴ Source: [Rigetti Investor Presentation](#), October 2021 (56 slides).

⁷⁹⁵ See [A Practical Quantum Instruction Set Architecture](#) by Robert S. Smith, Michael J. Curtis and William J. Zeng, Rigetti Computing, 2017 (15 pages).

⁷⁹⁶ In [Quantum Kitchen Sinks: An algorithm for machine learning on near-term quantum computers](#), July 2018 (8 pages).

Cloud. Rigetti offers access to its quantum computers via the cloud, like IBM and D-Wave do with their Quantum Cloud Services. It started running in beta in January 2019. Since early 2020, they are also distributed in the cloud by Amazon in its Braket service.

Acquisition. Rigetti acquired QxBranch in July 2019 to complete its software offering. It was established in the USA, UK and especially in Australia. In September 2020, their UK-based subsidiary announced the launch of a collaborative project to accelerate the commercialization of quantum computers, funded with £10M private/public money. To do so, they will use a latest-generation Proteox cryostat from Oxford Instruments.

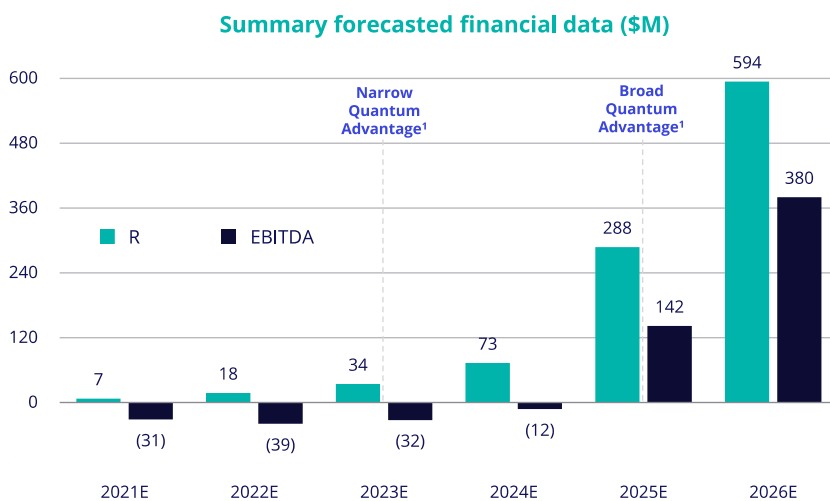


Figure 328: Rigetti's revenue and EBITDA forecasts until 2026. In the first quarter of 2022, they made \$2.1M. It seems their 2022 forecast was optimistic. Source: [Q1 2022 quarterly report](#).

SPAC. After having raised about \$200M through classical VCs, they went into the stock market after being acquired by a SPAC company in March 2022, Supernova Partners Acquisition Company II. It brought on the table \$345M of funding for a valuation of \$1,152M. As of December 2021, the company had 140 people in the United States, UK and Australia. At their SPAC time, they were forecasting a revenue of \$594M by 2026, based on the release of their 1000 qubits system in 2024.

In May 2022, they announced a one-year delay on their roadmap⁷⁹⁷.

Patents. They have a portfolio of 100 patents and applications in interchip coupling and multi-die chipsets, cabling, processor design, cloud quantum computing and quantum software tools.

Partnerships. On top of **Amazon**, **Microsoft**, **Zapata Computing** and **Strangeworks** for cloud deployments, they announced in 2022 a new partnership with **Ampere Computing** (USA) to create hybrid quantum-classical computers designed to run machine learning applications, with **Keysight** for control electronics and **Bluefors** for cryogeny. Ampere is a fabless company designing 128-core arm chipsets for servers⁷⁹⁸. They have also various business and academic partnerships running in the UK, which led to the deployment in the UK of a 32-qubit Aspen system in June 2022 (why not the more recent 40 or 80 qubit Aspen?). With **Zapata**, they are building hybrid quantum-classical compilation tools with the support of the 80Q Aspen-M QPU and Rigetti cloud services. At last, they announced a partnership with **Riverlane** (UK) in June 2022 to work on error correction.

Rigetti is also working with DARPA in the USA, having been selected to provide hardware, software and benchmarks for phase two of the DARPA ONISQ program (Optimization with Noisy Intermediate-Scale Quantum). The aim is to create quantum computers able to solve complex optimization problems. This work is jointly done with Universities Space Research Association (USRA) and NASA's Quantum Artificial Intelligence Laboratory (QuAIL). Rigetti has also a strong R&D partnership with the DoE **Fermilab**, which conducts testing and material designs in its Superconducting Quantum Materials and Systems Center (SQMS) led by Anna Grassellino⁷⁹⁹.

⁷⁹⁷ See [Rigetti Pushes Back Roadmap on Development of 1,000-Qubit, 4,000 Qubit Models](#) by Matt Swayne, The Quantum Insider, May 2022.

⁷⁹⁸ See [Ampere Goes Quantum: Get Your Qubits in the Cloud](#) by Ian Cutress, AnandTech, February 2022.

⁷⁹⁹ See [Superconducting Quantum Materials and Systems Center](#) by Anna Grassellino, June 2021 (40 slides).

Customer wise, they have a couple early adopters like **Nasdaq** who plans to use their systems to detect fraud, optimize order matching and handle risk management.



IQM (2018, Finland, 167M€) is a spin-off from the Quantum Computing and Devices group of the Aalto University and from the VTT research center. Its funding is a mix of dilutive capital investment and debt financing through the European Investment Bank.

In June 2020, IQM received 15M€ capital funding from the European Commission's EIC Accelerator, supplemented by a 2.5M€ grant. A new funding round of 128M€ was announced in July. All-in-all, IQM raised 167M€ making it the best funded quantum startup in Europe.

They develop superconducting qubits QPUs after having initially created an on-chip refrigeration system technology for superconducting and silicon chipsets based on electron transfer using an electron tunnel-effect⁸⁰⁰. The company states that their qubits are operable with a faster clock speed than competing superconducting qubits thanks to optimizations applied to qubits reset, gates and readout. They use tunable couplers for qubits entanglement. They also developed a fast graphene-based bolometer for qubit readout able to detect a single microwave photon. Its benefits is some power saving compared to parametric amplifiers⁸⁰¹.

On the R&D stage, IQM participates to a research consortium including Aalto University and VTT which proposed in 2021 a qubit on-chip circuit to create microwaves pulses that could be used to drive superconducting qubits and working at 10 mK⁸⁰². Its size is one mm and would remove the need to use cables to feed the processor with microwave pulses. So far, it only creates a sinus wave at 1 GHz, still far from what is needed to drive a superconducting qubit, i.e., a short duration pulse with a precise waveform added to some carrier frequency at around 5 GHz. It is closer to a local oscillator source! IQM also uses a TWPA from VTT in the first stage amplification of qubit readout microwaves⁸⁰³. This enables them to enable 5 to 10 qubits readout multiplexing with using different frequencies for qubits readouts with resonators of different lengths.

In March 2022, IQM introduced a new superconducting-qubit type nicknamed the unimon which has better fidelities, of about 99.9% with single-qubit gates. It is using a single Josephson junction in a resonator, combining high anharmonicity in the superconducting loop, different anharmonicities for each qubit, better insensitivity to low frequency charge noise and insensitivity to magnetic flux noise. As of 2022, they had tested three unimon qubits given they use tunable couplers to create two-qubit gates.

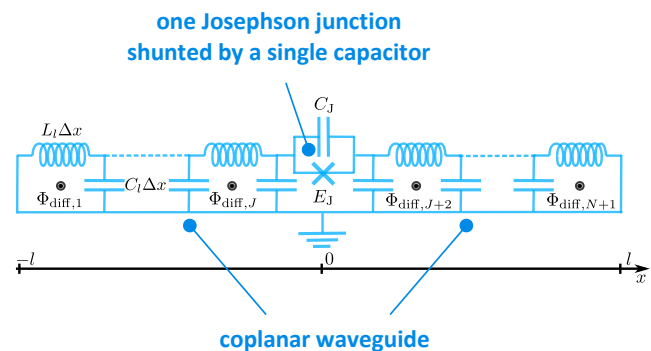


Figure 329: IQM's unimon circuit layout. Source: [Unimon qubit](#) by Eric Hyyppä, Mikko Möttönen et al, IQM and VTT, April 2022 (72 pages).

They obtained two-qubit CPHASE gates fidelity above 99% and fidelities of 99.9% for X and Y gates. All with fast 13 ns gate (good), readout probe pulses of 100 ns (fine) and a T_1 of 8,6 μ s (not good).

⁸⁰⁰ See [Quantum-circuit refrigerator](#) by Kuan Yen Tan et al, 2017 (8 pages) and [video](#).

⁸⁰¹ See [Bolometer operating at the threshold for circuit quantum electrodynamics](#) by R. Kokkonen, Mikko Möttönen et al, Nature, September 2020 (19 pages).

⁸⁰² See [A low-noise on-chip coherent microwave source](#) by Chengyu Yan et al, Nature Electronics, December 2021 (14 pages) and [A new super-cooled microwave source boosts the scale-up of quantum computers](#), December 2021 that is clearly overselling this technology development. It also requires pulse shaping with other techniques (AWG, DAC).

⁸⁰³ See [Broadband continuous variable entanglement generation using Kerr-free Josephson metamaterial](#) by Michael Perelshtein, Pertti Hakonen et al, March 2022 (15 pages).

It now must be tested with a large number of qubits and with two qubit gates⁸⁰⁴. In August 2022, they also published an arXiv preprint explaining how they will implement long-distance reliable two-qubit gates⁸⁰⁵.

After relying on VTT Micronova 2600 m² clean-room fab, they inaugurated their own Espoo 560 m² and 20M€ fab in November 2021 to manufacture their chipsets, a self-sufficiency strategy also seen with Rigetti. In 2020, the Finland government granted VTT with a 20,7M€ funding to acquire an IQM system. It should reach 50-qubit by 2024. They had 5 operational qubits as of November 2021.

The company had over 190 people as of September 2022. They opened a research lab in Germany in March 2020, one office in Spain in 2021 and one in Paris in 2022.

IQM's business model is based on selling quantum computing system to research and supercomputing centers as well as proposing customized hybrid analog/digital "Co-Design QC" quantum processors. The latter could be classified as "quantum ASICs", based on superconducting qubits⁸⁰⁶. These systems are adapted to the execution of hybrid algorithms such as VQE (Variational Quantum Eigensolvers) and QAOA (Quantum Approximate Optimization Algorithm). IQM will also implement a digital-analog quantum processor together with other partners like Infineon at the LRZ supercomputing center in Garching, near Munich in Germany⁸⁰⁷.

Their co-design offering is based on **KQCcircuits**, an open sourced software tool based on KLayout for qubit design, using the OASIS format for masks that is lighter. It enables a graphic-based creation of circuits elements and contains a library with SQUIDS, complex waveguides, coplanar capacitors, qubits, flipchip connectors, indium bumps and other templates. They are partnering since August 2022 with **Multiverse Computing** for the software implementation of these co-designed QPUs, relying on Multiverse's Singularity SDK. They also announced a partnership with **Atos** together with the Finnish supercomputing center **CSC** which bought a classical QLM emulator for their services. This machine is used both to simulate the operation of IQM's quantum accelerator qubits and to drive it⁸⁰⁸. CSC will provide scientific computing resources to the country's researchers, much like GENCI/TGCC/IDRISS do in France and JSC in Germany. Atos has also announced its interest to distribute an IQM quantum accelerator, among other market solutions, including the Pasqal simulator.



Oxford Quantum Circuits (2017, UK, \$45M) was launched by Peter Leek from Clarendon Laboratory Oxford. The startup is run by Ilana Wisby and had a team of 60 people as of mid-2022. The company wants to remove the identified barriers that prevent superconducting qubits from scaling.

⁸⁰⁴ See [Unimon qubit](#) by Eric Hyyppä, Mikko Möttönen et al, IQM and VTT, April 2022 (72 pages) which provides a good scientific and technical documentation of unimon qubits.

⁸⁰⁵ See [Long-distance transmon coupler with CZ gate fidelity above 99.8%](#) by Fabian Marxer, Mikko Möttönen, Johannes Heinsoo et al, IQM, QCD Lab and VTT, August 2022 (24 pages).

⁸⁰⁶ Their method is described in [Approximating the Quantum Approximate Optimization Algorithm](#) by David Headley et al, February 2020 (14 pages) and [Improving the Performance of Deep Quantum Optimization Algorithms with Continuous Gate Sets](#) by Nathan Lacroix, Alexandre Blais, Andreas Wallraff et al, May 2020 (14 pages).

⁸⁰⁷ See [New EU Consortium shaping the future of Quantum Computing](#), IQM, February 2021. In November 2021, IQM was officially selected to provide its quantum computer to LRZ (Leibniz Supercomputing Centre) in association with an HPC to set-up an hybrid computing system as part of the Q-Exa project. It's part of a €45.3M consortium project funded by BMBF (German Federal Ministry of Education and Research) with €40.1M. Although it was not detailed in the announcement, we can suspect that the provided QPU will have 50 qubits as planned by IQM in 2025.

⁸⁰⁸ See [Atos, CSC and IQM join forces to accelerate the commercialization of European quantum technologies](#), June 2020.

OQC's technology is based on their "coaxmon" superconducting qubits that are composed of highly coherent planar qubits⁸⁰⁹ and using a 3D structure connecting the qubit chipset with an interposer and using a layer for controlling the qubits on top of the chipset and another one below for qubit readouts⁸¹⁰.

It's based on various works from MIT and the University of Oxford, on an idea from Peter Leek⁸¹¹.

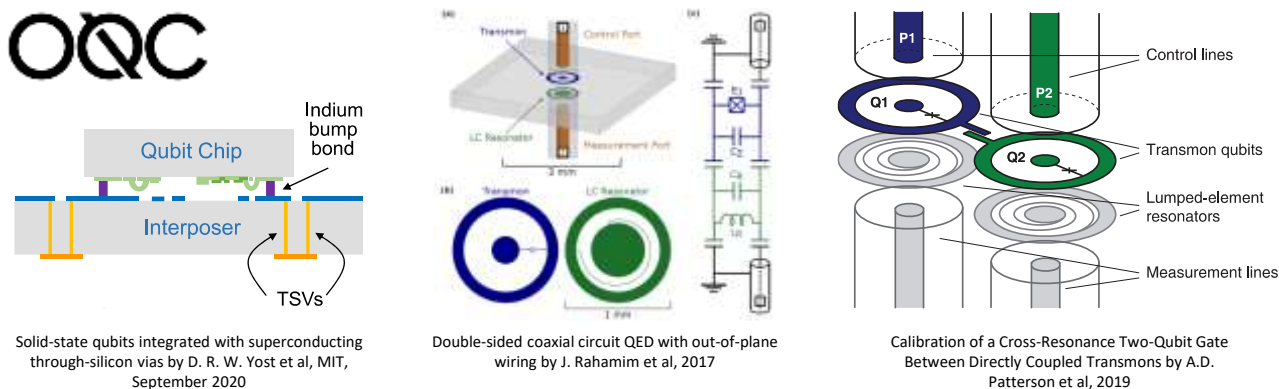
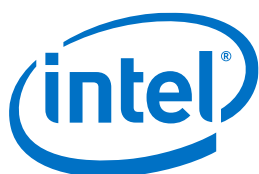


Figure 330: OQC coaxmon schematics showing how microwave controls are distributed vertically onto the qubits and their resonator. Source: OQC.

They are partnering with Cambridge Quantum Computing (CQC) which is developing a quantum compiler dedicated to their qubits. In April 2020, OQC obtained collaborative project funding from the British government of £7M. As part of this project, they are associated with SeeQC UK, Oxford Instruments, Kelvin Nanotechnology, the University of Glasgow and the Royal Holloway University of London.

In July 2021, OQC announced that they were making their first system available only as a QCaaS solution, in private beta (quantum cloud as a service) without even saying how many qubits were deployed. They then announced in December 2021 that an 8-qubit version of their processor nicknamed Lucy would be made available on Amazon Braket and revealed that their July 2021 system had a mere 4 qubits. The OQC system became live on Braket in February 2022.



Intel is another player in the superconducting qubits field. With no commercial solution so far as it's only a research field at this stage, completed by to the more natural avenue of electron spin silicon qubits they are also pursuing. At CES 2018, Intel's CEO proudly showcased a 49-qubit superconducting chipset during his keynote, stuck between a passenger drone demonstration and a broad talk on artificial intelligence.

Named Tangle Lake, the chipset was tested at **Qutech** in the Netherlands. They were at 7 qubits at the end of 2016, 17 qubits at the end of 2017 and 49 (uncharacterized) qubits in January 2017. Since then, no news. It seems that Intel is now entirely focused on electron spin qubits, along with their partner Qutech in The Netherlands, where they invested \$50M back in 2015.



Anyon Systems (2014, Canada) was created by Alireza Najafi-Yazdi. Their physics team is managed by Gabriel Éthier-Majcher and the startup has over 20 employees as of mid-2021.

⁸⁰⁹ See [Surface acoustic wave resonators in the quantum regime](#), 2016 (40 slides).

⁸¹⁰ The 3D layering and TSV structure is inspired from [Solid-state qubits integrated with superconducting through-silicon vias](#) by D. R. W. Yost et al, MIT, September 2020 (9 pages). This project was funded by IARPA.

⁸¹¹ See [Double-sided coaxial circuit QED with out-of-plane wiring](#) by J. Rahamim, Peter Leek et al, 2017 (4 pages), [Calibration of a Cross-Resonance Two-Qubit Gate Between Directly Coupled Transmons](#) by A.D. Patterson, Peter Leek et al, 2019 (8 pages) and [Superconducting microwave circuits for quantum computing](#) by Peter Leek, 2018 (42 slides).

They started with creating their Quantum Device Simulator (QDS), a software tool used in quantum computer design and simulation that can run on supercomputers. It was used by John Martinis' Google team in 2017 for their design of a superconducting 6- and then 20-qubit qubit processor⁸¹². Their software was mainly used to predict the level of adjacent qubits cross-talks. It's part of Snowflake, an open source library for creating quantum circuits running both on quantum emulators and quantum computers.

But their main goal then became to create gates-based superconducting qubits quantum computers in a full stack approach, creating their own control electronics and cryogenics systems. They are also implementing some sort of topological error correction codes. In December 2020, they announced that they would provide such a system to the Canadian Department of Defense using their Yukon processor. It was put online in 2021. They published qubit fidelities data in March 2022 with 99,7% for single qubit gates in parallel and 95,6% for two qubit gates⁸¹³. Their T_1 is 10 μ s and T_2 is 8 μ s. Is that good? If it were with fewer than 20 qubits, it would be less than stellar, particularly compared with the recent IBM systems who have T_1 over 100 μ s and 99,9% two-qubit gate fidelities with 27 qubits (Falcon R10 processor as of November 2021).

If it was achieved with over 50 qubits, that would be better! But there's no open way to have some clues on the number of their qubits. I'd guess it is fewer than 30 qubits. Otherwise, you'd hear about it. In June 2022, they announced the delivery of their quantum computer to Calcul Québec, a Canada's public supercomputing center hosting Narval, the 92th HPC in the world Top 500 and 28th in the Green 500 as of June 2022.

They also published an impressive 3D picture of their Qube computer which shows well that they use a cryostat, that is said to be homemade, at least for the dilution part, but with no more information on the of qubits that we thus suspect to be very low and under 10.



Figure 331: artist rendering of Anyon's quantum computer, with all the traditional nuts and bolts of a superconducting quantum computer. Source: Anyon.



Bleximo (2017, USA, \$1.5M) was founded by Alexei Marchenkov and Richard Maydra, two former Rigetti employees.

It develops superconducting qubits processors tailored for specific needs and adapted to different markets including biotech and financial services⁸¹⁴. It seems similar to Finland's IQM strategy.

They focus on improving the classical control electronics driving their qubits and are partnering with Q-CTRL which develops error correction codes quantum software. As of 2022, they had created a 8-qubit processor which is less than stellar compared to IBM and Rigetti but in line with OQC from the UK⁸¹⁵. Their qubits lifetime sits around 100 μ s. They would need to assemble at least 40 to 50 functional physical qubits, if not 100, to enable real-life applications with their customers.

They also develop quantum software solutions (aka "QCO") for typical use cases like optimization, physics simulation and machine learning. In their team, Anastasia Marchenkova is a researcher producing a lot of [educational video content](#).

⁸¹² See [Google's 'supreme' 20-qubit quantum computer](#) by Tushna Commissariat, 2017.

⁸¹³ See [Update on Performance Metrics](#), Anyon Systems, March 2022.

⁸¹⁴ See [Application-Specific Quantum Hardware is the Most Promising Approach for Early Practical Applications](#) by Fabio Sanches, Chiara Pelletti, and Alexei Marchenkov, February 2022.

⁸¹⁵ See [Superconducting Quantum Processor Design at Bleximo](#) by Chiara Pelletti and Fabio Sanches, March 2022 and [Bleximo builds its competitive advantage with an application-specific approach](#), PhysicsWorld, June 2022.

Their customer based seems made of US research labs (Berkeley University, DoE Berkeley Lab⁸¹⁶, Syracuse University, John Hopkins Applied Physics Laboratory). So, we're not far from a contract research company. This is exemplified by their willingness to create application-specific hardware, like IQM, which doesn't make much sense from an economical and even practical standpoint⁸¹⁷. It would make sense if it brought similar benefits like FPGA (slower operations, low fixed cost, higher variable costs) vs ASICs (fast operations, higher fixed costs, low variable costs). But the costs here are still high, and they are not yet providing any quantum advantage with their system.



QuantWare (2021, Netherlands, \$7M) is a designer and manufacturer of superconducting qubits processors created by Matthijs Rijlaarsdam and Alessandro Bruno⁸¹⁸. They offer their 25 qubits Contralto processor and a customizable connectivity that could for example help prototype specific quantum error corrections codes.

The chipsets have AirBridges and a proprietary TSV configuration (through-silicon via). It seems to be very classical transmon superconducting qubits. They propose custom processors and a product design-to-delivery cycle of 30 days, leveraging the Van Leeuwenhoek Lab cleanroom at TU Delft.

They don't build full-fledged quantum computers. Their first 5-qubit Soprano QPU had a modest T_1 of 10 μs and a single-qubit gate fidelity of 99,99%. Contralto's 25-qubit processor (pictured below) could reach a T_1 of 60 μs . They don't provide data on the most important figures of merit: dual-qubits gates and readout fidelity. Who could use these QPUs? Seemingly, research labs and vendors developing enabling technologies for superconducting qubits, like their colleagues from Qblox and Delft Circuits. They plan to double the number of qubits in their QPUs each and every year. QuantWare has various partnerships in place, including with SeeQC (USA), with QuantrolOx (UK) and QphoX (The Netherlands).

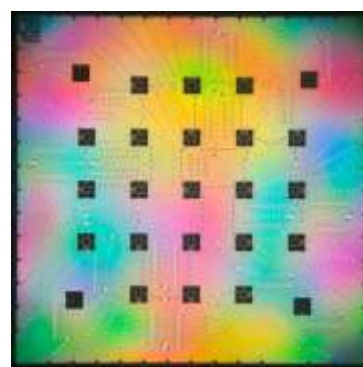


Figure 332: QuantWare's 25 qubit processor.

As we'll see later in the [cryoelectronics section](#), QuantWare also designs Crescendo, a TWPA (qubits readout traveling waves parametric amplifiers). In September 2022, the company got a subsidy funding of 1.1M€ from Quantum Delta NL, the foundation running the Dutch quantum national plan, to develop superconducting qubits based on undefined novel materials.



Atlantic Quantum (2022, USA/Sweden, \$9M) is a startup cofounded by Jonas Bylander from Chalmers University in Sweden, along with Bharath Kannan (CEO), Simon Gustavsson, Youngkyu Sung, William D. Oliver, Shereen Shermak and Tim Menke, from the MIT.

⁸¹⁶ See [Raising the Bar in Error Characterization for Outrit-Based Quantum Computing](#), Monica Hernandez, Lawrence Berkely National Laboratory in HPCwire, September 2021.

⁸¹⁷ See [Application-Specific Quantum Hardware is the Most Promising Approach for Early Practical Applications](#) by Fabio Sanches, Bleximo, February 2022.

⁸¹⁸ Among their scientific advisors are Charlie Marcus, formerly running the Microsoft Quantum Lab in Copenhagen, Denmark. He left Microsoft in November 2021.

The startup develops scalable fluxonium superconducting qubits-based quantum computers with experts covering all aspects of the quantum computing stack, from chip design and device fabrication to gate calibration and quantum algorithms. The cofounder's research group develops superconducting quantum electronic devices for quantum computing and simulation. Jonas Bylander recently published a paper on an efficient qubit readout solution using two microwave pulses and getting rid of the parametric amplifier, but it doesn't tell if it's in Atlantic Quantum's roadmap⁸¹⁹.

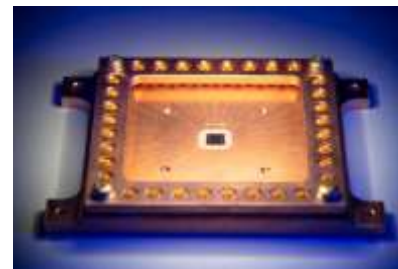


Figure 333: Atlantic Quantum fluxonium superconducting chipset. Which is insufficient to have an idea of its qubit fidelities, that is not yet published. Source: Atlantic Quantum.



Alibaba is active in using the resources of its datacenters to simulate quantum algorithms exceeding 50 qubits. China's leading e-commerce company is also partnering with the **University of Science and Technology of China (USTC)** of the Chinese Academy of Sciences (CAS) to create superconducting quantum computers with superconducting qubits.

They offer cloud access to 11 qubits since early 2018, on a technology platform developed with USTC. They even announced in 2018 that they were creating a subsidiary, **Ping-Tou-Ge**, which develops NPUs (neuromorphic processors for AI) and, eventually, superconducting quantum chipsets⁸²⁰. They work on superconducting qubits, using the fluxonium variation, which could bring some coherence advantage. They announce qubit lifetimes T_1 and T_2 over 100 μs and a 99,5% iSWAP gate fidelity.



In April 2021, the Japanese research center **RIKEN** and **Fujitsu** created the RIKEN RQC-Fujitsu Collaboration Center to do joint research and create a superconducting qubit computer, with a goal of reaching 1000 physical qubits and develop an associated software platform.

It will leverage RIKEN's existing work on superconducting qubits and Fujitsu's computing know-how. The research plan is quite classical: improving qubit manufacturing, reducing the size and noise of driving electronics components and wiring and improve error correcting codes.

Some plans roadmaps were uncovered in August 2022. Fujitsu plans to release a first 64 qubits QPU by spring 2023, to be expanded to 1000 qubits in 2026. Fujitsu has created a research center in Wako City, Japan, to work on these systems with Riken with about 20 researchers.



Toshiba has been conducting fundamental research in quantum computing since at least 2008, in quantum photonics and with superconducting qubits in its Frontier Research Laboratory.

Here, Hayato Goto is a prolific scientist working in many disciplines. In 2022, he created a double-transmon coupler that turns on/off coupling between two superconducting qubits in an efficient manner, enabling fast computing and two-qubit gate fidelities of 99.99% and time of 24 ns⁸²¹.



Baidu announced in August 2022 its Qian Shi QPU with 10 superconducting qubits, to be later expanded to 36 qubits using couplers to run two-qubit gates, reusing a concept first pioneered by Google in 2019.

⁸¹⁹ See [Transmon qubit readout fidelity at the threshold for quantum error correction without a quantum-limited amplifier](#) by Liangyu Chen, Jonas Bylander, Giovanna Tancredi et al, August 2022 (8 pages).

⁸²⁰ See [Alibaba Launches Chip Company "Ping-Tou-Ge"; Pledges Quantum Chip](#), September 2018.

⁸²¹ See [Double-Transmon Coupler: Fast Two-Qubit Gate with No Residual Coupling for Highly Detuned Superconducting Qubits](#) by Hayato Goto, PRA, March-September 2022 (10 pages).

These qubits are said to showcase high fidelities. Let's look at the numbers: $T_1 = 31 \mu\text{s}$, $T_2 = 8.7 \mu\text{s}$, single qubit gate at 99,8% and two-qubit gates at 96,4% (CX) and 96,8% (CZ). For 10 qubits, it's less than stellar and the numbers look like those of some average transmon qubits.



Origin Quantum Computing (2017, China, \$163.4M) is a startup created in Hefei by Guo Guoping out of the CAS quantum lab in Hefei. It closed an amazing \$148M Series B funding round in July 2022.

The company works on a full-stack quantum offering including a 24 superconducting qubits system, working on semiconductor quantum dots qubits as well, on qubits control electronics (Quantum AIO), cryogenic equipment, on quantum software with an operating system (Origin Pilot), a programming framework (QPanda), the EmuWare virtual machine, a quantum machine learning framework (VQNet), a quantum programming language (QRunes), an integrated development environment (Qurator), and some applications frameworks for quantum chemistry (ChemiQ), fluid dynamics (OriginQ QCFD) and financial optimization.

Initially, it worked mainly on developing quantum algorithms and quantum emulation software. They were behind one of the records for 64-qubit quantum algorithm emulation on a supercomputer⁸²². They also created cloud based emulation appliances supporting 32 and 64 qubits. They then started to create their own quantum chipsets, including superconducting qubits chipsets with 6 qubits (KF C6-130) and 100 qubits (XW B2-100), using tunable couplers. A bit like IBM, they expect to reach 1024 qubits by 2025 with intermediate steps of 64 qubits in 2021 and 144 qubits in 2022.

Now, on to cat-qubit and other bosonic qubits vendors...



ALICE & BOB

Alice&Bob (2020, France, \$33M) was created by Théau Peronin (ENS Lyon) and Raphaël Lescanne (ENS Paris). They are designing a fault-tolerant gate-based quantum computer associating superconducting technology and stabilized photon-based (in the microwave regime) cat-qubits. Their technology main benefit is its capability to implement a complete universal fault-tolerant quantum computer with a much lower ratio of physical per logical qubits than traditional transmon based superconducting qubits. It saves at least two orders of magnitude, moving from 1000 to 1 down to 30 to 1 (about $\sqrt{1000}$)!

Alice&Bob's technology is based on the PhD thesis from the startup founders and the associated work of the **Mazyar Mirrahimi's** Quantic team from Inria where Raphaël Lescanne was a doctoral student and where **Zaki Leghtas** as well as **Jérémié Guillaud** also work or worked⁸²³, the CNRS and ENS Lyon and ENS Paris. **Pierre Rouchon** from MinesParistech is also a key contributor⁸²⁴. We'll see how all these works were influential, up to inspire Amazon in its own cat-qubits engineering efforts, documented later.

Cat-qubits encode the state of a qubit with superposing opposite quantum states in micro-wave photon cavities, precisely, in the two-dimensional Hilbert space spanned by two coherent states of micro-waves of same amplitude and opposite phase⁸²⁵.

⁸²² See [Researchers successfully simulate a 64-qubit circuit](#), June 2018.

⁸²³ Mazyar Mirrahimi did work in Michel Devoret's team at Yale University around 2012. See [Dynamically protected cat-qubits: a new paradigm for universal quantum computation](#) by Mazyar Mirrahimi, Zaki Leghtas and Michel Devoret, 2013 (28 pages). Jérémié Guillaud is now Chief of Theory at Alice&Bob.

⁸²⁴ See [Quantum computation with cat qubits](#) by Jérémié Guillaud, Joachim Cohen and Mazyar Mirrahimi, March 2022 (75 pages).

⁸²⁵ See [Exponential suppression of bit-flips in a qubit encoded in an oscillator](#) by Raphaël Lescanne et al, July 2019 (18 pages) and [Repetition Cat Qubits for Fault-Tolerant Quantum Computation](#) by Jérémié Guillaud and Mazyar Mirrahimi, July 2019 (23 pages).

These cat-qubits have a very low bit-flip error rate given it decreases exponentially with the average number of microwave photons used in the cat qubit cavity⁸²⁶. Phase-flip errors can be corrected with repetition error codes having a rather low overhead⁸²⁷.

Cat-qubits can support a native implementation of 3-qubits Toffoli gates which, combined with Clifford gates, form a universal set of quantum gates. The implementation of such a universal gate set is a prerequisite to run quantum algorithms with a proven exponential speed-up. The Toffoli gate is an alternative to the usual (non-Clifford) T gate used in QFT-based algorithms. This gate can be corrected efficiently with avoiding magic state distillation, enabling fault-tolerance, and limiting error propagation between ancilla qubits⁸²⁸.

These qubits are more complex to design and operate but it would only take about 30 of them to create a well-corrected logical qubit, which would make it possible to create a better scalable architecture whereas with the current technologies of IBM, Google and Rigetti, about 1,000 to 10,000 physical qubits are required to create a functional logical qubit given their expected fidelities. These corrected qubits could also play the role of associative quantum memory. Moreover, their system avoids microwave radiations leaks between adjacent qubits.

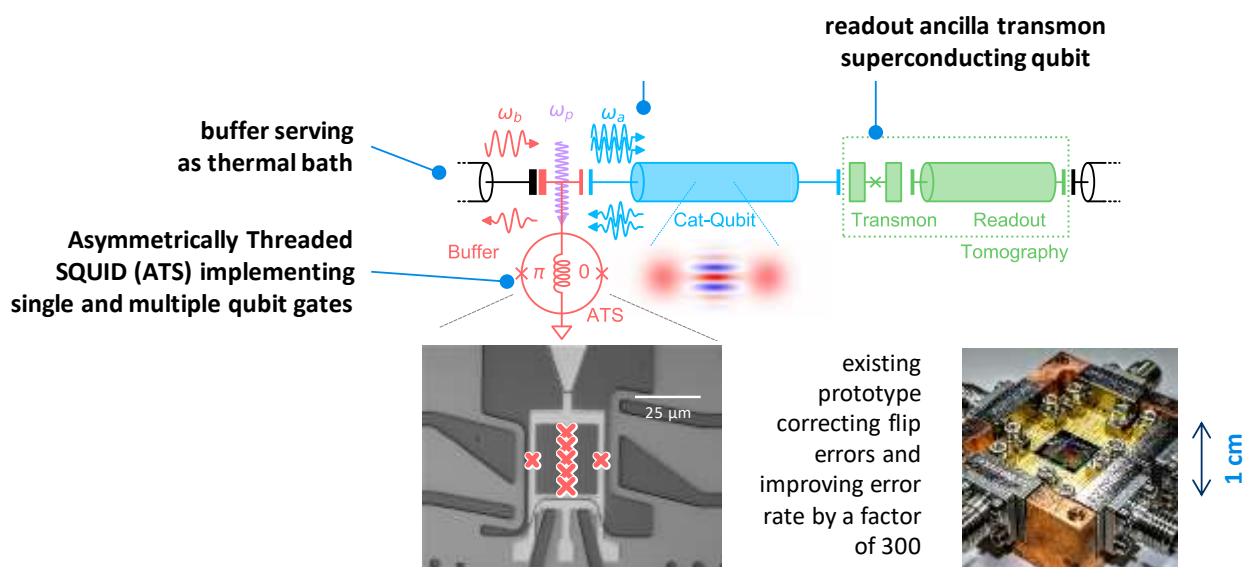


Figure 334: Alice&Bob cat-qubit cavity and its coupling to a transmon qubit and the ATS (asymmetrically threaded SQUID) that implements single and multiple qubit gates. Source: Alice&Bob.

The gates they implement on top of a Toffoli gate are a CNOT and a Hadamard gate. SWAP gates are built with three CNOTs in a classical fashion.

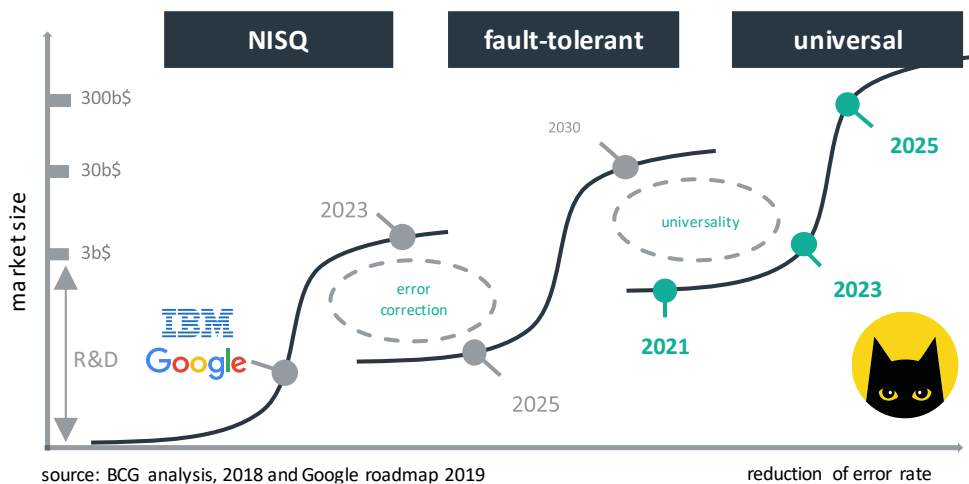
These are heavily used to circumvent the absence of many to many qubits connectivity in most 2D qubits layouts. All this will require a specific compiler, to be created later in the startup product lifecycle.

⁸²⁶ See [One hundred second bit-flip time in a two-photon dissipative oscillator](#) by C. Berdou, Zaki Leghtas, Maryar Mirrahimi, Pierre Rouchon, Raphael Lescanne, Théau Peronnin, Taki Kontons et al, April 2022 (20 pages).

⁸²⁷ See [Error Rates and Resource Overheads of Repetition Cat Qubits](#) by Jérémie Guillaud and Mazyar Mirrahimi, March 2021 (17 pages). Based on numerical simulation, it estimates that a fault-tolerant cat-qubits computer with a logical error probability of 10^{-10} can be realized using 140 physical cat-qubits for Clifford gates and an average number of 15 photons per mode. A Toffoli gate could be implemented with only 180 physical cat-qubits including all required ancilla qubits.

⁸²⁸ They propose a ‘pieceable fault-tolerant’ implementation of the Toffoli gate, following the method introduced in [Universal Fault-Tolerant Gates on Concatenated Stabilizer Codes](#) by Theodore J. Yoder, Ryuji Takagi and Isaac L. Chuang, September 2016 (23 pages). This is a substitute to the transversal gates technique.

On a practical way, these cat-qubits drive require some more corrections than regular transmon qubits. A continuous pulse tone drives the cat-qubit photons buffer. The qubit error corrections makes use of an ATS (Asymmetrically Threaded SQUID), a nonlinear element that is flux biased with an AC current in the 4-8 GHz range. A one qubit gate requires two pulses (cat drive and dissipation phase). A cat-qubit readout uses two pulses on the coupling transmon and a readout pulse. Readout uses 3 in-bound pulses and one reflected pulse. And in total, cat-qubits require about 6 control lines.



source: BCG analysis, 2018 and Google roadmap 2019
 Figure 335: Alice&Bob roadmap which ambitions to directly create a fault-tolerant QPU and then a universal quantum computer (although the definition of universal quantum computer is not agreed upon. Source: Alice&Bob.



Amazon (USA) started first to announce late 2019 its Amazon Braket cloud offering, based on using third-party quantum computers from D-Wave, Rigetti and IonQ, covered in the cloud section of this book, page 677.

In December 2020, they went out of the woods with announcing their detailed plan to build their own quantum computers, using cat-qubits, in a thorough 118 pages paper⁸²⁹.

This work is getting the help from Caltech, including John Preskill, in connection with Yale University where some Caltech students did their PhDs in the teams of Rob Schoelkopf and Michel Devoret. The Amazon effort is led by **Simone Severini** (Director of Quantum Computing at AWS), **Oskar Painter** (Head of Quantum Hardware at AWS), **Fernando G.S.L. Brandão** (Head of Quantum Algorithms at AWS and also researcher at Caltech) and **Richard Moulds** (GM Amazon Braket).

The bulk of Amazon's quantum team are based in the new 21,000-sq-ft AWS Center for Quantum Computing building next to Caltech in Pasadena, North of Los Angeles. It was inaugurated in October 2021.

The Amazon proposed architecture is largely inspired by what the French teams at Inria have investigated since 2013 with Mazyar Mirrahimi et al, including the founders of Alice&Bob⁸³⁰. They want to create a FTQC. As of 2020, Amazon was planning to use an electro-acoustic resonator to host the cat qubits while the circuit element, the Asymmetrically Threaded SQUID (ATS) invented by Raphaël Lescanne and Zaki Leghtas, used by Alice&Bob to stabilize the cat-qubit is superconducting. While Alice&Bob QEC is based on dissipating excess qubit energy to maintain it in low-energy states with encoding it in a linear oscillator driven by 10 GHz microwaves, Amazon chose a variant that uses

⁸²⁹ See [Building a fault-tolerant quantum computer using concatenated cat codes](#) by Christopher Chamberland, John Preskill, Oskar Painter, Fernando G.S.L. Brandão et al, 2020 (118 pages). It is summarized in [Designing a fault-tolerant quantum computer based on Schrödinger-cat qubits](#) by Patricio Arrangoiz-Arriola and Earl Campbell, April 2021. See also [Fault-tolerant quantum computing with biased-noise hardware](#) by Earl Campbell, November 2020 (40 mn).

⁸³⁰ On top of France's founding work on cat-qubits, Amazon is also relying on many US Universities research like Caltech, Stanford, Chicago University and Yale University.

linear harmonic oscillators-based cat-qubits using very compact piezoelectric nanostructures and phonons. Like with Alice&Bob, these cat-qubits self-corrects flip errors at the hardware level while phase errors are being handled by some QEC requiring, supposedly about 20 physical qubits.

Cat-qubits encode information with microwaves put in coherent states with opposite phases, $|+\rangle$ and $|-\rangle$. The qubit computational basis states are defined as even and odds coherent states cats, meaning using positive and negative sign superpositions for these two cat-states. Like Alice&Bob, they will implement a universal gate set comprising X, Z, CNOT and Toffoli gates. They use two new ideas for implementing fault-tolerant Toffoli gates: an extremely small chip layout (“bottom-up Toffoli”) and a technique to lower the bit-flip error rate (“top-down Toffoli”). They also avoid crosstalk between cat-qubits with using four cat-qubits connected to a single dissipating reservoir. This compact layout is compatible with a scalable architecture but may generate significant crosstalk errors, which could be mitigated with a well-chosen filter design cutting the frequencies to remove crosstalk errors.

They first plan to implement a 9-qubit QEC to obtain a logical error rate of 2.7×10^{-8} . As a result, they expect to use 2000 superconducting qubits to create a 100 logical qubits system. If this works, as with Alice&Bob, it will make a significant difference with IBM and Google who plan to obtain the same number of logical qubits with one million physical qubits. The scalability constraints are much different in both cases, whether it deals with cryogenics, microwave generations and readouts, or cabling.

In April 2021, University of Sydney science undergraduate Pablo Bonilla Ataidés published in Nature Communications a paper on its ZXXZ surface code that would reduce the number of required physical qubits to create a logical qubit thanks to a lower error threshold. It brought the attention of Amazon researchers⁸³¹. This surface code could be used by Amazon who made a choice to use a relatively low number of photons per cat qubit (8 to 10, compared to about 15 for Alice&Bob, but the optimum number of photons is still to be determined experimentally), still requiring some first level bit-flip error correction on top of phase-flip correction. That’s where a ZXXZ surface code QEC could come into play. ZXXZ QEC codes are indeed mentioned as an option QEC technique in Amazon’s technical paper from December 2020.

The AWS Center for Quantum Computing opened at Caltech in October 2021 and houses all Amazon teams working on quantum computing⁸³². They even then showcased a picture of a prototype quantum processor, maybe the one with 9 qubits.

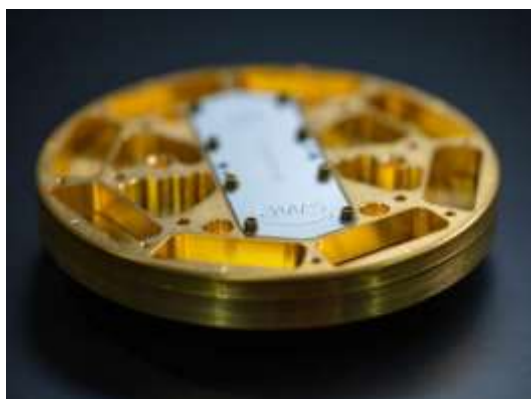


Figure 336: the first prototype Amazon cat-qubit chipset of undisclosed characteristics, and their lab in Caltech opened in October 2021.

⁸³¹ See [Student's physics homework picked up by Amazon quantum researchers](#) by Marcus Strom, University of Sydney, April 2021, [Sydney student helps solve quantum computing problem with simple modification](#) by James Carmody April 2021 and [The XZZX surface code](#) by J. Pablo Bonilla Ataidés et al, April 2021, Nature Communications (12 pages).

⁸³² See [Announcing the opening of the AWS Center for Quantum Computing](#) by Nadia Carlsten, October 2021.



QCI (2015, USA, \$18M) or Quantum Circuits Inc is a spin-off from Yale University co-founded by Rob Schoelkopf, Luigi Frunzio and Michel Devoret. Michel Devoret left the company in 2019, preferring to be a full-time researcher at Yale University.

Their technology is also based on cat-qubits that solve noise and coherence problems, using Rob Schoelkopf's teamwork at Yale. They have a long track-record in that space although they are not very talkative. They announced in 2019 that their system should be available some day on Microsoft Azure Quantum cloud. But so far, they have not delivered any functional QPU.

Technically, their planned cat-qubit are stabilized by discrete parity measurement using a transmon⁸³³ and their two qubit gates are implemented using SNAP gates (Selective Number-dependent Arbitrary Phase (SNAP) using the same transmon⁸³⁴. They also planned to use micromachined 3D cavities with a good Q factor⁸³⁵. They plan to obtain a linear gain in qubit lifetime with the number of physical qubits. It will still require some surface codes to fully correct flip-errors (on top of phase errors).

They are also at the origin of the **qbsolv** framework that is part of their **Mukai** middleware and development platform launched in January 2020⁸³⁶. It supports D-Wave computers, Fujitsu digital-annealed computers and Rigetti superconducting qubits.



Nord Quantique (2019, Canada, \$7.6M) is a startup from the Institut Quantique from the University of Sherbrooke that is working on creating a superconducting quantum computer using more efficient error correction, using another variation of bosonic codes that would have fast quantum gates, but with no further publicity on how they implement this and on their roadmap.

The company was created by Julien Camirand Lemyre and Philippe St-Jean with the scientific support from Alexandre Blais and their investors are BDC Capital (USA), Quantonation (France) and Real Ventures (Canada).

Quantum dots spins qubits

Electron spins qubits are a new promising qubit technology with a lot of variations. Its related research started later than superconducting qubits. Its potential benefits are miniaturization and scalability. It could leverage existing manufacturing processes for standard CMOS semiconductors⁸³⁷.

History

Electron spin qubits quantum state is generally the spin orientation of an electron trapped in a potential well or of an electron hole, i.e. a missing electron and its virtual inverse impact on structural spin.

⁸³³ See [Demonstrating Quantum Error Correction that Extends the Lifetime of Quantum Information](#) by Nissim Ofek, Zaki Leghtas, Steve Girvin, Liang Jiang, Mazhar Mirrahimi, Michel Devoret, Rob Schoelkopf et al, February 2016 (44 pages).

⁸³⁴ See [Cavity State Manipulation Using Photon-Number Selective Phase Gates](#) by Reinier W. Heeres, Eric Holland (who now works at Keysight), Liang Jiang, Robert Schoelkopf et al, March 2015 (9 pages).

⁸³⁵ See [Multilayer microwave integrated quantum circuits for scalable quantum computing](#) by Teresa Brecht, Michel Devoret, Rob Schoelkopf et al, Nature, 2015 (5 pages) and the related thesis [Micromachined Quantum Circuits](#) by Teresa Brecht, 2017 (271 pages).

⁸³⁶ See [QCI Qbsolv Delivers Strong Classical Performance for Quantum-Ready Formulation](#) by Michael Booth et al, May 2020 (7 pages).

⁸³⁷ CMOS ("Complementary Metal Oxide Semiconductor") is the dominant technology used to produce microprocessors, for CPUs (Intel, AMD), GPUs (Nvidia, AMD), chipsets for smartphones (Qualcomm, Samsung, MediaTek, HiSilicon, etc.) and in a whole host of specialized sectors (microcontrollers, radio components, etc.).

It is usually considered that Daniel Loss with David DiVincenzo and Bruce Kane are the first to have devised ideas to use electron spins to create a quantum computer, a couple years after Peter Shor created his famous integer factoring eponymous algorithm.

Daniel Loss (University of Basel) and **David DiVincenzo** (then at IBM Research) published a similar paper in 1996-1997 where they proposed the concept of quantum dots to create qubits with controlling the spin of electrons in a potential well⁸³⁸. Their design used a two-qubit gate (SWAP) using an electrical control of the tunneling barrier between neighboring quantum dots. A low gating voltage creates a coupling – *aka* Heisenberg coupling - between the neighbor qubits. The design also implemented single qubit gates. The Loss-Vincenzo concept was later extended with using pairs of quantum dots electron spins, one being the qubit itself, and the other, capacitively coupled with the first one and being used for qubit readout with a spin-to-charge conversion using conductance measurement, usually with some radio-frequency reflectometry using a microwave pulse, a bit like with superconducting qubit readout.

The first electron spin qubit was created in 2005 by a USA and Brazil team using GaAs on Si substrates⁸³⁹. But GaAs qubits suffers from a major limitation, a strong hyperfine coupling together with a nonzero nuclear spin that leads to dephasing. So physicists looked at Si and SiGe alternatives, which showcase lower hyperfine coupling. They could even provide quasi-noiseless environment for spins thanks to their nuclear-free isotopes ²⁸Si and ⁷²Ge isotopes. But they are much more challenging in terms of manufacturing, regardless of the supply of isotopically purified materials.

The first demonstration of silicon spin qubit was made in 2012 by UNSW teams. In 2016, silicon qubits were demonstrated using industry-grade manufacturing processes by a French team from CEA-Leti and IRIG in Grenoble⁸⁴⁰.

This belongs to the Si-MOS category, the most generic and easier to manufacture. Qubits are derived from planar MOS bulk or FDSOI technologies as well as with Fin-FET that are inspired from the latest CMOS manufacturing technologies. These spin qubits have a size of about 100x100 nm, leading to potential high densities when it will scale⁸⁴¹.

Bruce Kane (UNSW) presented in 1998 another spin-based quantum computer concept based on placing individual phosphorous atoms (³¹P) in a pure silicon lattice structure⁸⁴². This approach is labelled “donors spin”. It is a hybrid scheme using quantum dots and single atom nuclear magnetic resonance (NMR) since qubits associate phosphorus atoms nuclear spin and silicon donors electron spins. The qubits are controlled by electrical and magnetic fields⁸⁴³. The main benefit is the long coherence of nuclear spins, which can theoretically extend to several seconds⁸⁴⁴.

⁸³⁸ See [Quantum computation with quantum dots](#) by Daniel Loss and David DiVincenzo, 1997 (20 pages).

⁸³⁹ See [Coherent Manipulation of Coupled Electron Spins in Semiconductor Quantum Dots](#) by Jason Petta et al, Science, 2005 (5 pages).

⁸⁴⁰ See [A CMOS silicon spin qubit](#) by Romain Maurand, Maud Vinet, Marc Sanquer, Silvano De Franceschi et al, 2016 (12 pages).

⁸⁴¹ See [The path to scalable quantum computing with silicon spin qubits](#) by Maud Vinet, Nature Nanotechnology, December 2021 and [Scaling silicon-based quantum computing using CMOS technology](#) by M. F. Gonzalez-Zalba, Silvano de Franceschi, E. Charbon, Tristan Meunier, Maud Vinet and Andrew S. Dzurak, [Nature Electronics](#), December 2021 (16 pages).

⁸⁴² See [A silicon-based nuclear spin quantum computer](#) by Bruce Kane, Nature, 1998 and [Silicon-based Quantum Computation](#) by Bruce E. Kane, 2000 (14 pages).

⁸⁴³ See [The Race To Make Better Qubits](#) by Katherine Derbyshire, Semiconductor Engineering, November 2021.

⁸⁴⁴ The Bruce Kane concept is well described in [Toward a Silicon-Based Nuclear-Spin Quantum Computer](#) by Robert G. Clark, P. Chris Hammel, Andrew Dzurak, Alexander Hamilton, Lloyd Hollenberg, David Jamieson, and Christopher Pakes, Los Alamos Science, 2022 (18 pages). It shows linear array of phosphorous donor atoms buried into a pure silicon wafer, operating in the presence of a large magnetic field and at sub-K temperatures. The donor atoms nuclear spins are be aligned either parallel or antiparallel with the magnetic field, corresponding to |0> and |1> qubit basis states. The metal gates are above an insulating barrier of SiO₂. The A-gates above the ³¹P atoms enable single qubits gates while the J-gates in between the donors regulate an electron-mediated coupling between adjacent nuclear spins, for two-qubit operations. At last, qubit readout is done with either a single electron transistor (SET) or with a magnetic-resonance force microscope (MRFM, not shown).

The challenges lie with the way to precisely position the phosphorus atoms in the silicon lattice and how to handle qubits entanglement and readout. This is the path chosen by Michelle Simmons at UNSW and in her startup SQC. The individual atoms are positioned in the silicon structure with lithography using a scanning tunneling microscope (STM).

The first processor fully implementing this architecture was announced by SQC in 2022 (we cover it later). Similar options are pursued like the use of antimony nucleus embedded in silicon lattice structures and controlled by microwaves by Andrea Morello from UNSW⁸⁴⁵.

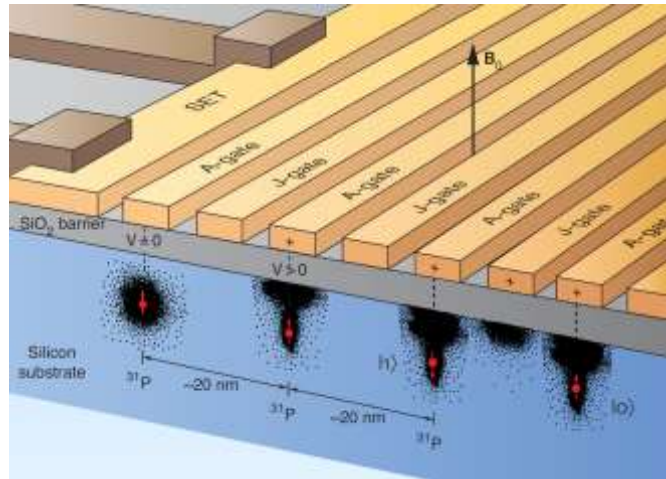


Figure 337: the donor spin architecture with phosphorous atom implanted in a silicon substrate under a SiO₂ isolation layer. Source: [Toward a Silicon-Based Nuclear-Spin Quantum Computer](#) by Robert G. Clark, P. Chris Hammel, Andrew Dzurak, Alexander Hamilton, Lloyd Hollenberg, David Jamieson, and Christopher Pakes, Los Alamos Science, 2022 (18 pages).

Later, Andrea Morello and Patrice Bertet designed another hybrid approach, coupling transmon superconducting qubits (for computing) and phosphorus in silicon nuclear spins with a donor electron (for creating a quantum memory)⁸⁴⁶.

On top of the above two mainstream paths (Si-MOS/CMOS and donors), several other avenues are investigated in the quantum dots based spin qubit realm:

- **Silicon/silicon germanium (Si/SiGe)** heterostructures qubits (Qutech, CEA IRIG) where germanium is used for the stability of its spin holes, large band gaps, higher electron mobility, stronger spin-orbit coupling, its insensitiveness to exchange coupling oscillations and long coherence times. It is however more difficult to manufacture and scale, with gates that are far from the qubits⁸⁴⁷. A record breaking 4 entangled qubits was announced late 2020 by TU Delft, based on germanium. Germanium allows the creation of very fast quantum gates ranging from 0.5 to 5 ns⁸⁴⁸.
- **Gallium-arsenide (GaAs)**, first tested in 2005, but with very short coherence times due to spin interferences from gallium and arsenic atoms nuclei.
- **Electrons trapped** on solid (inert) neon⁸⁴⁹ or on superfluid helium.
- **Electron spin trapped in carbon nanotubes (C12 Quantum Electronics)** or **carbon nanospheres** (Archer Materials). These structures better protect the spin of a trapped electron, at the expense of more complicated interfaces and controls

⁸⁴⁵ See [Coherent electrical control of a single high-spin nucleus in silicon](#) by Serwan Asaad, Andrea Morello, Kohei M. Itoh, Andrew S. Dzurak et al, 2019 (56 pages).

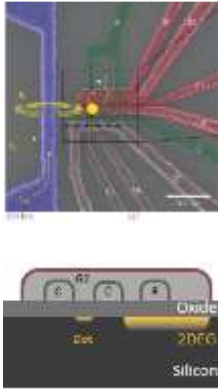
⁸⁴⁶ See [Donor Spins in Silicon for Quantum Technologies](#) by Andrea Morello, Patrice Bertet and Jarryd Pla, 2020 (17 pages).

⁸⁴⁷ See this excellent germanium review paper: [The germanium quantum information route](#) by Giordano Scappucci, Silvano De Franceschi et al, 2020 (18 pages).

⁸⁴⁸ See also [Quantum control and process tomography of a semiconductor quantum dot hybrid qubit](#), 2014 (12 pages).

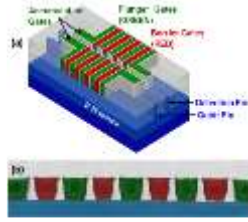
⁸⁴⁹ See [Single electrons on solid neon as a solid-state qubit platform](#) by Xianjing Zhou, Kater W. Murch, David I. Schuster et al, Nature, May 2022 (16 pages). The trapped electrons are coupled to a superconducting resonator on top of solid neon at 10 mK. It should bring better coherence but their current T₂ is at 200 ns.

Si-MOS, CMOS



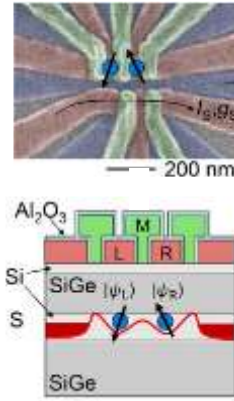
UNSW, Sandia Labs, CEA-Leti

Fin-FET



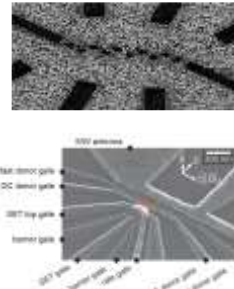
Intel, TU Delft, IBM, U. Basel

Si/SiGe



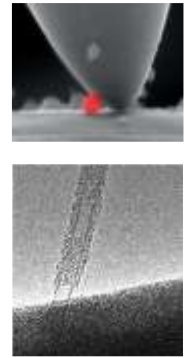
Princeton, RIKEN, HRL, TU Delft, CEA IRIG

donors



UNSW, SQC

carbon nanotubes/spheres



C12 Quantum Electronics, Archer Materials

Figure 338: various silicon spin qubits. (cc) Olivier Ezratty, 2022, inspired by a compilation by Maud Vinet, CEA Leti.

These qubits small dimensions and the possibility to integrate control electronics in or around the qubit chipset make it an interesting candidate for large-scale quantum computing⁸⁵⁰. There are however many challenges to overcome, particularly with materials design⁸⁵¹.

| | specs | Pros | cons |
|---|--|---|---|
| Si-MOS | silicon quantum dot | mastered fabrication technique and scalability potential | qubit decoherence, poor entanglement, disordered potential in materials |
| FinFET | silicon quantum dot | mastered fabrication technique and scalability potential | disordered potential in materials |
| SiGe | holes or spin in Si Ge heterostructures | longer coherence time, entanglement, relatively high temperature (>1K), clean epitaxial barrier | valley degeneracy making it difficult to differentiate qubit states |
| GaAs | first Si- GaAs qubits in 2005 | stable dopants, single conduction band valley, easy to manufacture, test platform for many characteristics with knowledge transferable to Si-MOS/FinFET/SiGe qubits | nuclear spins effect and very small coherence time (T_2) |
| atom donors | phosphorus atom spin donor | long coherence time | complicated to manufacture, impact of impurities |
| electrons on neon or helium | trapped electrons on superfluid helium. | long coherence, high connectivity, fast gates | not very vocal company (EeroQ) on progress made |
| carbon nanotubes and nanospheres | electron spin trapped in carbon nanotubes or nanospheres | long coherence time, reuse components from other qubit types for qubit control | more complex wiring and control, entanglement |

Figure 339: specificities with pros and cons of each silicon spin qubit variety. (cc) Olivier Ezratty, 2022.

⁸⁵⁰ A good up-to-date overview of silicon qubits can be found in [Scaling silicon-based quantum computing using CMOS technology: Challenges and Perspectives](#) by Fernando Gonzalez-Zalba, Silvano de Franceschi, Tristan Meunier, Maud Vinet, Andrew Dzurak et al, 2020 (16 pages).

⁸⁵¹ See [Democratizing Spin Qubits](#) by Charles Tahan, November 2021 (19 pages) which describes the many challenges with quantum dots spin qubits and [Quantum Technologies for Engineering: the materials challenge](#) by Kuan Eng Johnson Goh, Leonid A Krivitsky and Dennis L Polla, IOP Publishing, March 2022 (14 pages).

Science

Spin qubits may allow the integration of a large number of qubits in a circuit, with potentially up to billions of qubits on a single chipset. It seems to be the only technology that can achieve this level of integration. These qubits would have a rather long coherence time and an error rate at least as low as with superconducting qubits⁸⁵².

The control microwaves used have a higher energy level which explains why silicon qubits can theoretically operate around 1K instead of 15 mK for superconducting qubits. This level corresponds to microwaves with a frequency higher than 20 GHz, compared to the 4 to 8 GHz control microwaves of superconducting qubits. This higher temperature makes it possible to place denser control electronics around the qubits without heating up the circuit too much. The reference data are as follows: only one milliwatt of energy can be consumed at 100 mK⁸⁵³.

This limits the control electronics to about 10,000 transistors in CMOS technology⁸⁵⁴. Once developed, silicon qubits will require the use of massive error correction codes, such as surface codes or color codes.

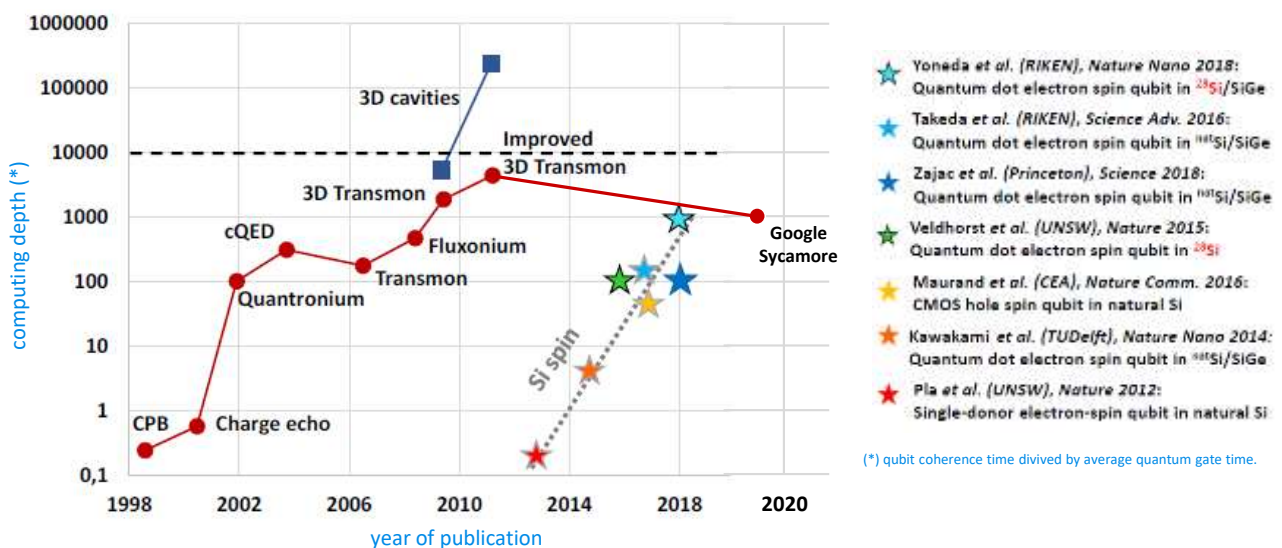


Figure 340: a perspective chart showing how silicon qubit progressed in the last 10 years with respect of computing depth. It requires some updates. First adapted by Maud Vinet from [Superconducting Circuits for Quantum Information: An Outlook](#) by Michel Devoret and R. J. Schoelkopf, *Science*, 2013. Then updated by Olivier Ezratty in April 2020.

Advances in spin qubits are more recent in a race against superconducting qubits. The diagram in Figure 340 illustrates this evolution over time between 2013 and 2020⁸⁵⁵, and would require some updating.

⁸⁵² A record silicon qubit coherence time was broken in 2020 by a team from the University of Chicago, reaching 22 ms (T₂). This is 10,000 times longer than the usual coherence times around 100μs found in superconducting qubits. These qubits use double gaps in silicon carbide structures. See [Universal coherence protection in a solid-state spin qubit](#) by Kevin C. Miao, David D. Awschalom et al, August 2020 (12 pages). University of Chicago.

⁸⁵³ A milli-Watt of cooling power can be achieved with a double pulsed tube cryostat such as the BlueFors XLD1000 or the Oxford Instruments TritonXL.

⁸⁵⁴ This is explained in [28nm Fully-Depleted SOI Technology Cryogenic Control Electronics for Quantum Computing](#), 2018 (2 pages), from CEA-Leti and STMicroelectronics. It discusses the good performance of CMOS components manufactured in FD-SOI technology and operating at 4K, where the available cooling budget is even higher than at 100 mK. At 4K, the cooling power is in the order of a quarter of a Watt to a Watt.

⁸⁵⁵ This diagram is by Maud Vinet and is inspired by [Superconducting Circuits for Quantum Information: An Outlook](#) by Michel Devoret and Robert Schoelkopf, 2013 (7 pages). Being quite old, it does not indicate the progress made since then in superconducting qubits as well as on spin qubits. "Operations per error" is proportional to the ratio between the lifetime of the qubits and the speed of the quantum gates on these qubits. It does not take into account the impact of the qubit error rate, which generally occurs well before reaching the limit of the number of theoretically executable gates.

They use a single parameter of comparison, the number of quantum gates that can be executed before reaching qubit decoherence time T_2 .

At the state-of-the-art level, the Australians, Dutch researchers from QuTech⁸⁵⁶ and Jason Petta at Princeton have demonstrated two-qubit gates in different geometries. To get to the next step, the challenge is to control the electrostatic potential between the quantum wells where the electrons are stored - and thus their spin - with a number of grids that allow the qubits to be arranged not too far apart, typically on the order of a few tens of nanometers. Also, a lot has to be done in materials design and process manufacturing⁸⁵⁷.

Note that these qubits can be associated with photonics for long range connectivity. The states of these qubits can be transmitted via photons, which would enable distributed quantum computing architectures⁸⁵⁸.

Qubit operations

The general principle of quantum dots spin qubits consists in confining a spin carrier (an electron or an electron hole) in an electrostatically defined quantum well that is surrounded by tunnel barriers. A static magnetic field enables the creation of a 2-level system with spin up and down. Single gate rotations are handled with submitting the spins/holes to a radio frequency magnetic field. The spin being affected only by this field protects it against electrical noise and other undesirable interactions like phonons (atomic vibrations). Two-qubit gates are created with lowering the tunnel barrier between adjacent dots. Spin state measurement is implemented with a spin-to-charge conversion.

Let's now look at the details⁸⁵⁹:

- **Qubit quantum state** is generally the spin of a trapped individual electron in a potential well. The electrons are confined in a two-dimensions layer semiconductor structure, such as at the interface between two different semiconductors as in GaAs/AlGaAs, in a small quantum well as in Si/SiGe, or between an insulator and semiconductor (MOS), with the two-dimensional conducting layer known as a two-dimensional electron gas (2DEG)⁸⁶⁰. In normal temperature, the energy levels of valence electrons with different spin is the same, or "degenerate". This spin degeneracy is lifted with using cryogeny at very low temperature (below a couple K) and with exposing the material under a magnetic field.
- **Single-qubit quantum gates** use the principle of electron spin resonance (ESR). As with superconducting qubits, these gates rely on the irradiation of the qubit by microwaves pulses, either using electromagnetic cavities, or with radio-frequency lines in which an alternating current creates a magnetic field, or finally, using micro-magnets. The related microwaves use frequencies between 8 and 20 GHz. These gates are usually R_x and R_y gates with the microwave pulse phase driving the gate rotation around axis X or Y and their amplitude and duration driving the rotation angle.

⁸⁵⁶ See [A Crossbar Network for Silicon Quantum Dot Qubits](#) by R Li et al, 2017 (24 pages).

⁸⁵⁷ See the review paper [Materials for Silicon Quantum Dots and their Impact on Electron Spin Qubits](#) by Andre Saraiva, Wee Han Lim, Chih Hwan Yang, Christopher C. Escott, Arne Laucht and Andrew S. Dzurak, December 2021 (22 pages).

⁸⁵⁸ See [Coherent shuttle of electron-spin states](#) by Lieven Vandersypen et al, 2017 (21 pages).

⁸⁵⁹ See [Silicon Qubits](#) by Thaddeus D. Ladd 2018 (19 pages) which describes various methods other than the one discussed here.

⁸⁶⁰ See the review paper [Quantum Dots / Spin Qubits](#) by Shannon Harvey, April 2022 (20 pages).

- **Two-qubit quantum gates** are created by controlling a tunneling interaction between two neighboring qubits with a significant number of electrodes. These interact with each other by modifying the potential barrier that separates the two qubits. The manipulations, as in single-qubit gates, are performed by applying square pulse currents to qubit barrier and plunger gates.

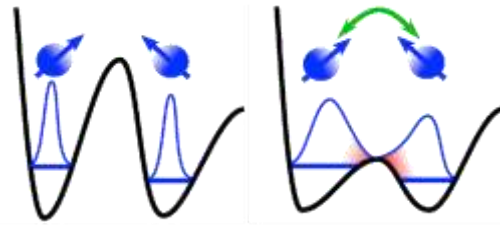


Figure 341: how a two-qubit gate is implemented with reducing the tunnel barrier between two spins. Source: Maud Vinet.

Common low-level gates of this type are the square root of a SWAP gate and a phase controlled gate.

- **Qubit readout** uses the conversion of the electron spin into electrical charge ("spin to charge") which is then exploitable by traditional electronics. It's frequently using a second electron-spin positioned next to each and every computing qubit. It's based on a microwave pulse sent on the qubit and a reflected signal phase/amplitude analysis, *aka* gate reflectometry⁸⁶¹.

In typical circuits, qubit drive is usually implemented with several wirings: L (lead, providing the electron for the quantum dot), P (plunger, control the electron population), T (for tunnel coupling between quantum dots), S (source) and D (drain).

Research

Here are now the main research laboratories that are exploring the silicon spin path, very often in multi-laboratory and multi-country partnership ventures. We'll focus first on the Netherlands, Australia, France and the USA, and will then cover other countries.



In **The Netherlands**, TU Delft and QuTech are among the most active research organizations in Europe around quantum dots based qubits. This activity is centered in Lieven M. K. Vandersypen's lab at QuTech.

Two main technology paths are explored there with Si-MOS quantum dots in partnership with Intel since 2015, and on silicon-germanium qubits under the leadership of Menno Veldhorst and Giordano Scappucci. On top of his main role at Forschungszentrum Jülich in Germany, David DiVincenzo is also a professor at the EEMCS Department at the TU Delft and a contributing scientist at QuTech. TU Delft collaborates on germanium qubits with Purdue University in Indiana and Wisconsin-Madison University.

In 2020, Menno Veldhorst's team demonstrated the feasibility of germanium qubits with two entangled qubits with fidelities of respectively 99.9% and 98% for one and two qubit gates, using germanium electron holes and with two-qubit gate time of 75 ns over a coherence time of about 1 μ s⁸⁶². These qubits are built on a SOI substrate⁸⁶³.

⁸⁶¹ See an implementation with [Gate-reflectometry dispersive readout and coherent control of a spin qubit in silicon](#) by Alessandro Crippa, Silvano De Franceschi, Maud Vinet, Tristan Meunier et al, July 2019 (6 pages).

⁸⁶² See [Fast two-qubit logic with holes in germanium](#) by N.W. Hendrickx, Menno Veldhorst, Giordano Scappucci et al, January 2020 in Nature et on arXiv in April 2019 (6 pages) also described in [Reliable and extremely fast quantum calculations with germanium transistors](#), Qutech, January 2020.

⁸⁶³ The SOI for "silicon on insulator" is a technology from the French CEA-Leti and SOITEC. It adds a layer of silicon oxide insulator (SiO₂ or "BOX" for "buried oxide") over the silicon wafers and on which are then etched transistors and other circuits conductors

Also in 2020, they implemented the same types of qubits in a 2x2 qubit array with a coherence time of 0.5 ms with 10 ns single qubit gate time⁸⁶⁴ (the qubits are labelled P₁ to P₄ in Figure 342).

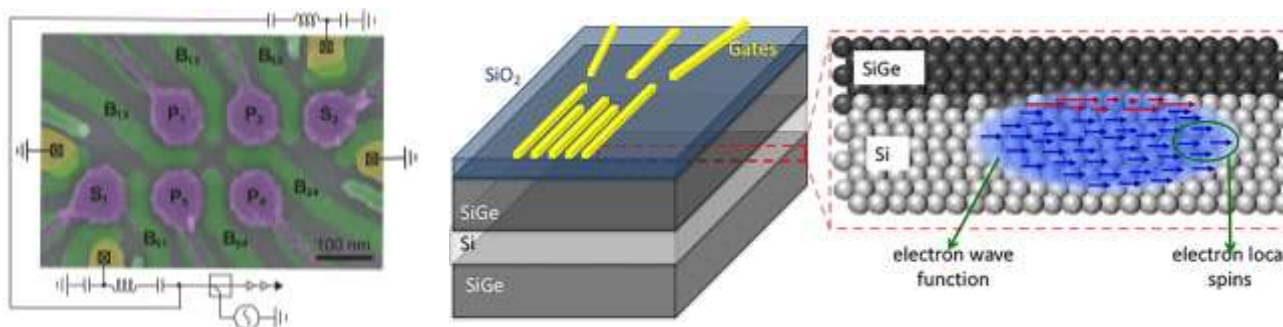


Figure 342: silicon-germanium prototype qubits. Source: [A two-dimensional array of single-hole quantum dots](#) by F. van Riggelen, Giordano Scappucci, Menno Veldhorst et al, August 2020 (7 pages) and [Silicon provides means to control quantum bits for faster algorithms](#) by Kayla Wiles, Purdue University, June 2018.

In 2022, they prototyped a Si-Ge spin qubits phase error correction proof of concept using the same 4 SiGe qubits⁸⁶⁵. They then extended the number of qubits to 6 while preserving good fidelities of 99.77% for single-qubit gates and reaching 71% to 84% for two-qubit gates, with a T₂ coherence time of several μ s⁸⁶⁶. They also achieved interesting results based on two SiGe qubits, with two-qubit gate fidelities exceeding 99%, paving the road for fault-tolerance (although surface codes QEC would probably require much better fidelities in the 99,99% range and with way above 2 qubits)⁸⁶⁷.

Sideways, the QuTech team in collaboration with research teams from ICREA and IC2N in Spain also made interesting inroads with interfacing their SiGe qubits with a germanosilicide superconducting material.

It could be useful in topological qubits design, to create gate-tunable superconducting qubits (gate-mons), to create long-range coupling between spin qubits using superconductivity and microwave guides⁸⁶⁸. At last, they demonstrated also in 2022 a 36x36 gate electrode crossbar supporting 648 narrow-channel field effect transistors (FET) to drive SiGe qubits⁸⁶⁹.

Qutech is also the testing arm of Intel with its HorseRidge system and Si-MOS double quantum dots qubits. In 2020, QuTech and Intel announced having developed "hot" silicon qubits operating at around 1K, more precisely at 1.1K⁸⁷⁰.

⁸⁶⁴ See [A two-dimensional array of single-hole quantum dots](#) by F. van Riggelen, Giordano Scappucci, Menno Veldhorst et al, August 2020 (7 pages) and [A four-qubit germanium quantum processor](#) by N.W. Hendrickx et al, September 2020 (8 pages).

⁸⁶⁵ See [Phase flip code with semiconductor spin qubits](#) by F. van Riggelen, M. Veldhorst et al, QuTech, February 2022 (8 pages).

⁸⁶⁶ See [Universal control of a six-qubit quantum processor in silicon](#) by Stephan G.J. Philips, Menno Veldhorst, Lieven M.K. Vandersypen et al, February 2022 (38 pages).

⁸⁶⁷ See [Quantum logic with spin qubits crossing the surface code threshold](#) by Xiao Xue, Lieven M. K. Vandersypen et al, Nature, January 2022 (17 pages).

⁸⁶⁸ See [Hard superconducting gap in a high-mobility semiconductor](#) by Alberto Tosato, Francesco Borsoi, Menno Veldhorst, Giordano Scappucci et al, June 2022 (20 pages).

⁸⁶⁹ See [A quantum dot crossbar with sublinear scaling of interconnects at cryogenic temperature](#) by P. L. Bavdaz, James Clarke, Menno Veldhorst, G. Scappucci et al, Nature, 2022 (6 pages) and [Shared control of a 16 semiconductor quantum dot crossbar array](#) by Francesco Borsoi, Giordano Scappucci, Menno Veldhorst et al, September 2022 (33 pages).

⁸⁷⁰ See [Hot, dense and coherent: scalable quantum bits operate under practical conditions](#) by QuTech, April 2020 which refers to [Universal quantum logic in hot silicon qubits](#) by L. Petit, Menno Veldhorst et al, April 2020 in Nature and October 2019 in pre-print (10 pages).

At the same time, UNSW researchers were testing similar qubits at 1.5K⁸⁷¹.



Australians are among the most active around silicon qubits, whether in the CQC2T teams at UNSW (University of New South Wales) or in other laboratories. Australian Universities are also teaming up with Microsoft Research⁸⁷².

UNSW's CQC2T (Center for Quantum Computing & Communication Technology) laboratory is led by Michelle Simmons. She also cofounded and runs SQC, a silicon qubit startup that spun-out of UNSW. Their specialty is donors spin qubits using phosphorous atoms implanted in silicon wafers, along the Bruce Kane model already described in the [History](#) part and created in 1998 at UNSW. This is a home run! In 2020, a team from the University of Melbourne showed how machine learning could help calibrate the placement of phosphorus atoms in a 2D structure of qubits on a silicon substrate⁸⁷³. We'll cover these phosphorus-based qubits in the part dedicated to SQC a bit later in the [vendors part](#).

Two other key scientists at UNSW are Andrew S. Dzurak and Andrea Morello. Andrea Morello's team working with DoE's Sandia Labs published in 2022 results with a single-qubit gate fidelity of 99.95%, a C-Z two-qubit gate fidelity of 99.37% and 98.95% readout fidelity with two phosphorus nuclear spins coupled with a single silicon spin donor electron. They even produced a three-qubit entangled state (GHZ) with a fidelity 92.5%. This was interesting but was not a "scalable" demonstration⁸⁷⁴.

Still, Morello and Dzurak usually work on more classical silicon quantum dots qubits. In 2018, they proved the feasibility of creating silicon qubits and developed protocols for reading the state of the spins of these qubits without the need for averaging via a process called "Pauli spin blockade", paving the way for error correction codes implementation and the creation of large-scale quantum computers⁸⁷⁵. They also obtained in 2019 a 2% error rate for two-qubit quantum gates and a 99.96% fidelity for one-qubit gates⁸⁷⁶.

Andrew S. Dzurak found in 2021 a way to improve the scalability of spin qubits with removing some the microwave circuits within the qubit chipset and providing these microwaves to the qubits quantum dots with a dielectric microwave resonator (DR) made in potassium tantalate and activated by a discrete loop coupler, made of a simple wire⁸⁷⁷. It drives the ESR (Electron Spin Resonance) magnetic field that enables spin rotations and single qubit gates as well as spin state readout. All this saves at least two microwave circuits in the quantum dots chipset, reducing heating and simplifying the chipset design and, potentially, qubits topology.

⁸⁷¹ See [Hot qubits made in Sydney break one of the biggest constraints to practical quantum computers](#) by UNSW, April 2020 referring to [Silicon quantum processor unit cell operation above one Kelvin](#) by C. H. Yang, Andrea Morello, Andrew Dzurak et al, February 2019 (15 pages).

⁸⁷² UNSW also received in 2018 a funding of \$53M from the telecom operator Telstra, the Commonwealth Bank and the governments of Australia and the New South Wales region.

⁸⁷³ See [Machine learning to scale up the quantum computer](#) by Muhammad Usman and Lloyd Hollenberg, University of Melbourne, March 2020. Also seen in [To Tune Up Your Quantum Computer, Better Call an AI Mechanic](#) by NIST associated with UNSW, March 2020.

⁸⁷⁴ See [Precision tomography of a three-qubit donor quantum processor in silicon](#) by Mateusz Madzik, Andrea Morello et al, January 2022 (51 pages).

⁸⁷⁵ See [Tests show integrated quantum chip operations possible](#), October 2018 and [Integrated silicon qubit platform with single-spin addressability, exchange control and single-shot singlet-triplet readout](#) by M. A. Fogarty, Andrea Morello, Andrew S. Dzurak et al, Nature Communications, October 2018 (7 pages).

⁸⁷⁶ See [Quantum World-First: Researchers Reveal Accuracy Of Two-Qubit Calculations In Silicon](#), May 2019.

⁸⁷⁷ See [Single-electron spin resonance in a nanoelectronic device using a global field](#) by Ensar Vahapoglu, Andrew S. Dzurak et al, August 2021 (7 pages) and [Supplemental Materials](#) (12 pages).

The global magnetic field generated by this system comes from a dielectric microwave resonator of $0,7*0.55*0.3\text{mm}$ and the discrete loop coupler is even larger, while quantum spin qubits can scale down as low as $100\text{ nm} \times 100\text{ nm}$. The team communicates on this technology as one that could enable scaling quantum dots to million qubits. So how are individual qubits controlled? Individual spin control and readout is activated by some classical direct current tension sent to each quantum dots in the qubit chipset, replacing the usual microwave signals sent and reflected in the chipset. The next step is to implement the qubit circuit on isotopically purified ^{28}Si and check qubits coherence. While the solution simplifies the qubit chipset wiring for some of the microwave lines, the prototype is based on using external microwave generators and readout systems, which doesn't scale at all. It circles back to a cryo-CMOS component that was developed by another Australian team and with Microsoft, which we describe in the [cryo-CMOS section](#), page 498.

single-electron spin resonance (ESR) in a global field

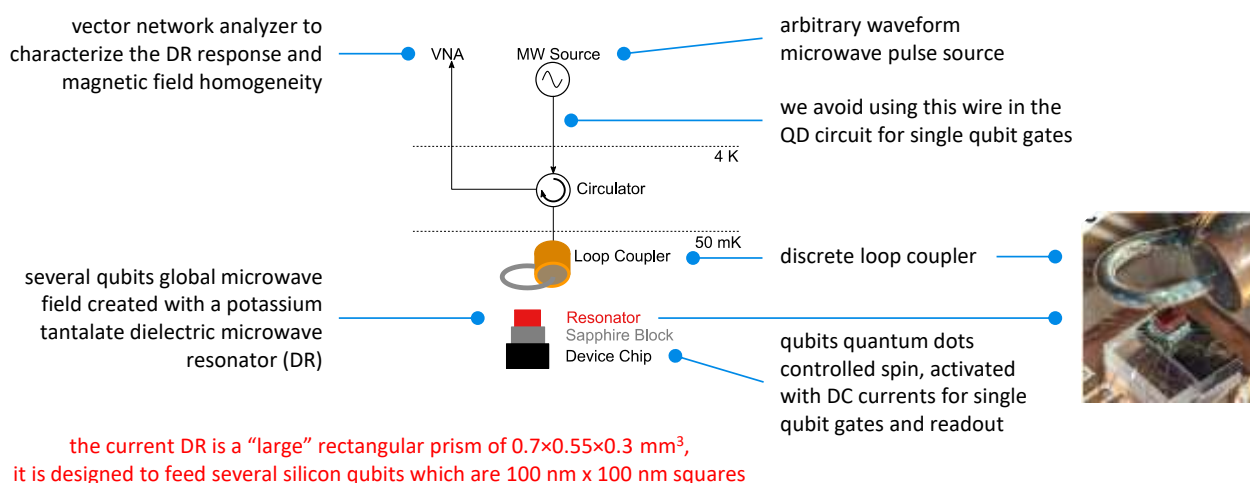


Figure 343: a proposal to improve the scalability of spin qubits with removing some the microwave circuits within the qubit chipset and providing these microwaves to the qubits quantum dots with a dielectric microwave resonator. Source: [Single-electron spin resonance in a nanoelectronic device using a global field](#) by Ensar Vahapoglu, Andrew S. Dzurak et al, August 2021 (7 pages).

Andrea Morello's team is also studying the remote coupling of electron spins via photons in the visible or in radio waves spectrum. His team created silicon qubits exploiting the control of electron spin of intermediate layers of silicon atoms, increasing stability and reducing flip (or charge) errors⁸⁷⁸. It also managed, by chance, to control the spin of antimony atomic nuclei with an oscillating electric field⁸⁷⁹.



In France, the silicon qubit effort is driven out of a group of research labs in Grenoble with CEA-Leti, CEA-LIST, CEA-IRIG, CNRS Institut Néel and UGA (Université Grenoble Alpes).

⁸⁷⁸ See [UNSW use flat electron shells from artificial atoms as qubits](#) by Chris Duckett, February 2020 and [Engineers Just Built an Impressively Stable Quantum Silicon Chip From Artificial Atoms](#) by Michelle Starr, February 2020 which refers to [Coherent spin control of s-, p-, d- and f-electrons in a silicon quantum dot](#) by Andrea Morello et al, 2020 (7 pages).

⁸⁷⁹ See [Engineers crack 58-year-old puzzle on way to quantum breakthrough](#) by UNSW, March 2020 and [Chance discovery brings quantum computing using standard microchips a step closer](#) by Adrian Cho, March 2020.

In October 2018, the Grenoble-based team of Silvano De Franceschi (INAC, CEA), Tristan Meunier (Institut Néel, CNRS) and Maud Vinet (CEA-Leti) obtained a €14M **ERC Synergy Grant** for their QuQube project, spread over 6 years to produce a 100-qubit electron spin CMOS quantum processor⁸⁸⁰. Since March 2020, the Grenoble team is also coordinating the 4-year European Quantum Flagship project **QLSI** which was formally launched in February 2021⁸⁸¹.

It consolidates fundamental research in silicon qubits and brings together CEA, CNRS Institut Néel, Atos, SOITEC and STMicroelectronics for France, IMEC (Belgium), Quantum Motion and UCL (UK), Infineon, IHP, U Konstanz, Fraunhofer and RWTH Aachen (Germany), UCPH (Denmark), TU Delft, U Twente and TNO (Netherlands) and U Basel (Switzerland). With a budget of 15M€ to be shared between all these entities, the objective is to enable the manufacture and testing of 16 silicon qubits with gate fidelity of over 99%, and the preparation of a roadmap to be able to scale beyond a thousand qubits.

The Grenoble silicon qubit project was led until 2022 by **Maud Vinet** (CEA-Leti) and **Tristan Meunier** (CNRS) until they launched **Siquance** in November 2022. This story started about 10 years earlier when CEA-Leti got interested in silicon qubits as a way to extend a then flailing Moore's law. CEA-Leti implemented their first silicon quantum dots qubits in 2016⁸⁸².

Here are some of the specifics of this endeavor.

Different techniques. The Grenoble team mainly bets on Si-MOS silicon spin qubits. But they are still investigating SiGe qubits (CEA-IRIG), well as GaAs (for testing and calibration purpose) as well as silicon spin holes qubits, which are easier to control with a tension on the quantum dot transistor gate⁸⁸³.

Manufacturing capacity is a key asset from CEA-Leti, being one of the few public laboratories in the world with a CMOS component test production platform (IMEC is their counterpart in Europe, in Belgium). It includes all the tools required to produce 200 mm and 300 mm wafers.

It allows the production of all kinds of components in silicon, germanium and III-V materials (photonics, gallium arsenide, gallium nitride, etc.).

⁸⁸⁰ See [An ERC Synergy Grant for Grenoble research on quantum technologies](#), October 2018 (6 pages). A European Research Council Synergy Grand funds "moonshots" in European research involving at least two research laboratories. 14M€ is the maximum funding for such projects. 10M€ of core funding and 4M€ which can fund heavy investments or access to large infrastructures.

⁸⁸¹ See [New EU Quantum Flagship consortium launches a project on silicon spin qubits as a platform for large-scale quantum computing](#), February 2021. QLSI was a follow-up project from the European collaborative project **Mos-quito**, a 3-year project from 2016 to 2019 with 4M€ funding for studying the performance of different types of individual silicon spin qubits to provide recommendations for their large-scale implementation.

⁸⁸² See [A CMOS silicon spin qubit](#) by Romain Maurand, Maud Vinet, Marc Sanquer, Silvano De Franceschi et al, 2016 (12 pages) that was already mentioned.

⁸⁸³ See [Dispersively probed microwave spectroscopy of a silicon hole double quantum dot](#) by Rami Ezzouch, Maud Vinet, Matias Urdampilleta, Tristan Meunier, Marc Sanquer, Silvano De Franceschi, Romain Maurand et al, 2020 (13 pages) and [A single hole spin with enhanced coherence in natural silicon](#) by Nicolas Piot, Boris Brun, Vivien Schmitt, Maud Vinet, Matias Urdampilleta, Tristan Meunier, Yann-Michel Niquet, Silvano De Franceschi et al, Nature, September 2022 (15 pages).

The CEA-Leti clean rooms are spread over several buildings, with the main one being 185 m long on 8000 m² ⁸⁸⁴. Here, CMOS qubits manufacturing process uses 300 mm SOI wafers on with an additional thin layer of 99.992% purified 28-isotope silicon⁸⁸⁵. Validated production is to be later transferred to volume production in commercial fabs such like those from STMicroelectronics in Crolles, France, or GlobalFoundries in the USA or Germany.



Figure 344: the CEA-Leti's pre-industrial 200/300 fabs in Grenoble.

In its early stages, the size of the quantum computer market will be modest. In a conventional batch of 25 wafers alone, you can produce several thousand quantum chips in a single run, enough to power a large base of quantum supercomputers. But industry-grade clean room ensure quality processes that are not necessarily found in pre-production clean rooms.

Staging progress with the Grenoble team expecting to progress in stages over a six-year period starting in 2019: demonstration of a two-qubit silicon-based gate, demonstration of quantum simulation in a 4x4 array based on III-V material, demonstration six qubits in silicon, development of error correction codes and adapted algorithms, and fabrication of 100 2D array qubits in silicon at the end of this journey.

Control electronics with the Grenoble team creating control electronics operating at cryogenic temperature. The 2D architecture of Leti's CMOS chipset contains several layers with silicon qubits and then the integrated electronics for control and qubit readout wiring. The qubits are distributed in 2D, but the integration of the components is also vertical within the components.

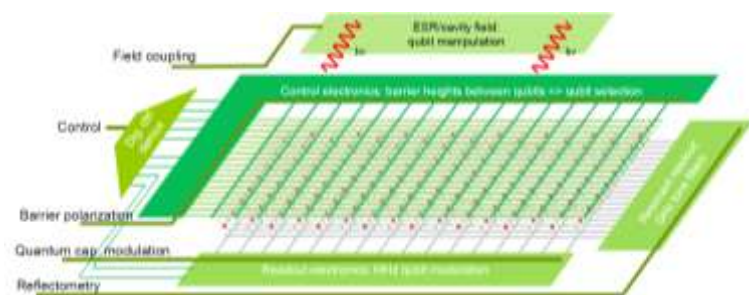


Figure 345: 2D wiring to access spin qubits with scalable wiring. Source: [Silicon Based Quantum Computing](#), Maud Vinet 2018 (28 slides).

The measurement layer is located below the qubits while the layer for activating the qubits with quantum gates is above. For N^2 qubits, they would need $2N$ control lines (horizontal, vertical) instead of $2N^2$, which would generate an appreciable gain in connectivity. The technique would work to generate one- and two-qubit quantum gates⁸⁸⁶.

⁸⁸⁴ Other research clean rooms exist in France: the C2N clean room in Palaiseau, the IEF in Orsay, the Thales TRT clean room in Palaiseau, the IEMN clean room in Lille, Femto-ST clean room in Besançon and the Laas clean room in Toulouse. In production are mainly the fab 200 and 300 at STMicroelectronics in Crolles, near Grenoble. Some of these laboratories are associated in the National Network of Large Technology Plants (Renatech). They make their platforms available to companies in project and contract mode.

⁸⁸⁵ The first test of spin control with isotopically purified silicon was achieved in 2011. See [Electron spin coherence exceeding seconds in purified silicon](#) by Alexei Tyryshkin, Kohei Itoh, John Morton et al, 2011 (18 pages).

⁸⁸⁶ The technique is described in [Towards scalable silicon quantum computing](#) by Matias Urdampilleta, Maud Vinet, Tristan Meunier, Yvain Thonnart et al, 2020 (4 pages) as well as in the presentation [Silicon Based Quantum Computing](#), Maud Vinet, 2018 (28 slides).

The great challenge of these architectures is their variability, i.e., the differences in behavior from one qubit to another and from one circuit to another. This leads to a need for precise calibration, qubit by qubit, of the microwaves controlling and reading the state of the qubits. As for superconducting qubits, this calibration can be done using dedicated machine learning software. They use superconducting materials for the metal layer of these circuits, based on titanium nitride. This provides low resistance and reduces the noise of qubit state measurement.

3D stacking is used to arrange chipsets components in 3D⁸⁸⁷, which can help solve various scalability problems. CEA-Leti is using it CoolCube technology. The reference publications of these teams on CMOS qubits are numerous⁸⁸⁸.

Spin-photon coupling could be used to create a communication link between remote qubits. At the Néel Institute, the aim is to move electron spins over long-distances ("Long-distance coherent spin shuttling"). Here, a long-distance means 5 μm ! But it makes enough to link qubits together, so it's worth it⁸⁸⁹.



In the USA, on top of Intel, several research labs are working on electron spin qubits. Let's factor in the already mentioned **DoE Sandia Labs** with sites in New Mexico and California, and **Purdue** and **Wisconsin-Madison Universities**.

They work on the physics of silicon qubits and their error correction codes. They are targeting an operating temperature of 100 mK.

Princeton University and Jason Petta's team are working on the realization of a two-qubit silicon CNOT gate with a very high level of reliability and low operating time, respectively 200ns and 99%⁸⁹⁰.

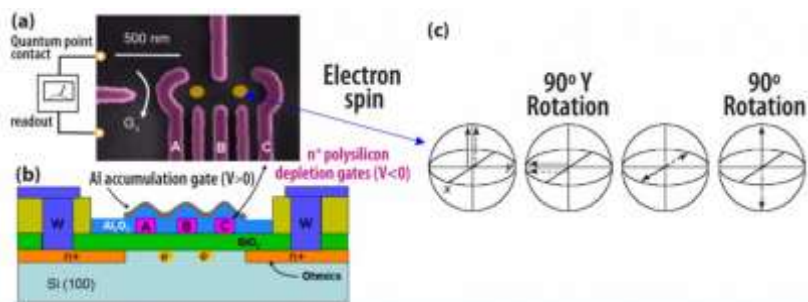


Figure 1: (a) scanning electron microscope image of Sandia's dual quantum dot structure fabricated in silicon (the dots suggest the approximate location of the electron position); (b) schematic cross section of the quantum dot structure showing the position of the single electron locations; and (c) schematic representation of spin manipulation using rotation and precession of two different spins.

Figure 346: a typical double quantum dots spin qubit. Source: [Toward realization of a silicon-based qubit system for quantum computing](#) by Malcolm Carroll, Sandia Labs, 2016.

These are also double quantum dots qubits using silicon and germanium. In October 2018, this Princeton team had succeeded in monitoring the state of its CMOS qubits with light and exploiting a microwave field to exchange a quantum between an electron and a photon⁸⁹¹.

UCLA and **Virginia Commonwealth University** are working on nanomagnets to drive silicon qubits⁸⁹².

⁸⁸⁷ See [CoolCube: A True 3DVLSI Alternative to Scaling Resource Library, Technologies Features](#) by Jean-Eric Michallet, 2015.

⁸⁸⁸ These include [A CMOS silicon spin qubit](#) by Romain Maurand, Maud Vinet, Marc Sanquer, Silvano De Franceschi et al, 2016 (12 pages) which defines the basis of double quantum dot CMOS qubit, [SOI technology for quantum information processing](#), 2016 which completes this description as well as [Conditional Dispersive Readout of a CMOS Single-Electron Memory Cell](#) by Simon Schaal et al, 2019 (9 pages) which describes, in the framework of a partnership with the University of London, the work on reading the state of a CMOS quantum dot. And then [Towards scalable silicon quantum computing](#) by Maud Vinet et al, 2018 (4 pages).

⁸⁸⁹ See [Coherent long-distance displacement of individual electron spins](#), 2017 (27 pages) and [Quantum Silicon Grenoble, the project on which the Forteza report relies for a quantum computer made in France](#) by Manuel Moragues, January 2020.

⁸⁹⁰ Seen in [Quantum CNOT Gate for Spins in Silicon](#), 2017 (27 pages).

⁸⁹¹ See [How old-school silicon could bring quantum computers to the masses](#), October 2018 and [In leap for quantum computing, silicon quantum bits establish a long-distance relationship](#) by University of Princeton, December 2019.

⁸⁹² See [Quantum Control of Spin Qubits Using Nanomagnets](#) by Mohamad Niknam et al, March 2022 (11 pages).

At last, **HRL Malibu**, a joint research subsidiary of Boeing and General Motors located in California is working on both GaAs and Si / SiGe spin qubits. In 2022, they achieved a CNOT gate fidelity of $96.3 \pm 0.7\%$, SWAP fidelity of $99.3 \pm 0.5\%$ with 6 silicon qubits arranged in a 1D array⁸⁹³. They also work on triple-dot qubits with long lifetimes and better self-error correction⁸⁹⁴.

Let's finish this list with a couple other countries:

Switzerland: the Swiss National Science Foundation launched **SPIN (Spin Qubits in Silicon)**, an electron spin qubits project in December 2019 with a funding of \$18M. The end goal is to create a scalable universal quantum computer with more than a thousand logical qubits. The project led by the University of Basel also gathers researchers from ETH Zurich, EPFL and IBM Research Zurich. It looks like a "Plan B" for IBM who is so far focused commercially on superconducting qubits⁸⁹⁵. We've also seen the key role of Daniel Loss in silicon qubits. He still works in Switzerland⁸⁹⁶! Another key researcher is EPFL's Andrea Ruffino, who is working with the Hitachi Cambridge Laboratory in the design of a mixed silicon qubit and cryo-CMOS readout control circuit⁸⁹⁷.

UK: is another active country on silicon qubits, particularly in **Oxford University**, **Cambridge University** and **UCL**, and with their startup **Quantum Motion**.

Germany: at the **University of Aachen**, researchers created double quantum dots of silicon with graphene⁸⁹⁸. Also involved are Infineon, Leibniz Institute IHP Microelectronics, Universität Konstanz and Fraunhofer IPMS with its own cleanroom.

Denmark: **Niels Bohr Institute** and **CEA-Leti** collaborated to build a silicon qubit 2x2 matrix using single electrons quantum dots. These were fabricated on a classical 300 mm SOI wafer coming out of the CEA-Leti fab in Grenoble. While not being operational qubits, these quantum dots electrons were controllable with voltage pulses bases gates. They also implemented electron swaps, that could be useful in optimizing SWAP gates in future systems⁸⁹⁹. In another work with Purdue University in the USA, NBI researchers implemented four GaAs qubits in a 2x2 array⁹⁰⁰.

China also explores silicon qubits. Their work is difficult to evaluate and they don't publish much on this type of qubits compared to photon-based qubits, boson sampling and superconducting qubits⁹⁰¹.

Japan silicon qubits are investigated at **RIKEN**. Their Semiconductor Quantum Information Device Theory Research Team is led by... Daniel Loss, yes, the same one. They were able in 2020 to measure the state of silicon qubits without altering it.

⁸⁹³ See [Universal logic with encoded spin qubits in silicon](#) by Aaron J. Weinstein et al, HRL, February 2022 (12 pages).

⁸⁹⁴ See [Full-permutation dynamical decoupling in triple-quantum-dot spin qubits](#) by Bo Sun et al, HRL, August 2022 (12 pages).

⁸⁹⁵ See for example [A spin qubit in a fin field-effect transistor](#) by Leon C. Camenzind et al, March 2021 (14 pages) which describes a FinFET hole spin qubit potentially operating at 4K.

⁸⁹⁶ See [Fully tunable longitudinal spin-photon interactions in Si and Ge quantum dots](#) by Stefano Bosco, Daniel Loss et al, EPFL, March 2022 (18 pages) and [A hot hole spin qubit in a silicon FinFET](#), IBM, March 2021.

⁸⁹⁷ See [A cryo-CMOS chip that integrates silicon quantum dots and multiplexed dispersive readout electronics](#) by Andrea Ruffino, Edoardo Charbon et al, Nature Electronics, December 2021 (14 pages). The circuit was implemented for three qubits

⁸⁹⁸ See [Bilayer graphene double quantum dots tune in for single-electron control](#) by Anna Demming, March 2020.

⁸⁹⁹ See [Single-electron operations in a foundry-fabricated array of quantum dots](#) by Fabio Ansaloni, Benoît Bertrand, Louis Hutin, Maud Vinet et al, December 2020 (7 pages).

⁹⁰⁰ See [Simultaneous Operations in a Two-Dimensional Array of Singlet-Triplet Qubits](#) by Federico Fedele et al, October 2021 (12 pages) and [Roadmap for gallium arsenide spin qubits](#) by Ferdinand Kuemmeth and Hendrik Bluhm, 2020 (4 pages).

⁹⁰¹ See [Semiconductor quantum computation](#) by Xin Zhang Hai-Ou Li et al, December 2018 (23 pages). The document provides an overview of CMOS quantum technology but does not specify the specific contribution of Chinese research laboratories.

This non-destructive measurement uses an Ising interaction model based on ferromagnetism that evaluates the spin of atoms neighboring the atom containing the qubit spin electron⁹⁰².

Teaming up with Qutech, they also work on shuttling electrons to connect distant silicon QPUs⁹⁰³, on SiGe high fidelity qubits⁹⁰⁴ and on quantum error correction⁹⁰⁵.

quantum dots spins qubits

- **good scalability potential** to reach millions of qubits, thanks to their size of 100x100 nm.
- **works at around 100 mK - 1K** => larger cooling budget for control electronics.
- **average qubits fidelity** reaching 99% for two qubits gates in labs.
- adapted to **2D architectures** usable with surface codes or color codes QEC.
- can leverage existing semiconductor fabs.
- good quantum gates speed.

- **active research** in the field started later than with other qubit technologies and spread over several technologies (full Si, SiGe, atom spin donors).
- **so far, only 4 to 15 entangled qubits** (QuTech, UNSW, Princeton, University of Tokyo).
- **qubits variability** to confirm.
- **scalability** remains to be demonstrated.
- **high fabs costs** and quality manufacturing constraints.
- **less funded** startup scene.

Figure 347: quantum dots spin qubits pros and cons. (cc) Olivier Ezratty, 2022.

Vendors

Key silicon based qubits industry vendors and startups are **Intel** (USA), **SQC** (Australia), **Diraq** (Australia), **Quantum Motion** (UK), **Siquance** (France), **C12 Quantum Electronics** (France), **Equal1.labs** (Ireland/USA) and **Archer Materials** (Australia).



Silicon
Quantum
Computing

Silicon Quantum Computing or **SQC** (2017, Australia, \$66M) is a spin-off from UNSW and CQC2T launched by Michelle Simmons. In 2017, their goal was to reach 10 qubits by 2022⁹⁰⁶ and they expect to reach 100 qubits by 2028.

The 40+ people company recruited John Martinis from Google at the end of September 2020 but he left the team less than a year later. SQC uses the spin donors technique, trapping phosphorus atoms on a silicon substrate. Their qubit is made with controlling the association of the phosphorus atom nucleus spin and a silicon donor electron spin. They create two-qubit gates with two phosphorus atoms that are a few nanometers apart, using quantum tunneling. They showcased single-gates fidelity of about 99.99% and two-qubit gates speed of less than one nanosecond⁹⁰⁷. In 2022, they touted having produced the “*first ever quantum circuit*”⁹⁰⁸.

⁹⁰² See [Scientists succeed in measuring electron spin qubit without demolishing it](#), RIKEN, March 2020, mentioning [Quantum non-demolition readout of an electron spin in silicon](#) by J. Yoneda et al, 2020 (7 pages).

⁹⁰³ See [A shuttling-based two-qubit logic gate for linking distant silicon quantum processors](#) by Akito Noiri et al, February 2022 (25 pages).

⁹⁰⁴ See [Fast universal quantum control above the fault-tolerance threshold in silicon](#) by Akito Noiri, Giordano Scappucci et al, 2022 (27 pages).

⁹⁰⁵ See [Quantum error correction with silicon spin qubits](#) by Kenta Takeda, Giordano Scappucci et al, Nature, January-August 2022 (23 pages).

⁹⁰⁶ This is documented in [Silicon quantum processor with robust long-distance qubit couplings](#) by Guilherme Tosi, Andrea Morello et al, 2017 (17 pages).

⁹⁰⁷ See [Exploiting a Single-Crystal Environment to Minimize the Charge Noise on Qubits in Silicon](#) by Ludwik Kranz, Michelle Simmons et al, 2020 and [A two-qubit gate between phosphorus donor electrons in silicon](#) by Y. He, Michelle Simmons et al, 2019.

⁹⁰⁸ See how the media buy in such outrageous claim in [A Huge Step Forward in Quantum Computing Was Just Announced: The First-Ever Quantum Circuit](#) by Felicity Nelson, Science Alert, June 2022. Hopefully, The Quantum Insider is not parroting the fancy claim and titled [Silicon Quantum Computing Announces its First Quantum Integrated Circuit](#) by James Dargan, June 2022.

It was a way to fulfill their 2017 goal and showcase a 10-qubit processor, implemented in a 1D lattice. It was presented in an article published on Nature, implementing a particular physics simulation, the many-body Su–Schrieffer-Heeger (SSH) model. Of course, with just 10 qubits, it can't showcase any quantum advantage. Unfortunately, the paper doesn't provide qubit fidelities data⁹⁰⁹. The paper was published as SQC announced it was starting a new financial round with a goal to obtain \$130M⁹¹⁰.

Mid-2021, Andrea Morello and Andrew Dzurak quit SQC where they were involved since the beginning. They preferred to focus on SiMOS qubit instead of phosphorus and donors qubits. It led to the creation of their startup Diraq, which we'll discuss later. As a result, SQC sold in May 2022 its patent portfolio and special equipment related to SiMOS to SiMOS Newco, a company created in December 2021, and probably related to Diraq, created a month later⁹¹¹.



Diraq (2022, Australia) is a startup spun out of UNSW created by Andrew Dzurak that develops quantum dots electron spin qubits. The company set a goal to build a one billion qubits computer, the largest I've seen so far with commercial vendors.

Their first planned steps are to reach 9 and then 256 qubits. The team is already set up with a bunch of scientists and engineers like Arne Laucht, Henry Yang. Andrea Morello from UNSW is also a scientific advisor for the venture. Morello and Dzurak were previously working with Michelle Simmons in her company SQC and they parted away in 2021. The founding team has a good track record in the advancement of quantum dots based qubits with many "firsts" achieved since 2014, including many patented processes (SiMOS - Silicon-Metal-Oxide-Semiconductor qubits, resonators and qubit electrical control, etc).



Siquance (2022, France) is the silicon qubits startups launched in November 2022 by Maud Vinet, Tristan Meunier and François Perruchot out of CEA-Leti and CNRS Institut Néel. They ambition to release a 100 physical qubit system by 2026.



Quantum Motion Technologies (2017, UK, \$9.7M) is an Oxford University spin-off that wants to create high-density silicon quantum computers. They have received unspecified seed funding from the UK fund Parkwalk Advisors in 2017.

The startup co-founded by John Morton (UCL) and Simon Benjamin (Oxford University) wants to industrialize a process created by Joe O'Gorman's team at Oxford University, which consists of clearly separating silicon qubits and their measurement.

Measurement was supposed to be carried out with a magnetic probe mechanically moved on the surface and making "square" movements, guided by a MEMS (micro-electro-mechanical device). This probe system was designed to avoid the use of control electronics and allow a better separation between the qubits⁹¹². A data rate separation process with intermediate mediation rates was limiting leakage effects⁹¹³. This process protected by one granted US patent and four patents pending. But it seems that this technology is finally not the one they will implement!

⁹⁰⁹ See [Engineering topological states in atom-based semiconductor quantum dots](#) by M. Kiczynski, Michelle Simmons et al, Nature, June 2022 (11 pages).

⁹¹⁰ See [Quantum star kicks off crucial \\$130m funding push](#) by Paul Smith, Financial Review, June 2022.

⁹¹¹ See [UNSW Sydney spin-out buys quantum computing hardware technology](#) by Lauren Croft, Lawyers Weekly, May 2022.

⁹¹² See [A silicon-based surface code quantum computer](#) by Joe O'Gorman et al, 2015 (14 pages). The paper is co-authored by John Motin and Simon Benjamin who are two co-founders of the startup Quantum Motion Technologies. Their Si-MOS qubits are mixing planar and 3D SOI components and are laid out to enable surface code error correction.

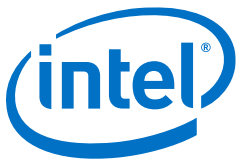
⁹¹³ See [A Silicon Surface Code Architecture Resilient Against Leakage Errors](#) by Zhenyu Cai (Quantum Motion Technologies) et al, April 2018 (19 pages).

In January 2021, Quantum Motion presented with Hitachi Cambridge, University of Cambridge and EPFL a 50 mK cryo-CMOS including quantum dots qubit arrays, row-column control electronics lines and analog LC resonators for multiplexed readout, using 6-8 GHz microwave resonators. This was a first step to implement time- and frequency-domain multiplexing scalable qubits readout⁹¹⁴.

In March 2021, Quantum Motion announced a record of stability of 9 seconds for an isolated silicon qubit. The chipsets were manufactured by CEA-Leti in Grenoble and the French team led by Maud Vinet coauthored the paper associated with this performance⁹¹⁵. Quantum Motion and UCL are part of the Quantum Flagship QLSI on silicon qubit that is led by Maud Vinet. So, this explains that.

Their roadmap consists of producing 5 qubit "small cells" by 2022 in a structure that could then be reproduced in matrix patterns. They believe they can create a quantum computer with 100 logical qubits by 2029, a classical milestone for most quantum computer vendors. They provided an update on their architecture in an arXiv paper in August 2022⁹¹⁶.

In the software area, Quantum Motion developed QuEST, an open source, hybrid multithreaded and distributed, GPU accelerated simulator of quantum circuits. It works both on any laptop or on supercomputers. It supports pure (computational state vector) and mixed states (density matrices) to reproduce the effects of noise and decoherence⁹¹⁷.



Intel is a key contender in the race for silicon qubits. They started working on superconducting qubits but it seems it was a secondary route for them. They started with producing a wafer with 26 qubit chipsets in 2017 and made some progress since they, although it is rather hard to evaluate.

Intel's quantum work is managed under the direction of **Anne Matsuura**⁹¹⁸ and **James Clarke** for hardware.

In June 2018, Intel made another announcement with a highly integrated chip using SiMOS qubits, with 1500 qubits, fabricated in the D1D fab located in Portland, Oregon, with an etch density of 50 nm, six times greater than the early 2018 generation.

But this chipset, like many that did follow, were produced to test their manufacturing capacity and their material designs. They were not functional particularly with regards to two-qubit gates. In 2022, Intel did show again some interesting data related to their qubits manufacturing capacity, producing chipsets with 3 to 55 quantum dots on 300 mm wafers and a >95% production yield, using 193 nm Deep UV immersion photolithography instead of electron beam lithography⁹¹⁹. These SiGe qubits have a relaxation time of >1s (T_1), coherence times of >3 ms (T_2) and single qubit gates of >99% (and no published data for two-qubit gates...). These qubits are to be characterized by the DoE Argonne lab in Chicago in its Q-NEXT research center⁹²⁰.

⁹¹⁴ See [Integrated multiplexed microwave readout of silicon quantum dots in a cryogenic CMOS chip](#) by A. Ruffino, January 2021 (14 pages).

⁹¹⁵ See [Spin Readout of a CMOS Quantum Dot by Gate Reflectometry and Spin-Dependent Tunneling](#), by Virginia N. Ciriano-Tejel, Maud Vinet, John Morton et al, 2021 (18 pages). This followed [Remote capacitive sensing in two-dimensional quantum-dot arrays](#) by Jingyu Duan, Michael A. Fogarty, James Williams, Louis Hutin, Maud Vinet and John J. L. Morton, 2020 (31 pages) which described the coupling technique using silicon nanowires (SiNW) to measure qubits spins with remote capacitive charge sensing.

⁹¹⁶ See [Silicon edge-dot architecture for quantum computing with global control and integrated trimming](#) by Michael A. Fogarty, August 2022 (13 pages).

⁹¹⁷ See [QuEST and High Performance Simulation of Quantum Computers](#) by Tyson Jones et al, December 2018 (8 pages).

⁹¹⁸ See [Intel's quantum efforts tied to next-gen materials applications](#), January 2019 and [Intel's spin on qubits and quantum manufacturability](#), both from Nicole Hemsath, November 2018 and [Leading the evolution of compute](#), Anne Matsuura, June 2018 (26 slides).

⁹¹⁹ See [Qubits made by advanced semiconductor manufacturing](#) by A.M.J. Zwerver, Menno Veldhorst, L.M.K. Vandersypen, James Clarke et al, 2021 (23 pages).

⁹²⁰ See [Intel to install quantum computing test bed for Q-NEXT](#), April 2022.

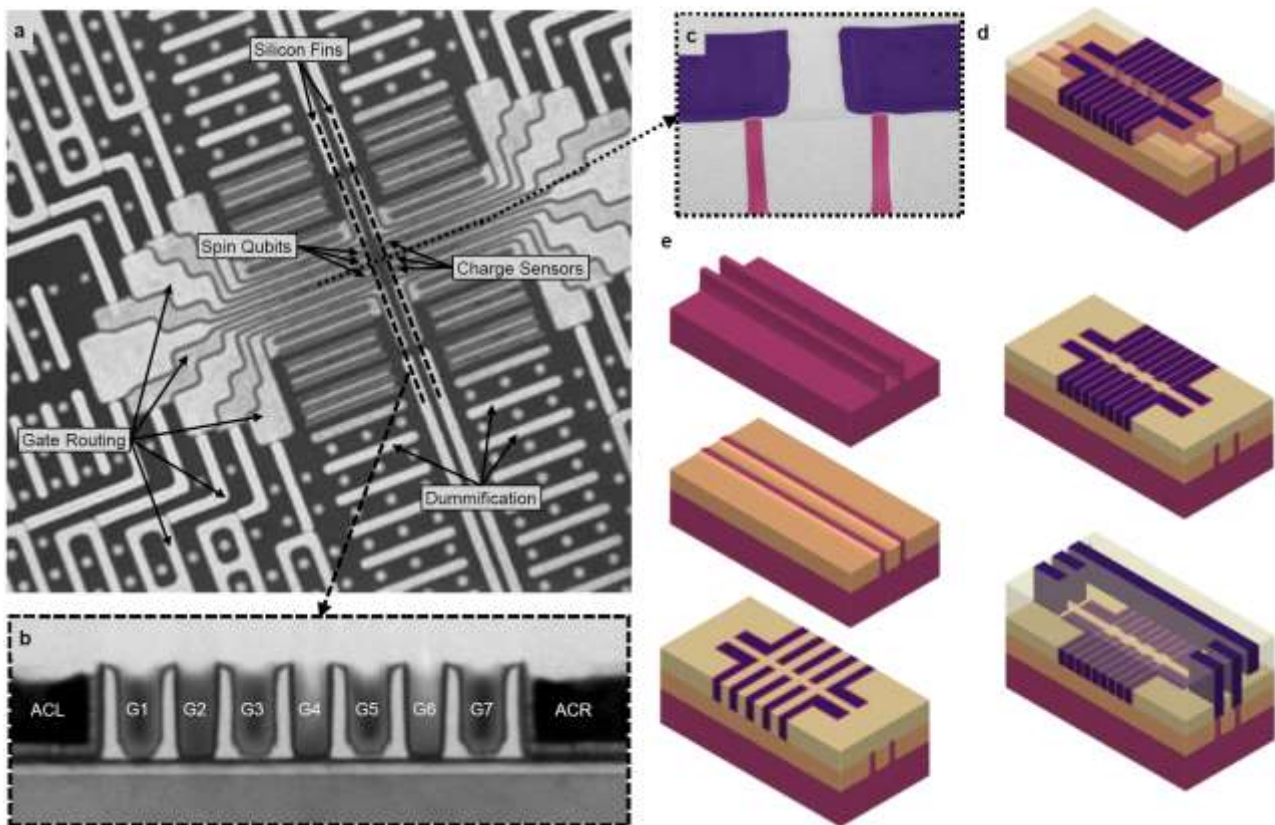


Figure 348: Intel SiGe quantum dots circuit implementation and process quality. Source: [Qubits made by advanced semiconductor manufacturing](#) by A.M.J. Zwerver, Menno Veldhorst, L.M.K. Vandersypen, James Clarke et al, 2021 (23 pages).

As part of their efforts in manufacturing, they are now using, like CEA-Leti, a cryo-wafer prober provided by Afore and Bluefors, that enables testing entire wafers at 1.6K, significantly accelerating the testing and characterization process (on the left, below).



Figure 349: how Intel is saving time with a Bluefors/a-Fore cryo-prober. Source: Intel.

QuTech and Intel work well together on these qubits. QuTech got a \$50M investment from Intel in 2015 to explore it. Intel announced in 2018 that it had succeeded in controlling a two-qubit SiMOS processor with single and two quantum gates running Deutsch-Jozsa and Grover algorithms on a very small scale. These silicon-germanium qubits manufactured by Intel were tested by the Vandersypen Laboratory at the University of Delft, part of QuTech⁹²¹. Since 2018, Intel has kept a rather low profile on its silicon qubit advances⁹²².

⁹²¹ See [A programmable two-qubit quantum processor in silicon](#) by T F Watson et al, TU Delft, May 2018 (22 pages).

⁹²² See [What Intel Is Planning for The Future of Quantum Computing: Hot Qubits, Cold Control Chips, and Rapid Testing](#) by Samuel Moore, August 2020, which provides a rather pedagogical overview of Intel's approach to silicon qubits.

At the beginning of 2020, Intel announced that it had developed with QuTech the **HorseRidge** cryo-component. It is a CMOS component operating at 4K that is used to generate the microwaves used to drive both superconducting and silicon qubits. A second version was announced in 2021. We cover it in the section dedicated to cryo-CMOS electronics.

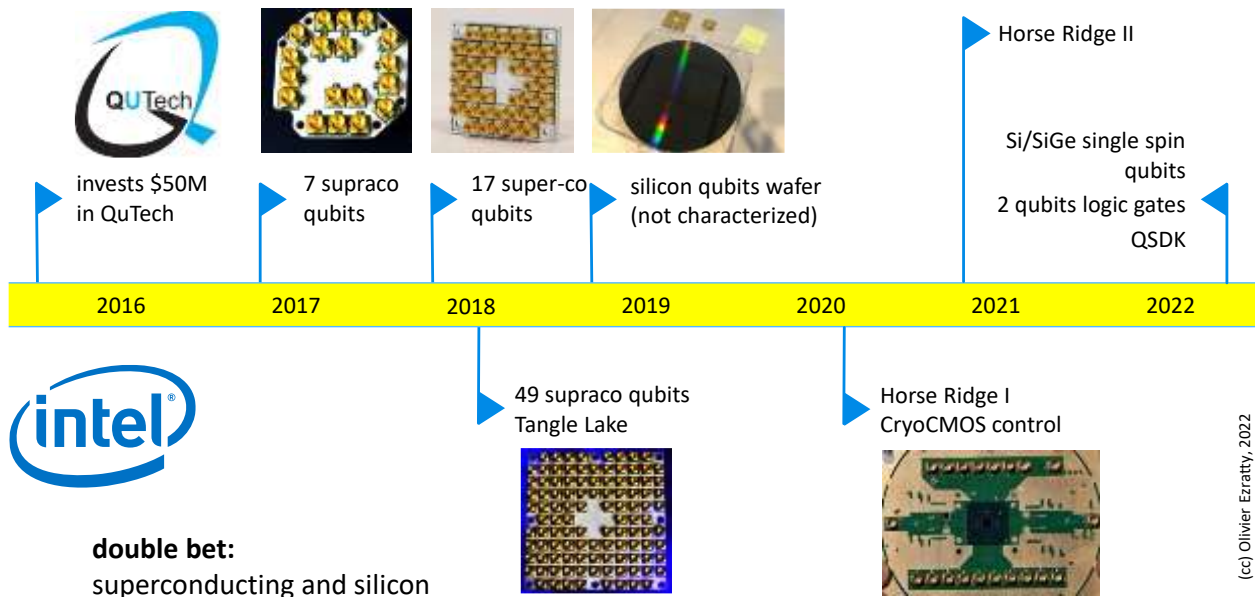


Figure 350: Intel quantum computing timeline. (cc) Olivier Ezratty, 2022.

equal1.labs (2017, Ireland/USA, 6M€) is creating a charge electron spin qubits chipset manufactured in 22 nm FD-SOI technology at GlobalFoundries in Dresden, Germany.

They announced in 2021 a 422 qubits test chipset embedded in a full-rack system with its cryogeny, Alice mk1. At this stage, they are just able to inject single electrons in their quantum dots and simulate numerically some one- and two-qubit quantum gates, but not much more⁹²³. Their next generation Aquarius is to fit in a desktop packaging, planned for 2022, and is to house one million qubits. They position their systems to run quantum neural networks for imaging applications.

In May 2021, equal1 uncovered a prototype chipset operating at 3.7K and including 10 million transistors handling qubits controls and readout with arbitrary waves generation (AWGs), all coupled to an external FPGA, as well as some classical cryogenic memory. There's a caveat with their coherence time being only 150 ns. Equal1 also designs its own cryogenic system.

The company was created by Dirk Leipold, Mike Asker and Bogdan Staszewski from the University of Dublin. Elena Blokhina is their CTO and expect to raise \$50M by 2022.

EeroQ Quantum Hardware (2016, USA, \$7.5M) develops an exotic quantum processor using trapped (and more or less flying/moving) electrons on superfluid helium ("eHe"). The startup was created by Johannes Pollanen from the University of Michigan (CSO), Dave Ferguson, Nick Farina (CEO) and Faye Wattleton (EVP)⁹²⁴.

⁹²³ See [A Single-Electron Injection Device for CMOS Charge Qubits Implemented in 22-nm FD-SOI](#) by Imran Bashir, Elena Blokhina et al, 2020 (4 pages).

⁹²⁴ See [Helium surface fluctuations investigated with superconducting coplanar waveguide resonator](#) by N.R. Beysengulov, Johannes. Pollanen et al, 2022 (10 pages). It deals with a superconducting resonator and not with a qubit.

In May 2021, they appointed Princeton University Professor Steve Lyon as CTO. It has benefited from US public (NSF) and private funding. Johannes Pollanen's bio indicates that he conducted research in superconducting and two-dimensional qubits (silicon, graphene)⁹²⁵.

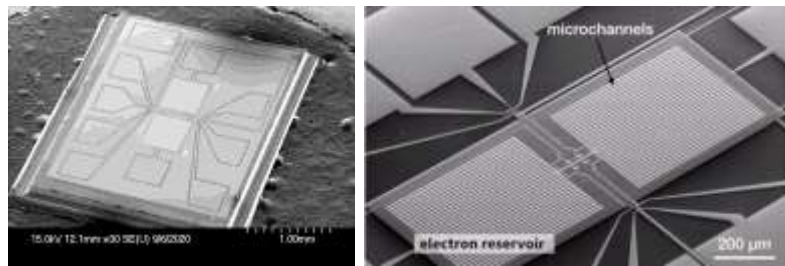


Figure 351: EeroQ silicon qubit prototype processor. Source: EeroQ.

They want to associate the long coherence and high connectivity of trapped ions and the fast gates of electron spin and superconducting qubits. The chipset is built using CMOS technology and electrodes driving electron spins. It is probably complicated to tune given we've not heard from them for a while, with any functional and programmable system. They still got an undisclosed investment from VCapital in 2022.

C12

C12 Quantum Electronics (2020, France, \$10M) was launched by Matthieu Desjardins and his twin brother Pierre. It is a project originating from the LPENS at ENS Paris and 15 years of research from Takis Kontos in this lab, with contributions from Jérémie Vienot at Institut Néel Grenoble.

french startup created by Matthieu and Pierre Desjardins

with the help from Taki Kontos (LPENS)

electron spins qubits trapped in carbon nanotubes

5 qubits demonstrator planned for 2021/2022

qubits are based on a **single electron spin** isolated in a 2 nm diameter carbon nanotube

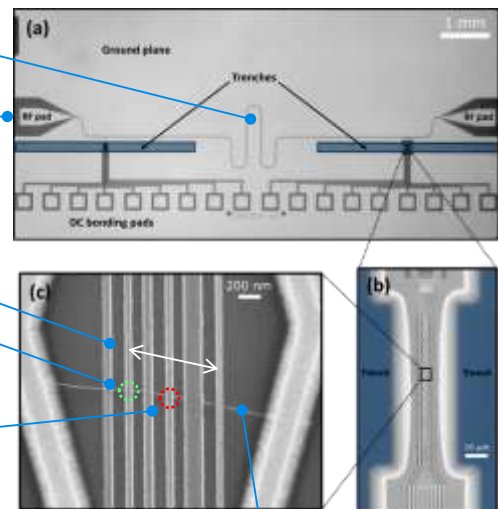


multiple spins can be coupled for **2-qubit gate** to the same resonator enabling all-to-all connectivity between qubit

spin qubit manipulated and read-out with a **7 GHz microwave** superconducting resonator

electrons move in **one direction** it can be trapped in a **quantum dot** by defining an electrostatic potential with underneath control electrodes.

coupling to the resonator can be switched on and off by freezing the motion of electron in one of the two quantum dots.



decoherence is limited with using **zero spin isotope C₁₂** in nanotubes, suspending the tube above the substrate and removing the oxide

Figure 352: C12 Quantum Electronics carbon nanotubes and how it is controlled. Source: C12.

Their goal is to use carbon nanotubes to trap electrons used in electron spin qubits and build the surrounding control circuitry on silicon substrate. This technology can improve qubits isolation and coherence time by a factor of 100, up to one second, while keeping a strong coupling for fast qubit manipulation. The qubits are controlled by spin-photon coupling in the microwave regime, using frequency multiplexing to avoid crosstalk.

Qubit readout uses spin to charge coupling with a single charge coupling with 8 qubits⁹²⁶. The challenges sit in materials, design, control electronics, connectivity, topology and error correction codes.

⁹²⁵ See [Integrating superfluids with superconducting qubit systems](#) by Johannes Pollanen et al, 2019 (11 pages).

⁹²⁶ A related technique is described in [Charge Detection in an Array of CMOS Quantum Dots](#) by Emmanuel Chanrion, Pierre-André Mortemousque, Louis Hutin, Silvano de Franceschi, Franck Balestro, Maud Vinet, Tristan Meunier, Matias Urdampilleta et al, Grenoble CEA-LETI, CNRS Institut Néel and UGA, August 2020 (8 pages).

The nanotubes are mechanically integrated into the circuit at the end of the manufacturing process⁹²⁷. The carbon nanotubes are grown by C12 using a CVD process (chemical vapor deposition). The connection between two qubits is based on microwave cavities, exploiting QEDC (Quantum Electrodynamic Cavity). Of course, there are still many challenges to develop this kind of qubits but it is worth exploring. It could even have some use cases beyond computing, in quantum sensing. In March 2022, C12 announced it was starting a manufacturing partnership with CEA-Leti. These will provide their quantum chips on silicon on 200 mm wafers. These will contain the superconducting electronics controlling the state of their carbon nanotubes that will be positioned on the chipsets.

On the software engineering side, Atos works with C12 to develop its quantum compiler, to create digital simulation models of its qubits and for co-designing quantum gates.



Archer Materials (2017, Australia) develops quantum computing and sensing technologies based on carbon nanospheres that operate at room temperature⁹²⁸.

The company was cofounded by Mohammad Choucair who invented their ¹²CQ chipset design and by Martin Fuechsle who contributed to the development of the single electron transistor and worked at UNSW with Michelle Simmons⁹²⁹. The 12 is not a number of qubits but the isotopic weight of the zero spin carbon atoms used in these nanospheres trapping some electron and its spin. Electrons are delocalized around the nanosphere and not setting inside it, contrarily to the C12 Quantum Electronics electrons that are stored inside nanotubes.

They built their first three-nanospheres chipset in 2019, in red, in the picture, the 50 nm nanospheres being surrounded by driving electrodes, but without any visible coupling between these qubits. In February 2021, Archer announced that they had achieved “electronic transport” in a single qubit at room temperature in its ¹²CQ quantum computing qubit processor chip.



Figure 353: Archer qubits.
Source: Archer.



Figure 354: Archer-EPFL spin-resonance circuit. Source: Archer.

It however does not mean that it is a fully functional qubit that can be operated with quantum gates⁹³⁰. In July 2021, they announced that they were embedding some parts of their qubits control electronics in the qubit chipset, that records the Continuous Wave Electron Spin Resonance (cwESR) signals generated by a superconducting on-chip resonator.

In February 2022, through a collaboration with EPFL, they demonstrated the use of a single-chip integrated electron spin resonance (ESR, seemingly at 9.4 GHz according to their patent) detector based on high electron mobility transistor (HEMT) to detect and characterize their qubit at room

⁹²⁷ It is described in [Nanoassembly technique of carbon nanotubes for hybrid circuit-QED](#) by Tino Cubaynes, Matthieu Desjardin, Audrey Cottet, Taki Kontos et al, September 2021 (6 pages).

⁹²⁸ See [Archer Materials granted trading halt ahead of quantum computing chip agreement](#) by Quantum Analyst, 2020 and [Room temperature manipulation of long lifetime spins in metallic-like carbon nanospheres](#) by Bálint Náfrádi, Mohammad Choucair et al, 2016 (32 pages) which describes in detail this technique of electron spin trapping in a 35 nm wide carbon nanosphere. In April 2021, Archer Materials announced it would sell off all its mineral traditional business to iTech Minerals, to focus on quantum technologies.

⁹²⁹ Their ¹²CQ processor is patented in the USA, Japan and Europe (since February 2022). See [WO2017091870 - A QUANTUM ELECTRONIC DEVICE](#) (55 pages). The patent dates from 2017 and is very sketchy with regards to single and multiple qubit gates operations. We can still learn they use SiO₂ isolation layers of 200 to 400 nm between control electrodes and nanospheres. Conductors can use unspecified graphene structures. The spin stability in their device is amazingly small, at around 115 ns, not sufficient to run several quantum gates.

⁹³⁰ Their electron spin T₁/T₂ is very low, at 175 ns at 27°C. They also said they tested microwave pulses from 4 GHz to 420 GHz. Seen in their video [Archer's Quantum Computing Q&A Webinar](#), April 2020.

temperature⁹³¹. The resonator was manufactured by OMMIC (France), a fab company specialized in III-V wafer processes. This technology is as mature as superconducting qubits were in the mid 1990's when it became possible to create the first qubits.

What would be needed are some tomographies for their qubit state, showing real superposition, and a full cycle of reset, flip and phase single qubit quantum gates and qubit readout, then implement this with a couple entangled qubits. One can wonder how they will drive their qubits with microwave pulses at room temperature given the ambient thermal noise will be larger than the pulse themselves. The road ahead is still quite long for them. Based on this 2022 milestone, the company CEO forecasted “*mobile quantum computing*” use-cases. That is quite an oversold proposal. It deserves scrutiny, if not strong skepticism.

In December 2020, Archer launched a partnership with **Max Kelsen**, another Australian company, specialized in QML software development. Max Kelsen and Archer will develop QML algorithms based on Qiskit, eyeing a future execution on Archer's processor. They also announce that Global-Foundries would become the manufacturer of their 12Q qubit chipset.

The company is also developing graphene-based biosensor chip aka “lab on chip”. This is a more short-term and credible product proposal than their room temperature spin qubits.



Qpi (2019, India) is a QML software and hardware development company, providing the QpiAI library. They are working on creating the ASGP (AI System Generating Processor), a hybrid classical-quantum compute chip.

Practically speaking, they planned first to introduce a qubit control chip in September 2021 operating at 4K and produced in a 22 nm TSMC CMOS process⁹³². This chipset was to control the microwaves sent to both superconducting and electron spin qubits processors. They later announced a room temperature control chipset named QpiAISense. They are now developing a full-stack classical and silicon qubit solution in a single package. It is supposed to contain a classical chip for optimization (ASGP for “AI System Generating Processor”), their microwaves cryogenic control chip and a silicon spin-qubit based QPU (quantum processing unit). They signed a partnership with QuantrolOx in April 2022 to develop their QPU and set-up a lab in Finland for that purpose, where part of QuantrolOx team is installed. Their goal is to start with releasing a functional 25 qubits system. They plan later to create a one million electron spin quantum dots qubits processor. Overselling seems not to be an issue for them. QpiAI Tech is a subsidiary selling software services for quantum computing and AI to transportation, materials, manufacturing, finance, and pharmaceutical business.

NV centers qubits

This qubit technology is based on the control of electron spins trapped in artificial defects of crystalline carbon structures in which one carbon atom is replaced by one nitrogen atom and another carbon atom is replaced by a void, gap or cavity. Practically speaking, it's a bit more complex since the qubits themselves are stored in nuclear spins of surrounding carbon and nitrogen atoms⁹³³.

History

Defects in diamonds have been studied from 1930 with the examination of infrared absorption. This made it possible to distinguish two categories of diamonds: type I with an absorption band of 8 μm in the infrared and type II without this band. The defects explain the color of diamond gems.

⁹³¹ See [Quantum information detected using mobile compatible chip technology](#), Archer Materials, February 2022.

⁹³² Source: [QpiAI in Partnership With IISc Launches Joint Certification for AI and Quantum Computing to Upskill Enterprises, Schools and Colleges](#), March 2021.

⁹³³ See the review paper [Diamond Integrated Quantum Photonics: A Review](#) by Prasoon K. Shandilya et al, July 2022 (31 pages) which provides a good 360° overview of NV centers, and not only for quantum computing.

It was not until 1959 that these impurities were found to be related to the presence of nitrogen, at 7.8 μm and that nitrogen atoms were well isolated in the diamond crystal. In 1975, it was discovered that some heat treatment could control the diffusion of nitrogen atoms in the diamond. These nitrogen centers explain the diamond color. It has four types: one nitrogen atom isolated in a gap, two nitrogen atoms, three nitrogen atoms surrounding a gap and four nitrogen atoms.

It is the first type that is interesting for both quantum computing and quantum sensing. We can visualize these defects with a confocal microscope (having a very shallow depth of field) by illuminating them with a green laser beam that will generate some red light.

These NV centers diamonds are slightly pink. These properties make it possible to generate single-photon sources thanks to the isolation of a NV center.

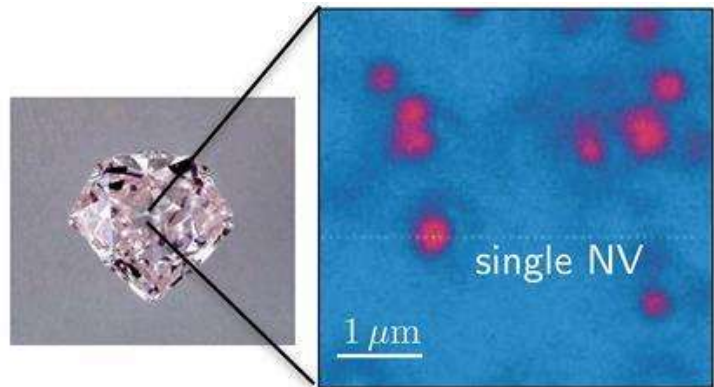


Figure 355: how NV center cavities look in real diamonds. Source: TBD.

Nitrogen-rich artificial diamonds are used to manufacture these NV centers. Gaps are generated with irradiation.

Vacuum annealing at about 800°C-900°C moves the vacancies next to the nitrogen atoms in the crystal structure⁹³⁴. This is explained by nitrogen atoms being as large as carbon atoms. The gap creates a small bar of electrons that serve as a virtual magnet via their spin.



Figure 356: how are nitrogen vacancies created. Source: [NV Diamond Centers from Material to Applications](#) by Jean-François Roch, 2015 (52 slides).

Diamonds can also be produced at NV centers with vacuum deposition of hydrogen and methane (CVD, for Chemical Vapor Deposition) to create a perfect diamond crystal structure and then with ion implantation with nitrogen ion beams⁹³⁵.

⁹³⁴ See [NV Diamond Centers from Material to Applications](#) by Jean-François Roch, 2015 (52 slides) for an historical view of NV centers and a thesis that describes the different techniques of NV centers creation in [Engineering of NV color centers in diamond for their applications in quantum information and magnetometry](#), Margarita Lesik, 2015 (139 pages).

⁹³⁵ See a description of this manufacturing process in [CVD diamond single crystals with NV centres: a review of material synthesis and technology for quantum sensing applications](#) by Jocelyn Achard, Vincent Jacques and Alexandre Tallaire, 2019 (41 pages).

The carbon structure surrounding a NV center protects the cavity area well. The state of the gap is unstable and quantum. It is excited by lasers and microwaves. The reading of the qubit state is performed by a fluorescence brightness measurement.

Science

The cavity contains a free electron that is generated by an electrical voltage applied to an n-p junction obtained by doping the diamond. The free electron is coupled to another one from the nitrogen atom near the cavity. The cavity includes two other pairs of electrons from the nitrogen atom in the cavity, with a total zero spin.

The process involves controlling the collective spin of these two free electrons as well as the spin of the nitrogen nucleus of the cavity and possibly of the neighboring ^{13}C carbon atoms⁹³⁶. The cumulative spin of the two electrons of the cavity is 0, 1 or -1 because it adds the spins of two electrons that are either $\frac{1}{2}$ or $-\frac{1}{2}$. These electron spins are controlled by a combination of microwave and magnetic field.

Commonly used NV centers are called NV^- because of the addition of an external electron into the cavity. The cavity has 6 electrons, three from the surrounding carbons, two from the nitrogen valence shell and one captured from the bulk. There are other variations like vacancies without this captured electrons (NV^0), or with missing electrons (NV^{+1} , NV^{+2}) that are not commonly used.

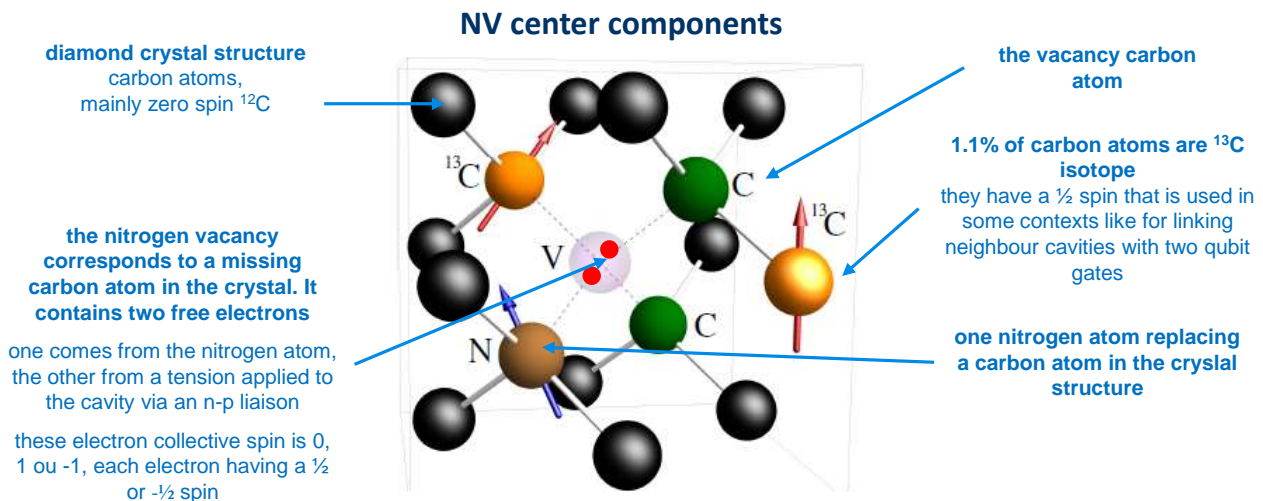


Figure 357: the nitrogen vacancy contains two free electrons. Their spin is controlled as well as nuclear spins from surrounding ^{13}C and nitrogen atoms. (cc) Olivier Ezratty, 2021, image source TBD.

Below is a diagram that describes what a NV center can look like in practice considering that there are many different implementations, knowing that NV centers are used not only for computing but, in a dominant manner, in quantum sensing. NV centers can be integrated in circuits fabricated on an SOI silicon wafer with a layer of SiO_2 insulator. It is covered with a matrix Fresnel lens, used to focus a control and readout laser⁹³⁷. It is frequently associated with other photonics components when the NV center spins are used to generate photons for quantum communications⁹³⁸.

⁹³⁶ Approximately 1.1% of the carbon atoms in diamond are of the ^{13}C isotope. The most common isotope is ^{12}C . ^{14}C is present in trace amounts and is used to date carbonaceous objects due to its half-life of 5730 years. See [Coherent control of an NV- center with one adjacent \$^{13}\text{C}\$](#) by Burkhard Scharfenberger et al, 2014 (24 pages).

⁹³⁷ See [Spin Readout Techniques of the Nitrogen-Vacancy Center in Diamond](#) by David Hoper et al, 2018 (30 pages).

⁹³⁸ See [Hybrid Quantum Nanophotonics: Interfacing Color Center in Nanodiamonds with \$\text{Si}_3\text{N}_4\$ -Photonics](#) by Alexander Kubanek et al, July 2022 (55 pages) that describes such hybrid nanophotonic circuits.

NV center implementation and controls

microlens focusing a laser beam for qubits control and readout in the cavity

the lens base contains light guide that are one fourth micron large

images source: Spin Readout Techniques of the Nitrogen-Vacancy Center in Diamond par David Hoper & Al, 2018 (30 pages).

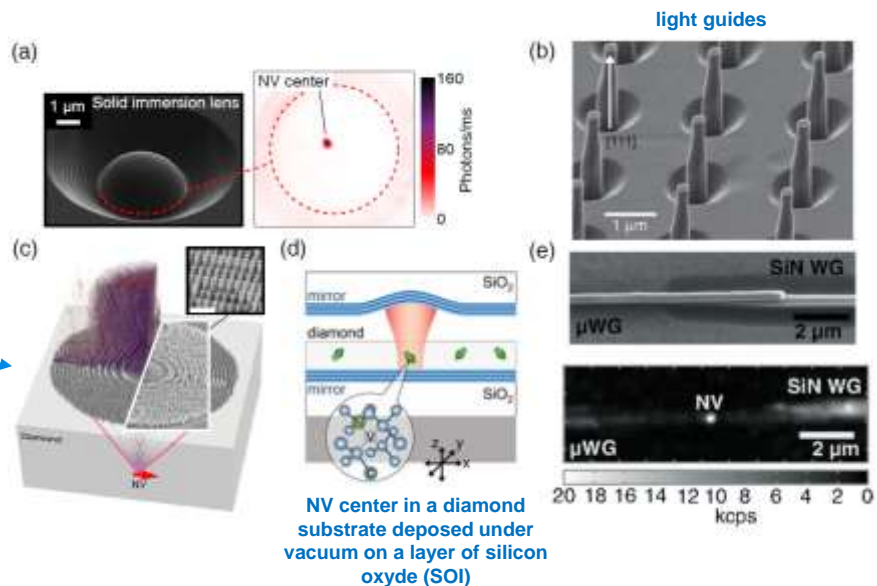


Figure 358: examples of NV centers implementation and controls to guide laser light on the cavities. Source: [Spin Readout Techniques of the Nitrogen-Vacancy Center in Diamond](#) by David Hoper et al, 2018 (30 pages).

Next is a diagram explaining how these rather complex qubits operate with the various energy levels and transitions of the cavity and its free electrons using microwaves and green photons. The vertical arrows represent useful energy transitions⁹³⁹. This is applicable to the NV^- species.

The vacancy qubit state is controlled with 2.87 GHz microwaves that change the spin state of the vacancy electrons and switches the vacancy state between $|0\rangle$ and $|1\rangle$. The degeneracy of the spins 1 and -1 at the 3A level (meaning: same energy level for different quantum properties) is removed with exposing the qubit to a static magnetic field. Other techniques are used to change the qubit state of the surrounding ^{13}C and ^{14}N nucleus spins.

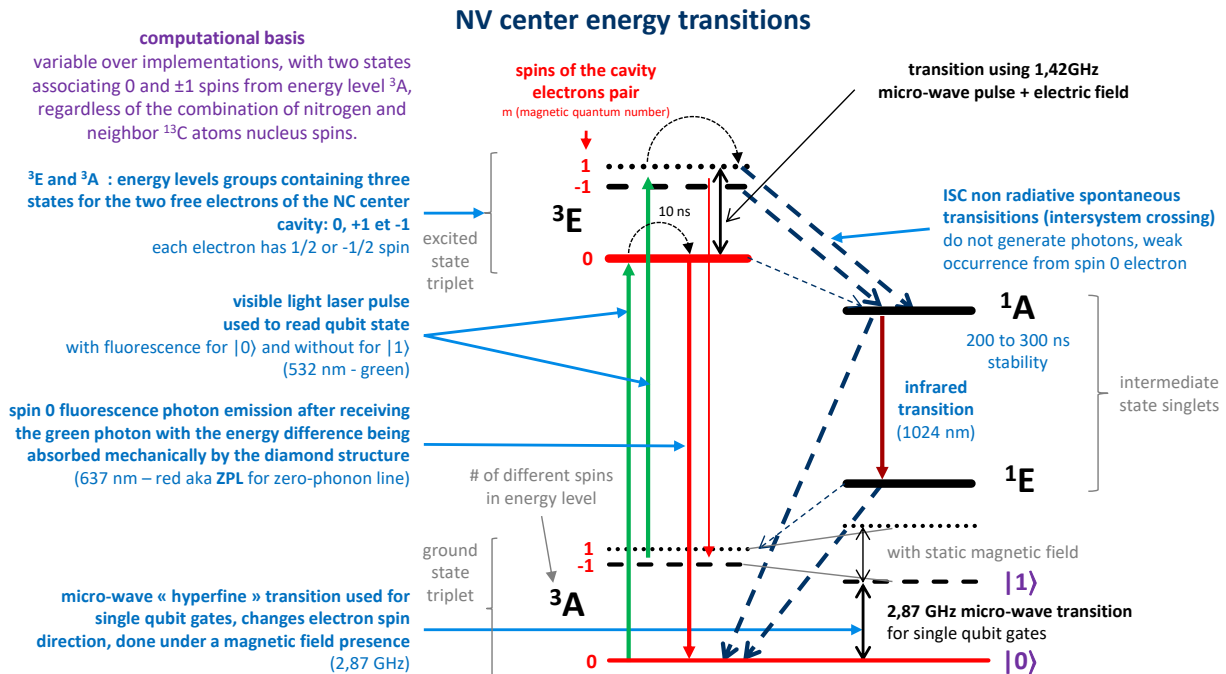


Figure 359: energy transitions in an NV center. (cc) compilation by Olivier Ezratty, 2022.

⁹³⁹ See the excellent review paper [Quantum computer based on color centers in diamond](#) by Sebastien Pezzagna and Jan Meijer, May 2020 (17 pages).

For qubit readout, an incoming green photon, usually at 532 nm, from a laser generates two possible outcomes:

- For $|0\rangle$ at a zero spin, a change of state to 3E which then degenerates via the 1A state into a spontaneous non-radiative transition which does not emit a photon but transmits some mechanical energy to the crystal structure and returns to the basic state $|0\rangle$. This happens when the related electron has a zero spin.
- For $|1\rangle$ at a non-zero-spin, an emission of a fluorescence 637 nm red photon, part of the energy being also mechanically absorbed by the diamond structure. There is still a residual red photon emission, that creates some qubit readout noise.

NV centers qubits operate theoretically at room temperature⁹⁴⁰. Recent experiments have reached a $400 \mu\text{s } T_1$ at ambient temperature⁹⁴¹.

NV centers have a too low DWF of 3%. This Debye-Waller factor which is measured by the ratio between the ZPL (zero-phonon lines) red emission and the total ZPL plus the phonon sideband emission (PSB). The ZPL is the sharp zero-phonon lines of luminescence of NV center in the visible spectrum that is of interest.

The phonon sideband is a thermal effect that is problematic⁹⁴². Also, the DWF gets improved with low operating temperatures. This reduces qubit readout errors and explains why, on practice, a temperature of 4K is frequently used⁹⁴³! Another reason is that at low temperature, the spectral lines of the different energy states of the cavity are different, better spaced and easier to distinguish⁹⁴⁴.

A joint QuTech-Fujitsu-Element Six team demonstrated in 2022 a fault-tolerant operation of a NV centers based QPU with logical qubits made of 5 physical spin qubits and two additional measurement qubits in a 29-qubit QPU running at 10K⁹⁴⁵.

As shown in Figure 361 in page 370, the configuration was using different qubits: the NV center cavity was used as an auxiliary qubit with its two electrons, then the nuclear spin of the nearby nitrogen and five nuclear spins of ^{13}C were used for one flag and five data qubits.

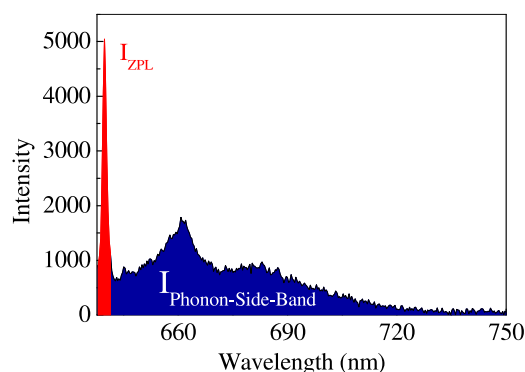


Figure 360: visualizing a ZPL and phonon-side-band. Source: [Suppression of fluorescence phonon sideband from nitrogen vacancy centers in diamond nanocrystals by substrate effect](#) by Hong-Quan Zhao et al, Hokkaido and Osaka Universities, Japan, Optics Express, 2012 (8 pages).

⁹⁴⁰ See [A programmable two-qubit solid-state quantum processor under ambient conditions](#) by Yang Wu of Hefei's USTC in China, 2018 (5 pages). He describes an NV center managing two qubits at ambient temperature exploiting the cavity electron spin and the associated nitrogen atom nucleus spin. See also the review paper [Quantum information processing with nitrogen-vacancy centers in diamond](#) by Gang-Qin Liu et al, 2018 (15 pages).

⁹⁴¹ See [Success in mass production technology for ultra-high-purity 2-inch diamond wafer; expected to spur realization of quantum computing](#), August 2022 and [Long spin coherence times of nitrogen vacancy centers in milled nanodiamonds](#) by B. D. Wood et al, PRB, May 2022 (11 pages).

⁹⁴² See [Suppression of fluorescence phonon sideband from nitrogen vacancy centers in diamond nanocrystals by substrate effect](#) by Hong-Quan Zhao et al, Hokkaido and Osaka Universities, Japan, Optics Express, 2012 (8 pages).

⁹⁴³ The technique is documented in [Quantum information processing with nitrogen vacancy centers in diamond](#) by Gang-Qin Liu and Xin-Yu Pan, 2018 (15 pages) and in [Diamond NV centers for quantum computing and quantum networks](#) by Lilian Childress and Ronald Hanson, 2017 (5 pages).

⁹⁴⁴ This interdependence between hyperfine spectral lines and temperature is not unique to diamond cavities. They are common in crystalline structures because temperature modifies many parameters such as the relative arrangement of the atoms in the crystals which leads to changes in electrical and magnetic gradients and therefore spins, etc.

⁹⁴⁵ See [QuTech and Fujitsu realise the fault-tolerant operation of a qubit](#) by QuTech, May 2022 and [Fault-tolerant operation of a logical qubit in a diamond quantum processor](#) by M. H. Abobeih et al, May 2022 (11 pages).

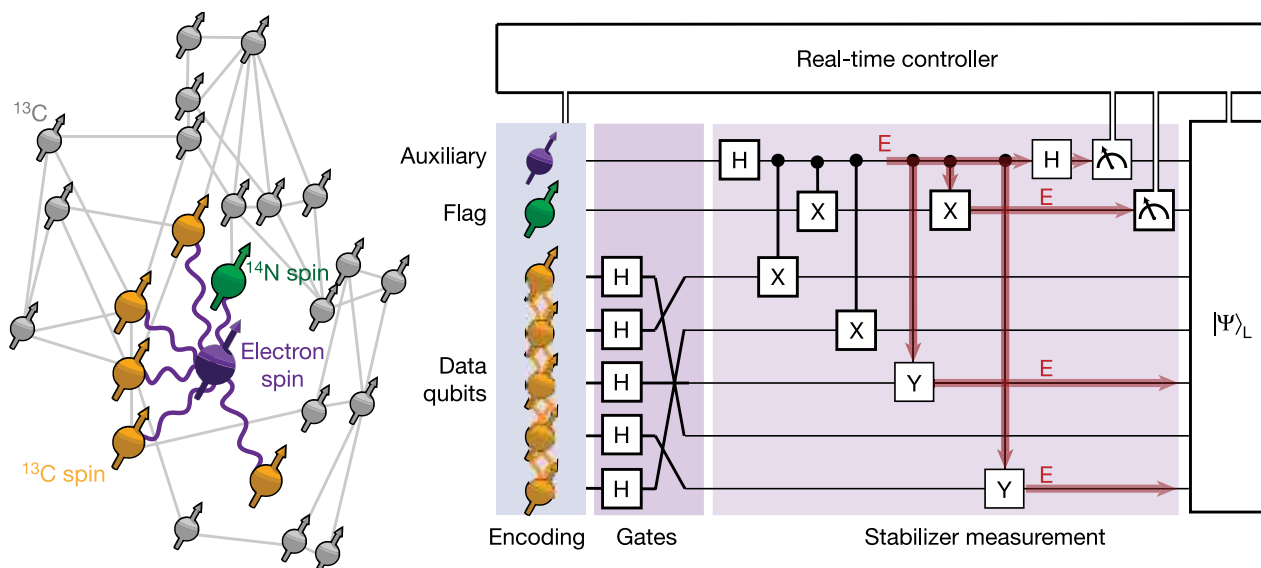


Figure 361: an error correction code implemented with NV centers qubits. Source: [Fault-tolerant operation of a logical qubit in a diamond quantum processor](#) by M. H. Abobeih et al, May 2022 (11 pages).

Another team, in Japan, implemented a similar error correction code with a Shor-3 codes using 6 qubits⁹⁴⁶.

Qubit operations

The general principle of operation for these qubits is as follows⁹⁴⁷:

- **Qubit quantum state** is based on a two-state computational basis, with $|0\rangle$ corresponding to the 3A energy zero spin base level and $|1\rangle$ to the same level but with a non-zero spin. The computational basis is sometimes $|+1\rangle$ and $|-1\rangle$ corresponding to the two non-zero spin levels of the 3A basis. Most techniques use the neighboring ^{13}C and ^{14}N atoms nuclear spins as qubits and are arranged in clusters. The NV center electrons spin is used as a mediator to control the neighbor atomic spins.
- **Single-qubit quantum gates** are microwave-activated and exploit hyperfine energy transitions at a frequency of 2.87 GHz⁹⁴⁸. These transitions work together with a magnetic field for zone A and an electric field for zone E.
- **Two-qubit quantum gates** use different methods: coupling NV centers with entangled photons which doesn't work well, magnetic coupling, or with coupling the NV center with the nucleus spin of neighboring ^{13}C and ^{14}N atoms with microwaves⁹⁴⁹. There are many variations of two-qubit gates like a CNOT⁹⁵⁰, a CZ or even a weird $\exp(i\pi S_z \otimes I_z)$ ⁹⁵¹.

⁹⁴⁶ See [Quantum error correction of spin quantum memories in diamond under a zero magnetic field](#) by Takaya Nakazato et al, Nature Communications Physics, April 2022 (7 pages).

⁹⁴⁷ I was initially inspired by a diagram from [lecture 3](#) of H el ene Perrin's course, February 2020. Then I integrated other sources of information. See in particular [The nitrogen-vacancy color center in diamond](#) by Marcus Doherty, Joerg Wrachtrup et al, 2013 (101 pages) which describes in particular the energy levels variations of NV centers as a function of their temperature.

⁹⁴⁸ As we have seen about trapped ions, hyperfine transitions are energetic transitions of low energy electrons, here in the microwave regime, which are generally related to the interaction between the magnetic polarities of the nucleus of the atoms with the magnetic field generated by the electrons. Knowing that here we are talking about electrons that do not rotate around the nucleus of an atom but in a cavity.

⁹⁴⁹ See some explanations in [Entanglement in NV centers](#) by Alexander Okupnik, Andrei Militaru and Ramon Gao, ETH Zurich, 2017 (34 slides).

⁹⁵⁰ See some detailed explanations in [Colour centers in diamond](#) by Joerg Wrachtrup, 2017 (36 slides).

⁹⁵¹ See [A programmable two-qubit solid-state quantum processor under ambient conditions](#) by Yang Wu et al, NPJ, 2019 (5 pages).

- Qubits readout** uses the capture of the fluorescence of the cavity activated by a laser and with an APD (avalanche photodiode) or a CCD sensor, similar to what is done with trapped ions and cold atoms. It consists in illuminating the cavity with a green (546 nm) laser. This excites level 3A in 3E but without changing the spin⁹⁵². The non-zero spin state 3E will generate a non-radiative transition passing through the 1A state. The null spin state 3E will generate the emission of a red photon (689 nm) which will be detected by the CCD sensor. This optical readout of single isolated qubits works only at low temperatures to avoid the creation of perturbation affecting neighbor qubits. The measurement of the cavity electron spin can exploit other techniques, each with their advantages and disadvantages: SCC (spin to charge conversion⁹⁵³), NMR (readout is assisted by the nucleus spin of neighboring atoms) and only by photonics means, knowing that lasers are used in all cases. Only a nuclear spin readout can be nondestructive (QND)⁹⁵⁴.

The technology is not easy to industrialize on a large scale, whether it is the chipset itself or the control lasers. In Figure 362 is a schematic diagram of the control mechanism for these qubits⁹⁵⁵.

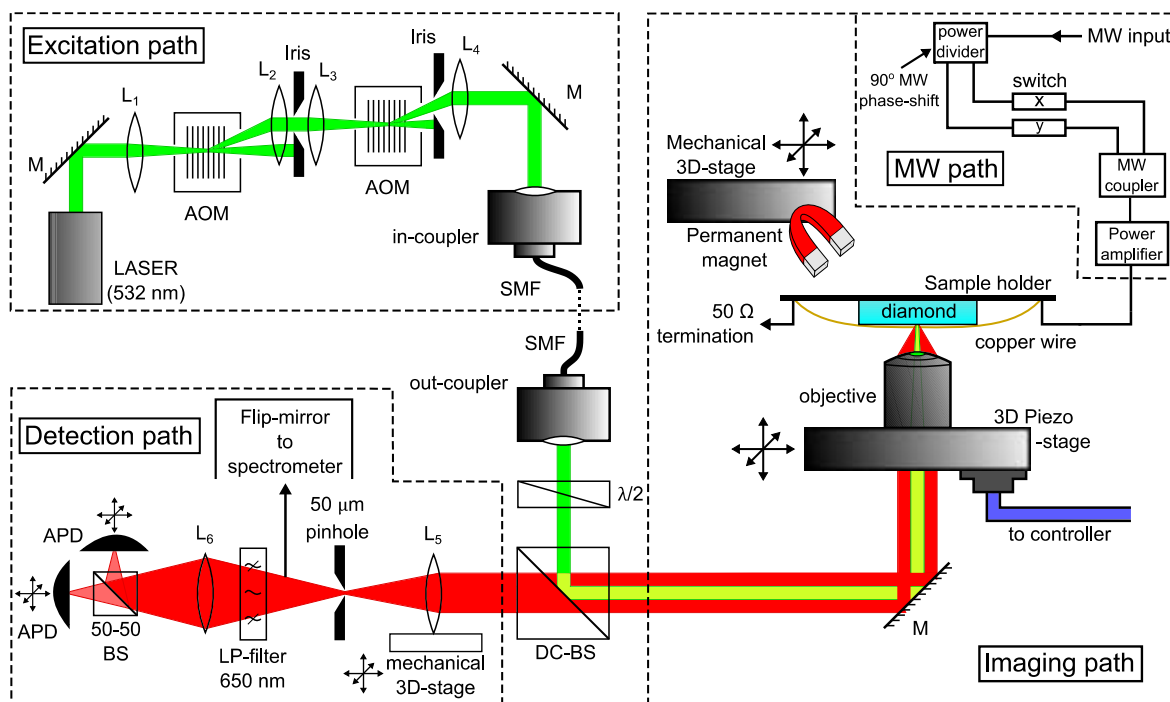


Figure A.1.: Schematic representation of the utilized setup for the characterization of NV centers. Experimental setup utilized for optical characterization and coherent spin manipulation of NV centers, comprising of a home-built confocal microscope, a scanning-stage for the imaging of diamond, and external magnet and microwave apparatus. The excitation wavelength is 532 nm. In the figure, mirrors are represented by M, lenses by L_i , single-mode optical fiber by SMF, beam-splitters by BS, and avalanche photo-diodes by APD.

Figure 362: characterization of NV centers setup. Source: [Forefront engineering of nitrogen-vacancy centers in diamond for quantum technologies](#) by Felipe Favaro de Oliveira, 2017 (235 pages).

⁹⁵² This technique is labelled ODMR for optically detected magnetic resonance.

⁹⁵³ Explained in detail in [Spin readout via spin-to-charge conversion in bulk diamond nitrogen-vacancy sets](#) by Harishankar Jayakumar, September 2018 (5 pages).

⁹⁵⁴ See [Color Centers in Diamond](#) by Andreas Wallraff, ETH Zurich, 2017 (34 slides).

⁹⁵⁵ Seen in [Forefront engineering of nitrogen-vacancy centers in diamond for quantum technologies](#) by Felipe Favaro de Oliveira, 2017 (235 pages).

Research

The main countries involved are China, the Netherlands (TU Delft and Qutech⁹⁵⁶), Australia (University of Melbourne, Quantum Brilliance), Germany (University of Ulm), Japan (NII and NTT), some laboratories in France (such as CEA SPEC) and of course in different labs in the USA.

NV centers qubits

- works at 4K, with simple cryogeny without dilution and helium 3.
- can also work at **ambient temperature**, with some limitations on entanglement.
- long **coherence time** > 1 ms.
- **strong and stable diamond structure**.
- can also help create **quantum memory** for other qubits types, like superconducting qubits.
- possible to integrate it with **optical quantum telecommunications**.

- only **two startup** in this field, Turing and Quantum Brilliance

TURING  QUANTUM BRILLIANCE

- **qubits controls complexity with lasers and microwaves** => not easy to scale.
- complexity of NV centers manufacturing.
- NV centers applications are more centered on quantum magnetometry and sensing than computing.

Figure 363: pros and cons of NV centers qubits. (cc) Olivier Ezratty, 2022.

One of the challenges of NV centers is their implantation in diamonds. One promising technique created by Berkeley Labs is using gold ions-based implantation that could scale to thousands of qubits. But this is just about fabrication and not functional qubits⁹⁵⁷.

NV Centers based quantum computers have been very low key for a few years.

Indeed, it seems that NV centers have more promising uses in quantum sensing for the creation of precision magnetometers or for quantum memories interoperable with qubits realized with other technologies such as superconducting qubits in hybrid systems. This is a path recently explored by the University of Delft⁹⁵⁸, in Japan⁹⁵⁹ and by CEA-SPEC with Patrice Bertet as shown in Figure 364, with a superconducting qubit linked to a NV center memory qubit.

There are also variants of NV center techniques with defects introduced in phosphorus-doped silicon carbide.

It would have the advantage of creating qubits whose readout is more accurate since being based on the emission of a narrow frequency fluorescence⁹⁶⁰.

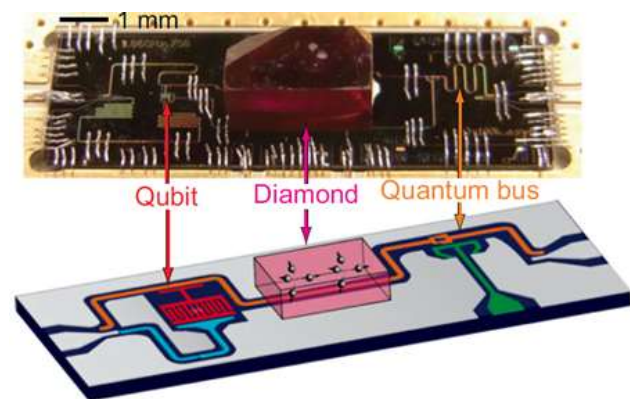


Figure 364: NV center used as a quantum memory for a superconducting qubit, which could lead to create heterogeneous qubits. Source [Quantum technologies with hybrid systems](#), Patrice Bertet et al, 2015 (8 pages).

⁹⁵⁶ Qutech demonstrated a 10-qubit prototype with a coherence time of one minute and working at 3.7K in 2019. See [Fully controllable and highly stable 10-qubit chip paves way for larger quantum processor](#), Qutech, 2019.

⁹⁵⁷ See [Ion-Trap Advance: Berkeley Lab Pioneers Way That Could Increase Scalability to Over 10,000 Qubits for Quantum Sensing, Quantum Computing](#) by Matt Swayne, May which refers to [Direct formation of nitrogen-vacancy centers in nitrogen doped diamond along the trajectories of swift heavy ions](#) by Russell E. Lake et al, March 2021 (5 pages).

⁹⁵⁸ See [Diamond-based 10-qubit register with coherence more than one minute](#), November 2019.

⁹⁵⁹ See [Coherent Coupling between a Superconducting Qubit and a Spin Ensemble](#) by Shiro Saito et al, 2012 (7 pages).

⁹⁶⁰ See [Study Takes Step Toward Mass-Producibile Quantum Computers](#), 2017.

In a similar fashion, MIT prototyped in 2020 a NV centers chipset replacing nitrogen with silicon and germanium. They assembled 128 qubits but these are not operational ⁹⁶¹. China researchers are also experimenting NV center qubits but so far, their prototype has only 3 qubits ⁹⁶². In another work, Australian researchers were able to implement single Clifford group qubit gates with NV⁻ centers with a fidelity of 99.3%⁹⁶³.

Manufacturing

Artificial diamonds are produced either with high-pressure high-temperature processes (HPHT) or with chemical vapor deposition (CVD)⁹⁶⁴. The latter is used for quantum use cases.

NV centers are manufactured with various methods of precise defects implantation. NV vacancies are usually produced by electrons, neutrons, protons or ions irradiation to create the vacancies followed by thermal annealing at temperatures above 650 °C to move the vacancies close to the defect atoms (here, nitrogen). A tiny share of nitrogen atoms impurities are deposited during the CVD (chemical vapor deposition) production of artificial diamond. One technique makes use of targeted ion depositions of ion beams with masking and ebeam lithography nanopatterning⁹⁶⁵.

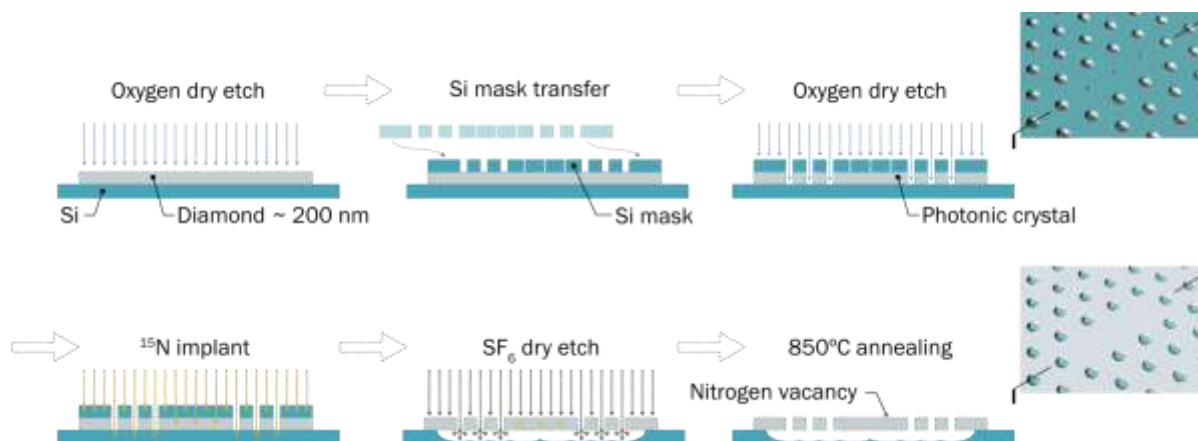


Figure 365: example of NV center implantation technique using a mask. Source: [Scalable fabrication of coupled NV center – photonic crystal cavity systems by self-aligned N ion implantation](#) by T. Schroder and A. Stein, May 2017 (13 pages).

Vendors

Quantum Brilliance (2019, Australia), **Turing Inc** (2016, USA) and **XeodQ** (2021, Germany) are the few companies dedicated to creating NV center-based quantum computers.



Quantum Brilliance (2019, Australia/Germany, \$29.4M) is developing a NV centers quantum processor that operates at room temperature, created by ANU (Australian National University) researchers, Andrew Horsley (CEO) and Marcus Doherty (CSO).

⁹⁶¹ See [Large-scale integration of artificial atoms in hybrid photonic circuits](#) by Noel H. Wan, Dirk Englund et al, MIT, UC Berkeley, Sandia Labs, Nature, 2020 (11 pages).

⁹⁶² See [Quantum anomaly detection of audio samples with a spin processor in diamond](#) by Zihua Chai et al, January 2022 (8 pages).

⁹⁶³ See [High Fidelity Control of a Nitrogen-Vacancy Spin Qubit at Room Temperature using the SMART Protocol](#) by Hyma H. Valabhapurapu et al, UNSW, August 2022 (7 pages). Clifford group gates are the simplest to implement and are not sufficient to create a universal gate set. It misses either a 3-qubit Toffoli gate or a T gate.

⁹⁶⁴ See the thesis [Engineering of NV color centers in diamond for their applications in quantum information and magnetometry](#) by Margarita Lesik, 2015 (138 pages) and the review paper [Chemical vapour deposition diamond single crystals with nitrogen-vacancy centres: a review of material synthesis and technology for quantum sensing applications](#) by Jocelyn Achard, Vincent Jacques and Alexandre Tallaire, 2020 (30 pages).

⁹⁶⁵ See [Scalable fabrication of coupled NV center – photonic crystal cavity systems by self-aligned N ion implantation](#) by T. Schroder and A. Stein, May 2017 (13 pages).

They estimate that their solution will be size/weight/performance/cost/power competitive and bring some quantum advantage earlier than competing systems from Google and IBM that they brand « quantum mainframes ». They want to create “quantum desktops” and why not pushing the envelope a bit too far with “smartphone quantum computers”⁹⁶⁶.

They introduced in March 2021 a 5-qubits prototype fitting into a 2U classical 19-inch server form factor⁹⁶⁷. They expect to reach 50 qubits by 2026 and to then scale up this architecture with connecting several units together⁹⁶⁸. The next step is to fit their whole system in a large PCI board as shown in Figure 366. To learn more about these systems, you need to look at the scientific papers coauthored by Marcus Doherty⁹⁶⁹.



Figure 366: a Quantum Brilliance PCI board. Source: Quantum Brilliance.

You find that they have an error rate of 10^{-5} for single qubit gates, which is fine, and expect to have a similar level for two-qubit gates. But what is documented is a 99,2% two-qubit gate fidelity, which is not stellar nor sufficient to implement fault-tolerant quantum computing.

In April 2021, Quantum Brilliance also announced a partnership with **Quantum-South** (Uruguay) and to develop proof of concepts optimization quantum applications for air and maritime cargo companies. This is a bit early given their existing 5-qubits but why not exploring the path.

In January 2022, Quantum Brilliance announced DE-Brill, a joint research project with the Fraunhofer Institute for Applied Solid State Physics IAF and the University of Ulm funded by the German government quantum plan. The partnership is focused on the development of manufacturing (Fraunhofer) and control (Ulm) techniques of NV center qubits. The total investment of this 5-year project starting in December 2021 is €19.9M with 78.4% funded by BMBF, the German ministry of research. In April 2022, the company launched a joint R&D hub with La Trobe University and RMIT University around material design and manufacturing. This and other German universities working on NV centers⁹⁷⁰ create a critical mass of skills in NV centers aimed at quantum computing. Germany’s involvement deals with manufacturing these NV center based chipsets with high precision.

At home in Australia, the **Pawsey Supercomputing Research Centre** announced in June 2022 the installation of a Gen1 Quantum Brilliance quantum accelerator. There was no precision whatsoever on the specifications of this system.

⁹⁶⁶ See [Breakthrough: Quantum computers will soon fit in your phone](#) by Maija Palme, Sifted, August 2021.

⁹⁶⁷ In some sources, the number of available qubits is two and not five! I found out in a December 2022 preprint that their current commercial GPU has only two qubits fitting in a 6U rack. See [Software for Massively Parallel Quantum Computing](#) by Thien Nguyen et al, November-December 2022 (21 pages).

⁹⁶⁸ See [Diamond-Based Quantum Accelerator Puts Qubits in a Server Rack](#) by Charles Q. Choi, March 2021. The illustrative picture comes from Quantum Brilliance. See also some technical details in [Quantum accelerators: a new trajectory of quantum computers](#) by Marcus Doherty, Quantum Brilliance, March 2021.

⁹⁶⁹ See [Optimisation of diamond quantum processors](#) by YunHeng Chen, Marcus W. Doherty, et al, September 2020 (42 pages), [Spin-to-Charge conversion with electrode confinement in diamond](#) by Liam Hanlon, Marcus W. Doherty et al, August 2021 (16 pages) and [Optical activation and detection of charge transport between individual color centers in room-temperature diamond](#) by Artur Lozovoi, Marcus W. Doherty et al, October 2021 (15 pages).

⁹⁷⁰ See [Optically coherent nitrogen-vacancy defect centers in diamond nanostructures](#) by Laura Orphal-Kobin et al, Humboldt-Universität and Ferdinand-Braun-Institut both in Berlin, 2022 (26 pages).

TURING

Turing Inc (2016, USA, \$15.5M) is a startup willing to create quantum computing hardware and software, based on NV centers qubits and operating at 4K⁹⁷¹.

They also develop error correction systems that they market to other industry specialists. A way to avoid putting all your eggs in the same basket!



XeedQ (2021, Germany) is developing XQ1, an NV-center-based multi-qubit mobile quantum processor running at room-temperature. It fits in a desktop format with 4 qubits and consuming only 150 W. Two-qubit gate fidelity is >90% and single qubit gate >95% which is quite average.

They plan to release a version with 256 qubits by 2026. You may wonder what are the exact quantum computing skills of the founding team when their web site touts that “*quantum systems offer encryption standards that are virtually impossible to breach. Welcome to future-proof quantum secure communications on a mobile footprint*”. Someone should tell them that PQC doesn’t need a quantum computer to run. The company created by Gopalakrishnan Balasubramanian, formerly at the Max Planck Institute for Biophysical Chemistry in Göttingen and is based in Leipzig. He published a wealth of [papers](#) on the physics of NV centers but not on NV-centers-based quantum computers nor how do you entangle such qubits at room temperatures.

SiC and other spin cavities variants

Besides NV centers, another similar technique is investigated at the research stage that uses various vacancies in silicon carbide crystal structures (SiC) or silicon. Vacancies can be missing nearby couples of carbon and silicon atoms, called divacancies ($V_{Si}V_C^0$) or just a missing silicon atom (V_{Si}^-)⁹⁷²

Others use transition metal defects with chromium, vanadium, molybdenum, tungsten, erbium⁹⁷³ and also hexagonal boron nitride (h-BN)⁹⁷⁴. In 2022, a research team from the DoE Argonne National Lab created a prediction model of the coherence time of vacancies depending on their characteristics, which can help investigate new materials⁹⁷⁵.

As with NV centers, SiC qubits could theoretically work at ambient temperature⁹⁷⁶. While these vacancies could be used to create qubits and quantum processors like with NV centers, they are currently aimed mostly at quantum photonics applications. One of the reasons is that some SiC vacancies have fluorescence wavelengths corresponding to fiber optics telecom wavelengths in the near infrared band around 1,5 μm , in the so-called 4H-SiC hexagonal lattice version⁹⁷⁷.

⁹⁷¹ See [Turing Inc: Large Scale Universal Machines](#), 2017, which details this a little bit.

⁹⁷² See [Single artificial atoms in silicon emitting at telecom wavelengths](#) by W. Redjem et al, 2020 (4 pages).

⁹⁷³ See [Roadmap for Rare-earth Quantum Computing](#) by Adam Kinos, Alexandre Tallaire et al, March 2021 (47 pages).

⁹⁷⁴ See [First-principles theory of extending the spin qubit coherence time in hexagonal boron nitride](#) by Jaewook Lee, Huijin Park and Hosung Seo, npj, September 2022 (9 pages).

⁹⁷⁵ See [A mathematical shortcut for determining quantum information lifetimes](#) by Leah Hesla, Argonne National Lab, April 2022 and [Generalized scaling of spin qubit coherence in over 12,000 host materials](#) by Shun Kanai, David D. Awschalom et al, PNAS, April 2022 (8 pages). It shows that the coherence time T_2 of vacancies is dependent on the cavity spin density (n_i) of nucleus i , the crystalline structure, the nuclear spin-factor (g_i), and the nuclear spin quantum number (I_i) according to the formula $T_{2,i} = 1.5 \times 10^{18} |g_i|^{-1.6} I_i^{-1.1} n_i^{-1.0}$ (s).

⁹⁷⁶ The DoE Argonne National Laboratory together with researchers from Hungary, Sweden and Russia published in 2019 a work on SiC qubits operating at room temperature. See [Scientists Find Yet Another Way to Get Qubits Working at Room Temperature](#) by David Nield, March 2020 and [Novel Qubit Design Could Lead to Quantum Computers That Work at Room Temperature](#) by Matt Swayne, March 2020 which references [Quantum well stabilized point defect spin qubits](#) by Viktor Ivády et al, May 2019 (20 pages).

⁹⁷⁷ See the excellent review paper [Quantum Information Processing With Integrated Silicon Carbide Photonics](#) by Sridhar Majety et al, March 2022 (50 pages).

SiC vacancies can indeed be used as interesting sources of single or entangled photons in quantum communications and cryptography. SiC photon sources are implanted on nanophotonic devices⁹⁷⁸.

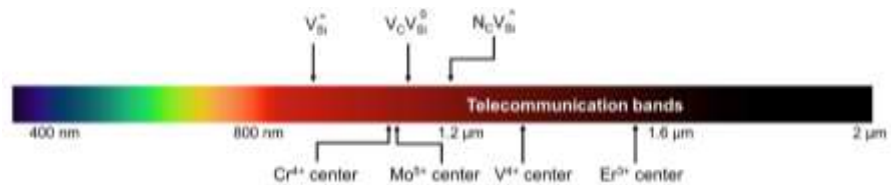


Figure 367: other cavities are interesting due to their transition frequencies that sit in the telecommunication wavelengths. Source: [Quantum Information Processing With Integrated Silicon Carbide Photonics](#) by Sridhar Majety et al, March 2022 (50 pages).

It could also be used in quantum repeaters thanks to relatively long spin coherence times above 50 ms. Also, SiC vacancies can show a much better DWF (Debye-Waller factor) than diamond NV centers. However, their readout contrast has to be improved⁹⁷⁹.

In quantum information processing, SiC vacancies are investigated in various areas such as with quantum simulation and measurement-based quantum computing. There are some specific technology paths like using SiC spin qubits that are coupled by photons⁹⁸⁰.

SiC vacancies have very long coherence times in the seconds range⁹⁸¹. It leads to theoretically long computing time, although, it would work with solving many other problems like large entanglement capacities and high two-qubit gate fidelities. Thus, when you read in the media that SiC could achieve a hundred million operations, you may get skeptic and right to be so⁹⁸². Indeed, the related paper simply compute this number of operations with dividing SiC qubit coherence time of 5 seconds by a single-qubit gate time. They have not implemented it yet, particularly given it's useless to do that on a single qubit. It would be nice to have a tomography of a 2-qubit gate...:)



Photonic (2019, Canada) is a spin-off from the Silicon Development Lab at Simon Fraser University in Vancouver. They develop silicon based chipsets quantum computers with the aim of putting on million qubits on two square-cm.

They tout having reached 1000 electron spin qubits in 2020 and 100,000 in 2021. Their technology seems to be based on defects in silicon, using similar techniques as SiC and NV vacancies⁹⁸³. Too bad they are probably overselling their achievements.

Topological qubits

In this category of qubits and quantum computing, we must create a distinction between the notion of "topological" which defines a type of qubit based on anyons and the "Majorana fermions" which are a variant of anyons to create topological qubits. Of all the types of qubits, they are the most mysterious and complex to understand⁹⁸⁴! It's part of the broad field of topological matter.

⁹⁷⁸ See [Integrated quantum photonics with silicon carbide: challenges and prospects](#) by Daniil M. Lukin, Melissa A. Guidry and Jelena Vuckovic, October 2020 (20 pages) and [Fabrication and nanophotonic waveguide integration of silicon carbide colour centres with preserved spin-optical coherence](#) by Charles Babin, Florian Kaiser et al, November 2021 (18 pages).

⁹⁷⁹ See [Room temperature coherent manipulation of single-spin qubits in silicon carbide with a high readout contrast](#), by Qiang Li et al, July 2021 (10 pages).

⁹⁸⁰ See [Silicon photonic quantum computing with spin qubits](#) by Xiruo Yan et al, 2021 (28 pages).

⁹⁸¹ See [Five-second coherence of a single spin with single-shot readout in silicon carbide](#) by Christopher P. Anderson, David D. Awschalom et al, 2021 (9 pages).

⁹⁸² See [Quantum Computing: Researchers Achieve 100 Million Quantum Operations](#) by Francisco Pires, Tom's Hardware, February 2022.

⁹⁸³ See [Silicon-Integrated Telecommunications Photon-Spin Interface](#) by L. Bergeron et al, 2020 (15 pages).

⁹⁸⁴ See [Topological Quantum Computing](#) by Torri Yearwood, January 2020 and [A Short Introduction to Topological Quantum Computing](#) by Ville Lahtinen and Jiannis K. Pachos, May 2017 (44 pages).

History

Ettore Majorana predicted in 1937 the existence of a new class of particles that are its own anti-particles. It was labelled “Majorana fermions.

The notion of anyon, "quasi-particle", i.e. particle representation models that describe the state of electron clouds around atoms, in the superconducting regime and in 2D was first proposed by Jon Leinaas and Jan Myrheim from the University of Oslo in 1976 and then elaborated by Frank Wilczek in 1982⁹⁸⁵. Majorana fermions are a specific type of these quasiparticles organized along a small superconducting wire in 1D structures. They have collective electron behaviors in crystalline networks at very low temperature⁹⁸⁶.

Alexei Kitaev then had the idea in 1997 to use anyons for quantum calculations when he was a researcher at Microsoft. He published two foundational papers in 2000 describing the category of fermionic quantum computers and a model of spinless fermions in a 1D superconducting nanowire, *aka* a Kitaev chain⁹⁸⁷. There are several various variations of fermionic quantum computing being investigated, including analog quantum computing with cold atoms⁹⁸⁸.

In 2008, Liang Fu and C.L. Kane from the University of Pennsylvania predicted that Majorana bound states can appear at the interface between topological insulators and superconductors⁹⁸⁹.

In 2012, Leo Kouwenhoven then at TU Delft announced the detection of Majorana Zero Modes quasiparticles at TU Delft and later on in 2018 when he was at Microsoft Research in Delft.

Some other advances came out in 2016 from the MIT and in 2018, from a group of three American universities UC Irvine, UCLA and Stanford, who said they discovered real Majorana fermions. In May/June 2019, German and Austrian researchers said they succeeded in creating two-dimensional topological phenomena like Majorana zero modes⁹⁹⁰.

Princeton researchers also published in June 2019 the results of their work that led them to control the state of a quasi-particle⁹⁹¹.

⁹⁸⁵ See [On the theory of identical particles](#) by J.M. Leinaas and J. Myrheim, 1976 (23 pages) and See [Quantum Mechanics of Fractional-Spin Particles](#) by Frank Wilczek, PRL, 1982. See also the essay [Quanta of the Third Kind](#) by Frank Wilczek, November 2021 that provides an excellent simplified view of what are anyons, braiding and quasi-particles. The author explains three specifics of quasi-particles: fractionalization (where quasiparticles have properties that are subparts of usual whole-number multiples like spins or unit of electron electric charge or angular momentum), flux tubes (fractional angular momentum made possible by particles orbiting around tubes of magnetic flux like in type II superconductors) and dimensional reduction (with point-like structures).

⁹⁸⁶ This is the thesis of Hugo de Garis in [Topological Quantum Computing The TOC Shock Wave and its Impact on University Computer Science Teaching](#), 2011 (29 pages).

⁹⁸⁷ See [Fermionic quantum computation](#) by Serguei B. Bravyi and Alexei Y. Kitaev, 2000 (18 pages) and [Unpaired Majorana fermions in quantum wires](#) by Alexei Kitaev, 2000 (16 pages).

⁹⁸⁸ See [The Power of Noisy Fermionic Quantum Computation](#) by Fernando de Melo et al, April 2013 (21 pages) and [Quantum register of fermion pairs](#) by Thomas Hartke et al, MIT, March 2021 (10 pages). Fermionic quantum computing was defined by Serguei B. Bravyi and Alexei Y. Kitaev in [Fermionic quantum computation](#), 2000 (18 pages).

⁹⁸⁹ See [Superconducting proximity effect and Majorana fermions at the surface of a topological insulator](#) by Liang Fu and C.L. Kane, 2008 (4 pages) and [Josephson Current and Noise at a Superconductor-Quantum Spin Hall Insulator-Superconductor Junction](#) by Liang Fu and C.L. Kane, 2008 (4 pages).

⁹⁹⁰ See [Computing Faster With Quasi-Particles](#), May 2019 referring to [Topological superconductivity in a phase-controlled Josephson junction](#) by Hechen Ren et al, Nature, April 2019.

⁹⁹¹ See [Mysterious Majorana Quasiparticle Is Now Closer To Being Controlled For Quantum Computing](#), June 2019 mentioning [Observation of a Majorana zero mode in a topologically protected edge channel](#) by Ali Yazdani et al, Science, June 2019 (12 pages).

2021 marked the beginning of a crisis winter for Majorana fermion. It started with an expression of concern and a withdrawal of Leo Kouwenhoven's 2018 Nature paper⁹⁹². In a [March 2022 Twitter thread](#) Sergey Frolov made an impressive inventory on many other unreliable Majorana research papers with other retracted papers⁹⁹³ or that should be retracted.

He used to work at TU Delft with Leo Kouwenhoven on Majorana fermions and moved in 2012 to the University of Pittsburgh⁹⁹⁴.

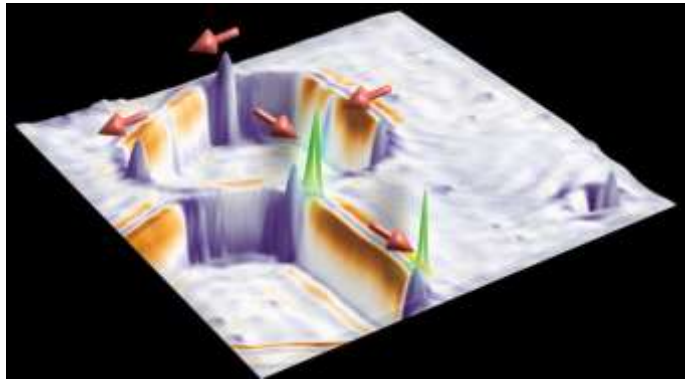


Figure 368: a Majorana Zero mode discovered at Princeton in 2019. Source: [Mysterious Majorana Quasiparticle Is Now Closer To Being Controlled For Quantum Computing](#), June 2019.

The withdrawal came after Sergey Frolov and his fellow Pittsburgh researcher Vincent Mourik tried to reproduce Kouwenhoven's experiment and couldn't reproduce its results⁹⁹⁵. Early in 2022, Leo Kouwenhoven left Microsoft in March 2022⁹⁹⁶. Charlie Marcus from Microsoft Research in Denmark also quit Microsoft late 2021 to return to academic research at the Niels Bohr Institute⁹⁹⁷.

The same Sergei Frolov is himself making discoveries on Majorana bound states using the 4π Majorana-Josephson effect using a fluxonium superconducting qubit, the ensemble being branded a braidonium⁹⁹⁸. He also reported in 2022 that looking at research experimental data from 2012 did show the presence of Majorana modes in nanowire devices⁹⁹⁹. Other researchers in Germany succeeded in integrating a topological insulator into a superconducting qubit in 2022, following on a 2013 proposal from researchers from Caltech and Harvard¹⁰⁰⁰. Another 2020 proposal is to couple a Majorana qubit playing the role of a well-protected quantum memory and a superconducting qubit for computation and to implement a SWAP gate between these¹⁰⁰¹.

⁹⁹² See [Quantized Majorana conductance](#) by Leo Kouwenhoven et al, 2017 (26 pages) which was followed by an "[expression of concern](#)" from the authors warning readers about the veracity of the published results, which were not reproducible due to a problem with the calibration of measuring instruments. The coverage on the paper withdrawal in 2021 was dense, starting with [Data manipulation and omission in 'Quantized Majorana conductance'](#), Zhang et al, Nature 2018 by Frolov et al, March 2021 (31 slides) which spurred [Microsoft's Big Win in Quantum Computing Was an 'Error' After All](#), by Tom Simonite, Wired, February 2021. Another of their paper was later retracted. See [Retraction Note: Epitaxy of advanced nanowire quantum devices](#) by Sasa Gazibegovic, Leo Kouwenhoven et al, Nature, April 2022.

⁹⁹³ See [Chiral Majorana fermion modes in a quantum anomalous Hall insulator–superconductor structure](#), Science, 2017 (7 pages) was the subject of an [expression of concern](#) in December 2021.

⁹⁹⁴ See [Signatures of Majorana fermions in hybrid superconductor-semiconductor nanowire devices](#), Kavli Institute of Nanoscience, Delft University of Technology, 2012.

⁹⁹⁵ The story is well told in [Major Quantum Computing Strategy Suffers Serious Setbacks](#) by Philip Ball, Quanta Magazine, September 2021. The same Philip Ball that was mentioned in the part of this book related to [quantum matter taxonomy](#), page 116.

⁹⁹⁶ See [Kouwenhoven departs, Microsoft presents Majoranas](#), Delta GTU Delft, March 2022.

⁹⁹⁷ As shown in his LinkedIn profile: <https://www.linkedin.com/in/charles-marcus-02984597>.

⁹⁹⁸ See [Braiding quantum circuit based on the \$4\pi\$ Josephson effect](#) by John P. T. Stenger, Michael Hatridge, Sergey M. Frolov and David Pekker, University of Pittsburgh, Physical Review B, 2019 (10 pages).

⁹⁹⁹ See [We cannot believe we overlooked these Majorana discoveries](#) by Sergey Frolov and Vincent Mourik, University of Pittsburgh and FZ Jülich, March 2022 (9 pages).

¹⁰⁰⁰ See [Integration of Topological Insulator Josephson Junctions in Superconducting Qubit Circuits](#) by Tobias W. Schmitt et al, FZ Jülich, March 2022 (14 pages). And [Proposal for Coherent Coupling of Majorana Zero Modes and Superconducting Qubits Using the \$4\pi\$ Josephson Effect](#) by David Pekker, Chang-Yu Hou, Vladimir E. Manucharyan and Eugene Demler, PRL, 2013 (8 pages).

¹⁰⁰¹ See [SWAP gate between a Majorana qubit and a parity-protected superconducting qubit](#) by Luca Chirulli et al, Berkeley, May 2022 (7 pages).

In August 2019, NIST physicists led by Nick Butch announced the discovery by chance of interesting properties of uranium ditelluride (UTe₂). It would be superconducting at 1.7K with the ability to do so via Cooper pairs with identical spins in addition to opposite spins, allowing three types of pairs. This would give it a rare ability to get a magnetic flux resistant superconductivity. This material would thus have topological properties in this framework allowing to create topological qubits that are more stable and less subject to decoherence¹⁰⁰². Related work was published by researchers from John Hopkins University in 2018 with superconducting topological qubits made of a bismuth-palladium alloy¹⁰⁰³.

And the story goes on and on around Majorana fermions that are discovered, believed to be discovered or rediscovered depending on the case.

They are found on gold¹⁰⁰⁴, on the surface of superconducting nanowires¹⁰⁰⁵, in crystals¹⁰⁰⁶, in 2D graphene¹⁰⁰⁷, not to mention other publications that are not obvious to analyze¹⁰⁰⁸, all this in 2020.

Science

The principle of topological quantum computing is based on the notion of anyon which are "quasi-particles" integrated in two-dimensional systems, given that there are Abelian and non-Abelian anyons! Anyons are asymmetrical and two-dimensional physical structures whose symmetry can be modified. This makes it possible to apply some topology principles with sets of successive permutations applied to pairs of anyons that are in close proximity in circuits.

The related algorithms are based on the concepts of topological braid or node organizations ("braids"). Their representation explains this, with a temporal evolution of the permutations of temporal anyons going from bottom to top, knowing that in other representations, it may go from top to bottom¹⁰⁰⁹.

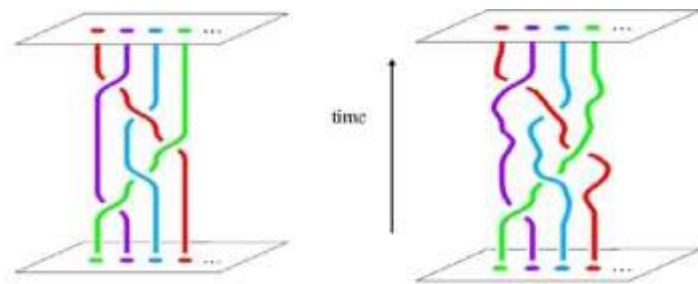


Figure 369: anyon braiding explained topologically.

The diagram in Figure 370 clarifies this a little. Topological quantum gates require a long sequence of anyonic permutations as with the CNOT gate shown at the bottom of the diagram. They are a sort of quantum error correction code.

¹⁰⁰² See [Newfound Superconductor Material Could Be the 'Silicon of Quantum Computers' Possible "topological superconductor" could overcome industry's problem of quantum decoherence](#), August 2019, mentioning [Nearly ferromagnetic spin-triplet superconductivity](#) by Sheng Ran et al, 2019.

¹⁰⁰³ See [Observation of half-quantum flux in the unconventional superconductor \$\beta\$ -Bi₂Pd](#) by Yufan Li & Al, October 2018 (12 pages).

¹⁰⁰⁴ See [Quantum Computing Breakthrough: First Sighting of Mysterious Majorana Fermion on Gold](#) by Jennifer Chu, MIT, Indian Institute of Technology, University of California & Hong Kong University, 2020. And [Signature of a pair of Majorana zero modes in superconducting gold surface states](#) by Sujit Manna et al, MIT, 2019 (35 pages).

¹⁰⁰⁵ See [Alternative route to topological superconductivity Hub](#), April 2020. University of Copenhagen in collaboration with Microsoft. Refers to [Flux-induced topological superconductivity in full-shell nanowires](#) by S. Vaitiekėnas et al, March 2020 (38 pages).

¹⁰⁰⁶ See [Building block for quantum computers more common than previously believed](#) by Chanapa Tantibanchachai, Johns Hopkins University, April 2020.

¹⁰⁰⁷ See [Observation of Yu-Shiba-Rusinov states in superconducting graphene](#) by E. Cortés-del Río, Pierre Mallet et al, 2020 (22 pages) and published in *Advanced Materials* in April 2021.

¹⁰⁰⁸ See [The observation of photon-assisted tunneling signatures in Majorana wires](#) par Ingrid Fadelli, May 2020, [Quantum computers do the \(instantaneous\) twist](#) by Chris Cesare, August 2020 on a topological error correction system and [Fractional statistics of anyons in a two-dimensional conductor](#), C2N, April 2020.

¹⁰⁰⁹ Topological qubits could also be realized in photonics-based architecture. See [New photonic chip promises more robust quantum computers](#), September 2018, involving researchers in Australia, Italy and Switzerland.

You need two Majorana fermions to create a single two-level quantum system, *aka* a qubit. With Majorana modes, you implement XX, YY and ZZ two-qubit measurements which are well protected and a CNOT is built with two consecutive such measurements. But a T gate is not natively protected making it hard to implement FTQC. Some researchers in China still found a workaround to create non-Clifford single-qubit phase gates¹⁰¹⁰.

By the way, let's clarify a little bit the weird vocabulary from this field. Majorana fermions are non-Abelian excitations. They are also called Majorana Zero Modes (MZM) or Majorana bound states or even Majorinos. You have also Majorana Edge Modes (MEM) and Majorana Pi Modes (MPM)¹⁰¹¹. Others non-Abelian anyons exist like Ising anyons, Fibonacci anyons¹⁰¹² and Jones-Kauffman anyons.

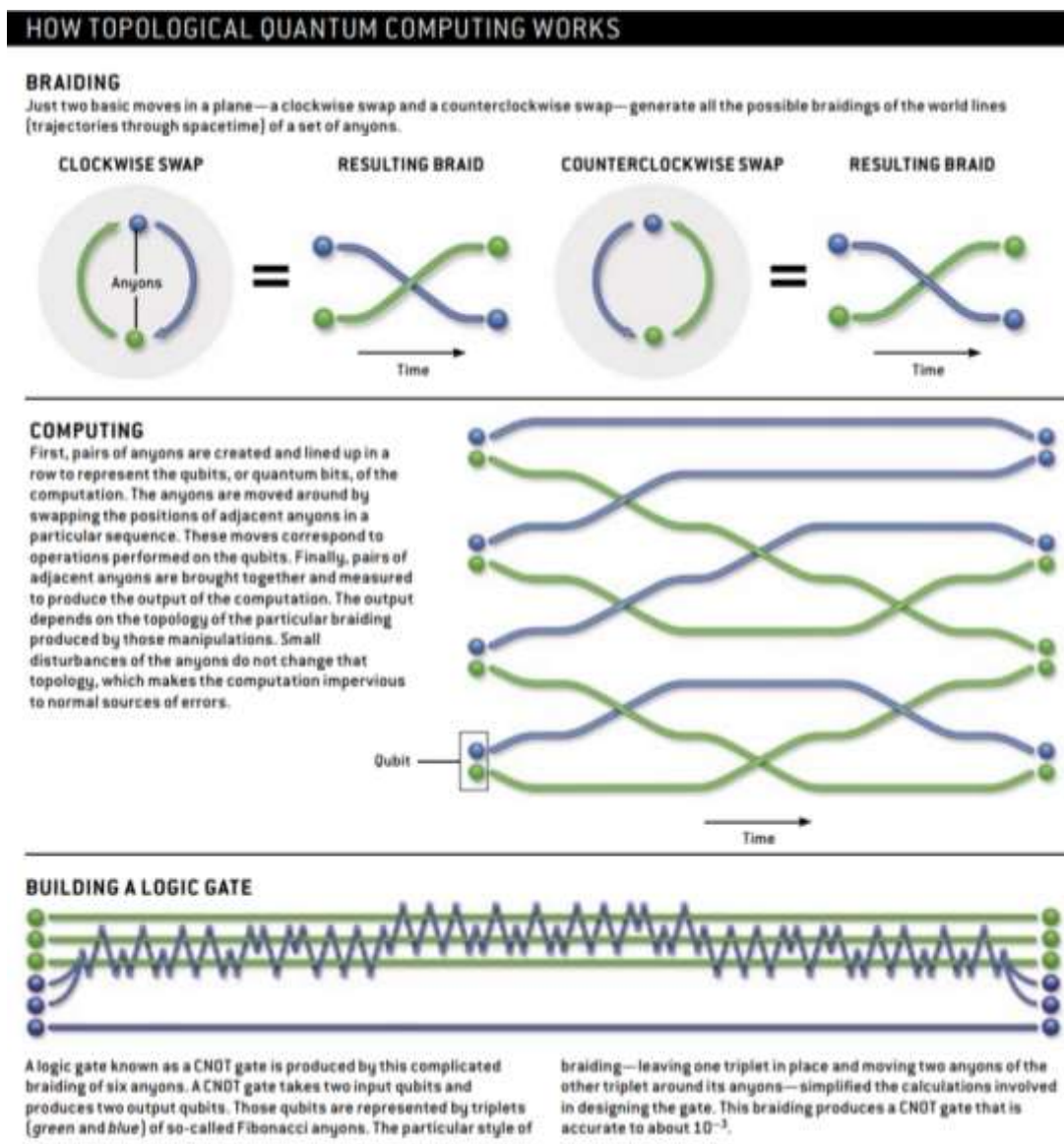


Figure 370: how topological quantum computing is supposed to work. Source: [Computing with Quantum Knots](#) by Graham Collins, *Scientific American*, 2006 (8 pages).

¹⁰¹⁰ See [Universal topological quantum computation with strongly correlated Majorana edge modes](#) by Ye-Min Zhan et al, March 2022 (18 pages) which is about creating non-Clifford $\pi/10$ gates.

¹⁰¹¹ To sort things out, see the excellent thesis [Quantum Field Theories, Topological Materials, and Topological Quantum Computing](#) by Muhammad Ilyas, August 2022 (204 pages).

¹⁰¹² See [A short introduction to Fibonacci anyon models](#) by Simon Trebst, Matthias Troyer et al, 2009 (24 pages).

Research

On top of the above-mentioned labs, different physics laboratories are working on topological qubits, notably in the USA, China, the Netherlands, Denmark, Finland¹⁰¹³ and also in France.

Maryland¹⁰¹⁴, **Caltech**¹⁰¹⁵ and **Purdue**¹⁰¹⁶ Universities also have teams working on topological quantum computing and/or Majorana fermions, the two later working with Microsoft Research.

It is also the case of the Quantum Science Center (QSC) from the DoE **ORNL**.

The KouBit Lab from the **University of Illinois** and led by Angela Kou also investigate topologically protected superconducting qubits.

Even IBM is working on Majorana fermions. In 2022, an **IBM Research** team published a paper showing how they could simulate Majorana Zero Modes (MZM), Majorana Pi Modes (MPM) and Majorana braiding on 27-qubits quantum computers¹⁰¹⁷. A large **Google AI** team did a similar experiment with 47 qubits from its Sycamore processor and simulating Majorana Edge Modes¹⁰¹⁸.

Research on topological qubits still goes on at **TU Delft** with some recent work on the way to stabilize entanglement of topological qubits¹⁰¹⁹. Teams in **Finland** and **Russia** also work on topological qubits¹⁰²⁰.

In **France**, a team at the CEA-IRIG in Grenoble (Manuel Houzet, Julia Meyer and Xavier Waintal), Pierre Mallet of CNRS Institut Néel in Grenoble, Hugues Pothier at the CEA in Saclay and Pascal Simon at the LPS in Orsay¹⁰²¹ do not work on Majorana fermions per se, but on topological matter at the fundamental level and particularly on Andreev's states, the linked states and the physics of weak links, different areas that remain to be explored in these lines. Some of these researchers are conducting joint projects with TU Delft.

Majorana zero modes (MZMs) were also found by researchers in **China** in 2022 with iron-based superconductors showcasing topological vertices¹⁰²². In February 2020, **John Preskill** (father of the notions of quantum supremacy and NISQ) predicted that by 2030, we will be able to demonstrate two entangled topological qubits, against **Jonathan Dowling** (photonicist) who did not believe it could

¹⁰¹³ See [Ultra-thin designer materials unlock quantum phenomena](#), Aalto University, December 2020 and [Topological superconductivity in a van der Waals heterostructure](#) by Shawulien Kezilebieke et al, March 2021 (27 pages).

¹⁰¹⁴ See [On-demand large conductance in trivial zero-bias tunneling peaks in Majorana nanowires](#) by Haining Pan and Sankar Das Sarma, University of Maryland, March 2022 (8 pages) and [Euler-obstructed Cooper pairing: Nodal superconductivity and hinge Majorana zero modes](#) by Jiabin Yu, Yu-An Chen and Sankar Das Sarma, University of Maryland, Physical Review B, March 2022 (47 pages).

¹⁰¹⁵ See [Dephasing and leakage dynamics of noisy Majorana-based qubits: Topological versus Andreev](#) by Ryan V. Mishmash, Bela Bauer, Felix von Oppen and Jason Alicea, November 2019 (22 pages).

¹⁰¹⁶ See [Ternary Logic Design in Topological Quantum Computing](#) by Muhammad Ilyas et al, Purdue and Portland Universities, April 2022 (53 pages).

¹⁰¹⁷ See [Observing and braiding topological Majorana modes on programmable quantum simulators](#) by Nikhil Harle et al, Yale University, MIT & IBM Research, March 2022 (14 pages). Tested with 27-qubit superconducting systems.

¹⁰¹⁸ See [Noise-resilient Majorana Edge Modes on a Chain of Superconducting Qubits](#) by Xiao Mi et many al, Google AI, April 2022 (24 pages).

¹⁰¹⁹ See [Topological Entanglement Stabilization in Superconducting Quantum Circuits](#) by Guliuxin Jin and Eliska Greplova, TU Delft, May 2022 (10 pages).

¹⁰²⁰ See [Half-quantum vortices and walls bounded by strings in the polar-distorted phases of topological superfluid ³He](#) by J.T. Makinen, G.E. Volovik et al, 2018 (17 pages).

¹⁰²¹ See Pascal Simon's presentation [Majorana zero modes around skyrmionics textures](#), 2021 (75 slides).

¹⁰²² See [Ordered and tunable Majorana-zero-mode lattice in naturally strained LiFeAs](#) by Meng Li et al, Nature, May 2022 (38 pages). See also [Topologically protected quantum entanglement emitters](#) by Jianwei Wang et al, February 2022 (10 pages) which deals with topologically protected matter although not formally a Majorana fermion.

be created! The object of this symbolic wager? A good beer and a pizza. Jonathan Dowling died in 2020 and will therefore not be able to see if he won or lost his bet in 2030.

Majorana fermions qubits

- **theoretically very stable qubits** with low level of required error correction.
- **long coherence time and gates speed** enabling processing complex and deep algorithms.
- **potential qubits scalability**, built with technologies close to electron spin qubits.
- some researches in the topological matter field could be fruitful with no Majorana fermions.

- **no Majorana fermion** qubit demonstrated yet.
- **topological qubits programming** is different and requires an additional software layer.
- **rather few laboratories** involved in this path.
- **no startup** was launched in this field. Microsoft is the only potential vendor. IBM is investigating the field in Zurich.
- works at **low cryogenic temperatures** like superconducting qubits < 20mK.

Figure 371: pros and cons of Majorana fermions and topological qubits. (cc) Olivier Ezratty, 2022.

Vendors



Microsoft

Microsoft Research has investigated topological quantum computing and Majorana fermions for quite a few years but has no prototype at this stage.

The company is making a bet there, up to say that if they fail, everybody will also fail in quantum computing. While being a little arrogant and a very risky bet, it would bring lots of strategic advantages if it worked!

Indeed, Majorana qubits would be much more reliable and generate fewer errors (10^{-30}), with the implication that we could avoid using some of the classical quantum error correction codes that are implemented with other types of qubits¹⁰²³.

A Fields Medal in 1986 for his work on the Poincaré conjecture, Fields Medal winner **Michael Freedman** joined Microsoft in 1997, coming from the University of Santa Barbara, the same where John Martinis came from when he joined Google in 2014. Freedman demonstrated with Alexei Kitaev the possibility of doing quantum computing with a hypothetical particle, the Majorana fermion, conceptualized in 1937 by the Italian Ettore Majorana from the resolution of mathematical equations of Dirac¹⁰²⁴. This fermion is a strange particle, whose charge and energy are zero and which is its own antiparticle.

Freedman and Kitaev were recruited by Microsoft Research. Created by Michael Freedman, Microsoft Quantum Santa Barbara (Station Q) is located on the campus of the University of Santa Barbara. They were complemented by **Leo Kouwenhoven**'s team based in Microsoft's Delft Lab in the Netherlands and with **Charles Marcus** from the Niels Bohr Institute who also joined Microsoft Research who both left Microsoft in 2022 and 2021. Microsoft also collaborates with **Purdue University** in Indiana, where it has a dedicated research team **Microsoft Quantum Purdue**, working on III-V superconductors.

¹⁰²³ Here are a few leads to find out more: [Microsoft Ready to Build a Quantum Computer](#) by Juliette Raynal, 2016, [A Software Design Architecture and Domain-Specific Language for Quantum Computing](#), 2014 (14 pages), Quantum [Computing at Microsoft](#) (56 slides) and [Quantum Computing Research at Microsoft](#) (59 slides) by Dave Wecker and [A short introduction to topological quantum computation](#) by Ville Lahtinen and Jiannis Pachos, 2017, (43 pages). And some videos: [keynote of November 2017](#) with Leo Kouwenhoven (43 mn), [Build conference of May 2018](#) on Q# (1h15mn) and [Majorana qubits](#) by Xiao Hu, in May 2017 (22 mn).

¹⁰²⁴ In [Topological Quantum Computation](#) published in 2002 and updated in 2008 (12 pages).

Majorana fermions are strange behaviors of electrons and their spin that are found at both ends of superconducting wires. They operate at very low temperatures, as for superconducting and silicon-based qubits, at about 15-20 mK¹⁰²⁵.

Seen up close, these qubits are sophisticated variants of superconducting qubits. These "topological" mesh associations provide protection against qubit decoherence because the shape of the braids does not matter as long as their topology is stable.

Microsoft announced at the Build conference in May 2018 that they would release their first fermion-based quantum computer from Majorana in 2023¹⁰²⁶. After Leo Kouwenhoven's 2017 paper withdrawal in 2021, this planning seems somewhat challenging¹⁰²⁷. But let's not count Microsoft out of the game too rapidly. All discoveries have their up and downs. If a failure meant *stop all research*, Thomas Edison would not have discovered the light bulb and many vaccines and cancer treatments wouldn't see the light of day!

In 2022, as Kouwenhoven was leaving Microsoft, the company published some new results related to Majorana fermions and scalable quantum computing. They seem not having learned from their past errors and were emphatically overselling their recent work¹⁰²⁸. It dealt with the observation of a 30 μeV topological gap in indium arsenide-aluminum heterostructures. But it seemed that this topological qubit was only digitally simulated and not implemented practically.

Just before, in February 2022, another Microsoft team published a paper related to a quantum error correction code (planar Floquet code) that was suitable for topological qubits and with a very high threshold exceeding 1% (meaning, qubits with 1% error rates are sufficient to implement error correction which seems a very high error-rate compared to what would be needed with superconducting qubits and surface codes, that require errors way below 0.1%)¹⁰²⁹.

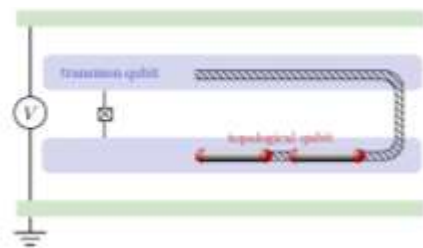


Fig. 6: Read out of a parity qubit in a Cooper pair box. Two superconducting islands (blue), connected by a split Josephson junction (crosses) form the Cooper pair box. The topological Majorana qubit is formed by four Majorana fermions (red spheres), at the end points of two undepleted segments of a semiconductor nanowire (striped ribbon indicates the depleted region). A magnetic flux Φ enclosed by the Josephson junction controls the charge sensitivity of the Cooper pair box. To read out the topological qubit, two of the four Majorana fermions that encode the logical qubit are moved from one island to the other. Depending on the quasiparticle parity, the resonance frequency in a superconducting transmission line enclosing the Cooper pair box (green) is shifted upwards or downwards by the amount which is exponentially small in E_J/E_C .

Figure 372: typical combination of a topological and a superconducting qubit. Source: [Majorana Qubits](#) by Fabian Hassler, 2014 (21 pages).

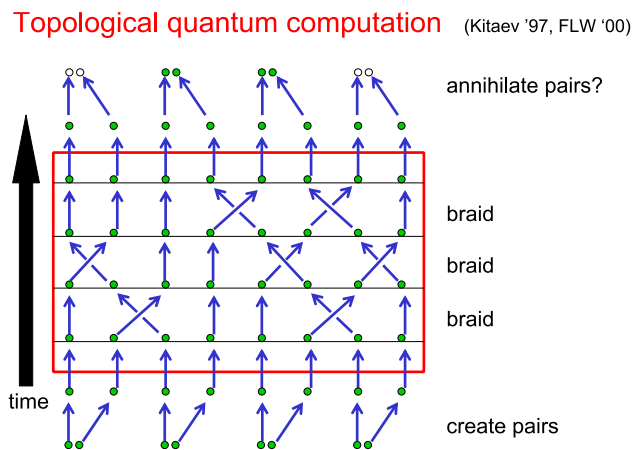


Figure 373: how braiding is sequenced during topological computing. Source: [Topological quantum computing for beginners](#), by John Preskill (55 slides).

¹⁰²⁵ See [Majorana Qubits](#) by Fabian Hassler, 2014 (21 pages).

¹⁰²⁶ See this video ad: [Introducing Quantum Impact \(Ep. 0\)](#), February 2020 (4 minutes).

¹⁰²⁷ See [Topological quantum computing for beginners](#), by John Preskill (55 slides).

¹⁰²⁸ See [In a historic milestone, Azure Quantum demonstrates formerly elusive physics needed to build scalable topological qubits](#) by Jennifer Langston, March 2022, [Microsoft has demonstrated the underlying physics required to create a new kind of qubit](#) by Chetan Nayak, March 2022, based on [Protocol to identify a topological superconducting phase in a three-terminal device](#) by Dmitry Pikulin et al, March 2021 (28 pages).

¹⁰²⁹ See [Performance of planar Floquet codes with Majorana-based qubits](#) by Adam Paetznick, Nicolas Delfosse et al, February 2022 (20 pages).

Overall, these Microsoft's research results have a very low TRLs have not been successful so far. We have for example no idea about the number of physical or logical qubits that they could implement, and how these are driven from the control and readout standpoint.

Microsoft obviously also invested on software development, first with its Liquid platform, then with F# for scripting and with the Q# language used for quantum programming, launched at the end of 2017.

One of the contributors to these efforts is researcher **Krysta Svore** from Columbia University. In 2018, Microsoft recruited a certain **Helmut Katzgraber**, one of the apostles of D-Wave quantum annealing and MBQC (measurement-based quantum computers)¹⁰³⁰.

| | Realizations | Lifetimes | Gate Speed |
|-----------------|------------------------|--------------------|------------------------|
| supraconducting | Topological (Majorana) | 1 minute | Nanoseconds |
| | Flux Qubit | / 10 ¹⁰ | same |
| | Charge Qubit | / 10 ¹⁰ | same |
| | Transmon | / 10 ⁷ | same |
| | Ion Trap | / 10 ² | 10 ³ slower |

better stability qubits
low decoherence noise
few errors
long coherence time
high gate speed

} nothing demonstrated so far
} no prototype
} different algorithms

Figure 374: timing benefits from Majorana fermions. Source: Microsoft, 2018.

NOKIA **Nokia's Bell Labs** in the USA, located in Murray Hill, New Jersey, work *or worked* on topological qubits¹⁰³¹.

Nokia also supports Oxford University's [Quopal](#) initiative on the use of quantum in machine learning. Nokia likes to remind us that Grover and Shor's algorithms were discovered by their creators when they worked at the Bell Labs. Nokia is also working on quantum cryptography, at least at the level of its transport on optical fibers, as demonstrated by this [partnership](#) with SK Telecom of 2017.



There is even a private research company, **Quantum Gravity Research** (2009, USA) with an overarching goal to create a unified physics theory encompassing gravity and quantum physics that also undertakes research in topological computing¹⁰³². The organization created by Klee Irwin employs about 20 researchers like Fang Fang, Raymond Aschheim, Marcelo Amaral, Dugan Hammock, Richard Clawson and Michel Planat. They envision “*a specific substructure of spacetime at the smallest scale, so that in this view physical reality is like a mosaic tiling language of Planck scale, 3-dimensional, tetrahedron-shaped pixels*”. Let's say it is quite difficult to fact-check these sorts of claims and their practicality!

Trapped ions qubits

Trapped ions are positively ionized atoms that are trapped by electrodes and sometimes also magnetically in a confined space and placed next to each other. The atoms are generally alkaline metals from the second column of Mendeleev's table (called "Group IIA" in Mendeleev's notation or group 2 in the modern notation, with beryllium, magnesium, strontium, barium and calcium), then as ytterbium which is a rare earth in the lanthanide family or even mercury, and finally, quite rarely, metals of group IIB or 12 (zinc, cadmium, mercury)¹⁰³³.

¹⁰³⁰ See [Quantum Driven Classical Optimizations](#), August 2018 (28 min video).

¹⁰³¹ See [Quantum computing using novel topological qubits at Nokia Bell Labs](#) published in 2017, which describes their approach with topological [qubits](#).

¹⁰³² See [Exploiting Anyonic Behavior of Quasicrystals for Topological Quantum Computing](#) by Marcelo Amaral et al, Quantum Gravity Research, July 2022 (20 pages).

¹⁰³³ See this interesting perspective on trapped ions qubits in [Introduction to Trapped Ion Quantum Computing](#) by Gabriel Mintzer from MIT, February 2020.

trapped ions qubits

- **identical ions** => no calibration required like with superconducting/electron spin qubits.
- **good qubits stability** with best in class low error rate.
- **long coherence time** and high ratio between coherence time and gate time => supports deep algorithms in number of gates.
- **entanglement** possible between all qubits on 1D architecture. It speeds up computing.
- works at **4K to 10K** => simpler cryogeny than for superconducting/electron spins.
- **easy to entangle ions with photons** for long distance communications.

- **entanglement** doesn't seem to scale well with a large number of ions.
- **questionable scalability options** beyond 50 qubits (ions shuttling, 2D architectures, photon interconnect).
- **relatively slow computing** due to slow quantum gates which may be problematic for deep algorithms like Shor integer factoring.

Figure 375: pros and cons of trapped ions qubits. (cc) Olivier Ezratty, 2022.

History

Before the very notion of a qubit even existed, scientists tried to control ions in space. **Wolfgang Paul** created in 1953 a way to control ions with a mass spectrometer avoiding the use of a magnetic field, named the “Paul trap”. He got the Nobel Prize in Physics in 1989. Later, in 1959, **Frans Penning** and **Hans Dehmelt** were able to control individual electrons with a magnetron trap that was later named the “Penning trap”. Penning traps are still being studied, particularly in their 2D variant.

In the USA, **David Wineland** from NIST created the laser cooling technique starting in 1979, using Doppler effect with magnesium ions. He got the Nobel prize in physics in 2012 along with Serge Haroche. In 1989, he used the technique to cool ions at their zero-point energy of motion with the sideband cooling technique that goes farther than Doppler cooling¹⁰³⁴.

Juan Ignacio Cirac and **Peter Zoller** from the University of Innsbruck in Austria proposed in 1995 a blueprint to create a gate-based quantum processor with a linear trap of ions controlled by laser beams¹⁰³⁵. They initiated a long-lasting experience in the field at Innsbruck, which led to the creation of the startup **AQT** in 2017.

Science

Here Are some specifics of trapped ions qubits...

Why ions? The interest of exploiting ions is to allow to trap them magnetically or with electrodes. It is also possible to couple them at long distance, of the order of several tens of microns. It can also be hybridized with several ion types mixed together, like calcium and strontium, to get their related benefit such as fast gates for calcium and stability for strontium¹⁰³⁶. The used elements have several common characteristics related to their electron layer configuration such as excitation levels from the ground state that are of short duration and allow their use for atoms cooling with laser and the Doppler effect. The basic energy state corresponding to the $|0\rangle$ and the excited energy level corresponding to $|1\rangle$ state are stable over time, which facilitates the implementation of quantum gate operations.

¹⁰³⁴ It is too complex to describe the Doppler cooling limit and how sideband cooling works. See [Laser cooling of trapped ions](#) by Jürgen Eschner, Giovanna Morigi, Ferdinand Schmidt-Kaler and Rainer Blatt, 2003 (13 pages) which describes various ions cooling techniques.

¹⁰³⁵ See [Trapped Ion Quantum Computing: Progress and Challenges](#) by Colin Bruzewicz et al from MIT, April 2019 (56 pages). This is a very well-documented state-of-the-art review of trapped ion technology. And the founding article [Quantum Computations with Cold Trapped Ions](#) by Juan Ignacio Cirac and Peter Zoller, 1995 (4 pages).

¹⁰³⁶ See [Benchmarking a high-fidelity mixed-species entangling gate](#) by A. C. Hughes et al, Oxford University, August 2020 (7 pages).

Long coherence time. Trapped ions have a rather long coherence time of up to several tens of seconds, but this is compensated by equally long gate times in proportion. The ratio between coherence time and gate time is however currently quite good at 10^6 , while it is 10^3 for superconducting qubits and about 200 for cold atoms qubits.

Qubit fidelities. Trapped ions show a fairly low error rate with up to single-qubit 99.999% and two-qubit gates 99.9% fidelity. The table below illustrates these fidelities depending on the quantum gate implementation and used ions. This and long coherence time make it possible to theoretically execute "deep algorithms" with a large number of quantum gates and to obtain a good quantum volume, to use IBM's terminology. However, this error rate seems to increase with the number of qubits, at least in 1D architectures like the one from IonQ.

| Type | Method | Fidelity | Time (μ s) | Species | Ref. |
|------------|------------|----------|-----------------|---------------------|---------------|
| 1-qubit | Optical | 0.99995 | 5 | $^{40}\text{Ca}^+$ | Bermudez 2017 |
| | Raman | 0.99993 | 7.5 | $^{43}\text{Ca}^+$ | Ballance 2016 |
| | Raman | 0.99996 | 2 | $^9\text{Be}^+$ | NIST 2016 |
| | Raman | 0.99 | 0.00005 | $^{171}\text{Yb}^+$ | Campbell 2010 |
| | Raman | 0.999 | 8 | $^{88}\text{Sr}^+$ | Kessler 2011 |
| | μ wave | 0.999999 | 12 | $^{43}\text{Ca}^+$ | Harty 2014 |
| μ wave | | | 0.0186 | $^{25}\text{Mg}^+$ | Opelkam 2011 |

Adapted from Bruzewicz et al.

source desschémas : lecture 1 de 77 slides du cours d'Hélène Perrin à l'Université Paris 13 en quatre parties, février 2020.

| Type | Method | Fidelity | Time (μ s) | Species | Ref. |
|--------------------|------------|-----------|---------------------|---------------------------------------|---------------|
| 2-qubit (1 sp.) | Optical | 0.996 | — | $^{40}\text{Ca}^+$ | Erhard 2019 |
| | Optical | 0.993 | 50 | $^{40}\text{Ca}^+$ | Berhelm 2008 |
| | Raman | 0.9991(6) | 30 | $^9\text{Be}^+$ | NIST 2016 |
| | Raman | 0.999 | 100 | $^{43}\text{Ca}^+$ | Ballance 2016 |
| | Raman | 0.998 | 1.6 | $^{43}\text{Ca}^+$ | Schafer 2018 |
| | Raman | 0.60 | 0.5 | $^{43}\text{Ca}^+$ | Schafer 2018 |
| | μ wave | 0.997 | 3250 | $^{43}\text{Ca}^+$ | Harty 2016 |
| μ wave | 0.985 | 2700 | $^{171}\text{Yb}^+$ | Weidt 2017 | |
| 2-qubit (2 sp.) | Ram./Ram. | 0.998(6) | 27.4 | $^{40}\text{Ca}^+ / ^{43}\text{Ca}^+$ | Ballance 2015 |
| | Ram./Ram. | 0.979(1) | 35 | $^9\text{Be}^+ / ^{25}\text{Mg}^+$ | Tan 2015 |

Figure 376: some trapped ions fidelities obtained with different atoms. Source: [lecture 1](#) on trapped ions, Hélène Perrin, February 2020 (77 slides).

There's a tendency with trapped ions vendors like IonQ and Quantinuum to measure qubit fidelities with the SPAM method which encompasses the whole process from state preparation to measurement. In March 2022, IonQ tested its new barium ions and improved fidelities with a record 99,96% SPAM fidelity. Quantinuum reached simultaneously a SPAM fidelity of 99,9904% also with barium ions¹⁰³⁷, which is clearly best-in-class in the qubit world.

Connectivity. Trapped ions qubits can all be entangled with each other with using phonons or micro-waves, but it depends on how they are distributed in space¹⁰³⁸. This simplifies the implementation of many algorithms, avoiding the usage of costly SWAP gates to connect distant qubits.

No calibration. Since these qubits are atoms, they are identical and do not require calibration adjustments like with superconducting qubits whose physical properties vary from one qubit to another depending on their materials and manufacturing.

Ions variations. There are five main variations of trapped ions being used, depending on the energy transitions applied to manage the two states of a qubit¹⁰³⁹. Each of these modes correspond to different transition frequencies:

- **Zeeman qubits** use electromagnetic waves of a few MHz with magnetic field control. They are very sensitive to it but allow to have qubits with a very low error rate once this field is well controlled¹⁰⁴⁰. They are rather used in quantum sensing since their control frequency is too low to allow a precision control of several qubits close to each other.

¹⁰³⁷ See [High fidelity state preparation and measurement of ion hyperfine qubits with \$I > 1/2\$](#) by Fangzhao Alex An et al, March 2022 (5 pages).

¹⁰³⁸ See [Benchmarking an 11-qubit quantum computer](#) by Christopher Monroe et al, March 2019 (8 pages).

¹⁰³⁹ See [Ion traps you never knew existed](#) by M. Malinowski, February 2022 which makes an interesting inventory of trapped ions settings.

¹⁰⁴⁰ See [Comparing Zeeman qubits to hyperfine qubits in the context of the surface code: \$^{174}\text{Yb}^+\$ and \$^{171}\text{Yb}^+\$](#) by Natalie Brown, April 2018 (7 pages).

- **Hyperfine structure qubits** use microwaves of a few GHz and laser-based Raman transitions¹⁰⁴¹. This works with ions having a non-zero spin nucleus. The other cases concern ions with zero spin nuclei, i.e. those whose proton and neutron numbers are both even. This explains why some elements such as calcium are sometimes used in several of these categories, with different isotopes such as ⁴⁰Ca+ in optical qubits and ⁴³Ca+ in qubits of hyperfine structure. The number of neutrons in these ions changes the spin of the nucleus of atoms and its hyperfine energy states. In this category, IonQ and Honeywell are using hyperfine structure qubits driven by lasers and Oxford Ionics is using microwave gates.
- **Fine structure qubits** use submillimeter waves of a few THz.
- **Optical qubits** use photons of a few hundred THz. AQT is using this type of qubits.
- **Rydberg qubits** use so-called Rydberg energy states controlled by VUV ultraviolet rays (vacuum ultraviolet, not transmitted in air, needs vacuum), with wavelengths under 122 nm¹⁰⁴². It is used by the new startup Crystal Quantum Computing (France).

Figure 377: contains a description of these variants based on ion energy levels and transitions. On the left, a generic structure of ion energy levels with the transitions allowing the change of qubit state and those used to prepare the qubit state or to read it. These charts showing atoms electronics energy transitions including fine and hyperfine transitions are called Grotrian diagrams. In the middle and on the right, the different energy transitions used to define the $|0\rangle$ and $|1\rangle$ of the qubit. The height between the two levels characterizes the energy level that separates these two states. The higher it is, the higher the frequency used to modify the qubit state, going from radio waves of a few MHz to extreme ultraviolet in the case of Rydberg qubits.

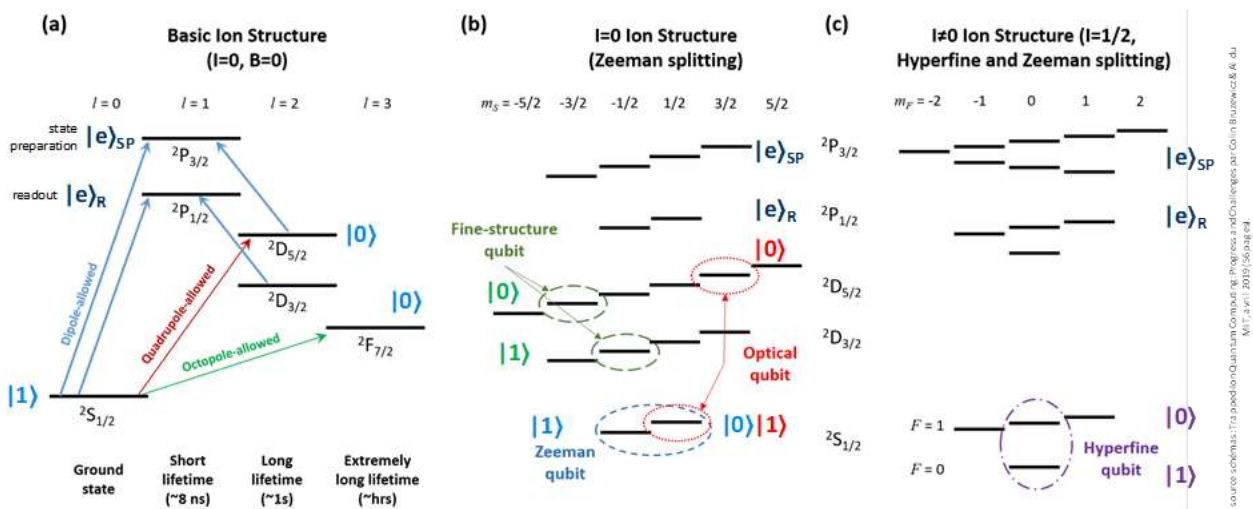


Figure 377: various types of trapped ions and their respective energy transitions. Source: [Trapped Ion Quantum Computing: Progress and Challenges](#) by Colin Bruzewicz et al from MIT, April 2019 (56 pages).

The spatial stabilization of trapped ions is achieved in two main ways with ion traps that allow individual control of their position¹⁰⁴³:

¹⁰⁴¹ See [Controlling Qubits With Microwave Pulses Reduces Quantum Computer Error Rates, Increases Efficiency](#) by Matt Swayne, 2020, which references [Robust and resource-efficient microwave near-field entangling ⁹Be+ gate](#) by G. Zarantonello, November 2019 (6 pages). See glossary for Raman transition.

¹⁰⁴² See for example [Speeding-up quantum computing using giant atomic ions](#) by Stockholm University, April 2020.

¹⁰⁴³ See many details in [Multi-wafer ion traps for scalable quantum information processing](#) by Chiara Decaroli, 2021 (248 pages).

- With a **magnetic field** and an **electric quadrupole**: these are the Penning traps, invented in 1959. Among other places, they have been tested at the ETH Zurich in Jonathan P. Home's team and in a 2D version which has the advantage of being theoretically scalable¹⁰⁴⁴.

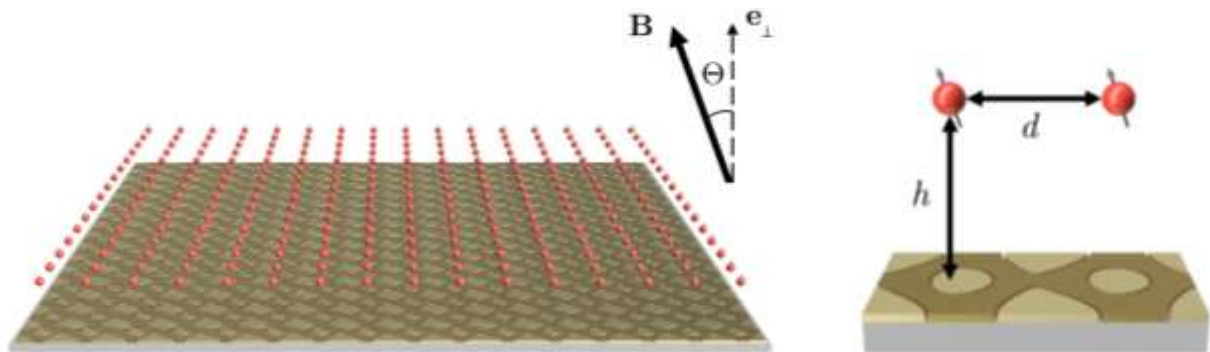


Figure 378: proposal for an array of trapped ions. Source: [Scalable arrays of micro-Penning traps for quantum computing and simulation](#) by S. Jain, Jonathan P. Home et al, April 2020 (21 pages).

- With a **variable electric field**: these are the Paul traps named after Wolfgang Paul. These traps are either linear in 1D structure (in Figure 379 in (f)) or flattened to create 2D structures. They are the most often used. The flat version corresponds to the technique used by Quantinuum and IonQ.

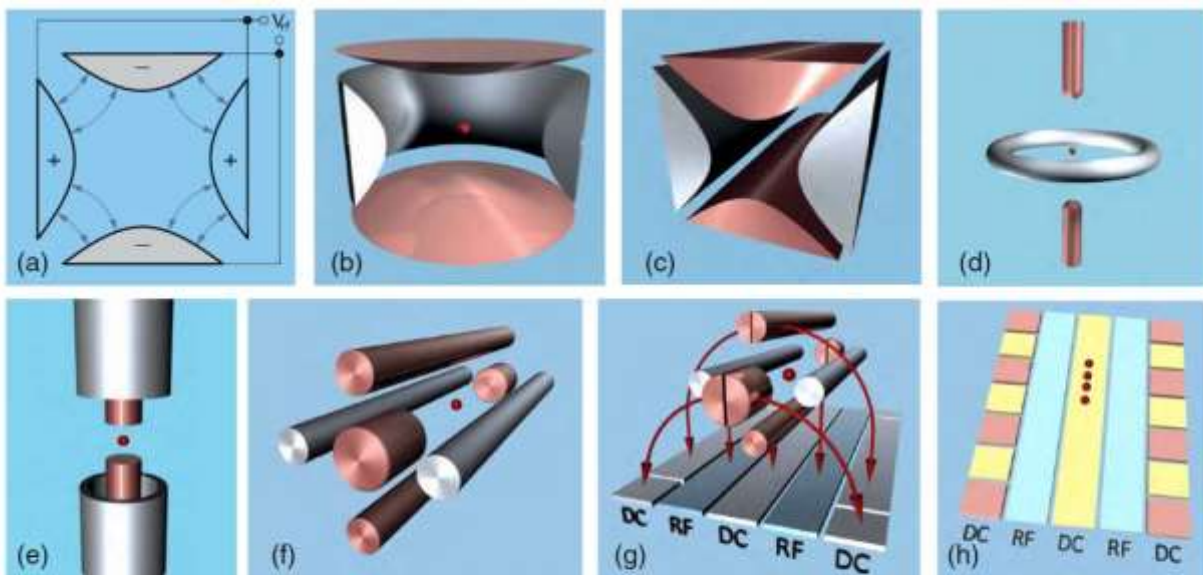


FIG. 2. (Reproduced from [68].) RF Paul trap geometries. (a) The basic concept of RF trapping, where quadrupolar fields oscillating at an RF frequency are produced using a set of (parabolic) electrodes. (b) The simplest cylindrically symmetric version of the basic RF trap. This is of the “ring and endcap” point-trap geometry. (c) The simplest translationally symmetric version of the basic RF trap. This will form a quadrupole mass filter and can be used to make a linear trap. (d,e) Topologically equivalent deformations of the geometry shown in (b). (f) Topologically equivalent deformations of the geometry shown in (c) with additional endcap electrodes added to form a four-rod, linear trap. (g) The four-rod trap in (f) may be deformed such that all electrodes reside in a single plane, forming a linear “surface-electrode trap.” (h) A subset of the electrodes in a linear trap [a surface-electrode trap is depicted here, but segmentation may be applied to other linear trap geometries, such as that shown in (f)] may be segmented to allow trapping in multiple zones, along the axial direction.

Figure 379: the various ways to trap ions. Source: [Trapped Ion Quantum Computing: Progress and Challenges](#) by Colin Bruzewicz et al from MIT, April 2019 (56 pages).

¹⁰⁴⁴ See [Scalable arrays of micro-Penning traps for quantum computing and simulation](#) by S. Jain, Jonathan P. Home et al, April 2020 (21 pages).

These various traps are implemented on integrated circuits using variations of direct current and radio-frequency electrodes and/or laser wave guides. Lasers play several roles in trapped ions control: they are used to cool the ions with the Doppler effect and by sideband cooling to slow down phonons (these are inter-ions vibrations, kind of shock waves), to initialize the energy state of the qubits to its ground $|0\rangle$ state, to create quantum gates and finally, for qubits state readout¹⁰⁴⁵.

The main disadvantage is that the solution will probably not scale well, particularly with laser light control that goes through a light splitter and some lenses to focus it on the controlled ions. The ions are aligned in rows and separated by about 2 to 5 μm .

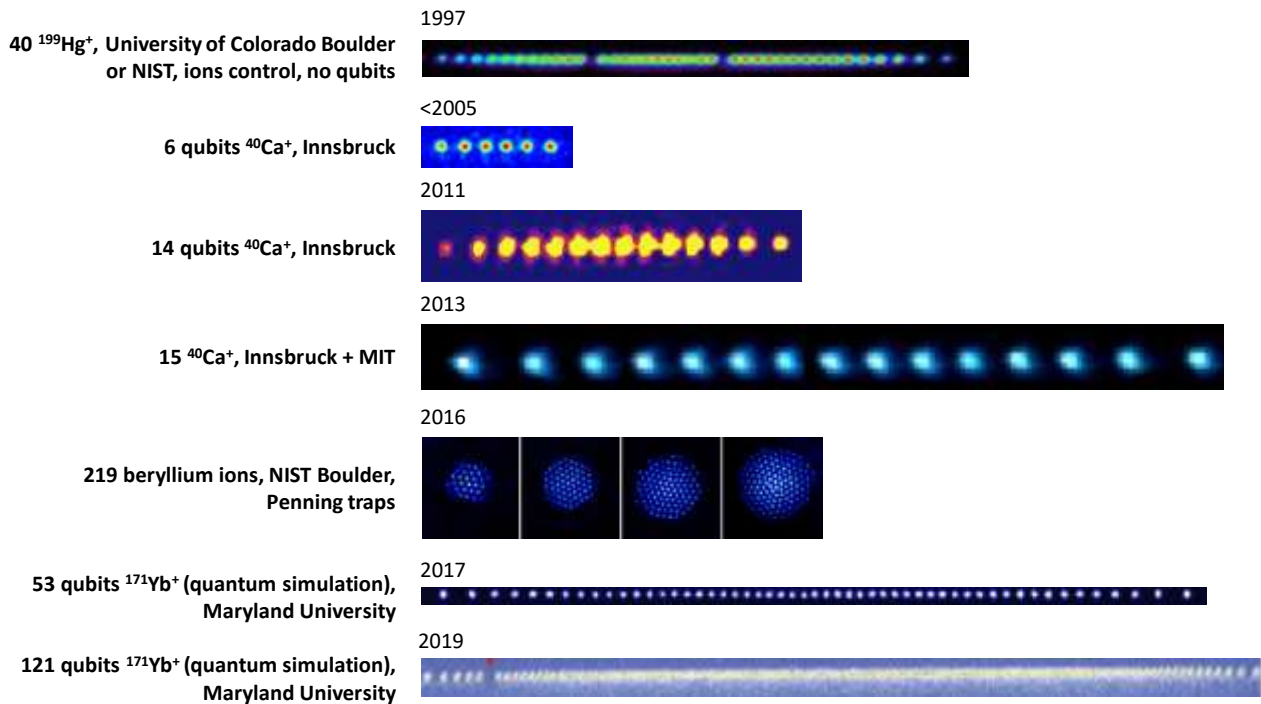


Figure 380: different lines of trapped ions over time. Compilation: Olivier Ezratty, 2020.

Temperature. Trapped ions are supposed to operate at room temperature. In practice, they generate an annoying heating effect, which is not fully explained at the moment. This requires some cooling between 4K and 10K¹⁰⁴⁶. The interest of such a cooling is also to improve the quality of the ultra-high vacuum chamber. Lasers and ions readout imagers also need some cooling at reasonable temperatures (from 10K to -35°C depending on the case).

Researchers from the University of Innsbruck and from ETH Zurich are thinking about making the trapped ion technology "portable", forgetting the vacuum system and the cryostat, necessary for their operation¹⁰⁴⁷. They are part of the EU-funded **PIEDMONS** project (E2020). It also involves Infineon Austria¹⁰⁴⁸.

¹⁰⁴⁵ See [Quantum information processing with trapped ions](#) by Christian Roos, 2012 (53 slides) on how trapped ion qubits are driven.

¹⁰⁴⁶ See [Closed-cycle, low-vibration 4 K cryostat for ion traps and other applications](#) by P. Micke et al, May 2019 (15 pages) which describes a cryostat for ion trapped processors using a pulsed head.

¹⁰⁴⁷ See [Quantum computers to become portable](#), August 2019.

¹⁰⁴⁸ See [2D Linear Trap Array for Quantum Information Processing](#) by Philip C. Holz, Rainer Blatt et al, September 2020 (20 pages).

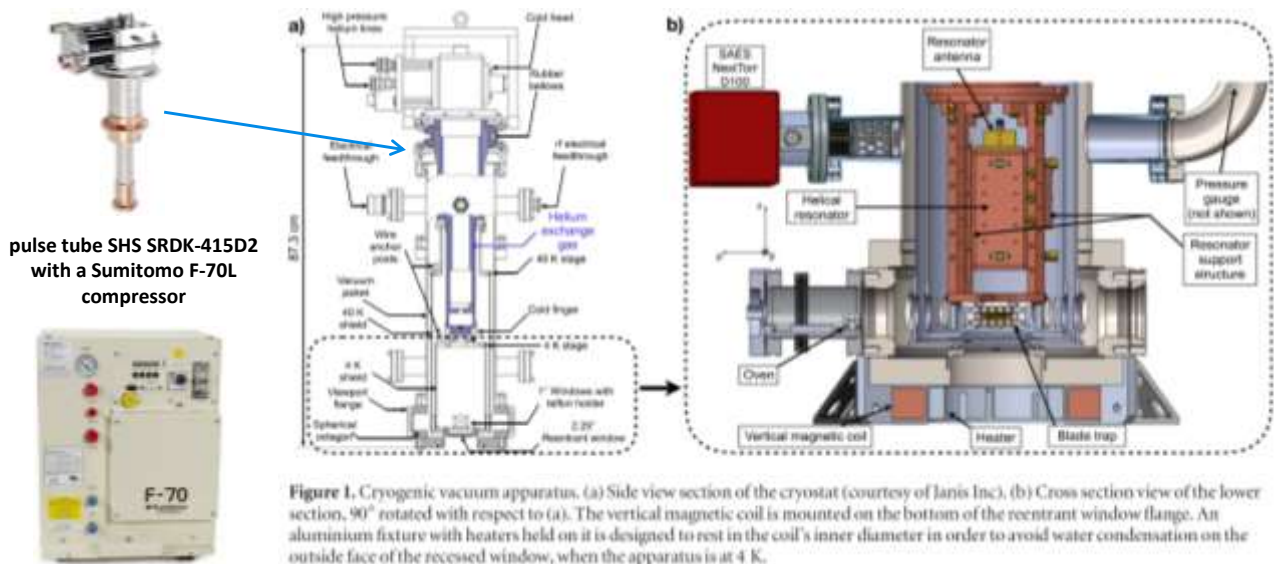


Figure 1. Cryogenic vacuum apparatus. (a) Side view section of the cryostat (courtesy of Janis Inc). (b) Cross section view of the lower section, 90° rotated with respect to (a). The vertical magnetic coil is mounted on the bottom of the reentrant window flange. An aluminium fixture with heaters held on it is designed to rest in the coil's inner diameter in order to avoid water condensation on the outside face of the recessed window, when the apparatus is at 4 K.

Figure 381: the 4K cryostat used a while ago by Christopher Monroe's team at the University of Maryland to trap more than a hundred ytterbium ions. It operated a 4.2K SHS pulse tube and a Sumitomo compressor¹⁰⁴⁹. Source : [Cryogenic trapped ion system for large scale quantum simulation](#) by Christopher Monroe et al, 2018 (17 pages).

Scale-out. Trapped ions have at least two other use cases: quantum memories, and their integration in quantum repeaters for secure quantum telecommunications, including quantum keys distribution¹⁰⁵⁰. This involves interactions between trapped ions and photons, using cavities. It is already possible to entangle trapped ions via a photonic link of several hundred meters, a feat done over a distance of 400 m at the University of Innsbruck. This would enable the creation of distributed quantum computing architectures, a plan devised by IonQ to circumvent the scalability limitations of their qubits¹⁰⁵¹.

Other avenues are explored to scale-out trapped ions processors like with shuttling ions from computing units to other computing units¹⁰⁵². This is the basis of rather old research and is still pursued practically by Quantinuum in their future 2D architecture.

¹⁰⁴⁹ See also the thesis [Towards Cryogenic Scalable Quantum Computing with Trapped Ions](#) by Matthias Brandl, 2016 (138 pages) which documents very well the overall engineering of a quantum computer based on trapped ions.

¹⁰⁵⁰ See [Single-qubit quantum memory exceeding 10-minute coherence time](#) by Ye Wang (China), 2017 (6 pages).

¹⁰⁵¹ See [Large Scale Modular Quantum Computer Architecture with Atomic Memory and Photonic Interconnects](#) by Christopher Monroe et al, 2014 (16 pages).

¹⁰⁵² See [Building a prototype for the world's first large-scale quantum computer](#), 2022, related to [Blueprint for a microwave trapped ion quantum computer](#) by Bjoern Lekitsch et al, ScienceAdvances, February 2017 (11 pages). It deals with microwave gates using a static magnetic field with high fidelities and low crosstalk, a technique proposed by Mintert and Wunderlich in 2001. It adds ions transport between trapped ions modules. Laser-based gate control doesn't scale well due to the way phonons work and also due to the complexity of laser beams alignment. They plan to use silicon circuits and X-junction plus on-chip control electronics. Trapping ions would require an area of 103.5×103.5 m² and 23x23 connected vacuum chambers corresponding to the estimate in 2017 of what was needed to factorize an RSA key of 2048 bits. Now, it's 100 times fewer qubits. It still makes 10,3x10,3 m² with a power dissipation of 300W per module, so, with 4 modules now. It is surprisingly low and deserves some recalculation. See also [A Shuttle-Efficient Qubit Mapper for Trapped Ion Quantum Computers](#) by Suryansh Upadhyay et al, April 2022 (7 pages) which is also pursuing a ions shuttling approach.

Qubit operations

The general principle of trapped ion qubits is as follows:

- **Preparation** with neutral atoms being first heated in a small heating oven and then ionized and cooled by laser beams. Ions are then confined in vacuum in different ways by a magnetic and/or electric fields with variants of Paul and Penning traps as seen earlier. Qubits initialization is relying on electric dipole or quadrupole transitions driven by lasers to set them up at the right energy level corresponding to the $|0\rangle$ ground state. All this happens in an ultra-vacuum chamber.
- **Qubit quantum state** corresponds to two relatively stable energy levels of the trapped ions that are controllable by optical or microwave transitions.
- **Single-qubit quantum gates** are activated by microwaves, lasers or magnetic dipoles electric fields.
- **Two-qubit quantum gates** often use lasers with entangled photons and exploit the phonon phenomenon that links atoms together by vibrations that propagate from one atom to another, which is valid for qubits aligned in linear Paul traps¹⁰⁵³. It however doesn't scale well beyond a couple dozen ions. More scalable variants use microwave fields distributed through the ions supporting circuit¹⁰⁵⁴ or efficiently distribute laser beams on nanophotonic circuits¹⁰⁵⁵.
- **Qubits readout** uses the detection of the cavity fluorescence with either superconducting photon detectors¹⁰⁵⁶ or CCD image sensors after ions are excited by a laser¹⁰⁵⁷. The excited ions corresponding to the $|1\rangle$ state are visible while the unexcited ions corresponding to the $|0\rangle$ state are not.



Figure 382: examples of image sensors for trapped ions qubits readout with an **Oxford Instrument Andor iXon Ultra 888 UVB** (left) and a **Hamamatsu H10682-210 PMT** (right).

Setup

The typical trapped ions setup contains a vacuum chamber containing a chipset where the ions are “floating on”. They are driven by microwave and laser pulses, thus the associated control electronics. Like with cold atoms, an imager sensor is involved in the qubit readout. Some cooling is frequently used, but at reasonable temperatures of about 4K. All of this can fit into two standard data-center racks.

¹⁰⁵³ Photon mediated entanglement was invented in 2004 by Christopher Monroe et al. See [Scalable Trapped Ion Quantum Computation with a Probabilistic Ion-Photon Mapping](#) by L.-M. Duan, B. B. Blinov, D. L. Moehring and Christopher Monroe, University of Michigan, 2004 (6 pages).

¹⁰⁵⁴ Trapped ions single and two qubit gates can be generated with only microwave magnetic fields and radiofrequency magnetic field gradients and no lasers. See [High-fidelity laser-free universal control of two trapped ion qubits](#) by R. Srinivas et al, February 2021 (40 pages).

¹⁰⁵⁵ See [Integrated optical multi-ion quantum logic](#) by Karan K. Mehta, Jonathan P. Home et al, ETH Zurich, Nature, October 2020 (12 pages).

¹⁰⁵⁶ See [State Readout of a Trapped Ion Qubit Using a Trap-Integrated Superconducting Photon Detector](#) by S. L. Todaro, David Wine-land et al, NIST, University of Colorado Boulder, University of Oregon, PRL, 2020 (7 pages).

¹⁰⁵⁷ See [Real-time capable CCD-based individual trapped ion qubit measurement](#) by S. Halama et al, April 2022 (16 pages) which compares a fast CCD camera with PMT (photomultiplier tubes) and superconducting nanowire single-photon detectors (SNSPDs). It is an Andor iXon Ultra 888 UVB from Oxford Instruments of 1024x1024 pixels and operating at -35°C and 200 frames per seconds with reasonable noise. It works in UV light. The reference PMT comparison example is a Hamamatsu H10682-210.

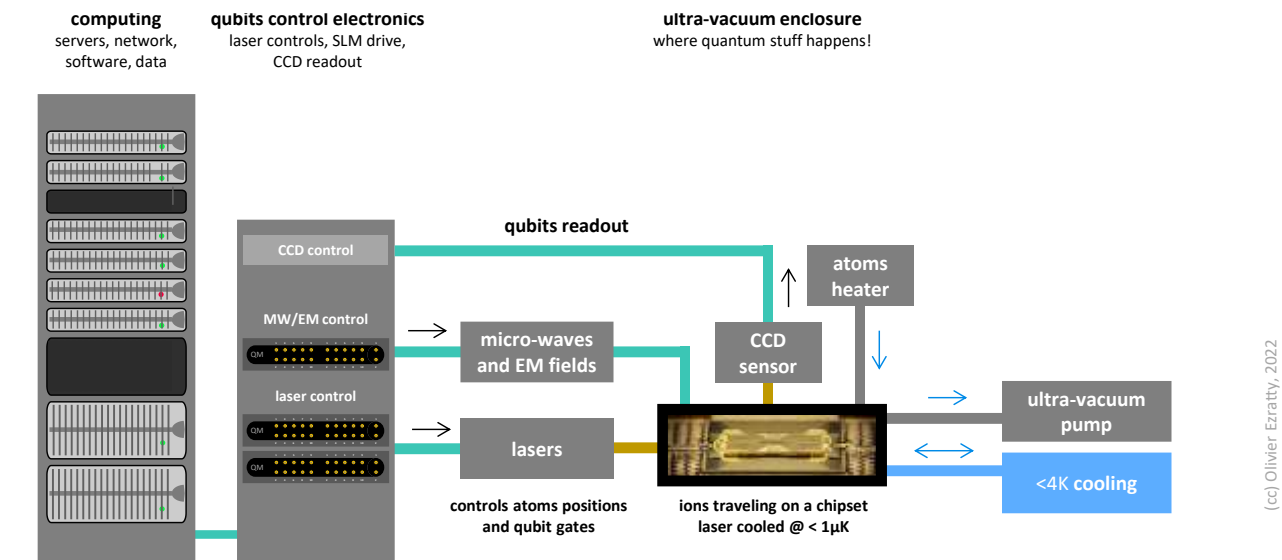


Figure 383: generic architecture of a trapped ion quantum computer which fits into a 2-rack system. (cc) Olivier Ezratty, 2022.

Research

About a hundred research teams around the world are working on trapped ion qubits in almost every country working on quantum technologies (Australia, Austria, Canada, China, Denmark, Finland, France, Germany, India, Israel, Japan, Netherlands, Singapore, Switzerland, UK, USA)¹⁰⁵⁸.

Rainer Blatt from the University of Innsbruck is one of the pioneers in this field. He created a register of 14 addressable qubits in 2011 and increased it to 20 addressable and individually controllable qubits in 2018, using calcium ions. Rainer Blatt then cofounded **Alpine Quantum Technologies** (2017, Austria) where he [characterized](#) up to 10 high quality ion trapped qubits. In 2021, his team also demonstrated the use of trapped ions to create qudits with 3, 5 and 7 levels, potentially opening the path for more powerful trapped ion based quantum computing¹⁰⁵⁹.

Quantum simulation using trapped ions, and an Ising model as with the D-Wave, is also investigated by some laboratories such as at **ETH Zurich** in Jonathan P. Home's Trapped Ions Quantum Information Group (TIQG), the **University of Maryland**, elsewhere in the USA¹⁰⁶⁰ and also in China¹⁰⁶¹.

In May 2020, Wesley Campbell's **UCLA** team associated with UNSW announced that they had stabilized barium ions ($^{133}\text{Ba}^+$) to build quality qubits in a linear trap¹⁰⁶². The quality of these barium ions is compared to that of 2,014 qubits with a 10-fold improvement. This quality is evaluated only with the SPAM indicator which measures a fidelity on a qubit after preparation, some initialization single qubit gates and measurement (SPAM = "state preparation and measurement").

¹⁰⁵⁸ There were 98 research laboratories in the world working on trapped ions in 2020. See this table listing them all in [List of Ion Trapping Groups](#), February 2020.

¹⁰⁵⁹ See [A universal qudit quantum processor with trapped ions](#) by Martin Ringbauer et al, September 2021 (14 pages). 8 levels for a calcium-based trapped ion qubit.

¹⁰⁶⁰ See [Digital Quantum Simulation with Trapped Ions](#) by Kenny Choo and Tan Li Bing, 2016 (29 slides) and [Programmable Quantum Simulations of Spin Systems with Trapped Ions](#) by Christopher Monroe et al, 2019 (42 pages) and a follow-up with [Programmable quantum simulations of bosonic systems with trapped ions](#) by Or Katz and Christopher Monroe, July 2022 (7 pages).

¹⁰⁶¹ See [Probing critical behavior of long-range transverse-field Ising model through quantum Kibble-Zurek mechanism](#) by B.-W. Li et al, August 2022 (10 pages).

¹⁰⁶² See [Physicists develop world's best quantum bits](#) by Stuart Wolpert of UCLA, May 2020 which refers to [High-fidelity manipulation of a qubit enabled by a manufactured nucleus](#) by Justin Christensen et al, May 2020 (5 pages). First precaution of use: identify the author of the article. It happens to be a certain Stuart Wolpert from UCLA, in charge of media relations at the University where the published work comes from. So he does the PR for the laboratory and publishes his article on a site where it is possible (Physorg).

Let's also mention the **IQOQI** (Austria, see Rainer Blatt, one of their laboratories) and the **IQST** (Germany), and their calcium based 20 qubits prototype¹⁰⁶³ as well as the Ion Quantum Technology Group from the **University of Sussex** (UK) that is run by Winfried Hensinger and its 10 qubits prototype, proposing an architecture design to scale up to 1,000 qubits through a cluster of quantum processors¹⁰⁶⁴. The group led to the creation of the startup **Universal Quantum** (2019, UK).

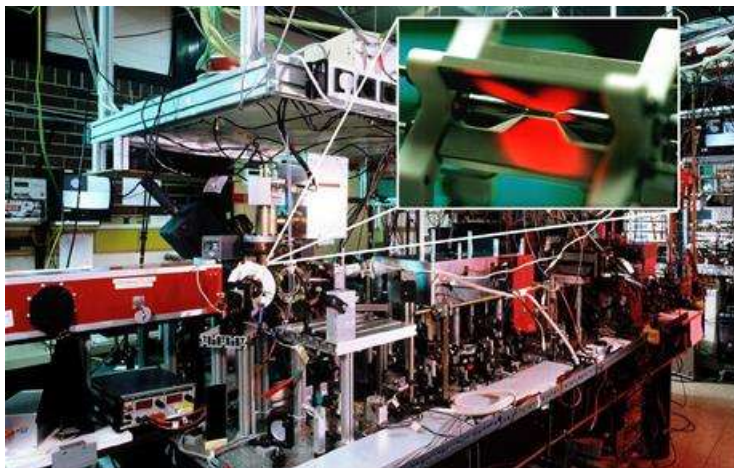


Figure 384: Rainer Blatt's lab in Innsbruck.

In March 2021, the DoE **Sandia Labs** launched the QSCOUT (Quantum Scientific Computing Open User Testbed), a cloud quantum computing resource available to selected researchers from universities and other government research agencies¹⁰⁶⁵. It is an ^{171}Yt based trapped ions system of 3 qubits used for benchmarking and for algorithms development, particularly in computational chemistry. It will later be expanded to a 10 and then 32 bits system, by 2023, on par with 2021's IonQ's capacity. At a low-level, this system is programmed with the in-house assembly language Jaqal ("Just Another Quantum Assembly Language").

Also, in the USA, a team from **Georgia Tech** led by Creston Herold and including NIST and DoE Oak Ridge's quantum lab and funded by DARPA is working on rare-earth trapped ion systems using the less used Penning traps, that controls the position of the trapped ions with magnetic and electric fields, using permanent magnets made of neodymium and samarium cobalt¹⁰⁶⁶. At this point, they control 10 trapped ions.

The European Flagship includes the **AQTION** project, which is led by the University of Innsbruck and has a budget of €9.57M. The objective is to reach 50 operational qubits to prepare the next phase, beyond 100 qubits, by adopting a distributed architecture with photonic links. Alpine Quantum Technologies (AQT), the University of Oxford, ETH Zurich, Fraunhofer IOF and Atos are participating. Atos works on the solution software stacks and applications.

In **Israel**, a team of researchers from the Weissman Institute announced in 2022 the creation of the first local quantum computer using 5 strontium ions¹⁰⁶⁷. It is less than stellar at this point. They plan to reach 64 qubits someday.

In **Russia**, the Russian Quantum Center, the P.N. Lebedev Physics Institute of the Russian Academy of Sciences and Rosatom presented in 2021 a prototype of a trapped ions computer, starting with 4 qubits. Looks like they are late in the catch-up game behind the USA, UK and Austria!

¹⁰⁶³ They coauthored [Observation of Entangled States of a Fully Controlled 20-Qubit System](#), April 2018 (20 pages).

¹⁰⁶⁴ See [Blueprint for a microwave trapped ion quantum computer](#) by Winfried Hensinger et al, 2017 (12 pages) and their review paper [Quantum control methods for robust entanglement of trapped ions](#) by C H Valahu, Winfried Hensinger et al, Journal of Physics B: Atomic, Molecular and Optical Physics, 2022 (27 pages).

¹⁰⁶⁵ See [Rare open-access quantum computer now operational](#), Sandia Labs, March 2021.

¹⁰⁶⁶ See [DARPA Probing Quantum Computing Capabilities](#) by Meredith Roaten, June 2022 and [Universal Control of Ion Qubits in a Scalable Microfabricated Planar Trap](#) by Creston D. Herold et al, February 2016 (17 pages). Back in 2016, their single qubit gate fidelities was 97% which is far from being stellar for trapped ions.

¹⁰⁶⁷ See [Trapped Ion Quantum Computer with Robust Entangling Gates and Quantum Coherent Feedback](#) by Tom Manovitz, Yotam Shapira, Lior Gazit, Nitzan Akerman and Roei Ozeri, March 2022 (12 pages).

Vendors



IonQ (2016, USA, \$736M¹⁰⁶⁸) is a spin-off from the University of Maryland specialized in the design of universal quantum computers based on ytterbium trapped ions, and later, barium ions¹⁰⁶⁹.

Co-founded by Christopher Monroe, professor at the university who is also their Chief Scientist, the company CEO is Peter Chapman, a former e-commerce executive at Amazon. IonQ's cap table includes Google Ventures, Amazon, Samsung Ventures, Microsoft, Lockheed Martin, Bosch and HPE. In June 2020, they created an advisory board including David Wineland, Umesh Vazirani, Margaret Williams (ex Cray) and Kenneth Brown (Duke University). In March 2021, IonQ announced a new round of funding with a merger agreement through the Special Purpose Acquisition Company (SPAC) mechanism, with the fund dMY Technology Group III that will yield a \$650 million investment. The funding was made of \$350M coming from investors including Hyundai, Kia Corporation¹⁰⁷⁰ and Breakthrough Energy Ventures. The remaining \$300M came from dMY and an IPO¹⁰⁷¹. The IPO was finalized in October 2021.

IonQ's architecture use 1D arrays of ions of variable length. They are controlled by lasers for both cooling, quantum gates and readout. Trapped ions enable all-to-all connectivity between ions, making it easier to run algorithms and avoiding the usage of costly SWAP gates.



Figure 385: IonQ trapped ion drive system, the small vacuum enclosure where the ions are located, and the chipset controlling the ions position. Sources: IonQ and [Ground-state energy estimation of the water molecule on a trapped ion quantum](#) by Yunseong Nam, Christopher Monroe et al, March 2019 (14 pages).

This allows implementing a very good optimization of quantum algorithms to minimize the number of gates to be executed as shown in the example in Figure 386.

But, as with all trapped ions qubits QPUs, this is achieved at the expense of relatively slow gates in comparison with superconducting and silicon qubits QPUs. The scalability of trapped ions is being questioned and it shows-up well in the history of the company. At the beginning of 2018, they announced a record of 53 coherent and entangled qubits but these were used for quantum simulation and not with gate-based computing.

¹⁰⁶⁸ This amount includes \$84M from VCs and the 2021 SPAC. It excludes the total \$165M grants the company and Christopher Monroe's lab in Maryland University got from the US government, per their 2021 investor presentation.

¹⁰⁶⁹ See [A Reconfigurable Quantum Computer](#) by David Moehring, 2017 (20 slides).

¹⁰⁷⁰ They seem to have closed links with South Korea. These investors add up with a partnership with Q Center. See [IonQ and South Korea's Q Center Announce Three-Year Quantum Alliance](#), January 2021. To provide to the Q Center students to the IonQ computer online.

¹⁰⁷¹ See [QC ethics and hype: the call is coming from inside the house](#) by Scott Aaronson, October 2020, who found this IPO to be pushing the envelope of bullshit a bit too far.

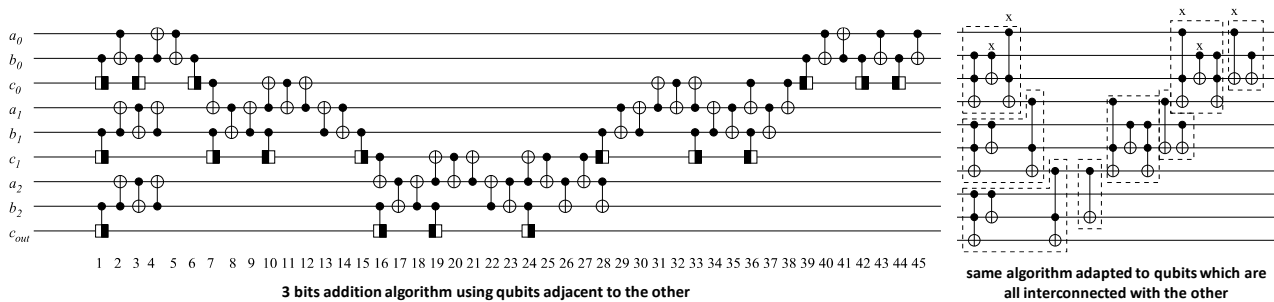


Figure 386: how the good connectivity with trapped ions enables a good compression of the code. Source: [Fast Quantum Modular Exponentiation](#) by Rodney Van Meter and Kohei Itoh, 2005 (12 pages).

At the end of 2018, they said they had reached 79 qubits associated with 160 storage qubits but with not fidelity numbers¹⁰⁷². In 2019, they had 11 characterized qubits¹⁰⁷³.

In October 2020, IonQ announced that it had created the world's most powerful quantum computer with 32 qubits and a quantum volume of 4,000,000 but it took over a year and a half for this system to become live and tested¹⁰⁷⁴ and made available on Amazon Braket, Microsoft Azure Quantum and Google cloud offerings. They claimed to handle error correction codes with 13 (and sometimes, 16) physical qubits per logical qubits. They also announced the creation of a Quantum Data Center sized to host 10 of their quantum computers.

In December 2020, IonQ unveiled its 5 years roadmap with plans to use rack-mounted modular quantum computers small enough to be networked together in a datacenter by 2023. IonQ adopted a new benchmark metric of their own: algorithmic qubits, using \log_2 of IBM's quantum volume and a different calculus mode that we cover in the benchmarking section of this book, using a set of QED-C benchmarks.

Their 32 qubits support 22 algorithmic qubits with plans to reach 29 algorithm qubits by 2023, 64 by 2025 with using a 16:1 error-correction encoding (meaning: 16 physical qubits per logical qubits). Later on, they will rely on a 32:1 ratio.

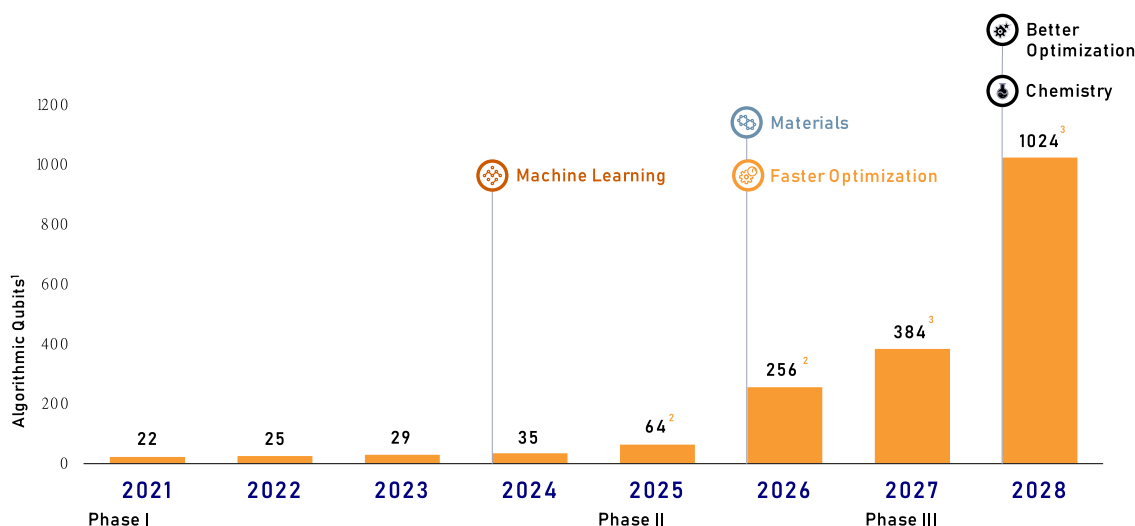


Figure 387: IonQ's qubits roadmap as published in March 2021.

¹⁰⁷² See [IonQ Has the Most Powerful Quantum Computers With 79 Trapped Ion Qubits and 160 Stored Qubits](#) by Brian Wang, December 2018.

¹⁰⁷³ See [Benchmarking an 11-qubit quantum computer](#) by K. Wright et al, November 2019.

¹⁰⁷⁴ See [IonQ Unveils World's Most Powerful Quantum Computer](#), IonQ, October 2020.

Then, they expect to scale beyond 64 and reach a broad quantum advantage with 256 then 1024 algorithmic qubits by 2026 and 2028. The caveat is that this can be achieved only with scaling-out their quantum processors, assembling several units of 64 qubits through photonic links in a distributed computing manner. Something that has not been tested yet beyond one-to-one qubit connectivity¹⁰⁷⁵.

IonQ announced in August 2021 their Reconfigurable Multicore Quantum Architecture (RMQA) detailing how they would create 64 ions chipsets ([video](#)). It would assemble 4 chains or lines of 16 ions, 12 being usable as qubits and the 4 remaining for cooling, in a single chipset manufactured on a glass support (Evaporated Glass Traps) replacing their previous silicon-based platform built by Sandia Labs and Honeywell. These chunks of 16 ions can be moved around, paired and entangled, to create dynamic 32 ions units. IonQ stated that this architecture could scale-up and support even more blocks of 16 ions. Well, if that actually works in practice, why not!

A team associating IonQ, Duke University in Durham and ColdQuanta published an interesting paper describing the architecture of a trapped ions systems cryostat from Montana Instruments that is optimized to minimize the vibrations coming from the pulse tube. This seems to be one of the figures of merit to ensure the stability of the trapped ions qubits and their control devices like lasers¹⁰⁷⁶. The qubits are cooled at 5K while laser-based cooling using the Doppler effect cool it at an even lower temperature.

In February 2022, IonQ and Duke University presented a new way to create 3-qubit gates including a Toffoli gate using state squeezing¹⁰⁷⁷. This sort of gate is interesting since it can be the basis for a universal gate-set enabling fault-tolerance. It can help speeding up many algorithms including Grover and variational quantum eigensolvers (VQEs).

In December 2021, after they had finalized their SPAC and IPO, IonQ announced they were switching from ytterbium to barium ions (precisely $^{133}\text{Ba}^{+}$ ¹⁰⁷⁸). The reasons were well explained: it provides better gates and readout fidelities and the ions are primarily controlled with visible light rather than ultraviolet light, using standard silicon photonics technology, which can better enable QPU photonics interconnect¹⁰⁷⁹. They also secured the provisioning of these atoms with a partnership with **DoE's** PNNL (Pacific Northwest National Laboratory) in February 2022.

¹⁰⁷⁵ The associated concepts were laid out in [Scaling the ion trap quantum processor](#) by Christopher Monroe and J. Kim, Science, 2013 (7 pages). It consists in associating one qubit of two ions QPUs with probabilistic entangled photons. See also [Large-scale modular quantum-computer architecture with atomic memory and photonic interconnects](#) by Christopher Monroe, Robert Raussendorf et al, PRA, 2013 (16 pages).

¹⁰⁷⁶ See [High stability cryogenic system for quantum computing with compact packaged ion traps](#) by Robert F. Spivey et al, August 2021 (12 pages). ColdQuanta seems involved here given a cold atoms system can reuse some of the experimental setting crafted for trapped ions. Interestingly, in its 2021 investor presentation, IonQ pretended that their system was operating at room temperature!

¹⁰⁷⁷ See [SNS-body interactions between trapped ion qubits via spin-dependent squeezing](#) by Or Katz, Marko Cetina and Christopher Monroe, February 2022 (7 pages).

¹⁰⁷⁸ See [Ba-133: the Goldilocks qubit?](#) by UCLA Hudson Lab.

¹⁰⁷⁹ See [IonQ Announces New Barium Qubit Technology, Laying Foundation for Advanced Quantum Computing Architectures](#), IonQ, December 2021.

On May 3rd, 2022, IonQ was literally attacked by a short-seller financial company, **Scorpion Capital**, which published a scathing report on their business, presented as a scam¹⁰⁸⁰.

This 193-page report was very long, apparently detailed and based on many interviews. But it was misplaced.

It did criticize IonQ wrongly on many points like when explaining that quantum computers couldn't even do a 1+1 calculation. They pinpointed exaggerations that can be found in IonQ investor March 2021 presentation. They even said that their 32-qubit system was non-existent (which is not true at all). They also highlighted that their ions control chipset was produced by Sandia Labs, a DoE lab operated by Honeywell, but it was not a secret. The same with **Hyundai** being both one of their investors and also a customer, on far-fetched use-case plans related to battery designs. They could have been harsh on their aggressive roadmap, their scalability goals and their related QPU interconnect plans but lacked scientific background to do so¹⁰⁸¹.

All of this was border line defamation as was shown later. IonQ was then defended by preeminent quantum computing analysts¹⁰⁸². A couple days later, IonQ announced the "select" availability of their 31 bits Forte system a couple months after having released its 23-qubits Aria system supporting 20 algorithmic qubits (as of August 2022¹⁰⁸³). "Select" means, only for selected developers and customers, general availability being planned for 2023, a common and cautious practice with quantum hardware vendors. The system introduces an Acousto-Optic Deflector (AOD) which dynamically directs laser beams towards individual ions to drive qubit gates and supports up to 40 ions.

In November 2019, **Microsoft** announced the integration of IonQ's quantum accelerator support into its Azure Quantum cloud offering and its Q#, QDK and Visual Studio development tools. All this was made available to developers from late spring 2020. IonQ is also proposed by **Google** in its own cloud offering, on top of **Amazon** AWS Braket. IonQ became in 2021 the only quantum computer vendor available on Amazon, Google and Microsoft clouds (with 11 qubits, being extended to 32 qubits).

On the use cases side, IonQ works with a couple customers like **Goldman Sachs** on financial services on top of the above mentioned Hyundai. They also partner with **Accenture** to develop customer applications.

In September 2021, IonQ announced the creation of a joint laboratory with the University of Maryland (UMD), the **Q-Lab**, with \$20M funding. Among other things, the lab is tasked with training UMD students on quantum computing. In 2022, they also established business development subsidiaries in Germany and Israel.

IONQ (NYSE: IONQ)

The "World's Most Powerful Quantum Computer" Is A Hoax With Staged Nikola-Style Photos – An Absurd VC Pump With A Recent Lock-Up Expiration Takes SPAC Abuses To New Extremes

- A part-time side-hustle run by two academics who barely show up, dressed up as a "company"
- A useless toy that can't even add 1+1, as revealed by experiments we hired experts to run
- Fictitious "revenue" via sham transactions and related-party round-tripping
- A scam built on phony statements about nearly all key aspects of the technology and business
- CEO appears to be making up his MIT educational credentials

\$1.6B market cap | \$8/share | ADV 6.4MM shares | Short interest 7mm shares

Figure 388: Scorpion Capital review cover page with extreme and misleading statements.

¹⁰⁸⁰ See [The "World's Most Powerful Quantum Computer" Is A Hoax With Staged Nikola-Style Photos – An Absurd VC Pump With A Recent Lock-Up Expiration Takes SPAC Abuses To New Extremes](#) by Scorpion Capital, May 2022 (183 slides).

¹⁰⁸¹ I mention this in the paper [Mitigating the quantum hype](#), January 2022 (26 pages) that is quoted in Scorpion's presentation on slide 14. They may have just read its title!

¹⁰⁸² See [A short report has placed a spotlight on IonQ, a quantum computing champion. This should not deflect long term interest in this or other quantum technologies](#) by David Shaw, Doug Finke and André M. König, May 2022.

¹⁰⁸³ See [IonQ Aria: Past and Future \(Part Two\)](#) by IonQ, August 2022.



Quantinuum (USA/UK) is the result of the merger in June 2021 of Honeywell Quantum Systems (USA, a branch of Honeywell) and the software company Cambridge Quantum Computing (UK), with an investment of \$300M for a stake of 55% for Honeywell in the resulting company¹⁰⁸⁴. The Quantinuum renaming occurred in December 2021.

Quantinuum's CEO is Ilyas Khan who previously was the founder and CEO of CQC. The company now has more than 600 people overall. Honeywell started working in quantum computing in 2016 in "stealth" mode. Their team came in particular from the NIST Boulder lab and the University of Colorado with some alumni from the University of Maryland and Christopher Monroe's team (IonQ). In March 2020, they announced the development of a quantum computer that was bound to become be "the most powerful in the world", doubling the power of the previous record that was then held by IBM¹⁰⁸⁵. The initial announcement dealt with a four-qubit trapped ions-based quantum processor¹⁰⁸⁶, its power being evaluated using IBM's quantum volume benchmark.

Trapped ion QCCD is the trapped ions technique they are using (for "quantum charge-coupled device"). It uses ytterbium-based ions coupled with barium ions to cool the device. This technique was developed in 2002 by Christopher Monroe, David Wineland and Dave Kielpinski¹⁰⁸⁷. They are reusing many other works from various research laboratories spread out between 2008 and 2012.

Ions are generated from a jet of collimated atoms obtained by heating a solid ytterbium target. They are then "hit" by a laser, which removes an electron from the valence layer of the atom (the last one). Only one electron remains in this layer, giving rise to an ion with a positive charge, Yb^+ . The laser cooling of these ions is well-controlled thanks to their favorable energy level pattern. Thanks to their electrical charge, it is possible to trap and move these atoms using electrostatic and radiofrequency potentials. The ions quantum states correspond to two "hyperfine" energy states related to the interaction between the magnetic moment of the nucleus and that of the electrons of the ion. These hyperfine levels are also used in cesium atomic clocks. The transition frequency between the two hyperfine levels of ytterbium is 12.6 GHz¹⁰⁸⁸. The hyperfine states of the ytterbium ion are well suited for quantum computation because they are very stable, which allows them to have a long coherence time.

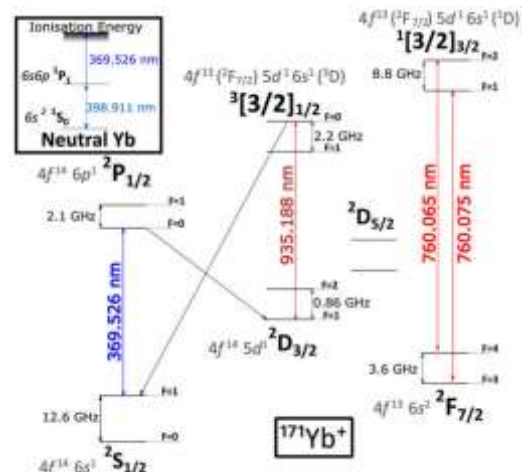


Figure 389: ytterbium atomic transitions used by Quantinuum. Source: [Laser-cooled ytterbium ion microwave frequency standard](#) by S. Mulholland et al, 2019 (16 pages).

¹⁰⁸⁴ See [Honeywell Quantum Solutions And Cambridge Quantum Computing Merge With Go-Public In Mind](#) by Paul Smith-Goodson, June 2021.

¹⁰⁸⁵ See [Honeywell Achieves Breakthrough That Will Enable The World's Most Powerful Quantum Computer](#) and [How Honeywell Made the Leap into Quantum Computing](#) by Honeywell, March 2020. In Honeywell [has it created the world's most powerful quantum computer](#), March 2020, I analyze the ad in detail, with the text embedded in the book as a compacted version.

¹⁰⁸⁶ The performance is described in detail in: [Demonstration of the QCCD trapped ion quantum computer architecture](#) by J. M. Pino et al, 2020 (8 pages). This can be complemented by the presentation [Shaping the future of quantum computing](#) by Tony Uttley, the head of Honeywell's quantum team at the Q2B conference at QC Ware in California in December 2019 ([slides](#)).

¹⁰⁸⁷ It is described in [Architecture for a large-scale ion-trap](#), 2002 (4 pages).

¹⁰⁸⁸ See [Laser-cooled ytterbium ion microwave frequency standard](#) by S. Mulholland et al, 2019 (16 pages).

Shuttling ions is a technique used to handle their connectivity. This is a rare case of shuttling qubits, the other one being shuttling electrons that still is in research labs. Usually, qubits based on electrons, cold atoms or ions don't move (too much) where they are installed. This idea was proposed in 2002 by Dave Wineland and co. This was the first working shuttling ions setup.

Their system prepares ytterbium atoms, ionizes them and sends them into a hole that feeds the chipset. It then uses about ten to twelve ions storage and sorting areas (in orange, yellow and blue in Figure 390).

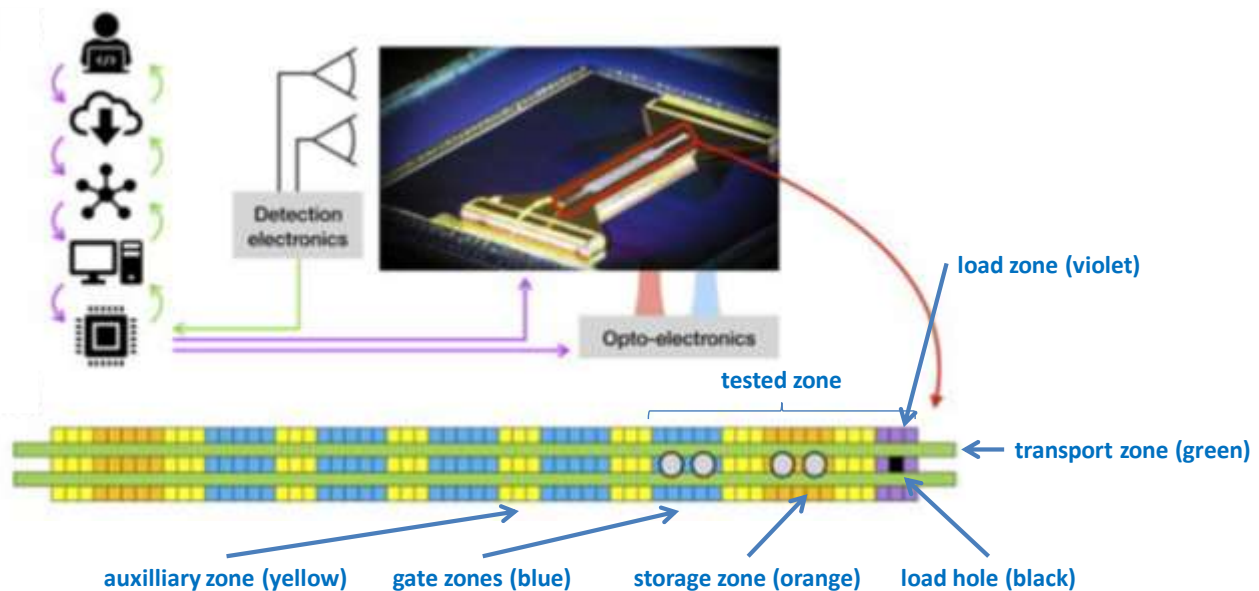


Figure 390: overall control architecture in 1D versions of Quantinuum's trapped ions, as presented in 2020.

The ytterbium ions are confined above a rail of three rows of electrodes whose variable voltage allows to control their position and to move them laterally. Their aim is to be able to demonstrate logical operations between several qubits while moving them at will between storage areas and interaction areas during operations.

Their initial system was using 198 direct current (DC) electrodes for controlling the displacement and positioning of ytterbium ions coupled with barium ions used for cooling. The chip uses cryogenic surface traps that dynamically rearrange the positioning of the ytterbium/barium ion pairs and implement quantum gates running in parallel on several areas of the circuit. Ions circulate above the green band, allowing arbitrary movements of the ions along the band. Once positioned, they are transferred to the middle band to get submitted to a single qubit quantum gate, or in the side bands for two-qubits quantum gates, as explained in the diagram below. One of these operations is a SWAP gate that allows the ions to be physically interchanged.

Slow gates. The disadvantage of the technique is its slow quantum gates. The time required to configure the ions to create a quantum gate is 3 to 5 ms, which is not negligible, especially for algorithms that require a large number of quantum gates.

Cooling. The system operates at a temperature of 12.6K and with a temperature stability of 2mK which avoids disturbing the ions and their superposed and entangled quantum states. Helium cooling is complemented by a so-called "sympathetic cooling" technique which combines the use of Doppler effect and Raman cooling on the barium ions next-door to the ytterbium ions. The Coulomb interaction between the barium ions cools the ytterbium ions next to the barium ions. A barium ion cooling operation takes place before each two-qubit gate execution. Ion laser cooling has been operating at room temperature for more than 30 years. Like many research groups, they cool the ion trap to 12.6K to minimize the effect of abnormal ions heating, which is a major problem that is not fully understood. This abnormal heating is greatly reduced when the trap is cooled.

Qubit gates. The system is built around four-qubit chunks and uses one- and two-qubit quantum gates that are activated by lasers, via the Raman effect that requires a pair of beams. The single-qubit gates are activated by a pair of 370.3 nm Raman beams in circular polarization. The system allows the generation of X, Y and Z gates for which quarter and half turns are performed around the three axes of the Bloch sphere. These rotations are done with very high precision according to Honeywell. This ensures a minimum error rate for single-qubit quantum gates.

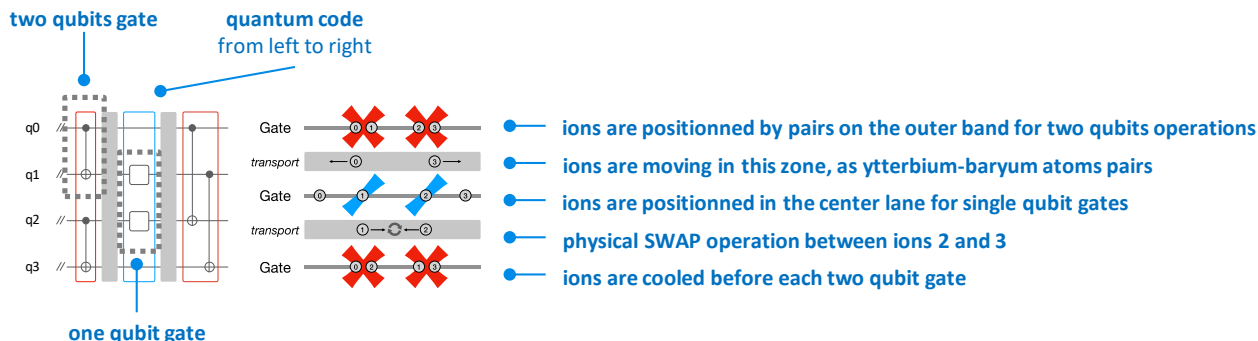


Figure 391: how single and two-qubit gates are implemented in Quantinuum trapped ions systems. Source: Honeywell, 2020.

Two-qubit gates use two additional pairs of laser beams that act on pairs of ytterbium atoms that have been brought closer together by the circuit's positioning control electrodes. Two ions are thus moved by the electrodes into the same potential well before being coupled by laser. The qubits can then be separated and moved elsewhere to interact with other qubits. I wrote all of this in 2020 and presume it has not changed since then.

Qubits readout is performed with a classical imager that detects the energetic state of the ions via their laser-activated fluorescence. This imager is a PMT array, i.e. a linear array of photomultipliers (Photo-Multiplier Tubes). Their architecture allows a qubit readout during processing, without disturbing the neighboring qubits. This would allow the implementation of conditional logic, with IF THEN ELSE like with classical programming. They are also using the mid-circuit measurement and qubit reuse technique (MCMR) which can be used to optimize the length of quantum algorithms.

The system includes an FPGA programmable electronic circuit for qubits controls, sitting outside the cryogenic enclosure.

Qubit fidelities seem very good. They launched their 6-qubit H0 system in June 2020, then their 10-qubits H1 system in October 2020 with an initial quantum volume of 128 (7 qubits x 7 gates depth). Their quantum volume reached 512 in March 2021 (9x9 qubits with 10 qubits). Single-qubit gate fidelity were above 99.991% and two-qubit gate fidelity above 99.76% while readout fidelity is at 99.75% with a measurement crosstalk at 0.2%, characterized as the decay of a qubit coherence in an equal superposition state, while repeatedly measuring the nearest qubit¹⁰⁸⁹. In July 2021, HQS announced the creation of the first logical qubits using color codes with their 10 trapped ions qubits¹⁰⁹⁰.

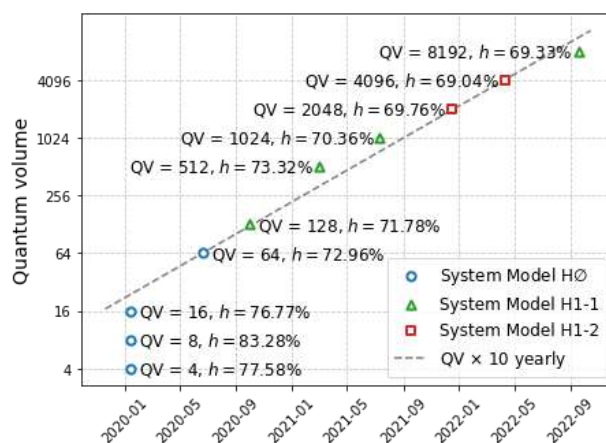


Figure 392: evolution of Quantinuum systems quantum volume. Source: [Quantinuum Sets New Record with Highest Ever Quantum Volume](#), Quantinuum, September 2022.

¹⁰⁸⁹ See [Get to Know Honeywell's Latest Quantum Computer System Model H1](#) by Honeywell, October 2020.

¹⁰⁹⁰ See [Realization of real-time fault-tolerant quantum error correction](#) by C. Ryan-Anderson et al, HQS, July 2021 (22 pages).

As of April 2022, they had 12 running qubits reaching a quantum volume of 2^{12} with their System Model H1-2. It is the only quantum processor where a quantum volume is reached with all its available qubits. Their related fidelities were 99.994% for single-qubit gates, 99.81% for two-qubit gates and 99.72% for qubits readout¹⁰⁹¹. Meanwhile, their H1-1 system launched in June 2022 has 20 qubits (despite a lower “version” number), which enabled them in September 2022 to reach a QV of 8,192 (2^{13})¹⁰⁹². This system adds arbitrary angle two-qubit gates which helps shorten the length of many algorithms, particularly those relying on a QFT (quantum Fourier transform).

From 1D to 2D. For now, Quantinuum is using a 1D trapped ion bar. They plan to adopt a 2D bar layout that would allow them to move the ions in two directions, and accumulate more of them and connect them with their neighbors in two dimensions¹⁰⁹³.

Partnerships. Quantinuum initially touted several partnerships: with **Microsoft**, for the integration of its systems in Azure Quantum which became operational in July 2020, an investment in **Cambridge Quantum Computing** (2014, UK, which they later merged with) and **Zapata Computing** (2017, USA, \$64M). In February 2022, **IBM** invested about \$25M in Quantinuum, probably more interested by its software branch (CQC) with which they had been partnering for a while.

Their first customers include **DHL**, **Merck**, **Accenture** and **Samsung**, who works on new batteries designs and **JPMorgan Chase** to create quantum algorithms in the financial sector. All of this for pilot projects. 12 or 20 qubits are way too few to enable production grade applications. They also work with **JSR Corporation** (Japan) to improve semiconductor design and research with organic and inorganic materials. In May 2022, Quantinuum launched InQuanto, a quantum computational chemistry software platform that was developed with the support of **BMW**, Honeywell, **JSR**, **Mitsui & Co**, **Nippon Steel Corporation** and **TotalEnergies**. The platform makes it possible to associate various quantum algorithms coupled with chemistry-specific noise-mitigation techniques running on NISQ systems. It also breaks down larger problems into smaller subproblems that fits existing NISQ machines. InQuanto is based on Quantinuum’s open source toolkit **TKET**, which had been downloaded 500,000 times as of September 2022. You can wonder whether there are that many quantum developers in the world!

Quantinuum is investing a lot in QNLP (quantum natural language). They released lambeq in March 2022, a Python library that “*converts any natural language sentence into a quantum circuit*” that contains Bobcat, a neural-based Combinatory Categorical Grammar (**CCG**) parser, Bobcat. It is used to pre-process natural language training data to be subsequently used for various NLP applications (classification, summaries, etc).

In July 2022, a team assembling researchers from **JP Morgan Chase Bank** and the **University of Maryland** published an amazing paper saying that a (Quantinuum) quantum computer may be better at summarizing long documents¹⁰⁹⁴. That was not exactly true. First, it was a hybrid algorithm with a lot of classical data preparation. The classical part analyzed a dataset of 300,000 news articles from CNN and the Daily Mail and precomputed it with a BERT NLP classical deep learning model that handles sentences extraction and converts them into vectors. Second, the experiment worked to summarize text from respectively 20 to 8 and 14 to 8 sentences, corresponding exactly to the number of used qubits in Quantinuum QPUs versions H1-1 and H1-2. On the H1-1, the quantum computing part executed at most 765 two-qubit gates with a computing depth of 159 and 2000 shots.

¹⁰⁹¹ See [Quantinuum Announces Quantum Volume 4096 Achievement](#) by Kortny Rolston-Duce, Quantinuum, April 2022.

¹⁰⁹² See [Quantinuum System Model H1 Product Data Sheet Version 5.00](#), June 14, 2022 (9 pages).

¹⁰⁹³ See [Transport of multispecies ion crystals through a junction in an RF Paul trap](#) by William Cody Burton et al, June 2022 (6 pages) where they describe how they can transport ytterbium and barium in 2D structures.

¹⁰⁹⁴ See [Long Story Short: Researchers Say Quantum Computers May be Better at Summarizing Long Documents](#) by Matt Swayne, The Quantum Insider, June 2022, referring to [Constrained Quantum Optimization for Extractive Summarization on a Trapped ion Quantum Computer](#) by Pradeep Niroula et al, June 2022 (16 pages).

The experiment was based on using three quantum optimization algorithms working under constraints: QAOA, L-VQE¹⁰⁹⁵ and XY-QAOA and the comparison was made vs a classical random guess, with XY-QAOA being the best. This was to date the best optimization under constraint problem ever solved by a quantum computer. But its capacity is obviously limited to simple and short texts. It could not summarize a 300 sentences document given there are not enough physical qubits available, and fidelities allowing very long depth computing accordingly. It couldn't of course summarize the scientific paper for you since it contains several hundreds of sentences that are way more complicated than short news from CNN and The Daily Mail. In the end, we always must find out if the thing scales well or not, and under which circumstances. That aspect wasn't addressed in the paper.



Alpine Quantum Technologies or **AQT** (2017, Austria, \$34.8M) is a spin-off from the University of Innsbruck created by Rainer Blatt, Peter Zoller and Thomas Monz. Ignacio Cirac (MPI) and Jonathan Home (ETH Zurich) are among their scientific advisors.

AQT drives its microwave trapped ions without the use of lasers, which simplifies the device. They use only one laser for photoionization of their calcium ions, which creates the ions at start-up, and another for measuring the qubit state by fluorescence after calculations. The fidelity of their qubits is 99.6% for two qubits and drops to 86% for 10 qubits¹⁰⁹⁶.

Although small and less visible than IonQ and Quantinuum, AQT has the largest trapped ions systems available in-store, with 20 working qubits working out of two 19-inches datacenter rack¹⁰⁹⁷. The associated research team had already entangled 14 ions back in 2011¹⁰⁹⁸! Their PINE system uses a linear Paul trap that supports up to 50 ions, including from multiple species. It can be used beyond quantum computing for quantum clocks or spectroscopy experiments.

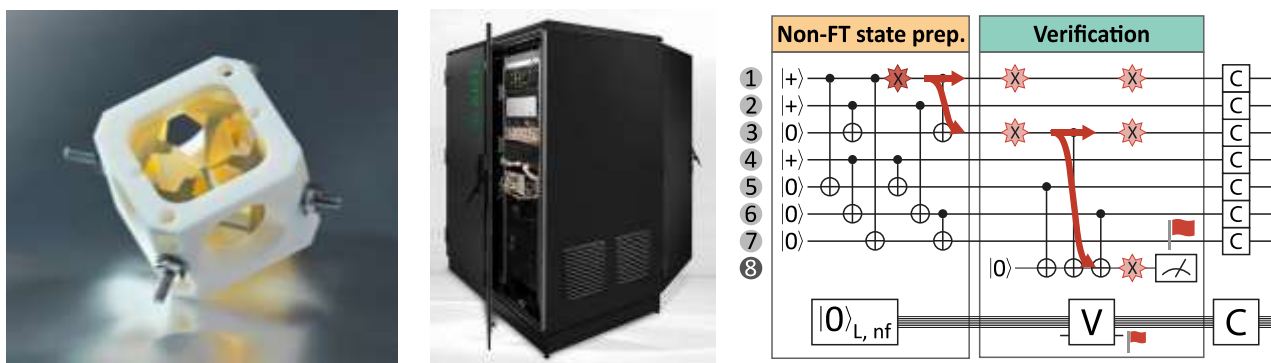


Figure 393: AQT's pane system to trap their calcium ions, the 2-rack system, and how they implemented a fault-tolerant T gate with magic state preparation. Source: [Demonstration of fault-tolerant universal quantum gate operations](#) by Lukas Postler, Rainer Blatt, Thomas Monz et al, *Nature*, November 2021 and May 2022 (14 pages).

AQT is also experimenting using qudits of dimension 5 with its ions¹⁰⁹⁹. In May 2022, Thomas Monz's team announced the first realization of a fault-tolerant CNOT gate across two logical qubits made with 16 physical qubits and using 7-qubits color codes quantum error correction plus one

¹⁰⁹⁵ See [Layer VQE: A Variational Approach for Combinatorial Optimization on Noisy Quantum Computers](#) by Xiaoyuan Liu et al, May 2022 (22 pages). So, we deal with a very recent algorithm!

¹⁰⁹⁶ See [Characterizing large-scale quantum computers via cycle benchmarking](#) by Alexander Erhard et al, 2019 (13 pages).

¹⁰⁹⁷ In [EU Team Make Progress Toward European-Only Compact Quantum Computer That Could Run on Solar Power](#) by Matt Swayne, The Quantum Insider, October 2021, we see them touting an energetic performance: a 24 qubits experimental system consumes only 1500W, like a kettle. Unfortunately, with 24 qubits can be emulated on a laptop that consumes less than 30W!

¹⁰⁹⁸ See [14-Qubit Entanglement: Creation and Coherence](#) by Thomas Monz et al, 2011 (pages).

¹⁰⁹⁹ See [Native qudit entanglement in a trapped ion quantum processor](#) by Pavel Hrmo, Rainer Blatt, Tomas Monz et al, June 2022 (9 pages).

measurement qubit (above, in Figure 393, *on the right*, so $16=2x(7+1)$). They also separately implemented a fault-tolerant T gate using magic state preparation with flag qubits, fully using their 16 qubits¹¹⁰⁰.

Their PINE system supports Qiskit, Cirq, PennyLane and Pytket. They team up with NTT on developing financial applications¹¹⁰¹.



Oxford Ionics (2019, UK, \$3.6M) is a spin-off from the Department of Physics at Oxford University created by Chris Ballance and Tom Harty which is developing a quantum computer based on trapped ions and low-noise control electronics.

They were originally called Nqie Limited. The company was founded by Thomas Harty and Christopher Ballance and also includes Jochen Wolf, all from Oxford University. They announced in July 2022 that they are teaming up with Infineon for the manufacturing of their trapped ions chipsets.



Universal Quantum (2018, UK, \$14.6M) is a spin-off from the Ion Quantum Technology Group at the University of Sussex in the UK led by Winfried Hensinger. They are developing a trapped ion system that uses microwaves transmitted by electrical circuits, and magnetic fields to control them instead of lasers. They won a \$67M deal with DLR in Germany in November 2022.

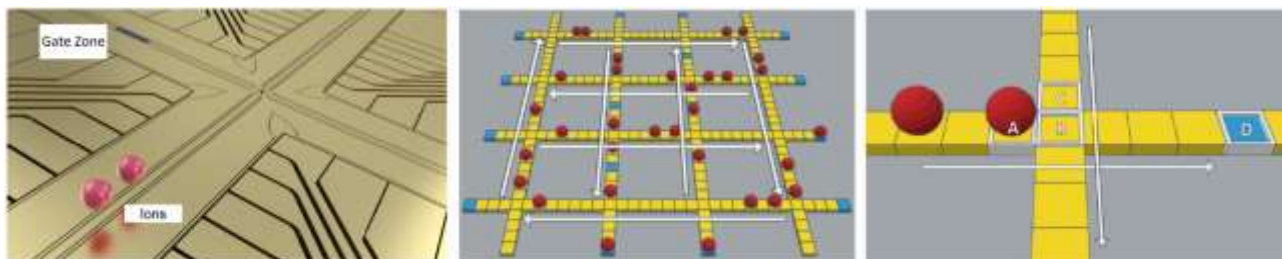


Figure 394: Universal Quantum's shuttling ion architecture in their Penning traps. Source: Universal Quantum.

They use Penning traps which are well known. The company presentation [video](#) gives the impression that they use a 2D process similar to Quantinuum's¹¹⁰². The cooling required is around 70K, which is done with liquid nitrogen. They still need to use lasers at least for the Doppler based ions cooling during their preparation, then for the qubit state readout combining the usual laser excitation and fluorescence readout with a CMOS or CCD sensor¹¹⁰³. They use electrodes to drive qubit gates. In 2022, they announced their plan to reach one million qubits, some day, with using a modular approach¹¹⁰⁴. They plan to use electric fields to connect several modules on their silicon based wafer.



Aquabits (2021, Canada) is developing a trapped ions qubit processor using 'aquaporins', that trap ions inside artificial water channels. It is supposed to avoid using lasers and micro-nano fabrication techniques, making these qubits highly scalable. There's no public way to find out how all these qubits are controlled, entangled and measured.

¹¹⁰⁰ See [Demonstration of fault-tolerant universal quantum gate operations](#) by Lukas Postler, Rainer Blatt, Thomas Monz et al, Nature, November 2021 and May 2022 (14 pages).

¹¹⁰¹ See [Quantum computing in finance - Quantum readiness for commercial deployment and applications](#), NTT, February 2022 (17 pages).

¹¹⁰² The ion routing process is described in [Efficient Qubit Routing for a Globally Connected Trapped Ion Quantum Computer](#) by Winfried Hensinger et al, February 2020 (13 pages). This is the origin of the illustration used in these lines.

¹¹⁰³ The ion control process with Penning Traps used by Universal Quantum seems to be described in [Microfabricated Ion Traps](#) by Winfried Hensinger et al, 2011 (28 pages).

¹¹⁰⁴ See [How Universal Quantum is rising to the million-qubit challenge](#), Universal Quantum, February 2022



eleQtron GmbH (2020, Germany, 50M€) develops a NISQ trapped ions quantum computer. They use their Magnetic Gradient Induced Coupling (MAGIC) to control the qubits.

The project involves the University of Siegen and Infineon. They are partnering with ParityQC (Austria) for software development within the ATIQ consortium with a total funding of 44.5M€ including 37M€ from the German government through DLR. They plan to release a 10-qubit processor in 2023.



Hon Hai / Foxconn (Taiwan) announced in December 2021 it is starting the development of a trapped ions quantum computer in its quantum computing research center, part of its Research Institute¹¹⁰⁵.

The lab is directed by Min-Hsiu Hsieh who was previously an associate professor at the Centre for Quantum Software and Information from University of Technology Sydney. He's more specialized in quantum machine learning than in trapped ions computing.



Crystal Quantum Computing (2021, France) was a stealth startup until 2022, created by Quentin Bodart (with a long-lasting experience with neutral atoms, including quantum microgravimeters) and Luca Guidon (from the CNRS MPQ laboratory in Paris).

Its goal is to create a trapped ion quantum computer using strontium 88 ions energized at Rydberg levels. Their ions would be easier to control than classical trapped ions, using UV lasers at 243 nm (generated with IR lasers and double frequency doubling) and THz microwave directive antennas, all being handled in a Penning trap on a chipset running at 30K.

Neutral atoms qubits

Neutral atoms, *aka* cold atoms, are another atomic form of qubits in addition to trapped ions¹¹⁰⁶. They are both trapped, but not exactly in the same way. Since these atoms are not used in ionized form, they are not trapped with electrodes but with lasers. The atoms preparation is done in multiple steps.

An atom cloud is first trapped and cooled in a MOT (magneto-optical-trap)¹¹⁰⁷. Then other lasers using the method of "optical tweezing" or "optical traps" will precisely control the position of the atoms and arrange them in patterns like 2D matrices¹¹⁰⁸.

Neutral atoms can be used to create qubits with their two states corresponding to different atomic energy levels, where transitions are controlled by a variable mix of laser beams and microwaves. These atoms have controllable high-energy so-called Rydberg states which can be used as the $|1\rangle$ qubit state and/or for coupling qubits with two-qubit gates or for setting-up a Hamiltonian for a quantum simulation run.

Indeed, neutral atoms qubits can be used in two ways: with gate-based computing using one and two-qubit gates and for quantum simulations, using a prepared state of interconnected qubits that are converging to a minimum energy level, helping to find a solution to chemical simulation and optimization problems.

¹¹⁰⁵ See [Hon Hai to develop trapped ion quantum computers](#), Taipei Times, December 2021.

¹¹⁰⁶ See this excellent review paper: [Quantum simulation and computing with Rydberg-interacting qubits](#) by Manuel Agustin Morgado and Shannon Whitlock, Laboratory of Exotic Quantum Matter, University of Strasbourg, December 2020 (28 pages).

¹¹⁰⁷ It creates a variable magnetic field and associate three pairs of lasers to cool down the atoms below the Doppler limit, using the Zeeman variable shift effect. The frequency of the lasers used for atoms cooling would have to be changed as they are cooled. A workaround is to progressively change their resonance frequency with a varying magnetic field so that it's aligned with the cooling laser frequency.

¹¹⁰⁸ See [Quantum information processing with individual neutral atoms in optical tweezers](#) by Philippe Grangier, (47 slides).

Quantum simulation also simulate the “Hubbard model” (*aka* Fermi-Hubbard model) which modelizes strongly correlated electronic materials like condensed matter and high-temperature superconducting materials¹¹⁰⁹.

However, neutral atoms are very versatile and have various other use cases on top of quantum computing and simulation, including quantum sensing, with applications in microgravity detection, electromagnetic spectrum analysis and atomic clocks and also quantum memories and repeaters¹¹¹⁰. We cover these various use cases in other parts of this book.

History

Neutral atom-based computing history starts a long time ago with fundamental physics research before quantum computing was even conceptualized. High energy atom states were formalized by Johannes Rydberg in Sweden in 1887 based on Johann Balmer’s series. It was later explained by Niels Bohr in 1913 with his semiclassical model of the hydrogen atom with discrete energy levels. An extended understanding of the observed hydrogen spectrum was done by Wolfgang Pauli in 1926¹¹¹¹.

In parallel with the many research on Bose-Einstein Condensate, which are not relevant for neutral atoms computing, mechanisms were developed in the 1980s to control individual atoms in vacuum using lasers¹¹¹². It was first demonstrated in 1985 at the Bell Laboratories by Steven Chu, creating what they called “optical molasses” due to the viscosity of the confined sodium atoms used in their experiment.

In 1985, Claude Cohen-Tannoudji, Alain Aspect and Jean Dalibard started to work on laser-based atoms cooling using Doppler effect. In 1987, David Wineland and Wayne Itano improved laser cooling, which led the way for various applications including ultrahigh resolution spectroscopy and atomic clocks. In 1988, scientists led by Claude Cohen-Tannoudji at ENS Paris and others from Stanford University developed new atoms cooling mechanisms based on laser optical pumping, light shifts and laser polarization gradients¹¹¹³. They invented “Sisyphus cooling” in 1989, a cold atom cooling, *aka* polarization gradient cooling, reaching temperatures below the Doppler cooling limit. This led Claude Cohen-Tannoudji to be awarded the Nobel prize in physics in 1997, together with Steven Chu.

Laser cooling of atoms then reached very low temperatures, in the nK range. It contributed in 1995 to the discovery in the USA, of gaseous Bose-Einstein condensates that was devised in the mid-1920s by Bose and Einstein.

Ultra-cold atoms were used to create more precise atomic clocks than the cesium-based ones running at room temperature starting in 1998 in France.

In the 1980s, Serge Haroche, started to work with Rydberg atoms and their integration in superconducting cavities, pioneering cavity electrodynamics (CQED), light-atoms interactions, cold atoms control and the understanding of quantum decoherence.

So, how about neutral atoms and quantum computing? First, we have the raw idea of a quantum simulator by Richard Feynman in 1981. In 1996, Seth Lloyd demonstrated that it “was possible” to implement such scheme, noticeably with controlled atoms¹¹¹⁴.

¹¹⁰⁹ See [Quantum simulation of the Hubbard model with ultracold fermions in optical lattices](#) by Leticia Tarruell (ICFO, Spain) and Laurent Sanchez-Palencia (CPHT, France), January 2019 (38 pages).

¹¹¹⁰ See [Highly-efficient quantum memory for polarization qubits in a spatially-multiplexed cold atomic ensemble](#) by Julien Laurat et al, 2018 (6 pages) and [Experimental realization of 105-qubit random access quantum memory](#) by N. Jiang et al, 2019 (6 pages).

¹¹¹¹ See [Rydberg Physics](#) by Nikola Šibalić and Charles S Adams, 2018 (28 pages).

¹¹¹² See [New Mechanisms for Laser Cooling](#) by Claude Cohen-Tannoudji and William D. Phillips, 1990 (8 pages).

¹¹¹³ See [Laser cooling and trapping of neutral atoms](#) by Jean Dalibard and Claude Cohen-Tannoudji (20 pages).

¹¹¹⁴ See [Universal Quantum Simulators](#) by Seth Lloyd, 1996 (7 pages).

While quantum simulation can be theoretically implemented with trapped ions and superconducting qubits, the cold atom way is the only one that is seriously investigated and which has reached the commercial stage.

Then things started to get serious with two-qubit gates proposals from Dieter Jaksch, J. Ignacio Cirac and Peter Zoller¹¹¹⁵ and from Gavin K. Brennen et al in 1998¹¹¹⁶, with improvements from Jaksch, Zoller and Mikhail Lukin in 2000¹¹¹⁷. In 2012, J. Ignacio Cirac and Peter Zoller proposed a set of criteria for quantum simulators similar to those from David DiVincenzo’s 2000 for gate-based quantum computing (in Figure 395)¹¹¹⁸.

TABLE I. Criteria for quantum simulators and quantum computers

| Criteria | Quantum computers ⁶⁴ | Quantum simulators ⁴ |
|----------------|--|--|
| Quantum system | A scalable physical system with well characterized qubits | A system of quantum particles (bosons, fermions, pseudo-spins) confined in space and collectively possessing a large number of degrees of freedom |
| Initialization | The ability to initialize the state of the qubits to a simple fiducial state, such as $ 000\dots\rangle$ | The ability to prepare (approximately) a known quantum state (typically a pure state) |
| Coherence | Long relevant decoherence times, much longer than the gate operation time | |
| Interactions | A “universal” set of quantum gates | An adjustable set of interactions used to engineer Hamiltonians/quantum master equations including some that cannot be efficiently simulated classically |
| Measurement | A qubit-specific measurement capability | The ability to perform measurements on the system: either individual particles or collective properties |
| Verification | | A way to verify the results of the simulation are correct |

Figure 395: comparisons of gate-based quantum computing (left) and quantum simulation (right). Source: [Quantum simulation and computing with Rydberg-interacting qubits](#) by Manuel Agustin Morgado and Shannon Whitlock, December 2020 (28 pages).

The first two-qubits gates with pairs of Rydberg atoms were implemented in 2009 by Mark Saffman from the University of Wisconsin (with “gg-qubits”, which we cover later) and at the Institut d’Optique in France (“gr-qubits”).

Many progresses were made in the 2010’s which encouraged many scientists to create their own companies. It started with the creation of ColdQuanta (2007), Muquans (2011), both using cold atoms for quantum sensing in micro-gravimetry, BraneCell (2015), Atom Computing (2018), Pasqal (2019) and QuEra (2020). Besides Muquans (now in France’s ixBlue), all the others are positioned in the quantum computing market although ixBlue is also a technology provider for Pasqal for lasers.

Science

Neutral atoms are simply non-ionized atoms with an equivalent number of protons in their nucleus and electrons in their shells. The neutral atoms that are used in cold atoms computing belong to the first column in the table of elements, having a single electron in the valence layer, such as hydrogen, sodium, lithium, cesium or rubidium, the last one being the most commonly used. This alkaline metal has interesting energy transitions that correspond to common lasers wavelengths as well as easily generated microwaves between 3 and 10 GHz. It is possible to manage with them so-called closed transitions which allow, with lasers, to make atoms transit between several states in a cyclic and controlled manner.

¹¹¹⁵ See [Entanglement of atoms via cold controlled collisions](#) by Dieter Jaksch, H.-J. Briegel, J. Ignacio Cirac, C. W. Gardiner and Peter Zoller, 1998 (4 pages).

¹¹¹⁶ See [Quantum Logic Gates in Optical Lattices](#) by Gavin K. Brennen, Carlton M. Caves, Poul S. Jessen, and Ivan H. Deutsch, PRL, 1998 (7 pages).

¹¹¹⁷ See [Fast Quantum Gates for Neutral Atoms](#) by D. Jaksch, J. Ignacio Cirac, Peter Zoller, Mikhail D. Lukin et al, PRL, 2000 (4 pages).

¹¹¹⁸ See [Goals and opportunities in quantum simulation](#) by J. Ignacio Cirac and Peter Zoller, Nature Physics, 2012 (3 pages).

On top of that, states are stable long enough to perform computations, i.e. about a hundred microseconds. Other elements are investigated like dysprosium and praseodymium who are lanthanide elements.

Cold atoms can be used in Rydberg states, which correspond to a very high level of energetic excitation, between 50 and 100 electron quantum number (layer position in atom against Bohr's model, labelled n or N). This creates very large electron orbits, scaling by N^2 . These high energy states are used to create entanglement between atoms and thus to operate multi-qubit quantum gates or large Hamiltonians in quantum simulation modes. These excited states have a fairly good stability level of about 100 μ s. They are several orders of magnitude longer than the classical excited states (hyperfine, which are used for cold atoms qubit states). This stability is somehow equivalent to the coherence time of superconducting qubits.

Cold atoms computing also exploits the Rydberg blockade effect, where a Rydberg atom excited with a high energy level (with $n > 50-70$) prevents neighboring atoms from reaching that level.

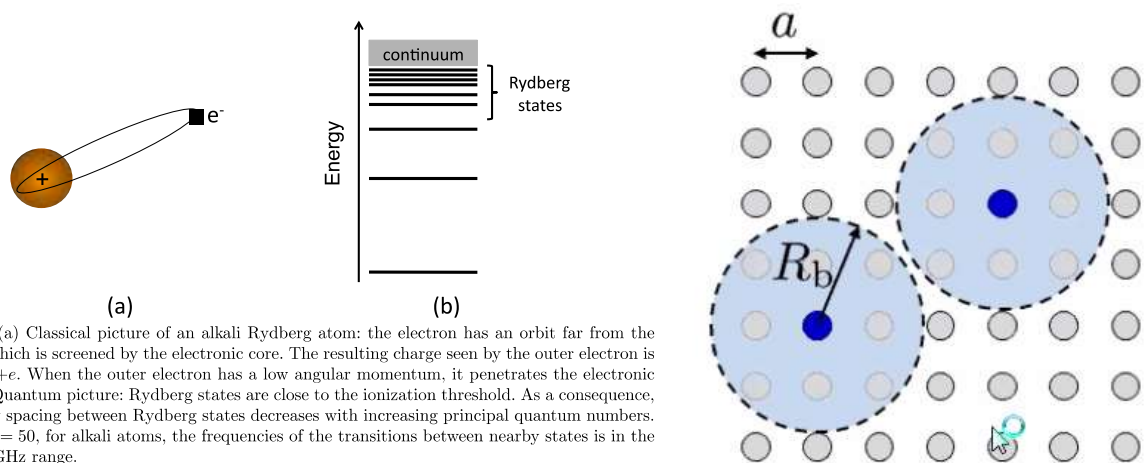


Figure 1: (a) Classical picture of an alkali Rydberg atom: the electron has an orbit far from the nucleus, which is screened by the electronic core. The resulting charge seen by the outer electron is therefore $+e$. When the outer electron has a low angular momentum, it penetrates the electronic core. (b) Quantum picture: Rydberg states are close to the ionization threshold. As a consequence, the energy spacing between Rydberg states decreases with increasing principal quantum numbers. Around $n = 50$, for alkali atoms, the frequencies of the transitions between nearby states is in the 10 – 100 GHz range.

Figure 396: Rydberg state are high-energy level of excited atoms that create a dipole in the atom. It enables entanglement with neighbor atoms. Source: [Interacting Cold Rydberg Atoms: a Toy Many-Body System](#) by Antoine Browaeys and Thierry Lahaye, 2013 (20 pages).

When excited, these atoms behave like accentuated dipoles, the orbit of the electrons of the valence layer being very inclined as shown in Figure 396.

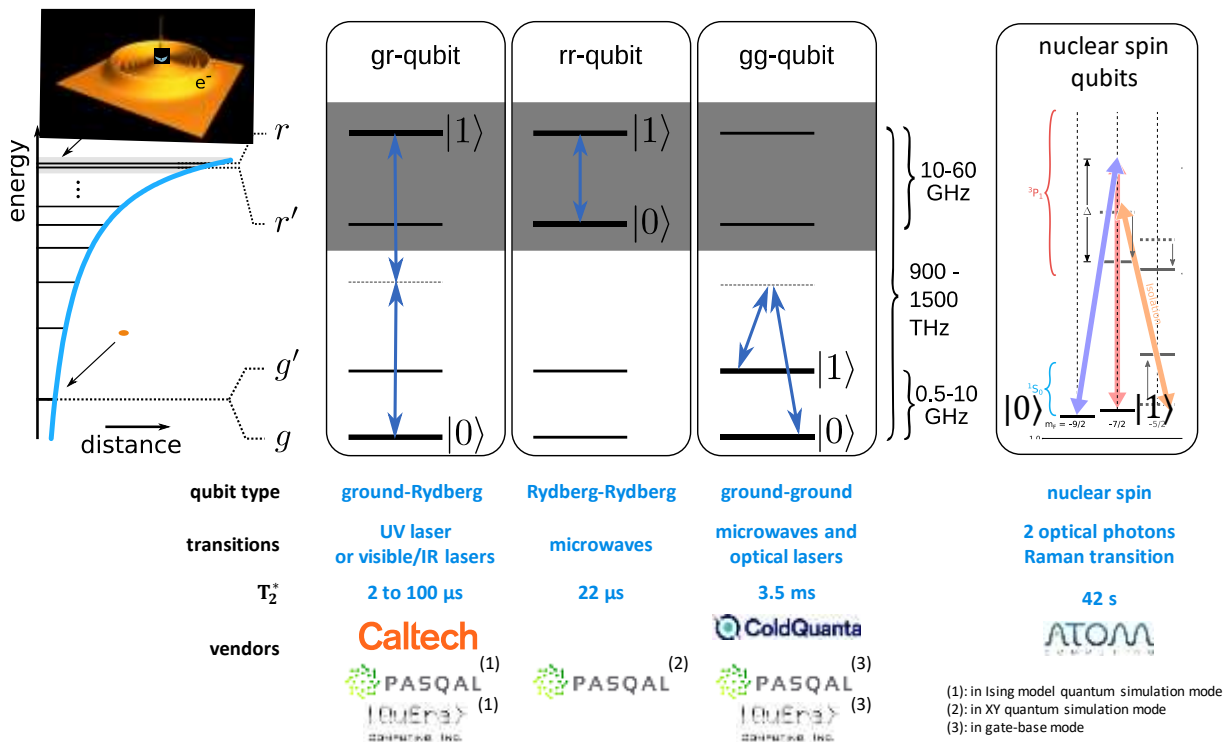
They also have a disproportionate size of up to one micron (μ m) in diameter for $n=100$ with ^{87}Rb . This is close to being in an ionized state¹¹¹⁹. Their electromagnetic characteristics make the atoms react with their neighbors whose excitation they block within a perimeter of up to 20 μ m, which is huge at the atomic scale.

Activated Rydberg atom can also be excited by lasers to generate well-isolated single photons that can be used in nonlinear optics¹¹²⁰. This provides yet another source of single photons, in addition to quantum dots. The Rydberg blockade phenomenon could also be implemented in quantum telecommunications, in spectroscopy and in atomic clocks¹¹²¹.

¹¹¹⁹ This [presentation of 52 slides](#) from 2014 describes well the history and geometry of the Rydberg atoms.

¹¹²⁰ See [Observation of coherent many-body Rabi oscillations](#) by Yaroslav Dudin and Alex Kuzmich, GeorgiaTech, 2012 (5 pages) and [Nonlinear quantum optics mediated by Rydberg interactions](#) by Sebastian Hofferberth et al, 2016 (26 pages).

¹¹²¹ See [Photon-Mediated Quantum Information Processing with Neutral Atoms in an Optical Cavity](#) by Stephan Welte, 2019 (124 pages).



schema source: Quantum simulation and computing with Rydberg-interacting qubits by Manuel Agustin Morgado and Shannon Whitlock, December 2020 and additions by Olivier Ezratty, 2022.

Figure 397: the various ways to control cold atoms. Source: [Quantum simulation and computing with Rydberg-interacting qubits](#) by Manuel Agustin Morgado and Shannon Whitlock, December 2020 (28 pages) and additions by Olivier Ezratty, 2022.

But as usual with all qubit types, there are many variations of cold atoms qubits. First, you have three breeds of qubits whose manifold is based on classical energy levels. With ground-Rydberg qubits which are controlled by UV, visible and infrared lasers, Rydberg-Rydberg qubits controlled by microwaves and lasers, ground-ground qubits controlled by microwaves and optical lasers, and at last, nuclear spin atoms controlled by optical lasers using Raman transitions. Some players like Pasqal have been investigating the first three types of qubits, seemingly favoring gr-qubits and rr-qubits for quantum simulation and gg-qubits for gate-based computing. Topological states allowing to create more reliable qubit-based computing systems are also studied¹¹²².

Cold atoms qubits are the most common ones that can be used in both gate-based quantum computing and in quantum simulation computing mode (*aka* analog quantum simulation). In the first case, qubits are individually controlled over time with single and two-qubit gates, to read qubit state at the end of processing¹¹²³. With quantum simulation¹¹²⁴, a so-called Hamiltonian is prepared with specific atoms geometry and connectivity, usually using Rydberg states, which then converges itself into an energy minimum leading to qubits measurement. Individual qubits are controlled only at the initialization stage and for readout. There is no sequential programming.

¹¹²² See [Topologically protected edge states in small Rydberg systems](#) by Antoine Browaeys et al, 2018 (6 pages) and [Observation of a symmetry protected topological phase of interacting bosons with Rydberg atoms](#) by Antoine Browaeys, Thierry Lahaye et al, 2019 (20 pages). Quantum simulation using cold atoms is also a tool to simulate topological matter. See [Scientists unveil first quantum simulation of 3-D topological matter with ultracold atoms](#) by Hong Kong University of Science and Technology, July 2019.

¹¹²³ See [Versatile neutral atoms take on quantum circuits](#) by Hannah J Williams, Nature, 2022 (2 pages) which describes two such methods, implemented by QuEra and ColdQuanta and mentioned later.

¹¹²⁴ See [Toward quantum simulation with Rydberg atoms](#) by Thanh Long Nguyen, 2016 (182 pages), [Quantum simulations with ultracold atoms in optical lattices](#) by Christian Gross and Immanuel Bloch, 2017 (8 pages), [Tunable two-dimensional arrays of single Rydberg atoms for realizing quantum Ising models](#) by Thierry Lahaye and Antoine Browaeys, 2017 (13 pages), [Quantum read-out for cold atomic quantum simulators](#), par J. Eisert et al, 2018 (20 pages), [Quantum critical behaviour at the many-body localization transition](#) by Markus Greiner et al, 2018 (10 pages), [Quantum Kibble-Zurek mechanism and critical dynamics on a programmable Rydberg simulator](#) by Alexander Keesling et al, 2019 (16 pages) and [Many-body physics with individually controlled Rydberg atoms](#) by Antoine Browaeys and Thierry Lahaye, 2020 (14 pages).

cold atoms qubits

- long qubit coherence time and fast gates.
- operational systems with 100-300 atoms.
- identical atoms, that are controlled with the same laser and micro-wave frequencies (but dual-elements architectures are investigated).
- works in both simulation and gate-based paradigms, but still with difficulty for gate-based.
- reuse trapped ions qubits tools for qubits readout with fluorescence and CCD/CMOS detection.
- no need for specific integrated circuits.
- uses standard apparatus.
- low energy consumption.

- acceptable quantum gates error rate although not “best in class”.
- crosstalk between qubits that can be mitigated with two-elements systems.
- adapted to simulation more than to universale gates computing.
- not yet operational QND (quantum non demolition) measurement that is required for QEC and FTQC.
- control lasers and optical not scaling well beyond one thousand qubits with the current state of the art.

Figure 398: pros and cons of cold atoms quantum computers and simulators. (cc) Olivier Ezratty, 2022.

Most neutral atoms systems and qubit types can be used in both paradigms, but it seems that the gate-based model is the most demanding and complicated to handle. Thus, three situations in the market can be observed: startups like Pasqal are explicitly saying that they start first with the quantum simulation paradigm, others like ColdQuanta tout their positioning on gate-based quantum computing but actually start with quantum simulation and at last, others like Atom Computing start readily with a gate-based approach but to no real avail.

Qubit operations

We’ll look here at the way qubits lifecycle works, from initialization to readout, with quantum gates in-between (for gate-based systems). The general principle is as follows:

- **Quantum state** for the $|0\rangle$ and $|1\rangle$ qubit basis corresponds to a ground and excited state, which depends on the qubit type as seen previously with ground-Rydberg, Rydberg-Rydberg, ground-ground and nuclear spin atoms qubits. The most commonplace for gate-based computing seems the ground-ground case. The qubit $|0\rangle$ state is usually prepared with laser pumping or with some microwave pulse. Contrarily to superconducting and quantum dots spin qubits who are static in nature in their electronic circuits, atoms have to be first arranged in space before any computing can start. The qubits can be arranged in 1D, 2D¹¹²⁵ or 3D matrices¹¹²⁶.

They are cooled, controlled, and positioned by several lasers organized in precision "optical tweezers". A qubit can be based on a single atom or on a group of atoms depending on the methods used. The atoms are prepared with a hot or cold source (some μK) which then feeds an ultra-vacuum chamber where laser control takes place.

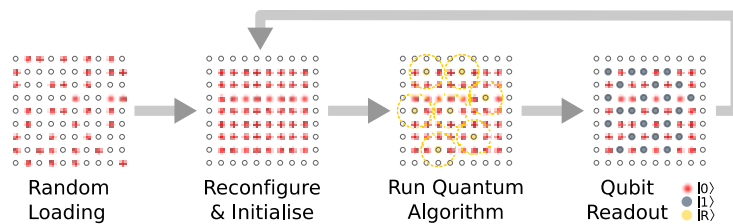


Figure 2. Schematic of a Rydberg array quantum computer. Atoms are initially loaded stochastically, followed by rearrangement to achieve a defect free qubit register. Coherent excitation to Rydberg states allows implementation of quantum algorithms exploiting long-range interactions to couple neighbouring qubits, followed by state-selective readout which is repeated many times to tomographically reconstruct the output state.

Figure 399: how an array of cold atoms is being prepared. Source: [Rydberg atom quantum technologies](#) by James Shaffer, 2019 (24 pages).

¹¹²⁵ See the thesis [Rydberg interactions in a defect-free array of single-atom quantum systems](#) by Daniel Ohl de Mello, 2020 (147 pages) which describes the way to fill a 2D matrix of a hundred heavy atoms.

¹¹²⁶ See [Three-Dimensional Trapping of Individual Rydberg Atoms in Ponderomotive Bottle Beam Traps](#) by Antoine Browaeys, Thierry Lahaye et al, 2019 (8 pages).

- **Single-qubit quantum gates** are activated by a mix of microwaves (a few GHz, compatible with hyperfine states in the case of Rydberg-Rydberg or ground-ground qubits) and laser pumping to change the energy state of the cold atom between its ground and excited state. These gates can also use Raman transitions driven by lasers on two frequencies or by a combination of the Stark effect of spectral line shifting under the effect of an electric field and microwaves. In most cases, cold atoms single qubit gates are $R_z(\theta)$ (arbitrary phase rotation). The best single-qubit gate fidelities are around 99.6% with a long-term objective of reaching an error rate of 10^{-4} ¹¹²⁷. Fortunately, there are optical systems for multiplexing laser beams, which make it possible to avoid having more lasers than qubits.
- **Two-qubit quantum gates** also use a variable mix of microwaves and lasers most of the time, using Rydberg state, the related Rydberg blockage phenomenon and dipole-dipole interactions¹¹²⁸. They are applied to atoms in their ground or excited state, which projects its valence layer electrons into a high orbit. For rubidium, there is only one electron to manage in this layer. These quantum gates can in practice involve more than two qubits, which is useful to set up a Hamiltonian in quantum simulation mode. The fidelity of two qubit gates was quite low in 2016 with a maximum of 75% with rubidium and 81% in 2016 with cesium. It increased to a better level of 99,1% in 2020¹¹²⁹. The decoherence of cold atoms qubits has different origins: photoionization, spontaneous emission of photons, transitions induced by black body radiation, stability of control lasers and laser pulse timing and precision control of atoms in space¹¹³⁰. The two-qubit gate set is variable. It can for example contain a CPHASE, CZ (ColdQuanta, QuEra) and XY gate. These gates usually work in a nearest neighborhood fashion. With cold-atoms, two-qubit gates are usually faster to operate than single qubit gates¹¹³¹.
- **Qubit readout** uses a CCD or CMOS camera that detects the atoms fluorescence with a method similar to the one used with trapped ions and NV centers. In Figure 400 is a simplified description a cold atom qubits system with laser and microwaves-based control tools and qubit measurement using fluorescence and a camera. This method is destructive of the qubit state so it's not a QND measurement.

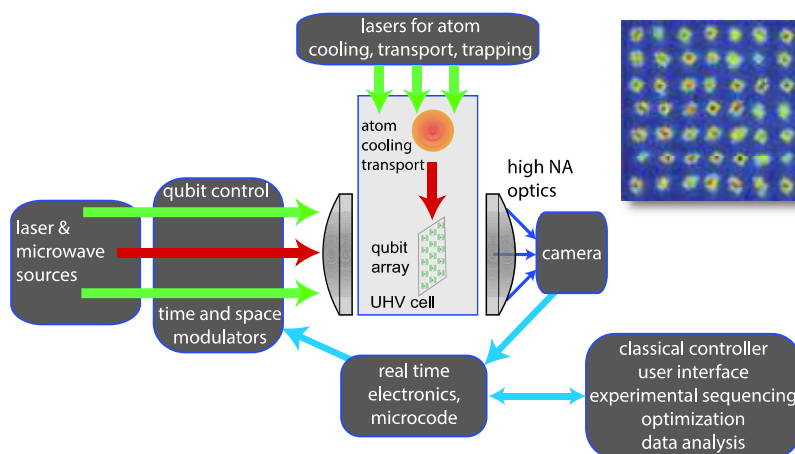


Figure 400: typical devices arrangement to control cold atoms. Source: [Quantum computing with atomic qubits and Rydberg interactions: Progress and challenges](#) by Mark Saffman, 2016 (28 pages).

¹¹²⁷ See [High-Fidelity Control, Detection, and Entanglement of Alkaline-Earth Rydberg Atoms](#) by Ivaylo Madjarov, January 2020 (13 pages) which uses strontium.

¹¹²⁸ In 2019, American researchers were able to create multi-qubit quantum gates with 95% fidelity based on cold atoms, in [Parallel implementation of high-fidelity multi-qubit gates with neutral atoms](#) by H. Levine et al, August 2019 (16 pages). Two-qubit gate bases in [Direct Measurement of the van der Waals Interaction between Two Rydberg Atoms](#) by Lucas Béguin, Antoine Browaeys et al, 2013 (5 pages). And [Quantum information processing with individual neutral atoms optical tweezers](#) by Philippe Grangier (47 slides).

¹¹²⁹ See [High-fidelity entanglement and detection of alkaline-earth Rydberg atoms](#) by Ivaylo S. Madjarov et al, November 2020 (16 pages).

¹¹³⁰ Source: [Quantum Computing with Neutral Atoms](#), 2013 (42 slides).

¹¹³¹ It could even reach the nanosecond scale as experimented in [Ultrafast energy exchange between two single Rydberg atoms on a nanosecond timescale](#) by Y. Chew et al, Nature Photonics, 2022 (7 pages).

As a result, cold atoms are not the easiest candidate to implement measurement-based quantum error correction for creating FTQC systems. There are however various investigated solutions¹¹³².

Setup

In general, cold atom-based systems operate at room temperatures but atoms are cooled at below 1 mK and in ultra-high vacuum. In practice, it is the ultra-high vacuum and the atoms laser cooling that ensures this thermalization. Preparing and controlling the qubits is based on a set of lasers, light structuring devices (SLM and AODs), polarizing beam splitters and microwaves devices. Microwaves are sent in a “one to many” mode and usually coupled with targeted photons to control individual gates. Neutral atom qubits vendors often argue that their system work at ambient temperature and do not require any refrigerant based cooling system. While they do not use cryostats like those that cool superconducting and silicon qubits, they still cool their qubits, using different methods combining ultra-vacuum pumps, magnetic traps and lasers. And now, some are even using a 4K cryostat to cool their ultra-vacuum pump to avoid the pollution of their tweezer-assembled 2D grid by spare atoms, at least, beyond 200 atoms.

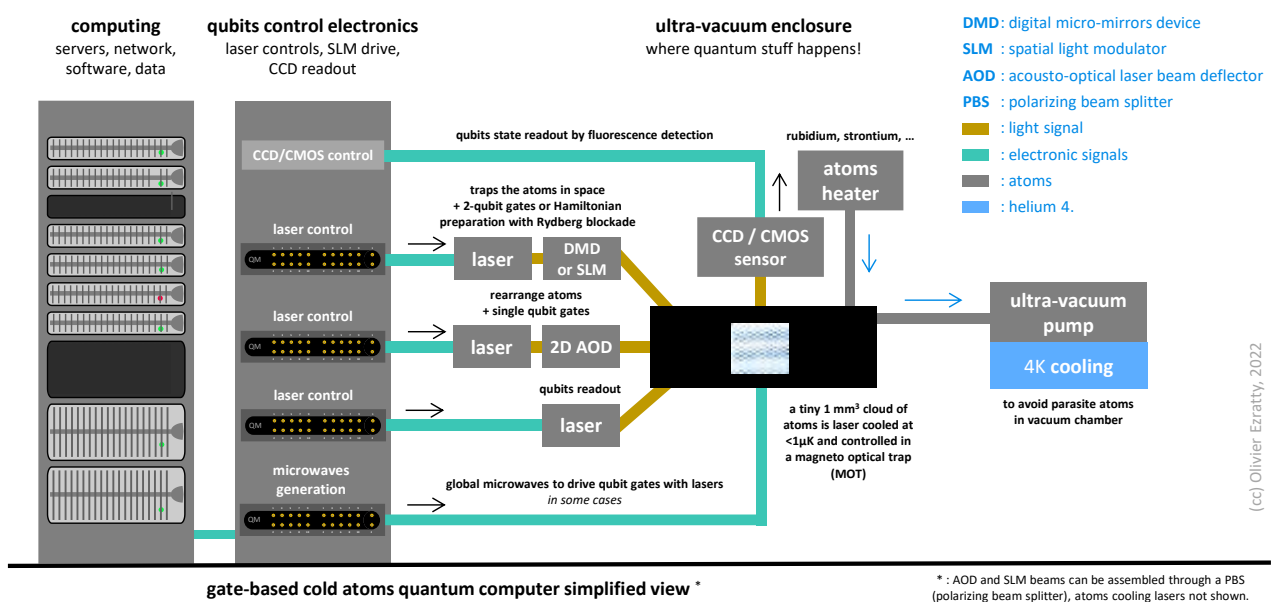


Figure 401: overall architecture of a cold atoms based computer. (cc) Olivier Ezratty, 2022.

I now owe you some explanations on the mentioned devices:

MOT (magneto-optical trap) uses laser cooling and a spatially-varying magnetic field to create a trap for our cold atoms where they are cooled with lasers and Doppler effect. The MOT contains a weak quadrupolar spatially-varying magnetic field generated by a coil of about 8 cm diameter and four to six glass doors letting through circularly-polarized red lasers beams which are slowing down the movement of the atoms at the center of the MOT. It enables the atoms to reach very low temperature under 1 mK. Next is the MOT chamber used by Pasqal. It’s quite heavy, weighting in excess of 25 kg. The MOT chamber is pumped to be under ultra-vacuum.



Figure 402: a vacuum chamber from Pasqal, which contains a MOT.

¹¹³² See for example [Monitoring Quantum Simulators via Quantum Nondemolition Couplings to Atomic Clock Qubits](#) by Denis V. Vasilyev, Andrey Grankin, Mikhail A. Baranov, Lukas M. Sieberer and Peter Zoller, October 2020 (22 pages).

SLM (spatial light modulator) are systems modulating light. Its main use is with video projectors, using LCD (liquid-crystal displays, transparent), LCOS (Liquid crystal on silicon, a reflective version of LCD chipsets) or DMD chipsets (using micro-mirrors reflecting light in various directions). The SLMs breeds used for cold atom tweezers modulate the light phase instead of just its intensity and creates sort of a hologram. Phase SLMs are usually based on LCOS chipsets thanks to their controllable birefringence. SLM main vendors are Hamamatsu, Holoeye and Thorlabs. SLM resolution can reach 4,160 x 2,160, equivalent to 4K in TV/PC formats. SLMs are used with neutral atoms to create optical tweezers that precisely control atoms position in vacuum and at the nanometer scale¹¹³³.

AOM (acoustic-optical modulators) *aka* **AOD** (acousto-optic deflectors) uses an acousto-optic effect to diffract and shift the frequency of light using sound waves at radio frequencies. It contains a piezoelectric transducer that is attached to a material such as glass. An oscillating electric signal creates transducer vibrations, producing sound waves within the material, changing the refraction index¹¹³⁴.

Research

The most active research laboratories with cold atom-based qubits are in the USA (Harvard with **Mikhail Lukin**, University of Wisconsin with **Mark Saffman**¹¹³⁵, **Adam Kaufman** from JILA in Colorado, Caltech with **Vladan Vuletic** and **Manuel Endres**, Princeton with **Jeff Thompson**, GeorgiaTech), in the UK at the University of Cambridge, in Austria at the University of Innsbruck and the University of Vienna, Germany (Max-Planck Institute, Free University of Berlin, University of Stuttgart).

In France we have Institute d'Optique Graduate School with **Antoine Browaeys** and **Thierry Lahaye** who cofounded **Pasqal**, and the **Unistra** laboratory in Strasbourg run by **Shannon Whitlock**, who is behind the project **aQCess** and the European Flagship **EuRyQa** (with Pasqal).¹¹³⁶ Another European H2020 project, **AtomQT**, covers research with cold atoms, both qubits and sensing. In France, it involves the Bordeaux Optics Institute and the LPMCM in Grenoble.

In Germany, **Johannes Zeiher** from the Mack Planck Institute of Quantum Optics created SNACQ in 2022, a research group on cold atoms ("Scalable Neutral Atom Quantum Computing"). Its ambition it to create the first error-corrected logical qubit¹¹³⁷. It complements **Immanuel Bloch**'s team (Quantum Many-body Systems) and **Gerhard Rempe**'s group (Quantum Dynamics).

In 2017, Mikhail Lukin's team from **Harvard** University and a team from **MIT** assembled 51 rubidium atoms¹¹³⁸. It went up to 256 qubits in July 2021¹¹³⁹. Antoine Browaeys's team at **Institut d'Optique** reached 72 cold atoms in a 3D structure in 2018, 196 in 2020¹¹⁴⁰. and 500 in 2021. Four startups are positioned in the cold atoms computing market: **ColdQuanta** (2007, USA, working initially on quantum sensing), **Atom Computing** (2018, USA), **Pasqal** (2019, France) and **QuEra Computing** (2020, USA, linked to Lukin and Harvard).

¹¹³³ See [High-Precision Laser Beam Shaping and Image Projection](#) by Jinyang Liang, 2012 (126 pages).

¹¹³⁴ See alternative and more scalable approaches as proposed in [An integrated photonic engine for programmable atomic control](#) by Ian Christen et al, MIT and CSEM, August 2022 (16 pages).

¹¹³⁵ See [Quantum computing with atomic qubits and Rydberg interactions: Progress and challenges](#) by Mark Saffman, 2016 (28 pages).

¹¹³⁶ See [Time-Optimal Two- and Three-Qubit Gates for Rydberg Atoms](#) by Sven Jandura and Guido Pupillo, February 2022 (24 pages).

¹¹³⁷ See [Johannes Zeiher launches new research group](#), February 2022.

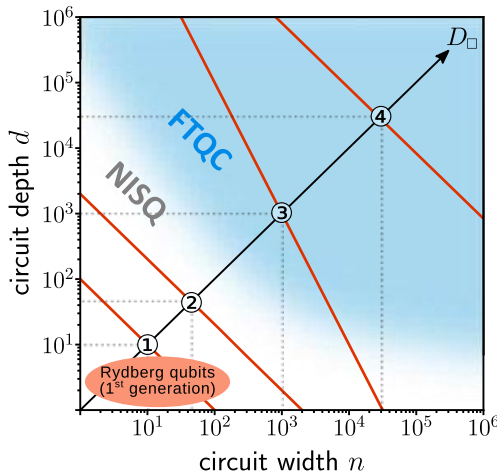
¹¹³⁸ See [Quantum simulator with 51 qubits is largest ever](#) by Matt Reynolds, 2017 which refers to [Probing many-body dynamics on a 51-atom quantum simulator](#) by Hannes Bernien, Mikhail Lukin et al, 2017 (24 pages).

¹¹³⁹ See [Harvard-led physicists take big step in race to quantum computing](#), Harvard, July 2021. Their work is like Pasqal/IOGS based on the same technique with rubidium atoms and SLM tweezers.

¹¹⁴⁰ See [Synthetic three-dimensional atomic structures assembled atom by atom](#) by Daniel Barredo, Antoine Browaeys et al, 2018 (4 pages).

You may obviously wonder whether China is also working on cold atom. You bet they are, like in all quantum fields. It includes the Key Laboratory of Quantum Optics in Shanghai and the Center for Cold Atom Physics in Wuhan, both from the **China Academy of Science**¹¹⁴¹. These labs are mainly focused on building cold atom based quantum sensors and also repeaters. They also investigate cold atoms quantum computing.

neutral atoms gate-based quantum computing scalability challenges



| limitations | T_1 | d | N_g | solution |
|--|-------------------|-----------------|-----------------|---|
| ① short dwell time of Rydberg excitations | $5 \mu\text{s}$ | 10 | 50 | blue detuned optical or magnetic traps that can simultaneously trap both ground and Rydberg states |
| ② atoms interaction with thermal and vacuum electromagnetic fields | $100 \mu\text{s}$ | 44 | 10^3 | embedding atoms inside cryogenic cavities to inhibit black-body transitions and spontaneous microwave emissions |
| ③ trap loss due to background gas collisions | 100s | 10^3 | 5×10^5 | cooling vacuum chamber |
| ④ | 100s | 3×10^4 | 5×10^8 | apply gates in parallel |

red lines: successive barriers associated with the finite lifetime T_1 of Rydberg qubits with barriers assuming each gate has a duration of 50 ns.

$N_g = d \cdot n/2$: multi-qubit gate count with $n/2$ two-qubit count per circuit layer.

schema source: Quantum simulation and computing with Rydberg-interacting qubits by Manuel Agustin Morgado and Shannon Whitlock, December 2020 and additions by Olivier Ezratty, 2022.

Figure 403: sorting out the cold atoms computing challenges per generation. Source: [Quantum simulation and computing with Rydberg-interacting qubits](#) by Manuel Agustin Morgado and Shannon Whitlock, December 2020 (28 pages) and text formatting by Olivier Ezratty, 2022.

The many challenges to overcome are, like with all other qubit types, about scalability and also, the implement non-destructive qubit measurement to enable QEC/FTQC.

Scalability can be improved mostly with increasing the lifetime of atom interactions as described in the above chart in Figure 403. It also requires the continuous improvement of gate fidelities, one goal being to reach three nines (99,9% for two-qubit gates)¹¹⁴². One approach, also tested with trapped ions, consists in mixing two types of neutral atoms. It is evaluated in a configuration prototyped at the **University of Chicago**. Shown in Figure 404, it packs 512 atoms in an array using an equivalent proportion of cesium and rubidium in alternating patterns. Since these atoms require a different laser wavelength for gate drive. The benefit is a reduction of qubit crosstalk¹¹⁴³.

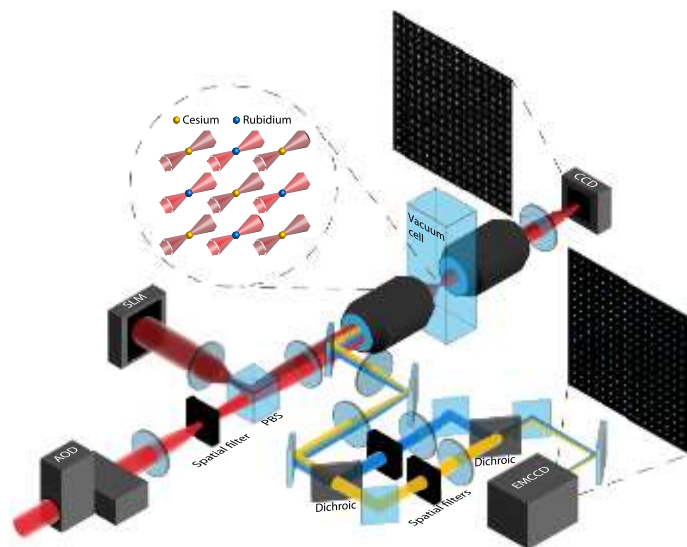


Figure 404: mixing two types of atoms, cesium and rubidium. Source: [Dual-Element, Two-Dimensional Atom Array with Continuous-Mode Operation](#) by Kevin Singh et al, University of Chicago, February 2022 (11 pages).

¹¹⁴¹ See [Two-qubit controlled-PHASE Rydberg blockade gate protocol for neutral atoms via off-resonant modulated driving within a single pulse](#) by Yuan Sun et al, October 2019 (16 pages) which deals with the improvement of CPHASE two-qubit gates on gg-qubits, with gate time at $1 \mu\text{s}$.

¹¹⁴² See [Two-qubit gate in neutral atoms using transitionless quantum driving](#) by Archismita Dalal and Barry C. Sanders, University of Calgary, June 2022 (22 pages). These researchers could improve CZ two-qubit gate with cesium with fidelities of 99,85%.

¹¹⁴³ See [Dual-Element, Two-Dimensional Atom Array with Continuous-Mode Operation](#) by Kevin Singh et al, University of Chicago, February 2022 (11 pages).

Vendors

Let's cover them by order of creation.



ColdQuanta (2007, USA, \$182.6M) is a company created by Dana Anderson, now his CTO, which develops laser-based solutions for cooling cold atoms and also designs cold atoms-based computers.

It is located in Boulder, Colorado, not far from the NIST Quantum Laboratory. Mark Saffman from the University of Wisconsin is their Chief Scientist for Quantum Information while Fred Chong from the University of Chicago is their Chief Scientist for Quantum Software (he also works for QCI).

Their initial core technology was the Quantum Core (*left* in Figure 405), a light guide that converges laser beams to control cold atoms that are usually cooled to less than 50 μK . It is integrated in QuCAL, a complete Bose-Einstein condensate generator, and in the Physics Station, a complete optical device for the control of cold atoms that can be used for various purposes. Atom chips are chips that can be integrated in these systems including miniaturized cold atom control optics. The startup uses these generic technologies to create a wide variety of systems, and above all for quantum sensing, especially for geopositioning instead of GPS, microgravimetry or cesium quantum clocks. They also offer ultra-high vacuum pumps for the control of cold atoms, called RuBECi as well as a cryogenic trapped ions package and magneto-optical traps, magnetic coils and cold atoms sources.

Their approach to the market is truly diverse. They have equipped the ISS space station with measuring instruments for NASA and JPL.



Figure 405: ColdQuanta Quantum Core (*left*), Physics Station (*middle*) and the atoms control chipset (*right*). Source: ColdQuanta.

Their overarching goal is to create and sell cold atoms-based quantum computers¹¹⁴⁴. They obtained some funding from DARPA in April 2020 under the ONISQ program with a \$7.4M collaborative project involving numerous universities and Raytheon BBN. The DARPA asked them to develop a scalable (>1000 qubits) system that can demonstrate quantum advantage on real-world problems. ColdQuanta is focused on creating gate-based systems with 100 qubits¹¹⁴⁵. Their first 2021 100-qubit “Hilbert” cloud-based quantum system was supposed to work in July 2021 but was said to be commercially available only by May 2022. It is using cesium atoms.

¹¹⁴⁴ See [ColdQuanta - Life in Quantum's Slow \(and Cold\) Lane Heats Up](#) by John Russell, April 2020 and the webinar [Powering the Quantum Information Age](#) with Bo Ewald, April 2020 (53 minutes).

¹¹⁴⁵ See [Demonstration of multi-qubit entanglement and algorithms on a programmable neutral atom quantum computer](#) by T. M. Graham, M. Saffman et al, ColdQuanta, February 2022 (25 pages) and published as [Multi-qubit entanglement and algorithms on a neutral-atom quantum computer](#) in Nature in April 2022. It describes their state of the art: a preparation of entangled Greenberger-Horne-Zeilinger (GHZ) states with up to 6 qubits, implementation of quantum phase estimation for a chemistry problem, and Quantum Approximate Optimization Algorithm (QAOA) for the MaxCut graph problem. Their gates set is made of local Rz phase gates and two-qubit CZ gates, run on a 7x7 grid spaced by 3 μm . The system is using cesium atoms. See the related See [ColdQuanta, Riverlane and University of Wisconsin–Madison Demonstrate Algorithms on a Programmable Neutral Atom Quantum Computer](#), April 2022.

During the summer of 2022, they released some interesting numbers on their gate-based system with fidelities of 99,4% for single qubit gates (lasting between 0.2 and 5 μ s) and 96,5% for two qubit gates (CZ, lasting 0.75 μ s), a measurement time of 1.5 ms, a T_2 of 1 second, all of this with 121 qubits.

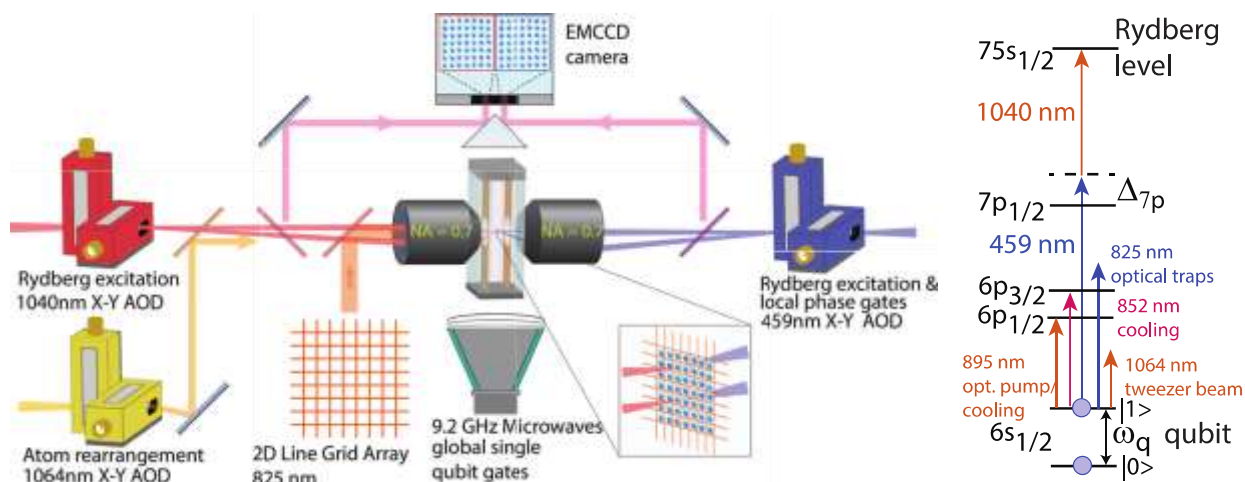


Figure 406: ColdQuanta's gate-based system architecture. Source: [Demonstration of multi-qubit entanglement and algorithms on a programmable neutral atom quantum computer](#) by T. M. Graham, M. Saffman et al, ColdQuanta, February 2022 (25 pages).

In May 2021, ColdQuanta joined a couple other quantum computers vendors like Pasqal with supporting IBM's Qiskit, formally joining the "IBM Quantum Network". The startup had about 170 people onboard as of mid-2022.

In May 2022, ColdQuanta acquired **Super.tech**, a software company providing pulse-level optimization, optimized transpilation and error mitigation techniques (SuperstaQ). It also provides benchmarking tools (SupermarQ). Fred Chong was their Chief Scientist from January 2021 until their acquisition in 2022. They are also teaming up with **Classiq** to handle code compilation¹¹⁴⁶ and with **ParityQC** (Austria) for the development of quantum software targeting optimization problems.

At last, in November 2022, ColdQuanta raised an additional \$111M making it the best funded neutral-atom startup, but seemingly to help them focus on developing and selling quantum sensors which are generating short and mid-term revenues.



Atom Computing (2018, USA, \$81M) aims to create a quantum computer based on optically controlled neutral atoms with qubit states using atoms nuclear spins initially with cesium and later with strontium 87¹¹⁴⁷.

The company was created by Ben Bloom (CTO, coming from Rigetti) and Jonathan King (Chief Scientist, directly coming from Berkeley), joined in 2021 by Bob Hays (CEO). The company based in Berkeley, in California, established an R&D facility in Boulder, Colorado in 2022.

They demonstrated in October 2021 their strontium-based 100-qubit Phoenix system with a 40 second qubits coherence time. They control their qubits with individual microwave drives. The qubit manifold states are in the atom electronic ground state, avoiding spontaneous decay and with a coherence time of 42 seconds. They can run simultaneous gates on individual atoms using two photon Raman transitions¹¹⁴⁸. As pictured below, it was demonstrated on 21-qubit arrays of 3x7 qubits.

¹¹⁴⁶ See [Classiq and ColdQuanta partner to provide a complete solution to creating and executing 100-qubit quantum circuits](#) and beyond, January 2022.

¹¹⁴⁷ See [Quantum computing with neutral atoms](#) by David Weiss 2017 (7 pages) and [Assembly and coherent control of a register of nuclear spin qubits](#) by Katrina Barnes et al, August 2021 (10 pages).

¹¹⁴⁸ See [Assembly and coherent control of a register of nuclear spin qubits](#) by Katrina Barnes et al, Atom Computing, August 2021 (11 pages).

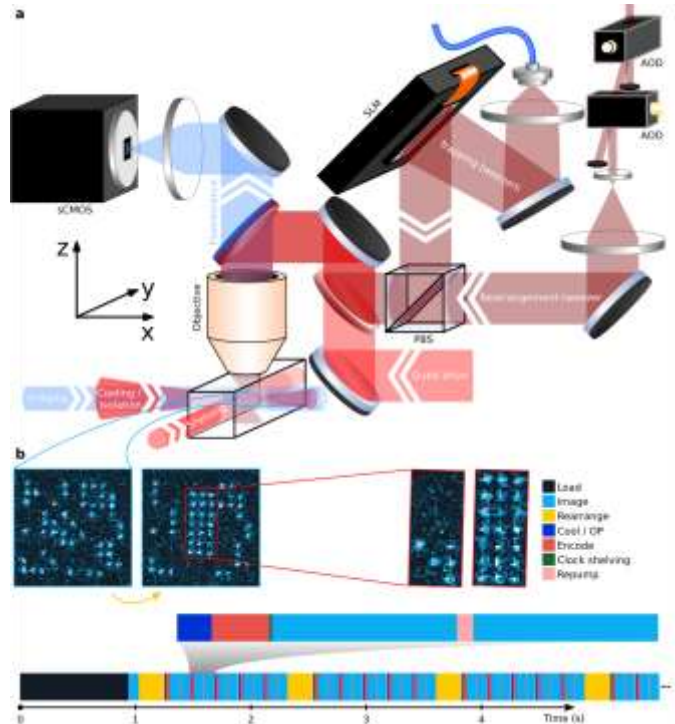
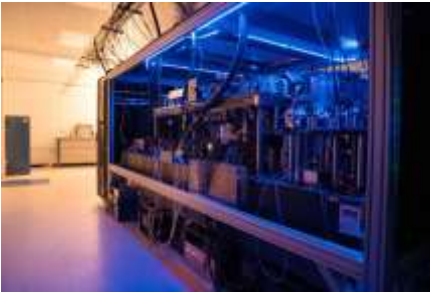
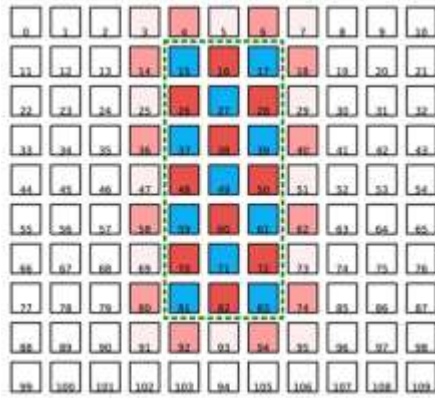


Figure 407: Atom Computing architecture for over 100-qubit gate-based computing. Source: [Assembly and coherent control of a register of nuclear spin qubits](#) by Katrina Barnes et al, August 2021 (10 pages).

They use the same apparatus as other vendors with SLMs for atoms trapping and rearrangement tweezers drive, AOD (acousto-optic deflector), EOM (electronic optical modulator) and a CMOS image sensor for qubits fluorescence readout. They plan to implement some form of QEC but don't provide many details on how they will handle non-demolition measurement (QND).



Pasqal (2019, France, 140M€) use magnetically confined rubidium atoms cooled by Doppler laser to reach mK and with a variant of the atomic Sisyphus effect to go down to $30 \mu\text{K}$ ¹¹⁴⁹. The atoms are trapped in 2D arrays with a spacing of a few microns between each of them.

Qubit states are managed with various modes depending on the use case: two levels of Rydberg-level energy (for XY quantum simulation model), ground-Rydberg levels (for Ising quantum simulation models¹¹⁵⁰) or with ground-ground states (for gate-based model, in future versions). Quantum gates are laser-activated to control the atom energy state. Qubits entanglement comes from atoms excitement in the Rydberg state which allows them to interact with other at long distance¹¹⁵¹.

¹¹⁴⁹ This method also uses lasers emitting orthogonally polarized photons. The method was invented by Claude Cohen-Tannoudji who was awarded the Nobel Prize in Physics in 1997.

¹¹⁵⁰ See [Efficient protocol for solving combinatorial graph problems on neutral-atom quantum processors](#) by Wesley da Silva Coelho, Mauro D'Arcangelo and Louis-Paul Henry, Pasqal, July 2022 (16 pages) that describes how they use a variational analog quantum computing and machine learning to solve graph problems. In that case, the atoms are arranged in a graph with specific distances between atoms that match the problem to be solved. It is not a simple regular 2D array.

¹¹⁵¹ See [Quantum Computing with Arrays of Atoms](#) by Lucas Béguin and Adrien Signoles from Pasqal, April 2020, which details the functioning of the startup's quantum processors. And their white paper [Quantum Computing with Neutral Atoms](#), June 2020 (41 pages).

Pasqal plans first to implement quantum simulators *aka* PQS (Programmable Quantum Simulator, or analog quantum computers) and then, to move to NISQ gate-based quantum computing¹¹⁵², with some hybrid analog/digital approach¹¹⁵³. The technology currently works with 100 qubits in simulation mode with plans to reach a thousand qubits by 2023¹¹⁵⁴.

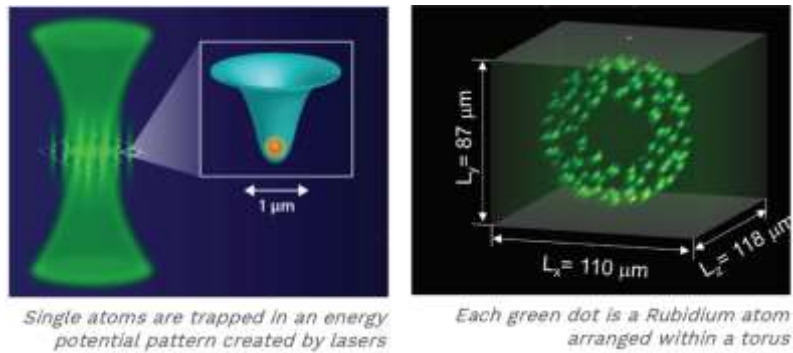


Figure 408: how atoms can be arranged, even in 3D. Source: Pasqal.

The computer will eventually fit into a 4-unit wide double-depth data center rack. It is based on rather standard components and does not require the creation of specific chipsets as it is the case for all other types of qubits.

In April 2020, startups **Pasqal** and **Muquans** announced a partnership that had been in preparation for a long time and on the use of a Muquans lasers system to control the cold atoms.

Milestone scientific papers and achievements happened between late-2020 and mid-2022, led by Pasqal and by the research team at IOGS behind Pasqal's cold atom-based system. The first one from December 2020 describes how a 2D matrix of 196 qubits was assembled using optical tweezers created with an SLM (a high-resolution Spatial Light Modulator) and an optimized arrangement technique using fewer than 200 steps¹¹⁵⁵. These SLMs enable phase grading and controlling phases spatial pattern. This atoms-positioning system will be extended to 3D arrays. It went on in 2022 with parallel gates execution¹¹⁵⁶. In July 2022, they announced having trapped up to 324 cold atoms in a 2D array, with using a 4K cryostat cooling the ultra-vacuum pump, which helps create a better vacuum and extend the atom qubit lifetime¹¹⁵⁷.

¹¹⁵² See [Why analog neutral atoms quantum computing is the most promising direction for early quantum advantage](#) by Jean-Charles Calbelguen, June 2022.

¹¹⁵³ See [Microwave Engineering of Programmable XXZ Hamiltonians in Arrays of Rydberg Atoms](#) by P. Scholl, Loic Henriët, Thierry Lahaye, Antoine Browaeys et al, PRX, April 2022 (10 pages) which presents an hybrid analog-digital architecture based on Hamiltonian evolutions and one-qubit gates. Qubits encoding will be different according to the use case. For gate-based computing, qubits are encoded with two hyperfine ground states. For Ising-like Hamiltonian, qubits use a ground state and a Rydberg state and for XY exchange Hamiltonian, they use two Rydberg states.

¹¹⁵⁴ Rydberg atoms have unsuspected uses, such as managing random music. See [Quantum music to my ears](#), June 2019. This is a change from music generated by deep learning!

¹¹⁵⁵ See [Enhanced atom-by-atom assembly of arbitrary tweezers arrays](#) by Kai-Niklas Schymik, Antoine Browaeys, Thierry Lahaye et al, November 2020 (10 pages).

¹¹⁵⁶ See [Pulse-level Scheduling of Quantum Circuits for Neutral-Atom Devices](#) by Richard Bing-Shiun Tsai, Loic Henriët et al, Pasqal, June 2022 (8 pages) and [Pulsar: An open source package for the design of pulse sequences in programmable neutral-atom arrays](#) by Henrique Silvério, Nathan Shammah, Louis-Paul Henry, Loic Henriët et al, January 2022 (21 pages).

¹¹⁵⁷ See [In-situ equalization of single-atom loading in large-scale optical tweezers arrays](#) by Kai-Niklas Schymik, Antoine Browaeys, Thierry Lahaye et al, PRA, July 2022 (5 pages).

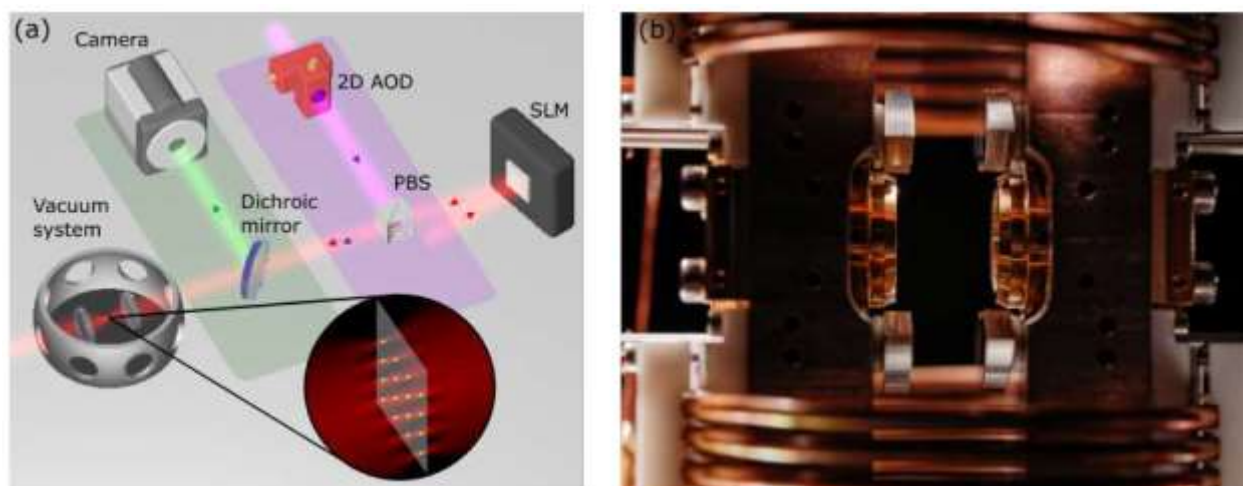


Figure 409: Pasqal's cold atom-based qubit control system includes a spatial light modulator (Spatial Light Modulator, SLM, based on LCoS liquid crystals¹¹⁵⁸) that controls the phase of the transmitted light in a focal plane with optical micro-traps. Laser tweezers or traps/pinches for rearranging the atoms and preparing the Hamiltonian to solve are controlled by the AOD (Acousto-Optic laser beam Deflector) and added to the beam from the SLM by a PBS (Polarizing Separator Filter). The fluorescent light emitted by the atoms during qubit readout is filtered by a dichroic mirror and analyzed by a CCD camera. The controlled atoms are confined in a small space of 1 mm³.

Applications wise, they published papers on quantum machine learning¹¹⁵⁹, on a financial risks assessment case study with CA-CIB in France¹¹⁶⁰ and for solving graph classification problems using the “quantum evolution kernel” method (QEK) with a first use case in 2021 in toxicity screening of chemical compounds and in the identification of optimal chemical reaction pathways. A 196 cold atoms setup was then used to program an Ising model simulating ferromagnetism and enabling quantum simulation¹¹⁶¹.

Then came the optimization of smart charging of electrical vehicles co-developed with EDF, using a QAOA hybrid algorithm and classical emulators of Pasqal systems and the QLM emulator from Atos¹¹⁶².

It was also funded through the PASQuanS flagship project. Atos researchers also evaluated the specifications of a cold atom simulator needed to reach some quantum advantage to solve an optimization task, the UD-MIS problem (Unit-Disk Maximum Independent Set problem)¹¹⁶³.

¹¹⁵⁸ See a description of an SLM in [Spatial Light Modulators](#) by Aurélie Jullien, 2020 (6 pages).

¹¹⁵⁹ See [Quantum evolution kernel: Machine learning on graphs with programmable arrays of qubits](#) by Louis-Paul Henry, Slimane Thabet, Constantin Dalyac and Loïc Henriët, PRA, September 2021 (19 pages) that is better explained in [Machine Learning – Pasqal's Quantum Computers can be used on concrete industrial problems](#), Pasqal, October 2021.

¹¹⁶⁰ See [Towards quantum advantage with efficient graph implementations](#), Pasqal, April 2022.

¹¹⁶¹ See [Programmable quantum simulation of 2D antiferromagnets with hundreds of Rydberg atoms](#) by Pascal Scholl, Thierry Lahaye, Antoine Browaeys et al, December 2020 (16 pages). Also published in [Nature](#) in July 2021. This was a result of a research funded through the European Flagship PASQuanS project in partnership with labs from Spain, Germany and Austria

¹¹⁶² See [Qualifying quantum approaches for hard industrial optimization problems. A case study in the field of smart-charging of electric vehicles](#) by Constantin Dalyac, Loïc Henriët, Emmanuel Jeandel, Wolfgang Lechner, Simon Perdrix, Marc Porcheron and Margarita Veshchezerova, 2021 (29 pages).

¹¹⁶³ A MIS problem consists in determining the size of the largest possible independent set in a graph and returning an example of such a set. The Unit-Disk MIS (UD-MIS) problem is the MIS problem restricted to unit-disk graphs. A graph is a unit-disk graph if one can associate a position in the 2D plane to every vertex such that two vertices share an edge if and only if their distance is smaller than unity.

They found out that over 1,000 qubits were required with a time budget of 0.2 seconds, if and when the system coherence could be improved by a factor ten¹¹⁶⁴.

Pasqal has created its own low-level programming environment that interfaces with high-level programming tools, including support for development platforms such as Google's **Cirq** that is supported in emulation mode, in digital gate-based programming mode¹¹⁶⁵, **TensorFlow Quantum** and IBM's **Qiskit**.

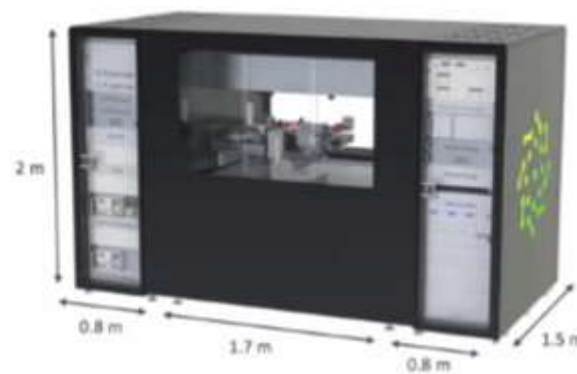


Figure 410: Pasqal Fresnel packaging.

In July 2020, **Cambridge Quantum Computing** (CQC) announced their support of Pasqal's qubits with their development tool (tket). Pasqal added a partnership with **ParityQC** with a 3-year collaboration to advance quantum optimization and parallelization¹¹⁶⁶ and released the open source library **Pulser**, co-developed with the **Unitary Fund** enabling the control of their processor at the level of laser pulses¹¹⁶⁷. They also announced a partnership with **Atos** in November 2020 to integrate a Pasqal accelerator with Atos supercomputers. At last, they also work with **Rahko** as well as with **Multiverse Computing**, in association with Cr dit Agricole CIB.

In January 2021, the Italian HPC consortium **CINECA** announced that will use Pasqal's Fresnel 100-qubits processor¹¹⁶⁸. The startup was also selected as part of the project HPC-QS from EuroHPC to provide two of their systems to HPC public datacenters, one in Germany (FZ J lich *aka* J lich Research Centre) and one in France (CEA TGCC). Both Pasqal systems will be connected to an Atos QLM for emulation and quantum system drive.

Pasqal funding came through an initial round of 2.5M  led by Quantonation and Christophe Jurczak who is their chairman, then a 4,5M  grant from the European Union EIC Accelerator¹¹⁶⁹, and finally a second round of funding of 25M  announced in April 2021. In January 2022, Pasqal and Qu&Co (The Netherlands) merged, creating an integrated hardware/software company. As of December 2022, they had a staff of >100 people. In January 2023, Pasqal raised an additional 100M .

2022 was a busy year with new partnership announced with **EDF**, **Thales**, **GENCI**, **Aramco** (for implementing QML algorithms in the energy business), **Siemens** (for computer-aided-design and engineering, simulation and testing), **BASF** (fluid dynamic problem solving algorithm), **BMW** (material science and material deformation algorithms) and the first sales of two 100-qubit quantum processor to **GENCI** and **FZJ** as part of the HPCQS EU consortium. They opened an office in Boston (USA) and in Sherbrooke (Canada) in June 2022. And their first 100-qubit quantum simulator web online with **OVHcloud** in May 2022 (in private beta) and will be online later with **Microsoft Azure Quantum**.

¹¹⁶⁴ See [Solving optimization problems with Rydberg analog quantum computers: Realistic requirements for quantum advantage using noisy simulation and classical benchmarks](#) by Michel Fabrice Serret, Bertrand Marchand and Thomas Ayr l, November 2020 (25 pages).

¹¹⁶⁵ See [Quantum circuits on Pasqal devices](#).

¹¹⁶⁶ See [ParityQC and Pasqal partner to build the first fully parallelizable quantum computer](#), Pasqal, October 2020. With other researchers in Austria, ParityQC is proposing a way to encode QAOA generic optimization problems into gate-based cold atoms computers using a specific 4-qubit gate as seen in [Quantum computing on neutral atoms: the novel four-body Rydberg gate](#), ParityQC, 2022, referring to: [Quantum Optimization via Four-Body Rydberg Gates](#) by Clemens D laska, Kilian Ender, Glen Bigan Mbeng, Andreas Kruckenhauser, Wolfgang Lechner, and Rick van Bijnen, PRL, March 2022 (11 pages).

¹¹⁶⁷ See [Pulser: a control software at the pulse-level for Pasqal quantum processors](#) by Pasqal, January 2021.

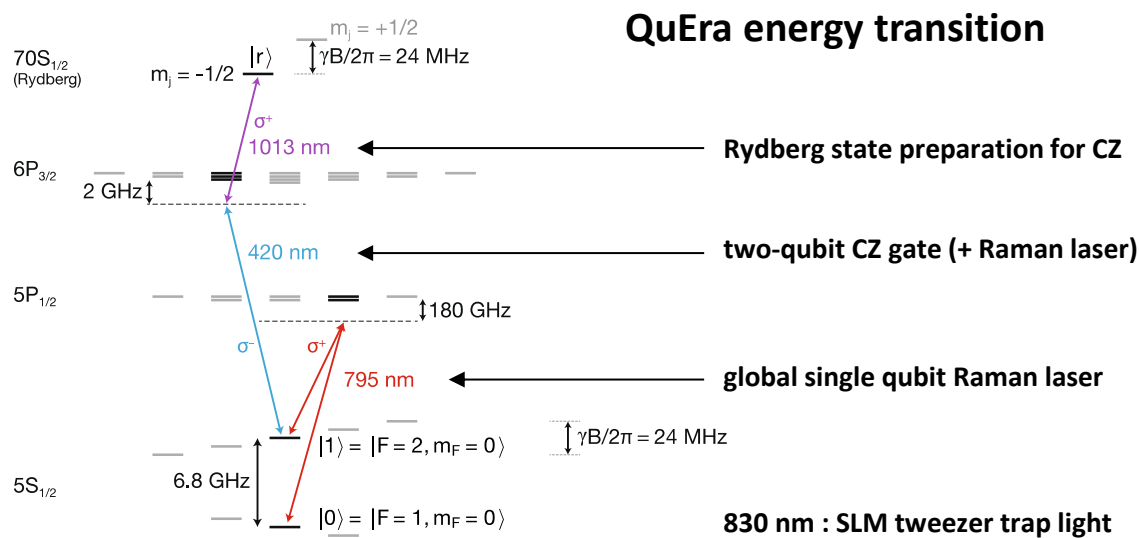
¹¹⁶⁸ See [CINECA-Pasqal agreement on quantum computing](#), January 2021.

¹¹⁶⁹ See [Europe is betting on quantum computing with neutral atoms](#), Pasqal, December 2020.



QuEra Computing (USA, 2018, \$17M) develops a cold atom gate-based quantum computer, their first generation being named Aquila. The startup was created by researchers from Harvard University and MIT.

With Nathan Gemelke, Alexei Bylinskii, Shengtao Wang and Mikhail D. Lukin, among others, who is one of their scientific advisors¹¹⁷⁰. They published a research paper on a 2D array 256 programmable cold atom system in 2021 and announced in November 2021 it would become a commercial product¹¹⁷¹. It is available on Amazon Braket since November 2022. What they brand “programmable quantum computers” are not gate-based systems and are still quantum simulators where they encode graph problems into a layout of cold atoms¹¹⁷². A graph problem is expressed as a “maximum weight independent set” (MWIS) problem that is then turned into several unit-disk graph sets (UDG) which are assemblies of nearby neutral atoms using the Rydberg effect for local entanglement. These sets are connected to each other with entangled neutral atoms at their edge. Various problems like QUBO, Ising models and even integer factorization can be mapped onto MWIS problems.



source: See A quantum processor based on coherent transport of entangled atom arrays by Dolev Bluvstein, Mikhail Lukin et al, Nature, April 2022.

Figure 411: QuEra atomic energy transitions used to control qubits and qubit gates. Source: [A quantum processor based on coherent transport of entangled atom arrays](#) by Dolev Bluvstein, Mikhail D. Lukin et al, Nature, April 2022 (21 pages).

They proposed in 2022 a way to transport qubits to handle two-qubit gates using atoms shuttling with tweezers. They implemented it with a Steane-7 quantum error correction code graph (but not with a full QEC), topological surface code and toric code states using mobile ancilla and with hybrid analog-digital quantum circuits using dynamically reconfigurable array and CZ gates¹¹⁷³.

They are also working on making non-demolition qubit measurement, a key feature to implement full QEC (quantum error correction) and FTQC (fault-tolerant quantum computing). This would be based on moving selected atoms “into a readout zone where their qubit state can be rapidly detected via fast, resonant photon scattering on a cycling transition”.

¹¹⁷⁰ See in particular [Parallel Implementation of High-Fidelity Multiqubit Gates with Neutral Atoms](#) by Harry Levine, Mikhail D. Lukin et al, August 2019 (16 pages).

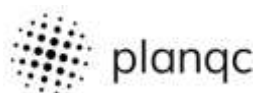
¹¹⁷¹ See [Quantum Phases of Matter on a 256-Atom Programmable Quantum Simulator](#) by Sepheer Ebadi, Mikhail D. Lukin et al, 2020 (20 pages).

¹¹⁷² See [This new startup has built a record-breaking 256-qubit quantum computer](#) by Siobhan Roberts, MIT Technology Review, November 2021 and the real stuff in [Quantum Optimization of Maximum Independent Set using Rydberg Atom Arrays](#) by Sepheer Ebadi, Mikhail Lukin et al, February 2022 (10 pages) and [Quantum optimization with arbitrary connectivity using Rydberg atom arrays](#) by Minh-Thi Nguyen, Mikhail D. Lukin et al, September 2022 (19 pages).

¹¹⁷³ See [A quantum processor based on coherent transport of entangled atom arrays](#) by Dolev Bluvstein, Mikhail D. Lukin et al, Nature, April 2022 (21 pages).

They could also use arrays with two atoms species such as two isotopes of the same element or two different atom elements, with the data atoms being encoded in one atomic species and ancilla atoms encoded in another species that can be easily measured¹¹⁷⁴.

In July 2022, QuEra launched Bloqade, their quantum emulation software package that is available on Github as a Julia package. It emulates on classical computers atom-based quantum simulations. This is akin to Pulser from Pasqal. They got help for this from Amazon and the Perimeter Institute.



Planqc (2022, Germany, 4.6M€) is a startup created in Garching near Munich by Alexander Glätzle (CEO, a researcher at the University of Oxford in the UK), Sebastian Blatt (CTO) who was a researcher at Ludwig-Maximilians-University Munich (and is a son of Rainer Blatt) and Johannes Zeiher (a researcher at MPQ).

Immanuel Bloch and Jose Ignacio Cirac from MPQ and Dieter Jaksch, Professor of Physics at the University of Oxford and the University of Hamburg are their scientific advisors. It's a neutral atom based qubits company that plans to scale its system to thousands of qubits. They are still semi-stealth and don't provide any details on their technology choices and roadmap. Looking at the research work from the founders, you may infer that they plan to implement MBQC on large cluster states of entangled cold atoms¹¹⁷⁵.

Let's note here that **M Squared** (2006, UK, \$56M) who was historically working on neutral atoms sensors entered the neutral atoms quantum computers market in November 2022.

NMR qubits

History and science

Nuclear Magnetic Resonance was an early technique investigated to create quantum computers. Qubit states are the spin of nuclei within large ensembles of up to 10^{15} molecules. The qubit states are readout using nuclear magnetic resonances, implementing a variant of nuclear magnetic resonance spectroscopy.

The NMR phenomenon was discovered in 1945 by **Edward Mills Purcell** (1912-1997, American) for which he was awarded the Nobel prize in physics in 1952, shared with Felix Bloch. Using nuclear spins for quantum computing was first proposed in 1993 by **Seth Lloyd** from the MIT¹¹⁷⁶ and refined in 1994 by **David DiVincenzo**, then at IBM Research, for the implementation of perfluorobutadienyl two-qubit gates¹¹⁷⁷.

¹¹⁷⁴ See [Hardware-Efficient, Fault-Tolerant Quantum Computation with Rydberg Atoms](#) by Iris Cong, Mikhail Lukin et al, May 2022 (31 pages) making references to [A dual-element, two-dimensional atom array with continuous-mode operation](#) by Kevin Singh et al, October 2021 (11 pages) on reduced cross-talk and QND with two mixed atom elements (cesium and rubidium), [Fast Preparation and Detection of a Rydberg Qubit using Atomic Ensembles](#) by Wenchao Xu et al, May 2021 (11 pages) and [Interaction enhanced imaging of individual atoms embedded in dense atomic gases](#) by G. Günter, Shannon Whitlock et al, June 2011 (6 pages) which also describes a QND measurement of cold atoms state.

¹¹⁷⁵ See [Realizing distance-selective interactions in a Rydberg-dressed atom array](#) by Simon Hollerith, Immanuel Bloch, Johannes Zeiher et al, October 2021 (5 pages), See [Quantum Information Processing in Optical Lattices and Magnetic Microtraps](#) by Philipp Treutlein, Immanuel Bloch et al, Max-Planck Institute, June 2006 (15 pages). This is a variation of cold atoms qubits adapted to cluster states and MBQC. See also [Quantum simulations with ultracold atoms in optical lattices](#) by Christian Gross and Immanuel Bloch, 2017 (8 pages).

¹¹⁷⁶ See [A potentially realizable quantum computer](#) by Seth Lloyd, Science, 1993 (4 pages).

¹¹⁷⁷ See [Two-Bit Gates are Universal for Quantum Computation](#) by David DiVincenzo, July 1994 (21 pages) and [Bulk Spin-Resonance Quantum Computation](#) by Neil A. Gershenfeld and Isaac L. Chuang, 1997 (7 pages).

It was refined by various proposals coming from the MIT, UCSB and Stanford researchers in 1997 with a computing method using liquid state NMR (molecules in a liquid) and enabling the measurement of the expectation value of quantum observables, ensuring an exponential computing speedup¹¹⁷⁸.

An expectation value of an observable is the average value of the observable and not a random value obtained by a projective measurement, the type of qubit readout measurement usually implemented with other techniques. Using another explanation, this measures a statistical mixture of pure states.

In 2001, **IBM** researchers even implemented Shor's algorithm with the number 15 on a 7-qubit NMR quantum processor using a perfluorobutadienyl iron complex where the spins come from the nuclear spins of fluor and carbon atoms (in red)¹¹⁷⁹. It is still the record to date! In these systems, qubit states where the ensemble nuclear spins $\frac{1}{2}$ in a magnetic field, quantum gates were operated by radiofrequency pulses and qubit readout was done with detecting spin states with a radiofrequency coil¹¹⁸⁰.

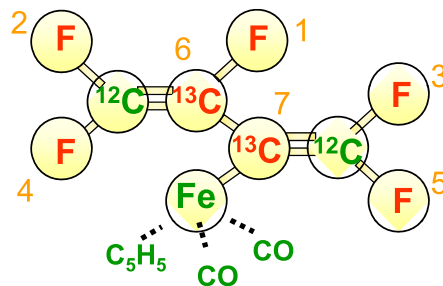


Figure 412: NMR can rely on complex molecule like perfluorobutadienyl. Source: IBM.

Afterwards, there were some developments with “Solid state NMR” (SSNMR) using nitrogen vacancies and interactions between carbon atomic spins and vacancies electron spins or nuclear spins of ²⁹Si in silicon structures¹¹⁸¹.

NMR was quite fashionable in quantum computing about 20 years ago. IBM was even planning for the existence of NMR-based tabletop quantum computers¹¹⁸². 22 years ahead, their (superconducting qubits) quantum computers are 3-meter wide cubes consuming in excess of 25 kW.



Still, research is still ongoing on NMR quantum computing. It goes on in Europe in the Europe 2020 project **FATMOLS** run by a research consortium led by Spain¹¹⁸³. Its ambition is to create a molecular spin quantum processor using artificial magnetic molecules implementing spin qubits controlled, read-out and linked with some superconducting circuits.

Quantum features are implemented with nuclear spins, electronic spins and circuits. Programming models range from quantum simulations to gate-based FTQC. The FATMOLS project's goal is to create a proof-of-concept of one of the repetition unit cells of this platform with at least two molecules with multiple and fully addressable levels and related algorithms.

¹¹⁷⁸ See [Ensemble quantum computing by NMR spectroscopy](#) by David G. Cory, Amr F. Fahmy and Timothy F. Havel, MIT, 1997 (6 pages).

¹¹⁷⁹ See [Experimental realization of Shor's quantum factoring algorithm using nuclear magnetic resonance](#) by Lieven M.K. Vandersypen, Isaac L. Chuang et al, December 2001 (18 pages).

¹¹⁸⁰ See [NMR Quantum Computing](#), 2012 (43 slides) and [NMR Quantum Computation NMR Quantum Computation](#) by Thaddeus Ladd, Stanford, 2003 (39 slides).

¹¹⁸¹ See [Solid-State Silicon NMR Quantum Computer](#) by E. Abe, K. M. Itoh, Y. Yamamoto et al, 2003 (5 pages).

¹¹⁸² See [Toward a table-top quantum computer](#) by Y. Maguire, E. Boyden and N. Gershenfeld, IBM, 2000 (17 pages).

¹¹⁸³ With CSIC, Aragón Materials Science Institute (ICMA), The Centre of Astrobiology (CAB), University of Barcelona, Universidad de Valencia / Instituto de Ciencia Molecular (UVEG), the Keysight team in Barcelona, and outside Spain: University of Manchester Molecular Magnetism Group, University of Oxford Department of Condensed Matter Physics, University of Parma and the Department of Chemistry at the University of Florence, Universität Stuttgart / Institute for Functional Matter and Quantum Technologies, Wolfgang Pauli Institut, Technische Universität Wien and IBM Zurich (Ivano Tavernelli).

The end-goal is to reach 100 to 1000 physical qubits¹¹⁸⁴. The project runs from March 2020 to August 2023 with a total cost of 3.2M€, entirely funded by the EU.

Research

Various NMR variants are still investigated like the use of large molecular spins¹¹⁸⁵, europium molecules with nuclear spins that can interact with luminescent photons carrying the nuclear spin information¹¹⁸⁶, with molecular ensembles¹¹⁸⁷ and optically addressable molecular spins¹¹⁸⁸.

DQC1 (Deterministic Quantum Computation with 1 quantum bit) is a curious quantum computing model created in 1998 by Emanuel Knill and Raymond Laflamme. It was designed for NMR qubits which were commonly developed in the late 1990s and were very noisy. It is described as a deterministic quantum computation using one qubit and a classical computer¹¹⁸⁹.

It computes deterministic functions on one bit and a classical computer is performing probabilistic computing. But there's more than one qubit in the story: the input is indeed constrained to a single qubit in a pure state but a set of n other qubits is prepared in an identity state and subject to a random unitary transformation U_n and in a completely mixed state. These systems use noise as a resource which is formalized with **quantum discord** mathematical tools¹¹⁹⁰. At the end of computing, a measurement takes place on the first qubit. It is not a universal quantum computing model, doesn't use massive entanglement and has a narrow set of use cases although it is supposed to bring some exponential speedups in some circumstances¹¹⁹¹.

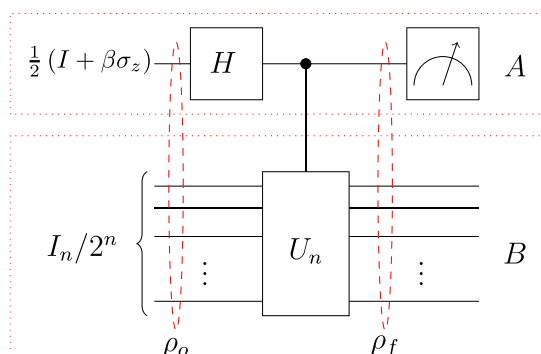


Figure 413: description of the DQC1 model. A qubit at the top is the only input. It is prepared then subject to an Hadamard gate and the result controls the application of the U_n unitary transformation to n other qubits. At the end of this processing, the first qubit is the only one measured, with the process being repeated several times. The output yields a trace of the unitary U_n . Source: [Measurement-Based Quantum Correlations for Quantum Information Processing](#) by Uman Khalid, Junaid ur Rehman and Hyundong Shin, *Nature Research Scientific Reports*, 2020 (9 pages).

Vendors

NMR quantum computers don't scale well due to noise affecting qubits and poor entanglement. It didn't prevent one company from China to manufacture and sell an NMR-based quantum computer. And fulfilling IBM's 2000 dream, it is a desktop product.

¹¹⁸⁴ See [A perspective on scaling up quantum computation with molecular spins](#) by S. Carretta et al, *Applied Physics Letters*, May 2021 (13 pages).

¹¹⁸⁵ See [Optically addressable molecular spins for quantum information processing](#) by S. L. Bayliss et al, April 2020 (9 pages) as well as [Chemical tuning of spin clock transitions in molecular monomers based on nuclear spin-free Ni\(ii\)](#) by Marcos Rubin-Osanz et al, 2021 (11 pages). It involves one lab in Spain and three in France (ICMM Orsay, LCPQ Toulouse and LNCMI Grenoble).

¹¹⁸⁶ See [Ultra-narrow optical linewidths in rare-earth molecular crystals](#) by Diana Serrano, Senthil Kumar Kuppasamy, Benoît Heinrich, Olaf Fuhr, David Hunger, Mario Ruben and Philippe Goldner, KIT, CNRS, University of Strasbourg and Chimie ParisTech, *Nature*, May 2021-March 2022 (19 pages).

¹¹⁸⁷ See [A New Approach to Quantum Computing Using Magnetic Resonance Imaging](#) by Zang-Hee Cho et al, June 2022 (9 pages).

¹¹⁸⁸ See [Enhancing Spin Coherence in Optically Addressable Molecular Qubits through Host-Matrix Control](#) by S. L. Bayliss, David Awschalom et al, April 2022 (13 pages).

¹¹⁸⁹ See [On the Power of One Bit of Quantum Information](#) by Emanuel Knill and Raymond Laflamme, 1998 (5 pages).

¹¹⁹⁰ See [Measuring geometric quantum discord using one bit of quantum information](#) by G. Passante, O. Moussa and Raymond Laflamme, 2021 (5 pages), [Introducing Quantum Discord](#) by Harold Ollivier, October 2001 (5 pages) and [Quantum Discord: A Measure of the Quantumness of Correlations](#) by Harold Ollivier and Wojciech H. Zurek, PRL, December 2001 (5 pages).

¹¹⁹¹ See [Power of Quantum Computation with Few Clean Qubits](#) by Keisuke Fujii et al, 2015 (45 pages).

SpinQ Technology (2018, China, \$14.4M) started with announcing in January 2021 their Gemini \$5K 2-qubit desktop quantum computer and their cloud quantum computing platform Taurus¹¹⁹². It followed an initial version launched in 2020 and sold at \$55K. The computer weighs 55 kg and works at ambient temperature. They plan to increase the number of qubits of this device in upcoming versions, up to a maximum 15 qubits. It would be nice since 2 qubits are totally useless even for quantum programming learning tasks. Meanwhile, you can test for free 7 real superconducting qubits on IBM Quantum Experience cloud systems.

The SpinQ computers use liquid dimethyl-phosphite molecules with two OCH₃ groups associated to a phosphorus atom plus one oxygen and one hydrogen atom. These molecules are controlled with permanent magnets and an RF pulse generation system. They followed on with the Gemini mini version (also with two qubits) and the Triangulum (with a hefty three qubits).



Photons qubits

Contrarily to all the previous qubits, photons have no mass and move at about the speed of light, modulo the optical refractive index of the physical media they pass through. While photons were used everywhere in solid qubits in control and readout features with microwaves or laser beams, they can be used to create qubits exploiting polarization or other physical characteristics such as frequency, amplitude, phase, mode, path or photon number. This is the vast field of linear and nonlinear optics¹¹⁹³. It is found in both the generation of qubits for quantum computation or simulation and with their application in telecommunications and quantum cryptography which we study in [another part](#) of this document, starting page 819.

photons qubits

- **stable qubits** with absence of decoherence.
- qubits processing at **ambient temperature**.
- **emerging nano-photonic** manufacturing techniques enabling scalability.
- **easier to scale-out** with inter-qubits communications and quantum telecommunications.
- **MBQC/FBQC** circumventing the fixed gates depth computing capacity.

- **not yet scalable** in number of operations due to probabilistic character of quantum gates and the efficiency of photon sources.
- **photons can't be stopped or be stored**, they can just be slightly delayed.
- **need to cool photon sources and detectors**, but at relatively reasonable temperatures between 2K and 10K, requiring lightweight cryogenic systems.
- **boson sampling based quantum advantage** starts to being programmable but a practical quantum advantage remains to be proven.

Figure 414: pros and cons of photon qubits. (cc) Olivier Ezratty, 2022.

¹¹⁹² See [SpinQ Gemini: a desktop quantum computer for education and research](#) by Shi-Yao Hou et al, 2021 (14 pages). It was updated with 3 qubits in September 2021 with their Triangulum version.

¹¹⁹³ Nonlinear optics is well described in [Nonlinear Optics](#) by Franz X. Kärtner and Oliver D. Mücke, University of Hamburg, December 2016 (255 pages). See also the reference book [Nonlinear Optics](#) by Robert W. Boyd, 2007 (620 pages).

Photonics is both an interesting solution for creating qubits as well as a transversal technology that is indispensable to other types of qubits because it is the only one that allows long-distance communications between quantum sensors, quantum networks and quantum computers. Photons are also used directly in quantum sensing, particularly for precision time measurement and even for pressure measurement.

The advantages of photonics are that it allows to manage quite stable qubits with a very low error rate at the quantum gate level thanks to their weak coupling with the environment. The main source of decoherence is related to the optical losses happening with photons propagation. Photons also operate at any temperature¹¹⁹⁴, do not require expensive nanoscopic manufacturing techniques and can be based on nanophotonic CMOS manufacturing processes¹¹⁹⁵. Their disadvantage lies in the fact that photons are even more probabilistic beasts than any of the other qubits. Scalability issues make it difficult to assemble more than a few dozens of qubits, at least for the moment. Photon sources must be more powerful to accommodate a larger number of entangled qubits.

Current technology developments are based on progresses made with more efficient single photon sources, better photon detectors, nonlinear optics, advanced quantum states preparation (multimode, spatial or spectral multiplexing, non-Gaussian states) with a larger computing space than traditional two-states qubits, using cluster-states measurement-based techniques (MBQC) to avoid the pitfalls of a physically limited quantum gates depth and quantum error corrections.

History

The roots of quantum photonics date back from 1963 with the introduction of Glauber states by Roy J. Glauber which created the notion of coherent states of light explained by the quantization of the electromagnetic field. This corresponded to the beginnings of the laser era which led, among many things, to its broad industry impact, including fiber optics in the telecom realm.

While the first physical qubits were experimented in the mid-1990 (trapped ions, NMR) and early 2000s (superconducting), photon qubits used for computation saw the light much later. Starting in the mid-1980s, quantum photonics were envisioned for implementing quantum key distribution protocols. 2001 was a foundational year with the creation of the KLM theory by Emanuel Knill and Raymond LaFlamme (then at the Los Alamos National Lab) and Gerald Milburn (University of Queensland, Australia)¹¹⁹⁶.

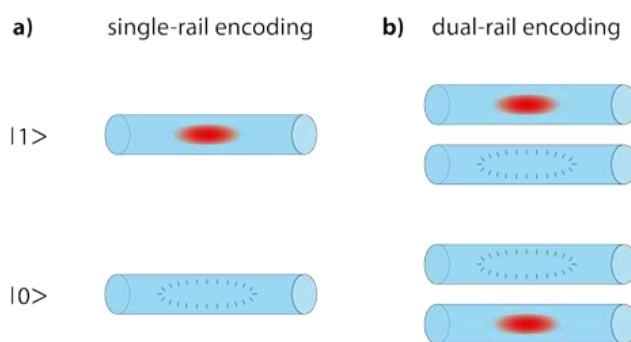


Figure 415: how dual-rail encoding works. Source: [No-go theorem for passive single-rail linear optical quantum computing](#) by Lian-Ao Wu et al, *Nature*, 2013 (7 pages).

¹¹⁹⁴ In general, solid-state light source must be cooled to 10K and the photon detectors output to about 2K to 4K. At least, one avoids going below 1K, which allows the use of cryogenic systems that are satisfied with helium 4 and do not require helium 3. These cryogenic systems are miniaturizable and require much less energy than the dilution systems used for superconducting and silicon qubits.

¹¹⁹⁵ See [Photonic quantum information processing: A concise review](#) by Sergei Slussarenko and Geoff Pryde of the Centre for Quantum Dynamics and the Centre for Quantum Computation and Communication Technology at Griffith University in Brisbane, Australia (20 pages) which describes the state of the art of photon qubits. This is the source of the diagram. See also the older [Why I am optimistic about the silicon-photon route to quantum computing](#) by Terry Rudolph, a cofounder of PsiQuantum, published in 2016 (14 pages).

¹¹⁹⁶ See [A scheme for efficient quantum computation with linear optics](#) by Emanuel Knill, Raymond Laflamme and Gerard Milburn, 2001 (7 pages).

This model could theoretically implement quantum computing without relying on some sort of non-linearity for creating entangling quantum gates¹¹⁹⁷. Implementing for example a CNOT gate with photons is not easy since photons do not easily interact with each other.

The KLM model was a breakthrough, making it possible to implement two qubit gates with using photon sources, beam splitters and photon detectors, using a dual-rail encoding, represented by the presence of a single photon in one of two spatial optical modes¹¹⁹⁸. It circumvents the need for non-linear interactions between photons with the use of post-selection with using ancilla photons, many executions and iterations being required. It creates significant overhead which makes the model impractical and not scaling well¹¹⁹⁹.

There were then many “firsts” with the first universal optical quantum computer in 2015 using a chipset handling 6 photons with 15 Mach-Zehnder interferometers and 30 thermo-optic phase shifters and a 12-single-photon detector system¹²⁰⁰, a programmable photonic quantum computer created by Xanadu in 2021 with 8 photons¹²⁰¹ and a first quantum computational advantage using gaussian boson sampling in China¹²⁰². Boson sampling was based on an idea from Scott Aaronson elaborated in 2011¹²⁰³. It led in 2022 to a similar experiment achieved by Xanadu with a programmable gaussian boson sampler. These systems however are not yet providing a quantum computing advantage with a real useful problem defined by some entry data.

Many fundamental research advances were also achieved:

- The MBQC model was created in 2000 by Robert Raussendorf and Hans Briegel. It circumvented some limitations of photon qubits beyond the nonlinearity already discussed, like the finite number of gates that could be executed, the photons being “flying qubits”. We’ll describe this later. The key figure of merit of this architecture is the ability to create large cluster states of entangled photons.
- Quality photon sources, like single and deterministic photon sources, and better, entangled photon sources. Two entangled photons can be created with a photon source and a polarizing crystal. More entangled photons can be created with a single deterministic indistinguishable photon sources and delay lines.
- Silicon-based or III-V Quantum Photonic Integrated Circuits (QPICs) that implement quantum gates with waveguides and electronically controllable optical elements like beam splitters and polarizing filters as well as photon sources and photons detectors. They enable miniaturization of these components. Their figures of merit are miniaturization and low photon losses¹²⁰⁴.

¹¹⁹⁷ See the review paper [The Category of Linear Optical Quantum Computing](#) by Paul McCloud, March 2022 (34 pages).

¹¹⁹⁸ See [No-go theorem for passive single-rail linear optical quantum computing](#) by Lian-Ao Wu et al, Nature, 2013 (7 pages).

¹¹⁹⁹ This part is inspired from [Twenty Years at Light Speed: The Future of Photonic Quantum Computing](#) by David D. Nolte, December 2021. See also [Photonic quantum technologies](#) by Jeremy L. O'Brien, Akira Furusawa and Jelena Vučković, Nature Photonics, 2009 (11 pages).

¹²⁰⁰ See [Universal linear optics](#) by Jacques Carolan, Jeremy O'Brien, Anthony Laing et al, Science, 2015 (6 pages).

¹²⁰¹ See [Quantum circuits with many photons on a programmable nanophotonic chip](#) by J. M. Arrazola et al, Nature, March 2021 (21 pages).

¹²⁰² See [Quantum computational advantage using photons](#) by Han-Sen Zhong et al, December 2020 (23 pages).

¹²⁰³ See [The computational Complexity of Linear Optics](#) by Alex Arkhipov and Scott Aaronson, 2010 (94 pages).

¹²⁰⁴ See the review paper [Silicon photonic devices for scalable quantum information applications](#) by Lantian Feng et al, August 2022 (20 pages).

Then, since about 2017, a wealth of startups have been created that are all pursuing the goal of creating photon qubits quantum computers, first in the NISQ and then the FTQC realms: **PsiQuantum**, **Xanadu**, **Quandela**, **Orca Computing**, **QuiX**, etc. They all adopt very diverse technological choices as we will see in the vendor section.

Science

To understand photons in quantum information systems, one needs to get a bit deeper in quantum optics and statistical optics. This section constitutes a very rudimentary primer, enabling you to understand some of the vocabulary used by quantum information photonicians. It can also help us segment the various kinds of photonic qubits like discrete variables and continuous variables qubits.

So far, we've mainly mentioned photons as wave-particles interacting with matter, with the photoelectric effect and atoms energy transitions. But exactly, what are photons? How do we define and classify it?

A photon is a moving perturbation of the electromagnetic field with orthogonal magnetic and electric field variations themselves orthogonal to the photon propagation direction.

Photons are described with their quantum numbers which are:

- **Mass and electric charge** that are equal to zero.
- **Wavelength** λ or frequency ν which define the photon energy and momentum. Several photons with same or different frequencies can be coherently superposed and create a “photon number” or a “wave packet”. Wave packets are usually generated by femto-lasers pulses, mostly in the visible and infrared ranges, or by digital-to-analog microwave generators like those used to drive superconducting and electron spin qubits.
- **Spin angular momentum** (SAM), which corresponds to their angular momentum having quantized values $+\hbar$ or $-\hbar$ (spin = +1 or -1 since spins are expressed in \hbar units) corresponding to circular right or left polarization. Any single monochromatic photon is a linear superposition of these two circular polarizations, including linearly horizontally or vertically polarized photons.
- **Orbital angular momentum** (OAM) where the electromagnetic field is rotating helically along its propagation axis or vector¹²⁰⁵. Equals $\ell\hbar$ with ℓ being any integer.

Photons interact with other particles, mainly electrons either tied to atom nucleus, for photons absorption and/or emission, or free electrons like with the Compton effect.

They can be created, destroyed and modified by many of these interactions. Pairs of photons can also be generated by the collision between particles and their antiparticles. Their behavior is mainly described with Maxwell's equations and its derivatives.

Photon directionality. Is a photon directional? Textbooks usually make a distinction between spontaneous emission with photons going in any direction, from a lightbulb or the Sun, and stimulated emission, with directional light, coming from lasers. Radio-frequency antennas can also create spherical radiations going in many directions.

But whatever its source and wavelength, a single photon is mostly always directional and moving in space as a planar wave. A photon electromagnetic wave is represented by orthogonal electric and magnetic fields variations travelling along a vector orthogonal to them. A photon direction can change when it traverses various materials having different refraction indices.

¹²⁰⁵ See [Quantum advantage using high-dimensional twisted photons as quantum finite automata](#) by Stephen Z. D. Plachta et al, February 2022 (20 pages) which proposes to use qubits encoded in orbital angular momentum to implement a Quantum finite automata (QFA) to solve binary optimization problems.

Can we have non-planar photons? “Any direction” photons can come from a statistical view of random multidirectional photons emissions or from a coherent superposition of photons emitted in several directions.

With light bulbs, many photons are emitted in various directions by random thermal processes, with various photon wavelengths. Laser coherent light is made of photons with the same wavelength, phase and direction. The distinction between a wave and a point-like particle is as blurred with photons as it is with electrons as far as their exact physical nature and dimensional scope is concerned.

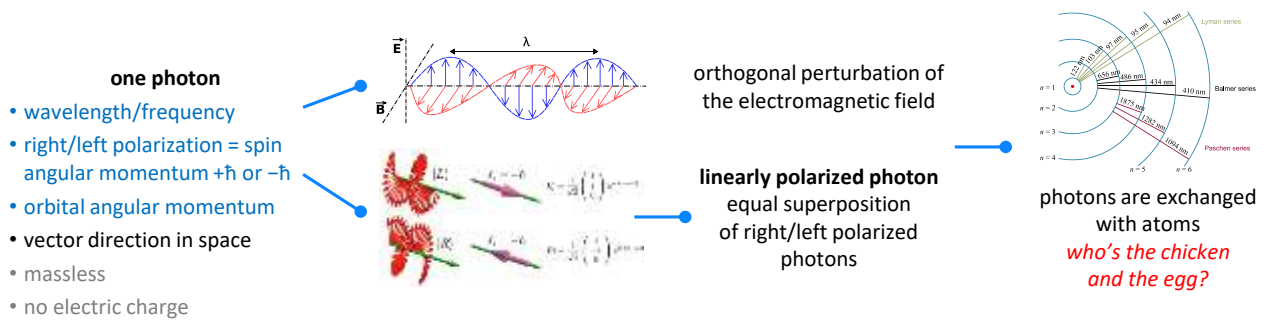


Figure 416: photon characteristics, polarization.

Photon length and size are thus notions that are rarely mentioned. According to the Hunter-Wadlinger electromagnetic theory of the photon established in 1985 and verified experimentally for some wavelengths, an optical photon has a shape similar to an elongated ellipsoid of length λ and diameter λ/π , λ being the photon’s wavelength.

What this means is the usual graphic representation in Figure 417 in green is not realistic! According to other literature, the longitudinal length of a single photon is half of its wavelength $(\lambda/2)^{1206}$.

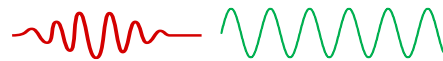


Figure 417: a photon wave packet or pulse, and a single frequency photon... of undetermined length. The first has many harmonic frequencies shaped like a Gaussian curve in their Fourier transform while the single frequency photon Fourier transform is a single point.

This length’s range is quite broad, with 1 nm for X-rays and several orders of magnitude smaller for gamma rays, to over one millimeter and up to several kilometers for radio waves. A classical representation in the above illustration with an EM field of 1,5 wavelengths doesn’t correspond to a single photon according to this interpretation, but to three or 1,5 consecutive single photons.

Nothing says that this can represent reality. On top of that, with a photon having half a wavelength, its Fourier transform won’t be decomposed with a single frequency, but with some harmonic frequencies. We’re safe since this can be explained with Heisenberg’s indeterminacy, related here to two complementary properties, the photon length, and its wavelength. In other words, if you try to describe with precision the length of the photon wave (time/space domain), you end up losing precision with its wavelength (energy domain). And vice versa!

Photon modes are not that easy to define and their simplified descriptions are diverse. These are defined by coherence and orthogonality properties of the EM field. These are orthogonal solutions of the EM wave equations. Different photon modes do not interfere. The energy of a linear superposition of modes equals the sum of the energy of the individual modes. Only photons with the same mode can be coherent and interfere.

¹²⁰⁶ See [Electromagnetic fields, size, and copy of a single photon](#) by Shan-Liang Liu, 2018 (4 pages) and [The Size and Shape of a Single Photon](#) by Zhenglong Xu, 2021 (22 pages).

There are two types of photon modes: spatial modes that are transverse to their direction of propagation and temporal modes in the direction of propagation (time and frequency)¹²⁰⁷.

We find these multimode photons in various quantum optics setups like with boson sampling experiment that we'll describe a bit later, as well as in quantum key distribution settings¹²⁰⁸.

Photon number is a way to describe groups of similar photons. Several photons with the same wavelength and polarization, can be at the same place and at the same time. They also share the same direction vector. These photons are indistinguishable. This is a property of bosons which are elementary or composite particles with the same quantum characteristics which can get together, following Bose-Einstein statistics, while fermions with the same quantum characteristics can't be together, following Fermi-Dirac statistics.

A group of similar photons form an electromagnetic wave whose energy $E = h\nu N = \hbar\omega N$, i.e. the energy of each photon multiplied by the number of added photons having that wavelength¹²⁰⁹.

A photon number is this number of "clustered" photons forming a higher energy EM field than a single photon¹²¹⁰. You can even create superpositions of multi-photons (or single-mode Fock state as we'll see later) with 0, 1, 2 and 3 photons. This can be used to create photon-number Bell states, namely entangled states of superposed photon numbers¹²¹¹. This is head twisting and hard to visualize!

Quantum optics is heavily based on the model of the **quantum harmonic oscillator**, the quantum-mechanical analog of the classical harmonic oscillator, with quantized energy.

The energy of a quantum oscillator can be described with a simple equation, N being the photon number. When $N=0$, the oscillator energy corresponds to the vacuum state energy.

$$\text{energy } E \text{ and photon number } N: E = \hbar\omega \left(N + \frac{1}{2} \right) \quad \text{photon wavenumber } k = \frac{2\pi}{\lambda}.$$

Photon wavenumber is the spatial frequency of a wave, measured in radians per unit distance. It is defined as k with the above right formula using the photon wavelength.

Creation and annihilation operators or ladder operators are mathematical operators used with quantum harmonic oscillators and many-particles systems. An annihilation operator \hat{a} reduces the number of particles in a given state by one and a creation operator \hat{a}^\dagger increases this number by one. It is the adjoint operator of the annihilation operator. These operators act on states of various types of particles, and with photons, as adding or removing a quantum of energy to and oscillator system.

The use of these operators instead of wavefunctions is part of the second quantization formalism. It explains why the canonical quantum physics postulates that we described in an [earlier part](#) (page 86) are not entirely applicable to quantum optics, particularly the time evolution postulate related to Schrödinger's wave equation that is applicable only to non-relativistic massive particles and even the structure of the quantum state ψ .

¹²⁰⁷ See [The concept of modes in optics and photonics](#) by René Dändliker, 1999 (6 pages).

¹²⁰⁸ See the review paper [Roadmap on multimode photonics](#) by Ilaria Cristiani et al, 2022 (39 pages) which also covers classical use cases of multimode photonics.

¹²⁰⁹ Here, ν is the photon frequency, h in Planck's constant, \hbar is Planck's reduced constant or Dirac's constant and ω is the photon angular frequency with $\omega = 2\pi\nu$, in radians per second, 2π radians corresponding to a 1 Hz frequency.

¹²¹⁰ A powerful radio of digital TV emitter is creating these kinds of photons, in the radiowave range! Same for a radar.

¹²¹¹ See [Generation of non-classical light in a photon-number superposition](#) by J. C. Loredó, Pascale Senellart et al, November 2018 (13 pages), [Generating superposition of up-to three photons for continuous variable quantum information processing](#) by Mitsuyoshi Yukawa et al, 2013 (7 pages), and [Generation of light in a photon-number quantum superposition](#), August 2019. And the entangled photon numbers in [Photon-number entanglement generated by sequential excitation of a two-level atom](#) by S. C. Wein, Pascale Senellart et al, June 2021 and in *Nature Photonics*, April 2022 (18 pages).

Mathematically, a photon occupation number operator is a Hermitian operator $\hat{N} = \hat{a}^\dagger \hat{a}$. And a photon number of n superposed photons created by the operator \hat{a}^\dagger applied n times to the vacuum state $|0\rangle$ creates the state $|n\rangle = \frac{1}{\sqrt{n!}} (\hat{a}^\dagger)^n |0\rangle$.

Second quantization is the broad field of quantum physics that deals with many-body quantum systems. It was introduced by **Paul Dirac** in 1927 and developed afterwards by **Vladimir Fock** and **Pascual Jordan**. While the first quantization dealt with individual quantum objects and their description by the Schrödinger wave equation, the second quantization describes many-body systems which are represented mathematically by Fock states and Fock spaces.

Its formalism introduces creation and annihilation operators to construct and handle the Fock states, providing the mathematical tools to the study quantum many-body systems.

Instead of describing such a system as a tensor product of all its constituent quantum objects, it is simplified with chaining $|n_{k_i}\rangle$ describing the n_i quantum objects that are in the same quantum state k_i as described in the above equation related to the creation operator.

A many-body system is described as the tensor product of the Fock states $|n_{k_i}\rangle$ corresponding to each individual quantum states in the system: $|n_{k_0}\rangle \otimes \dots \otimes |n_{k_n}\rangle$, given that the photon number n_i for the Fock state $|n_{k_i}\rangle$ can be 0 or 1 for fermions and any positive number for a boson. When all occupation numbers are equal to zero, the Fock state corresponds to the vacuum state.

A Fock state with only one non-zero occupation number is a single-mode Fock state. Contrarily, a multi-mode Fock state has several non-zero occupation numbers.

Quantum optics. This field of quantum physics started quite late. In 1956, the Hanbury-Brown-Twiss (HBT) experiment was about observing the intensity correlations of the radiation of a mercury lamp and from some bright stars. After traversing a beamsplitter (with a mercury lamp) or at two spatially separated points (for stars), the intensities measured by two detectors were fluctuating, and these fluctuations were correlated.

It was then explained by the emission of photon bunches coming from thermal sources. But it could be explained without using photons and quantum physics.

Quantum optics really started when it became possible to create non classical light sources like pairs of photons and single photons, respectively in 1967 and 1977. Photon pairs were first created with using cascaded atom decay and parametric down conversion¹²¹².

Semi-classical light. It describes interactions between quantized matter such as atoms and electrons with classical light fields. Continuous laser light belongs to this category.

Non-classical light. Light and photons are always quantum, just because it comes from quantized energy exchanges with matter. Still, light is considered to show non-classical and quantum effects when the electromagnetic field is quantized and photons are handled individually. This happens in a couple situations: creation of entangled Bell states, antibunching, photon noise and negative probabilities with the Wigner function. We'll look at each of these phenomena.

Bell states where single photons behave probabilistically and in the general case have no *a priori* properties like polarization, wavelength, wavevector before being measured. These properties are revealed while being measured and show correlations between entangled photons whose measured properties will be random.

¹²¹² Source: [Lecture 1. Basic concepts of statistical optics](#) (7 pages).

Anti-bunching corresponds to a light field where photons are equally spaced in time, much better than with a coherent laser field. It is detected with a HBT (Hanbury Brown & Twiss) intensity auto-correlator... with no correlations. It refers to sub-Poissonian photon statistics, that is a narrow photon number distribution.

It can be generated by single photon sources as well as from pulse mode lasers. A coherent state from a laser has a Poissonian statistics generating random photon spacing and a thermal source light field has super-Poissonian statistics and yields bunched photon spacing. All these aspects belong to the field of statistical optics.

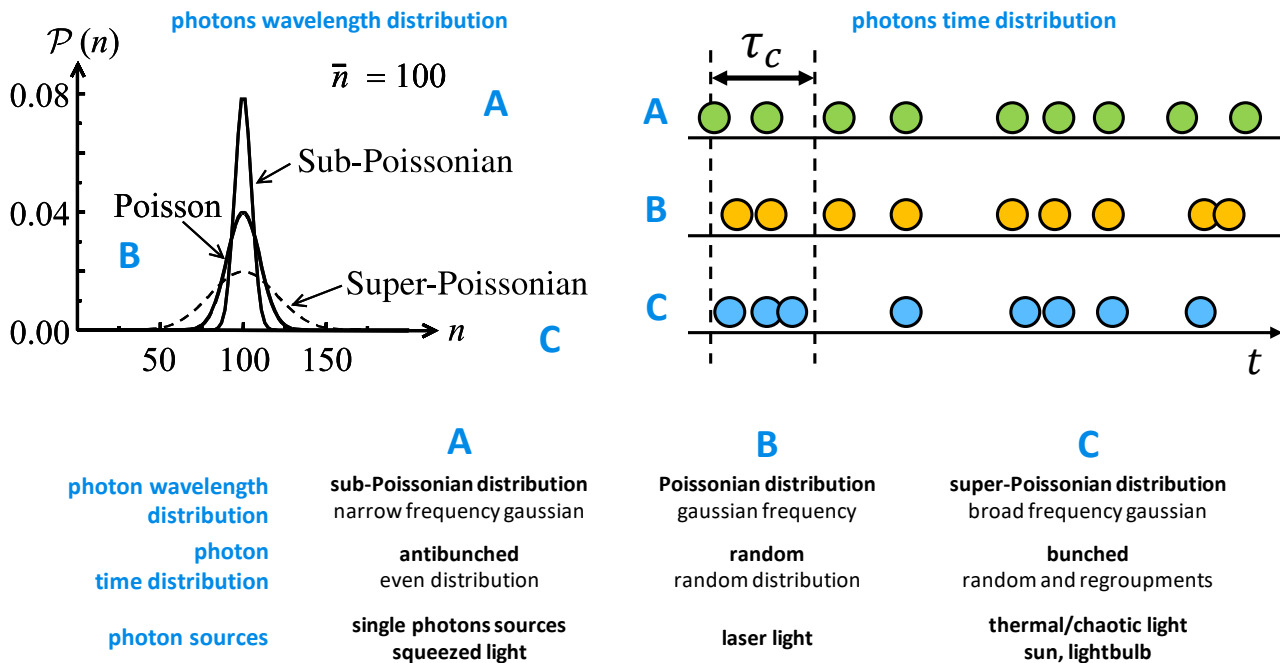


Figure 418: poissonian, sub-Poissonian and super-Poissonian photons wavelength distribution and photons time distribution. Compilation: Olivier Ezratty, 2021.

The quality of single photons source is measured with the data from two experiments. The first uses a variant of a **Hanbury Brown and Twiss** (HBT) intensity autocorrelator that checks the photons are emitted in a very regular way, like a metronome. From a starting click on one of the two photon detectors, it analyzes the time distribution of the appearance of the following photons. This produces the plots in Figure 419. The ideal model would be that of a high peak on either side of the center. The low peaks represent the system noise¹²¹³.

The second experiment called H.O.M. for **Hong-Ou & Mandel** and created in 1987 uses a Mach-Zehnder interferometer to validate the fact that the emitted photons are indeed identical and impossible to distinguish¹²¹⁴.

¹²¹³ This experiment, originally created to detect the size of stars, also allowed to validate the corpuscular nature of photons. The experiment can be easily interpreted in an intuitive way: photons pass through a one-way mirror, whether or not it crosses randomly. Behind this mirror are two photon counters, here with SPADs (avalanche diodes). The system detects when a photon is detected at the same time by both sensors. If the photons take the same way to reach both detectors, there will be no coincidence since the emitted photons are sent in well-ordered trains and can only be on one side or the other. By adding a delay line between the mirror and one of the sensors that is proportional to the period of emission of the photons, it creates many occurrences with photons arriving simultaneously in both sensors. This is what we see in the two curves, one of them being with a linear scale of coincidences (measured over a period of time sufficient to capture hundreds of them) and another logarithmic which allows to better characterize the noise of the system.

¹²¹⁴ See [High-performance semiconductor quantum-dot single-photon sources](#) by Pascale Senellart, Glenn Solomon and Andrew G. White, 2017 (14 pages) which describes the various ways to characterize the quality of single photons sources.

antibunching measurement

$$g^2(0) = 0.019$$

time correlation of second order or of intensity between pairs of photons with a zero delay. the closer to zero, the better. describes the level of noise in the system.

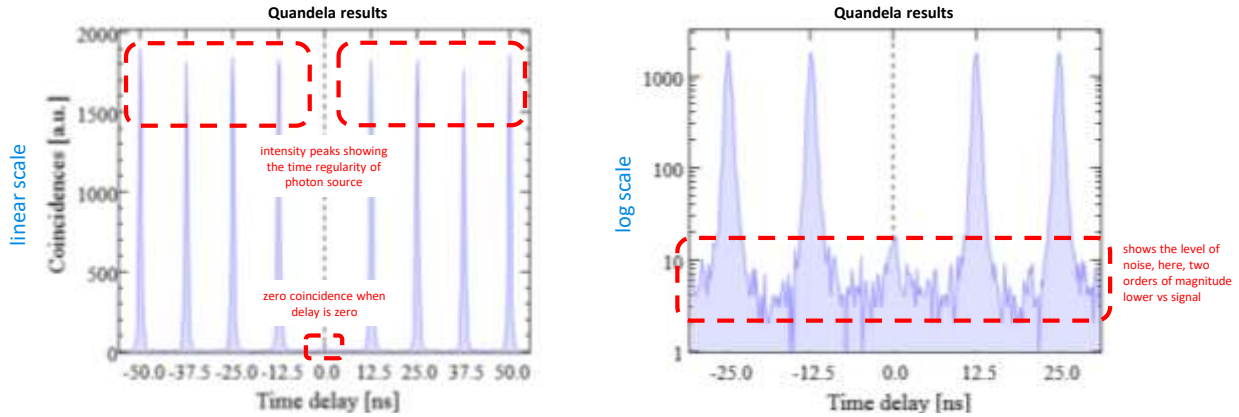
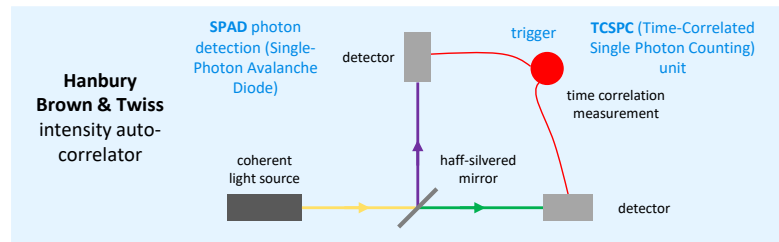


Figure 419: how antibunching is measured. Sources: various.

Quadratures representation is a way to describe the electromagnetic field and its related uncertainty. An EM wave is positioned in two axis X and Y or X_1 and X_2 corresponding to the rotation of the electric field in the EM field, thus the equations describing X_1 and X_2 below, with the cosine and sine of ωt (angular frequency \times time). Said otherwise, a quadrature describes the real and imaginary parts of a complex amplitude. This EM field complex amplitude is rotating so what's interesting is not the grey circle position in the chart but its shape and size which represents the photon measurement uncertainty. It is represented by the variation of the length of the vector which is the photon number and of the width of the circle, orthogonally to the vector, which corresponds to the phase uncertainty. For unsqueezed coherent light, this uncertainty is the same as the vacuum state.

Photon noise aka shot noise is found in the detection of light and corresponds to quantum fluctuations in the electromagnetic field. This noise or imprecision can be squeezed in one dimension.

Squeezed light corresponds, in a quadrature or phasor diagram representation, to wave functions which have an uncertainty in one of the quadrature amplitudes (phase or photon number) smaller than for the ground-state corresponding to the vacuum state. It can be generated by different means like a parametric down conversion¹²¹⁵. Balanced homodyne detectors are used to detect squeezed light.

Wigner function is yet another representation of a quantum state, richer than the phase diagram above which is used to measure the level of quantumness of a light pulse. It's not far from a probability distribution of the electric field in the (Q, P) plane that can take negative values in some conditions, for so-called non-Gaussian states¹²¹⁶. With coherent states, $W(Q, P)$ is a symmetric Gaussian function peaking at the average values of the sine and cosine components of the electric field with the peak width corresponding to the vacuum noise like in the quadrature representation.

¹²¹⁵ See [Generation of squeezed states by parametric down conversion](#) by Ling-An Wu et al, University of Texas, Physical Review Letter, 1986 (4 pages).

¹²¹⁶ See [Conversion of Gaussian states to non-Gaussian states using photon number-resolving detectors](#) by Daiqin Su et al, Xanadu, April 2019 (37 pages), the tutorial paper [Non-Gaussian Quantum States and Where to Find Them](#) by Mattia Walschaers, LKB - Collège de France, April 2021 (55 pages) and the review paper [Production and applications of non-Gaussian quantum states of light](#) by A. I. Lvovsky, Philippe Grangier et al, June 2020 (50 pages).

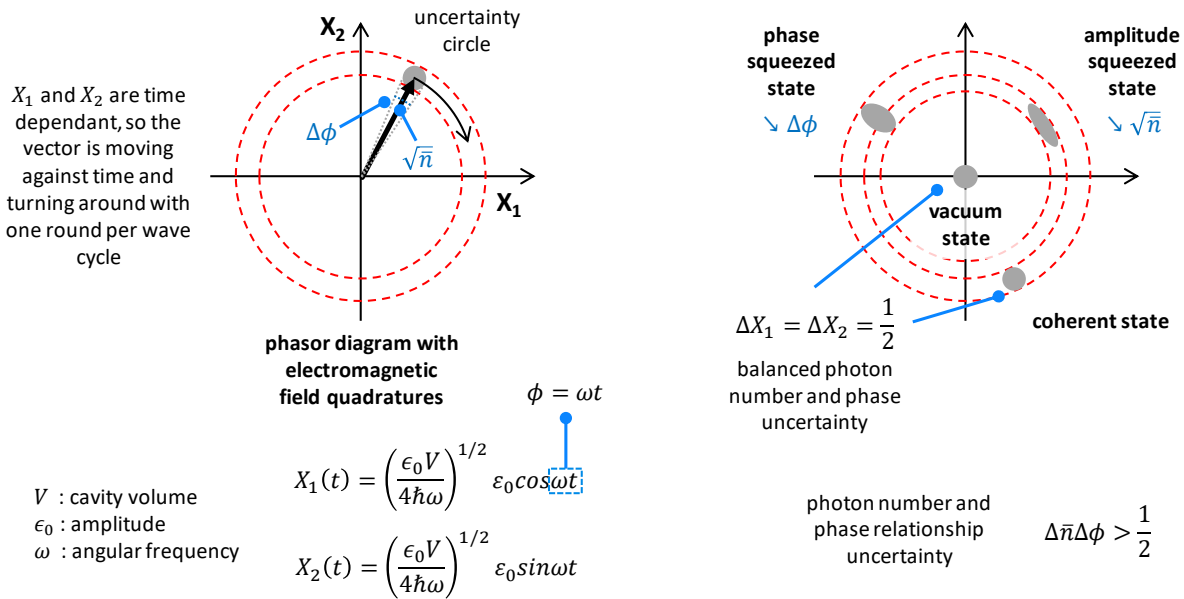


Figure 420: what squeezed light looks like when using quadratures representation. Sources: various.

The Wigner function equation looks like:

$$W(Q, P) = \frac{1}{\pi\hbar} \int_{-\infty}^{+\infty} \psi^*(Q + y)\psi(Q - y)e^{2iPy/\hbar} dy$$

Figure 421: Wigner function which helps measure the quantumness of light.

with ψ being the quantum object wave function, Q and P the position and momentum and y, the variable used in the integral. It returns a real value that can be positive or negative. Q and P could be replaced by the sine and cosine components of the quantized electric field like in the phasor diagram.

In Figure 422 are presented a set of Wigner functions, ranging from the most classical to the most quantum fields. A is a coherent state¹²¹⁷, B, a squeezed state, C a single-photon state and D a Schrödinger's-cat state. The projections or shadows of the Wigner function are the probability distributions of the quantum continuous variables Q or P. The Wigner function is a Gaussian function for A and B but takes negative values for the non-Gaussian strongly quantum states C and D¹²¹⁸.

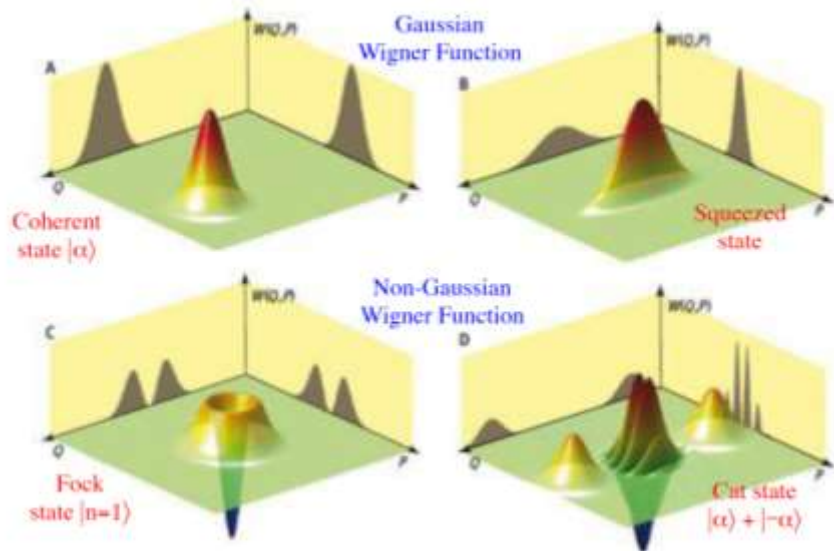


Figure 422: various 3D representations of the Wigner function, for Gaussian and non-Gaussian light. Source: [Make it quantum and continuous](#) by Philippe Grangier, Science, 2011.

¹²¹⁷ The vacuum state has a similar Wigner function, but centered around $P=0$ and $Q=0$.

¹²¹⁸ See [Recent advances in Wigner function approaches](#) by J. Weinbub and D. K. Ferry, 2018 (25 pages) which shows the various use cases of the Wigner function.

These negative values vanish very quickly with decoherence.

Parametric down-conversion is a nonlinear optical process converting one photon of high energy into a pair of photons of lower energy. It is used to generate pairs of entangled photons.

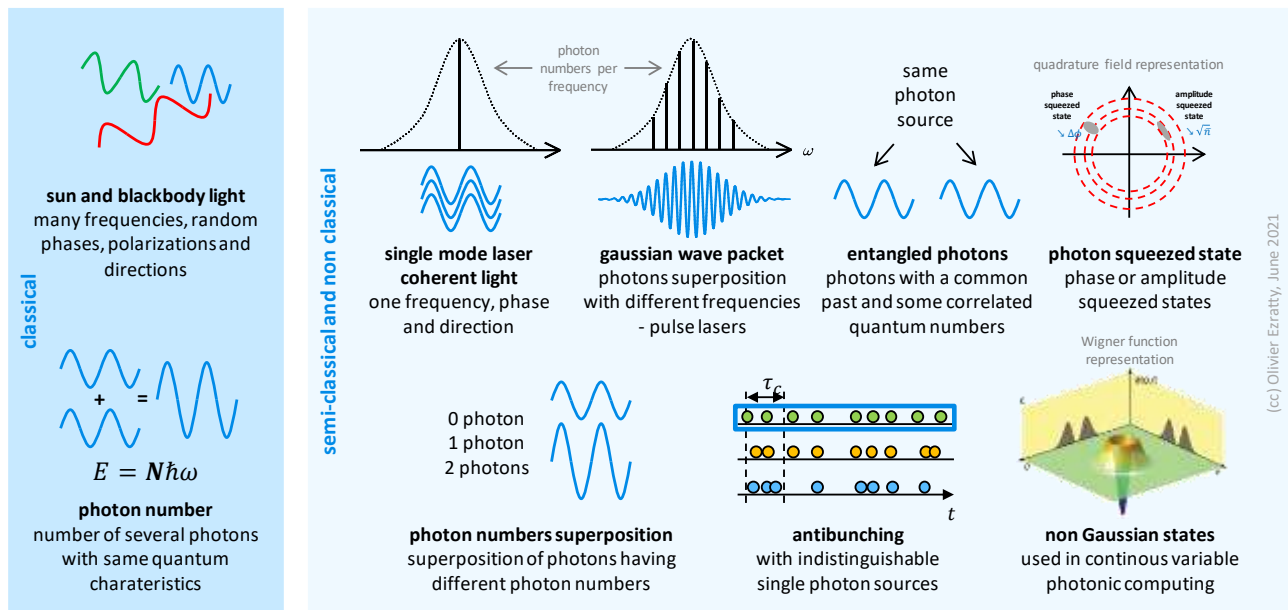


Figure 423: a zoo of photons. (cc) Olivier Ezratty, 2021.

Photons zoo. Figure 423 shows some various photon states as a summary of this section. Random photons in spontaneous light coming from the Sun or light bulb and “photon number” waves assembling several similar photons belong to classical light.

Other forms of light described here are semi-classical or non-classical: photon number superposition, squeezed states where the precision is improved in photon number, amplitude or phase at the expense of the others, single-mode coherent laser light, wave packets created by pulse lasers or microwave coming from waveform generators used with superconducting and electron spin qubits, entangled photons used in QKD and photon qubits, and non-gaussian states which are weird beasts too complicated to describe in a couple of words that are used to implement non-Clifford quantum gates with photon qubits.

Qubit operations

Photons are "flying qubits". They are the only ones having this characteristic with flying electrons, which are investigated at the fundamental research level. There are two main classes of photon qubits: discrete variable and continuous variable qubits¹²¹⁹.

Discrete Variable qubits use single photons and use a two-dimensional space like orthogonal polarizations or the absence and presence of single photons. DV systems can even be based on qudits using more than one degree of liberty. DV qubits rely on highly efficient, deterministic and indistinguishable single photon sources. They are using the “particle” side of photons. Their indistinguishability must exceed 95%, meaning this percentage of photons must be indistinguishable. The photon sources must also be efficiently connected to dynamically controllable photonic computing chipsets.

¹²¹⁹ See this good review paper: [Integrated photonic quantum technologies](#) by Jianwei Wang et al, May 2020 (16 pages) and [Hybrid entanglement of light for remote state preparation and quantum steering](#) by Adrien Cavaillès et al, LKB (41 slides) which positions well the difference between DV and CV computing.

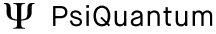





| | discrete variables | continuous variables | boson sampling |
|---------------------|---|---|---|
| quantum information | discrete degree of freedom of a photon Fock states: $ 0\rangle, 1\rangle, 2\rangle \dots$ single or many photon properties | quadrature of a light field coherent states, qumodes, spectral and time modes | multimode photons |
| photon sources | single indistinguishable photon sources | entangled photons sources squeezed states, ... | unique photons source |
| representation | density matrix | Wigner function | permanent |
| gates | KLM model, MZI (Mach-Zehnder Interferometer) gates | determinist gates modes measurement gaussian and non gaussian gates | MZI and interferometer |
| photon detectors | photon counters /detectors APD, SNSPD, VLPC, TES | homodyne and heterodyne detectors | single photons detectors |
| players |  PsiQuantum  ORCA Computing  QUANDELA  DUALITY QUANTUM PHOTONICS |  XANADU |  |

Figure 424: comparison of the main models of photon-based quantum computing. (cc) Olivier Ezratty, 2021.

Efforts are also undertaken to create cluster states of entangled photons used in MBQC and to create deterministic multi-qubit gates using spin-photon interactions like in NV centers or other silicon spin defects¹²²⁰.

Continuous Variable qubits encode information in the fluctuations of the electromagnetic field, in their quadrature components, in qubits that are sometimes baptized qumodes¹²²¹. We are playing here with the wave nature of photons.

Photons readout can be done with a Gaussian measurement comprising homodyne detection for one of the two quadrature components and heterodyne detection on one of these¹²²², and a non-Gaussian measurement implementing photon counting returning an integer. There, you hear about Wigner function amplitude, phase encoding, Gaussian states¹²²³, including squeezed states generated with nonlinear media and non-Gaussian gates to execute non-Clifford group gates bringing a real exponential speedup for quantum computing. Quantum gates can be deterministic, homodyne detectors are cheaper than single photons detectors, and quantum states are more robust. CV qubits are implementing larger cluster states for MBQC, using a large number of photon modes (in the thousands)¹²²⁴.

In the CV qubit domain, **PhotoQ** (Denmark) is a collaborative project implementing this architecture with using surface codes for fault-tolerance¹²²⁵. The project is built around research from DTU with participating organizations being AMCS Group, Aarhus University, Kvantify and NKT Photonics (lasers) with a public funding of 3M€ from Innovation Fund Denmark. They are (wonder why) focused on solving logistics and pharmaceutical industries problems.

¹²²⁰ See [Multidimensional cluster states using a single spin-photon interface coupled strongly to an intrinsic nuclear register](#) by Cathryn P. Michaels et al, University of Cambridge, April 2021 (11 pages).

¹²²¹ For an explanation of the difference between qumodes and qubits, see [Introduction to quantum photonics](#) from Xanadu.

¹²²² On the measurement of CV qubits, see [Optical hybrid architectures for quantum information processing](#) by Kun Huang, LKB, 2017 (215 pages). This is not the same Kun Huang as the discoverer of phonon-polaritons in 1951.

¹²²³ Understanding how Gaussian states work is already quite a challenge. See [Gaussian Quantum Information](#) by Christian Weedbrook, Seth Lloyd et al, 2011 (51 pages).

¹²²⁴ See [A fault-tolerant continuous-variable measurement-based quantum computation architecture](#) by Mikkel V. Larsen, January 2021 (16 pages).

¹²²⁵ See [A fault-tolerant continuous-variable measurement-based quantum computation architecture](#) by Mikkel V. Larsen et al, August 2021 (19 pages) and [Deterministic multi-mode gates on a scalable photonic quantum computing platform](#) by Larsen, Mikkel V. et al, Nature Physics, August 2021 (32 pages).

There you will also find cat-qubits and GKP states¹²²⁶. Hybrid DV/CV qubits approaches are also investigated¹²²⁷. CV computing can be used with universal gates quantum computing as well as with quantum simulations.

Quantum Walks based simulation is another computing technique using photons. Similarly to the CV/DV computing segmentation, you have two classes of photon-based quantum walk systems: discrete-time quantum walks with discrete steps evolutions¹²²⁸ and continuous-time quantum walks with a continuous evolution of a Hamiltonian coupling different sites¹²²⁹. A research team in China created a CV-quantum walk system handling a Hilbert space of dimension 400 as shown in Figure 425. It even takes the form of a seemingly packaged and designed product despite coming out of a public research lab and not a startup. There are even hybrid fermion/bosons approaches that are proposed but that are very theoretical and with very few hardware implementation details¹²³⁰.

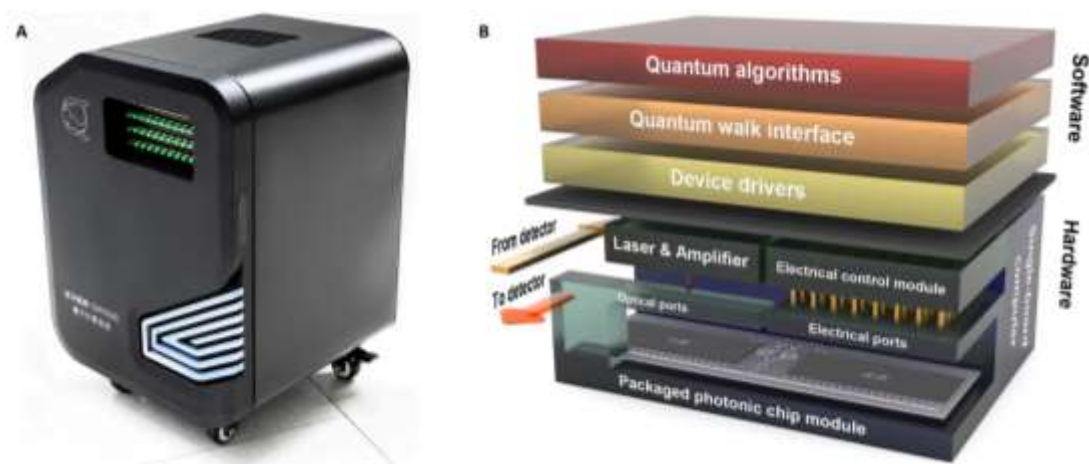


Figure 425: the continuous-variable quantum walk system YH QUANTA QW2020 from China. Source: [Large-scale full-programmable quantum walk and its applications](#) by Yizhi Wang et al, August 2022 (73 pages).

Boson sampling is a separate technique we'll cover later in a dedicated section, page 445. It's a research field that has not yet brought to life programmable computing.

Coherent Ising Machines is another technique based on using optical neural networks that can solve combinatorial optimization problems with mapping them onto NP-hard Ising problems¹²³¹.

¹²²⁶ These light states require specific preparation techniques. See for example [Robust Preparation of Wigner-Negative States with Optimized SNAP-Displacement Sequences](#) by Marina Kudra, Jonas Bylander, Simone Gasparinetti et al, Chalmers University, PRX Quantum, September 2022 (12 pages) with interesting cavity-based preparation of various quantum light states usable in CV photon qubit systems.

¹²²⁷ See [Hybrid Quantum Information Processing](#) by Ulrik L. Andersen et al, 2014 (13 pages) and [Hybrid discrete and continuous-variable quantum information](#) by Ulrik L. Andersen et al, 2015 (11 pages), [Visualization of correlations in hybrid discrete—continuous variable quantum systems](#) by R P Rundle et al, February 2020 (15 pages) and [Remote creation of hybrid entanglement between particle-like and wave-like optical qubits](#) by Olivier Morin, Claude Fabre, Julien Laurat, LKB France, 2013 (7 pages).

¹²²⁸ See for example [Quantum walks of two correlated photons in a 2D synthetic lattice](#) by Chiara Esposito, Fabio Sciarrino et al, April 2022 (18 pages).

¹²²⁹ See [Purdue University Scientists Say 'Quantum Rainbow' May Allow Room-Temperature Quantum Computing](#) par Matt Swayne, 2021 referring to [Probing quantum walks through coherent control of high-dimensionally entangled photons](#) by Poolad Imany et al, July 2020 (9 pages).

¹²³⁰ See [Two-level Quantum Walkers on Directed Graphs I: Universal Quantum Computing](#) by Ryo Asaka et al, December 2021 (20 pages) and [Two-level Quantum Walkers on Directed Graphs II: An Application to qRAM](#) by Ryo Asaka et al, April 2022 (23 pages).

¹²³¹ CIM is described in the presentation [Coherent Ising Machines: non-von Neumann computing using networks of optical parametric oscillators](#) by Peter McMahon, Cornell University, October 2020 (100 slides). It reminds us that HPE and Ray Beausoleil worked on a CIM before abandoning all quantum computing endeavors altogether. The source of the illustration was found on slide 55.

Practically speaking, Ising models can solve many problems: planning and scheduling, financial portfolio optimizations, graph problems and even material and molecular design. These problems are defined by couplings between a set of spins. The solution is the spin orientation that minimizes the energy function of the system. CIM systems use single-mode photon squeezing, oscillation at degenerate frequency, Optical Parametric Amplifiers in a Cavity (OPO) and a measurement feedback technique. Leveraging delay lines, time division multiplexing and measurement feedback, CIM can implement many-to-many connectivity. The largest CIM system was built in Japan in 2021 with 100,000-spins¹²³². It competed with quantum annealing (from D-Wave) and also classical CMOS-based annealing (from Fujitsu).

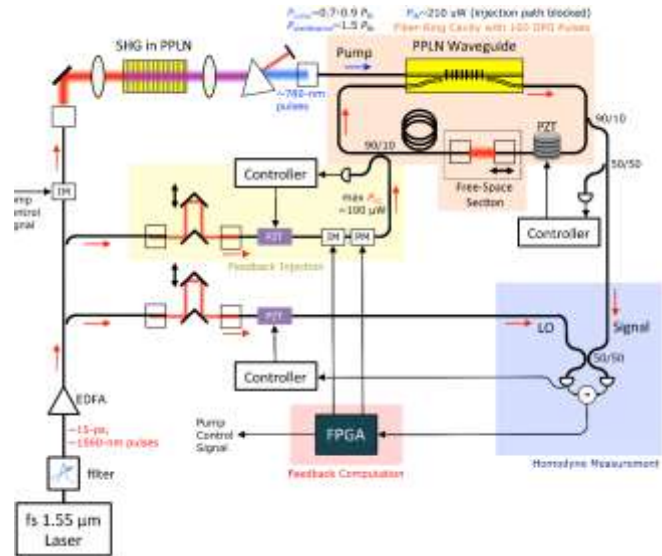


Figure 426: example of realization of a coherent Ising Machine. Source: [Coherent Ising Machines: non-von Neumann computing using networks of optical parametric oscillators](#) by Peter McMahon, Cornell University, October 2020 (100 slides).

A bit like the difference we discovered between (D-Wave) quantum annealing solving Ising “Z” problems¹²³³ and quantum simulation models implementing XY qubits connectivity, there are also photonic based coherent XY models that compete with CIM¹²³⁴.

Hybrid atoms-photons qubits. Stanford University researchers devised a new hybrid quantum photonic approach using a single atom that modifies photons states via quantum teleportation and implement quantum gates and qubit readout¹²³⁵.

It reduces the need for multiple photon emitters and greatly simplifies the hardware setting that makes use of a photons storage ring made of a fiber loop, optical switches in the loop, a beam splitter, a phase shifter, a photon scattering unit and a cavity containing a single atom controlled by a laser, the atom getting entangled with the photon.

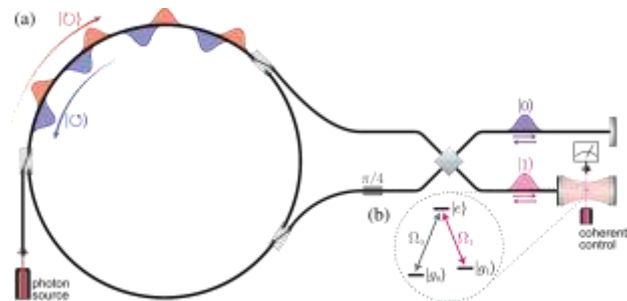


Figure 427: an example of hybrid atoms-photons system. Source: [Deterministic photonic quantum computation in a synthetic time dimension](#) by Ben Bartlett, Avik Dutt and Shanhui Fan, Optica, November 2021 (9 pages).

¹²³² See [100,000-spin coherent Ising machine](#) by Toshimori Honjo et al, September 2021 (8 pages).

¹²³³ CIM is supposed to work better than D-Wave that also implement Ising models according to [Practical Application-Specific Advantage through Hybrid Quantum Computing](#) by Michael Perelshtein et al, 2021 (14 pages) that is described in [A poor man’s coherent Ising machine based on opto-electronic feedback systems for solving optimization problems](#) by Fabian Böhm et al, Nature Communications, 2019 (9 pages). See also [Experimental investigation of performance differences between coherent Ising machines and a quantum annealer](#) by R. Hamerly et al, Sci. Adv., 2019 (26 pages) for the comparison with D-Wave 2000Q. The compared CIM machine is from NTT and Stanford. The Stanford CIM is described in [A fully programmable 100-spin coherent Ising machine with all-to-all connections](#) by Peter L. McMahon et al, 2016 (9 pages). The NTT CIM is described in [A coherent Ising machine for 2000-node optimization problems](#) by T. Inagaki et al, Science, 2016 (6 pages).

¹²³⁴ Coherent Ising machines models and challenges are described in [Coherent Ising machines - optical neural networks operating at the quantum limit](#) by Y. Yamamoto et al, npj Quantum, December 2017 (16 pages).

¹²³⁵ See [Deterministic photonic quantum computation in a synthetic time dimension](#) by Ben Bartlett, Avik Dutt and Shanhui Fan, Optica, November 2021 (9 pages) also described in [Researchers propose a simpler design for quantum computers](#) by McKenzie Prillaman, Stanford University, Physorg, November 2021.

The photon source is a single photon train source. But this is not a perfect solution. It has some requirements on the cavity quality, on low fiber attenuation, on very low insertion losses optical switches and can't implement quantum gates in parallel.

The general principle of quantum computing systems using photon qubits is as follows:

- **Photon sources** are lasers, often coupled with single and indistinguishable photon generators¹²³⁶. They are critical to generate simultaneously a large number of indistinguishable photons that will feed in parallel several qubits thanks to delay lines. These are well time-isolated unique and indistinguishable photons generated in well-spaced in time series. These single photons are individually detectable at the end of processing with single photon detectors. The key metrics of these photon sources are the system efficiency (probability that at least one photon is created per pulse), purity (probability of getting a maximum of one photon per pulse) and coherence (how generated photons are quantum mechanically identical or indistinguishable).

The purity and high probability to get a photon per clock cycle are the enabler of quantum interferences based multiple qubit gates with discrete variable qubits. High-efficiency sources are qualified as “on-demand” or “deterministic” with the alternatives of heralded sources, where the emission time can be accurately measured.

There are two main types of single photons sources (SPSs)¹²³⁷:

Quantum dot single-photon source are the best-in-class devices, able to generate photons with a 99.7% single-photon purity, and overs 65% extraction efficiency, which could potentially reach 80% (meaning, 4 photons generated out of 5 clock cycles). See below in Figure 428 how these efficiencies are improved. These sources also have an over 99% photon indistinguishability. In the second quantization formalism, they create a single Fock state with a photon number equal to one.

The leaders in this market are **Quandela**¹²³⁸ and **Sparrow Quantum**¹²³⁹. And many research labs are working on other varieties of quantum dots¹²⁴⁰. These photon sources must be cooled at about 3K to 4K. In their latest Prometheus generation, Quandela directly couples the quantum dot to a fiber, avoiding the use of cumbersome confocal microscopes and significantly increasing the photon generation yield. It creates a path to reaching a combined source–detector efficiency closer to the 2/3 threshold that is mandatory for scalable discrete variable optical quantum computing.

Others are trying to operate these quantum dots at ambient temperature. That's the case with the quantum dots single photon emitters developed at EPFL, with a mix of gallium nitride and aluminum nitride (GaN/AlN) on silicon substrate.

¹²³⁶ See [Near-ideal spontaneous sources in silicon quantum photonics](#) by S. Paesani et al, 2020 (6 pages) which describes a single photon source based on a photonics component. It is an Anglo-Italian research project.

¹²³⁷ See [Integrated photonic quantum technologies](#) by Jianwei Wang et al, May 2020 (16 pages).

¹²³⁸ See [The race for the ideal single-photon source is on](#) by Sarah Thomas and Pascale Senellart, Nature Nanotechnology, January 2021 (2 pages) which describes the various ways to improve the yields of single photon sources, [Sequential generation of linear cluster states from a single photon emitter](#) by D. Istrati, Niccolo Somaschi, Hélène Ollivier, Pascale Senellart et al, October 2020 and [Reproducibility of high-performance quantum dot single-photon sources](#) by Hélène Ollivier, Niccolo Somaschi, Pascale Senellart et al, October 2019 (10 pages) on benchmarking single photon sources.

¹²³⁹ See [Scalable integrated single-photon source](#) by Ravitej Uppu et al, December 2020 (7 pages) which describes the latest advancements of their technology.

¹²⁴⁰ See [Planarized spatially-regular arrays of spectrally uniform single quantum dots as on-chip single photon sources for quantum optical circuits](#) by Jiefei Zhang et al, University of Southern California and IBM, November 2020 (8 pages) describes an array with 32 quantum dots and a simultaneous purity of single-photon emission over 99.5%.

These are showcasing a single-photon purity of 95% at cryogenic temperatures (below 50K) and a purity of 83% at room temperature. The photon emission rates reaches 1 MHz with a single-photon purity exceeding 50%¹²⁴¹.

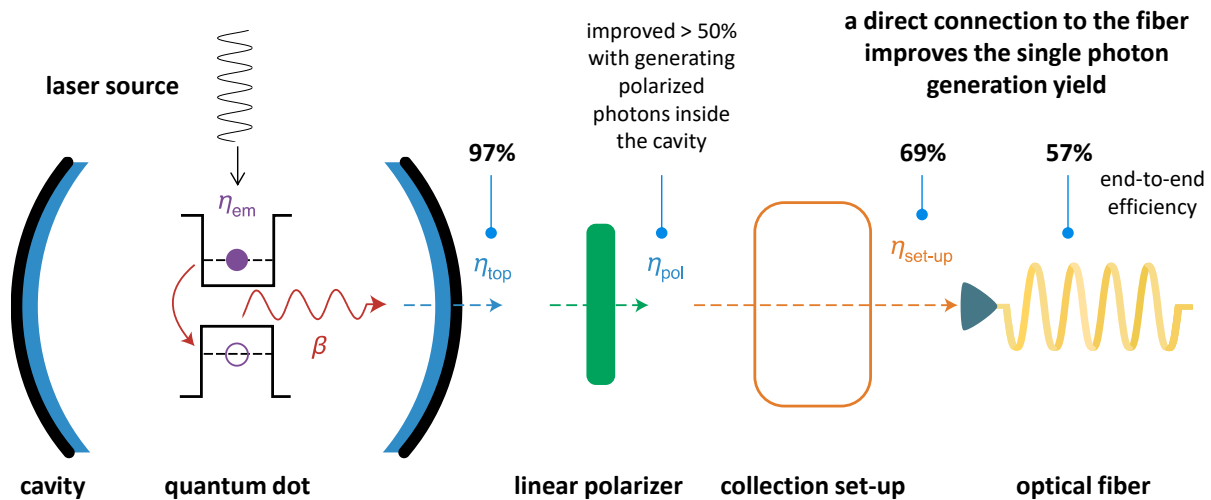


Figure 428: what characterizes the efficiency of a quantum dots photon generator. Source: [The race for the ideal single-photon source is on](#) by Sarah Thomas and Pascale Senellart, *Nature Nanotechnology*, January 2021 (2 pages) and comments by Olivier Ezratty, 2021.

Parametric photon-pair sources are laser pumping nonlinear optical waveguides or cavities that create photon-pairs. It can be integrated in nanophotonic circuits. They are using either spontaneous four-wave mixing (SFWM) or spontaneous parametric down-conversion (SPDC) processes in nonlinear crystals. The efficiency is lower than with quantum dots, reaching about 50% with a 95% photon indistinguishability from separated SPSs. Photons are created non-deterministically with a rather low 5% to 10% probability, which can be increased to above 60% with time and spatial domains multiplexing.

Such solutions are embedded in nanophotonic solutions like with **PsiQuantum**. SPDC sources work at room temperature but for efficient multiplexing (>95%), it is necessary to use SNSPD detectors running at low temperature. Progress is being made with nanophotonic-based single photons generation, although their performance still lags quantum-dots sources¹²⁴². Figure 429 shows a SPDC method to create pairs of entangled photons. The conversion creates pairs of orthogonally polarized photons in two light cones with entangled photons at their intersection.

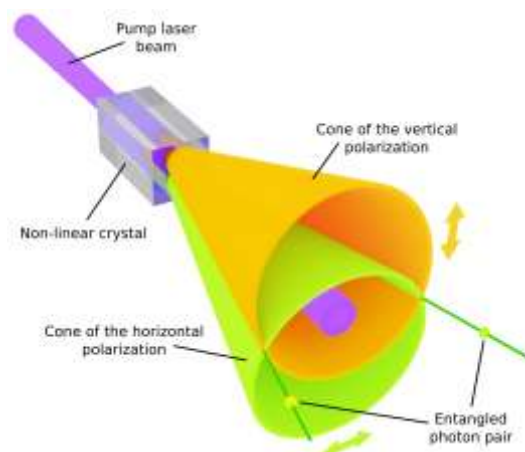


Figure 429: how entangled photons are generated with SPDC method.

¹²⁴¹ See [Toward Bright and Pure Single Photon Emitters at 300 K Based on GaN Quantum Dots on Silicon](#) by Sebastian Tamariz, Nicolas Grandjean et al, January 2020 (19 pages).

¹²⁴² See [High-efficiency single-photon generation via large-scale active time multiplexing](#) by F. Kaneda et al, October 2019 (7 pages), [Researchers create entangled photons 100 times more efficiently than previously possible](#) pointing to [Ultra-bright Quantum Photon Sources on Chip](#) by Zhaohui Ma et al, October 2020 (5 pages) and [A bright and fast source of coherent single photons](#) by Natasha Tomm et al, University of Basel and Ruhr-Universität Bochum, July 2020 (14 pages).

One key challenge with implementing MBQC, one dominant photonic quantum computing architecture that we'll cover later, is the ability to create large cluster-states of entangled photons. There are many options to implement it. Quantum dots source can be tailored for this need. Good indistinguishable and deterministic photon sources can be coupled with delay lines and mixers to create these cluster states. There are even solutions to create hundred pairs of entangled photons, as investigated by the University of Virginia, using frequency combs. Here, the photon source is a continuous laser emitting a single continuous wave, a small 3 mm Kerr microcavity creates a frequency comb generating pairs of entangled photons around the pump frequency as described below. This could lead to massive multimode photonic quantum computing¹²⁴³.

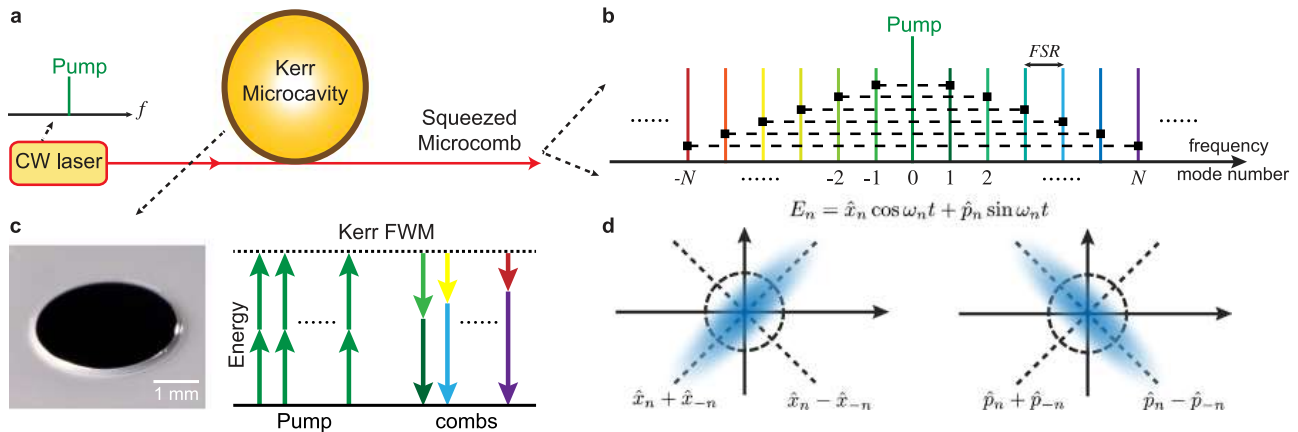


Figure 430: a frequency comb method to generate a large cluster state of entangled photons. Source: [A squeezed quantum microcomb on a chip](#) by Zijiao Yang et al, Nature Communications, August 2021 (8 pages).

- **Quantum state** is based on a single or several properties of the photons. The most common is their polarization with a computational basis based on horizontal and vertical polarization. Other parameters of photons are also explored to create qubits such as their phase, amplitude, frequency, path, photon number, spin orbital momentum and even orbital angular momentum¹²⁴⁴. This potentially allows the creation of qutrits or qudits managing more than two exclusive values. Photons are "flying qubits" because they move in space and are not static or quasi-static at the macroscopic scale unlike most other types of qubits¹²⁴⁵.

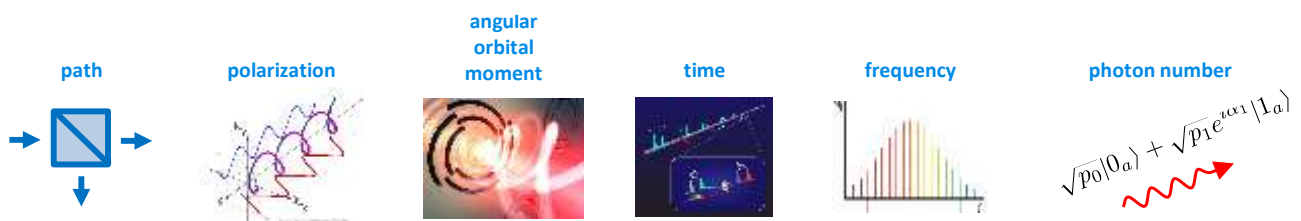


Figure 431: the various properties or observables of photons that can be used to create a qubit. You have many more solutions than the old-fashioned polarization! Compilation (cc) Olivier Ezratty, 2021.

¹²⁴³ See [A squeezed quantum microcomb on a chip](#) by Zijiao Yang et al, Nature Communications, August 2021 (8 pages) covered in [Researchers open a path toward quantum computing in real-world conditions](#) by Karen Walker, University of Virginia, August 2021.

¹²⁴⁴ This multiplicity of parameters also makes it possible to encode not only qubits but also qudits, with a greater number of states. But it is quite complex to manage and, if only to manage two-qubit quantum gates, we are happy with qubits instead of using qudits. See also [Forget qubits -scientists just built a quantum gate with qudits](#) by Kristin Houser, July 2019, which refers to [High-dimensional optical quantum logic in large operational spaces](#) by Poolad Imany et al, 2019 (10 pages). See the definition of orbital angular momentum in the glossary. It was discovered in 1992. See [Orbital angular momentum of light and the transformation of Laguerre-Gaussian laser modes](#) by Les Allen et al, 1992 (5 pages).

¹²⁴⁵ The other qubits are "non-flying": spin-controlled electrons trapped in a cavity, cold atoms (which are stabilized in space) and trapped ions (which can move, but in a limited space), NV centers (cavities do not move) and superconducting circuits (which are fixed in space even if they use pairs of circulating Cooper electrons).

One such implementation was achieved in 2022 by a China-international team using ququarts states (quantum objects with four dimensions instead of the two dimensions of qubits)¹²⁴⁶. The experiment shown below in Figure 432 was implemented in a programmable silicon CMOS photonic integrated chipset of 15 x 1.5 mm implementing linear optics and enhancing parallelism. It was tested with a QFT, Deutsch-Jozsa and Bernstein-Vazirani, quaternary phase estimation and factorization algorithms. The system creates four-level entangled state in an array of four integrated identical SFWM (spontaneous four-wave mixing) sources. Then the photons traverse wavelength-division multiplexing filters (WDM), Mach-Zehnder interferometers (MZI), thermal-optic phase shifters (TOPS), multimode interferometer beamsplitters (MMI) and qudit states measurement.

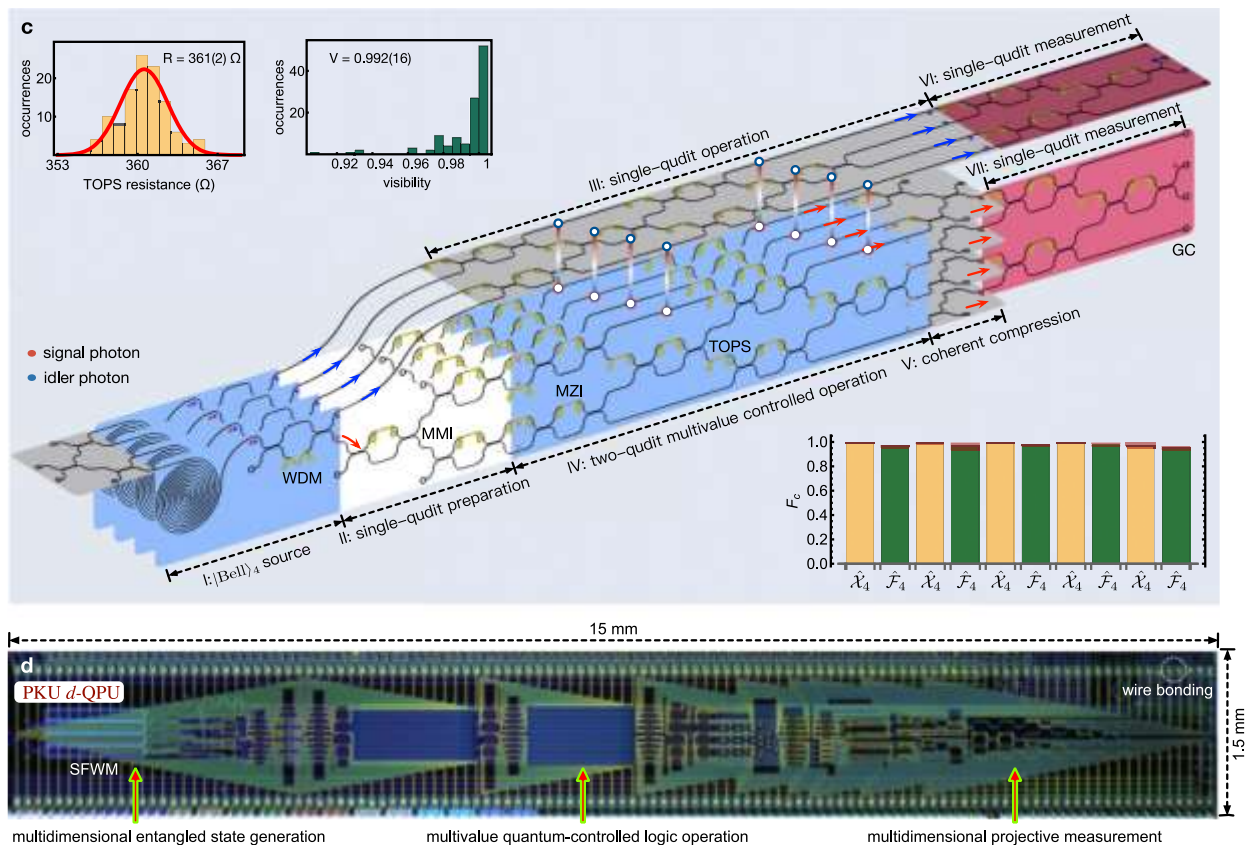
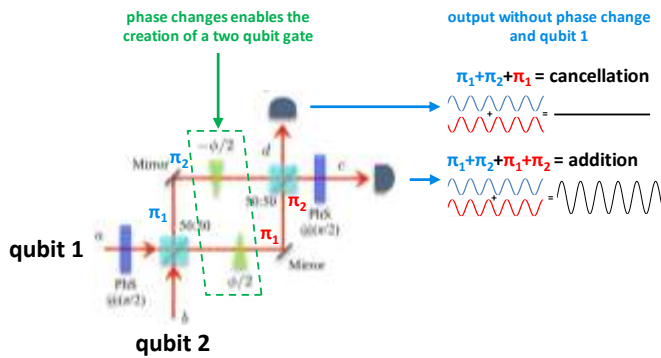


Figure 432: a ququart photons processor created in China. [A programmable qudit-based quantum processor](#) by Yulin Chi, Jeremy O'Brien et al, Nature, March 2022 (10 pages).

- **Single-qubit quantum gates** use simple optical circuitry, including beamsplitters, waveplates, mirrors and semi-reflective mirrors, and phase shifters¹²⁴⁷. For example, a Hadamard gate (H) uses a beamsplitter or waveplate, a Pauli X gate (bit flip) combines a beamsplitter and a Hadamard gate, and a Pauli Z gate (phase flip) uses a phase shifter causing a 180° phase change (π).

¹²⁴⁶ See [A programmable qudit-based quantum processor](#) by Yulin Chi, Jeremy O'Brien et al, Nature, March 2022 (10 pages) covered in [Scientists Make Advances in Programmable Qudit-based Quantum Processor](#) by Matt Swayne, The Quantum Insider, March 2022.

¹²⁴⁷ This is based on the KLM scheme proposed in [A scheme for efficient quantum computation with linear optics](#) by Emanuel Knill, Raymond Laflamme and Gerard Milburn, 2001 (7 pages).



Mach-Zehnder interferometer (MZI) creates an interference between two photons with introducing a dephasing linked to the number of mirrors reflections (the π s) and phase changers

The implementation of various quantum logic gates using optical MZI is tabulated in Table. 3.

| Quantum Logic Gate | Unitary Matrix | Relation for MZI implementation | Elements |
|------------------------------|--|---|---|
| Beam Splitter(B(θ)) | $\begin{bmatrix} \cos\theta & -\sin\theta \\ \sin\theta & \cos\theta \end{bmatrix}$ | | |
| 50-50 Beam Splitter(B) | $\frac{1}{\sqrt{2}} \begin{bmatrix} 1 & -1 \\ 1 & 1 \end{bmatrix}$ | | |
| Hadamard(H) | $\frac{1}{\sqrt{2}} \begin{bmatrix} 1 & 1 \\ 1 & -1 \end{bmatrix}$ | H=BZ | 50-50 Beam splitter |
| Phase flip gate (Z) | $\begin{bmatrix} 1 & 0 \\ 0 & -1 \end{bmatrix}$ | Z=HB | π Phase shifter |
| Bit Flip gate (X) | $\begin{bmatrix} 0 & 1 \\ 1 & 0 \end{bmatrix}$ | X=BH | Beam Splitter, Hadamard |
| T gate | $\begin{bmatrix} 1 & 0 \\ 0 & \exp(i\pi/4) \end{bmatrix}$ | | $\pi/4$ phase shifter |
| S gate | $\begin{bmatrix} 1 & 0 \\ 0 & i \end{bmatrix}$ | | Quarter wave plate |
| Pauli Y gate | $\begin{bmatrix} 0 & -i \\ i & 0 \end{bmatrix}$ | | |
| CNOT gate | $\begin{bmatrix} 1 & 0 & 0 & 0 \\ 0 & 1 & 0 & 0 \\ 0 & 0 & 1 & 0 \\ 0 & 0 & 0 & 1 \end{bmatrix}$ | $(I \otimes H) \times K \times (I \otimes H)$ | Kerr Media(K) Hadamard(H) Identity(I) |

MZI based quantum gates a one qubit gate can be created with introducing some dephasing in one or two of the circuits, and two qubit gate with using two entries and some dephasing. The table shows the correspondence between quantum gates and the used filters elements.

Figure 433: how a Mach-Zehnder Interferometer works. Source: [Quantum Logic Processor: A Mach Zehnder Interferometer based Approach](#) by Angik Sarkar and Ajay Patwardhan 2006 (19 pages).

- **Two-qubit quantum gates** are difficult to realize because it is not easy to have photons interact with each other, particularly when they are not perfectly indistinguishable. They use optical circuits based on beamsplitters or Mach-Zehnder interferometers with two inputs integrating phase changes on the optical paths, based on the KLM method already quoted in footnote.

This does not work well when the photons are uneven, such as those coming from lasers. Namely, in only a few % of the cases. With indistinguishable photons, gates are more than 95% efficient since photons can interfere with each other, and add or subtract. It facilitates Mach-Zehnder interferometry operations.

These sources have the additional advantage of being very bright, which allows them to multiply the incoming photons and then to pass through many quantum gates. There are also solutions based on cavities. Research is also active on the creation of nonlinearities to improve the reliability of these quantum gates¹²⁴⁸. Ideally, nonlinear separating cubes should be used¹²⁴⁹.

How about photonic gates execution times? It must be fast since photons traverse optical devices at nearly the speed of light in vacuum. Traversing a one meter long series of optical instruments would last only 3 ns. If the circuit is nanophotonic based, we'll get into the cm realm and reach tens of pico-seconds. But that's not the right way to evaluate the speed of quantum computing here, particularly when dealing with non-deterministic photon sources where computing has to be repeated many times. Then, you may need to take into account the speed of the electronics that define the various quantum gates along the photon route and we may end-up adding milliseconds.

- **Qubit readout** uses single photon detectors that also capture their quantum state. This detection is still imperfect. Several single-photons detection technologies are competing: SPAD (avalanche photodiodes, which detect photon occurrences but not photon number)¹²⁵⁰, transition edge sensor

¹²⁴⁸ See [Quantum Computing With Graphene Plasmons](#), May 2019 which refers to [Quantum computing with graphene plasmons](#) by Alonso Calafell et al, 2019. This is the creation of two-qubit quantum gates with graphene-based nonlinear structures. It comes from the University of Vienna in Austria and from Spanish and Serbian laboratories. As well as [Researchers see path to quantum computing at room temperature](#) by Army Research Laboratory, May 2020 which refers to [Controlled-Phase Gate Using Dynamically Coupled Cavities and Optical Nonlinearities](#) by Mikkel Heuck, Kurt Jacobs and Dirk R. Englund, 2020 (5 pages).

¹²⁴⁹ It is a function that can be realized with Quandela's single photon generation component, diverted from its original use. See also [Researchers see path to quantum computing at room temperature](#), May 2020 which refers to [Controlled-phase Gate using Dynamically Coupled Cavities and Optical Nonlinearities](#) by Mikkel Heuck, September 2019 (5 pages) and discusses a nonlinear cavity optical quantum gate technique.

¹²⁵⁰ See recent progress with SPADs in [Low-noise photon counting above 100 × 106 counts per second with a high-efficiency reach-through single-photon avalanche diode system](#) by Michael A. Wayne et al, NIST, December 2020 (6 pages).

(TES, which can detect photon numbers) and Superconducting Nanowire SPDs (SNSPDs, which also detect photon numbers). Fully integrated SNSPDs are based on GaAs, Si and Si₃N₄ waveguides. In order to limit the dark count phenomenon coming from thermal effects, these SNSPDs are usually cooled between 800 mK and 3K which requires a dilution refrigeration system¹²⁵¹. NbTiN-based SNSPDs could work with higher-temperature cooling, between 2.5K to 7K¹²⁵². One goal is to integrate these photon detectors directly in photonic computing circuits. Other detectors are specialized for analyzing continuous variables qubits, like homodyne and heterodyne detectors. There are even concepts of single photon detectors that can also detect their frequency with high precision¹²⁵³. In the continuous variable types of qubits, qubit readout uses homodyne detectors to detect the photon quadrature such as optical parametric amplifier (OPA)¹²⁵⁴. Others are experimenting photon detectors operating at a relatively hot temperature of 20K, using cuprates who are known for their relatively high superconducting temperature¹²⁵⁵.

From a physical point of view, these items are classical photonic components: single and identical photon sources, light guides, optical delay lines (optical fibers or voltage-controlled Pockels cells), Mach-Zehnder interferometers, beam splitters (splitters, which divide an optical beam into two beams, generally identical), birefringent filters (which have two different refractive indices), phase shifters and single photon detectors¹²⁵⁶.

To conduct experiments, these discrete and very affordable components are installed on carefully calibrated optical tables of a few square meters with lots of instruments and photons that circulate largely in the free space of a darkened room.

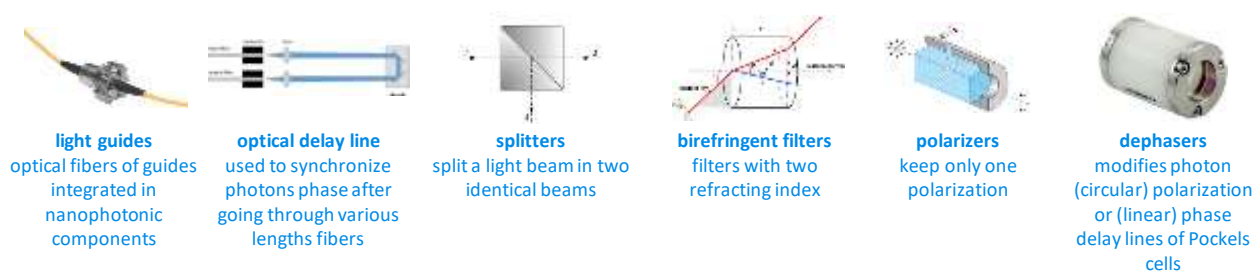


Figure 434: the various optical tools to control light in a quantum processor. These are made for experiments and can be miniaturized in nanophotonic circuits. Compilation (cc) Olivier Ezratty, 2021.

Fortunately, these optical components are miniaturizable on semiconductor integrated circuits. This is part of the vast field of nanophotonics. Nanophotonics components are etched with densities between 220 nm and 3 μm¹²⁵⁷.

¹²⁵¹ See [The potential and challenges of time resolved single-photon detection based on current-carrying superconducting nanowires](#) by Hengbin Zhang et al, October 2019 (19 pages) and [Superconducting nanowire single-photon detectors for quantum information](#) by Lixing You, June 2020 (20 pages). Dark counts are detected photons coming from the environment due to thermal or tunneling effects.

¹²⁵² See [Superconducting nanowire single photon detectors operating at temperature from 4 to 7 K](#) by Ronan Gourgues et al, Optics Express, 2019 (9 pages).

¹²⁵³ See [Nanoscale Architecture for Frequency-Resolving Single-Photon Detectors](#) by Steve M. Young et al, Sandia Labs, May 2022 (20 pages).

¹²⁵⁴ See [Towards a multi-core ultra-fast optical quantum processor: 43-GHz bandwidth real-time amplitude measurement of 5-dB squeezed light using modularized optical parametric amplifier with 5G technology](#) by Asuka Inoue et al, May 2022 (18 pages).

¹²⁵⁵ See [Two-dimensional cuprate nanodetector with single photon sensitivity at T = 20 K](#) by Rafael Luque Merino, Dmitri K. Efetov et al, August 2022 (27 pages). I also found out [Graphene-based Josephson junction single photon detector](#) by Evan D. Walsh, Thomas A. Ohki, Dirk Englund et al, September 2017 (12 pages) but it seems not applicable for photonic qubit readout. It works at 25 mK.

¹²⁵⁶ This is well explained in [Silicon photonic quantum computing](#) by Syrus Ziai, PsiQuantum, 2018 (72 slides) as well as in [Large-scale quantum photonic circuits in silicon](#), by Nicholas C. Harris, Dirk Englund et al, Nanophotonics, 2016 (13 pages).

¹²⁵⁷ See for example the work of InPhyNi discussed in [High-quality photonic entanglement based on a silicon chip](#) by Dorian Oser, Sébastien Tanzilli et al, 2020 (9 pages).

In nanophotonics, quantum gates are dynamically programmed by the conditional routing of photons in optical circuits and/or with their modes of generation (polarization, phase, frequency, ...).

These circuits are often etched on CMOS (silicon) or III/V (especially germanium) components. These components could be assembled in a modular way as shown in the functional diagram in Figure 435¹²⁵⁸. This enables a better management of processes heterogeneity used to create these different circuits.

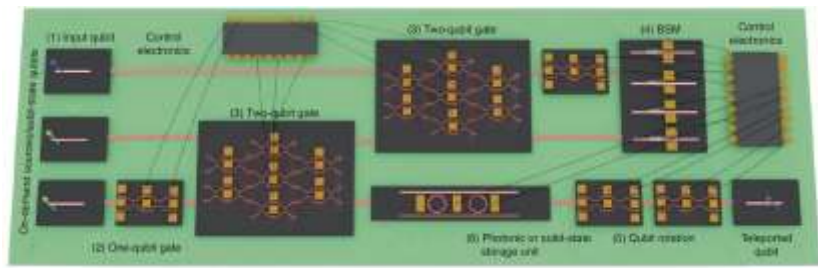


Figure 435: a nanophotonic circuit functional diagram. Source: [Hybrid integrated quantum photonic circuits](#) by Ali W. Elshaari et al, 2020 (14 pages).

Many semiconductor fabs in the world are helping photonicians design and prototype nanophotonic circuits to support photon qubits. We'll mention here only a few of them. Many fab technologies are investigated with classical silicon-based CMOS, hybrid CMOS with silicon nitride (SiN) and lithium niobate (LiNbO₃), III/V materials (GaAs¹²⁵⁹, InP, ...), etc¹²⁶⁰.

In France, **CEA-Leti** is also building an integrated silicon photonic qubits platform including single photons source, phase shifters and superconducting nanowire single-photon detectors (SNSPD) or CdHgTe avalanche photodiodes (APD), working at 2,5-4K that is compatible with single photon detectors. They are initially targeting secured QKD based telecommunications.

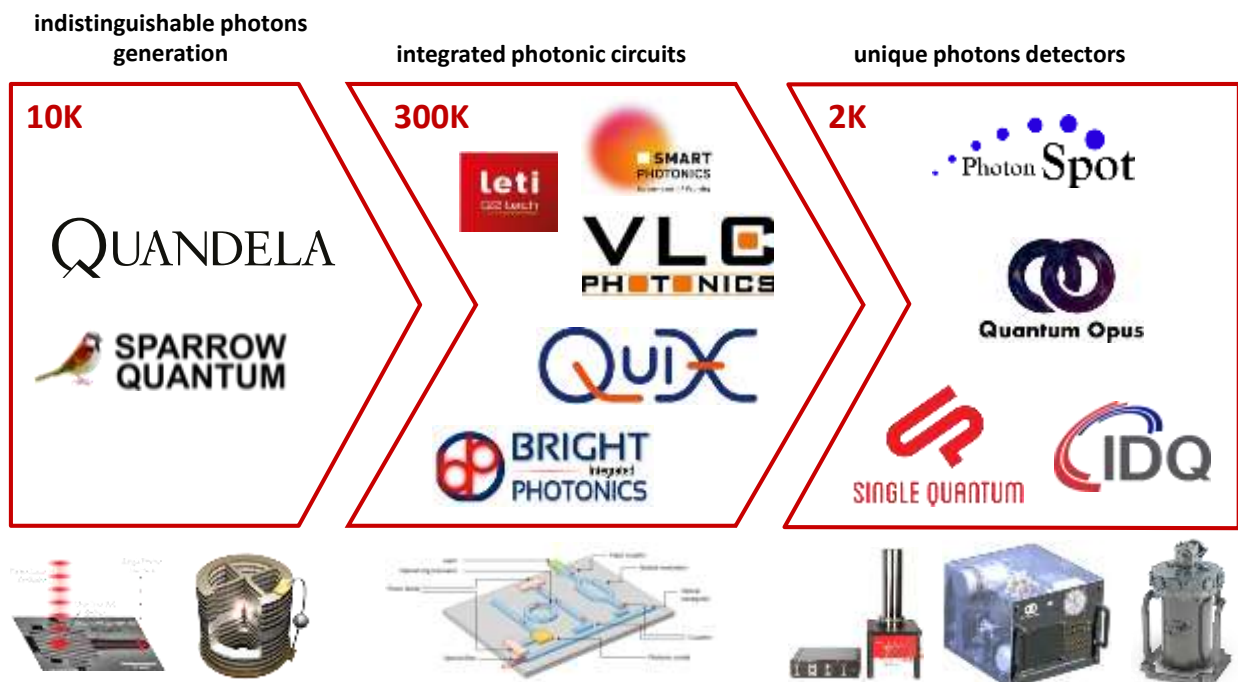


Figure 436: the key components of a photonic quantum computer: quality photon sources, preferably deterministic, nanophotonic circuits for processing, and photon detectors for readout. Source: adapted from [Photonic quantum bits](#) by Pascale Senellart, June 2019 (31 slides) in slide 11.

source : adapted from Photonic quantum bits by Pascale Senellart, June 2019 (31 slides)

¹²⁵⁸ See [Hybrid integrated quantum photonic circuits](#) by Ali W. Elshaari et al, 2020 (14 pages).

¹²⁵⁹ See [Expanding the Quantum Photonic Toolbox in AlGaAsOI](#) by Joshua E. Castro et al, May 2022 (9 pages). They implement non linear elements, edge couplers, waveguide crossings, couplers, and MZIs in Aluminum gallium arsenide-on-insulator (AlGaAsOI).

¹²⁶⁰ See the review paper [Roadmap on integrated quantum photonics](#) by Galan Moody, Jacqueline Romero, Eleni Diamanti et al, August 2021 (108 pages).

Ultimately, a photon qubits quantum computer would consolidate three key components as shown in Figure 436: a single photon generator, integrated photonic circuits and single photon detectors. The first and last ones are integrated with a cryogenic system operating at about 10K and 2K-4K respectively. But it seems also possible to integrate photon sources and detectors in a single photonic chipset¹²⁶¹.

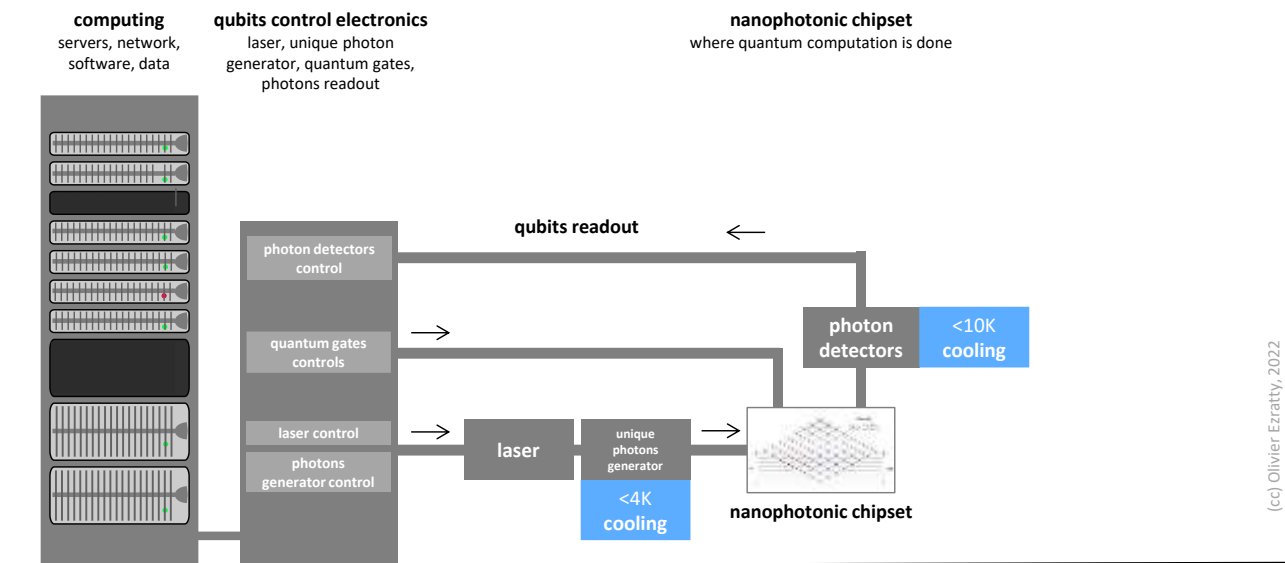


Figure 437: typical architecture of a photon qubits quantum computer. (cc) Olivier Ezratty, 2022.

The most active countries in the field seem to be China, the UK (particularly at the Universities of Oxford, Bristol, Cambridge and Southampton)¹²⁶², France (C2N, LKB, ...), Italy¹²⁶³, Germany (Universities of Stuttgart and Paderborn), Austria, Australia, Japan and of course the USA.

Photon qubits are the specialty of some startups like **PsiQuantum**, **Orca Computing**, **Tundra Systems Global**, **QuiX**, **Quandela**, **Nu Quantum**, and **Xanadu**.

Boson sampling

In photonics, the simulation of boson sampling is an experiment that is used to showcase the advancement of photon qubits. The idea of boson sampling came from **Scott Aaronson** and **Alex Arkhipov** from the MIT in a paper published in 2010¹²⁶⁴. They devised a linear optics-based experiment that would be impossible to easily emulate on a classical supercomputer¹²⁶⁵.

Boson sampling is about solving a problem of sampling the probability distributions of identical and indistinguishable photons being mixed in an interferometer and reaching single photon detectors. This physical process is impossible to emulate above a certain threshold, which generates yet another so-called "quantum supremacy" or "advantage".

¹²⁶¹ See [Integrated nanophotonics for the development of fully functional quantum circuits based on on-demand single-photon emitters](#) by S. Rodt and S. Reitzenstein, APL Photonics, December 2020 (14 pages).

¹²⁶² According to [Quantum Age technological opportunities](#) from the UK Government Office of Science in 2016 (64 pages).

¹²⁶³ Fabio Sciarrino of La Sapienza University in Rome, carried out in 2013 a sampling of bosons with a chip with 13 input ports and 13 output ports, with three photons. See [Efficient experimental validation of photonic boson sampling against the uniform distribution](#), 2013 (7 pages).

¹²⁶⁴ See [The computational Complexity of Linear Optics](#) by Alex Arkhipov and Scott Aaronson, 2010 (94 pages).

¹²⁶⁵ In quantum computing, we rely on only one type of boson: the photon. The other bosons are elementary particles such as gluons or Higgs bosons that can only be observed in particle accelerators. There are also composite particles such as the Cooper pairs (double electron) which are at the origin of superconducting currents. But when we talk about boson sampling, we always mean "photon".

A classical emulation requires extremely heavy matrix computing: the evaluation of square matrix permanents¹²⁶⁶. This sits in the "#P difficult" problem class of the complexity theories zoo¹²⁶⁷. The verification of the obtained result can't even be carried out by a classical computer¹²⁶⁸.

Boson sampling is the quantum and photonic analogue of the famous **Galton** plate experiment where balls cross rows of nails in a random way and end up in columns, with a Gaussian distribution.

This experiment is based on various probability concepts: convergence of a binomial distribution law towards a normal or Gaussian distribution, Moivre-Laplace theorem, etc. In the photon-based experiment, photons are injected into a series of interferometers combining them with their neighbor in a random way. On the other hand, the distribution at the end does not follow a Gaussian curve.

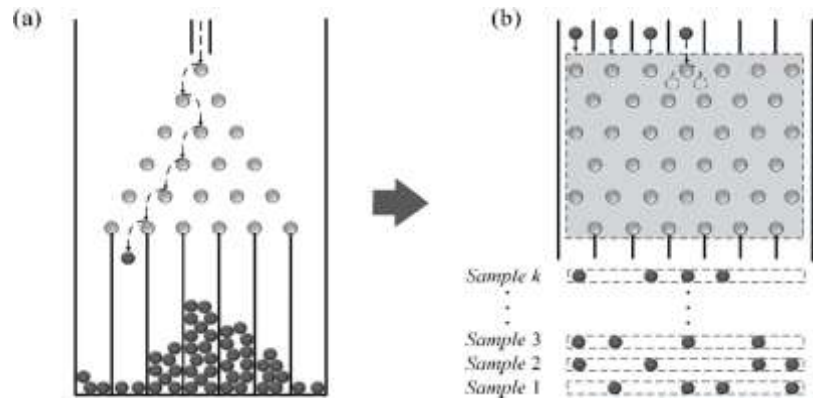


Figure 438: the typical Galton plate experiment that inspires Boson sampling. Source: [Quantum Boson-Sampling Machine](#) by Yong Liu et al, 2015.

It depends on the photons being sent upstream.

The appropriateness of the boson sampling style exercise is questionable. It implements a physical phenomenon with photons that is difficult to emulate in a classical way¹²⁶⁹. However, it is not strictly a form of calculation with some problem input data. There is not even a real notion of qubits, quantum gates and programming, except in the choice of the photons we send into the system. The optical components used are all passive and static, except the photon generators and detectors¹²⁷⁰.

It is a physics experiment generating additive and subtractive interferences and superposition of quantum states¹²⁷¹. The difficulty of the experiment lies mainly in the complexity of the production of identical and indistinguishable photons. At this stage, nobody has managed to transform (or reduce) a useful algorithm into boson sampling. However, this could eventually lead to applications in homomorphic encryption and blind computing¹²⁷².

¹²⁶⁶ If you want to explore the question, see for example [Lecture 3: Boson sampling](#) by Fabio Sciarrino, University of Rome, (63 slides) and [Experimental boson sampling with integrated photonics](#) (33 slides) by the same author who describes laser-based techniques for etching integrated photonic components. As well as [Permanents and boson sampling](#) by Stefan Scheel, University of Rostock, 2018 (21 slides). As for the definition of the notion of permanent in [Wikipedia](#), it uses notions and notations of linear algebra that are not even explained. The permanent of a matrix is a variant of its determinant. If the classical resolution of sampling requires the computation of matrix permanents, its resolution by linear optics system does not allow the computation of matrix permanents.

¹²⁶⁷ #P is the class of function problems that counts the number of solutions of NP problems.

¹²⁶⁸ In 2018, a Chinese team carried out a numerical simulation of 50 photon boson sampling using 320,000 processors from the Tianhe-2 supercomputer. See [A Benchmark Test of Boson Sampling on Tianhe-2 Supercomputer](#), 2018 (24 pages). With the 20 photons and 60 modes of the Chinese experiment published in October 2019, a supercomputer is no longer able to follow.

¹²⁶⁹ But this is a valid reality for the simulation of many complex physical phenomena, such as the folding of a protein or the functioning of a living cell, except that these remain in the realm of the living and are not simulated in a machine.

¹²⁷⁰ See [An introduction to boson-sampling](#) by Jonathan Dowling et al, 2014 (13 pages) which describes well the issues involved in conducting boson sampling.

¹²⁷¹ See the animation [Boson Sampling with Integrated Photonics](#), 2015 (3mn) which describes the path of photons in a boson sampling experiment as well as [Photonic implementation of boson sampling: a review](#) by Fabio Sciarrino, 2019 (14 pages) which describes in detail this kind of experiment.

¹²⁷² Seen in [Introduction to boson-sampling](#) by Peter Rohde, 2014 (34 minutes) which refers to [A scheme for efficient quantum computation with linear optics](#) by Emanuel Knill, Raymond Laflamme and Gerard Milburn, 2001 (7 pages) which theorized that quantum computation based on linear optics was plausible. We owe them the KLM scheme or protocol (their initials), a linear optics quantum computing (LOQC) programming model that has the disadvantage of being very heavy in terms of the number of hardware devices.

There are also some algorithms for simulating molecular vibrations based on boson sampling¹²⁷³. In 2020, a Chinese team was conducting an experiment similar to boson sampling to play a variant of the Go game¹²⁷⁴.

Chinese researchers are particularly active in the field¹²⁷⁵. In June 2019, the **Hefei** laboratory created a boson sampling using six photons with three degrees of freedom, therefore, based on qutrits (three-state qubits)¹²⁷⁶. The states of the photons were their traveled path, polarization and orbital angular momentum. With a gate error rate of 29%. In October 2019, Chinese researchers upgraded the feat to 20 photons with an experiment presented as reaching quantum supremacy, at the same time as the announcement of Google Sycamore¹²⁷⁷. In this experiment described in the diagram *below*, 20 indistinguishable photons were sent in a series of splitters and ended up in 60 photon detectors. The output Hilbert space was limited to 14 detectors, with a size of 3.7×10^{14} or 2^{48} . With the 60 activated detectors, this space should be able to reach a size of 60^{20} or 2^{118} .

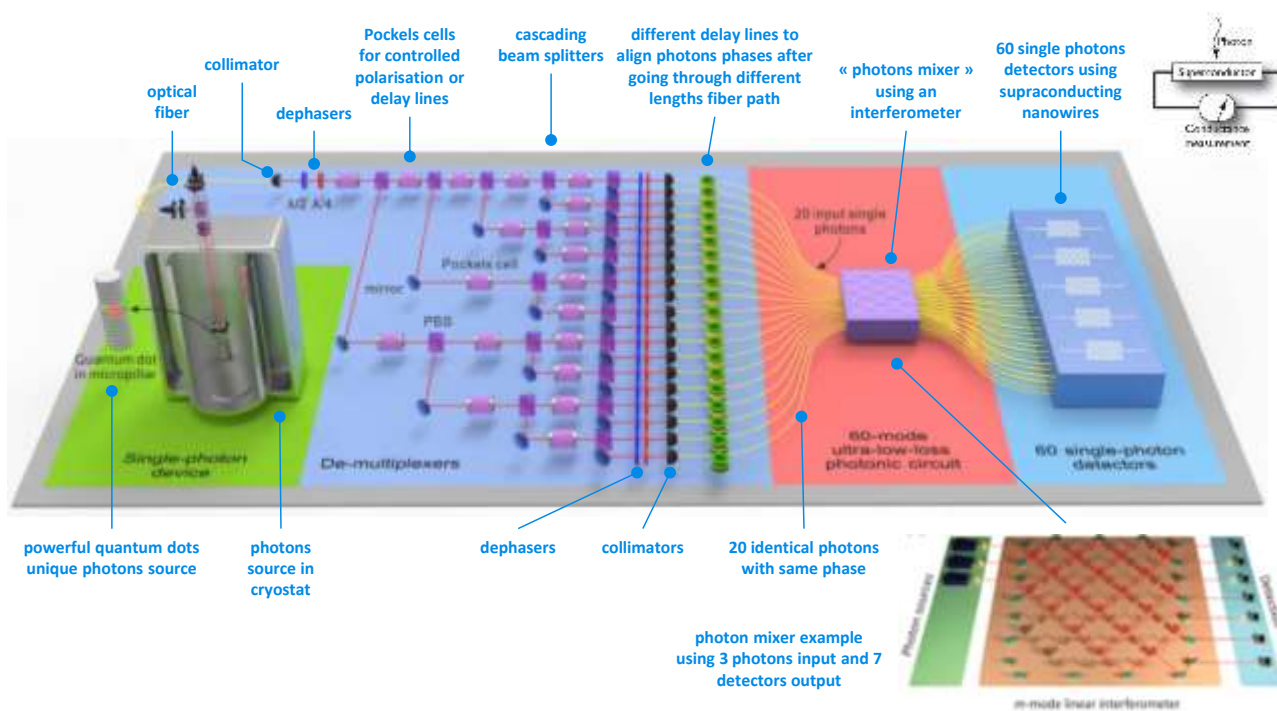


Figure 439: one of the first Boson sampling experiment made in China, in 2019, with 20 photon modes. Source: [Boson sampling with 20 input photons in 60-mode interferometers at \$10^{14}\$ state spaces](#) by Hui Wang et al, October 2019 (23 pages).

The size of Hilbert's space of such a device is evaluated with the size of the Fock space of M modes occupied by N photons. This would give a binomial space $\binom{M+N-1}{M}$ so $\binom{79}{60}$ which is equal in size to $\frac{79!}{60! \times 19!}$ ([source](#)).

¹²⁷³ See [Boson sampling for molecular vibronic spectra](#) by Joonsuk Huh, Alán Aspuru-Guzik et al, 2014 (7 pages) and [Vibronic Boson Sampling: Generalized Gaussian Boson Sampling for Molecular Vibronic Spectra at Finite Temperature](#) by Joonsuk Huh et al, 2017 (10 pages).

¹²⁷⁴ See [Quantum Go Machine](#) by Lu-Feng Qiao et al, July 2020 (16 pages).

¹²⁷⁵ See [Chinese researchers on the road to the 'ultimate' quantum processor?](#) by Bruno Cormier, September 2018 which points to [Building Quantum Computers With Photons Silicon chip creates two-qubit processor](#) by Neil Savage, September 2018 which discusses the creation of a two-qubit quantum processor. The original article is [Large-scale silicon quantum photonics implementing arbitrary two-qubit processing](#), September 2018 (23 pages). The researchers involved were Chinese, English and Australian.

¹²⁷⁶ See [18-Qubit Entanglement with Six Photons Three Degrees of Freedom](#) by Xi-Lin Wang et al, June 2019 (14 pages).

¹²⁷⁷ See [Boson sampling with 20 input photons in 60-mode interferometers at \$10^{14}\$ state spaces](#) by Hui Wang et al, October 2019 (23 pages).

The Chinese researchers indicated that they could use several hundred detectors in output and use a double encoding of photons (polarization and spatial encoding) to multiply the power of their system and thus make it able to create a NISQ (noisy intermediate scale quantum computer) system, except that the ability to program it does not seem obvious, nor its uses.

This represents the number of incoming photon detectors at the power of the incoming photon number. The previous record was 5 photons over 16 modes and the sampling was verifiable on a classical computer whereas with these 20 photons and 60 modes, it was no longer possible. The photon generator was realized with quantum dots in gallium and indium arsenide, placed in a 4K¹²⁷⁸ cryostat. The photon mixer used 396 beam splitters and 108 mirrors. For the experiment to work, one photon must arrive at the same time in all the inputs of the photon mixer.

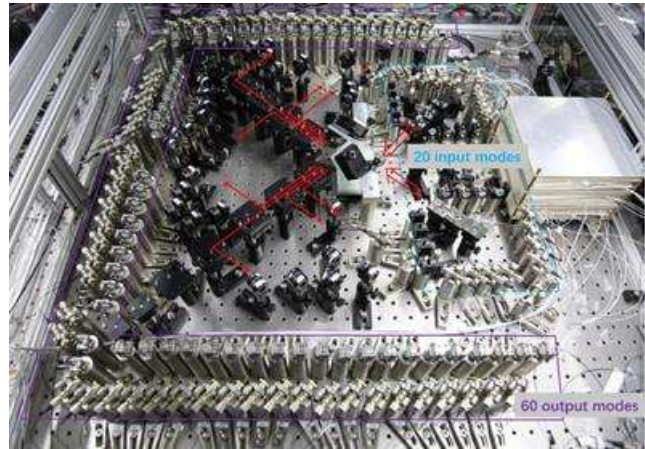
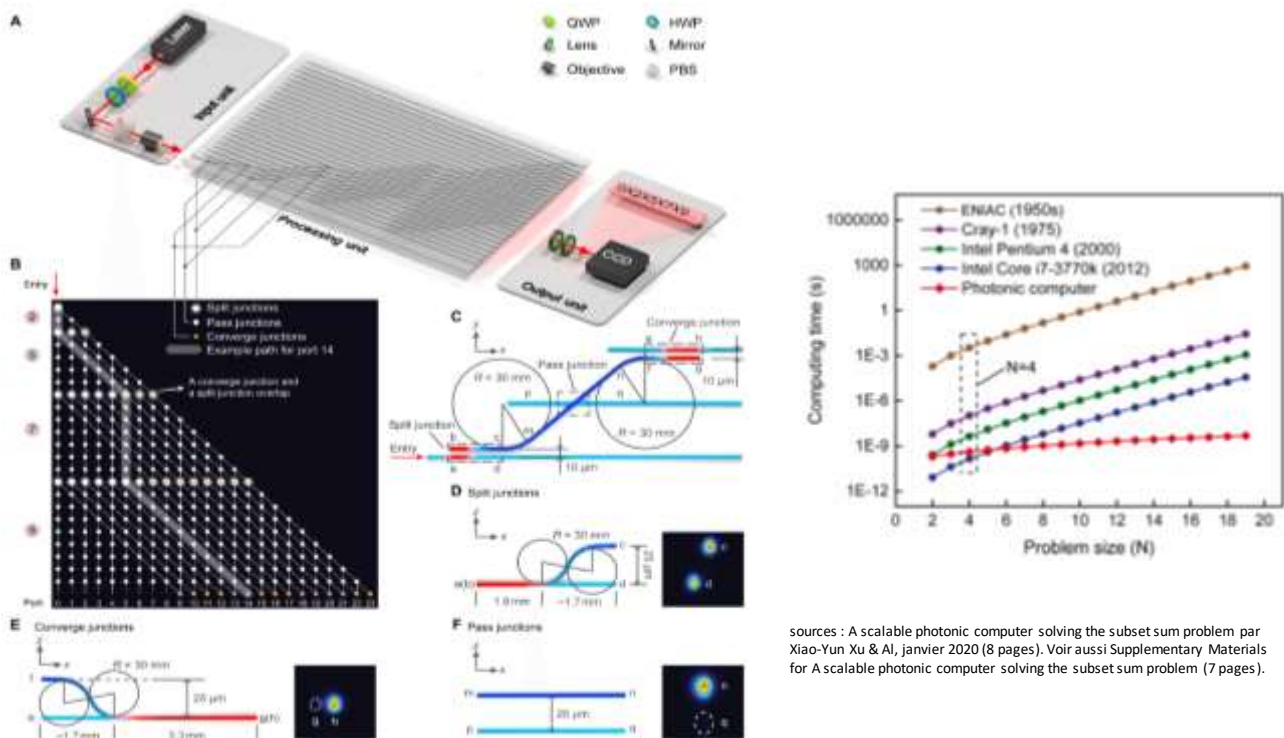


Figure 440: optics table of the 20 photons/60 modes China experiment.

The corresponding probability is very low. They use active demultiplexers with Pockels cells to demultiplex and direct the photons.

In 2020, other Chinese researchers used an optical quantum calculator to solve a useful problem, the subset-sum problem, which is complete NP. The system shown in Figure 441 uses a chipset much more miniaturized than the usual boson sampling experiments.



sources : A scalable photonic computer solving the subset sum problem par Xiao-Yun Xu & Al, janvier 2020 (8 pages). Voir aussi Supplementary Materials for A scalable photonic computer solving the subset sum problem (7 pages).

Figure 441: a first optical calculator to solve a useful problem created in 2020. Source: [A scalable photonic computer solving the subset sum problem](#) by Xiao-Yun Xu et al, January 2020 (8 pages).

¹²⁷⁸ The photon source would come from a German laboratory located in Würzburg, Bavaria. It is largely inspired by the reference work in the field of Pascale Senellart's team from the CNRS C2N.

The problem is to determine, apart from a set of signed integers, whether it is possible to add a subset of them together to obtain a given integer¹²⁷⁹. The system uses a laser as a source of photons. The benchmark has been realized with N=4 integers. They indicate that by extrapolating, their system would beat all other known methods of solving this kind of problem.

One of the perspectives of photon-based qubits is to bypass their flaws with the use of MBQC and cluster states, which we have already defined on page 450. Indeed, these use the implementation of an entangled state between all qubits and then a measurement of the progressive state of the others. This avoids the complexity of optical quantum gates, which are difficult to implement, whereas we now know how to create a set of well-entangled photons.

In December 2020, the stakes went higher with a **gaussian bosons sampling** done with 70 photon modes¹²⁸⁰. The experiment was even more impressive than the previous ones and the publicized quantum advantage reached new heights. But the system, shown in Figure 442, was not more programmable than the previous ones. So, any computing advantage claim was dubious.

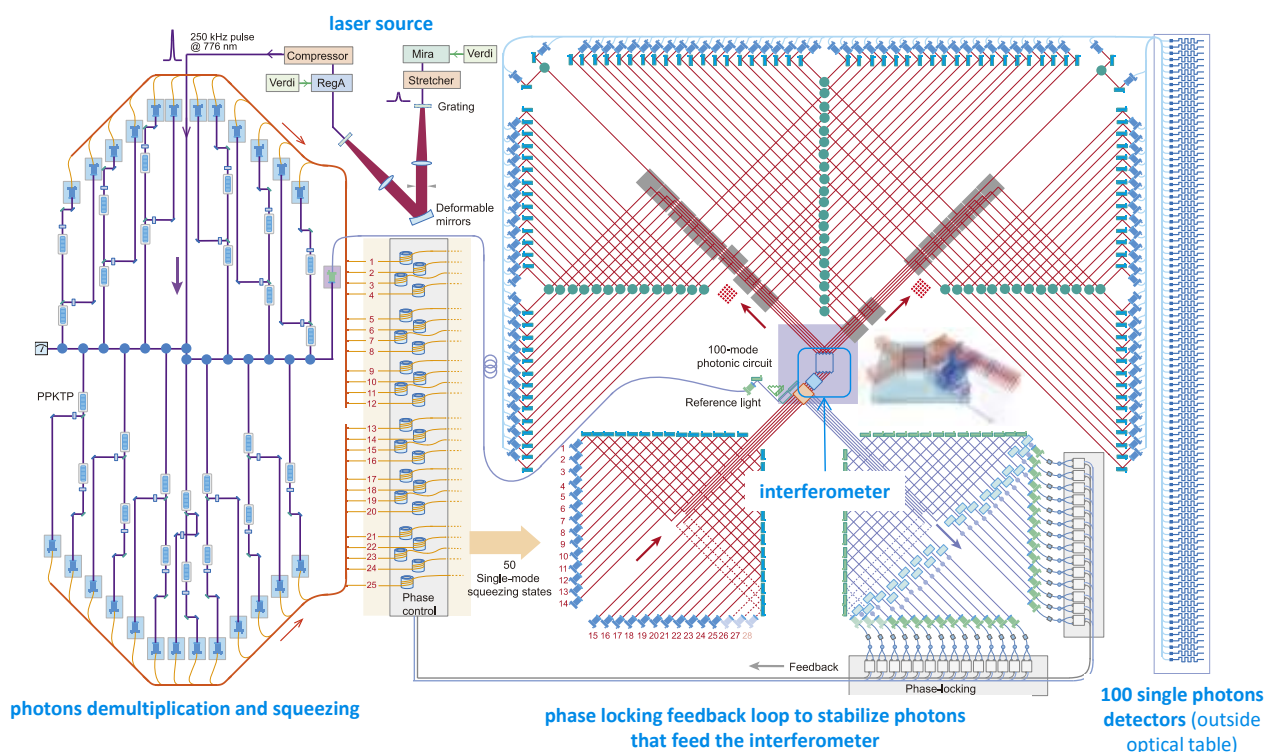


Figure 442: a 2020 generation China boson sampling experiment with up to 70 simultaneous photon modes. Source: [A scalable photonic computer solving the subset sum problem](#) by Xiao-Yun Xu et al, January 2020 (8 pages).

Late 2020, a competing Chinese team implemented another form of boson sampling using “membosonsampling” for which an emulation requires even more complicated Haar-random unitary matrix¹²⁸¹. But it was not programmable.

¹²⁷⁹ See [Photonic computer solves the subset sum problem](#), February 2020 which points to [A scalable photonic computer solving the subset sum problem](#) by Xiao-Yun Xu et al, January 2020 (8 pages). See also [Supplementary Materials for A scalable photonic computer solving the subset sum problem](#) (7 pages).

¹²⁸⁰ See [Chinese Scientists Begin Climb Toward Universal Quantum Computer](#) by Matt Swayne, December 2020, [Chinese scientists say they’ve achieved a quantum computing breakthrough](#) by Shiyin Chen et al, December 2020 and [Quantum computational advantage using photons](#) by Han-Sen Zhong et al, December 2020 (23 pages) and the [supplemental materials](#) (64 pages). See [Benchmarking 50-Photon Gaussian Boson Sampling on the Sunway TaihuLight](#) by Yuxuan Li et al, 2020 (12 pages) for the classical emulation on classical supercomputers.

¹²⁸¹ See [Quantum Advantage with Timestamp Membosonsampling](#) by Jun Gao, December 2020 (30 pages).

In June 2021, the China team from 2020's GBS upgraded their experiment and made it somewhat programmable, ramping it up to 113 detection events extracted from 144 photon modes circuit shown in Figure 443. The input squeezed photons are phase programmable before they enter the fixed part of the experiment in the interferometer. The experimenter still has to implement some real-world algorithms and benchmarks to demonstrate sort of quantum computing advantage¹²⁸².

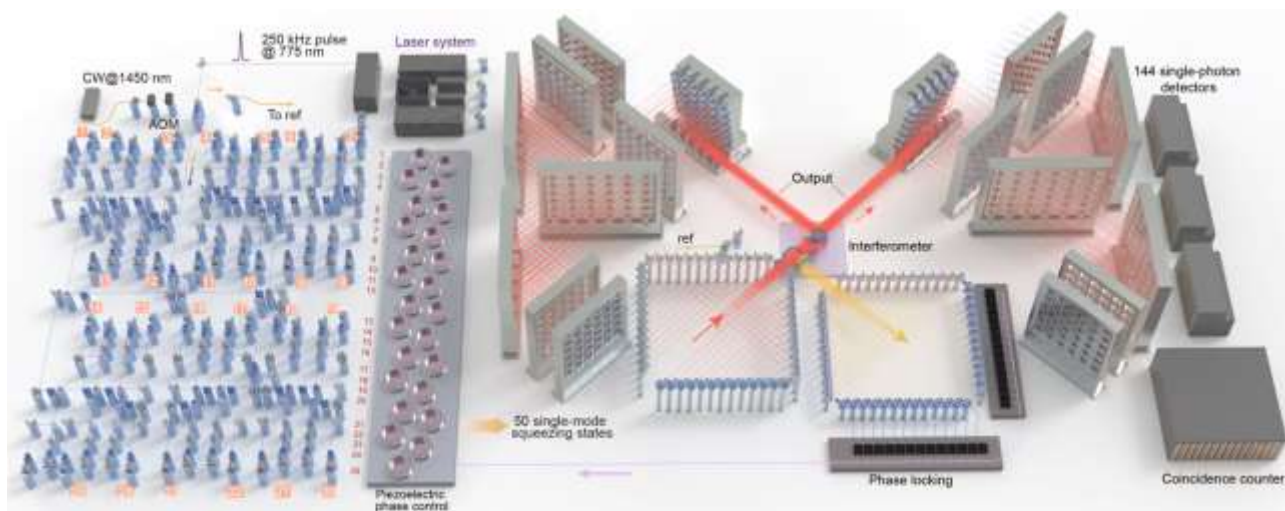


Figure 443: the latest Boson sampling experiment achieved in China in 2021 with 144 photon modes. Source: [Phase-Programmable Gaussian Boson Sampling Using Stimulated Squeezed Light](#) by Han-Sen Zhong, Chao-Yang Lu, Jian-Wei Pan et al, June 2021 (9 pages).

In 2022, Fabio Sciarrino did demonstrate that it was possible to create a programmable interferometer in a boson sampler¹²⁸³. And in 2022, Xanadu did up the ante with a new GBS experiment, more powerful than the last one from China, but simpler thanks to some time-bin multiplexing. It was also programmable and even made available in the cloud but with caveats we'll describe in the photonic qubits vendor section.

Measurement Based Quantum Computing

MBQC is a very particular approach to quantum computing. It consists in exploiting the initialization of entangled qubits and then performing step-by-step measurements on certain qubits to obtain a result on the last measured qubits at the end of the run. There are several variants, the *one-way quantum computing* (1WQC¹²⁸⁴) which uses two-dimensional qubits matrices to create cluster states and the *measurement-only QC* which only measures qubits, without prior entanglement. We will focus here on the first method which seems to be the most commonplace.

¹²⁸² See [Phase-Programmable Gaussian Boson Sampling Using Stimulated Squeezed Light](#) by Han-Sen Zhong, Chao-Yang Lu, Jian-Wei Pan et al, June 2021 (9 pages).

¹²⁸³ See [Reconfigurable continuously-coupled 3D photonic circuit for Boson Sampling experiments](#) by Francesco Hoch, Fabio Sciarrino et al, npj quantum information, May 2022 (7 pages).

¹²⁸⁴ MBQC was designed in 2000 by Robert Raussendorf and Hans Briegel. See [A computationally universal phase of quantum matter](#) by Robert Raussendorf, 2018 (41 slides), [Measurement-based Quantum Computation](#) by Elham Kashefi, University of Edinburgh (50 slides) and the extensive [Introduction to measurement based quantum computation](#) by Tzu-Chieh Wei from Stone Brook University, 2012- (88 slides) and a one pager: [Universal measurement-based quantum computation with Mølmer-Sørensen interactions and just two measurement bases](#). Other information sources include [Blind quantum computation](#) by Charles Herder (10 pages), [Cluster-state quantum computation](#) by Michael Nielsen, 2005 (15 pages), [Fault-tolerant quantum computation with cluster states](#) by Michael Nielsen and Christopher Dawson, 2004 (26 pages), [2D cluster state](#) (50 slides), [Quantum Computing with Cluster States](#) by Gelo Noel Tabia, 2011 (18 pages), [Quantum pictorialism for topological cluster-state Computing](#) by Clare Horsman 2011 (18 pages) and [Cluster State Quantum Computing](#) by Dileep Reddy et al, 2018 (11 pages). See also [Quantum computing with photons: introduction to the circuit model, the one-way quantum computer, and the fundamental principles of photonic experiments](#) by Stephanie Barz, 2015 (26 pages). At last, see the review paper [Realizations of Measurement Based Quantum Computing](#) by Swapnil Nitin Shah, December 2021 (7 pages).

MBQC allows the execution of classical quantum algorithms with universal gates. Where is it relevant? It is particularly interesting in qubit-based quantum systems where it is difficult to create multi-qubit quantum gates exploiting entanglement and where the number of chained gates is limited for physical reasons.

The model was initially created for cold atoms qubits but it later made more sense with photon qubits for which two-qubit gates are difficult to create. Photons are also indicated because they allow to easily manage rotation angles in the Bloch sphere that are used in the single-qubit quantum gates of the process, via a phase control of the photon qubits. It can also be implemented with other types of qubits like silicon carbide defects¹²⁸⁵.

With MBQC, things are done a bit backwards with respect to classical quantum computing: we first apply single-qubit gates and measure them progressively, whereas in classical quantum computing with universal gates, we only involve qubits progressively and then make measurements at the end of computation.

An MBQC calculation is **logically irreversible**, unlike a quantum algorithm based on universal quantum gates. Indeed, the process of measuring qubit states cannot be logically reversed except when the state of the qubits read corresponds exactly to their basis states $|0\rangle$ and $|1\rangle$.

A quantum computation executed with universal gates is the equivalent of applying a unitary transformation embodied by a giant square matrix of dimension 2^N to a set of N qubits initialized in the state $|0\rangle$. This matrix can be inverted by scrolling backwards the quantum gates that were used to create it. With MBQC, this is not possible. This irreversibility of MBQC calculations explains why it is also called 1WQC for One Way Quantum Computing. There is no way going back.

This model is also **probabilistic**, due to the probabilistic nature of the state measures of qubits at each step of the calculation. The successive measurements provide information on the state of the qubits, which makes it possible to become determinist again in the rest of the computation by applying a kind of error correction on the fly. A bit like using 3-qubit error correction codes.

By definition, MBQC is a **hybrid algorithms** method since its implementation depends on interactions between quantum computing and the exploitation of qubits readout data by a classical computer controlling the system.

Qubits used in the cluster state-based MBQC are of four different classes: those that are prepared and measured (the ancilla qubits), those that are only measured during computing, those that are only prepared (but measured at the end of computing) and those that are neither prepared nor measured (and are used for the rest of computing).

The principle is based on the sequencing of so-called NEMC sequences with four steps¹²⁸⁶:

- Using a set of **ancilla qubits** (step N), those of the first type which are measured with a Z projection.
- Creating **cluster-states of entangled qubits** (step E). With photons, there are many ways to generate these cluster states and it's one of the key scientific and technology challenges with MBQC. Theoretically, you could generate these cluster states with regular independent qubits and apply these a series of single and entangling quantum gates (H, CNOT, etc). Problem is, these entangling gates are difficult to create with photons and MBQC is a method that gets rid of these in the first place! So, scientists are looking for ways to generate these cluster states with other means.

¹²⁸⁵ In [Quantum Information Processing With Integrated Silicon Carbide Photonics](#) by Sridhar Majety et al, March 2022 (50 pages).

¹²⁸⁶ Information sources: [Advanced Quantum Algorithms](#) by Giulia Ferrini et al, 2019 (30 pages) and [An introduction to Quantum Computing](#) by Elham Kashefi, School of Informatics University of Edinburgh, 2020 (119 slides).

There are many figures of merits here: the source must be as deterministic as possible and avoid so-called heralding and post-selection methods that reduce the chance to get a full cluster state at a given moment. There are also 1D and 2D cluster states.

Photonic cluster states can be generated in many ways which have evolved over time with **SPDC** (spontaneous parametric down-conversion) using powerful laser single photons source heralding with a probabilistic outcome that is detected post-selectively and doesn't scale well beyond a dozen qubits¹²⁸⁷, atom based **cavity QED** generation¹²⁸⁸ that was later extended to **ensemble of Rydberg atoms**¹²⁸⁹, individual **neutral atoms**, **spin-photon entanglement** to deterministically generate linear cluster states aka the Lindner-Rudolph protocol¹²⁹⁰ with recent improvements¹²⁹¹, with **quantum dots molecules**¹²⁹², with the **entanglement of several single photon sources**¹²⁹³, **time-domain multiplexing** using indistinguishable photon sources which has the advantage to be theoretically unlimited¹²⁹⁴, **2D spin-photon** cluster states¹²⁹⁵, etc. You can also add **spectral domain multiplexing** on top of time-domain multiplexing as a complement to SPDC sources¹²⁹⁶.

¹²⁸⁷ See [12-Photon Entanglement and Scalable Scattershot Boson Sampling with Optimal Entangled-Photon Pairs from Parametric Down-Conversion](#) by Han-Sen Zhong, Jian-Wei Pan et al, PRL, 2018 (17 pages) with a ~97% heralding efficiency and ~96% photons indistinguishability. They generated 12-photon entanglement with a state fidelity of 0.572 ± 0.024 . It was used for early Boson sampling experiments.

¹²⁸⁸ See [Sequential generation of matrix-product states in cavity QED](#) C. Schön, K. Hammerer, M. M. Wolf, J. I. Cirac, and E. Solano, 2006 (11 pages) and [Efficient generation of entangled multiphoton graph states from a single atom](#) by Philip Thomas et al, Nature, August 2022 (12 pages) with a generation of 14 qubits GHZ states and linear cluster states of 12 photons.

¹²⁸⁹ See [Sequential generation of multiphoton entanglement with a Rydberg superatom](#) by Chao-Wei Yang, Jian-Wei Pan et al, December 2021 (11 pages). One disadvantage of this method is its slow emission rate.

¹²⁹⁰ See [Proposal for Pulsed On-Demand Sources of Photonic Cluster State Strings](#) by Netanel H. Lindner and Terry Rudolph, PRL, 2009, published initially as [A photonic cluster state machine gun](#) on arXiv (10 pages), a first demonstration obtained with semiconductor quantum dots spins in [Deterministic generation of a cluster state of entangled photons](#) by I. Schwartz, D. Gershoni et al, Technion and University of Washington, Science, 2016 (28 pages) with series of 5 entangled photons and recent improvements in [Probing the dynamics and coherence of a semiconductor hole spin via acoustic phonon-assisted excitation](#) by Nathan Coste, Niccolo Somaschi, Loic Lanco, Pascale Senellart et al, C2N and Quandela, July 2022 (6 pages).

¹²⁹¹ See the first results of high photon indistinguishability in [A deterministic source of indistinguishable photons in a cluster state](#) by Dan Cogan, David Gershoni et al, Technion, October 2021 (17 pages) where quantum dot emits indistinguishable polarization-entangled photons with a Gigahertz rate deterministic generation of >90% indistinguishable photons in a cluster state of over 10 photons and [High-rate entanglement between a semiconductor spin and indistinguishable photons](#) by Nathan Coste, Sophia Economou, Niccolo Somaschi, Alexia Auffèves, Loic Lanco, Pascale Senellart et al, July 2022 (17 pages). It is about the efficient generation of three qubits cluster state with one semiconductor spin and two indistinguishable photons with 2 and 3 particle entanglement with fidelities of 80 % and 63 % respectively, with photon indistinguishability of 88%. The spin-photon and spin-photon-photon entanglement rates exceed by three and two orders of magnitude respectively the previous state of the art.

¹²⁹² See [Deterministic generation of entangled photonic cluster states from quantum dot molecules](#) by Arian Vezvaei, Sophia Economou et al, June 2022 (5 pages).

¹²⁹³ See [Multi-photon entanglement from distant single photon sources on demand](#) by Almut Beige et al, 2006 (9 pages) and [Protocol for generation of high-dimensional entanglement from an array of non-interacting photon emitters](#) by Thomas J Bell et al, University of Bristol and NBI, New Journal of Physics, January 2022 (9 pages).

¹²⁹⁴ See [Sequential generation of linear cluster states from a single photon emitter](#) by D. Istrati, Pascale Senellart, H.S. Eisenberg et al, 2020 (8 pages), [Deterministic generation of a two-dimensional cluster state](#) by Mikkel Vilsbøll Larsen et al, Science, September 2019 (30 pages), using two OPOs (Optical Parametric Oscillator) and [Generation of time-domain-multiplexed two-dimensional cluster state](#) by Warit Asavanant et al, Science, 2019 (23 pages).

¹²⁹⁵ See [Multidimensional cluster states using a single spin-photon interface coupled strongly to an intrinsic nuclear register](#) by Cathryn P. Michaels et al, University of Cambridge, October 2021 (14 pages) and [Deterministic multi-mode gates on a scalable photonic quantum computing platform](#) by Mikkel V. Larsen et al, DTU, Nature Physics, July 2021 (30 pages) which deals with creating a universal gate set with cluster states, with CV qubits using telecommunication wavelengths (1550nm).

¹²⁹⁶ See [Spectrally shaped and pulse-by-pulse multiplexed multimode squeezed states of light](#) by Tiphaine Kouadou, Nicolas Treps, Valentina Parigi et al, September 2022 (9 pages) which is about generating continuous variables entangled field modes which could also be used for Gaussian boson sampling.

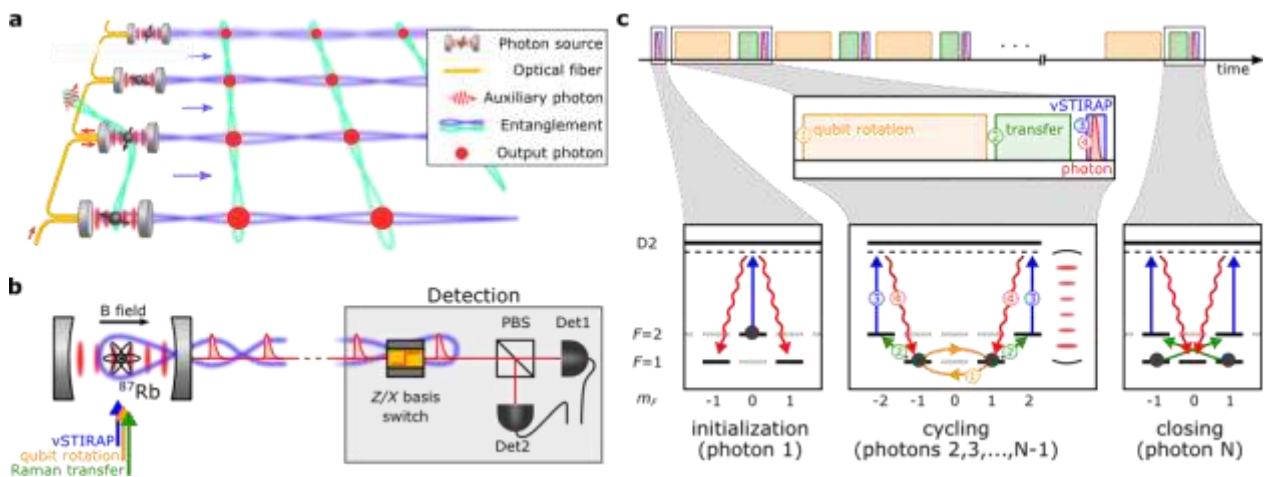


Figure 444: one solution to generate a cluster state of entangled photons for MBQC. Source: [Efficient generation of entangled multi-photon graph states from a single atom](#) by Philip Thomas, Leonardo Ruscio, Olivier Morin and Gerhard Rempe, MPI, May 2022 (10 pages).

- Measuring **state of intermediate qubits** during computing (M). It is carried out with a variation of projective measurement. It consists in first applying one or more X or Y gates to a qubit to create a rotation in their Bloch sphere and then to measure their state on the computational basis. It is a bit like rotating the Z ($|0\rangle/|1\rangle$) axis in the Bloch sphere to change the reference point.

$$|\pm\rangle = \frac{|0\rangle \pm |1\rangle}{\sqrt{2}}$$

$$|\pm_\alpha\rangle = \frac{|0\rangle \pm e^{i\alpha}|1\rangle}{\sqrt{2}}$$

The projective measurement basis is in the form of states of the type $|\pm_\alpha\rangle$, α being generally a half or quarter turn in Bloch's sphere. A measured qubit is always an intermediate resource and is not an output resource. This helps obtaining an information that can be used to manipulate the qubits afterwards to propagate computation. Projective Z measurements have the effect of removing the measured qubits from the cluster.

- These successive **corrections** make computing deterministic (step C) with X and Z gates. They are applied according to the result of the projective measurements made in (M). No correction gate acts here on a qubit already measured. This model makes it possible to apply any gate to a qubit which is in fact a combination of $Rz(\gamma)Rx(\beta)Rz(\alpha)$, i.e. rotations around the three axis of the Bloch sphere of angles γ , β and α ¹²⁹⁷.

What has just been described allows to interpret the lower right-hand part of the illustration in Figure 445 which explains how the MBQC equivalents of the CNOT (two-qubit), H or S quantum gate equivalents are realized in MBQC. Each X or Y circle is an X and Y projective measure that combines an X or Y gate followed by a qubit readout. The result conditions the type of projective measurement performed immediately afterwards in the order indicated (1 to 15 and 1 to 5).

Two forms of measurements affect the inner working of the qubit matrix: Z measurements separate the qubits by digging sort of grooves in the qubit matrix, a bit like pacmans, then classical measurements along the "wires" or on the "bridges" between these wires simulate single-qubit gates like Hadamard's and the two-qubit CNOT gates. The sequence of operations depends on the result of each measurement along the wires. The computation result is located in the last qubits whose state is not yet measured and which will be measured last¹²⁹⁸.

¹²⁹⁷ The decomposition of quantum gates into a computational method that can be used for MBQC has been [patented](#) by Krysta Svore of Microsoft, who leads the QuArC group there.

¹²⁹⁸ Illustrations sources: [Basics of quantum computing and some recent results](#) by Tomoyuki Morimae, 2018 (70 slides).

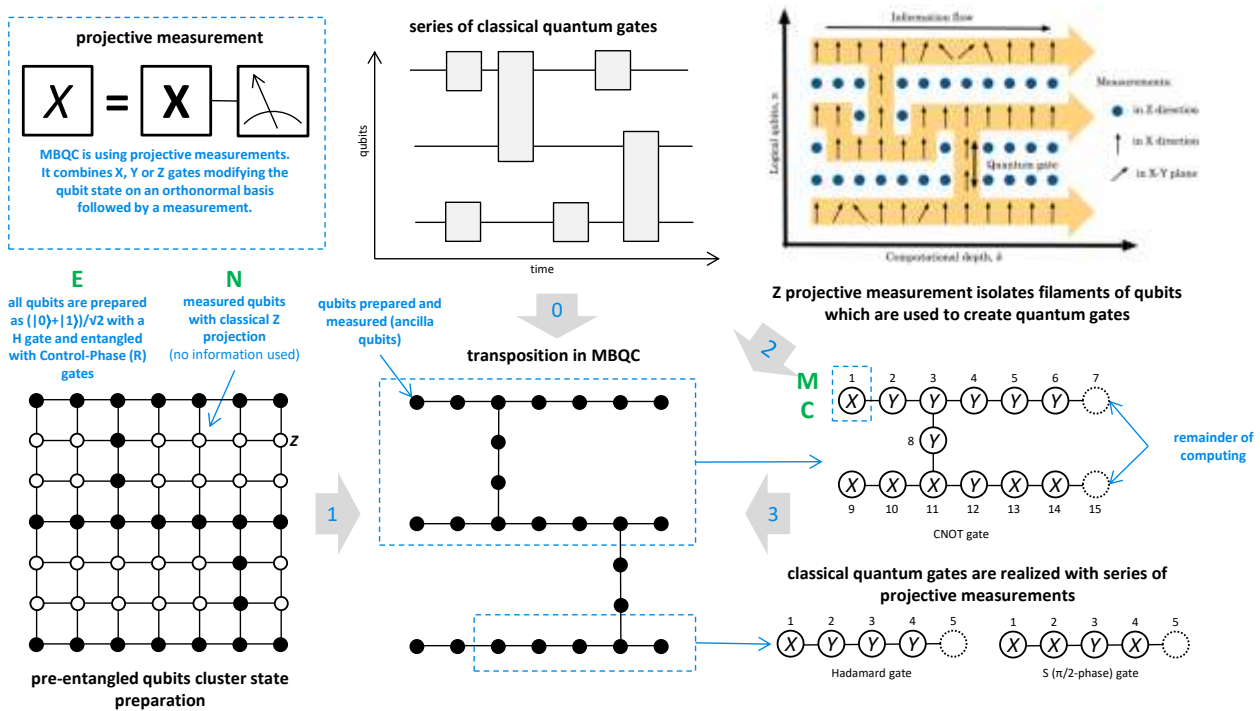


Figure 445: a tentative summary of how MBQC works. Usually, learning it works like a Write Once Read Never (WORN) memory!
 (cc) compilation, Olivier Ezratty, 2021, dedicated to my friend Jean-Christophe Gougeon.

This combination of NEMC sequences allows the reproduction of the operation of one- and two-qubit quantum gates. A complete quantum computation is a sequence of multiple NEMCs that ends with the measurement of the state of the remaining qubits!

The consequences of what we have just seen are multiple:

- MBQC requires way **more qubits** than in a conventional circuit-based model. We've seen that a single X or Y gate results from the combination of four X and Y gates and as many measurements. This in turn creates a "pressure" on the classical part of the calculation, linked to the measurement. But we'll catch up later with parallelism.
- MBQC still requires **error correction codes** such as those we have studied in a previous section, page 216. They too will multiply by several orders of magnitude the number of physical qubits necessary for computing any algorithm. It could be facilitated if we could organize the qubits in 3D matrices, the third dimension being used to align the qubits necessary for error correction, especially with surface codes. On the other hand, since MBQC models contains its own error correction mechanisms, it is less demanding in terms of additional qubits for error correction necessary for the creation of "fault tolerant" quantum computers¹²⁹⁹.
- The **temporal dimension** of computing is modified compared to classical gate-based quantum computing. As we can parallelize operations coupling gates and measurements, MBQC is a bit like Nutella on the breadcrumbs: we can spread it out! The depth of the available computation is no longer linked to the ability to chain quantum gates in time as in the middle-high diagram in the previous illustration, but to execute a large number of them in parallel over a very large number of qubits (modulo the required error correction). The sequences of measurements labeled 1, 2 ... n will be carried out simultaneously in groups 1, 2 ... n, n being limited to 15. Therefore, the required physical calculation depth if defined by the maximum number of physical gates to execute to create a CNOT. This is an argument in favor of photon qubits.

¹²⁹⁹ See one proposal of correction codes in [Error-protected qubits in a silicon photonic chip](#) by Caterina Vigliar et al, VTT, Nature Physics, September 2021 (31 pages).

The depth of an algorithm no longer depends on the ability to chain quantum gates with one and two qubits, but on the entanglement capacity of the qubits at startup in the model's cluster states. In short, sequential quantum computing is replaced by massively parallel quantum computing with a very shallow depth. This is the approach chosen by PsiQuantum.

- An MBQC model is easily exploitable to take advantage of teleportation and **distributed quantum computing** algorithms. Cluster states will be able to be linked together via remote optical links. It is also one of the tools of blind computing¹³⁰⁰.
- Finally, there is a direct link between the MBQC and the **ZX Calculus**. ZX Calculus is a graph model that help formalizing MBQC, its cluster states and the associated error corrections¹³⁰¹.
- The **algorithms** are specific to this kind of architecture¹³⁰². It is not yet experimental because it requires a large number of qubits that are not yet practically available.

Vendors

Ψ PsiQuantum **PsiQuantum** (2016, USA/Europe, \$728M) is a startup created by Jeremy O'Brien, a former Stanford and Bristol University researcher, who wants to create a photon-based quantum processor in CMOS silicon technology.

Other cofounders are Pete Shadbolt (co-inventor of the VQE algorithm with Jeremy O'Brien and Alán Aspuru-Guzik), Mark Thompson and Terry Rudolph, who discovered when he finished his physics thesis that he was a grandson of Erwin Schrödinger, which may have helped with fundraising! The company already employs over 150 people, most of them in Palo Alto in the USA, but some of them work remotely all over the world, including a couple ones in Europe.

Early in 2021, the company started to be more open on its technology¹³⁰³. It published a paper describing their qubit architecture, using an **FBQC** system, aka Fusion-based quantum computation, a variant of MBQC that we study a bit later. It uses micro-clusters states with groups of 4 qubits connected together and using Resource State Generators (RSGs). It's replacing measurement of entangled states by double measurement of non-connected adjacent qubits to create entanglements between them¹³⁰⁴. Qubits are encoded in path, in what they call dual-rail encoding with lines for photon states $|0\rangle$ and $|1\rangle$.

Two qubit gates use XX nondeterministic and ZZ deterministic measurements (measuring two photons simultaneously with the same polarization basis), implemented with a beam splitter then combining fusions to create small cluster states.

¹³⁰⁰ See [Measurement-based and Universal Blind Quantum Computation](#) by Anne Broadbent, Joseph Fitzsimons and Elham Kashefi, 2016 (41 pages).

¹³⁰¹ Seen in [Universal MBQC with generalised parity-phase interactions and Pauli measurements](#) by Aleks Kissinger and John van de Wetering, 2019 (21 pages).

¹³⁰² See for example [Changing the circuit-depth complexity of measurement-based quantum computation with hypergraph states](#), May 2019 (16 pages). The article describes an MBQC method based on the exploitation of Toffoli (CCZ) and Hadamard (H) gates. They allow to simulate topological quantum computation, reducing the error rate of quantum computation.

¹³⁰³ See [Silicon Photonic Quantum Computing - PsiQuantum at 2021 APS March Meeting](#) by Jeremy O'Brien, April 2021 (25 mn).

¹³⁰⁴ FBQC is fairly well explained in [Quantum Computing at the Speed of Light](#) by Terry Rudolph, November 2021 (1h13 video).

With that, the qubit computing depth is quite shallow, avoiding the pitfalls of qubits error rates. It's replaced by a large breadth of computing and commutative operations replacing "depth-computing" by "breadth-computing"¹³⁰⁵. Their ambition is to produce a system with one million physical qubits generating the equivalent of 100 logical qubits. Their photonic chipsets manufacturing is handled at the 300 mm wafers **Global-Foundries** Luther Forest Technology Campus in upstate New York.

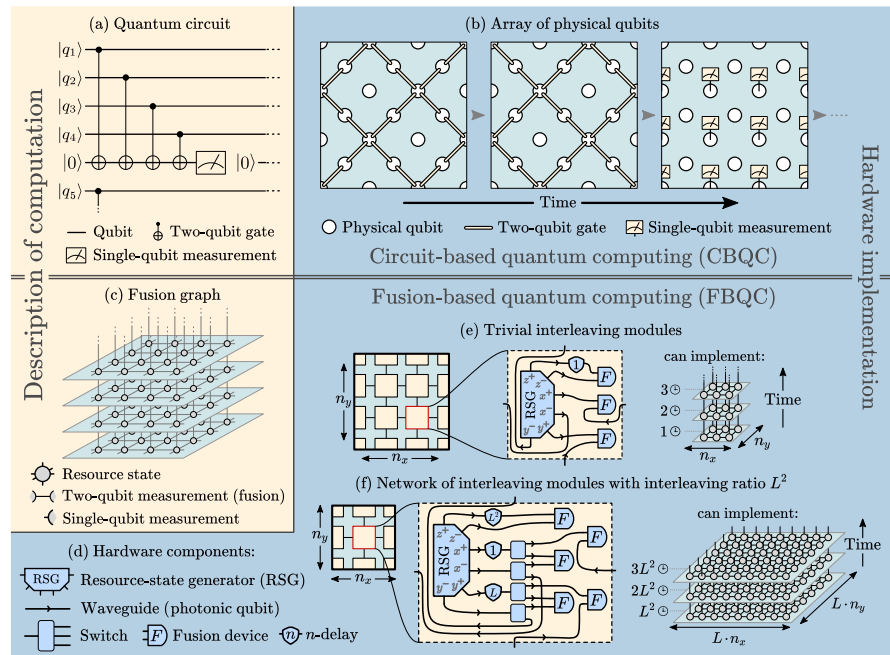


Figure 446: a description of the FBQC method for the amateur photonicist. Source: [Interleaving: modular architecture for fault-tolerant photonic quantum computing](#) by Hector Bombin et al, 2021 (22 pages).

They announced having produced a first q1 chipset sample in April 2021 integrating tens of thousands of single photon sources and detectors¹³⁰⁶. Their physical architecture is using sandwiches assembling a 22 nm CMOS electronic chipset of 750M transistors using superconducting nanowires bonded with 100K connections to a photonic chipset containing thousands of photon sources, detectors and other optical devices. The photonic chipset has 200 optical fiber entries and exits that are used to interconnect similar photonic chipsets together in a distributed architecture manner.

The final PsiQuantum one million physical qubits computer will be made of thousands of computing chips connected together so we can presume each chip is implementing fewer than 1000 physical qubits. The whole system will run at a temperature of 4K, requiring only a pulse tube refrigeration system, that is much simpler than a dilution system for sub 100mK temperatures and with more cooling power. They are also using fiber delay lines as optical memory thanks to its low loss rate. It is mixed with topological fault tolerance codes. This is supposed to multiply by 5000x the number of usable qubits¹³⁰⁷.

To date, PsiQuantum is the best funded startup in the world in quantum computing, even ahead of D-Wave and Rigetti and on par with IonQ and its 2021 SPAC. Originally from the United Kingdom, it moved part of the team to the USA¹³⁰⁸. They even have Microsoft as investors as well as Pascal Cagni's investment fund, C4 Ventures. Their last funding round of \$450M in July 2021 cemented this funding lead. In October 2022, PsiQuantum also got a funding from the US Federal Government through an US Air Force Research Laboratory contract of \$22.5M.

¹³⁰⁵ See [Percolation thresholds for photonic quantum computing](#) by Mihir Pant, 2017 (14 pages). The process is also documented in [Towards practical linear optical quantum computing](#) by Mercedes Gimeno-Segovia, 2015 (226 pages). This was the last publication on the PsiQuantum architecture until when they released [Fusion-based quantum computation](#) by Sara Bartolucci et al, January 2021 (25 pages). See also [QIP2021 Tutorial: Architectures for fault tolerant quantum computing](#) by Naomi Nickerson, January 2021 (3h).

¹³⁰⁶ See [PsiQuantum partners with GLOBALFOUNDRIES to bring up Q1 quantum system](#) by Mercedes Gimeno-Segovia, PsiQuantum, May 2021.

¹³⁰⁷ See [Interleaving: modular architecture for fault-tolerant photonic quantum computing](#) by Hector Bombin et al, 2021 (22 pages).

¹³⁰⁸ See the presentation [Measurement-based fault tolerance beyond foliation](#) by Naomi Nickerson of PsiQuantum in September 2019 and [Quantum Computing With Particles Of Light: A \\$215 Million Gamble](#) by Paul Smith-Goodson, April 2020.



Xanadu (2016, Canada, \$235.6M) is a startup created by Christian Weedbrook, a [prolific researcher](#) having started at MIT and the University of Toronto, among others. The startup is developing a photon qubit quantum computer in the FTQC realm (fault tolerant quantum computer).

In September 2020, they launched a cloud-based testing platform of 8 and 12 qubits. Their qubits are qumodes based on squeezed states using continuous variables encoding¹³⁰⁹. The 8-qubit silicon-nitride chipset is 4mm x 10 mm wide. It's fed by infrared laser pulses and generates "squeezed states" superposing multiple photons, then flowing through an interferometer made of beam splitters and phase shifters performing quantum gates, and exiting to superconducting photon detectors. They don't specify the detailed characteristics of these qubits, particularly in terms of fidelity¹³¹⁰.

In 2021, a team of Xanadu and Canadian researchers published a blueprint with more details on the Xanadu FTQC architecture. It's based on MBQC and three-dimensional resource states comprising both GKP bosonic qubits and squeezed states of light. This hybridization enables the implementation of both Clifford and non-Clifford gates. All of this will be implemented on 2D photonic chipsets¹³¹¹. In August 2021, Xanadu announced that their FTQC silicon-nitride chipsets would be manufactured by IMEC in Belgium. But in March 2022, Xanadu announced a partnership with GlobalFoundries for the manufacturing of their chipset on 300 mm silicon wafers, like PsiQuantum.

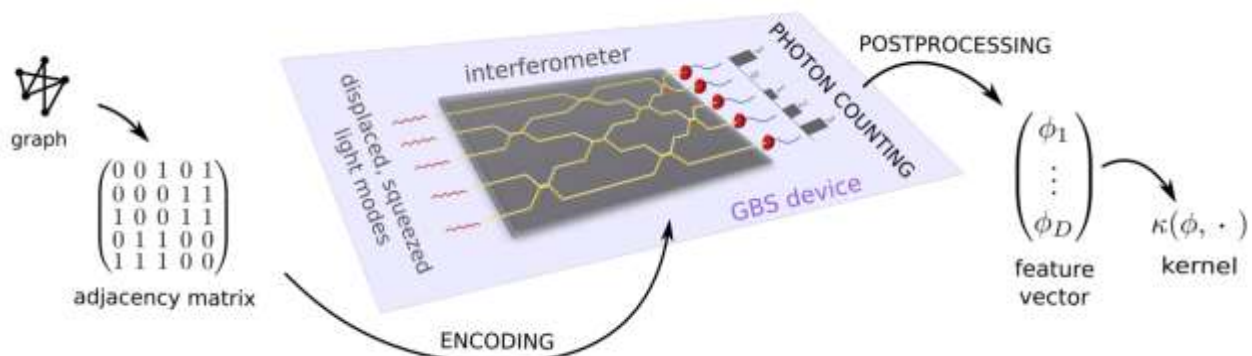


Figure 447: Xanadu's architecture for their 2022 GBS. Source: Xanadu.

In June 2022, Xanadu announced their own "quantum advantage" with their gaussian boson sampling architecture (GBS). Adding to China's 2021 similar performance, they increased the number of handled photon modes to 216 thanks to using frequency multiplexing and delay lines. Their system is programmable with parametrizable photon phases and it was put online on the cloud, seemingly with Amazon Bracket. However, Xanadu was cautious in saying that it didn't yet find use case with some useful quantum advantage¹³¹². Since then, it seems that Xanadu decided not to pursue the path of parametrizable GBS in its photonic computer roadmap.

¹³⁰⁹ Their process is documented in [The power of one qumode for quantum computation](#), 2016 (10 pages) with an example of implementation in [Continuous-variable gate decomposition for the Bose-Hubbard model](#), 2018 (9 pages). See also [Optical hybrid approaches to quantum information](#) by Peter van Loock, 2010 (35 pages). See also [Quantum computing with multidimensional continuous-variable cluster states in a scalable photonic platform](#) by Bo-Han Wu et al, 2020 (22 pages) and the review paper [Quantum computing overview: discrete vs. continuous variable models](#) by Sophie Choe, June 2022 (12 pages).

¹³¹⁰ See [In the Race to Hundreds of Qubits, Photons May Have "Quantum Advantage"](#) by Charles Q. Choi, March 2021.

¹³¹¹ See [Programmable optical quantum computer arrives late, steals the show](#) by Chris Lee, March 2021 referring to [Blueprint for a Scalable Photonic Fault-Tolerant Quantum Computer](#) by J. Eli Bourassa et al, February 2021 (38 pages).

¹³¹² See [Quantum computational advantage with a programmable photonic processor](#) by Lars S. Madsen et al, Xanadu, June 2022 (11 pages) and the earlier and more detailed [Quantum Computational Advantage via High-Dimensional Gaussian Boson Sampling](#) by Abhinav Deshpande et al, February 2021 and January 2022 (24 pages).

Xanadu develops the software platform **Strawberry Fields** and **PennyLane** in Python¹³¹³ (wondering about the inspiration...). It includes the Blackbird language and targets chemistry use cases, graph theory problems and quantum machine learning. All this is distributed in open source.

Their main application is the analysis of similarities between graphs to identify those that are similar and/or separate them into several classes of similarity. Classical methods for solving this kind of problem are similar to finding a matrix determinant¹³¹⁴.

QUANDELA **Quandela** (2017, France, €35M) decided in 2020 to expand its historical single photon source activity to create photon qubits computers as part of their project ROQC (Reconfigurable Optical Quantum Computer).

Their first quantum computer is MosaiQ, which handles 12 photon modes and consumes 1kW. It was first deployed online in November 2022. They first target use cases are certified QRNGs using Bell states with the Entropy solution, hybrid quantum machine learning algorithms and chemical simulations. They announced in October 2022 that their future photonic chipsets will be designed and manufactured by CEA-Leti in Grenoble. Their initial plans is to use a KLM model using Fock states and then, later, a MBQC cluster-states based model. Quandela is always teaming up with Pascale Senellart's C2N research lab. With Fabio Sciarrino's team from Sapienza University in Rome, Italy, they qualified the ability of Quandela's photon source to create entangled states that are used in MBQC computation. They developed an interferometer to assess the indistinguishability of 4 entangled photons generated by their quantum dots source¹³¹⁵.

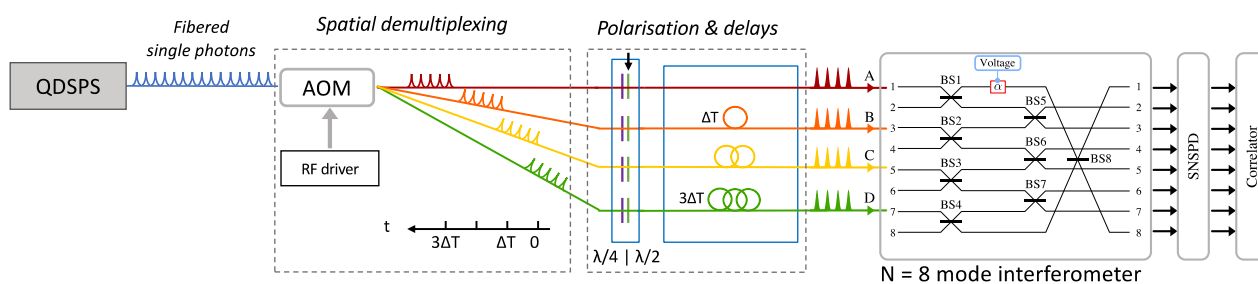


Figure 448: an interferometer used to validate the indistinguishability of a set of generated photons paving the way for the creation of cluster states of entangled photons. Source: [Quantifying n-photon indistinguishability with a cyclic integrated interferometer](#) by Mathias Pont, Fabio Sciarrino, Pascale Senellart, Andrea Crespi et al, PRX, January-September 2022 (21 pages).

In February 2022, Rawad Mezher and Shane Mansfield from Quandela proposed a single-number benchmark metric, the **Photonic Quality Factor** (PQF), defined as the largest number of input photons for which the output statistics pass all tests. It covers photons quantum computing using single photon sources, multi-mode linear optics and photon detectors, including boson sampling experiments¹³¹⁶. In April 2022, Quandela released **Perceval**, their photon qubits physical classical simulation software. It enables the simulation at low level of photonic linear circuits (PBS, ...), help understand how photon qubits work and create adapted algorithms like Grover, Shor, GBS, VQE and QML¹³¹⁷. They later announced that Perceval was proposed in the cloud in partnership with **OVH-cloud** and connector with popular programming frameworks like Qiskit.

¹³¹³ This is documented in [Strawberry Fields: A Software Platform for Photonic Quantum Computing](#), 2018 (25 pages).

¹³¹⁴ See [Measuring the similarity of graphs with a Gaussian Boson Sampler](#) by Maria Schuld et al, 2019 (11 pages).

¹³¹⁵ See [Quantifying n-photon indistinguishability with a cyclic integrated interferometer](#) by Mathias Pont, Fabio Sciarrino, Pascale Senellart, Andrea Crespi et al, PRX, January-September 2022 (21 pages).

¹³¹⁶ See [Assessing the quality of near-term photonic quantum devices](#) by Rawad Mezher and Shane Mansfield, Quandela, February 2022 (30 pages).

¹³¹⁷ See [Perceval: A Software Platform for Discrete Variable Photonic Quantum Computing](#) by Nicolas Heurtel et al, April 2022 (31 pages).



ORCA Computing (2019, UK, \$18.7M including some UK public funding) is developing a quantum computing platform based on qumodes photons and a proprietary photonic memory using delay lines plus programmable beam splitters¹³¹⁸. They currently use photon frequency multiplexing (PT-series) and plan to later add time and space multiplexing (PA-Series). Their chipset is manufactured by **Ligentec** in Switzerland.

The startup was cofounded by Richard Murray (CEO, former head of the UK quantum program), Josh Nunn (CTO, former Oxford University, and also working with VeriQloud) and Cristina Escoda (COO), an entrepreneur with a background in finance and deep tech¹³¹⁹. The startup leverages research done by Ian Walmsley's Ultra-fast and Nonlinear Quantum Optics Group from the University of Oxford.

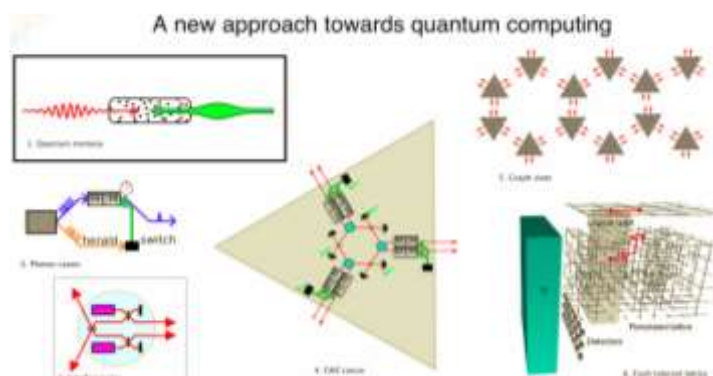


Figure 449: Orca's view of quantum computing. Source: Orca Computing.

In June 2022, the UK Minister of Defense announced the procurement of Orca's PT-1 quantum computer, which fits into a single rack and manages 8 qumodes. They plan to support 128 qumodes by 2024. Quantonation is among their investors. It supports machine learning and QUBO algorithms with their Python software library, seemingly¹³²⁰. Orca also sold a PT-1 QPU to Israel's Quantum Computing Centre managed by Quantum Machines in July 2022.



TundraSystems (2014, UK) is developing a linear optics quantum processor operating supposedly at room temperature. They seem to create a photonic microprocessor and not necessarily, a quantum computer with qubits using linear optics.

Their Advisory Board includes two Chinese scientists, Xinliang Zhang and Pochi Yeh who are specialized in optonics ([site](#)).



QuiX Quantum (2019, Netherlands, 5.5M€) is developing a photonic quantum processor using silicon nitrides (Si_3N_4) TriPlex waveguides generating low losses. It came out of a project from the University of Twente and the AMOLF laboratory in Amsterdam. The company is a subsidiary of the fab Li-onix.

Their fab also provides photonic components to other industry vendors, like Quandela. They presented in 2021 a record 12x12 programmable photonic processor. It uses thermo-optic phase shifters and tunable beam splitters. The circuit is labelled a 12x12 because it has 12 input photons and a depth of 12 quantum gates¹³²¹.

¹³¹⁸ See [One-Way Quantum Computing in the Optical Frequency Comb](#) by Nicolas C. Menicucci, Steven T. Flammia and Olivier Pfister, April 2018 (4 pages) and [High-speed noise-free optical quantum memory](#) by K. T. Kaczmarek et al, April 2018 (12 pages).

¹³¹⁹ See some details on their approach in [Photonic quantum processors](#), Orca Computing, April 2020 (27 slides).

¹³²⁰ See [Certain properties and applications of shallow bosonic circuits](#) by Kamil Bradler and Hugo Wallner, December 2021 (34 pages).

¹³²¹ See [A 12-mode Universal Photonic Processor for Quantum Information Processing](#) by Caterina Taballione et al, 2020 (11 pages).

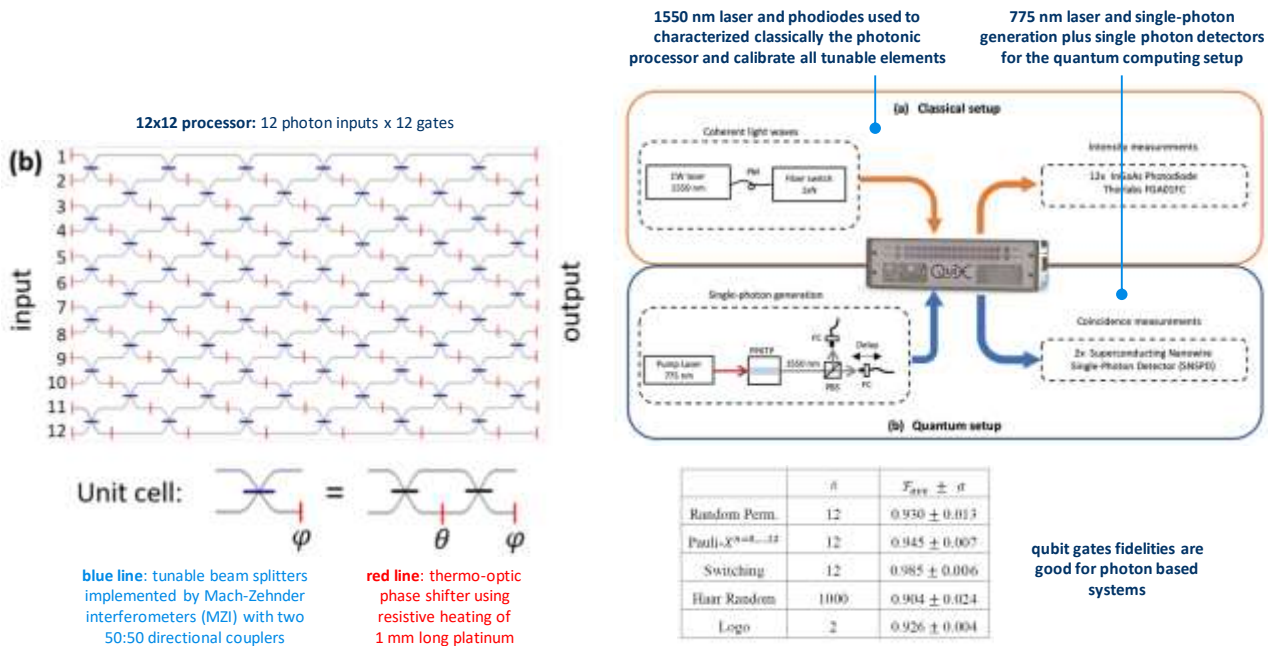


Figure 450: a QuiX circuit handling 12x12 photons (12 photons and 12 quantum gate depth using MZIs). Source: [A 12-mode Universal Photonic Processor for Quantum Information Processing](#) by Caterina Taballione et al, 2020 (11 pages).

In March 2022, QuiX announced the “world’s largest photonic quantum processor” expanding the previous 2021 performance from 12 to 20 “qumodes”¹³²². It contains 380 thermo-optic tunable elements and a photon source made of a Ti:Sapphire laser pumping a crystal. QuiX is now teaming up with PHIX (The Netherlands), an assembly subcontractor, to create an even larger quantum photonic processor with 50 qumodes, using over a hundred optical fiber connections and about 5000 electrical connections. In September 2022, the company signed a 14M€ contract with DLR, the German Aerospace Center, to build a 64-qubit quantum computer. The company plans to build a 10K qumodes system after 2030.

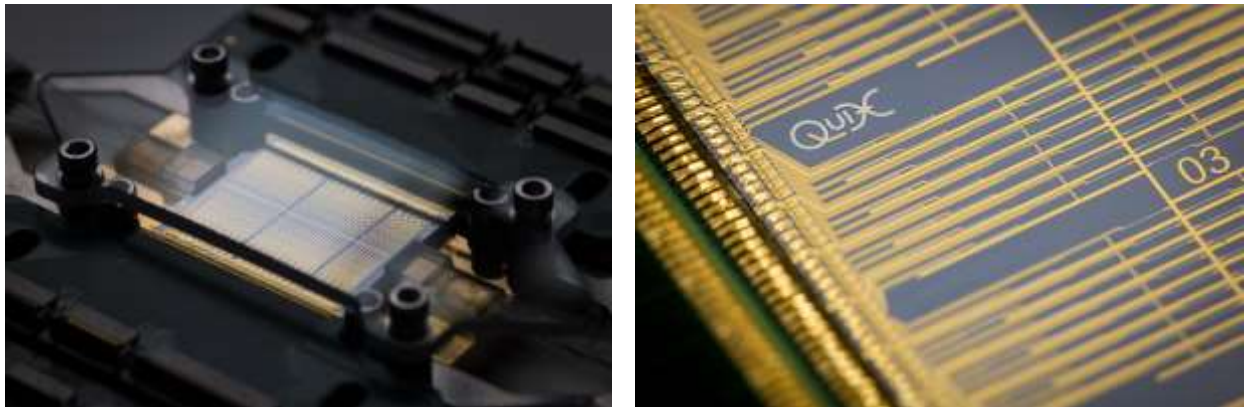


Figure 451: QuiX photonic processor. Source: QuiX.



QBoson (2020, China, \$3M) aka “Bose Quantum” was founded by Wen Kai in Chaoyang (200 km North-East of Beijing), who studied at Tsinghua University and later got a PhD from Stanford in quantum computing.

He also worked at Google AI in the USA. The company is creating photon-based quantum computers with, in sights, a hybrid AI applications approach.

¹³²² See [20-Mode Universal Quantum Photonic Processor](#) by Caterina Taballione, June 2022 (9 pages).

They claim to have completed the construction of a laboratory and of a 1,000 photon-based qubit quantum computer with a plan to reach 1 million-qubits in 3 to 4 years. The first part is probably a little oversold even if the second part is not far from PsiQuantum promises¹³²³. Another promise is that this computer works at ambient temperature, which is a highly dubious claim since you generally need some form of cooling for your light sources and photon detectors. On the left, the only visual of the laboratory that was inaugurated in July 2021 ([source](#))!



Figure 452: openness in China. You see the folks looking at the window of a lab. Go guess what they saw and understood!

I finally found out in August 2022 that they are working on some sort of coherent Ising machines using spiking neurons in an arXiv paper¹³²⁴.



Duality Quantum Photonics (2020, UK) is a Bristol-based startup created in February 2020. Its founder is Anthony Laing, from the Department of Physics at the University of Bristol where he developed a quantum simulator based on lithium niobate generated photons.

He targets drugs design for the pharmaceutical industry. They were supposed to create a prototype in 2021.



TuringQ (2021, China, \$79M) creates lithium niobate on insulator (LNOI) optical quantum computer chips and femtosecond lasers. Not to be confused with Turing Quantum (USA) who is specialized in NV centers computing and Turing (USA) who develops quantum software.



Quantum Computing Inc. (aka QCI), also covered in the software vendors section, announced in February 2022 a “*business partnership and exclusive marketing agreement with QPhoton, Inc*”.

In the current newspeak, it simply means an [acquisition](#)! QPhoton (USA) was a stealth quantum photonics computing and sensing company based in New Jersey. They hold a portfolio of patents on quantum hardware, authentication protocols, simulators, photonic Lidar, imaging and covert communications. They were mostly a contract research company working for DARPA, DoD, NASA and other US federal agencies who spent \$30M on these projects. The company was created and headed by Yuping Huang, a professor from Northwestern University (Evanston, Illinois) and the Stevens Institute of Technology (Hoboken, New Jersey).



Figure 453: QCI photonic quantum computer package. Source: QCI.

¹³²³ Wen Kais thesis is [Experimental study of tune-out wavelengths for spin-dependent optical lattice](#) in ⁸⁷Rb Bose-Einstein condensation by Kai Wen et al, September 2021 (9 pages). It relates to cold atoms qubits, not photons. But QBoson’s communication is about photonic qubits controlled by lasers ([source](#)). All in all, one thing is sure: these guys don’t want you to know what they are doing exactly.

¹³²⁴ See [Combinatorial optimization solving by coherent Ising machines based on spiking neural networks](#) by Bo Lu et al, August 2022 (6 pages).

How about their Quantum Photonic System (QPS)? It's a nonlinear system. That's all you need to know from them at this point!

QCI announced in July 2022 having solved a combinatorial problem with 3,854 variables with its "Entropy Quantum Computing" (EQC) hardware that was running 70x faster than QCI's 2021 hybrid DWave implementation¹³²⁵. We can suspect it is based on some form of photonic coherent Ising model and on QPhoton QPS architecture. In September 2022, its Dirac 1 Entropy Quantum Computer (EQC) was launched as a cloud-based subscription.

It'sQ

It'sQ (2022, Germany) is a photonic qubits startup created by Christine Silberhorn from the Institute for Photonic Quantum Systems (PhoQS) of the University of Paderborn.

The company is based on her research on frequency multiplexed qubits ("field-orthogonal temporal modes"), including the related pulsed photon pairs sources, and MBQC as well as quantum walks¹³²⁶, using LiNbO₃ on silicon oxide insulator circuits (lithium niobate). Christine Silberhorn is also investigating GBS (gaussian boson sampling) avenues as part of the German project PhoQuant led by Q.ANT. Quantonation is one of It's Q seed investors.



Quantum Source Labs (2022, Israel, \$15M) is a photonic computer startup created by Oded Melamed (CEO), Gil Semo (R&D VP), Dan Charash (Chairman) and Barak Dayan (Chief Scientist, Associate Professor at the Weizmann Institute of Science, head of the Weizmann Quantum Optics group).

Likewise to It's Q, there's not much data available on what they are doing. They seem to run some contract research programs and among others, work with PsiQuantum. Given their founders background, you can infer that they have skills in designing photon guides in nanophotonic circuits, qubit conversions, nanofibers, MBQC and photon detection.

LightOn (France) announced a quantum photonic processor in 2021. It implements 8 input quantum states onto 19 distinct optical railings, performing 19x19 unitary linear operations with up to 8 entangled photons at minimal loss and a reconfigurability rate of 10Hz. This is based on using multimode fibers. It must be further documented to be fairly evaluated¹³²⁷.



Hewlett Packard Enterprise

HP conducted research in quantum computing at its Bristol laboratory, UK, covering quantum computing, cryptography and quantum communications. They invested in "The Machine", conceptually far from a universal quantum computer and uses an optical bus to link the different components of a super-computer.

In partnership with HP, American and Japanese scientists proposed in 2008 the creation of an HPQC, High Performance Quantum Computer, with 3D qubit arrays realized in linear optics containing 7.5 billion physical qubits allowing to accumulate 2.5 million logical qubits¹³²⁸. This project was left aside. HPE abandoned quantum computing entirely and explained it in 2019. They said they preferred to focus on neuromorphic processors and memristors¹³²⁹.

¹³²⁵ See [QCI Solves 3,854-Variable Problem in Six Minutes in BMW Group, AWS Quantum Computing Challenge](#) by Matt Swayne, The Quantum Insider, July 2022.

¹³²⁶ See for example [Fabrication limits of waveguides in nonlinear crystals and their impact on quantum optics applications](#) by Matteo Santandrea, Michael Stefszky, Vahid Ansari and Christine Silberhorn, March 2019 (16 pages).

¹³²⁷ See [LightOn Qore, a novel Quantum Photonic Processor](#), June 2021 (2 pages).

¹³²⁸ See [High performance quantum computing](#) (7 pages).

¹³²⁹ See [Why HPE abandoned quantum computing research](#) by Nicole Hemsöth, April 2019.

Their photonics specialist is **Ray Beausoleil**, based in Silicon Valley. He was specialized in photonics and NV centers and abandoned this track, becoming a quantum computing skeptic. Somewhat along the lines of Gil Kalai, he believes that errors would increase faster than the growth in the number of qubits. Still, HPE invested in **IonQ** in October 2019 to show that it didn't entirely leave the quantum stage.

Quantum computing hardware key takeaways

- Superconducting qubits are the most common nowadays, implemented by IBM, Google and Rigetti among others. But they are noisy and do not scale well. One solution may be cat-qubits which combine trapped microwave photons in cavities and superconducting qubits for their manipulation and readout (Alice&Bob and Amazon).
- Quantum dots spin qubits could scale well due to their small size, the reuse of classical CMOS semiconductors manufacturing known-how, their higher working temperature enabling the usage of control cryo-electronics. They have however been demonstrated at a relatively low scale at this stage.
- NV centers qubits have the benefit to be stable and to work potentially at ambient temperature but there are not many vendors involved there, besides Quantum Brilliance (Australia and Germany).
- Topological qubits could bring the benefit of being resilient to some quantum errors and to scale better than other solid-state qubits. It doesn't really exist yet, particularly the Majorana fermions species looked after by Microsoft.
- Trapped ions qubits have the best fidelities so far, but they are hard to scale beyond about 40 qubits, at least with their main vendor, IonQ, Quantinuum and AQT.
- Cold atoms qubits are mostly used in quantum simulation where it could scale up to a thousand qubit and it could potentially also be used in gate-based quantum computing although it's not really demonstrated at a large scale. Pasqal (France), Cold Quanta (USA), QuEra (USA) and Atoms Computing (USA) are the industry vendors in this field.
- Photon qubits are flying qubits, moving from a source to detectors and traversing optical devices implementing quantum gates. There are many investigated techniques, with the distinction between single/discrete variable photons and continuous variable photons. Scalability is also an issue, particularly with photon sources and the probabilistic nature of photons generation. Their limited quantum gates computing depth requires the implementation of specific computing techniques like MBQC and FBQC, this last one being used by PsiQuantum, the best funded quantum computing startup with IonQ as of 2022. Quandela (France), Xanadu (Canada) and Orca (UK) are other key players in that space. One key capability to implement MBQC is the generation of high volume cluster states of entangled photons.

Quantum enabling technologies

Building a quantum computer and other second quantum revolution related products involve assembling a lot of various technologies, some being classical and others quantum-related themselves. This part of this book is dedicated to these various important enabling technologies. These are “enabling” in a sense that their characteristics and performances frequently have a direct impact on the performance and scalability, particularly with quantum computing. We’ll see this with cryogenics, cabling, classical electronics, lasers and photonics.

We’ll also look at the raw materials needed in quantum technologies, where it comes from, is it rare or not and how is it transformed. At last, we’ll have a look at other unconventional computing technologies. They can both compete and, in some cases, complete quantum computers. Whatever happens, this competition is also enabling innovation.



Figure 454: a market map of key enabling technology vendors. (cc) Olivier Ezratty, 2022.

Cryogenics

Cryogenics is an important enabling technology used with most types of qubits, the most demanding being the very low operating temperatures of superconducting qubits, at 15 mK. Other technologies like photon qubits require lightweight cryogenics operating at 4K to 10K for their photon sources and detectors¹³³⁰. Detectors must be cooled to avoid the photon dark count effect, when thermal noise originated photons are detected instead of useful photons.

In this part, we’ll focus on the 15mK dry dilution refrigeration systems used by superconducting qubits.

¹³³⁰ By definition, cryogenics operates below 123K or -150°C. Bearing in mind that -153.15°C is the temperature below which permanent gases, i.e. gases in the ambient air, all condense into liquid at ambient pressure.

These qubits must be cooled to this low temperature to avoid noise sources from the environment, particularly when compared with the microwave pulses used to control qubits and handle their readout¹³³¹.

These are the most complicated systems and also, those requiring some scalability in cooling power to accommodate the growth in number of physical qubits.

Wet and dry dilution refrigeration

Superconducting quantum computer from IBM, Google and others are frequently presented with these mysterious gold chandeliers where the processor is housed, surrounded by an unlikely set of wires, devices and several layers of circular plates. This system is a mix of passive and active control electronics reaching the qubits processor and low temperature cooling system¹³³². The chipset must be as isolated as possible in terms of temperature, magnetism, vacuum and even mechanical vibrations.

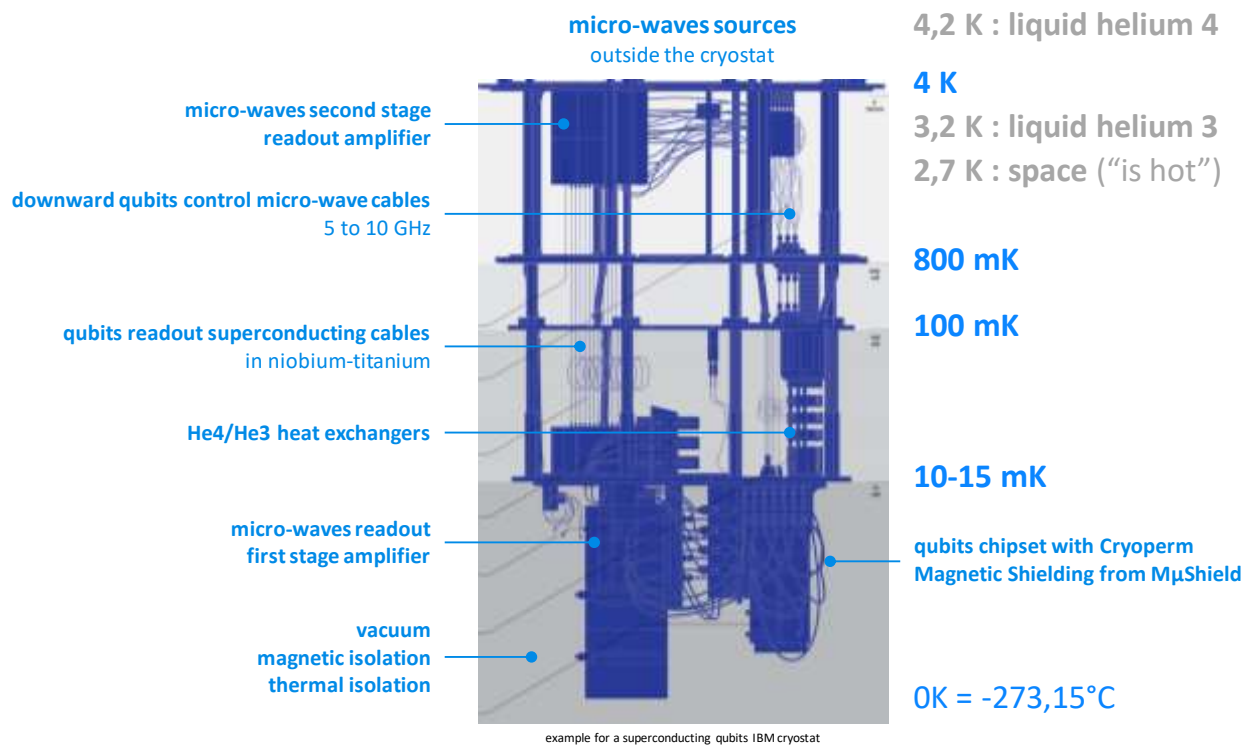


Figure 455: a documented interior of an IBM superconducting qubit cryostat. Image source: [Quantum Computers Strive to Break Out of the Lab](#), 2018. Legends by Olivier Ezratty.

The refrigerated part of a quantum computer with superconducting qubits or silicon is generally organized in stages, knowing that the lower you go down in the stages, the colder it gets:

- On the upper level, a plate that is not usually seen in diagrams and picture is thermalized at 50K. This is where both the electronic cables for controlling and reading the qubits as well as the fluids used for refrigeration arrive in the cryostat.

¹³³¹ It is governed by the equation $k_B T < \hbar \omega$. The Boltzmann constant multiplied by the temperature must be inferior to the product of the Dirac constant and the microwaves frequency in Hz. This leads us to adopt a temperature of about 15 mK for superconducting qubits.

¹³³² A tour of the IBM Q Lab is available in the 2016 video [A Tour of an IBM Q Lab](#).

- One level below, running at 4K, i.e. 4°C above absolute zero (273.15°C)¹³³³. That's where sits the lower part of the so-called pulse tube.
- The below plate is at around 800 mK. Between these two floors is the lowest temperature in space, which is 2.7 K and also corresponds to the cosmic background radiation.
- Another plate is generally located at a temperature of 100 mK.
- The lowest stage plate is where the quantum processor sits, and is cooled between 10 and 25mK, usually around 15mK. It is also called the "mixing chamber cold plate". A cold plate is a one-stage copper plate and the mixing chamber is the last level at the bottom of the dilution refrigeration system that we will explore later¹³³⁴.

We will now study the detailed characteristics of the very low temperature cryogenics used in these superconducting quantum computers¹³³⁵.

It uses a **dilution refrigeration**, which is based on the association of two helium isotopes: helium 4 and helium 3, which have different and complementary physical properties¹³³⁶. They have respectively a boiling temperature of 4.2K and 3.2K. Helium 4 is superfluid at 2.17K while helium 3 is superfluid at a much lower temperature of 2.5 mK, at ambient pressure. The cryostat exploits the combination of three phases: a gaseous ³He phase and two liquid phases, one with ³He and the other with a mixture of ³He and ⁴He, with evaporation of the ³He in a mixed chamber¹³³⁷. Let's explain first why helium is so important for low temperature cryogenics. Hydrogen becomes liquid at 20.3K¹³³⁸, nitrogen at 77.4K and oxygen at 90.2K. These gases are useless for low temperature cryogenics.

On the other hand, ⁴He liquefies at 4.2K at room temperature and a ⁴He cryostat can reach 1K while ³He cryostats can go as low as 300 mK. The mix of ⁴He and ³He is used in so called dilution refrigerators reaching 15 mK¹³³⁹. Note the low density of ⁴He which is 125g/L at 4.2K. There are two types of dilution refrigerators: "dry" and "wet".

¹³³³ The Kelvin scale starts at absolute zero. This temperature where atoms literally no longer move is unreachable. If it were, Heisenberg indeterminacy would be broken! It is approached asymptotically. The lowest temperature record is 38 pK (pico-kelvin), reached in 2021. See [Collective-Mode Enhanced Matter-Wave Optics](#) by Christian Deppner, David Guéry-Odelin, Ernst M. Rasel et al, PRL, August 2021 (7 pages). See how fast these records have been broken over the last decades in [Moore's Law for Low Temperature Physics](#) by Pramodh Senarath Yapa, December 2021.

¹³³⁴ In [Top 5 Trends in Quantum Technologies to Look for in 2020](#) by QuantumXchange, January 2020, we find: "Interestingly, IBM and Google are taking different approaches in the infrastructure of quantum computers. IBM's hardware resembles a chandelier with rings whereas the Google device looks like a chip". Which shows that they did not understand at all that IBM and Google had both a candlestick and a chipset. So they did not explore the hardware architecture of a superconducting quantum computer!

¹³³⁵ See [Cryostats Design ⁴He and ³He cryostats](#) by Guillaume Donnier-Valentin, CNRS Institut Néel, 2011 (91 slides), [Some Fundamentals of Cryogenic and Module Engineering with regard to SRF Technology](#), Bend Petersen, ESY Cryogenic Group MKS (95 slides) and [Development of Helium-3 Compressors and Integration Test of Closed-Cycle Dilution Refrigerator System](#), 2016 (5 pages).

¹³³⁶ Helium was discovered indirectly in 1868 through the discovery of an unexplained spectral line in the light spectrum of the sun by astronomers Pierre Jules Janssen (1827-1907, France) and Joseph Norman Lockyer (1836-1920, United Kingdom). It was then isolated for the first time in 1895 by the Scottish chemist William Ramsay (1852-1916).

¹³³⁷ See the video [Quantum Cooling to \(Near\) Absolute Zero](#) by Andrea Morello of UNSW which explains very well how dilutions work, 2013 (10 minutes). This illustration is inspired from a schema seen in inspired by [Cryostat design below 1K](#) par Viktor Tsepelin, October 2018. Bcc means body-centered cubic and hcp, hexagonal close-packed. These are two states of solid helium which are of no interest in dilution refrigerators. A phase diagram shows the phase of the element as a function of temperature (in X in logarithmic scale) and pressure conditions (in Y, 1 bar = atmospheric pressure). It shows that in the regime used below 1K, helium 3 is liquid and helium 4 is superfluid. This difference makes it possible to operate refrigeration at these low temperatures.

¹³³⁸ Liquid hydrogen cryogenics uses spin variations of hydrogen, instead of isotopic ones. H₂ molecule exists in two forms, with both hydrogen atoms having the same spin (orthohydrogen) or an opposite spin (parahydrogen). At 300K, the ratio is 75% orthohydrogen and 25% parahydrogen. At low temperature, the ratio is different and the conversion between orthohydrogen and parahydrogen is exothermic, used in the refrigeration process.

¹³³⁹ The first liquefaction of helium was achieved in 1908 in Leyden, Netherlands, by Kamerlingh Onnes. The dilution cryostat concept was proposed by Heinz London in 1951 and was tested in 1965 at the University of Leiden, when it reached 220 mK. The record temperature went down to 60 mK in 1972 and then to 1.75 mK in 1999.

In **wet dilution refrigerators**, a first system cools the enclosure to 4K with liquid ^4He . A second so-called dilution system uses a mixture of liquid ^4He and ^3He with a flow circulating in ducts connecting the metal plates down to less than 15 mK in the bottom stage.

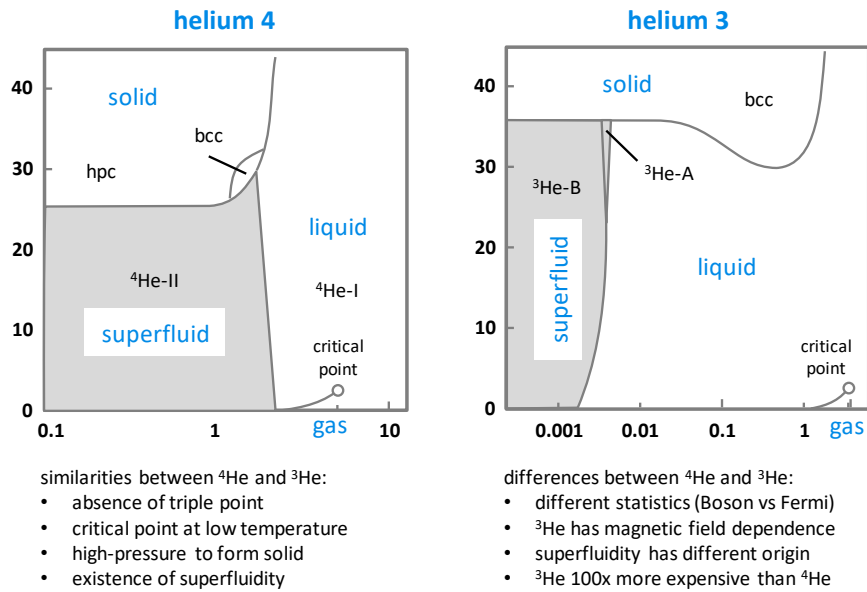


Figure 456: phase differences between helium 3 and helium 4. Source: [Cryostat design below 1K](#) by Viktor Tsepelin, October 2018 (61 slides).

Wet dilutions system was used until the early 2000s. It was then replaced by dry dilution systems that are simpler to operate, especially to create quantum computers that are easy to install at customer sites, thanks to avoiding liquid helium. However, wet dilution systems are still used for various physics experiments where the dry system is not appropriate, but usually not for quantum computing.

wet dilution refrigeration

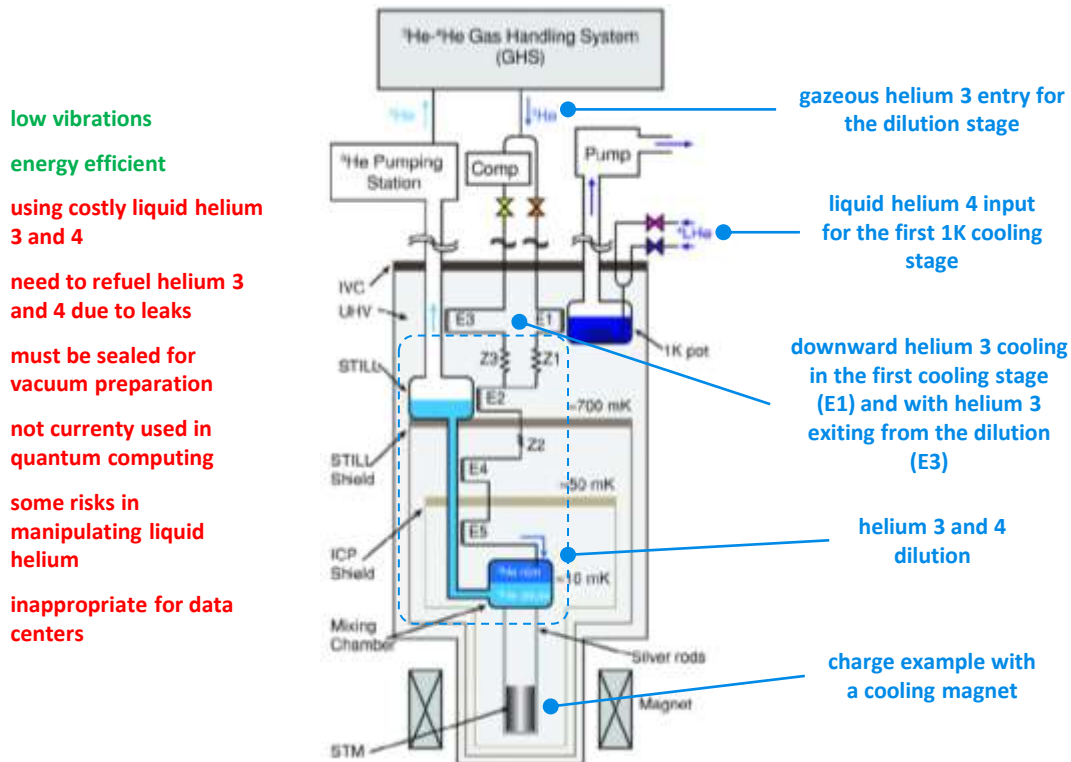


Figure 457: wet dilution refrigerator operations. Schema from Source: [Cryostat design below 1K](#) by Viktor Tsepelin, October 2018 (61 slides) and legends from Olivier Ezratty, 2020.

One interesting breed of wet dilution cryostats are inverted dilution refrigerators (IDR). I saw many of them at CNRS Institut Néel in Grenoble which has a dedicated cryogeny lab crafting custom cryostats for various use cases, including for astronomy. These inverted cryostats enable fast and easy experiment samples loading and fast cooling as well. Below is an example IDR from Nicolas Roch's laboratory at Institut Néel.

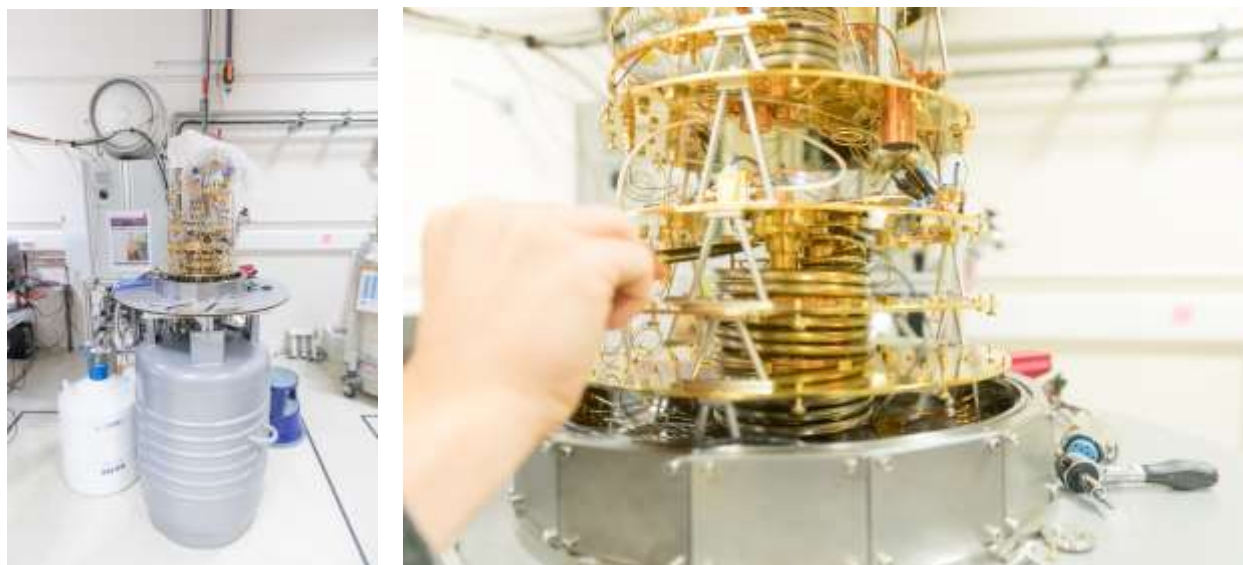


Figure 458: custom made bottom-up cryostats made at CNRS Institut Néel in Grenoble. Pictures source: Olivier Ezratty.

While most cryostats for quantum computers use dry dilutions, Fermilab is currently putting the final touch on an impressive wet dilution system developed to house a 3D supercomputing system, probably co-developed with Rigetti. Its numbers are impressive: it's got 625W of cooling power at 4.5 K. 50W at 2K and, above all, 300 μ W at 20 mK for a load fitting in a 2m wide cylinder. And it's using 2000 liters of liquid helium¹³⁴⁰. What is interesting here is that 625K cooling power at 4.5K could have another application: superconducting (non-quantum) computing.

Dry dilution refrigerators or so-called cryogen-free refrigerators do not use liquid helium. They are using only gaseous helium 3 and 4. Like wet systems, they have two stages: the lower dilution stage is about the same with controlled expansion of helium 3 which is bathed at the bottom in liquid helium 4 in a dilution chamber. This covers cooling to temperatures lower than 1K.

The upper stage relies on the pulsed tube technique that manages cryogenics down to about 2.8K with helium 4 gas and a large external water-cooled compressor. This technique has been mastered for about twenty years and has been progressing incrementally since then. Its arrival coincides with the first experiments with superconducting qubits. Dry dilution refrigerators are generally used for the cryogenics of qubits requiring to go below 1K. The schematic in Figure 459 explains how it works.

The pulsed tube is associated with a **Stirling** or **Gifford-McMahon** type compression and expansion system. The latter seems to be the most frequently used, particularly at **CryoMech**. It uses a piston. Stirling engines are used to cool infrared devices but not in dilution systems.

It can be seen in the curve on the right of Figure 461 that the available cooling power decreases rapidly with temperature. It is currently around 1W at 4K¹³⁴¹. There are no moving mechanical parts inside the cryostat, both in the pulse tube and in the dilution.

¹³⁴⁰ See [A large millikelvin platform at Fermilab for quantum computing applications](#) by Matthew Hollister, Ram Dhuley and Grzegorz Tatkowski, Fermilab, August 2021 (10 pages).

¹³⁴¹ With larger liquid helium cryogenic installations like Helial SF from Air Liquide, a cooling power of 100W to 1kW can be generated at 4K.

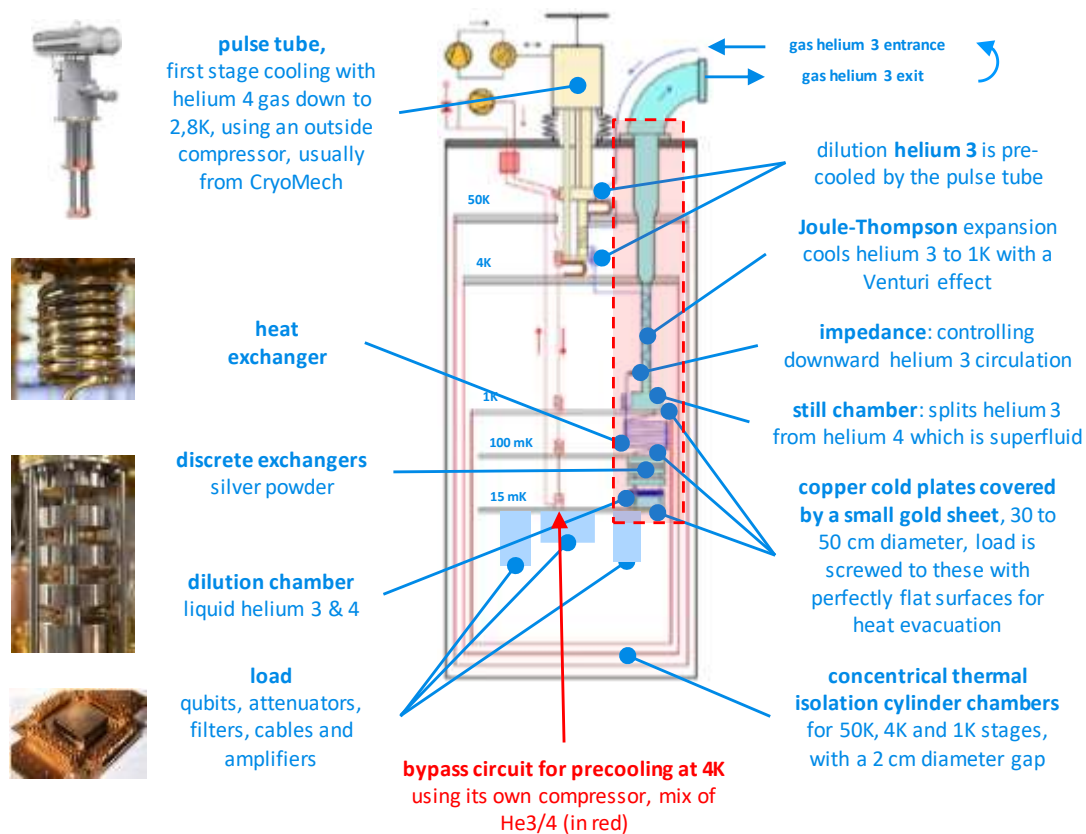


Figure 459: dry dilution schematic inspired from [Cryostat design below 1K](#) by Viktor Tsepelin, October 2018 (61 slides), illustrations from CryoMech documentation, Janis, [Dry dilution refrigerator with 4He-1K-loop](#) by Kurt Uhlig, 2014 (16 pages) and IBM.

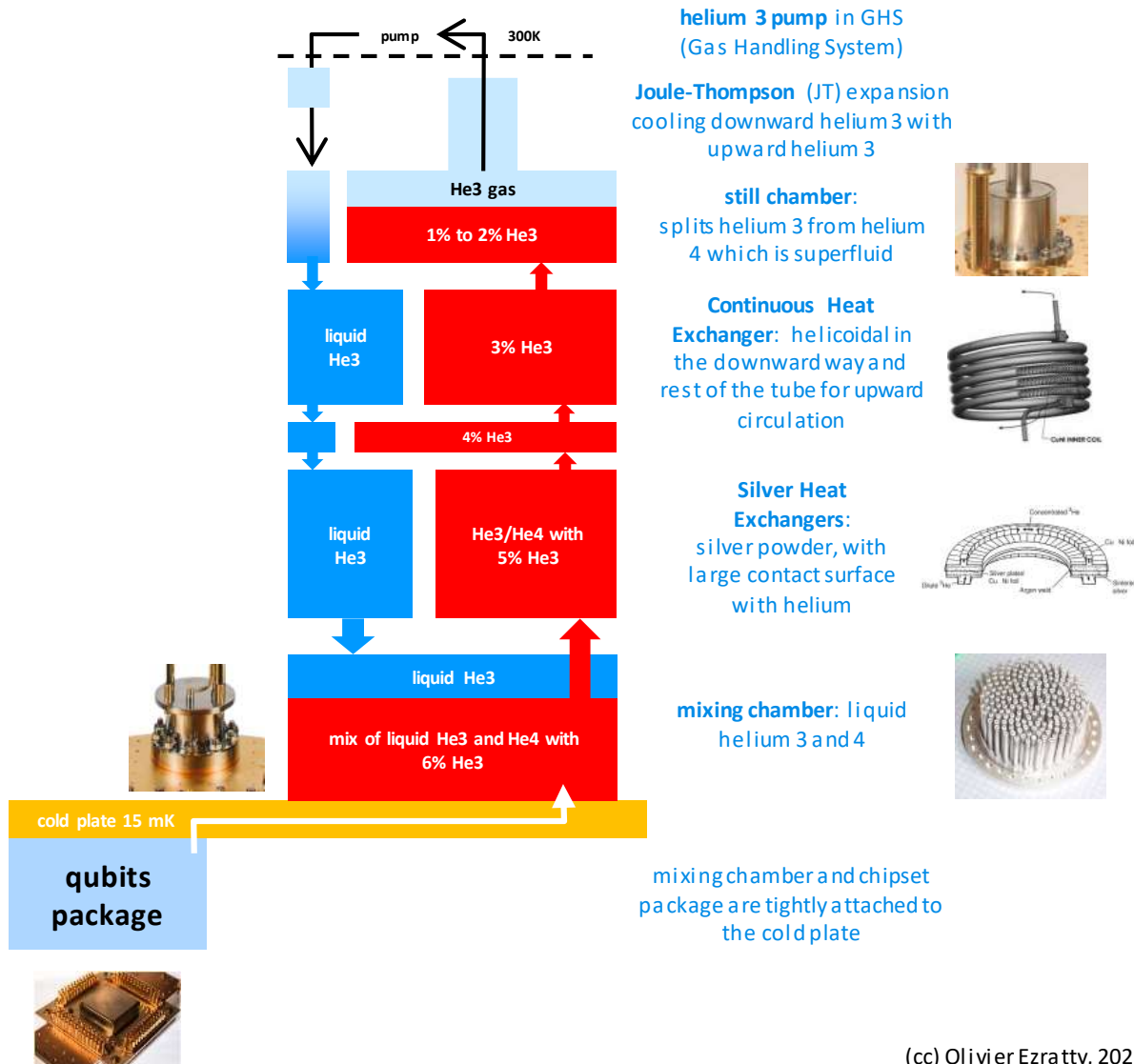
This avoids the generation of unwanted vibrations that could disturb the wiring and the qubits which are very sensitive beasts. The flow of gases and liquids produces very little disturbance in the dilution process.

A refrigeration system is often evaluated in % of the Carnot cycle. This cycle describes a perfect thermodynamic cycle using four perfectly reversible thermodynamic processes involving work-heat exchange¹³⁴². The efficiency of a thermal machine is never perfect with 100% of this cycle.

For a pulsed tube, a perfect Carnot efficiency would be about 1.4%, i.e. it would take 70W of energy to extract 1W at 4.2K¹³⁴³! In practice, it requires about 10 kW, i.e. 152 times more! We thus obtain a **Carnot efficiency** of less than 1%. That's <1% of 1.4%! Indeed, we spend more than 10 kW to get 1W of power at 4.2K. So... at 15 mK to get 10 μ W? We do not evaluate the efficiency of the 15 mK stage of Carnot because it operates isobarically, i.e., at constant pressure, the thermal cycle being linked to a phase variation of helium 3. This stage is powered by heat exchanges between the pulsed tube and the helium 3 gas circuit.

¹³⁴² See Cryogenic Systems by Pete Knudsen, 2018 (71 slides) which describes well the Carnot cycle principle.

¹³⁴³ See [Lecture 5 Refrigeration & Liquefaction \(Part 1\)](#) by J. G. Weisend II (17 slides).



(cc) Olivier Ezratty, 2021

Figure 460: details of the dilution inner working and the phases of helium 3 and 4 that are used. (cc) Olivier Ezratty, 2021.

There is a circuit, shown in red in Figure 460, that is used to pre-cool the cryostat in the thermalization preparation. This is done in three steps: first, by starting the pulse tube which cools the 50K and 4K stages with helium 4 gas and the external compressor of about 12 kW¹³⁴⁴ (in yellow in the diagram). Then by using the pre-cooling circuit which will circulate a helium 3 and 4 mixture to the lower stages, and which will have been cooled by the pulse tube, in the circuit in red in the diagram.

Finally, the dilution system takes over from the second one and is launched to be able to go down to 15 mK in the lower cold plate (in light blue in the diagram).

By adopting a rocket analogy, the pulsed tube and its 7 to 12 kW compressor are the equivalent of the first stage of a Saturn V rocket. The pre-cooling system is the analogue of the rocket second stage and the dilution system is the equivalent of the third stage that sends the lunar module and the LEM to the moon, here, the chipset. Extracting the Earth's gravity over a large mass is equivalent to cooling a large metal mass inside the cryostat to 50K and 4K. While the dilution system is responsible for cooling a smaller mass from 4K to 15 mK, the lower cold plate and the payload attached to it.

¹³⁴⁴ At CryoMech, the compressors adapted to these dilution systems consume from 7.9 to 12kW; from PT410 to PT420. About 4kW must be added for the GHS (Gas Handling System) which manages the dilution circuits with their pumps and controls as well as for the computer and the assembly dashboard.

Pulse Tube Cryocoolers

- Two general types
 - Stirling type
 - High frequency = 60 Hz
 - High efficiency: 25% of Carnot
 - Operation down to 10 K
 - GM type
 - Low frequency = 1-2 Hz
 - Split design = very low vibration
 - Ideal for 4 K operation (< 1 watt)

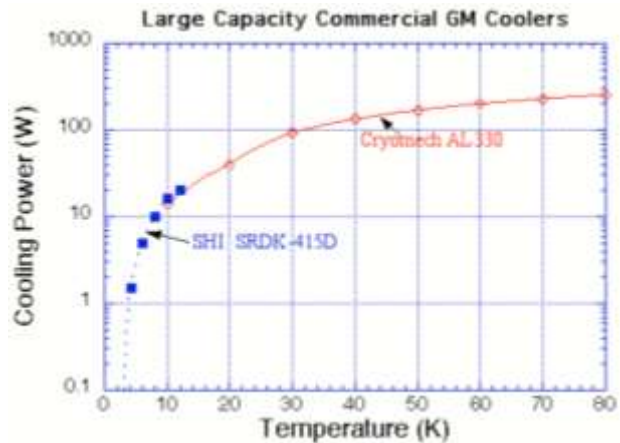
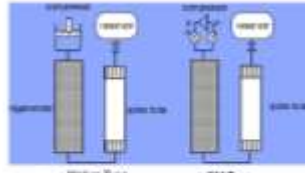


Figure 461: pulse tubes models with Stirling and Gifford-McMahon types. And commercial capacities available. Source: [Lecture 2.2 Cryocoolers](#), University of Wisconsin (25 slides).

These systems require optimization with a large number of parameters. The modeling of a cryostat could one day benefit from quantum computation, especially since the fluids used are in a superfluid quantum state.

A good part of the power is used to lower the temperature to 1K, because the mass to be cooled is the most important. The cylinder that protects the part cooled at 4K receives the thermal radiation from the part at 50K. This makes a big thermal difference to absorb.

In a cryostat of about 16 kW, only about one third of this power is used in the dilution system, which is used to lower to 15 mK. It corresponds to the pumps in the GHS, the Gas Handling System, which contains all the pumps and gas circuits outside the cryostat, and to the share of the energy spent in the pulse tube to cool the dilution system.

The dilution system does not use a compressor. The helium 3 circulating outside is just driven by a pump located in the GHS. The reason is that the helium 3 that returns to the cryostat is cooled by the pulse tube. In practice, all the cryostat heat is evacuated by the compressor of the pulse head which is itself cooled by water.

The above diagram in Figure 460 details the operation of the dilution system as well as the phase (liquid or gaseous) and the concentration of helium 3 and 4 in each stage and component. It shows the descending circuit of helium 3 which becomes liquid from the condensation at the boiler.

In the circuit going up from the mixing chamber, a liquid mixture of helium 3 and 4 rises and the concentration of helium 3 goes down as the stages go up. It is only in the boiler that helium 3 becomes gaseous. Helium 4 remains liquid and is evacuated downwards. It has moreover a tendency to rise due to superfluidity. A trick is to cut this rising film and send helium 4 back down.

The helium 3 landing in the dilution chamber at the bottom must end up there at a temperature barely above 1mK of the chamber temperature. It is pre-cooled by the helium 3 that is moving upward. The only way to achieve this is to increase the contact surfaces, which is done in the discrete heat exchangers just below the cold plate at the 100 mK level.

These dry cryostats still use a cryogen, liquid nitrogen at 77K, to filter helium gas and remove impurities¹³⁴⁵. This filtration is based on zeolite powder, made of microporous aluminosilicate crystals.

¹³⁴⁵ LN₂ for liquid nitrogen, gaseous nitrogen being a molecule of two nitrogen atoms.

The liquid nitrogen tank used for this pre-cooling is called a "cold trap"¹³⁴⁶. This filtering is completed in the cryostat 4K stage by another filtering system based on activated carbon powder which works better at low temperatures and increases the contact surfaces with the gas to better filter it.

As a general rule, the complete thermalization of a quantum computing cryostat takes about 24 hours. The so-called "1K" stage was actually cooled at about 1.2K in wet cryogenics and is around 800 mK for dry cryogenics. The power consumption is identical between the thermalization phase and the temperature maintenance of the instruments once the thermalization is completed.

Cryogenics at 10-20 mK is specific to quantum computers whose qubits must be cooled at very low temperatures, mainly those based on electrons (superconductors, electron spin, Majorana fermions). Theoretically, silicon qubits should only be cooled down to 1K but for the moment, they are still cooled down to about 15mK. An Australian team created a proof of concept of silicon qubits running even at 1.5K and another one from Intel and Qutech at 1.1K¹³⁴⁷.

To reach **lower temperatures**, below 3 mK, a complementary technique is used, adiabatic nuclear demagnetization (ADR or Adiabatic Demagnetization Refrigeration)¹³⁴⁸. It is not necessary for quantum computing. This type of refrigeration can be added to a wet or dry dilution cryostat. The principle consists in using a paramagnetic salt which is magnetized with a strong enough field, of 6 Tesla or more. This will heat the salt. The heat is evacuated via a 4K liquid helium bath. The suppression of the magnetic field cools the salt by expansion. The process complexity lies in the heating-cooling cycle which can disturb the cooled equipment. It is treated by combining several devices that take turns to smooth the temperature curve of the system. The process has been tried and tested for a long time, but the cooling power available is very low.

Even colder temperatures can be obtained with neutral atom cooling and Bose-Einstein condensates, below the nK threshold¹³⁴⁹. It is based on using laser-based cooling, magneto-optical traps and the likes.

kiutra (2017, Germany) uses this technique to obtain more classical temperatures of a few hundred mK, one of its advantages being that it does not generate vibrations¹³⁵⁰. These temperatures are interesting for cooling silicon qubits.

It is a startup from the TUM (Technical University of Munich) launched by Alexander Regnat. It was seed financed by APEX Ventures and German investors, but the amount is not known. Their cryostat range goes down to 100 mK (in pulsed mode) or 300 mK (in continuous mode), which is insufficient to cool superconducting Josephson effect quantum computers but could possibly be suitable for electron spin silicon chipsets that can theoretically be satisfied with a temperature of 1K.

¹³⁴⁶ Liquid nitrogen is also sometimes used to pre-cool the metallic structure of the cryostat during the warm-up. This is unrelated to the helium circuit. This can save up to five hours for the cryostat thermalization. But this process is not commonly used for quantum computer cryostats. It is used for precooling heavier payloads for physics experiments using equipment weighing up to several hundred kilograms, including superconducting magnets. This technique is not used for quantum computing.

¹³⁴⁷ See [Hot qubits made in Sydney break one of the biggest constraints to practical quantum computers](#) by UNSW, April 2020 related to [Operation of a silicon quantum processor unit cell above one kelvin](#) by Andrew Dzurak et al, April 2020 (in nature) and in February 2019 on arXiv. The test was performed on 2 qubits with a unit gate reliability rate of 98.6% quite average but in line with what is currently obtained with silicon qubits. See also [Universal quantum logic in hot silicon qubits](#), 2019 (11 pages).

¹³⁴⁸ We owe the creation of the process to William Giaouque (1895-1982, USA) in 1927. He was awarded the Nobel Prize in Physics in 1949.

¹³⁴⁹ See an interesting discussion on the limits of cooling in [Landauer vs. Nernst: What is the True Cost of Cooling a Quantum System?](#) by Philip Taranto, Marcus Huber et al, June 2021-September 2022 (61 pages) which makes a connection between Landauer's bound, the creation of quantum pure states and Nernst's unattainability principle, according to which infinite resources (time, energy) are required to cool a system to absolute zero temperature. They create a new Carnot-Landauer limit that generalizes Landauer's principle

¹³⁵⁰ See also [Cryogenic Fluids](#) by Henri Godfrin (now retired), 2011 (50 slides), from Institut Néel in Grenoble, which includes a leading research team on cryogenics. With a record of 100 μ K obtained with the DN1 cryostat using nuclear demagnetization.

Their system uses the magnetocaloric effect which was discovered in stages in 1881, 1917 and demonstrated in 1933 to reach a temperature of 250 mK.

The Kiutra process is based first on this classical effect also called adiabatic demagnetization. It consists in magnetizing a solid material with magnetocaloric properties.

This makes it rise in temperature. This temperature increase is evacuated by a conventional heat transfer fluid, which is not specified. It may be helium 4 if it is a question of going down to a temperature of less than a few Kelvins. Then, the magnetization is stopped which leads the material to cool down.

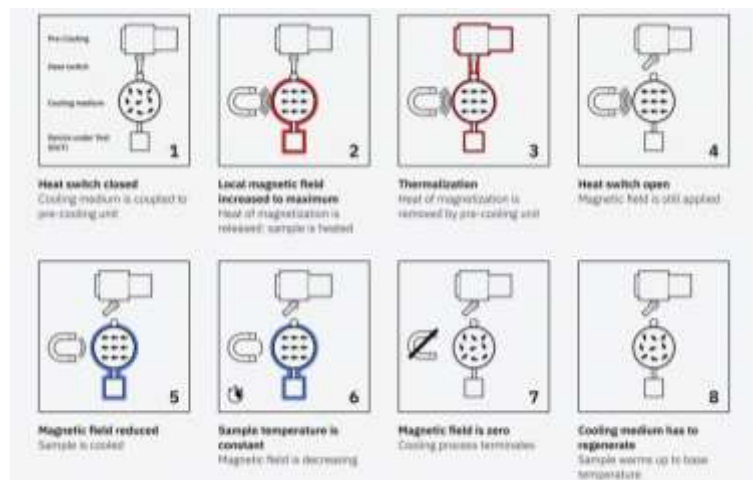


Figure 462: the Kiutra magnetic refrigeration process. Source: Kiutra.

To smooth in time and space this heating/cooling cycle, they combine several cooling units with what they call cADR (continuous Adiabatic Demagnetization Refrigeration)¹³⁵¹.

The apparatus proposed by Kiutra seems to be mainly designed to cool small samples and does not seem to be yet adapted to the usual architectures of quantum computers with their cooling stages stacked between 4K at the top and 15 mK at the bottom. On the other hand, some dry cryostats can reach temperatures situated between 5 and 10 mK.

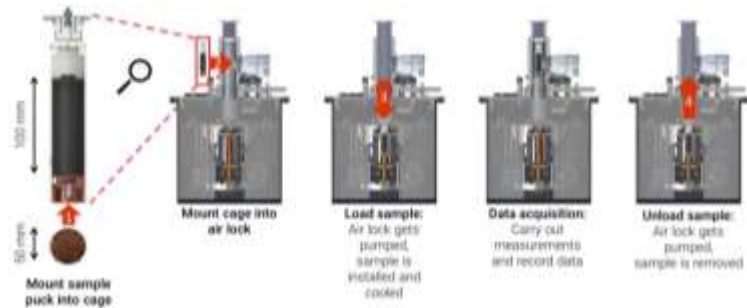


Figure 463: Kiutra cooling process. Source: Kiutra.

They are dedicated to physics experiments unrelated to quantum computing such as the search for dark matter (for the detection of WIMP, Weakly Interacting Massive Particles) and the analysis of cosmic radiation using calorimeters operating between 5 mK and 7 mK¹³⁵².

Dry dilution installation

A dry dilution refrigeration system is divided into two large parts with the compressor, pumps, liquid nitrogen and helium gas reservoirs positioned in one room, and the refrigerated enclosure in another room. This is quite logical since the compressor will generate heat that will have to be dissipated, via an incoming and outgoing water pipe¹³⁵³.

¹³⁵¹ I discovered occasionally that this technique was also being explored at the Institut Polytechnique de Grenoble. See in particular the thesis [Magnetic Refrigeration: Conceptualization, Characterization and Simulation](#) by Morgan Almanza, 2015 (160 pages).

¹³⁵² This is the case, for example, of the **CUORE** (Cryogenic Underground Observatory for Rare Events) bolometer installed in Italy. The cryostat comprises five pulse tubes and cools a 750 kg payload of tellurium dioxide to 10 mK. It was looking for signs of beta decay that could prove the existence of Majorana fermions. In the end, it did not find any.

¹³⁵³ See this well crafted detailed explanation of how a dry dilution cryostat works: [Design and Analysis of a Compact Dilution Refrigerator](#) by Jacob Higgins, 2017 (47 pages) and [Dilution Refrigerators for Quantum Science](#) by Matthew Hollister, 2021 (47 slides).

With dry dilution refrigerators, the safety constraints are quite light compared to wet versions. Wet dilution uses up to 80 liters of liquid helium which could drive a cryostat explosion if heated too abruptly because the expansion of the gas is important compared to its liquid state, with a ratio of 1 to 700. It was necessary to handle liquid helium canisters and fill tanks with protective equipment against splashes.

The oxygen level in the room could also dangerously decrease due to the accidental evaporation of nitrogen or liquid helium. Contact with cryogenic materials, particularly carbon steel, should also be avoided. Rooms must be large enough and care must be taken of in the higher zones in the room where helium can be concentrated since it is lighter than air.

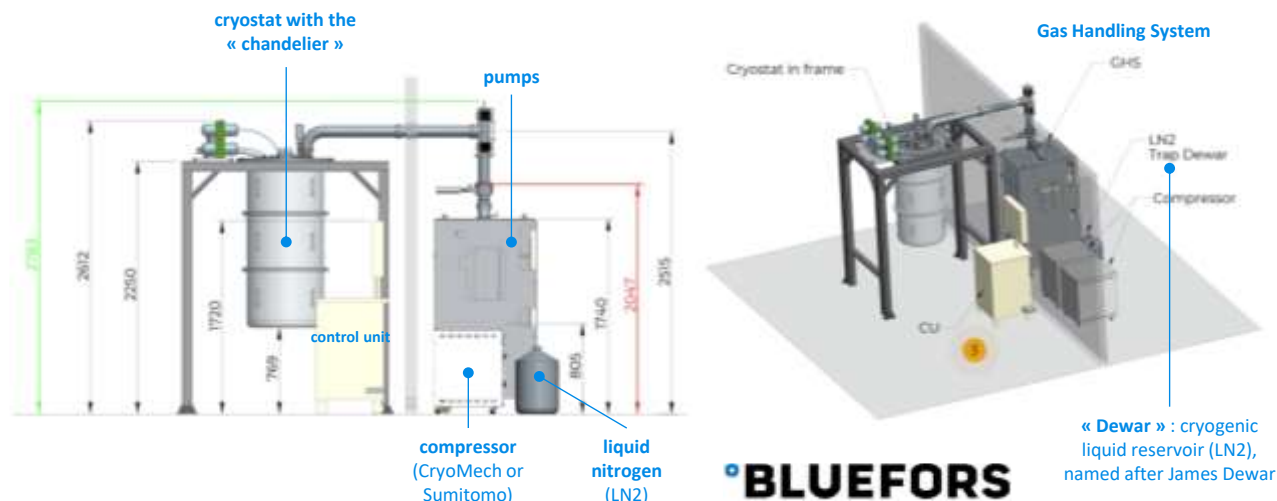


Figure 464: Bluefors recommendations for setting up one of their dilution refrigerators. Source: Bluefors documentation.

The wet dilution installation below is from CEA-IRIG in Grenoble, which deployed in June 2019 two systems from **Bluefors**. I visited it at the end of June 2019. These systems cost about €1 million each. The CEA teams installed a device that allows the tested sample to be changed in just 7 hours. Thermalization can thus be planning at night, and in the early morning, the experiments can be resumed.

The phenomena of materials **expansion and compression** are significant at very low temperatures. This has an impact on the design of the whole device and the choice of materials. The materials that can be used are special steels with nickel, chromium, aluminum, bronze, copper, composite materials, niobium-titanium for wiring, nickel-copper alloys, indium for joints, kapton and mylar for insulation.

The refrigerated system is usually placed in **vacuum**. The management of high vacuum and ultra-high vacuum (UHV) are industrial specialties. Knowing that cryostats of superconducting and silicon quantum computers only require high vacuum between 5 and 10 mBar. They use commercially available pumps from e.g. **Pfeiffer** (Germany). Pumping only takes place when the system starts up and is deactivated once the system is thermalized at low temperature. Cooling down to 15 mK does not require ultra-vacuum pumping because in practice, at this temperature, all the gases become solid and settle on the walls of the material, generating a very good vacuum.



Figure 465: Bluefors installation at CEA IRIG in Grenoble. Photos: Olivier Ezratty.

Using too much pumping to generate ultra-high vacuum could propagate dust from these solidified gases, damaging the qubits or the rest of the equipment in the cryostat. Ultra-high vacuum is used for cold atom-based computers.

Thermal leaks are coming from cables entering and leaving the enclosure or radiation. Numerous layers of thermally insulating materials are integrated in the cryostat. They are cylinders stacked upside down like Russian dolls. It is made of aluminum, copper and steel. Each cylinder and plate acts as a thermal insulator vs the lower cylinder.

The quantum chipset is **magnetically isolated** from the outside. Magnetic isolation uses several Russian doll enclosures made of various alloys, including **Mu-metal**, an alloy of nickel, iron and molybdenum, aluminum alloys and other superconducting alloys. The quantum processor can also be magnetically shielded. IBM uses a Cryoperm Magnetic Shielding from **M μ Shield**.

Apart from this magnetic isolation, cryostats in research laboratories may be supplemented by **superconducting magnet** systems that occupy the lower part of the cryostat cylinder. They have a cylindrical shape that surrounds a measuring instrument. These magnets are also supplied with liquid helium to guarantee the superconducting effect that is used to generate intense magnetic fields of several Teslas.

These fields are used to set up various experiments, particularly in astronomy or fundamental physics. They are sometimes used in quantum computing, especially with silicon qubits for electrons spin control¹³⁵⁴. At D-Wave, the magnetic field is reduced to one nano-Tesla (nT) in the computer enclosure, compared to the Earth's magnetic field, which can reach 65 micro-Teslas, giving us a ratio of 1 to 65,000. D-Wave communicates on a ratio of 1 for 50,000.

¹³⁵⁴ At CryoConcept, 8 or 14 Tesla magnets can be installed on the 4K stage next to the dilution unit.

The **cold plates** at each stage of the cryostat are generally made of 99.99% pure copper with very low oxygen content to maximize their thermal conductivity¹³⁵⁵. It is covered with a thin a few microns thick layer of gold which serve as a protection against oxidation and radiation. It also has good thermal conductivity and is soft, which is very useful for solidly anchoring and cooling all the attached components.

On the right, an example of a BlueFors cryostat cold plate. These plates are custom perforated to allow all the cables to pass through, not including the cryostat components. All the holes must be used to avoid thermal leaks between the bottom and top of these cold plates.



Figure 466: cold plate with a gold finish which is used to facilitate the assembly with experimental devices and optimize thermal conductivity. Photo: Bluefors.

Infrared rays must be prevented from passing from one level to another and generating downward heat leakage.

These plates must be optically totally watertight screens so as not to let a single photon pass through! The trend is to increase the size of the cold plates, with a diameter reaching 50 cm. Knowing that their size is slightly decreasing from the top to bottom cold plates because of the concentric cylinders shields surrounding them.

In cryostats for quantum computers, the current standard for the bottom plate is 30 cm to 40 cm for research and 50 cm in production, to accommodate more electronic components. It could soon reach 100 cm. Infrared photons are filtered with an **Eccosorb** resin that surrounds the superconducting cables in the lowest stage of the system. This resin is a mixture of epoxy and metal powder. It is injected into copper filters (OFHC) that surround the cables in the coldest stage of the cryostat as shown in Figure 467¹³⁵⁶. The resin is usually supplied by **Laird Performance Materials** (UK).



(A) ECCOSORB injection. Inject slowly and at a flat angle such that the liquid creeps onto the edge of the fill opening and into the cavity. Injecting too fast or steep will cause a planar bubble to form which blocks the opening (see Figure 3.8b).

Figure 467: how the Eccosorb resin is injected in the filters.

To reach ultra-low temperatures of 1 mK, the **Continuous Nuclear Demagnetization Refrigerator** technique can also be used, in complement with dry refrigeration¹³⁵⁷. This temperature is required for some physics experiments but not with solid-state based quantum computers (superconducting or electron spin qubits). At such a low temperature, the cooling budget is equally super low, at just 20 nW.

¹³⁵⁵ It is OFHC for oxygen-free high thermal conductivity. Source of this information: [Flying Qubit Operations in Superconducting Circuits](#) by Anirudh Narla 2018 (219 pages).

¹³⁵⁶ See some explanations of the Eccosorb resin in [Improving Infrared-Blocking Microwave Filters](#) by Graham Norris, 2017 (114 pages) and [Development of Hardware for Scaling Up Superconducting Qubits and Simulation of Quantum Chaos](#) by Michael Fang, 2015 (56 pages). Eccosorb is a product from Laird, a subsidiary of Dupont. It came from the acquisition of Emerson and Cuming in 2012. Eccosorb is a laminated structure of polyurethane foam generating a controlled conductivity gradient.

¹³⁵⁷ See [Development of a sub-mK Continuous Nuclear Demagnetization Refrigerator](#) by David Schmoranzer, Sébastien Triqueneaux et al, Institut Néel, 2020 (7 pages).

Cryostats vendors

The main suppliers of cryostats for quantum computers are **BlueFors Cryogenics** (Finland), which equips IBM, Rigetti and many others, **Oxford Instruments** (UK), which is used by D-Wave and Microsoft, **Form Factor** (USA), used by Google, **Maybell Quantum** (USA), **Leiden Cryogenics** (Netherlands)¹³⁵⁸, which manufactures the most powerful cryostats on the market, used mainly for physics experiments, and **CryoConcept** (France), a branch of **Air Liquide** since 2020. The world market for cryogenic systems, all categories combined, was about \$1.8B in 2020¹³⁵⁹. Market share wise, BlueFors leads the pack with over 60% and >\$100M revenue, followed by Oxford Instruments and the rest.

Let us recall that the science of low temperatures used in quantum computing has benefited from numerous advances from other fields: space and especially space telescopes where a large part of the instruments needs to be cooled such as infrared sensors or bolometers, particle accelerators with their superconducting magnets and finally, medical imaging, especially MRI, which also needs low temperatures to cool its superconducting magnets.

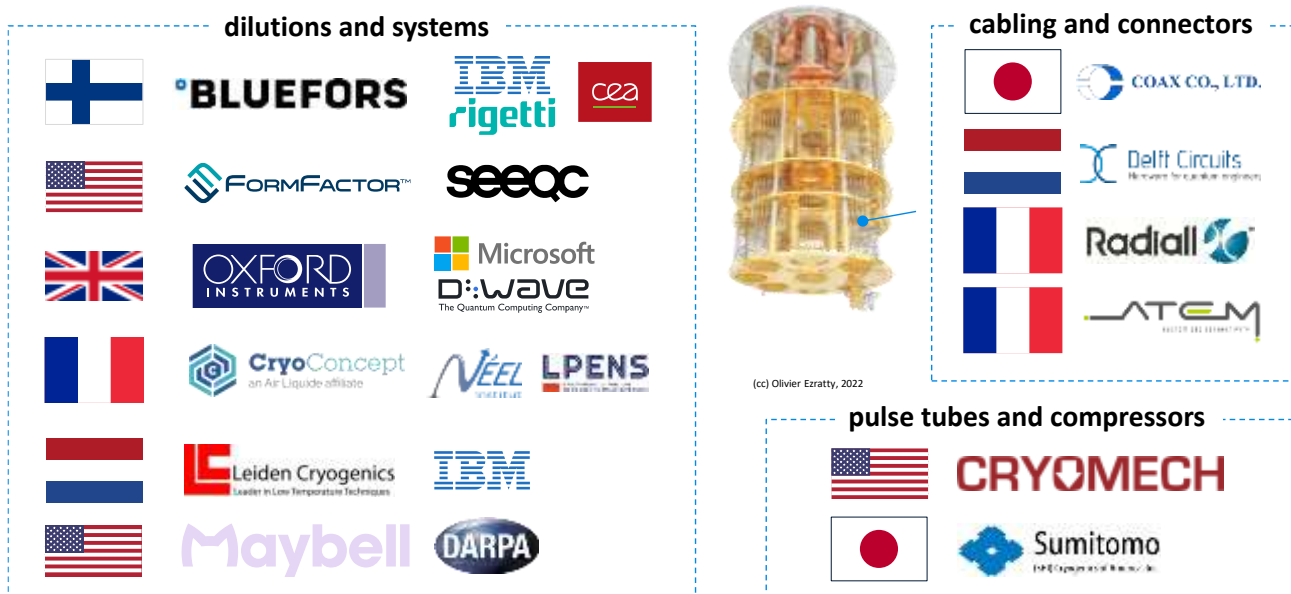


Figure 468: the main vendors for quantum computer low temperature cryostats, their compressor, cabling and connectors. (cc) Olivier Ezratty, 2020-2022.

BLUEFORS Bluefors (2007, Finland) is the worldwide leader of low temperature cryogenic systems, using dry dilution. It's focused on the quantum computing market.

The spin-off from Aalto University delivered 600 systems with its 250 employees. It has a broad range of dry dilution systems, with some cabling (coaxial, ribbon, optical) and filters, QDevil X, codeveloped with QDevil.

¹³⁵⁸ See [Leiden Cryogenics BV](#) brochure (28 pages).

¹³⁵⁹ See [Cryocooler Market by Type \(GM, PT, JT, Stirling, and Brayton Cryocoolers\), Services \(Technical Support, Repair, Preventive Maintenance\), Heat Exchanger Type \(Recuperative and Regenerative\), Application, and Geography - Global Forecast to 2022](#), December 2019. This market represented \$1.4B in 2018 and is expected to grow 9.3% annually by 2027. But beware, the market for quantum computers cryostats is a rather small share of this market.

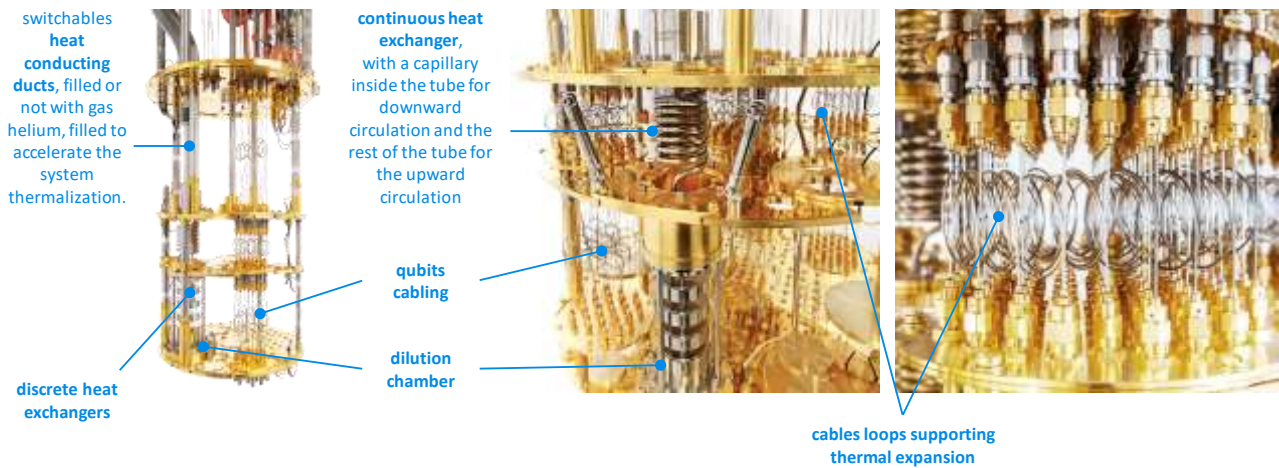


Figure 469: details of a BlueFors cryostat with custom comments. Source: Bluefors.

In March 2021, Bluefors announced a partnership with **Linde** (Germany) to create high-capacity cryogenic systems dedicated to scalable quantum computers. Linde is a gas producer competing with Air Liquide!

They also developed with **Afore** (Finland) a Cryogenic Wafer Prober, a system used for the characterization of 300 mm wafers at 4K. It was acquired by **CEA-Leti** in 2021 to test the quality of their silicon qubits wafers. **Intel** acquired a similar tool as well, for their own silicon qubits development efforts in their D1D fab in Hillsboro, Oregon, USA.



Figure 470: the Bluefors/Afore cryoprober used by Intel and CEA-Leti.

In November 2021, Bluefors announced KIDE, its new generation of cryostats, that has a hexagonal shape to make it easier to assemble them next to each other for distributed QPU setups and with 9 pulse tubes and three dilutions each. It will be produced in 2023 and used among others by IBM and Rigetti.



JanisULT (1961, USA) was initially Janis, a generalist cryostat manufacturer. In 2020, they sold their 'classical' laboratory cryostats business to Lake Shore.

They kept their ultra-low temperature cryostat business under the brand Janis ULT. They have an offering of wet and dry dilution refrigerators for various use cases, including quantum computing. Their high-end wet dilution refrigerator is the JDry-500-QPro with a 508 mm cold plate and >450 μ W of cooling power at 100 mK achieved with a single pulse tube, coming from Sumitomo SHI.



FormFactor (1993, USA) is a provider of electronics test and measurement tools for the semiconductor industry with some products dedicated to quantum technologies.

They acquired in early 2022 the dry-refrigerator business line from Janis ULT. Their offering covers chipsets inspection and metrology, characterization, modeling, reliability, and design debug, to qualification and production test. They sell HPD IQ3000, a cryogenic probe stations for on-wafer and multi-chip measurements. It can embed IR-sensor test, radiometric test and DC and RF measurements. It supports 150 mm and 200 mm wafers at 4 K (while Bluefors' probe station also supports 300 mm wafers). They sell dry dilution refrigerators supporting 10 mK and below temperatures that are used for test and measurement (JDRY-250, JDRY-500, and JDRY-600, this last one offering a 630 μ W cooling power at 100 mK and 17 μ W at 20 mK), all coming from Janis ULT. They also sell one or two-stage ADR (Adiabatic Demagnetization Refrigerators) using a salt crystal to strong magnetic fields, complementing dilution refrigerators. Among others, FormFactor partners with SeeQC and Keysight.



Oxford Instruments (1959, UK) is an established British company, listed on the London Stock Exchange since 1999, specializing in scientific instrumentation including cryogenic systems capable of reaching 5 mK¹³⁶⁰.

They also provide CCD cameras to detect the state of trapped ion qubits, electron microscopes, vacuum deposition systems, X-ray sources and cameras, and nuclear magnetic resonance spectrographs. The company had acquired VeriCold Technologies (Germany) in 2007 to gain control of pulsed tubes used in the first stage refrigeration for dry dilution cryostats. Their last product is the Proteox, a high-end and flexible dry dilution system with removable cabling.

ProteoxLX – Maximise experimental capacity



Enabling the future of Quantum Computing scale-up

- Exceptional capacity for signal lines and cold electronics
 - 530 mm diameter mixing chamber plate
 - Two large Secondary Inserts with 117 mm x 252 mm fully customisable space – up to 256 UT85 SMA lines per system
 - 10 KF50 non line of sight ports for DC wiring
- Highest cooling power system
 - 25 μ W at 20 mK
 - Twin pulse tubes at 1.5 W or 2.0 W per Pulse Tube Refrigerator (PTR) provide up to 4.0 W cooling power at 4 K
- Low base temperature < 7 mK



Figure 471: Oxford Instruments ProteoxLX. Source: Oxford Instruments.

In March 2021, they launched the ProteoxLX. It expands the qubits hosting capacity with a larger sample space and coaxial wiring capacity, low vibration and integration of cryo-electronics components. It offers a cooling power of 25 μ W at 20 mK and 850 μ W at 100 mK with twin pulse tubes providing up to 4 W cooling power at 4 K.

¹³⁶⁰ See [Principles of dilution refrigeration](#) by Oxford Instrument (20 pages) which also documents well the architecture of a cryostat.

They also designed a Q-LAN, a cryogenic link that could be used to connect two dilution fridges. The payload can reach 20 kg at 20 mK and 125 kg at 4K.



CryoConcept (2014¹³⁶¹, France, acquired by Air Liquide in July 2020) stands out with cryostats ensuring a very low-level of vibration via their UltraQuiet technology.

They have deployed more than 120 cryostats in 13 countries for various players such as the CEA in Saclay and the ENS¹³⁶². Since 2018, CryoConcept has been collaborating with CEA-Leti to deliver two large cryostats to equip the QuCube project for silicon qubits. They sell worldwide including in the USA, Japan and South Korea in a market driven by dark matter research and bolometry. The unique low-level of vibrations of their cryostat is related to the absence of mechanical contact between the pulse tube and the cryostat.

By this mean, vibrations are reduced in the range from 1Hz to 1kHz. This absence of vibration is useful to preserve qubits coherence as for cryostats installations containing bolometers that are used to perform physics experiments such as in dark matter research. This experience in bolometry enabled CryoConcept to develop highly reliable dilution fridges, with systems running for more than one year without interruption. This reliability is a key attribute sought after to operate future quantum data centers.

Historically, CryoConcept started by manufacturing wet cryostats and kept an expertise in this field even though dry systems are now the most commonly manufactured dilutions. Now associated with Air Liquide, CryoConcept is working on coupling helium liquefiers with dilution refrigerators in order to overcome the current cooling power limitation at 4K, thanks to their refrigeration technology from 300 K down to 20 mK. This will ensure cooling power adapts as the number of qubits in the related quantum processors is growing.



Leiden Cryogenics (1992, Netherlands) was founded by Giorgio Frossati and Alex Kamper. The former had been working on dilution refrigeration since the 1970s. Among other things, he invented silver powder heat exchangers.

He started to work at the Centre de Recherche sur les Très Basses Températures in Grenoble, which became the research center on Condensed Matter and Low Temperatures (MCBT) of the Institut Néel of the CNRS. He then became a professor at the University of Leiden in the Netherlands. He designed there a dilution refrigerator reaching a record temperature of 1.85 mK with a cooling power of 25 μ W at 10 mK. The heat exchanger technologies he developed were licensed to Oxford Instruments. At last, BlueFors was created by Giorgio Frossati's post-docs! What a small world!

Leiden is behind what looks like the largest very low temperature cryostat ever build for a large load as shown in Figure 472. It was achieved between 2016 and 2018 for CUORE (Cryogenic Underground Observatory for Rare Events).



Figure 472: the CUORE mega-cryostat cooling a load of one ton.

¹³⁶¹ CryoConcept was in fact created in 2001 by technology transfer from the CEA where Olivier Guia had worked. The company has had several different owners including French company Segula Technologies and American company CryoMagnetics. Olivier Guia took over the company in 2014. They then reintegrated the in-house R&D and in particular recovered the technological mastery that was at the CEA.

¹³⁶² See the quantum equipment of the ENS (Ecole Normale Supérieure, in France) in their [Labtour](#).

It is a bolometric experiment for neutrinoless double-beta decay detection in TeO_2 (tellurium dioxide) that is installed at the underground facility of Laboratori Nazionali del Gran Sasso (LNGS) in the Alps. The CUORE cryostat is cooling a one ton mass of metal with a one cubic meter size to 7mK. It is using a three stage cooling system with liquid Helium vapors for the first stage at 50K, 5 CryoMech PT415 pulse-tubes and compressors for the 4K stage and only a single Leiden modified dilution for the <10mK stage. Interestingly, the cooling power of the lowest stage is only of 3 μW at 12 mK, lower than the max cooling power at 15mK of most dilutions analyzed in this section. The difference is it took 26 days to cool down the experiment, including only 4 days for the last stage of one ton after 22 days to reach 3.4K¹³⁶³.



ICE (2004, UK) aka ICEoxford was created in 2004 by Chris Busby and Paul Kelly to design and manufacture custom wet and dry Ultra Low Temperature (ULT) cryostats (but not below 300 mK) and High Magnetic Field equipment for research applications.



Maybell Quantum (2022, USA, \$500K) is a new company created in Colorado by Corban Tillemann-Dick (CEO, formerly at the BCG), Kyle Thompson (CTO, from the MIT Lincoln Labs and Janis ULT) and Brian Choo.

It develops a dilution refrigerator, the Icebox, that is intended to support three times more qubits in 10% of the usual space, all at a temperature below 10 mK. Above all, they announce a capacity of 4,500 cables to drive qubits with microwaves up to 12 GHz (meaning: superconducting qubits and electron spin qubits) thanks to their Flexlines, ultra-high-density RF ribbon cables and Super-Flex NbTi ribbons cables for the lower stages of the cryostat. Their Resito-Flex (CuNi-NbTi, BeCu-NbTi, CuNi-CuNi) and Atenu-Flex (SS-NbTi, SS-SS, SS-CuNi) ribbons are adapted to higher-temperature stages. It is optimized for 1000 qubits QPUs. They also provide classical coaxial cabling and fiber optics connectivity. The whole cryostat fits into two 19" server racks formats with extra space available for 9U of electronics and computing.

But it doesn't contain the compressor and the GHS (gas handling system) that controls the flow of helium in and out of the compressor and requires a space equivalent to their own system. The helium compressor can be cooled with air or water. All this looks like a game changer. On top of that, the Maybell Icebox experimental part is supposedly accessible with a simple door. It would probably require many Russian-doll doors given a cryostat have about five layers of isolations as portrayed in their own schematics below.

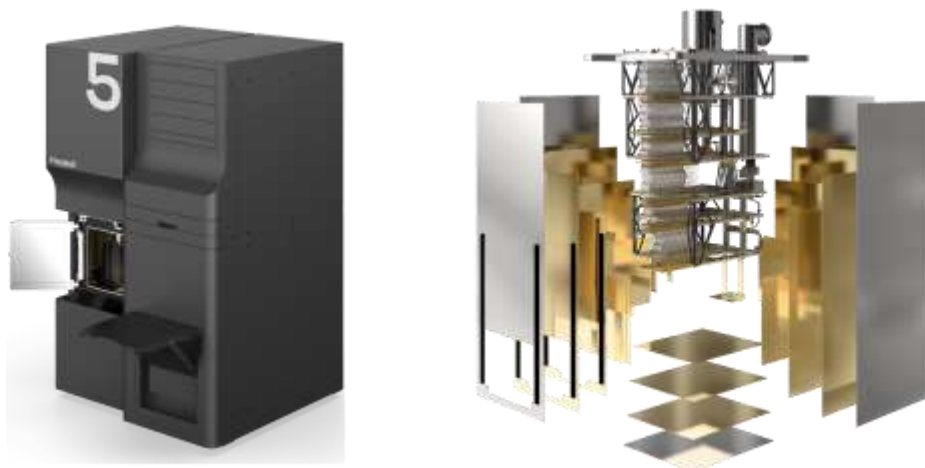


Figure 473: the Maybell Quantum cryostat unveiled at the APS March meeting 2022 in Chicago. Source: Maybell Quantum.

¹³⁶³ See [The CUORE cryostat](#) by A. D'Addabbo et al, August 2018 (8 pages).

The company initial funding came from Colorado's Advanced Industry Accelerator (AIA) venture fund and the US DoD National Security Innovation Capital fund (NSIC) which belongs to the Defense Innovation Unit. The company said it already has some contracts from DARPA.



Absolut System (2010, France) was created by Alain Ravex, former head of the low temperature department of the CEA in Grenoble in the 1980's and 1990's, then a consultant for Air Liquide. He sold the company to his partners and now consults for them and other players in the cryogeny field.

The company develops custom cryostats running at temperatures higher than 1.8K and targets a wide range of applications in research and in the industry, particularly for the production of liquid nitrogen. Their customers include CEA-Leti, Thales and Air Liquide. They are based near Grenoble.

They developed the ACE-Cube (Advanced Cryogenic Equipment), a cryogen free helium cryostat using a remote cooling technique. It is implemented for specific infrared detectors and semiconductor characterization and above 10K.

They also launched AFCryo (2017), a joint subsidiary in New Zealand, with Fabrum Solutions (2004) also based in New Zealand¹³⁶⁴.



MyCryoFirm (2013, France) produces dry cryostats, running at 3K with a cold plate of 250 mm diameter with a 300 mW cooling power at 4,2K. They rather target the field of research in quantum optics, quantum physics and quantum sensing.

They propose various experiment decks/plates adapted to creating magnetic fields, spectroscopy applications and the likes. In 2022, they did add a dilution option on their Optidry250 cryostat and made it operate at 50 mK at Météo France.



Cryomech (1963, USA) is a supplier of components for cryostats and in particular dry cooling systems comprising a pulsed tubes and a compressor which are integrated in the cryostats of most market players such as BlueFors and CryoConcept.

These pulse tubes and compressors are the first stage of dry dilution refrigeration systems. They use an expansion system of compressed gas outside the cryostat with no rotating parts in the cryostat¹³⁶⁵. The compressor is water-cooled, with a flow rate of 5 to 12 liters per minute depending on the incoming temperature. But this water must also be cooled, and it can require up to an additional 10 kW of electric power unless the computer is located in a cool region.

Their pulse tubes range includes the PT415 and PT420 (*right*). Its main competitor is the SHI Cryogenics Group subsidiary of **Sumitomo** (Japan, *left*)¹³⁶⁶. These compressors are sold combined with their related pulsed tubes.

¹³⁶⁴ See [Commercial Cryocoolers for use in HTS applications](#) by Christopher Boyle, Hugh Reynolds, Julien Tanchon and Thierry Trollier, 2017 (29 slides).

¹³⁶⁵ These pulsed tubes are used in particular in the semiconductor industry, in vacuum deposition machines (CVD, MOCVD) and plasma deposition machines. They are down to 10K, which is sufficient for semiconductor production.

¹³⁶⁶ There are other pulse head and compressor manufacturers such as Fabrum Solutions (New Zealand) but the latter only targets temperatures of 77K for liquid nitrogen production.



Figure 474: a Cryomech compressor, that is connected to a pulse tube (on the right).



Figure 475: Cryomech pulse tubes, that cool a cryostat down to 4K. It is also used to cool down the helium 3 and 4 mixture circulating in a dilution.



High Precision Devices (1993, USA) develops cryogenic instruments adapted to superconducting quantum computers and in particular sensors. It is very specialized low-level instrumentation. They also develop ADR (Adiabatic Demagnetization Refrigeration) type cryogenic systems. It was acquired by **FormFactor** (1993, USA) in 2020, an advanced SoC and memory probe cards designer for the semiconductor industry.



Intelline (2018, Canada) produces customized cryogenic refrigeration systems that are expected to be more affordable than those of its competitors. But they seem to target markets other than quantum computer cryogenics, at least at temperatures below 1K.



CryoFab (1971, USA) provides liquid helium containers and related accessories.



Cryogenic Limited (1991, UK) provides a various set of cryogenic systems and superconducting magnets. It includes liquid helium systems and ultra-low temperature systems using their own magnet and an off-the-shelf cryostat from Leiden.



Qinu (Germany) is a new company selling mK and 4K cryostats. It was created by a former researcher from Institut Néel in Grenoble, which has its own cryostats design laboratory.



Attocube Systems (2001, Germany) has different line of businesses including cryostats mainly targeting the research community. It sells the attoDry series, closed-cycle dry cryostats (with cooling temperatures ranging from 1.65K to 4K), and the attoLIQUID series (300 mK), liquid helium cryostats.



Montana Instruments (2009, USA) develops cryostats and vacuum pumps, used in trapped ions (including IonQ) and NV centers computers as well as photon-sources (Sparrow Quantum).

One of their added value is to reduce the vibrations coming from the pulse tube. They cover temperatures ranging from 3.2K to 4.9K.

There are many other cryostats and cryogenic devices vendors but they are less specialized in serving the needs of quantum technologies providers¹³⁶⁷.

Cooling budgets

The level of cooling power at ultra-low temperature is quite low. This limits the energy that can be released by the qubits themselves and by the microwave attenuation and amplification circuits used to read the state of the qubits. See in Figure 476 a comparison of these cooling power budgets by supplier.






| | cryostat | pulse tubes | minimum temperature | 20mK stage | 100mK stage | MC cold plate |
|---|---------------|-------------|---------------------|------------|-------------|---------------|
|  | LD250 | 1 | 10 mK | 12 μW | 250 μW | 30 à 50 cm |
| | XLD400 | 2 | 8 mK | 14 μW | 450 μW | 30 à 50 cm |
| | XLD1000 | 2 | 8 mK | 34 μW | 1000 μW | 30 à 50 cm |
|  | JDry-500-QPro | 1 | 7 mK | 14 μW | 500 μW | 50 cm |
|  | TritonXL | 2 | 5 mK | 25 μW | 1000 μW | 43 cm |
| | TritonXL-Q | 2 ou 4 | 7 mK | 25 μW | 850 μW | 50 cm |
| | Proteox | 1 | 10 mK | >25 μW | 500 μW | 36 cm |
|  | HD200 | 1 | 10 mK | 11 μW | 350 μW | 30 à 50 cm |
| | HD400 | 1 | 10 mK | 10 μW | 400 μW | 30 à 50 cm |
|  | CF2400 Maglev | 2 | 4 mK | ? μW | 2000 μW | 49 cm |
| | CF1400 Maglev | 2 | 8 mK | ? μW | 1000 μW | 49 cm |

Figure 476: cooling power per temperature and cryostat vendor. (cc) Olivier Ezratty, 2020-2022.

The **BlueFors'** refrigeration thermal budget ranges from 12 μW (LD250) to 30 μW (XLD1000) at 20 mK, and from 250 μW (LD250) to 1000 μW (XLD1000) at 100 mK.

Oxford Instruments' TritonXL also has a thermal budget of 1000 μW at 100 mK but with two pulsed tubes, while the new Proteox reaches 500 μW ... with only one pulsed tube. It is completed by a removable system for qubit control cables supporting up to 140¹³⁶⁸.

The **Janis JDry-500-QPro** has a thermal budget of 14 μW at 20 mK and 450 μW at 100 mK (*above*, in-house compilation).

The current record can be found at **Leiden Cryogenics** with a recent cryostat with a thermal budget of 2000 μW on the 100 mK stage, but the budget at 20 mK is not indicated in their literature. On the 4K stage, the available thermal budget is around 1W. But beware, these extreme performances above 500 μW are often obtained with two pulsed tubes instead of one and thus, double the external compressor and power drain. All this with a double dilution refrigeration system to go below 1K. It is also possible to have systems with a single pulse tube and two dry dilution systems.

The thermal budget of the coldest stage is conditioned by the equation: $Q_m = 84\dot{n}_3 T^2$ where Q_m is the cooling power in W, \dot{n}_3 is the flow velocity in mol/s of helium 3 in the cryostat at this stage and T is the temperature of the stage in Kelvin. This law that can be simply called "Q=84NT²" explains that the thermal budget at 15 mK is very low compared to the cooling budget available at the upper stages (up to 25 μW at 15 mK, 1 mW at 100 mK and 1.5W at 4K).

There is another constraint related to the Kapitsa resistance. It limits heat exchanges between helium 3 and the heat exchanger. These exchanges are proportional to T^4 . If we therefore want to multiply heat exchanges by 10, the exchange surfaces in the lower parts of the dilution system would have to be multiplied by 10,000! This is done with using silver powders integrated into the discrete heat exchangers above the dilution chamber. These powders are structured to maximize the heat exchange surface area with the helium gas flowing through them. Their deposition process must maximize the flat contact surface with the small tanks where they are located.

¹³⁶⁷ See [61 Ice Hot Companies Transforming The Cryogenics & Alternative Cooling Systems Industries](#), January 2021.

¹³⁶⁸ See the very interesting presentation [50 years of dilution refrigeration](#), by Graham Batey of Oxford Instruments, 2015 (26 slides).

It is possible to increase cryostats cooling power with adding more cooling stages, improving their Carnot efficiency and with multiplying the pulse tubes and dilutions (like what IBM has done with its Goldenye cryostat).

Other cryogenics

For the other types of qubits, the cooling requirements are different: trapped ion qubits are not theoretically refrigerated, but Honeywell's prototype ion trapped processors announced in early March 2020 are cooled to 12.6K, a temperature that can be obtained with helium 4 based cryostats.

In photon-based quantum processors, the optical components traversed by the photons (mirrors, prisms, interferometers, whether miniaturized in nanophotonics or not) are not refrigerated, but the photon sources and photon detectors are, at temperatures between 1K and 10K. The associated cryogenics is much lighter and consumes less energy compared to dilution cryostats.

Other techniques allow very localized cooling. This is the case of the **Doppler effect** which works on cold atoms suspended in a vacuum. Another solution developed by researchers from the VTT Technical Research Centre in Finland would cool silicon components with a phonon-based electronic cooling technique. It seems that this cooling's capacity is very low, very localized, and still requires pre-cooling the system to at least 244 mK. It is therefore still necessary to operate a helium 3 and 4 dilution cryostat¹³⁶⁹.

Thales Cryogenics

Thales Cryogenics (France, The Netherlands) is a subsidiary of Thales Group which creates various specialized cryocoolers for military and commercial applications.

It includes rotary and linear Stirling coolers, mini-coolers, high-pressure gas compressors, miniature DC/AC rotary and linear converters, linear pulse tube cryocoolers etc.

Thales' NV centers-based quantum sensors use miniaturized cooling using liquid nitrogen and occupying only half a cubic decimeter¹³⁷⁰. The required temperature is lower, around 70K which is quite hot compared to 15 mK! These cryostats are used for various breeds of quantum sensors.



Figure 477: a small Stirling cooler for embedded systems. Source: [Closed Cycle Refrigerator](#) by John Wilde, 2018 (11 slides).

Qubits control electronics

Most of the times, driving qubits with quantum gates and for their state readout requires sending them some sort of photons. For superconducting qubits and electron spin qubits, these photons are in the microwave spectrum. In a counterintuitive fashion, these microwaves are transmitted in coaxial cables and not over the air like radio waves. Their frequencies range between 4 and 8 GHz for superconducting qubits and between 12 and 26 GHz for electron spin qubits. These are in between higher-frequencies photons that can be transmitted in optical fiber and lower frequencies signals which are transmitted as classical electrical current in wires. These photons are generated as pulses of various shapes and duration (cosine signals shaped with an envelope, base pulses of diverse forms, cosine or other, and direct-current pulses which are the simplest to generate).

¹³⁶⁹ See [Thermionic junction devices utilizing phonon blocking](#) by Emma Mykkänen et al, 2020 (9 pages). It reads: "The cooling power for this sample is about 2 pW/μm² at 300 mK". "Our best-performing sample is S2 (subchip with 1-mm diameter and 0.4-mm height). Its maximal absolute and relative temperature reductions are 83 mK (at 244 mK) and 40% (at 170 mK), respectively". Therefore, it is already necessary to reach 244 mK before starting, and it is therefore necessary to use a helium 3 and 4 cryostat.

¹³⁷⁰ These are usually systems using a Stirling engine. Thales Cryogenics produces such miniaturized refrigeration systems. The [RM2](#) cools a payload to 77K for a mass of 275g and a thermal budget of 400 mW at this temperature. It is notably used for cooling infrared cameras in embedded systems. This type of small cryostats can also be found at SunPower (USA), capable of cooling down to 40K and with a larger mass of 1.2 kg. Ricor (1967, USA) is another manufacturer of this kind of mini-cryostats.

We'll look here into two sorts of micro-wave generation technologies: those coming from room temperature electronics and those generated within the cryostat at cryogenic temperature, including cryo-CMOS, SFQ superconducting electronics and other discrete electronic components working at these low temperatures like the TWPAs used for qubits microwave readout signals amplification.

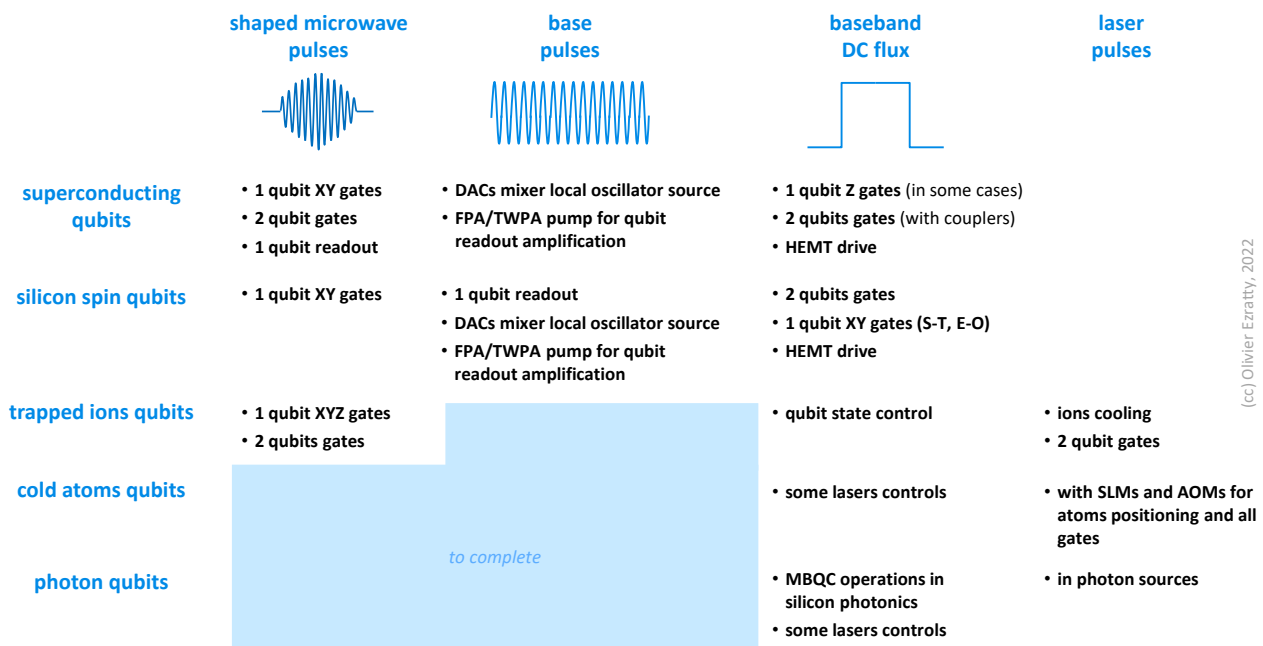


Figure 478: compilation of the various electronic and photonic signals used to drive various types of qubits. This diagram will later be completed with more signals used to drive atoms and photon qubits. (cc) Olivier Ezratty, 2022.

Direct current signals are also used to drive qubits, like with Z gates with some superconducting qubits and to drive some amplifiers¹³⁷¹. To be complete, we'll then also look at cabling and filtering components and their vendors.

With photon, cold atoms and trapped ions qubits, control techniques involve photons and lasers operating in the infrared and near visible spectrum which we don't cover here. There are missing parts in the schema above in Figure 478 with regards to the shaped and base pulses that may be used for the control of various electronic and photonic devices used in atom and photon based systems.

We'll try here to answer many questions: how are all these electronics affecting the quality of qubits? How is it scaling as you need to significantly increase the number of physical qubits to accommodate the requirements of fault-tolerant quantum computing? How do you optimize the existing cumbersome wiring? What are the solutions to run all or part of these electronic systems inside the cryostat? What is the power consumption of these various solutions? How can we scale with room temperature electronics and cryogenic electronics?

Wiring. How many wires are needed to control solid states qubits? It depends but there are usually half a dozen wires are needed to control a superconducting or quantum dot spin qubit. One or two microwave wires to drive qubit gates, one or two DC pulses wires to control other gates and then, two microwave wires for qubit readout (one in and one out of the qubit). One DC bias is sometimes used to change energy spacing for tunable superconducting qubits. When you scale the number of qubits, this creates a massive number of wires.

¹³⁷¹ This excellent review paper [Microwaves in Quantum Computing](#) by Joseph Bardin et al, January 2021 (25 pages) provides an excellent overview of the challenges of microwave based qubit controls for superconducting, electron spin and trapped ion qubits. The table/chart in this page is inspired from this document. Z gates are driven by direct currents with Google's Sycamore qubits while IBM's are driven by microwaves, like the XY gates. See also [Engineering cryogenic setups for 100-qubit scale superconducting circuit systems](#) by S. Krinner et al, 2019 (29 pages) which makes a good inventory of energy consumption sources in the cryostat.

Multiplexing. Work is being done to multiplex these signals with different methods. One is frequency domain multiplexing that is already implemented for qubit readout with up to 8 microwaves frequencies in a single wire. A second would be frequency multiplexing with up and down convert to higher frequencies such as in the optical domain. Nanophotonic circuits sitting very close to qubit chipsets could be used for microwave up/down frequency conversion from microwave photons to optical photons and their multiplexing¹³⁷². One proposed conversion technique uses VCSEL (Vertical-cavity surface-emitting lasers) that are known to operate at low temperature of 2.6K, which is still high¹³⁷³. A third method consists in using time domain multiplexing which probably has some limitations in scaling, making it impossible to run several gates simultaneously and therefore potentially slowing down computing and quantum error correction¹³⁷⁴. To ensure scalability, these solutions must demux the signal as close as possible to the qubit chipset and have a very low power drain, compatible with the very low cryostat cooling budget at low cold-plate stages, and if not, at the 4K stage.

Cryo-electronics options. Many options exist that we'll cover in this part. Cryo-electronics can operate at the 4K stage (HorseRidge) down to the lower stages (15 mK to 100 mK). What are their limitations? Also, what are the pros and cons of cryo-CMOS vs SFQ electronics? All these cryo-electronics solution must be compared with detailed specifications. The generated microwave quality depends on the sampling rates used in their DAC and ADCs, on the number of points used in generating the wave envelope (16,384 points for HorseRidge 2, aka 14-bit sampling), their power consumption per qubit, their frequency range (targeting superconducting and/or electron spin qubits), their clock, their noise level and their real scalability potential with a large number of qubits. These electronic components must also be as isolated as possible from the qubit chipsets.

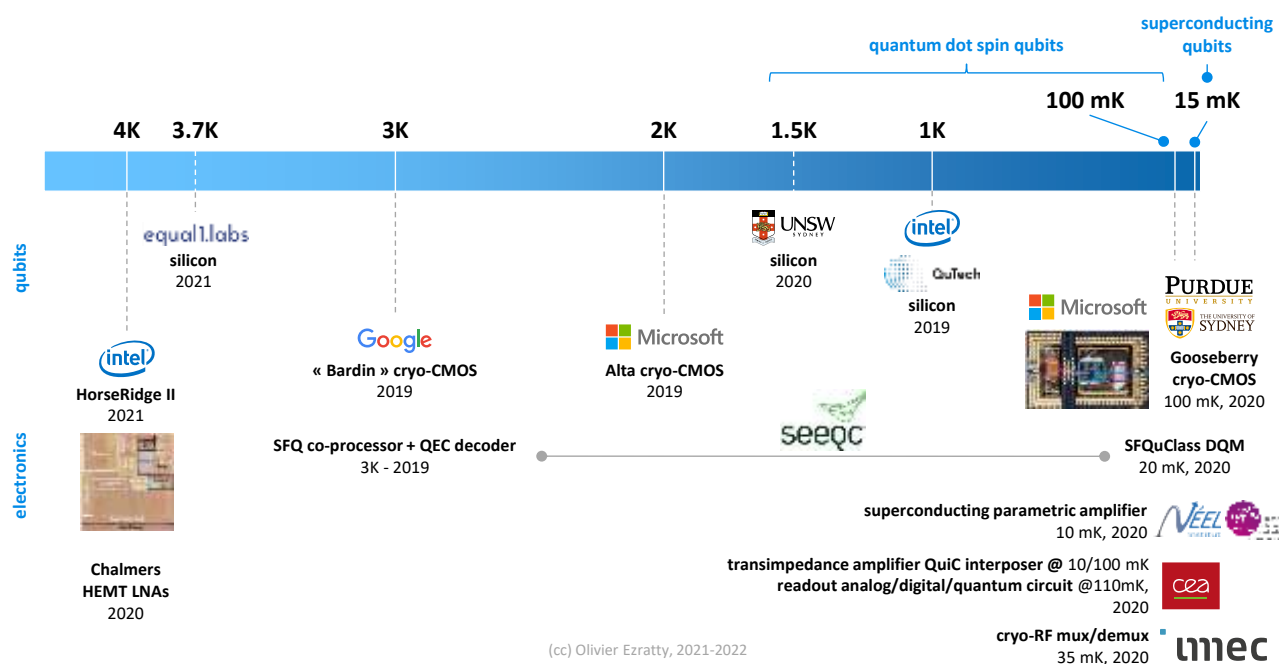


Figure 479: comparison of the temperature and feature of various qubits and cryo-electronic chipsets. (cc) Olivier Ezratty, 2022.

¹³⁷² See [Supporting quantum technologies with a micron-scale silicon photonics platform](#) by Matteo Cherchi et al, VTT, 2022 (17 pages) and [Control and readout of a superconducting qubit using a photonic link](#) by F. Lecocq et al, NIST, September 2020 (13 pages).

¹³⁷³ See [Recent Advances in 850 nm VCSELs for High-Speed Interconnects](#) by Hao-Tien Cheng et al, February 2022 (27 pages) and [Microwave-optical quantum frequency conversion](#) by Xu Han et al, Optica, 2021 (15 pages). See also [Scaling up Superconducting Quantum Computers with Cryogenic RF-photonics](#) by Sanskriti Joshi et al, University of Washington, October 2022 (10 pages).

¹³⁷⁴ See [Overcoming I/O bottleneck in superconducting quantum computing: multiplexed qubit control with ultra-low-power, base-temperature cryo-CMOS multiplexer](#) by Rohith Acharya et al, IMEC, September 2022 (22 pages). The “1 to 4” drive multiplexer has a power consumption of around 0.24 μ W of static power and 0.5 μ W of dynamic power, with \sim 0.2 μ W power consumption per qubit channel making it suitable to control 100 qubits and 1000 qubits with some optimizations, within the constraints of today’s cryostats.

Optimization. Cryo-electronics are an interesting solution for many respects: it potentially reduces the wiring burden as seen above, it creates miniaturized electronics that can help constrain the total size and weight of a quantum computer, it has the potential to minimize the control/readout/processing cycle latency and its energy consumption can be much smaller than room temperature electronics.

If the cryo-electronics components are not at the same stage as the qubits, you'll still need some (expensive superconducting) wiring. And it has a significant indirect energetic cost. These cryo-electronics components generate heat that must be extracted from the cryostat. As you get in the lower cryostat stages, its cooling power gets drastically reduced proportionally to T^4 , T being the cryostat stage temperature.

The current cooling budget at 15 mK is lower than 40 μ W and goes up to 1W at the 4K stage. You can still bet on the creation of larger cooling power cryostats but their energetic cost will skyrocket. It explains why some cryo-electronics components are designed to stay at intermediate stages (2K to 4K). This balance depends also on the qubit operating temperature.

For superconducting qubits, the constraint is much bigger than with spin/silicon qubits which could operate at higher temperatures (100 mK to 1K). Recent modelling did show that for superconducting qubits, the control electronics energetic cost is surprisingly optimized with room temperature electronics¹³⁷⁵.

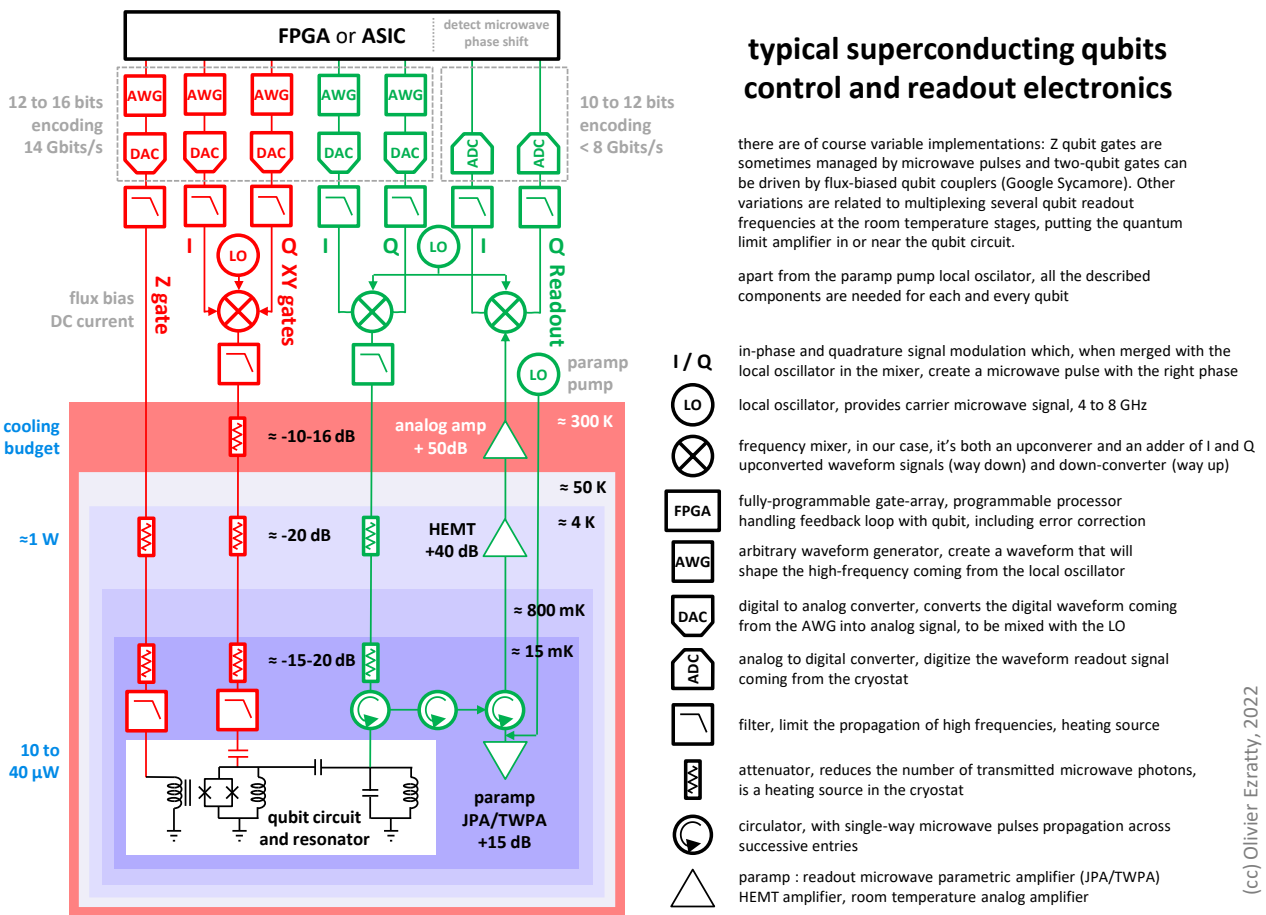


Figure 480: description of the various electronic tools that control superconducting qubits. (cc) Olivier Ezratty, 2022.

¹³⁷⁵ See [Optimizing resource efficiencies for scalable full-stack quantum computers](#) by Marco Fellous-Asiani, Jing Hao Chai, Yvain Thonnart, Hui Khoon Ng, Robert S. Whitney and Alexia Auffèves, arXiv , September 2022 (39 pages)

Control electronics and qubit fidelities. The relation between qubit fidelities (one and two qubit gates + idling + qubit readout) and control electronics precision has been widely studied. A paper from Intel and Dutch researchers from 2019 did show this correlation and created a model to reach 99,9% fidelities for all these operations. With solid state qubits, two sorts of control signals are generated: DC pulses and waveformed pulses in the microwave regime.

There's a clear link between qubit fidelities and the precision of microwave signal generation with regard to their duration, amplitude, frequency and phase. It demonstrated that it was a reachable goal for state of the art classical room temperature electronics¹³⁷⁶. The noise affecting qubits and coming from control electronic comprises many aspects: phase noise coming from source clock jitter feeding the master and local oscillators, AWGs and DACs originated harmonics, leakage signals from mixers, various amplitude signal to noise ratios (SNR) and noise coming from reference voltage sources like the BVGs (bias voltage generators) that are used to generate DC pulses.

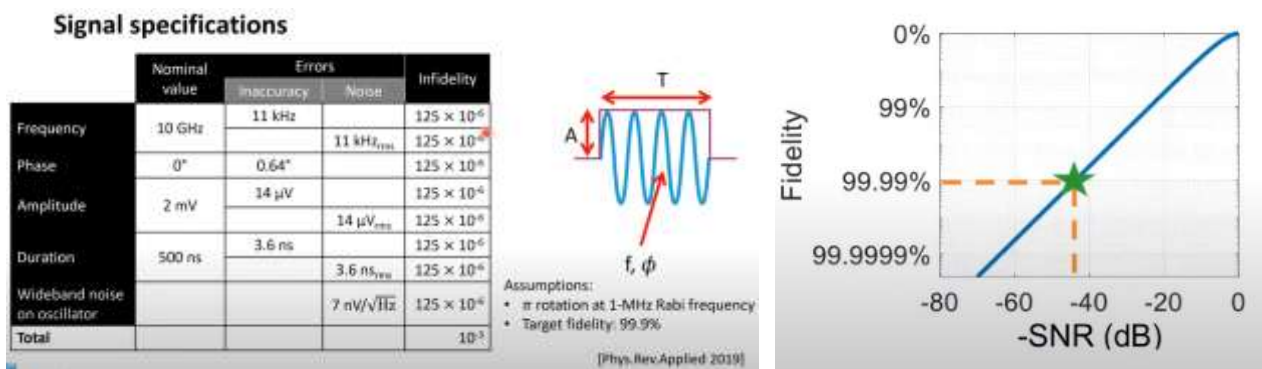


Figure 481: specifications of a qubit control microwave pulse and of the infidelity sources. Data source: [Impact of Classical Control Electronics on Qubit Fidelity](#) by J.P.G. van Dijk, Menno Veldhorst, L.M.K. Vandersypen, E. Charbon, Fabio Sebastiano et al, PRA, 2019 (20 pages).

Various improvements are thus sought in qubit control electronics:

LO Phase Noise. The local oscillators used in the AWG (arbitrary waves generators) must have a reasonable phase noise¹³⁷⁷. Phase error noise becomes important as qubit fidelities are improved with better control of environmental sources of decoherence. Lab-grade oscillators may already limit the performance of qubits having microsecond scales gate times, like with trapped ions. Thus, the need to use low phase noise high precision local oscillators instead of traditional lab-grades LOs.

Table 2. Time until a qubit physical error rate p is reached solely due to phase fluctuations in the LO

| Time to Reach LO-Induced Error Rate p | | | | | |
|---|-----------|-----------|-----------|-----------|-----------|
| p | 10^{-3} | 10^{-4} | 10^{-5} | 10^{-6} | 10^{-7} |
| Lab-Grade LO | 4.0 μs | 900 ns | 200 ns | 30 ns | < 10 ns |
| Precision LO | > 100 ms | > 100 ms | > 100 ms | 80 ms | 600 μs |

These times may be viewed as an upper bound on the allowable QEC cycle period. Achievable cycle periods will be reduced because of other error sources. Error rates are derived from free-evolution calculations presented in Figure 2b. Driven operation error rates (see Figure 2c) yield similar results.

Figure 482: [The role of master clock stability in quantum information processing](#) by Harrison Ball et al, NPJ Quantum Information, November 2016 (8 pages)

There's a 10^{-4} difference in phase noise errors between lab-grade and precision LOs! Given superconducting gates time span 10 ns to 600 ns, a 10^{-5} error rate only due to LO phase noise could be reached during this time. We're not far from the required threshold for QEC!

¹³⁷⁶ See [Impact of Classical Control Electronics on Qubit Fidelity](#) by J.P.G. van Dijk, Menno Veldhorst, L.M.K. Vandersypen, E. Charbon, Fabio Sebastiano et al, PRA, 2019 (20 pages).

¹³⁷⁷ See [The role of master clock stability in quantum information processing](#) by Harrison Ball et al, NPJ Quantum Information, November 2016 (8 pages) and [A 2–20-GHz Ultralow Phase Noise Signal Source Using a Microwave Oscillator Locked to a Mode-Locked Laser](#) by Meysam Bahmanian and J. Christoph Scheytt, 2021 (11 pages).

Low Latency control/readout cycles. There's also a need to minimize the duration of the qubit control and readout cycle. It minimizes the impact of the errors that can happen during the cycle due to decoherence, enabling a higher quality QEC. The quantum feedback latency must be several orders of magnitude under superconducting qubits coherence times that are in the range of 50 μ s to 100 μ s, and could potentially exceed 1 ms. So, we're in for a maximum of a few 100 ns.

The control system must also be well synchronized across all qubits, which can be achieved with a distributed synchronous clock and trigger architecture¹³⁷⁸. Labs also makes use of spectrum analyzers. Another feedback loop optimization comes with handling qubits gates AWGs, their DACs and readout data acquisition in the same FPGA¹³⁷⁹.

From FPGA to ASIC. At this point, the most advanced qubit control systems are FPGA based. Their advantage is sound economics for small scale use cases but at an energetic cost. Using CMOS ASICs could bring some energetic advantage on top of further reducing control cycle latency, but it has a significant cost few qubit developers can afford at least in research labs. Also, the ASIC design and manufacturing cycle is much longer than with an off-the-shelf FPGA board.

Memristors DC control. A Canadian-French team proposed to control spin qubits quantum-dot gate biases with DC sources with a cryogenic solution using Al₂O₃-TiO₂-based tunable memristors with a ± 1 V range and 100 μ V resolution. Memristors are non-volatile systems with tunable resistance. It fits the need to tune these DC pulses due to qubits variability. It was demonstrated at 4.2K¹³⁸⁰. It doesn't support the other needed type of electronic controls, microwave pulses, that are needed to drive single qubit gates. This solution simplifies the DC wiring between room temperature control electronics and the 4K stage in the cryostat, but it still requires DC lines between this stage and the qubits chipset at below 1K. These memristors are dissipating 1.77 mW. As a result, a current generation cryostat with 1.5W cooling power at 4.2K could accommodate about 800 such memristors. We're still far from the LSQ realm.

Pulse control optimization. At the software level, pulse control can benefit from some optimization techniques, requiring a verticalized approach crossing the usual layers between high-level gate-based code and pulse control. Such cross-layers optimizations are proposed by IBM and Q-CTRL¹³⁸¹.

Consolidated projects. Several qubit control and electronics research and development projects were recently launched in Europe. In Germany alone, you have three related projects:

QuMIC (Qubits Control by Microwave Integrated Circuits, 6,3M€, 2021-2024) which involves four academic and two industry partners (Infineon, Supracon AG) and deals with miniaturization of RF electronics to control superconducting and trapped ions qubits.

qBriqs (2M€, 2021-2024) which also involves four academic and two industry partners (Rosenberger and Stahl Electronics) and deals with compact cryogenic connectors, qubit readouts TWPA and HEMT amplifiers, filters and attenuators, DACs and ADCs and DC flux current generators.

¹³⁷⁸ In [FPGA-based electronic system for the control and readout of superconducting quantum processors](#) by Yuchen Yang et al, USTC China and Alibaba, February 2022 (12 pages), a Chinese team describes how it implemented such a system, to control 2 qubits for a starter. It's based on using FPGAs in 3U (3 units heights in electronics racks) PXIe modules, the instrumentation equivalent of the PCIe bus used in microcomputers and created by National Instruments in 1997. As an example, the 3U PXIe-1095 below has 18 slots. The team used a FS725 Rubidium Clock running at 10 MHz with ultralow phase noise, coming from Stanford Research Systems (1980, USA). They are also using the physical layer "Low Voltage Differential Signaling" system (LVDS) which has a low latency.

¹³⁷⁹ See [Hardware for multi-superconducting qubit control and readout](#) by Zhan Wang et al, 2021 (11 pages). In this work, the feedback latency reached 178.4 ns. It's using a 28 nm Xilinx XC7K325T FPGA with 326K logic cells.

¹³⁸⁰ See [Memristor-based cryogenic programmable DC sources for scalable in-situ quantum-dot control](#) by Pierre-Antoine Mouny et al, March 2022 (13 pages).

¹³⁸¹ See [Summary: Chicago Quantum Exchange \(CQE\) Pulse-level Quantum Control Workshop](#) by Kaitlin N. Smith, February 2022 (17 pages).

HIQuP (2021-2024, 2,2M€) with, again, four academic and two industry partners (Supracon AG and IQM Germany) which works on superconducting and cryogenic qubit control electronic circuits.

In France, the **QRYOlink** project combines CEA-Leti and Institut Néel from Grenoble, Radiall, ATEM, Air Liquide, C12 and Alice&Bob to develop a scalable architecture for cryogeny and cabling aimed at supporting solid-state qubits. Other related projects also cover scalable control electronics targeting large scale quantum computing architectures.

Room temperature electronics

Room temperature electronics is the dominant solution used both in research labs and with most commercial vendors (IBM, Google, Rigetti, IQM, etc).

The key components are on the way in for each and every qubit:

- **AWGs** (arbitrary waveform generators) which create microwaves pulse forms and usually generate about 2 GigaSamples/s. These are used to create single qubit gates and also readout pulses. Alternative techniques are proposed which generate pulses width modulation (PWM) that would be less costly without jeopardizing qubit fidelities ¹³⁸².
- **DACs** (digital to analog converters) who use a 14-bit to 16-bit amplitude resolution to convert into analog format the output of the AWGs.
- A **mixer** of the waveform and a **LO** (local oscillator) signal in the used microwave range (around 5 GHz for superconducting qubits). The output is called a “heterodyne” signal.
- Some **direct current** sources to drive certain types of qubit gates *aka* bias drives.

Since we mentioned heterodyne measurement, let’s make a pause with describing the three main different techniques used to measure an electromagnetic signal with homodyne measurement (one observable), heterodyne measurement (two orthogonal observables like in-phase and quadrature) and photon measurement or counting. These three techniques are used for optical frequencies photons and radio-frequency photon signals, with, of course, many differences and variations.

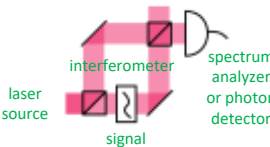
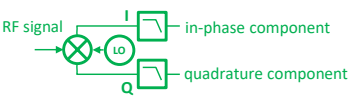
| | homodyne measurement | heterodyne measurement | photon counting |
|-----------------------|---|---|---|
| definition | extracts information encoded as modulation of the phase and/or frequency of an oscillating signal with comparing that signal with a standard oscillation carrying no information. | extracts information along two orthogonal components in phase space like, for RF signals, the in-phase and quadrature signals coming out of an I/Q mixer, use a reference oscillator source (LO). | measure the excitation quanta as degree of freedom in an electromagnetic signal |
| process |  |  | |
| pros/cons | better precision | more information but less precision | photon losses |
| output data | signal phase or frequency, signal spectrum | signal quadrature (in-phase and quadrature) | number of superposed photons or the presence of photons |
| implementation | homodyne interferometry | RF I/Q mixer, heterodyne interferometer, I/Q components analysis with ADC+digital signal processing | photodetection with SPAD, SNMPD, FMCW lasers, ... |
| use cases | QKD detection with balanced homodyne detection (BHD) | qubit microwave readout processing, CV photon qubits readout | DV photon qubits readout |

Figure 483: explanation of the various ways to detect a photon or electronic signal with homodyne and heterodyne measurement and photon counting. (cc) Olivier Ezratty, 2022.

(cc) Olivier Ezratty, 2022

¹³⁸² See [Quantum Optimal Control without Arbitrary Waveform Generators](#) by Qi-Ming Chen et al, Aalto University, Princeton and Tsinghua University, September 2022 (14 pages). The paper however doesn’t provide some indications of the associated power savings.

On the way out of the cryostat, we have:

- A last-stage **analog amplifier**, following the cryogenic amplification stages (TWPA and HEMT).
- **ADCs** (analog to digital converter) of the readout microwave signal, usually with a 1 GigaSamples/s sampling rate and a 8 to 12-bit encoding.
- **SoC** (systems on chip), **FPGA** or **ASIC** circuits used to interpret the output of the ADCs to get the qubit state, and which may manage a closed-loop control of the whole cycle to implement error correction (QEC).

All these components are more or less integrated in one or several boxes, or boxes with interchangeable modules. The FPGAs are programmable, usually with Python and some extension (library or language extension).

This field is well covered by electronics industry vendors addressing research and commercial quantum computing markets. Beforehand, many quantum computing research laboratories were relying on generic micro-wave generator and readout systems coming from vendors like **Rohde & Schwarz**, **Tektronix** and **Keysight**¹³⁸³. Over time, some of these vendors have developed specialized offerings for quantum computing, particularly through some acquisitions (for Rohde & Schwarz and Keysight). Specialized quantum computing electronics emerged like **Zurich Instruments**, **Qblox** and **Quantum Machines**. Large shops like **Google** also developed their own electronics.

Some hardware and software open source control systems have also been proposed like the **QICK** (Quantum Instrumentation Control Kit) from Fermilab¹³⁸⁴ and **QubiC** from Lawrence Berkeley National Lab, both from the DoE¹³⁸⁵. They are cost efficient when compared to commercial solutions and adapted to the needs of research labs. These kits are all based on Xilinx FPGAs containing their own DACs and ADCs. Researchers from Chalmers and KTH in Sweden created **Presto**, a fully integrated room-temperature system on chip using a Zynq UltraScale+ RFSoc from Xilinx with full control operations for superconducting qubits¹³⁸⁶.



Zurich Instruments (2008, Switzerland, \$112K) is a manufacturer of electronic test and measurement equipment, including a range of microwave generation and analysis tools.

The company was acquired by Rohde & Schwarz in July 2021. Their offer is built around their Quantum Computing Control System, which bridges the gap between the quantum computer software control tools and the associated electronic instrumentation.

This system consists of several components.

¹³⁸³ Tektronix provides an AWG that can be used to drive qubit signals, the 16-bit AWG5200 supporting up to 32 output channels with 2 Gbits/s sampling (and local oscillator frequency go up to 5 GHz) and the 6 Series Low Profile Digitizer for 4-channel qubits readout (up to 8 GHz).

¹³⁸⁴ See [The QICK \(Quantum Instrumentation Control Kit\): Readout and control for qubits and detectors](#) by Leandro Stefanazzi et al, Fermi Lab, Princeton University, Seconda Università degli Studi di Napoli, GE Healthcare Institute, CNEA - Argentina, and University of Chicago, March 2022 (15 pages). It's based on Xilinx based RFSoc (Radio-Frequency System-on-chip) ZCU111 Evaluation Kit with a Xilinx XCZU28DR FPGA containing 8 14-bit DAC and 8 12-bit ADC. This is an "hybrid FPGA" with a programmable logic part and a more classical SoC part with a quad-core Arm Cortex A53 cores, various I/Os and memory. It supports microwaves output up to 6 GHz. The toolkit is programmed in Python. The QICK power consumption is 50 W and it seems able to drive 4 qubits. It could support up to 100 qubits with frequency domain multiplexing.

¹³⁸⁵ See [QubiC: An Open-Source FPGA-Based Control and Measurement System for Superconducting Quantum Information Processors](#) by Yilun Xu, Irfan Siddiqi et al, Lawrence Berkeley National Laboratory and University of California at Berkeley, September 2021 (11 pages). QubiC uses a Xilinx Virtex-7 FPGA and separate DACs and ADCs from the Abaco Systems FMC120 and its four 16-bit ADC and four 16-bit DACs. The conversion circuits come from Texas Instruments (ADS54J60 ADC and DAC39J84).

¹³⁸⁶ See [Measurement and control of a superconducting quantum processor with a fully-integrated radio-frequency system on a chip](#) by Mats O. Tholén et al, Chalmers, May-October 2022 (14 pages). This type of chipset has a power drain of at least 70W ([source](#)). It seems it can handle about 8 qubits in total in a 2U 19-inch package.

First, the PQSC (Programmable Quantum System Controller, left of Figure 484 which is used to program and control all the devices. It is equipped with a Xilinx UltraScale+ FPGA that can be driven by the LabOne software using Python, C, MATLAB, LabVIEW and Microsoft's .NET framework. It controls up to 18 HDAWG (High-Density Arbitrary Waveform Generator, in Figure 484 *in blue*) microwave generators and manages up to a hundred qubits. LabOne became LabOne Q in October 2022 with some extensions easing the setting and optimization of Zurich Instruments tools.

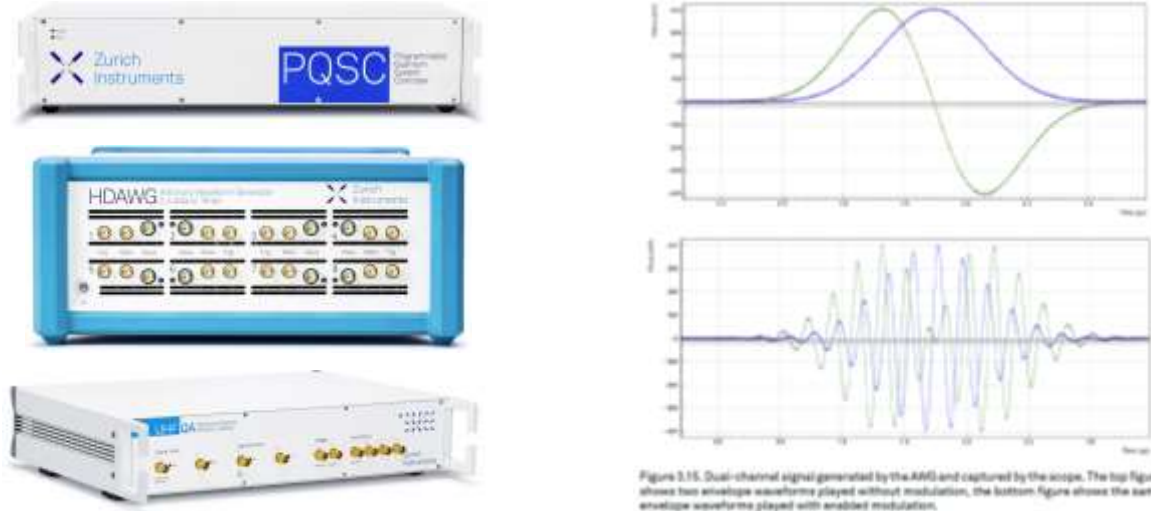


Figure 484: Zurich Instruments PQSC and UHFQA for qubit control and readout. On the right, the types of microwave pulse signals generated. Source: Zurich Instrument product documentation.

These are sold at 23K€. These generators create microwave pulses that combine a waveform (Gaussian or other, in Figure 484 *on the right*) modulated by a high-frequency signal, usually between 5 and 10 GHz, adapted to superconducting qubits drive and readout. It can control up to 8 channels. These microwaves are sent to the qubits to reset them to zero, activate quantum gates or handle state readout. The single-qubit quantum gates are generated by sending a modulated microwave that modifies the energy level of the qubits and change its state.

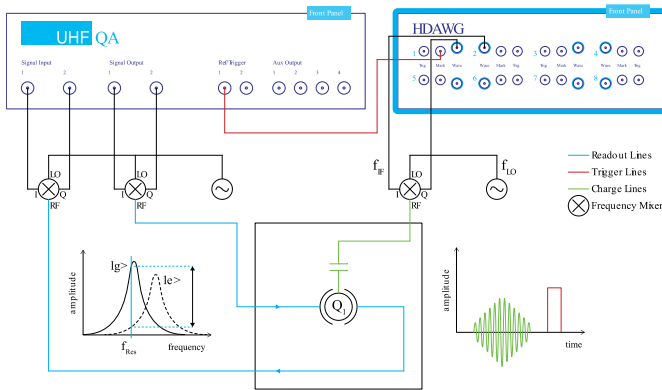


Figure 485: UHFQA and HDAWG cabling. Source: Zurich Instruments.

This is complemented by the UHFQA (Ultra-High Frequency Quantum Analyzer) which can analyze the readout state of 10 qubits. In the diagram, F_{LO} is the frequency of the microwave signal to be modulated and F_{IF} is the modulation waveform.

On the UHFQA side, the system detects the modulation or phase modification of the signal recovered through a resonator associated with the qubits, I_g and I_e respectively for ground states and excited states.

In April 2021, Zurich Instruments launched a new signal generator, the SHFSG with better microwaves signal spectral purity and stability. It can handle up to 144 qubit control channels and is accommodated with 4 or 8 channels, controlling up to 8 qubits. In August 2022, they introduced their SHFPPC (Super High Frequency Parametric Pump Controller), a room temperature tone pulse generator that feeds the parametric amplifiers like the TWPAs sitting at the lowest stage of the cryostat.



Figure 486: an SHFQC can control up to 16 qubits.

It was then completed by the software reconfigurable and programmable SHFQC launched in November 2021, which bundles 6 signal generator control channels and a readout channel analyzer supporting up to 16 qubits. Several SHFQC can be combined to support up to 100 qubits and “beyond”.



Qblox (2018, Netherlands, \$5M) is a spin-off from QuTech that develops scalable control electronics for superconducting qubits. Their latest generation controls up to 20 qubits with a 4U rackable system.

These clusters consume about 1 kW. The device contains both micro-wave generators for qubits gates (QCM module, blue) and qubits readout and electronics for qubit readout (QRM module, white). Each unit relies on small custom FPGAs. In a classical manner, it creates waveforms mixed with a microwave carrier signal after DAC conversion. Readout uses an ADC and a phase detection system.



Figure 487: this Qblox system can control up to 20 qubits.

Their DACs/ADCs have a high sampling rate of 16 bits. A high sampling rate is important to create precise waveformed microwaves. This precision is a way to ensure a good fidelity for qubit gates generated by these generated microwave pulses.

Their architecture could scale up to controlling 1000 superconducting qubits. Calibration is done with the help from **Orange Quantum Systems** and cabling comes from **Delft Circuits**, two other spin-offs of QuTech in the Netherlands.

They also sell the desktop Pulsar QRM (quantum readout module) that handles a few qubits control in small factor format. As their Cluster modules, these can be coupled and synchronized together with using their homegrown protocols SYNQ (synchronized start within $\ll 1$ ns) and LINQ (distributing measurement outcomes in < 200 ns).



Quantum Machines (2018, Israel, \$100M) provides a qubit control layer for superconducting quantum computers that combines hardware and software¹³⁸⁷. It is a spin-off from the Braun Center for Submicron Research Laboratory at the Weizmann Institute.

They developed their own classic qubit control processor, an FPGA operating at room temperature, which generates the pulses for controlling qubits and measuring their states either with microwaves and lasers¹³⁸⁸. Packaged as their OPX/OPX+ systems, it supports superconducting, electron spin, NV centers, trapped ions and cold atoms qubits. In March 2022, they announced the availability of Octave.



Figure 488: OPX+ is a full-stack solution for qubit control and measurement, enabling closed-loop error correction.

¹³⁸⁷ See [The Story of the First Israeli Quantum Computing Startup](#) by Eliran Rubin, December 2018.

¹³⁸⁸ See the video [MLQ2021 Session Th2: Quantum Machines](#), March 2021 (46 mn) explaining their process.


It is a compact and rack-mountable all-in-one RF up/down-conversion module which completes their OPX systems. It contains its own built-in Local Oscillator (LO) sources and provides continuous self-calibration features.

They already have more than a dozen customers, including, in France, ENS Paris, ENS Lyon, Alice&Bob and Pasqal (just in France...). The company was created by Itamar Sivan (CEO, who did a Master's degree at the ENS Paris between 2009 and 2011), Yonathan Cohen (CTO, former Weizmann Institute managing director) and Nissim Ofek (Chief Engineer, who had a post-doc position in Rob Schoelkopf's lab in Yale University where he developed a FPGA based control and QEC code).

They also partner with Q-CTRL which develops qubits firmware level control software. Their processor is integrated into their "Quantum Orchestration Platform", which also combines a software layer¹³⁸⁹. In June 2020, they announced the creation of the **QUA** language, positioned as a language for creating hybrid quantum and classical algorithms, such as VQE and QAOA, which need rapid feedback between classical and quantum processors. This programming language works with all types of qubits, superconductors, silicon, cold atoms and trapped ions. The compiler thus takes into account the differences in the implementation of qubits: their connectivity, the homogeneity or heterogeneity of their coupling, the coherence times, the error rates, etc.

In April 2022, Quantum Machines, together with their customers Alice&Bob, Benjamin Huard's team from ENS Lyon and Florian Marquardt of the Max Planck Institute for the Science of Light in Germany, announced the launch of [Artemis](#), a 3-year EU funded project (900K€) as part of QUANTERA to use a real-time neural network to improve the accuracy of quantum controls and quantum error correction. It will lead to the creation of a full-stack QEC universal quantum controller. It will be complemented by an (unspecified) cloud-based quantum processor.

In March 2022, Quantum Machines made the acquisition of QDevil (Denmark) which gives them a foothold in the cryogenic electronics space with filters and a low noise DAC. The company had a total staff of 80 as of March 2022.

 **KEYSIGHT** **Keysight Technologies** (USA) is an electronics measurement company spun-out of Agilent in 2014, which itself was coming from Hewlett Packard in 2000.

It then expanded its portfolio through several acquisitions: Signadyne (FPGA-based PXI digitizers and AWGs) in 2016, Ixia (software), Liberty Cal (calibration services) and ScienLab (test solutions in eMobility systems) in 2017, Labber Quantum in 2019 (MIT spun-out specialized in qubits control and software) and Quantum Benchmark in 2021 (quantum error diagnosis and suppression, and benchmarking software). The company has now a broad portfolio of measurement and control electronic systems widely used in the quantum real, in its three markets: computing, sensing and communications, including optical instruments. Most quantum research labs already have some Keysight test and measurement systems. In qubits control electronics, they provide pulse laser controls, basebands pulse controls and pulsed microwaves controls (AWGs like the M3202A PXIe Arbitrary Waveform Generator with 1 GSa/s, 14 bit sampling, DAC) as well as ADCs for qubit readout (like the M3102A 14-bit PXIe Digitizer). Interestingly, they address one source of electronics signals quality variability: the fluctuating room temperature. Thus, a solution to control rack temperature with air flow operating at 35°C.

¹³⁸⁹ See [Quantum Machines raises \\$17.5M for its Quantum Orchestration Platform](#) by Frederic Lardinois, March 2020, [Israel gets ready to join global quantum computing race](#) by Amitai Ziv, December 2019 and [The quantum computer is about to change the world. Three Israelis are leading the revolution](#) by Oded Carmeli, February 2020.

Their Quantum Control System which assembles various software and hardware components to drive single and multi-qubit lab experiments. The hardware part is the Quantum Engineering Toolkit (QET) and contains a PC workstation with a PXIe Interface Module, a PXIe chassis containing an AWG, a DAC, and In-Phase and Quadrature modulator and demodulator, a Vector Signal Generator and other optional electronics. Among other places, this toolkit is used since 2020 at the MIT EQuS (Engineering Quantum Systems Group) testbed.

Keysight is involved in several quantum computing related projects like the Boulder Cryogenic Quantum Testbed launched in 2019, a joint effort of Google, the NIST and the University of Colorado Boulder, housed in the JILA laboratory on the CU Boulder campus. It helps US researchers working on superconducting qubits at the characterization level. The lab is equipped with a 10 mK Janis JDry 250 mini dilution refrigerator. They also participate to MATQu, an EU funded German project which ambitions to produce superconducting qubits on 300 mm silicon-based process flows.

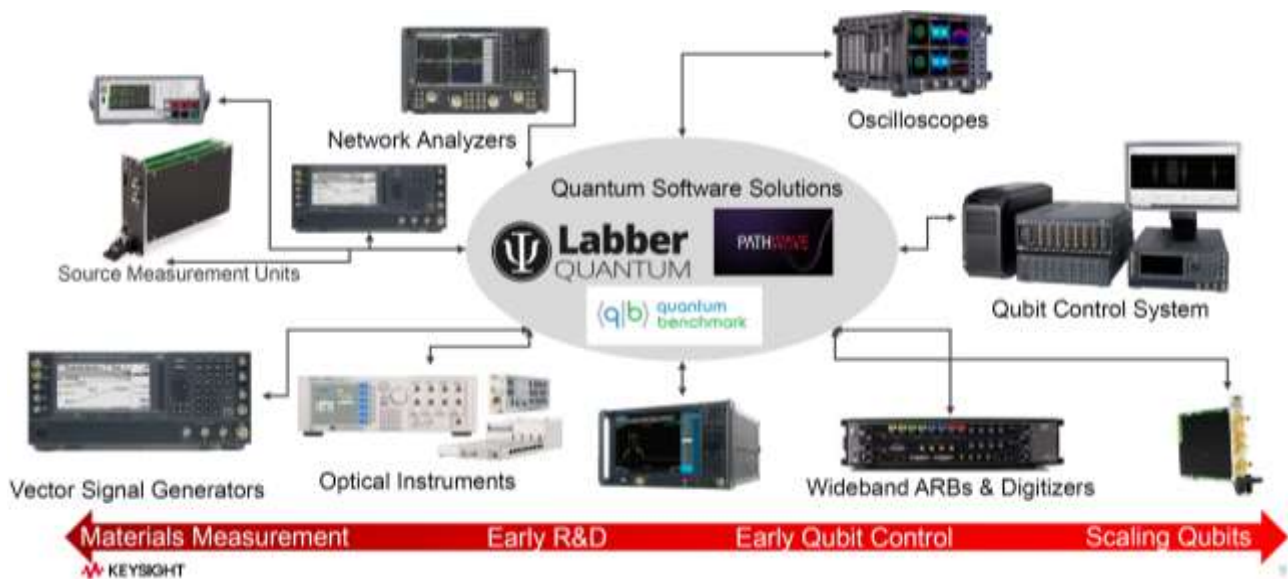


Figure 489: the Keysight control electronics family, mostly used in research laboratories.

Keysight hardware is also used in quantum sensing (AWGs, ADCs, DACs, analog signal generation, measurement of current-voltage (“I-V”) and capacitance-voltage (“C-V”), oscilloscopes) and CV-QKD signal generation and detection (with waveform/pattern generation, oscilloscopes, lightwave detectors and variable optical attenuators). In the vendors space, they partner with IBM on Qiskit Metal, an open source software solution to design your own superconducting qubits to understand qubits crosstalk effects.

In most of their solutions, Keysight uses Xilinx FPGAs but it also has its own cleanroom facilities to design custom ASICs, like in photonics. They plan to implement control electronics with cryo-CMOS only in the long term, after 2030-2040. Until then, classical electronics will make the job.

Keysight announced in June 2022 its new generation of qubit control electronics, Quantum Control System (QCS), based on a proprietary ASIC integrating microwave signals AWGs, 14-bit DACs and 12-bit readout ADCs with the effect of reducing phase jitter in the generated signals and enabling fast closed-loop quantum error correction. It is packaged in PXIe cards format and a 4U box can control 20 qubits. It is completed by a Python API. It seems to be the first offering of this type with some ASIC drive components. The readout lag is only 20 ns, from the reception of the readout microwave to outputting its result. The first announced customers of QCS are Alice&Bob and Rigetti.



Figure 490: Keysight PXIe Quantum Control System.

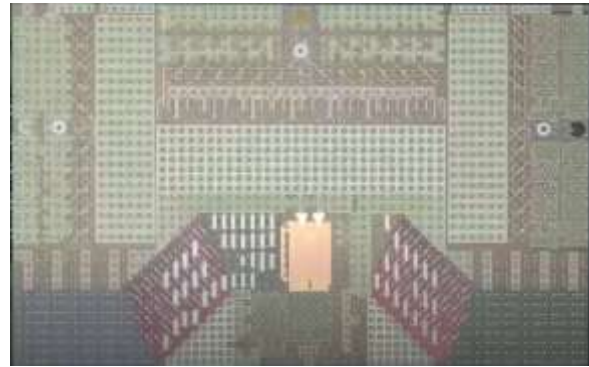


Figure 491: Keysight's first ASIC to control qubits.



QuantrolOx (2021, Finland-UK, \$1.4M) is an enabling technology company creating a deep learning software solution to optimize the automatic tuning and optimization of qubits settings¹³⁹⁰.

Their solution that was developed with the help from DeepMind is using small training data sets and works in two steps: one with coarse tuning and a second with fine tuning. It efficiently adjusts the parameters of a large number of qubits and is applicable to all sorts of qubits but particularly with those who express the largest variability like superconducting and electron spins qubits. The company has already about a staff of 10 including Vishal Chatrath (CEO, UK), Andrew Briggs (Executive Chair, UK, Professor of Nanomaterials, University of Oxford), Natalia Ares (Chief Scientist, UK, with a strong background on quantum thermodynamics and machine learning, Professor at University of Oxford), Dominic Lennon (Head of Quantum Technologies, UK, also from Oxford University) and Juha Seppä (CTO, Finland). Mostly based in the UK, the startup is positioned as a Finish one, maybe to make it easier to get some EU funding! Their first investors are Nielsen Ventures, Hoxton Ventures, Voima Ventures, Remus Capital, Hermann Hauser (cofounder of Arm) and Laurent Caraffa.

We can also mention a Chinese project, a superconducting microwave generator for the control of superconducting qubits based on a Xilinx FPGA¹³⁹¹. In other similar and older projects, China's research teams showcased scalability claims that were not really sustained by a real scalable architecture¹³⁹².



Active Technologies (2003, Italy) is a spin-off of University of Ferrara creating AWGs and Pulse/Pattern Generators. It can control experimental solid state qubits as well as electro-optical and electro-acoustic modulators used with cold atoms qubits. Its flagship product is the AWG-5000, a fast 16-bit AWG with 8 output channels.

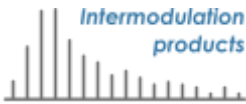


CIQTEK (2016, China, \$15M) aka Guoyi Quantum develops high-precision pulse generator (ASG) and arbitrary waveform generator (AWG) used in qubits control, electron parametric resonance spectrometers and scanning electron microscopes. They also manufacture NV centers-based magnetometers and <Diamond I>, a 2-qubit computing system for educational purpose. It is based in Hefei and has 500 employees.

¹³⁹⁰ See [Machine learning as an enabler of qubit scalability](#) by Natalia Ares, Nature, 2021 (3 pages) and [Learning Quantum Systems](#) by Valentin Gebhart, Natalia Ares et al, July 2022 (26 pages) which provides a broad view on machine learning use-case for various types of qubits quantum error mitigation.

¹³⁹¹ See [Scalable and customizable arbitrary waveform generator for superconducting quantum computing](#) by Jin Lin, 2019 (9 pages).

¹³⁹² See [High Performance and Scalable AWG for Superconducting Quantum Computer](#) by Jin Lin et al, 2018 (5 pages).



Intermodulation Products (2018, Sweden) is a spin-off company of KTH, the Royal Swedish Institute of Technology. They market Vivace, a microwave generator in the 4 GHz band used to drive superconducting qubits.



Quaxys (2020, USA) provides hardware and software solutions for superconducting and spin qubits electronic control, including Quantuware 4840, a compact qubit control and measurement unit.



Teledyne E2V (USA/UK/France) is a designer, manufacturer and provider of DACs and ADCs circuits used for microwave processing with superconducting qubits, noticeably with IBM. These are designed and manufactured near Grenoble, France.

VIQTHOR (2022, France) is a stealth startup aiming to create scalable room temperature control electronics solutions for solid state qubits.

Cryo-CMOS

Cryo-electronics sit inside the cryostat, control the qubits and manage their readout in place of the some of the external electronic devices we're just covered, totally or partially depending on the systems generation. Many research team and industry vendors are working on this strategic set of technologies which may help to unlock qubit scalability. We have among others the **University of Sidney**, **TU Delft** in the Netherlands¹³⁹³, **VTT** in Sweden, **CEA-Leti** and **CNRS Institut Néel** in France, **POSTECH** in South Korea and US vendors like **Intel** and **IBM**. Cryo-electronics could help save a lot of quite expensive and embarrassing cabling, filters, attenuators, amplifiers, and reduce thermal losses in the cryostat. It can also contribute to shorten the qubit gate to qubit readout cycle which can fasten the execution of quantum correction codes that will be required when operating large scale quantum processors.

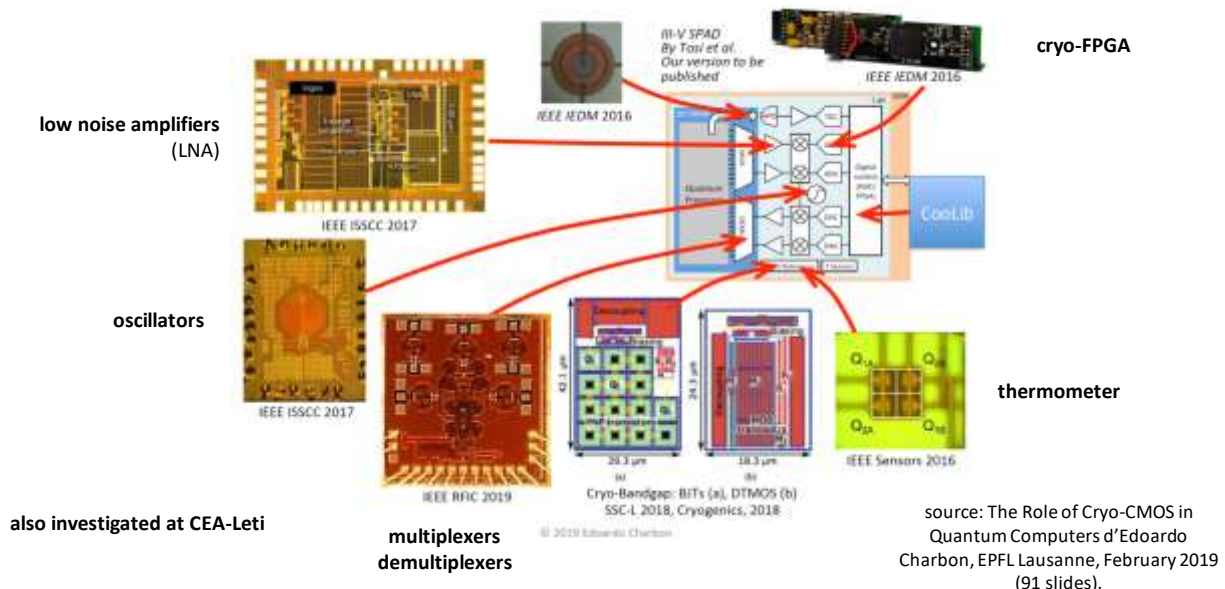


Figure 492: initially, research labs tried to build specific cryo component chipsets for many qubit control functions. Then, players like Intel tried to consolidate these in fewer components. There are still many components around, even with integrated cryo-CMOS for qubit control and readout, like the parametric amplifiers and HEMT. Source: [The Role of Cryo-CMOS in Quantum Computers](#) by Edoardo Charbon, EPFL Lausanne, February 2019 (91 slides).

¹³⁹³ See [Large-Scale Quantum Computers: The need for Cryo-CMOS](#) by Fabio Sebastiano, TU Delft, April 2021 (57 mn video).

It must meet rigorous specifications¹³⁹⁴. Figure 492 describes the variety of component functions that can be integrated in the 1K-4K stages and even, when possible, at the qubit chipset stage at less than 20 mK¹³⁹⁵. These components must be certified to operate at these temperatures. These are data multiplexers and demultiplexers, local oscillators, AWGs, DACs, ADCs, low-noise amplifiers, DC flux bias generators, thermometers and other various sensors.

The trend is to put within the cryostat a maximum of these electronic components. However, the heat they released is limited by the dilution refrigeration system cooling power¹³⁹⁶. It also conditions at which cold plate stage these components can operate. There's a complicated trade-off between the cryostat power overhead and what is saved by cabling and filters.

Starting in 2016, separate solid-state electronic components started to be designed and tested at cryogenic temperatures.

IMEC (Belgium) developed in 2020 a cryo-CMOS RF MUX multiplexing the in and out microwave signals used in qubit readouts and operating at 32 mK. Working at up to 10 GHz, it is suitable for superconducting qubits readouts and not yet for all electron spin qubits¹³⁹⁷. It greatly simplifies the cabling between RF control and readout electronics.

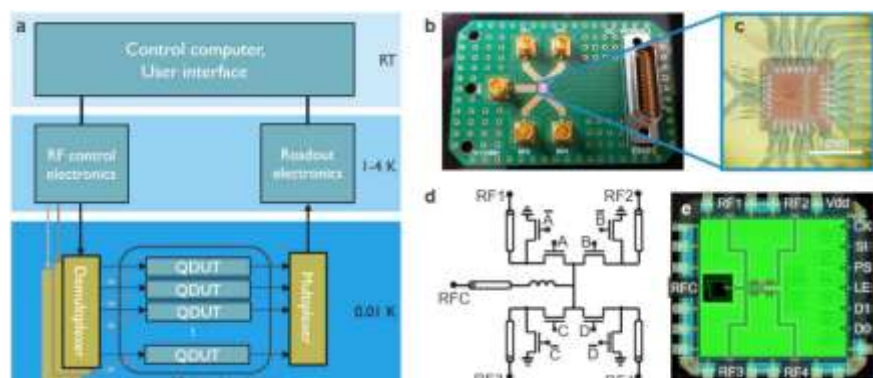


Figure 493: a qubit control multiplexing solution developed by IMEC. Source: [Millikelvin temperature cryo-CMOS multiplexer for scalable quantum device characterisation](#) by Anton Potočnik et al, IMEC, November 2020 (35 pages).

It sits at 4K and the qubit chipset sitting at below 20 mK. They created a similar solution operating at 15 mK in 2022 and suitable for time-domain microwaves multiplexing for the drive of superconducting qubits.

The trend is to integrate all these components in a minimum number of chipsets, preferably one, and working as close as possible to the qubits chipset. The best level of integration so far was reached with **Intel HorseRidge 2** announced in 2021 and the coldest operation was achieved with the **Gooseberry** chipset from **Microsoft** and the **University of Sidney** as well as with a cryo-CMOS from **CEA-Leti**.

¹³⁹⁴ See [Engineering cryogenic setups for 100-qubit scale superconducting circuit systems](#) by S. Krinner et al, 2019 (29 pages) which describes the issues with superconducting qubit control. In 2018, they proposed an optimized approach of wiring and electronics allowing up to 150 superconducting qubits to be embedded in a cryostat.

¹³⁹⁵ Source of the diagram: [The Role of Cryo-CMOS in Quantum Computers](#) by Edoardo Charbon, EPFL Lausanne, February 2019 (91 slides). See also an earlier work from Purdue University and Australian colleagues: [Cryogenic Control Architecture for Large-Scale Quantum Computing](#) by J. M. Hornibrook, 2014 (8 pages) which describes well what should be done where in the cryostat.

¹³⁹⁶ See [Cryogenic Control Beyond 100 Qubits](#) by Ian Conway Lamb, 2017 (103 pages) which describes the technological challenges of components operating at cryogenic temperature, here for superconducting qubits. And the short version: [Cryogenic Control Architecture for Large-Scale Quantum Computing](#) by Ian Conway Lamb et al, 2017 (8 pages). See also [Semiconductor devices for cryogenic amplification](#) by Damien Prêre, 2013 (30 slides) and [Cryo-CMOS Circuits and Systems for Quantum Computing Applications](#) by Bishnu Patra et al, 2018 (14 pages).

¹³⁹⁷ See [Millikelvin temperature cryo-CMOS multiplexer for scalable quantum device characterisation](#) by Anton Potočnik et al, IMEC, November 2020 (35 pages).

The first approach was to miniaturize these circuits at the 4K stage of the cryostat. It was studied in 2019 at **TU Delft** for silicon qubits state readout with their QuRO, for Quantum Read-Out¹³⁹⁸. The readout was using microwaves photon reflectometry. It sent an unmodulated RF frequency and evaluated the amplitude and phase of the reflected RF photon. The technique allows multiplexing qubits readout before sending the information out of the cryostat. This simplifies the output wiring. The prototype was based on a CMOS low noise amplifier (LNA) supplemented by a SiGe (silicon-germanium) transistor amplifier, followed by an analog-to-digital converter (ADC) implemented in a Xilinx Artix 7 FPGA. This FPGA made it possible to multiplex the readout state of several qubits. They use some copper cooling radiator in the 4K stage of the dilution refrigeration. They relied on standard market off-the-shelf passive and active components operating correctly at 4K. This prototyping did not deal with the waveform generation and DAC circuits driving qubit gates. The energy saving of this kind of system is related to the quantum error correction load on qubit measurement. Bringing readout electronics closer to qubits speeds up error correcting codes. It's also interesting for simplifying the connectivity and improving quantum computers scalability.

A similar approach was initially adopted by **Intel** in collaboration with **QuTech** for its 2020 HorseRidge superconducting and silicon qubits driver component capable of handling the microwave pulses of this frequency driver from 2 to 20 GHz. This component is sitting at the 4K stage of the cryostat¹³⁹⁹.

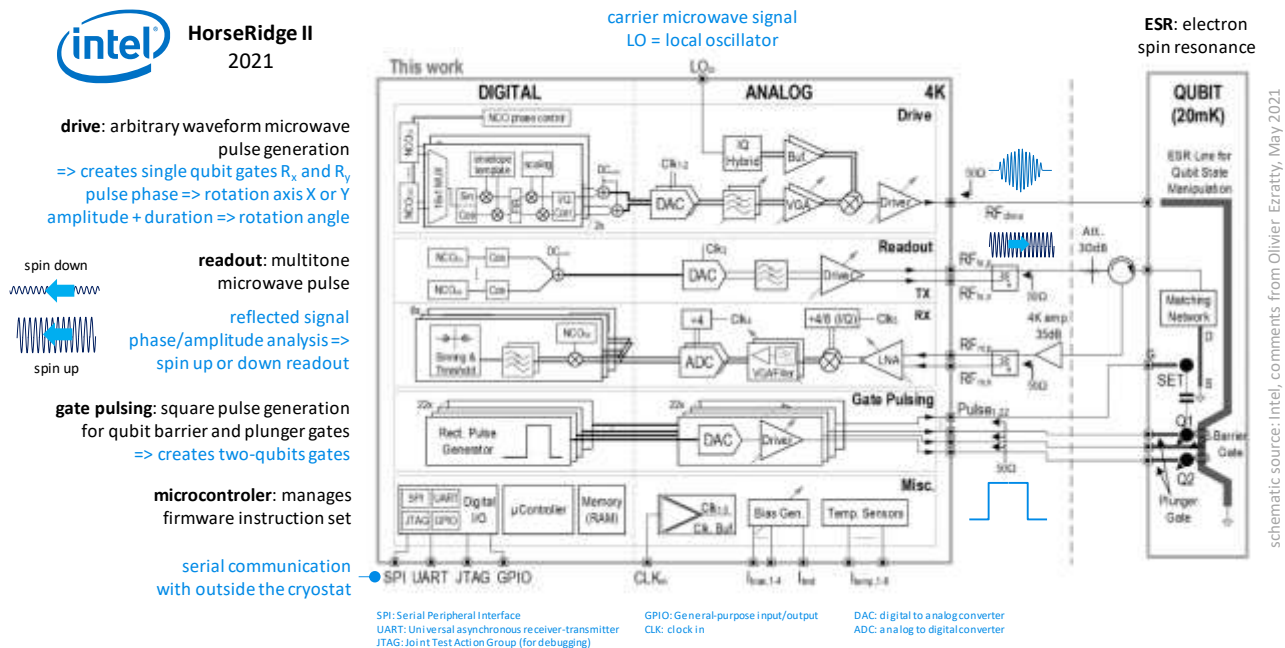


Figure 494: Intel HorseRidge 2 presented in 2021 is probably the most integrated qubit control chipset being developed. Source: [A Fully Integrated Cryo-CMOS SoC for Qubit Control in Quantum Computers Capable of State Manipulation, Readout and High-Speed Gate Pulsing of Spin Qubits in Intel 22nm FFL FinFET Technology](#) by J-S. Park et al, February 2021 (3 pages).

Introduced in 2021, **HorseRidge 2** improved cryo-electronics integration to an unprecedented level. It added multigate pulsing making it possible to control several qubits simultaneously, qubit readout and a programmable microcontroller. Gate pulsing create multi-qubit gates with square DC signals controlling the barrier and plunger gates of the quantum dots while single-qubit gates use modulated RF signals and qubit readout use regular RF signals. The chipset uses frequency multiplexing to reduce the number of RF cables for qubits drive and readout. It drives up to 16 spin qubits with frequency ranges between 11 and 17 GHz. It reads the state of up to 6 qubits simultaneously.

¹³⁹⁸ See [Cryogenic electronics for the read-out of quantum processors](#) by Harald Homulle, TUDelft, 2019 (185 pages).

¹³⁹⁹ See [Cryo-chip overcomes obstacle to large-scale quantum computers](#) by QuTech, February 2020.

The control chip contains 22 DACs to simultaneously control the gate potentials for many qubits. The chipset is manufactured in a 22nm low-power FinFET technology (22FFL), operates at 4K and contains 100 million transistors¹⁴⁰⁰. In May 2021, Intel and Qutech demonstrated high-fidelity two-qubit control with this HorseRidge 2 control chipset.

In 2022, **POSTECH** from South Korea proposed a similar architecture to HorseRidge 2 with a CMOS SoC sitting at 3.5K. It adds local oscillators¹⁴⁰¹. It was prototyped in 40 nm TSMC bulk CMOS and consumes about 15 mW per qubit.

In 2019, an American-Australian team from the **University of Sydney, Purdue University and Microsoft Research** designed Gooseberry, a CMOS circuit to control superconducting, electron spin or (yet to be seen) Majorana fermion qubits¹⁴⁰². Designed by David Reilly's team from the joint Microsoft Quantum Laboratories at the University of Sydney, it is operating at 100mK, just next to the qubit circuit on the same PCB support but without supposedly disturbing the qubits (in that case, only for silicon qubits since superconducting qubits would sit at the 15 mK cold plate stage). It seems to save power with a low sampling rate in AWG/DAC/DACs (4 bits).

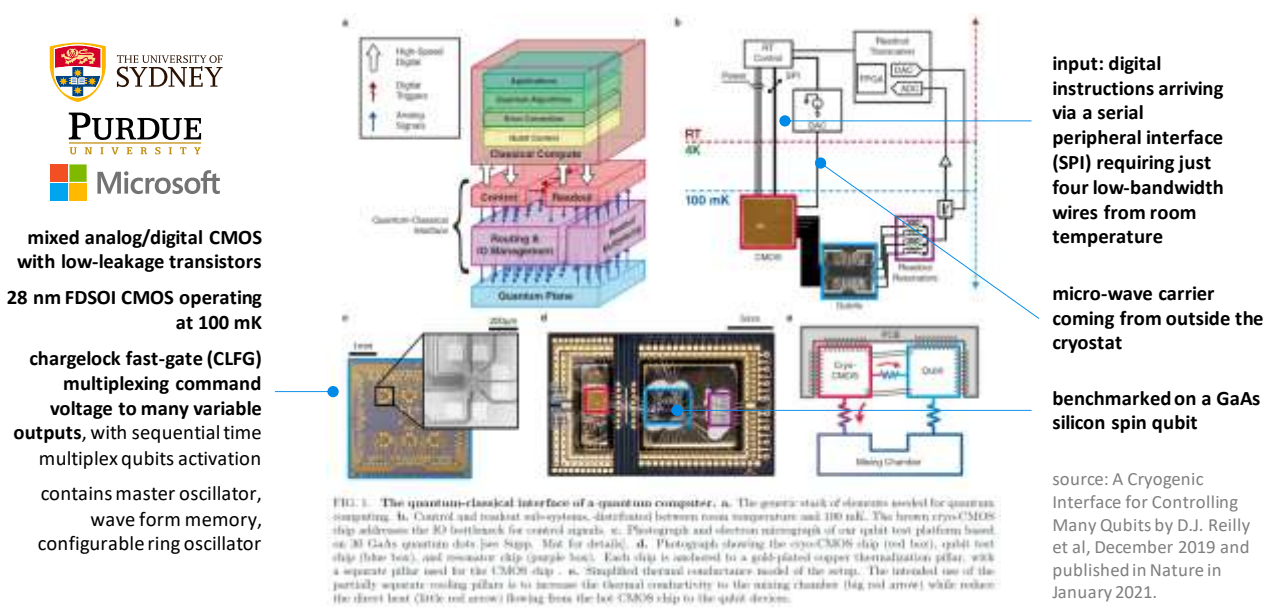


Figure 495: Microsoft prototype another control chipset that support fewer functions than HorseRidge but it run next to the qubit chipset at lower temperature, suitable for silicon spin qubits. Source: [A Cryogenic Interface for Controlling Many Qubits](#) by D.J. Reilly et al, December 2019 (7 pages).

The circuit is using a microwave carrier signal source (LO or local oscillator) sitting outside the cryostat. It is using a round-robbing scheme to distribute modulated micro-waves to each and every qubit in a sequential way. Qubit readout is done here with external circuits (ADC and FPGA). It is a bit the opposite of Harald Homulle's solution from TUDelft. The test CMOS is realized in FDSOI in 28nm. The chipset greatly simplifies the control circuitry coming from outside. This low-power chipset is generating control pulses of 100 mV at 18 nW per cell.

¹⁴⁰⁰ See [A Fully Integrated Cryo-CMOS SoC for Qubit Control in Quantum Computers Capable of State Manipulation, Readout and High-Speed Gate Pulsing of Spin Qubits in Intel 22nm FFL FinFET Technology](#) by J-S. Park et al, February 2021 (3 pages) and 41 slides (not free access).

¹⁴⁰¹ See [A Cryo-CMOS Controller IC for Superconducting Qubits](#) by Kiseo Kang et al, August 2022 (14 pages). Computing the power per qubit was not obvious since the drain per function is not clearly presented in the paper (readout pulses vs readout pulses analysis).

¹⁴⁰² See [A Cryogenic Interface for Controlling Many Qubits](#) by D.J. Reilly et al, December 2019 (7 pages). It was then published in [Nature](#) in January 2021.

The control of the qubits can also use superconducting microwave generation and reading circuits, their interest being a much lower thermal dissipation¹⁴⁰³.

In 2020, CEA-Leti in Grenoble created a mixed analog, digital and quantum cryo-CMOS circuit manufactured in 28 nm FDSOI and operating at 110 mK. It handles all the qubits driving and readout cycle with charge pumping, generating continuous tone GHz microwaves and measuring the induced current with a multiplexed transimpedance amplifier (TIA). At this experimental stage, it drives only a couple qubits but looks promising with regards to the ability to control quantum dots qubits at their operating temperature, at least for silicon qubits working between 100 mK and 1.5 K depending on their type and experimental settings. And the quantum dot qubits were in the circuit itself!

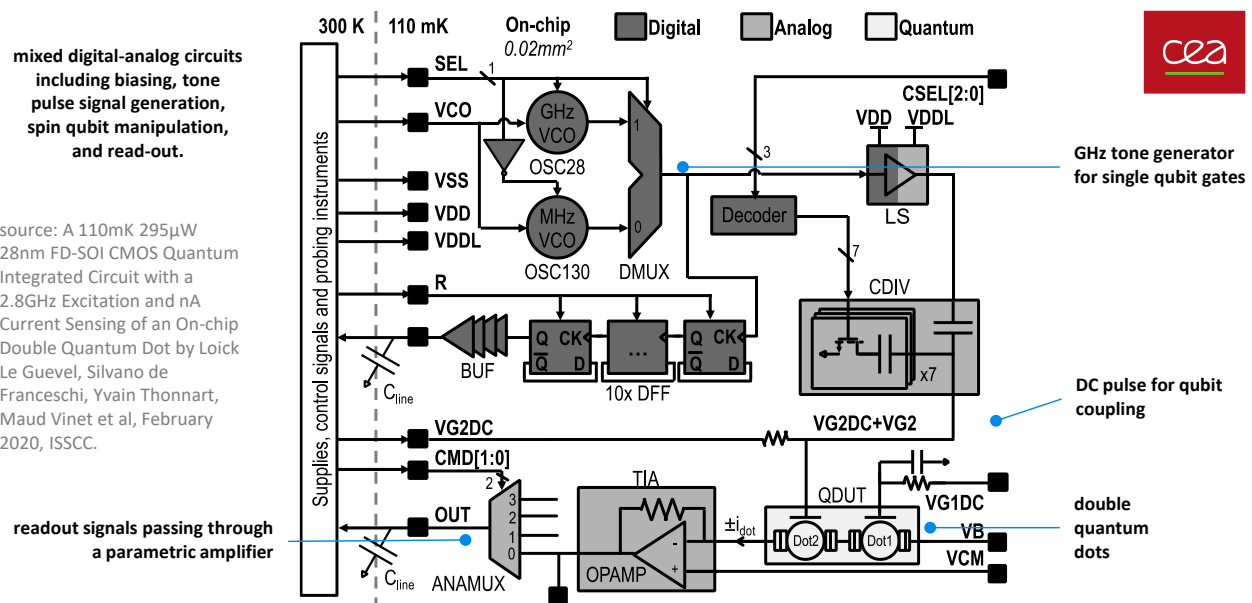


Figure 496: this chipset from CEA-LIST runs at the same temperature as Microsoft's chipset seen before. It is tailored for silicon spin qubits control. Source: [A 110mK 295μW 28nm FD-SOI CMOS Quantum Integrated Circuit with a 2.8GHz Excitation and nA Current Sensing of an On-chip Double Quantum Dot](#) by Loick Le Guevel, Silvano de Franceschi, Yvain Thonnart, Maud Vinet et al, February 2020, ISSCC (12 pages).

One key technology to master when assembling electronic components at the qubit level is packaging and connectivity. That's where a French team from CEA-Leti, CEA LIST and CNRS-Institut Néel made progress in February 2021 with building a prototype interposer enabling the integration of quantum and control chips fabricated from different materials, processes and sources. Named QuIC (Quantum integrated circuits with cryo-CMOS), the prototype demonstrator controls quantum chipsets with integrated control electronics and operating at below 1K. The integration uses a 3D flip-chip process. The control electronics are made on standard FDSOI 28nm by STMicroelectronics. Passive elements and filter devices will be integrated in future versions.

The integrated packaging increases the number of qubits that can be controlled with reducing the number of coaxial cables flowing through the cryostat from the upper stages. It also avoids chipset wire bonding since qubits and control electronics are coupled by routing lines on the interposer. The packaging allows thermal decoupling between the quantum chipset and the electronics control chipset. They also use a die-to-wafer process from CEA-Leti that are used to build interconnects working at under 1K.

¹⁴⁰³ See [Quantum Computer Control using Novel, Hybrid Semiconductor-Superconductor Electronics](#) by Erik P. DeBenedictis of Zettaflops, 2019 (15 pages), which describes an approach for controlling qubits mixing superconductors (JJ) and adiabatic circuits, Cryogenic Adiabatic Transistor Circuits (CATCs). The paper gives an overview of the energy efficiency of cryo-CMOS components and various known superconductors (RQL, AQFP, ...).

CEA is also replacing indium bumps with other materials that are compatible with existing CMOS manufacturing processes, like SnAg microbumps and directly bonded Cu pads from Cu/SiO₂¹⁴⁰⁴.

In another work published by an EPFL team in January 2021, a 40 nm CMOS chip operating at 50 mK hosts both 9 silicon quantum dots qubits organized in a 3x3 array and some digital electronics using analog LC resonators implementing time- and frequency-domain multiplexing for qubit readout, all operating at 50 mK¹⁴⁰⁵.

| | DC pulses | LO | AWG | DAC | I/Q mixers | I/Q demod | readout parametric amplification | readout ADC | readout signal analysis | temp | power / qubit | |
|-----------|--|-----|---|---------------------------------------|-------------|-----------|----------------------------------|---|--------------------------|-------------------------------------|---------------------------------|------------------|
| cryo-CMOS | Google - Bardin 2019 | | | for X and Y gates | yes | yes | | | | 3K | 2 mW | |
| | Microsoft/Sydney/Purdue, FD-SOI 28 nm, 2019 | yes | yes | only external signal routing to qubit | | | | | | 100 mK | N/A, low power | |
| | CEA List/Leti FD-SOI 28 nm 2020 | Yes | yes | | | | Yes TIA amplification | | | 110 mK | 295µW | |
| | QuTech& Intel FinFET 22 nm 2020 | | | Yes, 8-10 bits | Yes | yes | | | | | 12 mW | |
| | HorseRidge 2 FinFET 22 nm, Intel 2021 | yes | | yes, 14-bit | yes | Yes | yes | only LNA between paramp and HEMT | yes | | 4K | 27 mW (to check) |
| | EPFL, CMOS 40 nm 2021 | | | | | | yes | time and frequency domain readout signal multiplexing | | 50 mK | | |
| | POSTECH Korea CMOS 40 nm 2022 | | 2 | yes, 4 bits | yes, 4 bits | yes | yes | LNA | yes | | 3.5K | 15 mW |
| | IBM, FinFET 14 nm 2022 | | | Yes | | Yes | | | | | 3.5K | 23 mW |
| SFQ | SeeQC, SFQ 2019 DigiQ, USC, Chicago, Nvidia 2022 (*) | yes | replaced by series of single amplitude pulses | | | | yes | | | 3K/600 mK (SFQ copro) & 20 mK (DQM) | 0,24 mW (*) | |
| | IBM QEC, SFQ 2022 | | | | | | | | partial surface code QEC | 4K | 10µW to 500µW per logical qubit | |

(cc) Olivier Ezratty, 2022

Figure 497: compilation of various cryo-chipsets developed so far. (cc) Olivier Ezratty, 2022. Sources: Google – Bardin: [A 28nm Bulk-CMOS 4-to-8GHz <2mW Cryogenic Pulse Modulator for Scalable Quantum Computing](#), February 2019 (13 pages), Intel HorseRidge 2: [A Fully Integrated Cryo-CMOS SoC for Qubit Control in Quantum Computers Capable of State Manipulation, Readout and High-Speed Gate Pulsing of Spin Qubits in Intel 22nm FFL FinFET Technology](#) by J-S. Park et al, February 2021 (3 pages), Microsoft / Sydney / Purdue: [A Cryogenic Interface for Controlling Many Qubits](#) by D.J. Reilly et al, December 2019 (7 pages), CEA List/Leti: [A 110mK 295µW 28nm FD-SOI CMOS Quantum Integrated Circuit with a 2.8GHz Excitation and nA Current Sensing of an On-chip Double Quantum Dot](#) by Loïck Le Guevel et al, February 2020, ISSCC (12 pages). QuTech: [A Scalable Cryo-CMOS Controller for the Wideband Frequency-Multiplexed Control of Spin Qubits and Transmons](#) by Jeroen Petrus Gerardus Van Dijk, Menno Veldhorst, Lieven M. K. Vandersypen, Edoardo Charbon et al, November 2020 (17 pages). EPFL: [Integrated multiplexed microwave readout of silicon quantum dots in a cryogenic CMOS chip](#) by A. Ruffino et al, EPFL, January 2021 (14 pages), POSTECH: [A Cryo-CMOS Controller IC for Superconducting Qubits](#) by Kiseo Kang et al, August 2022 (14 pages). IBM: [A Cryo-CMOS Low-Power Semi-Autonomous Qubit State Controller in 14nm FinFET Technology](#) by David J Frank et al, IBM Research, ISSCC IEEE, February 2022 (no free access), SeeQC: [Hardware-Efficient Qubit Control with Single-Flux-Quantum Pulse Sequences](#) by Robert McDermott et al, 2019 (10 pages), DigiQ: [A Scalable Digital Controller for Quantum Computers Using SFQ Logic](#) by Mohammad Reza Jokar et al, February 2022 (15 pages). IBM QEC: [Have your QEC and Bandwidth tool: A lightweight cryogenic decoder for common / trivial errors, and efficient bandwidth + execution management otherwise](#) by Gokul Subramanian Ravi et al, August 2022 (14 pages).

At last, IBM is also working on their own Cryo-CMOS component. They piloted the first one manufactured in a 14 nm process. It supports 4.5-to-5.5GHz RF AWG for pulse control generation, and doesn't rely on TDM or FDM (time or frequency multiplexing)¹⁴⁰⁶.

¹⁴⁰⁴ See [Die-to-Wafer 3D Interconnections Operating at Sub-Kelvin Temperatures for Quantum Computation](#), September 2020.

¹⁴⁰⁵ See [Integrated multiplexed microwave readout of silicon quantum dots in a cryogenic CMOS chip](#) by A. Ruffino et al, EPFL, January 2021 (14 pages).

¹⁴⁰⁶ See [A Cryo-CMOS Low-Power Semi-Autonomous Qubit State Controller in 14nm FinFET Technology](#) by David J Frank et al, IBM Research, ISSCC IEEE, February 2022 (no free access).

For a helicopter view, all these cryo-CMOS projects seem to make more sense to drive silicon spin qubits than superconducting qubits. One reason is the available cooling budget is much higher at the operating temperature of spin qubits that sits between 100 mK and 1 K while superconducting qubits operate at about 15 mK. Figure 497 contains a quick comparison of the various cryo-chipsets studied in the section and the next on superconducting logic. It shows a discrepancy of power consumption per qubit which is explained by several factors: the different electronic features supported by the chipsets, their mutualization across a given number of qubits and the manufacturing node technology.

It is completed by Figure 498 which lists which part in the table corresponds to which function in the pulse management sequences from qubit drive to qubit readout.

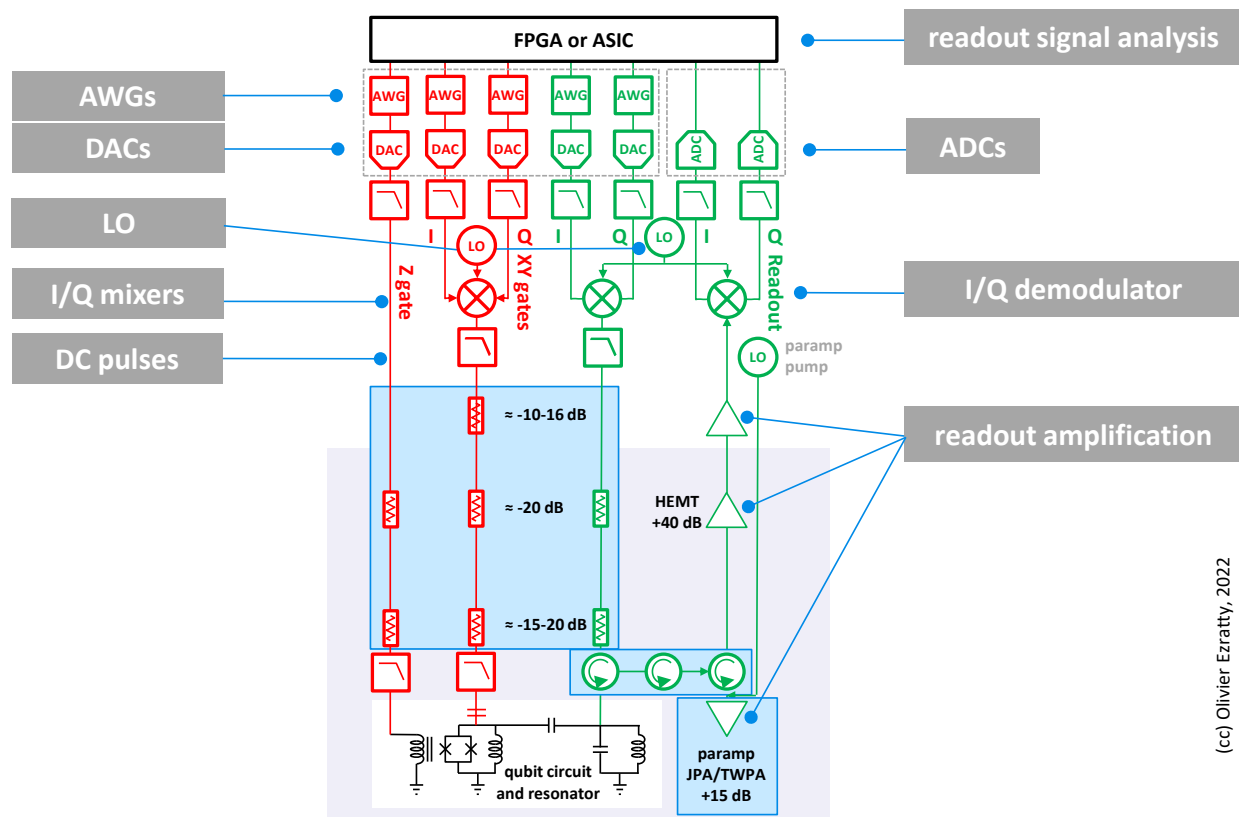


Figure 498: feature list chosen for the table in Figure 497. (cc) Olivier Ezratty, 2022.

Superconducting electronics

The other option for qubit control and readout at low temperature is to rely on superconducting logic based on Josephson junctions¹⁴⁰⁷. The most common one are SFQ, for “single flux quantum” and RSFQ for “rapid SFQ”¹⁴⁰⁸. Their potential benefit is a very low power consumption, up to 500 times less than CMOS logic¹⁴⁰⁹, the ability to operate at the same temperatures as superconducting qubits, and their enablement of a much simple cabling scheme within the cryostat¹⁴¹⁰.

¹⁴⁰⁷ See [Superconducting electronics at 4 K for control and readout of qubits](#) by Adam Sirois et al, NIST, ASC 2020 (27 slides) and [Flux Quantum Electronics](#) by NIST which cover their broad research in the domain.

¹⁴⁰⁸ SFQ logic families are divided into two groups: ac-biased and dc-biased. Reciprocal Quantum Logic (RQL) and Adiabatic Quantum Flux Parametron (AQFP) are in the first group, and Rapid Single Flux Quantum (RSFQ), Energy-efficient RSFQ (ERSFQ) and energy-efficient SFQ (eSFQ) are in the second group. The dc-biased logic family with higher operation speed (as high as 770GHz for a T-Flip Flop (TFF)) and less bias supply issues are more popular than ac-biased logic family. Source: [NISQ+: Boosting quantum computing power by approximating quantum error correction](#) by Adam Holmes et al, Intel, University of Chicago and USC, April 2020 (13 pages).

¹⁴⁰⁹ Source: [Superconducting Microelectronics for Next-Generation Computing](#) by Leonard M. Johnson, February 2018 (27 slides).

¹⁴¹⁰ With room temperature classical control electronics on a 1000 qubit system, you’d need between \$5M and \$10M of niobium-titanium cables for the 4K to 15 mK stages. Each such cable costs in excess of \$2K.

The eSFQ variant can even potentially be 10^4 more efficient than cryo-CMOS for some functions¹⁴¹¹.

However, this technology has some shortcomings: it may be a significant source of noise affecting qubits fidelities with so-called quasiparticle poisoning¹⁴¹², there are some constraints on high-frequency power sources, classically generated AWG wave formed pulses are replaced by trains of single amplitude SFQ pulses of less than 2 ps duration which drives its own preparation overhead to create qubit gates¹⁴¹³, limited Josephson junctions density and at last, SFQ logic can't be used to store data. Many solutions are investigated but are still in the making: cryogenic spintronics, magnetic tunnel junction (MTJ)¹⁴¹⁴, RQL (reciprocal quantum logic)¹⁴¹⁵, SQUID-based, hybrid Josephson-CMOS, JMRAM and OST-MRAM memories (I'll pass on the whereabouts of these various technologies).

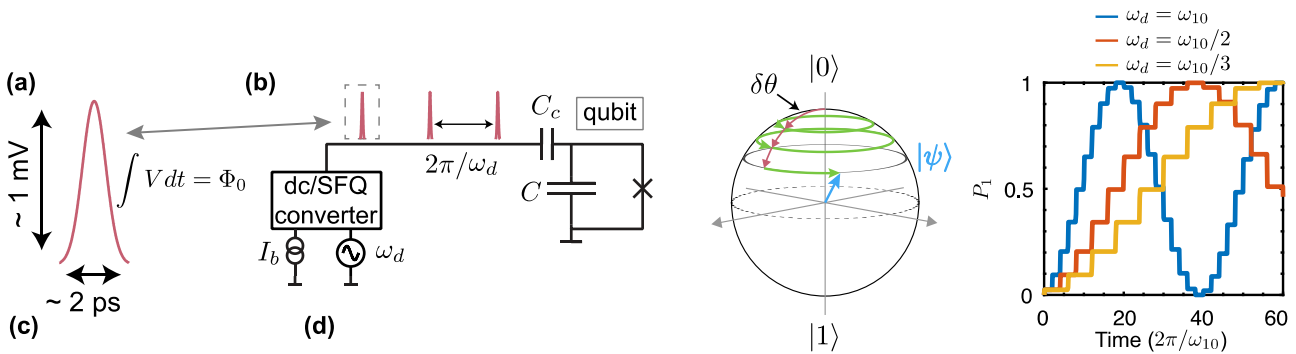


Figure 499: SFQ based wave pulse generation process. Source: [Digital coherent control of a superconducting qubit](#) by Edward Leonard, Robert McDermott et al, 2018 (13 pages).

There are many interconnected research fields here, and SFQ qubits drive logic is frequently of sub-product of more general research in superconducting electronics. Since the 1970s, there were many ups and downs with research in using superconducting electronics to override the apparent limitations of Moore's law with classical semiconductors. Also, superconducting electronics have other use cases like with single photon detection, magnetism sensing with SQUIDs and analog amplifiers working at the quantum limits (JPAs, SPMs, TWPA, that we'll cover in the next part).

Qubit readout function can also be implemented with SFQ with readout signal generated through a JPM amplifier¹⁴¹⁶ and converted with ADCs¹⁴¹⁷. Tone signal generation can also be implemented in SFQ logic¹⁴¹⁸.

¹⁴¹¹ See [Quantum-Classical Interface Based on Single Flux Quantum Digital Logic](#) by Roger McDermott, Oleg A. Mukhanov, Thomas A. Ohki et al, October 2017 (16 pages).

¹⁴¹² See [Single Flux Quantum-Based Digital Control of Superconducting Qubits in a Multi-Chip Module](#) by Chuan-Hong Liu, R. McDermott et al, January 2023 (15 pages) that addresses the quasiparticle poisoning problem with separating the SFQ chipset from the qubit chipset.

¹⁴¹³ At this point, in D-Wave annealers, SFQ circuits create DC signals and ramp currents with DACs (digital-to-analog converters) to configure the system and drive the magnetometers used for qubits readouts.

¹⁴¹⁴ See [Cryogenic Memory Architecture Integrating Spin Hall Effect based Magnetic Memory and Superconductive Cryotron Devices](#) by Minh-Hai Nguyen et al, 2020 (11 pages).

¹⁴¹⁵ See [Superconducting logic circuits operating with reciprocal magnetic flux quanta](#) by O.T. Oberg, 2011 (337 pages).

¹⁴¹⁶ See [Interfacing Superconducting Qubits With Cryogenic Logic: Readout](#) by Caleb Howington, Alex Opremcak, Robert McDermott, Alex Kirichenko, Oleg A. Mukhanov and Britton L. T. Plourde, August 2019 (5 pages) with more details in the related thesis [Digital Readout and Control of a Superconducting Qubit](#) by Caleb Jordan Howington, December 2019 (127 pages).

¹⁴¹⁷ See [History of Superconductor Analog-to-Digital Converters](#) by Oleg Mukhanov, 2011 (19 pages) and [Superconductor Analog-to-Digital Converters](#) by Oleg A. Mukhanov et al, 2010 (21 pages).

¹⁴¹⁸ See [A low-noise on-chip coherent microwave source](#) by Chengyu Yan, Mikko Möttönen et al, November 2021 (14 pages) and [Digital Control of a Superconducting Qubit Using a Josephson Pulse Generator at 3 K](#) by L. Howe et al, PRX Quantum, 2022 (11 pages).

IBM studied classical electronics based on the Josephson junction from the 1960s to 1983, using lead and then lead/niobium. The technology was only supported by IBM and could not compete with CMOS processors, drive by Moore's law and the whole semiconductor industry, particularly with Intel. Japan's MITI had also launched a superconducting computing initiative throughout the 1980s leading to a 4-bit machine using 1 Kbits of RAM. The Bell labs also worked on niobium/aluminum oxide Josephson junctions.

Hypres. Then, the invention of the more efficient and energy efficient RSFQ in USSR in 1985 led to its transfer to the USA via its coinventor Oleg Mukhanov when he joined Hypres in 1991. It led to a short lived superconducting supercomputing project (1997-2001). Starting in the early 2000s, attention then turned to superconducting qubits with investments throughout the world (USA, France, Japan, ...) leading to major developments from IBM, Google and others. Hypres did use superconducting electronics for non-quantum use cases, particularly in the defense industry and with radars, and quantum sensing using SQUIDs. Interestingly, some of the interest in classical electronics made with SFQ and RSFQ came with quantum computing and the need for energy efficient control electronics.

D-Wave was probably the first to use SFQ electronics in its systems and since its inception. At their beginning, they hired skilled engineers coming from IBM, Stony Brook University in New York and coming from Stellenbosch University in South Africa having a good experience in superconducting physics and electronics.

D-Wave's quantum annealers contain flux superconducting qubits and superconducting SFQ circuits handling signals control generation, control and qubit state readout, and for up to 5000 qubits. This is a little-known technological feat from D-Wave. It allows them to greatly simplify the wiring that leads to the quantum processor since all their SFQ electronics sits in the same chipset handling the qubits. Figure 500 shows how it looks like.

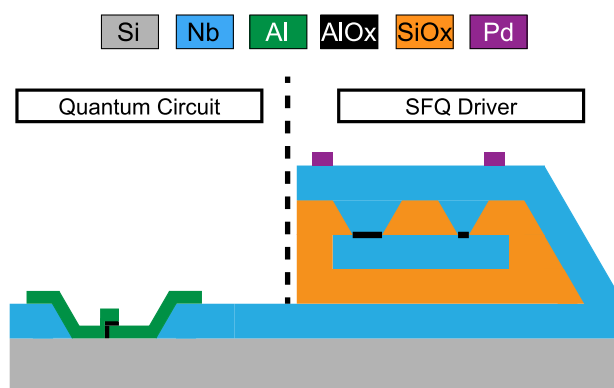


Figure 500: a side-by-side comparison of the stacking of elements in a superconducting qubit (left) and with SFQ logic (right). Source: [Digital coherent control of a superconducting qubit](#) by Edward Leonard, Robert McDermott et al, 2018 (13 pages).

Who else is working with SFQ electronics to control solid state qubits? Let's start with the USA who are the most active here.

- **SeeQC**, a spin-off / split-off from Hypres that we'll detail later and is specialized in superconducting electronics for qubits control.
- **Raytheon BBN (USA)** is investigating the usage of SFQ systems and a mix of SFQ and spintronics for controlling qubits¹⁴¹⁹. They have a wide-ranging partnership with IBM and some IBM researchers worked with BBN on SFQ back in 2018 but it doesn't tell whether IBM is keen to adopt SFQs to control their superconducting qubits.

¹⁴¹⁹ See [Quantum Engineering and Computing Group](#) by Thomas Ohki, March 2021 (39 slides). The team has a staff of 20 and [Digital coherent control of a superconducting qubit](#) by Edward Leonard, Robert McDermott et al, 2018 (13 pages). It identifies a shortcoming of SFQ: quasi-particles poisoning that negatively impacts qubit fidelities. Back in 2018, they said it could be addressed with putting SFQ logic on a separate chip that would be bonded (with indium) to the qubit chipset. Nowadays, this is an available technology.

- **University of Wisconsin-Madison** has a Department of Physics run by Robert McDermott that investigates SFQ logic. He pioneered qubit control with trains of SFQ pulses¹⁴²⁰. They authored the paper with Raytheon BBN on SFQ qubit control mentioned with Raytheon above.
- **MIT Lincoln Labs** has been working for a while on SFQ logic in the “beyond CMOS” roadmap funded by IARPA as part of the Quantum Enhanced Optimization (QEO) and Logical Qubit (LogiQ) programs¹⁴²¹. In 2017, they developed a 3D Integrated Superconducting Qubit Platform using three layers: the qubit chipset, an interposer with through-substrate vias and a supporting chipset with a routing layer and a TWPA for qubit readout microwave amplification. They are also leveraging their own superconducting cleanroom. The Lincoln Lab is even providing many labs across the world with their own custom TWPA and for free.
- **University of Chicago** is also involved in the design of SFQ-based qubit control electronics. In 2022, they demonstrated low-error two-qubit operations using SFQ pulses drive working with fluxonium superconducting qubits¹⁴²². They also led the DigiQ project launched by the NSF.

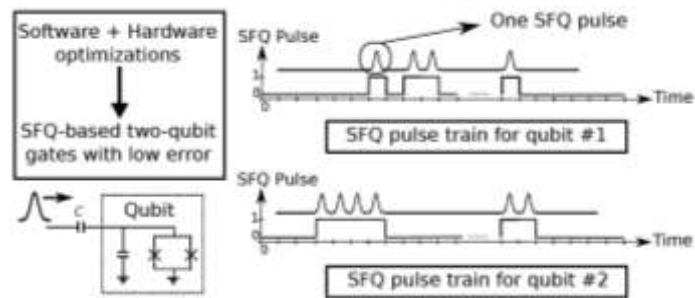


Figure 501: SFQ wave packet optimization. Source: [Practical implications of SFQ-based two-qubit gates](#) by Mohammad Reza Jokar et al, February 2022 (11 pages).

It was funded as part of the Enabling Practical-scale Quantum Computation (EPiQC)¹⁴²³.

- **Northrop Grumman** is also working on SFQ for qubit controls and even patented one related solution back in 2008¹⁴²⁴. They also developed RQL techniques.
- **IBM** together with the Universities of Chicago and Southern California, and Super.tech (from ColdQuanta) presented in August 2022 the development of an SFQ-based cryogenic circuit to implement part of the logic of the most common errors in quantum error correction for surface codes¹⁴²⁵. The decoder could support between 2000 and 100,000 logical qubits depending on the code distance.

And in the rest of the world:

- **Japan** has a very active group in SFQ, the group of Nobuyuki Yoshikawa from Yokohama National University. They are working in the field of superconducting electronics, SFQ and adiabatic circuits mostly as “beyond than Moore” solutions¹⁴²⁶.

¹⁴²⁰ See [Accurate Qubit Control with Single Flux Quantum Pulses](#) by Robert McDermott and M.G. Vavilov, 2014 (10 pages), [Quantum-Classical Interface Based on Single Flux Quantum Digital Logic](#) by Robert McDermott et al, 2017 (16 pages) and [Scalable Hardware-Efficient Qubit Control with Single Flux Quantum Pulse Sequences](#) by Kangbo Li, Robert McDermott and Maxim G. Vavilov, 2019 (10 pages).

¹⁴²¹ See [Superconducting Microelectronics for Next-Generation Computing](#) by Leonard M. Johnson, February 2018 (27 slides).

¹⁴²² See [Practical implications of SFQ-based two-qubit gates](#) by Mohammad Reza Jokar et al, February 2022 (11 pages).

¹⁴²³ See [DigiQ: A Scalable Digital Controller for Quantum Computers Using SFQ Logic](#) by Mohammad Reza Jokar et al, February 2022 (15 pages). The project is run with Amazon, Nvidia, Super.tech and USC. The qubits are driven by series of small SFS pulses, not by arbitrary waveform pulses. Theoretically, SFQ logic could still create these waveforms thanks to clock speed exceeding 100 GHz. It could create waveforms with basebands of 4 to 25 GHz. But this would require superconducting DACs and ADCs which happen to need resistances, thus being irreversible and dissipative, creating some thermal constraints.

¹⁴²⁴ See [Method and apparatus for controlling qubits with single flux quantum logic](#) patent.

¹⁴²⁵ See [Have your QEC and Bandwidth too!: A lightweight cryogenic decoder for common / trivial errors, and efficient bandwidth + execution management otherwise](#) by Gokul Subramanian Ravi et al, August 2022 (14 pages).

¹⁴²⁶ See a review paper he coauthored in 2004: [Superconducting Digital Electronics](#) by Hisao Kayakawa et al, 2004 (15 pages).

He participated to the development to AQFP (Adiabatic Quantum-Flux-Parametron), an energy-efficient superconductor logic element¹⁴²⁷. Although they contribute significantly to the field of SFQ, they still do not seem to work on its implementation for qubits control.

- **Germany** has a couple labs and fabs looking at superconducting electronics and their potential usage in qubits control. You can count with Per J. Liebermann and Frank K. Wilhelm from Saarland University who work on improving qubit fidelities with varying the time distance between SFQ pulses in the train using control theory and (classical) genetic algorithms¹⁴²⁸. The Leibniz-IPHT in Jena, Thuringia, has a cleanroom that works, among other things, on producing RSFQ circuits and SQUIDs for quantum sensing. Leibniz-IPHT is coordinating the German project HIQuP dealing specifically with superconducting qubit control electronics and partnering with IQM Germany and Supracon AG, itself a spin-out of the Leibniz-IPHT that is specialized in SQUID based magnetometers. The PTB has also investigated SFQ circuits in the past¹⁴²⁹. There was also the EU project RSFQubit from 2004 to 2007, involving many German players and coordinated by Chalmers University, Sweden, with a funding of 2,6M€.
- **Finland** also conducts some research in SFQ logic at VTT under the leadership of Matteo Cherchi¹⁴³⁰. Their aCryComm project develops converters and input/outputs for simple SFQ processors. This work could also lead to some potential collaboration with IQM.
- **China** launched a 200M€ project on SFQ electronics. The Shanghai Institute of Microsystem and Information Technology's (SIMIT) Laboratory of Superconducting Electronics is studying SQUIDs (Superconducting quantum interference device used in sensing), SNSPD (superconducting nanowire single-photon detectors) and Superconducting large scale integrated circuits with a 50 persons team. They ambition to create a 64 bits SFQ-based microprocessor. They have their own cleanroom. As side-project of the later could well become SFQ-based qubits control chipsets.
- **Russia** has some researchers working on superconducting electronics and even on SFQ qubit drive electronics, particularly at Lomonosov Moscow State University and Lobachevsky State University of Nizhny Novgorod¹⁴³¹.



SeeQC (2017, USA, \$34,2M) was created as a subsidiary of Hypres, an American company specialized in the creation of superconducting electronics, by John Levy, Matthew Hutchings and Oleg Mukhanov¹⁴³².

Its parent company Hypres (1983, USA, \$50K) is a long-time specialist in superconducting electronic circuits. It was created by Sadeg Faris, a Libyan who invented the quiteron at IBM, a superconducting transistor. He created Hypres the same year IBM pulled the plug on superconducting electronics and used IBM patents under license.

¹⁴²⁷ See [Adiabatic Quantum-Flux-Parametron: A Tutorial Review](#) by Naoki Takeuchi, Nobuyuki Yoshikawa et al, January 2022 (14 pages)

¹⁴²⁸ See [Optimal Qubit Control Using Single-Flux Quantum Pulses](#) by Per J. Liebermann and Frank K. Wilhelm, Saarland University, 2016 (5 pages).

¹⁴²⁹ See [Low-noise RSFQ Circuits for a Josephson Qubit Control](#) by M Khabipov, D Balashov, E Tolkacheva and A B Zorin, PTB, 2008 (7 pages).

¹⁴³⁰ See [Superconducting chips to scale up quantum computers and boost supercomputers](#) by Matteo Cherchi, March 2021.

¹⁴³¹ See [Beyond Moore's technologies: operation principles of a superconductor alternative](#) by Igor I. Soloviev et al, 2017 (22 pages), [Flux qubit interaction with rapid single-flux quantum logic circuits: Control and readout](#) by N. V. Klenov, Low Temperature Physics, 2017 (11 pages), the excellent review presentation [Superconducting digital electronics](#) by Igor Soloviev, 2021 (115 slides) and [Genetic algorithm for searching bipolar Single-Flux-Quantum pulse sequences for qubit control](#) by M.V. Bastrakova et al, September 2022 (9 pages) that deals with the optimization of SFQ pulses to drive qubits, using a genetic machine learning algorithm.

¹⁴³² See [Seeqc Cuts Its Own Path to the Quantum Era With Integrated Circuit Approach](#) by Matt Swayne, The Quantum Daily, September 2020. By setting up offices in Milan and the UK, the startup found a way to secure European funding for its research. Otherwise they collaborate with Robert McDermott's team at the University of Wisconsin and the Syracuse team in upstate New York.

They've been the only superconducting electronics company for three decades and lived out of SBIR funding and some defense business, like with radars and spectrum analysis. They are a mix of nationalities with Indians, Russians, and a Lebanese. Hypres split in two in 2020. The RF business did stay at Hypres and SeeQC specialized in SFQ based qubit drive while keeping Hypres's cleanroom. The remained of Hypres then worked with other cleanrooms like with SkyWater and the MIT Lincoln Labs.

SeeQC stands for "Superconducting Energy Efficient Quantum Computing". It focuses on the creation of superconducting circuits completed with spintronic technology memories¹⁴³³. The company was initially funded under IARPA's C3 project launched in 2016. Then SeeQC created a lab at Federico II University of Naples, Italy, and the UK, mostly to capture EU/UK public funding. It fared better with the UK than with the EU. They got grants from Innovate UK's Industrial Challenge Strategy Fund as part of four consortiums.

- The first, announced in April 2020, totaling £7M, is led by Oxford Quantum Circuits includes Oxford Instruments, Kelvin Nanotechnology, University of Glasgow (Martin Weides' team) and the Royal Holloway University of London, to create a superconducting qubit computer.
- The second, launched in September 2021, is NISQ.OS, totaling £5,363M, is focused on building an operating system and an hardware abstraction layer is led by Riverlane and includes, Hitachi Europe, Universal Quantum, Duality Quantum Photonics, Oxford Ionics, Oxford Quantum Circuits, arm and the UK National Physical Laboratory, another SeeQC partner in the UK. SeeQC and Riverlane announced in June 2021 that they had integrated Riverlane's operating system Deltaflow.OS with SeeQC's qubit driving components.
- The third consortium was launched in November 2021 in partnership with Merck who is also an investor in SeeQC as well as with Riverlane, Oxford Instruments, the University of Oxford and Medicines Discovery Catapult, with a total funding of £6.85M grant from Innovate UK's Industrial Strategy Challenge Fund (ISCF) to build a "*commercially scalable application-specific quantum computer designed to tackle prohibitively high costs within pharmaceutical drug development*" (aka QuPharma project). A bit like IQM's strategy, SeeQC is to create "*an application-specific quantum computer*" to simulate quantum chemistry, an idea that I found a bit questionable. The announcement didn't mention either a number of qubit or expected fidelities, but the project is due for completion "*in 18 months*".
- The fourth consortium is a project led by sureCore, with £6.5M to support the integration of SeeQC's technology with cryo-CMOS components for qubit controls. SeeQC's role is to "*determine what IP blocks the project will need to create for the Cryo-CMOS chips*". Other partners are Oxford Instruments, SemiWise, Synopsys, Universal Quantum and the University of Glasgow.

In December 2021, SeeQC also announced a partnership with QuantWare (The Netherlands) for the development of a QPU containing QuantWare's superconducting qubits and SeeQC's RSFQ cryogenic control electronics. It adds another superconducting vendor to SeeQC's partners, on top of OQC (UK). The difference here is that QuantWare will embed SeeQC's technology in its QPU.

SeeQC's architecture is based on two chipsets: a classical SFQ control chipset and the SFQClass DQM, both using Josephson junctions in SFQ superconducting circuits. The first chipset runs at 3K or as low as 600 mK and uses an energy efficient ERSFQ or eSFQ variant of RSFQ logic.

¹⁴³³ See [Single Flux Quantum Logic for Digital Applications](#) by Oleg Mukhanov of SeeQC/Hypres, August 2019 (33 slides). Oleg Mukhanov also worked on a TWPA, in [Symmetric Traveling Wave Parametric Amplifier](#) by Alessandro Miano and Oleg Mukhanov, April 2019 (6 pages).

It controls the DQM and handles error corrections without requiring an external classical computer. The SFQuClass DQM (Digital Quantum Management) includes the microwave generators used to drive the qubits (with DACs, digital-to-analog signal converters) and for qubits readouts (with ADCs, analog to digital microwave signal converters).

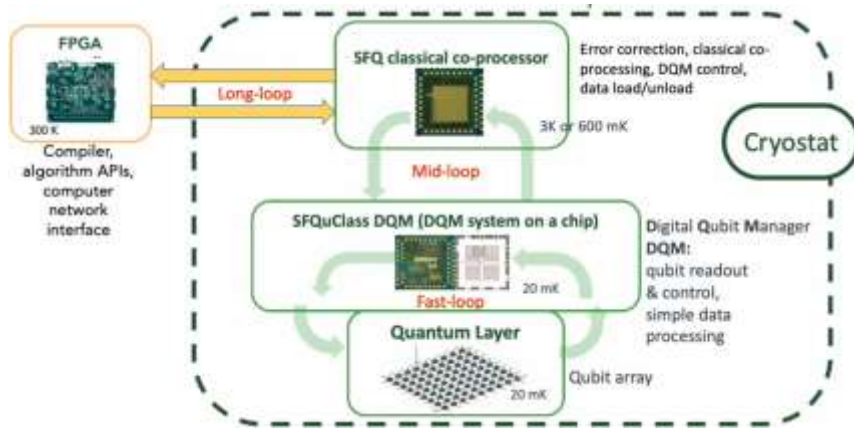


Figure 502: SeeQC overall architecture with a classical coprocessor running at 3K/600mK and the DQM that sits close to the qubit chipset at 20 mK. Source: SeeQC.

Its power drain is only 0,0002 mW per qubit when it could reach over 20 mW per qubits with cryo-CMOS but we have to check these kinds of comparison making sure the same electronics functions are implemented or not implemented.

The mid-loop between the SFQ co-processor and the DQM also reduces the latency for qubits controls and is particularly interesting for implementing error correction codes¹⁴³⁴.

When we can generate qubit control signals inside the cryostat, it still must be exchanged both ways digitally with the outside of the cryostat. This can be done through signals multiplexed on copper, fiber optics, or even, it is under study, radio waves at very high frequencies (in THz). It also helps maximizing the thermal and vacuum insulation with the outside.

An optical fiber has the advantage of being made of glass, which does not generate thermal expansion and is a weak heat conductor. Still, SeeQC has scalability plans that will require using a growing number of wires with the number of qubits, with a better “Rent’s rule” than with classical control¹⁴³⁵.

| "Quantum" Rent's Rule | | | |
|-----------------------|-------------------------------|--------|--------------------------|
| Qubit Count | Qubit Control Wiring Overhead | | Application |
| | Google | seeQC | |
| 2 | 4 | 3 | Prototype |
| 10 | 20 | 3 | Prototype |
| 100 | 200 | 31 | Prototype |
| 1k | 2,000 | 76 | Optimization / chemistry |
| 10k | n/a | 330 | Optimization / chemistry |
| 100k | n/a | ~1,600 | Big data / ML |
| 1m | n/a | ~6,000 | Encryption |

Figure 503: how many wires are necessary for controlling qubits comparing Google’s Sycamore system and SeeQC’s solution. Source: SeeQC.

¹⁴³⁴ See [Quantum-classical interface based on single flux quantum digital logic](#) by Robert McDermott, 2018 (19 pages), [Digital coherent control of a superconducting qubit](#) by Edward Leonard Jr. et al, 2018 (13 pages). The diagram on page 10 suggests that microwave generation is always performed outside the cryostat. This is related to the fact that the experiment contains a double control of the qubits: by direct current to drive the microwave generation by the SFQ near the qubits, and in the traditional way outside the cryostat. This allows them to compare the fidelity of the two methods. And then [Digital coherent control of a superconducting qubit](#), by Oleg Mukhanov (CTO and co-founder of SeeQC), Robert McDermott et al, September 2019 (39 slides) and [Hardware-Efficient Qubit Control with Single-Flux-Quantum Pulse Sequences](#) by Robert McDermott et al, 2019 (10 pages).

¹⁴³⁵ Rent’s rule compute the maths of connections needed to control an electronic system and how it scales with size. See [Microminiature packaging and integrated circuitry: The work of E. F. Rent, with an application to on-chip interconnection requirements](#), 2005 (28 pages) which describes the history of Rent’s rule that dates from 1960 and [Rent’s rule and extensibility in quantum computing](#) by D.P. Franke, James Clarke, L.M.K. Vandersypen and Menno Veldhorst, 2018 (8 pages) that describes how these rules could be applied in quantum computing.

Circulators

Another key component are the circulators used in qubits readouts at the lowest level of a cryostat.

The generic role of a n-way circulator is to send the microwave from input i to input $i+1$ in a directional *aka* non-reciprocal way. The signal from $i+1$ can't be sent, or is sent with strong attenuation to input i . It is used to convey the readout microwave from their AWG/DAC source to the qubit resonator and its response microwave to the first amplification stage. The amplified microwave is sent upwards to the next amplification stage, without being sent back to the resonator. There are settings variations based on using between one and four circulators to improve the various components isolation in the readout food chain.

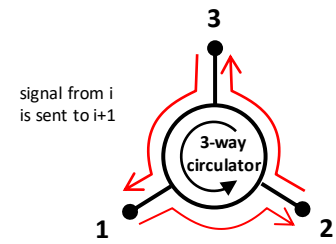


Figure 504: principle of operation of a circulator which circulates microwaves in a one-way fashion.

Indeed, the reciprocal protection is not perfect, as measured in decibels and is usually of about 17 to 18 dB. So, chains of circulators enable a protection of about 35 dB, if not over 50 dB. The circulator protection must exceed the first amplifier (or paramp) gain.

Circulators protect the qubits from unwanted noise coming from the output measurement chain. It avoids so-called back-action of the amplifier. They are key contributors to the qubit readout being “nondestructive” of the resulting quantum state (*aka* QND for quantum non-demolition measurement).

Isolators are similar symmetry breaking devices, but with only two connectors they enable a one-way microwave circulation. Conceptually, these are like “microwave diodes”, letting microwaves be transmitted in only one direction.

Traditional circulators are passive devices using a ferrite magnet. A microwave entering the circulator through one port is subject to a Faraday rotation in the ferrite, changing its phase¹⁴³⁶. It creates a constructive microwave interference in one direction of circulation and a destructive interference in the other direction. Such circulators can't be integrated in or near qubit circuits due to their ambient magnetism. Circulators can still be mutualized for the readout of several qubits with frequency-domain multiplexing used at the AWG/DAC and ADC/FPGA levels in the upper data processing stages¹⁴³⁷.



Figure 505: a typical commercial bulky circulator.

Nowadays, this multiplexing is not exceeding 8 qubits, but it could theoretically reach 100 qubits, such as with a 10 MHz bandwidth and equivalent 10 MHz spacing, spread in a 2 GHz bandwidth centered at 6.5 GHz, although 20-qubit multiplexing seems more reasonable given the specifications of existing parametric amplifiers (mostly TWPAs).

Existing Faraday circulators used with superconducting qubits are relatively large components of several centimeters wide. This length is conditioned by the microwave length, which is 5 cm for 6 GHz wavelengths. With cabling, filters and attenuators, circulators are the key components located in the cryostat that limit qubit scaling, thus the need for other solutions.

¹⁴³⁶ This effect was described first in [The Ferromagnetic Faraday Effect at Microwave Frequencies and its Applications](#) by C. L. Hogan, 1952 (31 pages).

¹⁴³⁷ See the interesting presentation [Hall Effect Gyrotors and Circulators](#) by David DiVincenzo, Quantum Technology - Chalmers, 2016 (53 slides).

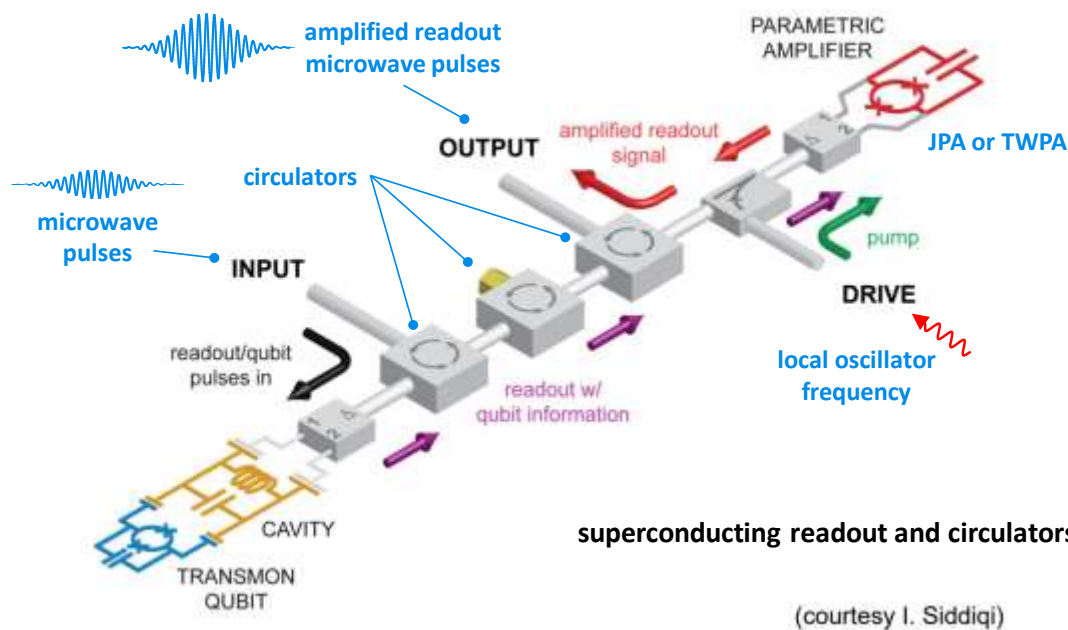


Figure 506: several circulators are actually used for each set of qubits controlled through frequency multiplexing. Source: Irfan Siddiqi.

Many alternatives are investigated to circumvent the shortcomings of existing ferrite-based circulators. Ideal circulators would fit into the qubit chipsets and use compatible (superconducting) circuits, have a high protection (in the 20 dB region), a large and controllable bandwidth (between 500 MHz and up to 2 GHz, to enable qubit readout multiplexing) and low power drain if they are active and depending on the cryostat stage where they are operating (15 mK or 4K). They'd also be combined with the first stage quantum-limit low-noise amplifier like a TWPA.

These new types of circulators can be segmented by their underlying physical process. I'll simplify this and have, first, classical electronics systems:

- **Hall effect circulators** as developed by David DiVincenzo in Germany and whose size is not constrained by the readout microwave wavelength¹⁴³⁸.
- **LC based cryo-CMOS circulators** as prototyped at TU Delft¹⁴³⁹.

And then, various superconducting circuits using Josephson junctions like:

- **Interferometric Josephson circulators**, developed at IBM¹⁴⁴⁰ and RIKEN¹⁴⁴¹, with the advantage of being very low power hungry.

¹⁴³⁸ See [Hall Effect Gytrators and Circulators](#) by Giovanni Viola and David DiVincenzo, 2014 (18 pages) and [On-Chip Microwave Quantum Hall Circulator](#) by A. C. Mahoney et al, 2017 (9 pages) which is based on III/V GaAs and AlGaAs electronics.

¹⁴³⁹ See [A Wideband Low-Power Cryogenic CMOS Circulator for Quantum Applications](#) by Andrea Ruffino, Fabio Sebastiano and Edoardo Charbon, IEEE & EPFL, 2020 (15 pages). It uses resonant LC circuits level combining inductance (L) and capacitors (C). The circuit provides a 18 dB isolation and consumes a total of 10.5 mW. It runs at 4.2K and not at the lowest 15 mK. It was tested with a 40 nm node with an active area of 0.45 mm² in an experimental 1,5 mm wide square circuit.

¹⁴⁴⁰ See [Active protection of a superconducting qubit with an interferometric Josephson isolator](#) by Baleegh Abdo, Jerry M. Chow et al, IBM Research, 2018 (10 pages) and [High-fidelity qubit readout using interferometric directional Josephson devices](#) by Baleegh Abdo et al, IBM Research, 2021 (32 pages).

¹⁴⁴¹ See [Magnetic-Free Traveling-Wave Nonreciprocal Superconducting Microwave Components](#) by Dengke Zhang and Jaw-Shen Tsai, RIKEN, 2021 (18 pages), with a bandwidth of 580 MHz around 6 GHz and an isolation of 20 dB.

- **Superconducting quantum tunnelling capacitors**, developed by Clemens Mueller at ETH Zurich and the University of Queensland¹⁴⁴². These are passive systems or can be controlled with just some DC (direct current) input, as shown in Figure 507¹⁴⁴³. These could be potentially directly implemented in superconducting qubit chipsets.
- **On-chip microwave circulators** with a wide tunable frequency, developed at the University of Colorado in Boulder¹⁴⁴⁴, a variation with SQUIDs superconducting components.

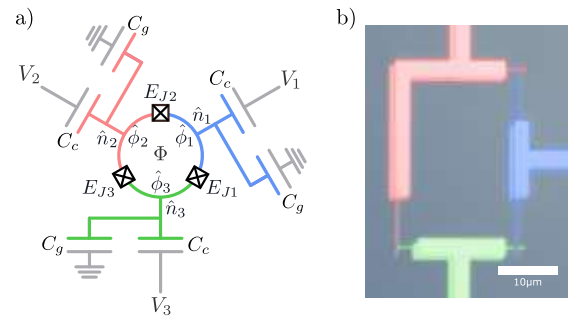


Figure 507: a) prototype passive superconducting circulator that could potentially be integrated in a superconducting qubit chipset. Source [Passive superconducting circulator on a chip](#) by Rohit Navarathna, Thomas M. Stace, Arkady Fedorov et al, August 2022 (11 pages).

While there are many such prototype solutions, and we’ve not covered them all, they seem not having reached the commercial stage at this point, although some have use cases beyond qubits control like in the telecom and radar markets.

Amplifiers

Analog qubit readout microwave signals have to be amplified several times before they are converted digitally with an ADC and then analyzed, usually with an FPGA programmable circuit. Superconducting readout microwaves are amplified at least three times: first, at the lowest cryogenic stage (15 mK) with a parametric amplifier (“paramp”) operating at the quantum limit (JPA, TWPA), then at the 4K stage with an HEMT amplifier, then at ambient temperature with a classical RF analog amplifier that may also be an HEMT. The paramp serves as a low-noise signal preamplifier before the noisier HEMT. They all add a gain of respectively about 15 dB, 40 dB and 50 dB to readout microwaves.

Paramps. To make things short, two main generations of parametric amplifiers have been used for qubits readout. They are based on exciting and pumping a material with nonlinear polarization using an intense electromagnetic field. A weak microwave signal can then get amplified via the interaction with the medium. The first paramps used with qubit readouts were the JPAs (Josephson Parametric Amplifiers)¹⁴⁴⁵. These are simple amplifiers, using one or two Josephson junctions, easy to manufacture, with a good gain of about 15 to 20 dB¹⁴⁴⁶. Their main shortcoming is their narrow bandwidth which prevents their implementation with frequency-domain qubits readout multiplexing, where a single amplifier processes a readout signal coming from several chained qubits using different resonant frequencies. It is due to JPAs being based on cavities.

¹⁴⁴² See [Breaking time-reversal symmetry with a superconducting flux capacitor](#) by Clemens Müller, Thomas M. Stace et al, 2018 (10 pages). This circulator uses a small superconducting capacitor, using the quantum tunnelling of the magnetic flux around it, allowing a flow of microwave energy in one direction.

¹⁴⁴³ See [Passive superconducting circulator on a chip](#) by Rohit Navarathna, Thomas M. Stace, Arkady Fedorov et al, August 2022 (11 pages).

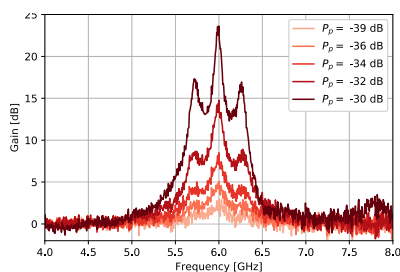
¹⁴⁴⁴ See [Widely Tunable On-Chip Microwave Circulator for Superconducting Quantum Circuits](#) by Benjamin J. Chapman, Alexandre Blais et al, 2017 (16 pages) and the related thesis [Widely tunable on-chip microwave circulator for superconducting quantum circuits](#) by Benjamin J. Chapman, 2017 (144 pages). See also [Design of an on-chip superconducting microwave circulator with octave bandwidth](#) by Benjamin J. Chapman et al, 2018 (12 pages).

¹⁴⁴⁵ See [Superconducting Parametric Amplifiers](#) by Jose Aumentado, IEEE Microwave Magazine, August 2020 (15 pages) (*not open access*).

¹⁴⁴⁶ A Japanese team was able to reach a gain of 40 dB with a JPA in 2022, but with a narrow bandwidth. With a 20 dB gain, they obtain a bandwidth of only 400 kHz. See [A three-dimensional Josephson parametric amplifier](#) by I. Mahboob et al, May 2022 (5 pages).

This explains the interest for a relatively new generation of paramps, the TWPAs (travelling waves parametric amplifiers) which were pioneered by Bernard Yurke (USA) in 1996¹⁴⁴⁷ and successfully implemented in an array of SQUIDs in 2007 by Manuel A. Castellanos-Beltran from JILA (USA)¹⁴⁴⁸, and then, in 2008, with an intrinsic noise below the standard quantum limit (SQL) and over 20 dB of power gain¹⁴⁴⁹. These amplifiers are used for qubit readout, in high-energy particle physics, radioastronomy and astrophysics for the detection of dark matter. TWPA (*aka* usually JTWPA) practically emerged in 2015¹⁴⁵⁰. Recent TWPAs are based on long arrays of about 2000 series of Josephson junctions and as such are considered to be “meta-materials”. They are more complicated to manufacture. Their broader bandwidth could potentially enable up to 10-20 qubits readout multiplexing¹⁴⁵¹. Their other figures of merit are their saturation and dynamic range (linked to minimum and maximum input signal power), and noise level (noise temperature, under 1K). New options arise with Floquet mode TWPAs from MIT, decreasing noise level and across a wide bandwidth of 6 GHz, further increasing qubits readout multiplexing capabilities. And it has a better directionality¹⁴⁵².

Both JPAs and TWPAs are active components that are driven by a constant microwave pulse acting as a “pump”. JPAs are fed with a pulse of -80 dB while TWPAs use a -70 dB or just a tiny 0,1nW. This is the power reaching the paramps. It is much larger from the outside local oscillator and has to be attenuated on the way down in the cryostat.



Gain curves for a JPA as a function of applied pump power in three-wave mixing mode.

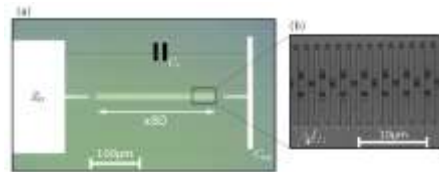


Figure 6.1 - 3/4 resonator. (a) Optical micrographs picture. The left-most pad is the bonding pad, the right-most thin pad is the shunt capacitance denoted C_{out} . In between, there is the array of 80 SQUIDs. (b) Scanning electron microscope (SEM) picture of seven SQUIDs where a single junction has a $10.7 \mu\text{m} \times 0.17 \mu\text{m}$ area.

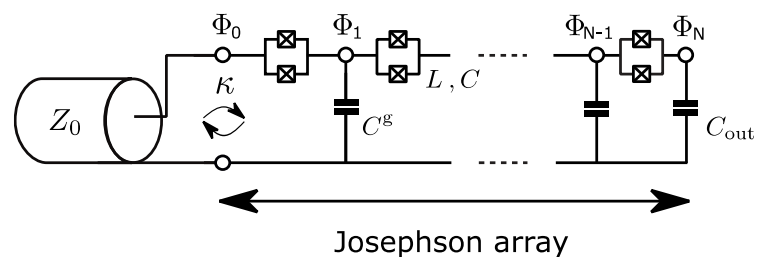
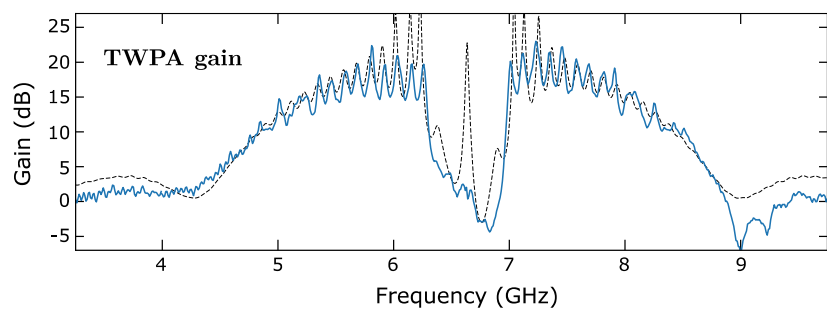


Figure 508: top left, the typical narrow-band response curve of a JPA, and top right, the typical frequency response curve of a TWPA that has over 2 GHz available with a gain superior to 15 dB in two parts, below 6.2 GHz and above 7 GHz. Bottom left is a typical TWPA circuit, with 2000 series of Josephson junction bridges, as described on the right. Source: [Resonant and traveling-wave parametric amplification near the quantum limit](#) by Luca Planat, June 2020 (237 pages).

¹⁴⁴⁷ See [A low-noise series-array Josephson junction parametric amplifier](#) by Bernard Yurke et al, 1996 (4 pages).

¹⁴⁴⁸ See [Widely tunable parametric amplifier based on a superconducting quantum interference device array resonator](#) by Manuel A. Castellanos-Beltran et al, 2007 (9 pages).

¹⁴⁴⁹ See this good TWPA review paper [Perspective on traveling wave microwave parametric amplifiers](#) by Martina Esposito, Arpit Ranadive, Luca Planat and Nicolas Roch, September 2021 (8 pages).

¹⁴⁵⁰ See [Traveling wave parametric amplifier with Josephson junctions using minimal resonator phase matching](#) by T.C. White, John Martinis et al, UCSB, 2015 (15 pages) and [A near-quantum-limited Josephson traveling-wave parametric amplifier](#) by C. Macklin, William D. Olivier, Irfan Siddiqi et al, 2015 (3 pages). Despite the first work involving John Martinis in 2015, Google Sycamore was using JPAs and not TWPAs. Google is still investigating, naturally, how to use TWPAs in their systems.

¹⁴⁵¹ TWPAs however generate undesired mixing processes between the different frequency multiplexed tones as described in [Intermodulation Distortion in a Josephson Traveling Wave Parametric Amplifier](#) by Ants Remm, Andreas Wallraff et al, October 2022 (11 pages).

¹⁴⁵² See [Floquet Mode Traveling-Wave Parametric Amplifiers](#) by Kaidong Peng et al, MIT, PRX Quantum, April 2022 (20 pages). This work from MIT was funded by Amazon AWS Center for Quantum Computing and by NEC.

With TWPAs, there are variations with three-wave mixing (3WM) using one pump photon yielding one signal photon and one idler residual photon and four-wave mixing (4WM) using two pump photons yielding one signal and one idler photon. The pump microwave usually comes from a local oscillator source outside the cryostat.

Other qubit readout options are investigated. One is based on a **JPM** (Josephson Photo Multiplier) that can be directly embedded in the qubit chipset. It doesn't require low-noise amplification with a JPA or a TWPA and provides a good readout fidelity in excess of 98% although it's a bit slow, lasting 500 ns¹⁴⁵³.

CEA-Leti prototyped in 2020 a low-noise cryo-CMOS amplifier that operates as low as 10 mK¹⁴⁵⁴. All this is used to handle the first stages of qubits state readout within the cryostat. In another recent work involving the UK and CEA-Leti in France, quantum-dots based readout amplification is studied, and is adapted to silicon spin qubits.

With some improvements, it could reach gains of classical JPAs (15 dB) although on a small bandwidth¹⁴⁵⁵.

Before looking at cryogenic amplification commercial vendors, let's mention the **MIT Lincoln Lab** team from William D. Oliver who has been pioneering TWPAs for a while, and is providing many labs in the world with its own TWPAs since 2015, and for free (pictured in Figure 509). A gift for science development! On the industry vendors side, **IBM** and **Rigetti** developed their own TWPAs. **IQM** uses TWPAs from VTT.

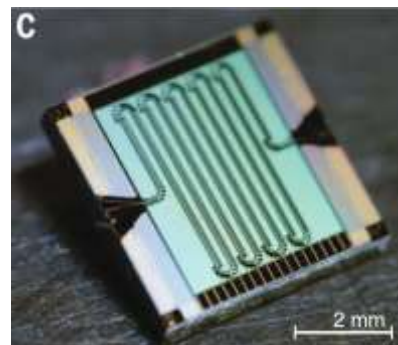


Figure 509: an MIT Lincoln lab TWPA. Source: [A near-quantum-limited Josephson traveling-wave parametric amplifier](#) by C. Macklin, William D. Oliver, Irfan Siddiqi et al, 2015 (3 pages)

In Finland, **VTT** is also manufacturing TWPAs using 1600 Josephson junctions. 40 nm CMOS. In Sweden, **Chalmers University** researchers are working on their own optimized 3WM TWPA¹⁴⁵⁶. In Italy, various labs launched DARTWARS, for designing a TWPA with very large bandwidth covering 5 to 10 GHz with low noise temperature of 600 mK. It will use two techniques with Josephson junctions (JTWPAs) and kinetic inductances (KITWPAs)¹⁴⁵⁷. There was also a 4-year EU TWPA project named **ParaWave**, run by German, Italian and British partners from 2018 to 2021¹⁴⁵⁸.

Google is not following the TWPA path but improving JPAs with their home-made SNIMPA or 'snake impedance matched parametric amplifier' which has a high dynamic range, large bandwidth, high saturation and where the active nonlinear element is implemented with an array of rf-SQUIDS¹⁴⁵⁹.

¹⁴⁵³ See [High-Fidelity Measurement of a Superconducting Qubit Using an On-Chip Microwave Photon Counter](#) by A. Opremcak, Robert McDermott et al, February 2021 (13 pages). On top of give researchers from Wisconsin University, this work involves six researchers from Google and one from Syracuse University in New York.

¹⁴⁵⁴ See [Low-power transimpedance amplifier for cryogenic integration with quantum devices](#) by L. Le Gueulet et al, March 2020 (13 pages).

¹⁴⁵⁵ See [Quantum Dot-Based Parametric Amplifiers](#) by Laurence Cochrane, Fernando Gonzalez-Zalba, Maud Vinet et al, PRL, May 2022 (7 pages).

¹⁴⁵⁶ See [Three-wave mixing traveling-wave parametric amplifier with periodic variation of the circuit parameters](#) by Anita Fadavi Roudsari, Per Delsing et al, September 2022 (6 pages).

¹⁴⁵⁷ See [Ultra low noise readout with travelling wave parametric amplifiers: the DARTWARS project](#) by A. Rettaroli et al, July 2022 (4 pages).

¹⁴⁵⁸ See [Josephson travelling wave parametric amplifier and its application for metrology](#), 2018 (7 pages).

¹⁴⁵⁹ See [Readout of a quantum processor with high dynamic range Josephson parametric amplifiers](#) by T.C. White, Charles Neil, Frank Arute, Joseph C. Bardin et many al, September 2022 (9 pages). They tested it on a 54-qubit Sycamore processor.

HEMT. At last, at the 4K cryostat stage sit the second qubit microwaves readout amplifiers named HEMT (High-electron-mobility transistor). They provide a large gain amplification of about 40 dB with high dynamic range and a large-bandwidth $>6\text{GHz}$ for the inbound microwave readout signal coming from the paramps from the first cryostat stage, which benefited from a first level 15 to 20 dB low-noise amplification at or near the quantum limit.

Many labs and vendors produce HEMTs for qubit readout, like Chalmers University of Technology in Sweden using indium phosphide (InP) transistors which are very efficient at 4K¹⁴⁶⁰. The main vendor here is **Low Noise Factory** (described later, below) as well as **Cosmic Microwave Technology**, with HEMTs designed at Caltech.

Still, commercial HEMT amplifiers dissipate 10 mW of power, which can be a problem when the number of qubits scale, even though the cooling power at the 4K stage is quite larger than at 15 mK, with about 1W to 2W.

One solution would be to use a variety of weakly dissipative TWPAs sitting at the 4K stage, using superconducting materials operating at this temperature like NbTiN and put an HEMT at the 70K cryogenic stage¹⁴⁶¹. This would reduce the heat generated at 4K.

Then, we have room temperature analog amplifiers adding about 50 dB to the signal coming from the HEMT at 4K. These amplifiers are also usually HEMT-based. They consume about 250 mW, which is shared for the multiplexed readout signals of several qubits, usually between 5 and 10 with the potential to grow to 20 and even 100 qubits, depending on the readout speed. Indeed, the shorter the readout pulse, the broader the pulse frequency spectrum will be, limiting multiplexing over a bandwidth of about 2 GHz. The longer the pulse, the smaller the pulse spectrum will be, but it will be detrimental to the efficiency of error correction. That's another design trade-off to take into account in designing these systems.

Now let's look at the amplification vendors I have identified so far.



Low Noise Factory (2005, Sweden) designs and produces low-noise amplifiers (HEMT) operating at ambient or cryogenic temperatures as well as circulators and JPAs. They are part of the European **OpenSuperQ** project, led by the University of Saarland in Germany, VTT in Finland and Chalmers in Sweden, to create commercial TWPAs. The consortium demonstrated in 2019 a TWPA with a maximal gain of 10 dB over a 1.4 GHz bandwidth.



Silent Waves (2022, France) is a spun-out startup from CNRS Institut Néel in Grenoble. It was founded by Luca Planat, Nicolas Roch and Baptiste Planat.

Their offering is a very efficient TWPA, based on the research conducted by CNRS-Institut Néel-UGA and the LPMCM in Grenoble¹⁴⁶². Their commercial TWPA added noise is near the quantum limit of noise. It enables high-fidelity single-shot qubit readout on a wide frequency band and with a gain than can exceed 20 dB. Based on a patented fabrication process, Silent Waves' amplifiers are currently being manufactured in the clean room of the Institut Néel¹⁴⁶³.

¹⁴⁶⁰ See [InAs/AlSb HEMTs for cryogenic LNAs at ultra-low power dissipation](#) by Giuseppe Moschetti et al, 2020, Solid State Electronics (7 pages).

¹⁴⁶¹ See [Performance of a Kinetic-Inductance Traveling-Wave Parametric Amplifier at 4 Kelvin: Toward an Alternative to Semiconductor Amplifiers](#) by M. Malnou et al, NIST and University of Colorado Boulder, October 2021 (11 pages). Their KI-TWPA dissipates only 1 μW .

¹⁴⁶² See [A photonic crystal Josephson traveling wave parametric amplifier](#) by Luca Planat et al, October 2019 (17 pages).

¹⁴⁶³ TWPAs could have applications beyond superconducting qubits readout, in microwave photonics, quantum sensing and quantum information with continuous variables as described in [Observation of two-mode squeezing in a traveling wave parametric amplifier](#) by Martina Esposito, Olivier Buisson, Nicolas Roch, Luca Planat et al, first published in November 2021 and revised in April 2022 (16 pages).

They address both superconducting and silicon spin qubits readout. As a first stage, they will enable 5 and 10 qubits readout multiplexing.



QuantWare (The Netherlands) is not just providing custom superconducting qubits chipsets but also their Crescendo TWPA. It provides a gain of >18 dB gain on a bandwidth of over 1.5 GHz.



Qubic Technologies (2020, Canada) is developing JPAs and TWPAs, the aim being to produce more correlations and better filtered noise. They also use this technology to improve radars. The company was created by Jérôme Bourassa (CEO), a former researcher from the Institut Quantique at the Université de Sherbrooke. He also collaborates with the Institute for Quantum Computing from the University of Waterloo.

Analog Quantum Circuits (2021, Australia) is a TWPA manufacturer created in October 2021.

At last, let's mention again **Cosmic Microwave Technologies** (2016, USA) which produces cryogenic LNAs (low noise amplifiers) used for qubits readouts and is a spin-out of Caltech.

Cabling, connectors and filters

In current quantum systems based on superconducting qubits, copper coaxial cables carry **microwave photon pulses** at frequencies between 5 and 10 GHz that act on the qubits for their reset, for implementing quantum gates and handling qubit readouts.

Microwaves are generated by devices generally located outside the refrigerated enclosure. Frequencies below 5 GHz and above 10 GHz are filtered out¹⁴⁶⁴. These microwaves are also attenuated and filtered at the input on the 4K cold plate. An attenuation of 60db, carried out in three steps of 20 dB which each time divide by 100 the transmitted power. It is used to limit the thermal noise that is conveyed in the cables. It is reduced so as not to represent by more than one thousandth of the photons that end up in the qubits. Each filter absorbs energy that must be dissipated at the stages where they are placed.

The thermal conductivity of a cable Q is calculated as follows, using the product of the cable conductivity k , its cross-section A , the temperature gradient T_2-T_1 and L the length of the cable.

$$Q = kA \frac{T_2-T_1}{L}$$

Coaxial superconducting cables - having theoretically zero resistance at low temperature - connect the qubits to their reading system (thus, in the upward direction in the diagrams). They are made of niobium and titanium alloy (NbTi). They include loops to absorb the metal contraction that occurs during cryostat cooling and warm-up¹⁴⁶⁵. With qubit readout, microwave signals are amplified at least twice before leaving the cryostat including once at superconducting temperature, below 1 K.

¹⁴⁶⁴ See [Engineering the microwave to infrared noise photon flux for superconducting quantum systems](#) by S. Danilin et al, 2022 (22 pages).

¹⁴⁶⁵ See [Challenges in Scaling-up the Control Interface of a Quantum Computer](#) by D. J. Reilly of Microsoft, December 2019 (6 pages) which states that superconducting cables have resistance and capacitance when microwaves are passed through them and therefore have a thermal release that must be taken into account.

These cables are used between the 4K and 15-100 mK cold plates in a cryostat. They come from various vendors including **CoaxCo** (Japan). This company seems to be the only one in the world that produces NbTi cables¹⁴⁶⁶. The 2 mm diameter cable consists of a conductive outer jacket and a central conductor, both made of niobium-titanium which are separated by a Teflon (PFTE) or Kapton insulation.

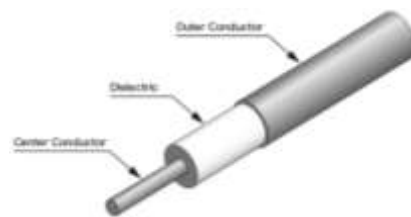


Figure 510: a typical CoaxCo niobium-titanium cable.

Source: [CoaxCo](#).

Other vendors like Delft Circuits are also proposing superconducting cables but they seem to rely on CoaxCo for the base cables they're then integrating in their own solutions.

Most vendors are now trying to miniaturize this cumbersome cabling, mostly with using flexible cables.

Other avenues are pursued, at the research level, using optical cables and frequency conversion from 5 GHz to 200 THz and the other way around, using phonon-based mechanical resonators cavity optomechanics, optomechanical crystal resonator¹⁴⁶⁷ or coplanar waveguide and optical cavity using the dark state protocol¹⁴⁶⁸. You then have to look at the thermal cost of demultiplexing this signal in the cryostat and the quality of the microwave signal after its dual transduction to and from optical wavelengths. This is an option IBM is investigating for scaling its superconducting computer systems¹⁴⁶⁹. Above 4K, the coax cables are using more regular materials like copper alloys.

Microwave qubit control downlink cables are made of various materials including copper-nickel, copper-beryllium or bronze alloys. After passing through the 4K stage, they are replaced by superconducting versions to limit their heat conduction. Between the two, 20 dB attenuators are inserted. In addition, conventional twisted pair cables carrying direct current are used to power the active electronic components integrated in the cryostat, in particular the qubit state readout amplifiers.

This creates significant **wiring clutter**. Figure 511 contains *on the left* a Google cryostat with its bunch of cables and wires connecting the different cold plates. This is the wiring for only 53 qubits (actually, you need to add the 88 coupling qubits). It seems that it is possible to miniaturize some of this, especially with flat ribbon cables. These various cables have another disadvantage: they are very expensive. The unit is several thousand dollars. For today's 53-qubit superconducting quantum computer, this cabling costs more than the entire cryostat, more than half a million dollars. This explains why cryostat manufacturers such as **Bluefors** also offer their own optimized cabling system, such as their 168-cable High-Density Wiring, which appears to be sized to support 56 qubits (*center*). The same is true with the removable cable system of the **Oxford Instruments** Proteox (*right*).

The most expensive cables are the niobium-titanium coax sitting between the 4K and 15 mK stages, up to \$3K each. A 1000 qubit QPU could have \$10M of cabling in its bill of materials!

¹⁴⁶⁶ See [We'd have more quantum computers if it weren't so hard to find the damn cables](#), by Martin Giles, January 2019.

¹⁴⁶⁷ See [Cavity optomechanics](#) by Markus Aspelmeyer, Tobias J. Kippenberg, and Florian Marquardt, Review of Modern Physics, 2014 (65 pages), [Two-dimensional optomechanical crystal cavity with high quantum cooperativity](#) by Hengjiang Ren, Oskar Painter et al, 2020 (21 pages) and the review paper [Mesoscopic physics of nanomechanical systems](#) by Adrian Bachtold et al, February 2022 (87 pages).

¹⁴⁶⁸ See [Proposal for transduction between microwave and optical photons using ¹⁶⁷Er:YSO](#) by Faezeh Kimiaee Asadi et al, University of Calgary, February 2022 (8 pages).

¹⁴⁶⁹ See [Optomechanics with Gallium Phosphide for Quantum Transduction](#) by Paul Seidler, May 2019.



Figure 511: from left to right, Google Sycamore cable clutter, BlueFors optimized cabling system and Oxford Instrument removable cabling system. Sources: Google, Bluefors, Oxford Instruments.

Now, onto the vendors in this space...



Delft Circuits (2016, The Netherlands) was created by Sal Jua Bosman (CEO), Daan Kuitenbrouwer (COO) and Paulianne Brouwer (CFO), the first two coming from TU Delft.

They offer cables and flexible mats used to carry the control microwaves of superconducting qubits such as CF3 (Cri/oFlex) and supporting frequencies ranging from 2 to 40 GHz with 8 embedded cables. Delft Circuit also introduced in March 2022 their Tabbi, an ultra-high density modular flexible microwave interconnect that consolidates the equivalent of 8 SMA cables in about 10 mm and embed its own filters. The startup had 24 people as of early 2022. They manufacture their products out of a 150 m² lab located at the Delft Quantum Campus. The company got financial support from many EU programs (AVaQus, MATQu and SPROUT).



Figure 512: a Delft Circuit Tabbi flat cable and connector.



QDevil (2016, Denmark, 1M€) sells filters used in cryostats including the QFilter, based on a collaboration between Harvard University and the University of Copenhagen. It's a cryogenic filter reducing electron temperatures below 100 mK.

They also sell the QDAC, a 24-channel low noise DAC, the QBoard, a PCB-based fast-exchange cryogenic chip carrier system, and the QBox, a 24-channel breakout box. They are partnering with Bluefors. The company was acquired by Quantum Machines (Israel) in March 2022.



XMA Corporation (2003, USA) provides the OmniSpectra product line comprising adapters, attenuators, couplers and other passive cryo-electronic components used in quantum computing.



Radiall (France) is an industry company specialized in connectors and cabling, very active in the aerospace vertical. They are now addressing quantum technology needs.



The company creates custom solutions for the quantum industry, including ultra-miniature microwave board-to-board connectors, 3D cabling and cryogenic switches. Radiall is currently expanding its product portfolio with microwave solutions supporting various quantum computing technology that require microwave components meeting strict electromagnetic compatibility/electromagnetic interference (EMC/EMI) constraints, cryogenic, non-magnetic and density specifications.



CryoCoax (UK/USA) is a division of **Intelliconnect** (UK/USA) that provides RF interconnect assemblies for various markets including quantum computing, based on niobium-titanium, cupro-nickel, beryllium-copper, stainless steel and brass.

They provide high-density multiway connectors using the SMPM interface (created by Carlisle Interconnect Technologies) that supports a 4.75mm pitch instead of a classical 15 mm pitch with SMA connectors. They also distribute the cabling solutions from Delft Circuits and passive components from OmniSpectra.



Atem (1990, France) is a coaxial cables designer and manufacturer. It wants to enter the quantum computers space with its Qryolink project to propose superconducting coaxial cables.

Rosenberger

Rosenberger Group (Germany) is involved in the German qBriqs projects to build connectors, attenuators components, niobium-titanium and stainless cables assembly to be incorporated in 80 channel multiport connectors and flat cables (with a 1 mm pitch) developed by **Supracon AG** and **LPKF**. They plan to produce these flat cables with 3D printers.

At last, let's mention the IARPA funded **SuperCables** US program that aims to develop high-data rate and low-power transport solutions for cryogenic electronics.

It started in 2019. Its goal is to optical fiber connectivity between room temperature and cryogenic electronics to limit heating. It works on creating electro-optic modulators converting digital signals into and from optical data. It was a 2-year effort targeting a bandwidth of 50 Gbits/s. Which in itself is insufficient for qubits control!

Other electronics vendors

Let's now look at other commercial vendors in the cryogenic electronics area, given they don't create any cryo-CMOS at this point.



Atlantic Microwave (1989, USA) produces and markets radio-frequency and microwave components operating at cryogenic temperatures.

They are used to control superconducting and silicon qubits in cryostats. This includes microwave attenuators, filters, microwave amplifiers and bias tees. It is a subsidiary of the British group ETL Systems, founded in 1984.



Raditek (1993, USA) is a designer and provider of RF signals processing systems, including the circulator magnet-based filters used between the first stage microwave amplifier (at 15 mK) and second stage amplifier (at 4K) used usually with superconducting qubits.



QuinStar Technology (1993, USA) is a vendor of cryogenic circulators, coming from the acquisition of **Pamtech** (USA) in 2010.



RF-Lambda (2003, USA) also provides circulators and low-noise amplifiers.



CryoHEMT (2019, France) is a company created by Quan Dong and Yong Jin in Orsay, France. It designs and manufactures low-noise HEMT microwave amplifiers which amplifies microwaves at the 4.2K cryostat stages.

Their technology is based on the PhD [thesis](#) from Quan Dong done under the supervising of Yong Jin in France in 2013. It seems not being used in quantum information systems.



Diramics (2016, Switzerland) is a spin-off from ETH Zurich creating ultra-low noise transistors in III-V materials (InP, indium-phosphorus) with a technology named pHEMT (pseudomorphic high-electron-mobility transistor, using junctions with two semiconductors with different band gaps).

It can be used in low temperature electronics. It is currently mostly used in astronomy applications.



Marki Microwave (1991, USA) is a supplier of microwave control components: amplifiers, bias tees, couplers, mixers and filters.



Quantum Microwave (2016, USA) creates microwave components operating at cryogenic temperatures for quantum computers, including JPA amplifiers, attenuators, frequency couplers, multiplexers, bias tees, diplexers, filters, image reject mixers and directional couplers.



One main applied research domain for **Raytheon** is related to superconducting qubits controls. They work on arbitrary pulse sequencers (APS) creating superconducting qubits control microwaves, an FPGA readout system using low noise parametric amplifiers and a custom made three-way mixing mode JPAs with 20 dB gain as show in Figure 513.

They are also exploring SFQ based control logic (Josephson gate-based logic) and spintronics based low-power memories. They are mainly found in superconducting qubits quantum computers (IBM, Google, Rigetti, D-Wave). However, they do not push forward the miniaturization of these components like what SeeQC is doing. In October 2021, they announce a technology partnership with IBM, with not many details¹⁴⁷⁰. On top of that, they also develop Josephson junction based infrared photon detectors¹⁴⁷¹.

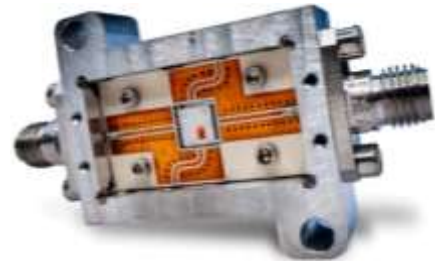
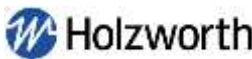


Figure 513: a Raytheon BBN JPA.



Wenteq Microwave Corp (2006, USA) provides low-noise amplifiers, attenuators, circulators and coaxial connectors, in the RF/microwave range.



Holzworth Instrumentation (2004, USA) is a provider of multi-channel RF sources and AWGs. They also provide phase noise analyzers. The company was acquired by Wireless Telecom in 2019.



apitech (1999, USA) is a provider of cryo-attenuators targeting the quantum computing market and covering signals from DC to 40 GHz, and with SMA, and SMPM connectors.

¹⁴⁷⁰ See [Raytheon, IBM partner for quantum in defense, aerospace](#) by Nicole Hemsoth, in TheNextPlatform, October 2021.

¹⁴⁷¹ See [Josephson junction infrared single-photon detector](#) by Evan D. Walsh et al, April 2021 (12 pages).



AnaPico (2005, Switzerland) is a provider of low phase noise RF signals generators, for the local oscillators used in qubits control and readout, running up to 6,1 GHz.



Scalingq (2022, Sweden) was created by a team coming from Chalmers University who wants to help superconducting quantum computers companies design larger QPUs.

It designs a QPU chipset sample holder named LINQER, with currently 16, 36 and 80 connectors, and the potential to scale up to 300 connectors. It provides low crosstalk, an innovative magnetic shielding technology, and supports chipset sizes up to $20 \times 20 \text{ mm}^2$. The company was created by Zaid Saeed (CEO), Lisa Rooth (VP) and Robert Rehammar (CTO).

Thermometers

It is possible to measure **pressure** (ambient, gas), **temperature** (everywhere) and **flow** (of gas) at cryogenic temperature. Specific sensors are therefore installed for this purpose in the cryostat enclosure, attached to different places in the "candlestick".

Temperatures are measured with cryogenic thermometers! These are found in particular at **Lake Shore Cryotronics** with its Cernox thermometers which go down to 100 mK and resist well to the ambient magnetic field and its ruthenium oxide thermometers which go down to 10 mK. At less than 20 mK, noise thermometers using Josephson junctions are used (and the loop is closed...). Some thermometers are placed on the plates opposite the heat exchange tubes and the mixing box. Still, progresses need to be done even in this area, noticeably to measure precise temperatures in the 10 mK range and with no delay¹⁴⁷².

Low Temperature Thermometers

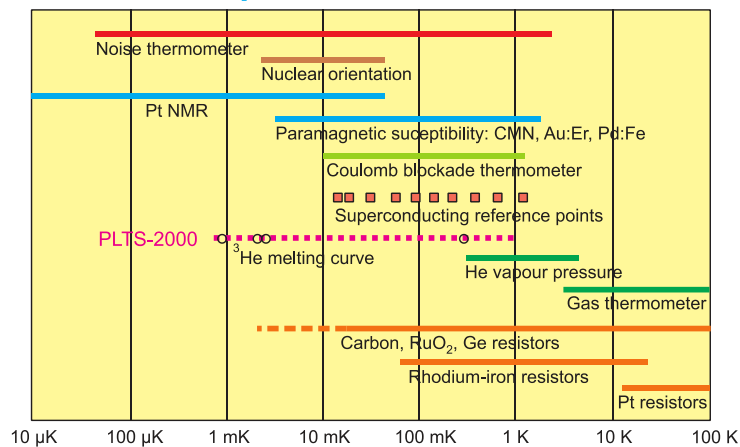


Figure 514: categories of low-temperature thermometers. Source: [Thermometry at low temperature](#) by Alexander Kirste, 2014 (31 slides). We can see that there are about ten types of thermometers that go down to less than 1K. The most commonly used one exploits the Coulomb block based on tunnel junction. The electrical voltage of the junction varies linearly with the cryogenic temperature.

Vacuum

Besides photon qubits, most other qubit types require some form of vacuum to isolate the qubits from their environment. We usually make a distinction between different levels of vacuum. The most stringent ones are used with trapped ions and cold atoms which require ultra-high vacuum (UHV) conditions whereas solid-state qubits like superconducting and electron spins are less demanding. UHV starts at 10^{-9} mbar.

¹⁴⁷² That's what researchers from Chalmers in Sweden achieved in 2020. See [Primary Thermometry of Propagating Microwaves in the Quantum Regime](#) by Marco Scigliuzzo, Andreas Wallraff et al, December 2020 (14 pages).

One problem to avoid when creating vacuum is outgassing. It manifests with particles being ejected from the internal enclosure surfaces and materials, including residual water coming from the air. The phenomenon is avoided with carefully selecting the materials.

Cold atoms qubits require a pressure of 10^{-10} mbar while trapped ions goes down to 10^{-12} mbar. In both cases, low pressures and outgassing are obtained with heating the system enclosure above 200°C for several hours while the vacuum pumps are operating. This “bake-out” process removes water and other trace gases sitting on the chamber surface. Heating is done with heater stripes placed around the chamber. The chamber exterior can also be cooled with liquid nitrogen to contain any further gassing.

There are many vacuum and ultra-high-vacuum systems vendors. The most commonly seen in research labs come from **Pfeiffer** (Germany). Some pumps must be cooled at low temperature, like the 4K pump used by Pasqal to cool their atoms.

At last, measuring pressure in vacuum is also a challenge. Classical mechanical pressure measurement is of no use in the UHV to XUV (extreme ultra-vacuum) ranges covering 1×10^{-6} to 1×10^{-10} Pa. The NIST in the USA is proposing a solution applicable to cold atoms to cover these ranges of pressures¹⁴⁷³. A dedicated part on quantum pressure measurement is located in page 906.

Lasers

Masers and lasers are applications of three successive discoveries and inventions:

- **Fabry-Pérot resonant cavities**, named after Charles Fabry¹⁴⁷⁴ (1867-1945) and Alfred Pérot (1963-1925). Their system invented in 1898 was originally used to create an interferometer.
- **Stimulated emission**, formalized by Albert Einstein in 1917. It occurs when an excited atom receives a photon of energy equivalent to a transition between two energy levels. It then re-emits two photons identical to the received one and the energy level of the atom is reduced to its ground state.
- **Optical pumping**, invented by Alfred Kastler in 1949 at ENS in France, which earned him the 1966 Nobel Prize in Physics.

It generates a population inversion, creating a high proportion of atoms excited at level E_2 in the diagram below compared to level E_1 . Optical pumping often excites atoms to energy levels higher than E_2 in Figure 515, with a non-radiative transition from these levels to the E_2 level and then from the E_1 level to the fundamental level of the E_0 atom. If pumping was performed only between levels E_1 and E_2 , their proportion would balance and the laser effect could not be triggered. Three-level pumping is used with pulse lasers and four-level pumping with continuous lasers.

A laser is based on a resonant cavity filled with a gain or amplifier medium. The pumping of this gain medium is optical, electrical or chemical. Once at the high energy level (E_2 in Figure 515), the atom drops to the E_1 energy level either spontaneously or stimulated.

¹⁴⁷³ See [Development of a new UHV/XHV pressure standard](#) (Cold Atom Vacuum Standard) by Julia Scherschligt et al, 2018 (15 pages).

¹⁴⁷⁴ We owe to Charles Fabry the creation of the Institut d'Optique, of which he was the first director in 1926 of the engineering school that was originally called SupOptique or Ecole Supérieure d'Optique.

laser and maser are applications of the photoelectric effect and light-matter interaction

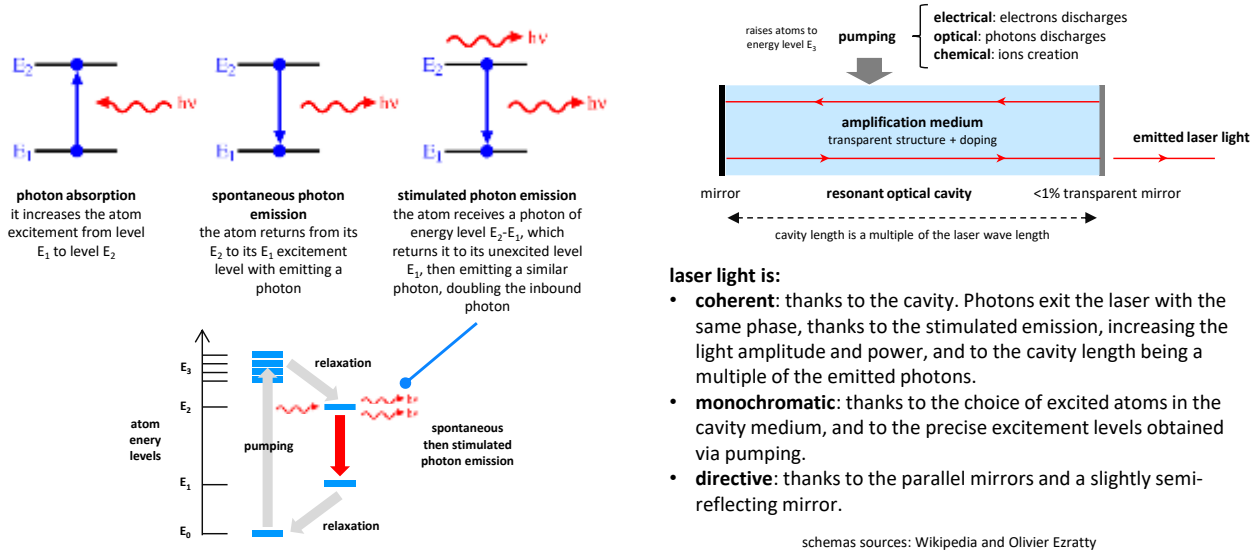


Figure 515: how lasers work. (cc) Olivier Ezratty, 2021.

The mechanism can be self-sustained since the spontaneously emitting photons then generate the stimulated emission of identical twin photons in frequency, phase and amplitude.

The stimulated emission is sustained by placing the atoms in a transparent cavity, filled with solid, liquid or gas, and parallel mirrors trapping the photons. One of the mirrors is slightly semi-reflective, allowing some of the amplified light to exit the laser.

This system of mirrors plays the role of a resonator. It reflects off-axis and thus undesirable photons out of the laser and the wanted on-axis photons back into the excited population where they can continue to be amplified thanks to the laser pumping.

The light resulting from this process is **directive** (thanks to the resonator and its parallel mirrors), **monochromatic** (thanks to the choice of excited atoms and the fineness of the cavity) and **coherent** (the photons are in phase and with the same wavelength/frequency thanks to the stimulated emission and the length of the cavity being a multiple of the laser wavelength). The laser photons frequency depends on the materials used in the cavity and the optical length of the cavity. As an order of magnitude, a 1mW red laser emits 3×10^{15} photons per second.

Lasers (light amplification by stimulated emission of radiation) appeared conceptually in 1958 in an article by Arthur Leonard Schawlow and Charles Hard Townes. The first **gas laser** was created in 1960 by Theodore Maiman, using helium-neon. **Excimer**-based gas lasers cover ultraviolet.

We then had successively **doped crystal lasers** (also named solid-state lasers, such as ruby which is Al_2O_3 doped with Cr^{3+} , or YAG, Yttrium garnet and Aluminum $\text{Y}^{33}+\text{Al}^{53}+\text{O}_{12}^{2-}$), **chemical lasers** (covering the infrared spectrum), **semiconductor diode lasers** (the most common today, usually based on gallium arsenide, or GaAs), **fiber lasers** (using rare earth elements like neodymium, erbium and thulium, mainly used in optical communications), and finally, **free electron lasers**, which we already briefly covered in relativistic quantum mechanics section.

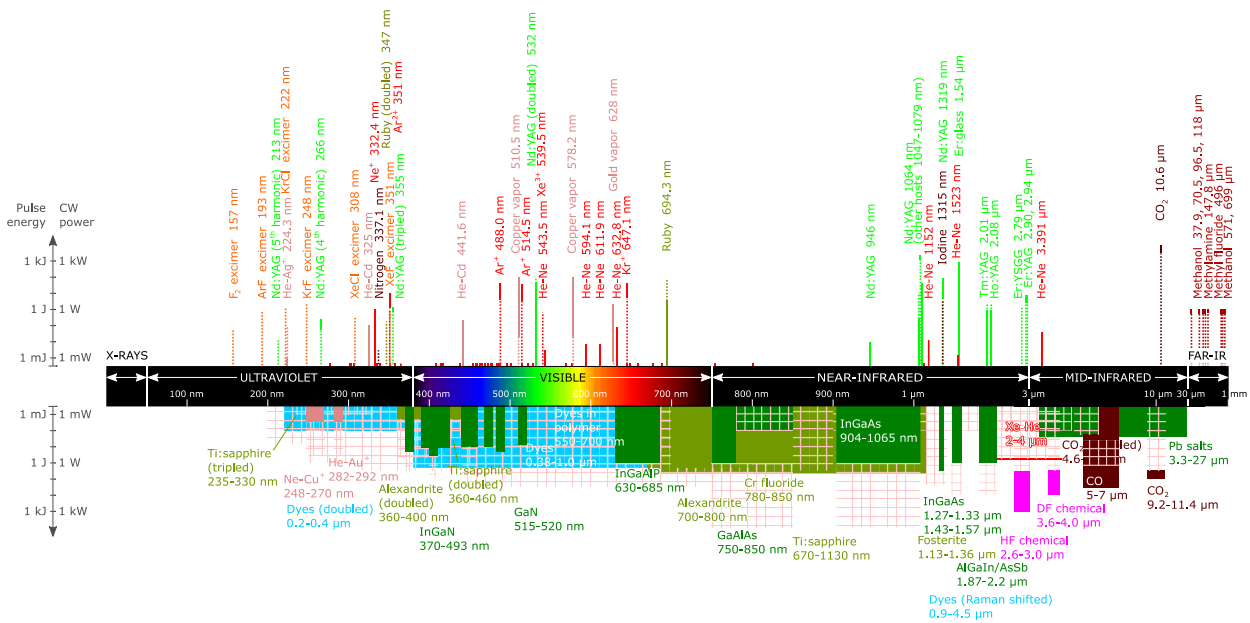


Figure 516: the great variety of lasers covering the electromagnetic spectrum from ultraviolet to mid-infrared waves. Source: [Wikipedia](#).

Lasers operate either in pulses or continuously. The first mode is used to create very high-power levels. To create very powerful lasers, laser amplifiers are created which consists of chains of lasers with a primer laser that is connected to a series of lasers that successively amplify the light generated by the previous laser.

Lasers applications are quite various: industrial diamond drilling and cutting (1965), barcode readers (1974), laser printing (1981), office scanners, Laserdisc (1978), audio CDs (1982), DVDs (1995), surgery, particularly in ophthalmology (glaucoma, retinal detachment, refractive surgery), cosmetic surgery, in dermatology, for tattoo and hair removal, telecommunications, laser pointers, depth sensors, focus sensors for smartphones, iPhone FaceID sensor, measurement and alignment in construction, all sorts of LiDARs, stereolithography 3D printing, confocal microscopy (very shallow depth images), flow cytometry (cell counting), DNA chips analysis, video projector light sources, velocity measurement, the stripping of certain materials, various weapons, nuclear fusion, telescopes adaptive optics, atoms cooling, quantum telecommunications, quantum cryptography and finally, quantum computing, and on and on and on. In short, lasers are everywhere!

The frequency ranges covered by lasers range from infrared to ultraviolet. There are even types of lasers with adjustable frequency. Free electron lasers go as far as X-rays. Gamma-rays lasers - or grasers - do not yet exist.

In quantum technologies, the most commonly used laser wavelengths are 775 nm (beginning of the near infrared region next to red) and 1550 nm (middle of the near infrared region). The first one is used for quantum computing thanks to efficient photon generation and single photon detection (particularly with APD, avalanche photo diodes). The second is used in optical fiber for long distance communications, data transmission and QKD systems.

There are many solutions to up and down convert photons from/to these two wavelengths. For example, these conversions are mandatory when connecting several photon-based quantum computers through a fiber optic link. Solid-state qubits require another type of conversion, mostly from microwaves to 1550 nm infrared photons, given the conversion must convert the quantum information in the solid-state qubit to some encoding in the resulting photons, like their polarization.

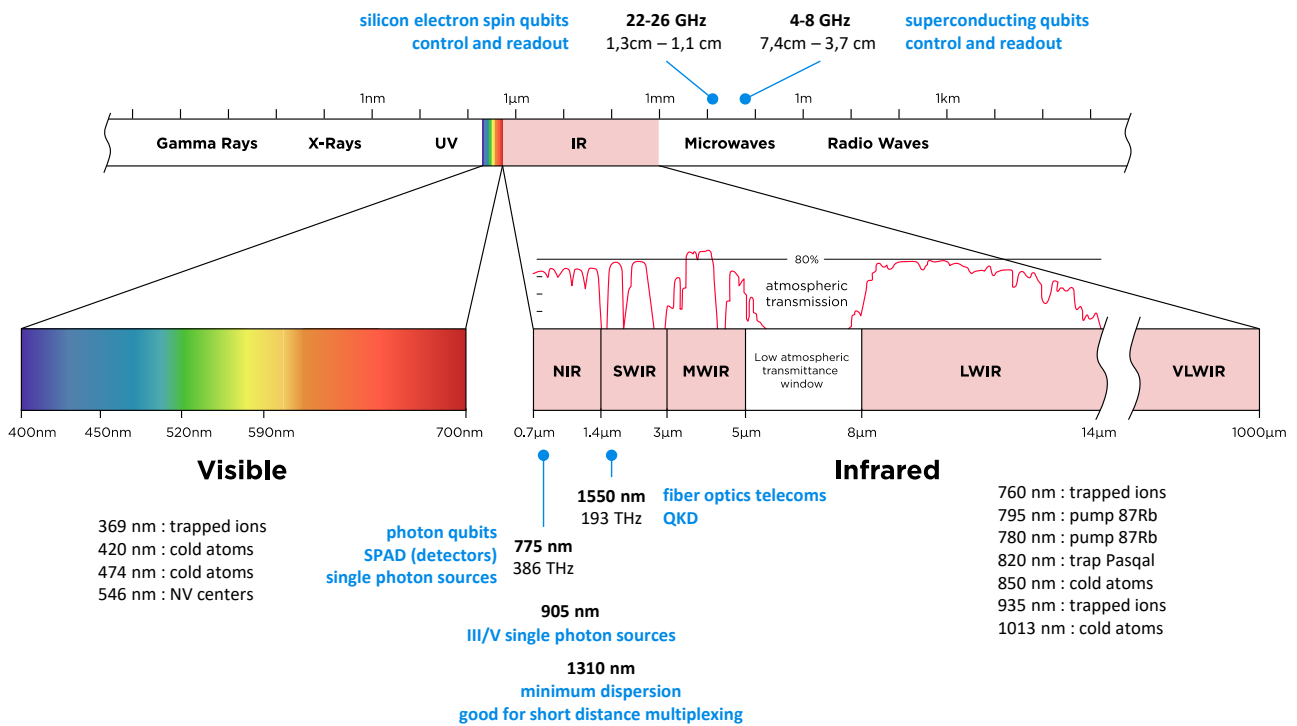


Figure 517: lasers used in the visible and infrared spectrum. Source: <http://www.infiniioptics.com/technology/multi-sensor/>.

Another breed worth mentioning are femtosecond lasers, which create short pulses of coherent light in the range from the femtosecond (10^{-15} s) to the picosecond (10^{-12} s). They are used in micro-machining and various other tasks, including quantum sensing in relation with frequency combs¹⁴⁷⁵.

The **Maser** (1953) or "Microwave Amplification by Stimulated Emission of Radiation" was invented before the laser, in 1953, by Nikolay Basov, Alexander Prokhorov and Charles Hard Townes, who were awarded the Nobel Prize in Physics in 1964.

It is the equivalent of the laser, but emits microwaves instead of visible light. The first masers were made with ammonia and generated 24 GHz microwave photons. Hydrogen Masers followed in 1960.

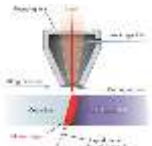


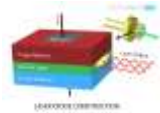

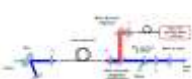

| gas | doped crystals | chemical | diodes | fibers | free electrons |
|---|---|---|--|--|---|
| ionized argon ionized krypton helium-neon copper-neon nitrogen CO ₂ excimers | rubis Nd-YAG rare earths titanium chromium OPO | hydrogen-fluoride deuterium-fluoride | AsGa DFB VCSEL | ytterbium erbium Nd ³⁺ | |
|  |  |  |   |  |  |

Figure 518: the various types of lasers and their cavity materials. (cc) Olivier Ezratty, 2021.

¹⁴⁷⁵ See [20 years of developments in optical frequency comb technology and applications](#) by Tara Fortier and Esther Baumann, NIST, 2019 (16 pages).

There are many laser vendors who play a role in second revolution quantum technologies, both with photon qubits, quantum telecommunications, quantum cryptography and quantum sensing. Lasers are also used to control cold atom and trapped ions qubits.



Toptica Photonics (1998, Germany) is a photonics equipment manufacturer developing laser sources covering a wide range of frequencies from 190nm (UV) to Terahertz waves, including laser diodes and frequency combs. Their lasers can be used to control trapped ions and cold atoms. They employ over 320 people for a revenue of \$82M and are a worldwide leader in their market.

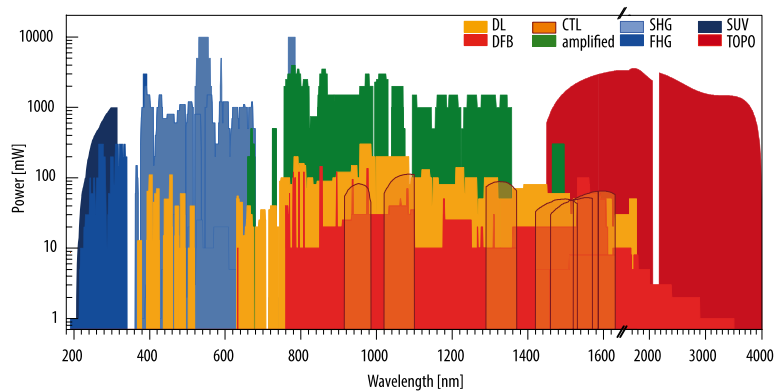


Fig 2 Each quantum system requires lasers with a specific combination of wavelengths and power levels. The broad wavelength coverage from 190 nm to 4 μm provided by Toptica's tunable diode lasers combined with reliable and convenient operation therefore enables many spectacular applications of quantum technologies. (Source: Toptica)

Figure 519: wavelengths coverage of Toptica lasers. Source: [The Control of Quantum States with Lasers in Photonics View, 2019 \(3 pages\)](#).

Their flagship product, the Chromacity OPO, has a tunable optical parametric oscillator that covers near-IR and mid-IR wavelengths. Some of their lasers can create entangled photons.



Stable Laser Systems (2009, USA) offers Fabry-Perot lasers and cavities that can be used for cold atom confinement.

The startup launched by Mark Notcutt is based in Boulder, Colorado, one of the nerve centers of quantum technologies in the USA, near NIST and the University of Colorado. His team also includes Jan Hall, winner of the 2005 Nobel Prize in Physics for the discovery of the effect that bears his name.



Lumibird (1970, France) is a supplier of lasers. Formerly Quantel and Keopsys, it is a large SME with more than 800 employees and a turnover of 110 M€, 80% of which is exported.



Chromacity (2013, UK) is a manufacturer of lasers targeting various industry and research needs, including quantum communications.



DenseLight Semiconductors (2000, Singapore) manufactures various laser products.



FemTum (2016, Canada) creates mid-infrared lasers which can be used in quantum optics and silicon photonics applications and quantum sensing using optical frequency combs. It is a spin-off from the Center of optics, photonics and laser (COPL) in Quebec City.



FocusLight Technologies (2007, China) produces laser diodes and laser optics components.



Freedom Photonics (2005, USA) manufactures lasers and photodiodes using InP and GaAs semiconductor, SiGe-based photonics and planar lightwave waveguides. It was acquired by **Luminar** in March 2022.



GLOphotonics (2011, France) sells hollow-core photonic crystal fiber (HC-PCF) and their functionalized form Photonic Microcells (PMC). These lasers use a proprietary fiber technology and gas photonics. They are partnering with CNRS XLIM lab in Limoges.



iPronics (2019, Spain) develops general-purpose integrated programmable photonic systems, where optical hardware complements software to perform multiple functions.



Q.ANT (2018, Germany, 11M€ public funding) has a product line organized in four segments: particle metrology, atomic gyroscope, magnetic sensing and photonic computing.

They develop a green laser optimized for NV centers quantum sensors. It is a subsidiary of the TRUMPF Group. It also manufactures powerful lasers used in ASML lithography machines and light channels on silicon for qubits transport. They are also working on photonic-based quantum computing using lithium-niobate circuits using path encoding, phase modulation, interferometers (MZI), fiber couplers, electro-optical modulators and resonators. They lead a relate German consortium with 50M€ funding including 42M€ public funding from the German government. As of November 2022, the company had 50 employees.



Silentsys (2021, France) created a closed-loop voltage regulation electronic system that complements lasers and their servo controller to reduce the emitted laser noise and improve its frequency precision.



UnikLasers (2013, UK, £4.1M) sells ultra-narrow linewidth, high power lasers at the specific wavelengths related to the exact atomic transitions targeted for quantum sensing applications.

It can transform a MHz linewidth laser into an Hz linewidth laser. It is currently adapted to continuous lasers running in the 1550 nm and 1050 nm wavelengths and fits in a 2U rack system. Their OFD system (optical frequency discriminator) delivers a continuous voltage signal driving the laser diodes that is proportional to the frequency fluctuations of the input laser beam. The technology core is optical, using frequency combs. They also propose low power voltage power systems. One of their OFD can drive two lasers.



Vexlum (2017, Finland) produces high-power narrow-linewidth vertical external-cavity surface-emitting lasers (VECSELs) including blue and UV lasers, used among other things, to control trapped beryllium ions.

It is a spinoff from Tampere University of Technology Optoelectronics Research Centre (ORC).

And also: **Spectra Physics** (1961, USA), **Altitun** (1997, Sweden, \$10M), **Calmar Laser** (1996, USA) and **Ampliconyx** (2016, Finland who manufactures short-pulses lasers), **Active Fiber Systems** (2009, Germany) which creates femtoseconds fiber lasers and is a spin-off from Fraunhofer IOF, **InnoLume** (2002, Germany, \$26.8M, which sells laser diodes), **FISBA** (1957, USA) which develops multi-wavelengths lasers, **Intense Photonics** (1994, USA, \$51M, which develops single and multi-mode monolithic laser array products, and high power laser diodes and was acquired by Orix Group), **Lytid** (2015, France) which manufactures terahertz cascade lasers, **Spark Lasers** (2015, France) and their picosecond and femtosecond lasers, **Amplitude Laser Group** (2001, France) and their femtosecond lasers, **neoLASE** (2007, Germany) a supplier of various laser products including laser amplifiers, **Alpes Lasers** (1994, Switzerland) which sell infrared quantum cascade lasers, **Luna Innovations** (1990, USA, \$13.1M), **Vector Photonics** (2020, UK, £1.6M) is a spin-off from the University of Glasgow which develops semiconductor lasers based on PCSELs (Photonic Crystal Surface Emitting Lasers) and **OEwaves** (2000, USA, \$15M) provides lasers, oscillators and optical/RF tests and measurement systems.

Photonics

Let's now look at other photonics equipment manufacturers. They sometimes also manufacture lasers but even more.



Accelink (1976, China) sells optoelectronic components, including fiber optics modulation and demodulation systems, lasers and SiO₂/Si material plane optical waveguides. They probably play a role in the deployment of quantum telecommunication networks.



Aurea Technology (2010, France) is a photonics equipment manufacturer targeting various markets including quantum communications (QKD) and quantum sensing.

It sells twin photon sources (TPS), time correlated single photon detectors (Picoxea), ultra-low-noise NIR single-photon counting detection modules (SPD_A and SPD_OEM_NIR¹⁴⁷⁶), time correlators (Chronoxea) and high-resolution fiber sensors (q-OTDR) and picosecond pulse lasers (Pixea). They also developed Fluoxea, a fluorescence lifetime imaging mapping system using time-correlated single photon counting that can be used to characterize semiconductors, qualify quantum dots or measure local magnetic fields (with the help of NV centers). The company has its own assembly plant in Besancon, France. It's a spin-off company from the optics department of FEMTO-ST, a public research lab based as well in Besancon.



Azurlight Systems (2010, France) develops high-power laser amplification systems in the visible and near-infrared spectra (from 488 nm to 1065 nm) using ytterbium-based fibers with low thermal dissipation. These can be used for atoms cooling and trapping.



Qontrol Systems (2016, UK) develops photonics components including photonics device status readout modules and backplanes (boards) on which several of these modules can be installed. These modules drive photonics devices via a 12V voltage and read signals with 18-bit accuracy. This is control electronics.



Cailabs (2013, France, \$46.2M) is a company based in Rennes, France, which is a spin-off from the LKB of ENS Paris and markets photonics equipment and in particular spatial multimode multiplexing systems for optical fibers supporting up to 45 nodes.

This is what makes it possible to multiply the speed of the optical fibers of the telecom operators' networks. In particular, they have KDDI (Japan) as a customer. The startup is managed by Jean-François Morizur (CEO) and Guillaume Labroille (CTO) with Nicolas Treps from LKB being their scientific advisor.



Quandela (2017, France, €35M) is a startup specialized in the generation of indistinguishable photons with quantum dot fed by a laser. They target research, telecommunications and quantum computing use cases.

Quandela's team is composed of Valérian Giesz (CEO), an engineer from the Institut d'Optique with a PhD in photonics¹⁴⁷⁷, Niccolo Somaschi (CTO), PhD from the University of Southampton and Pascale Senellart (CSO), CNRS research director at C2N from CNRS and Université Paris-Saclay.

¹⁴⁷⁶ The SPD_OEM_NIR is using an InGaAs single photon avalanche diode (SPAD in the 900 to 1700 nm wavelength range with very low dark count rate noise (DCR < 700 Hz). It is cooled with the Peltier effect. The supported wavelengths make it suitable to photon counting in telecom wavelengths based QKDs (1,550 nm). It also fits into a standard datacenter rack in a 2U package.

¹⁴⁷⁷ See his thesis in [Cavity-enhanced Photon-Photon Interactions With Bright Quantum Dot Sources](#) by Valérian Giesz, 2016 (228 pages) where he describes his work in Pascale Senellart's team and the various evolutions of their quantum dot photon source that led in 2017 to the creation of Quandela.

It had a staff of about 50 people in Summer 2022 and several international customers, mainly in Europe, Russia and Asia. Their team also includes Shane Mansfield, who works on theory, algorithms and software.

With a trapped artificial atom comprised of a couple thousand atoms forced to emit periodically single photons in a given direction by laser-activated cavity quantum electrodynamics, they are able to generate photon streams that are well separated in time and with stable quantum characteristics, with wavelengths from 924 nm to 928 nm in the near infrared, this range being progressively extended¹⁴⁷⁸. This creates a very bright photon source that can then be multiplied to create indistinguishable photons used in quantum photon processors and various other applications such as quantum telecommunications and quantum key distribution¹⁴⁷⁹.

They are developing single photon sources running at telecom wavelength as part of the project Paris-RegionQCI, a regional project, led by Orange, with an end goal to deploy a QDK-fibered link between Paris and the Paris-Saclay University. They also work on the generation of cluster states of entangled photons as part of the European Union FET Open Qcluster project (2019-2023).

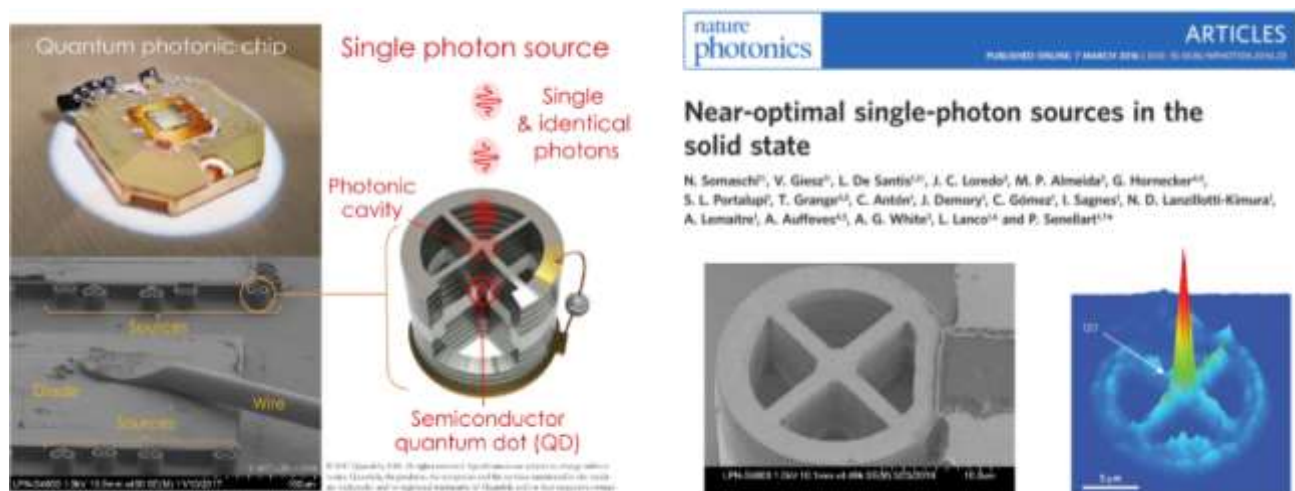


Figure 520: Quandela's quantum dots single photon source. Source: [Near-optimal single-photon sources in the solid-state](#) by Niccolò Somaschi, Valerian Giesz, Pascale Senellart et al, 2015 (23 pages).

The photon source must be cooled down to a temperature range of 5K-10K, which is achievable with compact cryostats costing only a few thousand Euros and using helium 4, such as the attoDRY800 from **Attocube** (Germany). These cryostats use a simple pulsed tube, reminiscent of the first cooling stage of the dry dilution cryostats used with superconducting and quantum dot spin qubits. These single photons are particularly indicated to allow the creation of quality quantum qubit gates and for measurement-based quantum computing (MBQC, which we cover starting page 450).

¹⁴⁷⁸ See [Near optimal single-photon sources in the solid state](#), Niccolò Somaschi, Valerian Giesz, Pascale Senellart et al, 2016 (23 pages). The quantum dot is made with InGaAs (indium, gallium, arsenide) and is surrounded by stacked Bragg-reflectors made respectively with GaAs and Al_{0.9}Ga_{0.1}As (aluminum, gallium, arsenide). Pascale Senellart describes in detail how Quandela's photon generators are made in her talk [Quantum optics with artificial atoms](#) in a Rochester Lecture in June 2018 (1h10mn). The prestigious [Rochester Lectures](#) are held once a year in Durham, UK. The 2017 edition welcomed Peter Knight and the 2012 edition Alain Aspect.

¹⁴⁷⁹ The process was improved in Pascale Senellart's laboratory in 2020 to generate even brighter and purer photon sources from a spectral and polarization point of view thanks to quantum dot excitation with phonons. See [Efficient Source of Indistinguishable Single-Photons based on Phonon-Assisted Excitation](#) by S. E. Thomas, Pascale Senellart et al, July 2020 (10 pages).

Quandela's photon generator was previously offered as a combination of two packaged products:

- The **Qubit Control Single Unit** which allows complete filtering of the single photons emitted by the sources in an Attocube cryostat of the laser used for quantum dot excitation. It is mainly composed of filters tuned to the energy of the optical transition of the emitter.



Figure 521: Quandela Control Single Unit.

- The **QShaper** is a more compact device that generates femto/pico-second laser pulses on an optical fiber that will then feed the QCSU quantum dot above. It is powered at the input by the customer's laser. It is used to prepare the laser beam with the right spatial and temporal shape. It is a device made up of various filters. It is calibrated to supply the semiconductor sources.

Quandela launched in 2020 a compact and integrated version of this whole set, fitting into a datacenter rack named Prometheus. The fiber is glued to the photon source, which will eliminate the mechanical part of the calibration. The pulsed head of the 4K cryostat is also integrated in this 3U rack, the compressor being outside and water-cooled at first. Eventually, it will be integrated in the rack and cooled by air.

The rack was designed by **Pentagram**, the same British designer that IBM used for the Q System One launched in January 2019. It is 1.75m high and 80cm wide. It stacks all the elements: the QShaper, the new QCF and a control computer with its keyboard. The whole thing consumes about 5 to 6 kW, the bulk of it coming from the cryostat.

Quandela and the C2N laboratory collaborate with research labs around the world to create advanced photonics platforms. In 2020, they published with a team from the **Hebrew University of Jerusalem** a paper on the creation of a photon cluster state for quantum computing (Figure 522). The idea is to use single photons and to entangle them with each other via a delay line, and inject them into a computing circuit based using cluster states and MBQC (measurement based quantum computing) method.

In Europe, they collaborate mainly with **Fabio Sciarrino's** team in Italy, in the Netherlands with **QuiX**, in Spain with **INL** and other teams in Austria, the United Kingdom, Slovakia and Israel. They are part of the European FET project PHOQUSING for boson sampling led by Fabio Sciarrino's team.

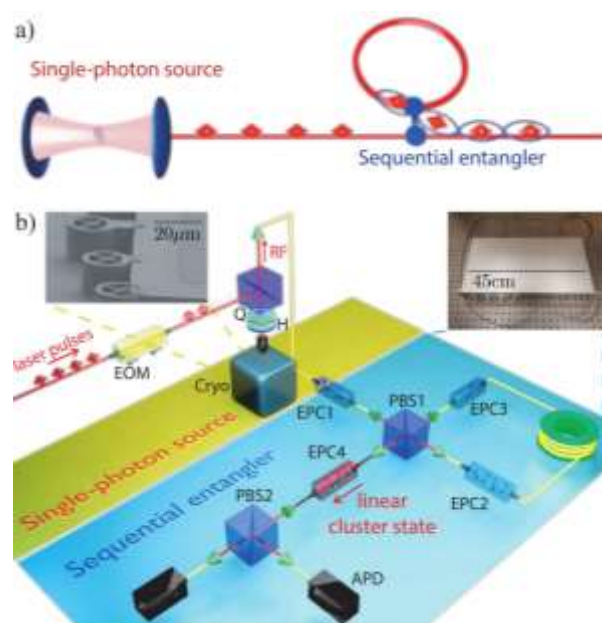


Figure 522: creation of cluster state photons with a serial entangler using a delay line. Source: [Sequential generation of linear cluster states from a single photon emitter](#) by D. Istrati et al, 2020 (14 pages).

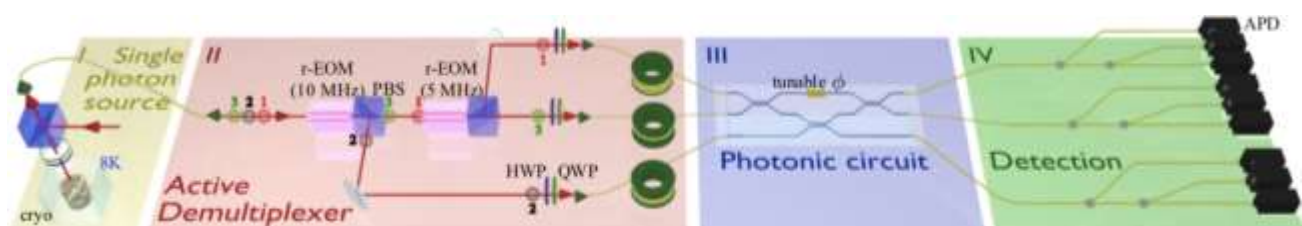


Figure 523: three entangled photon source using Quandela quantum dots. Source: [Interfacing scalable photonic platforms: solid-state based multi-photon interference in a reconfigurable glass chip](#) by Pascale Senellart et al, 2019 (7 pages).

In 2019, they experimented with Quandela's photon source to demultiplex it into three photons which were then injected into a photonic integrated circuit integrating a programmable quantum gate. The photonic circuit was precisely etched with a femtosecond laser (Figure 523).

At last, since 2020, Quandela has started working on creating a photon-based quantum computer using their own photon source. We cover this aspect of their business in the photonic qubits vendor section that starts page 455.



Quantum Opus (2013, USA) develops single photon detectors based on superconducting nanowires, the Opus One. The compact version Opus Two is an 8U data center rack-mount package, including cryostat¹⁴⁸⁰. This company benefited from US federal funding, including \$100K in 2015 and \$1.5M in 2015 from DARPA and \$125K from NASA in 2018. They are a provider of the Chinese team who did run the gaussian boson sampling experiment announced in December 2020.



Qubitekk (2012, USA, \$5M) is a supplier of photon and entangled photon sources for use in the context of quantum cryptography (QKD). This technology can also be used to manage part of the communication between qubits in some types of quantum computers. It competes to some extent with Quandela.



Scotel (2004, Russia) offers single photon detectors in the visible and infrared (SSPD, for Superconducting Single Photon Detecting Systems). These detectors are cooled at 2.2K helium-4 using a Sumitomo SRDK 101 pulse head system with a water-cooled HC-4E compressor.



Single Quantum (2012, The Netherlands) offers Qos single photon detectors integrated in a 2.5K liquid helium cooled cryostat.

Their sensor uses the SNSPD (superconducting nanowire single photon detector) technique, made of a thin film of superconducting nanowires shaped into a flattened serpentine coil. This device captures a single photon from an optical fiber and have a detection efficiency of 85% to 90%, covering wavelengths from 800 nm to 1550 nm.

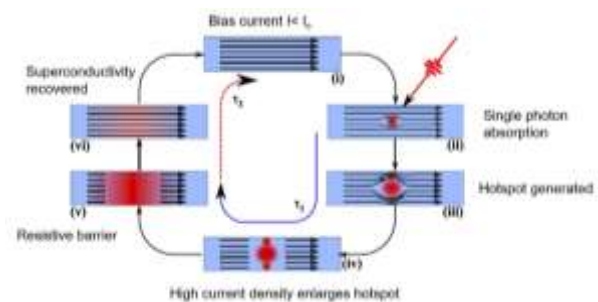
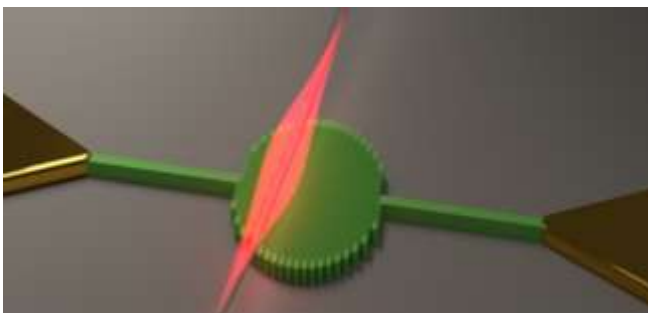


Figure 524: SingleQuantum SNSPD photon source.



Sparrow Quantum (2016, Denmark, \$2.2M) is a spin-off from the Niels Bohr photonics research laboratory. Like Quandela and Qubitekk, they offer single photon sources.

Their solution is based on InAs quantum dots. Their engineering differentiation lies with the quantum dot efficient coupling with a slow-light photonic-crystal waveguide.

¹⁴⁸⁰ See [Introduction to Quantum Opus and revolutionary superconducting detection systems](#) (14 slides).

A laser is illuminating the quantum dots with using a confocal microscope. Their photon coherence indistinguishability is between 95% and 98% with their Sparrow Chip 2021 Resonant. They are generated in the 920-980 nm wave range. The photon generation system is cooled at 6K.



VLC Photonics (2011, Spain) produces photonics equipment and fables design of photonic integrated circuits. The company is involved in European Flagship projects.

It is a spin-off of the University of Valencia. The company was founded by Iñigo Artundo, Pascual Muñoz, José Capmany and José David Domenech. They also market technical reports at prices ranging from 4K€ to 5.4K€ per piece.



Excelitas (2010, USA) sells various photonics devices including Single-Photon Counting Modules (SPCMs).



Pixel Photonics (2020, Germany, 1.45M€) develops single photon detectors (SNSPD) targeting quantum computing, QKD and imaging markets. With HTGF (Germany) and Quantonation (France) as seed investors.



Hamamatsu Photonics (1953, Japan) provides silicon photodiodes, electron multipliers for detecting electrons, ions, and charged particles, photon counters, LCoS based spatial Light Modulators (SLM) used for cold atoms controls, laser cooling systems, quantum imaging and image sensors for the detection of neutral atoms, trapped ions and NV centers fluorescence.



Miraex (2019, Switzerland) has two main quantum technologies in its portfolio: photonic based quantum sensors for vibration, acceleration, acoustic, pressure, electrical field and temperature measurement and a quantum system converting matter qubits into photon qubits and vice versa. It's a spin-off from EPFL.



Micron-Photons-Devices (2004, Italy) aka MPD creates Single Photon Counting Avalanche Diodes, "SPAD", fabricated using custom silicon, standard CMOS and InGaAs/InP technologies. It also sells photon counting based QRNGs.



Qubitrium (2020, Turkey) develops entangled photon sources, laser current drivers and single photons detectors.



Teem photonics (1998, France) creates lasers and integrated photonics components including erbium doped waveguide amplifiers and arrayed-waveguide gratings. Not the same AWGs than the arbitrary waveform generators used to control solid-state qubits, although these can be used to signals multiplexing/demultiplexing.



Alcyon Photonics (2018, Spain, \$560K) is a spin off from IO (Instituto de Óptica) in Spain. Its expertise is on sub-wavelength grating (SWG) technology. They create complex photonic circuits like high-performance Application Specific Photonic Integrated Circuits (APICs). The company was cofounded by the researcher Aitor Villafranca.



Scintil Photonics (2018, France) develops mixed silicon and III/V photonic components, using their BackSide-on-BOX process, that mixes active and passive optical components.

Their technique bonds InP/III-V dies on the backside of processed Silicon-On-Insulators (SOI) wafers, only where it is needed. Their fabrication process is classical CMOS. Their components integrate lasers (WDM laser arrays and tunable lasers), modulators, waveguides, wavelength filters, surface fiber couplers, semiconductor optical amplifiers (SOA), and photodetectors.

Muquans/ixBlue (France) is also a provider of laser and intelligent frequency tunable lasers, laser frequency doublers and narrow-linewidth lasers used in various quantum technologies.

Photon Force (2015, UK) creates single-photons cameras of 32x32 pixels. It can be used in various photonic based quantum sensing applications. It enables time-tagging of incoming photons with a time resolution of 55 pico-seconds.

Covesion (2009, UK) develops laser frequency conversions devices that are used in many quantum optics applications. It's a spin-off from the University of Southampton.

We also have **Ibsen Photonics** (1991, Denmark) which provides spectrometers and various photonic equipment, **Lumiphase** (2020, Switzerland) which develops optical modulators, **Pixel Photonics** (2020, Germany, 1.8M€) which designs Single Photon Detectors (SNSPD), **Bay Photonics** (2007, UK) which provides photonic circuits assembly and packaging, **MenloSystems** (2001, Germany) and their optical frequency combs, terahertz systems and femtosecond lasers, **Qubig** (2008, Germany) which develops light modulators (amplitude and phase modulators, phase shifters, Pockels cells) that can be used in quantum computing or communications, etc.

Fabs and manufacturing tools

Many quantum technologies components are nanofabrication based and must be manufactured somewhere. It's the case with superconducting qubits, superconducting electronics, quantum-dots based electron spin qubit circuits, quantum nanophotonic circuits, NV center based qubits and sensors, single-photon generating quantum dots, photon detectors, trapped ions supporting circuits, travelling wave parametric amplifiers and the likes. You could wonder how these circuits are manufactured and where. Like your regular smartphone chipset processor, is it coming from a giant \$20B TSMC 5 nm fab in Taiwan? Well, most of the time, no!

Foundries

We are in a very different technology and market realm. Quantum related components have some distinct characteristics compared to mass market semiconductors that you'll find in your TV, smartphone, laptop or tablet. They are very specialized and use sometimes special manufacturing processes and/or materials like III/V semiconductors or niobium/aluminum deposition for superconducting qubits and electronics. They are most of the time experimental with many try/error cycles. They are sometimes manufactured with specialized tools. And at last, they are produced in rather small quantities. Surprisingly, given the experimental nature of many components, the related fabs are usually less impressive in size and cost.

Fabs contain cleanrooms, where the concentration of airborne particles is controlled on top of temperature, humidity and sometimes, other parameters like ambient magnetism and vibrations. Cleanrooms are classified according to the number and sizes of particles suspended in the atmosphere. Cleanroom ISO classes range from 1 to 9, with an (exponential) increased number and size of particles per volume unit, 1 being the "cleaner". Most specialized quantum technologies fabs have a less stringent cleanroom class requirement than the most expensive and modern semiconductor fabs since they are not creating high-density chipsets and do not care so much about yield. They are rather class 100 to class 1000 cleanrooms.



Figure 525: research and industry cleanrooms fabricating semiconductors for quantum use cases. (cc) Olivier Ezratty, 2022.

We can segment quantum technologies fabs in a couple categories:

Research fabs. These are most of the time fabs from national research organizations labs and universities. These fabs have cleanrooms with sizes ranging from 100 m² to 4,000 m². Their teams and the associated researchers are creating the “recipe” of new semiconductor technologies. These fabs usually produce 200 mm or smaller wafers. You have for example the famous MIT Lincoln Labs in the USA (superconducting electronics and qubits, trapped ions chipsets, with 1,629 m² of clean rooms), Princeton (1,350 m² cleanroom, silicon and III/V, up to 100 mm wafers), HRLabs in California (all sort of things in a 900 m² clean room), UCSB Nanofab (1,170 m², superconducting qubits, MEMS, photonics, imaging sensors), Harvard CNF (966 m²), Yale University (108 m², superconducting qubits), Stanford (180 m², various quantum techs), NIST NanoFab (1,800 m² cleanroom), VTT in Finland (2,600 m² cleanroom for 150 and 200 mm wafers, superconducting qubits and electronics, photonics), CNRS C2N (2,900 m² clean room near Paris, photon quantum dots sources in GaAs, polaritons circuits, etc), CNRS Institut Néel (220 m², near Grenoble, superconducting electronics and qubits, graphene, diamonds growth¹⁴⁸¹), Van Leeuwenhoek Lab at TU Delft (3,500 m² cleanroom used by Qutech and TNO in The Netherlands), MyFab (Sweden), Fraunhofer IPM (400 m² clean room in Freiburg, various optical quantum sensors), Fraunhofer IPMS near Dresden (200 mm wafers 1,500 m² cleanroom) and also PTB, Leibniz IPHT and Jülich in Germany, EPFL and ETH Zurich in Switzerland and others like RIKEN and AIST (superconducting electronics, but also a strong CMOS 300 mm manufacturing capacity) in Japan or UNSW in Australia. PoliFAB from Politecnico di Milano created an interferometer used by Pascale Senellart’s team to demonstrate the indistinguishability of photon clusters¹⁴⁸². The Shanghai Institute of Microsystem And Information Technology (SIMIT) has also its own fab.

Pre-industry research fabs. These are the likes of IMEC (Belgium) and CEA-Leti (France) who create new semiconductor components and design new manufacturing processes before they are volume-produced in commercial fabs. These are larger fabs than the aforementioned research fabs. CEA-Leti operates 11,000 m² of cleanroom in Grenoble. IMEC cleanrooms totals 12,000 m² in Leuven, Belgium. CEA-Leti produces silicon qubits wafers for its own usage as well as for vendors like Quantum Motion (UK). These fabs produce wafers up to 300 mm.

¹⁴⁸¹ See [Fabrication of superconducting qubits](#) by Vladimir Milchakov (IQM), September 2020, who describes the Institut Néel superconducting manufacturing capability and process. This fab also produces the TWPA electronics from Silent Waves, a spin-off startup from Institut Néel created in 2022.

¹⁴⁸² See [Quantifying n-photon indistinguishability with a cyclic integrated interferometer](#) by Mathias Pont, Pascale Senellart, Fabio Sciarino, Andrea Crespi et al, January 2022 (21 pages).

Likewise, the Center for Advanced Technology in Nanomaterials and Nanoelectronics (CATN2) from SUNY Polytechnic Institute in New York State has a cleanroom of 12,000 m² producing 200 mm and 300 mm wafers for AI, photonics, CMOS spin qubits, superconducting qubits and digital electronics.

Foundry vendors. These are independent foundries manufacturing semiconductors for third parties. GlobalFoundries manufactures nanophotonic chipsets for PsiQuantum and Xanadu in Malta, New-York State in their 41,400 m² clean room on top of classical CMOS chipsets like the IBM Power processors. Infineon's Villach fab in Austria manufactures trapped ions chipsets in its 23,000 m² cleanroom for Oxford Ionics¹⁴⁸³. In Germany, Infineon is an industry partner of many other projects with superconducting qubits, qubit control electronics and NV centers qubits and sensing¹⁴⁸⁴. In the USA, SkyWater is the largest foundry for superconducting electronics, working among others for D-Wave, on top of working on various space applications and with DARPA. Formerly Cypress Semiconductor, Control Data and VTC, they consolidate a 7,360 m² clean room in Minnesota and another one of 3,300 m² in Florida and support 90 nm features geometries on 200 mm wafers. Lionix in The Netherlands manufactures nanophotonic circuits for its subsidiary QuiX. Larger foundries are usually needed for high-density chipsets, particularly with silicon qubits where patterns are relatively small, down to about 10 nm. OMMIC (2000, France) is a small foundry specialized in manufacturing III-V MMIC (monolithic microwave integrated circuit) which could comprise cryogenic amplifiers used in quantum computing.

In-house vendor fabs. These are the fabs from quantum technology vendors who are self-sufficient for this respect. Intel manufactures its own quantum dots spin qubits chipsets in one of its clean rooms at its Hillsboro facility in Oregon. IBM also has its own manufacturing capacity for superconducting qubits and high-density silicon chipsets with a cleanroom of 3,600 m² in Yorktown, New York State. Rigetti in the USA and IQM in Finland have their own small \$20M fabs for their superconducting qubits chipsets. Google has also an in-house fab in Santa Barbara, California. SeeQC has a small 150 mm wafers 200 m² cleanroom dedicated to manufacturing superconducting electronics. Keysight also has its own III/V 1,200 m² cleanroom, the High Frequency Technology Center (HFTC) in Santa Rosa, California¹⁴⁸⁵. Qilimanjaro relies on a fab that was put in place in 2021 at TII in Abu Dhabi. At last, Thales has an in-house 4000 m² III/V fab with CEA-leti as a partner. Having your own fab makes sense when you need to have a fast turn-around and test repetitively many generations of qubit chipsets. It is relatively affordable for producing superconducting qubits on small wafers.

The USA, European Union and China all want to increase their share, self-reliance and supply security with semiconductor manufacturing. In February 2022, the European Union launched the European Chips Act to “*foster development of capacities in advanced manufacturing, design and system integration as well as cutting-edge industrial production*”, with a public/private funding of €43B until 2030. It includes international partnerships like when Intel is installing a new fab in Germany. The plan contains a provision for quantum technologies, to “*set up advanced technology and engineering capacities for quantum chips in the form of design libraries for quantum chips, pilot lines, and testing and experimentation facilities*”. This may provide some additional funding for the extension of the many quantum-related fabs mentioned before.

In March 2022, the US Senate voted the CHIPS Act, with \$52B funding. It was finally signed by POTUS in August 2022.

¹⁴⁸³ See [Development of novel micro-fabricated ion traps](#) by Gerald Stocker, November 2018 (96 pages) and [Trapped ion quantum computing](#), Infineon.

¹⁴⁸⁴ See [Infineon Participates in 6 Research Projects, Expands Commitment to Quantum Computing](#) by Matt Swayne, The Quantum Insider, February 2022.

¹⁴⁸⁵ Their equipment is well documented in [Keysight High Frequency Tech Center \(HFTC\)](#) (15 pages).

It contains additional Federal budget of \$152M per year for quantum technologies for the 2023-2027 period, although seemingly not specific to components manufacturing. Chipsets USA manufacturing market share is in the 12% mark, above EU's that sits around 9%. The rest is in Asia, mostly Taiwan, South Korea, China and Japan.

Generic processes

We'll describe here the generic processes used to produce chipsets regardless of their use case, the most commonplace being bipolar, CMOS and BiCMOS chipsets¹⁴⁸⁶. The story always begins with a wafer.

Wafers are usually made of monocrystalline silicon sliced with wired diamond saws out of ingots manufactured with the Czochralski crystal growth method. They are sometimes completed with a thin buried layer of SiO₂ (aka SOI, for silicon on insulator) and another thin layer of regular Si, using the SmartCut process invented by CEA-Leti and implemented by SOITEC and its licensing partners¹⁴⁸⁷. SOI wafers have many interesting characteristics like reduced parasitic capacitances and low leakage currents. They are frequently used for nanophotonic circuits (like those from PsiQuantum manufactured by GlobalFoundries) or for silicon qubits chipsets (CEA-Leti, Qutech, ...).

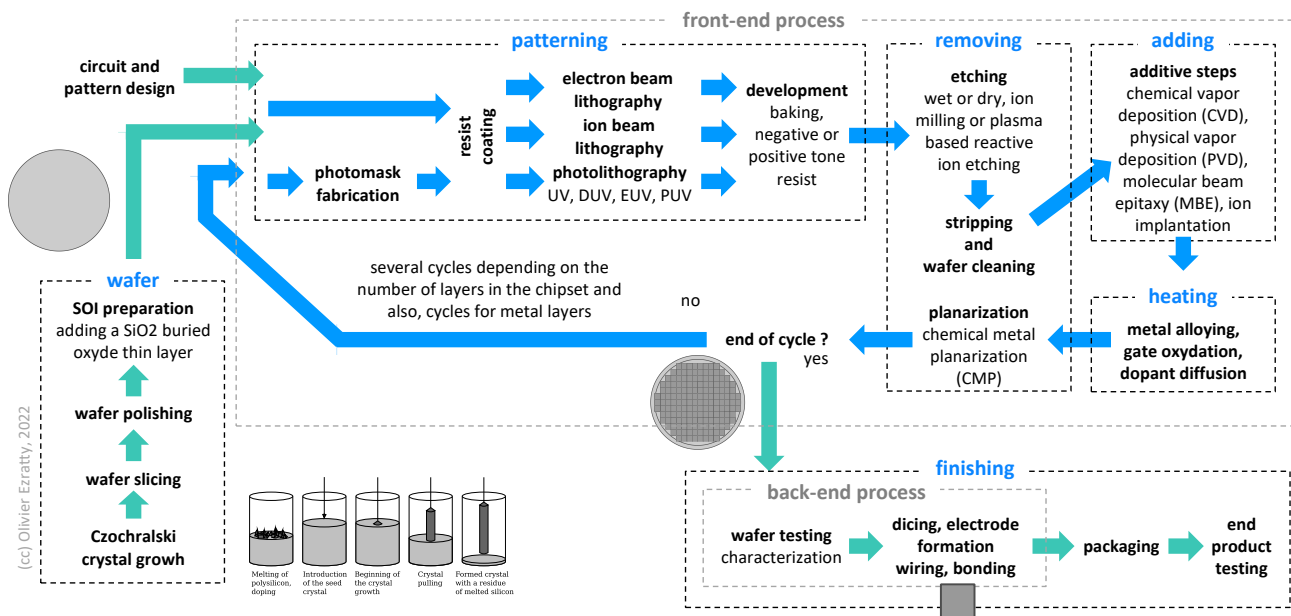


Figure 526: a generic layout of a chipset manufacturing process. (cc) Olivier Ezratty, 2022.

In other cases, wafers are made of III/V semiconducting materials (like GaAs or GaN, for manufacturing some nanophotonic circuits) or even sapphire (for some superconducting qubits and trapped ion circuits).

¹⁴⁸⁶ Bipolar transistors have a very high speed and are used in analog devices. CMOS transistors are slower and do not handle such high power as bipolar transistors but are aggressively scaled down in density and require far less power to operate. BiCMOS used both bipolar and CMOS logic that are co-integrated within the same chip, which requires additional process steps and incur higher costs.

¹⁴⁸⁷ The SmartCut process is not using a wire diamond saw like the ones used to slice wafers out of silicon ingots. It first creates a layer of SiO₂ on a Si wafer using Si thermal oxidation in wet atmosphere, PECVD or CVD. Then, an ionic implantation of H or He is made on another Si wafer creating a sort of “glue”. The SiO₂ side of the first wafer is bounded with this “glued” Si wafer and a thin layer of Si of that wafer is deposited on the SiO₂ using a “layer splitting” process created by thermal annealing. The second Si wafer can be reused for another Si deposit cycle. Both the SiO₂ and the overlay Si layers can be as thin as 10 nm. A variant of the SmartCut process is also used to deposit a thin Si layer on sapphire wafers and thermal annealing is created with laser beams in a so-called “LLO” process, for laser lift-off. I found interesting SmartCut process descriptions in [The advanced developments of the SmartCut technology: fabrication of silicon thin wafers & silicon-on-something hetero-structures](#) by Raphaël Meyer, 2018 (252 pages).

A wafer has a thickness ranging from 40 μm to 700 μm and its diameter ranges from a couple inches (for III/V and other small volume processes) to 300 mm and even 450 mm (for volume CMOS processes).

The most generic chipsets production processes then involve several cycles with the following successive steps with a repeat cycle ranging from resist coating to planarization including patterning, removing and adding matter.

When this cycle is over will all chipset layers added on top of the other, the process ends with various finishing steps up to a packaged chipset ready for integration.

Patterning

These are the process steps that define the places in the wafer where matter has to be removed with etching or added afterwards. It involves several steps that are defined during the design stages exploiting automated electronic design automation (EDA) software tools like those from ANSYS, Cadence, Keysight Technologies, Synopsys, Xilinx and Mentor Graphics (in Siemens group).

Resist coating is applied on the wafer with a photoresist liquid that will be later exposed during the lithography process and selectively removed during development. The coating is mechanically added with a dispenser nozzle positioned above the center of the rotating wafer attached to a chuck and spindle with vacuum pumping¹⁴⁸⁸.

EBR (edge bead removal) removes excess coating at the wafer edge with a solvent. Then a N_2 based soft bake evaporates most of the solvent.

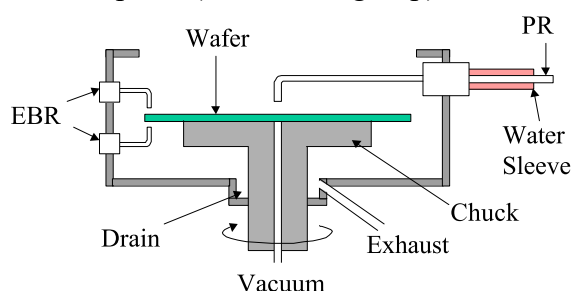


Figure 527: resist spin coating. Source: [Introduction to Semiconductor Manufacturing Technology](#) by Hong Xiao (2148 slides).

Photolithography is used to expose a special coating on selected areas. The photolithography technique makes use of a photomask and ultra-violet rays exposing a photoresist film or coating. It's being used to produce silicon qubits and nanophotonic chipsets. The usual photolithography process involves a stepper which moves the wafer under the camera to expose the wafer for each and every chipset to produce, and with a very high precision (<1 nm). It replaces mask aligners that are used when the photolithography process exposes the whole wafer in a single step. The size of the chipset is limited by the size of the photolithography reticle, which conditions the mask maximum size. Across time and density improvements, various ranges of ultraviolet wavelengths have been used. It started with UV, to DUV or deep ultra-violet under 248 nm, then to EUV (extreme ultra-violet) at 13 nm and PUV at 6,5 nm which is border line to soft X Rays. Starting with EUV, there is only one provider of photolithography system, ASML.

Electron beam lithography (EBL) is another lithography technique, that is focusing a beam of electrons on an electron-sensitive resist film to remove matter in specified areas, without requiring a mask like with photolithography. EBL can reach precisions of 1 nm which is excellent and better than photolithography. It is used to create precision nanostructures like with photon-generating quantum dots and also superconducting qubit chipsets. It is a very slow process compared with photolithography, so adapted to low volume and custom productions. An EBL looks like an electron microscope. Existing electron microscopes can be converted to run EBL tasks.

Other less used varieties of lithography are ion-beam (using helium), laser lithography, the latter being used for resolutions above 500 nm, and STM (Scanning Tunnelling Microscopy) that can reach sub-nm resolutions.

¹⁴⁸⁸ See the incredibly rich [Introduction to Semiconductor Manufacturing Technology](#) by Hong Xiao (2148 slides) and its eponymous book published in 2012 (524 pages).

Development which removes the photoresist coating where it was or wasn't exposed during the photolithography or electron beam lithography step. It depends on the photoresist material used which is either a negative (insoluble after exposure) or positive resist material (soluble after exposure).

Positive photoresist enables better lithography resolution but is more expensive than negative photoresist. It uses so-called hard baking above 100°C to polymerize and stabilize the photoresist coating.

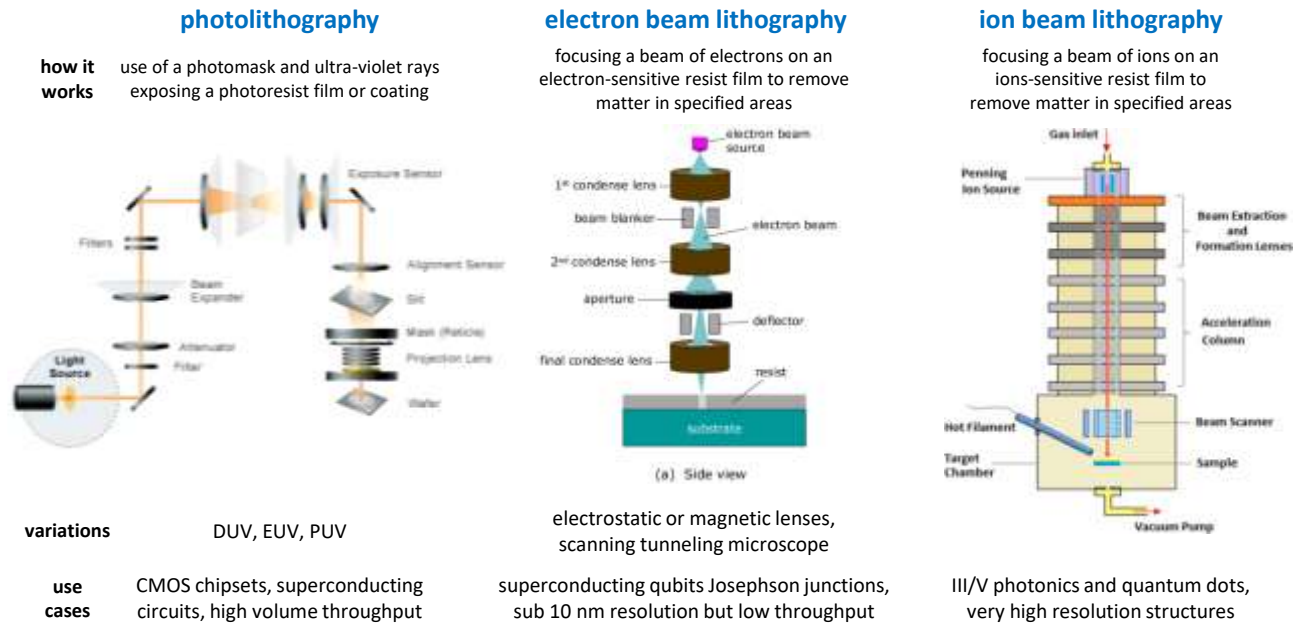


Figure 528: the three main lithography techniques used for semiconductors manufacturing. Compilation (cc) Olivier Ezratty, 2022.

There are many resist coatings depending on the process (photolithography or electron beam lithography) and whether we are using a negative or positive resist. With positive resist, coating can be made of long polymer chains with weak chain bonds. Exposure creates chain scission in the exposed areas. These are dissolved during the chemical development process while the longer chains do not dissolve. Another process consists in using resist creating hydrophilic product when exposed, which are then dissolved by water. Negative coating can be made of monomers that polymerize when exposed to light, and become non-dissoluble by the solvent used in the development process.

The photolithography process contains in total about 10 stages (coating, soft-baking, exposure, cleaning, hard-baking, ...). In volume production, these are handled in cluster tool systems, using one or several robotized systems to move the wafer from one tool to the next in a controlled environment. This ensures both productivity and production quality. Photolithography cluster vendors include Dainippon Screen, who partners with ASML. Cluster tools are also in place for other parts of manufacturing seen later, like etching and additive steps. Multi-axis robots and roof conveyors like those from Kuka and Muratec move wafer cassettes (handling 25 wafers) from one cluster to the other.



Figure 529: two examples of such cluster tools, on the left with a Kurt Lesker OCTOS Automated Thin Film Deposition Cluster Tool [\(source\)](#) and on the right an Applied Materials Endura Clover MRAM PVD System [\(source\)](#).

Removing matter

These steps correspond to the removal of matter on the wafer based on the zones defined by the lithography process.

Etching which removes matter in the uncovered areas, using wet chemical or dry physical methods, the dry methods being the most commonplace for high-density (VLSI) circuits. Various dry etching techniques include ion milling or sputter etching, and plasma based reactive ion etching. The first uses the projection of inert ionized noble gas while the second uses neutrally charged free radicals that react with the target surface. In general, a plasma is an ionized gas with the same proportion of positive and negative charges. There are also variants with anisotropic (orientation independent) or directional etching (orientation dependent).

| | ion milling or sputter etching | ion beam etching (IBE) | plasma based reactive ion etching |
|---------------------|--|---|--|
| how it works | the ions of an inert noble gas like argon are accelerated from a wide beam ion source on the target in vacuum to mechanically remove material on the target. | the ions of active molecules like CF_4 , Cl_2 or CHF_3 are accelerated from a wide beam ion source on the target in vacuum to mechanically remove material on the target. | energetic and neutrally charged free radicals reacting at the surface of the wafer, attacking the wafer from all angles, aka, being anisotropic. |
| | | | |
| variations | reactive ion etching deep reactive ion etching | ion polishing, ion cutting, reactive ion beam etching (RIBE, RIE), chemically assisted ion beam etching (CAIBE). | MEMS, nanophotonics, niobium resonators in superconducting qubits |
| use cases | superconducting qubits | III/V chipsets, single photon quantum dots shapes, MEMS | |

Figure 530: the various ways to remove matter in semiconductor manufacturing. Compilation (cc) Olivier Ezratty, 2022. Illustration sources: Wikipedia, others.

Stripping and cleaning which removes the remainder of the photoresist material. In volume production clean rooms, etching and stripping is handled by cluster tools with robotized handlers moving wafers from the etcher to the stripper tool, with a loading and unloading station extracting wafers from its carrier box (usually, containing 25 wafers in volume production environments).

Planarization of the wafer uses physical polishing. It can be based on CMP (Chemical Metal Planarisation). It is generally implemented after additive steps.

Adding matter

Additive steps consist in adding some materials in the visible areas, like silicon or doped silicon in classical CMOS transistors, using boron or indium (for p-doping) and arsenic (As), phosphorus (P), antimony (Sb) or aluminum (Al) (for n-doping). Some of these processes are implementing an epitaxy, creating a perfect crystalline structure with the added material, in the feature layers (doped silicon, gates). Other processes like PVD and sputtering are not epitaxial and are used for the production of superconducting qubits.

Additive steps can use various techniques like ion implantation, CVD (chemical vapor deposition, where the target surface is exposed to one or more volatile precursors, which chemically react and/or decompose on the target surface to leave a thin film deposit on the target, e.g. using silane SiH_4 to deposit Si on the wafer, generating 2 H_2 molecules), ALD (atomic layer deposition, a variation of CVD to create highly precise epitaxial atomic layers using repeat cycles), PVD (physical vapor deposition under low pressure, where the material to deposit with evaporation, sputtering or plasma and then condenses on the target surface), sputtering being one type of PVD (using ion projection to pull material from a source and deposit it on the target wafer or ionized gas like argon that, thanks to a high-voltage applied to the target, is projected on the target and creates a plasma with the target atoms that then condenses on the surface of the chipset), e-beam deposition (another variety of PVD using electron beams to evaporate the matter to deposit on the wafer), PLD (pulse laser deposition, using femtoseconds laser pulses to extract matter from a source and then sent to the target), MBE which is a variety of PVD (molecular beam epitaxy, for thin-film deposition of single orderly crystal structures). CVD can be plasma based.

In the last process cycles, these steps are related to the creation of several superposed metal layers connecting the various semiconducting circuits created in the earlier steps. With superconducting qubits, aluminum, and aluminum oxide (or niobium) sputtering is implemented in this step.

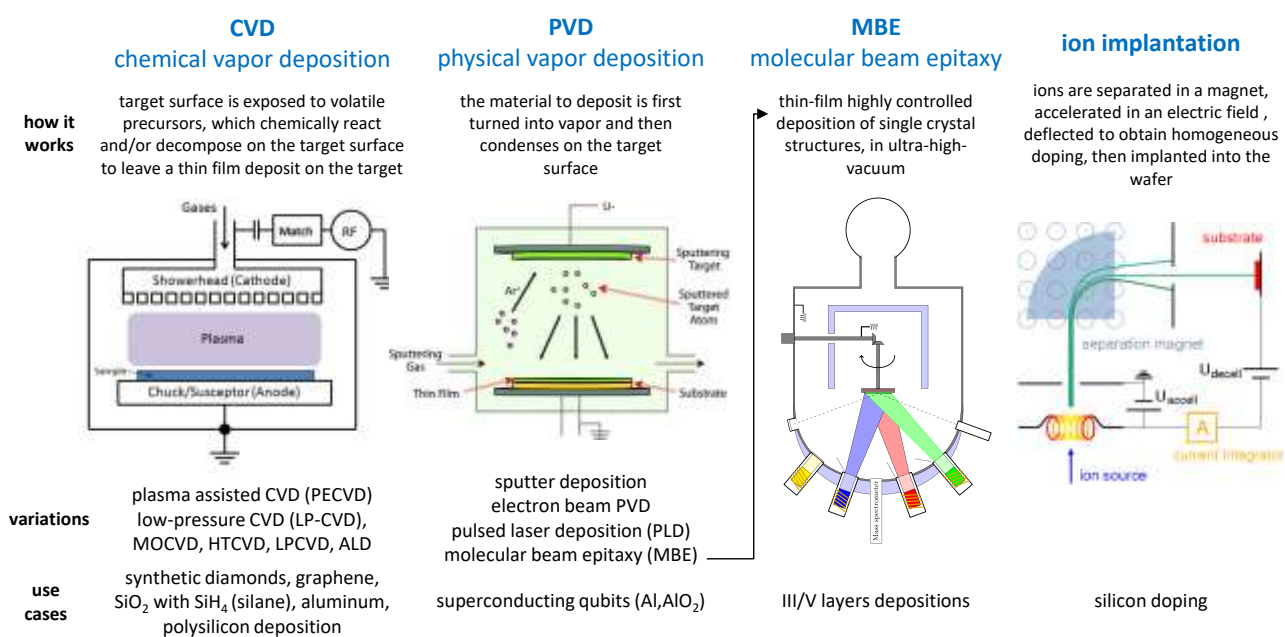


Figure 531: the various ways to add matter in semiconductor manufacturing. Compilation (cc) Olivier Ezratty, 2022.

Metal layers. When all cycles related to the functional parts of the circuits are finished, some electrodeposition of metal is made to connect the chipset to the outside world, usually copper or aluminum (in the case of superconducting qubits and electronics) and copper-aluminum alloys. Metal layers are created with a mix of lithography-etching and PVD/CVD. As metal layers are added, their density is decreasing. Then, some wiring may be added and bonding or bumps plus packaging. In CMOS designs, the “front-end-of-line” (FEOL) contains the individual active elements (transistors, capacitors, etc.) while the “back end of line” (BEOL) contains the metal layers.

So-called 3D chipsets like the superconducting qubits chipsets from IBM, OQC and others result from the assembly and perfect alignment of stacked chipsets. CEA-Leti (France) is collaborating with Intel in the design of such innovative 3D packaging technologies. 3D stacking makes use of TSV or through silicon vias, which establishes a metal connection from top to bottom of a chipset or from the active layer to the front plane through the wafer.

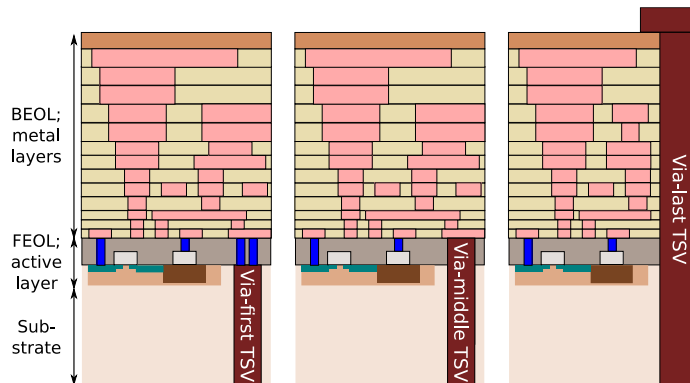


Figure 532: typical metal layers of a semiconductor.

A TSV hole is created with reactive ion etching, copper electrochemical deposition for creating a seed layer and electroplating to fill the hole¹⁴⁸⁹.

Heating

Thermal processes are implemented for various purposes like dopant activation and diffusion, gate oxidation ($\text{Si} + 2\text{O} \rightarrow \text{SiO}_2$), metal reflow which smooths its surface usually in an atmosphere of N_2 or H_2O , metal alloying and chemical vapor deposition. One used technique involves rapid thermal annealing, using a vertical or horizontal furnace.

Finishing

These are the product finishing tasks undertaken when the patterning-removing-adding-heating cycle is completed (the front-end process). The aim here is to turn the chipset on its wafer into a functional component with its connectivity. It's also called the back-end process.

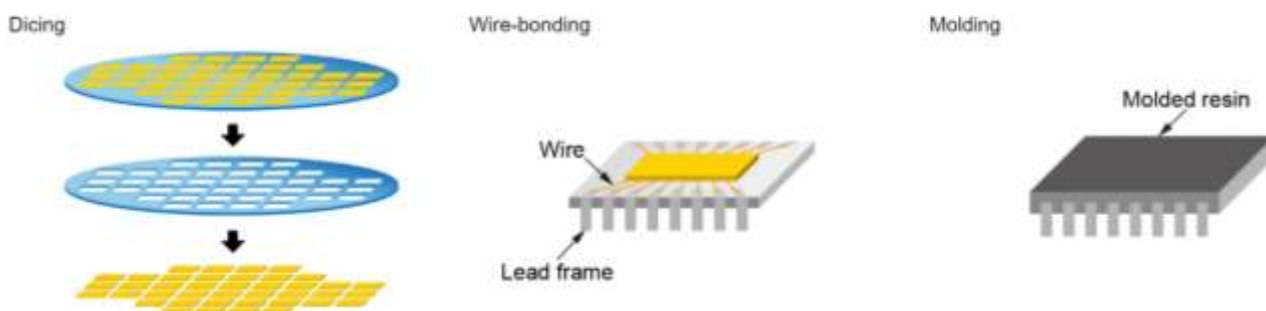


Figure 533: the finishing steps of semiconductor manufacturing with dicing, wire bonding and molding. Compilation (cc) Olivier Ezratty, 2022 and [The semiconductor manufacturing process \(back-end process\)](#), Matsusada, February 2022.

¹⁴⁸⁹ See [Tutorial on forming through-silicon vias](#) by Susan L. Burkett et al, January 2020 (16 pages).

Wafer testing. Then, testing and characterization is done to make sure the manufactured components meet the required quality. One inspection tool used is electron microscopes, which can also be used to analyze the patterning quality between each patterning cycle. Wafers containing chipsets operating at cryotemperatures can be tested by a cryo-prober like the one provided by Bluefors/Afore and being used by Intel in Oregon and CEA-Leti in Grenoble.

Electrode formation, wiring and bonding. These are more traditional steps to add macro-elements to the circuit that will connect them to the outside world. This is done after the chipsets are extracted from the wafer with dicing.

Packaging. It is mostly about putting plastic and sometimes metal shielding for specific applications (space, military, quantum) around the chipset and its bonds/wires. The component can be then integrated in a system with its surrounding electronics.

End-product testing. The electronic circuit is fully functionally tested here before being used.

The manufacturing yield is the percentage of functional chipsets at the end of manufacturing. Each intermediate manufacturing step has its own yield, and the end yield is the result of the multiplication of each step yield.

Quantum process specifics

Each and every chipset is manufactured with a specific recipe with many steps involving different tooling and dozens of parameters (tool, chemical compounds, temperature, pressure, angles, ...). Putting in place such processes is tedious and require very specialized skills. The whole manufacturing process for a chipset can last from a couple hours to a couple months depending on its complexity. All in all, a new chipset design, manufacturing and testing can last between a couple weeks to 2,5 years depending on the product and process.

Superconducting qubits

Manufacturing a superconducting qubit chipset is both rather specific and simple, at least, compared to classical silicon CMOS chipsets and their epitaxy processes, creating pure crystalline semiconducting structures. It explains why so many labs in the world have their own cleanroom able to prototype such chipsets. A superconducting chipset wafer can usually be produced in less than a week when it can last months for CMOS chipsets¹⁴⁹⁰. There are of course many variations and as the superconducting chipsets become more complicated, assembling up to three stack chiplets, and with more lithography steps, the production cycle gets longer.

We'll describe here one of the methods to create a superconducting qubit chipset which is derived from the bridge-based Niemeyer-Dolan bridge technique¹⁴⁹¹. The superconducting qubit core feature is its Josephson junction made of three layers: a conducting metal like aluminum and its oxide insulator variant in between. It's surrounded by metal structures for creating capacitances and a resonator¹⁴⁹².

¹⁴⁹⁰ See a couple examples of superconducting qubits manufacturing process descriptions in [Manufacturing low dissipation superconducting quantum processors](#) by Ani Nersisyan et al, Rigetti, January 2019 (9 pages), [Simplified Josephson-junction fabrication process for reproducibly high-performance superconducting qubits](#) by A. Osman et al, Chalmers, November 2020 (7 pages) and the thesis [Micromachined Quantum Circuits](#) by Teresa Brecht, Yale University, December 2017 (271 pages).

¹⁴⁹¹ There are other Josephson junction techniques like the Manhattan bridge. See [Improving Quantum Hardware: Building New Superconducting Qubits and Couplers](#) by Thomas Michael Hazard, Princeton, 2019 (136 pages).

¹⁴⁹² The schema below comes from [Resonant and traveling-wave parametric amplification near the quantum limit](#) by Luca Planat, June 2020 (237 pages). It describes the process for the creation of a Josephson junction in a TWPA, and is very similar to a superconducting qubit.

- The wafer substrate is made of either sapphire or intrinsic silicon (meaning monocrystalline and undoped). Silicon is commonplace but has its shortcomings: it must be deoxidized, since SiO_2 is damaging the qubit's quality. Sapphire can't be oxidized but is less commonplace. The wafer may be gold plated on its unpolished side to ensure good electric and thermal contacts between the chipset and the chip-carrier.
- Resist deposition is done using the spin-coating technique and with two layers of resist one on top of each other. The bottom one is more sensitive to the e-beam than the one above.
- E-beam lithography exposes some of the resist to an electron beam. This is a rather slow process. It uses a double insolation process with different strengths to attack the two resins layers.
- Development where the resist is removed from the hole exposed by the e-beam and etching which creates an undercut carved in the resist.
- First metal evaporation where a first layer of aluminum is deposited with an angle $+\theta$. It creates the first layer of the Josephson junction.
- An aluminum oxide layer is grown during an oxidation step. The gate can be less than 1 nm thick.
- Second angled metal evaporation to create a new layer above the oxidized aluminum from the Josephson junction gate. It is done in the opposite angle $-\theta$ to cover a different area in the hole.
- The residual resist may in some situations be removed with a CMP process or more classically dissolved in solvent during the lift off step. For these, no additional layer or isolation layer is added on the Josephson junction.

All of this process was just about creating a single Josephson junction that is usually 200 nm wide. A classical superconducting qubit contains at least two other circuits: capacitances (about 100 μm to 600 μm wide), a resonator (*aka* superconducting coplanar waveguide) and a microwave network.

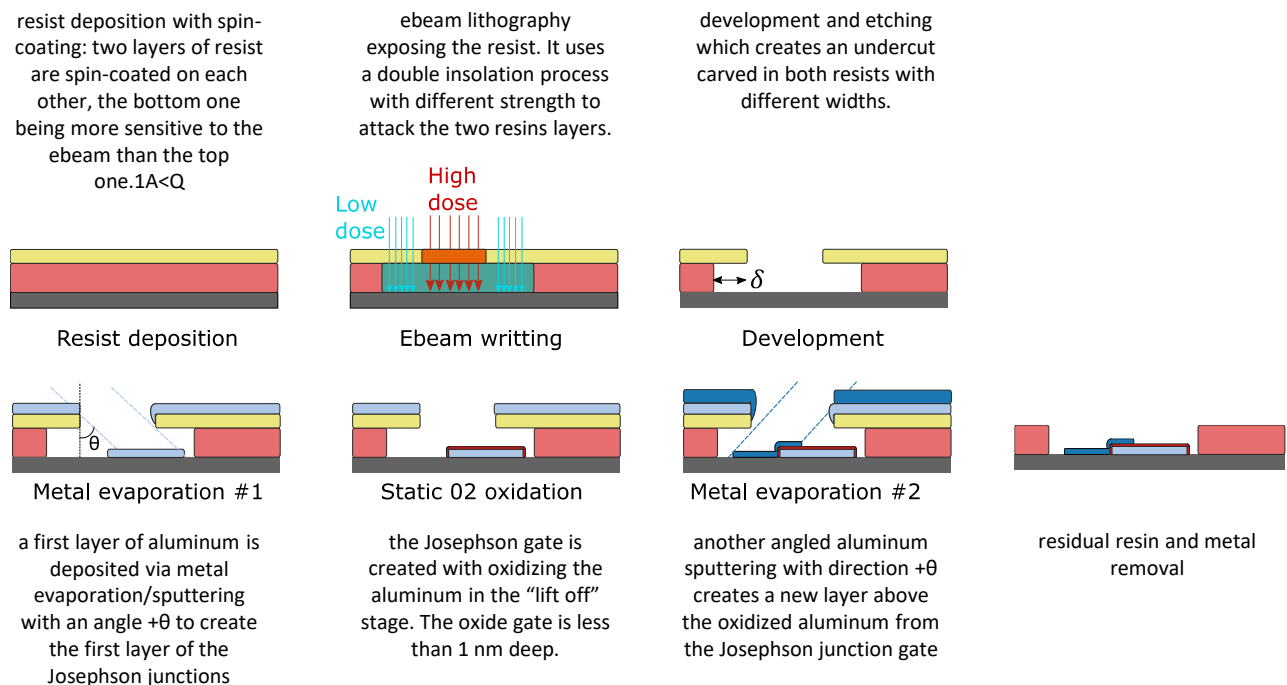


Figure 534: the process of manufacturing a superconducting qubit or superconducting component like a TWPA. Source: [Resonant and traveling-wave parametric amplification near the quantum limit](#) by Luca Planat, June 2020 (237 pages). Comments added by Olivier Ezratty in 2022.

The network and resonator can be created using 193 nm UV lithography or laser lithography and negative resist etching, meaning the metal is first deposited everywhere (except on the Josephson junction) and then, the resist coating is removed where it was not exposed. RIE (reactive ion etching) can also be used, particularly for creating resonators. This process can make use of aluminum, niobium, TiN (titanium nitride) as developed by John Martinis in 2013 and even indium¹⁴⁹³. TiN is appreciated thanks to its ability to avoid oxidation. Titanium nitride (TiN) can be used as an isolation layer on top to a sapphire substrate to avoid dielectric losses between the various qubit's components¹⁴⁹⁴.

Superconducting qubits circuits are usually rather simple and only 2D with no additional metal layers and no insulator since there are no good insulators available. There's an empty space of a minimum 2 mm height above and below the chipset in its (copper) packaging. On the other hand, superconducting electronics dies can superpose up over 10 alternating layers of niobium and dielectric, usually SiO₂. The surrounding connections are themselves superconducting and the chipset edge is connected to gold or aluminum wires and bonds. Andreas Fuhrer Janett from IBM Zurich labs developed a process and apparatus to put the chipset in ultra-high vacuum (UHV) during assembly¹⁴⁹⁵. According to IBM, the UHV can contribute to create less noisy qubits.

The connectivity constraints explain for example the limitations of the chimera structure in D-Wave superconducting qubits layout. The trend is to create 3D structures, assembling several chipsets, with one being dedicated to electronic signals controlling the qubits, like with Google, IBM and OQC.

The chipsets are assembled using wafer bonding, connecting metal layers using indium thanks to its ductility, even in low temperatures and at relatively low temperature (156°C).

The chipset density is not very high as compared with classical CMOS chipsets. The quality and fidelity of the superconducting qubits depends on several factors including materials purity¹⁴⁹⁶. The manufacturing yield of superconducting chipsets can however be as low as 1% but is usually above 70%¹⁴⁹⁷. One avenue to potentially improve the manufacturing quality of superconducting qubits would be to produce them with 300 mm CMOS fab technologies. That's what IMEC has been experimenting in 2022 with producing qubits of rather good quality (but not stellar), using argon milling and subtractive processes¹⁴⁹⁸.

We mentioned a lot aluminum so far. It is not the only superconducting metal used with Josephson junctions. While aluminum is used for superconducting qubits, niobium is used for superconducting electronics (SFQs, already covered) and SQUIDS sensors with the advantage of being a superconductor at 9K versus 1.2K for aluminum.

Superconducting nanowire single photon detectors

Superconducting nanowire single photon detectors (SNSPDs) can be manufactured with NbTiN sputtering on sapphire¹⁴⁹⁹.

¹⁴⁹³ See [Sputtered TiN films for superconducting coplanar waveguide resonators](#) by S. Ohya, John Martinis et al, UCSB, 2013 (9 pages).

¹⁴⁹⁴ See [Titanium Nitride Film on Sapphire Substrate with Low Dielectric Loss for Superconducting Qubits](#) by Hao Deng et many als, Alibaba, May 2022 (10 pages). The use of TiN enables qubit lifetimes of up to 300 μ s.

¹⁴⁹⁵ See [Ultrahigh vacuum packaging and surface cleaning for quantum devices](#) by M. Mergenthaler, Andreas Fuhrer et al, 2021 (6 pages).

¹⁴⁹⁶ See [Material matters in superconducting qubits](#) by Conal E. Murray, IBM Quantum, 2019 (98 pages).

¹⁴⁹⁷ It was the yield with IBM's 17 qubits chipsets in 2018 according to [Towards Efficient Superconducting Quantum Processor Architecture Design](#) by Gushu Li et al, 2019 (15 pages).

¹⁴⁹⁸ See [Path toward manufacturable superconducting qubits with relaxation times exceeding 0.1 ms](#) by J. Verjauw et al, npj, August 2022 (7 pages).

¹⁴⁹⁹ See [NbTiN for improved superconducting detectors](#) by Julien Zichi, KTH Sweden, 2019 (86 pages).

Trapped ions circuits

These circuits implementing Paul or Penning traps are manufactured using a mix of techniques with e-beam metal evaporation-based deposition of titanium and gold, etching process, and femtosecond-laser machining for 3D surfaces shaping using tools like those from **FEMTOprint**¹⁵⁰⁰.

Photon-generating quantum dots

Like the ones from CNRS C2N and Quandela are manufactured with adding about 100 layers alternating GaAs and GaAsAl compounds using molecular beams epitaxy. Adding these many layers can still be implemented in a couple hours. In the middle of the road, special techniques are used to deposit the planar λ cavity made of a couple hundred of InGaAs. The cylinder cut for the quantum dot enclosing is implemented with ion milling¹⁵⁰¹.

Silicon qubits

Their manufacturing is very close to traditional CMOS manufacturing techniques. It requires UV/EUV photolithography due to the relatively high features density in the chipsets (which can go as low as 10 nm). The etching processes are also rather similar. The materials purity is an important figure of merit to ensure the quality of the manufactured qubits as it is with superconducting qubits.

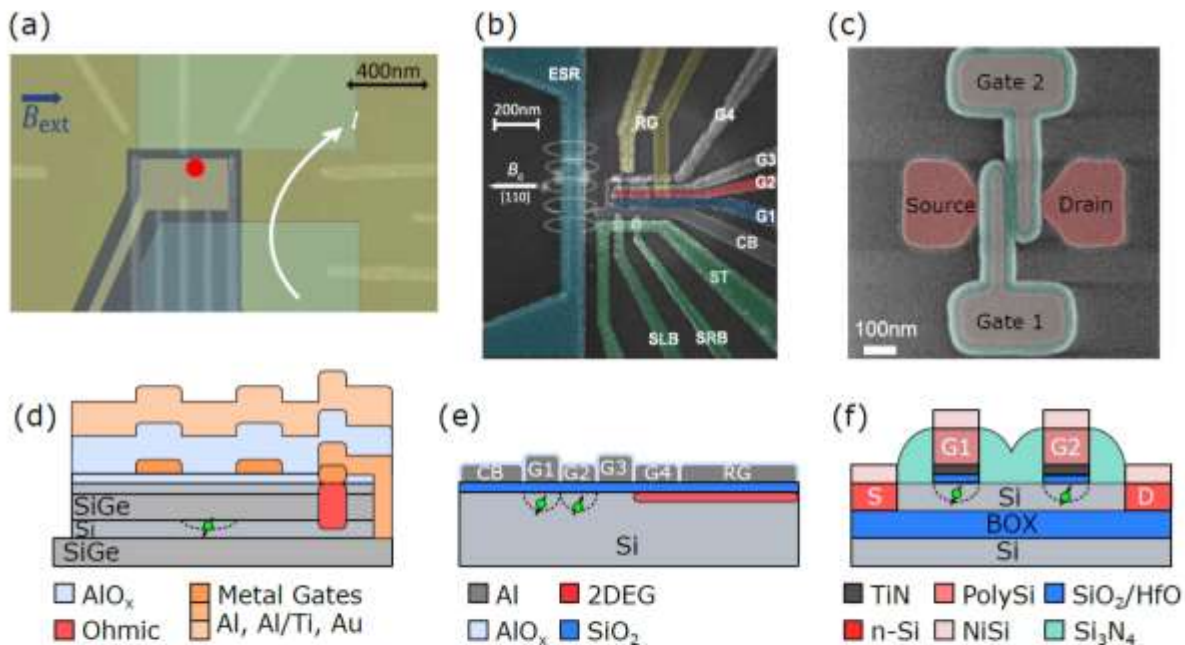


FIG. 1. Silicon quantum dot devices. (a) Scanning electron microscope (SEM) image of an accumulation mode Si/SiGe heterostructure. Two layers of gates, bottom (light grey) and top (dark green) are designed to form two quantum dots (centre of image) and a single-electron transistor for readout (right). The structure contains a micromagnet in an upper metal layer (light green) to produce a magnetic field gradient. The red dot indicates the position of a quantum dot used in ref. [16]. (b) SEM image of a metal-oxide-semiconductor multi quantum dot device with quantum dot gates (G1-4), confinement gate (CB), reservoir gate (RG), an integrated single-electron transistor (green) and microwave antenna for magnetic resonance spin control (blue) used in ref. [17]. (c) SEM image of a CMOS p-type double quantum dot on an etched silicon-on-insulator nanowire used in ref. [18]. Cross-sectional view of the Si/SiGe quantum dot device (d) MOS double quantum dot device (e) and CMOS double quantum dot device (f) shown above in (a-c).

Figure 535: various implementations of silicon spin qubits. Source: [Scaling silicon-based quantum computing using CMOS technology: State-of-the-art, Challenges and Perspectives](#) by M. F. Gonzalez-Zalba, Silvano de Franceschi, Edoardo Charbon, Maud Vinet, Tristan Meunier and Andrew Dzurak, November 2020 (16 pages).

¹⁵⁰⁰ See the thesis [Multi-wafer ion traps for scalable quantum information processing](#) by Chiara Decaroli, ETH Zurich, 2021 (248 pages) which provides a lot of insights on trapped ion architectures and circuits manufacturing.

¹⁵⁰¹ See the details in [Near-optimal single-photon sources in the solid-state](#) by Niccolò Somaschi, Valerian Giesz, Pascale Senellart et al, 2015 (23 pages).

The silicon wafers used to create spin qubits are covered by a layer of about 100 nm of ^{28}Si using a wafer scale CVD process.

All the other functional and isolation layers using silicon are also based on ^{28}Si , mostly through silane (SiH_4). There are many variants with Si/SiGe heterostructures, Al/ AlO_x structures, etc.

The chipset vertical structure is relatively simple, with only a few metal layers, and some control electronics usually placed in a separate chipset that is bonded to the qubits in a 3D fashion. In its various research papers published at APS March meeting in 2022, **Intel** did showcase how manufacturing quality had an impact on the quality of quantum dots spin qubits. In October 2022, they added some information on the quality and yield of their silicon qubits wafers¹⁵⁰².

Tools

We'll cover here some specific manufacturing tools that are used for producing quantum technologies semiconductor components. The breadth of tools in semiconductor fabs is much broader with tools from vendors like **ASML** (UV and EUV photolithography) and **Applied Materials** (PVD, CVD, etching and stripping, ...). Their tools are used in high-volume large fabs while many of the quantum-specific production tools are used more for research purpose and for small scale industrial production.



Plassys Bestek (1987, France) develops and manufactures vacuum and ultra-high-vacuum thin film deposition systems with a turnover of about 7M€. Most of their tools are based on physical vapor deposition (PVD) processes (vaporization of metal or compounds for deposition on a substrate, all under vacuum).

Positioned at the end of the 1990s as a key supplier of equipment for the fabrication of superconducting qubits, they have developed a wide range of electron beam deposition systems dedicated to controlled angle evaporation under the name "MEB" which makes Plassys the leader for this technology (Yale University, Rigetti Computing, QCI, NTT, Oxford, CEA Saclay, Qilimanjaro, TU Delft, VTT... rely on their tools). The "MEB" tools used an electron beam to melt and to evaporate materials that allows the deposition of aluminum films for forming the Josephson junctions or for resonators as well as of niobium as underlayer or as resonators. They also provide sputtering tools for depositing various kind of superconducting films (Al, Ti, Nb, Ta, MoSi, MoGe, nitrides...) and other elemental materials or more or less complex compounds. Sputtering tools integrates cathodes on which a bias voltage is applied under a controlled atmosphere of gas mixture including argon for generating a plasma around $10^{-3} - 10^{-2}$ mbar. Positive ions from the plasma are attracted by the cathodes on which a "target" made from the material source you want to deposit. The high energy of the ions sputters the target inducing then the generation of a vapor that condensates on to the substrate.

They also supply the SDDR150 chemical vapor deposition (CVD) reactor for the growth of ultra-pure diamonds which is the raw material for the development of NV center based technologies. This CVD process is using hydrogen and methane (CH_4) at a pressure around 100millibars¹⁵⁰³ with the assistance of a microwave source generating a high density plasma. They also handle diamond doping with nitrogen, boron, phosphorus....

Their R&D and production machines dedicated to quantum technologies are now grouped under the Qutek Series brand. In addition to the MEB systems, Qutek series includes MP systems (sputtering deposition for superconducting or photonic devices) and thermal evaporation system for indium bumps (used for connecting superconducting qubits).

¹⁵⁰² See [Intel Hits Key Milestone in Quantum Chip Production Research](#), Intel, October 2022.

¹⁵⁰³ The CVD diamond growth process is described in [Diamond growth by chemical vapour deposition](#) by J. J. Gracio et al, 2011 (75 pages).



Figure 536: various production machines from Plassys-Bestek. Source: Plassys-Bestek.



Angstrom Engineering (1992, Canada) is a manufacturing tool vendor. Their Quantum Series line of physical vapor deposition (PVD) systems is adapted to the creation of Josephson Junctions, from using an electron beam source to deposit aluminum, magnetron sputtering for niobium and ion beam cleaning.



Kelvin Nanotechnology (2020, UK) is an electron beam lithography and nanofabrication tooling company. It manufactures various miniaturized MEMS and photonic components used in quantum technologies.

These include 3D ion traps, various photonic devices, MEMS gravimeters and lasers built on 200 mm wafers in features going as low as 20 nm. They are based at the James Watt Nanofabrication Centre (JWNC) in Glasgow, Scotland.



Orsay Physics (1989, France) is a subsidiary of **Tescan Orsay Holdings** (Czech Republic - France). It provides manufacturing tools for focused ion and electron beam processes.

Out of these, their nitrogen-FIB (i-FIB, for focused ion beam) is being used to create NV centers in nano- and micro-structures with high precision, like in NV center arrays with 2 μm separations between the centers¹⁵⁰⁴.



Riber (1987, France) is a manufacturer of MBE reactors, used mostly in III/V and II/VI multi-layers epitaxy processes.

They handle various MBE processes: solid sources MBE, Plasma-Assisted MBE (PAMBE), Metal-Organic MBE (MOMBE), Gas Source MBE (GSMBE) and full gaseous Chemical Beam epitaxy (CBE). A Riber MBE reactor is being used to manufacture the 100+ layers quantum dots based photon sources from Quandela.



Raith (1980, Germany) provides nanofabrication and electron beam lithography instruments. These tools are involved in the manufacturing of all sorts of qubits, trapped ions, superconducting, electron spin, topological qubits, NV centers and nanophotonics.



Picosun Group (2003, Finland, 17.4M€) is a manufacturer of atomic layer deposition (ALD) tooling used in the production of various electronic components (imaging sensors, LEDs and OLEDs, MEMS, etc).

Their technology can be used to create graphene structures among other things.

¹⁵⁰⁴ See [i-FIB application note](#).

They are one of the Finish industry partners of **QuTI**, a 10M€ collaborative research project on quantum related components manufacturing and testing. They partner with VTT, Bluefors, Afore, IQM, Quantastica, Saab, Vexlum and the Finish offices from Rockley Photonics (USA) and CSC (USA).



Encapsulix (2011, France) develops ultra-short cycle time ALD systems. It's mostly used in the production of OLED in encapsulated quantum dots.



Samco Inc (Japan) is a provider of thin film deposition, microfabrication and surface cleaning, CVD and other treatment machines.

Their tooling includes PECVD systems (plasma-enhanced CVD), SiC CVD systems, ALD (atomic layer deposition) systems, reactive-ion etching (RIE) systems, Inductively Coupled Plasma (ICP) etching systems, Silicon Deep Reactive Ion Etching (DRIE) systems for MEMS device fabrication and TSV (through-silicon-vias) via-hole etching and plasma cleaners. These systems are used to produce various sorts of quantum components like niobium and tantalum based superconducting circuits, from qubits to surface acoustic waves filters¹⁵⁰⁵ and GaAs photonic components.



ADNANOTEK (Taiwan, 1999) is a provider of MBE, PLD (pulsed laser deposition which is a variation of PVD) and Laser MBE PLD, various sputtering systems, EBE (electron beam evaporators), Ion Beam Sputter Deposition (IBSD), ALD (atomic layer deposition), Plasma Enhanced Atomic Layer Deposition (PEALD) and various ultra-high vacuum equipment.



CVD Equipment Corporation (USA) is specialized in CVD and dry etching systems that can be used for various semiconductor production, including III/V and nanophotonic chipsets.



Plasma-Therm (USA) has a broad range of plasma and ion beam etching and deposition used among other things in GaAs components manufacturing.

The company made several acquisitions: Advanced Vacuum Europe of Lomma (1993, Sweden) in 2011, Nanoplas France in 2015, Nano Etch Systems (2009, USA) in 2016, Kobus and Corial (France) in 2018, JLS Designs Ltd (UK) in 2020. The company opened in 2018 its European Head Office in Grenoble, France, and in 2020, one process and technical support office in Singapore.



Izovac Photonics (Lithuania) provides the IZOVAC range of products vacuum coating equipment using vacuum sputtering (magnetron sputtering, Ion Beam Assisted Deposition, Ion beam sputtering, DLC (Diamond-Like Carbon) coating by PECVD (Plasma Enhanced Chemical Vapor Deposition). Their main market are the display and touch screen manufacturing. They also develop customized vacuum deposition equipment.



Evatec (Switzerland) provides a family of evaporation, sputtering and PECVD products covering various needs including in MEMS and photonics applications. They also develop and sell wafer cassette-to-cassette processing tools in their Clusterline family.



Prevac (Poland) has a breadth of semiconductors manufacturing tools including an UHV Magnetron Sputtering System working with 3-inches wafers and PLD systems. They also sell an UHV multichamber cluster tool to automate a process with a thin film layer growth deposition chamber, load-lock chambers and a transferring tunnel.

¹⁵⁰⁵ See [Towards practical quantum computers: transmon qubit with a lifetime approaching 0.5 milliseconds](#) by Chenlu Wang et al, NPJ, January 2022 (6 pages) and [Niobium \(Nb\) Plasma Etching Process \(RIE or ICP-RIE\)](#), Samco.



Seki Diamond Systems (Japan) is a subsidiary of **Cornes Technologies** (USA) that sells CVD diamond reactors producing synthetic diamonds and supporting Microwave Plasma CVD, Hot-Filament CVD and Low Temperature CVD. It covers broad industry use cases.



Polyteknik (2005, Denmark) provides PVD and coating systems, including their Flextura e-beam PVD system.



Besil

Besil (1995, The Netherlands) or BE Semiconductor Industries, is the worldwide leader in semiconducting assembly machines (die attach, packaging, plating). One key use case is 3D chiplets assemblies. The company participates to the EU project MATQu to create a manufacturing capacity of superconducting chipsets on 300 mm silicon wafers.



SOITEC (1992, France) is a company producing SOI wafer which contain an isolation layer of SiO₂. These wafers are commonplace in many quantum technologies semiconductor components.

SOITEC acquired EpiGaN (2010, Belgium, 4M€) in 2019. It adds GaN wafers production to their portfolio.

Some other vendors can be mentioned like **RECIF Technologies** (France) with its wafers handling and sorters, **Heidelberg** (Germany) and its mask writer, **Süss MicroTec** (Germany) and its photomask handling and mask aligners, Keysight Technologies (and its NX5402A silicon photonics hybrid wafer testing system), **Oxford Instruments** (UK) and its RIE plasma etchers from the Plasmalab family and ALD systems, **Vistec** (USA) and **STS Elionix** (USA) and their e-beam writers, **Transene Company** (USA) and their etching systems, **Pureon** with its diamond based Chemical Mechanical Planarization tools (CMP)¹⁵⁰⁶, **Polygon Physics** (2013, France) which provides ion, electron, plasma and atom sources based on ultracompact and ultralow power electron cyclotron resonance plasma technology (ECR) and Multi Beam Sputtering tools (MBS), **JEOL** (Japan) and **Multibeam** (USA) and their e-beam lithography systems, **Thermo Fisher** (USA) and its e-beam lithography and ion milling systems, **Veeco** (USA) and its lithography, MBE, CVD, PVD, ion beams, ALD and dicing systems, **Aixtron** (1983, Germany) and its CVD systems, **NuFlare** (Japan) and its mask writers and epitaxial growth reactors, **AJA International** (1989, USA) and its thin film deposition systems including magnetron sputtering, e-beam evaporation, thermal evaporation, and ion milling systems and **Denton Vacuum** (1964, USA) and its evaporation, sputtering, PE-CVD and ion beam deposition tools.

Let's add a couple software design tools:



NanoAcademic Technologies (2008, Canada) is a company created by Hong Guo from McGill University and Yu Zhu and Leil Liu (all coming from China) which sells quantum materials software simulation tools like NanoDCAL. It is used to simulate the physics of quantum chipsets like superconducting qubits.



QuantCAD (2021, USA) is a company created by Michael Flatté and based in Iowa that develops and sells CADtronics and qNoise, a suite of simulation software that models noise and current in quantum devices. It is used to design various quantum components, including quantum sensors and optoelectronic devices.

¹⁵⁰⁶ In 2020, Microdiamant (Switzerland) acquired Eminess Technologies from Saint Gobain and was rebranded as Pureon.

Other enabling technologies vendors

These companies are developing physical components and enabling technologies that can play a role in building quantum computers.

More often, as this market remains limited to research, these startups are more generalist and target broader markets than quantum computing, covering physics research in general and even various industrial applications.



Aeponyx (2011, Canada, \$11,4M) is a fabless micro-optical switch semiconductor chips designer and manufacturer, specialized in Micro-Electro-Mechanical-Systems (MEMS) and Silicon Photonics.



Alter Technology (2006, Spain/Germany) is a subsidiary of the German group TÜV NORD specialized in micro and optoelectronics engineering for space and harsh environment applications.

It has labs in UK, France, Spain and Italy. They develop several quantum enabling technologies like frequency-stabilized lasers used to control cold atoms, an ion-trap chip carrier, entangled sources of photons for space based QKD, a squeezed light quantum MEMS gravimeter.



AuroraQ (2017, Canada) creates communication systems based on superconducting qubits, including quantum communication repeaters. It is complemented by the QSPICE Design software which allows the design of superconducting quantum circuits. In other words, this is an ultra-niche market¹⁵⁰⁷.



DiamFab (2019, France) is a spin-off of Institut Néel in Grenoble specialized in the growth of doped diamond layers on a diamond wafer substrate.

Among other markets, they also target NV center use cases in quantum technologies. Diamond is also used as a high-performance semiconductor for power applications for diodes and field-effect transistors.

HiQuTe Diamond (2022, France) is a company created by Riadh Issaoui, Ovidiu Brinza, Fabien Bénédic, Alexandre Tallaire and Jocelyn Achard, who are researchers from LSPM in Paris, France (Laboratoire des sciences des procédés et des matériaux). They produce high quality diamond crystals used in quantum technologies.



Elementsix (1946, Luxembourg) is a subsidiary of De Beers Group, the world's leading diamond producer, which, among other things, manufactures synthetic diamonds for use in NV centers based systems, mostly used in quantum sensing.

They hold a large number of patents in the related processes. In September 2021, they launched DNV-B14, a new chemical vapor deposition (CVD) made quantum-grade diamond with a uniform and x 10 higher density of NV spin centers.



HumminK (2020, France) developed a patented technology combining a nanometric “pen” with an oscillating macro-resonator to perform a capillary deposition of various liquids.

It can print conducting materials with an existing choice of 10 different materials. It can be used to add precision items on devices in 3D.

¹⁵⁰⁷ See [The Geometry of a Quantum Circuit and its Impact on Electromagnetic Noise](#), 2018 (15 pages).



Labber Quantum (2016, USA) develops software solutions for controlling the qubits of experimental quantum computers with Python scripting handling electronics hardware control (AWGs, DACs, ADCs), data storage and visualization. They are used to calibrate qubits. The startup was acquired by **Keysight Technologies** in March 2020.



LakeDiamond (2015, Switzerland, €2M) produced synthetic diamonds used to create NV centers qubits in diamonds or with quantum sensing.

They use vacuum deposition with the CVD method (Chemical Vapor Deposition). The company closed in February 2020 after getting funding from an ICO in 2018 (Initial Coin Offering, using some crypto currency).



Lucigem (2016, Australia) manufactures fluorescent nano-diamonds that can be used in various quantum applications, particularly for medical imaging. The company is the result of work carried out at Macquarie University in Sydney.



Diatope (2021, Germany) creates diamonds with NV centers for quantum sensing and quantum computing applications. It is a spinoff from the Institute for Quantum Optics at Ulm University by Johannes Lang, Christoph Findler and Christian Osterkamp.

They produce NV centers using isotopically purified ^{12}C and do provide NV centers benchmarking services.

Qzabre (2018, Switzerland) creates NV center-based tips and probes to be used in scanning microscopes. They also sell a NV center microscope, the QSM. The startup was created by Christian Degen from ETH Zurich.



Adamas Nano (2010, USA) sells nanodiamond particles for various use cases including NV centers-based sensors. **Bikanta** (2013, USA, \$1.7M), **Cymaris Labs** (2004, USA) and **FND Biotech** (2016, Taiwan) sell fluorescent nanodiamond targeting medical imaging applications. **Diamond Materials** (2017, Germany) is a manufacturer of various variations of diamonds including NV centers. **Quantum Diamant** (Germany) also produces NV centers diamonds, for quantum sensing.

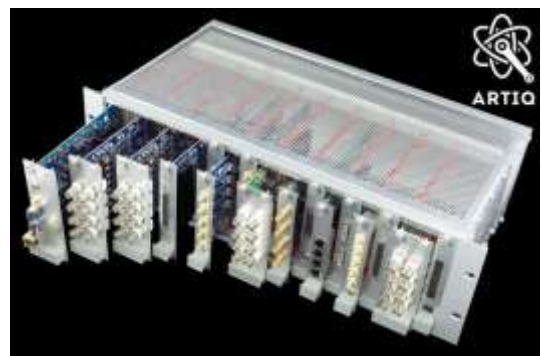
It is a spin-off from TUM (the Technical University of Munich). **Photonanometra** (2011, Russia) is another producer of diamond with NV-center defects.



M-Labs (2007, Hong Kong), formerly known as Milkymist, is working on the ARTIQ (Advanced Real-Time Infrastructure for Quantum physics) project.

This system combines hardware and a real-time operating system to control quantum computer hardware based on trapped ions. It's a bit like the trapped counterpart of startups such as the Israeli Quantum Machines. They have developed their own FPGA circuit for ARTIQ, all programmed in Python. The solution has been developed with the Ion Storage Group team at NIST in the USA, working on ion trapped qubits.

The company was founded by a French engineer, Sébastien Bourdeauducq.





Nano-Meta Technologies (2010, USA) is a spin-off from the University of Perdue that aims to create a quantum information storage system. It is in fact a private contract research laboratory.

It commercializes intellectual property on technologies associating photonics and nanomaterials that could be used in quantum cryptography systems.



Photon Spot (2010, USA) develops nanowires based single photon detectors. They have received a DARPA funding of \$100K in 2014 and \$1.5M in 2015.



QBee.eu (2020, Belgium) is a sort of quantum accelerator or incubator created by Koen Bertels, who also leads the Quantum Computer Architectures Lab in TU Delft and also works at Qutech.

They run various research projects like defining a quantum micro-architecture for quantum accelerators using the OpenQL language from TU Delft, a quantum computing emulator, quantum genomics and quantum finance plus some services in education and consulting.



Q-Lion (2019, Spain) develops an error correction code solution for trapped ion qubits. The startup is a spin-off from the Bank of Santander's Explorer incubation program. It was created by Andrea Rodriguez Blanco, who was still working on a thesis in 2020.

QuantTera (2005, USA) is a contract R&D company created by Matt Kim that develops nano-engineered photonic devices targeting photonic telecommunications and wireless applications. It is mainly using silicon-germanium based photonics. It says it target quantum applications, with no details.



QuTech (2014, The Netherlands) is the quantum hardware spin off from TU Delft University. It collaborates with Intel in the development of superconducting qubits and with Microsoft in topological quantum.

The company is an applied contract research laboratory. It also develops software, such as the **Quantum Inspire** development platform, which enables quantum algorithms to be run on conventional computers in emulation mode. It provides a graphical programming interface in the QASM language. The code can then be executed in emulation mode in the cloud on a classic machine, the Dutch national supercomputer Cartesius, with 5, 26 and 32 qubits, depending on the chosen package.

Cartesius is equipped with thousands of Intel Xeon and Xeon Phi CPUs and a few dozen Nvidia Tesla K40m GPUs with 130 TB of memory delivering 1.84 PFLOPS. The equipment comes from Atos. Quantum Inspire also provides cloud access to QuTech 5 superconducting qubits and 2 electron spin qubits since April 2020.



S-Fifteen Instruments (2017, Singapore) is a spin-off from the renowned CQT laboratory and develops qubit control systems, entangled photon sources, single photons detectors and quantum cryptography solutions covering QKD and QRNGs.



StarCryo Electronics (1999, USA) creates SQUIDs sensors used mostly in quantum sensing and other cryo-electronics products (cables, connectors, ...).

Vapor Cell
Technologies



Vapor Cell Technologies (2020, USA) provides alkaline atom capsules, mainly rubidium, for use in various miniaturized solutions using cold atoms¹⁵⁰⁸. The company was founded by Doug Bopp, a former NIST researcher from Boulder, Colorado.

Zyvex Labs (1997, USA) develops atomic precise manufacturing (APM) solutions based on STM (Scanning Tunneling Microscopy) that can be used to produce components for use in quantum computing (such as the deposition of dopants for superconducting qubits and silicon) and quantum metrology.

They were funded by NIST, DARPA and the Department of Energy SBIR research programs. The company was founded by Jim Von Ehr. Zyvex announced in September 2022 a sub-nm version of its STM solution, the ZyvexLitho1.

Raw materials

For any new hardware technology, it is now a common practice to wonder about its environmental friendliness. We've already been dealing with the energetic dimension of quantum computing. Another key aspect to investigate is the raw materials that are used. What are their sources of supply, their global reserves, their economic and environmental cost of extraction, consumable raw materials if any, and finally, the recycling processes of these materials?

In this exclusive content, I propose a first broad inventory of the different raw materials used in and around quantum technologies of all types, particularly in quantum computers. All these elements are positioned in an in-house Mendeleev periodic table of elements, *below*¹⁵⁰⁹.

We mainly have two types of materials to study: those used in qubits and the supplemental materials, particularly for cables and other supporting structures as well as the gases used in cryostats, mostly helium 3 and 4.

The materials used in qubits are sometimes quite rare (strontium, ytterbium, beryllium). Their selection is based on their energy transitions which correspond to laser or microwave wavelengths that can be used practically with market sources.

Other constraints explain their choice such as the stability of some of these energy levels. Some materials are very rare but their needs in quantum technologies remain marginal in proportion to their production and world consumption.

This is at least the case as long as millions of quantum computers using them are not manufactured. We are not yet at the stage where the consumption of certain elements would come mostly from quantum technologies, as may be the case for smartphones concerning certain rare earths and minerals such as the famous coltan¹⁵¹⁰.

How about rare earth elements? Out of the 17 elements in that category who mainly sit in the lanthanum row in Mendeleev's elements table, about 6 of them are used in quantum technologies: yttrium, praseodymium, dysprosium, europium, erbium and ytterbium, the two later being commonplace in trapped ions computing.

¹⁵⁰⁸ See [Chip-scale atomic devices](#) by John Kitching, 2018 (39 pages) which makes a very interesting inventory of measurement components using this technology: magnetometers, gyroscopes, atomic clocks. You will say that this should go in the metrology section and you will be right.

¹⁵⁰⁹ See also this very nice illustrated poster: [The Periodic Table of the Elements](#), in Pictures.

¹⁵¹⁰ The coltan is the contraction of columbite-tantalite. It is used to recover tantalum and niobium. If it is an important source for tantalum, it is in fact secondary for niobium compared to other minerals. See USGS [Mineral Commodity Summaries 2020](#), the equivalent of the French BRGM (204 pages) that helped me create this part.

In July 2022, Turkey announced the discovery of large reserves of rare earths minerals potentially exceeding China's reserves. But the announcement was probably overstated, preprocessed minerals getting out of mines and rare earth oxides produced after separation¹⁵¹¹.

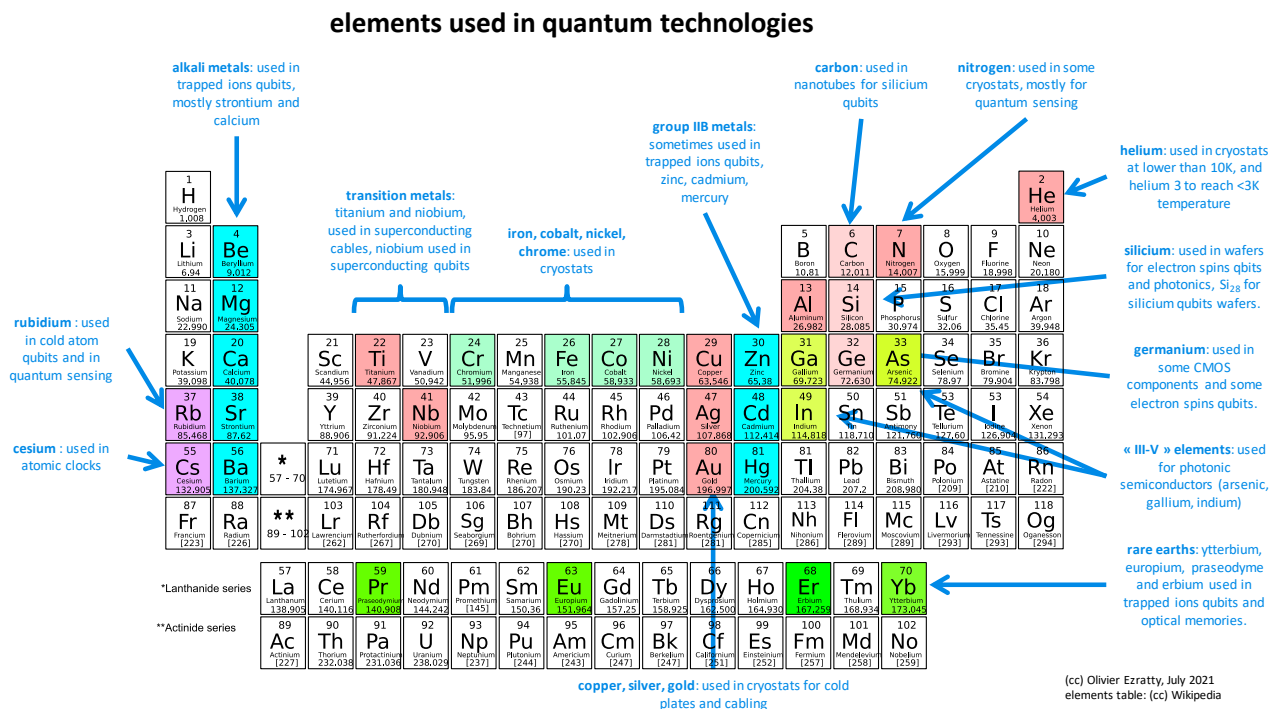


Figure 537: table of elements and those who are used in quantum technologies. (cc) Olivier Ezratty, 2021.

One differentiating aspect of quantum technologies relates to the isotopes used which are sometimes the rarest of their elements. This is the case for helium (3) used in cryogenics below 4K or for cesium (133) for atomic clocks or rubidium (87) in cold atoms. Silicon (28) is used in silicon qubits and, although it is the most abundant isotope, requires costly refining. Carbon (12) is also used in nanotubes like with the startup C12 Quantum Electronics, while Carbon 13 is used in some NV center structures. Some of these isotopes are purified with centrifugal separation, a technique well known in nuclear physics, both civil and military.

I do not mention in this inventory the materials used in the production of semiconductors, such as fluorine and other various solvents. And there are many of these!

We will also not deal with the recycling of quantum computers, an issue that has not yet arisen due to their current very limited number. However, it can be reduced to the more generic issue of recycling various electronic devices.

Helium

Helium is a great paradox in the table of elements. It is the second most abundant element in the Universe after hydrogen. Nuclear fusion does the rest to create all the other elements in first- and second-generation stars. Yet, this element is quite rare on Earth and its reserves are dwindling. It is a noble, inert gas that does not interact chemically with any other element because its electron layer is complete with two electrons. Lighter than air, it tends to leave the atmosphere. As we have seen in detail in the cryostats section, page 465, helium is used for cooling superconductors and electron spins qubits systems.

¹⁵¹¹ See [Turkey Discovers 694 million mt of Rare Earth Element Reserves, with Infrastructure Construction Starting This Year](#), July 2022 and [Turkey Probably Hasn't Found the Rare Earth Metals It Says It Has](#) by Chris Baraniuk, Wired, July 2022.

As soon as one needs to go below 1K, one must use a mixture of two helium isotopes, ^4He which is the most common and stable (with two neutrons) and ^3He which is much rarer (with only one neutron). For cryogenics above 1K, ^4He is sufficient.

For at least a decade, many specialists have been concerned about a shortage of ^4He supply. It is commonly used for cooling superconducting magnets in particle accelerators such as the CERN LHC and in MRI scanners or to inflate balloons. It is also used as a neutral gas for the production of semi-conductors. Fortunately, new sources of natural gas from which ^4He can be extracted have emerged, notably in Tanzania and Qatar¹⁵¹².

But a low annual growth in demand of just 1.6% is too high compared to production forecasts. Air Liquide is one of the major players in this global market, operating a large ^4He extraction and production unit in Qatar, linked to their gas operations. It seems however than the shortage is temporarily gone¹⁵¹³.

The ^3He isotope is rather rare, therefore quite expensive! It was historically a by-product of the storage of tritium-based H-bombs. Tritium gradually disintegrated to produce ^3He . It was therefore recovered from H-bomb stockpiles!

With the reductions in nuclear weapons stockpiles, the production of ^3He is now coming from specialized nuclear power plants. Tritium can be produced with irradiating lithium or with tritium-controlled decay in specialized nuclear facilities, such as those controlled by the US Department of Energy. Tritium is an isotope of hydrogen with one proton and two neutrons.

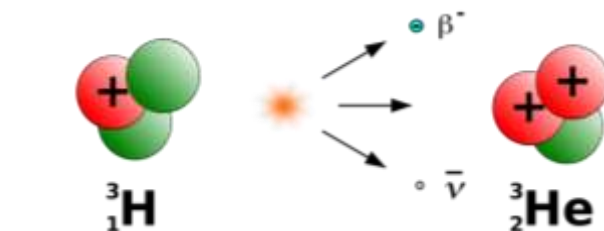


Figure 538: Helium 3 is a by-product of tritium, an isotope of hydrogen with two neutrons.

^3He is produced at the U.S. Department of Energy's Savannah site in South Carolina and at the Canadian CANDU power plant¹⁵¹⁴.


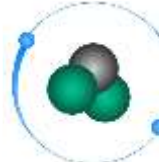
| | |
|---|---|
|  <p>helium 4 2 protons 2 neutrons <i>relatively abundant</i></p> <p>\$5-\$20 per liter of gas >100L per computer</p> |  <p>helium 3 2 protons 1 neutron <i>rare</i></p> <p>\$1500 to \$2000 per liter of gas >\$10K helium 3 per computer</p> |
|---|---|

Figure 539: price tags for helium 3 and 4... as gas!

The price of ^4He gas is around €20 per liter while the price of ^3He gas is between €2K and €3K per gas liter.

A typical dilution-based cryostat requires 15 to 18 liters of ^3He gas for a little over 100 liters of ^4He gas! The gases are purchased separately and mixed at the right dosage by the manufacturer of the dry cryostat.



U.S. DEPARTMENT OF ENERGY





DoE Savannah River Site in South Carolina



The Tritium Extraction Facility began operating in 2017.

Figure 540: Savannah River Site is one of the few places where helium 3 is produced in the world.

At the end, it is therefore necessary to pay at least 30 to 40K€ of ^3He and ^4He per dry cryostat.

The ^4He which feeds the pulsed head and passes through the large compressor must be highly purified.

¹⁵¹² See [Helium - Macro View Update](#), Edison Investment Research, February 2019 (21 pages).

¹⁵¹³ See [Helium shortage has ended, at least for now](#), June 2020.

¹⁵¹⁴ See [Savannah River Tritium Enterprise](#) (4 pages). Helium-3 is also exploited in various specialized applications: in neutron detectors used in security systems, in oil exploration, in medical imaging and in nuclear fusion research. Also see [CANDU Reactor](#), Wikipedia.

France has some ^3He production capacities located in a CEA nuclear reactor in Grenoble. But it does not necessarily use them for quantum computers because this production is too expensive¹⁵¹⁵.

We can also find ^3He on the surface of the Moon but it is not very practical to extract it and ship it back to Earth even if it is technologically possible¹⁵¹⁶! This isotope could be interesting to feed nuclear fusion reactions, pending its complicated technological development.

^3He is therefore a real bottleneck in the production of superconducting and electron spin quantum computers! It cannot even be avoided for the latter, which requires a temperature of about 1K¹⁵¹⁷.

Silicon

Silicon is the key element in many semiconductor components used in or around quantum processors. While being the second most abundant element in the Earth's crust after oxygen, the silicon used in semiconductors comes from a few quartz mines. This is because quartz is composed of at least 97% silicon, which is easier to refine. After chemical-based refinement, silicon is turned into large cylindrical ingots which are then sliced into thin wafers. Wafers are then processed in semiconductor fabs with transistors that combine silicon oxide and different doping materials such as hafnium.

Silicon qubits require using ^{28}Si , because the null spin of its nucleus does not interfere with the spin of the trapped electrons used as the qubit observable. The silicon wafers on which the qubits are etched are covered with a thin layer of ^{28}Si . ^{28}Si is the most abundant variant of the element while ^{29}Si represents less than 4%.

^{28}Si made headlines in 2010 when some German researchers created a perfect crystal ball made of ^{28}Si to accurately determine the Avogadro number, which determines the number of elements, here atoms, in a mole¹⁵¹⁸. The tests were carried out on a 5 kg sample at a cost of 1M€ In 2014, an American team improved the purity of ^{28}Si to 99.9998% with pumping silicon ions in a magnetic field, allowing it to be separated by mass¹⁵¹⁹.

This continued in 2017 with 99.999%¹⁵²⁰ ^{28}Si produced by a team of Russian and German researchers. The interest of ^{28}Si was to allow a precise counting of the number of silicon atoms in the mass considered, because of its perfect crystal structure, dimensioned by X-ray interferometry. The Avogadro number determined by the 2010 experiment was $N_A = 6.022\,140\,84(18) \times 10^{23}$. The ambition of these two projects was to create a new material standard of the kilogram, the 1889 material standard preserved in France that degrades by oxidation.

¹⁵¹⁵ See [Isotope Development & Production for Research and Applications \(IDPRA\). Supply and Demand of Helium-3](#), 2016, [Responding to The U.S. Research Community's Liquid Helium Crisis](#), 2016 (29 pages) and [How helium shortages will impact quantum computer research](#) by James Sanders, April 2019.

¹⁵¹⁶ See [There's Helium in Them Thar Craters!](#). China is planning to harvest Helium 3 on the Moon.

¹⁵¹⁷ Helium-4 is used to cool superconducting magnets in MRI systems. It is also used to cool the magnets of the LHC at CERN. The constraints are different: it is just a matter of obtaining superconductivity for the magnets that focus the particle beams. The required temperature is between 1.8K and 4.5K, much "hotter" than the 15 mK of electron-based quantum processors (superconductors, silicon, NV Centers, Majorana fermions). On the other hand, the volumes to be cryogenized are much larger. In some cases, however, the required temperature can fall below 1K, particularly for the search for dark matter. In CERN's LHC, 9 Tesla magnets are cooled to 1.8K with 18 kW cryostats that handle 120 tons of helium 4.

¹⁵¹⁸ See [An accurate determination of the Avogadro constant by counting the atoms in a \$^{28}\text{Si}\$ crystal](#) by B. Andreas, 2010 (4 pages). Silicon 28 was obtained by centrifuging silicon fluoride (SiF_4) gas, then transformed into SiH_4 which was then used to create the crystal by vacuum deposition of purified silicon. All this was carried out in different laboratories in Russia, in Nizhny-Novgorod and Saint Petersburg. The researchers involved also came from Italy, Australia, Japan, Switzerland and BIPM in France, from their respective weights and measures offices.

¹⁵¹⁹ See [Purer-than-pure silicon solves problem for quantum tech](#) by Jonathan Webb, 2014 which refers to [Enriching \$^{28}\text{Si}\$ beyond 99.9998% for semiconductor quantum computing](#) by K J Dwyer et al, 2014 (7 pages).

¹⁵²⁰ See [A new generation of 99.999% enriched \$^{28}\text{Si}\$ single crystals for the determination of Avogadro's constant](#) by N V Abrosimov et al, 2017 (12 pages) which describes very well the process of purification of ^{28}Si , the source of the illustration on this page.

Finally, in 2018, the Avogadro number was redefined in the international measurement system as a slightly different constant of $6.022\,140\,76 \times 10^{23} \text{ mol}^{-1}$. Indirectly, however, these two experiments did advance the know-how of ^{28}Si purification, at a time when its interest in creating silicon qubits was barely in the radar. What a good illustration of serendipity in science!

The silicon purification process is complex. It involves the production of silicon tetrafluoride (SiF_4) of all isotopes. Enrichment in ^{28}Si is carried out in a centrifuge, originally at the Central Design Bureau of Machine Building in St. Petersburg, in fact, a former plutonium enrichment plant reassigned for this use in 2004.



Figure 541: silicon 28 was initially produced to create a replacement for the reference kilogram used in the international metric system, as a way to determine the Avogadro number. Purifying silicon 28 was a figure of merit of this quest that is now reused in the silicon spin realm.

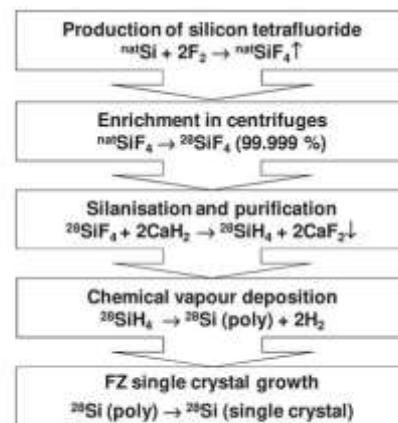


Figure 4. Main technological steps of the ^{28}Si crystal production (^{nat}Si : silicon of natural isotopic composition).

The gas is transformed into silane ($^{28}\text{Si H}_4$) at the **Institute of Chemistry of High-Purity Substances** of the Russian Academy of Sciences in Nizhny-Novgorod. It can then be deposited by vapor deposition (CVD) on silicon, releasing hydrogen. The resulting ingot can then be stretched to create a perfectly crystalline silicon ready to be sliced into wafers. CEA-Leti researchers are also working with Russian teams at Nizhny-Novgorod on the process for vacuum deposition of ^{28}Si on 300 mm wafers¹⁵²¹. In October 2021, **Orano** announced its ambition to produce ^{28}Si in France.

Air Liquide is also partnering with the Nizhny-Novgorod laboratory for this process of CVD (chemical vapor deposition) of ^{28}Si on a 30 to 60 nm thin film that is 99.992% pure¹⁵²² above a conventional silicon wafer. Knowing that Air Liquide also masters the conversion of SiF_4 into silane.

Germanium

Germanium is a semiconductor metalloid that is part of the III-V family. It is used in many fields: in photonics, in SiGe heterojunction bipolar transistors which are used for the amplification of weak microwave signals as well as in electron spin qubits chipsets.

¹⁵²¹ See [99.992% \$^{28}\text{Si}\$ CVD-grown epilayer on 300 mm substrates for large scale integration of silicon spin qubits](#) by V. Mazzocchi of CEA-Leti and colleagues from France and Russia, 2018 (7 pages).

¹⁵²² See [Quantum computing: progress toward silicon-28](#), April 2018.

With spin qubits, it must be isotopically purified to generate ^{73}Ge which corresponds to 7.36% of its proportion (in purple in the chart *opposite*). It is a stable, natural and non-radioactive isotope. Germanium is generally extracted from zinc ores and also from zinc-copper ores. In 2019, 130 tons of germanium were produced, with China being the main supplier with 85 tons¹⁵²³. Data on known reserves are variable and are estimated at approximately 9,000 tons, mainly located in China, Canada and the USA. Along with gallium and indium, which are also III-V materials, germanium is considered a critical resource.



Isotopic purification of germanium is carried out by the same Russian teams at Nizhnii Novgorod as those producing ^{28}Si . It uses a germanium tetrafluoride centrifugation process similar to the one used to produce germanium tetrafluoride and explained in Figure 541¹⁵²⁴.

Rubidium

Rubidium is an alkali metal used to create cold atom qubits that are excited into highly energetic Rydberg states. It is also used in quantum sensing, notably to create atomic clocks and micro-gravimeters. It is an alkaline, soft, silvery metal with a melting temperature of only 39.3°C (in Figure 542).

In a neutral atom computer, the metal is used very sparingly. It is supplied in ampoules of a few solid grams. It is heated in a small box to be sublimated into gas which then feeds the vacuum chamber where the lasers will trap individual atoms. The metal costs about \$85 per gram and about \$1600 per 100g. It is readily available from chemical companies.



Figure 542: rubidium in molten state. , in molten state.
Source [Wikipedia](#).

Only 5 tons are produced annually worldwide, including China, Canada, Namibia and Zimbabwe¹⁵²⁵. It is a by-product of the extraction of cesium and lithium. The isotope ^{87}Rb is the most used and represents 27.8% of available rubidium. It is radioactive but with a half-life longer than the age of the Universe, so it is very stable. World reserves are estimated at 100,000 tons, which is enough to keep up with the current rate of production and consumption.

Niobium

Niobium is a transition metal used in superconducting qubits as well as in microwave cables driving superconducting and electron spin qubits. **Coax Co** (Japan) has a monopoly in the manufacturing of these cable, which are very expensive, about \$3K per half a meter segment. And three are needed per superconducting qubits, positioned between the 4K and 15mK cryostat cold plates.

In industry, it is used in the production of high-strength special steels, in superconducting magnets, in particle accelerators, in arc welding, in bone prostheses associated with titanium, in optics, as a catalyst for rubber synthesis, in aircraft engines and in gas turbines.

¹⁵²³ See [Refinery production of germanium worldwide in 2021](#), by country, Statista.

¹⁵²⁴ See [Production of germanium stable isotopes single crystals](#) by Mihail Fedorovich Churbanov et al, April 2017 (6 pages).

¹⁵²⁵ Each human weighing 70 kg contains about 0.36g of it. However, we are not going to create a variant of Soylent Green to exploit it. Rubidium mining in Canada is carried out by Tantalum Mining Corporation, which belongs to the Chinese group Sinomine Resources since June 2019.

World production was estimated at 68,000 tons per year in 2018, with Brazil accounting for 88%, followed by Canada for just over 9%, generated by a single mine. It comes from the exploitation of pyrochlore, an ore combining calcium, sodium, oxygen and niobium.

It is not very expensive and is priced at \$45 per kilogram, but in its ferro-niobium form. The reserves are of 9 million tons, enough to last 130 years at the current usage rate. But in practice, niobium is considered a "risky" resource because its demand is growing rapidly even though it comes from relatively safe geopolitical places.



Figure 543: niobium is a relatively cheap metal.

Ytterbium

Ytterbium is a rare earth of the lanthanide series which is used in trapped ions qubits, quantum memories, atomic clocks, doping of certain lasers and, more rarely, in cold atom qubits.

Otherwise, it is used to reinforce certain specialized steels.

The metal is extracted from monazite, a tetrahedral crystalline rock structure of phosphorus oxide associated with various rare earths, which contains only 0.03% of it. Production follows a complex cycle using sulfuric acid and ions exchange. Quantum applications use isotope 171, one of the 7 non-radioactive isotopes of the element. It represents 14% of its proportion in the rocks from which it is extracted. This isotope is probably more expensive than the regular multi-isotope version which is sold between \$500 and \$1K per kilogram.

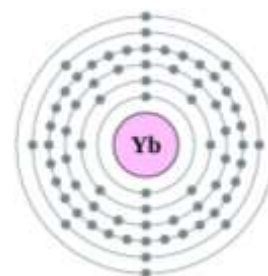


Figure 544: ytterbium atomic structure.

Approximately 50 tons are produced annually, mainly in China, the USA, Brazil, India and Australia, with reserves estimated at one million tons. Creating trapped ions computers require about one gram per quantum processor.

Erbium

This rare earth of the lanthanide family is used in quantum memories, in some fancy cold atom qubits and in certain lasers (Er:YLF type for yttrium lithium fluoride or Er:YAG type for yttrium aluminum oxide). It is found in some optical fibers used in optical amplifiers.

Finally, it can be used to create vanadium alloys found in cryostats thanks to its high thermal mass heat absorption capacity. China is the main producer, followed by the USA. It comes from extracting xenotime (phosphate ore) and euxenite (an ore also containing niobium, titanium and yttrium). The ore is processed with hydrochloric or sulfuric acid and then neutralized with soda ash. After a bunch of chemical treatments, erbium ions are extracted by ion exchange on polymer resins.



Figure 545: erbium.

Erbium is then obtained by heating its oxide with calcium at 1450°C in a neutral argon atmosphere. All this is a long and expensive chemical process, probably polluting of lot but carried out on small volumes. Erbium is produced at a rate of about 500 tons per year. Its price per gram is about \$20, which is quite affordable to integrate it in memories or cold atoms qubits.

Strontium

Strontium is the most common alkali metal used to create trapped ions qubits, with its isotope 87, representing 7% of its five isotopes. It is used as a red dye in fireworks.

Mexico and Germany are the main producers, with an estimated world production of 220,000 tons per year and reserves of over one billion tons. It is notably used in bones anti-cancer radioactive chemotherapies.

Strontium is considered to be toxic. This is the case of all these rare metals which, being pure, oxidize quickly whatever happens. In particular, it explodes when being in contact with water.

Gold

In quantum technologies, gold is mainly used as a thin layer covering the copper plates of the cold plates in cryostats. It prevents copper oxidation and adds good thermal conductivity. The volume used is quite small in relation to gold production and global reserves. About 3000T of gold are produced every year worldwide.

Titanium

Titanium is mainly used in association with niobium in superconducting microwave cables.

In industry, it is used for its resistance to corrosion, particularly in the aerospace industry. Some submarines have an all-titanium hull. Titanium oxide is used as a painting white pigment. It is found in great quantities on Earth since it is the fifth most abundant metal. But only a few ores contain a high enough concentration of it to make its production profitable. The main producing countries are Australia, South Africa, Canada and Norway at a rate of 4.2 million tons per year. Reserves are in excess of 600 million tons.

Nitrogen

Liquid nitrogen is used in cryostats to clean the gaseous helium that feeds them. It is also found in small quantities in NV Centers crystals. It is not a rare commodity. But its production in liquid form is quite energy consuming.

Other materials

Many other relatively common materials are used in quantum technologies.

Copper is found in cryostat cold plates and with some of the various electrical connectors. It is purified at 99.99% to become free of impurities and oxygen (OFHC for oxygen-free high conductivity), in order to improve its thermal conductivity and electrical conductance. It is also widely used in trapped ions chambers. As far as its depletion is concerned, its consumption in quantum technologies is minor.

Carbon is exploited in a variety of places, including with carbon nanotubes from C12 Quantum Electronics. This carbon must be purified to keep only its isotope ^{12}C is acquired in the form of methane in bottles acquired in the USA for \$10K. It is 99.997% purified. The isotopic separation of ^{12}C uses a chemical process applied to CO_2 . Carbon is also used in NV centers.

Aluminum¹⁵²⁶ is used in some superconducting qubits as well as for part of the connector technology in cryostats. It is abundant.

Manganese is used in very small quantities as a dopant in some superconducting qubits and can be used with trapped ions qubits.

Silver is mainly used in powder form in some heat exchangers in dilution refrigeration systems.

Iron is a commodity used in the form of steel in the structure of quantum computers.

¹⁵²⁶ The spelling is aluminum in American and Canadian English and aluminium elsewhere. This document is mostly in American English.

Cesium is mainly used in atomic clocks, in its isotope 133. Reserves are sufficiently abundant in relation to identified needs. They are mainly located in Canada.

In addition to germanium, **gallium** and **indium** play a key role in III-V components used mainly in photonics and **Neodymium** is used in lasers. This is one of the few areas of quantum technologies where there is a strong dependence on China as a source of supply. Finally, **beryllium**, **calcium**, **zinc**, **cadmium** and **mercury** can be used in trapped ion qubits, but the most commonly used are ytterbium, barium and calcium.

The below table in Figure 546 is a summary of this part with a list of materials, their main usage in quantum technologies, their main countries of production, rarity and production cleanliness.

| Element | Quantum computing | Quantum sensing and others | Main country sources | Rarity | Cleanliness |
|------------|-------------------------|----------------------------|---|--------|-------------|
| Helium 3 | Cryostats | | USA, Canada | | |
| Helium 4 | Cryostats | Cryostats | Qatar | | |
| Silicon 28 | Silicon Qubits | | Russia, France | | |
| Rubidium | Cold Atoms | Cold Atoms | China, Canada, Namibia and Zimbabwe | | |
| Niobium | Cables, supra qubits | | Brazil, Canada | | |
| Ytterbium | Trapped ions, memory | | China, USA, Brazil, India and Australia | | |
| Europium | Memories | Repeaters | Mongolia, China, Russia | | |
| Erbium | Cold atoms, memory | | China | | |
| Barium | Trapped ions | | UK, Romania, Russia | | |
| Strontium | Trapped ions | | Mexico, Germany | | |
| Neodymium | Lasers | Lasers | China, United States, Brazil, India, Sri Lanka, Australia | | |
| Gold | Cold plates | | Peru, Mexico, Indonesia | | |
| Titanium | Cables | | Australia, South Africa, Canada, Norway | | |
| Gallium | | Photonics | China, Germany, Kazakhstan, Ukraine | | |
| Germanium | | Photonics | China, Canada, Finland, Russia, USA | | |
| Indium | | Photonics | China, Belgium, Canada, Japan, Peru, South Korea. | | |
| Nitrogen | Cryostats | NV Centers | | | |
| Aluminum | Cryostats, supra qubits | | China, India, Russia, Canada | | |
| Silver | Cryostats | | Mexico, China, Peru, Chile, Poland | | |
| Caesium | | Clocks | Canada, Zimbabwe, Namibia | | |
| Carbon | NV Centers, nanotubes | NV Centers | | | |

Figure 546: table with elements used in quantum technologies with their country or origin, rarity and environmental footprint. Consolidation (cc) Olivier Ezratty.

Quantum enabling technologies key takeaways

- Cryogeny is a key quantum computing enabling technology particularly for solid-state qubits which work at temperatures between 15 mK and 1K. These systems rely on a mix of helium 3 and 4 in so-called dry-dilution refrigeration systems. Other simpler cooling technologies target the 3K to 10K temperature ranges that are used with photon sources and detectors, as used with photon qubits systems.
- Cabling and filters play another key role, particularly with solid-state qubits. Superconducting cables are expensive with 3K€ per unit and come from a single vendor source from Japan. Signals multiplexing is on the way!
- Microwave generation and readout systems used with superconducting and quantum dots electron spin qubits are other key enabling technologies. The challenge is to miniaturize it and lower their power consumption and, if that makes sense, to put them as close as possible to the qubits, operate them at cryogenic temperatures and simplify system cabling. It's a key to physical qubits scalability. A lot of different technologies compete here, mostly around cryo-CMOS and superconducting electronics. Other components deserve attention like circulators and parametric amplifiers that we cover in detail in this new edition.
- Many lasers and photonics equipment are used with cold atoms, trapped ions and photon qubits and also quantum telecommunications, cryptography and sensing. It includes single indistinguishable photon sources as well as single photon detectors. The lasers field is also very diverse with product covering different ranges of wavelengths, power, continuous vs pulsed lasers, etc.
- Manufacturing electronic components for quantum technologies is a strategic topic covered extensively in this book for the first time with a description of generic fab techniques and some that are specific to quantum technologies like with the fabrication of superconducting qubits and quantum dots.
- Quantum technologies use a lot of various raw materials, some being rare but used in very small quantities. While some materials may have some incurred environmental costs, most of them do not seem to be scarce and they have multiple sources around the planet.

Page intentionally left blank.

The remainder of “Understanding Quantum Technologies” is in Volume 2.

It contains the following parts: quantum algorithms, quantum software tools, quantum computing business applications, unconventional computing, quantum telecommunications and cryptography, quantum sensing, quantum technologies around the world, corporate adoption, quantum technologies and society, and quantum fake sciences, plus a glossary, table of figures and index for both documents using a continuous pagination numbering.

Page intentionally left blank.

back cover back page

le lab quantique

$|0\rangle$



$|1\rangle$